



FEDERAL UNIVERSITY OF TECHNOLOGY, MINNA
SCHOOL OF ELECTRICAL ENGINEERING AND TECHNOLOGY &
SCHOOL OF INFRASTRUCTURE, PROCESS ENGINEERING AND TECHNOLOGY

3rd **INTERNATIONAL
ENGINEERING CONFERENCE
IEC 2019**

THEME THE ROLE OF ENGINEERING AND
TECHNOLOGY IN SUSTAINABLE DEVELOPMENT

BOOK *of*
PROCEEDINGS



DATE:
24TH - 26TH
SEPTEMBER 2019

VENUE:
CHEMICAL ENGINEERING
LECTURE THEATER, FEDERAL
UNIVERSITY OF TECHNOLOGY,
MINNA, NIGER STATE

EDITED BY

ENGR. DR. S.M. DAUDA, ENGR. DR. A.U. USMAN, ENGR. DR. U.S. DAUDA,
ENGR. M. ABUBAKAR, ENGR. DR. E.A. AFOLABI, ENGR. DR. I.M. ABDULLAHI,
ENGR. DR. (MRS) I.H. MUSTAPHA, ENGR. A.S. AHMAD, ENGR. J.G. AMBAFI,
ENGR. T.A. FOLORUNSO, ENGR. U.U. BUHARI, ENGR. DR. OPE OSANAIYE,
ENGR. A. YUSUF



FEDERAL UNIVERSITY OF TECHNOLOGY, MINNA
SCHOOL OF ELECTRICAL ENGINEERING AND TECHNOLOGY &
SCHOOL OF INFRASTRUCTURE, PROCESS ENGINEERING AND TECHNOLOGY



DATE: 24TH - 26TH SEPTEMBER 2019

**THEME THE ROLE OF ENGINEERING AND
TECHNOLOGY IN SUSTAINABLE DEVELOPMENT**

MEMBERS OF THE CONFERENCE ORGANISING COMMITTEE

Engr. Dr. S.M. Dauda	Chairman	Engr. Dr. U.S. Dauda	Member
Engr. Dr. A.U. Usman	Co-Chairman	Engr. Dr. M.D. Yahya	Member
Engr. Prof. R.A. Muriana	Member	Engr. Dr. B.A. Orhevba	Member
Engr. Dr. T.W.E. Adejumo	Member	Engr. Dr. Michael David	Secretary

TECHNICAL COMMITTEE

Engr. Dr. U.S. Dauda	Chairman
Engr. Dr. Eytayo Afolabi	Member
Engr. Dr. A.I. Mohammed	Member
Engr. Dr. (Mrs) H.I. Mustapha	Member
Engr. A.S. Ahmad	Member
Engr. J.G. Ambafi	Member
Engr. T.A. Folorunso	Member
Engr. Buhari U. Umar	Member
Engr. Dr. Ope Osanaiye	Member
Engr. A. Yusuf	Member
Engr. M. Abubakar	Secretary

WELFARE COMMITTEE

Engr. Dr. M.D. Yahya	Chairman
Engr. Prof. R.A. Muriana	Member
Engr. Dr. A.J. Otaru	Member
Engr. Dr. E.A. Afolabi	Member
Engr. A. Yusuf	Member
Engr. Dr. B.A. Orhevba	Secretary

LOGISTIC COMMITTEE

Engr. Prof. R.A. Muriana	Chairman
Engr. D.N. Kolo	Member
Engr. Essien Akpan	Member
Mr. Idris Akintunde	Member
Mr. Mohammed Shehu	Member
Engr. Dr. T.W.E. Adejumo	Secretary

FINANCE COMMITTEE

Engr. Dr. B.A. Orhevba	Chairman
Engr. Prof. O.A. Olugboji	Member
Engr. Dr. M.D. Yahya	Member
Engr. Dr. H.I. Mustapha	Member
Engr. Bello Abdulkadir	Member
Engr. Buhari Umar	Member
Engr. Dr. M. Alhassan	Secretary

ICT COMMITTEE

Engr. Dr. Bala A. Salihu	Chairman
Mr Emmanuel Abba	Member
Mr Alenoghena Benjamin	Member



CONTENTS

Content	Page
Cover Page	i
Table of Content	ii
Forward	ix
Acknowledgement	x
Statistical Optimization of Biodiesel Production from Jatropha Oil Using Calcined Snail Shell Catalyst Afangide, U. N., Olutoye, M. A, & Aberuagba, F.	1 – 5
Development of AgNPs-MWCNTs Adsorbent for Seawater Treatment Mohammed, S. M., Muriana, R. A, Agboola, J. B, Abdulkareem, A. S., Kariim, I., & Yahya, M. D.	6 – 14
The Role of Engineering and Technology and Sustainable Development Reducing Carbon Emission with Green and Sustainable Build Environment Hashimu, L., Halilu, A, A., & Sani, I.	15 – 23
Optimization and Kinetics Study of Biodiesel Synthesis from Beef Tallow Using Calcium Oxide from Limestone Ogunjobi, T. O., Olutoye, M. A. & Aberuagba, F.	24 – 33
Column Adsorption Studies of Textile Wastewater Using Iron Oxide Nanoparticles doped Zeolite A Alaya-Ibrahim, S., Kovo, A.S., Abdulkareem, A.S., Adeniyi, O.D. & Yahya, M.D.	34 – 43
A Comprehensive Review on Use of Poly Electrolyte Complex PEC as an Adsorbent for the Removal of Heavy Metals From Aqueous Solution. Achanya, B. E. & M., Auta	44 – 52
Computational Fluid Dynamics Simulation of FCC Regenerator of a Refinery Usman, A. A., Onifade, K.R., Mohammed, I. A., & Garba, M.U.	53 – 60
Assessment of Factors Affecting Stakeholder Management in Nigeria Construction Projects Okosun, B. O., Idiake, J.E., Oyewobi, L.O., & Shittu, A.A.	61 – 64
Effect of Partial Replacement of Fine Aggregate with Sawdust in Light Weight Concrete Production using Bida Natural Stone as Coarse Aggregate Alhaji B., Abubakar M., Yusuf A., Oritola S. F, Mohammed S. & Kolo D. N.	65 – 69
Quality Assessment of Locally Available Selected Cements in Nigeria Muftau, O. S., Abdullahi, M., & Aguwa, J. I.	70 – 76
Development of Mix Design Guide for Normal Weight Concrete using Locally Available Materials Okoh S. O.; Abdullahi M.; & Alhaji, B.	77 – 82
Comparative Evaluation of Strength of Compacted Lateritic Soil Improved with Microbial-Induced Calcite Precipitate K. J. Osinubi, E.W. Gadzama, A. O. Eberemu, & T. S. Ijimdiya	83 – 91
Effects of Urban Growth on Surface Temperature in Parts of Katsina State, Nigeria Abdulsamad Isah & Abubakar A.S.	92 – 98



2nd International Engineering Conference (IEC 2017)
Federal University of Technology, Minna, Nigeria



Kinetic Modelling and Error Analysis of the Bioremediation of Used Motor Oil Contaminated Soil Using Palm Bunch Ash as Stimulant Abdulyekeen, K. A., Aliyu, A, Abdulkarim, A. Y, Salis , A., & Abdulkarim, A. S.	99 – 103
Quantitative Risk Analysis for Communication Satellite Payload Babadoko, D . M, & Ikechukwu, A. D.	104 – 113
Characterization and Grading of South Eastern Nigerian Grown <i>Mangifera Indica</i> Timber in Accordance with British Standard 5268 Mbakwe C.C., Aguwa J.I., & Oritola S.F.	114 – 120
Characterization of Palm Kernel Shell as Lightweight Aggregate in Concrete Production Sunday I .O., Aguwa J.I. & Auta S.M.	121 – 125
Integrated Geophysical Investigation of the Failed Portion of Minna-Zungeru Road, Minna Niger State Osheku, G. A., Salako, K. A, & Adetona, A. A	126 – 132
Partial Replacement of Fine Aggregate with Waste glass in Concrete made from Bida Natural Aggregate Alhaji B., Kolo, D. N., Abubakar M., Yusuf A., Abdullahi, A. and Shehu, M.	133 – 137
Assessment of the Compressive Strength of Concrete Produced with Fine Aggregate from Different Locations in Minna Aminulai, H. O., Abdullahi, A., Abdulrahman, H. S., Alhaji, B., Joseph, O. F., Aliyu, S. Y.	138 – 143
Response Surface Optimisation of the Adsorption of Cu (II) from Aqueous Solution by Crab Shell Chitosan Babatunde E. O., Akolo S. A., Ighalo J. O. & Kovo A. S.	144 – 151
The Linear Transformation of a Block Hybrid Runge-Kutta type Method for Direct Integration of First and Second Order Initial Value Problem Muhammad, R., Yahaya, Y.A., & Abdulkareem, A.S.	152 -154
Groundwater Potential Mapping in Bosso Local Government Area, Niger State, Nigeria Abubakar, U.B. & Muhammed, M.	155 – 159
Optimization of Synthesis Parameters of Silica from Bentonite Clay Using Acid Leaching Ogwuche, A. S., Auta, M., & Kovo, A. S.	160 – 163
Chemical and Mineralogical Characterization of Locally Sourced Nigerian Clay Sumanu, O. M., Dim, P.E. & Okafor, J. O.	164 – 167
Production and Optimization of Bioethanol from Watermelon Rind using <i>Saccharomyces Cerevisiae</i> Igbonekwu, C . A., Afolabi, E. A., Nwachukwu, F.O.	168 – 173
Use of Carbide Waste as a Mineral Filler in Hot Mix Asphalt Murana, A.A. & Musa, Y.	174 – 182
Review of Bio Oil Upgrading from Biomass Pyrolysis Abdullahi, M. A, Garba, M. U, Eterigho E. J, & Alhassan, M.	183 – 192



2nd International Engineering Conference (IEC 2017)
Federal University of Technology, Minna, Nigeria



Optimization study of Deacetylation Process in the Synthesis of Chitosan from Red Shrimp Using Response Surface Method Atanda, A. S, Jimoh, A. & Ibrahim, A.A.	193 – 204
Optimisation Study on the removal Pb(II), Cd(II) and Ni(II) from Pharmaceutical Wastewater using Carbonized African Giant Snail Shell (<i>Archachatina marginata</i>) as an Adsorbent. Olanipekun, O., Aboje, A. A, Auta, M.	205 – 215
Ground Electromagnetic Prospecting for Potential Ore Mineralisation Zones in Tsohon- Gurusu Area of Minna, North Central Nigeria Ogale, O. D, Rafiu, A. A., Alhassan, D. U., Salako K. A., Adetona A. A. & Unuevho C.	216 – 222
Magnetic and Geoelectrical Prospecting for Gold Mineralisation Within Tsohon-Gurusu Area, Part of Sheet 164 Minna, North-Central Nigeria Omugbe, L. E, Salako, K. A, Unuevho, C.I, Rafiu, A. A, Alhassan, D. U, Ejepu, J. S, & Adetona, A. A.	223 -228
Road Stabilization Using Cold Bitumen for Low Traffic Road Kolo S. S., Jimoh, Y. A., Alhaji, M.M, Olayemi, J. & Shehu, M.	229 – 233
Sawdust Ash Stabilization of Weak Lateritic Soil Kolo S. S., Jimoh Y. A., Yusuf I. T, Adeleke O. O., Balarebe, F. & M. Shehu	234 – 238
Radio Refractive Index and Refractive Index Gradients Variation in a Tropical Environment I.M. Tukur, K.C. Igwe & J.O. Eichie	239 - 243
Vocational and Technology Education: A Viable Entrepreneurship Tool for Rapid Economic Growth Kareem, W.B., Abubakar, H.O. (Mrs.), Onuh, J., Abdulrahaman, T.S., Abdullahi S.M.	244 – 249
A 2-Step Hybrid Block Backward Differentiation Formula for the Approximation of Initial Value Problems of Ordinary Differential Equations Akintububo, Ben.G & Umaru Mohammed	250 – 254
Significant Delay Factors Affecting Completion Time of Public Sector Construction Projects in Niger State Mamman, J. E., Abdullahi, A. H., Isah, L. M.	255 – 260
Communication Frequency and Effectiveness on Construction Sites in Abuja, Nigeria Mamman, J.E., Abdullahi, A.H. & Isah, M.L.	261 – 269
Contribution of Quality Management Practices towards Building Collapse in Nigeria Yunusa, H., Makinde, J. K., & Oke, A. A.	270 – 277
Assessment of Ethical Practices at Different Stages of Public Housing Delivery in Nigeria Oluwadare, D. O. & Idiake, J. E.	278 – 285
Participation of Female Quantity Surveyors in the Nigerian Construction Industry Nnamoko, C. E	286 – 292
Performance Evaluation of WUPA Wastewater Treatment Plant Idu-Industrial Area, Abuja Saidu, M., Adesiji, A. R., Asogwa, E.O., Jiya, A.M. & Haruna, S.I.	293 – 296
Evaluation of Strength Characteristics of Compacted Deltaic <i>Chikoko</i> Clay Stabilized with Rice Husk Ash T.W.E. Adejumo & B. B. Olanipekun	297 – 303



2nd International Engineering Conference (IEC 2017)
Federal University of Technology, Minna, Nigeria



Empirical Impact Evaluation of Sales Promotional Mix on Sachet -Water Product Distribution on Enterprise Performance: A Survey of Selected Sachet- Water Outfits in Niger State Adima Julius Osaremen	304 - 312
Assessing the Level of Readiness to Adopt Building Information Modelling (BIM) Amongst Built Environment Professionals In Selected Northern Nigerian States Abubakar, I. T. & Oyewobi, L. O.	313 – 323
Design and Implementation of an SMS-based dynamic matrix LED Display Board Habibu, H., Chukwu , E. C., Latifa , Y., Haris, M. Y.& Okosun, O. E.	324 – 329
An Improved User Pairing, Subchanneling, and Power Allocation Algorithm For 5G Noma System. Muhammad Z.Z., Tekanyi A.M.S., Abubilal K.A., Usman A. D., Abdulkareem H. A. & Kassim A. Y.	330 – 337
Automation of Agricultural Machinery Operation Systems; An Imperative for Sustainable Development Bala Ibrahim	338 – 343
Electricity Generation using Locust Bean Waste and Coal in a Molten Carbonate Direct Carbon Fuel Cell Yakubu E., Adeniyi, O.D., Alhassan M., Adeniyi, M.I., Uthman H., and Usman A.A.	344 – 349
Design of a Programmable Solid State Circuit Breaker Ajagun, A. S., Abubakar, I. N., Yusuf, L. & Udochukwu P. C.	350 – 354
Design of an Arduino Based RFID Line Switching Using Solid State Relay with Individual Phase Selection Ajagun, A. S., Yusuf, L., Abubakar, I. N. & Yusuff, S. D.	355 – 361
Development of an Improved Adaptive Hybrid Technique to Mitigate Cross-Tier Interference in a Femto-Macro Heterogeneous Network Kassim, A. Y., Tekanyi, A. M. S., Sani, S. M., Usman, A. D., Abdulkareem, H. A. & Muhammad, Z. Z.	362 – 370
The Level of Awareness of Electrical Safety Among Energy Users in Sokoto State Umar, A., Abubakar, I. N., Yusuf, H. M. & Okosun, O. E.	371 – 376
Phytoremediation of Soil Contaminated with Brewery and Beverage Effluents using <i>Cynodon dactylon</i> Mustapha, H., Ehichoya, C. S & Musa, J. J	377 – 384
Application of Dreyfus Model of Skills Acquisition in Curbing Youth Unemployment Among the Motor vehicle Mechanic Students' in Nigeria Aliyu Mustapha, Abdulkadir Mohammed, Abubakar Mohammed Idris & Benjamin Oke	385 – 390
A Numerical Analysis of Convective Heat Transfer Rate from A Wavy Fin Projecting Horizontally From A Rectangular Base Okon, J. O.	391 – 396
Towards A Hybrid MQTT-COAP Protocol for Data Communications In Wireless Sensor Networks Nwankwo, E. I, Onwuka, E. N& Michael, D.	397 – 403
Toward a Hybrid Technique for Friends Recommendation System in Social Tagging Usman Bukar Usman	404 – 410
Towards A Model for Aspect Based Sentiment Analysis of Online Product Review Abdulganiyu, O. H. & Kabiru, U.	411 – 418



**2nd International Engineering Conference (IEC 2017)
Federal University of Technology, Minna, Nigeria**



Parametric Oscillations in Electric Oscillatory System Enesi A.Y., Ejiogu. E. C.	419 – 423
Fenestration Effect on the Adequacy of Classroom UDD Azodo, A. P., Onwubalili, C. & Mezue T. C.	424 – 431
Prediction of Upper Limb Functional Ability in Post-Traumatic Patients Using Machine Learning. Zaiyanu Nuhu, Yeong Che Fai, Elijah David Kure, Ibrahim B. Shehu, Mahmoud Mustapha, Rabiu Al-Tanko & Khor Kang Xiang	432– 441
Arduino Based Automatic Irrigation System Ibrahim Bashir Shehu, Zayyan Nuhu & Rbiu Altanko Ummaisha	442 – 448
Production and Application Potentials of Sugarcane Bagasse Reinforced Polymer Composites for Acoustic Control Sanda Askira Damboama	449 – 456
Electromagnetic Field analysis of a Single-phase Induction Motor based on Finite Element Method Omokhaje J. Tola, Edwin A. Umoh, Enesi A. Yahaya, Chika Idoko, Ayo Imoru	457 – 463
Parameter Investigation and Analysis for Elite Opposition Bacterial Foraging Optimization Algorithm Maliki, D, Muazu, M.B, Kolo, J.G, & Olaniyi, O.M.	464 – 471
Multi-Access Edge Computing Deployments for 5G Networks Mosudi, I. O, Abolarinwa, J, & Zubair, S.	472– 479
Suitable Propagation Models for 2.4 GHz Wireless Networks: Case Study of Gidan Kwano Campus, FUT MINNA. Ogunjide, S. B., Usman, A. U., & Henry, O. O.	480 – 488
A Survey on Mobile Edge Computing: Focus on MEC Deployment, Site Selection Problems and Application Scenarios. Atolagbe, M. I, Osanaiye, O.	489 – 496
Influence of Processing Techniques and Packaging Materials on Anti- Nutritional Properties of Soybean Flour Orhevba, B. A., Anehi, A. & Obasa, P. A.	497 – 503
Prospects and Challenges of Off-Grid Power Generation For Rural Communities in Nigeria – Theoretical Perspective Dangana Audu & Ikechuku A. Diugwu	504 – 509
Spectrum Occupancy Measurement in the VHF Band- Results and Evaluation in the Context of Cognitive Radio Ajiboye, J.A, Adegboye, B.A, Aibinu, A.M, Kolo, J.G	510 – 514
Modelling and Simulation of Adaptive Fuzzy-PID Controller for Speed Control of DC Motor Timothy Onyechokwa, Adegboye B. A. & A.S. Mohammed	515 – 520
Implementation of Remote Patient Monitoring System using GSM/GPS Technology Umar Abdullahi, Salihu Aliyu Oladimeji, Waheed Moses Audu, Muslim Saidu, Manasseh Wayo	521 – 527
Comparism of Adaptive Neuro Fuzzy Inference System and Support Vector Machine for the Prediction of Immunotherapy Warts Disease Abisoye,B.O, Abisoye, O.A, Kehinde Lawal, Ogunwede E mmanuel	528 – 536



**2nd International Engineering Conference (IEC 2017)
Federal University of Technology, Minna, Nigeria**



Prediction of Epileptic Seizure using Support Vector Machine and Genetic Algorithm Abisoye, O. A, Abisoye, B.O, Ekundayo Ayobami, & Ogunwede Emmanuel	537 – 542
The Prediction of Cervical Cancer Occurrence Using Genetic Algorithm and Support Vector Machine Abisoye, O. A, Abisoye, B.O, Ekundayo Ayobami & Kehinde Lawal	543 – 549
Performance Evaluation of Ant Lion Optimization and Particle Swarm Optimization for Uncapacitated Facility Location Problem (UFLP) Shehu Hussaina & Morufu Olalere	550 – 558
Potential, Barriers and Prospects of Biogas Production in North- Central Nigeria Ahonle Jennifer Eferi & Adeoye Peter Aderemi	559 – 564
Design Analysis of Manually Operated Machine for On-Row Transplanting of Paddy Rice Ibrahim, T. M., Ndagi, A., Katun. I. M. & Anurika, U. A.	565 – 572
Investigation of Vulnerability of Oil and Gas Critical Infrastructures and Developing a Tracking Algorithm to track Malicious Attacks on the Streams Isah, A.O., Alhassan, J.K, Idris, I., Adebayo, O.S., Onuja, A. M.	573 – 580
Optimization of Process Variables in Bio-Waste Based Activated Carbon Preparation Using Response Surface Methodology. Onuoha, D. C., Egbe, E. A. P., Abdulrahman, A. S. & Abdulkareem, A. S.	581 – 589
Development of a Petroleum Pipeline Monitoring System for Detection, Location and Characterization of Damages in Pipes Aba, E. N, Olugboji, O. A, Nasir, A, Oyewole, A, & Olutoye, M. A.	590 – 598
Analysis of Maximum Power Point Tracking (MPPT) Techniques under Different Atmospheric Conditions: Technical Review Dania, D. E, Tsado, J, Nwohu, M, & Olatomiwa, L.	599 – 608
Development OF Briquette-Powered Water Distiller Muhammadu M. M, Unugbai, J. A, Bako M. D., Abubakar J. A.	609 – 614
Impact of SVC and DG Coordination on Voltage Constrained Available Transfer Capability (VSATC) Sadiq A. A, Adamu S. S, Abubakar I. N. & Yusuf L.	615 – 619
Construction of a Solar Powered Battery Forge Adimula, M. G., Abubakre, O. K., Muriana, R. A.	620 – 625
Financial Assessment of the Flood Risk Preparedness of Some Selected States in Nigeria Idachaba, A, Makinde, J & Oke, A.	626 – 631
Development of Spin Dryer Machine Alhassan T. Yahaya & Muhammadu M. M.	632 – 641
Assesment of Quality Control Management in Sachet Water Packaging T.J Bolaji and A.A. Abdullahi	642 – 648
Survey of Tractor Usage and Parts Breakdown in Niger State, Nigeria Dauda, S. M., Abdulmalik M.K., Isyaku M. I., Francis A.A. & Ahmad D.	649 – 654



**2nd International Engineering Conference (IEC 2017)
Federal University of Technology, Minna, Nigeria**



Development of an Inspection Methodology for Peugeot 508 Bala Dauda & James Oseni Abu	655 – 660
Design and Fabrication of Banana Fiber Extractor machine and Performance Evaluation for the Reinforcement of Composites Odii Kinsley Chika & Ademoh N.A.	661 – 667
Optimisation of Biodiesel Production from Sandbox (<i>Hura Crepitans</i>) Seed Oil Usman M., Adebayo S., Aliyu M. & Dauda, S. M.	668 – 676
A Multi-source Broadband Radio Frequency Energy Harvester with Cascaded Diversity Combiner for Mobile Devices Ihemelandu, J. C., Onwuka, E. N., David, M., Zubair, S. & Ojerinde O. A.	677 – 683
Artificial Neural Network (ANN), a Formidable Tool for Atmospheric Forecasting. A Review Usman M.N., Aku I.G. & Oyedum O.D.	684 – 692
Development of a Model for Generation of Examination Timetable Using Genetic Algorithm Ahmed A., Umar B. U., Abdullahi I. M., Maliki. D., Anda I. & Kamaldeen J. A.	693 – 700
Smart Protection of Vehicle using Multifactor Authentication (MFA) Technique S. Aliyu , Umar Abdullahi, Majeedat Pomam, Mustapha Hafiz, Adeiza Sanusi, & Sodiq Akanmu	701 – 710
Development of Production Frame Work to Mitigate Corrosion in Under Groung Tanks Emenuwe Vincent & Aliyu Abdullahi	711 – 715
Physical Property Modification of Vegetable Bio-Cutting Oil Using Garlic as EP Additive Sanni John	716 - 719
Soil Moisture and Nutrients Control: An Automated Design Proposal Mustapha Mohammed, Elijah David Kure & Yusuf Mubarak	720– 727



**2nd International Engineering Conference (IEC 2017)
Federal University of Technology, Minna, Nigeria**



FORWARD

The School of Engineering and Engineering Technology, Federal University of Technology, Minna, organized the 1st and 2nd International Engineering Conference in 2015 and 2017 respectively. With the emergence of the new School of Electrical Engineering and Technology and the School of Infrastructure, Process Engineering and Technology, the two schools came together to organize this 3rd International Engineering Conference (IEC 2019) with the theme: “The Role of Engineering and Technology in Sustainable Development” considering the remarkable attendance and successes recorded at the previous conferences. The conference is aimed at offering opportunities for researchers, engineers, captains of industries, scientists, academics, security personnel and others who are interested in sustainable solutions to socio-economic challenges in developing countries; to participate and brainstorm on ideas and come out with a communiqué, that will give the way forward. In this regard, the following sub-themes were carefully selected to guide the authors’ submissions to come up with this communiqué.

1. Engineering Entrepreneurship for Rapid Economic Growth.
2. Regulation, Standardization and Quality Assurance in Engineering Education and Practice for Sustainable Development.
3. Solutions to the Challenges in Emerging Renewable Energy Technologies for Sustainable Development.
4. Electrical Power System and Electronic as a Panacea for Rapid Sustainable Development
5. Promoting Green Engineering in Information and Communication Technology
6. Reducing Carbon Emission with Green and Sustainable Built Environment
7. Artificial Intelligence and Robotics as a Panacea for Rapid Sustainable Development in Biomedical Engineering
8. Petrochemicals, Petroleum Refining and Biochemical Technology for Sustainable Economic Development.
9. Advances and Emerging Applications in Embedded Computing.
10. Traditional and Additive Manufacturing for Sustainable Industrial Development.
11. Emerging and Smart Materials for Sustainable Development.
12. Big Data Analytics and Opportunity for Development.
13. Building Information Modeling (BIM) for Sustainable Development in Engineering Infrastructure and Highway Engineering.
14. Autonomous Systems for Agricultural and Bioresources Technology.

The conference editorial and Technical Board have members from the United Kingdom, Saudi Arabia, South Africa, Malaysia, Australia and Nigeria. The conference received submissions from 4 countries namely: Malaysia, South Africa, the Gambia and Nigeria. It is with great joy to mention that 123 papers were received in total, with 0.9 acceptable rate as a result of the high quality of articles received. Each of the paper was reviewed by two personalities who have in-depth knowledge of the subject discussed on the paper. At the end of the review process, the accepted papers were recommended for presentation and publication in the conference proceedings. The conference proceedings will be indexed in Scopus.

On behalf of the conference organizing committee, we would like to seize this opportunity to thank you all for participating in the conference. To our dedicated reviewers, we sincerely appreciate you for finding time to do a thorough review. Thank you all and we hope to see you in the 4th International Engineering Conference (IEC 2021).

Engr. Dr. S. M. Dauda

Chairman, Conference Organizing Committee



**2nd International Engineering Conference (IEC 2017)
Federal University of Technology, Minna, Nigeria**



ACKNOWLEDGEMENT

The Chairman and members of the Conference Organizing Committee (COC) of the 3rd International Engineering Conference (IEC 2019) wish to express our gratitude to the Vice Chancellor and the management of the Federal University of Technology, Minna, the Deans and all staff of the School of Electrical Engineering and Technology (SEET) and the School of Infrastructure, Process Engineering and Technology (SIPET) for the support towards the successful hosting of this conference. We also thank the entire staff of the university who contributed in one way or the other. We are sincerely grateful to you all.



Statistical Optimization of Biodiesel production from Jatropha oil using Calcined Snail Shell Catalyst

* Afangide, U. N¹, Olutoye, M. A¹, & Aberuagba, F¹.

¹Chemical Engineering Department, Federal University of Technology, PMB 65 Minna Niger State, Nigeria

*Corresponding author email: unwana2007@yahoo.com, +2348036427410

ABSTRACT

In this research, calcium oxide was prepared from snail shells as a heterogeneous catalyst for biodiesel production through a quick and easy calcination method at 900 °C. Response surface technique (Box-Behnken Design) was used to evaluate the impact of temperature, catalyst quantity (wt %) and response time (min) on biodiesel processing using the synthesized calcium oxide catalyst from snail shell for transesterification of Jatropha oil. A second quadratic equation to estimate the percentage of biodiesel output was achieved. The most appropriate transesterification reaction condition for maximum biodiesel production were temperature, 60 °C; catalyst quantity, 4 wt %; and reaction time, 105 min, based on the experimental evaluation and response surface methodology study. The optimal biodiesel yield of 83.68% was obtained.

Keywords: Biodiesel, Calcium oxide, Optimization, Snail Shell, Transesterification.

1 INTRODUCTION

Biodiesel as natural gas is a fatty acid methyl ester (FAME) generated by pure plant oils transesterification. More than 95% of the raw material produced by biodiesel comes from vegetable oils, e.g. maize oil, canola oil, corn syrup, soybean oil, rice bran oil, coconut oil, fish oil, olive oil, macadamia oil, nut oil, hemp oil, peanut oil, etc., which adds to biodiesel costs. The cost of petroleum feedstock usually affects the price of biodiesel by 70–80%. Biodiesel is, therefore, more costly than petrodiesel (Knothe, 2002). Biodiesel generated from vegetable oils of good quality is thus not economically viable at the moment. Manufacturing of petroleum feedstock cultivation from edible oil may result in competition with food plants. Many scientists are concerned about the use of non-edible oils to address these issues, which would decrease the cost of producing biodiesel (Talebian-Kiakalaieh *et al.*, 2013).

El-Glendy *et al.* (2009) reported that for biodiesel production, investigators have used different kinds of the binary or different catalyzed transesterification process. Though with high biodiesel outputs and limited side reactions, the homogeneous catalyzed biodiesel production process is comparatively quick, it is still not competing with petrodiesel. Since the catalyst cannot be retrieved or reused, the washing step is a must for biodiesel neutralization and removal of unreacted glycerides and catalysts, resulting in large quantities of wastewater resulting in waste management issues (El-Glendy *et al.*, 2009). Homogenous catalysts such as H₂SO₄, KOH are anticipated to be substituted in the nearest future by heterogeneous catalysts such as CaO, ZnO, SrO, MgO. They are recorded to also have high performance at low temperature and atmospheric pressure and can be readily detached, recycled and the washing step eliminated, leading to lower manufacturing expenses and being able to be utilized in a constant fixed bed method (Borges and Diaz, 2012). CaO is estimated to be made from naturally occurring animal

sources such as calcite, dolomite, oyster shells, eggshells, shells of crabs, cockle shells and shells of mollusks. (Ngamcharussrivichai *et al.*, 2010; Boey *et al.*, 2011). This not only eliminates disposal management costs, but it is also possible to obtain catalysts with high price efficiency for the biodiesel sector at the same time.

El-Glendy *et al.* (2009) reported that every year, thousands of liters of snail shell are dumped in drainage systems in Nigeria. It, therefore, pollutes rivers, causing many waste disposal issues and thus adding to the expense of effluent treatment. Biodiesel production from non-edible Jatropha oil using CaO derived from snail shell would, therefore, give a three-fact alternative: financial, environmental, and waste management (El-Glendy *et al.*, 2009).

In this study, the conversion of Jatropha oil biodiesel was explored using snail shell modified CaO. By introducing the Box-Behnken design technique for the response surface, the mechanism was established and optimized.

2 METHODOLOGY

2.1 MATERIALS

Snail shell was selected for this study. It was purchased from Ungwan Sunday market of Kaduna South metropolis located in Kaduna state, Nigeria. The sample was carefully chosen to avoid difference in characteristics.

2.2 COLLECTION OF JATROPHA OIL

In this research, pre-treated Jatropha oil was obtained from the National Research Institute for Chemical Technology, Zaria, Nigeria.

2.3 CATALYST PREPARATION

Snail shell purchased from Ungwan Sunday market of Kaduna South metropolis located in Kaduna state, Nigeria was cleaned with distilled water, dried in an oven at 100 °C for 12 hours, and then crushed using a rolling mill. It was then sieved into various particle sizes, and particle

size of 850 microns was used for this study. At a temperature of 900 °C for 150 min, calcination was conducted in a carbolite furnace. The calcined catalysts were then placed in a desiccator to prevent humidity and CO₂ reactions in the atmosphere before use.

2.4 OPTIMIZATION OF TRANSESTERIFICATION PROCESS

The above transesterification procedure was repeated for various temperatures, time, and catalyst weight to investigate these transesterification parameters on the amount of biodiesel (yield) using RSM based Box-Behnken. This was carried out by varying the levels of factors for optimization of these parameters, as shown in Table 1. The designed experimental matrix for the catalyst synthesis is presented in Table 1.

TABLE 1: EXTREME OPERATING CONDITIONS FOR TRANSESTERIFICATION REACTION PROCESS PARAMETERS

Independent variables	Coded Levels		
	-1	0	+1
A: Reaction Temperature (°C)	30	45	60
B: Reaction Time (min)	60	120	180
C: Amount of Catalyst (wt% of oil)	1	2.5	4

The developed experimental matrix based on the RSM Box Behnken Design and the +/- Alpha values in Table 1 are as shown in Table 3.4. Each experimental run consisted of three samples, and the sequence of the experiment following the randomly assigned run number as reflected in Table 2.

TABLE 2: RESPONSE SURFACE METHODOLOGY EXPERIMENTAL RUN AND RESULTS OF BIODIESEL YIELD

SN	A (°C)	B (min)	C (wt% of oil)	Yield (%)
1	45	120	2.5	72.81
2	30	180	2.5	68.58
3	60	60	2.5	74.28
4	30	60	2.5	43.88
5	45	120	2.5	72.82
6	45	180	1	45.79
7	60	120	1	54.79
8	30	120	1	37.69
9	30	120	4	77.49
10	60	180	2.5	74.07
11	60	120	4	79.57
12	45	60	4	73.87
13	45	60	1	32.57
14	45	120	2.5	72.8
15	45	180	4	76.77

2.5 TRANSESTERIFICATION

The catalytic activity of the snail shell catalyst was evaluated by transesterification of Jatropha oil with methanol in a batch process. The reaction was carried out using the conical flask, magnetic stirrer, and beaker. The process was carried out by mixing a requisite amount of catalyst and methanol, followed by the addition of oil. The desired reaction temperature, time and catalyst amount obtained from the experimental design shown Table 2 was maintained. Finally, the mixture was transferred to the separating funnel for the separation of biodiesel. The set up was left undisturbed for the phase separation. The lower phase (glycerol) was withdrawn, and the upper phase containing biodiesel was measured for calculating biodiesel yield. The catalyst settled at the bottom was removed and regenerated. The value of the yield of the biodiesel, according to Boro *et al.* (2011) is shown in equation 1.

$$\%Yield = \frac{\text{Weight of produced biodiesel}}{\text{Weight of used Jatropha oil}} \times 100 \quad (1)$$

This was calculated for all the runs of experimental design of Table 2.

3.0 RESULTS AND DISCUSSION

The results of the yield of biodiesel obtained were used to carry out the response surface analysis and optimization using Minitab 17. The experimental result of Table 2 was used to obtain the second-order empirical model coefficients of Equation 2. The empirical model equations for the biodiesel yield as a function of reaction temperature, time, and catalyst loading was developed using experimental data of Table 1 and are represented as Equation 2 below. The quadratic equation model terms are shown in Table 3.

TABLE 3: MODEL COEFFICIENT TABLE FOR BIODIESEL YIELD RESPONSE SURFACE REDUCED QUADRATIC MODEL

Term	Effect	Coef	SE Coef	T-Value	P-Value	VIF
Cons		-113.4	1.85	39.46	0.000	
tant						
A	13.77	2.201	1.13	6.09	0.002	1.00
B	10.15	0.892	1.13	4.49	0.006	1.00
C	34.21	42.77	1.13	15.14	0.000	1.00
A*A	-2.47	-0.00549	1.66	-0.74	0.491	1.01
B*B	-12.74	-0.00177	1.66	-3.83	0.012	1.01
C*C	-18.38	-4.084	1.60	-5.52	0.003	1.01
A*B	-12.45	-0.00692	1.60	-3.90	0.011	1.00
A*C	-7.51	-0.1669	1.60	-2.35	0.066	1.00
B*C	-5.16	-0.0287	1.60	-1.61	0.167	1.00

The uncoded biodiesel yield empirical model is shown in Equation 2.

$$\text{Yield} = -113.4 + 2.201A + 0.892 B + 42.77C - 0.00549 A^2A - 0.001770B^2B - 4.084C^2C - 0.00692 A^*B - 0.1669 A^*C - 0.0287 B^*C \quad (2)$$

The ANOVA result of Table 4 shows that reaction values having a p-value less than 0.05 are seen to be significant for biodiesel yield response factor. The backward elimination technique was used to screen the insignificant parameters from the model. Biodiesel yield ANOVA result of Table 4 shows that the reaction temperature (A), the reaction time (B), catalyst amount (C), the interaction terms (AB, AC, and BC) and the quadratic terms (A², B², C²) are significant and affect biodiesel yield.

TABLE 4: ANALYSIS OF VARIANCE (ANOVA) TABLE FOR BIODIESEL YIELD RESPONSE SURFACE REDUCED QUADRATIC MODEL

Source	DF	Adj SS	Adj MS	F-Value	P-Value
Linear	3	3595.71	399.52	39.11	0.000
Interaction		2926.57	975.52	95.51	0.000
A	1	379.09	379.09	37.11	0.002
B	1	206.15	206.15	20.18	0.006
C	1	2341.33	2341.33	229.22	0.000
Square	3	430.99	143.66	14.06	0.007
A*A	1	5.64	5.64	0.55	0.491
B*B	1	149.88	149.88	14.67	0.012
C*C	1	311.75	311.75	30.52	0.003
2-Way Interaction	3	238.15	79.38	7.77	0.025
A*B	1	155.13	155.13	15.19	0.011
A*C	1	56.40	56.40	5.52	0.066
B*C	1	26.63	26.63	2.61	0.167
Error	5	51.07	10.21		
Lack-of-Fit	3	51.07	17.02	170237.92	0.180
Pure Error	2	0.00	0.00		
Total	14	3646.78			

The statistical inferences of Table 5 show that biodiesel yield model developed is significant as it has a lack of fit value of 18.06885833 relative to the pure error. Therefore, there is a 30.14 % probability that lack of fit value of 18.06885833 and Model F-value of 1702 could occur due to noise. Therefore, the non-significant lack of fit attained for the empirical equation indicates that the model truly represents the experiment.

TABLE 5: MODEL SUMMARY STATISTICS FOR BIODIESEL YIELD RESPONSE SURFACE REDUCED QUADRATIC MODEL

Std. Dev.	R-Squared	Adj R-Squared	Pred R-Squared
3.19598	98.60%	96.08%	77.59%

3.19598 98.60% 96.08% 77.59%

The Predicted R² of 77.59% of Table 5 agrees with the Adjusted R² of 96.08%." Suitable Precision" measures the signal to noise ratio. The low-value standard deviation of 3.19598 showed that the model can be used to predict the design space. Also, the model terms (A, B, C, AB, AC, BC, A², B², C²) are significant as their "Prob> F" less than 0.0500 as presented in Table 4.6.

The primary diagnostic tool for residual analysis was also examined. Figure 1 shows the normal probability plot of the residuals. The data points are normally distributed as it follows a straight line. Figure 1 shows that the model expectations are correct as the actual values follow the predicted values.

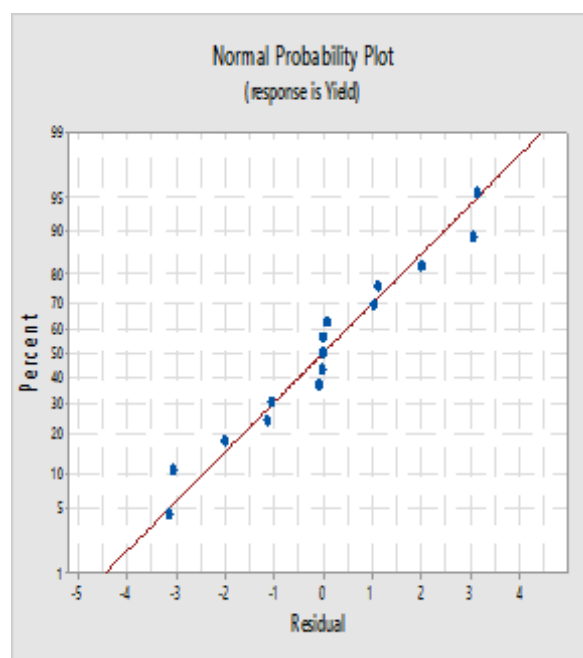


Figure 1: Normal Plot of Residual for Biodiesel Yield

The objective of the biodiesel production process is to find optimum settings of reaction process variables that maximize biodiesel yield. Concerning this need, the results of the reaction process variables that will maximize biodiesel yield are shown in Figure 2 – 3.

Figures 2 and 3 display the 2-D contour plot and 3-D surface of the yield model, respectively. The contour and response surface plots are used to discover the relationship between the experimental levels of each process factor and biodiesel yield. The plot displays the effect of varying two process parameters while holding the catalyst loading constant at zero points. Figures 2 and 3 indicate the influence of the quadratic function of reaction temperature and significant influence of reaction

time on biodiesel yield while ignoring the catalyst loading and keeping it constant at zero. The plots display that increased biodiesel yield was observed with increasing reaction time and temperature values. Figures 2 and 3 show increased biodiesel yield was observed with increasing reaction temperature and time values. However, a further increase in reaction temperature above the optimum value of 60 °C and below the reaction time of 104.85 min caused a decrease in the biodiesel yield. At reaction temperature higher than 60 °C, the biodiesel yield began to decrease as reaction time decreases below 104.85 min.

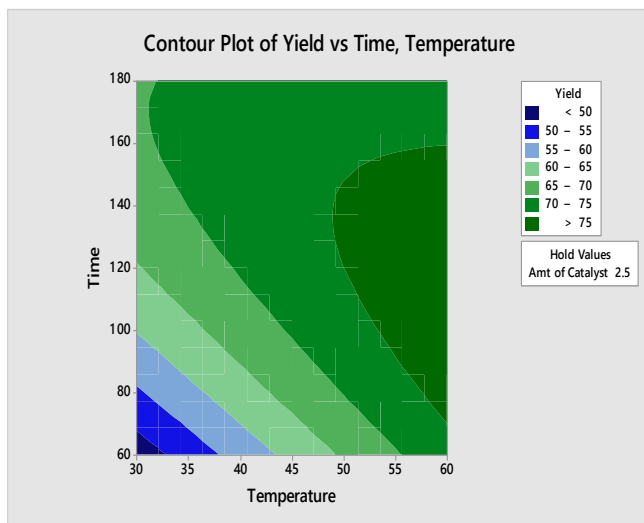


Figure 2: Model Contour Plot Showing the Effect of Reaction Temperature and Time on Biodiesel Yield for Simultaneous Optimization of Biodiesel Yield Model.

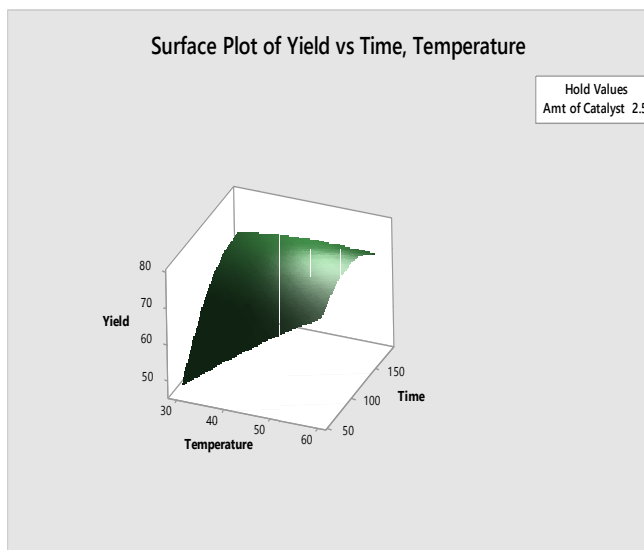


Figure 3: Mean Model Response Surface Plot Showing the Effect of Reaction Temperature and Time on

Biodiesel Yield for Simultaneous Optimization of Biodiesel Yield Model.

The RSO objective is to find a suitable operating condition of process values that will satisfy the objective. Figure 4 show that the reaction temperature of 60 °C, the reaction time of 105 min and catalyst loading of 3.64 produced maximum biodiesel yield of 83.68%. The condition of response optimization using Suich and Derringer Approach is the value of desirability to be between 0 and 1.0. The value of desirability depends on how close the lower and upper limits are to the actual optimum (Aggarwal, *et al.*, 2009). The response optimization carried out for the specified design space constraints for biodiesel yield models using Minitab shows that optimum solutions were obtained at the desirability of 0.77, as shown in Figure 4.

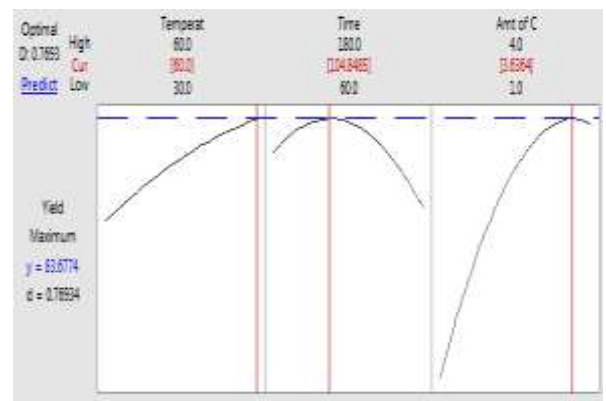


Figure 4: Response Surface Plot Showing the Effect of Reaction Temperature, Time and Catalyst Loading on Biodiesel Desirability for Response Optimization of Biodiesel Yield Model.

4.0 Conclusions

Optimization of biodiesel production from Jatropha oil using catalyst prepared from snail shell was studied. The influence of the transesterification parameters on the yield of the biodiesel was studied by optimization using response surface Box-Behnken Design method. The result of the statistical optimization shows that optimum biodiesel yield of 83.7% was obtained at transesterification temperature of 60 °C, the reaction time of 105 min and catalyst weight of 3.6%. The results of the optimization revealed that the composite desirability (0.7693) was obtained. However, the desirability shows that the limits of factors were aimed at maximizing yield (0.98077). The results of the plot of experimental and predicted data for the yield of biodiesel showed that both the experimental and optimized yield fall within statistical acceptability with regression coefficient (R^2) = 0.7759. The contour and surface plots showed that there are



interactions between the factors and the yield of the biodiesel.

References

- Aggarwal, A., Singh H., Kumar, P. and Singh, M. (2008). Modeling of machining parameters and cooling conditions in hard turning of AISI P-20 tool steel using response surface methodology and desirability graphs, *International Journal of Machining & Machinability of Materials*, 4(1), 95-110.
- Boey, P. L., Maniam, G. P., Abd Hamid, S., and Ali, D. M. H. (2011). Utilization of waste cockle shell (*Anadara granosa*) in bio-diesel production from palm olein: Optimization using response surface methodology. *Fuel* 90:2353–2358.
- Borges, M. E., and Diaz, L. (2012). Recent developments on heterogeneous catalysts for bio-diesel production by oil esterification and transesterification reactions: A review. *Renew. Sustain. Energy Rev.* 16:2839–2849.
- Boro, J., Thakur, A. J., and Deka, D. (2011). Solid oxide derived from waste shells of *Turnonilla striatula* as a renewable catalyst for bio-diesel production. *Fuel Process. Technol.* 92:2061–2067.
- El-Gendy, N. Sh., and Madian, H. R. (2013). *Ligno-cellulosic Biomass for Production of Bio-energy in Egypt*. Saarbrücken, Germany: Lambert Academic Publishing.
- Knothe, G. 2002. Current perspectives on bio-diesel. *Information* 13:900–903.
- Ngamcharussrivichai, C., Nunthasanti, P., Tanachai, S., and Bunyakiat, K. 2010. Bio-diesel production through transesterification over natural calciums. *Fuel Process. Technol.* 91:1409–1415.
- Talebian-Kiakalaieh, A., Amin, N. A. S., and Mazaheri, H. 2013. A review on novel processes of bio-diesel production from waste cooking oil. *Appl. Energy* 104:683–710.
- Widayat, W., Darmawan, T., Hadiyanto, H., & Rosyid, R.A. (2016). Preparation of heterogeneous calcium oxide catalysts for biodiesel production. *International Conference of Energy Sciences (ICES2016)*, 315 - 325.
- Win, T.T., & Khine, M.M. (2016). Chicken egg shell waste as a suitable catalyst for transesterification of palm oil: optimization for biodiesel production. *Proceedings of the 5th International Conference on Food, Agricultural and Biological Sciences (ICFABS2016)*, 25-26.
- Wong, Y.C., Tan, Y.P., Taufiqyap, Y.H., & Ramli, I. (2015). An Optimization study for transesterification of palm oil using response surface methodology. *Sains Malaysiana* 44(2), 281-290.
- Woodgate S., & van der Veen J.T. (2004) The use of fat processing and rendering in the European Union animal production industry. *Biotechnology, Agronomy, Society and Environment* 8(4), 283–294.



Development of AgNPs-MWCNTs Adsorbent for Seawater Treatment

* Mohammed, S. M¹, Muriana, R. A², Agboola, J. B³, Abdulkareem, A. S⁴, Kariim, F⁵, & Yahya, M. D⁶

¹National Environmental Standards and Regulations Enforcement Agency, Niger State Field Office Minna, Nigeria

^{2,3}Materials and Metallurgical Engineering Department, Federal University of Technology, P.M.B. 65 Minna Niger State, Nigeria

^{4,5,6}Chemical Engineering Department, Federal University of Technology, P.M.B. 65 Minna Niger State, Nigeria

*Corresponding author email: msabamkutigi@yahoo.com, +2348031185292

ABSTRACT

Multi-walled carbon nanotubes (MWCNTs) were synthesized using Fe-Co/Al₂O₃ bimetallic catalyst synthesized via the wet impregnation method. Also, silver nanoparticles (AgNPs) was synthesized via the green synthesis route using extract from *Piptadeniastrum africanum* (*P. africanum*) leaves. The synthesized silver nanoparticles was then doped with MWCNTs to form (AgNPs-MWCNTs) nano adsorbent. The adsorbent produced was characterized using TGA, TEM, EDS and BET. The adsorption efficiency and antibacterial activity of the adsorbent was tested on sample of seawater collected from Lagos, Nigeria. Evaluation of antimicrobial potentials of the nano-formulated adsorbent was carried out via bacteria counts. Also, adsorption capacity towards selected parameters of nano-formulated adsorbent treated seawater were investigated in order to determine the adsorption capacity of the nanocomposite. Parameters such as pH, turbidity, conductivity, TSS, TDS, COD, BOD, DO and ions such as Cl⁻, Na⁺, Mg²⁺, Ca²⁺, F⁻, SO₄²⁻, HCO₃⁻, Br⁻, Sr²⁺ and K⁺ were analysed. The antibacterial activity of the adsorbent was investigated against microorganisms *Salmonella typhimurium*, *Pseudomonas aeruginosa*, *Escherichia coli*, *Staphylococcus aureus*, fungi and non-pathogenic bacteria. Results obtained shows that the adsorbent was very effective in the removal of dissolved ions, contaminants and microorganisms present in the seawater. The dissolved ions, microorganisms and other pollutant in the water were reduced to within the limits recommended in the National Standard for Drinking Water Quality guidelines (NSDWQ). It can be concluded that AgNPs-MWCNTs adsorbent have superior potential for seawater treatment and thus, recommended as a cost effective and energy saving alternative for seawater treatment.

Keywords: Adsorbent, Nanoparticles, Seawater, Silver, Treatment.

1 INTRODUCTION

Water plays a vital role for our planet and its inhabitants and has often been summed up with the expression that water is life (Brown, Martinez and Uche, 2010; Jimenez and Perez-Foguet, 2010). According to (Rahmanian *et al.*, 2015) clean drinking water is now recognised as a fundamental right of human beings. To this end, any obstacle to the supply of potable water is tantamount to disturbing the perpetual existence and survival of humanity as a whole (Harvey and Reed, 2007). However, access to this very vital resource is becoming increasingly difficult as a result of population growth, urbanization, climate change impacts and increases in household and industrial uses (WHO, 2011; Tayalia and Vijaysai, 2012). More than half of the world population has been under water stress since 2015 (GE Reports, 2011). Francisco *et al.* (2014) reported that potable water supply shortages give room to public health associated problems, conflicts, reduced agricultural produce and ultimately endangering the ecosystem via climate change. This global issue of clean water scarcity owing to the accelerating population growth, environmental deterioration and climate change is threatening the lives of human beings all over the world (Bates *et al.*, 2008; McGinnis and Elimelech, 2008; Immerzeel *et al.*, 2010). Currently, growing number of people are losing access to clean water, a basic necessity of every human being (Shannon *et al.*, 2008). Thus the

increasing demand for clean water impels the initiatives for water reuse and clean water production from brackish or seawater to avoid the aforementioned crisis (Glueckstern *et al.*, 2008; Greenlee *et al.*, 2009).

Thermal and membrane technologies are two primary methods being used for seawater treatment (Helal *et al.*, 2003). Thermal treatment methods consume large thermal energy (200~400MJ/ton) (Borsani and Rebagliati, 2005). Membrane filtration process has been widely used for seawater desalination (McGinnis and Elimelech, 2008; Greenlee *et al.*, 2009; Ling *et al.*, 2010) but without associated issues, such as, secondary pollutants, unpleasant odor and heat energy consumption, poor salt rejection and biological attack (Zhu and Elimelech, 1997; Fritzmann *et al.*, 2007; Niksefat *et al.*, 2014; Linares *et al.*, 2014). Furthermore, the broad applications of these technologies (thermal and membrane processes) are severely limited by the worsen energy crisis globally (Chow *et al.*, 2003; Semiat, 2008; McGinnis and Elimelech, 2008; Hightower and Pierce, 2008). Consequently, the desire for an alternative and cost effective methods of treating seawater is on the increase and adsorption technology has been identified as a means for the removal of dissolved ions from water (Li *et al.*, 2002; Mamba *et al.*, 2010).

The rapid development of nanomaterials opens a new window for the creation of ideal nano sorbents for seawater desalination. Mass transport resistance is greatly reduced when nano-materials are used as adsorbents, due to size of adsorbents, high surface area and high adsorption capacity (Amiri *et al.*, 2011). Among conventional method of water treatment, adsorption offers flexibility in design and operation, in many cases it generates high-quality treated effluents (Bharathi and Ramesh, 2013). Also, owing to the reversible nature of most adsorption processes, adsorbents could be regenerated by suitable desorption processes for multiple uses (Bharathi and Ramesh, 2013 and Elabbas *et al.*, 2015). As a result of its large surface area, high adsorption capacity and surface reactivity, adsorption using suitable adsorbents can remove metals from inorganic effluents (El Muguana *et al.*, 2018). Carbon nanotubes (CNTs) are new adsorbents that have been shown to possess great potential for removal of pollutants such as organic compounds and inorganic pollutants from various aqueous environments (Shah and Murthy, 2013; Kecili and Hussain, 2018). Also nanoparticles such as silver nanoparticles are biocompatible and non-toxic. In this study, the antimicrobial merit of AgNPs (Shahverdi *et al.*, 2007; Edwards-Jones, 2009; Rai *et al.*, 2009; Krishnaraj *et al.*, 2010; Vijayakumar *et al.*, 2012; Sankar *et al.*, 2013; Morones *et al.*, 2013; Hamed *et al.*, 2015) and good adsorption capability of carbon nanotubes (CNTs) (Lu and Chiu 2006; Kuo *et al.*, 2008; Yang *et al.*, 2009; Azodi-Deilami, *et al.*, 2014; Purkayastha *et al.*, 2014; Kecili and Hussain, 2018) were integrated in order to reduce the concentration of dissolve ions and eliminate undesirable microbes from the seawater thereby removing the odour, stabilizing the composition of the seawater, and other parameters like conductivity, biological oxygen demand and chemical oxygen demands in conformity to acceptable standard.

2 METHODOLOGY

All the chemicals used are of analytical grade with the percentage purity in the range of 95-99.6% and no further purification was done. The acetylene and argon gases were sourced from BOC Nigeria. Iron nitrate, Cobalt nitrate, Alumina and Silver nitrate were purchased from BDH, England, Distilled water was purchased from Dana Pharmaceuticals Co. Ltd, Minna. Nitric Acid and Sulphuric Acid were purchased from Burgoyne & Co., Mumbai India and Guangdong Guanghua Sci-Tech Co., Ltd, China respectively.

2.1 PREPARATION OF LEAF EXTRACT

10g of dried powder *Piptadeniastrum africana* (*P. africana*) leaf was mixed with 100ml of distilled water in a 250ml beaker and the mixture was boiled at 50°C for 30mins. The extract was obtained by filtration method

through whatman no. 2 filter paper and stored in a brown bottle at 4°C.

2.2 SYNTHESIS OF SILVER NANOPARTICLES

An aqueous solution of silver nitrate (AgNO_3) was initially prepared by weighing 0.016987g of the silver nitrate salt and dissolved in 100cm³ of distilled water (1mM stock of AgNO_3). The obtained silver nitrate solution was stored at room temperature in a brown reagent bottle. For the reduction of Ag^+ ions, 1ml of aqueous extract solution of *Piptadeniastrum africana* (*P. africana*) was added to 10 ml of aqueous solution of 1mM AgNO_3 . pH was adjusted to 8.0 and the reaction was allowed to take place at room temperature for at least 10 min

2.3 SYNTHESIS OF BIMETALLIC CATALYST AND CNTS

The Fe-Co/ Al_2O_3 bimetallic catalysts supported on alumina was prepared using the wet chemical impregnation method. The synthesized catalysts was used in the CVD machine for the synthesis of MWCNTs.

2.4 PURIFICATION OF AS-SYNTHESIZED MWCNTS

Acid treatment method was employed in removing residual Fe, Co, amorphous carbon and support material (alumina) in the as-synthesised MWCNTs. As-synthesized MWCNTs was placed in 1000 mL solution containing 10% H_2SO_4 (100 mL) and 30% HNO_3 (300 mL) (v/v 1:3) to remove amorphous carbon, Fe, Co alumina impurities. The resultant mixture was sonicated for 90 minutes at 40°C in an ultrasonic bath to introduce oxygen to the surface of the CNTs. The CNTs were cooled to room temperature and thereafter washed with distilled water until a pH of 7 was obtained and then filtered using a filter unit. The wet CNTs were oven dried for 12 hours at 393K.

2.5 DOPING OF SILVER NANOPARTICLES WITH MWCNTS

1g of CNTs was dissolved in 10ml of AgNPs broth solution under ultrasonic mixing for 30min to obtain a homogenous black suspension. The solution was then allowed to continue to react for another 15min. Finally, the mixture was dried under the temperature of 80°C.

2.6 COLLECTION AND CHARACTERIZATION OF SEAWATER SAMPLE

The seawater used in this study was collected from Lagos Lagoon. The seawater was stored in a tight container and transported to the Laboratory for further analysis. Before treatment, the sample water was analysed at Jesil Pharmaceutical Industries Limited, Minna for its initial physicochemical and microbial concentrations. The result of each parameter was compared to the guidelines and

standards set by the Standard Organization of Nigeria (SON) i.e National Standard for Drinking Water Quality (NSDWQ).

2.6.1 PHYSICOCHEMICAL/ORGANOLEPTIC CHARACTERIZATION OF SEAWATER SAMPLE BEFORE TREATMENT

The concentrations of the conservative ions- Chloride (Cl^-), Sodium (Na^+), Magnesium (Mg^{2+}), Calcium (Ca^{2+}), Strontium (Sr^{2+}), Sulphate (SO_4^{2-}), Bicarbonate (HCO_3^-), Bromide (Br^-) Fluoride (F^-) (table 2) before treatment are beyond acceptable guideline limit for drinking-water. Fluoride (F^-) has the least concentration (12.71 mg/l) and Chloride (Cl^-) has the highest concentration (581.38 mg/l). The physical/organoleptic requirements (colour, taste, odour, temperature, turbidity, pH and conductivity) are all within the NSDWQ limits except the taste and conductivity of the water sample. The sample water taste is salty and its conductivity of 1680 $\mu\text{S}/\text{cm}$ is above the 1000 $\mu\text{S}/\text{cm}$ limit set by SON. The Manganese, Iron, Nitrate and Nitrite concentrations all falls outside the (SON, 2017) guideline values. Furthermore, biochemical parameters- Biological Oxygen Demand (BOD), Dissolved Oxygen (DO), Total Dissolve Solid (TDS), Total Suspended Solid (TSS) and Chemical Oxygen Demand (COD) of the sample water under study fall within limits, except Total Dissolve Solid (TDS).

2.6.2 MICROBIAL CHARACTERIZATION OF SEAWATER SAMPLE BEFORE TREATMENT

There are a number of diverse organisms that often have no public health significance but which are undesirable because they produce taste and odour. However, the principal risk associated with water supplies is that of infectious disease related to faecal contamination. Hence, it is important that microbiological examination of drinking-water be undertaken to assess hygienic quality of water. This requires the isolation and enumeration of organisms that indicate the presence of faecal contamination. The microbial analysis carried out include *Pseudomonas aeruginosa* (*P. aeruginosa*), Non-Pathogenic Bacteria, *Escherichia coli* (*E. coli*), *Salmonella typhimurium* (*S. typhimurium*), *Staphylococcus aureus* (*S. aureus*) and Fungi (yeast/moulds). Compare to the National Standard for Drinking Water Quality (NSDWQ) guidelines for drinking water, the bacteriological and pathogenic properties of the sample water under study falls outside the recommended limits. With exception of *P. aeruginosa*, all other microbial analysis results for the sample water were far higher than the national guideline limit.

2.7 ADSORPTION STUDIES

0.3 gram of AgNPs-MWCNTs composite material was transferred into 100ml beakers and 25ml of the seawater sample was added into the beakers. The beakers were placed in a water batch shaker rotating at 150 rpm for 70 minutes. The experimental temperature was set at 30°C. After completion of the adsorption process, the aliquots was then filtered using a filter unit into a sample bottle for post treatment analysis.

3 RESULTS AND DISCUSSION

3.1 CHARACTERIZATION OF AgNPs-MWCNTs NANO ADSORBENT

The AgNPs-MWCNTs adsorbent produced was characterized using thermogravimetric analysis (TGA), transmission electron microscopy (TEM), energy dispersive x-ray spectroscopy (EDS) and Brunauer Emmett Teller (BET).

3.1.1 TEM ANALYSIS OF AGNPS-MWCNTs NANO ADSORBENT

AgNPs-MWCNTs composites were successfully synthesized with an average of 10ml AgNPs broth per gram of MWCNTs. TEM images of the AgNPs-MWCNTs are presented in Figure 1a and 1b.

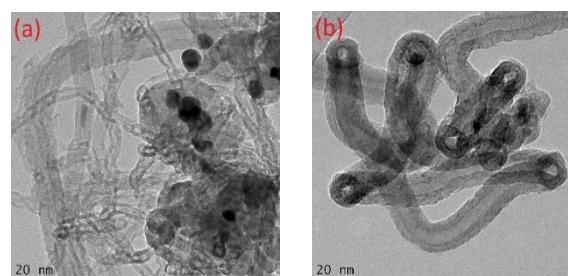


Figure 1a & 1b: Transmission electron microscope images of AgNPs-MWCNTs nano adsorbent

The AgNPs-MWCNTs have open tips suggesting that the acid purification process was highly effective (Zhao *et al.*, 2006). The kinks or bends observed at the edges are a common feature in CNTs after oxidation for longer times or heating at high temperature or even applying stress on the tubes (Zhao *et al.*, 2006). The successful doping with silver was also confirmed by the presence of dark spherical spots and bamboo compartment (Figure 1a and 1b) within the inner walls of the AgNPs-MWCNTs adsorbent materials.

3.1.2 EDS ANALYSIS OF AGNPS-MWCNTs NANO ADSORBENT

The EDX spectroscopy was used to investigate the presence of elements in the AgNPs-MWCNT composite

material. The EDX spectroscopy and its corresponding elemental analysis is presented in Figure 2.

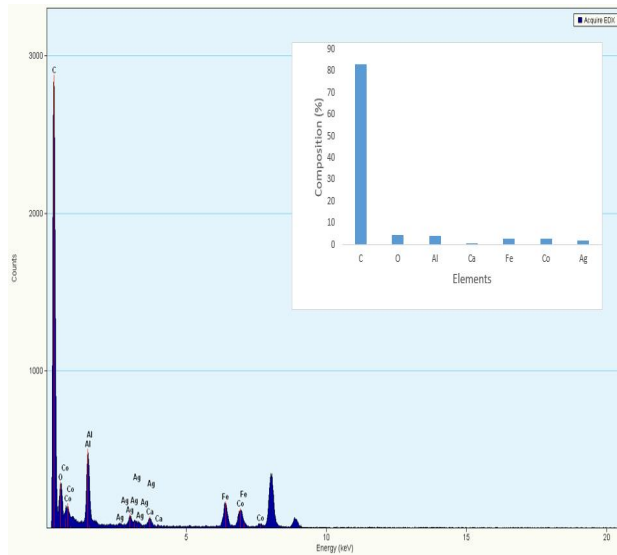


Figure 2: Energy Dispersive X-ray (EDX) for AgNPs-MWCNTs nano adsorbent

It can be seen that the prepared AgNPs-MWCNTs composite contained different elements such as C, Al, O, Ca, Fe, Co and Ag in varying amounts. The predominant deposit was carbonaceous material with percentage carbon content of about 84%. The element Aluminium (Al) possibly originated from the support material. Iron (Fe) and Cobalt (Co) and Oxygen (O) observed in the result were from the precursor salts used in synthesizing the catalyst. The calcium (Ca) presences in the sample originated from the holey calcium grid used during the EDS analysis (Aliyu *et al.*, 2017).

3.1.3 TG ANALYSIS OF AGNPS-MWCNTS NANO ADSORBENT

TGA was performed to investigate the thermal stability of the AgNPs-MWCNTs composite. The TGA and DTG profile for AgNPs-MWCNTs composite is shown in Figure 3.

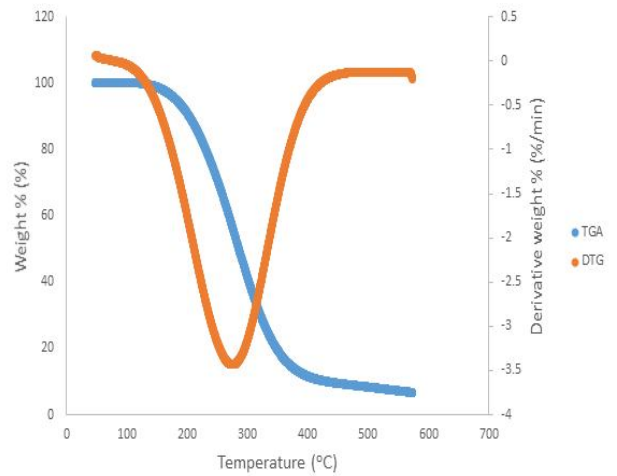


Figure 3: TGA and DTG profiles of AgNP-MWCNTs nano adsorbent

The decomposition peak for the AgNPs-MWCNTs composite occurs at 276°C as shown on the derivative weight profiles (Figure 3). After incorporation of the AgNPs unto the MWCNTs via the conventional method, there was no significant reduction in the decomposition temperature of the MWCNTs at that temperature. This suggests that addition of AgNPs to MWCNTs has little or no effect on the thermal stability of the MWCNTs due to the strong bond formed between the AgNPs and the MWCNTs. Thus, the doping of the silver nanoparticles with MWCNTs is not expected to have any negative effect on the application of this adsorbent material in water purification since temperatures used during treatment processes are low. The TGA profile also indicates that the AgNPs-MWCNTs composite had a lot of moisture which was lost at 100°C.

3.1.4 BET ANALYSIS OF AGNPS-MWCNTS NANO ADSORBENT

The BET surface area, pore volume and pore size of the AgNPs-MWCNTs composite material was determined under nitrogen multilayer adsorption measurement. The BET surface area, pore volume and pore size of AgNPs-MWCNTs nano adsorbent material are 125.80 m²/g, 0.1522 cm³/g and 2.6470nm respectively. Similarly the BET surface area, pore volume and pore size of purified CNT are 468.2 m²/g, 0.220 cm³/g and 2.427nm respectively. A decrease in the BET surface area was obtained after incorporation of silver nanoparticles on the carbon nanotubes, and this indicates appropriate incorporation of the metal nano particles onto the carbon nanotube surfaces. The decrease in the surface area after doping might be as ascribed to the structural changes that occur after incorporation of AgNPs onto the lattice structure of MWCNTs.

3.2 CHARACTERIZATION OF SAMPLE WATER AFTER ADSORPTION

3.2.1 PHYSICOCHEMICAL/ORGANOLEPTIC CONCENTRATION OF SEAWATER AFTER ADSORPTION

The treated seawater was characterized for its physicochemical/organoleptic properties after adsorption. The result of physicochemical/organoleptic characteristics of seawater sample after adsorption is shown in Table 1.

TABLE 1: PHYSICOCHEMICAL/ORGANOLEPTIC CHARACTERISTICS OF SEAWATER AFTER ADSORPTION PROCESS WITH NANO ADSORBENT MATERIAL

PARAMETERS	RAW	AgNPs-CNTs	NSDWQ Limit
Chloride (mg/l)	581.38	55.12	100
Sodium (mg/l)	261.04	27.33	100
Potassium (mg/l)	14.00	0.02	--
Magnesium (mg/l)	2.24	1.89	2.0
Flouride (mg/l)	12.71	0.84	1.0
Bicarbonate (mg/l)	227.13	63.01	--
Calcium (mg/l)	513.02	91.02	--
pH	7.40	7.97	6.5-8.5
Taste	Salty	Unobjectionable	Unobjectionable
Clarity	Clear	Clear	N/A
Colour (TCU)	Colourless	Colourless	3.0
Odour	Odourless	Odourless	Unobjectionable
Temperature (°C)	16.7	22.8	Ambient
Turbidity (NTU)	0.5	0.1	5
Conductivity (µS/cm)	1680	101.6	1000
TDS (mg/l)	1125.6	107.30	500
TSS (mg/l)	5.0	0.00	--
DO (mg/l)	2.70	2.68	--
BOD (mg/l)	1.80	0.00	--
COD (mg/l)	3.00	0.00	--
Bromide (mg/l)	14.02	0.01	--
Sulphate (mg/l)	81.06	33.10	100
Strontium (mg/l)	5.70	1.30	--
Iron (mg/l)	29.91	0.12	0.3
Manganese (mg/l)	62.15	0.00	0.1
Nitrate (mg/l)	54.03	2.70	10
Nitrite (mg/l)	0.08	0.002	0.02

Key:

N/A = Non available

-- = No limit establish

From Table 1, with the exception of colour and odour, all other physical/organoleptic parameters were largely influenced by the treatment process. Both colour and odour of the sample water after treatment with the nano adsorbent material remains unchanged. This implies that the nano adsorbent material does not contaminate or negatively affect the water treatment process. Although pH usually has no direct impact on consumers, it is one of the most important operational water quality parameters. To protect water and make it useful and beneficial to living organisms, the pH of the water should be maintained between 6.5 - 8.5 range (WHO, 2011 and SON, 2017). The pH of the untreated water was 7.40 but

increased to 7.97 after treatment with the nano-adsorbent material and this agrees with WHO and SON standard. Before treatment of the water sample with the nano adsorbent material, the water taste was salty because of high chloride and sodium ions concentration. Lowering the concentrations of these ions by the nano adsorbent results in neutralizing the salty taste of the water. Thus confirming the results of high chloride and sodium removal from the water after treatment with the nano adsorbent material. Turbidity is an important indicator of the possible presence of contaminants that would be of concern for health. The maximum National recommended turbidity limit is 5 NTU. The turbidity value obtained in the untreated water sample was 0.5 NTU. This is far below the maximum limit set for NSDWQ. Treatment of the water sample with the nano sorbent material further lowered the turbidity to 0.1 NTU. The conductivity of the sample water decreased from 1680 to 101.6 µS/cm. This decrease was mainly due to the reduction of chloride ion concentration in the seawater after treatment (WHO, 2011). Concentration of sodium in drinking-water in excess of 200 mg/l may give rise to unacceptable taste (WHO, 2011). Sodium concentration in the original sample water was 261.04mg/l. This is far above the National limit of 100mg/l recommended for drinking-water. Treatment of the water sample with nano adsorbent material led to reduction in the sodium concentration (27.33mg/l). This value falls within NSDWQ guidelines. Biological Oxygen Demand (BOD) values are good parameters in ascertaining the level to which a particular water body has been polluted. Water bodies with high BODs is an indication of high amount of organic wastes present in the water, because the higher the amounts of these wastes, the higher the amount of oxygen needed to biologically break down these organic wastes and thereby resulting into higher BOD values. Less polluted water bodies often depicts comparatively lower BOD values (Bichi and Amatobi, 2013). The 0.00 mg/l BOD value obtained for the treated water as against the value of 1.80 mg/l of the sample water is an indication of elimination of organic wastes from the water after treatment with the nano adsorbent material. Higher forms of aquatic life require DO for survival. Similarly, the micro-organisms present in water bodies often act on wastes materials for their survival. During this process, the metabolic activities require oxygen which is achieved through the dissolved oxygen (DO) in water body (U.S. EPA, 2015). Conversely, depletion of dissolved oxygen in water can encourage the microbial reduction of nitrate to nitrite and sulphate to sulphide (WHO, 2011). No health-based guideline value is recommended for DO, however, very high levels of dissolved oxygen may exacerbate growth of micro-organisms. The DO value of 2.68 mg/l recorded for the water sample after treatment with the adsorbent is slightly lower than the DO value of 2.70mg/l for the raw water sample. This indicate that the nano sorbent material only slightly influence the DO value. Chemical Oxygen

Demand (COD) is a measurement of the oxygen required to oxidize soluble and particulate organic matter in water. COD is an important water quality parameter as it provides an index to assess the effect water will have on consumers. Higher COD levels means a greater amount of oxidizable organic material in the water sample, which will reduce the dissolve oxygen (DO) levels leading to anaerobic conditions which encourage nitrate conversion nitrite and sulphate to sulphide if present in water. A 0.00 mg/l value was obtained for the COD after treatment. This COD value obtained for the treated water is a further indication of elimination of organic wastes from the water after treatment with the nano adsorbent material. Total dissolved solids (TDS) comprise inorganic salts (principally calcium, magnesium, potassium, sodium, bicarbonates, chlorides and sulphates) and small amounts of organic matter that are dissolved in water. Although, the palatability of water with a total dissolved solids (TDS) level of less than about 600 mg/l is considered to be good, drinking-water becomes significantly and increasingly unpalatable at TDS levels greater than about 1000 mg/l (WHO, 2011). Also noticeable aesthetics such as smell, taste or colour may become obvious in water with high TDS. The maximum national limit for Total Dissolved Solid in drinking-water is 500 mg/l. The water sample has a TDS of 1125.6 mg/l before treatment. However, treatment of the water sample with nano sorbent material reduced the TDS concentration to 107.30 mg/l. This value falls within the guideline limit of 500mg/l recommended for drinking. The most common pollutant in the world is "dirt" in the form of Total Suspended Solids (TSS). Practically, these are particles large enough to not pass through the filter used to separate them from the water. In considering waters for human consumption or other uses, it is important to know the concentrations of suspended solids. High concentrations of suspended solids decreases the aesthetic quality of drinking water. There is no standard limit recommended for TSS concentration in the NSDWQ guidelines. However, after treating the water with the nano adsorbent material, no trace of suspended solid was found in the water. 100mg/l is the National limit recommended for chloride concentration in drinking water, however, the original water sample contains far higher than the recommended standard. After treatment with the nano adsorbent material, the chloride concentration was lowered to within the National limit recommended for drinking-water. Sulphate content of the original sample water is 81.06 mg/l. Although, this is below the national standard limit of 100 mg/l, sulphate concentration further reduced to 33.10 mg/l after treatment with nano adsorbent material. After treatment with the nano adsorbent material, the manganese was completely removed. This suggest a 100 percent efficiency of the nano adsorbent to manganese adsorption. There is no standard limit recommended for potassium concentration in the NSDWQ guidelines. However, the 14mg/l potassium concentration in the water sample

reduced to 0.02 mg/l after treatment with the nano adsorbent material. Iron concentration in the original sample water was 29.91mg/l. This is far above the limit (0.3 mg/l) recommended for drinking water. Treatment of the water sample with nano adsorbent material lowered the iron concentration and falls within the NSDWQ recommended limit. Strontium concentration in the water sample was 5.70 mg/l. After treatment with the nano adsorbent material, concentration of strontium reduced to 1.3 mg/l. There is no standard limit recommended for bicarbonate concentration in the NSDWQ guidelines. However, the 227.13 mg/l bicarbonate concentration in the water sample decreased to 63.01 mg/l after treatment with the nano adsorbent material. Similarly, no standard limit is recommended for calcium and bromide concentration in the NSDWQ guidelines. However, the 513.02 mg/l calcium and 14.02mg/l bromide concentrations in the water sample reduced to 91.02 mg/l and 0.01 mg/l after treatment with the nano adsorbent material. The fluoride content of the untreated sample water has concentration of 12.71 mg/l as against the 1 mg/l maximum limit for the Nigerian Standard for Drinking Water Quality. After treatment with nano-adsorbent material, the fluoride concentration reduced to within the acceptable (SON, 2017) guidelines limit. Magnesium concentration in the original sample water was 2.24 mg/l. This is slightly above the National limit of 2 mg/l recommended for drinking water. Treatment of the water sample with nano adsorbent material lowered the magnesium concentration to 1.89 mg/l. As a result of the possibility of the simultaneous occurrence of nitrate and nitrite in drinking-water, WHO recommended that the sum of the ratios of the concentration (C) of nitrate and nitrite to their respective guideline value (GV) should not exceed 1. A value of 0.37 was obtained for the sum of ratio of the concentration (C) of nitrate and nitrite to their respective guideline value (GV) in this work. This value agrees with the WHO recommendation for nitrate and nitrite concentrations in drinking water.

3.2.2 BACTERIOLOGICAL CONCENTRATION OF SEAWATER SAMPLE AFTER ADSORPTION

The bacterial community structure and its dynamics were analysed using bacteria plate count. Based on the analysis, it can be observed from Table 2 that *S. typhimurium*, *S. aureus*, Fungi (yeast/moulds), Non-Pathogenic Bacteria and *E. coli* were present in the water sample in different amounts. Only *P. auruginosa* was not detected in the water sample.

TABLE 2: MICROBIAL CONCENTRATION OF SEAWATER SAMPLE AFTER TREATMENT

PARAMETERS	A	B	C
Non-Pathogenic Bacteria (cfu/100ml)	20	NIL	$\leq 1 \times 10^3$
<i>E. coli</i> (cfu/100ml)	30	NIL	NIL
<i>S. typhimurium</i> (cfu/100ml)	60	NIL	NIL
<i>P. auruginosa</i> (cfu/100ml)	NIL	NIL	NIL

<i>S. aureus</i> (cfu/100ml)	30	NIL	NIL
Fungi (yeast/moulds) (cfu/100ml)	10	NIL	≤1*10 ²

Key

A = Raw water sample

B = Nano adsorbent treated water

C = NSDWQ limit

The presence of *E. coli* in water provides evidence of recent faecal contamination (Ashbolt *et al.*, 2001 and WHO, 2011). 30cfu/100ml of *E. coli* was present in the water sample before treatment. However, treatment of the seawater sample with the nano adsorbent material reveals zero colony of *E. coli*. The national limit for fungi (yeast/mould) is $\leq 1 \times 10^2$. Before treatment, fungi colony count in the water sample was 10 cfu/100ml. This is within the NSDWQ limit. However, after subjecting the water through the treatment cycle, all colonies of fungi in the water sample were eliminated. Similarly, before treating the water sample with the AgNPs-MWCNTs adsorbent material, 30cfu/100ml of *S. aureus* was found in the water sample but after treatment with the nano adsorbent material there were no count of the microorganism, thus, further indicating the effectiveness of the nano adsorbent composite material in the seawater treatment. *S. typhimurium* recorded the highest value (60cfu/100ml) of all the microbial analysis of the water sample. However, after treating the water with the AgNPs-MWCNTs material there were no colonies of *S. typhimurium* in the treated water. The sample water contain 20 cfu/100ml of Non-pathogenic bacteria. Although this value satisfy the national limit of $\leq 1 \times 10^3$ cfu/100ml recommended for drinking water, the post treatment analysis reveal no count of this bacteria in the water sample. The post treatment analysis of the water shows no evidence of *P. aeruginosa* in treated water indicating that there was no introduction of this bacteria during the handling process. In summary, it is evident from table 2 that the treatment of the water sample with the AgNPs-MWCNTs nano adsorbent led to complete elimination of community of the diverse microorganism that were present in the sample prior to treatment.

4 CONCLUSION

Nano-sized AgNPs-MWCNTs adsorbent have been successfully synthesized and used for the treatment of seawater. The AgNPs-MWCNTs composite have been characterized by a variety of analytical techniques such as TEM, EDS, TGA and BET. The doping of silver nano particles with carbon nano tubes display high anti-microbial tendencies. Results obtained shows that the nano-adsorbent was very effective in the removal of dissolved ions, contaminants and micro-organisms present in the seawater. The dissolved ions, micro-organisms and other pollutant in the water were reduced to within the limits recommended in the National Standard for Drinking Water Quality guidelines (NSDWQ). Finally it

can be concluded that AgNPs-MWCNTs adsorbent have superior potential for seawater treatment.

ACKNOWLEDGEMENTS

The authors wish to acknowledge the Nanotechnology Research Group, Centre for Genetic Engineering and Biotechnology (CGEB), Federal University of Technology, P.M.B 65, Bosso, Minna, Niger State, Nigeria. Standard Organization of Nigeria (SON) and Jesil Pharmaceuticals Company Limited Minna are also acknowledge for technically assisting with inputs for this paper.

REFERENCE

- Amiri, A., Maghrebi, M., Baniadam, M., Zeinali, H. S. (2011). One-pot, Efficient Functionalization of Multi-walled Carbon Nanotubes with Diamines by Microwave Method. *Applied Surface Science*, 257, 10261-10266.
- Ashbolt, N. J., Grabow, W. O. K. & Snozzi, M. (2001). Indicators of Microbial Water Quality. In L. Fewtrell, J. Bartram, (Eds), *Water Quality-Guidelines, Standards and Health: Assessment of Risk and Risk Management for Water-related Infectious Disease* (pp. 289-315). London: IWA Publishing.
- Azodi-Deilami S, Najafabadi AH, Asadi E, Abdouss M, Kordestani D. (2014). Magnetic Molecularly Imprinted Polymer Nanoparticles for the Solid-Phase Extraction of Paracetamol from Plasma Samples, Followed Its Determination By HPLC. *Microchim. Acta*, 181, 1823.
- Bates, B., Kundzewics, Z. W., Wu, S. & Palutik, J. (2008). Climate Change and Water, Technical Paper of the Intergovernmental Panel on Climate Change, IPCC Secretariat, Geneva, 201.
- Bharathi, K. S. & Ramesh, S. T. (2013). Removal of Dyes Using Agricultural Waste as Low-Cost Adsorbents: A Review. *Applied water Science*, 3, 773-790
- Bichi, M. & Amatobi, D. (2013). Assessment of the Quality of Water Supplied by Water Vendors to Households in Sabon Gari Area of Kano, Northern Nigeria. *The International Journal of Engineering and Sciences*, 2(7), 9-17.
- Borsani, R., & Rebagliati, S. (2005). Fundamentals of Costing of MSF Desalination Plants and Comparison with other Technologies. *Desalination*, 182, 29-37
- Brown, M. T., Martinez, A. & Uche, J. (2010). Energy Analysis Applied to the Estimation of the Recovery of Cost for Water Services under the European Water Framework Directive. *Journal of Ecological Model*, 22(1), 2123-2132

- Chow, J., Kopp, R. J. & Portney, P. R. (2003). Energy Resources and Global Development. *Science*, 302, 1528-1531.
- Edwards-Jones V. (2009). The benefits of silver in hygiene, personal care and health care. *Letter of Applied Microbiology*, 49, 147-152
- El Muguana, Y., Elhadiri, N., Bouchdoug, M., Benchanaa, M. & Boussetta, A. (2018). Optimization of Preparation Conditions of Novel Adsorbent from Sugar Scum Using Response surface Methodology for Removal of Methylene Blue. *Journal of Chemistry*. Article ID 2093654, <https://doi.org/10.1155/2018/2093654>
- Elabbas, S., Mandi, L., Berrekhis, F., Noelle, M., Pierre, J. & Quazzani, N. (2015). Removal of Cr(III) from Chrome Tanning Wastewater by Adsorption Using Two Natural Carbonaceous Materials: Eggshell and Powdered Marble. *Journal of Environmental Management*, 166, 589-595
- Francisco, O., Tanya, H., Francisco, A. & Daniele, C. (2014). Developing Sustainable and Replicable Water Supply Systems in Rural Communities in Brazil. *The International Journal of Water Resources Development*, 4(5), 3-25
- Fritzmann, C., Löwenberg, J., Wintgens, T., & Melin, T. (2007). State-of-the-art of Reverse Osmosis Desalination. *Desalination*, 216, 1-76
- GE Reports (2011). Water Reuse Gains as Urban and Industrial Demand is Set to Double, Retrieved from <http://www.gereports.com/water-reuse-gains-as-urban-industrial-demand-is-set-to-double/>
- Glueckstern, P., Priel, M., Gelman, E. & Perlov, N. (2008). Wastewater Desalination in Israel. *Desalination*, 222, 151-164
- Greenlee, L. F., Lawler, D. F., Freeman, B. D., Marrot, B. & Moulin, P. (2009). Reverse Osmosis desalination: Water sources, Technology, and today's Challenges. *Water Research*, 43, 2317-2348.
- Harvey, E. & Reed, R. (2007). Community-Managed Water Supplies in Africa. Sustainable or Dispensable? *Community Development Journal*, 42(3), 365.
- Helal, A. M., El-Nashar, A. M., Al-Katheeri, E. & Al-Malek, S. (2003). Optimal Design of Hybrid RO/MSF Desalination Plants Part 1: Modelling and Algorithms. *Desalination*, 154, 43-66
- Hightower, M. & Pierce, S. A. (2008). The Energy Challenge. *Nature*, 452, 285-286.
- Immerzeel, W. W., Beek, L. P. H. v. & Bierkens, M. F. P. (2010). Climate Change will affect the Asian Water Towers. *Science*, 328, 1382-1385.
- Jimenez, A., & Perez-Foguet, A. (2010). Challenges for Water Governance in Rural Water Supply: Lessons Learned from Tanzania. *Water Resources Development*, 26(2), 235-248
- Kecili, R. & Hussain, C. M. (2018). Mechanism of Adsorption on Nanomaterials. *Nanomaterials in Chromatography*, 89-115
- Krishnaraj, C., Jagan, E. G., Rajasekar, S., Selvakumar, P., Kalaichelvan, P. T. & Mohan N. (2010). Synthesis of Silver Nanoparticles Using *Acalypha indica* Leaf Extracts and its
- Li, Y.-H., Wang, S., Wei, J., Zhang, X., Xu, C. Luan, Z., Wu, D. & Wei, B. (2002). Lead Adsorption on Carbon Nanotubes. *Chemical Physics Letters*, 357, 263-266
- Linares, R. V., Li, Z., Sarp, S., Bucs, S. S., G. Amy, G. & Vrouwenvelder, J. S. (2014). Forward Osmosis Niches in Seawater Desalination and Wastewater Reuse: A Review. *Water Research*, 66, 122-139
- Ling, M. M., Wang, K. Y. & Chung, T. S. (2010). Highly Water-soluble Magnetic Nanoparticles as Novel Draw Solute in Forward Osmosis for Water Reuse. *Industrial and Engineering Chemistry Research*, 49, 5869-5876.
- Mamba, G., Mbianda, X. Y., Govender, P. P., Mamba, B. B. & Krause, R. W. (2010). Application of Multiwalled Carbon Nanotube-Cyclodextrin Polymers in the Removal of Heavy Metals from Water. *Journal of Applied Sciences*, 10(11), 940-949
- McGinnis, R. L. & Elimelech, M. (2008). Global Challenges in Energy and Water Supply: The Promise of Engineered Osmosis. *Environmental Science and Technology*, 42, 8625-8629.
- Morones, J. R., Elechiguerra, J. L., Camacho, A., Holt, K., Kouri, J. B., Ramirez, J. T. & Ykaman, M. J. (2005). The bacterial effects of silver nanoparticles. *Nanotechnology*, 16, 2346-2353.
- Niksefat, N., Jahanshahi, M., & Rahimpour, A. (2014). The Effect of SiO₂ Nanoparticle on Morphology and Performance of the Thin Film Composite Membrane for Forward Osmosis Application. *Desalination*, 343, 140-146
- Purkayastha, D., Mishra, U. & Biswas, S. (2014). A Comprehensive Review on Cd(II) Removal from Aqueous Solution. *Journal of Water Process Engineering*, 2, 105-128.
- Rahmanian, N., Siti Hajar Bt Ali, Homayoonfard, M., Ali, N. J., Rehan, M., Sadeh, Y. & Nizami, A. S. (2015). Analysis of Physicochemical Parameters to Evaluate the Drinking Water Quality in the State of Perak, Malaysia. *Journal of Chemistry*, Article ID 716125, <http://dx.doi.org/10.1155/2015/716125>
- Rai, M., Yadav, A. & Gade, A. (2009). Silver Nanoparticles as a New Generation of Antimicrobials. *Biotechnology Advances*, 27, 76-83



- Sankar, R., Karthik, A., Prabu, A., Karthik, S., Shivashangari, K. S. & Ravikumar, V. (2013). *Origanum vulgare* Mediated Biosynthesis of Silver Nanoparticles for its Antibacterial and Anticancer Activity. *Colloids and Surfaces B: Biointerfaces*, 108, 80-84
- Semiati, R. (2008). Energy Issues in Desalination Processes. *Environmental Science and Technology*, 42, 8193-8201.
- Shah, P. & Murthy, C. N. (2013). Studies on the Porosity and Control of MWCNT/Polysulfone Composite Membrane and its Effect on Metal Removal. *Journal of Membrane Science*, 473, 90-98
- Shahverdi, A. R., Fakhimi, A., Shahverdi, H. R. & Minaian, S. (2007). Synthesis and Effects of Silver Nanoparticles on the Antibacterial Activity of Different Antibiotics against *Staphylococcus aureus* and *Escherichia coli*. *Nanomedicine: Nanotechnology, Biology and Medicine*, 3, 168-171
- Shannon, M. A., Bohn, P. W., Elimelech, M., Georgiadis, J. G., Marinas, B. J. & Mayes, A. M. (2008). Science and Technology for Water Purification in the Coming Decades. *Nature*, 452, 301-310.
- Standard Organisation of Nigeria (2017). Standard for Bottled/Packaged Drinking Water (Other than Natural Mineral Water)
- Tayalia, Y. & Vijaysai, P. (2012). Process Intensification in Water and Wastewater Treatment Systems. Proceedings of the 11th International Symposium on Process Systems Engineering, 33-40
- U.S. EPA (2015). Benchmark dose software (BMDS) version 2.6.0.1. Software available for download from the U.S. Environmental Protection Agency. Available at: www.epa.gov/NCEA/bmds/index.html.
- World Health Organization (2011). *Guidelines for Drinking Water Quality* (4th ed.). Geneva, Switzerland: WHO Press
- Yang, S., Li, J., Shao, D., Hu, J. & Wang, X. (2009). Adsorption of Ni(II) on Oxidized Multi-walled Carbon Nanotubes: Effect of Contact Time, pH, Foreign Ions And PAA. *Journal of Hazardous Materials*, 166, 109-116
- Zhao, N., He, C., Li, J., Jiang, Z. & Li, Y. (2006). Study on Purification and Tip-opening of CNTs Fabricated by CVD. *Materials Research Bulletin*, 41, 2204-2209
- Zhu, X., & Elimelech, M. (1997). Colloidal Fouling of Reverse Osmosis Membranes: Measurements and Fouling Mechanisms. *Environmental Science and Technology*, 31, 3654-3662



THE ROLE OF ENGINEERING AND TECHNOLOGY AND SUSTAINABLE DEVELOPMENT REDUCING CARBON EMISSION WITH GREEN AND SUSTAINABLE BUILD ENVIRONMENT

BY

¹HASHIMU, L, ²HALILU, A, A, & ³SANI, I.

Department of Chemistry, School of Secondary Education, Zamfara State College of Education Maru.

E-Mail; lawalhashim22@gmail.com. Phone Number; 08069289623.

ABSTRACT

Global warming is caused by the emission of greenhouse gases. 72% of the totally emitted greenhouse gases are carbon dioxide (CO₂), 18% Methane and 9% Nitrous oxide. Carbon dioxide emissions therefore are the most important cause of global warming. CO₂ is inevitably created by burning fuels e.g. oil, natural gas, diesel, organic-diesel, petrol, and organic-petrol. The emissions of CO₂ have been dramatically increased within the last 50 years and are still increasing by almost 3% each year. The concept of reducing carbon emission with green building is put forward under the ground that all people over the world are taking action to deal with climate change. Reducing carbon emission with green or sustainable buildings use key resources like energy, water, materials, and land more efficiently than buildings that are just built to code. With more natural light and better air quality, green buildings typically contribute to improved employee, employer, student health, comfort, and productivity. In this paper the ways and challenges of reducing carbon building are pointed out, which are new energy develop, clean technique use, green planning, green building and reducing carbon life style.

Keywords: *carbon, reducing carbon, global warming, climate change, global policy, green building; sustainable material.*

1. INTRODUCTION

Building Construction sector is the largest global consumer of materials, and buildings are the sector with the largest single energy use worldwide [1]. Consequently, buildings are also responsible for 19% of global greenhouse gas (GHG) emissions [2]. In the beginning of the industrial revolution, concentration of carbon dioxide in the atmosphere was 270 parts per million. This concentration, which has now risen to 377 parts per million, has been unprecedented not only in the past 740 thousand years, but also perhaps even 55 million years ago [3]. There are two main reasons for climate change: natural reasons arising from changes in the orbit of the sun and in the parameter of earth orbit, and human related causes, the most important of which is excessive emissions of greenhouse gases through human activities [4].

2. LITERATURE REVIEW

Recent studies have suggested that buildings offer the greatest abatement opportunities for reducing GHG emissions in the short-term [5]. Policy-makers have responded to this through the introduction of regulation requiring improvements in building fabric and performance, such as the European Union (EU) Energy Performance of Buildings Directive. These regulations have principally focused on the operational GHG emissions associated with energy use in activities such as space heating, cooling and lighting. However, these regulatory drivers have not extended to the embodied carbon associated with the initial production of structures as shown in figure-1.

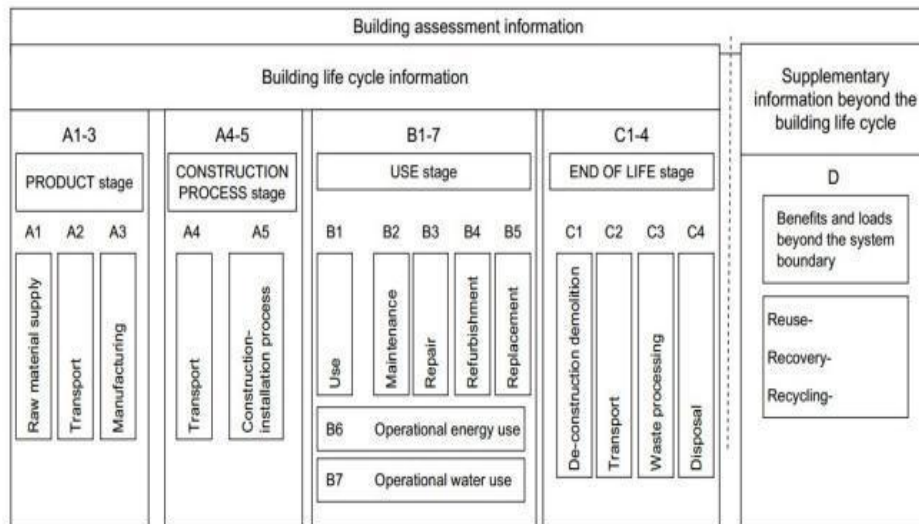


Figure 1: Life cycle stages of construction works [6]

A recent review of building life cycle assessments demonstrated that embodied carbon can account for anywhere between 2% and 80% of whole-life carbon emissions [6]. The precise proportion depends upon a number of characteristics including building use, location, material palette, and assumptions about the service life and future energy supply. The proportion tends to be higher in certain structure types, such as industrial warehousing, where embodied emissions can contribute up to 90% of the total [7]. The share of life cycle emissions attributable to embodied carbon is expected to increase further with reductions in operational emissions owing to improved operational performance and reductions in the carbon intensity of the electricity supply [8]. Meanwhile, absolute increases in embodied carbon can be expected with an anticipated growth in building activity and higher performance buildings typically requiring greater material use.

The importance of embodied emissions further increases when taking account of the temporal allocation of emissions. As cumulative emissions, not annual emissions, are the critical component in preventing unacceptable levels of climate change [9], some researchers have

increasingly argued that a greater weighting should be attached to current rather than future emissions savings in economic analyses and policy-making [10]. When the temporal allocation of emissions is considered in building assessments, research demonstrated that the swift release of emissions, or a ‘carbon spike’, associated with construction phase emissions can dominate life cycle emissions in the time horizon relevant to adopted climate mitigation goals [11]. This conclusion led the same author’s subsequently to question the merits of building new developments as a means of climate change mitigation. In many cases, however, new development is unavoidable and, in such instances, a greater focus on embodied carbon mitigation is essential.

Numerous past studies have addressed barriers to particular forms of ‘green building’ or ‘sustainable building’. Some of these studies take broad definitions of sustainability, incorporating economic and social factors [12] whilst others have focused specifically on the environmental aspects of sustainability. However, these studies have tended to consider only operational emissions [13], the adoption of energy-efficient technologies [14], or the achievement of



regulatory targets, such as zero carbon homes [15] that exclude the embodied emissions of materials used in construction. Few, if any, have focused specifically upon the barriers to alternative material choice as a means of mitigating embodied carbon emissions. The following review therefore draws upon literature from two streams. The first stream features studies that offer insight into the cultural and institutional barriers preventing sustainable innovation within the construction industry. The second stream contains detailed studies that address the adoption of specific alternative materials.

2.1 OBJECTIVE OF THE STUDY

Emissions generated from burning of these fossil fuels are huge threats to the environment. Industrial revolution, sudden increase in consumption of natural resources and invention of technologies that use non-renewable energy sources all together affected our environment in many ways. The problems associated with global warming and climate change move us towards more sustainable approaches in building design. These problems do not affect only our environment but our social and economic life as well. Therefore it is necessary to take global actions towards reducing these emissions specially in building sector which opportunities are numerous.

2.2 CO₂ EMISSIONS IN BUILDINGS LIFE CYCLE

Early description of reducing carbon buildings highlighted balance between the need of living organisms, buildings and climate. Throughout recent years the development of passive low energy building has referred reducing carbon building in the framework of sustainability. Henceforth, we may redefine the

reducing carbon building as a sustainable building or 'green building' base on human ecology with the sustainable development of economy, society and architecture simultaneously [16]. The Brutland definition of sustainability is meeting the needs of the present without compromising the ability of future generations to meet their own needs [17]. That is why it is important to construct buildings which have least possible impact on the nature, and to preserve natural sources for future generations too

Zero carbon buildings are the core driver for sustainable design to mitigate against further climate change.

To produce useful information concerning carbon dioxide emissions in the building construction industry, many researchers have studied energy consumption at different stages of the building life cycle and have concluded that each phase has different effects [18]. Carbon dioxide emissions are commonly expressed in terms of the life cycle stages involved that is, planning, design, construction, installation, test, commissioning, operation and disposal

[19]. USEPA categorize these stages into the three consecutive phases, namely 'cradle to entry gate', entry gate to exit gate and exit gate to grave'. Another study, have represented these in three distinct stages: (a) initial impact covering the content of materials in the construction process; (b) operational impact from the operational to maintenance phases; and (c) end of life impact – the deconstruction process to waste materials [20]. Alternatively, the life cycle of buildings can be represented in five phases, including (a) design phase; (b) materials phase (c) distribution phase; (d) use phase (e) the refurbish/demolition phase (as shown in figure-2).

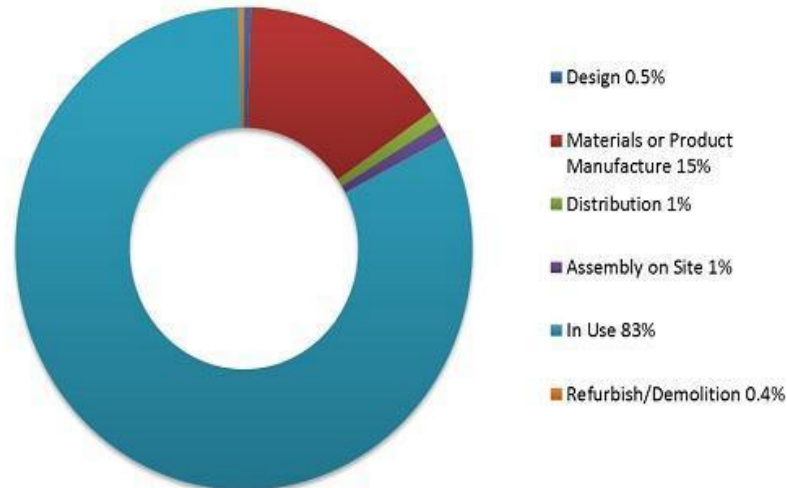


Figure 2: Carbon dioxide emissions in the building life cycle

The planning and design phase is of paramount importance for carbon dioxide reduction as decisions made during this stage are influential on operational efficiency [21]. Correct selection of materials and technology during the planning and design phase can provide an opportunity for carbon dioxide reductions in the industry [22]. To facilitate clients and design team members finding out how environmentally responsible the design is, various building environmental assessment tools such as the leadership in energy and environmental design (LEED) in the USA have been developed.

2.3 HOW GREEN BUILDINGS REDUCE CARBON DIOXIDE

As the serious consequences of climate change or global warming have been better understood by modern climate models, focus has rested on the reduction in overall carbon dioxide emission. While the effect of carbon dioxide on the climate are taught in most schools in United States and picture of the so called “greenhouse effect” on climate are ingrained into most of our minds, the link between green buildings and reduction in carbon dioxide emission is often passed over. This link however is vitally important to understand so

that builders, architects, and engineers understand the great societal value of green building, not to mention value in their pockets. There are two main ways that green building reduce carbon dioxide emission which in turn helps the overall climate [23].

2.3.1 Reduce Losses during Fabrication

For many green buildings, the raw materials and components themselves are purchased from green suppliers. These suppliers adhere to strict standards and controls to ensure that their production methods conserve natural resources and reduce overall carbon dioxide emissions. Some of the ways that they do this include more efficient processes designed to reduce energy consumption during fabrication, transporting goods on more efficient means of transportation and leveraging new and growing technologies like solar power to reduce dependence on fossil-fuel based (heavily carbon dioxide emitting) power plants. Furthermore, green buildings are erected in a way that minimizes inefficiencies and leverages modern materials science in a way to reduce overall emissions even during construction.



Contemporary green building materials can dramatically reduce the overall carbon dioxide emissions, both in their construction and in their installation.

2.3.2 Reduce Energy Consumption during Operation

Some of the greatest benefits to the environment from green buildings come after the construction phase is concluded, and the building settles to a daily operation grind. Because most of the power grid around the world, and especially in the united, state, Nigeria e.t.c relies heavily on fossil fuel-natural gas, coal, and oil for the production of energy, every kilo watt hour used by a building is indirectly releasing carbon dioxide to the air.

Advantage of green building that uses less energy:

A reduced overall, usage of energy whether from energy efficient appliances, passive heating and cooling, or sustainable architectures can dramatically shrink a buildings overall carbon footprint or even make it a net positive on the environment. The great thing about building with a mind toward sustainability is that the same practices which protect the environment from excessive carbon dioxide production have beneficial site effect of often reducing a building owners overall expenditures on building maintenance. Sustainable architecture by, designed to last without needing continual repair or refurbishment, but instead to work with, instead of against, the natural world. Using constructed, stable materials in concert with made equipment can save the building owner money while also leading toward environmental benefits [23].

2.4 CONSTRUCTION MATERIALS

Cement is an important construction element around the world, and therefore, cement

production is a significant cause of global carbon dioxide CO₂ emissions, making up to nearly 2.4 percent of global CO₂ emissions from industrial and energy sources [23]. Cement manufacturing is extremely energy demanding, because of the extreme heat required to produce it. Producing a ton of cement requires 4.7 million BTU of energy, equals to about 400 pounds of coal, and produces nearly a ton of CO₂. Given its high emissions and serious importance to society, cement is an obvious place to look to lessen greenhouse gases emissions [24].

2.4.1 SUSTAINABLE BUILDING MATERIAL

Materials which produce less pollution and waste during manufacturing and construction process are being considered as sustainable building materials. Natural materials are less toxic and their embodied energy is less as compared to artificial materials. Therefore, most of the natural materials are sustainable building materials. Recyclability and biodegradability are also important measures of sustainability. Some materials such as steel and glass are recyclable whereas concrete cannot be recycled, it can only be grounded up and used as aggregate in new concrete. From biodegradability point of view organic materials decompose rapidly, but steel for example takes much longer time. Another important factor is life span of the material. Materials which have longer life need not to be replaced therefore less natural resources are required for manufacturing and less landfill waste is generated. Some sustainable building materials are mentioned below:

2.4.2 RAMMED EARTH

Not to be confused with mud brick, rammed earth is a precisely controlled mixture of gravel, clay, sand, cement, and sometimes lime or waterproofing additives. The contents are



carefully proportioned and mixed, and then machine-compacted in removable formwork to yield a stone-like wall that is massive, water resistant, load bearing and long lasting. Recent Study shows that, rammed earth can also contribute in building energy consumption and thermal comfort [25].

2.4.3 STRAWBALE

Strawbale building like mudbrick is a good sustainable choice as it is made from natural materials they are a sustainable, recyclable, non-toxic and healthy form of building construction. Rectangular strawbales are stacked up to form walls, fixed in place with metal or wooden pins, and then trimmed and shaped before being rendered with mud or cement based renders.

2.4.4 TRIPLE GLAZED WINDOWS

The three layer glass acts as better insulation as compared to double glazed windows. It avoids air infiltration. Therefore, keeps the building warm in winters, and cool in summers. In double glazed windows argon is injected in each layer of glass whereas in triple glazed windows krypton which is better insulation is injected.

2.4.5 SUSTAINABLE CONCRETE

While, 95% of buildings CO₂ emissions are outcome of the energy used during its life, there is ample that can be done to reduce that 5% related with construction. Concrete is a perfect place to start, partially because nearly every building uses it, and mostly due to the fact that concrete accounts for 7-10% of global CO₂ emissions. More sustainable forms of concrete exist, that use combination of recycled materials. Crushed glass can be added, as can wood chips or slag – a byproduct of steel manufacturing. Though, these changes aren't radically transforming concrete, by simply using a material

that would have otherwise gone to waste, the CO₂ emissions related to concrete are decreased [26].

2.4.6 AERATED AUTOCLAVED CONCRETE

Manufacturing of AAC blocks and panels does not have high energy requirements. Besides, since AAC is light weight, it also saves energy required for transportation and leads to reduced CO₂ emissions by transport vehicles. Since AAC blocks are made from fly ash – an industrial left-over product – produced by thermal power plants, it offers a low price and sustainable solution for present and future.

2.4.7 COMPRESSD STABILIZED EARTH BLOCK

CSEB usually made with adding sand and Jute fiber as reinforcement. Stabilizer (cement) was kept constant for each type of block as 10%. Different type of curing like air curing, sun curing and polythene wrapping curing were incorporated and tested for three days, seven days, fourteen days, and twenty eight days. Beneficial climatic performance in most regions due to its high thermal capacity, low thermal conductivity and porosity, thus it can moderate extreme outdoor temperatures and maintain a satisfactory internal temperature balance.

2.4.8 ADOBE

Adobe is material made up of combination of sand, clay; water, and fibrous or organic material, builders make bricks out of adobe and dry it in the sun. Some of the advantages of adobe structures is that they have long life and great thermal mass, in hot climates. A disadvantage which can be mentioned is that they are not earthquake resistant and have poor behavior in case of earthquake

3. DISCUSSION



In addition to the examples above, there are many other innovative reducing carbon products available and many more are undergoing research and development. These CO₂ emission studies confirm the construction industry's high levels of energy consumption and production of a significant amount of carbon dioxide throughout buildings life cycles. Each phase of the life cycle contributes a different level of carbon dioxide emissions. The operational phase is the highest contributor, followed by the materials and construction process phase, the maintenance and renovation phase, the deconstruction and disposal waste material phase, and the planning and design phase. It is argued, however, that the most significant influence on emissions occurs in the early stages of the project life cycle as the greatest potential carbon dioxide savings can be realized in the design phase before construction. As this involves building design and materials, any changes will affect the other phases, generating waste materials that eventually produce carbon dioxide emissions. When choosing materials, it is clear that the embodied energy of building materials must be carefully considered along with the operating energy in order to reduce the total life cycle energy use. By replacing those materials that require a significant amount of energy to produce with those consuming minimal energy during the production process, this will help cut down on the energy embodied in buildings.

4. CONCLUSION

Reducing embodied carbon is one of the simple and practical mitigation options for the building sector by utilizing carbon sink and low or reduced carbon materials and products in buildings. Not all building materials can be carbon-sinks. In such cases, low or reduced carbon building materials should be used as much as possible. Low or reduced-carbon building materials can be sourced from materials with both low embodied energy and carbon in their

production, assembly, and transportation processes. By following the suggested techniques during different stages of building's life cycle, lower carbon emissions from buildings could be achieved, which will help in development of more sustainable, ecofriendly environments. Fortunately, though buildings account for large amount of GHG emissions, there are also lots of opportunities to reduce these emissions. This is where low carbon green building comes into the picture. To have sustainable environment friendly world, not only buildings need to be designed and operated based on sustainable considerations, but the whole communities and cities need to be sustainable.

Many countries have made efforts to decrease carbon emissions by framing development planning and taking measures from aspects of energy, transportation, industrial structure etc. Facing the increasingly serious challenge of environmental change (levels of carbon dioxide in the atmosphere have risen by more than a third since the industrial revolution and are now increasing faster than ever before) and decline of indigenous energy supplies different government bodies are working together.

In order to have sustainable eco-friendly environment sustainable rules should be passed by governments which obligate builders to follow the rules regarding reducing the carbon emissions in building industry.

REFERENCES

- [1] Krausmann et al., 2009; De la Rue du Can & Price, 2008; Sectorial trends in global energy use and greenhouse gas emissions. *Energy Policy*, 36(4), 1386–1403. doi:10.1016/j.enpol.2007.12.017
- [2] Intergovernmental Panel on Climate Change (IPCC), 2014



- [3] Farshchi, R. (2009). Architecture in the Age of Climate Change, 48
- [4] Azizi, Q. Climate change, 2004
- [5] McKinsey & Co., Intergovernmental Panel on Climate Change (IPCC), 2014
- [6] Ibn-Mohammed, Greenough, Taylor, Ozawa-Meida, & Acquaye, 2013
- [7] Sturgis & Roberts, 2010; Redefining Zero: Carbon profiling as a solution to whole life carbon emission measurement in buildings. RICS Research.
- [8] Ibn-Mohammed et al., 2013; Operational vs. embodied emissions in buildings—A review of current trends. *Energy and Buildings*, 66, 232–245. doi:10.1016/j.enbuild.2013.07.026
- [9] Matthews, Solomon, & Pierrehumbert, 2012; Cumulative carbon as a policy framework for achieving climate stabilization. *Philosophical Transactions of the Royal Society. Series A, Mathematical, Physical, and Engineering Sciences*, 370(1974), 4365–4379. doi:10.1098/rsta.2012.0064
- [10] Rhys, J. (2011). Cumulative carbon emissions and climate change: Has the economics of climate policies lost contact with the physics? <http://www.oxfordenergy.org/wpcms/wp-content/uploads/2011/07/EV-571.pdf>
- [11] Heinonen, Saynajoki, and Junnila, 2011; A longitudinal study on the carbon emissions of a new residential development. *Sustainability*, 3(12), 1170–1189
- [12] Williams & Dair, 2007; what is stopping sustainable building in England? Barriers experienced by stakeholders in delivering sustainable developments. *Sustainable Development*, 15, 135–147. doi:10.1002/sd.308
- [13] Kershaw & Simm, 2013; Thoughts of a design team: Barriers to low carbon school design. *Sustainable Cities and Society*, 11, 40–47. doi:10.1016/j.scs.2013.11.006
- [14] Pinkse & Dommisse, 2009; overcoming barriers to sustainability: An explanation of residential builders' reluctance to adopt clean technologies. *Business Strategy and the Environment*, 18(8), 515–527.
- [15] Osmani & O'Reilly, 2009; Feasibility of zero carbon homes in England by 2016: A house builder's perspective. *Building and Environment*, 44(9), 917–924. doi:10.1016/j.buildenv.2009.01.005
- [16] Li J and Colombier M (2009) Managing carbon emissions in China through building energy efficiency. *Journal of Environmental Management* 90(8): 2436–2447.
- [17] World Commission on Environment and Development, 1987
- [18] Bevington and Rosenfeld, 1990; Energy for buildings and homes. *Scientific American* 263(3): 77–86
- [19] Gangoelle et al., 2009; A methodology for predicting the severity of environmental impacts related to the construction process of residential buildings. *Building and Environment* 44(3): 558–571.
- [20] Sodagar and Fieldson, 2009; towards a framework for early estimation of life cycle carbon foot printing of building in the UK. *Construction Information Quarterly* 11(2): 66–75.
- [21] Erlandsson and Borg, 2003; Generic LCA-methodology applicable for buildings, constructions and operation services – today's practice and development needs. *Building and Environment* 38(7): 919–938.
- [22] Gerilla et al., 2007; an environmental assessment of wood and steel reinforced concrete housing construction. *Building and Environment* 42(7): 2778–2784.
- [23] Boma et al., 2019; green building consultant.
- [23] <http://blogs.ei.columbia.edu/2012/05/09/emissions-from-the-cement-industry>, 2012
- [24] <http://thisbigcity.net/five-sustainable-building-materials-that-could-transform-construction>, 2013.
- [25] Jaher Wasim, AKM Hasan Julker Nine. "Assessment of rammed earth as external cladding on thermal comfort and energy



**2nd International Engineering Conference (IEC 2017)
Federal University of Technology, Minna, Nigeria**



consumption of a low cost house in Bangladesh." *Seminar on—
“Housing, Building Material and Construction
Technology:*

Bangladesh Context”. Housing and Building
Research Institute(HBRI), Bangladesh,
2016.

[26] <http://aac-india.com/aac-bloc>

**1 MATHEWS, J., BERRETT, D., &
BRILLMAN, D. (2005, MAY 16).**

Other winning equations. Newsweek, 145(20), 58-
59.

1. Newspaper with no author:

Generic Prozac debuts. (2001, August 3). The
Washington
Post, pp. E1, E4.



Optimization and Kinetics study of Biodiesel synthesis from beef tallow using Calcium Oxide from Limestone

*Ogunjobi, T. O¹, Olutoye, M. A¹, & Aberuagba, F¹

¹Chemical Engineering Department, Federal University of Technology, PMB 65 Minna Niger State, Nigeria

*Corresponding author email: toxylee20021@gmail.com, +2347030392217

ABSTRACT

Biodiesel is an eco-friendly fuel substitute for Petro-diesel. Biodiesel is a mixture of mono alkyl esters (C₁₄ – C₂₂). This study was undertaken to investigate the optimization and kinetics study of Biodiesel synthesis from beef tallow (BT) using Calcium Oxide from Limestone. The optimization study was carried out using Design expert version 7.0 for the esterification and transesterification experiments. The process parameters considered for the optimization study of the esterification reaction resulted in an optimum FFA of 0.60 at operating conditions of catalyst amount of 7.1 wt.%, methanol to oil ratio of 9:1, reaction temperature of 60 °C and a reaction time of 96 minutes while that of the transesterification reaction resulted in an optimum Biodiesel yield of 72.0 % at methanol to oil ratio of 7:1, catalyst loading of 4 wt.%, reaction temperature and time of 60 °C and 106 minutes respectively. It was observed that a close correlation exists between the experimental and predicted results as confirmed by the validation experiment and the square of the correlation coefficient (R²) for both the esterification reaction and transesterification reactions were estimated to be 0.9592 and 0.9595, respectively. The kinetics data for the CaO catalysed transesterification reaction of Biodiesel from Beef Tallow resulted in activation energy and the pre-exponential factor of 82.845 KJ/mol. K and 4.805*10¹¹ min⁻¹ with the Arrhenius plot giving an R² value of 0.9109 which shows a good correlation with the experimental data.

Keywords: *Beef Tallow, Biodiesel, Calcium oxide, Kinetics, Transesterification.*

1 INTRODUCTION

The increase in demand for energy, a growing worldwide concern for environmental protection and the conservation of non-renewable natural resources have led to search for an alternative fuel which can supplement or replace fossil fuel (Niju, *et al.*, 2014).

Bio-fuel on the other hand has received worldwide attention as one of the key solutions to issues of sustainable energy development, energy security, and reduction of green gas emissions (Omotoso & Akinsanoye, 2015).

Biodiesel is a type of bio-fuel that is currently accepted as a valid contributor to reduce fossil fuels dependency, either by its use as an extender or in total substitution of diesel fuel (Berenguer & Sierra, 2015). Biodiesel is a mixture of mono alkyl esters (C₁₄ – C₂₂) that can be derived from renewable lipid feedstock majorly plant oil and animal fat (Feddern, *et al.*, 2011).

Of the numerous advantages attributed to biodiesel is the fact that it has a higher cetane number and flash point than Petro-diesel, has no aromatics, it is biodegradable and non-toxic. Key issues to be considered in biodiesel production include source of oil (animal or plant), type of oil (edible or inedible oil), cost of production, feasible pretreatment and production method (Abdulrahman, *et al.*, 2016).

Recent trends have placed emphasis on the use of non-edible feedstocks as the demand for these feedstocks is not affected by dietary needs. The use of Animal fats as an example of source of biodiesel feedstock has been considered. This animal fat could include tallows, lard,

pork and chicken fat which are all readily available (Abdulrahman, *et al.*, 2016).

However, their suitability as biodiesel feedstocks is hampered by their high Free Fatty Acid (FFA) values as reported by Días, (2012). This hurdle is overcome by introducing a pretreatment process for the animal fat known as esterification. This esterification step is aimed at reducing the excess free fatty acid.

According to Leung, *et al.*, (2010), Transesterification reaction is one of the most successful processes of converting lipid feedstocks into biodiesel.

A typical transesterification process involves a reaction with an alcohol in the presence of a catalyst which may be homogeneous or heterogeneous. Musa, (2016) reported that in terms of choice of alcohol used, primary alcohols such as methanol were the most widely used for biodiesel production in that when they were used the reaction proceeded rapidly and completely.

A good catalyst for biodiesel production must have a high surface area, be thermally stable, have low deactivation rate, activated at low temperature and have high selectivity (Rafaat, *et al.*, 2010). Based on this premise the three main classification of catalyst employed in transesterification are acid catalysts, base catalysts and biocatalysts (Tshizanga, 2015; Pathak, 2015).

These catalysts can also be classified as either homogeneous or heterogeneous depending on which phase the catalysts exists. The use of heterogeneous catalysis has become more prominent in biodiesel production because it is insensitive to high FFA, easily removed from reaction mixture, reusable, and readily available (Shu, *et al.*, 2010).

On the other hand, heterogeneous catalysts could be acidic or basic with Tshizanga, (2015) reporting that heterogeneous basic catalysts have faster reaction rate and higher product yield than heterogeneous acid catalyst.

2 METHODOLOGY

The major feedstock used in this research work was beef tallow, a hard fat rendered from the fatty tissues of cattle that is removed during processing of beef. Tallow was purchased from Kure Market in Minna, Niger State. Limestone used as source of calcium oxide catalyst was obtained from Obajana in Kogi State.

2.1 CATALYST PREPARATION

The calcium oxide catalyst was prepared from raw limestone which was sourced from Obajana in Kogi State. The limestone was crushed and the Thermo-gravimetric Analysis (TGA) of the limestone sample was carried out. The calcium oxide catalyst was prepared at different temperature of 600 °C, 700 °C, 800 °C, and 900 °C while Brunnauer, Emmitt and Teller (BET) analysis was done to determine the surface area, pore size and pore volume of the sample.

2.1.1 Catalyst characterization

The chemical, physical and morphological properties of calcium oxide catalyst was evaluated using Scanning Electronic Microscopy (SEM) and X-ray diffraction (XRD).

2.1.1.1 Scanning Electron Microscope (SEM) Analysis

The physical surface morphology of catalyst sample obtained was examined using LEO S-440 Scanning Electron Microscope. A thin layer of calcium oxide catalyst sample was mounted on an aluminum holder by a double-sided tape. To avoid poor image resolution and discharge of electrostatics, the catalyst sample was coated with gold (Au) to thickness of 1.5 to 3 nm. The test was conducted at different magnifications and data generated was recorded.

2.1.1.2 X-ray Diffraction (XRD) Spectrometry

First, 2 g sample of size 100 µm was pressed in stainless steel holder and then identification of the crystalline phase was conducted by X-ray diffractor (X'Pert MPD – PAN analytical X-ray B.V.) using Cu-Kα radiation operated at 45 kV, 35 mA in which the incidence angle spanned from 5° to 85°2θ at 0.02°2θ step size with a scan speed of 0.5 s/step. This method was used to obtain a high-quality diffraction data of the sample.

2.2 FEEDSTOCK PREPARATION

The feedstock (Beef Tallow) was washed and air dried. The beef tallow was rendered into smaller pieces and placed in a pan which was heated to a temperature of

400 °C for 10 minutes. This led to the melting of rendered beef tallow, suspension of solid particles and evaporation of residual water contained in the tallow (Hinnach, 2016). The hot mixture was then filtrated using a cotton sieve to the liquid substrate (oil) which was then extracted. The oil was used as the feedstock for biodiesel production.

2.2.1 Feedstock characterization

The beef tallow was characterized for color, odor, fatty acid content, moisture, specific gravity and viscosity to ascertain its physical and chemical properties.

2.2.1.1 Determination of Moisture Content

The moisture content was measured using the procedure described in ASTM D445 test method for opaque and viscous liquids. BT was kept in the oven at 105 °C for a time period of 1 hour and after then, it was kept in the desiccators for 15 minutes and then the weight was taken. The percentage (%) moisture content was determined using the equation:

$$\% \text{ Moisture content} = \frac{W_2 - W_3}{W_1} \times 100 \quad (1)$$

Where W_0 = weight of empty petri dish, W_1 = wet sample, W_2 = weight of wet sample + empty petri dish. W_3 = weight of petri dish + dry sample.

2.2.1.2 Determination of Specific gravity (S.G.) / Density

Specific gravity and density of the fat sample was measured in accordance to the procedure described by standard ASTM D5355-95 (2012) using 25 ml Pycnometer. Dry empty bottle of 25 ml capacity was weighed to give W_0 and then filled with the oil and reweighed to give W_1 . The oil was then substituted with water and reweighed after the bottle had been washed and dried which then gave a weight W_2 . Specific gravity was then calculated using the expression:

$$\text{Specific gravity} = \frac{W_1 - W_0}{W_2 - W_0} \quad (2)$$

$$\text{Density } (\rho) \text{ of the oil} = \frac{\text{weight of oil}}{\text{volume of oil}} \quad (3)$$

2.2.1.3 Determination of Kinematic Viscosity

Kinematic viscosity was measured using the procedure described in ASTM D445 test method for opaque and viscous liquids.

2.2.1.4 Determination of Acid Value/Free Fatty Acid

Both values were determined using the procedure reported in ASTM D5555 – 95 (2011) standards. 10 g of the oil sample was poured into a 250 ml conical flask and a few drops of phenolphthalein was also added. 25 ml of ethanol and 25 ml of diethyl ether were mixed in a separate beaker to which 0.2 ml of phenolphthalein

solution was also added and then poured into the conical flask. The mixture was agitated continuously and titrated with the solution of potassium hydroxide until a pink color was noticed which lasts for at least 10 seconds, the titration was stopped.

$$\text{Acid Value} = \frac{V_{\text{KOH}} \times N \text{ of KOH} \times W_{\text{KOH}}}{W} \quad (4)$$

Where N = normality (concentration) of KOH, W = weight of sample; V = volume of KOH used in titration; W_{KOH} = molecular weight of KOH

$$\% \text{ Free Fatty Acid (FFA)} = AV \times 0.503 \quad (5)$$

2.3 TWO-STEP TRANSESTERIFICATION OF BEEF TALLOW

Two-step transesterification experiment was conducted for synthesis of biodiesel. Acid catalyzed esterification was carried out on the extracted oil from beef tallow in order to reduce the free fatty acid (FFA) and moisture which leads to saponification and poor-quality biodiesel yield (Abdulrahman, *et al.*, 2016). Then, transesterification was conducted with methanol using the refined oil obtained.

2.3.1 Design of experiment

Response surface methodology (RSM) with five-level-four-factor central composite design (CCD) was applied to optimize free fatty acid (FFA) reduction during esterification reaction and also to optimize the transesterification of the refined oil into biodiesel. DESIGN EXPERT (Version 7.0.0, Stat Ease, Inc., USA) software was used.

The process parameters considered in the esterification phase are methanol to oil ratio, catalyst amount (H_2SO_4), reaction time and reaction temperature while for the transesterification phase the methanol to oil ratio, catalyst loading, reaction time and reaction temperature were considered. Table 1 and Table 2 show the range of independent factors considered in this study for both the esterification and transesterification stage respectively.

TABLE 1: INDEPENDENT FACTORS USED FOR CCD IN ESTERIFICATION OF BEEF TALLOW

Variables	Low	High
Catalyst (H_2SO_4) Amount (%)	4	10
Sample to Methanol ratio (w/v)	1:9	1:12
Reaction Temperature ($^{\circ}\text{C}$)	45	60
Reaction Time (minutes)	50	120

TABLE 2: INDEPENDENT FACTORS USED FOR CCD IN TRANSESTERIFICATION OF BEEF TALLOW

Variables	Low	High
Sample to Methanol ratio (w/v)	6:1	10:1
Catalyst Loading (% vol)	4	10
Reaction Temperature ($^{\circ}\text{C}$)	42	60

Reaction Time (minutes)	60	120
-------------------------	----	-----

2.3.2 Characterization of produced biodiesel

The synthesized biodiesel was characterized and its properties were compared against the ASTM D6751.

2.3.2.1 Determination of flash point

The flash point of biodiesel was tested in accordance to ASTM D93. Sample of biodiesel was heated in a close vessel and ignited. When the sample burns, the temperature was recorded; the pensky-martens cup tester measures the lowest temperature at which application of the test flame causes the vapor above the sample to ignite. The biodiesel was placed in a cup in such quantity as to just touch the prescribed mark on the interior of the cup. The cover was then fitted onto the position on the cup and Bunsen burner was used to supply heat to the apparatus at a rate of about 5°C per minute. During heating, the oil was constantly stirred. As the oil approaches its flashing, the injector burner is lighted and injected into the oil container after every 12 second intervals until a distinct flash was observed within the container. The temperature at which the flash occurred was recorded. The above step was repeated three times and the average taken.

2.3.2.2 Determination of Cetane number

Cetane Number is a measure of the fuel's ignition delay. Higher Cetane numbers indicate shorter times between the injection of the fuel and its ignition. Higher numbers have been associated with reduced engine roughness and with lower starting temperatures for engines. This was obtained from the empirical formula.

$$CN = 46.3 + \left(\frac{5458}{S}\right) - (0.225 \times I) \quad (6)$$

2.4 KINETICS DATA

The kinetics of the reaction was determined by measuring the effect of the reaction time and temperature. Several assumptions were made, one of which was that the catalyst used is of sufficient amount with respect to the oil in order to cause a change in the reaction equilibrium bringing about the formation of FAME (Krishnakumar & Sivasubramanian 2017). Similarly, the reverse reaction can be ignored and the catalyst concentration during the course of the reaction is assumed to be negligible.

3 RESULTS AND DISCUSSION

This section presents a comprehensive view of the results obtained from the experimental study. It also contains statistical analysis of the results as well as evaluation of the effect of selected process parameter on the Acid catalyzed esterification and heterogeneous catalyzed transesterification of the beef tallow leading to the formation of biodiesel.

3.1 CATALYST CHARACTERIZATION

3.1.1 Thermo-gravimetric analysis (TGA)

The TGA analysis of the raw limestone sample was carried out and presented in Figure 1

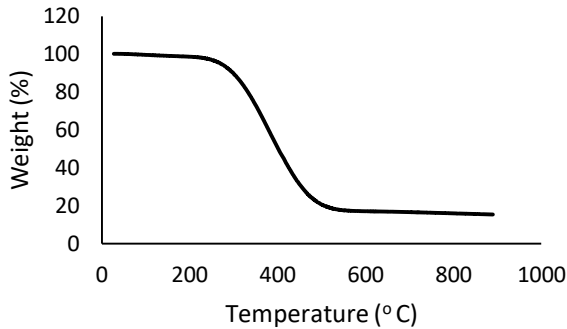


Figure 1: TGA curve for Limestone sample

From the TGA plot in Figure 1 it was observed that calcium oxide catalyst would be obtained at temperatures exceeding 600 °C at which temperature all the moisture and volatile components in the limestone would have evolved leaving behind the calcium oxide catalyst (CaO). The limestone sample was thermally treated (calcined) at different temperatures of 600 °C, 700 °C, 800 °C, and 900 °C to obtain the calcium oxide catalyst.

3.1.2 Brunauer Emmet Teller (BET) analysis

Brunauer, Emmitt and Teller (BET) analysis was carried out at the various temperature ranges in other to determine the surface area, pore size and pore volume of the sample.

TABLE 3: BET ANALYSIS RESULT FOR THE LIMESTONE SAMPLES CALCINED AT DIFFERENT TEMPERATURES

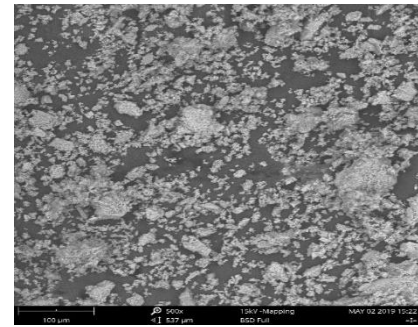
Samples	Surface area (m ² /g)	Pore volume (cc/g)	Pore size (nm)
Raw Limestone	418.33	0.2201	2.128
C-600	479.558	0.2878	2.115
C-700	507.004	0.1919	1.777
C-800	545.472	0.3066	2.124
C-900	586.272	0.2936	2.125

From Table 3, the BET analysis revealed that the calcium oxide catalyst produced at 900 °C has the largest

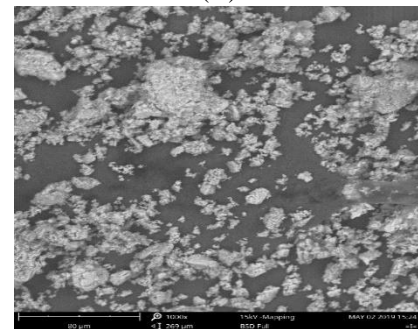
surface area as such show's suitability for use as the catalyst for biodiesel production.

3.1.3 Scanning electron microscopy (SEM) analysis

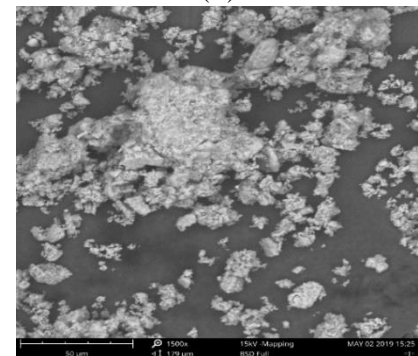
The SEM micrograph shows the honey comb surface morphology of the synthesized calcium oxide catalyst (CaO).



(A)



(B)



(C)

Figure 2: SEM micrograph of CaO catalyst at different magnifications of A (500X) B (1000X) and C (1500X)

3.1.4 X-ray diffraction (XRD) spectrometry

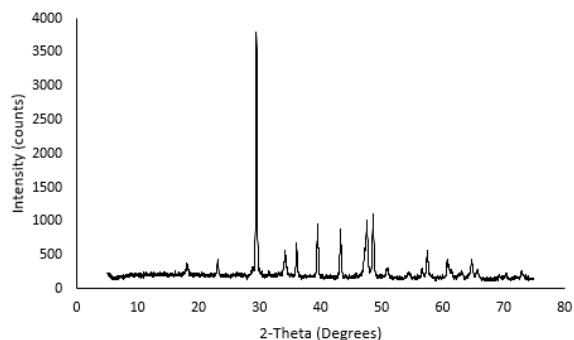


Figure 3: X-ray Diffraction (XRD) pattern of CaO calcined at 900 °C

According to Minaria and Risfidian (2016) standard peaks for CaO occur at 2θ : 32.3°, 37.5°, 47.1°, 64.3°, 67.5°. The XRD patterns observed in the X-ray Diffraction Spectrometry of the synthesized CaO catalyst bear a close resemblance to already established standard CaO peaks. The synthesized CaO catalyst 2θ peaks occurred at 30.3°, 37.5°, 47.5°, 64.3° and 66.7°.

3.2 FEEDSTOCK QUALITY CHARACTERIZATION

The suitability of a feed stock for biodiesel production relies heavily on its properties like free fatty acid value (FFA), viscosity, specific gravity and moisture content. The results obtained in the characterization of the feed stock (Beef Tallow) are presented in Table 4.

TABLE 4: CHARACTERIZATION OF BEEF TALLOW

S/N	PROPERTY	UNIT	PRESENT STUDY
1.	% Moisture Content	wt. %	14.6
2.	Density	g/cm ³	0.943
3.	Specific Gravity at 40 ° C	-	0.93
4.	Kinematic Viscosity at 40 ° C	mm ² /s	24.6
5.	Free Fatty Acid (FFA)	wt. %	2.41

3.3 OPTIMIZATION OF ACID CATALYZED ESTERIFICATION

The optimization of the acid catalyzed esterification process of beef tallow was conducted using the DESIGN EXPERT (Version 7.0.0, Stat Ease, Inc., USA) software. The parameters evaluated are Methanol to oil ratio, Catalyst Amount, Reaction time and Reaction temperature. Table 5, shows the ANOVA of the acid catalyzed esterification of BT.

TABLE 5: ANALYSIS OF VARIANCE OF THE ACID CATALYZED ESTERIFICATION OF BEEF TALLOW

Source	Sum of Square	Degree of Freedom	Mean Square	F Value	p-value
					Prob > F
Model	8.56	14	0.61	25.21	0.0001
A- Acid Catalyst amount	2.84	1	2.84	117.20	0.0001
B- Methanol to Oil ratio	1.5E-4	1	1.5E-4	6.184E-3	0.9384
C- Reaction Temperature	2.36	1	2.36	97.14	0.0001
D- Reaction Time	1.51	1	1.51	62.25	0.0001
AB	0.011	1	0.011	0.45	0.5105
AC	0.19	1	0.19	7.98	0.0128
AD	0.32	1	0.32	13.39	0.0023
BC	3.6E-3	1	3.6E-3	0.15	0.7055
BD	6.4E-3	1	6.4E-3	0.26	0.6150
CD	0.11	1	0.11	4.35	0.0544
A ²	0.59	1	0.59	24.19	0.0002
B ²	4.286E-5	1	4.286E-5	1.767E-3	0.9670
C ²	0.40	1	0.40	16.62	0.0010
D ²	0.48	1	0.48	19.85	0.0005
Residual	0.36	15	0.024		
Lack of Fit	0.31	10	0.031	3.01	0.1180
Pure Error	0.052	5	0.010		
Cor Total	8.93	29			

The significant factors from ANOVA analysis are the Acid catalyst amount with a p-value of 0.0001 which is less than 0.05. Other significant factors are the Temperature and Time factors with p values of 0.0001 respectively. Also significant are the interaction effect

factors of the Acid catalyst amount and Reaction temperature and Reaction time with p-values of 0.0128 and 0.0023. The quadratic effects of the Acid catalyst amount, the Reaction temperature and also the Reaction time are also significant factors with p-values of 0.0002, 0.0010 and 0.0005. The other factors of the model have no statistically significant effect.

In this study, the value of the determination coefficient ($R^2 = 0.9592$) indicates that the sample variation of 95.92% is attributed to independent variables and 4.08% of the total variations is not explained by the model.

3.3.1 The effect of interaction between process parameters

The Three-dimensional response surfaces are plotted on the basis of the generated model equation to investigate the interaction among the variables and to determine the optimum condition of each factor for minimum FFA.

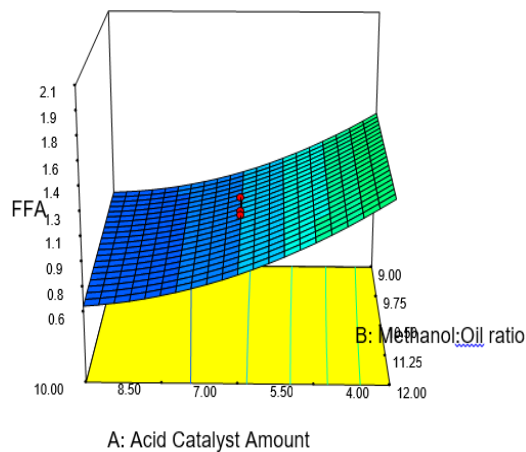


Figure 4a: Response Surface Plot of the Interaction Effect of Methanol: Oil ratio and Acid Catalyst amount on FFA at a Reaction Time of 85 minutes and a Reaction Temperature of 52.5 °C.

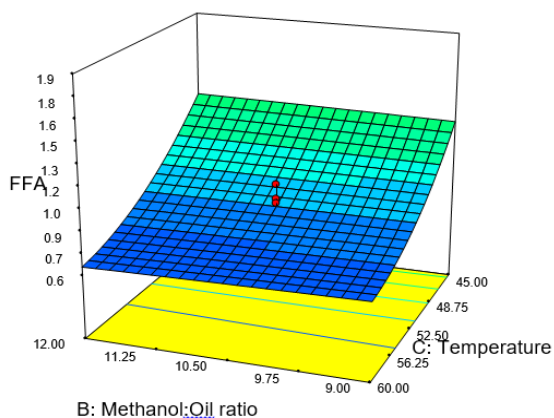


Figure 4b: Response Surface Plot of the Interaction Effect of Methanol: Oil ratio and Reaction Temperature on FFA at a Reaction Time of 85 minutes and Acid Catalyst amount of 7%.

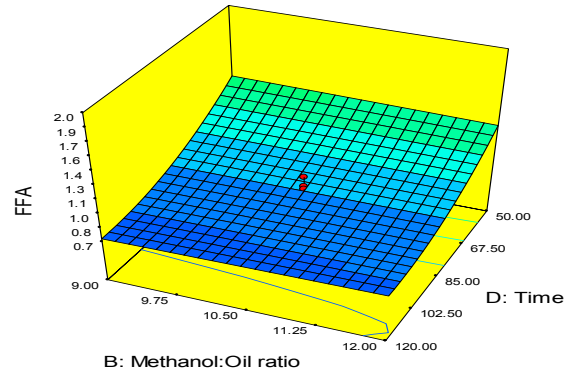


Figure 4c: Response Surface Plot of the Interaction Effect of Methanol: Oil ratio and Reaction Time on FFA at a Reaction Temperature of 52.5 °C and Acid Catalyst amount of 7%.

From Figure 4a the interaction effect of the methanol to oil ratio and the acid catalyst amount on the FFA resulted in an optimum FFA yield of 0.64 which was obtained at a methanol to oil ratio of 12:1 and acid catalyst amount of 10% at a constant reaction temperature and time of 52.5 °C and 85 minutes respectively.

Similarly, the RSM plots of the interaction effect of other reaction parameters against the FFA yield as represented by Figure 4a-c resulted in different FFA results at various operating conditions. However, the optimization solution obtained shows that an FFA of 0.60 at operating conditions of Acid catalyst amount of 7.1%, Methanol to Oil ratio of 9:1, Reaction temperature of 60 °C and a reaction time of 96 minutes respectively.

3.4 OPTIMIZATION OF BIODIESEL PRODUCTION FROM BEEF TALLOW

Optimization of the transesterification process from Beef Tallow was conducted using the DESIGN EXPERT (Version 7.0.0, Stat Ease, Inc., USA) software. The parameters considered are Methanol to oil ratio, catalyst loading, Reaction time and Reaction temperature as shown in Table 6. Table 7 however, shows the ANOVA of the transesterification of BT.

TABLE 6: DESIGN MATRIX FOR THE OPTIMIZATION OF BIODIESEL PRODUCTION FROM BEEF TALLOW

Run No.	A: Methanol to Oil ratio (v/v)	B: Catalyst Loading (%wt)	C: Reaction Temperature (°C)	D: Reaction Time (mins)	Actual FFA (%)	Predicted FFA (%)

1	8.00	7.00	51.00	90.00	56.00	61.17						
2	12.00	7.00	51.00	90.00	68.00	67.75						
3	8.00	7.00	33.00	90.00	34.00	33.75						
4	10.00	10.00	42.00	60.00	55.00	56.88						
5	6.00	4.00	42.00	60.00	38.00	36.38						
6	8.00	13.00	51.00	90.00	62.00	59.58						
7	6.00	10.00	60.00	120.00	56.00	60.88						
8	10.00	4.00	60.00	60.00	64.00	64.38						
9	8.00	7.00	51.00	90.00	61.00	61.17						
10	10.00	4.00	60.00	120.00	67.00	69.04						
11	10.00	4.00	42.00	120.00	61.00	59.87						
12	10.00	10.00	60.00	60.00	71.00	68.54						
13	6.00	4.00	60.00	60.00	71.00	69.54						
14	6.00	4.00	60.00	120.00	74.00	70.71						
15	10.00	10.00	60.00	120.00	69.00	69.21						
16	4.00	7.00	51.00	90.00	44.00	44.08						
17	8.00	7.00	51.00	90.00	60.00	61.17						
18	6.00	10.00	42.00	60.00	32.00	31.54						
19	10.00	10.00	42.00	120.00	58.00	61.04						
20	8.00	7.00	51.00	90.00	63.00	61.17						
21	8.00	1.00	51.00	90.00	62.00	64.25						
22	6.00	10.00	42.00	120.00	34.00	32.21						
23	8.00	7.00	51.00	30.00	48.00	51.75						
24	8.00	7.00	51.00	90.00	64.00	61.17						
25	8.00	7.00	51.00	90.00	63.00	61.17						
26	8.00	7.00	51.00	150.00	61.00	57.08						
27	6.00	4.00	42.00	120.00	37.00	41.04						
28	6.00	10.00	60.00	60.00	64.00	63.71						
29	8.00	7.00	69.00	90.00	75.00	75.08						
30	10.00	4.00	42.00	60.00	55.00	51.71						
							Model	4213.62	14	300.97	25.40	0.0001
							A- Methano l to Oil ratio	840.17	1	840.17	70.90	0.0001
							B- Catalyst Loading	32.67	1	32.67	2.76	0.1176
							C- Reaction Tempera ture	2562.67	1	2562.67	216.26	0.0001
							D- Reaction Time	42.67	1	42.67	3.60	0.0772
							AB	100.00	1	100.00	8.44	0.0109
							AC	420.15	1	420.15	35.46	0.0001
							AD	12.25	1	12.25	1.03	0.3254
							BC	1.00	1	1.00	0.084	0.7754
							BD	16.00	1	16.00	1.35	0.2634
							CD	12.25	1	12.25	1.03	0.3254
							A ²	47.25	1	47.25	3.99	0.0643
							B ²	0.96	1	0.96	0.081	0.7793
							C ²	78.11	1	78.11	6.59	0.0214
							D ²	78.11	1	78.11	6.59	0.0214
							Residual	117.75	15	11.85		
							Lack of Fit	134.92	10	13.49	1.57	0.3216
							Pure Error	42.83	5	8.57		
							Cor Total	4391.37	29			

TABLE 7: ANALYSIS OF VARIANCE OF THE TRANSESTERIFICATION OF BEEF TALLOW

Source	Sum of	Degree	Mean	F Value	p-value
--------	--------	--------	------	---------	---------

The significant factors from ANOVA analysis are the Methanol to Oil ratio and the Reaction Temperature with p-values of 0.0001 respectively which is less than 0.05.

The other significant factors are the interaction effect of the Methanol to Oil ratio and catalyst loading and the interaction effect of Methanol to Oil ratio and Reaction temperature with p-values of 0.0109 and 0.0001. Similarly, the quadratic effects of the Reaction

temperature and the quadratic effect of Reaction time are also significant factors with p-values of 0.0214 respectively. The other factors of the model have no statistically significant effect.

In this study, the value of the determination coefficient ($R^2 = 0.9595$) indicates that the sample variation of 95.95% is attributed to independent variables and 4.05% of the total variations is not explained by the model.

The Biodiesel yield is governed by the equation
Biodiesel Yield = $61.17 + 5.92A - 1.17B + 10.33C + 1.33D + 2.50AB - 5.12AC + 0.88AD - 0.25BC - 1.00BD - 0.87CD - 1.31A^2 + 0.19B^2 - 1.69C^2 - 1.69D^2$ (7)

The linear effect of A and C, the interaction effect of AB and AC and the quadratic effect of C² and D² are the general determining factors of transesterification of Beef Tallow as they have the larger coefficients.

3.4.1 The effect of interaction between process parameters

The Three-dimensional response surfaces are plotted on the basis of the generated model equation to investigate the interaction among the variables and to determine the optimum condition of each factor for maximum Biodiesel yield.

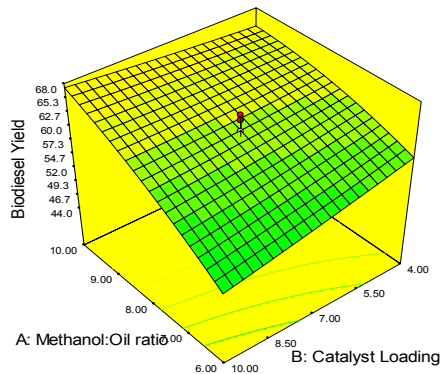


Figure 5a: Response Surface Plot of the Interaction Effect of Methanol: Oil ratio and Catalyst loading on the Biodiesel yield at a Reaction Time of 90 minutes and a Reaction Temperature of 51 °C.

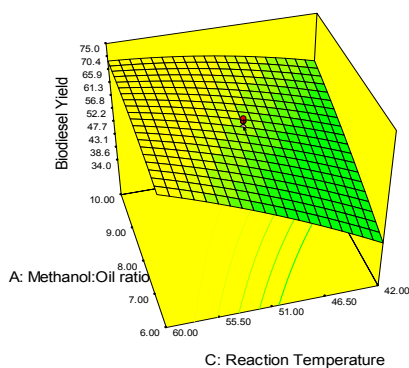


Figure 5b: Response Surface Plot of the Interaction Effect of Methanol: Oil ratio and Reaction Temperature on the Biodiesel yield at a Reaction Time of 90 minutes and a Catalyst loading 7%.

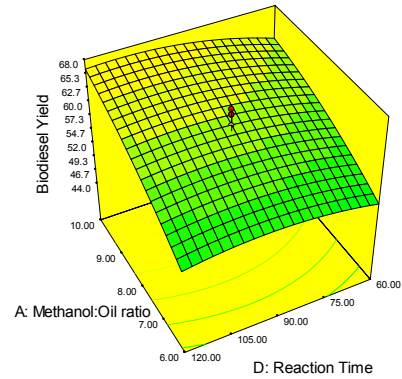


Figure 5c: Response Surface Plot of the Interaction Effect of Methanol: Oil ratio and Reaction Time on the Biodiesel yield at a Reaction Temperature of 51 °C and a Catalyst loading 7%.

From Figure 5a, an optimum Biodiesel yield of 67.19% was obtained at a methanol to oil ratio of 10:1 and catalyst loading of 10% at a constant reaction temperature and time of 51 °C and 90 minutes respectively.

Similarly, the RSM plots of the interaction effect of other reaction parameters against Biodiesel yield as represented by Figure 5a-c resulted in different Biodiesel yield results at various operating conditions. However, the optimization solution obtained shows that a biodiesel yield of 72.0% was obtained at a methanol to oil ratio of 7:1, a catalyst loading of 4%, a reaction temperature and time of 60 °C and 106 minutes respectively.

3.4.2 Kinetics of biodiesel production

According to Permsuwan et al., (2011) and Alam et al., (2014) the overall reaction rate is given as

$$-r_A = -\frac{d[TG]}{dt} = k_1[TG][MeOH]^3 \quad (8)$$

Which the reduces to

$$-r_A = -\frac{d[TG]}{dt} = k[TG] \quad (9)$$

And then

$$-\ln(1 - X_{fame}) = kt \quad (10)$$

The Arrhenius equation which is used to determine the activation energy is given by

$$k_A(T) = Ae^{-E/RT} \quad (11)$$

Which reduces to

$$\ln k_A = \ln A - \frac{E}{R} \left(\frac{1}{T} \right) \quad (12)$$

Where k_A = Temperature dependent specific rate constant. A = preexponential factor or frequency factor. E = Activation energy. R = gas constant and T = absolute temperature.

The linear relationship obtained from the plot of $-\ln(1 - X_{fame})$ against t gives the rate constant k which is inputted into the Arrhenius equation to determine the activation energy. The value of the reaction rate constant k was determined at various temperatures.

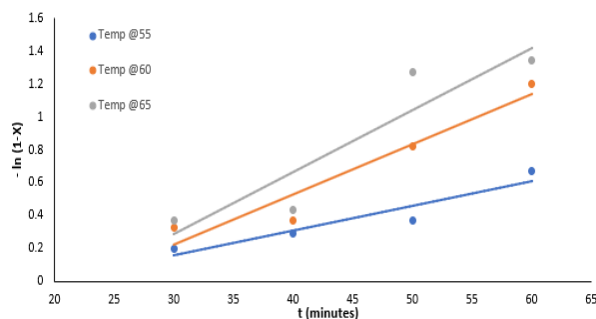


Figure 6: $-\ln(1-X)$ plot versus reaction time plot at different temperatures (methanol:Oil ratio of 8:1 and catalyst loading of 7 wt%).

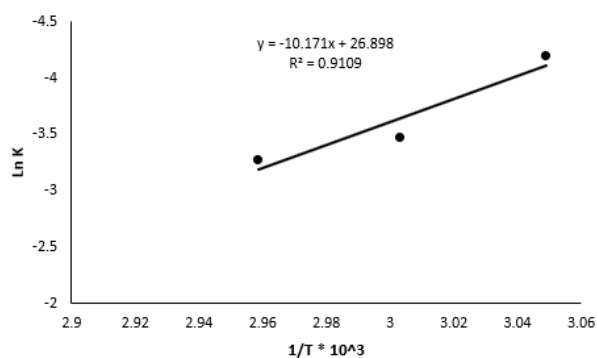


Figure 7: Arrhenius plot of $\ln k$ versus $1/T \cdot 10^3$ for the transesterification of Beef Tallow by CaO derived from limestone

From the plot, the activation energy and the preexponential factor are calculated as 82.845 KJ/mol. K and $4.805 \cdot 10^{11} \text{ min}^{-1}$. The Arrhenius plot gives an R^2 value of 0.9109 which shows a close correlation with the experimental data.

3.4.3 Biodiesel quality determination

The produced biodiesel was characterized and compared against established biodiesel standards like the American Standards and Testing Materials. The ASTM D6751 serves as a guideline which provides information on the properties and quality of good Biodiesel. Table 8 reveals the property of BT diesel.

TABLE 8: CHARACTERIZATION OF PRODUCED BIODIESEL FROM BEEF TALLOW

S/N	Property	Unit	Result Obtained	ASTM D6751
1.	Flash Point	$^{\circ}\text{C}$	154	130 min
2.	Kinematic Viscosity at 40°C	mm^2/s	5.4	1.9 – 6.0
3.	Cetane Index		56	47 min
4.	FFA	wt %	0.418	-
5.	Pour Point	$^{\circ}\text{C}$	5	18°C max

4 CONCLUSION

The four parameters studied in the acid catalyzed esterification of (BT) resulted in an optimum FFA of 0.60 at operating conditions of Acid catalyst amount of 7.1%, Methanol to Oil ratio of 9:1, Reaction temperature of 60°C and a reaction time of 96 minutes. The obtained FFA from the actual experimental data showed a close correlation with the predicted FFA result where a predicted FFA of 0.61 was obtained.

The statistical analysis of the Acid catalyzed esterification reaction, the quadratic model was selected as the most suitable with a correlation coefficient (R^2) of 0.9592 and a p value less than 0.05. The significant factors from the ANOVA analysis are the Acid catalyst amount, the reaction temperature and the reaction time with p -values of 0.0001 respectively.

Similarly, the four parameters studied in the transesterification of Beef Tallow resulted in an optimum Biodiesel yield of 72.0 % at a methanol to oil ratio of 7:1, a catalyst loading of 4%, reaction temperature and time of 60°C and 106 minutes respectively. The obtained Biodiesel yield from the actual experimental data showed a close correlation with the predicted Biodiesel result where a predicted Biodiesel yield of 72 % was obtained.

From the statistical analysis of the CaO catalyzed transesterification reaction of Biodiesel from BT, the

quadratic model was selected as the most suitable with R^2 value of 0.9595 and p value less than 0.05.

The significant factors from the ANOVA analysis are the Methanol to Oil ratio and the Reaction Temperature with a p -values of 0.0001 respectively which is less than 0.05.

The Kinetics data for the CaO catalyzed transesterification reaction of Biodiesel from BT resulted in activation energy and the preexponential factor of 82.845 KJ/mol.K and $4.805 \times 10^{11} \text{ min}^{-1}$ with the Arrhenius plot giving an R^2 value of 0.9109 which shows a correlation with the experimental data.

REFERENCE

- Abdulrahman, R.K., Zangana, M.H., Ali, J.A., Aziz, R.I., Kareem, R.M., & Hussain, B.M. (2016). Biofuel from cow tallow: A case study. *European Scientific Journal*, 12(6), 299-306. doi: 10.19044/esj.2016.v12n6p299.
- Alam, J., Shawon, A.Z., Sultana, M., Rahman, W., & Khan, M.R. (2014). Kinetic study of biodiesel production from soybean oil. *Proceedings of Power & Energy Systems: Towards Sustainable Energy (PESTSE2014)*, 15 - 21.
- Berenguer, M.B., & Sierra, M. P. (2012). Animal fats for biodiesel. *Bio-resource Technology*, 98(1), 1–14.
- Dias, J., Alvim-Ferraz, C., Almeida, F., Méndez, D., Sánchez, P., & Rivera, U. (2012). Selection of heterogeneous catalysts for biodiesel production from animal fat. *Fuel. International Journal of Renewable Energy Research*, 94, 418-425. Retrieved from <https://www.ijrer.com>
- Feddern, V., Anildo, C.J., Celant De Prá, M., Giovanni de Abreu, P., Jonas, I.F., Higarashi, M.M., Sulenta, M., & Arlei, C. (2011). Animal fat wastes for biodiesel production: Biodiesel - feedstocks and processing technologies, Dr. Margarita Stoytcheva, Ed., ISBN: 978-953-307-713-0, ch.3, 45 – 63.
- Hinnach, S. (2016). Valorization of waste animal fats into Biodiesel. *Int. J. Environ. Sci. Tech.*, 7 (1), 1-33.
- Krishnakumar, U. & Sivasubramanian, V. (2017). Kinetics study of preparation of Biodiesel from crude rubber oil over a modified heterogeneous catalyst. *Indian Journal of Chemical Technology*, 24(1), 430 – 434.
- Leung, D.Y.C., & Guo, Y. (2010). Transesterification of neat and used frying oil: Optimization for biodiesel production. *Fuel Process Technol*, 87, 883–900.
- Minaria & Risfidian, M. (2016). Preparation and characterization of calcium oxide from crab shells (*portunus pelagicus*) and its application in biodiesel synthesis of waste cooking oil, palm and coconut oil. *Science & Technology Indonesia*. 1(2016), 1 – 7.
- Musa, I.A., (2016). The effects of alcohol to oil molar ratios and the type of alcohol on biodiesel production using transesterification process. *Egyptian Journal of Petroleum*, 25, 21-31. doi:10.1016/j.ejpe.2015.06.007
- Niju, S., Begum, K.S., & Anantharaman, N. (2014). Enhancement of biodiesel synthesis over highly active calcium oxide derived from natural white bivalve clam shell. *Arabian Journal of Chemistry*, 9, 633-639. doi:10.1016/j.arabjc.2014.06.006.
- Omotoso, M. A., & Akinsanoye, O. A. (2015). A review of biodiesel general from nonedible seed oil crops using nonconventional heterogeneous catalysts. *Journal of Petroleum Technology and Alternative Fuels*, 6, 1- 12. doi:10.5897/JPTAF2014.0108.
- Pathak, S. (2015). Acid catalysed transesterification. *Journal of Chemical and Pharmaceutical Research*, 7(3), 1780-1786.
- Permsuwan A., & Tippayawong, N., Kiatsiriroat, T., Thararux, C., & Wangkarn, S. (2011). Reaction kinetics of transesterification between palm oil and methanol under subcritical conditions. *Energy Science and Technology*, 2(1), 35–4, doi.10.3968/j.est.1923847920110201.672.
- Refaat, A. A. (2010). Different techniques for the production of biodiesel from waste vegetable oil. *Int. J. Environ. Sci. Tech.*, 7 (1), 183-213.
- Shu, Q., Gao, J., Nawaz, Z., Liao, Y., Wang, D., & Wang, J. (2010). Synthesis of biodiesel from waste vegetable oil with large amount of free fatty acids using a carbon based solid acid catalyst. *Applied Energy*, 87, 2589-2596
- Tshizanga, N., Aransiola, E.F., & Oyekola, O. (2017). Optimization of biodiesel production from waste vegetable oil and egg shell ash. *South African Journal of Chemical Engineering*, 23, 145-156. Retrieved from <http://www.journals.elsevier.com/south-african-journal-of-chemical-engineering/>



Column Adsorption Studies of Textile Wastewater using Iron Oxide Nanoparticles doped Zeolite A

*Alaya-Ibrahim, S^{1,2}, Kovo, A.S.^{1,2}, Abdulkareem, A.S.^{1,2}, Adeniyi, O.D.² & Yahya, M.D.²

¹Nanotechnology Group, Centre for Biotechnology and Genetic Engineering, Federal University of Technology, PMB 65 Minna, Niger State, Nigeria;

²Chemical Engineering Department, Federal University of Technology, PMB 65, Minna, Niger State, Nigeria.

*Email of the Corresponding author: neekyai@yahoo.com, 08032877199

ABSTRACT

In this work, iron oxide nanoparticles were doped on zeolite A (MZA) for treatment of textile wastewater via column adsorption studies. The physicochemical parameters of the wastewater were conducted using standard methods. The effects of bed heights, flow rates and inlet concentrations on the breakthrough curves were studied to examine the performance of the adsorbent. The column studies revealed that the exhaustion and breakthrough time increased with increase in bed height while they decreased with increase in flow rates and inlet concentrations. The maximum adsorption of the chemical parameters was 45.83 %, 53.09 %, 45.50 %, 54.23 %, 49.48 %, 34.63 % for chloride, cyanide, chemical oxygen demand (COD), biological oxygen demand (BOD), nitrite and total organic carbon (TOC) respectively at 5 cm bed height, 4 ml/min flow rate and 10 % inlet concentrations. The Thomas model was found to predict the breakthrough of the pollutants better than Adams-Bohart with high R^2 values of 0.882-0.978, 0.899-0.984 and 0.876-0.981 for bed height, flow rate and inlet concentrations accordingly. The presented results show that FeONP-ZA developed is suitable for textile wastewater.

Keywords: *chemical parameters, column studies, MZA, textile wastewater.*

1 INTRODUCTION

Textile industry is an important manufacturing process which involves various stages of dry and wet processes for the production of fabrics. The wet processes such as desizing, scouring, bleaching, mercerizing, dyeing and finishing are of great concern as they pose potential risk to the ecosystem (Tafesse et al., 2015). As a result of these aforementioned processes, large amount of wastewater is generated from textile industries which are not treated prior to its discharge into the surface water (Elango et al., 2017) despite the strict legislations by the governments of most countries. Textile waste waters are highly coloured, salty and contain non-biodegradable compounds; they are also high in BOD and COD, which make their treatments difficult (Tafesse et al., 2015). However, the high cost of the conventional adsorbent has been identified as one of the factors responsible for non-compliance to this legislation, adversely resulting to degradation of water quality. Thus, developing a low cost adsorbent from local material will be economical and sustainable alternative for textile wastewater treatment. This will treat or at least reduce the pollutants to permissible limits to obtain cleaner water, thereby; protecting the environment as well as ensuring healthy lives of human beings and the aquatic lives.

Adsorption has been recognized as a technology in wastewater treatment and has been successfully employed by many researchers (Bankole et al., 2017; Yusuf-Alaya, 2014; Dada et al., 2012; Piccin et al., 2011) in that regards. Similarly, nanotechnology has recently revealed high

impacts on society and environment due to their various industrial applications, especially in water remediation and treatments (Balamurugan et al., 2014). Iron nanoparticles just like any other nanoparticles have much larger surface areas than bulk particles which make them applicable in water treatments. They can be synthesised and functionalized using various chemical functional group in order to increase their affinity towards target compound (Dhermendra et al., 2008). They have unique properties to develop high capacity and selective sorbents for metal ions and anions. Different nanomaterials can help to purify water through different mechanisms such as adsorption of pollutants, removal and inactivation of pathogens and transformation of toxic materials into less toxic materials (Gholamreza et al., 2014).

However, applying nanoparticles directly might result to aggregation in aqueous solution which consequently reduces their efficiencies (Girilal et al., 2015). Thus, loading nanoparticles within the pores of substrates such as mesoporous silica, zeolite, ceramics, activated carbon and chitosan have been reported to be efficient in wastewater/water treatments (Thamilselvi and Radha, 2017). Zeolites have been identified to be a potential support for nanoparticles due to their well-defined structures and microporous cavities (Kaya et al., 2013; Alfadul, 2007; Yamaura and Fungaro, 2013). Thus, doping iron oxide nanoparticles synthesised from biosynthesis route using mango leaf extract on the surface of synthesised zeolite A for treatment of textile waste water will eliminate the problem of nanoparticles agglomeration and

environmental problem posed by by-product of conventional treatment methods.

Even though several works have been conducted on wastewater treatments using batch adsorption mode (Bankole et al., 2017; Yusuf-Alaya, 2014; Dada et al., 2012; Piccin et al., 2011), however batch mode can only be used on laboratory scale. Thus, it is paramount to ascertain the applicability of the adsorbents using column/continuous adsorption mode (Tamilselvi and Asaithambi, 2015). More so, continuous studies can be used in treatment of large volume of wastewater, which has been useful and reliable in removal of pollutants from industrial wastewater (Biswas and Mishra, 2015).

This study therefore focuses on the green synthesis of iron oxide nanoparticles with mango leaves extract as the reducing agent. The synthesized nanoparticles was doped on the surface of zeolite A, developed from Ahoko kaolin for the treatment of textile wastewater using continuous process.

2 METHODOLOGY

The materials used, the synthesis of the iron oxide nanoparticles doped zeolite A (MZA) and the characterizations have been discussed in our conference paper (Alaya-Ibrahim *et al.*, 2018).

2.1 COLLECTION AND CHARACTERIZATION OF THE TEXTILE WASTEWATER (TWW)

The textile wastewater used in this study was collected from Unique Tie and Dye textile Industry in Ilorin, Kwara State, Nigeria. The wastewater was analysed based on recommendations of standard methods of water and wastewater analysis at Regional Water Quality Laboratory, Federal Ministry of Water Resources, Minna, Niger State, Nigeria. The chemical oxygen demand (COD), biochemical oxygen demand (BOD), total dissolved solid (TDS), alkalinity, the total amount of nitrate, nitrite, sulphate, phosphate, ammonium, chloride, cyanide and fluoride were determined by HACH instruments, USA using American Public Health Association (APHA, 2017) method. Other parameters investigated are Turbidity (Turbidity meter); pH (a multi-parameter analyser C3010); electrical conductivity (a multi-parameter analyser 2510B) and dissolved oxygen (dissolved oxygen meter).

2.2 COLUMN ADSORPTION STUDIES

The column adsorption studies were carried out based on the work of Patel and Vashi, 2015 with little modifications. The study was carried out with the aid of a glass column of 3 cm internal diameter and a height of about 30 cm. The iron oxide nanoparticles doped zeolite A (MZA) was packed on the glass wool in the column which serves as a support to prevent it from flowing through the outlet while an improvised device was used in controlling the flow rate

of the effluent from the tank into the glass column. Various parameters such as bed height, flow rate and inlet concentrations were studied at a predetermined interval. The effects of bed height were studied from 3 cm- 5 cm, the flow rate from 3 ml/min-5 ml/min while that of inlet concentration were in the range of 10 %-20 %. All the experiments were performed with 10 % inlet concentrations of the wastewater, 4 cm bed height of the MZA at a flow rate of 4 ml/min except those studies where bed heights, inlet concentrations and flow rates were studied accordingly. The initial and final concentrations of the parameters studied were obtained using HACH instruments in all cases. The schematic diagram of the experimental setup is given in the Figure 1

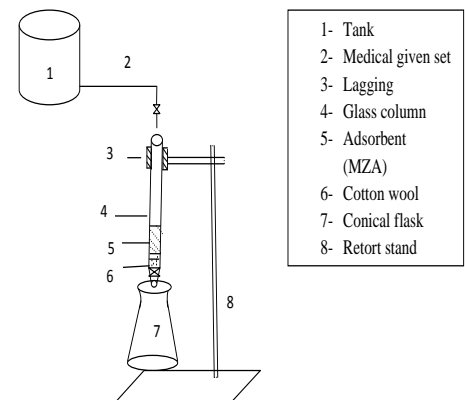


Figure 3.2 Schematic Diagram of the Column Experimental Setup
Figure 1: Schematic Diagram of the Column Experimental Setup

2.3 MATHEMATICAL MODELING OF COLUMN STUDIES

The various parameters associated with column adsorption studies were adopted from the work of Shadeera Rouf (2015) and were calculated as described thus;

$$\text{Effluent volume } V = Q t_T \quad (1)$$

Where the effluent volume in ml is V , Q is the flowrate in ml/min and t_T is the total flow time in min.

The maximum column bed capacity, q for the textile wastewater concentration and the influent flow rate was calculated using (2)

$$q_{max} = \frac{Q}{1000} \int_{t=0}^{t=t_T} C_{ad} dt \quad (2)$$

q_{max} is the maximum bed capacity in mg; C_{ad} , the adsorbed pollutants concentration in mg/L. The integral values were obtained from the area under the plot of C_{ad} versus time.

The maximum adsorption capacity at the exhaustion time was calculated using (3);

$$q_{exp} = q_{max}/m \quad (3)$$

The amount of the MZA in the column in (g) is m.

The total amount of pollutant concentration sent to the column M_T (mg) was obtained from (4);

$$M_T = \frac{C_o Q t r}{1000} \quad (4)$$

C_o = The initial concentration of pollutants in mg/L

The percentage removals of the pollutants were calculated via (5);

$$\% \text{ removal} = \frac{q_{max}}{M_T} \times 100 \quad (5)$$

2.4 BREAKTHROUGH CURVE MODELLING

The breakthrough curves and times are very important in column adsorption studies as they are used in defining the operation and dynamic response of the study (Biswas and Mishra, 2015). In order to predict the breakthrough data for the textile wastewater for a successful design of the adsorption process, the following breakthrough curve models were used;

Adams-Bohart Models

This model assumes that the rate of adsorption, residual adsorbent capacity and the adsorbate concentration are proportional; and are mainly determined by the surface site of the adsorbents. This model is used in describing the initial part of the breakthrough curve and can be linearly expressed (Tamilselvi and Asaithambi, 2015; Trgo *et al.*, 2011) as (6);

$$\ln \frac{C_t}{C_o} = K_{AB} (C_o t - N_o (Z/U_o)) \quad (6)$$

Where C_o and C_t are the initial concentration and concentration of the wastewater at time t in mg/L respectively, K_{AB} is the rate constant (L/mg.min), N_o is the saturation concentration (mg/L), t is flow time (min), Z is the bed height of the column (cm) and U_o is the superficial velocity.

Thomas Model

This is the most commonly used breakthrough model and it is used in calculating the maximum adsorption of the adsorbates by the adsorbents and the adsorption rate constant of the adsorption column. This is linearly expressed (Trgo *et al.*, 2011) as (7);

$$\ln \left[\frac{C_o}{C_t} - 1 \right] = K_{TH} \frac{q_o}{Q} (m - V_o) \quad (7)$$

K_{TH} is the rate constant (ml/min.mg), q_o is the amount of pollutants adsorbed per gram of adsorbent (mg/g) and m is the amount of adsorbent used for the column adsorption (g). K_{TH} and q_o are obtained from the plot of $\ln \left[\frac{C_o}{C_t} - 1 \right]$ versus V_o .

3 RESULTS AND DISCUSSION

3.1 PHYSICOCHEMICAL ANALYSIS OF TEXTILE WASTEWATER

The physicochemical parameters, heavy metals and methylene blue analyses (before and after treatment) were conducted on the local textile wastewater and the results with their various permissible limits based on WHO/EPA and NIS are presented in Table 1;

According to the presented results in Table 1, the colour, and turbidity concentration of the textile wastewater was 124620 TCU and 7638 NTU respectively. This is due to the different types of dyes used in imparting colour to the fabrics during production (Elango *et al.*, 2017). Colour is easily noticed to human eyes even in small amount, which is not desirable. Moreover, they alter the photosynthesis in plants and affect the growth of bacteria (Sanni *et al.*, 2016). However, after treatment with MZA, the colour reduced to 120 TCU while the turbidity reduced to 75 NTU respectively. The values of turbidity and colour obtained after treatment are higher than those sets by WHO/EPA/NIS (see Table 1) for drinking water. This might be due to the very high concentrated wastewater treated and as it is known that the rate of removal of pollutant also depends on its initial concentrations (Margata *et al.*, 2013). Nonetheless, the developed adsorbent removed 99.02 % and 99.9 % % for turbidity and colour accordingly.

The total dissolved solid of the raw water was 36723 mg/L which reduced to 500 mg/L; while the electrical conductivity was 54810 mg/L and reduced to 860 mg/L after treatment. These values conformed well to the standard set by WHO/EPA /NIS (see Table 1).

TABLE 1:PHYSICOCHEMICAL PARAMETERS OF WATER AT 5 CM BEDHEIGHTS, 10 % INLET CONCENTRATIONS AND 4 ML/MIN FLOWRATE

Physicochemical Parameters	Raw Value	Treatment with MZA	Standard limits (WHO/ EPA)	Standard limit (NIS)
Colour (TCU)	124620	120	20/100	15
pH	11.4	8.5	6.5-8.5/6.5-9.5	6.5-8.5
TDS (mg/L)	36723	500	1000/-	500
Conductivity ($\mu S/cm$)	54810	860	-/1000	1000
Dissolved oxygen (mg/L)	2.65	4.25	-	-
Turbidity (NTU)	7638	75	5.0	5.0
Total alkalinity (mg/L)	16443	380	-/400	-
Nitrate (mg/L)	1804	20.0	50/50	50
Ammonium (mg/L)	276	3.5	1.3-3.5/ 0.2-4.0	-
Chloride (mg/L)	9711	31.0	250/250	250
Phosphate (mg/L)	113	0.5	-/0.5-0.7	-
Cyanide (mg/L)	22.2	0.01	-/0.05	0.01
Fluoride (mg/L)	226	1.48	1.5/1.7	1.5
Sulphate (mg/L)	7111	25	500/250	100
COD (mg/L)	31044	36.7	-/40	-
BOD (mg/L)	6287	2.35	-/5.0-7.0	-
TOC (mg/L)	2990	20	-	5.0
Carbonate (mg/L)	780	20	-	-
Nitrite (mg/L)	21.9	0.04	3.0/5.0	0.2
Iron (mg/L)	3.6477	0.0549	-/0.3	0.2
Chromium (mg/L)	0.1240	0	0.05/0.05	0.05
Nickel (mg/L)	0.0045	0	0.07/0.02	0.02
Zinc (mg/L)	1.1476	0	-/3	-
Lead (mg/L)	0.0748	0	0.01/0.01	0.01
Cadmium (mg/L)	0.5431	0	0.003	0.005
Copper (mg/L)	2.1347	0.0057	2/1	2
Manganese (mg/L)	0.0128	0	-/0.2	0.05

Key: World Health Organization (WHO, 2011), Environmental Protection Agency (EPA, 2001) , Nigerian Industrial Standards (NIS, 2007)

The chemical inorganic parameters studied are nitrate, nitrite, ammonium, phosphate, cyanide, chloride, fluoride and sulphate. The values of nitrite, nitrate and ammonium were 21.9 mg/L, 1804 mg/L and 276 mg/L, which were reduced to 0.04 mg/L, 20 mg/L and 3.5 mg/L accordingly. Whilst that of sulphate, fluoride, chloride, cyanide, and phosphate were 7111 mg/L, 225 mg/L, 9711 mg/L, 22.2 mg/L, 113 mg/L, which were reduced to 25 mg/L, 1.48 mg/L, 31 mg/L, 0.01 mg/L, 0.5 mg/L and 25 mg/L accordingly, after having contact with the developed adsorbent in the column. This is evident that the pollutants were able to diffuse into the pores of the MZA and did not clog it (Zainal Abadin *et al.*, 2017). These values correlated well with all the standards, suggesting that the treated water can be used for drinking and other purposes (WHO, 2011; EPA, 2001; NIS, 2007).

The organic contents of the textile wastewater were also examined before and after passing through the columns and the results are presented in Table 1. As presented in the table, the dissolved oxygen, COD, BOD and TOC were 2.65 mg/L, 31044 mg/L, 6287 mg/L and 2990 mg/L which were brought to 4.25 mg/L, 36.7 mg/L, 2.35 mg/L and 20 mg/L accordingly. They all conformed to all the standards except for the TOC which is slightly above the standard set by NIS for drinking water as WHO/EPA did not see it as a factor of concern in drinking water. This might be due to the fact that TOC is the measure of total carbon in organic compounds in aqueous system and carbon has the ability to form complex molecules with the structural iron present in the MZA, thereby making its binding onto the surface of MZA not as fast as others (Pouran *et al.*, 2014).

The heavy metals investigated on the raw textile wastewater include; Fe, Cr, Ni, Zn, Pb, Cd, Cu and Mn. These were treated with MZA and the obtained results are presented in Table 1. The Fe concentration in the effluent was 3.6477 mg/L, which was above all the permissible limit by WHO/EPA/NIS of the range of 0.2-0.3 mg/L According to Cadmus *et al.*, (2018), the concentration of iron above 1 mg/L can damage the gills of fishes and the toxicity depends on the species and size of the fish (Cadmus *et al.*, 2018). Thus, consuming these fishes has detrimental effects on the consumers. However, this was reduced to 0.0549 mg/L which conformed well to all the standards (WHO, 2011; EPA, 2001; NIS, 2007). The Chromium was 0.1240 mg/L which was reduced to a value below detectable limits (see Table 1). Exposure to chromium can cause allergic reactions, nose irritation, kidney and liver damage and long term effects can lead to death (Oliveira, 2012).

The copper content of the effluent was 2.1347 mg/L and this was reduced to 0.0057 mg/L after treatment. Whilst the concentration of lead and cadmium were 0.0748 mg/L and 0.5431 mg/L respectively which were found to be undetected after treatment with MZA. This is an indication that these metals were completely removed and as such compared well with the standards. Acute exposure to both lead and cadmium causes pulmonary and gastrointestinal

disease, brain and kidney damages (Mahino *et al.*, 2014; Oliveira, 2012).

All the heavy metals treated conformed to all the standards (see Table 1), the efficient removal of these pollutants by MZA is attributed to the isomorphical substitution of Fe in the magnetite by these metals. More so, this adsorbent has octahedral sites at the surface of the crystal structure, which made binding easier (Uddin, 2017). Therefore, the treated water can be used for drinking and other domestic purposes.

3.1.1 EFFECTS OF BEDHEIGHTS ON BREAKTHROUGH CURVE

The results of effects of bed height on the breakthrough curves of the chemical parameters are presented in Figure 2;

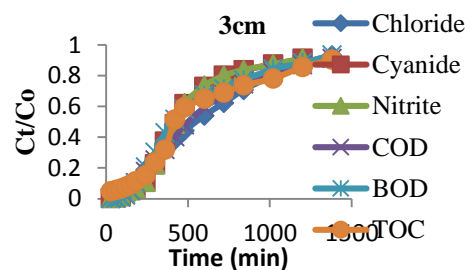


Figure 2a: Effect of Bedheight at 3 cm, 10 % inlet concentration and flowrate of 4 ml/min

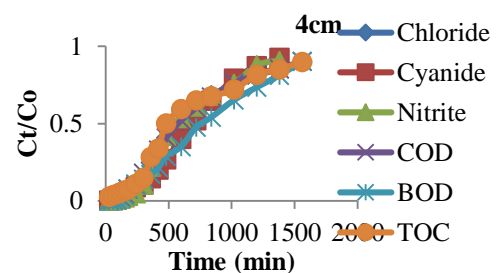


Figure 2b: Effect of Bedheight at 4 cm, 10 % inlet concentration and flowrate of 4ml/min

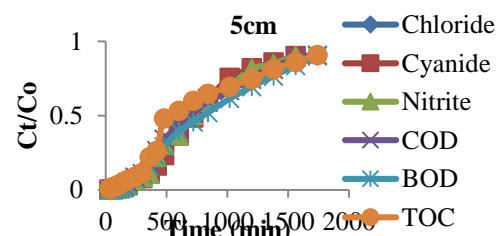


Figure 2c: Effect of Bedheight at 3 cm, 10 % inlet concentration and flowrate of 4 ml/min

From the presented results, it is evident that increase in bed height resulted to increase in breakthrough time as well as exhaustion time. For instance, the breakthrough time and exhaustion time of chloride, COD, BOD and TOC increased from 180-300 minutes and 1380-1740 minutes with increase in bed height from 3 cm to 5 cm respectively. Whilst that of cyanide and nitrite increased from 240-360 minutes and 1200-1560 min respectively for breakthrough and exhaustion time respectively. It can also be observed that the chloride, COD, BOD and TOC with higher concentration reached the breakthrough time earlier than cyanide and nitrite with lower concentration; this might be due to the fact that increase in concentration affects the saturation rate which consequently reduced the breakthrough time of these pollutants (Rouf and Nagapadma, 2015). This observation can be attributed to the fact that increase in bed height gave rise to more contact between the MZA and the contaminants due to higher dosage of MZA in the bed, thus, increasing the adsorption efficiency (Rouf and Nagapadma, 2015; Han *et al.*, 2009). The column adsorption data and parameters obtained in the course of studying the effects of bed height on removal of chemical parameters and MB are shown in Table 2

TABLE 2: EXPERIMENTAL DATA OF COLUMN STUDIES WITH RESPECT TO DIFFERENT BED HEIGHTS

Parameters	3cm					
	Chloride	CN	COD	BOD	Nitrite	TOC
V (mg)	5520	4800	5520	5520	4800	5520
q_{max} (mg)	23376.75	43.36	72003.18	13196.08	42.53	5137.8
q_{exp} (mg)	1948.06	3.61	6000.27	1099.67	3.54	428.15
M_r (mg)	53604.72	106.56	171362.9	34704.41	105.12	16504.8
% removal	43.61	40.69	42.02	38.02	40.56	31.13
4cm						
V (mg)	6240	5520	6240	6240	5520	6240
q_{max} (mg)	26775.53	62.023	84575.39	20187.81	57.06	6047.40
q_{exp} (mg)	1673.47	3.88	5285.96	1261.74	3.57	377.96
M_r (mg)	60596.64	122.54	193714.60	39230.88	120.89	18657.6
% removal	44.19	50.61	43.66	51.46	47.20	32.41
5cm						
V (mg)	6240	5520	6240	6240	5520	6240
q_{max} (mg)	30973.42	73.54	98316.35	23730.01	67.62	7206.6
q_{exp} (mg)	1548.67	3.68	4915.82	1186.50	3.38	360.33
M_r (mg)	67588.56	138.53	216066.20	43757.52	136.66	20810.40
% removal	45.83	53.09	45.50	54.23	49.48	34.63

According to Table 2, increase in bed height resulted to increase in amount of contaminants adsorbed as well as the percentage removal in all cases; the percentage removal of chloride, cyanide, COD, BOD, nitrite, TOC increased from 43.61-45.83 %, 40.69-53.09 %, 42.02-45.50 %, 38.02-54.23 %, 40.56-49.48 % and 31.13-34.63 % respectively. This might be due to increase in the quantity of the MZA, giving rise to more binding sites for adsorption (Lopez-Cervantes *et al.*, 2018; Han *et al.*, 2009)

3.1.2 EFFECTS OF FLOWRATE ON BREAKTHROUGH CURVE

The results of effects of flow rate on the breakthrough curves of the chemical parameters and MB are presented in Figure 3;

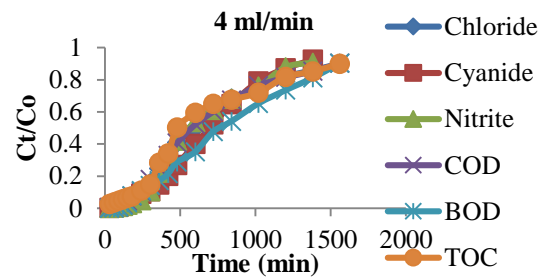


Figure 3a: Effect of Flow rate at 4 ml/min, 10 % concentration and bed height of 4cm

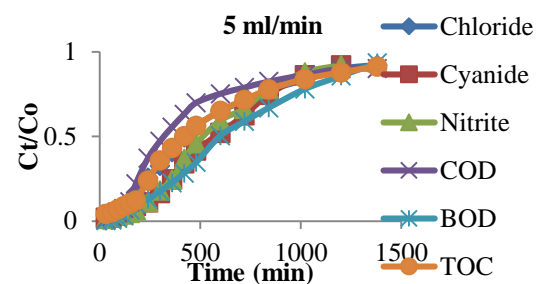


Figure 3b: Effect of Flow rate at 5 ml/min, 10 % concentration and bed height of 4cm

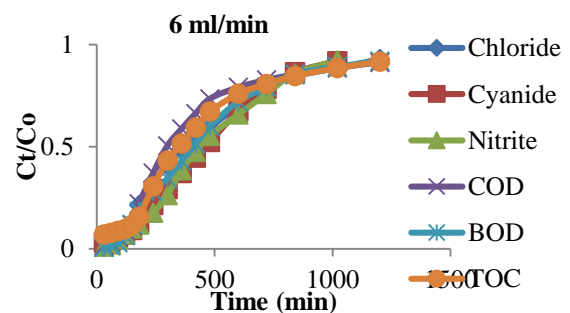


Figure 3c: Effect of Flow rate at 6 ml/min, 10 % concentration and bed height of 4cm

The results as presented in Figure 3 show that increase in flow rate consequently brought about decrease in breakthrough and exhaustion time. The breakthrough time and exhaustion time of chloride, COD, BOD and TOC reduced from 240-150 minutes and 1560-1200 min respectively, when the flow rate was increased from 4 ml/min to 6 ml/min. whilst that of cyanide and nitrite are 300 -150 min and 1380-1020 min. This observation is attributed to the MZA getting saturated faster as the flow rate increased (Lopez-Cervantes *et al.*, 2018; Patel and Vashi, 2015).

The column adsorption data and parameters obtained in the course of studying the effects of flow rate on removal of chemical parameters as shown in Table 3;

TABLE 3: EXPERIMENTAL DATA OF COLUMN STUDIES WITH RESPECT TO FLOW RATE

Parameters	4 ml/min Chloride	CN	COD	BOD	Nitrite	TOC
V (ml)	6240	5520	6240	6240	5520	6240
q_{max} (mg)	26775.53	62.0	84575.39	20187.81	57.06	6047.40
q_{exp} (mg/g)	1673.47	3.88	5285.96	1261.74	3.57	377.96
M_T (mg)	60596.64	122.54	193714.60	39230.88	120.89	18657.6
% removal	44.19	50.61	43.66	51.46	47.20	32.41
	5 ml/min					
V (ml)	6900	6000	6900	6900	6000	6900
q_{max} (mg)	25348.63	61.76	68285.73	18950.24	56.64	5955
q_{exp} (mg/g)	1584.29	3.86	4267.86	1164.39	3.54	372.19
M_T (mg)	67005.9	127.42	214203.6	40157.32	121.78	20631
% removal	37.83	48.47	31.88	47.19	46.51	28.86
	6 ml/min					
V (mg)	7200	6120	7200	7200	6120	7200
q_{max} (mg)	24923.04	61.58	67868.23	17080.39	56.32	5796
q_{exp} (mg/g)	1557.69	3.84	4241.77	1067.52	3.52	362.25
M_T (mg)	67487.25	135.86	223516.8	45266.4	122.89	21528
% removal	36.93	45.83	30.36	37.73	45.83	26.92

With respect to Table 3, it is evident that increase in flow rate led to subsequent reduction in maximum adsorption of contaminants (q_{max}), the uptake capacity of the contaminants by MZA (q_{exp}) and percentage removal in all cases. The percentage removal of chloride, cyanide, COD, BOD, nitrite and TOC reduced from 44.16 %, 50.61 %, 43.66 %, 51.46 %, 47.20 %, 32.41 %, 49.40 % to 36.93 %, 45.83 %, 30.36 %, 37.73 %, 45.83 % and 26.92 % respectively with increase in flow rate from 4 ml/min to 6 ml/min. This is because as the flow rate increase, the mass transfer rates also increase which consequently lead to faster saturation of the MZA. Similar effect was observed in literature (Lopez-Cervantes *et al.*, 2018; Han *et al.*, 2009).

3.1.3 EFFECTS OF INLET CONCENTRATIONS ON THE BREAKTHROUGH CURVE

According to the presented results, the breakthrough time and exhaustion time of the pollutants reduced with increase in the inlet concentrations of the textile wastewater. The breakthrough time and exhaustion time of chloride, COD, BOD, TOC reduced from 240-150 min and 1560-1200 min accordingly when the inlet concentration was increased from 10 % to 20 %. Whilst that of cyanide and nitrite decrease from 300 min to 180 min, in order to attain the breakthrough; and 1380-1200 min to get exhausted. These results demonstrated that the breakthrough time and saturation rate are greatly influenced by change in concentration (Chowdhury *et al.*, 2013). This is because of more active sites coverage as the concentration increased which consequently increase the rate of exhaustion. More so, more volume of effluent can be treated with decrease in inlet concentration as a result of slower transport of mass transfer reduction (Lopez-Cervantes *et al.*, 2018). The column adsorption parameters are presented in Table 4;

TABLE 4: EXPERIMENTAL DATA OF COLUMN STUDIES WITH RESPECT TO INLET CONCENTRATION

Parameters	10 % Chloride	CN	COD	BOD	Nitrite	TOC
V (ml)	6240	5520	6240	6240	5520	6240
q_{max} (mg)	26775	62.0	84575.39	20187.8	57.0	6047
q_{exp} (mg/g)	1673.47	3.88	5285.96	1261.74	3.57	377.96
M_T (mg)	60596.6	122.5	193714.6	39230.8	120.8	18657.6
% removal	44.19	50.61	43.66	51.46	47.20	32.41
	15 %					
V (ml)	5520	4800	5520	5520	4800	5520
q_{max} (mg)	27463.0	62.42	86243.46	20708.8	58.18	6115.2
q_{exp} (mg/g)	1716.44	3.91	5390.22	1294.31	3.64	382.2
M_T (mg)	61645.1	122.5	185928.7	39882.5	120.9	13137.6
% removal	44.55	50.93	46.39	51.92	48.11	46.55
	20 %					
V (ml)	4800	4080	4800	4800	4080	4800
q_{max} (mg)	27964.2	64.22	90843.19	21143.9	58.60	6221.4
q_{exp} (mg/g)	1747.76	4.01	5677.70	1321.50	3.66	388.84
M_T (mg)	55935.3	116.8	178813.4	37920	111.3	12384
% removal	49.99	54.96	50.80	55.76	52.65	50.24

With respect to Table 4.29, it can be deduced values of q_{max} and q_{exp} increased as the initial concentration increased in all cases. However, the volume of effluent reduced with increase in concentration. This is due to the faster transport of molecules as the concentration increased resulting to treatment of less effluent (Han *et al.*, 2009).

3.2 MODELING OF COLUMN ADSORPTION STUDIES

Three models (Adams-Bohart, Thomas and Yoon-Nelson) were used in studying the column adsorption behaviour through the estimation of the kinetic model of the column as well as the breakthrough curve.

3.2.1 ADAMS-BOHART MODEL

The initial part of breakthrough curve was investigated through the application of Adams-Bohart model to experimental data. Using linear regression analysis on the breakthrough curves, the values of kinetic constants K_{AB} and maximum adsorption capacity N_o were estimated and presented in Tables 5-7. According to Table 5, there was no substantial changes in the values of K_{AB} when the bed depth was increased from 3-5 cm, however the values of N_o decreased with increase in bed height in all cases. The N_o values of chloride, cyanide, COD, BOD, nitrite and TOC from 3-5 cm are 1902.32-1454.47 mg/L, 3.66-2.97 mg/L, 5960.55-4551.53 mg/L, 1172.41-1016.02 mg/L, 3.61-2.93 mg/L and 600.09-467.23 mg/L respectively. In addition, the K_{AB} (see Table 6) for chloride, cyanide, COD increased with increase in flow rate while that of BOD, TOC, decreased and no significant change in the value of

K_{AB} for nitrite. Nonetheless, the N_o values increased in all cases with increase in flow rate as presented in Table 6. Furthermore, the values of K_{AB} reduced with increase in concentration while that of N_o increased when the concentration was increased from 10 % to 20 % as shown in Table 7. It can be observed from these results that the N_o increased with increase in flow rates and concentrations, while it decreased with bed height. This is because N_o is also related to saturation concentration (Biswas and Mishra, 2015) and as such observation is expected.

Although, Adams-Bohart model is based on assumption that the equilibrium is instantaneous and the adsorption rate is proportional to adsorption capacity remaining on the adsorbents (Tamilselvi and Asaithambi, 2015; Trgo et al., 2011). However, this model cannot be used to describe the experimental data in the present study due to the low R^2 (0.550-0.878) values obtained in all cases.

TABLE 5: ADAMS BOHART PARAMETERS AT BEDHEIGHTS OF 3-5 CM, 10 % INITIAL CONCENTRATION AND FLOWRATE OF 4 ML/MIN

Contaminants	$K_{AB} (\frac{L}{mg}/min)$	$N_o (mg/L)$	R^2
3 cm			
Chloride	3.4×10^{-4}	1902.32	0.649
Cyanide	1.85×10^{-1}	3.66	0.689
COD	1.13×10^{-4}	5960.55	0.622
BOD	5.73×10^{-4}	1172.41	0.572
Nitrite	1.87×10^{-1}	3.61	0.691
TOC	7.69×10^{-4}	600.09	0.764
4 cm			
Chloride	3.3×10^{-4}	1593.28	0.674
Cyanide	1.71×10^{-1}	3.32	0.754
COD	1.03×10^{-4}	5120.55	0.623
BOD	5.25×10^{-4}	1077.13	0.641
Nitrite	1.83×10^{-1}	3.24	0.729
TOC	7.69×10^{-4}	507.50	0.755
5 cm			
Chloride	2.99×10^{-4}	1454.47	0.692
Cyanide	1.71×10^{-1}	2.97	0.693
COD	1.00×10^{-4}	4561.53	0.632
BOD	5.09×10^{-4}	1016.02	0.616
Nitrite	1.69×10^{-1}	2.93	0.724
TOC	7.79×10^{-4}	457.23	0.705

TABLE 6: : ADAMS-BOHART PARAMETERS AT FLOW RATES OF 4-6 ML/MIN, 10 % INITIAL CONCENTRATION AND BED HEIGHT OF 4 CM

Contaminants	$K_{AB} (\frac{L}{mg}/min)$	$N_o (mg/L)$	R^2
4 ml/min			
Chloride	3.3×10^{-4}	1593.28	0.679
Cyanide	1.71×10^{-1}	3.32	0.754
COD	1.03×10^{-4}	5120.55	0.623
BOD	5.25×10^{-4}	1077.13	0.641
Nitrite	1.83×10^{-1}	3.24	0.729
TOC	7.69×10^{-4}	507.50	0.755
5 ml/min			
Chloride	3.09×10^{-4}	1709.15	0.568
Cyanide	1.40×10^{-1}	3.79	0.844
COD	8.05×10^{-5}	5434.79	0.550
BOD	5.40×10^{-4}	1168.39	0.681
Nitrite	1.69×10^{-1}	3.54	0.801
TOC	7.36×10^{-4}	559.11	0.720
6 ml/min			
Chloride	3.09×10^{-4}	1826.30	0.624

Cyanide	1.58×10^{-1}	3.81	0.825
COD	9.34×10^{-5}	5630.67	0.605
BOD	5.56×10^{-4}	1150.17	0.614
Nitrite	1.83×10^{-1}	3.66	0.755
TOC	8.03×10^{-4}	571.63	0.734

TABLE 7: ADAMS-BOHART PARAMETERS AT INITIAL CONCENTRATION OF 10-20 % , FLOW RATE OF 4 ML/MIN AND BED HEIGHT OF 4 CM

Contaminants	$K_{AB} (\frac{L}{mg}/min)$	$N_o (mg/L)$	R^2
10 %			
Chloride	3.3×10^{-4}	1593.28	0.679
Cyanide	1.71×10^{-1}	3.32	0.754
COD	1.03×10^{-4}	5120.55	0.623
BOD	5.25×10^{-4}	1077.13	0.641
Nitrite	1.83×10^{-1}	3.24	0.729
TOC	7.69×10^{-4}	507.50	0.755
15 %			
Chloride	3.0×10^{-4}	1647.75	0.65
Cyanide	1.57×10^{-1}	3.40	0.77
COD	9.5×10^{-5}	5422.29	0.636
BOD	4.98×10^{-4}	1079.46	0.622
Nitrite	1.59×10^{-1}	3.50	0.719
TOC	1.05×10^{-4}	520.46	0.79
20 %			
Chloride	2.83×10^{-4}	1663.07	0.649
Cyanide	1.47×10^{-1}	3.44	0.814
COD	8.32×10^{-5}	5865.56	0.60
BOD	4.68×10^{-4}	1084.16	0.653
Nitrite	1.47×10^{-1}	3.63	0.756
TOC	1.0×10^{-4}	536.91	0.798

3.2.2 THOMAS MODEL

The column adsorption data was also fitted with the Thomas model to establish the behaviour of the contaminants breakthrough with respect to MZA. The Thomas rate constant K_{TH} and q_o were evaluated from the slope and intercept of plots of $\ln(\frac{C_t}{C_o} - 1)$ against volume as presented in Table 8-10.

With respect to Table 8, increase in bed height from 3 cm to 5 cm, brought a corresponding decrease in the values of K_{TH} as well as the q_o . This result is in agreement with that obtained by Nwabanne and Igbokwe, (2012). On the other hand, the K_{TH} increased while the q_o decreased with increasing flow rates (see Table 9). The K_{TH} reduced, while the q_o increased with increase in inlet concentrations. These results are in line with literature (Lopez-Cervantes *et al.*, 2018; Nwabanne and Igbokwe, 2012). The high R^2 values (0.882-0.978), (0.899-0.994), (0.876-0.981) for bed heights, flow rate and inlet concentrations accordingly shows the provision of good correlation between the experimental and calculated data. Hence, this model can be used to predict the breakthrough curve of the pollutants.

TABLE 8: THOMAS PARAMETERS AT DIFFERENT BED HEIGHTS OF 3-5 CM, 10 % INITIAL CONCENTRATION AND FLOW RATE OF 4 ML/MIN

Contaminants	$K_{TH}(\frac{ml}{min}.mg)$	$q_o(mg/g)$	R^2
3 cm			
Chloride	1.03x10 ⁻³	1352.68	0.933
Cyanide	0.5063	2.79	0.933
COD	3.33x10 ⁻⁴	4306.01	0.913
BOD	1.73x10 ⁻³	831.95	0.882
Nitrite	0.5151	2,74	0.935
TOC	2.52x10 ⁻³	385.81	0.967
4 cm			
Chloride	9.1x10 ⁻⁴	1277.34	0.950
Cyanide	0.4450	2.77	0.974
COD	2.90x10 ⁻⁴	4045.29	0.920
BOD	1.39x10 ⁻³	886.26	0.910
Nitrite	0.4749	2.69	0.962
TOC	2.31x10 ⁻³	370.88	0.978
5 cm			
Chloride	8.90x10 ⁻⁴	1102.78	0.959
Cyanide	0.4180	2.70	0.941
COD	2.85x10 ⁻⁴	3449.04	0.930
BOD	1.37x10 ⁻³	784.09	0.916
Nitrite	0.4475	2.44	0.965
TOC	2.27x10 ⁻³	350.36	0.966

TABLE 9: THOMAS PARAMETERS AT DIFFERENT FLOW RATES OF 4-6 ML/MIN, 10 % INLET CONCENTRATION AND BED HEIGHT OF 4 CM

Contaminants	$K_{TH}(\frac{ml}{min}.mg)$	$q_o(mg/g)$	R^2
4 ml/min			
Chloride	9.1x10 ⁻⁴	1277.34	0.950
Cyanide	0.4450	2.77	0.974
COD	2.90x10 ⁻⁴	4045.29	0.920
BOD	1.39x10 ⁻³	886.26	0.910
Nitrite	0.4749	2,69	0.962
TOC	2.31x10 ⁻³	370.88	0.978
5 ml/min			
Chloride	1.35x10 ⁻³	1126.91	0.912
Cyanide	0.5495	2.67	0.991
COD	3.56x10 ⁻⁴	3177.76	0.899
BOD	2.18x10 ⁻³	820.38	0.960
Nitrite	0.6370	2.62	0.991
TOC	3.53x10 ⁻³	331.92	0.973
6 ml/min			
Chloride	1.34x10 ⁻³	976.78	0.934
Cyanide	0.5865	2.29	0.994
COD	4.09x10 ⁻⁴	2943.51	0.910
BOD	2.20x10 ⁻³	569.86	0.934
Nitrite	0.6493	2.30	0.974
TOC	3.73x10 ⁻³	282.65	0.969

TABLE 10: THOMAS PARAMETERS AT DIFFERENT INLET CONCENTRATIONS OF 10 %-20 %, FLOW RATE OF 4 ML/MIN AND BED HEIGHT OF 4 CM

Contaminants	$K_{TH}(\frac{ml}{min}.mg)$	$q_o(mg/g)$	R^2
10 %			
Chloride	9.1x10 ⁻⁴	1277.34	0.950
Cyanide	0.4450	2.77	0.974
COD	2.90x10 ⁻⁴	4045.29	0.920
BOD	1.39x10 ⁻³	886.26	0.910
Nitrite	0.4749	2,69	0.962
TOC	2.31x10 ⁻³	370.88	0.978
15 %			
Chloride	7.99x10 ⁻⁴	1363	0.929
Cyanide	0.367	3.08	0.965
COD	2.68x10 ⁻⁴	4166.89	0.917

BOD	1.21x10 ⁻³	950.05	0.886
Nitrite	0.3970	2.96	0.950
TOC	2.85x10 ⁻³	393.25	0.981
20 %			
Chloride	7.1x10 ⁻⁴	1374.12	0.916
Cyanide	0.316	3.27	0.965
COD	2.3x10 ⁻⁴	4430.82	0.878
BOD	1.06x10 ⁻³	996.97	0.879
Nitrite	0.362	3.02	0.961
TOC	2.63x10 ⁻³	412.17	0.981

4 CONCLUSION

In the studies, iron oxide nanoparticles synthesized using mango leaf extract as a reducing agent was doped on zeolite A and used for treatment of textile wastewater, the following were deduced;

- Biosynthesis of iron nanoparticles was carried out with mango leaf extract as a reducing agent and the synthesized FeONPs was doped onto the surface of zeolite A to produce Nano adsorbents (MZA) for textile wastewater treatment via column studies.
- The column studies showed that the exhaustion and breakthrough time were influenced by increase in bed height, flow rates and inlet concentrations; and the breakthrough time and exhaustion time increased with increase in bed height while they decreased with increase in flow rates and inlet concentrations. The percentage removal of chemical parameters increased with increase in bed heights and inlet concentrations and decreased with increase in flow rates. The maximum adsorptions of the chemical parameters by MZA are 45.83%, 53.09 %, 45.50 %, 54.23 %, 49.48 % and 34.63 % for chloride, cyanide, COD, BOD, Nitrite and TOC accordingly, at 5 cm bed heights, 4ml/min flow rates and 10 % in let concentrations. The Thomas model was found to predict the breakthrough of the pollutants better than Adams-Bohart with R^2 values (0.882-0.978), (0.899-0.994), (0.876-0.981) for bed heights, flow rate and inlet concentrations respectively. This shows the provision of good correlation between the experimental and calculated data.

Thus, It can be informed from various analysis conducted that the developed adsorbent is suitable for textile wastewater treatments

REFERENCES

- Alaya-Ibrahim, S., Kovo, A.S., Abdulkareem, A.S., Adeniyi, O.D. & Yahya, M.D. (2018). Synthesis and characterization of magnetic zeolite A for removal of methylene blue from textile wastewater. A paper presented at the Nigerian Society of Chemical Engineers (NSChE) 48th Annual Conference,



- Exhibition & Annual General Meeting, Abeokuta, Ogun State. <https://pdfs.semanticscholar.org/9da4/648925199ce9659969c7d3a5fb4e895426a9.pdf>
- Alfadul, S.M. (2007) *Using Magnetic Extractants for Removal of Pollutants from Water via Magnetic Filtration*. PhD Dissertation, Oklahoma State University, Stillwater
- American Public Health Association (APHA), (2017). Standards methods for the examination of water and wastewater, American Water Works Association (AWWA), Water Environment Federation (WEF). ISBN: 9870875532875
- Balamurugan, M., Saravanan, S., & Soga, T. (2014). Synthesis of iron oxide by using Eucalyptus Globulus plant extract. *Journal of Surface Science & Nanotechnology* 12, 363-367
- Bankole, M.T., Abdulkareem, A.S., Tijani, J.O, Ochigbo, S.S., Afolabi, A.S & Roos, W.D. (2017). Chemical oxygen demand removal from electroplating wastewater by purified and polymer functionalized carbon nanotubes adsorbents. *Water Resources and Industry* 18, 33-50, <http://dx.doi.org/10.1016/j.wri.2017.07.001>
- Biswas, S. & Mishra, U. (2015). Continuous fixed bed column studies and adsorption modelling; removal of lead ion from aqueous solution by charcoal originated from chemical carbonization of rubber wood sawdust. *Journal of Chemistry* 2015, 1-9. doi:10.1155/2015/907379
- Cadmus, P., Brinkman, S.F. and May, M.K. (2018). Chronic toxicity of ferric iron for North American aquatic organism; derivation of a chronic water quality criterion using single species and mesocosm data. *Archives of Environmental Contaminants and Toxicology* 74(4), 605-615, doi: 10.1007/s00244-018-0505-2
- Chowdbury, Z.Z., Zain, S.M., Rashid, A.K., Rafique, R.F. & Khalid, K. (2013). Breakthrough curve analysis for column dynamics sorption of Mn (II) ions from wastewater using *Mangostana garcinia* peel based granular activated carbon. *Journal of Chemistry* 2013,1-8. doi: 10.1155/2013/959761
- Dada, A.O., Olalekan, A.P., Olatunya, A.M., & Dada, O. (2012). Langmuir, Freundlich, Temkin, and Dubinin-Radushkevich Isotherms studies of equilibrium sorption of Zn²⁺ unto phosphoric acid modified rice husk. *Journal of Applied Chemistry* 3(1),38-45. Retrieved from
- Dhermedra,K.T., Behari, J., & Prasengt, S., (2008). Application of nanoparticles in wastewater treatment. *World Applied Sciences Journal* 3(3), 417-433
- Elango, G., Rathika, G., & Elango, S. (2017). Physicochemical parameters of textile dyeing effluent and its impact with casestudy. *International Journal of Research in Chemistry and Environment* 7(1): 17-24. Retrieved on 1st December, 2017 from www.ijrc.org
- Environmental Protection Agency (EPA) (2001), *Parameters of water quality; Interpretation and Standards* (pp. 27-116). Ireland P.O. Box 3000, Johnstown Castle, Co. Wexford, ISBN 1- 84096-015-3
- Gholamreza, G., Momenpour, M., Omidi, F., Hosseini, M.R., Ahani. M. & Barzegari, A. (2014). Application of nanomaterials in water treatment and environmental remediation. *Frontier of Environmental Science & Engineering* 8(4), 471-482, doi:10.1007/s11783-014-0654-0
- Girilal, M., Varghese, A., K & Kalaichelvan, P.T. (2015). Adsorption of textile dyes using biogenic silver nanoparticles modified yeast cells. *Scientific Article*, 1-8
- Han. R., Wang, Y., Zhao, X., Wang, Y., Xie, F., Cheng, J., & tang, M. (2009). Adsorption of methylene blue by phoenix tree leaf powder in a fixed bed column experiment and prediction of breakthrough curve. *Desalination* 245: 284-297, doi:10.1016/j.desal.2008.07.013
- Kaya, E.M.O., Ozean, A.S., Gok, O., Ozean, A., (2013). Adsorption kinetics and isotherm parameters of Naphthalene onto Natural and Chemically Modified Bentonite from Aqueous Solutions. *Adsorption* 19, 879-888. <http://dx.doi.org/10.1007/s10450-013-9542-3>
- Lopez-Cervantes, J. Sanchez-Machado, D.I., Sanchez-Duarte, R.G., & Correa-Murriata, M.A., (2018), Study of a fixed bed column in the adsorption of azo dye from an aqueous medium using a chitosan-glutaraldehyde biosorbent. *Adsorption science and Technology* 36(1-2) 219-232, doi: 10.1177/0263617416688021
- Mahino, F., Nazura, U., & Hossaini, M.M. (2014). Heavy metals in aquatic ecosystem emphasising its effect on tissue bioaccumulation and histopathology: A review.



- Journal of Environmental Science & Technology* 7, 1-15. doi: 10.3923/jest.2014.1.15
- Nigerian Industrial Standard (NIS), (2007). Nigerian standard for drinking water quality; NIS SS4: 2007; ICS 13.060-20 by Standard Organization of Nigeria (SON); 1-29
- Nwabanne, J.T., & Igbokwe, P.K. (2012). Kinetic modelling of heavy metals adsorption on fixed bed column. *International Journal of Environmental Resources* 6 (4): 945-952
- Oliveira, H. (2012). Chromium as an environmental pollutants: Insight on induced plant toxicity. *Journal of Boteng* 2012: 1-8, doi: 10.1155/2012/375843
- Patel, H. & Vashi, R.T., (2015). Characterization and column adsorptive treatment for COD & colour removal using activated neem leaf powder from textile wastewater, *Journal of Urban and Environmental Engineering* 9(1), 45-53, doi:10.4090/juee.2015.v.9n1.04505
- Piccin, J.S., Dotto, G.L., Vierra, M.L.G & Pinto, L.A.A. (2011). Kinetic and mechanism of the dye FD& C Red 40 binding onto chitosan. *Brazilian Journal of Chemical Engineering* 28(2), 295- 304. Retrieved from <http://www.repositorio.furg.br/bitstream/handle/1/4602/31->
- Pouran, S.R., Abdulrahman, A., & Wan Daud, W.M. (2014). Review on the application of modified iron oxides as heterogeneous catalyst in Fenton process. *Journal of Cleaner Production* 64, 24-25. doi:10.1016/j.clepro.2013.09.013
- Rouf, S., & Nagapadma, (2015). Modelling of fixed bed column studies for adsorption of azo dye on chitosan impregnated with a cationic surfactant. *International Journal of Scientific Engineering Research* 6(2): 538-544
- Sanni, S.E., Adeeyo, O.A., Efevbokhen, V., Ojewumi, M., Ayoola, A. & Ogunbiyi, A. (2016). Comparative analysis of adsorption of methylene blue dye using carbon from palm kernel shell activated by different active agents. *3rd International Conference on African Development Issues (CU-ICADI 2016)*; 176-181
- Shadeera Rouf, M.N. (2015). Modelling of fixed bed column studies for adsorption of azo dye on chitosan impregnated with a cationic surfactant. *International Journal of Scientific & Engineering Research* 6(2), 538-545. Retrieved from www.ijser.org/%20ADSORPTION%20ISOTHERMS%20AND.pdf?sequence=1
- Tafesse, T.B., Yetemegne, A.K. & Kumar, S. (2015). The physico-chemical studies of water in Hawassa Textile Industry. *Environmental Analytical Chemistry* 2(11), 1-6, <http://dx.doi.org/10.4172/2380-2391.1000153>
- Tamilselvi, S. & Asaithambi, M. (2015). Column studies adsorption studies of acid dye using a novel adsorbent. *Rasayan Journal of Chemistry* 8(1), 84-91. Retrieved from <http://www.rasayanjournal.com>
- Thamilselvi, V. & Radha, K.V. (2017). Silver nanoparticles loaded silica adsorbents for wastewater treatment. *Korean Journal of Chemical Engineering* 34(6), 1801-1812, doi: 10.1007/s11814.017-0075-4
- Trgo, M., Medvidovic, N.V & Peric, J. (2011). Application of Mathematical empirical models to dynamic removal of lead on natural zeolite clinoptilolites in a fixed column. *Indian Journal of chemical Technology* 18; 123-131
- Uddin, M.K. (2017). A review on the adsorption of heavy metals by clay minerals with special form with the past decades. *Chemical Engineering Journal* 308, 438-462
- World Health Organization (WHO) (2011), *Guidelines for drinking water quality* (fourth edition) (pp. 120-350). Geneva, Switzerland. ISBN 978-92-4-15481.5, NLM Classification: WA 675, WHO Press
- Yamaura, M. & Fungaro, D.A. (2013) Synthesis and Characterization of Magnetic Adsorbent Prepared by Magnetite Nanoparticles and Zeolite from Coal Fly Ash. *Journal of Materials Science*, 48, 5093-5101. <http://dx.doi.org/10.1007/s10853-013-7297-6>
- Yusuf- Alaya, S. (2014). *Synthesis, intercalation and characterization of zeolite A for adsorption studies of methylene blue*. A Master's Thesis, Federal University of Technology, Minna, Niger state, Nigeria.
- Zainal Abidan, A., Abubakar, N.H.H., Ng, E.P., & Tan, W.L. (2017). Rapid degradation of methyloange by Ag doped zeolite X in the presence of borohydrides. *Journal of taibah University of Science* 11(6), 1070-1079, doi: 10.1016/j.jtusci.2017.06.004



A Comprehensive Review on Use of Poly Electrolyte Complex PEC as an Adsorbent for the Removal of Heavy Metals From Aqueous Solution.

*Achanya, B. E¹ & M, Auta²

^{1,2}Chemical Engineering Department, Federal University of Technology, PMB 65 Minna, Niger State, Nigeria

*Corresponding author email: achanyaene@yahoo.com, +2347036681700

ABSTRACT

Water pollution has become a 21st century problem because of industrialization. Adsorption is one of the most cost effective ways of removing noxious heavy metals from the solvent phase. This paper presents a detailed information and review on the adsorption of noxious heavy metal ions from wastewater effluents using polyelectrolyte complex PEC formed by Natural-Natural, natural-synthetic, synthetic-synthetic interaction of polyelectrolyte as adsorbents. In addition to this, the mode of preparation, efficiency of developed PEC for adsorption of the heavy metals ions is discussed in detail along with the comparison of their maximum adsorption capacity in tabular form. The results of searches show that PECs, which have low or almost no economic value because most are derived from waste, can be used as adsorbents for the adsorption of heavy metal ions from the solution.

Keywords: Adsorption, Heavy metals, Metal ions, Polyelectrolyte complex PEC, Wastewater.

INTRODUCTION

Nowadays researchers are looking for novel ways to remove metals from wastewater; this environmental pollution is caused by rapid industrialization. The using of various metallic materials have a negative impact on the environment, namely the emergence of cases of environmental pollution caused by waste containing heavy metals (Hastuti, et al 2017). This pollution can cause harm to the people around the industry producing the metallic waste. Refining metal factory, metal plating, painting and manufacturers of battery are a source of heavy metal contaminants. Waste containing the remains of these heavy metals is dangerous if not properly treated. Many methods are being used to remove heavy metal ions include chemical precipitation, ion-exchange, adsorption, membrane filtration, electrochemical treatment technologies etc. According to Hastuti et al Adsorption is one of the physicochemical treatment processes which have been found to be effective in removing heavy metals from aqueous solutions. adsorption has gained much attention because of its ease of operation, effectiveness, low cost etc. different adsorbents have been used in the adsorption of metals, however poly electrolyte complex PEC, have recently received a great deal of attention because of the fact that they represent renewable resources and are more environmentally friendly, nontoxic, than traditional materials. Poly electrolyte complex PEC is formed through combined electrostatic

interactions, which are predominate, between poly cations and poly anions upon mixing of aqueous solutions of oppositely charged poly electrolyte PE leading to the formation of a dense phase that is separated from the solvent, and the formation of multitudinous charges and functional groups such as -OH, -NH, -SH and -COOH on the surface of the PEC. (Meka, et al. 2017). PECs have a three-dimensional network structure, which was used in medical treatment when it was first discovered. Due to its ability to absorb water, it is used in agriculture, health care and so on. In recent years, it has been found that the PECs have a polyfunctional structure so that it also exhibits excellent performance as an adsorbent for heavy metal ion treatment (Yin, et al, 2018). Taking into account the importance of water quality and emerging benefits of polyelectrolyte complex, attempts have been made to discuss various issues of water treatment using low cost adsorbents. Critical analysis of various PEC used in the removal of various heavy metals, their performance, selectiveness and the optimum conditions in which they were operated. Furthermore, knowledge gaps, uncertainties, and future challenges involved in the fabrication and regeneration of PEC are also identified.

2.1 POLYELECTROLYTE COMPLEX PEC

Poly electrolyte complex results from electrostatic interactions between poly cations and poly anions, there are other bonds which can be formed between poly cations and poly anions such as hydrogen bonds, Vander Waals forces and covalent bond which results from crosslinking macro molecules (Chan, et al, 2010). PEC are formed from poly electrolyte PE, these PEs are divided into natural, chemically modified/semi-synthetic and synthetic PE (Meka, et al, 2017). PECs has the ability to attract water molecules, the super-hydrophilicity characteristics and porous structure networks; they can swell quickly in the aqueous solution, which is necessary for shortening the time to reach the adsorption equilibrium (Abd El-Mohdy, et al, 2013). The functionalization of PEC can improve its water uptake capacity and also act as a support for molecular species and metal ions. As hydrogels these hydrogels possess functional groups it increases their metal uptake capacity.

Table 1: polyelectrolytes (PEs) and their ionic nature

polyelectrolytes (PEs) and their ionic nature

PE type	Polyanion	Polycation	Reference
Natural	Galactorunic acid, Nucleic acids, poly(L-glutamic acid), carrageenan, sodium alginate, hyaluronic acid, chondroitin sulfate, gellan gum, gum kondagogu, gum karaya, Cieba pentandra gum, Termianlia catappa gum,	Poly(L-lysine), lysozyme, gelatin, chitosan, dextran, starch	Meka, et al, 2017
Chemically modified/semi-	N-carboxymethyl chitosan, cellulose-	Chitosan (deacetylation of chitin), N-trimethyl	Meka, et al, 2017

synthetic	based (sodium carboxymethyl cellulose), carboxymethyl konjac glucomannan, pectin, sodium dextran sulfate, xanthan gum	chitosan, chitosan-g-poly(ethylene glycol) monomethyl ether	7
Synthetic	Poly(acrylic acid)/carbopol, poly(methacrylic acid), Eudragit1 (Eudragit1 L 100, Eudragit1 S 100, Eudragit1 FS 30 D), poly(acrylamide-2-methylpropane sulfonate), poly(3-sulfopropyl methacrylate), dextran sulfate, poly(sodium styrene sulfonate), poly(vinyl sulfate), poly(acrylic acid-co-maleic acid), poly(p-styrenesulfonic acid), poly(p-styrenecarboxylic acid), poly(metaphosphoric acid), poly(4-	Poly(ethyleneimine), poly(allylamine hydrochloride), Eudragit1 E polymer (Eudragit1 E PO, Eudragit1 E 100), poly(N,N,N-trimethyl-2-methacryloyl ethyl ammonium bromide, poly(diallyldimethyl ammonium chloride), poly(4-vinyl-N-methylpyridinium iodide), poly(acrylamide-co-dimethyldiallylammonium chloride), poly(vinylbenzyl trialkyl ammonium), poly(acryloyloxyalkyl-trialkyl ammonium), poly(acrylamidoalkyl-trialkyl ammonium), poly(2-vinylpyridine), poly(aminoethyl	Meka, et al, 2017

methacryloyl oxyethyl trimellitate), poly (itaconic acid), poly(vinyloxy -4-butyric acid), poly(sodium 4-vinylbenzoate), poly(sodium acrylate)	methacrylate), poly(2-ethyloxazoline), poly[4-(N,N-dimethylamino methylstyrene)], poly(b-amino ester), poly(sulfoneamine)	
	hydrochlorate, poly(methacrylox yethyl trimethylammonium chloride)	

method depends on some factors, such as degree of ionization and charge distribution on the PEs, density of the PEs as well as their charges, PE chain stiffness, concentration, strength of the ionic sites, mixing ratio, order, duration and intensity, ionic group nature, chain flexibility, molecular weight, polymer structure, hydrophobicity, temperature conditions during process, degree of complexation, pH and ionic strength (Meka, et al, 2017).

2.1.3.1 EFFECT OF PH

pH is a very important factor in the formation of PECs because it determines the yield of PEC formed. At a very low pH polyanions will not dissociate and will not form complexes owing to the lack of dissociated carboxylate anions. As the pH is increased or upon dilution, polyanions can form a stable complex with oppositely charged polycations because the quantity of dissociated carboxylate anionic sites exceeds the critical value. At this stage, the complex is formed in the form of a curdy precipitate (Meka et al, 2017). At a pH higher than 7 (pH >7) an equimolar electrolyte complex aggregate is formed because of a complete dissociation of the poly anions.

2.1.3.1 EFFECT OF CONCENTRATION

The size of PEC formed depends greatly on the ratio of the poly cation and poly anion mixed, at a higher concentration of PEs, the PEC formed has large size.

2.1.1 TYPES OF PECs ON THE BASIS OF INTERACTION (SHAILESH ET AL, 2016)

1. Polyelectrolyte complex between natural polyelectrolyte
2. Polyelectrolyte complex between synthetic polyelectrolyte
3. Polyelectrolyte complex between natural and synthetic polyelectrolyte
- 4 Protein – polyelectrolyte complexation

2.1.2 PROCESS FOR THE FORMATION OF PECs

The process involved in the formation of PECs can be subdivided into three classes (Meka, et al., 2017):

Primary complex: Primary complex can form immediately after mixing of the two oppositely charged PE solutions owing to the binding forces. This process is fast.

Intra complexes. This is an intermediate complex formation usually taking 1–2 h from the time of mixing. It is at this process, new electrostatic bonds can form and/or alterations in the polymeric chains can occur.

Inter complex/aggregation. This process involves the aggregation of intermediate complexes through hydrophobic interactions. Such an aggregation is caused by some factors, for example the structure of the polymer components and the complexation conditions

2.1.3 FACTORS INFLUENCING PECs FORMATION

The nature, structure, quantity and application of PECs depend on the method by which it was prepared. This

2.2 POLY ELECTROLYTES COMPLEX USED AS Pb²⁺ ADSORBENT

Lead is a byproduct of industrial activities; these industries include battery and fuel industry, foundry and refinery industries. The presence of lead in the environment can wreak havoc in the lives of humans. These damages include kidney failure, brain damage, liver damage etc. Hastuti, et al, 2016 used carboxymethyl chitosan CMC and pectin to remove lead from aqueous solution. Chitosan is a copolymer of glucosamine and N-acetylglucosamine with reactive groups of amine and hydroxyl groups. Pectin is a polysaccharide derived from plant walls especially orange peel and apple pomace, it is a galacturonic acid with carboxylate group as its functional group (Zhang et al, 2017). CMC-pectin complex formed was characterized by using IR the active groups of the PEC was hydroxyl (OH) and carboxylate (-COOH) groups. The optimum mass ratio CMC: pectin to form the polyelectrolyte complex was 70%: 30%. The optimum conditions for Pb (II) ion adsorption was 10 mg of the adsorbent mass, 75 min of contact time, and pH 5. The material was effectively used to adsorb Pb (II) ions, where up 91% Pb (II) metal ions was adsorbed from

aqueous solution and the adsorption capacity of the adsorbent was 41.63 mg/g.

Cellulose is the most abundant biopolymer in plant, it is nontoxic, biodegradable. Due to the multiple hydroxyl groups in its molecular chain, cellulose can be an ideal carrier for tannin immobilization via epichlorohydrin activation (Ying, et al, 2019). Tannin/cellulose microspheres (T/C) were used in the removal of Pb²⁺ by Ying, et al, 2019. The microsphere had a maximum adsorption capacity of 23.75 mg/g from the Langmuir isotherm evaluation at 308K with an initial pH of 5, the optimum conditions for Pb (II) in their experiment was 2 mg of the adsorbent mass, 60 min of contact time, adsorbate initial concentration 100mg/L and pH 5. Ying 2019 reported that lead adsorption by Tannin/cellulose microspheres was driven by pH as seen from ZETA potential. The removal efficiency of the PEC was 95%. The results suggested that tannin/cellulose microspheres could be a low-cost and effective adsorbent for removing Pb (II) ions from aqueous solution. The mechanism of adsorption for lead from wastewater was via ionic interaction and chelation (Ying et al., 2019).

PEC was synthesized between N, N-dimethylacrylamide (DMAa) and 2-hydroxyethyl methacrylate (HEMA) for the adsorption of lead by free-radical type bulk copolymerization of equal volumes of each monomer (Ramos-Jacques et al, 2018). The PEC was formed between synthetic poly electrolytes, the uptake of water of the adsorbent was 3.5 times its weight at a period of 6 hrs which is necessary for shortening the time to reach the adsorption equilibrium (Abd El-Mohdy, et al, 2013), and their optimum condition for the uptake of Pb²⁺ was 5hrs of contact time, optimum temperature of 270C. As the Pb (II) initial concentration was increased gradually from 10 to 200 ppm, the amount of sorbed Pb(II) at equilibrium increased. As a result, different Q_e values were obtained when higher initial concentration solutions (C_i) were used. This continued until a critical point QC was reached where there was no change in Q_e (Ramos-Jacques et al, 2018). The final concentration C_e remained unchanged after equilibrium was reached. The Pb(II) adsorption on the p(HEMA-co-DMAa) copolymer followed the Langmuir model than the Freundlich model. Therefore, the p(HEMA-co-DMAa) copolymer behaves preferably as an energetically homogeneous surface during the Pb(II) sorption process. The adsorption capacity was 61.41mg/g and the removal efficiency was 60%.

2.1.3.2 POLY ELECTROLYTE COMPLEX USED AS PB²⁺ AND CD²⁺ ADSORBENT

The composite formed between polyaniline and chitosan is between a natural and a synthetic poly electrolyte (Shailesh et al, 2016). Polyaniline grafted chitosan PGC was prepared by grafting polyaniline into the matrices of chitosan, the reactive group in PGC is hydroxyl and carboxylate group (Karthik, 2014). Karthik 2014 reported that the adsorption of Cd (II) and Pb (II) reached equilibrium at pH 6, beyond pH 6, the experiments were not carried out due to the formation of lead hydroxide and cadmium hydroxide. The percentage removal increased as the dosage increased from 0.05 to 0.15 g/L due to an increase in the available adsorption sites and that the removal efficiency for Pb (II) was 100% while that of Cd(II) was 96.95%. PGC showed a greater affinity towards Pb(II) than Cd(II) because the binding energy that is constant b from langmuir isotherm, of Pb(II) was greater than that of Cd(II). Karthik 2014 revealed that the adsorption process using PGC was spontaneous, endothermic and freundlich isotherm was the suitable model for the adsorption process. The sorption capacity of PGC will increase with increase capacity. The adsorption capacity for Pb(II) and Cd(II) was 13.23mg/g and 12.87mg/g respectively.

TABLE 2: SHOWING PEC FOR REMOVAL OF PB

PEC(adsorbent)	Type of Interaction	Optimum conditions				Q _e (mg/g)	Removal %	Reference
		pH	Dosage	Temp	Time			
CMC-pectin complex	Natural-Natural	5	10	-	75	41.63	91	Hastun et al, 2017
Tannin/cellulose microspheres (T/C)	Natural-Natural	5	2	-	60		95	Ying et al, 2019
(HEMA-co-DMAa)	Synthetic-Synthetic	<3	-	27	300	61.41	60	Ramos-Jacques et al, 2018
Polyaniline grafted chitosan PGC	Natural	6	0.15	-	60	13.23	100	Karthik, 2014

2.3 POLY ELECTROLYTES COMPLEX USED AS CU²⁺ ADSORBENT

Cellulose is the most abundant biopolymer in plant, it is nontoxic, biodegradable. Due to the multiple hydroxyl groups in its molecular chain (Ying et al., 2019). Gelatin is an ionic hydrophilic linear polymer which exhibits properties of water solubility, non-toxicity, and biodegradability (Wang 2013). It has proven to be able to

improve the strength, hydrophilicity, and functional properties of hydrogel. Cellulose and gelatin was used to form composite for the removal of Cu^{2+} , the performance of the adsorbent was evaluated and from the characterization of the PEC, Teow et al, 2018 reported that the functional group is the O-H and N-H group. from Zeta potential, it was also reported that PEC had Higher negative charge of cellulose/gelatin hydrogels at higher weight percent of gelatin was due to the presence of dipolar polarization effect inherent by N-H functional group attributed to the addition of gelatin. The optimum pH for the adsorption of Cu^{2+} was 4.7, because at pH 4.7, Cu^{2+} is at its Natural pH. At this pH H^+ ions concentration was lowest and the O—H and N—H groups were existed in neutral forms. Hence, the competition between H^+ ions and Cu^{2+} ions on adsorption sites of hydrogel was less significant and the electrostatic repulsion between the active sites and Cu^{2+} ions was weaker. As a result, more Cu^{2+} ions could be adsorbed onto the hydrogel (Teow et al, 2018). An increase in the concentration of Cu^{2+} ions in aqueous solution, caused the concentration gradient between the adsorbent (hydrogel) and adsorbate solution (Cu^{2+} ions aqueous solution) to induced a stronger driving force to transport the large number of Cu^{2+} ions from the bulk solution to the active sites on the surface of hydrogel (Wang et al, 2013). The optimum time was observed to be 6hrs, the adsorbent dosage was 20 mg and the adsorption capacity was found to be 52.3mg/g. It was concluded from the success of the research study that cellulose/gelatin composite hydrogel and is a sustainable and environmental-friendly adsorbent for the removal of heavy metal from wastewater.

Chitosan/polyvinyl alcohol (CTN/PVA- Fe^{3+}) was investigated by Karaer et al, 2017 for the removal of copper. Poly (vinyl alcohol) (PVA) is a water-soluble matter containing large amounts of -OH groups and it has a lot of advantages such as low price,chemically stable, biocompatibility, high durability and non-toxic. The effect pH was not conduct in a basic medium due to precipitation in a $\text{pH}>6$ (Karaer et al, 2017). The ractive group of the PEC determined from FTIR was OH and NH_2 group. The PEC swelled up to 93%, the water absorbency of the composite was found very high. From the experiment the initial concentration increased from 25 to 400 mg/L with increase in time and reached equilibrium at 200 mins. kinetic experimental data of this work be fit better pseudo second-order adsorption indicating that adsorption process was dependent on ion concentration, and chemical sorption was the rate-controlling step. The optimum pH was observed to be 5,

the adsorption was fitted for Langmuir isotherm and the thermodynamics parameters showed it was spontaneous and endothermic. The adsorption capacity was found to be 62-143 mg g-1.

2.4 POLY ELECTROLYTES COMPLEX USED IN REMOVAL OF MULTI METAL

Lessa et al, 2017, investigated the adsorption capacity of pectin/cellulose microfibers (Pec-CF) beads towards the removal of multi-metals ions from water. For this, a series of experiments were performed and rationalized to establish the optimum conditions for the adsorption of copper (Cu), cadmium (Cd) and iron (Fe) on Pec-CF beads. The composite was prepared by factorial design approach. The optimized analytical conditions set for the further experiments were: adsorbent dosage – 150 mg; pH of the medium – 4; and content of CF – 5.5 wt%. This pH (pH 4) was chosen because it is an intermediate value between the optimum pHs verified for the removal of Cd (II), Cu(II), and Fe(II) ion (Lessa et al, 2011). The result from batch experiment carried out by Lessa et al, showed that amount of metal adsorbed on beads increased with increasing initial metal concentration in the medium. It also showed that above 20 min, the adsorption capacity values tend to level off and they showed slight variation up to the end of the experiment. The removal efficiencies were slightly affected by the initial metals concentration. The maximum removal of Cd(II), Cu(II), and Fe(II) ions was ca. 58%, 77%, and 94% when the initial concentration of such metals falls in the range of 50–150 mg/L. the adsorption capacity for this study was 192.3, 88.4 and 98.0 mg/g. the adsorption capacities and removal efficiencies followed the order $\text{Fe(II)} > \text{Cu(II)} > \text{Cd(II)}$. The Pec-CF beads can be utilized as an efficient and reusable adsorbent material for removing of multi-contaminants from wastewater (Lessa et al, 2011).

Jiang. C, et al, 2019 reported the performance of Glucan/chitosan (GL/CS) in the removal of Cu^{2+} , Co^{2+} , Ni^{2+} , Pb^{2+} and Cd^{2+} . Glucan is homologous polysaccharide composed of glucose monosaccharide it is linked by glycoside bonds. The glycosidic bond can be divided into alpha-glucan and beta-glucan. Alpha-glucan, is also known as glucan, it is found in the mucus secreted by certain microorganisms during their growth (Jiang. C, et al, 2019). GL/CS PEC was synthesized by ultrasonic assisted method using glucan and chitosan as the main raw materials. The swelling capacity of the adsorbent was observed and it was reported that the absorption rate increased rapidly within 40mins and reached a saturation point at 60 mins. Adsorption increases when the

adsorption rate is fast but decreases with a decrease in adsorption rate (Jiang, C, et al, 2019). q_e increases with an increase in pH value and the minimum value of q_e is at pH=1 for all the ions. The reactive group in the PEC is (-COO-, -NH-, -O-), the optimum adsorbent dosage was 0.02mg, beyond this, the adsorption capacity of the adsorbent decreased. This was true for all the ions. The adsorption capacity of Cu^{2+} is 365 mg g⁻¹, Co^{2+} is 251 mg g⁻¹, Ni^{2+} is 207 mg g⁻¹, Pb^{2+} is 424 mg g⁻¹, and Cd^{2+} is 356 mg g⁻¹. The thermodynamic parameter of the adsorption process is a spontaneous endothermic chemical monolayer adsorption. The adsorbent was selective towards $Pb^{2+} > Cu^{2+} > Cd^{2+} > Co^{2+} > Ni^{2+}$.

Carboxymethyl cellulose/polyacrylamide CMC/PAM composite hydrogel was prepared via free-radical polymerization for the removal of Cu^{2+} , Pb^{2+} and Cd^{2+} (Godiya et al, 2018). For multiple metal-ion adsorption, the q_e values are much lower than those for the single metal-ion adsorption, this result reveals that the adsorption of metal ions (Cu^{2+} , Pb^{2+} or Cd^{2+}) is negatively affected by the existence of the other two metal ions (Godiya et al, 2018), this is because the metal ions will compete for the binding site (Burakov, et al, 2018). The CMC/PAM composite hydrogel showed a preference of $Cu^{2+} > Pb^{2+} > Cd^{2+}$. The adsorption follows the Langmuir model and exhibits a pseudo second-order kinetics. The adsorption capacities for the metal ions were observed to be 151.5, 185.2 and 144.9 mg/g. The adsorption of the three ions followed the Langmuir model rather than the Freundlich model, indicating a monolayer adsorption manner of the investigated metal ions in the CMC/PAM hydrogels. The optimum time for this work was 7hrs.

He, et al, 2017 investigated the use of β -cyclodextrin (β -CD) polymer, for the removal of lead (Pb), copper (Cu) and cadmium (Cd). The adsorption took place in the chelating sites and ion exchange sites of the PEC. β -cyclodextrin (β -CD) is inexpensive, sustainable produced macro cycle of glucose, But it has low surface areas and poor removal performance compared to conventional adsorbents like activated carbons, it was cross linked with tetrafluoroterephthalonitrile to improve the surface area. The adsorption of Pb, Cu and Cd on β -CD polymer was fit better with Freundlich model, indicating that the adsorption process of Pb, Cu and Cd took place on heterogeneous surfaces that varied with surface coverage (He, et al, 2017). The adsorption capacities Was found to 215.2, 192.8 and 163.2 mg/g. the optimum pH beyond which no adsorption will take place was pH 5,

temperature was 45°C, and the optimum time was 5mins. The PEC was preferential towards $Pb > Cu > Cd$.

Cellulose-graft-poly (acrylic acid (AA)- co-acrylamide (AM)) was used as a biosorbent in the removal of Cu (II), Pb (II) and Cd (II) from aqueous solutions (Zhao et al, 2019). The effect on pH on MCC-g-(AA-co-AM), above pH 6, the metal hydroxides would be precipitated from the solution, the adsorption reached equilibrium at a pH 3. The optimum time at which equilibrium was reached was 15 mins. The adsorption capacity of the PEC increased with increase in initial concentration of the metal ions, the increased rate of mass transfer resulted from increased driving force of ions, which led to a high adsorption capacity (Garg et al., 2008). the adsorption capacity was 177.02, 556.69 and 306.22 mg/g for Cu (II), Pb (II) and Cd (II), respectively. The adsorption kinetics parameters showed the adsorption was a pseudo-second-order kinetic equation better described metal adsorption by the PEC, which meant chemisorption dominates the adsorption process (Chen et al., 2004; Li et al., 2017). Langmuir was the best fit for describing the adsorption process, which illustrated monolayer adsorption dominant. The PEC was preferential towards $Pb^{2+} > Cd^{2+} > Cu^{2+}$. the adsorption capacity from this experiment showed that it was good for metal removal.

Table 3: Showing Optimum Conditions for Adsorption

PEC (adsorbents)	Types of interaction	Optimum conditions					References
		pH	Dosage (mg)	Temperature (°C)	Initial concentration (mg/L)	Time (Mins)	
Pec-CF	Natural-Natural	4	150		50-100	20	Lessa, et al., (2011)
GL/CS	Natural-Natural		0.02	-	-	60	Jiang et al., (2019)
CMC/PAM	Natural-	-	-	-	-	-	Godiya et al., 2018
(β -CD)	Natural-synthetic	5	-	25	-		He, et al., 2017
MCC-g-(AA-co-AM)		3	-		-	15	Zhao et al., 2019

Table 4: Showing Adsorption Capacities of the PEC

PEC (adsorbents)	Metal Ion						References
	Cu ²⁺	Pb ²⁺	Co ²⁺	Cd ²⁺	Ni ²⁺	Fe ²⁺	
Pac-CF	88.4	-	-	98.4	-	192.3	Lessa, <i>et al.</i> , 2011
GL/CS	365	424	251	366	207	-	Jiang, <i>et al.</i> , 2019
CMC/PAM	185.2	151.5	-	185.2	-	-	Godiya, <i>et al.</i> , 2018).
β-CD)	192.8	215.2	-	163.2	-	-	He, <i>et al.</i> , 2017
MCC-g-(AA-co AM)	177.02	556.69	-	306.22	-	-	Zhao <i>et al.</i> , 2019

2.6 FUTURE DIRECTIONS IN THE DEVELOPMENT OF PECS FOR ADSORPTION

Heavy metal ions varies in complex matrixes, such as groundwater, stream waters, oceans, lake, and impoundment water which contain amount of alkaline metal ions (He, et al, 2017). So, it's necessary to do researches in the presence of impurities such as Na⁺, Mg²⁺ and Ca²⁺. To investigate practical applications, of the effects of Na⁺, Mg²⁺ and Ca²⁺ on the adsorption. The use of PEC in the removal of heavy metals has not been applied in real life scenario because exhaustive work has not been carried out on it, to show its viability. There are little of no comparative studies amongst the PECS, because the mode of preparation of the PECS differs. Further studies should be carried out to determine the mechanism behind the preferences of metal ions by PECs.

CONCLUSION

Large amounts of industrial, agricultural, and domestic wastewater need to be treated before being discharged into the environments. Polyelectrolyte complex showed great potential compared to other adsorbent because of renewability, low cost, nontoxicity, environmental compatibility and high adsorption capacity. PEC remains a superior alternative for the removal of heavy metal ions, dyes, and antibiotics. PECs for pollutants mainly depends on the corresponding adsorption mechanism, which in turn is determined by the modification method employed. Ion exchange, electrostatic attraction, hydrogen bonding,

and pore-filling are the predominant mechanisms controlling the adsorption of heavy metal ions.

ACKNOWLEDGEMENT

I wish to acknowledge Dr. Auta Manasseh for his support and guidance during the process of the research. My husband Emmanuel Audu for his love and encouragement. I will want to thank the Achanya's for being a big part of my life, Isaac kunle you were a big help to me. Most importantly God for bringing me to the end of this program.

REFERENCES

- Alexander E. Burakov, Evgeny V. Galunin, Irina V. Burakova, Anastassia E. Kucherova, Shilpi Agarwal, Alexey G. Tkachev & Vinod K. Gupta. (2017). Adsorption of heavy metals on conventional and nanostructured materials for wastewater treatment purposes: A review, *Ecotoxicology and Environmental Safety*, 148, 702-712. <https://doi.org/10.1016/j.ecoenv..11.034>.
- A.L. Ramos-Jacques, J.A. Lujan-Montelongo, C. Silva-Cuevas, M. Cortez-Valadez, M. Estevez, & A.R. Hernandez-Martínez. (2018). Lead (II) removal by poly (N,N-dimethylacrylamide-co-2-hydroxyethylmethacrylate), *European Polymer Journal*, 101, 262–272. <https://doi.org/10.1016/j.eurpolymj.2018.02.032>
- Adewoye, L.T., Mustapha, S.I., Adeniyi, A.G., Tijani, J.O., Amoloye, M.A. & Ayinde, L.J. (2017). Optimization of nickel (ii) and chromium (iii) removal from contaminated water using sorghum bicolor. *Nigerian Journal of Technology (NIJOTECH)*, 36(3), 960 – 972.
- Archana, D., Upadhyay, L., Tewari, R.P., Dutta, J., Huang, Y.B. & Dutta, P.K. (2013). chitosan pectin alginate as a novel scaffold for tissue engineering application. *Indian Journal of Biotechnology*, 12(1), 475 – 4.
- Baron, R.D, Perez, L.L, Salcedo, J.M, Cordoba, L.P, Amaral, P.J. (2017). Production and characterization of films based on blends of chitosan from blue crab (*Callinectes sapidus*) waste and pectin from Orange (*Citrus sinensis* Osbeck) peel. *International Journal of Biological Macromolecules*, 1(1), 1 – 26. <http://dx.doi.org/doi:10.1016/j.ijbiomac.2017.02.004>
- Chen, Q, Zheng, J.W., Zheng, L.C, Dang, Z, & Zhang, L.J. (2018). Classical theory and electron-scale view of exceptional Cd adsorption onto mesoporous cellulose



- biochar via experimental analysis coupled with DFT calculations. *Chemical Engineering Journal*, 350,1000-1009.
- Emanuele F. Lessa , Aline L. Medina b, Anderson S. Ribeiro & Andre´ R. Fajardo, 2016, Removal of multi-metals from water using reusable pectin/cellulose microfibers composite beads, *Arabian Journal of Chemistry*.<http://dx.doi.org/10.1016/j.arabjc.2017.07.011>.
- Elwakeel, K.Z., El-Bindary, A.A., Kouta, E.Y., & Guibal E. (2018). Functionalization of polyacrylonitrile/Na-Y-zeolite composite with amidoxime groups for the sorption of Cu (II), Cd (II) and Pb (II) metal ions. *Chemical Engineering Journal*,332,727-736.
- Gerente, C., du Mesnil, P.C., Andres, Y., Thibault, J.F., Le Cloirec, P., 2000. Removal of metal ions from aqueous solution on low cost natural polysaccharides – sorption mechanism approach. *React. Funct. Polym.* 46, 135–144.
- Gomes, R.F., de Azevedo, A.C.N., Pereira, A.G.B., Muniz, E.C., Fajardo, A.R., Rodrigues, F.H.A., 2015. Fast dye removal from water by starch-based nanocomposites. *J. Colloid Interface Sci.* 454, 200–209.
- H.L. Abd El-Mohdy , E.A. Hegazy, E.M. El-Nesr &M.A. El-Waha. (2013). Metal sorption behavior of poly(N-vinyl-2-pyrrolidone)/(acrylic acid-co-styrene) hydrogels synthesized by gamma radiation, *Journal of Environmental Chemical Engineering*, 1, 328–338, <http://dx.doi.org/10.1016/j.jece.2013.05.013>.
- Hatice Karaer & Ismet Kaya. (2017). Synthesis, characterization and using at the copper adsorption of chitosan/polyvinyl alcohol magnetic composite. *Journal of Molecular Liquids*.
doi:10.1016/j.molliq.2017.01.030
- H. Yan, J. Dai, Z. Yang, H. Yang, R. Cheng, Enhanced and selective adsorption of copper (II) ions on surface carboxymethylated chitosan hydrogel beads. *Chemical Engineering Journal*, 174(2) (2011) 586-594.
- H.T. Kahraman, Development of an adsorbent via chitosan nano-organoclay assembly to remove hexavalent chromium from wastewater, *International journal of biological macromolecules*, 94 (2017) 202-209.
- Jain, M., Garg, V.K., Kadirvelu, K., Sillanpaa, M., 2016. Adsorption of heavy metals from multi-metal aqueous solution by sunflower plant biomass-based carbons. *Int. J. Environ. Sci. Tech.* 13, 493–500.
- J. Wang, L. Wei, Y. Ma, K. Li, M. Li, Y. Yu, L. Wang, H. Qiu, Collagen/cellulose hydrogel beads reconstituted from ionic liquid solution for Cu(II) adsorption, *Carbohydrate Polymer*,98(1) (2013) 736-743.
- Jiang C, Wang X, Wang G, Hao C, Li X, Li T. Adsorption performance of a polysaccharide composite hydrogel based on crosslinked glucan/chitosan for heavy metal ions, *Composites Part B* (2019).
doi: <https://doi.org/10.1016/j.compositesb.2019.03.082>.
- L. Zhang, S. Tang, F. He, Y. Liu, W. Mao & Y. Guan. (2019). Highly efficient and selective capture of heavy metals by poly (acrylic acid) grafted chitosan and biochar composite for wastewater treatment, *Chemical Engineering Journal*.
doi: <https://doi.org/10.1016/j.cej.2019.122215>
- Kong, J.J., Yue, Q.Y., Sun, S.L., Gao, B.Y., Kan, Y.J., Li, Q., & Wang, Y. (2014). Adsorption of Pb (II) from aqueous solution using keratin waste - hide waste: Equilibrium, kinetic and thermodynamic modeling studies. *Chemical Engineering Journal*,241,393-400.
- Lessa, E.F, Gularte, M.S, Garcia, E.S & Fajardo, A.R, (2016). Orange waste: a valuable carbohydrate source for the development of beads with enhanced adsorption properties for cationic dyes. *Carbohydrate Polymer*, 57, 660–668. Retrieved from (<http://creativecommons.org/licenses/by-nc-nd/4.0/>).
- M. Auta & B.H. Hameed. (2010). Coalesced chitosan activated carbon composite for batch and fixed-bed adsorption of cationic and anionic dyes. *Colloids and Surfaces B: Biointerfaces*,
doi:10.1016/j.colsurfb.2012.12.021
- Opanasopit, P., Apirakaramwong, A., Ngawhirunpat, T., Rojanarata, T., Ruktanonchai, U., 2008. Development and characterization of pectinate micro/nanoparticles for gene delivery. *AAPS PharmSciTech* 9, 67–74
- R. Karthik & S. Meenakshi. (2014). Removal of Pb(II) and Cd(II) ions from aqueous solution using polyaniline grafted chitosan. *Chemical Engineering Journal*.
doi: <http://dx.doi.org/10.1016/j.cej.2014.11.0>
- Shailesh L. Patwekar¹, Ashwini P. Potulwar, Snehal R. Pedewad, Manoj S. Gaikwad, Shaz & A Khan, Arvind B Suryawanshi. (2016). Review on Polyelectrolyte Complex as Novel Approach for Drug Delivery System.



Ijppr.Human, 2016; Vol. 5 (4): 97-109. Retrieved from www.ijppr.humanjournals.com.

Teow YH, Ming KL, Mohammad AW, Synthesis of cellulose hydrogel for copper (II) ions adsorption, Journal of Environmental Chemical Engineering (2018), <https://doi.org/10.1016/j.jece.2018.07.010>.

Venkata S. Meka, et al, A comprehensive review on polyelectrolyte complexes, Drug Discovery Today Volume 22, Number 11 November 2017, <http://dx.doi.org/10.1016/j.drudis.2017.06.008>.

W. Wang, Y. Kang, A. Wang, One-step fabrication in aqueous solution of a granular alginate-based hydrogel for fast and efficient removal of heavy metal ions, Journal of Polymer Research, 20(3) (2013) 1-10.

Yin N, Wang K, Xia YA, Li Z. Novel melamine modified metal-organic frameworks for remarkably high removal of heavy metal Pb (II). Desalination 2018; 430: 120-7.

Zhao B, Jiang H, Lin Z, Xu S, Xie J, Zhang A, Preparation of Acrylamide/Acrylic Acid Cellulose Hydrogels for the Adsorption of Heavy Metal Ions, Carbohydrate Polymers (2019), <https://doi.org/10.1016/j.carbpol.2019.115022>.

Zhang, Dongyue Lin, Lingtao Kong, & Jinhui Liu. (2017). Rapid adsorption of Pb, Cu and Cd from aqueous solutions by -cyclodextrin polymers. Applied Surface, Science <http://dx.doi.org/10.1016/j.apsusc.2017.07.103>.

Zetty Azalea Sutirman, Mohd Marsin Sanag, Khairil Juhanni Abd Karim, Ahmedy Abu Naim, & Wan Aini Wan Ibrahim. (2018). Chitosan-Based Adsorbents For The Removal Of Metal Ions From Aqueous Solutions. Malaysian Journal of Analytical Sciences, Vol 22, No 5, 839 – 850.
DOI: <https://doi.org/10.17576/mjas-2018-2205-11>.



Computational Fluid Dynamics Simulation of FCC Regenerator of a Refinery

* Usman, A. A¹, Onifade, K.R², Mohammed, I. A³, & Garba, M.U⁴

^{1,2,4} Chemical Engineering Department, Federal University of Technology, PMB 65 Minna Niger State, Nigeria

³ Chemical Engineering Department, University of Ilorin, Ilorin Kwara State, Nigeria

*Corresponding author email: abdullahialfa85@gmail.com +2348032606357

ABSTRACT

The aim of this study is to simulate a Fluid catalytic cracking (FCC) Regenerator, of a refinery using the Fluent Ansys.15 program. The commercial CFD code Ansys.15 was used for the Geometry, Meshing, model setup and solving. The results showed that the carbon solid mass content (used to represent the coke) decreases from 0.39 to 0.18. There was a significant amount of carbon dioxide formed after burning of and the temperature of the catalyst increased from 973K to 1570K which is a requirement for catalytic cracking inside the riser. There is also increase in temperature with increase with more combustion, a confirmation of an exothermic reaction. Model results were validated with both analytical and literature data, coke combustion, carbon monoxide and carbon dioxide formed were in agreement.

Keywords: *Computational Fluid Dynamics (CFD), Fluid Catalytic Cracking (FCC), Regenerator.*

1 INTRODUCTION

Petroleum refineries are large industrial facilities with complex processing units. The plant convert crude oils and other input streams into refined co-products such as liquefied petroleum gas (LPG), gasoline, jet fuel, kerosene, diesel fuel etc.

Different refineries have their unique physical design, operating characteristics and economics. These performance characteristics and design configurations are determined by availability of funds for capital investment, source crude oils, product quality requirements, demand, environmental regulations and standard.

Refining involves several processes which includes distillation, cracking, upgrading, treating, separation, blending and utilities.

Cracking processes involves chemical reactions that break large boiling point hydrocarbon molecule that have low economic value into smaller, lighter molecules which are blended after processing into gasoline, jet fuel, diesel fuel, petrochemical feedstock and other high value light products (Sadeghbeigi, 2012).

Cracking units form the important core of modern refining operations, this allows for high yields of transportation fuels and other valuable light products, provide operating flexibility for maintaining light product output.

The cracking processes of primary interest are Fluid Catalytic Cracking (FCC), hydrocracking and Coking.

The single most important refining process downstream of crude distillation is the FCC, this is so in terms of both industry-wide throughput capacity and its overall effect on refining economics.

The process operates at a high temperature and low pressure, it uses a catalyst to convert heavy gas oil from crude distillation to light gases and other petrochemical feedstock. In large transportation fuels oriented refinery, FCC accounts for about 45% of all gasoline (Almeida, 2016)

The FCC has several pieces of equipment but the prime focus of this paper is the regenerator.

The main function of the regenerator is to remove the coke, coke comprises of mainly carbon, it may contain from 3 to 12 wt-% hydrogen and a small amount of sulfur and organic nitrogen molecules (Palmas and Johnson, 2013). Also in the regenerator with the spent catalyst is a small fraction of hydrocarbon vapor that was not removed from the stripping section (Sadeghbeigi, 2012). The oxygen for the combustion of coke is from air which is supplied by one or more air blowers. The air enters the regenerator from the bottom through an air distribution system. The design of the air distributor is important for the unit efficiency and reliable catalyst regeneration (Sadeghbeigi, 2012).

The regenerator usually operate in a turbulent fluidization regimen and are characterized by two zones, the dense zone in the lower part where there is high solid



concentration and almost all coke is burned and the dilute zone with lower concentration of solid particles which was dragged to the top by the gas. The solid particles are separated from the gas by a two stage cyclone.

Fluid flows are governed by partial differential equations which represents conservation laws for the mass, momentum and energy. Computational Fluid Dynamics (CFD) software is widely used to solve these equations. CFD provides a qualitative and quantitative prediction of fluid flows by means of mathematical modeling, numerical methods and software tools.

It also allows chemical engineers to maximize equipment yield and enable petroleum engineers to devise optimal oil recovery strategies.

Important works have been published in the area of CFD simulation of FCC units. (Ahsan,2012) used commercial CFD to predict the mass fraction profiles of gas oil, gasoline, light gas and coke. (Sheng Chen et al, 2015) focused on the feedstock injection zone in a FCC riser. (Nazik et al, 2015) worked on the FCC regenerator of a local refinery in Khartoum. Their predictions showed good agreement with data and they captured secondary flow phenomena.

The aim of this research is to model and simulate the catalyst regeneration unit using the data of Kaduna Refinery and Petrochemical Company, Kaduna Nigeria. The simulated result will be analyzed and compared with operational data from literature, analytical data and also check the effectiveness of the unit.

2 METHODOLOGY

2.1 TOOLS

The FCC Regenerator is simulated using Fluent Ansys15 package. The FCC was simulated without a cyclone or air grid. Coke (assumed as solid Carbon) reacts with the oxygen in the air separately with an inflow of matrix represented by pure solid Aluminium and Silicon. The profiles for the velocity, pressure and temperature were evaluated to access the performance of the Regenerator.

2.2 METHODOLOGY

The CFD simulation involves four simple steps.

- i. Geometry: As shown in Figure. 1

Table i shows the actual dimensions of KRPC Regenerator with the exceptions of the inlet and outlet diameters.

The Geometry has been divided symmetrically as shown in Figure 2 (less meshing elements will be generated)

- ii. Mesh (allows for discretization and solving at nodes and elements)
- iii. Setup for the data
- iv. Solution setup before results is generated.

Mesh

The following named selections were applied and mesh generated as shown in Figure. 3

1. Catalyst inlet
2. Air inlet
3. Outlet
4. Symmetry
5. Fluid

The following selections were made for the meshing which are most suitable for this kind of turbulent process and computational capacity of the computer used.

Size Function is set to **Curvature**

Maximum face size **0.1m**

Inflation **Programmed Controlled**

Smoothing **High**

Body sizing is also inserted with element size of **0.1m**

Other items are left at default values

Generated Mesh had the following statistics

Elements: 1593271

Setup

The following sequence was followed for setup

GENERAL

Scale: Made sure all dimensions are in meters

Check: For minimum and maximum values.

Solver Type: Pressure based

Velocity Formulation: Absolute

Time: Steady

Gravity: Checked

Input the value of -9.81m/s^2 as the flow runs from the bottom to the top in the y direction.

MODELS

Energy: Checked

Viscous Model – **k-epsilon (2 eqn)** This is suitable for turbulent reactions

k-epsilon model – **Standard**

Near-wall Treatment – **Standard Wall Functions**

Species Model – **Species Transport**

Reactions – **Volumetric**

Turbulence-Chemistry Interactions – **Eddy Dissipation**

MATERIAL

Material Type: Mixture

The following were added from the fluent database

Aluminium solid Al<s>, Carbondioxide CO₂

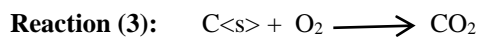
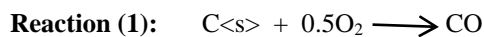
Carbonmonoxide CO, Carbon solid C<s>

Silicon solid Si<s>, Steel

These materials are the nearest elemental and compound composition to the catalyst.

REACTIONS

The following reactions were used



BOUNDARY CONDITIONS

Catalyst Inlet: Mass flow inlet

Turbulent intensity of 10% and mass fraction of 0.39 for C<s>

Other data for catalyst inlet is shown on Table 2.

Air Inlet: Mass flow inlet

Turbulent intensity of 10% and mass fraction of 0.23 for O₂

Other data for air inlet is shown on Table 3

Outlet: Pressure outlet

Symmetry: Symmetry

Wall Material: Steel

Solution Method: Coupled

SOLUTION

The solution is initialized

The calculation is run with 250 iterations

FIGURES AND TABLES

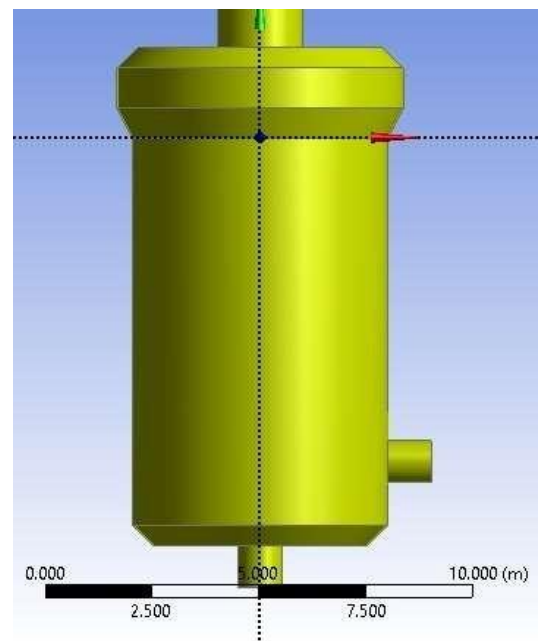


Figure 1: Full Geometry

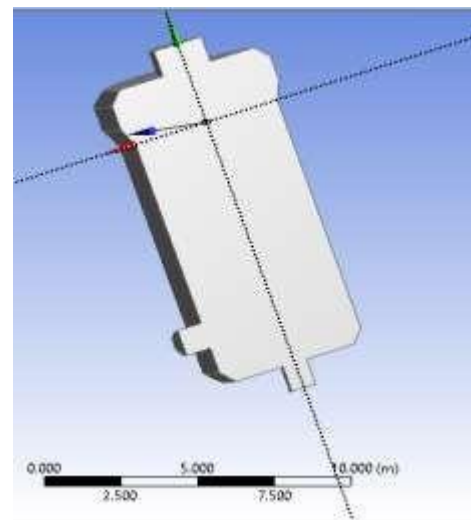


Figure 2: Symmetry of the Geometry



Figure 3: Mesh

Table 1. FCC Regenerator Dimensions

Parameters	
Length of regenerator (m)	12.45
Length of top section (m)	2.150
Length of middle section (m)	0.700
Length of bottom section (m)	9.600
Diameter of top section (m)	6.700
Diameter of bottom section (m)	6.000
Diameter of catalyst inlet (m)	1.000
Diameter of air inlet (m)	1.000
Diameter of outlet (m)	2.000

Table 2: Data for Catalyst Inlet

Parameter	Value
Mass flow rate (kg/s)	288
Pressure (kPa)	240
Hydraulic diameter (m)	1
Temperature (K)	973

Table 3: Data for Air Inlet

Parameters	Values
Mass flow rate (kg/s)	148
Pressure (kPa)	300
Hydraulic diameter (m)	1
Temperature (K)	473

3 RESULTS AND DISCUSSION

3.1 MESH INDEPENDENCE STUDY

Three (3) different mesh sizes were used for the solution, the mesh densities used were 1.6M, 1.2M and 0.9M. The results for the Carbon Solid Mass Fraction were the same for the three cases as shown in figure 4 below.

The mesh with 1.6M elements was selected for a finer and more accurate solution.

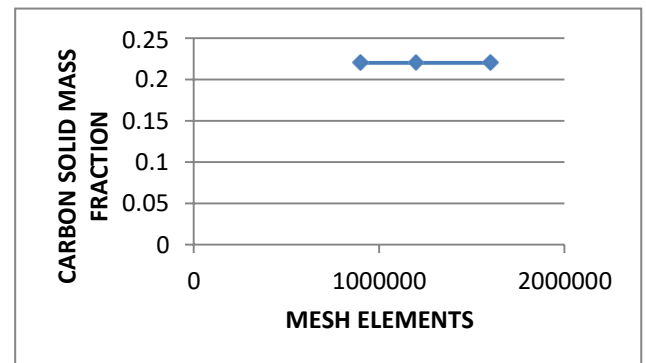


Figure 4: Plot of Mesh Independence Analysis

3.2 RESULTS AND DISCUSSION

The Results of the simulation and discussions are shown below.

Figure 5 shows the residual plot at the end of iterations. Figures 6a, b, c, d, e, and f shows the temperature, carbon solid, carbon dioxide, carbon monoxide, velocity and pressure contour profile respectively.

Details of the different component mass fractions, temperature, pressure and velocity at different regenerator heights (RH) are shown in tables 4 and 5 below.

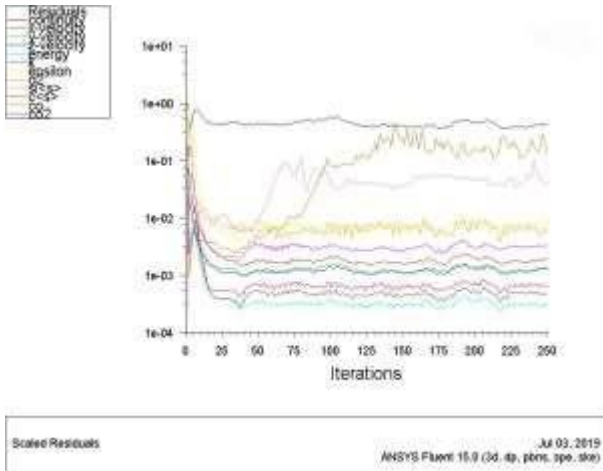


Figure 5: Residual Plot

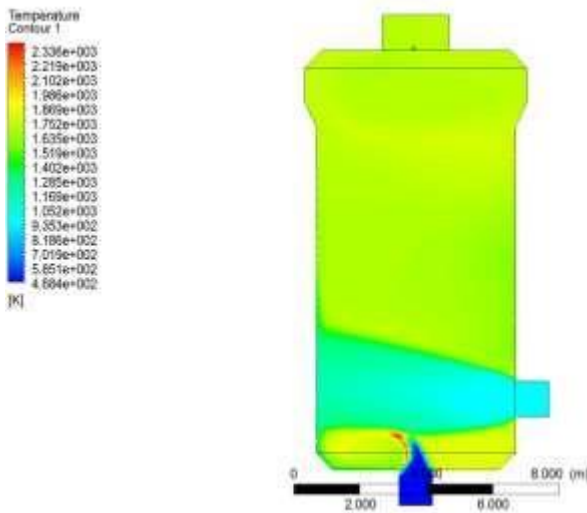


Figure 6a: Temperature Profile

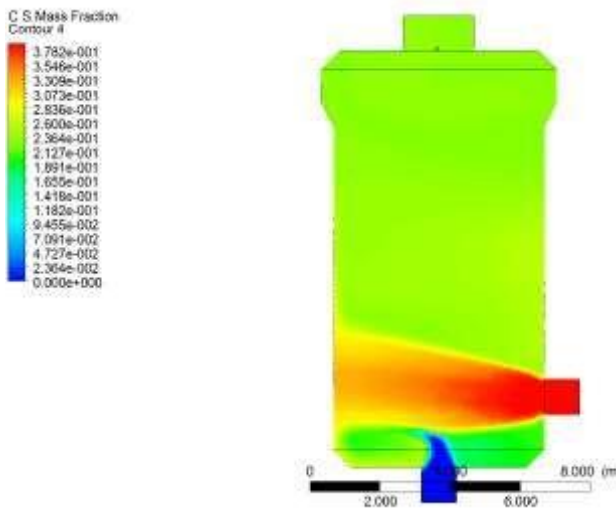


Figure 6b: Carbon solid profile

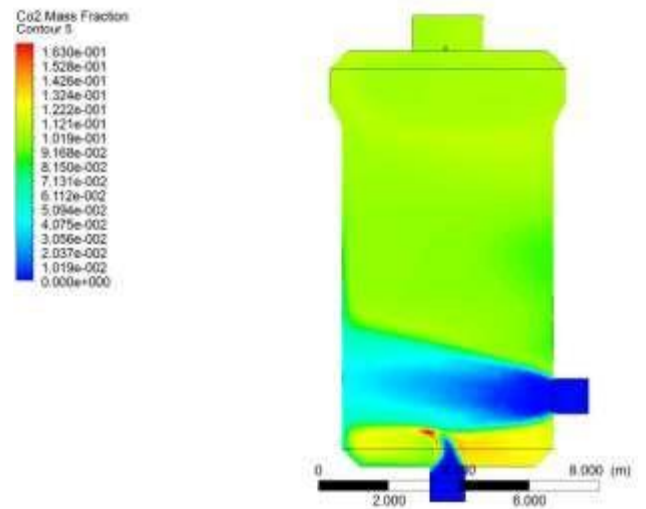


Figure 6c: Carbon dioxide profile

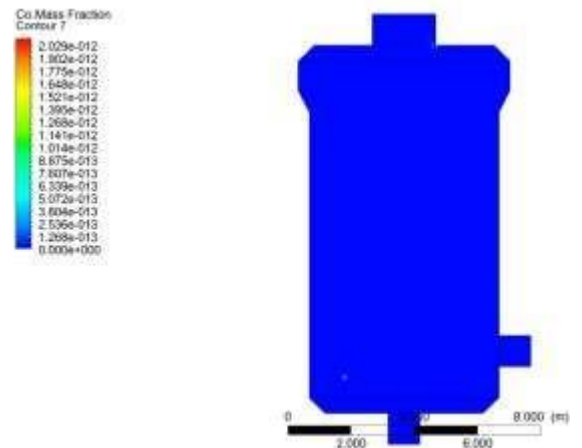


Figure 6d: Carbon monoxide profile

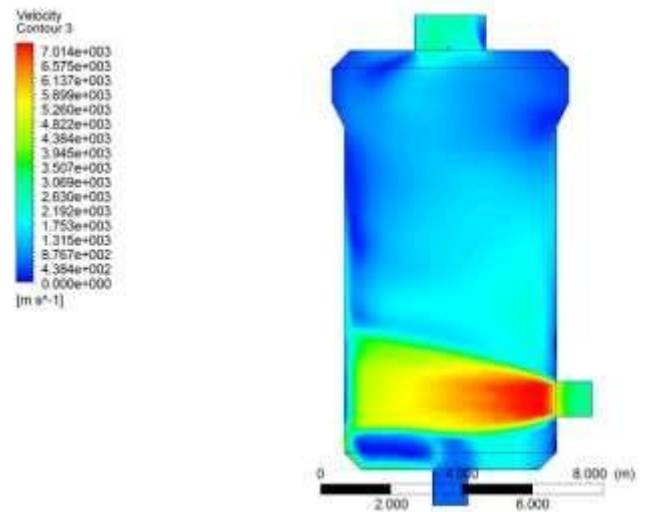


Figure 6e: Velocity profile

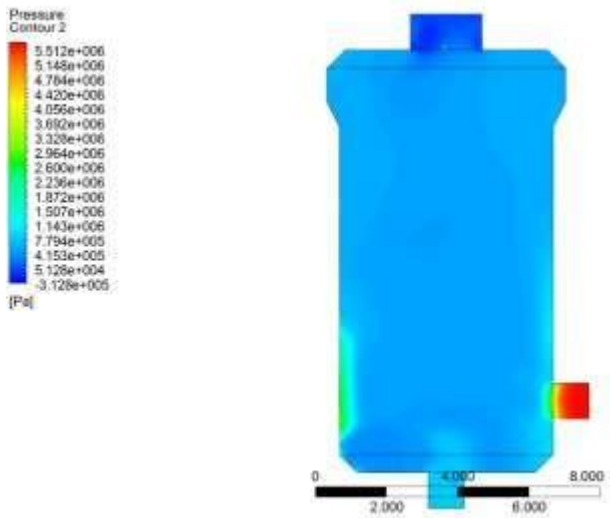


Figure 6f: Pressure profile

Table 4: Regenerator Height RH and Components Mass Fraction Data

RH (M)	CARBON M/F	CARBON MONOXIDE M/F	CARBON DIOXIDE M/F	OXYGEN M/F
0	0.00	0.00	0	0.23
0.5	0.00	0.00	0.01	0.22
1	0.32	0.00	0.05	0.00
1.5	0.34	0.00	0.03	0.00
2	0.36	0.00	0.02	0.00
2.5	0.35	0.00	0.03	0.00
3	0.32	0.00	0.05	0.00
3.5	0.23	0.00	0.1	0.00
4	0.23	0.00	0.1	0.00
4.5	0.24	0.00	0.1	0.00
5	0.24	0.00	0.1	0.00
5.5	0.24	0.00	0.1	0.00
6	0.24	0.00	0.1	0.00

6.5	0.24	0.00	0.1	0.00
7	0.24	0.00	0.1	0.00
7.5	0.23	0.00	0.1	0.00
8	0.23	0.00	0.1	0.00
8.5	0.23	0.00	0.11	0.00
9	0.22	0.00	0.11	0.00
9.5	0.23	0.00	0.11	0.00
10	0.23	0.00	0.1	0.00
10.5	0.23	0.00	0.1	0.00
11	0.23	0.00	0.1	0.00
11.5	0.23	0.00	0.1	0.00
12	0.23	0.00	0.1	0.00
12.5	0.23	0.00	0.1	0.00

Table 5: Temperature, Pressure and Velocity at Various Regenerator Heights RH

RH (M)	TEMPERATURE (K)	PRESSURE (Pa)	VELOCITY (m/s)
0	474	747460	623
0.5	573	748157	618
1	1205	591475	5325
1.5	1107	463847	5981
2	1058	494388	6038
2.5	1123	489648	5656
3	1248	493142	4506
3.5	1707	491188	1531
4	1694	492182	1707
4.5	1674	496357	1841
5	1670	498044	1666

5.5	1672	492714	1561
6	1674	482522	1536
6.5	1680	475887	1522
7	1690	476792	1478
7.5	1704	482490	1427
8	1722	491093	1374
8.5	1744	503393	1302
9	1772	506586	1169
9.5	1736	497882	1142
10	1708	490784	1171
10.5	1708	487259	1134
11	1711	459866	1265
11.5	1711	323190	1806
12	1711	105834	2425
12.5	1711	17215	2606

Results from the tables above were further analyzed using 2D plots for better interpretation.

The results from figure 7 below shows oxygen was completely used up after reacting with carbon, also there is a negligible amount of carbon monoxide after the combustion. The result also showed the carbon monoxide were mostly converted to carbon dioxide which confirms it is a complete combustion (Sadeghbeigi, 2012).

The result also showed most of the carbon dioxide were generated in the dense bed which is expected because that is where most of the combustion take place.

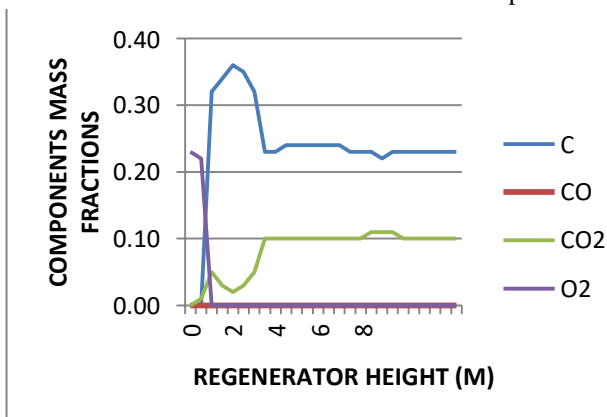


Figure 7: 2D Plot of Different Components Mass Fractions at Different Regenerator Heights.

Figure 8 below shows a significant drop in carbon content from dense bed where most of the combustion reaction takes place. However, it can be observed that the carbon content at the dilute phase is also high, this could indicate there is a high flow of carbon content flowing out with the flue gas.

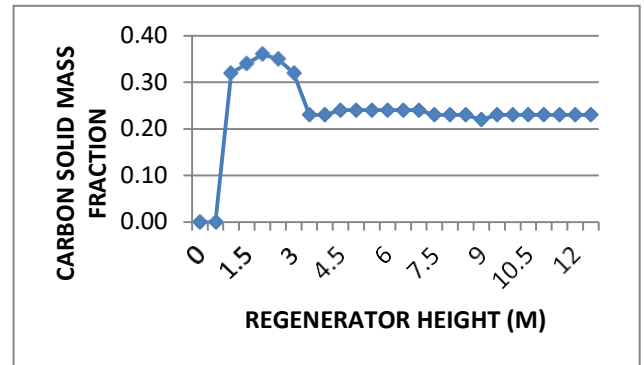


Figure 8: 2D Plot of Carbon Solid Mass Fractions at Different Regenerator Heights.

Results from figure 9 shows a temperature increase in the regenerated catalyst, this increase in temperature is a major requirement for the cracking reaction in the riser using the regenerated catalyst (Sadeghbeigi, 2012).

The result also shows more carbon dioxide is formed at the same temperature where there is maximum coke combustion. The result also showed as more carbon burned there is a net release of energy which gives rise to increase in temperature.

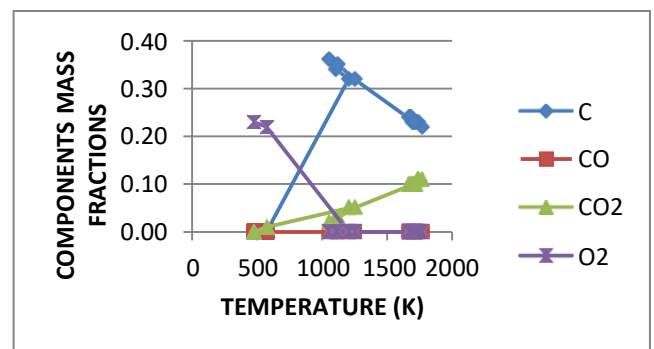


Figure 9: 2D Plot of Components Mass Fraction at Different Temperature.

Figure 10 below shows the different temperature distributions at different heights of the regenerator, the temperature increases at the point of mixing and combustion of carbon with oxygen and remains almost the same up to the top of the regenerator. This is expected as most of the reactions inside the regenerator are exothermic.

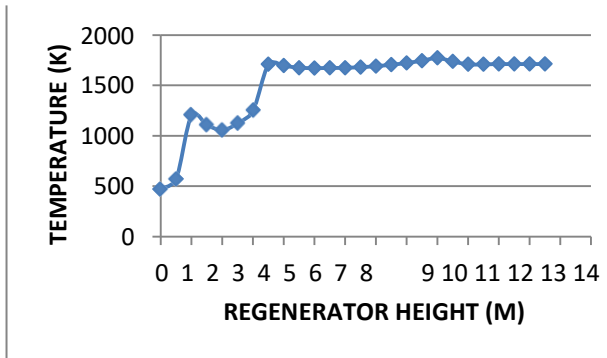


Figure 10: 2D Plot of Temperature at Various Regenerator Heights.

3.3 MODEL VALIDATION

The results of the flue gas outlet for the model were validated by comparing them with analytical data and literature data. The error margin of the carbon, carbon monoxide and carbon dioxide mass fraction between model data with analytical data is sufficient, also with literature. Error from temperature, and pressure could be as a result of different model assumptions and operational data like hydraulic diameter.

The model data validation is shown below.

Parameter	Model Data	Analytical Data (Nazik et al 2015)	% Error	Literature (Sadeghbeigi, 2012).
Temperature (K)	1711	1479	15	-
Pressure (Pa)	323 190	557 149	42	-
Velocity (m/s)	1806	295.7		-
Carbon Mass Fraction	0.23	0.23	0	<10% carbon reduction
Carbon monoxide Mass Fraction	0.00	0.00	0	0.00
Carbon dioxide Mass Fraction	0.10	0.13	23	unspecified

4 CONCLUSION

The CFD simulation for the fluid catalytic cracking regenerator has been done with data obtained from Kaduna Refinery and Petrochemical Company Kaduna. Ansys.15 CFD code was used for the simulation. Results of simulation showed similarity with data found from literature. The results also gave good results on carbon conversion and temperature inside the regenerator. The regenerated catalyst had an increase in temperature which is needed for the cracking reaction in the riser. Future work can be carried out on the model such as a temperature variation to investigate the burning of carbon and other operational bottlenecks such as catalyst attrition.

REFERENCE

1. Reza Sadeghbeigi, 2012, Fluid catalytic cracking hand book, An Expert Guide to the Practical Operation, Design and Optimization of FCC Unit, third edition, United States of America
2. Muhammad Ahsan, 2012, Computational fluid dynamics (CFD) prediction of mass fraction profiles of gas oil and gasoline in fluid catalytic cracking (FCC) riser, Ain Shams Engineering Journal, Volume 3, Issue 4, Pages 403-409.
3. Sheng Chen, Yiping Fan, Zihan Yan, Wei Wang, Jinghai Li, Chunxi Lu, 2015, CFD simulation of gas–solid two–phase flow and mixing in a FCC riser with feedstock injection Powder Technology, In Press, Accepted Manuscript, Available online 8 September 2015.
4. Nazik Abdullahi M.Ahmed, 2015, Computational fluid dynamics (CFD) simulation of a fluid catalytic cracking regenerator, University of Khartoum Engineering Journal, Volume 5, Issue 1, Pages 30-40.
5. Rashmi Pahwa, 2012 CFD Modeling of Fluid Catalytic Cracking Riser Reactor, Masters of Technology Thesis, Department of Chemical Engineering, Thapar University.
6. Juan David Alzate-Hernandez, 2016 CFD Simulation of an Industrial FCC Regenerator, Masters of Science Thesis, Chemical Engineering Department, University of Cambodia.
7. Varun Arasu, 2014, CFD Modeling and Simulation of FCC Riser, Masters of Technology Thesis, Department of Chemical Engineering, Indian Institute of Technology, ROORKEE India.
8. Miguel Andre Freire de Almeida, 2016, Modeling of Regenerator Units in Fluid Catalytic Processes, Masters of Science Thesis, Department of Chemical Engineering, University of Lisbon.
9. Ansys Fluent Tutorial Guide Release 18.0 January 2017.



Assessment of Factors Affecting Stakeholder Management in Nigeria Construction Projects

*Okosun, B. O¹, Idiake, J.E², Oyewobi, L.O³, & Shittu, A.A⁴

^{1,2,3,4}Quantity Surveying Department, Federal University of Technology, PMB 65 Minna Niger State, Nigeria

*Corresponding author email: blissing.odia@futminna.edu.ng, +2348033738630

ABSTRACT

Managing multiple stakeholders and maintaining an acceptable balance between their interests are crucial to successful project delivery. Several factors impede the management of stakeholders for sustainable construction projects. This study assessed 86 factors affecting stakeholder management which was sub grouped into 12 main factors. The study employed the use of questionnaires. Data gotten was analysed using reliability analysis, Mean Item Score and correlation matrix. The study found out that management, conflict and marginalization factors are significant factors to be considered and improved upon in future construction projects.

Keywords: *Construction, Factors, Management, Projects, Stakeholders*

1 INTRODUCTION

Construction projects are traditionally divided into series of operations undertaken by different individuals or groups who may have different levels of interest in the project (Heravi et al., 2015). Therefore, the process of design and execution of construction projects constitutes a complex system which involves collaboration and negotiations among many stakeholders. Managing multiple stakeholders and maintaining an acceptable balance between their interests are crucial to successful project delivery (Takim, 2009; Jurbe, 2014).

Disagreement among stakeholders during the implementation of projects adversely affects the ability of the management teams to deliver the construction project within the time and allocated budget and expected degree of quality. These disagreements are often caused by inappropriate identification and management of the different stakeholders involved (Olander and Landin, 2005).

Conflicting objectives among the project stakeholders impede the achievement of best value in construction projects (Aapaoja and Haapasalo 2014). Karlsen (2002) considered poor management of stakeholders to be a recipe for potential and serious challenges that are often associated with construction projects. These problems include factors such as incessant change order in scope of work, poor definition of work and scope, poor allocation of scarce resources to projects, poor communication, conflicts and controversies which are majorly the origin of delays and attendant time and cost overruns.

Despite several contributions on management of stakeholders in the construction industry, several studies point towards critical success factors hence boycotting the root problems that contribute to poor stakeholder management (Jergeas et al., 2000; Chinyio and Akintoye, 2008; Olander and Landin, 2008; Yang et al., 2009; Jepsen

and Eskerod, 2009; Li et al., 2011). Contributing factors also appear limited in literature (Karlsen (2002), thereby considering more in-depth studies to be done in this area as stipulated by (Golder and Gawler, 2005).

Therefore a need arises to assess the factors that affect stakeholder management on construction projects in Nigeria.

2 METHODOLOGY

A Quantitative research approach was adopted for this study. The scope of the study was limited to North Central Nigeria and higher institutional construction projects were the focal point of the study. Internal stakeholders within the eight (8) sampled institutions in the study area were selected using stratified and purposive sampling techniques. 210 questionnaires were self-administered on the respondents while 170 were returned giving an 81% response rate which was very suitable for the study.

Data gotten for the study was analyzed using Mean Item Score, reliability analysis and correlation matrix. The results were discussed and conclusions were drawn for the study.

3 RESULTS AND DISCUSSION

A reliability analysis was done to check the internal consistency and reliability of the data. The Cronbach's Alpha coefficient of 0.70 (DeVellis, 2003) was used as the indicator. Table 1 shows that the alpha value of 0.842 is greater than 0.70 which suggest a very good internal consistency reliability for the scale.

TABLE 1: RELIABILITY ANALYSIS

Cronbach's Alpha	Cronbach's Alpha Based	N of Items
0.836	0.842	10

TABLE 2: FACTORS AFFECTING STAKEHOLDER MANAGEMENT

Coding	Factors	Mean	Std. Dev.	Rank
OGF	Management factors	3.77	0.67	1
COS	Conflict management factors	3.76	0.63	2
COF	Communication factors	3.72	0.61	3
MGF	Cost factors	3.65	0.61	4
STE	Relationship factors	3.65	0.67	5
CMF	Contractual factors	3.63	0.60	6
STR	Stakeholder requirements	3.61	0.61	7
REF	Organization factors	3.61	0.55	8
CTF	Stakeholder Engagement	3.58	0.69	9
MAR	Marginalization	3.24	0.85	10

Table 2 showed the factors affecting stakeholder's management on construction projects. Management related factors ranked first with a mean item score of 3.77, followed by conflict management factors with a mean of 3.76. Next in line was communication factors and cost factors with mean scores of 3.72 and 3.65 respectively. This is in agreement with the findings of Aaltonen and Kujala (2010) that conflicts have a resultant effect on stakeholder management which affects the overall success of a project. However marginalization factor ranked least with a mean of 3.24. This particular factor adds contribution to knowledge that agrees with Golder and Gawler (2005) that gender is an important factor to be considered in stakeholder management as this affects the performance of a project.

The results in Table 3, 4 and 5 give a detailed breakdown of the most significant factors that affect stakeholder management which calls for attention for future construction projects.

TABLE 3: MANAGEMENT RELATED FACTORS

Management Related Factors	Mean	Rank
Inadequate Planning, coordinating and programming	3.92	1
lack of wide and deep knowledge / understanding of the concepts of project and stakeholder management by stakeholders	3.86	2
Poor feedback mechanism	3.77	3
Poor strategies to manage stakeholder responsibility	3.71	4
Lack of technical capacity and support on the part of the stakeholders	3.69	5
stakeholder competencies	3.66	6
Decision making problems	3.66	7
Difficulty in identifying stakeholders	3.59	8
Lack of ability to understand the implications of the project	3.55	9
non - existence of formal / systematic process of project stakeholder management	3.55	10
lack of knowledge about stakeholder groups and their expertise	3.54	11
inability to clearly identify the attitudes of stakeholders either positively or negatively towards the project	3.53	12

The results in Table 3 showed the management related factors that affect stakeholder management. Inadequate planning, coordinating and programming, lack of wide and deep knowledge / understanding of the concepts of project and stakeholder management by stakeholders, Poor feedback mechanism most affect stakeholder management in management related factors with a mean score of 3.92, 3.86 and 3.77

TABLE 4: CONFLICT RELATED FACTORS

Conflict Related factors	Mean	Rank
poor approaches in solving conflict and controversies among stakeholders	3.86	1
poor implementation and non adherence to conflict contract condition by project stakeholders	3.84	2
Consequences of mismanagement of stakeholders	3.67	3
different perceptions of the same issue	3.53	4
Analyzing conflicts and coalition among stakeholders	3.33	5

The conflict related factors in Table 4 showed that there are poor approaches in solving conflicts amongst stakeholders which ranked 1st with a mean score of 3.86, followed by poor implementation and non-adherence to conflict contract condition by project stakeholders, Consequences of mismanagement of stakeholders, different perceptions of the same issue, and Analyzing conflicts and coalition among stakeholders with mean scores of 3.86, 3.84, 3.67, 3.53 and 3.33 respectively. The findings agree with Olander and Landin (2005) and Jurbe (2014) that disagreements amongst stakeholders can have adverse effect on construction project as a whole.

TABLE 5: MARGINALIZED RELATED FACTORS

Marginalization Factors	Mean	Rank
Poor incentives and benefits	3.73	1
influence of the stakeholders	3.52	2
Type of stakeholder (indigenous, foreign, etc)	3.31	3
sensitivity of stakeholders	3.30	4
social and economic characteristics of the stakeholder.	3.28	5
the position of the stakeholders in the project	3.21	6
discrimination of gender	3.12	7
status of stakeholders	3.05	8
potentials of men and women in the stakeholder group	3.05	9
gender inequalities	3.01	10
volume of allocation of task to men and women	3.01	11
Gender differences	2.91	12

As seen in Table 5, poor incentives and benefits, influence of the stakeholders, type of stakeholders, sensitivity of stakeholders, ranked highest with mean scores of 3.73, 3.52, 3.31 and 3.30 in that order. However, volume of allocation of task to men and women, Gender

differences ranked the least with mean scores of 3.01 and 2.91 respectively. These are new findings and are lacking in the findings of Yogita (2016), hence call for consideration for future projects.

TABLE 6: CORRELATION MATRIX OF FACTORS

Inter-Item Correlation Matrix										
Factors	M G F	C M F	C O F	C O S	R E F	C T F	S T R	O G F	S T E	M A R
Management factors	1	0.6	0.4	0.3	0.2	0.2	0.3	0.2	0.2	0.2
Conflict management factors	0.6	1	0.6	0.3	0.2	0.3	0.3	0.3	0.3	0.2
Communication factors	0.4	0.6	1	0.5	0.4	0.4	0.3	0.3	0.3	0.1
Cost factors	0.3	0.3	0.5	1	0.6	0.3	0.3	0.3	0.4	0.2
Relationship factors	0.2	0.2	0.4	0.6	1	0.6	0.4	0.4	0.4	0.3
Contractual factors	0.2	0.3	0.4	0.3	0.6	1	0.7	0.4	0.3	0.3
Stakeholder requirements	0.3	0.3	0.3	0.3	0.4	0.7	1	0.4	0.3	0.3
Organization factors	0.2	0.3	0.3	0.3	0.4	0.4	0.4	1	0.5	0.4
Stakeholder Engagement	0.2	0.3	0.3	0.4	0.4	0.3	0.3	0.5	1	0.4
Marginalization	0.2	0.2	0.1	0.2	0.3	0.3	0.3	0.4	0.4	1

Table 6 showed the correlation matrix of the variable factors. 12 major factors were analyzed. From the result it can be seen that the value of 1.0 is above 0.70 which was used as the indicator. This implies that there is a strong significant relation among the variables and that these factors studied affect stakeholder management.

4 CONCLUSION

The study concluded that management related factors, conflict, communication and cost factors have a significant effect on the stakeholder management of construction projects. However, a new contribution to knowledge is being made on additional factor such as marginalization factor which is lacking in other studies. These factors calls for serious considerations for future construction projects.

In order to improve the management of stakeholders on projects, the study recommended that a management support group should be put in place to manage stakeholders, adherence to conflicts contract conditions



and consideration of gender in stakeholder analysis. These will improve construction performance for future projects.

This study is part of a doctoral research and hence further research in the aspect of developing a model that will curb these factors assessed to enhance project success, is in view. The researcher acknowledges the efforts of the supervisory committee which contributed to the success of this paper.

REFERENCE

- Aaltonen, K., and Kujala, J. (2010). A Project Lifecycle Perspective on Stakeholder Influence Strategies in Global Project. *Scandinavian Journal of Management*. 26 (4), 381 - 397.
- Aapaoja, A., and Haapasalo, H. (2014). A Framework for Stakeholder Identification and Classification in Construction Projects. *Journal of Business and Management*. 2, 43 – 55.
- Chinyio, E. and Akintoye, A. (2008). Practical Approaches for Engaging Stakeholders: Findings from the UK, *Construction Management and Economics*, 26 (6), 591-599.
- Heravi, A., Coffey, V., and Trigunaryyah, B. (2015). Evaluating the Level of Stakeholder Involvement during the Project Planning Processes of Building Projects. *International Journal of Project Management*. Elsevier 20, 1 – 13.
- Jepsen, A.L. and Eskerod, P. (2009). Stakeholder analysis in projects: Challenges in using current guidelines in the real world. *International Journal of Project management*, 27, 335-343.
- Jurbe, J.M. (2014). Stakeholder Management in Construction Projects: A Life Cycle Based Framework. Published Phd Thesis. Heriot Watt University, Edinburgh.
- Karlsen, J.T. (2002). Project Stakeholder Management, *Engineering Management Journal*, 14 (4), 19-24.
- Olander, S. & Landin, A. (2005). Evaluation of Stakeholder Influence in the Implementation of Construction Projects, *International Journal of Project Management*, 23 (4), 321-328.
- Olander, S. and Landin, A. (2008). A comparative studies of factors affecting the external stakeholder management process, *Construction Management and Economics*, 26(6), 553.
- Takim, R. (2009). The Management of Stakeholders' Needs and Expectations in Needs and Expectations in the Development of Construction Project in Malaysia. *Modern Applied Science*, 3 (5), 167-175.
- Yang, J., Shen, Q., and Ho, M. (2009). An Overview of Previous Studies in Stakeholder Management and its Implications for Construction Industry. *Journal of Facilities Management*, 7 (2), 159 – 175.



EFFECT OF PARTIAL REPLACEMENT OF FINE AGGREGATE WITH SAWDUST IN LIGHT WEIGHT CONCRETE PRODUCTION USING BIDA NATURAL STONE AS COARSE AGGREGATE

Alhaji B.¹, Abubakar M.¹, Yusuf A.¹, Oritola S. F.¹, Mohammed S.¹ and Kolo D. N.¹

¹Department of Civil Engineering, Federal University of Technology, Minna
E-mail: balhaji80@yahoo.com

ABSTRACT

This study investigated the effect of sawdust as partial replacement for Fine Aggregate in light weight concrete production. Sawdust was used to replace Fine Aggregate from 0% to 40% in steps of 5%. 150 x 150 x 150mm concrete cubes were cast for each replacement level, the concrete was cured and the compressive strengths were determined at 7, 21 and 28 days curing period respectively. Increase in percentage of sawdust in concrete led to a constant reduction in the compressive strength values with a corresponding reduction in weight. From the result obtained, 5% replacement of Fine Aggregate with sawdust gave a maximum compressive strength 13.11 N/mm². It was however concluded that the optimum replacement level of 5% can be used as plain concrete for blinding works.

Keywords: Bida, Compressive Strength, Light Weight Concrete, Sawdust

1. INTRODUCTION

The overall relevance of concrete in virtually all Civil Engineering Practice and Building Construction Works cannot be overemphasized (Adewuyi and Adegoke, 2008). Concrete is a combination of cement, aggregates and water, which are mixed in a right proportion to arrive at the strength. The cement and water react together chemically to form a paste, which binds the aggregate particles together. The mixture sets into a rock-like solid mass, which has considerable compressive strength but little resistance to tension (Agbede and Menessh, 2009). However, the construction industry relies heavily on conventional materials such as cement, granite and sand for the production of concrete. The high and increasing cost of these materials has greatly hindered the development of shelter and other infrastructural facilities in developing countries (Olutoge, 2010). Scientists,

Engineers and Technologists are continuously on the lookout for new materials which can be used as substitutes for conventional materials, especially where their properties would enable their use in new designs and innovative applications. There is also an increasingly awareness of the need to re-use or recycle waste. The growing concern of resource depletion and global pollution has challenged many researchers and engineers to seek and develop new materials relying on renewable resources. These include the use of by-products and waste materials in building construction. Many of these by-products are used as aggregates for the production of light weight concrete (Adewuyi and Adegoke, 2008). The most widely used fine aggregate for the making of concrete is the natural sand mined from the river beds. However, the availability of river sand for the preparation of concrete is becoming scarce due to the excessive nonscientific methods of mining from the river beds, lowering of water table and sinking of the bridge piers among others, is becoming common treats (Mageswari and Vidivelli, 2010). The Worldwide consumption of sand as fine aggregate in concrete production is very high and



several developing countries have encountered some strain in the supply of natural sand in order to meet the increasing needs of infrastructural development in recent years (Divakar *et al.*, 2012). Nonetheless, accumulation of unmanaged wastes especially in developing countries has resulted in an increasing environmental concern. However, the increase in the popularity of using environmental friendly, light weight construction materials in building industry has brought about the need to investigate how this can be achieved by benefiting environment as well as maintaining the material requirements affirmed in the standards. Sawdust is an industrial waste in the timber industry constitute a nuisance to both the health and environment when not properly managed (Elinwa and Abdulkadir, 2011). Wood sawdust wastes are accumulated from the countries all over the world and cause certain serious environmental problems and health hazards. Generation of wood waste in sawmill is an unavoidable hence a great efforts are made in the utilization of such waste (Zziwal *et al.*, 2006). Thus, this research investigates the potential use of wood sawdust wastes to produce a low cost and light weight concrete for construction and engineering purpose.

2. MATERIALS AND METHOD

2.1 Sourcing of materials

The sawdust for this study was collected from a saw mill point at Gidan Kwano, opposite Federal University of Technology Minna, Niger State Nigeria. The sample was carefully collected to avoid mixing with the sand. The natural stones of maximum size of 20mm used as coarse aggregate were obtained from Bida Niger state, Nigeria. Natural sand (having smooth and more rounded particles) passing sieve 5mm used and was collected from a river bed at Gidan Kwano road, Federal University of Technology Minna, Niger State. For use in this concrete production, it was ensured that the sand was clean, sound and well graded according to requirement set by BS812, 1990. Ordinary Portland cements (OPC) conforming to BS12, 1996 was used.

Dangote was used being the most widely recommended material of its kind. Bags of the cement were bought at a retail store in Minna, Niger State.

The water which is used for mixing the materials was obtained from a borehole at Gidan Kwano Campus which confirmed to BS3148 (1980) requirements. Therefore, the water is fit for drinking, free from suspended particles and organic materials which might affect hydration of cement.

2.2 Sample preparation

Prior to mixing of the concrete components, tests such as specific gravity tests, moisture content, particle size analysis, loose and compacted bulk density tests, water absorption of aggregates were conducted on sand, saw-dust and gravel. Fine aggregates, cement, sawdust, and water were mixed to form a paste (on which slump and compacting factor tests were conducted) which used to fill the voids around the coarse aggregates. A chemical process called hydration occurred which transformed the semi- liquid mass into a hard, strong engineering material. In this investigation, sawdust was used as partial replacement for the fine aggregate (sand). This work attempts to establish that the mixture of cement, sand – sawdust and gravel might have an equal advantage as the standard mix of cement, sand and gravel. Both mixes are in the proportion 1: 2: 4 (cement, fine aggregate and coarse aggregate) respectively. Eighty one cubes were cast with the same volume proportions. After placing in 150 x 150x 150mm moulds, they were left to set for 24 hours, and kept afterwards in a curing tank. The cured samples were tested after 7, 21 and 28 days for compressive strengths in accordance with BS1881, 1983.



3.0 RESULTS AND DISCUSSION

Table 1: Physical properties of Constituent Materials

Properties	Sawdust	Sand	Gravel
Loose bulk density (g/cm ³)	1.225	1.264	1.367
Compacted bulk Density (g/cm ³)	1.414	1.415	1.488
Water content (%)	7.79	6.19	1.57
Water absorption (%)	14.95	13.55	5.07
Specific gravity	1.37	2.66	2.17

Specific gravity value of 1.37 place the sawdust in the same category as lightweight aggregate while the specific of the sand and the gravel place them in the category of common rock group whose gravities range from 2.62- 3.00 (Neville, 2000). However, the loose and compacted bulk densities for both

Sawdust and that of sand are relatively the same, which makes the two material complimentary. Saw dust was found to have a greater water content value than sand with the difference in the region of 0.19%. This, thus, will cause a reduction in the workability of the fresh concrete.

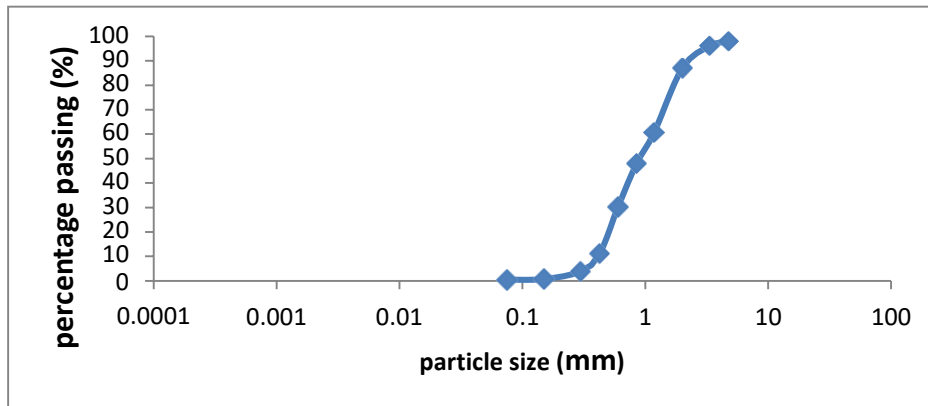


Figure 1: Particle Size Distribution Curve for Saw dust

It can be seen from the particle size distribution that the sawdust can act as sand and even as minerals fillers by virtue of the distribution.



Table 2: Result of Compressive Strength Test

% Replacement	7 Days Curing	21 Days Curing	28 Days Curing
0	15.69	21.82	26.27
5	9.20	12.58	13.11
10	6.31	5.73	7.4
15	4.09	5.20	5.42
20	2.98	4.13	5.40
25	2.76	3.02	3.24
30	2.40	2.76	2.93
35	2.09	2.31	2.53
40	1.60	2.13	2.22

It is seen from Table 2 that for control cube, the compressive strength increased from 15.69N/mm² at 7days to 26.27N/mm² at 28 days (about 10.58% increment). This is equivalent to grade 25 concrete that has a specified value of 25N/mm² (BS 8110, 1997). The 10% replacement sample gave a value of 7.4N/mm² at 28days which is equivalent to grade 7 concrete that has a value of 7N/mm² specified for plain concrete. It could also be observed that the weight of the cube reduced from 8.5kg for 0% replacement to 7.53kg for 10% replacement at 28 days, which is about 20% reduction in weight. This is evident that presence of sawdust in concrete hinders strength development of cement, thus causing decrease in the compressive strength.

4. CONCLUSION

From the results of the physical and mechanical property test conducted, it was concluded that sawdust is a light weight aggregate which is in agreement with the work of Mageswari and Vidivelli (2010) and thus, could be used as partial replacement for sand in plain concrete for blinding work.

However, to achieve best result in the use of sawdust in concrete production, optimum replacement level of 5% is recommended. It is also recommended that further works should be conducted with varying w/c ratios to determine the optimum.

REFERENCES

- Adeyuyi A.P & adegoke T., (2008). Exploratory study of periwinkle shells as coarse aggregate in concrete works. *Journal of Applied Sciences Research*, 4 (12), 1678-1681.
- Agbede O.I and Monash J. (2009). Suitability of periwinkle shell as partial Replacement for Gravel in Concrete. *Leonardo Electronic Journal of Practice and Technologies*, (15), 56-66.
- BS 812: part 2 (1990), Physical properties of aggregate. British Standard Institution, Her Majesty Stationary office London
- BS 812 (1990), Physical properties of aggregate. British Standard Institution, Her Majesty Stationary office London
- BS 8110: Structural use of concrete; Part 1: Code of practice for design and construction, 1997; Part 2: Code of practice for special circumstances, 1985; British Standards Institute, London
- BS 1881 Part 116 (1983). Method for Determining Compressive Strength of Concrete Cubes, British Standard Institution, Her Majesty Stationary office London
- BS 3148 (1980). Specification for concrete water. British Standard Institution, Her Majesty Stationary office London
- Divatar Y., Manjunath S., & Aswath M. U., (2012). Experimental Investigation on Behaviour of Concrete Fines. *International Journal of Advance Engineering Research*, 1 (4), 23-30
- Elinwa A.U & Abdulkadir S., (2011). Characterizing Saw Dust Ash for Use as an Inhibitor for Reinforcement Corrosion. *New Clues in Sciences*, 1, 1-10



3rd International Engineering Conference (IEC 2019)
Federal University of Technology, Minna, Nigeria



-
- Mageswari M. & Vidivelli B., (2010). The Use of Sawdust Ash as Fine Aggregate Replacement in Concrete. *Journal of Environment Research and Development*, 3 (3), 720-726.
- Mageswari M. & Vidivelli B., (2010). The Use of sheet Glass Powder as Fine Aggregate Replacement in concrete. *The open Civil Engineering Journal*, 4, 65-71.
- Marthong C. (2012). Size Effect study of Saw Dust Ash Concrete under compressive load. *IOSR Journal of mechanical and Civil Engineering (IOSRJMCE)*, 2(5), 27-32.
- Murali G. & Ramkumar V.R. (2012). Properties of Concrete with partial Replacement of Coarse Aggregate. *International Journal of Emerging Trends in Engineering and Development*, 4 (2), 585-589.
- Neville A.M. (2000). Properties of Concrete. 4th Edition, Pitman Publishing Ltd, 39 parker Street, London
- Olotoge F.A (2010). Investigations on Sawdust and Plam kernel Shells as Aggregate Replacement. *ARP Journal of Engineering and Applied Sciences*, 5 (4) 8-12.
- Turgut P. & Algin M.H. (2012). Lime Dust and Wood Sawdust as Brick Materials. *Building and the Environment*. 42, 3399-3403.
- Turgut P. (2007). Cement Composite with Limestone Dust and Different Grades of Wood Sawdust. *Building and Environment*, 42, 3801-3807

Quality Assessment of Locally Available Selected Cements in Nigeria

*Muftau, O. S¹, Abdullahi, M¹, & Aguwa, J. I¹

¹Department of Civil Engineering, Federal University of Technology, PMB 65 Minna Niger State, Nigeria

*Corresponding author email: salawumuftau@gmail.com, +2348185783380

ABSTRACT

The study assessed the quality of three major selected cement brands in Nigeria, designated as A, B and C. The chemical composition, standard consistence and setting time and compressive strength of the cement were determined. The percentage compositions of the major oxides of the brands are within the ranges stipulated by BS EN 196-2:1995. The mineral compositions indicated that C₃S in A and B were within the stipulated range for general purpose cement, but for C, C₃S is higher than the stipulated limit. On the other hand, C₂S of C brand fell short of the limit. The percentage compositions of C₃A and C₄AF were within the stipulated range for the three brands. The initial setting time of samples were between 80 and 100 minutes. The compressive strengths of the cements were 22.6 N/mm², 21.43 N/mm², and 24.28 N/mm² at 7 days; and 35.84 N/mm², 36.88 N/mm², and 34.22 N/mm² at 28 days respectively, these satisfied the requirements for high early strength (≥ 16.0 N/mm² at 7 days) and for normal strength development (≥ 32.5 N/mm² and ≤ 52.5 N/mm² at 28 days) classes of cement. The early highest strength observed in C was attributed to high percentage composition of C₃S. At 28 days, B had highest strength due to the significant high percentage composition of C₂S which was responsible for high strength at later age. Hence, this study established that the three brands are suitable for use in normal construction works as they relatively comply with the relevant standards.

Keywords: *Compressive strength, mineral composition, ordinary Portland cement, quality assessment.*

1 INTRODUCTION

Concrete is an indispensable construction material and employed in most infrastructure such as buildings and roads (Cao, 2012). Cement is one of the major basic constituents of concrete, others are aggregates and water; it acts as a hydraulic binder in concrete. Cement chemistry dictates the chemistry of concrete and influences the quality of the concrete so produced with it (Taylor, 1997; Olonade *et al.*, 2015). The use of concrete in the construction industry is widespread. Nigeria has been witnessing massive infrastructural development in the recent years where a lot of housing projects are springing up with concrete structures. Despite this development, many concrete structures have suffered from lack of durability and have exhibited signs of distress even though they are within their design life (Gambhir, 2013).

Structural failure remains challenging in our society today, several efforts have been made in ensuring that these failures are minimized. In recent years, Nigeria has witnessed frequent cases of collapsed building; several cases of such collapses are being recorded in many parts of the country claiming several lives (Adegoroye, 2010; Adewole *et al.*, 2014). Omoniyi and Okunola (2015) averred that the use of poor materials is the leading cause of frequent collapse of buildings in Nigeria. However, since cement is a major constituent in concrete or reinforced concrete (RC) for building construction and the major role played by cement in ensuring structural integrity of a building marks it out as the first culprit in building collapse.

One of the most important considerations to make before embarking on the construction of a building is the cement that would be used; the commonest type of cement used across the world is Portland cement (Omoniyi and Okunola, 2015). The primary reason for its global use is its composition and essential characteristics in the setting and hardening of the concrete, durability when dry, fire-proof nature, effective protection of iron or timber structures, ability to prevent corrosion, its use in ships, tanks and bunkers. About 90 - 95% of Portland cement is composed of four main cement minerals, tricalcium silicate (C₃S), dicalcium silicate (C₂S), tricalcium aluminate (C₃A) and tetracalcium aluminoferrite (C₄AF) with each of them playing different roles in the hydration process that converts the dry cement into hardened cement paste (Tennis and Bhatt, 2005). About 5 – 10% of the remaining compositions are calcium sulphate, alkali sulphates, unreacted calcium oxide, magnesium oxide and other minor constituents left over during the clinkering and grinding steps (Taylor, 1997; Omoniyi and Okunola, 2015).

Olonade *et al.* (2015) averred that the quality of cement may differ from plant to plant due to changes in raw material properties, kiln temperatures, as well as fineness upon grinding. These changes can significantly affect the concrete properties, when different cements are used. The quality information presently available on the bag of different brands of cement as given by the producers is not adequate to enable an assessment of the behaviour of cement in a concrete mix. For instance, setting behaviour of the cement is not highlighted on the container of these cements. Recently, poor quality of

cement has been implicated as one of the major causes of incessant building collapses in Nigeria (The Nation Newspaper, 2014). The need for regular sampling and testing of cement becomes imperative. Hence, research in this direction is not only timely but may also serve as a basis for many contractors to select appropriate cement for their construction works. Therefore, the present study aims at assessing the quality of three major selected cement brands in Nigeria by determining the chemical composition of the locally produced cement brands; the physical properties of the cement; and the compressive strength of the cement.

2 METHODOLOGY

2.1 MATERIALS

The materials used in achieving the objective of the study include potable water which was gotten from the Civil Engineering Department, Federal University of Technology, Minna. The water satisfied the requirement outlined in BS EN 1008:2002 being colourless, odourless, tasteless and free from organic matter of any type. The fine aggregates used was river sand obtained from Minna. It was sieved through 5 mm sieve to take away any impurities and larger size aggregates in accordance to BS 882:1992. The three brands of Portland cement were chosen and used based on availability and popularity, these brands were designated as A, B and C samples respectively. A bag of each of these cement brands was collected from the retail shops of the cement dealers around Minna, Niger State. This was to ensure that the sample used is true representative of what most construction sites use.

2.2 SAMPLE PREPARATIONS

2.2.1 Chemical composition of the cements

The cement samples were analysed to determine the oxide composition of the cements. This was conducted at the Chemistry Laboratory, Ahmadu Bello University, Zaria, Kaduna State. The mineral compositions were determined using X-Supreme 8000, an innovative X-Ray Fluorescence analytical solution from Oxford Instruments. The mineral compositions of the cement products were evaluated from the oxide concentrations of the cement using Bogue's equation in accordance with ASTM C 150 as follows:

$$C_3S = (4.071 \times \% CaO) - (7.600 \times \% SiO_2) - (6.718 \times \% Al_2O_3) - (1.430 \times \% Fe_2O_3) - (2.852 \times \% SO_3) \quad (1)$$

$$C_2S = (2.867 \times \% SiO_2) - (0.7544 \times \% C_3S) \quad (2)$$

$$C_3A = (2.650 \times \% Al_2O_3) - (1.692 \times \% Fe_2O_3) \quad (3)$$

$$C_4AF = 3.043 \times \% Fe_2O_3 \quad (4)$$

When performing chemical analyses of Portland cement, relationship existing between the percentage of lime on one hand and the combination of silica, alumina and iron oxide on the other are expressed in terms of Lime Saturation Factor (LSF), Silica Ratio (SR) and Alumina to Iron ratio (AF). These parameters were calculated from oxide concentrations using (Sam *et al.*, 2013; Alemayehu and Sahu, 2013; Omoniyi and Okunola, 2015):

$$LSF = \frac{100(CaO + 0.75MgO)}{2.85SiO_2 + 1.18Al_2O_3 + 0.65Fe_2O_3} \quad (5)$$

$$SR = \frac{SiO_2}{Al_2O_3 + Fe_2O_3} \quad (6)$$

$$AR = \frac{Al_2O_3}{Fe_2O_3} \quad (7)$$

2.2.2 Standard consistence of cement paste

The consistence test of the cement paste was carried out according to BS EN 193-3:2005. 400g of cement sample was weighed and spread out on a steel plate for about 30 minutes to cool to the temperature of the mixing room ($27 \pm 5^\circ C$). 30% water content of the mass of dry cement was added as a start. The mixture was mixed for 4 ± 0.25 minutes by using a trowel to give a paste and was immediately transferred into the mould laying on the steel plate. The top of the mould was smoothed off as quickly as possible with the aid of the trowel. The mould and paste were placed under the plunger in the vicat apparatus and the plunger lowered gently to contact the surface of the paste. This material was released quickly and allowed to sink into the paste. The scale reading of the vicat apparatus was noted after 1 minute and recorded. If the plunger penetrates to a point 5 to 7 mm above the bottom of the mould, the water-cement ratio is taken as the consistency, if not, a new water-cement ratio is taken and the procedure repeated. The standard cement paste was obtained using:

$$\text{Percentage consistency} = \frac{\text{Water consumed} \times 100}{\text{Weight of the cement sample}} \quad (8)$$

2.2.2 Compressive strength test

Mortar was prepared from each sample in the ratio of 1:3 (cement:standard sand) with a water/cement ratio of 0.4 in accordance with BS 4550-3.4:1978 specification. The mixtures were cast into 70.7 mm x 70.7 mm x 70.7 mm moulds and puddled for 27 times per specimen with a puddling rod and the demoulded after 24 hours and were marked for identification. This material was then immersed in clean water for curing and later removed for crushing after a 7, 14 and 28 days respectively. The specimens were tested in accordance with BS EN 12390-3:2009. The compressive strength was determined using universal testing machine at the Department of Civil Engineering, Federal University of Technology, Minna.

3 RESULTS AND DISCUSSION

3.1 CHEMICAL COMPOSITION

The percentage oxide composition of the selected brands of Portland cement determined by X-ray fluorescence (XRF) spectrometry technique is presented in Table 1. The results of the major oxide contents were comparatively analysed against the compositional ranges stipulated by BS EN 196-2:1995.

TABLE 1: CHEMICAL COMPOSITION OF THE SELECTED CEMENT BRANDS

Element	A	B	C	BS EN 196-2:1995
CaO	65.27	64.41	66.03	61.0 – 69.0
SiO ₂	20.68	22.14	19.43	18.0 – 24.0
Al ₂ O ₃	5.54	4.96	5.82	2.6 – 8.0
Fe ₂ O ₃	2.91	2.87	2.69	1.5 – 7.0
MgO	1.06	1.23	2.07	0.5 – 4.0
Na ₂ O	0	0	0	–
K ₂ O	0.6	0.67	0.24	0.2 – 1.0
SO ₃	2.23	2.16	2.88	0.2 – 4.0
P ₂ O ₅	0.09	0.09	0.35	–
TiO ₂	0.24	0.25	0.35	–
Mn ₂ O ₃	0.04	0.04	0.18	–
Cr ₂ O ₃	0.01	0.01	0.02	–
ZnO	0	0	0.01	–
SrO	0.56	0.46	0.04	–

The percentage compositions of CaO, SiO₂, Al₂O₃, Fe₂O₃, MgO, K₂O and SO₃ in the three brands are all within the stipulated BS EN 196-2:1995 specification. The chemical analysis also indicated the presence of other minor oxides such as Na₂O, P₂O₅, TiO₂, Mn₂O₃, Cr₂O₃, ZnO, and SrO. Aitcin (2016) stated that the term minor indicates only that their percentage is not very high but if in high concentration may have significant influence on the cement properties. The results of the major oxide compositions are similar to that obtained by Olonade *et al.* (2015) and Omoniyi and Okunola (2015) which were found to be within the stipulated range given same standard. The percentage mineral composition of the cement was evaluated from the oxide concentrations using Bogue's equation; the standardized Bogue's equations given in ASTM C 150 were used to compute the mineral

compositions. Though the equation does not give the exact mineral composition but it is still considered as approximate representation of the mineral composition and usually the values are quite close (Shetty, 2009; Faleye *et al.*, 2009; Sam *et al.*, 2013; Omoniyi and Okunola, 2015; Olonade *et al.*, 2015; Aitcin, 2016). The results obtained for the samples are presented in Table 2.

TABLE 2: MINERAL PERCENTAGE COMPOSITION

Mineral parameter	A	B	C	ACI 225R-99
C ₃ S (%)	60.81	50.36	69.98	40 - 63
C ₂ S (%)	13.42	25.48	2.91	9 - 31
C ₃ A (%)	9.76	8.29	10.87	6 - 14
C ₄ AF (%)	8.86	8.73	8.19	5 - 13
Total	92.84	92.87	91.95	

The percentage composition of C₃S (tricalcium silicate) in the cement samples A, B and C studied are 60.81, 50.36 and 69.98 % respectively. According to ACI (1999), this compound exists in clinker in the impure form known as alite. Alite is extremely complex and may take on six or seven crystal forms and contain the elements sulfur (S), sodium (Na), potassium (K), iron (Fe), magnesium (Mg), and fluorine (F) in addition as trace elements. The result showed that C₃S values for A and B are within the 40 – 63% limit as stated in ACI 225R-99:1999 for general purpose cement. However, C₃S values for C is higher than the stipulated range. Omoniyi and Okunola (2015) avered that the hydration of C₃S is responsible for most of cement pastes strength, particularly at early times.

On the other hand, the percentage composition of dicalcium silicate (C₂S) in A, B and C were 13.42, 25.48 and 2.91% respectively. The value of C₂S for A and B are within the limit as stated in ACI 225R-99:1999 for general purpose cement while that of the C falls short of the limit. C₂S exists as belite with at least five crystal forms; the different forms of belite, unlike those of alite, differ greatly in performance (ACI 225R-99, 1999). The compound has a very stable crystal structure that is completely unreactive in water, and an excess of it introduces impurities in cement compared to C₃S (Taylor, 1997). C₂S contributes slightly to strength at ages as early as 1 or 2 days and significantly to 28-day strength. Tran (2007) stated that C₃S and C₂S react to form calcium silicate hydrate gel (C-S-H = CaO·SiO₂·4H₂O) when cement mixes with water, which is primarily responsible for strength development.

The study also showed that tricalcium aluminate (C₃A) percentage compositions in A, B, and C were 9.76, 8.29,

and 10.87% respectively. These values were within the ACI 225R-99:1999 specification for general purpose cement. C_3A is largely responsible for setting of concrete and the degree of heat generated within in the first few days and may cause premature stiffening without significant strength development (ACI 225R-99, 1999). The hydration of C_3A occurs very quickly to produce calcium aluminate hydrate (C-A-H), which in return can lead to rapid heat of hydration; the process consumes water quickly and can often lead to flash set, which is undesirable (Tran, 2007). Omoniyi and Okunola (2015) expressed that C_3A , in the presence of sulphate ions, can harm concrete, by participating in expansive reactions that can lead to stress and cracking.

Moreover, the percentage compositions of tetracalcium aluminoferrite (C_4AF) in A, B, and C were 8.86, 8.73, and 8.19% respectively. The obtained values were within the ACI 225R-99:1999 specification for general purpose cement. Though C_4AF makes a smaller contribution to the strength of Portland cement when compared to other mineral; it is present because it facilitates burning of the cement clinker and formation of the strength-producing silicates (ACI 225R-99, 1999; Olonade *et al.*, 2015). C_4AF reacts very similar to C_3A except it produces less heat of hydration and does not cause premature stiffening (Tran, 2007).

The relationship existing between the percentage of lime on the one hand and the combination of silica, alumina and iron oxide on the other are expressed in terms of Lime Saturation Factor (LSF), Silica Ratio (SR) and Alumina to Iron ratio (AF). Each of these parameters also influences performance of cement in a way and is often used for control purposes (Alemayehu and Sahu, 2013; Abdula and Khailany, 2015). The calculated LSF, SR and AR are presented in Table 3.

TABLE 3: CALCULATED LSF, SR AND AR

Control parameter	A	B	C	Abdula and Khailany (2015); Winter (2019)
LSF	99.43	93.59	107.04	90 – 98
SR	2.45	2.83	2.28	2 – 3
AR	1.90	1.73	2.16	1.3 – 2.5

LSF = Lime saturation factor, AR = Alumina ratio, SR = Silica ratio

The LSF controls the ratio of alite (C_3S) to belite (C_2S) in the clinker. A clinker with a higher LSF will have a higher proportion of alite to belite than will a clinker with a low LSF (Winter, 2019). In other word, it is the ratio of the actual amount of lime to the theoretical lime required by the other major oxides in the clinker; when $LSF > 100\%$ the ordinary clinker will always contain some free lime (Alemayehu and Sahu, 2013). The LSF of

A is within the range recommended by Abdula and Khailany (2015) and Winter (2019) while that of B is slightly higher and value for C is significantly higher than the range. C might have surplus free lime that could not combine with other constituents as indicated by their LSF values being greater than 100%.

The values of SR (also known as the Silica Modulus) obtained were 2.45, 2.83, and 2.28 for A, B, and C respectively (Table 4.3). The normal range of Silica Ratio (SR) was recommended to be between 2 and 3 (Abdula and Khailany, 2015; Winter, 2019). The effect of the SR is that if the SR value is less than 2, the burning process becomes very easy although excessive liquid phase and low strength cement will occur. However, if the SR value reaches up to 3, the burning become very difficult and the high strength cement is obtained. If the SR exceeds 3, then no clinkerization process occurs at all (Taylor, 1997). The SR values for all the samples are within the acceptable 2 – 3 range recommended by Abdula and Khailany (2015) and Winter (2019).

The values of AR obtained are 1.90, 1.73, and 2.16 for A, B, and C respectively (Table 3). The AR is used to determine ratio of aluminum oxide to ferric oxide (Al_2O_3/Fe_2O_3). AR acceptable range is between 1.3 and 2.5 (Abdula and Khailany, 2015; Winter, 2019). The effect of the AF is that if the obtained value is greater than 2.5, it indicates an occurrence of high early strength, but if it is less than 1.3, then this leads to low early strength and low heat of hydration (Taylor, 1997; Abdula and Khailany, 2015). The AR values for all samples are within the acceptable range.

3.2 SETTING TIME AND STANDARD CONSISTENCE

Consistency of a concrete mix for a given mixture design is important to achieving uniformity. The initial setting time of the three samples lies in the range of 80 – 100 minutes while the final setting time occurs between 190 – 260 minutes as shown in Table 4.

TABLE 4: SETTING TIME AND STANDARD CONSISTENCE

Cement Sample	Initial Setting Time (mins)	Final Setting Time (mins)	Standard Consistence (%)
A	80	265	30
B	100	240	35
C	90	220	31

According to EN 197 -1:2011 standards requirements, initial setting time should be higher than 60 minutes. The differences observed in setting times may be as a result of the selective hydration of C_3S and C_2S in the samples. The influence of C_3S and C_2S on setting and hardening of fresh concrete is very crucial; an increase in the C_3S and

C₃A in cement could result into a rapid hardening. C₃S is significantly attributed to early setting and hardening as well, C₃A imposes the formation of AFt phases at fresh state, leading to a rapid hardening of Portland cement (Hewlett, 2004; Kim *et al.*, 2016). Thus, the three samples of cement are within the limits stated. However, no value is specified for final setting time in EN standards but Bundoo (2014) suggested that final setting times should be less than 600 minutes. The standard consistence of the samples A, B and C are 30%, 35% and 31% respectively (Table 5). B would likely require more water to obtain consistence mix than others for having highest standard consistency value of 35% followed by C (31%) and then A (30%). This can be explained as the C₃S (tricalcium silicate) of B is lower than that of A and C which might exhibit lower heat of hydration compared to using A and C.

3.3 COMPRESSIVE STRENGTH

Cement quality is typically assessed by its compressive strength development in mortar and concrete; this is important as it commonly represents the overall quality of cements (Alemayehu and Sahu, 2013; Broni-Bediako *et al.*, 2015). The compressive strength of the cements was determined at different curing ages of 7, 14, and 28 days as shown in Figure 1.

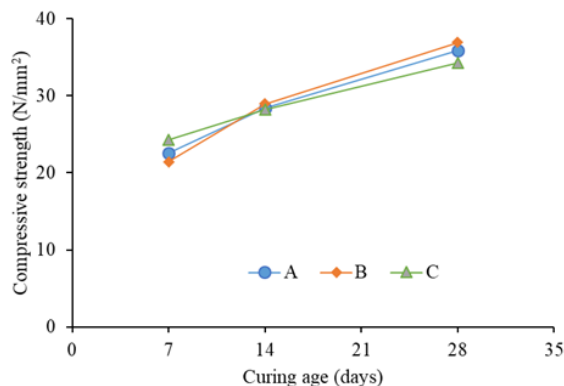


Figure 1: Rate of Strength Development for Various Cement Brands

At 7 days curing age with water cement (w/c) ratio of 0.4, the compressive strength of A, B, and C were 22.6 N/mm², 21.43 N/mm², and 24.28 N/mm² respectively. The compressive strength of A, B, and C at 14 days are 28.40 N/mm², 28.96 N/mm² and 28.21 N/mm² respectively. The compressive strength of A, B, and C at 28 days are 35.84 N/mm², 36.88 N/mm², and 34.22 N/mm² respectively. These satisfied the requirements for high early strength (≥ 16.0 N/mm² at 7 days) and normal strength development (≥ 32.5 N/mm² and ≤ 52.5 N/mm² at 28 days) classes of cement as stipulated by EN 197 -1. The strength characteristics of the cement are as a result of different cement mineral compositions. C₃S, C₂S, and C₃A are the principal strength-producing phases in

Portland cement but the two calcium silicate minerals, C₃S and C₂S, are largely responsible for the early strength development and the long-term structural and durability properties of hydrated cement (Taylor, 1997; ACI, 1999; Olonade *et al.*, 2015).

The proportions of these can be varied in the manufacturing process and can change both the early strength characteristics and the long-term strength; increasing the proportion of C₃S increases strength at ages from 10 to 20 h through 28 days. On the other hand, C₂S contributes slightly to strength at ages as early as 1 or 2 days and significantly to 28-day strength. Its major effect is to increase later age strengths (ACI 225R-99, 1999). The long-term strength contributions of C₂S are dependent on extended availability of moisture. In the meantime, C₃A contributes principally to strength at 24 h or less, and C₄AF makes a smaller contribution to the strength of Portland cement. It is present because it facilitates burning of the cement clinker and formation of the strength-producing silicates.

The result indicates that at 7 days, C has the highest compressive strength (24.28 N/mm²) followed by A (22.6 N/mm²) while B (21.43 N/mm²) has the lowest, this result can be justified by the amount of C₃S present in each sample (brand) meaning that increasing the proportion of C₃S increases strength at ages from 10 to 20 h through 28 days. As the curing age increased to 14, it was observed that the strengths of the three brands are close meaning that the amount of C₂S is higher in A and B leveraging the effect of C₃S at later age; C₂S increase later age strengths. At 28 days, the effects of C₂S was significant that B exhibited higher strength but was at earlier age 7 days had lowest strength.

4 CONCLUSION

The quality of three most commonly used cements in construction industries in Nigeria was assessed based mineral compositions, setting time and standard consistence, and compressive strength. Based on the outcome of the results, it is concluded that the percentage compositions of the major oxides are within the stipulated BS EN 196-2:1995 specification; the mineral compositions of the cements satisfied the requirements except that the tricalcium silicate (C₃S) and dicalcium silicate (C₂S) in C are at variance with the standard; and the control parameters of the cements are within acceptable range, though the LSF of C was significantly higher than the range leading to excess free lime.

The initial setting time of the three samples were between 80 minutes and 100 minutes which satisfied the specification given by EN 197 -1:2011 standard; sample B had the highest standard consistence value which would likely require more water to obtain consistence mix than the other two brands, this was as a result of the low C₃S which might exhibit lower heat of hydration compared to A and B samples. The compressive strengths of the

cements were 22.6 N/mm², 21.43 N/mm², and 24.28 N/mm² at 7 days and 35.84 N/mm², 36.88 N/mm², and 34.22 N/mm² at 28 days, these satisfied the requirements for high early strength (≥ 16.0 N/mm² at 7 days) and for normal strength development (≥ 32.5 N/mm² and ≤ 52.5 N/mm² at 28 days) classes of cement as stipulated by EN 197-1:2011.

Hence, it is recommended that for rapid hardening requirements such as in repair works and in cold weather environments, sample C is recommended due to higher percentage composition of C₃S and C₃A which are responsible for rapid early setting and hardening. For large concrete work such as earth dam and where low rate of hardening is required such as hot weather, sample B is recommended due to its lower percentage compositions of C₃S and C₃A which are responsible for rapid early setting and hardening and with higher C₂S which is responsible for later age strength. It is therefore recommended that government agencies/parastatals such as Standard Organisation of Nigeria and Nigerian Building and Road Research Institute (NBRRI) implement effective monitoring policies to control standard.

A conclusion should review the main points of the paper and should state concisely the most important propositions of the paper. It should state the author's views of the practical implications of the results. In addition to the deductions that can be made from the results. Do not replicate the abstract as the conclusion. A conclusion might also elaborate on the importance of the work or suggest applications and extensions.

REFERENCE

- Abdula, R. A., & Khailany, R. N. (2015). Shiranish Formation in Garota (Shaqawa, North Iraq) as Raw Material for Portland Cement Manufacturing. *Iraqi Bulletin of Geology and Mining*, 12(1), 65 – 72.
- ACI 225R-99. (1999). *Guide to the Selection and Use of Hydraulic Cements*. New York: American Concrete Institute.
- Adegoroye, B. (2010). Disaster Everywhere. *Daily Sun*. Retrieved from <http://www.dailysunnewspaperonline.com/webpages/news/nat>
- Adewole, K. K., Oladejo, J. O., & Ajagbe, W. O. (2014). Incessant collapse of buildings in Nigeria: The possible role of the use of inappropriate cement grade/strength class. *International Journal of Civil, Architectural, Structural and Construction Engineering*, 8(7), 818-823.
- Aitcin, P. -C. (2016). Portland cement. In P. -C. Aitcin, & R. J. Flatt, *Science and Technology of Concrete Admixtures* (pp. 26 - 51). Cambridge, UK: Elsevier Ltd.
- Alemayehu, F., & Sahu, O. (2013). Minimization of variation in clinker quality. *Advances in Materials*, 2(2), 23-28.
- ASTM C150-05:2017. *Standard Specification for Portland Cement*. West Conshohocken, PA, United States: ASTM International.
- Broni-Bediako, E., Joel, O. F., & Ofori-Sarpong, G. (2015). Evaluation of the Performance of Local Cements with Imported Class 'G' Cement for Oil Well Cementing Operations in Ghana. *Ghana Mining Journal*, 15(1), 78 - 84.
- BS 4550-3.4:1978. *Methods of testing cement —Part 3: Physical tests —Section 3.4 Strength tests*. London: British Standards Institution (BSI).
- BS 882:1992. *Specification for aggregates from natural sources for concrete*. London: British Standards Institution (BSI).
- BS EN 1008:2002. *Methods of test for water for making concrete*. London: British Standard Institute (BSI).
- BS EN 12390-3:2001. *Testing Hardened Concrete - Part 3: Compressive Strength of Test specimen*. London: British Standard Institute (BSI).
- BS EN 193.3:2005. *Methods of testing cement - Part 3: Determination of setting times and soundness*. London: British Standards Institution (BSI).
- BS EN 196-2:1995. *Methods of testing cement —Part 2: Chemical analysis of cement*. London: British Standards Institution (BSI).
- Bundoo, F. T. (2014). *Investigation of Cement Mortar and Steel used in Reinforced Concrete in Nigeria*. Abuja: African University of Science and Technology.
- Cao, Q. (2012). *Investigation into Lowering Cement Clinker Content using Available Materials*. Kansas City: University of Missouri. MSc Thesis
- EN 197 -1:2011:2011. *Cement. Composition, specifications and conformity criteria for common cements*. London: British Standards Institution (BSI).
- Faleye, F. J., Ogunnubi, S., & Olaofe, O. (2009). Chemical and physical analysis of selected cement samples in Nigerian market. *Bangladesh Journal of Scientific and Industrial Research*, 44(1), 41-50.
- Gambhir, M. L. (2013). *Concrete Technology: Theory and Practice*. New Delhi: Tata McGraw-Hill Education.
- Hewlett, P. C. (2004). *Lea's Chemistry of Cement and Concrete* (4th ed.). Oxford: Butterworth-Heinemann.
- Kim, M. J., Kim, K. B., & Ann, K. Y. (2016). The Influence of C₃A Content in Cement on the Chloride Transport. *Advances in Materials Science and Engineering*, 5962821, 1 - 8.
- Olonade, K. A., Jaji, M. B., Rasak, S. A., & Ojo, B. A. (2015). Comparative Quality Evaluation of Cement Brands used in Southwest Nigeria. *Academy Journal of Science and Engineering*, 9(1), 53 - 63.
- Omoniyi, K. I., & Okunola, O. J. (2015). Comparative Studies of Physico-chemical Properties of Some Selected Cements in Nigeria. *Nigerian Journal of Technological Development*, 12(2), 54 - 60.



- Sam, R. A., Bamford, S. A., Fletcher, J. J., Ofosuand, F. G., & Fuseini, A. (2013). Assessment of quality of the various brands of Portland cement products available in the Ghanaian market. *International Journal of Science and Technology*, 2(3), 252 – 258.
- Shetty, M. S. (2009). *Concrete Technology: Theory and Practice*. Schaad and Company: New Delhi.
- Taylor, H. F. (1997). *Cement chemistry*. London, UK: Thomas Telford Publishing.
- Tennis, P. D., & Bhatti, J. I. (2005). Portland cement characteristics-2004. *Concrete Technology Today*, 26(3).
- The Nation Newspaper. (2014, November 16). Curbing building collapse through cement standardization. *The Nation*. Retrieved October 20, 2018, from <https://thenationonline.net/curbing-building-collapse-through-cement-standardization/>
- Tran, K. N. (2007). *The Durability of Concrete using Concrete Plant Wash Water*. Waterloo, Canada: University of Waterloo. MSc Thesis.
- Winter, N. B. (2019). *Clinker: compositional parameters*. Retrieved January 31, 2019, from Understanding Cement: Interpreting Cement Science Since 2005: <https://www.understanding-cement.com/parameters.html>

Development of Mix Design Guide for Normal Weight Concrete using Locally Available Materials

*Okoh S. O.¹; Abdullahi M.¹; & Alhaji, B.¹

¹Department of Civil Engineering Federal University of Technology, Minna

*Corresponding author email: okohsundaynimi@gmail.com

ABSTRACT

Concrete is a very variable composite since its material composition bear different properties depending on their sources. This therefore makes mix design a laborious task. Design of concrete mixes using codes from different countries are being done which results into several trials before acceptable mix compositions are arrived at. This problem can be averted if tabular data and charts are developed from experimental data using our locally available materials. In this study several mix ratios were considered with modification. Eventually the mix that gave reasonable workability are 1:2:3, 1:2:4 and 1:2.5:4 with varying amount of w/c ratio of 0.5, 0.6, and 0.7 respectively. The physical properties of the aggregates were carried out to enable the computation of the mix constituents. The slump and compressive strength of concrete were determined at 7 and 28 days respectively after curing. Test result showed that, the compressive strengths at 7 days ranges from 11.35 N/mm² to 20.68 N/mm² and 28 days ranges from 14.76 N/mm² to 25.08 N/mm². The graphical data produced is capable of conducting mix design of normal weight concrete.

Keywords: *Aggregate, concrete, experiment, mix design.*

1 INTRODUCTION

Concrete is one of the most important, versatile and widely used construction materials worldwide; it is extensively used in buildings, bridges, roads and dams (Kalgal, 2019). Concrete is a composite material basically comprising cement, fine aggregate, coarse aggregate, water in a required proportion. The mixture (a workable paste) when placed in forms and allowed to set, gradually hardens over time and this hardening is caused by the chemical reaction between the water and the cement which results to concrete getting stronger with age (Amsterdam, 2000). The strength, durability and other characteristics of concrete among other things depends upon the constituent materials, proportion of mix, method of compaction and controls during placing (Shetty, 2009; Somayaji, 2000).

Remarkably, the constituent materials of the concrete, most especially the aggregates, are more often than not locally sourced which may invariably fail to satisfy the requirements of the commonly used British and American Standards and be apparently considered unacceptable. In this context, Gifford and Partners (1997) described local materials as aggregates, cement or water which may be at variance with the commonly used standards. They further explained that these materials can often be used to make good concrete provided due care is taken with the mix proportioning and production. This indicates that nature of the constituent materials is a crucial factor when considering mix design in order to achieve good properties of concrete (Mindess *et al.*, 2003).

Moreover, the aggregates used in normal weight concrete in most developing countries including Nigeria are mostly natural aggregates (sand and gravel) which come into being as a result of weathering, water

transportation, sorting, and stacking as well as other types of natural conditions (Zhang, 2011; Adewole *et al.*, 2015). Due to different sources with respect to geographic locations, the aggregates may exhibit different physical, chemical and mechanical properties different from aggregates used in the regions where those standards emanated from. The incessant collapse of building in Nigeria and elsewhere resulting to loss of lives and properties is at large blamed upon lack of adherence to material specification/poor building material specification, and poor concrete mix ratio (Adewole *et al.*, 2015; Kolawole, 2018). However, this situation can be curtailed if proper and suitable mix design is considered in the production of concrete production. Obtaining a good mix design using the local materials requires adjusting the commonly used standards before workable mixes can be achieved. Hence, mix proportioning adjustment is imperative so that structural failure could be avoided or minimised. Therefore, this study is aimed at developing a mix design guide for the appropriate mix ratios for normal weight concrete structures using locally available materials in Nigeria.

2 METHODOLOGY

2.1 MATERIALS

The materials used in the study were water, cement, fine and coarse aggregates. The fine aggregate was natural river sand gotten in Minna, Nigeria which was sieved through 5 mm sieve according to BS 882:1992. The coarse aggregate was gravel from a local Quarry in Minna and was sieved through 20 mm sieve. The physical properties of the aggregates such as particle size distribution, specific gravity, bulk density, moisture content and water absorption were determined in

accordance with BS 812:1995. The water used was potable water of drinkable quality which was obtained from the Civil Engineering Laboratory, Federal University of Technology, Minna, and considered to satisfy the requirements of BS EN 1008:2002. The cement used was Dangote ordinary Portland cement (42.5N) with specific gravity of 3.15. The fineness modulus, coefficient of uniformity C_u and coefficient of curvature C_c were evaluated from the sieve analysis using the following equations (Oyedepo, 2016):

$$C_u = \frac{D_{60}}{D_{10}} \quad (1)$$

$$C_c = \frac{(D_{30})^2}{D_{10}D_{60}} \quad (2)$$

where D_{60} is the particle diameter at 60% passing, D_{30} is the particle diameter at 30% passing, and D_{10} is the particle diameter at 10% passing.

2.2 PREPARATION OF SAMPLES

The mix design was conducted using absolute volume method. Several mixes were considered and workable mixes were identified. The mixes used in the work were 1:2:3, 1:2:4, and 1:2.5:4 at different water-cement (w/c) ratio of 0.5, 0.6, and 0.7. The constituent materials

computed were used to produce the require batch quantities in accordance with BS 1881-125, 2013. Slump test was conducted on the fresh concrete mixes in accordance with BS EN 12350-2:2009. Cast mould of 150 mm x 150 mm x 150 mm dimension was used for the production of the concrete cube samples. The mixing, casting, curing and crushing of the concrete were done in Civil Engineering Laboratory, Federal University of Technology, Minna. The samples were cured for 7 days and 28 days respectively, and compressive strength of the concrete cubes was tested according to BS EN 12390-3:2009.

3 RESULTS AND DISCUSSION

3.1 PROPERTIES OF THE MATERIALS

3.1.1 Particle Size Distribution of the Aggregates

The gradation of the aggregates (coarse and fine) as determined by the sieve analysis is shown in Figure 1. The results of the sieve analysis of fine aggregate are shown in Table 1 as capered with British and American Standards. The fineness modulus, coefficient of uniformity C_u and coefficient of curvature C_c were evaluated from the sieve analysis to adjudge the fineness/coarseness of the sand.

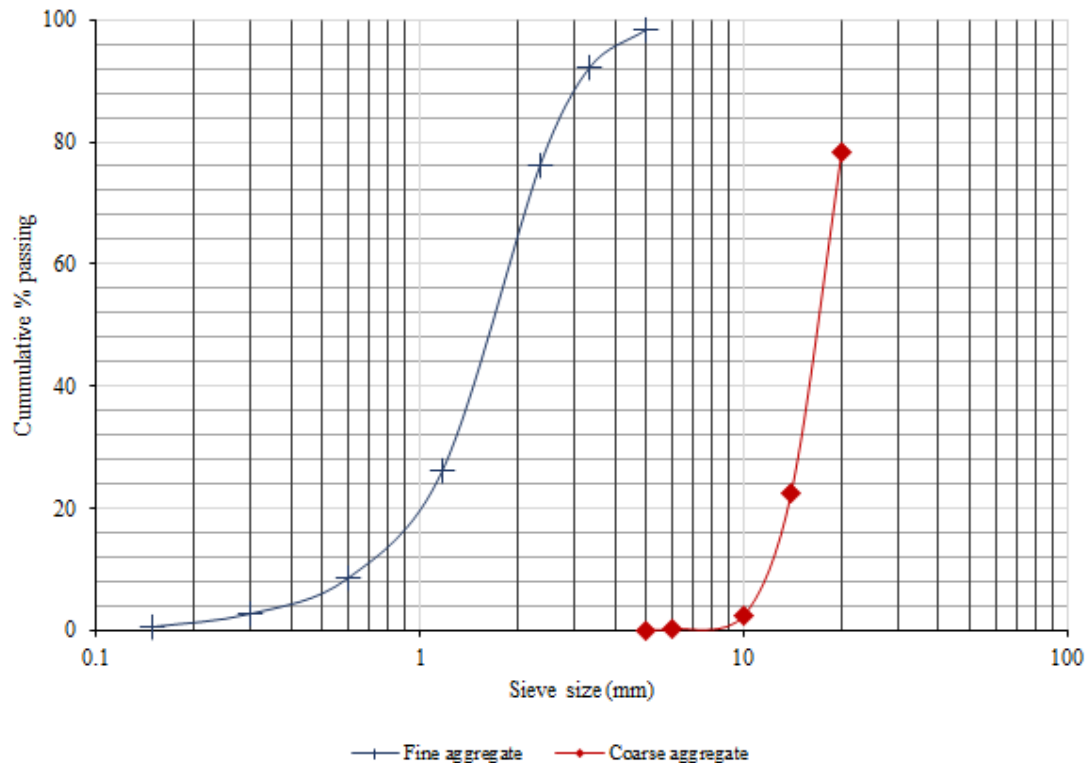


Figure 1: Particle size distribution of the aggregates

TABLE 1: SIEVE ANALYSIS OF FINE AGGREGATE COMPARED WITH BRITISH AND AMERICAN STANDARDS

Sieve size (mm)	Sand (mass passing (%))	ASTM C 33/C 33M – 8	BS 882:1992		
			C	M	F
10.00	100	100	100	100	100
5.00	98.37	95 – 100	89 - 100	89 - 100	89 - 100
2.36	76.26	80 – 100	60 - 100	65 - 100	80 - 100
1.18	26.28	50 – 85	30 - 90	45 - 100	70 - 100
0.60	8.54	25 – 60	15 - 54	25 - 80	55 - 100
0.30	2.75	5 – 30	5 - 40	5 - 48	5 - 70
0.15	0.6	0 – 10	0 – 15	0 – 15	0 – 15

C – coarse sand, M – medium sand, and F – fine sand

The Nigerian commonly used local fine aggregate barely meets the requirements of ASTM C 33/C 33M – 8 and BS 882:1992 standards, and is classified as “C” (coarse sand). The fineness modulus (FM) of the fine aggregate is 3.87 indicating that the average aggregate size is in between 0.6 mm and 1.18 mm corresponding to the 3rd sieve and 4th sieve respectively. The coefficient of uniformity C_u and coefficient of curvature C_c of the fine aggregate were found to be 2.92 and 1.05 respectively. However, the sand is considered to be poorly graded as it fails to satisfy $C_u \geq 6$ and $1 < C_c < 3$ conditions (Holtz *et al.* 2010) and $2.3 < FM < 3.1$ grading requirements (ASTM C 33/C 33M – 8). On the other hand, the C_u and C_c of the coarse aggregate were found to be 1.58 and 1.12 respectively; in the same vein, the gravel is poorly graded having failed to satisfy $C_u \geq 4$ and $1 < C_c < 3$.

3.1.2 Physical and mechanical properties

The results of the specific gravity, bulk density moisture content, and water absorption of the materials are presented in Tables 2 and 3. The specific gravities of the fine aggregate, coarse aggregate and cement were 2.7, 2.85 and 3.16; both aggregates satisfied the acceptable limits of natural aggregate range. The bulk densities of the materials are within the range suggested in the literature and the ratios of loose (uncompacted) bulk density to compacted bulk density of fine and coarse aggregates are 0.92 and 0.87 respectively, the values are within the range 0.87 to 0.96 suggested by Neville (2012). Thus, the materials (aggregates) are suitable for the production of concrete. In addition, the moisture content and water absorption of the aggregates are within the acceptable range.

TABLE 2 SPECIFIC GRAVITY AND BULK DENSITY

Aggregate	Specific gravity	Zhang (2011)	Bulk density (kg/m ³)	Zhang (2011) (kg/m ³)
Fine	2.7	2.6 – 2.8	1865.9	1450 – 1700
Coarse	2.85	2.6 – 2.9	1731.7	1400 – 1700

TABLE 3 MOISTURE CONTENT AND WATER ABSORPTION

Aggregate	Moisture content (%)	ACI (2007) (%)	Water absorption (%)	ACI (2007) (%)
Fine	0.4	0 – 10	22.45	10 – 20
Coarse	1.7	0.2 – 2	0.65	0 – 4

3.2 WORKABILITY OF THE FRESH CONCRETE

All mixes were tested for workability using the slump test and the results are presented in Table 4. The slump was 70 mm, 85 mm, and 100 mm at mix proportion of 1:2:3 for w/c 0.5, 0.6, and 0.7 respectively; 75 mm, 95 mm, and 110 mm at mix proportion of 1:2:4 for w/c 0.5, 0.6, and 0.7 respectively; and 85 mm, 100 mm, and 120 mm at mix proportion of 1:2.5:4 for w/c 0.5, 0.6, and 0.7 respectively. A similar pattern of slump was observed as it increases with an increase in w/c ratio from 0.5 to 0.7 for all the mixes.

TABLE 4 SLUMP OF THE CONCRETE

Mix ratio	Water/cement (w/c) ratio	Slump (mm)
1:2:3	0.5	70
	0.6	85
	0.7	100
1:2:4	0.5	75
	0.6	95
	0.7	110
2:2.5:4	0.5	85
	0.6	100
	0.7	120

It was also observed that the slump increases as mix proportion changes from 1:2:3 to 1:2:4 and further increases at 1:2.5:4. Bhatt *et al.* (2006) classified slump as very low workability (< 25mm), low workability (25 – 50 mm), medium workability (50 – 100 mm), and high workability (100 – 175 mm). The slump values obtained fall in the category of medium to high workability from 70 mm to 120 mm. The obtained slump is suitable for normal weight concrete as this requires fresh concrete of medium workability (Bhatt *et al.*, 2006).

3.3 CHARACTERISTIC STRENGTH

The compressive strength is a major parameter for the structure design and the indicator for the quality assessment of concrete (Zhang, 2011; Broni-Bediako *et al.*, 2015). The compressive strength of the concrete was determined at curing ages of 7 and 28 days for all the mixes as shown in Figure 2. The maximum strength obtained at 7 days curing age with various mix proportions is 20.68 N/mm² (1:2:3), 21.54 N/mm² (1:2:4), and 20.50 N/mm² (1:2.5:4). At 28 days, the maximum compressive strength is 25.08 N/mm² (1:2:3), 22.07 N/mm² (1:2:4), and 18.19 N/mm² (1:2.5:4). The mix 1:2:3 has the maximum compressive strength 25.08 N/mm² of all mixes at 28 days and w/c ratio of 0.5.

The compressive strength increases for all the mixes as the curing age from increased 7 days to 28 days. In contrast, the strength exhibited a downward shift as the mix proportion changed from 1:2:3 to 1:2:4 and further at 1:2.5:4. It was further observed that the strength of all the mixes decreases with increase in w/c ratio indicating that more water in the concrete weakens it. It is clear that the use of a lower w/c ratio of 0.5 in the samples was more effective in terms of strength than a higher w/c ratio of 0.6

and 0.7; this could be attributed to relatively low moisture content and water absorption of the aggregates used. This result is in agreement with what was obtained by Mallikarjuna *et al.* (2013); Choi *et al.* (2015); and Otunyo and Jephter (2018).

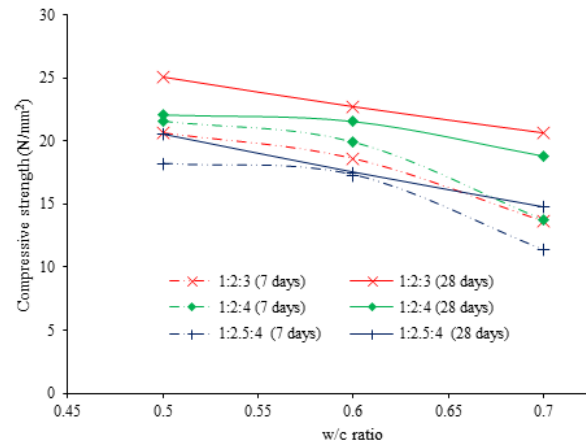


Figure 2 Variation of compressive strength with w/c ratio at different mixes

The comprehensive strength increases for all the mixes as the curing age from increased 7 days to 28 days. In contrast, the strength exhibited a downward shift as the mix proportion changed from 1:2:3 to 1:2:4 and further at 1:2.5:4. It was further observed that the strength of all the mixes decreases with increase in w/c ratio indicating that more water in the concrete weakens it. It is clear that the use of a lower w/c ratio of 0.5 in the samples was more effective in terms of strength than a higher w/c ratio of 0.6 and 0.7; this could be attributed to relatively low moisture content and water absorption of the aggregates used. This result is in agreement with what was obtained by Mallikarjuna *et al.* (2013); Choi *et al.* (2015); and Otunyo and Jephter (2018).

3.4 MIX DESIGN GUIDE: COMPUTATION OF MIX CONSTITUENTS

An evaluation of the experimental data was performed to provide a mix design guide for the appropriate mix ratios for normal weight concrete structures using locally available materials in Nigeria as shown in Figure 3. This provides real-time information on the strength and workability of the concrete produced with locally available materials if the w/c ratio changes by tracing the corresponding compressive strength and slump on the plots for the w/c ratio.

It is required to compute mix proportion for concrete with slump of 90mm. Figure 3 (a – c) is capable of giving the following mix constituents.

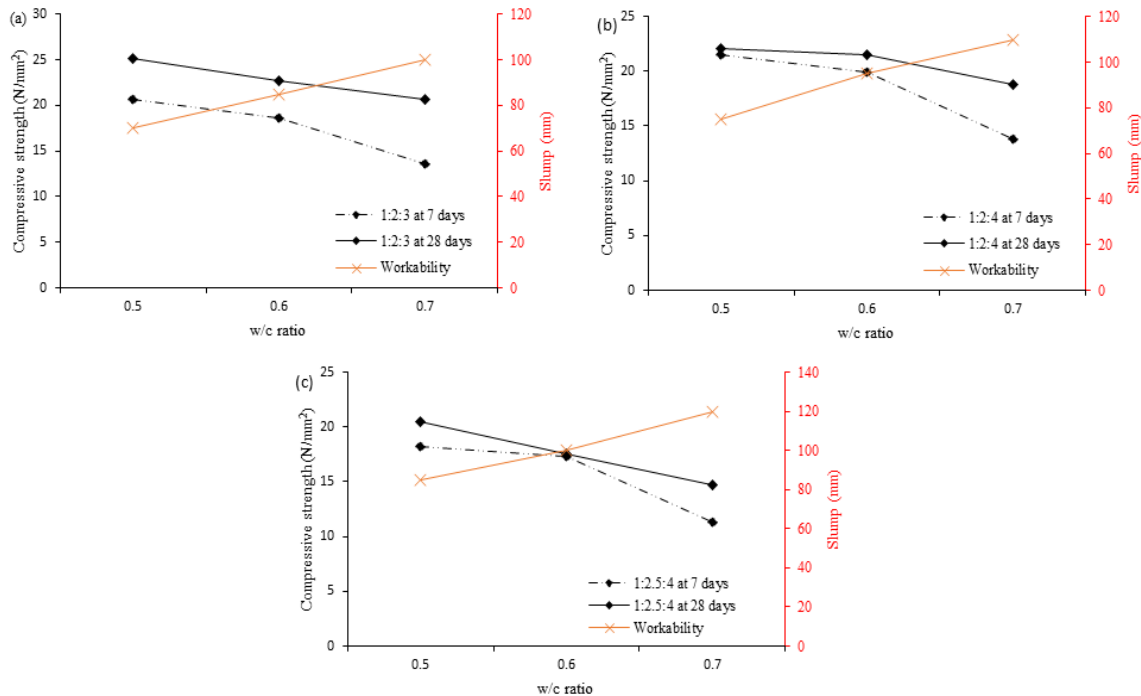


Figure 3 Evaluation of mix ratios 1:2:3, 1:2:4, and 1:2.5:4 at different curing days

- 1) Using Figure 3 for 90 mm slump
 - a) w/c = 0.63, for 1:2:3
 - b) w/c = 0.57, for 1:2:4
 - c) w/c = 0.53, for 1:2.5:4

Further Figure 3 gives the target compressive strength at 28 days as

- a) 22 N/mm²
- b) 21.5 N/mm²
- c) 18 N/mm²

Hence, the graphical data developed from experimented results are useful paradigm in expressions for a quick determination of a required major properties in mix design. At a glance, one may tell a required w/c ratio that can give a specific walkability and strength at a determined mix ratio.

4 CONCLUSION

An evaluation of experimental data was carried out in the study to provide a mix design guide for appropriate mix ratios required for normal weight concrete based Nigeria locally available materials. The following are drawn from the study:

1. The aggregates (fine and coarse) are within the recommended standard but poorly graded.
2. The physical and mechanical properties of aggregates within the recommended standard and therefore suitable for concrete production.
3. The slump values obtained fall in the category of medium to high workability from 70 mm to 120 mm.
4. The mix 1:2:3 has the maximum compressive strength 25.08 N/mm² of all mixes at 28 days and w/c ratio of 0.5; the strength increased for all the mixes as the curing age increased from 7 days to 28 days. In contrast, the strength of all the mixes decreases with increase in w/c ratio.
5. The study was able to develop mix design guide which can provide real-time information on the strength and workability with various mix ratios if the w/c ratio changes.
6. The graphical data developed in this work is capable of providing the mix constituent of concrete.

REFERENCE

- ACI. (2007). *Aggregates for Concrete*. Farmington Hills: American Concrete Institute ACI.
- Adewole, K. K., Ajagbe, W. O., & Arasi, I. A. (2015). Determination of appropriate mix ratios for concrete grades using Nigerian Portland-limestone grades 32.5 and 42.5. *Leonardo Electronic Journal of Practices and Technologies*, 26, 79 - 88.
- Amsterdam, E. V. (2000). *Construction Materials for Civil Engineering*. Cape Town, South Africa: Juta and Company Ltd.
- ASTM C 33/C 33M – 8. (2016). *Standard Specification for Concrete Aggregates*. West Conshohocken, PA: ASTM International.
- Bhatt, P., MacGinley, T. J., & Choo, B. S. (2006). *Reinforced Concrete Design: Theory and Examples* (3rd ed.). New York: Taylor and Francis.
- Broni-Bediako, E., Joel, O. F., & Ofori-Sarpong, G. (2015). Evaluation of the Performance of Local Cements with Imported Class 'G' Cement for Oil Well Cementing Operations in Ghana. *Ghana Mining Journal*, 15(1), 78 - 84.
- BS 1881-125:2013. *Testing concrete —Part 125: Methods for mixing and sampling fresh concrete in the laboratory*. London: The British Standards Institution.
- BS 812-2:1995. *Testing aggregates. Methods for determination of density*. London: British Standard Institute (BSI).
- S 882:1992. *Aggregates From natural sources of concrete*. London: British Standards Institution (BSI).
- BS EN 1008:2002. *Methods of test for water for making concrete*. London: British Standard Institute (BSI).
- BS EN 12350-2:2009. *Testing fresh concrete. Slump-test*. London: BSI.
- BS EN 12390-3:2001. *Testing Hardened Concrete - Part 3: Compressive Strength of Test specimen*. London: British Standard Institute (BSI).
- Choi, H., Kang, D., Seo, G. S., & Chung, W. (2015). Effect of Some Parameters on the Compressive Strength of MWCNT-Cement Composites. *Advances in Materials Science and Engineering*, 340808, 1 - 8.
- Kalgal, M. R. (2019, June). *Role of Concrete in - Road Infrastructure*. Retrieved from NBM&CW: Intra Construction and Equipment Magazine: <https://www.nbmcw.com/tech-articles/roads-and-pavements/40160-role-of-concrete-in-road-infrastructure.html>
- Kolawole, O. M. (2018). Assessment of Building Collapse in Nigeria: The Major Causes and Practical Remedies. *Civil and Environmental Research*, 10(5), 35 - 40.
- Mallikarjuna, R. V., Seshagiri, R. M., Srilakshmi, P., & Sateesh, K. B. (2013). Effect of W/C Ratio on Workability and Mechanical Properties of High Strength Self Compacting Concrete (M70 Grade). *International Journal of Engineering Research and Development*, 7(1), 06 - 13.
- Mindess, S., Young, J. F., & Darwin, D. (2003). *Concrete* (2nd ed.). New Jersey: Prentice-Hall.
- Neville, A. M. (2012). *Properties of Concrete* (5th ed.). New Jersey: Prentice Hall.
- Otunyo, W. O., & Jephther, B. G. (2018). Predictive Model for Compressive Strength of Concrete made from Recycled Concrete Coarse Aggregates. *Nigerian Journal of Technology*, 37(3), 633–639.
- Oyedepo, O. J. (2016). Evaluation of the Properties of Lightweight Concrete Using Periwinkle Shells as a Partial Replacement for Coarse Aggregate. *Journal of Applied Science and Environmental Management*, 20(3), 498-505.
- Shetty, M. S. (2009). *Concrete Technology: Theory and Practice*. Schand and Company: New Delhi.
- Somayaji, S. (2000). *Civil engineering materials* (2nd ed.). New Jersey: Prentice Hall.
- Zhang, H. (2011). *Building materials in civil engineering*. Beijing: Science Press.



Comparative Evaluation of Strength of Compacted Lateritic Soil Improved with Microbial-Induced Calcite Precipitate

K. J. Osinubi¹, *E.W. Gadzama², A. O. Eberemu¹, and T. S. Ijimdiya.¹

¹Department of Civil Engineering, Ahmadu Bello University, Zaria, Nigeria

²Department of Civil Engineering, Modibbo Adama University of Technology, Yola, Nigeria

*Corresponding author email: gadzymo@yahoo.com +2348054358847

ABSTRACT

Soil improvement methods often target strength gain as one of the key parameters to be considered. Negative environmental issues associated with conventional (i.e., cement, lime, bitumen, etc.) soil improvement methods prompted researchers to the discovery of microbial induced calcite precipitation (MICP) technique. An A-4(3) lateritic soil was treated with *Sporosarcina pasteurii* (*S. pasteurii*) suspension density up to 2.40×10^9 cells/ml. The soil was prepared at different moulding water content and compacted with reduced British Standard light (RBSL) and British Standard light (BSL). Specimens were permeated with cementation reagent to initiate the MICP processes before being subjected to index and strength tests. Peak unconfined compressive strength (UCS) values of 2,011 kN/m² and 2,232 kN/m² for specimens prepared at -2 % moulding water content relative to optimum when compacted with RBSL and BSL energy, respectively. However, UCS values decreased with increase in *S. pasteurii* suspension density and moulding water content relative to optimum for the compactive efforts considered. It is recommended that *S. pasteurii* suspension density of 1.20×10^9 cells/ml be used for the improvement of lateritic soil in the construction of liners and covers in municipal solid waste (MSW) containment systems.

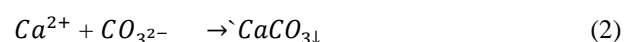
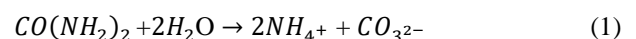
Keywords: *Cementation reagent, Compactive efforts, , Lateritic soils, MICP, Sporosarcina pasteurii .*

1 INTRODUCTION

The improvement of the engineering properties of soil is one of the major professional tasks to every civil engineer involved in engineering practice that has to do with soil (Sotoudehfar *et al.* (2016). Targeting strength gain is also one of the reasons why a particular method of soil improvement for engineering use is adopted. Unlike manufactured products, some soils have to be improved to meet the engineering specifications for the intended use, this is because they come with some deficiencies due to the geologic processes the soil has undergone during formation (Jayanthi and Singh, 2016). Several soil improvement methods documented in the literature have negative environmental related issues and therefore not sustainable (Faurel and Laloui, 2011). The search for a sustainable soil improvement method led researchers to the discovery of a novel and innovative method called microbial induced calcite precipitation (MICP). This emerging and active research area has recently prompted researchers to engage in multi-disciplinary studies that involve civil engineering, microbiology, chemical engineering and chemistry (Whiffin *et al.*, 2007; van Paassen *et al.*, 2010a&b; Hamdan *et al.*, 2011;2016; Dawoud *et al.*, 2014; Achal and Pan 2014; Feng and Montoya, 2016; Ijimdiya, 2017; Osinubi *et al.*, 2017; 2018; 2019 and Mujah *et al.*, 2019).

MICP is a natural biologically motivated process that makes the use of ureolytic bacteria to hydrolyse urea thus producing calcite and related carbonate ions (Mujah *et al.*, 2016). According to Reichle (1977), microorganisms constitute 70 - 85 % of biotic activity within soil systems. It is also pertinent to state that microorganisms relate with the immediate environment through enzymatic action, and nearly two-third of the results of such interaction are calcite minerals or other related minerals that have the needed role for cementation (Xu *et al.*, 2017).

According to The discovery of MICP technique has provided engineers with the idea to look at soil not only as an engineering material nevertheless as an ecosystem in which the engineering properties of soils can be enhanced (Mujah *et al.*, 2017). In MICP, calcite (CaCO₃) is the product of a two-stage chemical reaction (see equations (1) and (2)) responsible for improving the soil properties through bio-cementation and bio-clogging.



In equation (1), urea is hydrolyzed by the urease positive bacteria breaking it into ammonium and carbonate, while in equation (2) the product of the hydrolyzed urea, in the presence of calcium source yields to calcite as a precipitate.



The study focused on the comparative evaluation of the strength developed in compacted lateritic soil treated with *S. pasteurii* suspension density up to 2.40×10^9 cells/ml using the RBSL and BSL energy to be used as a liner and cover material in MSW systems.

2 MATERIALS AND METHODOLOGY

2.1 MATERIALS

Soil: The soil used in this study was collected using the disturbed sampling technique at depths of between 0.5 m and 3.0 m from Abagana (Latitude $6^{\circ}10'15''$ N and Longitude $6^{\circ}58'10''$ E), Anambra state, Nigeria. It is a lateritic soil classified as A-4(3) according to AASHTO soil classification system.

Bacteria: The type of bacteria used in the study is *S. pasteurii*, which is commonly found in soil. The urease positive bacteria is rod-shaped, spore-forming and Gram-positive was cultured and grown from the lateritic soil sample.

Cementation reagent: The cementation reagent is composed of 20 g Urea, 10 g NH_4Cl , 3 g Nutrient broth, 2.8 g CaCl_2 and 2.12 g NaHCO_3 per litre of distilled water, which has been used in several studies (e.g., Stocks-Fischer *et al.*, 1999; Dejong *et al.*, 2006; Al Qabany *et al.*, 2011; Park *et al.* 2014; Venkata *et al.* 2016; Tirkolaei and Bilsel, 2017). In all the cited studies, 3 g/l of nutrient broth was added to the cementation reagent because it is the most viable amount for survival of bacteria (Sharma and Ramkrishnan, 2016).

2.2 METHODS

Urease production: The ability of the test organism inoculated on urea agar slant incubated at 37°C for 24 hours to break down urea agar slant which allows the culture media to become alkaline in nature and change of colour to red-pink that indicates the test organism to be a urease positive

Bacteria cell suspension density: The suspension density of bacteria cells was changed in stepped suspensions of McFarland standard 0.5, 2, 4, 6 and 8 (i.e., equivalent to 0/ml, 1.5×10^8 /ml, 6.0×10^8 /ml, 1.2×10^9 /ml, 1.8×10^9 /ml and 2.4×10^9 cells/ml, respectively). The determined volume of organisms added to the soil was one-third (1/3) of the pore volume as reported by Rowshanbakht *et al.* (2016). Individual pore volumes were determined for each compactive effort used.

Index properties: Natural moisture content, specific gravities, Atterberg limits and sieve analysis were conducted in accordance with tests procedures specified in BS 1377: 1990.

Compaction characteristics: Compaction of specimens was conducted in accordance with the guidelines specified in BS 1377 (1990) to compute the required parameters. Two compactive efforts were used namely, reduced British Standard light (RBSL) and British Standard light (BSL). The RBSL compaction is the energy resulting from 2.5 kg rammer falling through a height of 30 cm onto three layers, each receiving 15 blows, while for BSL compaction each layer receives 27 blows.

Preparation of specimen: 3000 g of the crushed air-dried soil sample passing through BS No. 4 sieve was thoroughly mixed with moulding water content in the range -2 % to +4 % relative to optimum moisture content (OMC) with each having 1/3 of its pore volume as the *S. pasteurii* suspension density. This mixture was kept in sealed polythene bags and cured for 12 hours at $24 \pm 2^{\circ}\text{C}$ to enable the proper distribution of the microorganisms held onto the soil surface before compaction using the RBSL and BSL energies described above. Compacted specimens were percolated with cementation reagent in three circles each with 2/3rd of their pore volume, as earlier described, to initiate the MICP process.

Unconfined compressive strength (UCS): The test was conducted according to procedure described in BS, 1377: (1990). The treated specimens were prepared at moulding water contents of -2 %, 0 %, +2 % and +4 % relative to OMC and compacted with RBSL and BSL energies. The compacted specimens were cured for 24 hours in the moulds before extrusion and trimming as well as curing for another 24 hours in the laboratory at temperature of $24 \pm 2^{\circ}\text{C}$. After the second curing period, the specimens were kept in sealed polyethene bags for another 24 hours (making a total of seventy-two (72) hours curing period) before testing at a regulated strain of 0.02 %/min. Samples used had a height to diameter ratio of 2:1. The average of three (3) crushed specimens was recorded and used for the computation of the unconfined compressive strength.

Microanalysis: Microanalysis using scanning electron microscope (SEM) was conducted on both the natural and treated lateritic soil to investigate the changes in morphological features owing to the development and distribution of calcite links on the inter particle surface in the micro-structure of the soil. The test was carried out using Phenom World Pro desktop SEM with a software tool that could programme data collection and duplicate analysis. The specimens were positioned on an electrically powered tilt and rotating specimen holder which was regulated by a dedicated motion regulator which initiates an infinite 360° turning with a pseudo-eucentric tilting adjusted focus oscillating from 10° to 45° , which allows the creation of exact size and information from micro and nano fibre samples (Phenom World, 2017).

3 RESULTS AND DISCUSSION

Urea hydrolysis is a common and straight forward method used in MICP; its effectiveness in the conversion of the chemical reaction into calcite is over 90% in less than 24 hours (Al-Thawadi, 2011; Mujah *et al.*, 2017). The result of urease test conducted on the test organism is shown on Plate I, for a microorganism to be used in MICP when the ureolysis method adopted, it is required that the organism must be urease positive (i.e., ability to secret the urease enzyme). The pink colouration observed on Plate I indicates that the test organism is urease positive. Its reaction with urea in the cementation reagent results in the precipitation of calcite which is the required product for MICP process.

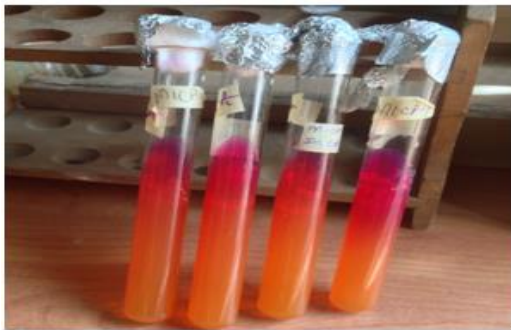


Plate I: Urease test on micro-organism

Index properties of the natural and treated lateritic soil:

The index properties of the natural and *S. pasteurii* treated lateritic soil are shown in Table 1. The fraction passing No 200 sieve is 36 % (see Figure 1), with silt and clay contents of approximately 22 % and 14 %, respectively. The soil is classified as A-4 (3) according to AASHTO soil classification system (AASHTO,1986) and SC according to Unified Soil Classification System, USCS (ASTM, 1992). X-Ray Diffraction (XRD) analysis of the sample shows that the dominant clay mineral is kaolinite whose peak are indicated by arrows (see Figure 2), which is a stable mineral. The oxide composition of the soil also summarized in Table 2 indicates that the soil is lateritic with a silica - sesquioxide ratio value {i.e., $SiO_2 / (Al_2O_3 + Fe_2O_3)$ } of 1.64 which lies between 1.33 and 2.00 for lateritic soils as recommended by Bell, (1993).

Table 2: Oxide composition of the natural lateritic soil

Oxide	SiO ₂	Al ₂ O ₃	CaO	TiO ₂	V ₂ O ₅	Cr ₂ O ₃	Fe ₂ O ₃	MnO	CuO	ZrO ₂	LOI	Total
Concentration (%)	56.5	19.00	0.33	2.89	0.061	0.051	15.41	0.075	0.056	0.290	4.54	99.20

TABLE 1: PROPERTIES OF THE NATURAL LATERITIC SOIL

Property	Quantity
Natural Moisture Content (%)	11.3
Percentage Passing No. 200 Sieve (Wet Sieve)	36.0
Liquid Limit (%)	44.0
Plastic Limit (%)	21.6
Plasticity Index (%)	22.4
CEC (Meq/100g)	5.50
Specific Gravity	2.62
AASHTO classification	A – 4(3)
USCS	SC
Colour	Reddish-brown
Dominant Clay Mineral	Kaolinite

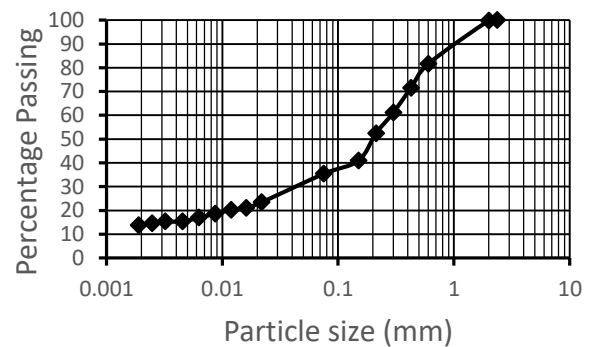


Figure 1: Particle size distribution curve of the natural soil

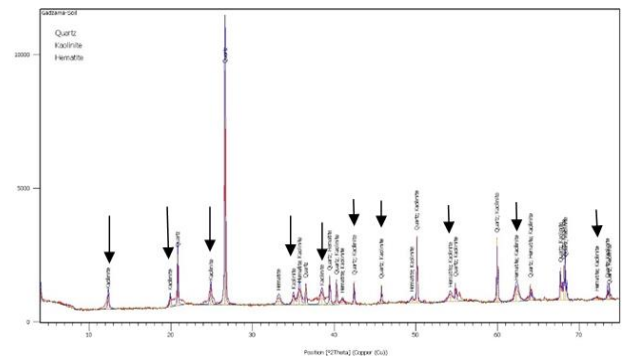


Figure 2: X-ray diffractogram of the natural lateritic soil.

Atterberg limits: Atterberg limits (i.e., Liquid Limit (LL), Plastic Limit (PL) and Plasticity Index (PI)) are used to evaluate the plastic behaviour of soils in connection to the amount of water content in the soil as it transits from solid to liquid phase. The variation of Atterberg limits with *S. pasteurii* suspension density is shown in Figure 3. The LL, PL and PI values generally decreased from 44.0 %, 21.6 % and 22.5 % for the natural soil to minimum values of 38.0 %, 16.0 % and 17.8 %, respectively, at *S. pasteurii* suspension density of 2.40×10^9 /ml. It is pertinent to state that decrease in PI value is desirable for any method adopted for the improvement of soil for engineering use. The results obtained suggest that the current method employed for soil improvements in this study is therefore appropriate Soon *et al.*, (2014).

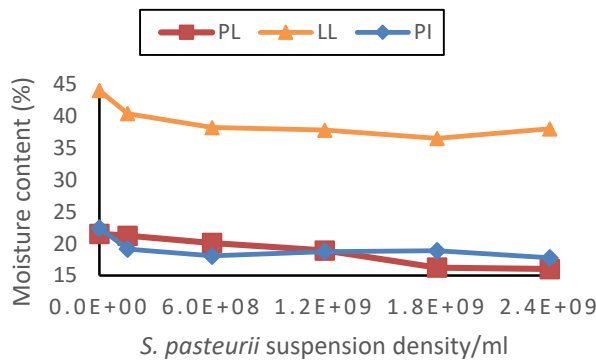


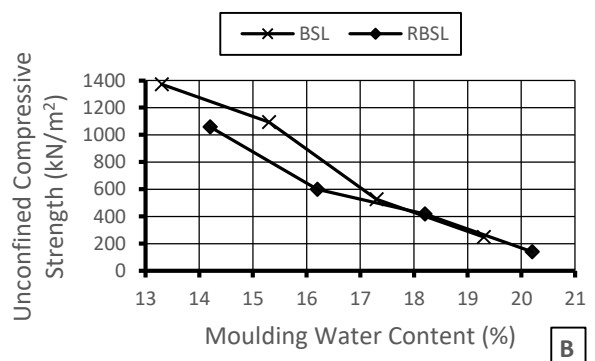
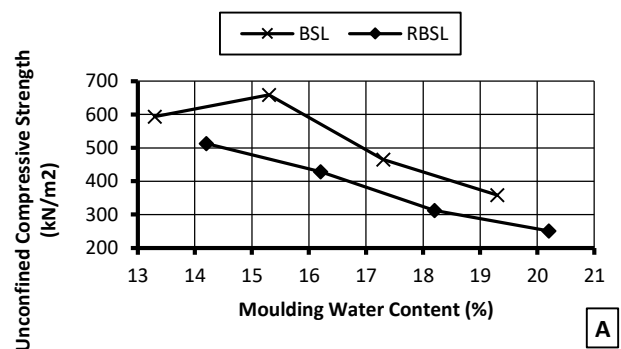
Figure 3 Variation of Atterberg limits of lateritic soil with *S. pasteurii* suspension density

Effect of moulding water content on unconfined compressive strength

The change in unconfined compressive strength (UCS) of lateritic soil with moulding water content for varying *S. pasteurii* treatment is presented in Figure 4A-F. Generally, UCS values decreased with increasing moulding water content regardless of the *S. pasteurii* suspension density or compactive effort considered. All the specimens of the natural soil satisfied the recommended minimum strength requirement of not less than 200 kN/m² for liners (Daniel and Wu, 1993). At *S. pasteurii* suspension density of 1.50×10^8 /ml, specimens compacted with RBSL energy satisfied the recommended minimum strength requirement at moulding water content of 19.6 %, while all specimens compacted with BSL, satisfied the requirement at the moulding water contents considered. At *S. pasteurii* suspension density of 6.0×10^8 /ml the strength requirement was satisfied by specimens prepared at moulding water contents of 19.8 and 19.0 % for RBSL and BSL compactations respectively. At *S. pasteurii* suspension density of 1.20×10^9 /ml the strength requirement was satisfied by specimens prepared at moulding water contents of 18.6 and 18.9 % for for RBSL and BSL compactations, respectively. At *S. pasteurii* suspension density of $1.80 \times$

10^9 /ml the strength requirement was satisfied by specimens prepared at moulding water contents of 18.5 % for RBSL compaction, while all the specimens prepared using BSL energy satisfied the strength criterion. Finally, at *S. pasteurii* suspension density of 2.40×10^9 /ml the strength requirement was satisfied by specimens prepared at moulding water contents of 19.6 % for RBSL compaction, while all the specimens prepared using BSL energy satisfied the strength criterion for the use of the material in the construction of liners.

The observed trend could probably be attributed to the existence of large volume of voids in soils compacted with lower energy than at higher energy. This enhanced the percolation of the cementation reagent which interacted with *S. pasteurii* and resulted in the deposition of higher amount of calcite precipitate at the particle-particle surfaces of the soil. This increased the inter-particle bonding among the soil particles and consequently improved the strength and stiffness of the soil. Higher strength gains were recorded for all treated soil at lower moulding water content, but decreased with increasing moulding water content irrespective of the *S. pasteurii* suspension density and compactive efforts used. The presented results are in agreement with the findings reported by Dejong *et al.* (2017).



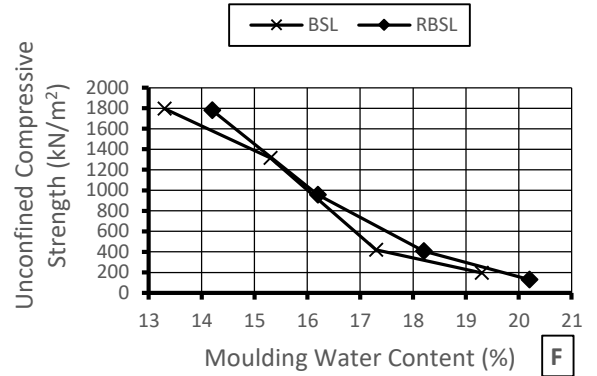
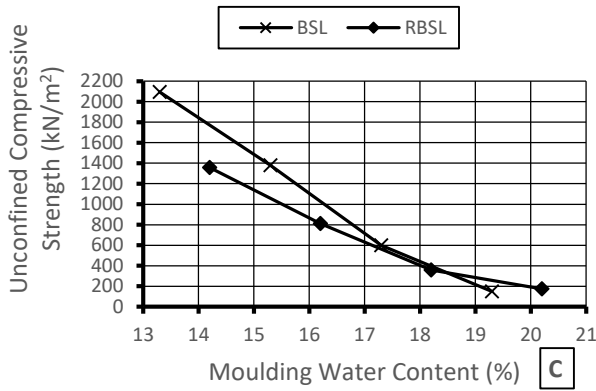
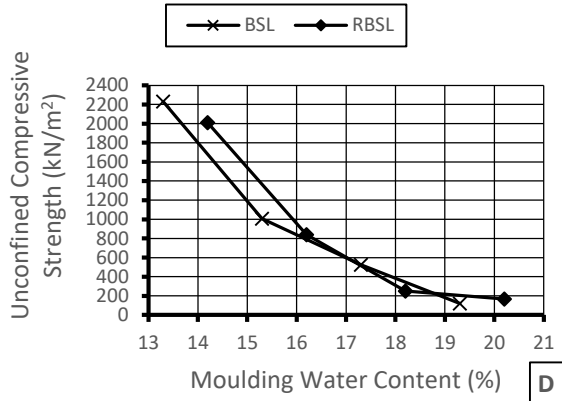
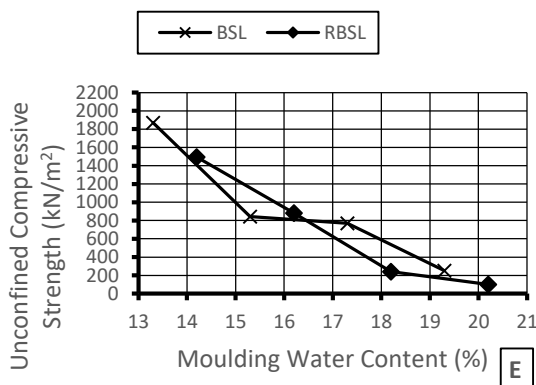


Figure 4: Variation of unconfined compressive strength with moulding water content for varying *S. pasteurii* suspension density: A= natural soil, B= 1.50×10^8 , C= 6.0×10^8 , D = 1.20×10^9 , E= 1.80×10^9 , F = 2.40×10^9 cells/ml.



Effect of *S. pasteurii* suspension density on strength

The variation of unconfined compressive strength (UCS) of lateritic soil with *S. pasteurii* suspension density is shown in Figure 5A-D. Peak UCS values of 2,011 kN/m² and 2,232 kN/m² were obtained at *S. pasteurii* suspension density of 1.20×10^9 cells/ml for specimens prepared at -2 % OMC and compacted with RBSL and BSL energy, respectively.



A typical strength improvement trend shown in Figure 5A and 5D for BSL compaction recorded the highest and lowest UCS values of 2,232 kN/m² and 120 kN/m², respectively, at *S. pasteurii* suspension density of 1.20×10^9 /ml is used to explain the percentage gain in strength. The strength improvement ratios of 392.03 % and 375.92 % were recorded for RBSL and BSL compaction, respectively. The observed trend could probably be due to higher voids within the soil compacted at -2 % OMC enabled the formation of calcite that bridged the soil particle surfaces and consequently resulted in higher UCS values of the specimens. This result is in agreement with the findings reported by Cheng and Cord-Ruwisch (2012) as well as Cheng *et al.*, (2013).

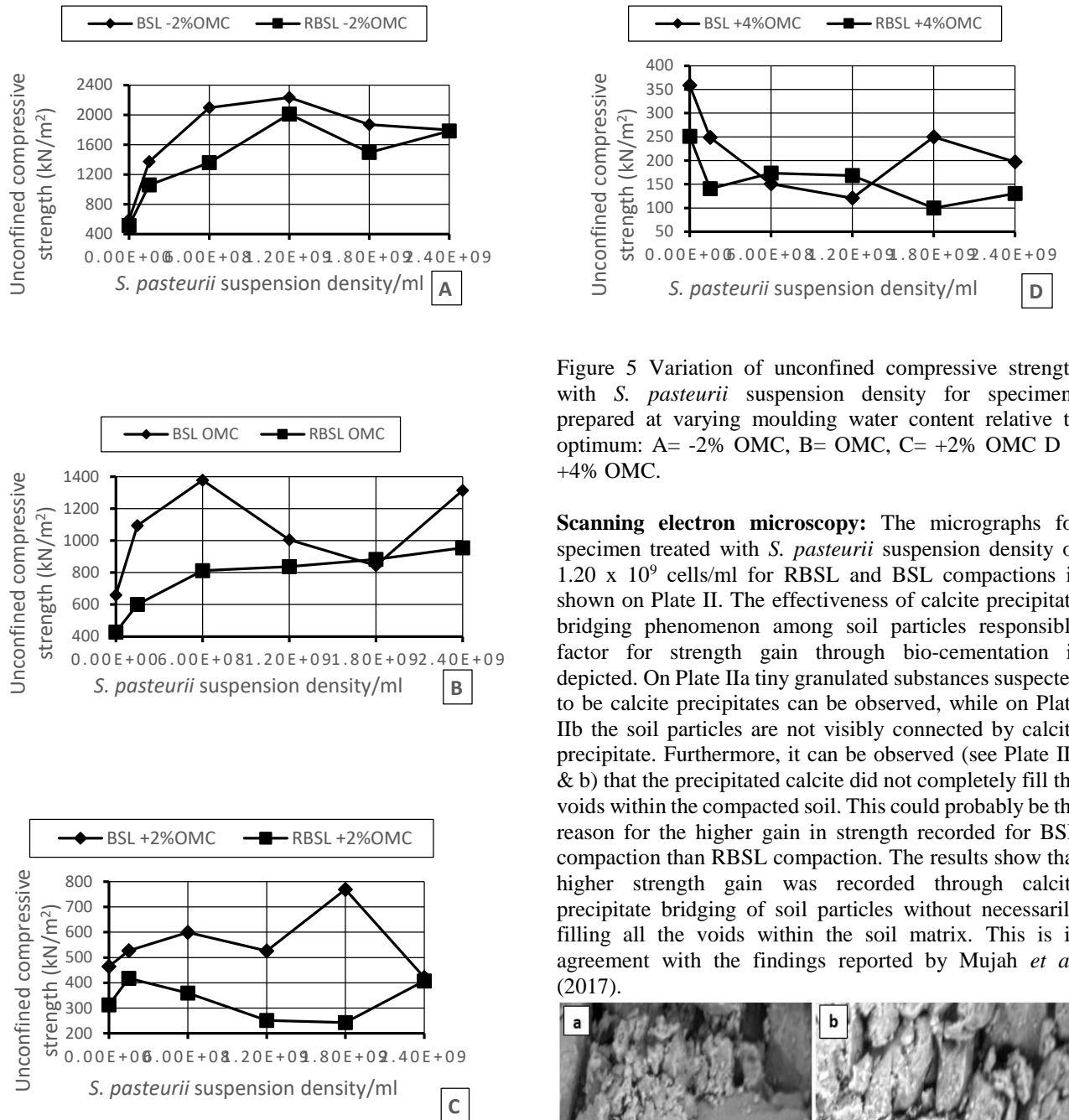


Figure 5 Variation of unconfined compressive strength with *S. pasteurii* suspension density for specimens prepared at varying moulding water content relative to optimum: A= -2% OMC, B= OMC, C= +2% OMC D = +4% OMC.

Scanning electron microscopy: The micrographs for specimen treated with *S. pasteurii* suspension density of 1.20×10^9 cells/ml for RBSL and BSL compactions is shown on Plate II. The effectiveness of calcite precipitate bridging phenomenon among soil particles responsible factor for strength gain through bio-cementation is depicted. On Plate IIa tiny granulated substances suspected to be calcite precipitates can be observed, while on Plate IIb the soil particles are not visibly connected by calcite precipitate. Furthermore, it can be observed (see Plate IIa & b) that the precipitated calcite did not completely fill the voids within the compacted soil. This could probably be the reason for the higher gain in strength recorded for BSL compaction than RBSL compaction. The results show that higher strength gain was recorded through calcite precipitate bridging of soil particles without necessarily filling all the voids within the soil matrix. This is in agreement with the findings reported by Mujah *et al.* (2017).

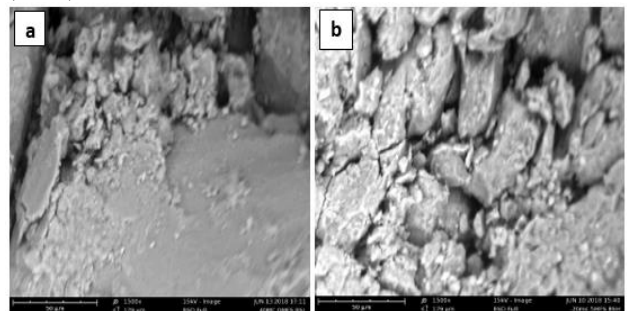


Plate II Microrgraphs of specimens treated with *S. pasteurii* suspension density of 1.20×10^9 cells/ml at x1500 magnification: a = RBSL compaction b = BSL compaction



CONCLUSION

The results of the study carried out show that higher strength gains were recorded for specimens prepared at lower moulding water content, but decreased with increasing moulding water contents irrespective of the *S. pasteurii* suspension density and compactive efforts used. Peak UCS values of 2,011 kN/m² and 2,232 kN/m² were obtained at *S. pasteurii* suspension density of 1.20 x 10⁹ cells/ml for specimens prepared at -2 % OMC and compacted with RBSL and BSL energy, respectively.

RECOMMENDATION

It is recommended that *S. pasteurii* suspension density of 1.20 x 10⁹ cells/ml be used to treat A-4(3) lateritic soil compacted with BSL energy to be used as liner and cover material in MSW containment system.

REFERENCES

- AASHTO (1986). *Standard Specifications for Transport Materials and Methods of Sampling and Testing*. 14th Edition, American Association of State Highway and Transport Officials (AASHTO), Washington, D.C
- Achal, V. and Pan, X. (2014). 'Influence of calcium sources on microbially induced calcite precipitation calcite precipitation by bacillus sp. CR2. *Appl Biochem Biotechnol*. 173 307–317. DOI: 10.1007/s12010-014-0842-1.
- Al Qabany, A., Mortensen, B., Martinez, B., Soga, K., and Dejong, J. (2011). 'Microbial Carbonate Precipitation: Correlation of S-Wave Velocity with Calcite Precipitation. *Pro. Geofrontiers in geotechnical engineering 2011: Technical Papers, ASCE*, 3993-4001.
- Al-Thawadi, S.M., (2011) Ureolytic bacteria and calcium carbonate formation as a mechanism of strength enhancement of sand. *Journal of advanced science and engineering research* 1 (2011) 98-114.
- ASTM, Annual book of ASTM standards, Vol. 04.08, 1992. Philadelphia.
- Bell, F.G. 1993. *Engineering Geology*, pp. 104. Blackwell Scientific Publications Oxford, London, Edinburgh, Boston, Melbourne, Paris, Berlin, Vienna.
- BS 1377 (1990). *Method of Testing Soils for Civil Engineering Purpose*. British Standard Institute, BSI, London.
- Cheng, L., and Cord-Ruwisch, R. (2012) "In situ soil cementation with ureolytic bacteria by Surface percolation". *Ecological Engineering*. 42 54–72. doi: 10.1016/j.ecoleng.2012. 01.013.
- Cheng L, Cord-Ruwisch R, Shahin M. A. 2013. Cementation of sand soil by microbially induced calcite precipitation at various saturation degrees. *Canadian Geotechnical Journal* 50:81–90.
- Daniel, D. E. and Wu, Y. K. (1993). 'Compacted clay liners and covers for arid site.' *Journal of Geotechnical Engineering ASCE*. Vol. 119. No. 2. Pp.223–237.
- Dawoud, O., Chen, C. Y., and Soga, K., (2014). 'Microbial induced calcite precipitation for geotechnical and environmental applications. *Pro. New frontiers in geotechnical engineering 2014: Technical Papers, ASCE, Geotechnical Special Publication*. 234, 11-18.
- Dejong, J. T., Fritzes, M.B., and Nusslein, K., (2006). 'Microbial induced cementation to control sand response to undrain shear. *ASCE, Journal of Geotechnical and Geoenvironmental Engineering*. 132 (11), 1381 – 1392. DOI: 10.1061/(ASCE)1090-0241(2006)132: 11(1381).
- Dejong, J. T., Gomez, M. G., Waller, J.T. and Viggiani, G. (2017) Influence of Bio-Cementation on the Shearing Behavior of Sand Using X-Ray Computed Tomography. *Geotechnical frontiers 2017: Technical Papers, ASCE, Geotechnical Special Publication*. 280, 871-880.
- Eberemu, A.O. (2013) Evaluation of bagasse ash treated lateritic soil as a potential Barrier material in waste containment application, *Acta Geotechnica* DOI 10.1007/s11440-012-0204-5
- Faurel, S., and Laloui, L., (2011). 'A bio-hydro-mechanical model for propagation of biogrowth in soils. *Pro. Geo-Frontiers 2011: Advances in Geotechnical Engineering, Dallas TX, ASCE, Geotechnical Special Publication*. 211, 4041-4048.
- Feng, K., and Montoya, B. M., (2016). 'Influence of confinement and cementation level on the behaviour of microbial-induced calcite precipitated sands under monotonic drained loading. *ASCE, Journal of Geotechnical and Geoenvironmental Engineering*. 142 (1), 040150571–9. DOI:10.1061/(ASCE)GT.1943-5606. 0001379.
- Hamdan, N., Kavazanjian, J., Rittman, B.E., and Karatas I. (2011). 'Carbonate Mineral Precipitation for Soil Improvement through Microbial Denitrification. *Pro. Geo-Frontiers 2011: Advances in Geotechnical Engineering, Dallas TX, ASCE, Geotechnical Special Publication*. 211, 3925-3934.



- Hamdan, N., Kavazanjian Jr. E., Rittmann, B.E. and Karatas, I. (2016): Carbonate Mineral Precipitation for Soil Improvement through Microbial Denitrification, *Geomicrobiology Journal*, DOI: 10.1080/01490451.2016.1154117
- Ijimdiya, T. S. (2017). Bioremediation of oil contaminated soils using NPK as nutrient for use in Road Subgrade. *Nigerian Society of Engineers Technical Transactions*. Jan. - March.51 (1);56–63.
- Jayanthi, P. N. V. and Singh, D. N. (2016) “Utilization of Sustainable Materials for Soil Stabilization: State-of-the-Art,” *Advances in Civil Engineering Materials*, 5(1), pp. 46–79, doi: 10.1520/ACEM20150013. ISSN 2165-3984
- Mujah, D., Shahin, M.A., and Cheng, L. (2016): Performance of biocemented sand under various environmental conditions, *XVIII Brazilian Conference on Soil Mechanics and Geotechnical Engineering. The Sustainable Future of Brazil goes through our Minas COBRAMSEG 2016 — 19-22 October, Belo Horizonte, Minas Gerais, Brazil*.
- Mujah, D., Shahin, M.A., and Cheng, L. (2017): State-of-the-Art Review of Biocementation by Microbially Induced Calcite Precipitation (MICP) for Soil Stabilization, *Geomicrobiology Journal*, DOI: 10.1080/01490451.2016.1225866.
- Mujah, D., Cheng, L. and Shahin, M.A. (2019) Microstructural and Geo-Mechanical Study on Bio-cemented Sand for Optimization of MICP Process. *ASCE Journal of Materials in Civil Engineering* 31(4): 04019025-10. DOI: 10.1061/(ASCE)MT.1943-5533.0002660.
- Osinubi, K.J., A.O. Eberemu, T.S. Ijimdiya, S.E. Yakubu and J.E. Sani (2017) Potential Use of *B. pumilus* in Microbial-Induced Calcite Precipitation Improvement of Lateritic soil. *Proceedings of the 2nd Symposium on Coupled Phenomena in Environmental Geotechnics (CEG2)*, Leeds, United Kingdom, 6-8 September, 2017.
- Osinubi, K.J. Eberemu, A.O. Ijimdiya, T.S. Gadzama, E.W. and Yakubu, S. E. (2018). ‘Improvement of the Strength of Lateritic Soil Treated with *Sporosarcina pasteurii*-Induced Precipitate.’ 2018 Nigerian Building and Road Research Institute International Conference. Theme: Sustainable Development Goals (SDGs) and the Nigerian Construction Industry – Challenges and the Way Forward. 12 – 14 June, Abuja, Nigeria.
- Osinubi, K. J., Gadzama, E. W., Eberemu, A. O., Ijimdiya, T. S. and Yakubu, S. E. (2019). Evaluation of the strength of compacted lateritic soil treated with *Sporosarcina pasteurii*. *Proceedings of the 8th International Congress on Environmental Geotechnics (ICEG 2018)*, “Towards a Sustainable Geoenvironment” Edited by Liangtong Zhan, Yunmin Chen and Abdelmalek Bouazza, 28th October – 1st November, Hangzhou, China, © Springer Nature Singapore Pte Ltd., Vol. 3, pp. 419–428, On-line: https://doi.org/10.1007/978-981-13-2227-3_52
- Park, S., Choi, S., Kim, W., and Lee, J., (2014). ‘Effect of microbially induced calcite precipitation on strength of cemented sand. *Pro. New frontiers in geotechnical engineering 2014: Technical Papers, ASCE, Geotechnical Special Publication*. 234, 47-56.
- Phenom World (2017). Fibermetric. <https://www.phenom-world.com/software/fibermetric>, 17th September, 2017.
- Reichle, D. E. (1977) The Role of Soil Invertebrates in Nutrient Cycling. *Ecological Bulletins* No. 25, Soil Organisms as Components of Ecosystems, pp. 145-156
- Rowshanbakht, K., Kamehchiyan, M., Sajedi, R.H., and Nikudel, M.R., (2016). ‘Effects of injected bacterial suspension volume and relative density on carbonate precipitation resulting from microbial treatment. *Ecological Engineering*, 89,49–55. [Dx.doi.org/ 10.1016/j.ecoleng.2016.01.010](https://doi.org/10.1016/j.ecoleng.2016.01.010).
- Sharma, A. and Ramkrishnan, R. (2016) Study on effect of Microbial Induced Calcite Precipitates on strength of fine grained soils. *Perspectives in Science* 8, 198–202. [dx.doi.org/10.1016/j.pisc.2016.03.017](https://doi.org/10.1016/j.pisc.2016.03.017)
- Soon, N., Lee, L., Khun, T., and Ling, H., (2014). ‘Factors affecting improvement in engineering properties of residual soil through microbial-induced calcite precipitation. *ASCE, Journal of Geotechnical and Geoenvironmental Engineering*. 140 (5), 04014006 1 – 11. DOI: 10.1061/(ASCE)GT.1943-5606.0001089.
- Sotoudehfar, A.R., sadeghi, M.M., Mokhtari, E., and Shafiei, F. (2016) Assessment of the Parameters Influencing Microbial Calcite Precipitation in Injection Experiments Using Taguchi Methodology, *Geomicrobiology Journal*, 33:2, 163-172, DOI:10.1080/01490451.2015.1025316.
- Stocks-Fischer, S., Galinat, J. K., and Bang, S. S., (1999). ‘Microbiological precipitation of CaCO₃. *Soil Biol. Biochem.*, 31 (11), 1563– 1571. PII: S00 3 8- 07 1 7(99)0 0 08 2 -6.
- Tirkolaei, H. K., and Bilsel, H., (2017) Estimation on ureolysis-based microbially induced calcium carbonate precipitation progress for geotechnical applications, *Marine Georesources and Geotechnology*, 35:1, 34-41, DOI:10.1080/1064119X.2015.1099062



van Paassen, L. A., Daza, C. M. Staal, M. Sorokin, D. Y. van der Zon, W. and van Loosdrecht, M. C.M. (2010a). Potential soil reinforcement by biological denitrification. *Ecological Engineering*. 36, 168 – 175. doi: 10.1016/j.ecoleng.2009.03.026.

van Paassen, L. A., Ghose, R., Van der Linden, T. J. M., Van der Star, W. R. L., and Van Loosdrecht, M.C.M., (2010b). ‘Quantifying biomediated ground improvement by ureolysis. Large-scale biogROUT experiment. *ASCE, Journal of Geotechnical and Geoenvironmental Engineering*. 136 (12), 1721 – 1728. DOI: 10.1061/(ASCE)GT.1943-5606.0000382.

Venkata P. N., Velpuri, Yu, X., Lee, H. and Chang, W. (2016). Influence Factors for Microbial-Induced Calcite Precipitation in Sands. Pro. Geo-China 2016: *Technical Papers, ASCE Geotechnical Special Publication 263*, 44-52

Whiffin, V.S., Van Paassen, L. A., and Harkes, M. P., (2007). ‘Microbial carbonate precipitation as a soil improvement technique. *Geomicrobiology Journal*. 24 (5), 417–423, DOI: 10.1080/01490450701436505.

Xu, G., Li, D., Jiao, B., Li, D., Yin, Y., Lun, L., Zhao, Z. and Li, S. (2017). Bio-mineralization of a calcifying ureolytic bacterium micro bacterium sp. GM-1. *Electronic Journal of Biotechnology* 25, 21-27. dx.doi.org/10.1016/j.ejbt.2016. 10.008.

Effects of Urban Growth on Surface Temperature in Parts of Katsina State, Nigeria

*Abdulsamad Isah¹ and Abubakar A.S¹

¹Department of Geography Federal University of Technology Minna, Nigeria.

*Corresponding Author Email: isahabdulsamad01@gmail.com, +2348032583692

ABSTRACT

An unprecedented urban population growth create the needs for the development of more urban infrastructures. In order to meet these demands, vegetated areas are converted to non- vegetated areas such as asphalt and bricks which has the ability to absorb heat and the later release it. This change in land use and land cover has increased the land surface temperature. A number of studies have demonstrated the impact of land use and cover on land surface temperature. Moreover, there is need to quantify the extent to which temperature has increased so as to identify areas where measure needs to be addressed. In this study, integration of remote sensing and geographical information system (GIS) was employed to evaluate the effect of rapid urban growth on land surface temperature in part of Katsina State, Nigeria. The result shows that urban land development raised land surface temperature by more than 17°C between 1999 and 2017. This study has demonstrated that the direct effects of urban land use and cover changes on one environmental element can have indirect effects on others. Therefore, planting of trees and vegetation should be encouraged to reduce the increase in surface temperature

Keywords: Effects, Urban growth, Surface Temperature, Remote Sensing.

1 INTRODUCTION

Since 1950 there has been a huge worldwide increase in the percentage of population living within cities (Kaya, et al., 2012). Approximately, 59% of the world's population currently lives in urban areas, and this Figures are further expected to increase especially in the developing countries where the fraction of the population that live in cities is comparatively lower than the developed countries (Kaya, et al., 2012). In the near future, it is expected that the global rate of urbanisation will increase the world urban population up to 67% by 2030, as urban agglomerations emerge and population migration from rural to urban suburban areas continue (Kaya, et al., 2012). The first fifty years of the 20th century witnessed unprecedented urbanisation in Nigeria. The urban population in Nigeria over the last three decades according to Alkali (2014) has been growing close to 5.8 percent per annum. In fact, the population of the urban centres in Nigeria constitute about 48.2 per cent of the country's total population and projections indicate that more than 60 per cent will live in urban centres by year 2025 (Alkali, 2015). Studies have shown that, in Nigeria, there are more than 840 urban centres and more than 10 cities with populations of over a million (Ayedun, Durodola & Akinjare, 2015).

In Katsina, land use and land cover patterns have undergone a rapid change due to accelerated expansion over the years. Urban growth has increased tremendously and extreme stress to the environment has occurred.

Katsina has been growing rapidly owing to favourable socio-economic, political, and physical factors.

The low values of albedo, vegetative cover, and moisture availability in combination with the presence of high levels of anthropogenic heating have given rise to a phenomenon known as the Urban Heat Island (UHI) effect. Hence, urban areas generally act as islands of elevated temperature relative to the natural areas surrounding them (Sailor, 1995) cited in (Lo & Quattrohi, 2013). The main cause of the Urban Heat Island is the modification of the land surface through urban development with the use of materials that effectively retain heat. As population increases, they tend to modify a greater area of land and have a corresponding increase in the average temperature (Rail, 2014). Urbanisation, on the other hand, negatively affects the environment due to pollution modifying the physical and chemical properties of the atmosphere and the soil surface. UHI is considered to be a cumulative effect of all these impacts. It is defined as the, rise in temperature of any man-made area (Kaya et al, 2012).

The integration of remote sensing and geographic information systems (GIS) have been widely applied and recognized as a powerful and effective tool in detecting urban land use and land cover change (Ehlers, Jadcowski, Howard and Brostuen, 1990; Treitz, Howard and Gong, 1992; Harris and Ventura, 1995) cited in Saleh (2016). Satellite remote sensing collects multispectral, multi resolution and multi temporal data, and turns them into

information valuable for understanding and monitoring urban land processes and for building urban land cover datasets. GIS technology provides a flexible environment for entering, analyzing and displaying digital data from various source necessary for urban identification, change detection and database development (Weng, 2015).

Many researchers have previously embarked on studies investigating the relationship between urban growth and surface temperature in major cities over Nigeria, such as; Suleiman and Tanko (2018) and Tanko et.al., (2017) in Kano metropolis; Tyubee and Anyadike (2013) in Makurdi, Benue State, Nigeria; and Zemba et.al, (2016) in Jimeta, Adamawa State, Nigeria. In Katsina state, one study which did very well in assessing urban growth and micro climate was that of Gide (2012), and the study used conventional climatic data as well as population figures for over 40 years in establishing the relationship between the air temperature and urban growth. The work of Gide (2012) was lacking in terms of GIS/Remote Sensing techniques. This study thus is aimed at filling that gap by using the GIS/Remote Sensing techniques in studying the same phenomenon. The study therefore aims to assess the effects of urban growth on surface temperature in parts of Katsina State, Nigeria with the objectives of evaluating the Land use/Land cover changes in the study area and analyzing the effect of urban growth on Surface Temperature in Katsina State.

1.1 THE STUDY AREA

The study area is Katsina state, Nigeria and it is located between latitude 12°30'N and 13°15'N, and longitude 7°31'E and 8°00'E. It has a tropical Continental type of climate that is hot and dry for most of the year with maximum day temperatures of about 38°C and the minimum temperature of 22°C (Abdulkadir I., 2016). It has an average rainfall of about 800mm. The vegetation is dominated by fine-leaved Acacia species and their associates such as baobab and their likes. (Danbuzu, 2012).

2 METHODOLOGY

In evaluating the Land use and Land cover changes in the study area. Landsat satellite imageries of 1999, 2007 and 2017 were utilized to get the land use and land cover classification which is necessary for detection of LULC changes as a result of urbanisation activities from 1999 to 2017. The classes considered include:-

Vegetation, Built-up area, Bare soil and water bodies. Each of these classes have a colour identifier.

Vegetation - Green

Built-up Area - Red

Bare Land - Brown.

Water bodies - Blue

The area coverage of each of their classes for each of the year under concern was estimated in Km² in order to ascertain the spatio-temporal changes.

This was achieved using model developer in ERDAS imagine 14 software. All bands of the satellite images with the exception of thermal and cloud bands were stacked together into a single image for each of the years put under concern using the maximum likelihood algorithm which is expressed as:

$$P(W) = \sum_{m=1}^M PCW_{/i} p \quad (1)$$

Where:

N = Number of classes

P(w) = Normalization constant to ensure that $\sum P(w/i) = 1$

P(w/i) = Likelihood function.

P(i) = Priori information, that is the probability the class occurred in the study area.

Thermal bands of the satellite images for the years put under concern in this study were imputed into ERDAS together with their tabular information of gain and bias obtained from the Landsat METADATA files. The Digital Numbers for each image was converted to radiance, radiance to reflectance, reflectance to emissivity, emissivity to corrected surface temperature, and finally to Land Surface Temperature (LST). Temperature values were converted from degree Kelvin (K) to degree Celsius (°C) by subtracting 272.15 from the Kelvin value, which is the conversion rate from Kelvin to Celsius.

In analyzing the effect of urban growth on LST in Katsina State, a regression analysis was done with urban growth values as independent variable and LST values as dependent variable in order to obtain the statistical effect of urban growth on LST in Katsina State. The regression model is expressed as:-

$$Y = a + bx \quad (2)$$

$$b = \frac{(N \sum XY - (\sum X)(\sum Y))}{(N \sum X^2 - (\sum X)^2)} \quad (3)$$

$$a = \frac{(\sum Y - b(\sum X))}{N} \quad (4)$$

Where:

X and Y are the variables

- b = the slope of regression line
- a = the intercept point of the regression line and the y axis
- N = number of values or elements
- Y = second score
- $\sum XY$ = sum of the product of first and second score
- $\sum X$ = sum of first scores
- $\sum Y$ = sum of second scores
- $\sum X^2$ = sum of square of first squares.

3 RESULTS AND DISCUSSION

The first part is on land use/land cover classification and evaluation of land use/land cover maps respectively. The second part is on land surface temperature distribution while the third section is on the relationship between surface temperature and land use/land cover. The results are presented in form of maps and statistical tables;

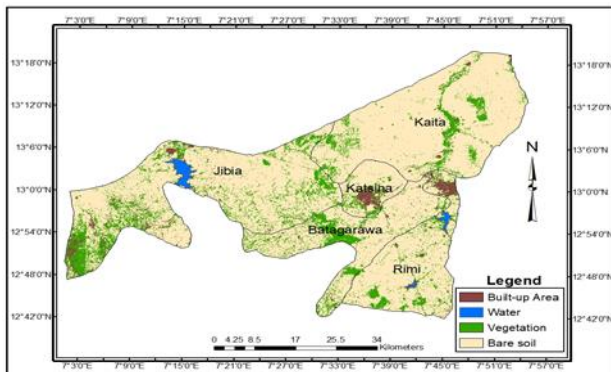


Figure 1: 1999 Land use/cover classification map of the study

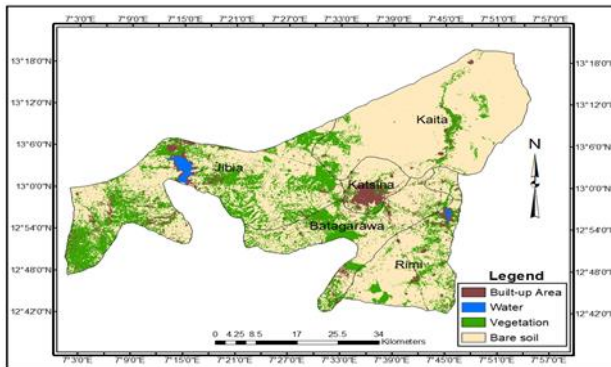


Figure 2: 2007 Land use/cover classification map of the study area

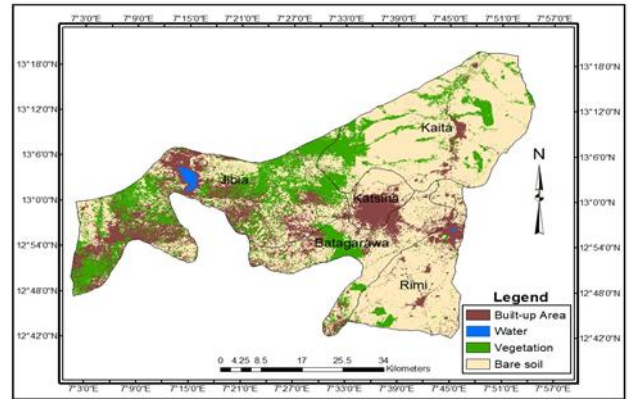


Figure 3: 2017 Land use/cover classification map of the study area

3.1 LAND USE LAND COVER MAPPING

Land use land cover maps for the three years of the study area were generated and presented in Figures 1, 2 and 3.

3.2 LAND USE LAND COVER CLASSIFICATION

Table I summarises the total area for each land use land cover class across the study area and the corresponding percentages of the total.

TABLE I: LAND USE LAND COVER STATISTICS

Years	1999		2007		2017	
	Area (km ²)	(%)	Area (km ²)	(%)	Area (km ²)	(%)
Built up area	94.3	3.2	165.5	5.5	580.3	19.4
Water body	22.8	0.8	18.2	0.6	12.7	0.4
Vegetation	470.11	15.7	715.3	23.9	641.9	21.5
Bare soil	2401.8	80.4	2090.0	70.0	1754.1	58.7
Totals	2,989.0	100.0	2989.0	100.0	2989.0	100.0

The land use/land cover classification for 1999 for TM satellite image (Figure1) indicates that most of the study area was under Bare soil accounting for 2401.8 km² (80.4%) followed by vegetation which occupied 470.1km² (15.7%), while built up area and water body amounted to 94.3km² (3.2%) and 22.8km² (0.8) respectively.

The image classification result generated from 2007 Landsat ETM+ (Figure 2) shows that Bare soil still

remain the major land use land cover but with a decrease to 2090.0km² (70.0%) of the total area. Vegetation has increased to 715.3 km² (23.9%), this change in Vegetation during the period under review was probably due to afforestation programmes funded under the European Economic Commission/Katsina State Government (EEC/KTSG) afforestation project in the State from 1999 to 2017, which mainly involved the planting of trees for shelter belts and wind breaks as well as private woodlots on communal land. Built-up area in this year has increased to 165.5 km² (5.5%). Water body has also decreased to 18.2km² (0.6%).

Result generated from 2017 Landsat 8 operational land imager (OLI) image (Figure 3) showed that the dominant class is Bare soil, even though it has decreased slightly to 1754.1km² (58.7%). Vegetation decreased to 641.9km² (21.5%) while Built-up area increased significantly to 580.3 km² (19.4%) and water body has also decreased to 12.7km² (0.4%).

3.3 ACCURACY ASSESSMENT OF IMAGE CLASSIFICATION

Evaluation of classification results is an important process in satellite image classification procedure. This is necessary to ascertain the level of correctness and reliability of the classification output. Kappa satisfied index which provides a more rigorous assessment of classification accuracy was also computed for each classified map. The Kappa coefficient expresses the proportionate reduction in error generated by a classification process compared with the error of a completely random classification. Tables II, III, and IV shows the accuracy assessment results for the years of 1999, 2007 and 2017 respectively.

TABLE II: ERROR MATRIX OF 1999 IMAGE CLASSIFICATION

	Built up Area	Water Body	Vegetation	Bare Soil	Kappa	P.A	U.A
Built of Areas	5	2	3	90	0.87	91%	90%
Water body	4	86	10	0	0.81	81%	86%
Vegetation	91	5	0	4	0.88	90%	91%
Bare soil	1	13	81	5	0.72	86%	81%

Overall classification accuracy =87%

Overall kappa statistics =0.83

TABLE III: ERROR MATRIX OF 2007 IMAGE CLASSIFICATION

	Built up Area	Water body	Vegetation	Bare Soil	Kappa	P.A	U.A
Built up area	0	2	2	96	0.95	93%	96%
Water body	89	7	4	0	0.85	87%	89%
Vegetation	3	90	1	6	0.87	90%	90%
Bare soil	10	1	88	1	0.84	93%	88%

Overall classification accuracy =91%

Overall kappa statistics = 0.88

TABLE IV: ERROR MATRIX OF 2017 IMAGE CLASSIFICATION

	Built up Area	Water Body	Vegetation	Bare Soil	Kappa	P.A	U.A
Built area	1	4	10	85	0.80	83%	85%
Water body	91	4	6	0	0.88	86%	91%
Vegetation	8	77	5	10	0.71	90%	77%
Bare Soil	6	1	85	8	0.80	81%	85%

Overall classification accuracy = 85%

Overall Kappa Statistic =0.79

Generally for the three images, the producer accuracy of bare soil (81%) was lower than other classes. This is as a result of error due to omission and misclassification to built-up area, water body and vegetation. The overall classification accuracy was 85% while the Kappa coefficient was 0.79.

3.4 LAND USE LAND COVER CHANGE

TABLE V: LAND USE LAND COVER CHANGE STATISTICS

Year	1999-2007		2007-2017		1999-2017	
	Change (km ²) (%)	Growt h (%/yr)	Change (Km ²)(%)	Growt h (%/yr)	Change (km ²)(%)	growt h (%/yr)
Built up area	71.2 (71.8)	8.9	414.8 (252.7)	25.2	486.0 (506.2)	28.1
Water body	-4.6 (-2.50)	-0.3	-5.5 (-33.3)	-3.3	-10.1 (-50.0)	-2.7

Vegetation	245.2 (52.2)	6.5	-73.4 (-10.0)	-1.0	-171.8 (-36.9)	-20
Bare soil	-311.8-12.9	-1.6	-335.9 (-16.1)	-1.6	-647.7 (-26.9)	-1.4

According to Table V, from 1999 to 2007, built-up area and vegetation increased by 71.2km² (71.8%) and 245.2km² (52.2%) respectively, while water body and Bare soil decreased by -4.6km² (-2.5%) and -311.8km² (-12.9) respectively. This may be due to the increase in population which may have increased the number of built-up areas. Similarly, during the second period between 2007 to 2017 water body decreased by -5.5km² (-33.3%), vegetation by -73.4 km² (-10.0%) and Bare soil -335.9km² (-16.1%), However, the built up area increased by 414.8km² (252.7%). In general, between 1999 and 2017 water body, vegetation and Bare soil decreased by -10.1km² (-50.0%), -171.8km² (-36.9%) and -647.7km² (-26.9%) respectively. While built up area increased by 486.0km² (506.2%).

The annual growth rate in built up area as determined by the land use and land cover change statistics was 8.9% from 1999 to 2007, 25.2% from 2007 to 2017 and 28.1% for the entire period of 1999 to 2017. This implies a dramatic urban growth and change in the morphology of the study area and to an extent, this was as a result of increase in housing and infrastructural development such as health, educational and other socio-economic reasons. On the other hand water body showed an annual reduction rate of 0.3% from 1999 to 2007, 3.3% from 2007 to 2017 and overall annual reduction rate of 2.7% for the entire study period of 1999 to 2017. Similarly, vegetation showed an annual increase of 6.5% from 1999 to 2007, but from 2007 to 2017, an annual reduction was experienced at a rate of 1.0%, and 2.0% for the entire study period of 1999 to 2017. Bare soil decreased annually at the rate of 1.6% from 1999 to 2017, 16.1% from 2007 to 2017. This result corroborate with the findings of Abdulkadir (2009) in which he used geomatics technology to analyze the pattern of spatial growth in parts of Katsina state.

In general, the land use land cover change statistics in Table V showed that increase in built-up areas mainly emanated from the conversion of other land use and land cover especially vegetation to built-up areas during the period under review (1999 to 2017), as a result of rapid urban growth within the study area. Besides the

land use land cover change statistics image classification result and visual assessment gives a general insight into the magnitude of the defined classes across the landscape and changes observed.

3.5 LAND SURFACE TEMPERATURE VARIATION IN THE STUDY AREA.

TABLE VI: STATISTICS OF LAND SURFACE TEMPERATURE

Years	1999	2007	2017
Maximum	24.55	39.11	42.59
Minimum	13.31	25.87	29.47
Mean	20.00	32.27	37.13

From Table VI, it could be seen that the maximum value of surface temperature (ST) in 1999 was 27.9°C while the maximum value was 25.0°C in 2007, the maximum and minimum ST values increased drastically to 30.9°C and 28.0°C respectively. The ST continued to increase in 2017 with a maximum value of 33.0°C and a minimum value of 31.0°C. From this study, the mean values of ST in 1999, 2007 and 2017 were 20.40°C, 29.48°C and 32.91°C.

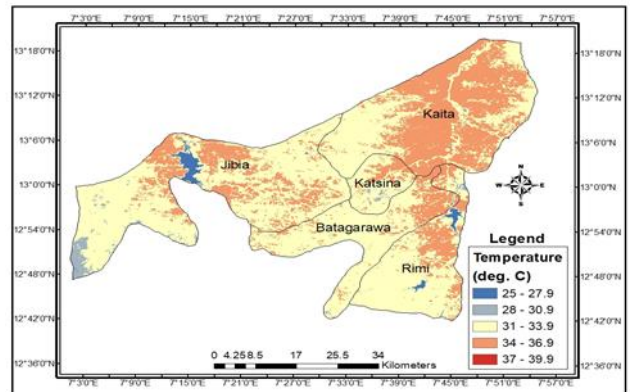


Figure 4: 1999 Surface Temperature Map

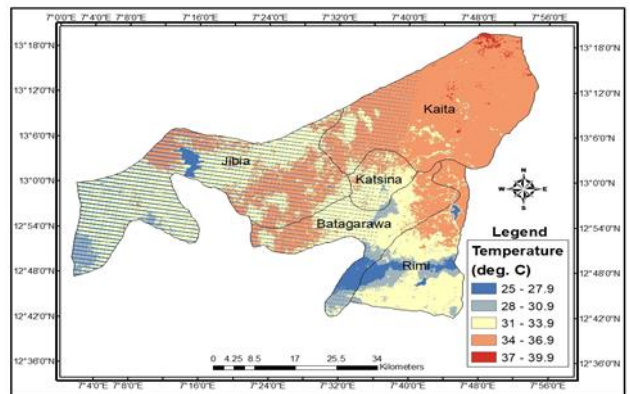


Figure 5: 2007 Surface Temperature Map

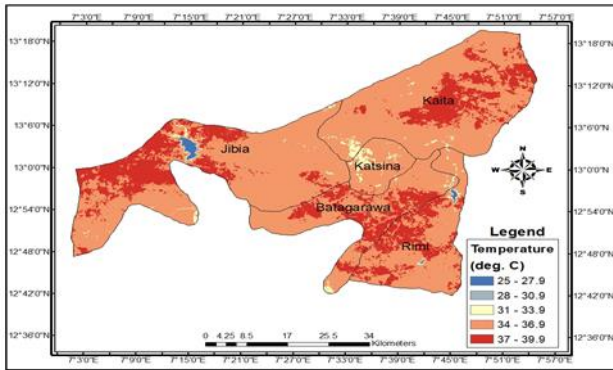


Figure 6: 2017 Surface Temperature Map

3.6 SURFACE TEMPERATURE OF LAND USE LAND COVER TYPES

Table VII; Shows the average value of surface temperature ($^{\circ}\text{C}$) for each of the land use/cover in 1999, 2007 and 2017.

TABLE VII: AVERAGE SURFACE TEMPERATURE ($^{\circ}\text{C}$) STATISTICS OF LAND USE/COVER TYPES

Class	1999 ($^{\circ}\text{C}$)	2007 ($^{\circ}\text{C}$)	2017 ($^{\circ}\text{C}$)
Built up	19.07	32.87	36.14
Farmland	20.19	31.94	38.15
Vegetation	16.03	28.08	33.41
Bare land	21.81	34.40	39.55

From Table VII, it is obvious that bare land exhibits the highest surface temperature (21.8°C in 1999, 34.40°C in 2007 and 39.55°C in 2017), followed by farmland (20.19°C in 1999, 31.94°C in 2007 and 38.15°C in 2017). In 1999, 2007, and 2017 the values of ST exhibited by built up are 19.07°C , 32.87°C and 36.14°C respectively. The lowest values of ST in this study are exhibited by vegetation (16.03°C in 1999, 28.08°C in 2007 and 33.41°C in 2017).

From 1999 to 2007, the surface of built-up areas, farmland, vegetation and bare land in the study area increased by 13.80°C , 11.75°C , 12.05°C and 12.58°C respectively. Similarly, during 1999 and 2017 the surface temperature of built up, farmland, vegetation and bare land appreciated by 3.27°C , 6.20°C , 5.33°C and 5.16°C . This represent a general increase in surface temperature of built up, farmland, vegetation and bare land by 17.06°C , 17.96°C , 17.74°C respectively during 1999 and 2017.

It is evident from Table VII that vegetation had shown considerably low ST during the three period because dense vegetation can reduce the amount of heat stored in the soil and surface structure through transpiration.

4 CONCLUSION

For the past 20 years, parts of Katsina state has been experiencing accelerated urban growth. This study has demonstrated how Landsat data can be used to evaluate the effect of urban growth on surface temperature in parts of Katsina state, Nigeria. Remote sensing and GIS were combined to examine the effect of urban growth on temporal variation of surface temperature. Findings from this study revealed that there is a general decline in natural surfaces, and an increase in developed surfaces from 1999 – 2017. The resulting GIS analysis shows that built-up area is increasing at an annual average range of 5.1%, and surface temperature has gone up by more than 17°C during the study period. If the built-up areas continues to increase at this rate, and vegetation continues to decline at an annual rate of 0.8%, ST will be on a very high scale in the near future and this may bring about the formation of the urban heat island over Katsina.

4.1 RECOMMENDATIONS

The variation in surface temperature of the identified land use/cover types in parts of Katsina state suggest that urban growth is a major factor responsible for land transformation in the study area. The increase in rate of surface temperature has its attendant effect on both the environmental and the health of residents. Therefore, planting of trees and vegetation in and around the study area should be encouraged to minimize the increase in surface temperature of the land use/cover types which may also affect the mean surface temperature of the study area. Future research works should be focused on integrating GIS and satellite remote sensing with high spectral, spatial and temporal resolution at the local scale to develop urban environmental monitoring models. Moreover, research works should draw attention to urban land use modeling and techniques integrating socio-economic data and GIS tools to predicting future pattern of change. Focus should be given to the effect of urban growth and growing impervious surfaces as well as water pollution and stress.

ACKNOWLEDGEMENTS

I am most grateful to Allah for granting me the wisdom, strength and needed resources to embark on his research. I wish to acknowledge my profound gratitude and regards to my able supervisor; Prof. A.S. Abubakar for his constant monitoring, guidance and encouragement throughout the period of this work. I appreciate the



support of Dr. M. A. Emiglati, Dr. M. Mairo and Dr. M. Y. Suleiman for their guidance and encouragements. My profound gratitude also goes to my lovely mum; Hajiya Mairo Garba Saulawa; my brother Dr. Hassan; My wife and daughters; as well as my close friends and colleagues, the likes of; Isah Abdullahi Tanko and Abba Aliyu Kasim for their prayers, support, guidance, and encouragements. May Allah reward you all abundantly.

REFERENCES

1. Journals

- Adesina, F.A., Siyanbola, W.O., Okelola, F.O., Pelemo, D.A., Ojo, L.O. & Adegbulugbe, A. O. (2014). Potentials of Agroforestry for Climate Change Mitigation in Nigeria. Some Preliminary Estimates. *Journal of Global Ecology Biogeography Letters*, 8, 163-173.
- Kaya, S., Basar, U.G., Karaca, M. & Seker, D.Z. (2012). Assessment of Urban Heat Islands Using Remotely Sensed Data Ekoloji. *Journal of Remote Sensing* 21(84), 107-113.
- Rail, A.N. (2007). Urban Thermal Plumes, their Possible Impact on Climate Change. *Kastell journal, Sudbury, Suffolk*.
- Sailor, D.J. (2015). Simulated urban climate response to modifications in surface albedo and vegetative cover. *Journal of Applied Meteorology*, 34(7), 1694-1704.
- Saleh, A.H.S. (2016), Impact of urban expansion on surface temperature in Baghdad, Iraq using remote sensing and GIS techniques, *Journal of Atmospheric Sciences*, 13(1), 48-59.
- Suleiman, Y.M. and Tanko, I. A. (2018). Assessing the Existence of the Atmospheric Urban Heat Island over Kano, Metropolis, Nigeria. *Journal of Environmental Planning and Sustainability*, 2(1), 1 – 14.
- Tanko, I. A, Suleiman Y. M, Yahaya T. I and Kasim A. A (2017). Urbanisation Effect on the Occurrence of Urban Heat Island over Kano Metropolis, Nigeria. *International Journal of Scientific and Engineering Research*, 8(9), 293 – 299.
- Tyubee, B. T. & Anyadike, R.N.C. (2012). Analysis of Surface Urban Heat Island in Makurdi, Nigeria. *Journal of Environmental Management*, 7(3).
- Weng, Q. (2001). A remote sensing-GIS evaluation of urban expansion and its impact on surface temperature in the Zhujlang Delta, China. *International Journal of Remote Sensing*, 22(10).
- Zemba, A. A., Adebayo, A. A. & Musa, A.A. (2010). Evaluation of the Impact of Urban Growth on Temperature in Jimeta. *International Journal of Geosciences*, 6(3), 234 -241.

2. Online journals without DOI

- Ayedun, C.A., Durodola, O.D. & Akinjare, O.A. (2011). Towards ensuring sustainable urban growth and development in Nigeria: Challenges and Strategies. *Business Management Dynamics*, 1(2), 99-104. Retrieved from <http://www.bmdynamics.com>

- United States Geological Survey (USGS). Complete Orthorectified Landsat images of Katsina Metropolis for the years of 1999, 2007 and 2017. Retrieved from <https://data.usgs.gov/datacatalog/>

3. Conference

- Abdulkadir, F.I. (2009). Application of geomatics technology in the analysis of the spatial Growth of Katsina metropolis. *A seminar paper presented at the Office of the Surveyor-General of the State, Nagogo Road Katsina Nigeria*.
- Alkali, J.L.S. (2005). Planning Sustainable Urban Growth in Nigeria: Challenges and Strategies. *A paper presented at the Conference on Planning Sustainable Urban Growth and Sustainable Architecture Held at ECOSOG Chambers, United Nations Headquarters, New York*.



Kinetic Modelling and Error Analysis of the Bioremediation of Used Motor Oil Contaminated Soil Using Palm Bunch Ash as Stimulant

ABDULYEKEEN, K. A¹, ALIYU, A², ABDULKARIM, A. Y³, SALIS, A⁴, & ABDULKARIM, A. S⁵
^{1,3,4,5}Chemical Engineering Department, Faculty of Engineering and Engineering Technology, Abubakar Tafawa Balewa University, Tafawa Balewa Way, P.M.B 0248, Bauchi, Nigeria

²Urban and Regional Planning Department, Faculty of Environmental Technology, Abubakar Tafawa Balewa University, Tafawa Balewa Way, P.M.B 0248, Bauchi, Nigeria

*Corresponding author email: avekeenkabir@atbu.edu.ng, +2347035863248

ABSTRACT

In view of the pollution of underground water, economic loss, decrease in agricultural productivity of soil, poor animal and human health caused by contamination of soil with used and unused motor oil, this study was conducted for the bioremediation of used motor oil contaminated soil using palm bunch ash (PBA) as stimulant in twelve treatment cells labelled T₁ to T₁₂ and kept at room temperature. D-optimal design of response surface methodology with one numerical factor (PBA) and a categorical factor at two levels (5% and 10% pollution) was employed to generate ten experimental runs for the biostimulation process. In this study, the bioremediation potential of the ash was evaluated for a period of ten (10) weeks by taking samples from each of the treatment cells for weekly analysis of Oil and Grease Content (O&G) and Total Heterotrophic Bacteria Count (THBC) at two-week interval. After ten (10) weeks, the results showed T₁, T₂, T₃, T₄, T₅, T₆, T₇, T₈, T₉, T₁₀, T₁₁, and T₁₂ exhibited 86.5%, 100%, 79.2%, 74.5%, 95.5%, 79.2%, 100%, 99.4%, 99.0%, 63.0%, 88.0%, and 58% oil and grease degradation, respectively. The biodegradation data were fitted to zero, first and second order kinetic models and the biodegradation constant (k) and half-life (t_{1/2}) values were obtained. The R² values showed that the first and second order kinetic models fitted the experimental data. Comparing the results of the error analysis of the studied kinetics, it was found that the first order kinetic model best fits the degradation of used motor oil in all the treatment cells. It was also observed that the THBC in all the treatment cells followed the batch growth culture of microorganisms. From the results of this work, it can be concluded that the application of PBA stimulates the growth of microorganisms that enhanced the consumption of used motor oil in the soil. Thus, can be applied to develop an environmentally safe, robust, and economically viable treatment strategy for oil contaminated soil.

Keywords: Biodegradation, biostimulation, palm bunch ash, kinetics, used motor oil.

1 INTRODUCTION

Pollution specifically, with petroleum and petroleum products has been acknowledged to be one of the most severe problems affecting lives of citizens and financial prudence of nations to which it quietly and undetectably spills mostly in mechanic workshop in Nigeria (Emmanuel et al., 2015). These oil spills are caused by used motor oil which is brown-to-black oily liquid due to the additional chemicals (such as chlorinated biphenyls, chlorodibenzofuran, lubricate additives) that are build up in oil after undergoing high temperature and pressure inside a running engine (Abdulsalam et al., 2012; Agarry and Ogunleye, 2012; Abdulyekeen et al., 2018).

The Release of persistent, bio accumulative and toxic chemicals (benzene, toluene, ethylbenzene, xylene and polycyclic aromatic hydrocarbon) caused health and environmental hazards. These pollutants find their way into plant tissues, animals and human being by the movement of hazardous elements in the environment (Ebenezer, 2013). Soil polluted with spent and fresh motor oil create a solmn effect on plant tissues, soil componrnnts, and its microorganisms, human and other animal health (Stephen and Ijah 2011; Adu et al., 2015).

There are many ways of remediating contaminated soil which includes physiochemical and biological methods (such as bioremediation) although the physical and chemical methods are expensive and less efficient than biological methods (Bijay et al., 2012; Abdulyekeen et al., 2018)

Bioremediation is the process of degrading pollutants in the environment by autochthonous or allochthonous microorganisms such as bacteria and fungi or plants to damage, destabilise, detoxify hazardous materials in soil or render them inoffensive by using them as their carbon and energy source (Anjana et al., 2014; Ebenezer, 2013; Abdulyekeen et al., 2018).

Contamination of soil through oil spills is the primary global concern today, and it has caused severe hazard to our health, lower ground water usage, environmental problems, causes economic loss (through bad products in our agricultural activities) by reducing the agricultural productivity of the soil (Bijay et al., 2012).

Many efforts have been made to reduce environmental pollution by using agricultural wastes for treating used motor oil polluted soil (Abdulsalam et al., 2012; Abdulyekeen et al., 2016; Abdulyekeen et al., 2018; Abdulyekeen et al., 2019) but there is little research on the use of palm bunch ash as stimulant for the treatment of used

motor oil polluted soil. Palm bunch ash is obtained from empty fruit bunch of *Elaeis Guineensis* palm tree species. Although the empty fruit bunches are normally thrown away, they have been found to be a source of Potassium Carbonate and Potassium Hydroxide (Yelebe *et al.*, 2015).

The aim of this research work is to compare the biostimulation potentials of palm bunch ash for the remediation of used motor oil contaminated soil as well as to obtain the kinetic model that best fits the experimental data obtained.

2 METHODOLOGY

2.1 SAMPLE CHARACTERIZATION

The analyses carried out on the contaminated soil and the PBA included the pH, total organic carbon, the phosphorus and nitrogen contents. The method adopted for each of the analyses is given in Table I. Also for soil, in addition to these parameters measured, the initial concentration of the oil and grease was determined.

2.2 DETERMINATION OF OIL AND GREASE CONTENT OF THE SOIL

The gravimetric method was used to determine the oil and grease content as described by (Chang, 1998). 5.0 g of the UMO polluted soil was weighed and transferred in to test tube after which 5.0 ml of n-hexane was added, and the mixture was agitated vigorously for 5.0 minutes. The mixture was allowed to settle and was decanted into a 50 ml beaker whose weight determined as w_1 in grammes. The procedure was repeated three times to bring the total solvent to 20 ml; the mixture was left open in the laboratory for 24 hours for the n-hexane to evaporates completely. The weight of the beaker after evaporation was weighed as w_2 in grammes. The oil and grease content was calculated using (1) and the percentage oil & grease removal was calculated using (2).

TABLE I: METHODS USED FOR DETERMINATION OF PHYSICOCHEMICAL AND MICROBIAL PROPERTIES DETERMINATION

Parameter	Method	Source
pH	Moisture adjustment in 1:1 (weight of soil to volume of water) followed by agitation of the mixture prior to pH Measurement	Ebenezer, 2013
Moisture content	Drying method based on moisture loss per dry weight	Motsara & Roy, 2008
Phosphorous content	Spectrophotometry	Abdulsalam <i>et al.</i> , 2012
Nitrogen content	Kjedahl method	Abdulsalam <i>et al.</i> , 2012
Total organic carbon	Titrimetry	Walkley & Black, 1934

$$O \& G (ppm) = \frac{w_2 - w_1}{W} \times 10^6 \quad (1)$$

Where, W = weight of soil sample taken.

$$Y_a (\%) = \frac{C_i - C_t}{C_i} \times 100 \quad (2)$$

where

C_i = initial concentration of O&G in ppm

C_t = concentration of O&G in ppm at a particular bioremediation time

2.3 DETERMINATION OF TOTAL HETEROTROPHIC BACTERIAL COUNT

The enumeration of the total bacterial count present in the treatment cells was determined by the spread plate techniques. The sample from each of the treatment cells was subjected to serial dilution which was plated on nutrient agar (NA) oxoid and incubated at $28 \pm 2^\circ\text{C}$ for 24 hour and plate that yields count between 30 – 300 colonies were counted (Agarry, Owabor, & Yusuf, 2010).

3 RESULTS AND DISCUSSION

3.1 RESULTS OF CHARACTERIZATION

The physicochemical properties of the used motor oil contaminated soil and palm bunch ash is presented in Table II. The higher the oil & grease, the higher the organic carbon whose oil and grease content was above the limit (500 mg/kg) set by the Nigeria Ministry of Environment (Abdulsalam *et al.*, 2011). Nitrogen and phosphorous content were also determined and presented in the Table II. The pH (6.6 and 6.9) for 5% and 10% respectively were within the acceptable limit of 5.5 - 8.5 for effective bioremediation by Vidali (2001).

TABLE II: PROPERTIES OF THE USED MOTOR OIL AND PALM BUNCH ASH

Type of analysis	Palm bunch ash	Soil	
		10% Pollution	5% Pollution
pH	12.3	6.9	6.6
Nitrogen (ppm)	3.7	2.5	1
Phosphorous (ppm)	2551.35	1156.76	1135.14
Total organic carbon (%)	12	13.5	7.8

3.2 OIL & GREASE CONTENT (O&G) FOR EACH OF THE TREATMENT CELLS

The result of the residual O&G is given in Figure I. From the figure, it can be seen that degradation occur in each of the treatment cells. The control (T₁₁ and T₁₂) undergo natural attenuation for the ten weeks' remediation period. Therefore, this result shows that the palm bunch ash increases the rate of the bioremediation.

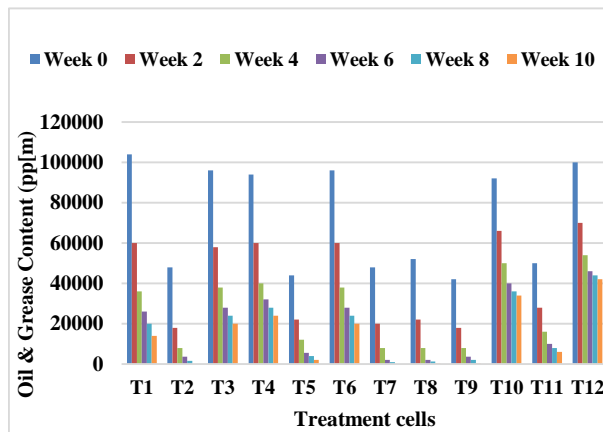


Figure I: Variation of Oil & Grease (ppm) with Bioremediation Time (week)

3.3 TOTAL BACTERIAL COUNT RESULT

Figure II illustrates the bacterial growth profile in the treatment cells. It was noticed that the bacterial growth profile followed the batch growth culture of microorganism with lag, exponential, stationary, and death phases. All the treatment cells followed a similar trend of lag phase, the period of adaptation to new environment and it lasted for one week. Between weeks two to six, it followed a similar pattern of the exponential phase, the period of maximum used oil consumption. Stationery phase was followed for a period of one week (between weeks six and eight) after which it was followed by death phase and this could be due to nutrients exhaustion or secretion toxic substances.

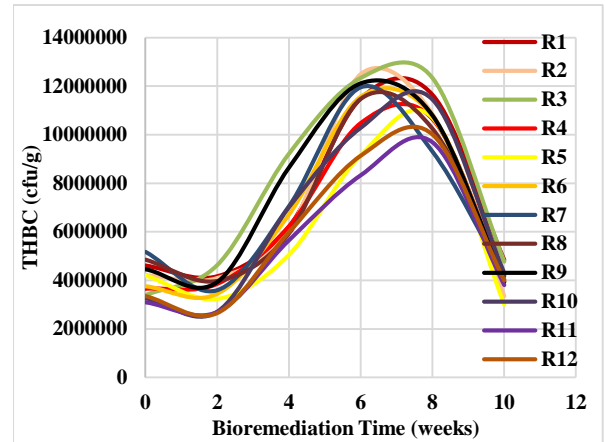


Figure II: Variation of Total Bacterial Count with Bioremediation Time (week)

3.4 KINETIC MODEL TESTING AND HALF-LIFE STUDY

Kinetic modelling was performed using zero, first and second order kinetic model equations to estimate the biodegradation rate of the pollutant in the used motor oil contaminated soil. The integral method is used for the degradation of the model equations. Equation (3a and 3b), (4a and 4b) and (5a and 5b) are zero, first and second order kinetic models respectively, whose summary of their plot is given in Table III (Abdulyekeen *et al.*, 2018)

$$C_A = -k_0 t + C_{A0} \quad (3a)$$

$$\ln C_A = -k_1 t + \ln C_0 \quad (4a)$$

$$\frac{1}{C_0} = k_2 + \frac{1}{C_{A0}} \quad (5a)$$

$$t_{1/2} = \frac{C_{A0}}{2k_0} \quad (3b)$$

$$t_{1/2} = \frac{0.693}{k_1} \quad (4b)$$

$$t_{1/2} = \frac{1}{C_{A0} k_2} \quad (5b)$$

Were C_A being the residual concentration of the oil and grease (mg/kg),

C_{A0} as the initial concentration of the oil and grease (mg/kg) at week zero,

t is the bioremediation time (week),

k_0 (mol.dm³week⁻¹), k_1 (week⁻¹) and k_2 (kgmg⁻¹week⁻¹) as the bioremediation constants for the zero, first, and second order kinetics.

TABLE III GIVES THE KINETIC MODEL TESTING RESULTS FOR ALL THE TREATMENT CELLS.

Sample	Zero k ₀	t _{1/2}	R ²	k ₁	First t _{1/2}	R ²	k ₂	Second t _{1/2}	R ²
T ₁	8285.7	6	0.8406	1.215311	0.570346	0.9797	0.000006	1.602564	0.9703
T ₂	5360	4	0.7909	1.522875	0.455157	0.9982	0.00007	0.297619	0.8419
T ₃	7028.6	9	0.8297	1.166724	0.594097	0.9495	0.000006	1.736111	0.9968
T ₄	6485.7	7	0.8319	1.142707	0.606583	0.9378	0.000003	3.546099	0.9925
T ₅	3862.9	6	0.8177	1.356218	0.511088	0.9932	0.00004	0.568182	0.8582
T ₆	7114.3	7	0.8381	1.168476	0.593206	0.951	0.000003	3.472222	0.9957
T ₇	5600	4	0.7569	1.652352	0.419491	0.991	0.00004	0.520833	0.8365
T ₈	4670	6	0.7487	1.669794	0.41511	0.9911	0.000003	6.410256	0.6541
T ₉	3720	6	0.771	1.549605	0.447306	0.9791	0.00004	0.595238	0.6004
T ₁₀	5571.4	8	0.8629	1.105503	0.626997	0.9322	0.000003	3.623188	0.9738
T ₁₁	4085.7	6	0.8233	1.236024	0.560788	0.9691	0.00004	0.5	0.9845
T ₁₂	5371.4	9	0.8049	1.087846	0.637174	0.8749	0.000003	3.333333	0.9284

3.5 ERROR ANALYSIS RESULTS

The use of the classical (correlation coefficient- R²) to find out best kinetic model for experimental data only measures the difference between theoretical data in linear plot and the experimental data but not the error in the kinetics curve as observed by El- Grandy *et al.* (2011). Due to the resulting bias from linearization, the first and second order kinetic models were compared using three error functions given by (6), (7) and (8).

The sum of square error (SSE)

$$SSE = \sum_{i=1}^p (C_{exp} - C_{cal})_i^2 \quad (6)$$

The hybrid fractional error function (HYBRID)

$$HYBRID = \frac{100}{p-n} \sum_{i=1}^p \left| \frac{(C_{exp} - C_{cal})^2}{C_{exp}} \right|_i \quad (7)$$

Marquardt's percentage standard deviation (MPSD)

$$MPSD = 100 \left[\sqrt{\frac{1}{p-n} \sum_{i=1}^p \left\{ \frac{(C_{exp} - C_{cal})}{C_{exp}} \right\}^2} \right] \quad (8)$$

Where n is number of parameters within the equation, p is the number of data points. C_{exp} is the experimental data and C_{cal} is the calculated data using the kinetic models.

The results of the three-error function analysis (presented in Table IV) shows that first order kinetic model best fit the experimental data which is in line with the results obtained by several researchers (Agarry and Latinwo, 2015; Agarry and Oghenejoboh, 2015; Agarry *et al.*, 2012; Abioye *et al.*, 2012).

TABLE IV: RESULTS OF ERROR ANALYSIS FOR FIRST AND SECOND ORDER KINETIC MODEL

Sample	Sum of square errors		Hybrid Fractional Error		MPSD	
	First	Second	First	Second	First	Second
T ₁	212175910.8	10851183155	144499	5245787.364	3801.304	22903.68
T ₂	12311233.15	3907057065	16377	8317496.414	1279.742	28840.07
T ₃	276746102.9	24217687.16	209531	17399.40447	4577.459	1319.068
T ₄	266914161.6	88791064.07	207662	88745.87862	4556.994	2979.025
T ₅	9475384.766	4784593056	20913	5507333.998	1446.128	23467.71
T ₆	248746653	37995464.94	198638	28709.18168	4456.887	1694.378
T ₇	13758428.87	3487196019	29803	7798922.902	1726.35	27926.55
T ₈	22186982.69	3406012253	40503	4173632.874	2012.524	20429.47
T ₉	13524616.22	2341434236	31906	3563560.268	1786.234	18877.39
T ₁₀	166469775.7	160589267.4	132964	134231.2935	3646.425	3663.759
T ₁₁	61723579.69	2582044523	95090	2832738.538	3083.666	16830.74
T ₁₂	318217747.4	951313744	220680	932092.8587	4697.661	9654.496

4 CONCLUSION

This research work has investigated the biostimulation potentials of palm bunch ash for the remediation of used motor oil contaminated soil. There was degradation of oil and grease in the whole treatment cells. Although, the application of palm bunch ash has successfully enhanced the degradation of the oil and grease in the polluted soil.

The correlation coefficient (R^2) of the kinetic study (zero, first and second order) showed that bioremediation process followed the first and the second order kinetics.

The results of the error analysis showed that first order kinetics model best fits this experimental data.

REFERENCES

- Abdulsalam, S., Bugaje, I. M., Bugaje, I. M., Ibrahim, S., (2011). Comparison of biostimulation and bioaugmentation for remediation of soil contaminated with spent motor oil. *International Journal of Science and Technology*, 8(1), 187–194.
- Abdulsalam, S., Adefia, S. S., Bugaje, I. M and Ibrahim, S. (2012). Bioremediation of soil contaminated with used motor oil in a closed system. *Journal of Bioremediation and Biodegradation*, 03(12), 3–9. <http://doi.org/10.4172/2155-6199.1000172>
- Abdulyekeen K.A., Ibrahim A.A., Aliyu A., Salis A., (2018). Kinetic Modelling and Half-Life Study of the Bioremediation of Used Motor Oil Contaminated Soil Using Animal Dung as Stimulants. *American Journal of Engineering Research*, Volume-7, Issue-8, pp-217-223.
- Abioye, O. P., Agamuthu, P., and Abdul Aziz, A. (2012). Bioremediation of used motor oil in soil using organic waste amendments. *Biotechnology Research International*, 8. <http://dio.org/10.1155/2012/587041>
- Adu, A.A., Aderinola, O.J., Kusemiju, V. (2015). Comparative effects of spent engine oil and unused engine oil on the growth and yield of *Vigna Unguiculata* (Cowpea). *International Journal of Science and Technology*, 4(3), 105–118.
- Agamuthu, P., Abioye, O. P., & Aziz, A. A. (2010). Phytoremediation of soil contaminated with used lubricating oil using *Jatropha curcas*. *Journal of Hazardous Materials*, 179(1-3), 891–894. <http://doi.org/10.1016/j.jhazmat.2010.03.088>
- Agarry, S., and Latinwo, G. K. (2015). Biodegradation of diesel oil in soil and Its enhancement by application of bioventing and amendment with brewery waste effluent as biostimulation-bioaugmentation agents. *Journal of Ecological Engineering*, 16(2), 82-91. <http://doi.org/10.12911/22998993/1861>
- Agarry, S. E., and Oghenejoboh K. M. (2015). Enhanced aerobic biodegradation of naphthalene in soil: Kinetic modelling and half-Life Study. *International Journal of Environmental Bioremediation & Biodegradation*, 3(2), 48-53 <http://doi:10.12691/ijebb-3-2-2>
- Agarry, S. E., Owabor, C. N., and Yusuf, R. O. (2012). Enhanced bioremediation of soil artificially contaminated with petroleum hydrocarbon oil mixtures: evaluation of the use of animal manure and chemical fertilizer. *Bioremediation Journal*, 14(4), 189-195. <http://doi.org/10.1186/2251-6832-3-31>
- Anjana, S., Poonam, K., and Meenal, B. R. (2014). Biodegradation of Diesel Hydrocarbon in Soil by Bioaugmentation of *Pseudomonas aeruginosa*: A Laboratory Scale Study. *International Journal of Environmental Bioremediation & Biodegradation*, 2(4), 202–212. <http://doi.org/10.12691/ijebb-2-4-8>
- Bijay, T., Ajay Kumar, K.C., Anish, G. (2012). A Review on Bioremediation of Petroleum Hydrocarbon Contaminants in Soil. *Kathmandu University Journal of Science, Engineering and Technology*, 8(1), 164–170.
- Bray, R. H. and Kurtz, L. T., (1945). Determination of Total, Organic and Available Forms of Phosphorus in Soil. *Soil Science*, 59: 39-45
- El-Gendy, N. S., and Farah, J. Y. (2011). Kinetic modeling and error analysis for decontamination of different petroleum hydrocarbon components in biostimulation of oily soil microcosm. *Soil and sediment contermination: An international journal*, 20(4), 432-446. <http://doi.org/10.1080/15320383.2011.571525>
- Ebenezer L. A. (2013). Bioremediation of Hydrocarbon Contaminated Soil Using Compost, NPK Fertilizer and Cattle Bile as Amendment Materials. *Kwame Nkrumah University of Science and Technology*.
- McAlpine, R., and Soule, B., (1933). Qualitative chemical analysis 476,575.
- Stephen, E. and Ijah, U. J. J., (2011). Comparison of Glycine Max and Sida Acutain the Phytoremediation of Waste Lubricating Oil Polluted Soil. *Natural and Science* 9(8): 190-193
- Walkley, A. and Black, I. A. (1934). "An examination of the method for determining soil organic matter, and a proposed modification of the chromic acid filtration method," *Soil Sci. Soc. Am. J.*, vol. 37, pp. 29–38.
- Vidali, M., (2001). Bioremediation. An overview. *Pure Appl. Chem*, 73(7), 1106-1115
- Yelebe, Z. R., Samuel, R. J. and Yelebe, B. Z., (2015). Kinetic Model Development for Bioremediation of Petroleum Contaminated Soil Using Palm Bunch and Wood Ash. *International Journal of Engineering Science Invention*, ISSN (Online): 2319 – 6734, Volume 4 Issue 5, PP.40-47. Retrieved from <http://www.ijesi.org>

Quantitative Risk Analysis for Communication Satellite Payload

*Babadoko, D. M¹, Ikechukwu, A. D²

¹Project Management Technology Department, Federal University of Technology, PMB 65 Minna Niger State, Nigeria

²Project Management Technology Department, Federal University of Technology, PMB 65 Minna Niger State, Nigeria

*Corresponding author email: babadokos74@gmail.com, +2348024563101

ABSTRACT

The application of risk management is a critical stage for any spacecraft project to achieve required components and system functionality for a successful mission, a risk management plan is high-level accounts and descriptions of risk concepts for any satellite mission to be successful. This research article investigates the application of criticality analysis and risk priority number analysis for communication satellite payload components by following industry standard and using MIL-STD-1628, MIL-STD-1629A termed as military standard and the ECSS-Q-STD-30-02C termed as European Cooperation for Space Standardization for space product assurance in conducting analysis of risk and determining mitigation techniques and also determined the sample correlation coefficient of criticality of components and risk priority.

Keywords: Correlation, Payload, Project, Risk, Satellite.

1 INTRODUCTION

The utilization of space technologies has increased substantially, bringing with it, a share of benefits, ranging from early environment and disaster threat detection and warnings, climatic changes, metrological forecasts, geographical information system (GIS), as well as enhanced communication (Spagnulo, 2013). A satellite system performs these multifaceted functions because of its design which consist of two functional areas, the Bus Systems and the Communication Payload Systems as in figure 1 and figure 2 respectively.

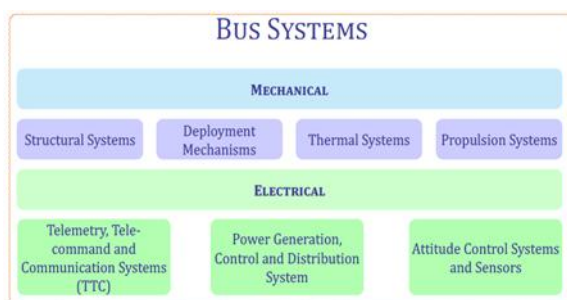


Fig. 1: Components of the functional areas of a satellite system. (Source: (GVF Training & MahdiBagh Computers PVT. Ltd., 2008)

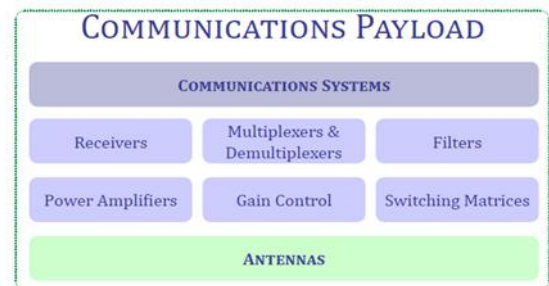


Fig. 2: Components of the functional areas of a satellite system. (Source: (GVF Training & MahdiBagh Computers PVT. Ltd., 2008)

While the Bus system consists of all the elements that support the communication payload, the communication payload provides support for all the functional aspects of the mission for which the satellite is launched (GVF Training & MahdiBagh Computers PVT. Ltd., 2008)

The increased utilization of space technologies necessitated an increased need for space research and explorations. Consequently, satellites are launched into space for either communication or environmental monitoring for disaster. Satellites have different functionalities, determined by their locations in space. Excerpts from existing literature (Braun, 2012; Stanniland & Curtin, 2013) suggest that Low Earth Orbit (LEO) satellites are used for navigation, space missions, and low latency communication, the Medium Earth Orbit (MEO) satellites, while performing the same function as the LEO satellites, are differentiated by the distance from the earth, and the Geostationary (GEO) satellites are commonly used for communication purposes.

Satellite has been recognised as driver for national growth and sustainable development, access to reliable and adequate geospatial information (GI) according to Akinyede and Agbaje (2006). The recognition of this fact, may have prompted the Nigerian government to initiate moves, the NIGCOMSAT-1, a Nigerian Communication Satellite Project (Zhicheng et al., 2006), aimed at addressing the problem of communication, seen as one of the greatest setbacks to the socio-economic development of the country, particularly in the areas of rural telephoning, broadcasting, tele-education, tele-medicine, e-government, e-commerce and real-time monitoring services (Chukwu-Okoronkwo, 2015). Boroffice (2008) noted that the NigComSat-1 project was to provide a platform for capacity-building and the development of satellite technology for the level of transformation in the telecommunication, broadcasting and broadband industry in Africa, as well as prospects increased businesses in rural and remote regions through access to strategic information.

Although the contribution of satellite systems has been substantial, Bargellini and Edelson (1977) noted that satellite communications systems will continue to expand because traffic growth forecasts indicate the need for greater communications capacity. Consequently, the financing of communications satellite has grown from a government organised, privately operated venture, to regulated and competitive part of the economic infrastructure. However, one critical factor confronting the satellite communication industry is the risk of damage, resultant disruption to service and liabilities due to collision as result of derelict satellite (Pelton et al., 2017).

The planning, building, launching, financing, and operating a communication satellite is a routine business for long term investment and its require a high up-front capital expenditure with a start-up period of 2 years, with a large number of high investment risk factors (Pelton et al., 2017). The effect of a satellite failure, in terms of cost and multiplier effect is huge, as noticeable in Zhicheng et al. (2006) containing an account of the failed NIGCOMSAT-1, which was de-orbited due to Electrical Power Subsystems defect in the Solar Array Drive Assembly (SADA), and replaced with NIGCOMSAT-1R.

The risk and cost associated with satellite failures like the NIGCOMSAT-1 is huge and by far outweighs the cost of carrying out a risk assessment of the space project. In the NIGCOMSAT-1 failure cited above, although the satellite was replaced at no cost to the Nigerian government, there were chances of collision with other satellite in the adjacent orbital slot when if it were not de-orbited. Even with the de-orbiting, the resulting space debris posed another risk for other satellites in orbit. To avert all these risk factors, the need for adequate and

thorough risk analysis of critical components and risk priority analysis before satellite launch become crucial.

Fales (1984) observes that given the fact that the development and production programme for satellite communications terminals are affected by a variety of risks from both satellite and terminal development, an understanding of the effect and impact of these risks on the terminals becomes a crucial step towards mitigating the overall system risk. Risk analysis of a communication satellite should provide an insight into risk areas with a view to designing a good mitigation strategy, identify areas where management reserve can be committed early to risk reduction activities, and determine the appropriate level of management reserve (Fales, 1984), as shown in table 1.

Inferences from existing studies is that the above, requires the development of a risk management plan to take account of risks by identifying, and conducting analysis, following the root cause of each risk and the consequences of each risk and providing mitigating plans (Gamble, 2015; Gamble & Lightsey, 2014; Gamble & Lightsey, 2015; Gamble & Lightsey, 2016)

TABLE 1: STEPS IN RISK MANAGEMENT PLAN

Main Step	Sub-steps
A.Risk identification	<ol style="list-style-type: none"> 1.Review the mission concept of operation 2.Identify root causes 3.Classify priority of risk 4.Name responsible person 5.Rank likelihood (L) and consequence(C) of root cause 6.Describe rationale for ranking 7.Compute mission risk likelihood and consequence values 8.Plot mission risks on L-C chart
B.Determine mitigation techniques	<ol style="list-style-type: none"> 1.Avoid the risk by eliminating root cause and/or consequence 2.Control the cause or consequence 3.Transfer the risk to a different person or project 4.Assume the risk and continue in development
C. Track progress	Plot the mission risk values on an L-C chart at life-cycle or design milestones to see progress

Table 1: Steps of Risk Management Plan. Source: Gamble (2015)

A risk may be assessed either qualitatively or quantitatively. Risk management process utilizes rating scales for each of the risk factors with impact, likelihood, and time frame (National Research Council (U.S.), 2005). The impact of a risk event can be to cost, schedule and technical performance. Qualitative risk assessment provides relative values of the likelihood of occurrence and potential consequences of each risk, in general qualitative risk assessment method would be adequately for making risk management decision. Quantitative risk assessment which is usually undertaken for high, critical, or unmanageable risks as determined through the qualitative risk assessment is aimed at establishing the amount of contingency to be included in the estimate for the risks undergoing this assessment, such that should the risk(s) occur, there would be sufficient budgeted amount to overcome the extra expenditure (Srinivas, 2019). This is possibly because quantitative methods require more precise analyses and understanding of the risk or allocation of resources for risk reduction (GOES, 2013).

Although Meyer (2015) notes that quantitative risk analysis is less common in risk management of projects due to insufficient data about the project to perform this analysis of risk quantitatively, the practice of quantitative risk methods would be appropriate to the schedule, budget and risk forbearance of communication satellite mission and will result in more informed knowledge and more successful communication satellite missions.

The results from quantitative risk and reliability analysis were an important input into decision making during design process. These results provided ways to compare relative risks and to inform the decision makers. Key programmatic decisions that were influenced by the risk assessment results in the satellite industry include; choice of Crew Launch Vehicle (CLV), choice of propulsion system, choice of lunar mission mode, elimination of unnecessary radiation shield and definition of acceptable risk in a space mission.

However, the approach for this work was to contribute to the risk analysis of communication payload in order to make improvement in the payload system under analysis, which was based on reliability of the payload components by combining both criticality and risk priority number analysis compared to other works which were based on quality, safety, control or depending on the purpose for the FMEA. By including the quantitative risk assessment into the design process effectively blend the performance and risk within time and budget constraint were achieved (Dale, 2005).

2 METHODOLOGY

This research utilized both qualitative and quantitative research approaches. A purposive sampling, a non-probability sampling technique, that focuses on a particular characteristics of a population of interest, thus enabling answers to research questions. Team of engineers from different background in satellite industry participated to come up with the decision on the parameters of the Risk Priority Number (RPN) of each component. Tables related to each of these parameters can be found in the associated standards (ECSS-Q-ST-30-02C, 2009) (European Cooperation for Space Standardization (ECSS), 2009).

Table 2 shows the charting of failure effects severity to the performance of a satellite communication payload. "Severity classification category shall be assigned to each failure mode and component according to the failure effect.

TABLE 2: THE FOUR SEVERITY LEVELS OF FAILURE AS DEVELOPED BY MIL-STD-1628

Cat egory	Effect	Criteria
4	Catastrophic	Failure mode capable of causing complete components, system and mission lost.
3	Critical	Failure mode capable of component damage, system degradation that could reduce the performance of the components or the system.
2	Major	Failure that could cause components damage, system damage that are not critical. It will lead to delay or loss of availability.
1	Minor	Failure that would not cause components damage, system degradation but could lead to unscheduled maintenance.

2.1 FAILURE MODE EFFECT CRITICALITY ANALYSIS (FME(C) A) APPLICATIONS FOR COMMUNICATION SATELLITE PAYLOAD

In line with the FMEA procedures of identifying the failure modes for each components of the system, it was essential to itemize failure modes for each component after decomposing the system into block diagram. The system design, assembly, and installation can provide the information needed for the failure modes for each unit component of the system (Harland & Lorenz, 2007).

The effect on the functional condition of the component under analysis caused by the loss or degradation of output shall be identified so the failure mode effect will be properly categorized” (MIL-STD-1629A, 1980) (Department of Defense United States of America, 1980).

Quantitative risk analysis data shortage gave room for organizations to come up with standards of requirement to meet up their needs, the military standard 1628 term as MIL-STD- 1628. (Liu at el 2013) came up with some ratings on failure occurrence, detection and severity as in table 3, table 4 and table 5 respectively below. These tables are used for computing and analysing the failure mode severity, occurrence and detection for the communication payload components risk analysis.

TABLE.3: SUGGESTED RATINGS FOR THE OCCURRENCE OF A FAILURE MODE

Probability of failure	Possible failure rates	Rank
Nearly impossible	≤ 1 in 150,000	1
Remote	1 in 150,000	2
Low	1 in 15,000	3
Relatively low	1 in 2000	4
Moderate	1 in 400	5
Moderately high	1 in 80	6
High	1 in 20	7
Repeated failures	1 in 8	8
Very high	1 in 3	9
Extremely high(failure almost inevitable)	≥ 1 in 2	10

Adapted from (Liu et al., 2013)

TABLE 4: SUGGESTED RATINGS FOR THE SEVERITY OF A FAILURE MODE.

Effect	Severity of effect	Rank
None	No effect	1
Very minor	Very minor effect on product or system performance	2
Minor	Minor effect on product or system performance	3
Low	Small effect on product performance. The product does not require repair	4
Moderate	Moderate effect on product performance. The product requires repair	5
Significant	Product performance is degraded. Certain functions may not operate	6
Major	Product performance is severely affected but functions. The system may not operate	7
Extreme	Product is inoperable with loss of primary function. The system is inoperable	8
Serious	Failure involves hazardous outcomes and/or noncompliance with government regulations or standards	9
Hazardous	Failure is hazardous, and occurs without warning. It suspends operation of the system and/or involves	10

	noncompliance with government regulations	
--	---	--

Adapted from (Liu et al., 2013)

TABLE 5: SUGGESTED RATINGS FOR THE DETECTION OF A FAILURE MODE

Detection	likelihood of detection by design control	Rank
Almost certain	Design control will almost certainly detect a potential cause of failure or subsequent failure mode	1
Very high	Very high chance the design control will detect a potential cause of failure or subsequent failure mode	2
High	High chance the design control will detect a potential cause of failure or subsequent failure mode	3
Moderately high	Moderately high chance the design control will detect a potential cause of failure or subsequent failure mode	4
Moderate	Moderate chance the design control will detect a potential cause of failure or subsequent failure mode	5
Low	Low chance the design control will detect a potential cause of failure or subsequent failure mode	6
Very low	Very low chance the design control will detect a potential cause of failure or subsequent failure mode	7
Remote	Remote chance the design control will	8

	detect a potential cause of failure or subsequent failure mode	
Very remote	Very remote chance the design control will detect a potential cause of failure or subsequent failure mode	9
Absolute uncertainty	Design control does not detect a potential cause of failure or subsequent failure mode. Or there is no design control	10

Adapted from (Liu et al., 2013)

2.2 ANALYSIS

1. Criticality Analysis

Critical components are focused on criticality number as a result of multiplying severity number and occurrence number of each failure mode. Criticality number for failure mode usually ranks the potential of components risk of failure which is centered on the component failure mode occurrence and consequence of the failure effect as shown in table 6 below using the MIL-STD-1628 to determine the severity of failure mode of each component.

TABLE 6: PAYLOAD COMPONENTS CRITICALITY NUMBER COMPUTATION

Part Name	Failure Mode	Severity Number	Occurrence Number	Criticality Number
Receiver Components				
Input Waveguide Filter	Opening of connections	3	1	3
Input Stage Components				
Low Noise Amplifier	Input signal to down converter	4	1	4

(LNA)	distortion			
	Unstable input signal to down converter	4	1	4
Down Converter				
Oscillator	Disorder in the performance of down converter	2	1	2
PLL	Frequency intermission or disorder of output signal	2	1	2
Mixer	Power loss in output signal of mixer/ increase in the level of unwanted signals	2	1	2
	Low isolation between the openings	2	1	2
High Power Amplifier				
TWTA	High output power	3	1	3
	Output power loss	4	1	4
	Failure of TWTA	4	1	4

	tube or cathode			
CAMP	Failure of transponder	4	1	4
Fixed Amplifier	Interruption of the output signal of down converter	2	1	2
Variable Attenuator	Interruption of the output signal of transmitter	2	1	2

Components with criticality value of four (4) shows tendency of high concern in the system, from this it shows that high power amplifier and low noise amplifier component in the system are critical in the functioning of the satellite communication payload system. To avoid risk of failure of these components is to make provision for redundancy of the active components of the payload as mitigation measures.

2. Risk Priority Number (RPN)

RPN method uses three rankings to come up with an RPN value and these rankings are the probability of the failure-mode occurrence (O), the severity of its failure effect (S) and the probability of the failure being detected (D). These three are measured on a numerical scale and then multiplied with one another to get the RPN value for each component in the system as shown in table 7. Components with a high value of RPN signified that, the component has high risk of failure.

TABLE 7: RISK PRIORITY NUMBER COMPUTATION

Part Name	Failure Mode	O	S	D	RPN
Receiver Components					
Input Waveguide Filter	Opening of connections	3	7	5	105
Input Stage Components					
Low Noise Amplifier (LNA)	Input signal to down converter distortion	5	7	3	105
	Unstable input signal to down converter	4	9	1	36
Down Converter					
Oscillator	Disorder in the performance of down converter	2	9	2	36
PLL	Frequency intermission or disorder of output signal	3	7	2	42
Mixer	Power loss in output signal of mixer/ increase in the level of unwanted signals	2	7	2	28
	Low isolation between the openings	2	7	5	70
High Power Amplifier					
TWTA	High output power	4	10	1	40
	Output power loss	3	10	1	30
	Failure of TWTA tube or cathode	3	10	1	40
CAMP	Failure of transponder	3	7	1	21
Fixed Amplifier	Interruption of output signal of down converter	4	7	28	
Variable Attenuator	Interruption of the output signal	2	5	5	50

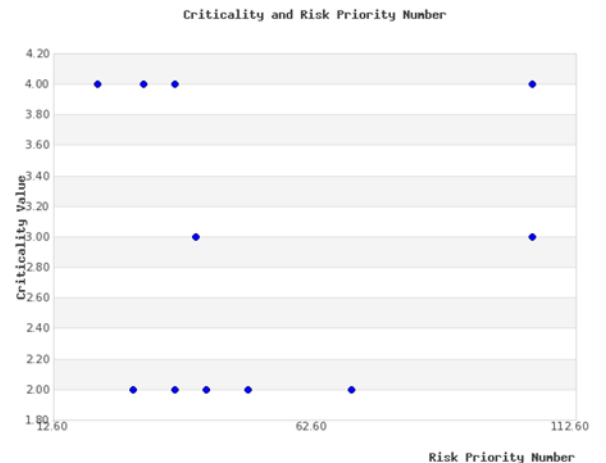
From the RPN analysis it's found that input filter, LNA, mixer has higher value of risk priority and translate to higher chances of risk failure.

3. Correlation Analysis

To establish the association between criticality of component (reliability) and component failure risk priority. Component criticality value is the independent variable while component risk priority number is the

TABLE 8: COMPONENT CRITICALITY AND RISK PRIORITY VALUES

Transponder Components	Components Criticality	Risk Priority Number
Input wave guide filter	3	105
Low Noise Amplifier 1	4	105
Low Noise Amplifier 2	4	36
Oscillator	2	36
Phase Lock Loop (PLL)	2	42
Mixer 1	2	28
Mixer 2	2	70
TWTA 1	3	40
TWTA 2	4	30
TWTA 3	4	30
CAMP	4	21
Fixed Amplifier	2	28
Variable Attenuator	2	50



3 RESULTS AND DISCUSSION

From the analysis of criticality of components using MIL-STD-1628 for the analysis, it shows that Low Noise Amplifier and High Power Amplifier components has critical value (4) four, and it means that at single point failure of these components would result to catastrophic severity effects on the satellite system and this might result to the total loss of signal from the payload and the mission would be at risk of failure.

While the RPN analysis, considering the suggested ratings adopted by Liu et al in their research and the ECSS-Q-STD-30-02C of space product assurance failure modes. The result shows that the input wave guide filter, Low noise amplifier, mixer and variable attenuator has high value of risk priority number 105,105,70, and 50 respectively. Some components with high criticality values like low noise amplifier of input stage component, High Power Amplifier components' has low value for risk priority number. In essence, these components with high RPN value signified high priority of risk

Theoretically, it would be that high critical components should have high risk failure priority and the correlation coefficient should be strong. The factors responsible for that not to happen in this study, is that some components with high severity rankings have low detection and occurrence rankings while some components with lower severity rankings with higher value of detection and occurrence rankings and this would definitely have higher value of risk failure priority when these rankings are multiplied out.

The result of the correlation coefficient shows a weak association with a value of $r = 0.0488$ between critical components and risk of failure, it would be expected that components with high criticality value should have strong association with risk priority of failure.

4 CONCLUSION

Considering single point failure mode of the communication payload components in Table 2, from the four severity level of failure developed by MIL-STD-1628 and components with failure effect of causing complete component, system and mission lost has criticality value of (4) four. Components such as low noise amplifier of the input stage, high power amplifier components are of high criticality values as a result of the criticality analysis of the sample data collected for the study as shown in table 6 and it implies that any failure of these components would bring about mission lost.

To avert or mitigates the effect of single point failure of these active components, a redundancy or back-up components should be incorporated in the design such that at the event of failure of any active components the back-up components would take active position to prevent total system failure.

The risk priority number, is similar to the criticality number, the difference is in computing for the criticality number to determine the critical components only the severity of failure and probability of failure occurrences are considered while in the risk priority number both the probability of failure mode, severity of failure effects and the probability of failure detection are computed.

Table 7 shows that components with high value of risk priority number are of high chances of failure, similar to criticality number. While performing correlation analysis to ascertain the association of criticality number and risk failure priority number, it shows a no correlation.

The study demonstrated that critical components are not necessary the components with high risk failure priority, in as much as components with high critical value are kept in watch likewise components with high risk failure priority number.

ACKNOWLEDGEMENTS

All glory is to All Mighty, I sincerely appreciate and grateful to the head and the entire staff of network operation center of NigComSat for their understanding and assistance.

REFERENCE

- Akinyede, J., & Agbaje, G. (2006). *Nigeria's Satellite Data Utilisation for Sustainable Development*. Paper presented at the Proceedings of the ISPRS Commission VII Symposium 'Remote Sensing: From Pixels to Processes', XXXVI (7), Enschede, The Netherlands.
- Bargellini, P. L., & Edelson, B. I. (1977). Progress and Trends in Commercial Satellite Communications—a Survey. In L. G. Napolitano (Ed.), *Space and Energy* (pp. 259-276): Pergamon.
- Boroffice, R. A. (2008). The Nigerian Space Programme: An Update. *African Skies*, 12, 40.
- Braun, T. M. (2012). *Satellite Communications Payload and System*. New Jersey: John Wiley & Sons, Inc.
- Chronaki, C. E., Berthier, A., Lleo, M. M., Esterle, L., Lenglet, A., Simon, F., . . . Braak, L.

- (2007). A Satellite Infrastructure for Health Early Warning in Post-Disaster Health Management. *Stud Health Technol Inform*, 129(Pt 1), 87-91.
- Chukwu-Okoronkwo, S. O. (2015). Nigerian Communication Satellite and the Quest for Sustainable National Development. *American Journal of Social Science Research*, 1(1), 1-8.
- Dale, F. C., Stephen Grey, Geoffrey Raymond and Phil Walker (2005). *Project Risk Management Guidelines* West Sussex England John Wiley and Sons Ltd.
- Department of Defense United States of America. (1980). Mil-Std-1629a - Procedures for Performing a Failure Mode, Effects, and Criticality Analysis. Washington, DC: United States Department of Defense.
- Dinas, P. C., Mueller, C., Clark, N., Elgin, T., Nasser, S. A., Yaffe, E., . . . Asrar, F. (2015). Innovative Methods for the Benefit of Public Health Using Space Technologies for Disaster Response. *Disaster medicine and public health preparedness*, 9(3), 319-328.
- ECSS-Q-ST-30-02C. (2009). *Space Product Assurance, Failure Modes and Effects Analysis (Fmea)*
- European Cooperation for Space Standardization (ECSS). (2009). Space Product Assurance: Failure Modes, Effects (and Criticality) Analysis (Fmea/Fmeca) ECSS- Q- ST- 30- 02C (pp. 74). The Netherlands: ESA Requirements and Standards Division (European Space Agency for the members of ECSS).
- Fales, R. L. (1984). *Risk Analysis and Satellite Communications Terminals*. Paper presented at the MILCOM 1984-IEEE Military Communications Conference.
- Gamble, K. B. (2015). *A Software Tool Suite for Small Satellite Risk Management*. (PhD Dissertation), The University of Texas at Austin, Austin Texas.
- Gamble, K. B., & Lightsey, E. G. (2014). Cubesat Mission Design Software Tool for Risk Estimating Relationships. *Acta Astronautica*, 102, 226-240. doi:<https://doi.org/10.1016/j.actaastro.2014.06.019>
- Gamble, K. B., & Lightsey, E. G. (2015). *Decision Analysis Applied to Small Satellite Risk Management*. Paper presented at the 53rd AIAA Aerospace Sciences Meeting.
- Gamble, K. B., & Lightsey, E. G. (2016). Decision Analysis Tool for Small Satellite Risk Management. *Journal of Spacecraft and Rockets*, 420-432.
- Garshnek, V. (1991). Applications of Space Communications Technology to Critical Human Needs: Rescue, Disaster Relief, and Remote Medical Assistance. *Space communications*, 8(3-4), 311-317.
- Risk Management Plan (2013).
- Goh, D. (2018). Satellite Technology and Disaster Management: Lombok Earthquakes. *SpaceTech Asia*. Retrieved from SpaceTech Asia website: <http://www.spacetechnology.com/satellite-technology-and-disaster-management-lombok-earthquakes/>
- GVF Training, & MahdiBagh Computers PVT. Ltd. (2008). *Satellites and Launch Vehicles*. Paper presented at the ITU Satellite Symposium 2018, Geneva, Switzerland. <https://www.itu.int/en/ITU-R/space/workshops/2018-SmallSat/>
- Harland, D. M., & Lorenz, R. (2007). *Space Systems Failures: Disasters and Rescues of Satellites, Rocket and Space Probes* (1 ed.). Switzerland: Springer Science & Business Media.
- Liu, H. C. (2016). *Fmea Using Uncertainty Theories and Mcdm Methods*: Springer Singapore.
- Meyer, W. G. (2015). *Quantifying Risk: Measuring the Invisible*. Paper presented at the PMI Global Congress, England Newtown Square.
- MIL-STD-1629A. (1980). *Procedures for Performing a Failure Mode, Effects and Criticality Analysis*: Springer.
- NASA. (2008). *Agency Risk Management Procedural Requirements*
- NASA AMES Research Centre. (March 29, 2008). Missions Operations Risk Management. Retrieved from https://www.nasa.gov/centers/ames/research/onepagers/mission_ops_risk_mngt.html
- National Research Council (U.S.). (2005). Risk Identification and Analysis The owner's role in project risk management. Washington, DC: National Academies Press.



- Pelton, J. N., Madry, S., & Camacho-Lara, S. (2017). *Handbook of Satellite Applications*: Springer Publishing Company, Incorporated.
- Pelton, J. N., Madry, S., & Camacho Lara, S. (2013). *Satellite Applications Handbook: The Complete Guide to Satellite Communications, Remote Sensing, Navigation, and Meteorology*. In J. N. Pelton, S. Madry, & S. Camacho-Lara (Eds.), *Handbook of Satellite Applications* (pp. 3-17). New York, NY: Springer New York.
- Spagnulo, M. F., R.; Balduccini, M.; Nasini, F. (2013). *Space Program Management Methods and Tools*.
- Srinivas, K. (2019). Process of Risk Management. In A. Hessami (Ed.), *Perspectives on Risk, Assessment and Management Paradigms*. London: IntechOpen Limited.
- Stanniland, A., & Curtin, D. (2013). An Examination of the Governmental Use of Military and Commercial Satellite Communications. In J. N. Pelton, S. Madry, & S. Camacho-Lara (Eds.), *Handbook of Satellite Applications* (pp. 187-219). New York, NY: Springer New York.
- Wagstaff, J. (2008). Space Technology: A New Frontier for Public Health: Satellite Technologies Are a Natural Ally in Public Health Emergencies for Tracking the Extent of Disease Outbreaks and Natural Disasters. Jeremy Wagstaff Explains Why They Have Only Become Really Useful over the Past 10 Years. *Bulletin of the World Health Organization*, 86(2), 87-89.
- Walter, L. S. (1990). The Uses of Satellite Technology in Disaster Management. *Disasters*, 14(1), 20-35. doi:10.1111/j.1467-7717.1990.tb00969.x
- Zhicheng, Z., Min, W., & Qiang, W. (2006, 2 - 6 October 2006). *Nigcomsat-1, the First Export Commercial Communications Satellite of China*. Paper presented at the 57th International Astronautical Congress (IAC2006, Valencia, Spain).



CHARACTERIZATION AND GRADING OF SOUTH EASTERN NIGERIAN GROWN *MANGIFERA INDICA* TIMBER IN ACCORDANCE WITH BRITISH STANDARD 5268

Mbakwe C.C¹, Aguwa J.I², & Oritola S.F³.

¹Civil Engineering Department, Federal University of Technology, PMB 65,
Minna Niger State, Nigeria.

²Civil Engineering Department, Federal University of Technology, PMB 65,
Minna Niger State, Nigeria.

³Civil Engineering Department, Federal University of Technology, PMB 65,
Minna Niger State, Nigeria.

Corresponding author email: mbakwechinemelum@yahoo.com, +2348061611455

ABSTRACT

The paper is aimed at characterization and grading of South Eastern Nigeria grown *mangifera indica* in accordance with British Standard 5268 (2002). The specimens used in the experiment were obtained from Olulufo in Alor Anambra State, South Eastern Nigeria. The samples were carefully selected, personally sliced into 600mm length and 300mm width for easy transportation in its green state. Samples were seasoned naturally for six months and prepared in accordance with British Standard 373(1957). The following laboratory test were carried out: bending parallel to the grain, tension parallel to the grain, tension perpendicular to the grain, compression parallel to the grain, compression perpendicular to the grain, shear parallel to the grain, moisture content and density. In accordance with British Standard 5268 the moisture content of 12% values were determined by adjusting the laboratory experiment of physical and mechanical properties of the timber specie. The analyses of the result were done statistically and computation of basic and grade stresses were done using experimental failure stresses. The result obtained from grade bending stress, density and mean modulus of elasticity shows that, *mangifera indica* can be graded and assigned to strength class C24 (softwood) . It can be used for cladding, decking, flooring, panelling, furniture and cabinets but cannot be used for load bearing structures.

Keywords: *Characterization, Grading, Nigeria grown timber, Soft wood, and Three point bending.*

1. INTRODUCTION

. The use of timber as a structural material has been dated over centuries ago, due to its availability in nature. Timber refers to wood in the form that is suitable for construction of carpentry, joinery or for reconversion for manufacturing purposes (Aguwa, 2010). There is high demand for timber as a building material. From building construction to furniture making, timbers have numerous uses. These uses have made timber an important building material.

Timber as a structural material serves various purposes which include bridge construction, beam, trusses, girder, piles, deck member, retaining structures and railways slippers.

Different wood species have different strength characteristics. And also within a species these characteristics may vary. Therefore, in practice, a classification system of strength classes is used (Jamala, et al., 2013). The strength of a timber depends on its species and the effects of certain growth characteristics

(Yeomans, 2003) therefore there is need to determine the physical and mechanical properties of each timber before it is used as structural materials in construction.

Grading of timber species is the process of grouping a timber with similar properties. Different species of timber used in construction can be grouped into two, softwood and hardwood. Softwood is the timber from conferral trees, they are gymnosperms, its leaves are needle like in shape, less dense, light in color, create more branches or shoots, they are usually wood from cones and occasionally nuts. Soft wood are used for home wood working projects , used for cladding, decking, flooring, paneling, structural framing, beams poles, bench tops, furniture and cabinets. Hardwoods are obtained from deciduous trees. They are basically angiosperms; the fibers are quite close and dense, normally these are dark coloured woods, durable and last for several decades. They are used for load bearing structures like railway sleepers and bridge beam.

Timbers as a natural product are not excluded from defect. A defect is any irregularity occurring in or on the timber which may lower its strength, durability, utility value or diminish its appearance. Defects may be 'natural' which occur whilst the tree is growing, or 'artificial' as a result of poor conversion, seasoning or handling after felling. Natural defects like Knots occur where branches have grown out of the tree trunk. Seasoning is the process of adjusting the moisture content of the wood, which can be achieved through exposing the felling timber to dryness within a given period of time or by the use of kiln to achieve its reduction in moisture content, during seasoning of timber, exterior or surface layer of the timber dries before the interior surface. So, stress is developed due to the difference in shrinkage. In a perfect seasoning process, stress is kept minimum by controlling the shrinkage. The process of cutting a fell timber into different market sizes is known as conversion of timber. Artificial defects can occur in a timber as a result improper cutting or machine notches during conversion.

Nigeria is one of the countries that have timber in surplus quantity (Jimoh and Aina, 2017). There is need to determine the strength properties and grading of our locally grown timber species so as to aid in choosing a timber that is free from defect and suitable for a specific construction, and also reduce the high rate of demand of concrete and steel in construction. Construction activities based on these locally available raw materials are major steps towards industrialization and economic independence for developing countries. This explains huge interest and considerable intellectual resources being invested in understanding the mechanical or structural properties of the Nigerian timber (Aguwa and Sadiku, 2011). The demand for timber is unlimited as it continues to increase rapidly in Nigeria.

Mangifera indica is a large, evergreen tree with a dark green, umbrella-shaped crown; it can grow from 11-46 metres tall. The long bole can be 0.7-1.5 metres in diameter. Mostly planted in south eastern part of Nigeria, and north central. There is need to determine the physical and mechanical properties of *mangifera indica* since it is locally grown and used as structural materials in construction. Some timber strength properties listed in British Standard or European code were based on timber obtained from trees in those areas and the laboratory tests were conducted there (Aguwa, 2010). The determined properties like density, grade bending stress and mean modulus of elasticity were used for grading and assigning strength class according to international code (British Standard 5268 part 2, 2002).

The aim of this study was to characterize and grade South Eastern Nigeria grown *mangifera indica* timber in accordance with British Standard 5268 (2002). The specific objectives were to collect, season, prepare

samples of *mangifera indica*, determine its physical and mechanical properties according to British Standard 373 (1957) and to grade *mangifera indica* timber specie in accordance with British Standard 5268 (2002).

2. METHODOLOGY

The materials used in this study were obtained from *mangifera indica* tree at its green condition sawn to size 200mm x 450mm x 4500mm and were reduced to 100mm x 300mm x 600mm for easy transportation to university of Ilorin for seasoning, preparation and testing.

PREPARATION OF TEST SPECIMENS IN ACCORDANCE WITH B.S 373 (1957)

Test specimens were seasoned for six months to attain equilibrium moisture condition at Department of Civil Engineering Laboratory, University of Ilorin, Nigeria. Natural seasoning method was adopted in line with Aguwa (2010). Thirty (30) samples each were prepared for six different laboratory tests which include three point bending strength parallel to the grain, shear strength parallel to the grain, tension strength parallel to the grain, tension strength perpendicular to the grain, compressive strength parallel to the grain, compressive strength perpendicular to the grain, natural moisture content and density according to BS 373 (1957).

DETERMINATION OF PHYSICAL AND MECHANICAL PROPERTIES.

Physical and mechanical properties were determined on the prepared samples in the Laboratory of university of Ilorin, Kwara State using Universal Testing Machine (UTM), Testometric M500-100AC of 300kN capacity. Thirty (30) samples of each of the following test were carried out three point bending strength parallel to the grain, shear strength parallel to the grain, tension strength parallel to the grain, tension strength perpendicular to the grain, compressive strength parallel to the grain, compressive strength perpendicular to the grain, total of one hundred and eighty (180) samples were carried out according to BS 373 (1957) including natural moisture content and density. In each set of the tests, failure loads were recorded for computation of failure stresses, mean failure stress, standard deviation and coefficient of variation. The corresponding load deformation graphs were plotted automatically.

STRESSES AT 12% MOISTURE CONTENT.

Failure stresses for bending parallel to the grain, tension parallel to the grain, compression parallel to the grain, compression perpendicular to the grain and shear parallel to the grain were adjusted to values at 12%

moisture content in accordance with BS 5268 (2002). Equation (1) was used for the adjustment.

$$FM12 = FW + \sigma(W - 12) \quad (1)$$

Thus
FM12= failure stress at 12% moisture content, w=experimental moisture content in (%), FW = experimental failure stress, σ = correction factor (Bending = 0.05, compression = 0.04 and shear = 0.03).

MODULUS OF ELASTICITY AT 12% MOISTURE CONTENT

Based on three points bending test, Equation (2) from the strength of materials applied to straight beams was used, in conformity with Izekor et al. (2010).

$$EL3 = \frac{L^3}{4EH^3} K, \quad (2)$$

Thus
EL3 is the three point bending modulus of elasticity, ℓ is the distance between the two supports (280mm), e is the width of the beam (20mm), h is the height of the beam (20mm) and k is the slope of load deformation graph that is $\frac{VP}{\Delta F}$. Minimum modulus of elasticity was determined with Equation (3) which shows the relationship between mean modulus of elasticity, E_{mean} and the minimum modulus of elasticity, E_{min} .

$$E_{minimum} = E_{mean} - \frac{2.33\sigma}{\sqrt{N}} \quad (3)$$

Thus
N is the number of specimens, σ is the standard deviation.

MODULUS OF ELASTICITY AT 12% MOISTURE CONTENT

Moduli of elasticity at experimental moisture content were adjusted to values at 12% moisture content in conformity with BS 5268 (2002). The adjusted values were computed with Equation (4).

$$Em12 = \frac{E_{measured}}{1 + 0.0143(12 - u)}, \quad (4)$$

Thus

$E_{measured}$ = the modulus of elasticity at experimental moisture content, $Em12$ = Modulus of elasticity at 12% moisture content and U = experimental moisture content.

DETERMINATION OF MOISTURE CONTENT

The pieces used for moisture content determination were from failed tested specimens. The samples were weighed and initial mass were recorded as M_1 which

represent masses of wood pieces before the oven dried. The samples were reweighed after oven dried at a temperature of $103 \pm 2^\circ\text{C}$ to a stable mass which were recorded as M_2 (final mass). The average mass of the species were recorded to determine the masses (M_1 and M_2) used for moisture content value.

$$MC = \frac{M1 - M2}{M2} \times 100\%, \quad (5)$$

Thus

M_1 (kg) =initial mass (mass of timber and moisture content)

M_2 (kg) = final mass (mass of timber alone) that is mass after oven dried.

DETERMINATION OF DENSITY

Five samples of the timber with size 20mmx20mmx20mm were used for the determination of the density in accordance with BS 373 (1957). Density was calculated using Equation (6).

$$\rho = \frac{m}{v}, \quad (6)$$

Thus

m= the mass of the specimen, v = volume of the specimen

DENSITY AT 12% MOISTURE CONTENT

The densities computed from test results in kg/m^3 were adjusted to values at 12% moisture content in accordance with BS 5268 (2002). Equation (7) was used for the adjustment.

$$\rho_{12} = \rho_w \left[1 - \frac{(1 - 0.5)(w - 12)}{100} \right], \quad (7)$$

Thus

ρ_{12} = density at 12% moisture content in kg/m^3 , ρ_w = density at experimental moisture content, w= experimental moisture content in percentage (%).

BASIC AND GRADE STRESSES

Basic stresses for bending, tensile, compressive, shear parallel to the grain, compressive stress perpendicular to the grain, were calculated from failure stresses. Equations (8) were used for the computation. Various grades stresses at 80%, 63%, 50% and 40% values respectively were calculated according to BS 5268 (2002).

$$fb = \frac{fm - kp\sigma}{kr}, \quad (8)$$

Thus

fb = Basic stress, fm = mean failure stress at 12% moisture content, σ = standard deviation of failure stress, kr = reduction factor and kp = modification factor = 2.33, Kr for bending, tension and shear parallel to the grain = 2.25. Kr for compression parallel to the grain = 1.4 while Kr for compression perpendicular to the grain = 1.2. fg80 = fb80%, fg63 = fb63%, fg50 = fb50%, fb40 = fb40%.

3. RESULTS AND DISCUSSION

Table 1 shows the mass of five samples of size 20mmx20mmx20mm for *mangifera indica*, the mean mass and mean density at experimental moisture content are equally shown in the Table 1.

TABLE 1: SAMPLES MASS AND MEAN DENSITY

SAMPLE NUMBER	MASS(g)	DENSITY(kg/m ³)
1	6.6	825
2	6.7	837.5
3	7.6	950
4	6.9	862.5
5	6.8	850
MEAN	6.92	865

Table 2 presents moisture content results of five (5) samples each of the following test: Bending parallel to the grain, tension parallel to the grain, compression parallel to the grain, compression perpendicular to the grain and shear parallel to the grain on *mangifera indica* samples and the average moisture content of the experiments.

TABLE 2: NATURAL MOISTURE CONTENT OF MAGINERFA INDICA

Test specimen	M1 initial mass of timber before oven drying(g)	M2 final mass of timber after oven drying(g)	MC $= \frac{m2 - m1}{m2} \%$
Compression parallel to the grain	40.6	36.2	12.154
Compression	342.7	272.9	25.577

perp. to the grain			
Tension parallel to the grain	62.7	53.4	17.415
Tension perpendicular to the grain	94.7	69.4	36.45
Bending parallel to the grain	337.8	280.6	20.38
Shear parallel to the grain	20.9	19	10
MEAN			20.330

Table 3 shows modulus of elasticity of five (30) samples at experimental moisture content, sample 12 have the least modulus of elasticity 8292.802 N/mm² while sample 22 with the highest value 15473.257 N/mm². The summary graph of bending test that was used for modulus of elasticity computation was used to confirm the samples with the values.

TABLE 3: MODULUS OF ELASTICITY AT NATURAL MOISTURE CONTENT

SAMPLE NO	M.O.E. (N/mm ²)
1	10100.617
2	13702.312
3	13391.999
4	10095.912
5	10413.145
6	13218.253
7	12011.994
8	12070.981
9	11147.251
10	8337.247
11	9381.749
12	8292.802
13	8953.258
14	13877.897
15	9451.386
16	14345.333
17	9282.586
18	11784.363
19	9929.698
20	9342.541
21	10881.638
22	15473.257
23	11223.954

24	9670.227
25	11437.090
26	9847.927
27	13313.685
28	8814.105
29	7013.942
30	3856.050
MINIMUM	3856.050
MEAN	10688.773
MEDIAN	10256.881
MAXIMUM	15473.257
STANDARD DEVIATION	2422.420
C. OR V.	22.663

Figure 1 (graph of Load on Y- Axis against Deflection on X-Axis).The graph shows the relationship between load and deflection of Timber beams (*mangifera indica*) under static bending load. Loads were applied at a constant speed of 0.11mm/s until the materials failed. These graphs confirm timber as an elastic structural material which does not undergo plastic stage of deformation (Aguwa, 2012). It was observed that deformation increased as load on the beam increased until elastic limits were reached.

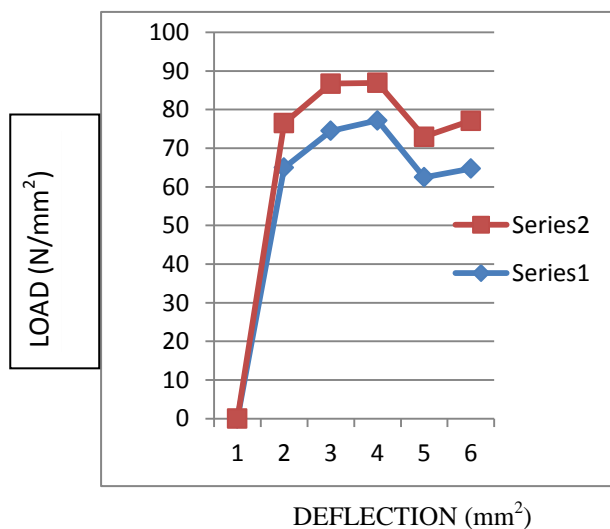


Table 4 shows modulus of elasticity and density of *mangifera indica* timber at 12% moisture content. *mangifera indica* properties are comparable with those timbers in strength class C24 because it has density of 865kg/m³, mean modulus of elasticity 10688.773N/mm² that is within the range of C24 in BS 5268 (2002). Based on these results *mangifera indica* belongs to timber strength class C24.

TABLE 4: MODULUS OF ELASTICITY AND DENSITY OF MANGIFERA INDICA AT 12% MOISTURE CONTENT

MODULUS OF ELASTICITY (N/mm ²)	VALUE
EMINIMUM (N/mm ²)	3856.050
EMEAN (N/mm ²)	10688.773
DENSITY (Kg/m ³)	865

table 5 shows basic stresses of mangifera indica at 12% moisture content calculated from mean failure stresses and standard deviation of failure stresses. basic stresses calculated were basic bending stress parallel to the grain, basic tensile stress parallel to the grain, basic compressive stress parallel to the grain, basic shear stress parallel to the grain and basic compressive stress perpendicular to the grain.

TABLE 5: VALUES GOTTEN FROM BASIC STRESSES OF MANGIFER INDICA AT 12 % MOITURE CONTENT.

TYPE OF STRESS	VALUE
BENDING PARALLEL TO THE GRAIN (N/MM ²)	70.6685
TENSION PARALLEL TO THE GRAIN (N/MM ²)	51.2605
COMPRESSION PARALLEL TO THE GRAIN	21.1435
COMPRESSION PERPENDICULAR TO THE GRAIN	226.1115
SHEAR PARALLEL TO THE GRAIN	9.8349

Table 6 shows basic stresses parallel and perpendicular to the grain as well as grade stresses at 12% moisture content. *mangifera indica* has grade bending stress of 18.09N/mm² which is comparable to range of grade bending stress of strength class C24 listed in Table 8 of BS 5268 (2002).

TABLE 6: VARIOUS STRESS FOR MANGIFERA INDICA AT 12% MOISTURE CONTENT.

TYPE OF STRESS	VALUE (N/mm ²)
MEAN FAILURES BENDING STRESS PARALLEL TO THE GRAIN	70.252
BASIC BENDING STRESS PARALLEL TO THE GRAIN	18.09
STANDARD DEVIATION OF FAILURE BENDING STRESS PAR. TO GRAIN	12.676
GRADE BENDING STRESS (80%) PARALLEL TO THE	14.477

GRAIN		STANDARD DEVIATION OF FAILURE COMP. STRESS PERP. TO GRAIN	98.686
GRADE BENDING STRESS (63%) PARALLEL TO THE GRAIN	11.40	GRADE COMPRESSIVE STRESS (80%) PERP. TO THE GRAIN	-2.8288
GRADE BENDING STRESS (50%) PARALLEL TO THE GRAIN	9.048	GRADE COMPRESSIVE STRESS (63%) PERP. TO THE GRAIN	-2.227
GRADE BENDING STRESS (40%) PARALLEL TO THE GRAIN	7.2384	GRADE COMPRESSIVE STRESS (50%) PERP. TO THE GRAIN	-1.768
MEAN FAILURES TENSILE STRESS PARALLEL TO THE GRAIN	50.844	GRADE COMPRESSIVE STRESS (40%) PERP. TO THE GRAIN	-1.4144
BASIC TENSILE STRESS PARALLEL TO THE GRAIN	4.625	MEAN FAILURES SHEAR STRESS PARALLEL TO THE GRAIN	9.585
STANDARD DEVIATION OF FAILURE TENSILE STRESS PAR. TO GRAIN	17.355	BASIC SHEAR STRESS PARALLEL TO THE GRAIN	0.1501
GRADE TENSILE STRESS (80%) PARALLEL TO THE GRAIN	3.7	STANDARD DEVIATION OF FAILURE SHEAR STRESS PAR. TO GRAIN	3.968
GRADE TENSILE STRESS (63%) PARALLEL TO THE GRAIN	2.915	GRADE SHEAR STRESS (80%) PARALLEL TO THE GRAIN	0.121
GRADE TENSILE STRESS (50%) PARALLEL TO THE GRAIN	2.3125	GRADE SHEAR STRESS (63%) PARALLEL TO THE GRAIN	0.094
GRADE TENSILE STRESS (40%) PARALLEL TO THE GRAIN	1.85	GRADE SHEAR STRESS (50%) PARALLEL TO THE GRAIN	0.075
MEAN FAILURES COMP. STRESS PARALLEL TO THE GRAIN	20.727	GRADE SHEAR STRESS (40%) PARALLEL TO THE GRAIN	0.060
BASIC COMPRESSIVE STRESS PARALLEL TO THE GRAIN	9.098		
STANDARD DEVIATION OF FAILURE COMP. STRESS PAR. TO GRAIN	3.429		
GRADE COMPRESSIVE STRESS (80%) PARALLEL TO THE GRAIN	7.27		
GRADE COMPRESSIVE STRESS (63%) PARALLEL TO THE GRAIN	5.73		
GRADE COMPRESSIVE STRESS (50%) PARALLEL TO THE GRAIN	4.55		
GRADE COMPRESSIVE STRESS (40%) PARALLEL TO THE GRAIN	3.64		
MEAN FAILURES COMP. STRESS PERPENDICULAR TO THE GRAIN	225.695		
BASIC COMPRESSIVE STRESS PERPENDICULAR TO THE GRAIN	-3.536		

Table 7: shows the summary results of the experiment for grading of *magnifera indica* in accordance with BS 5268 (2002). According to BS 5268 (2002), strength class may be assigned to a specie, if its characteristic value of grade bending stress and mean density equal or exceed the value for that class giving in Table 8 of BS 5268-2 (2002) and its mean modulus of elasticity in bending equal or exceed 95% of the value given in that strength class. Based on these criteria, *magnifera indica* was assigned to strength class C24 due to its grade bending stress parallel to the grain of 14.477N/mm², mean density of 865kg/m³ and mean modulus of elasticity of 10688.773N/mm². This is in agreement with strength class C24 listed in BS 5268-2 (2002) of grade bending stress of 7.5N/mm² and above, mean density of 420kg/m³.

TABLE 7: STRENGTH CLASS FOR MAGINFERA INDICA ACCORDING TO TABLE 8 BS 5268-2 (2002) .

GRADE STRESS OF BASIC BENDING PARALLEL TO THE GRAIN (80%) (N/mm ²)	14.477
--	--------

DENSITY (kg/m ³)	865
MEAN MODULUS OF ELASTICITY (N/mm ²)	10688.773
MINIMUM MODULUS OF ELASTICITY	3856.050
STRENGTH CLASS	C24

4. CONCLUSION

Maginfera indica is softwood (C Class) of C24 strength class according to BS 5268 (2002) with poor Engineering properties and cannot be used for a load bearing structures.

RECOMMENDATION

Having successfully characterized and grade this specie, *maginfera indica* timber can be compared with other species on international basis; hence this timber is recommended to engineers to be used according to its strength class. Further research can be carried out on characterization and grading of *mangifera indica* by comparing Euro code and British code.

ACKNOWLEDGEMENTS

My sincere gratitude goes to almighty God for his immeasurable love, care and favour granted to me throughout this program.

My unreserved thanks goes to my supervisor prof J.I Aguwa, my Parent Mr and Mrs A.E Mbakwe , my siblings Mr Ebuka Mbakwe, Mr Nonso Mbakwe, Mr ogechukwu Ezelibe, Miss Chidimma Mbakwe, and my lovely friends Chioma Okonkwo and Ifeoma Udeaja, for their guidance and support throughout the research work.

5. REFERENCES

1. **Reliability studies on the Nigerian timber as an orthotropic structural material**, Thesis submitted to Department Civil Engineering, Federal University of Technology, Minna. pp.50-67, 102-103. Aguwa, J.I.(2010),
2. **Reliability assessment of the Nigeria Apa(*Afzelia bipindensis*) timber bridge beam subjected to bending and deflection under limit state of loading**, International Journal of Engineering and Technology vol.2 No6 pp..1076-1087. Aguwa, J.I.(2012),
3. **Structural reliability analysis on the Nigeria Ekki timber bridge beam subjected to shearing force under Ultimate limit state**, Research Journal in Engineering and Applied Sciences vol.1 No4 pp..240-246. Aguwa, J.I., Sadiku, S (2012).
4. **Method of testing small Clear Specimens of Timber**, British Standard Institute, London. British standards 373, (1957),
5. **Structural use of timber**. Part 2 code of practice for permissible stress design, materials and workmanship. British Standard institute, London. British Standards 5268 (2002),
6. **Structural timber-Strength classes**. European committee for standardization, BS EN338 (2003), CEN, 2009, Brussels, Belgium
7. **Physical and Mechanical Properties of Selected Wood Species in Tropical Rainforest Ecosystem, Ondo State, Nigeria**. IOSR Journal of Agriculture and Veterinary Science (IOSR-JAVS). eISSN: 2319-2380, p-ISSN: 2319-2372, 5(3), 29–33, 2013. Jamala, G. Y., Olubunmi, S. O., Mada, D. A. and Abraham, P:
8. **Characterisation and Grading of two selected timber species grown in Kwara State Nigeria**. Nigerian Journal of Technonlogy (NIJOTECH), 36(4), 1002–1009. ISSN: 2467-8821, 2017. Jimoh, A.A and Aina, S.T:
9. **Nigerian standard code of practice; the use of timber for construction, Nigeria Standard Organisation**, Federal Ministry of Industries, Lagos, Nigeria. pp.10-18. NCP2 (1973),
10. **Strength Grading of Historical Timbers**. Cathedral Communications Limited, 2010 (<http://www.buildingconservation.com/articles/gradingtimbers.ht>), 2003. Yeomans, D:



CHARACTERIZATION OF PALM KERNEL SHELL AS LIGHTWEIGHT AGGREGATE IN CONCRETE PRODUCTION

*Sunday I .O.¹, Aguwa J .I.¹ & Auta S .M.¹

¹Department of Civil Engineering Federal University of Technology, P.M.B 65 Minna, Nigeria.

*Corresponding author: otegwus@gmail.com.

ABSTRACT

This study is on the Characterization of Palm Kernel Shell as Lightweight Aggregate in Concrete Production. The tests conducted were sieve analysis, water absorption test, bulk density, specific gravity to characterize aggregate and compressive strength. A design mix ratio of 1:3:5 and water-cement ratio of 0.65 were adopted for both PKSC and NWC (Control). Cubes (150mm×150mm×150mm) were cast and cured for periods of 3, 7, 14, 21 and 28 days and their compressive strengths were determined. The 28 days average compressive strength of PKSC was found to be 19.75N/mm², while that of control was found to be 23.28N/mm². The Specific gravities of crushed stone, and Palm Kernel Shell were found to be 2.62 and 1.32 while their bulk densities were 1755 and 632 kg/m³ respectively. Water absorption capacity of palm kernel shell was found to be 21.50%, while that of crushed stone was found to be 0.23% for 24hrs. In conclusion, palm kernel shell possess some characteristics of lightweight aggregate and could be used for structural lightweight concrete for small load bearing structures where compressive strength is not a major factor. It reduces the cost of construction, pollution associated waste disposal and enhance infrastructural development.

Keywords: Characterization, Compressive Strength, Concrete, Lightweight Aggregate, Palm kernel shells

1 INTRODUCTION

Palm Kernel Shell (PKS) is an inert, bio-renewable, non-toxic, abundantly available, stiff, corrosion resistant and a light weight organic solid waste by-product from processing of red oil from palm nuts. Palm kernel shell can also be defined as hard, carbonaceous and organic by-products of the processing of palm oil fruit (Alengaram, et al., 2010). In the same vain, Palm Kernel Shell Concrete (PKSC) is a concrete in which palm kernel shell serves as coarse aggregate replacing the granite or normal aggregate.

Concrete in the other hand, is defined as the artificial material resulting from a carefully controlled mixture of cement, fine and coarse aggregates and water, which when set or hardened form the shape of the container or form work that later turn to a solid mass when cured at the suitable temperate and humidity (Alawode et al, 2011).

Attempts have been made by various researchers to reduce the cost of concrete constituents and hence total construction cost by investigating and ascertaining the usefulness of materials which could be classified as agricultural or industrial waste. One of these wastes is palm kernel shells which are by-product of red oil producing company. PKS are hard stony endocarps that surround the kernel and the shells come in different shapes and sizes. They are light and naturally sized; they are ideal for substituting aggregates in LWC construction. Being hard and of organic origin, they will not contaminate or leach to produce toxic substances once they are bound in concrete matrix. Normally, the shells are flaky and of irregular shape that depend on the

breaking pattern of the nut. PKS are available in large quantities in palm oil producing countries in Asia and Africa. Malaysia alone produces nearly 4 million tons of PKS annually and this is likely to increase as more production is expected in the near future.

The research work carried out by Shafigh et al, on the new method of producing high strength palm kernel shell concrete have shown that palm kernel shell incorporated concrete possess ductility property, unlike normal aggregate concrete that fails without warning or notice. Another advantage of using palm kernel shell aggregate over normal granite coarse aggregate in concrete is cost and waste reduction which lead to the production of a cheaper structural light weight concrete and a cleaner environment.

Most coarse aggregates from quarries are very expensive and the operations that lead to the production of those aggregates pose danger to human being and his environment. In order to alleviate the incessant increasing demand for low cost and environmental friendly construction materials, while strengthening economic growth and competitiveness the use of palm kernel shell concrete (PKSC) becomes eminent in construction industries.

Moreover, Palm kernel Shell (PKS) is an ideal construction material for light weight concrete because of its excellent properties such as; non-toxic, inert, bio-renewable, readily available, strong, stiff, light weight, and corrosion resistant (attach, 2012).

In Nigeria, states that are considered to be largest producers of palm oil are Akwa- Ibom, Edo, Imo, Ondo, Bayelsa, Cross River and Delta. There are millions metric tons of palm kernel shell in open places in those states in Nigeria constituting nuisance and negative

impact on the environment. Some accumulate water for breeding of mosquitoes, while others also block water ways by clogging the local drains.

The high cost of production of coarse aggregate and the impact of the production processes on the environment have necessitated the replacement of coarse aggregate with palm kernel shells to produce concrete whose quality and standard satisfied the requirement of light weight concrete which can eliminate potential ecological disaster. High and continuous increase in the cost of construction is one of the major challenges the construction industries are facing. Great numbers of developmental projects are wholly dependent on some factors of production which is the cost of materials (Anthony 2000). In the light of this, Shetty (1999) affirmed that the price of concrete elements primarily depends on the cost of materials and labour. In every given volume of concrete, aggregates contains up to 70 to 80 %, according to Alexander et al, (2005) this means percentage of aggregate in concrete is of considerable important. The use of agricultural and industrial by-products has now become major important alternative to the use of granite that causes noise pollution during manufacturing according to (Falade et al, 2010).

Palm Kernel Shell (PKS) is agro-waste materials from oil mills, the disposal of (PKS) is an environmental problems of concern. The scarcity and high cost of aggregate is a great set back in terms of time and cost of construction, since aggregate forms the largest percentage of the content of concrete.

The use of agricultural wastes as aggregate in concrete has a lot of engineering potential and advantage especially in low-cost non-load bearing light weight concrete, where compressive strength is not important and also reduces the cost of construction greatly.

Earthquakes have been reported to occur in Abuja the city of Nigeria partly due to chipping production from the natural stone deposits. The continuous exploring of crushed granite for concrete in construction industries will also deplete the natural stone deposits and this will affect the environment negatively and cause a lot of imbalance in the ecosystem. The impact of aggregate production processes on environment and the proper disposal of palm kernel shell called for Civil engineering concern. Production of palm kernel shell (PKS) waste continuously endanger the environment by causing pollution, blocking of water ways and constitute nuisance in terms of its disposal. Palm kernel shell can be utilized as lightweight concrete to alleviate the high demand of aggregate and at the same time serve as a safe and proper way of palm kernel shell waste disposal. This research work will look into characterization of palm kernel shell aggregate for production of concrete in large volume for industrial use.

Abdullah (1984) was among the first researchers on palm kernel shell as light weight aggregate (LWA). He submitted that it is possible to replace completely the normal weight aggregate (NWA) with palm kernel shell.

Okafor (1988) work on the mechanical properties of palm kernel shell concrete (PKSC) and proved that similar to normal weight concrete (NWC), water to cement ratio (w/c) is one of the important factors affecting the mechanical properties of palm kernel shell concrete (PKSC).

Also, from the work of Alengaram et al (2010) on the investigation of physical and mechanical properties of different sizes of palm kernel shells as light weight aggregates (LWA) and their influences on the properties of palm kernel shell concrete (PKSC) submitted that the 28days compressive strength ranges from 21 to 26MPa. In the work he also shows that palm kernel shell consists of about 65 to 70% of medium size particles in the range of 5 to 10mm.

Acheampong et al, (2013) conducted a comparative study of the physical properties of palm kernel shells concrete (PKSC) and normal weight concrete (NWC) using different cement types and reported that the density of the palm kernel shell concrete was about 22 percent lower than that of the normal weight concrete for all the cement types. But here the same cement type will be used to characterize the aggregate.

A research carried out by Neville (2000) concluded that the use of palm kernel shell as a material of construction could have other advantages in concrete other than serving as light weight concrete. He further submitted that some of the usefulness is the reduction in the density of the concrete, which in other hand reduces the total dead load of the construction process, and the form work is also subjected to lower pressure than it will be if normal or heavy weight concrete is used.

In the same research, an assessment was carried out on the performance of palm kernel shells as a partial replacement for coarse aggregate in asphalt concrete production. Falad also carried out investigation on palm kernel shells and submitted that palm kernel shells are suitable for aggregate in lightweight concrete.

The aim of this research work is Characterization of palm kernel shell (PKS) as Lightweight aggregate for concrete production.

Some of the objectives are to determine the physical properties of palm kernel shell concrete such as water absorption test, bulk density, specific gravity test and sieve analysis and to determine the compressive strength of palm kernel shell concrete.

2 METHODOLOGY

(I) Palm Kernel Shell: Palm Kernel shells which serve as coarse aggregate for this research work is sourced from a local palm oil producing community of Ibagwa-aka in Igboeze South local government area of Enugu State Nigeria. Preparation of palm kernel shell is done by soaking the sample overnight in the detergent to remove all the oily dirty from the sample. After that, the shells were washed and sundried in the open air. Pre-treatment

was done to remove impurity such as oil coating and mud from the shells. In order not to reduce the performance of cement because of the presence of detergent, it was ensured that the sample is well-rinsed before sundry. After sundry the sample was kept in airtight water proof sacks.

(II) Cement: Ordinary Portland cement (Dangote) with specific gravity 3.0 was used. The cement conforms to the requirements of BS EN 197 (2011). The bags were observed to ensure they are airtight from the company and free from every moisture and fluid. The cement used for this research was sourced from Dangote mini-cement deport minna Niger state of Nigeria.

(III) Water: A portable water supply from Federal University of Technology Minna was used for the experiment. In fact, the water was drinkable and conformed to BS 3148 (1980).

(IV) Fine aggregate: The fine aggregate for this research work is naturally occurring clean river sharp sand (fine aggregate). They were sourced from Chanchagan River in Minna Niger state. It was ensured that the fine aggregate conformed to BS 812 (2002) for Testing Aggregates.

(V) Coarse aggregate: The coarse aggregate for this research work is Crushed Granite sourced from one of the on-going construction site within Federal University of Technology Minna. BS 812 (2002) that deals with "Testing Aggregates" was used in carrying out laboratory tests on the aggregates. The crushed granite was found to have maximum aggregates size of 8mm, specific gravity of 2.62, and a fineness modulus of 4.36. Subsection

2.1 CONCRETE MIX DESIGN (BS METHOD)

The method of mix design applied here is in accordance to the method published by the Department of Environment, United Kingdom (1998). From the design the quantities of different concrete constituents and mix ratio were arrived. The mix ratio was 1:3:5 while the quantities of concrete constituents were calculated using w/c ratio of 0.65.

2.2 SPECIFIC GRAVITY TEST The specific gravity of the materials was carried out in accordance with the specification of ASTM C 127, (2007). For this research, the specific gravity was carried out on both the fine aggregate and coarse aggregate to determine their strength and quality. Table 1 and 2 show the results.

2.3 SIEVE ANALYSIS

Sieve analysis was carried out on both the fine and coarse aggregate to determine their gradation and particle distribution of aggregate particle size. It was ensured that the experimental procedures conformed to the requirements of ASTM 136 (2003).

2.4 SLUMP TEST

Fresh concrete is said to be workable only when it can easily be placed, compacted, transported and casted without segregation. In this research, the slump test procedures were carried in accordance to BS 1881: Part 102: (1983).

2.5 WATER ABSORPTION TEST

The specimens were dried in an oven for periods of 1hr and 24hrs, and then placed in desiccator to cool. Immediately, upon cooling the specimen were weighed. The materials were also emerged in water at room temperature for 24hrs. The specimens were removed patted dry with a lint free cloth and weighed. The test was done in accordance to BS 1881-Part 122 (1983).

3 RESULTS AND DISCUSSION

The summary of the comparison of physical properties of the constituents materials used for the research work is shown in Table 1. The properties include the specific gravity, bulk density, water absorption test and sieve analysis. The coefficient of uniformity (Cu) and the coefficient of curvature (Cc) were arrived at through the sieve analysis.

Specific gravity has to do with estimation of voids in aggregates. From Table I it can be observed that the specific gravity of palm kernel shell is lower than that of crushed stone which serves as aggregate for the control concrete here. The high porosity of palm kernel shell is responsible for the low value compare with that of crushed granite which is higher. This implies that for any given mix design, the palm kernel shell concrete would contain a much higher volume of coarse aggregate than the normal weight concrete if batching by weight is adopted. It also indicates that the specific gravity of palm kernel shells fall within the ranges of Lightweight concrete. Hence, it can be deduced that Palm kernel shell aggregate can be regarded as light weight aggregate though it has low specific gravity.

The bulk density values for crushed stone and palm kernel shell in table I shows that the value for crushed stone fall within the range of bulk densities for normal weight aggregates according to ASTM C 330 (1999) while that of palm kernel shells lie within the range of bulk densities for lightweight aggregates. Hence, palm kernel shells fulfill the requirement for lightweight aggregates.

Also, from the results of sieve analysis for the aggregate, it can be deduced that the aggregates are well graded. This is because the value of coefficient of curvature, Cc for both crushed stone and palm kernel shells lie between 1 and 3 which satisfy the requirement of ASTM 33, (2003).

TABLE 1: PHYSICAL PROPERTIES OF CEMENT AND AGGREGATES

Property	Cement	Sand	PKS	Granite
Bulk Density(kg/m ³) Compressed	-	1737	632	1755
Bulk Density(kg/m ³) Uncompressed	-	1610	566	1680
Specific gravity	3.0	2.72	1.32	2.62
Water absorption (%) (1hr)		<1	11	<1
Water absorption (%) (24hrs)		<1	21.5	<1
Fineness modulus (FM)		2.66	3.80	4.36
Coefficient of Uniformity (Cu)		6.10	1.20	1.44
Coefficient of curvature (Cc)		1.28	2.10	0.92

From Table 2, it can be seen that the average density of palm kernel shell concrete fall within the range of structural lightweight concrete and this indicate that palm kernel shell concrete can be used as structural lightweight concrete in accordance with the requirements of ASTM C 330, (2004).

TABLE 2: AVERAGE DENSITIES OF PALM KERNEL SHELLS CONCRETE (PKSC) CUBES

CURING AGE (DAYS)	AVERAGE DENSITY OF PKSC CUBES (Kg/m ³)
3	1770.49
7	1692.94
14	1756.36
21	1789.63
28	1746.96

Table 3 shows that both the compressive strength of palm kernel shell concrete (PKSC) and that of normal weight concrete (NWC) which serves as control in research increases with the age of curing. It can also be

observed that the compressive strength of palm kernel shell concrete and normal weight concrete is directly depends on the unit weight of the concrete. The higher the unit weight the higher the compressive strength. It is of important to note that, the compressive strength of palm kernel shell concrete also depends on the density, the higher the density the higher the compressive strength, it is one of the most important variables to consider in the design of concrete structures. The results show that the average compressive strength of 19.75 N/mm² at 28 days curing fall within the limits of previous research findings that the compressive strength of palm kernel shell concrete ranges from 5 to 25 N/mm² by Okafor (1988).

TABLE 3: COMPRESSIVE STRENGTH OF PKSC AND NWC

Curing age (Days)	Average Compressive strength (N/mm ²)	
	PKSC	NWC (CONTROL)
3	11.51	12.34
7	14.13	15.60
14	15.61	16.21
21	17.72	19.63
28	19.75	23.28

4 CONCLUSIONS

From this research the results of the experiments conducted on the physical properties of palm kernel shell aggregates (PKSA) have shown that palm kernel shells possess some characteristics of lightweight aggregates and can be used as aggregates for production of lightweight concrete.

Similarly, from the results of the mechanical properties of Palm kernel shell concrete, comparable strength properties and structural characteristics similar to that of normal weight concrete has been observed. However, it can be concluded that the Palm kernel shell concrete is reliable and can be used as lightweight concrete because it has shown some properties that are similar to normal weight concrete with respect to compressive strength, though lower than that of normal weight concrete.

While recommending the use of palm kernel shell aggregates for mass concrete both in small scale concrete work and industries where concrete strength is not a major factor. It is necessary to intensify more efforts on research to reduce the density of palm kernel shell concrete without compromising the strength in order to produce high and



medium strength concrete. Further studies can also be conducted with other design mix and water cement ratio to further evaluate their influences on concrete strength

ACKNOWLEDGEMENTS

My sincere gratitude goes to almighty God for his immeasurable love, care and favour granted to me throughout this program. My unreserved thanks goes to my supervisor prof J.I Aguwa for his guidance and support throughout the research work.

REFERENCE

- Abdullah, A. A. (1984). Basic strength properties of lightweight concrete using Agricultural wastes as aggregates, Proceedings of International Conference on Low-cost Housing for Developing Countries, Roorkee, India
- Acheampong, A., Adom-Asamoah, M., Ayarkwa, J. and Afrifa, R. O. (2013). Comparative study of the physical properties of palm kernel shells concrete and normal weight concrete in Ghana. *Journal of Science and Multidisciplinary Research*, 5(1), 129-146
- Alawode, O and Idowu, O.I. (2011). Effects of Water-Cement Ratios on the Compressive Strength and Workability of Concrete and Lateritic Concrete Mixes. *The Pacific Journal of Science and Technology*, 12(2),
- Alengaram J. U, Jumaat M.Z and Mahmud H., (2008). Ductility Behaviour of Reinforced Palm Kernel Shell Concrete Beams. *European, Journal of Scientific Research*, 23(3), 406-420
- Alexander, M. and Mindness, S. (2005). Aggregates in Concrete. Taylor and Francis Group London and New York, 379-382
- Anthony, B. J. (2000). Physical Modeling in Geotechnics. PhD Thesis, Virginia Polytechnic Institute and State London, United Kingdom
- ASTM C136 (2003). Standard Test Method for Sieve Analysis of Fine and Coarse Aggregates. Annual Book of ASTM Standards.
- ASTM C127, (2007). Standard Test Method for Specific Gravity and Absorption of Coarse Aggregate. Philadelphia, PA, American Society for Testing and Materials.
- BS 1881: Part 102: (1983). Method for determination of slump. British Standards Institution, Her Majesty Stationery Office, London
- BS 1881: Part 108, (1983), Method for making test cubes from fresh concrete. British Standards Institution, Her Majesty Stationery Office, London.
- BS EN 197 (2011).Cement Part 1: Composition, specifications and Conformity criteria for common cements.
- Falade, F, Ikponmwosa, E. E and Ojediran, N. I (2010) Behaviour of lightweight concrete containing periwinkle shell at elevated temperature. *Journal of Engineering Science and Technology*, 5(4), 379 - 390
- Mosley, W.H and Bungey, J. H. (2000). Reinforced Concrete Design. 5th Edition. Macmillan Publishers Limited: London, UK.
- Ndoke, P. N. (2006). Performance of palm kernel shells as a partial replacement for coarse aggregate in asphalt concrete. *Leonardo Electronic Journal of Practices and Technologies*, 145-152.
- Neville, A. M. (2000). Properties of Concrete, 4th ed., England: Longman
- Okafor, F.O. (1988). Palm kernel shell as a lightweight aggregate for concrete. *Cement and Concrete Research*, 18, 901-910
- Shafiq P, Jumaat M.Z, Mahmud H.B and Alengaram U.J., (2011). A new method of producing high strength oil palm shell lightweight concrete. *Materials & Design*, 32(10), 4839-4843
- Shetty, M.S. (2005) Concrete Technology: Theory and Practice.



INTEGRATED GEOPHYSICAL INVESTIGATION OF THE FAILED PORTION OF MINNA-ZUNGERU ROAD, MINNA NIGER STATE

OSHEKU, G. A¹, SALAKO, K. A², & ADETONA, A. A³

Geophysics Department, Federal University of Technology, PMB 65 Minna Niger State, Nigeria
Corresponding author email: gregosheku@yahoo.com, +2348066270493

ABSTRACT

Very Low Frequency Electromagnetic (VLF EM) and Vertical Electrical Sounding (VES) geophysical methods were used to investigate the competency of kilometer 37 Minna – Zungeru road, Latitude 9^o38'37" N to Latitude 9^o39'06" N, Longitude 6^o16'09" E to Longitude 6^o15'20" E and altitude 682 feet to 597 feet. The study is aimed at investigating the causes of road failure other than the constructional factors that were generally believed. Two VLF – EM traverses which are 1.22 km long were established by the sides of the road segment, which cut across the unstable, fairly stable and stable portions. In these traverses, readings were taken at 20 m interval with SCINTEX ENVI VLF. The data were further filtered, analyzed and plotted with Karous Hject filtering. The inphase and quadrature were plotted against the distance which reveals the conductive zones (positive peak of the raw real). 16 VES were acquired with ABEM SAS 1000 tarrameter along the two traverses. These VES were sounded at the positive peak of the raw real VLF plot using Schlumberger array electrode spacing of 100 m. Geological sections were produced from the iterated VES curves produced with Winresist. The geoelectric sections revealed three geological layers which are the top soil, weathered layer and the fresh basement. The resistivity and depth of these layers ranges from 14 to 98, 81 to 990 and 1184 to 12, 940 Ω m 0.5 to 3.2, 1.6 to 39.4 and 3.5 m to ∞ respectively. The geological factors responsible for the road failure susceptibility are based on clayey subgrade beneath the road pavement, water fluctuation in the saturated zone and lateral inhomogeneity.

Keywords: Vertical Electrical Sounding (VES), Very Low Frequency (VLF)

1 INTRODUCTION

The usage of road has arrested the attention of all stakeholders in the maintenance of Nigeria highways. The problem is apparently more precarious on cut sections of roadways within the Precambrian basement complex terrain of the country (Oladapo *et al.*, 2008).

It has not only caused a setback to Nigerian economy but it has also led to loss of lives and properties in millions of Naira annually.

Since there is a very strong positive correlation between a country's economic development and the quality of its road network, a country's road network should be constructed in an efficient way in order to maximize economic and social benefits (Ighodaro, 2009).

However, in an attempt to unravel causes of persistent failure of roads across the country, various researchers have identified chiefly the underlying geological conditions among the other factors to be responsible for this mishap (Momoh *et al.*, 2008; Oladapo *et al.*, 2008; Adiat *et al.*, 2009). It therefore becomes imperative to investigate the subsurface geology upon which a road structure is to be founded rather than having recourse to a post-construction investigation and remedies.

1.1 Causes of Road Failure

There are several factors responsible for the failure of roads. These include geological, geotechnical, road usage and constructional practices and maintenance (Ajayi, 1987).

1.1.1 The geological Factors Influencing Road Failure Include; Geological structures (near surface linear features), lateral or lithological heterogeneity in competency of sub-surface, thinning out of faces, presence of cavities and existence of ancient stream channels and shear zones

Other factors are: poor soil compaction; can be difficult to obtain if roads are constructed on poor soil (flooded areas and soil with high clay content). **High water table and poor base;** An area subjects to fluctuation of ground water table, ground water always settle there. The high water table may be responsible for the settlement. If the base for the pavement section is improperly installed, then the pavement section will lack the required strength. Also, if a base fails, water can penetrate the pavement section and get into the sub-grade, causing the sub-grade to fail. **Poor compaction;** If the backfill on the utility trenches is not properly compacted, then the trench can be expected to settle. If the sub-grade

of the road is not properly compacted, then settlement can be expected along the road. Extensive compaction test have to be conducted through the life of any road project. **Poor Construction;** The Professional construction Engineer of a road is responsible for the determination of appropriate pavement section. In some cases, failure of the soil cement base is the main reason for the road failure. Ties have simplified this process by developing standard pavement sections to be used in their localities. **Construction in Wet Season;** When the soil conditions are extremely wet, proper compaction is very difficult to obtain therefore, de-watering is extremely important during trench excavation. **Poor Construction Methods;** Poor construction methods manifest when the contractor installing the utilities and preparing the road for paring is not experienced. Shortcuts and failure by some contractors to proper bed lying and backfill utilities are also another poor construction method. Adequate inspection during cement base preparation is of a paramount need.

1.2 Location and Description of the Study Area

The study area is located at Tudun Wada village of Bosso Local Government area of Niger State, North Central of Nigeria.

The road portion under investigation lies on Latitude 9038'37" N to Latitude 9039'06" N and Longitude 6016'09" E to Longitude 6015'20" E and altitude 682 ft to 597 ft. This portion of the road under investigation is about 1.22 km long. The road portion starts from 37 km to 35.78 km from Minna and 23 km to 24.22 km from Zungeru which falls between Beji and Tudun Wada (figure 1).

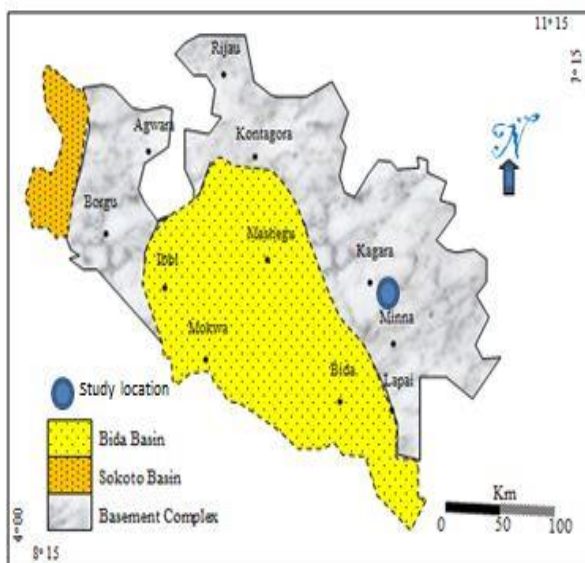


Figure 1: Geological map of Niger State showing the study area.

2 METHODOLOGY

2.1 Instrumentation and Field Procedure.

The equipment used for measurement are ABEM SAS 1000 Digital Resistivity Meter, Garmin etrex10 GPS, Compass clinometer, Measuring tapes, Electrodes, cutlasses, harmer and Scrintex Envi.

The methodology employed in the study involves very low frequency electromagnetic (VLF-EM) and the electrical resistivity methods. The electrical resistivity method utilizes schlumberger vertical electrical sounding (VES) which entails vertical probing of the sub-surface. The array utilizes electrode spacing for variable depth mapping which will be carried out at both stable and failed segments of the roadway.

These methods were employed to determine sections of the road with anomalous and also with the view of detailing the subsurface geoelectric sequences, mapping subsurface structural features, lithology, water saturation and delineating bed rock relief as a means of establishing the possible causes of the road failure.

The traverses covered both failed and stable segments of the roadway established parallel to the road pavement and extend above 1200 m in length (figure 2).

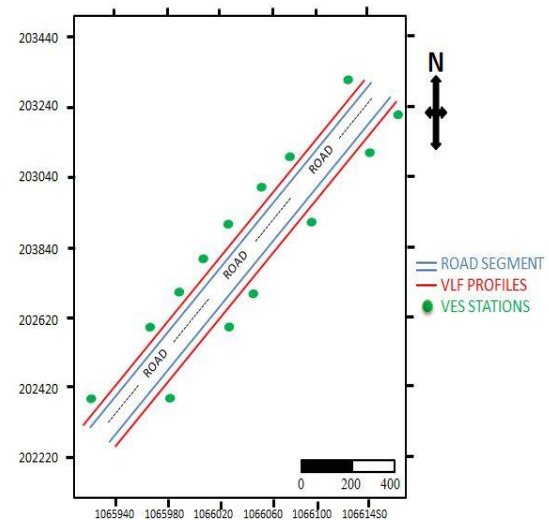


Figure 2: Data Acquisition map of the study area

2.2 Geophysical Methods

2.2.1 Electrical Resistivity Methods

In the electrical resistivity methods electric currents are generated artificially and are induced into the ground. The resulting potential differences are measured at the surface. In artificial field method of electrical prospecting, the voltage measured between the potential electrodes is the sum of the contribution of the entire earth material from various depths. The wider the spaces between the electrodes, the deeper the depth of investigation. The factors influencing the resistivity of the earth (Archie, 1942) are:

i. Porosity

$$\rho_r = a\phi^m \cdot S^n \rho_w \quad (1)$$

$$F = \frac{\rho_r}{\rho_w} = \frac{a}{\phi^m} \quad (2)$$

where:

ρ_r , is the formation resistivity (Ωm)

ϕ , is the porosity

S, is degree of fluid saturation

ρ_w , is the saturating fluid resistivity (a measure of saturating fluid concentration) (Ωm), and a, m, and n are constants peculiar to the rock type.

ii. Degree of fluid saturation;

iii. Nature of pore fluid;

iv. Nature and size of grains making up the matrix;

v. Degree of weathering and fracturing; and

vi. Degree of compaction and consolidation

2.2.2 VLF-EM Method

The VLF method has an excellent and simple tool for reconnaissance mapping of conductive mineralized bodies, water bearing fracture and delineation of saline water intrusion to fresh water zone. It is used in this study to delineation possible conductive zones (low resistivity zones).

2.2.2.1 Factors Affecting the VLF-EM Survey

The factors affecting the VLF-EM survey are:

i. The orientation of high tension power lines: Parallel electric power lines are capable of distorting the VLF-EM signals but perpendicularly oriented overhead or underground power lines are suitable.

ii Time: Radio waves utilized by VLF-EM equipment are very effective in the early hours of the day but the signals tend to be distorted as the evening approaches.

iii Equipment: The equipment must be held steady and horizontal while measurement is in progress.

iv Depth of penetration: It can only be used to detect near surface conductors.

v VLF-EM method: The method is totally dependent on an appropriate transmitter operation (Telford *et al.*, 1990).

2.3 Presentation and Interpretation of VLF-EM Data

The raw real and the real imaginary components of the VLF-EM data were filtered and processed with Karous Hjelt software. The processed data were presented as VLF-EM anomaly curves obtained by plotting the inphase (raw real) responses against the station positions.

The prominent VLF-EM anomalies were deeply considered as typical of the top linear features. Example is Basement fractures (Palacky *et al.*, 1981).

From the VLF-EM anomaly curves only the real components of the VLF-EM data were processed for quantitative interpretation despite the fact that both the real and the quadrature components of VLF-EM data were recorded. This is because signals from the inphase components (real components) are usually more diagnostic of linear features than the quadrature component (Amadi and Nurudeen, 1990).

The raw real (inphase) curves were used for the interpretation because they transform every genuine inflexion points of the real anomaly to positive peaks while reverse inflexions become negative peaks (Olorunfemi *et al.*, 2005).

The VLF-EM data was also inverted to produce a 2-D model section of the subsurface. This 2-D section reveals the nature of the conductive portions, the depth and the nature of the conductive zones using Karous and Hjelt, software.

2.4 Presentation and Interpretation of VES Data

The VES data were presented as depth sounding curves obtained by plotting the apparent resistivity (ρ_a) against the current electrode spacing (AB/2). The WINRESIST software was used to generate computer iterated result from the interpretative results of partial matching technique. The interpretation results were finally used to construct 2-D geoelectric sections which shows the thickness of the layers and the apparent depth of the overburden. The depth and the thickness of the Basement Complex were considered as infinity.

3.0 RESULT AND DISCUSSION

The profiles are quantitatively interpreted to provide locations of conductive zones and zones of anomaly (the inflexion points between the inphase and quadrature) which could be of further interest in investigation (figure 3b) (Nabighian, 1982; Adiat *et al.*, 2009; Reynolds, 1997).

Profile 1

There are points of positive high peaks in the VLF plot (figure 3). These positive peaks of the raw real are points of high conductivity which are indicative of the weak zones, fractures or cavities which serve as conduits for the passage of underground water and thus quicken the failure of the road. The plot indicates the conductive areas at 180, 450, 760, 1050, and 1210 m (figure 3a and 3b).

These portions of linear conductive bodies are also observed in the Karous-Hjelt filter plot of 2-D inversion geosection (figure 4) which shows pockets of conductive bodies. They are delineated in this plot by the red and fairly red colour (180, 450, 760, 1050, and 1210 m). The large conductive body at 620 to 780 m is inferred to be either a large portion of clay material or a cavity.

Vertical Electrical Sounding (VES) were taken at the points of positive peaks of conductive zones to delineate the nature of the conductive materials imbedded in it. Seven VES points were established on this traverse at 0, 180, 450, 600, 750, 1050 and 1120 m which are the points of the positive peaks in the raw real VLF plot (figure 3a). The data generated were used to produce geoelectric sections that delineate 3 zones of variations in resistivity and thickness values which are top layer, weathered layer and fresh basement of various thicknesses.

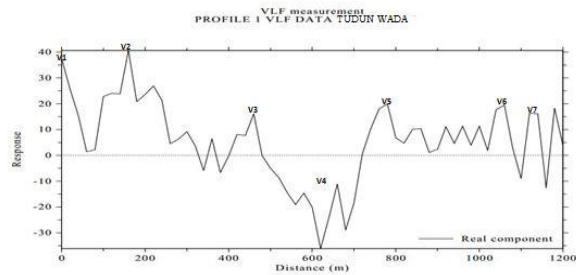


Figure 3a: VLF raw real plot

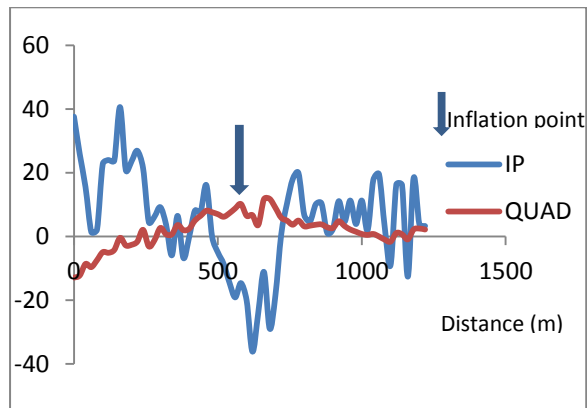


Figure 3b: VLF raw real and filter real excel plot

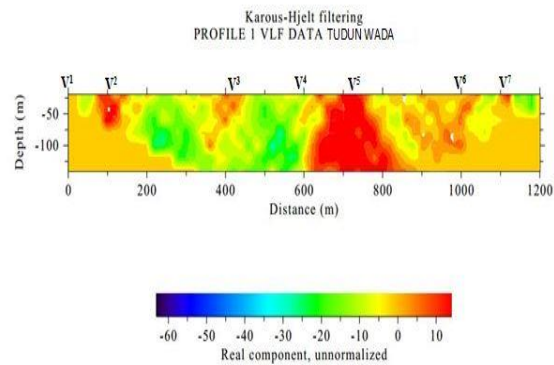


Figure 4: 2-D Karous Hjelt plot

* $V1V^1 - V7V^7$ are points of correlation.

The top soil has a range of 18 to 62.6 Ωm except VES stations 3 which has resistivity of 98.4 Ωm and a thickness of 1.3 m. These ranges of resistivity depict clay and sandy clay with an average thickness of 1.3 m. The variation in the estimated overburden thickness and resistivity ranges from 0.7 to 43.9 m and 7.59 to 991 Ωm respectively. There is an indication that weathered basement was encountered in all the VES locations at a very shallow depth (figure 5). The fresh basement was encountered in all the VES points except VES station 6 and 7 where fresh basement is not delineated. The resistivity of this basement range from 1114.5 Ωm to 6,977.1 Ωm . The clay content of the overburden and the weathered layer constitute the major cause of the road failure as investigated.

Table 1 : Summary of VES data traverse 1

VES	APPARENT		RESISTIVE (Ωm)	THICKNESS (m)	DEPTH (m)	INFERED LITHOLOGY
	CURVE LAYERS	TYPES				
1	1	A	60.2	2.3	2.3	Top soil (clay)
	2		187.3	6.6	8.9	Weathered layer
	3		2292			Fresh Basement
2	1	A	40.6	1.1	1.1	Top soil (clay)
	2		81.6	3.6	4.7	Sandy clay
	3		7090.2			Fresh Basement
3	1	A	98.4	1.3	1.3	Top soil (Sandy clay)
	2		286.4	8.7	10.0	Weathered layer
	3		15503			Fresh Basement
4	1	H	121.7	1.2	1.2	Top soil (Sandy clay)
	2		59.8	3.0	4.1	Clay
	3		1684			Fresh Basement
5	1		17.5	2.6	2.6	Top soil (clay)
	2	A	111.2	4.0	6.5	Sandy clay
	3		1189.8			Fresh Basement
6	1	K	41.6	0.9	0.9	Top soil (clay)
	2		162	4.3	5.1	Weathered layer
	3		433.7			Weathered layer
7	1		18.9	1.9	1.9	Top soil (clay)
	2	A	137.4	9.7	11.7	Weathered layer
	3		990.2			Weathered layer

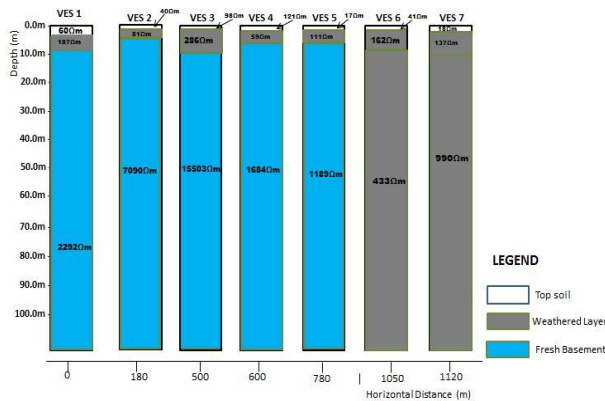


Figure 5: Geoelectric section of profile 1

Traverse 2

The plotting of the VLF raw real data and the distance generate a VLF signature which depict high and low conductive areas. The positive peak of the raw real shows the conductive zones which are zones of weakness, fracture or cavity. These areas are indicated on the VLF plot at distance 80, 240, 400, 450, 700, 830 and 1150 m (figure 6). There is a very high conductive body observed at 700 (figure 6). This is inferred as either fracture or a fault or an intrusion of a conductive body. This portion of the road experienced a major failure.

The Karous-Hjelt filtering was used to invert the VLF data to 2-D geosection model that shows the conductive bodies in various sizes and depth. The conductive zones are red colour while the low conductive areas are shown as green to deep blue colour (figure 7.). The high conductive zone identified at distance 700 m in the raw real VLF plot is inferred either as a fracture or an intrusion of a different body.

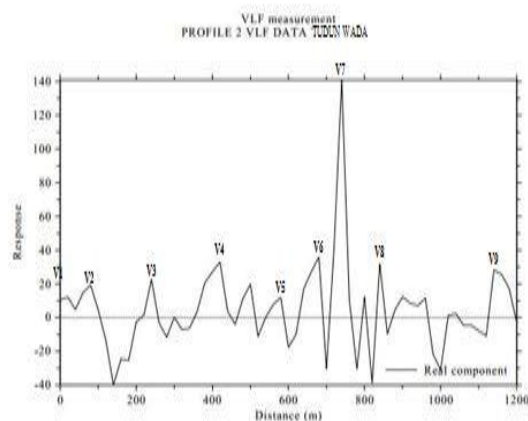


Figure 6: VLF raw real plot

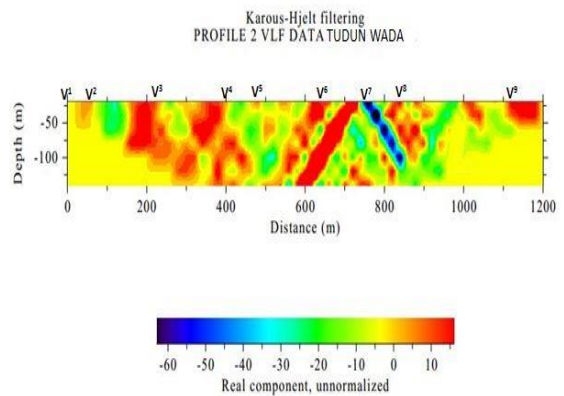


Figure 7: Karous-Hjelt plot 2

* $V1V^1 - V9V^9$ are points of correlation.

Nine VES points were established at the inflection points of positive peaks of the raw real VLF plot at distance 0, 100, 250, 400, 650, 700, 800 and 1150 m in the W-E direction of the traverse, and the data were used to produce a geoelectric section (figure 8). The geoelectric section shows the variation of resistivity and thickness values of the subsurface layers and this provides the information of the geoelectric sequences with the penetrated depth. The constructed geoelectric section revealed the presence of four geoelectric layers. These layers are: the top soil, the weathered layer, partly weathered (fractured basement) and the fresh basement.

The top soil has resistivity value ranging between 3.3 and 50.9 Ω m, except in VES 6 which has the resistivity of 150.85 Ω m. These resistivity values correspond to clay, clayey sand and sandy clay. The top soil is majorly characterized by relatively low resistivity values (less than 80.5 Ω m) suggesting weak zones that are capable of affecting the road stability. The weathered and partly weathered layer is characterized by resistivity ranging from 144.1 to 267.4 Ω m and its thickness varies from 1.4 to 78 m. This low resistivity corresponds to clayey sand and sandy clay as most predominant. This relatively low resistivity is inimical to the stability of the road structure. It should be stated that this low resistivity values may be attributed to water saturation in these weathered zones. The basement has resistivity ranging from 1717.1 to 9616.6 Ω m with thickness variation from 5 m to infinity. The depth to bedrock of the overburden is generally shallow. This also constitutes to the failure of the road.

Table 2 : Summary of ves data traverse 2

VES	LAYERS	CURVE TYPES	APPARENT RESISTIVITY (Ωm)	THICKNESS (m)	DEPTH (m)	INFERED LITHOLOGY
1	1	A	11.3	0.5	0.5	Top soil (clay)
	2		67.8	12.0	12.4	Sandy clay
	3		7026.1			Fresh Basement
2	1	H	36.7	2.8	2.8	Top soil (clay)
	2		2.5	5.7	8.5	clay
	3		192.5			Weathered layer (sand)
3	1	H	49.2	3.2	3.2	Top soil (clay)
	2		13.8	31.4	34.7	clay
	3		246.5			Weathered layer
4	1	H	14.2	1.9	1.9	Top soil (clay)
	2		8.9	1.6	3.5	clay
	3		1983			Fresh Basement
5	1	H	144.1	1.4	1.4	Top soil (sand)
	2		93	7.8	9.2	Sandy clay
	3		13,180			Fresh Basement
6	1	H	62.7	1.1	1.1	Top soil (sandy clay)
	2		36.7	4.3	5.4	clay
	3		1079.2			Fresh Basement
7	1	H	14.2	1.9	1.9	Top soil (clay)
	2		8.9	1.6	3.5	clay
	3		1983			Fresh Basement
8	1	H	62.7	1.1	1.1	Top soil (sandy clay)
	2		36.7	4.3	5.5	clay
	3		1079.2			Fresh Basement
9	1	H	45.4	1.2	1.2	Top soil (clay)
	2		12.3	3.0	4.2	clay
	3		4929.2			Fresh Basement

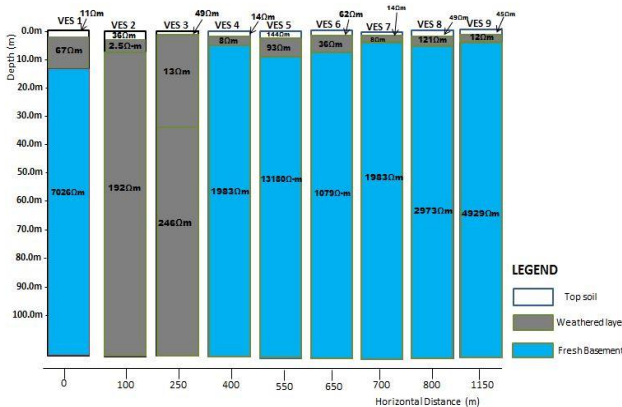


Figure 8: Geoelectric section of profile 2

3 CONCLUSION

The VLF Geophysical method was used to delineate the presence of near surface linear features such as sinkholes, cavity, faults, contact zones and conductive zones. It is however, important to state that limitation of the software used in processing the VLF data in the exaggeration of the probing depth particularly when the traverse is long (the longer the traverse the more the depth is exaggerated). Consequently the depth obtain from the VLF EM interpretation was not used.

Table 1 and 2 show the summary of the interpreted VES results of the study locations which were used to generate the geoelectric sections (figure 5 and 8). These suggest

three scenarios; the first is that the area is underlain by three geological layers which are the top soil, weathered layer and basement. The second is the weathered layer which occurs as the second layer at a shallow depth to the surface. The presence of the weathered layer can also undermine the stability of the road if not properly handled. The third scenario is that the study area is characterized by the occurrence of fresh basement at a very shallow depth (figure 8).

3.2 Recommendation

- 1 Clay formation is not a good engineering material for road sub base.
- 2 Lack of provision of drainages of the high way could obstruct the stability of the road.
- 3 There should be proper excavation of conductive materials in any road pavement.
- 4 Sinkholes that are detected should be filled with high resistivity materials.

REFERENCE

- Adelusi, A.O, K.A.N. Adiat & J.O. Amigun (2009).** Integration of Surface Electrical Prospecting Methods for Fracture Detection in Precambrian Basement Rocks of Iwaraja Area Southwestern Nigeria. *Journal of Applied Science*, 2(3):265- 280.
- Adiat, K.A.N., Adelusi, A.O. and Ayuk. M. A.,(2009).** "Relevance of geophysics in road failures investigation in a typical basement complex of Southwestern Nigeria". *Pacific Journal of Science and Technology*, Vol.5, pp 528 – 539.
- Ajayi, L.A., (1982).** Proposal for engineering classification of Nigeria soils, 1st National Conference Nigerian. Geotech. Association, Lagos State Nigeria.
- Archie, G.E., (1942).** The Electrical Resistivity Log as an Aid in determining some Reservoir Characteristics *Trans. A.I.M.E.* 146, pp. 54-62.
- Ighodaro, C.A.U., (2009).** Transport infrastructure and economic growth in Nigeria. *Journal of Research and National Development.* 7 (2) 14 – 19.
- Momoh, L.O., Akintorinwa, O., Olorunfemi, M.O., (2008).** Geophysical Investigation of Highway Failure; a case study from the Basement Complex terrain of South-Western Nigeria. *Journal of Applied Science Research*, 637-748.
- Nabighian, (1982).** Electromagnetic Methods in Applied Geophysics. *Society of Exploration Geophysics (SEG).* 9 (1) 11.
- Oladapo, M.I., Olorunfemi, M.O. and Ojo, J.S., (2008).** Geophysical investigation of road failure in the basement complex area of southwestern Nigeria. *Research Journal of Applied Sciences* 3(2): 103-112, 2008. ISSN 1815-932X.



Olorunfemi, M.O., Fatoba, J.O., and Ademilua, L.O., (2005). Integrate VLF-Electromagnetic and Electrical Resistivity Survey for F=Groundwater in a crystalline Basement Complex Terrain of southwestern Nigeria. *Global Journal of Geological Sciences*, Vol. 33 (1), pp. 71-80.

Palacky, G.J., (1987). Clay Mapping using Electromagnetic Methods. *First Break*, 5, Pp. 295-306.

Reynolds, J.M., 1995: *An Introduction to Applied and Environmental Geophysics*. Cambridge University Press, Cambridge, pp. 75-78.

Sharma, P.V., (1997). *Environmental and Engineering Geophysics*, Cambridge University Press, Cambridge, pp. 45-48.

Sinha, A.K. (1990). Interpretation of ground VLF-EM data in terms of vertical conductor models. *Geo-exploration*, 26:213-231.

Telford, W.M., Geldart, L.P. and Sheriff, R.E., (1990). *Applied Geophysics*. Second Edition, Cambridge University Press, New York, pp. 770



PARTIAL REPLACEMENT OF FINE AGGREGATE WITH WASTE GLASS IN CONCRETE MADE FROM BIDA NATURAL AGGREGATE

Alhaji B., Kolo, D. N., Abubakar M., Yusuf A., Abdullahi, A. and Shehu, M.

Department of Civil Engineering, Federal University of Technology, Minna
Email: balhaji80@yahoo.com, 08065260435

Abstract

This study reports the experimental investigation on the suitability of waste glass as partial replacement for fine aggregate in concrete made using Bida natural aggregates (BNA). Glass is widely used in our daily lives through manufactured products such as sheet glass, bottles, glassware, and vacuum tubing. It is an ideal material for recycling. The increasing awareness of glass recycling speeds up inspections on the use of waste glass with different forms in various fields. Mix ratio of 1:2:4 batched by weight with water – cement ratio of 0.55 was used. The percentage replacement varied from 0% to 40% at 5% intervals. Slump test was conducted to assess the workability of the fresh concrete. The compressive strengths and densities of cured concrete cubes of sizes 150mm x 150mm x 150mm were evaluated at 7, 21 and 28 days. A total of 81 concrete cubes were cast and tested. It was observed that an increase in the percentage replacement of fine aggregate with waste glass reduces workability, density and compressive strength. The compressive strength and density vary with days of curing. The findings of this study indicated that the optimum replacement percentage of waste glass with conventional fine aggregate was 20%. However waste glass can effectively be used as fine aggregate replacement (up to 40%) without substantial change in concrete strength.

Keywords: *Bida Natural aggregates, Concrete, Fine Aggregates, Recycling, Waste glass*

1.0 INTRODUCTION

Concrete is a man-made composite, a major constituent of which is natural aggregate such as gravel and sand or crushed rock. Alternatively, artificial aggregate such as blast furnace slag, expanded clay, broken bricks and steel shots may be used where appropriate. It is obtained by mixing cementitious material, water and aggregate (and sometimes admixtures) in required proportion. The mixture when placed in form and allowed to cure hardens into a rocklike mass known as concrete. The hardening of concrete is cured by chemical reaction between cement and water and continues for a very long time and consequently the concrete grows stronger with age (Bamigboye *et al.*, 2015). The hardened concrete may be considered as an artificial stone in which the voids of larger particles (coarse aggregate) are filled by the smaller particles (fine aggregate) and voids of fine aggregate are filled with cement. The cementitious material and water form a cement paste which in addition to the filling of the voids of fine aggregate coats the surface of fine and coarse aggregate together to form a compact mass (Bamigboye *et al.*, 2015). In its hardened stage concrete is a rocklike material with high compressive strength while in its plastic stage it can be easily moulded into virtually any shape. It may be used as an architectural advantage or solely for decorative purposes. Normal concrete

has a comparatively low tensile strength and for structural application it is normal practice to either incorporate steel bars to resist any tensile force (reinforced concrete) or to apply compressive forces to the concrete to counteract this tensile force (pre-stressed concrete). Concrete is also used in conjunction with other materials for example it may form a compression flange of a box section, the remainder of which, steel (composite construction) is used structurally in building, foundation, column, beams, slabs, shell construction, bridges (Shabana *et al.*, 2011). Concrete occurs in both fresh and hardened state. Its fresh state must undergo proper workability, consistence, setting, handling, placing, transportation and compaction for it to be satisfactory. This fresh concrete solidifies and hardens after placement and develops strength over time (Bartos *et al.*, 2002). Concrete can be considered to be an artificial stone made by binding together the particles of relatively inert fine and coarse materials with cement paste.

Glass is a transparent material produced by melting a mixture of materials such as silica, soda ash, and CaCO₃ at high temperature followed by cooling where solidification occurs without crystallization. Glass is extensively used in our lives through manufactured products such as sheet



glass, bottles, glassware, and vacuum tubing. Glass is an ideal material for recycling. The use of recycled glass saves lot of energy and the increasing awareness of glass recycling speeds up focus on the use of waste glass with different forms in various fields. One of its significant contributions is the construction field where the waste glass was reused for concrete production. The application of glass in architectural concrete still needs improvement. Several study have shown that waste glass that is crushed and screened is a strong, safe and economical alternative to sand used in concrete. During the last decade, it has been recognized that sheet glass waste is of large volume and is increasing year by year in the shops, construction areas and factories. Using waste glass in the concrete construction sector is advantageous, as the production cost of concrete will go down. The amount of waste glass is gradually increased over the years due to an ever-growing use of glass products. Most of the waste glasses have been dumped into landfill sites. The land filling of waste glasses is undesirable because they are non-biodegradable, which makes them environmentally less friendly. There is huge potential for using waste glass in the concrete construction sector. When waste glasses are reused in making concrete products, the production cost of concrete will go down (Topcu and Canbaz, 2004). Crushed glass or cullet, if properly sized and processed, can exhibit characteristics similar to that of gravel or sand. When used in construction applications, waste glass must be crushed and screened to produce an appropriate design gradation. Glass crushing equipment normally used to produce a cullet is similar to rock crushing equipment, it has been primarily designed to reduce the size or density of the cullet for transportation purposes and for use as a glass production feedstock material, the crushing equipment used is typically smaller and uses less energy than conventional aggregate or rock crushing equipment (Egosi,1992).

2.0 MATERIALS AND METHODS

2.1 SOURCING OF MATERIALS

Cement: in this work, ordinary Portland cement (OPC) was used. Cement is a kiln-dried and finely pulverized mixture of natural materials. The cement most commonly used for structural concrete is the ordinary Portland cement (OPC), other types of cement available include; Rapid- hardening Portland cement, Portland- Blast furnace cement, Low-heat Portland cement, sulphate-resisting cement, super-sulphate cement and High- alumina cement (Neville, 2000).

Typical Portland cement are mixture of Tricalcium silicate ($3\text{CaO}\cdot\text{SiO}_2$), Dicalcium Silicate ($2\text{CaO}\cdot\text{SiO}_2$),

Treicalcium Aluminates ($4\text{CaO}\cdot\text{Al}_2\text{O}_3$), and Tetracalcium Alumino ferrite ($4\text{CaO}\cdot\text{Al}_2\text{O}_3\cdot\text{Fe}_2\text{O}_3$), in varying proportions. In addition to the main compounds listed above there exist minor compounds, such as magnesium oxide. (MgO), titanium dioxide (TiO_2), manganese oxide (Mn_2O_3), potassium oxide (K_2O), sodium oxide (Na_2O); they usually amount to not more than a few percent of the mass of cement (Neville and Brookes, 2008).

Fine Aggregate: Aggregate passing B.S sieve 5mm are termed fine aggregates. Fine aggregates generally consist of natural sand, or crushed stone sand or crushed gravel with most particles smaller. The natural sand can be classified as coarse sand, medium sand and fine sand in accordance to Table 4 (B.S 882-103.1).

Coarse Aggregate (Bida Natural Aggregate): The coarse aggregate used for this study was obtained from Bida town. It passes through sieve size 20mm.

2.2 METHODOLOGY

In order to study the effect of waste glass as partial replacement of cement on the strength of concrete, 81 cubes of size 150 mm × 150 mm × 150 mm were cast with different percentage of demolished waste glass ranging from 5% to 40% and 0% as the control. An effort has been made here to compare the strength of cubes made up with different percentage of demolished waste to the respective strength of conventional concrete at the end of 7, 21 and 28 days of moist curing and to have an idea about the optimum percentage of demolished waste which does not affect the strength of recycled concrete considerably. Similarly, fine aggregate was also partially replaced by waste glass and only cubes were cast and tested after 7, 21 and 28 days for mix of 1:2:4 at a w/c of 0.55.

3.0 RESULTS AND DISCUSSION

Table 1.0: Physical properties of Aggregates

Properties	Waste Glass	Sand	Gravel
Loose bulk Density (g/cm^3)	1.53	1.96	1.34
Compacted bulk Density (g/cm^3)	1.65	1.8	1.5
Moisture content (%)	5.09	8.26	6.42
Specific Gravity	2.43	2.61	2.59
Water Absorption (%)	12.39	13.78	4.89

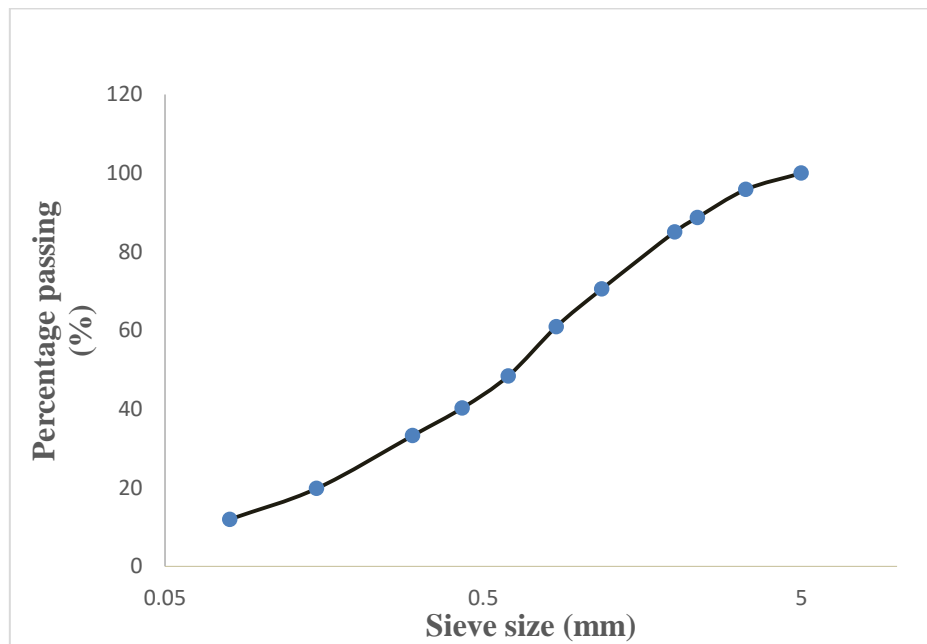


Figure 1.0: Particle Size Distribution for Waste Glass

Specific gravity value of 2.43 placed the waste glass in the same category as lightweight aggregate while the specific gravity of sand and the gravel were 2.61 and 2.59 respectively, both fall within the acceptable natural aggregates range of 2.0 – 2.6 (BS EN 1097-6, 2013). However, the compacted and loose bulk densities of waste glass are 1.65 and 1.53 respectively. Waste glass is found to have a lesser water content compared to the fine sand which in turn reduces the workability of fresh concrete.

Table 2 presents a summary of compressive strengths obtained utilising waste glass aggregate in concrete production.

Table 2.0: Compressive Strength Results (N/mm²)

% Replacement	7 Days	21 days	28 Days
0	15.61	15.97	16.61
5	15.10	14.93	16.56
10	13.93	14.34	15.51
15	13.75	14.30	15.41
20	13.35	13.55	14.12
25	13.3	13.54	13.90
30	12.58	13.40	13.80
35	12.45	13.10	13.20
40	11.87	11.73	12.10

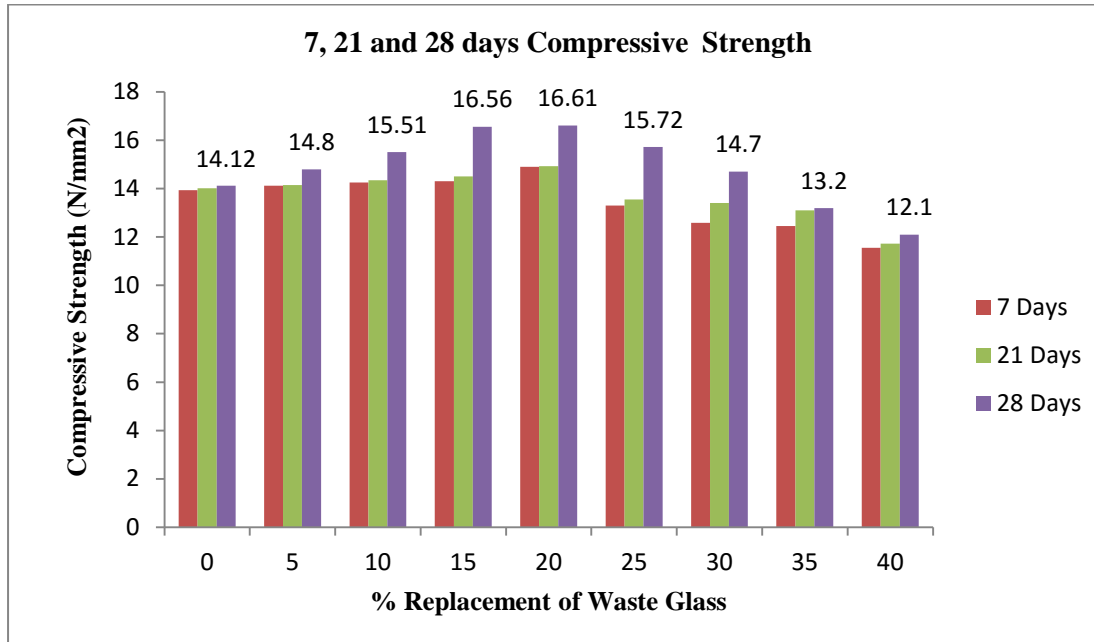


Figure 1.0: Compressive strength of concrete against percentage replacement of waste glass at 7, 21 and 28 days

It is observed from Table 2.0 and Figure 1 that for control (0% replacement), there is a minimal increase in compressive strength as the curing age increases. 7 days curing age has a compressive strength of 14.01 N/mm² while 28 days curing age has a compressive strength of 14.12 N/mm². The compressive strength however kept increasing as the percentage replacement level increased from 5% to 20% replacement level of waste glass with fine aggregate at the 7, 21 and 28 days replacement, after which a gradual reduction in strength was observed until the 40% replacement level. The results for the 28 days curing prove that waste glass can be used as a substitute for fine aggregate in concrete production, with the optimum strength obtained at 20% replacement of Fine aggregate with glass. This result is in line with that of Srivastava *et al.* (2017).

4.0 CONCLUSION

It can be seen from the results of this study that replacement of conventional fine aggregate with waste broken glass in the production of concrete for the construction industry would result in structures with reasonable structural characteristics. The following conclusions were drawn from the study:

While using waste glass as fine aggregate replacement, 28 days strength was found to slightly increase at 5-10% percentage replacement levels when compared to the control. A similar trend was observed in the variation of properties such as workability, unit weight and compaction factor of concrete with an increase in the percentage replacement of fine aggregate with waste glass.

Hence, Waste glass can effectively be used as fine aggregate replacement, with the optimum replacement level of 20%.

Waste glass is a reliable material that could be used in concrete to lower the amount of glass being land filled. The recycling of glass into aggregate applications is an economically feasible and environmentally friendly approach in tackling the problem of landfilling usually encountered with broken waste glass.

There exists a potential reduction in the cost of concrete production by replacing fine aggregate with waste glass.

Concrete containing glass as fine aggregate should be placed in applications where cracking and high strength are not of importance.



REFERENCES

- Bamigboye, G. O., Ede, A. N., Egwatu, C., and Jolayemi, J. (2015). Assessment of Compressive strength of Concrete produced from different brands of Portland Cement. *Civil and Environmental Research*. 7(8). ISSN 2225-05714.
- Bartos, P.J. M., Sonebi, M., and Tamimi, A.K. (2002). Workability and Rheology of Fresh Concrete: Compendium of Tests. Report of Technical Committee TC145 WSM. Rilem International Union of Testing and Research for Materials and Structures.
- BS EN 1097-6, (2013). Tests for Mechanical and Physical properties of aggregates. Determination of particle density and water absorption.
- Egosi, N. G. (1992). Mixed broken glass processing solutions. Proceedings of. Utilization of waste materials in Civil engineering construction conference USA. P.14.
- Neville, A. M. (2000). Properties of Concrete, 4th edition Pearson Education, Edinburgh, England.
- Neville, A. M. and Brookes J. J. (2008). Concrete Technology, Revised edition. Pearson Education Limited, Edinburgh gate, Harlow, Essex CM20 2JE, England.
- Shabana, E. H., Ibrahim, S. A., and Dessouki, A. K. (2011). Strength and Stability of lateral bracing for compression flange in L-shaped beams. *International Journal of Structural Engineering*. 2(3). 273 – 302.
- Srivastava, I., Gupta, D., Sehmi, S. S., Shivam, K., and Bharadwaj, J. (2017). Partial Replacement of Fine Aggregates with Waste Glass. *International Journal of Advance Research, Ideas and Information in Technology*. 3(4). 746-749.
- Topçu, İ. B., Bağcı, A.R., and Bilir, T., (2008). Alkali-silica reactions of mortars produced by waste glass.
- Topçu, İ. B. and Canbaz, M., (2004). Properties of concrete containing waste glass.



Assessment of the Compressive Strength of Concrete Produced with Fine Aggregate from Different Locations in Minna

*Aminulai, H. O¹, Abdullahi, A¹, Abdulrahman, H. S¹, Alhaji, B¹, Joseph, O. F², Aliyu, S. Y¹

¹Civil Engineering Department, Federal University of Technology, PMB 65 Minna, Niger State Nigeria

²Civil Engineering Department, Kogi State Polytechnic, PMB 101 Lokoja, Kogi State Nigeria

* Corresponding author email: aminulai.hammed@futminna.edu.ng, + 2347037751963

ABSTRACT

The construction industry in Nigeria has been witnessing serious collapse of buildings resulting from the qualities of materials used in their construction. This continuous collapse necessitates the need to investigate some of the materials used in the production of the building components in order to ascertain their appropriateness. This research thus investigates the compressive strength of concrete produced using fine aggregate from different locations in Minna. Fine aggregates were obtained from Chanchaga, Maikunkele, Bosso, Lapai Gwari and Garatu areas of Minna and subjected to series of tests namely: sieve analysis, Specific gravity, bulk density, moisture content, and water absorption. Concrete samples were produced using the mix ratio 1:2:4 and the water/cement ratio of 0.6. These samples were subjected to both the slump test and compressive strength test. For each of the fine aggregates, nine cubes of concrete (150mm x 150mm x 150mm) were cast, cured and tested at 7, 14 and 28 days. The results obtained for the mean compressive strength of the concrete produced shows that they all have mean strength greater than 20N/mm² with fine aggregate from Chanchaga having the highest mean of 25.17N/mm² at 28days of curing. Thus all the fine aggregates could be used in the production of structural lightweight concrete but for structures that require higher strength, the fine aggregate from Chanchaga is recommended

Keywords: *Building collapse, concrete, fine aggregate, compressive strength.*

1 INTRODUCTION

Concrete is one of the most popular artificial construction material on earth (Thandavamoorthy, 2014) and the most widely used construction material in Nigeria (Tsado, 2013). It is a composite material with natural aggregate as a major constituent. Traditionally, concrete is made up of cement, aggregate (coarse and fine) and water in an appropriate ratio which hardened up to form a rocklike mass (Gideon *et al*, 2015). This constituent has various influences on the strength of the concrete (Deodhar, 2009). Also, the strength, stiffness, and fracture energy of concrete for a given water/cement ratio depend on the type of aggregate used in its production (Abdullahi, 2012). Its quality could be impaired if the materials used in its production are not of good quality.

The collapse of buildings has been traced to many factors one of which is the qualities of the materials used during construction (Ayininuola and Olabisi, 2014, Ede 2010). The qualities of concrete depend on the type of cement, water, and aggregate used in its production. Since aggregate (coarse and fine) occupy up to 70 -75% of the concrete volume (Talbot and Richart, 1923), its quality need to be ascertained. The aggregates in concrete are of two types namely fine and coarse aggregate. The aggregate with size less than or equal to 5mm is termed fine aggregate while that with size above 5mm is termed coarse aggregate.

All aggregates for concrete works should be composed of hard particles and free of any amounts of clay, loam, and vegetable matter. The major characteristics of aggregates that affect the strength, durability, and workability of concrete are cleanness, grading, hardness, and shape. Usually, the aggregates are stronger than the concrete from which they are made. A coating of dirt or dust on the aggregate will reduce the strength of concrete because it prevents the particles from properly bonding to the mortar. A well-graded aggregate mix is essential to obtaining an economical concrete of good quality. If poorly graded, even clean, sound aggregates will require excessive water for workability, resulting in lower strength, or the mix will require an excessive amount of cement to develop a given strength.

Fine aggregate is one of the important constituents of concrete which contributes to the stability of the concrete produced (Gupta and Gupta, 2014). Various types of fine aggregates are being used in concrete production. The type of fine aggregate used changes the geometric properties of cement paste, and affect not only the shell formation during heat treatments but also the properties of concrete (Abdullahi *et al.*, 2017).

The fine/coarse aggregate ratio will influence the packing of concrete. It also influences the workability of concrete in the fresh stage. Increase of the sand to coarse aggregate ratio can lead to an increase of cohesiveness but reduces the consistency. Increasing the sand/coarse

aggregate ratio of concrete has proven to be the most effective measures for improving its cohesiveness (Li, 2011).

The commonly used fine aggregate in Nigeria is popularly referred to as sharp sand which may be sourced from the river or natural deposit. This is because of its tested nature which conforms to the British standard codes specifications. In Nigeria, especially Minna, sharp sand as fine aggregate used in construction are obtained from different locations but the location which gives the best quality of concrete is yet to be ascertained.

Production of concrete with fine aggregate from different locations in Minna will reveal the one that is most suitable for concrete work. Thereafter, in a construction project, the location of most suitable fine aggregate will be guaranteed and prevent usage of substandard material in the construction project so as to reduce the problem of collapsed structures.

2 METHODOLOGY

The approach of this study was to investigate the properties of the fine aggregates and fresh concrete and the compressive strength of the hardened concrete that is produced with it. Different concrete mixes were produced by using the fine aggregates from five different locations in Minna while using a uniform mix ratio 1:2:4 and water/cement ratio of 0.6. Nine cubes (150mm x 150mm x 150mm) were cast for each of the fine aggregates (BS 1881: Part 108:1983). These cubes were cured by completely immersing them in water for 7, 14 and 28 days (BS 1881: Part 111:1983).

2.1 MATERIALS

The materials described below were used for this study;

2.1.1 ORDINARY PORTLAND CEMENT

The cement used for this study is Ordinary Portland Cement (OPC). It was bought from a cement store beside Yellow house, Gidan Kwano, Minna, Niger State and conforms to BS EN 197-1 (2011) requirements.

2.1.2 AGGREGATES

The coarse aggregate used in the study was obtained from a quarry shop along Gidan Kwano to Kpakungu road. It was found to have conformed to PD 6682-1:2009+A1 (2013) as it was retained on BS sieve 5mm while the fine aggregates used also conformed to the specification of PD 6682-1:2009+A1 (2013) and passes through BS sieve 5mm. The samples of fine aggregates were obtained from the following five locations; Chanchaga, Maikunkele, Garatu, Bosso and Lapai Gwari within the region of Minna, Niger State.

All the aggregates were moisture-free before being used for concrete production.

2.1.3 WATER

The water used for the study was obtained from the borehole near the Civil Engineering Laboratory at the Main Campus, Gidan Kwano, Federal University of Technology Minna, Niger State. It conformed to BS EN 1008 (2002) specifications.

2.2 EXPERIMENTAL INVESTIGATIONS

The investigations include tests on all the fine and coarse aggregates, the fresh concrete and also the hardened concrete. The following tests were carried out on the aggregates used in order to determine their properties.

- i. Specific gravity, (G_s): This is the ratio of mass (weight in air) of a unit volume of material to the mass of the same volume of water at the same temperature. This test was carried out on the fine and coarse aggregates in accordance with BS EN 1097-6 (2000). The specific gravity is calculated as

$$G_s = \frac{W_2 - W_1}{(W_2 - W_1) - (W_3 - W_4)} \quad (1)$$

Where,

W_1 = Weight of vessel (g)

W_2 = Weight of vessel plus sample (g)

W_3 = Weight of vessel plus sample plus water (g)

W_4 = Weight of vessel plus water only (g)

- ii. Bulk density: This is the weight of a given material required to fill a given volume of container. It is also a measure of how dense or closely packed a sample is. The bulk density of a sample depends on the particle size distribution, the shape of particles and how densely the aggregate is packed. It is expressed in kilogram per meter cube (kg/m^3). Bulk density could either be compacted or un-compacted (loose) bulk density. The test was carried out on the fine and coarse aggregates in accordance with BS EN 1097-3 (1998). The bulk density of the un-compacted and compacted is calculated from:

$$\text{Un-compacted Bulk Density} = \frac{W_2 - W_1}{V} \quad (2)$$

$$\text{Compacted Bulk Density} = \frac{W_3 - W_1}{V} \quad (3)$$

Where:

W_1 = Weight of mould (g)

W_2 = Weight of mould plus un-compacted sample (g)

W_3 = Weight of mould plus compacted sample (g)

V = Volume of mould

- iii. Water Absorption: This is the increase in mass of aggregates due to the penetration of water into the pores of the particles during a period of time.

Water absorption is determined by measuring the decrease in mass of a saturated and dry sample after oven drying for 24 hours. Water absorption is expressed as a percentage of dry mass. This test was carried out in accordance with BS EN 1097-6 (2000). It is calculated as:

$$\text{Water Absorption} = \frac{W_3 - W_2}{W_4 - W_1} \times 100 \quad (4)$$

Where:

W_1 = Weight of container (g)

W_2 = Weight of container plus sample (g)

W_3 = Weight of container plus wet sample (g)

W_4 = Weight of container plus oven dry sample (g)

- iv. Moisture content (Mc): This is the amount of water that can be removed from a soil sample when it is dried at a temperature of 105°C. It is expressed in percentage as the relationship between the water content in the sample to the weight of the sample when it is completely dry. This test procedure was done on the fine and coarse aggregates in accordance with BS EN 1097-5 (2008). It is calculated as:

$$\text{Mc} = \frac{W_2 - W_3}{W_3 - W_1} \times 100 \quad (5)$$

Where:

W_1 = Weight of empty can (g)

W_2 = Weight of can plus sample (g)

W_3 = Weight of can plus oven-dried sample (g)

- v. Porosity: This is the amount of void present in an aggregate. it affects the bond between the aggregate and cement, the resistance of concrete, freezing, and thawing and, chemical stability of the aggregate (Neville and Brooks, 2010). According to Neville (2010), higher durable concrete can be achieved through aggregate with lower porosity.

$$\text{Porosity (\%)} = 1 - \frac{\rho_{\text{agg}}}{\rho_{\text{agg}} + \rho_{\text{cement}}} \times 100 \quad (6)$$

- vi. Particle size distribution (sieve analysis): This test commonly referred to as gradation test can simply be summarized as the process of dividing a sample of aggregate into fractions of the same particle size. The test was carried out in accordance with BS EN 933-1 (2012).

The slump test was done on the fresh concrete to determine its workability in accordance with BS EN 12350-2 (2009) while the compressive strength test was done on the hardened concrete in accordance with BS EN 12390-2 (2009) and BS EN 12390-3 (2009).

3 RESULTS AND DISCUSSION

This research aim at identifying the most suitable fine aggregate for concrete production in Minna and its environs. Here, the result of the physical properties of the fine and coarse aggregates as well as the workability test (slump test) done on fresh concrete mixes and the compressive strength test on the hardened concrete cubes at different curing ages are presented.

3.1 PROPERTIES OF FINE AND COARSE AGGREGATE

The particle size distribution curves of the fine and coarse aggregates are present in Figure 1. It showed that all the fine aggregates fall within a fine sand fraction with that obtained from Chanchaga being the most well graded. This shows that it requires less quantity of cement and water and is thus more economical and produce higher strength concrete, lower shrinkage and greater durability (Shetty, 2012). The coarse aggregate curve reveals medium gravel aggregate

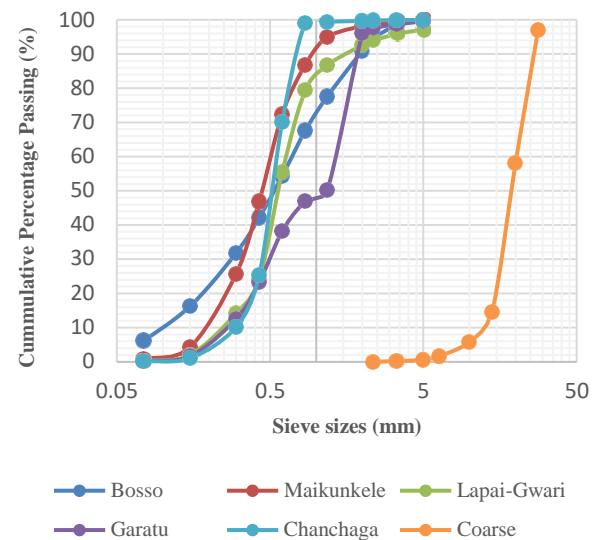


Figure 1: Particle size distribution of Fine and Coarse Aggregate

The results of the physical properties of the fine aggregates are as presented in Table 1 below.

The specific gravity of fine aggregates obtained from Lapai Gwari, Garatu, Maikunkele, Chanchaga, and Bosso are 2.58, 2.67, 2.63, 2.66 and 2.70 respectively. All the fine aggregates are within the standard range of 2.6 – 2.7 except that of Lapai Gwari. The specific gravity of the coarse aggregate (2.64) is also within the standard limit of 2.6 – 3.0 (Neville, 2010).

The results of bulk density for fine aggregates showed that all of them are in conformity with the standard limit of

1300-1800 kg/m³. Also, the coarse aggregates bulk density is within the standard limit of 1500-1700 kg/m³.

The results obtained for the porosity of the fine aggregates as shown in table 1 are 5.7%, 1.2%, 9.5%, 7.2% and 0.8% for Chanchaga, Maikunkele, Bosso, Lapai Gwari and Garatu respectively while the porosity for the coarse aggregate is 5.14%. The percentage porosity of these aggregates falls within the range of 1% to 15% (Neville, 2010). The lower values of porosity obtained for the aggregates specified that the aggregates can make a highly durable concrete (Neville, 1987). with fine aggregate from Garatu having the lowest value.

The results of water absorption test for the fine aggregate are 28.54%, 26.68%, 28.91%, 28.19%, and

24.08% respectively for Garatu, Lapai Gwari, Chanchaga, Maikunkele, and Bosso while that of coarse aggregate is 1.40%. This indicates a high water tolerance for the fine aggregates with Chanchaga having the tendency of absorbing more water than the others. Meanwhile, there is low water tolerance for the coarse aggregate.

The results of moisture content tests for the fine aggregates are 0.151%, 0.013%, 0.121%, 0.038% and 0.5045% for Garatu, Lapai Gwari, Chanchaga, Maikunkele, and Bosso respectively while that of coarse aggregate is 0.504%. These are within the standard ranges (Neville, 2010).

TABLE 1: Summary of the properties of fine and Coarse Aggregate used in the study

Properties	Bosso	Maikunkele	Lapai - Gwari	Garatu	Chanchaga	Coarse Aggregate	
Specific gravity	2.70	2.63	2.58	2.67	2.66	2.64	
Bulk density (kg/m ³)	Un-compacted	1545	1404	1444	1511	1388	1551
	Compacted	1708	1421	1556	1523	1472	1635
Water absorption (%)	24.08	28.19	26.68	28.54	28.91	1.40	
Porosity (%)	9.5	1.2	7.2	0.8	5.7	5.14	
Moisture content	0.089	0.038	0.013	0.151	0.121	0.504	

3.2 WORKABILITY TEST RESULTS (SLUMP TEST)

The slumps obtained for the concrete made with the fine aggregates types are as shown in table 2. The nature of the slumps obtained during the experiment revealed a true

slump for all the fine aggregates which indicate uniformity in the mix. The slumps are also classified as medium slump which indicates a highly durable and workable concrete except for Maikunkele with a slump of 30mm which is classed as low.

TABLE 2: Slump test result of concrete made from different fine aggregate types

Fine aggregate source	Trials	Water/ cement ratio	Mix ratio	Slump (mm)	Avg. slump	Slump Value	Type of slump
Lapai-Gwari	1	0.6	1:2:4	75	75	75	True slump
	2	0.6	1:2:4	75			
Maikunkele	1	0.6	1:2:4	32	30	30	True slump
	2	0.6	1:2:4	28			
Bosso	1	0.6	1:2:4	44	42	40	True slump
	2	0.6	1:2:4	40			
Chanchaga	1	0.6	1:2:4	45	45	45	True slump
	2	0.6	1:2:4	45			
Garatu	1	0.6	1:2:4	42	40	40	True slump
	2	0.6	1:2:4	38			

3.3 COMPRESSIVE STRENGTH TEST RESULTS

The results for the compressive strength test of hardened concrete for a constant mix ratio (1:2:4) and 0.6 water/cement ratio for 7, 14 and 28 days curing of concrete made from fine aggregates obtained from Lapai Gwari, Maikunkele, Bosso, Chanchaga and Garatu are as shown in Figure 2

The highest value of compressive strength was obtained for concrete made with the fine aggregate obtained from Chanchaga for all the days of the concrete curing.

From the values obtained for compressive strength, the concrete can be classified as lightweight concrete. The standard recommended in BS 1881: Part 116: (1983) and Barry (1999), indicates that a 28 days compressive strength range of 17.5N/mm² to 34N/mm² is specified for structural lightweight concrete, depending on factor such as aggregate grading, mix proportioning, and water/cement ratio. According to Neville (2010) concrete attain over 60% of their 28days strength at the age of 7 days; the compressive strengths obtained from concrete produced with all the fine aggregates were in conformity with this theory. Also, the graph showed that the compressive strength of concrete increase with curing ages.

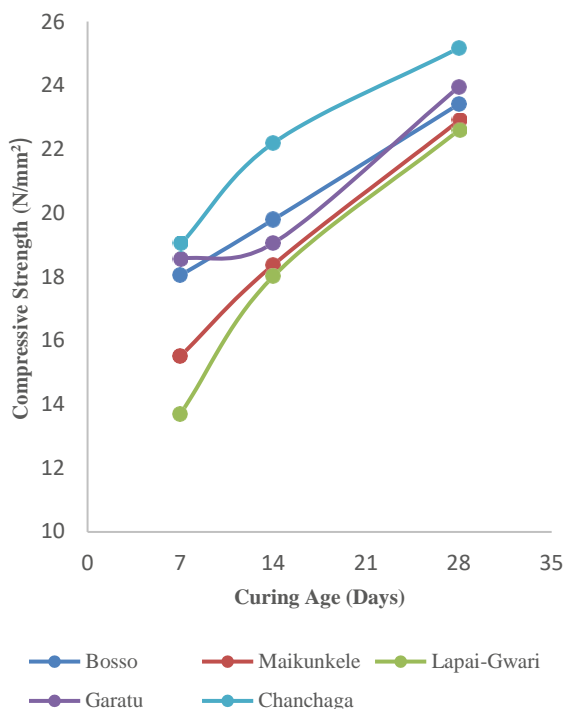


Figure 2: Compressive strength of concrete produced with fine aggregate from different locations

4 CONCLUSION

From the results obtained from the assessment of the compressive strength of concrete using fine aggregate obtained from different locations in Minna, the following conclusion can be drawn.

- The fine aggregate from Chanchaga is better graded in particle distribution than the other fine aggregates. Thus concrete produced from this will have better qualities than the others.
- The physical properties of fine aggregate obtained from different locations (sources) in Minna have varying values with most falling within the recommended standards. The specific gravity values ranges between 2.58 – 2.70, the bulk density from 1388kg/m³ - 1708kg/m³, the water absorption from 24.08% - 28.91%, the porosity of 0.8% - 9.5% while the moisture content ranges between 0.013 - 0.151.
- The fine aggregate from different locations in Minna produced concretes of different workability with constant mix ratio, w/c ratio, and coarse aggregate properties.
- All the fine aggregate used in the study produced concrete with mean strength greater than 20N/mm² with the fine aggregate obtained from Chanchaga having the highest mean compressive strength (25.17N/mm²) at 28days of curing.

It then means that all the aggregates could be used in the production of structural lightweight concrete but for structures that require high strength, then the fine aggregate from Chanchaga is recommended.

ACKNOWLEDGEMENTS

The authors acknowledge the support of all the technical staff in the Civil Engineering Laboratory, Federal University of Technology Minna. We would also like to acknowledge the effort of all the undergraduate students that assisted with the experimental work.

REFERENCES

- Abdullahi, M. (2012). Effect of aggregate type on Compressive strength of concrete. *International Journal of Civil and Structural Engineering*, 2(3), 791-800, ISSN 0976 –4399 (online)
- Abdullahi, M., Yakubu, A., & Aguwa, J. I. (2017). Compressive Strength of Concrete made from Natural Fine Aggregate Sources in Minna, Nigeria. *Arid Zone Journal of Engineering, Technology and Environment*, 13(6), 734–742. ISSN: 1596-2490 (Print), ISSN: 2545-5818 (Electronic)
- Ayininuola, G. M., & Olalusi, O. O. (2004). Assessment of building failures in Nigeria; Lagos and Ibadan case



- study. *Africa Journal of Science and Technology (AJST)* 5 (1), 72-78.
- Barry, R. (1999). *The Construction of Buildings: Foundations, Walls, Floors, Roofs - Vol 1, 7th Ed.*, Blackwell Science Ltd, Oxford, UK.
- BS EN 197-1 (2011). *Cement. Composition, specifications and conformity criteria for common cement*. British Standard Institute, London, U.K.
- BS EN 933-1(2012). *Tests for geometrical properties of aggregates. Determination of particle size distribution. Sieving method*. British Standard Institute, London, U.K
- BS EN 1097-3 (1998). *Tests for mechanical and physical properties of aggregates. Determination of loose bulk density and voids*. British Standard Institute, London, U.K
- BS EN 1097-5 (2008). *Tests for mechanical and physical properties of aggregates. Determination of the water content by drying in a ventilated oven*, British Standard Institute, London, U.K
- BS EN 1097-6 (2000). *Tests for mechanical and physical properties of aggregates. Determination of particle density and water absorption*. British Standard Institute, London, U.K
- BS EN 12350-2 (2009). *Testing Fresh Concrete – Slump test*, British Standard Institute, London, U.K.
- BS EN 12390-2 (2009). *Testing hardened concrete. Making and curing specimens for strength tests*. British Standard Institute, London, U.K
- BS EN 12390-3 (2009). *Testing hardened concrete, Compressive Strength of Test Specimens*. British Standard Institute, London, U.K.
- BS EN 1008 (2002). *Mixing water for concrete - Specification for sampling, testing and assessing the suitability of water, including water recovered from processes in the concrete industry, as mixing water for concrete*. British Standard Institute, London, UK.
- Deodhar, S. V. (2009). *Civil Engineering Materials, 6th Edition*. Khanna Publishers, Sarak, Delhi India. ISBN 81-7409-163-7.
- Ede, A. N. (2010). Building collapse in Nigeria: the trend of casualties in the last decade (2000 - 2010), *International Journal of Civil and Environmental Engineering*, 10(6), 32-42.
- Gideon, O. B., Ede, A. N., Egwuatu, C., Jolayemi, J., Oluwa, O., & Odewumi, T. (2015). Assessment of compressive strength of concrete produced from different brands of Portland cement, *Civil and Environmental Research*, 7 (8), 31-38. ISSN 2224-5790 (Paper) ISSN 2225-0514 (online)
- Gupta, B. L., & Gupta, A. (2014). *Concrete Technology*, Standard Publishers Distributors, New Delhi, India.
- Li, Z. (2011). *Advanced Concrete Technology*, John Wiley and Sons, Inc., New Jersey USA.
- Neville, A. M., (2010). *Properties of Concrete*. John Wiley and Sons Inc., London, UK.
- Neville, A. M., & Brooks, J. J. (2011). *Concrete Technology 2nd Edition*. Pearson Education Limited, London, UK.
- PD 6682-1:2009+A1:2013, *Aggregates. Aggregates for concrete. Guidance on the use of BS EN 12620*. British Standard Institute, London, U.K.
- Shetty, M. S. (2012), *Concrete Technology, Theory and Practice, Multicolour Illustrative Edition*, S. Chand and Company, New Delhi, India.
- Talbot, A. N., & Richart, F. E. (1923). The Strength of Concrete and its Relation to the Cement, Aggregate and Water, *Engineering Experiment Station, Bulletin 137, University of Illinois*.
- Thandavamoorthy, T. S. (2014). Feasibility of making concrete from soil instead of river sand, *ICI Journal April – June 2014*, 1 - 6.
- Tsado, T. Y. (2013). An investigation into structural strengths of laterized concrete. Extract from, <https://staff.futminna.edu.ng-journal>



Response Surface Optimisation of the Adsorption of Cu (II) from Aqueous Solution by Crab Shell Chitosan

*Babatunde E. O¹, Akolo S. A², Ighalo J. O³ & Kovo A. S⁴

^{1,3}Chemical Engineering Department, University of Ilorin, P. M. B. 1515, Ilorin, Kwara state, Nigeria.

²Prudent Energy and Services Limited, Bulk Petroleum and Gas Terminal Oghareki, Oghara, Delta state, Nigeria.

⁴Chemical Engineering Department, Federal University of Technology, P.M.B. 65, Minna, Niger state, Nigeria

* Corresponding author email: babatunde.eo@unilorin.edu.ng, +2348060265818

ABSTRACT

Adsorption of Cu (II) from aqueous solution by crab-shell derived chitosan was evaluated and optimised by response surface methodology alongside comparison with commercial chitosan. The commercial and locally developed chitosan was found effective in removal of copper (II) ion from aqueous solution and the results of the copper ion percentage removal was 99.57% for locally produced chitosan and 99.80% for commercial chitosan at pH of 6.0. Optimum metal uptake (99.57%) was observed at pH 4.75, 120 minutes equilibration time and dosage of 2 g/50ml. The monolayer adsorption capacity of the commercial and locally developed chitosan was 1.44 mg/g and 1.49 mg/g respectively. The isotherms modelling indicated that the Langmuir isotherm was the best fit. The kinetics for the adsorption of copper, onto chitosan was best described by a pseudo-second-order kinetic model. It has been shown that chitosan are excellent precursors for the removal of copper from aqueous solution and consequently for its use in remediating polluted industrial effluents.

Keywords: Adsorption, Chitosan, Crab shells, heavy metals, Optimisation.

1 INTRODUCTION

Environmental pollution by discharge of industrial waste into water streams is a major problem because of the toxic nature of industrial waste. Among various industrial wastes, heavy metals are of great concern because of their bioaccumulation and non-biodegradable nature (Bailey, Olin, Bricka, & Adrian, 1999). Methods of metal ion removal include filtration, chemical precipitation, adsorption, electrode position and membrane systems or even ion exchange process. Among these methods, adsorption is one of the most economically favourable and a technically easy method (Karthikeyan, Rajgopal, & Miranda, 2005). To remove trace levels of heavy metal ions, adsorption by natural occurring materials is one of the most effective and low cost methods (Bailey et al., 1999). Numerous materials have been studied for use as adsorbent for the removal of copper from aqueous solutions. They include fish scales (Das, Bhowal, & Datta, 2016; Eletta & Ighalo, 2019), cabbage leaves (Kamar, Nechifor, Nechifor, Al-Musawi, & Mohammed, 2017), *Terminalia catappa L.* fruit shell (Hevira, Munaf, & Zein, 2015), tea leaves (Ghosh, Das, &

Sinha, 2015), Pine bark (Cutillas-Barreiro et al., 2014) and many others.

Recently many statistical experimental design methods have been utilized in chemical process optimization (Gratuito, Panyathanmaporn, Chumnanklang, Sirinuntawittaya, & Dutta, 2008). Design of experiments is a very useful tool as it provides statistical models, which help in understanding the interactions among the parameters that have been optimized. Response surface methodology (RSM) is one of the experimental designing methods which can surmount the limitations of conventional methods collectively (Olmez, 2009). Response surface methodology is a combination of mathematical and statistical techniques used to determine the optimum operational conditions of the process or to determine a region that satisfies the operating specifications (Alam, Muyibi, & Toramae, 2007). The main advantage of response surface methodology is the reduced number of experimental trials needed to evaluate multiple parameters and their interactions (Karacan, Ozden, & Karacan, 2007). RSM has also been reportedly used in the optimisation of adsorption process (Garg, Kaur, Sud, & Garg, 2009; Ghosh et al., 2015; Kumar & Phanikumar, 2013; Madala, Mudumala, Vudagandla, &

Abburi, 2015; Mandal, Mondal, Mondal, Mukherjee, & Mondal, 2015; Olmez, 2009). In this study, bio sorption of Cu (II) from aqueous solution by crab-shell derived chitosan was evaluated and optimised by response surface methodology alongside comparison with commercial chitosan.

2 METHODOLOGY

2.1 COLLECTION OF SAMPLE

Crab shell was obtained from Lagos lagoon (Nigeria). The crab was washed with tap water to remove possible foreign materials present (dirt and sands). The commercial chitosan was from Sigma-Aldrich in Germany (purity >99%).

2.2 PREPARATION OF REAGENTS

The major chemicals used during experimental work include Sodium hydroxide (NaOH), sodium hypochlorite (NaClO), copper sulphate pentahydrate ($\text{CuSO}_4 \cdot 5\text{H}_2\text{O}$) and Hydrochloric acid (HCl) and they were all analytical grade (purity >99%). Sodium Hydroxide, hydrochloric and copper sulphate solution of different concentrations was prepared by dissolving calculated quantity of these chemicals in distilled water. The desired concentration of metal ion was freshly prepared from the stock solution. Copper (II) sulphate pentahydrate ($\text{CuSO}_4 \cdot 5\text{H}_2\text{O}$) was used as the source for copper stock solution. The solution was prepared with deionized water; the copper (II) stock solution (1000 mg/L) was made by dissolving 3.916 g of 99% $\text{CuSO}_4 \cdot 5\text{H}_2\text{O}$ in 1L deionized water. Samples of different concentrations of copper (II) are prepared from this stock solution by appropriate dilutions.

2.3 PRODUCTION OF CHITOSAN

Isolation of chitosan from crab shell wastes involves four traditional steps; deproteinisation (DP), demineralization (DM), decolourization (DC), and deacetylation (DA). The wet crab was washed and dried followed by grinding and sieving to a particle size of 750 μm , and then placed in a plastic bottle for storage at ambient temperature until used. Deproteinisation (DP) was then carried out on the crab shells. Four hundred grams of crab shell was placed in a solution of 3.5% NaOH (w/v) for 2 h at 65 °C, solid: solvent (1:10, w/v), then the solid was separated from the liquid and washed with distilled water until absence of colour in the medium which represents the absence of protein. The next step was to demineralise the shells. The deproteinised shell was placed in 1 N HCl for 30 minutes at room temperature, solid: solvent (1:15, w/v). Subsequently, the liquid was decanted and the solid was washed with

distilled water until neutral pH, the remaining was dried at 50 °C for 12 h and the product was chitin. The chitin was decolourized with 0.315% sodium hypochlorite (NaOCl) (w/v) for 5 minutes at room temperature solid: solvent (1:10, w/v) was poured into the vessel containing the solid and the suspension was agitated until the pigmentation of the solid disappeared. The white solid (chitin) was washed and dried at 50 °C for 12 h in the oven. The deacetylation of chitin was carried out by mixing chitin with 50% NaOH for 30 min at 121 °C, solid: solvent (1:10, w/v). The mixture was washed with distilled water several times to remove residual sodium hydroxide, until pH 7 was achieved. The chitosan was dried in an oven at 50 °C for 18 h.

2.4 DESIGN OF EXPERIMENTS

The experimental design for optimization of Cu(II) adsorption was done by applying Response Surface Methodology (RSM), categorical factor of 0 was engaged to optimize the adsorption parameters. The design was composed of three levels (low, medium and high, being coded as (-1, 0 and +1) and a total of 30 runs were carried out to optimize the level of chosen variables. Design Expert (Stat-Ease, Inc., version.7.0.0 Minneapolis, USA) software was used for statistical data analysis. In order to investigate the effect of various independent process parameters such as initial concentration (x_1), pH (x_2), adsorbent dose (x_3) and contact time (x_4) on percentage removal of Cu (II), batch experiments were conducted based on the central composite design (CCD).

2.5 BATCH ADSORPTION STUDIES

Batch adsorption studies were carried out at room temperature using 250 mL conical flasks with 50 mL of the working Cu(II) ion solution of different concentrations ranging from 20 to 30 mg/L on a magnetic stirrer at 300 rpm in view of the results from previous work (Liu & Cheng, 2009). The influence of pH (3.0–6.0) (The pH of each solution was adjusted by adding either 0.1 M of NaOH or HCL solution.), Cu(II) concentration (20-30 mgL^{-1}), contact time (45-120 min), adsorbent dose (1.0 -2.0 g/50 mL) were evaluated during the present study. Samples were collected from the flasks at predetermined time intervals for analysing the residual Cu(II) concentration in the solution. The adsorbate was removed by filtration through Whatmann filter paper. The residual concentration of Cu (II) was determined by atomic absorption spectroscopy (AAS). The experiments were performed in duplicates and the amount of Cu (II) ions adsorbed in milligram per gram was determined by using the following mass balance “Equation (1)”

$$q_e = \frac{(c_0 - c_e)V}{m} \quad (1)$$

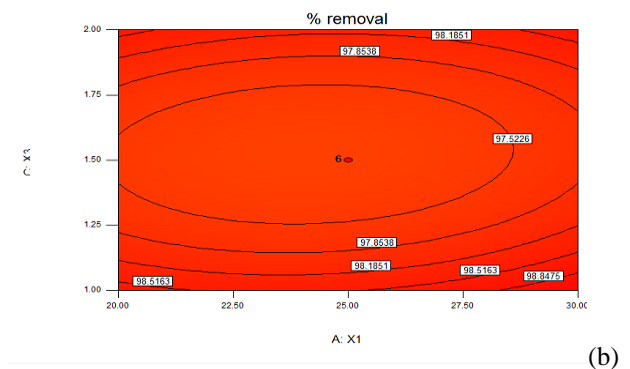
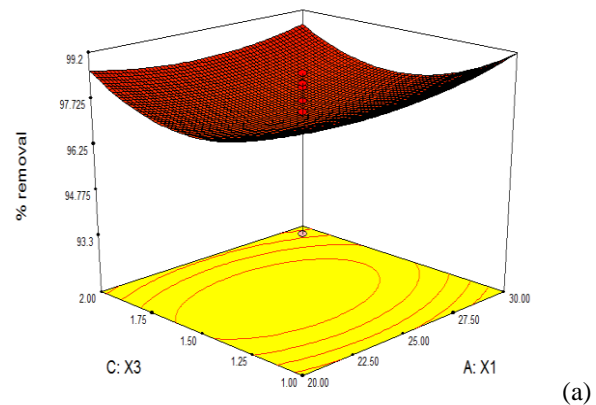
Where C_o and C_e are Cu (II) concentrations (mg/L) before and after adsorption respectively, V is the volume of adsorbate in litre and m is the weight of the adsorbent in grams. The percentage removal of Cu (II) ions was calculated from the following “Equation (2)”

$$(\%) \text{ Removal} = \frac{(C_o - C_e)}{C_o} \times 100 \quad (2)$$

3 RESULTS AND DISCUSSION

3.1 RESPONSE SURFACE PLOTS OF ADSORPTION FACTORS

The ultimate objective of the design used in this study was to find out the significant effects of the process parameters viz., initial concentration, pH, adsorbent dose and contact time on the removal efficiency of Cu (II). The response surface and contour plots were used to investigate the effect of all the factors on the responses. The 3D response surface plots are useful in investigating both the main and interaction effects of the factors. These figures also show the estimated Y parameter as a function of the normalized factor variables, the height of the surface represents the value of Y. A steep slope or curvature in a factor shows that the response is sensitive to that factor. A relatively flat line shows insensitivity to change in that particular factor great influence on the removal of Cu(II), initial metal concentration has less effect on the responses compared to other factors.



Figures 1(a-b): Interaction between adsorbent dose (x3) and initial concentration (x1) on Cu (II) removal, a-response plot, b-contour plot

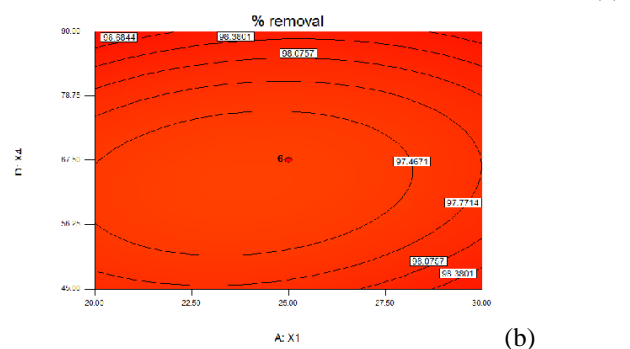
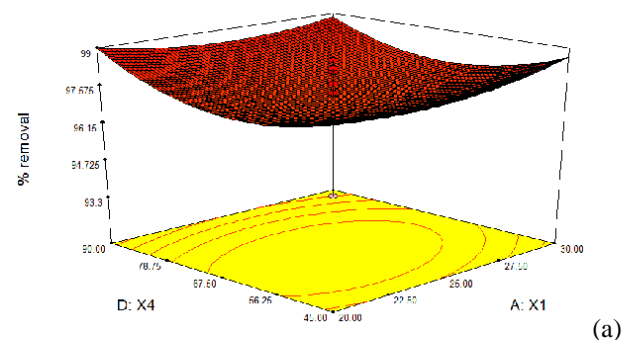
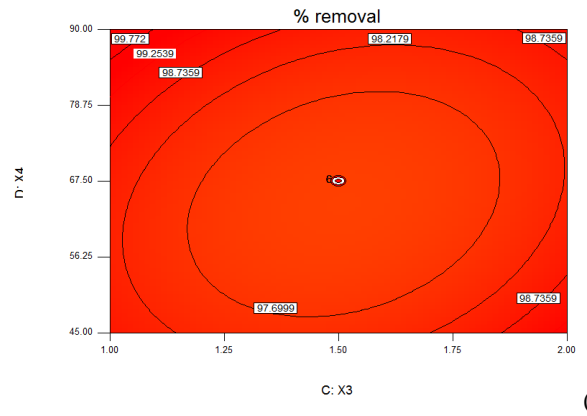
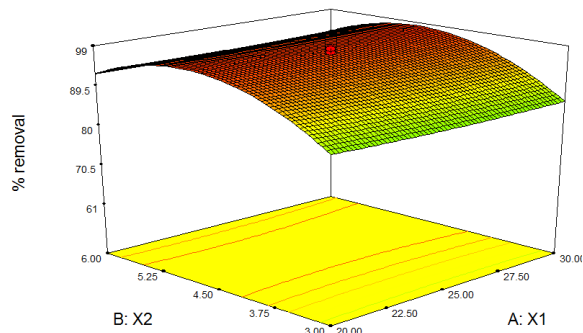
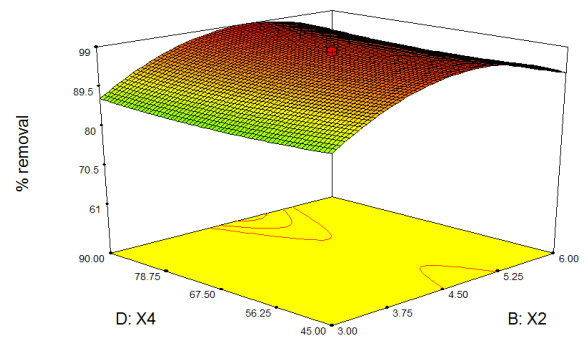
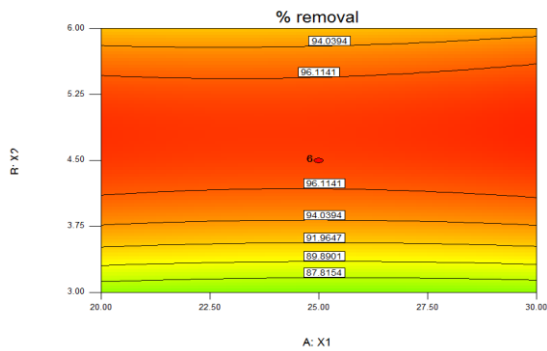


Figure 2(a-b): Interaction between contact time (x4) and initial concentration (x1) on Cu (II) removal, a-response plot, b-contour plot.



(a)

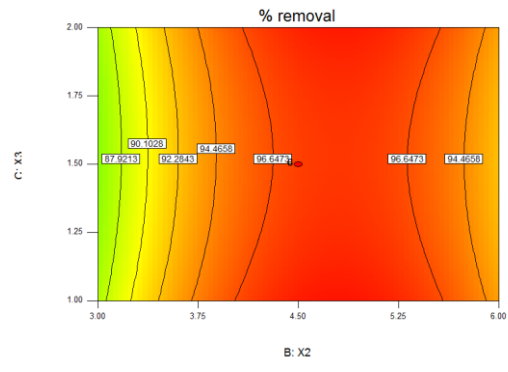
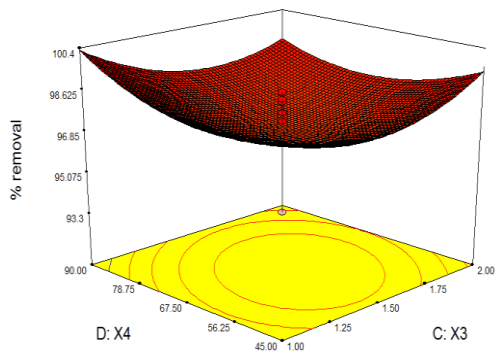
Figure 4(a-b): Interaction between contact time (x4) and adsorbent dose (x3) on Cu (II) removal, a-response plot, b-contour plot.



(b)

(a)

Figure 3(a-b): Interaction between pH (x2) and initial concentration (x1) on Cu (II) removal, a-response plot, b-contour plot



(a)

Figure 5(a-b): Interaction between contact time (x4) and pH (x3) on Cu (II) removal, a-response plot, b-contour plot.

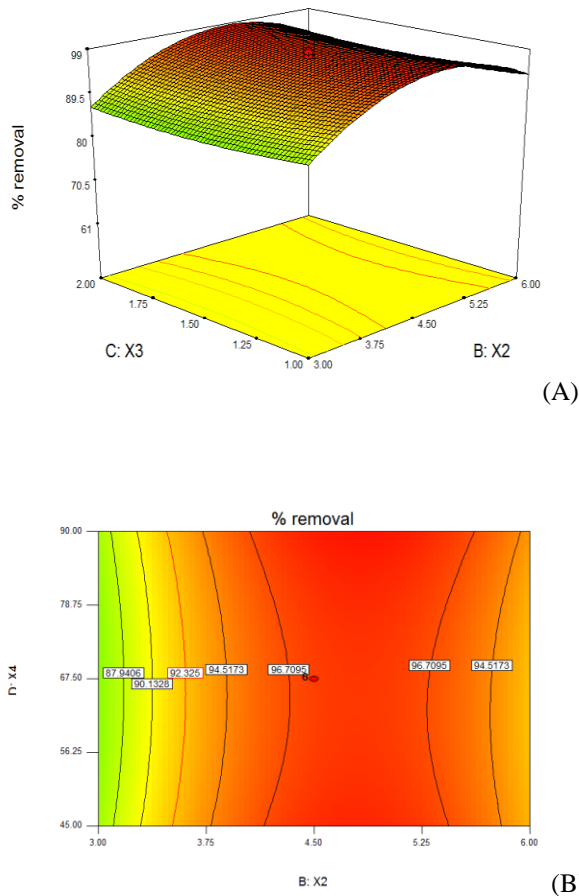


Figure 6(A-B): Interaction between pH (x2) and adsorbent dose (x3) on Cu (II) removal, a-response plot, b-contour plot.

The response and contour plots in figures 1 to 6 elucidate the relationship between the factors and how they affect the removal of copper from aqueous solutions. Figures 1 reveals that copper removal increases with increasing adsorbent dose and initial copper concentration does not have any effect on this trend. Figures 2 also reveal that copper removal increases with increasing time and initial copper concentration does not have any effect on this trend. Figure 3 reveals that copper uptake is optimum at about pH 4.75. The relationship of pH and metal uptake is not affected by initial copper concentration. Figures 4 reveals that metal uptake is maximum at the highest values of equilibration time and adsorbent dosage respectively. Figure 5 and 6 reveals that contact time and adsorbent dosage does not have any effect on the relationship between pH and metal uptake respectively. It can be surmised that metal uptake was maximum (99%) at

pH 4.75, 120 minutes equilibration time and dosage of 2 g/50ml.

3.2 EFFECT OF CONTACT TIME ON ADSORPTION OF COPPER ION

The relationship between contact time and the percentage removal of copper ion from solution using commercial and locally produced chitosan (pH = 6, Mass of chitosan = 1 g, initial concentration = 30 mg/L, and Agitation Speed 300 rpm) are shown in figure 7.

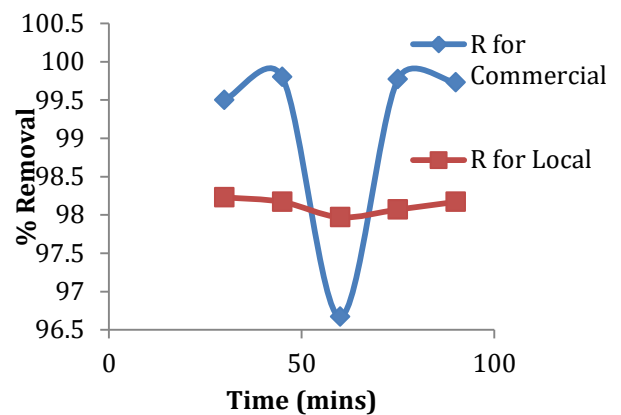


Figure 7: Effect of contact time on both commercial and locally developed chitosan

The contact time represents the time necessary for the adsorption process to reach equilibrium. For each sample the adsorption capacity was studied as a function of time. During short contact times, adsorption was fast due to the availability of plenty of active sites on the adsorbent surface. As the active sites were occupied, adsorption slowed down and finally an equilibrium stage was reached. The adsorption reached equilibrium at short contact time which was due to the availability of active sites on the adsorbent surface which was indicated by the fiber metric image measurements and pore histogram in figures 8 (a-b) and 9 (a-b). As the active sites were occupied, adsorption slowed down and finally an equilibrium stage was reached. It is evident that percentage metal ion removal reached equilibrium at within 40 minutes for Cu (II) for both commercial and locally produced chitosan from crab shell after which further increase in time did not bring about any further improvement.

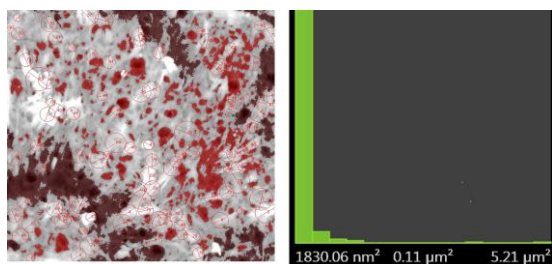


Figure 8 (a-b): Fibermetric Image and Pore Histogram of local developed chitosan

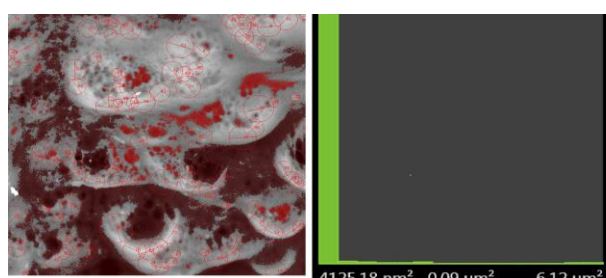


Figure 9 (a-b): Fibermetric Image and Pore Histogram of commercial chitosan

3.3 EQUILIBRIUM ISOTHERM MODELLING

Equilibrium isotherm are essential for describing the mechanism of adsorption, the equilibrium data of Cu^{2+} ion were subjected to five different adsorption isotherm models: Langmuir, Elovich, Temkin Freundlich and Dubinin-Radushkevich. The model constants are summarized in Table 1.

TABLE 1: Equilibrium isotherms parameters for Cu^{2+} adsorption on chitosan

Parameters	Locally developed chitosan	Commercial chitosan
Langmuir		
a(mg/g)	1.4435	1.4900
b (L/mg)	92.491	3728.56
R	0.000361	0.0000
R ²	0.9999	0.9999
Freundlich		
1/n	0.008	0.003
K _F	1.45	1.48
R ²	0.998	0.985
Temkin		
A _T (L/g)	4.297	4.41
b _T (×10 ³)	99.58	500.52

B	0.02488	0.00495
R ²	0.810	0.983
Elovich		
Q _m (mg/g)	0.0301	0.00502
K _F (L/mg)	0.0000	0.0000
R ²	0.9006	0.9915
Dubinin-Radushkevich		
K _{ad} (mol ² /kJ ²)	2.290 × 10 ⁻⁹	-
E (kJ/mol)	0.59	-
R ²	0.9901	-

The Langmuir and Freundlich isotherm models predict the adsorption data better than Elovich and Temkin because high correlation coefficients ($R^2 > 0.99$) were obtained at a higher confidence level. The Freundlich constants K_F and $1/n$ for Cu^{2+} were found to be 1.49 mg/g and 0.003 for commercial chitosan and 1.45 mg/g and 0.008 for locally developed chitosan respectively. The values of $1/n$ are between 0 than 1 for both the adsorbents, which indicate normal adsorption. The low $1/n$ suggested that any large change in the initial concentration Cu^{2+} ions would not result in a change in the amount of Cu^{2+} adsorbed by the chitosan. According to the values of the correlation coefficient (R^2), the best-fit isotherm model was the Langmuir isotherm model follow by the Freundlich model. The Elovich modelling of the experimental data also indicate chemisorption took place. High correlation coefficients were observed when the data were fitted to this model especially for the commercial chitosan and this also suggested that the adsorption of Cu^{2+} occurred by chemisorption. The Temkin model had the lowest value of correlation coefficient, which suggested that this model was not the best description of Cu^{2+} ion adsorption onto locally developed and commercial chitosan. However, the model did indicate that Cu^{2+} is an exothermic process, since $B > 0$ for both commercial and locally developed adsorbents. The numerical value of mean free energy E calculated from Dubinin–Radushkevich (D-R) isotherm model was 0.59 kJ/mol. If the value of E lies between 8 – 16 kJ/mol, the process is said to follow chemical ion exchange while $E < 8$ kJ/mol then the process follows physical adsorption (Horsfall, Spiff, & Ai, 2004). In the current study the biosorption process of Cu (II) onto locally developed chitosan follows physical adsorption.

3.4 ADSORPTION KINETICS

The data on the dependence of adsorption capacity on time were used for kinetic analysis. The results of the fitted data show that pseudo-second order kinetics model yielded linear plots compared to the pseudo-first-order reaction model, which is significantly scattered (non-linear).

Table 2. Kinetic parameters for Cu²⁺ adsorption on chitosan

Parameters	Locally developed chitosan	Commercial chitosan
Pseudo first order		
q _e cal (mg/g)	1.042	1.096
q _e exp (mg/g)	1.4735	1.4965
k ₁ (min ⁻¹)	0.085	0.104
R ²	0.0323	0.4965
Pseudo second order		
q _e cal. (mg/g)	1.4728	1.4993
q _e exp (mg/g)	1.4735	1.4965
k ₂ (g/mgmin)	66.02	10.35
R ²	0.999	0.999

Also the theoretical (calculated) value of q_e of, pseudo-second-order reaction model, are closer to the experimental value of q_e for instance, the calculated value of Cu²⁺ onto local chitosan was 1.4728 mgg⁻¹ which is in closed agreement with the experimental value of 1.4935 mgg⁻¹ compared to Cu²⁺ of pseudo-first-order reaction model, with calculated valued of 0.1042 mgg⁻¹ which differ greatly from the experimental value of 1.4735 mgg⁻¹. Also the calculated value of Cu²⁺ onto commercial chitosan was 1.4993 mgg⁻¹ which is in closed agreement with the experimental value of 1.4965 mgg⁻¹ compared to Cu²⁺ of pseudo-first-order reaction model, with calculated valued of 1.096 mgg⁻¹ which differ greatly from the experimental value of 1.4735 mgg⁻¹ these fact suggest that the adsorption of Cu²⁺ by commercial and locally produced chitosan from crab shells follows the pseudo-second-order reaction model which rely on the assumption that chemisorption is the rate-limiting step. In chemisorption the heavy metals stick to the adsorbent surface by forming a chemical usually covalent bond and tend to find sites that maximize their coordination with the surface (Yusuff, Popoola & Babatunde, 2019).

5 CONCLUSION

A detailed batch experimental study was carried out for the removal of copper (II) from aqueous solution using commercial and locally developed chitosan. The commercial and locally developed chitosan was found effective in removal of copper (II) ion from aqueous solution and the results of the copper ion percentage removal was 99.57% for locally produced chitosan and 99.80 for commercial chitosan at pH of 6.0. Optimum metal uptake (99.57%) was observed at pH 4.75, 120 minutes equilibration time and dosage of 2g/50ml. The results obtained from isotherms adsorption studies of Cu (II) ions by being analysed in five adsorption models, namely, Langmuir, Freundlich, Elovich, Temkin and

Dubinnin-Radushkevich. The isotherms equation indicated to be best fitted to the Langmuir isotherm equation under the concentration range studied. The kinetics for the adsorption of copper, onto chitosan was best described by a pseudo-second-order kinetic model.

ACKNOWLEDGEMENT

The authors would like to acknowledge the Department of Chemical Engineering, Federal University of Technology Minna, Nigeria for their immense support during execution of the work.

Abbreviations

- C_o initial concentration of metal ion in the liquid phase (mg/L)
- C_e equilibrium concentration of metal ion in the liquid phase (mg/L)
- K₁ rate constant of pseudo-first order adsorption (min⁻¹)
- k₂ rate constant of pseudo-second order adsorption (g·mg⁻¹·min⁻¹)
- K_F Freundlich isotherm constant is in (mg/g)
- b Langmuir isotherm constant (L/mg)
- m amount of chitosan membrane (g)
- n number of experimental data
- q adsorption amount (mg/g)
- q_e adsorption amount at equilibrium (pseudo-second order equation constant) (mg/g)
- a maximum adsorption capacity (Langmuir isotherm constant) (mg/g)
- q_t adsorption amount at time t (mg/g)
- t time (min)
- V volume of the solution (L)
- K_E is the Elovich equilibrium constant (L/mg)
- K is the Dubinin-Radushkevich constant (kJ²/mol)

REFERENCES

- Alam, M. Z., Muyibi, S. A., & Toramae, J. (2007). Statistical optimization of adsorption processes for removal of 2,4-dichlorophenol by activated carbon derived from oil palm empty fruit bunches. *Journal of Environmental Science and Health, Part B*, 19, 674–677.
- Bailey, S. E., Olin, T. J., Bricka, R. M., & Adrian, D. D. (1999). A Review Of Potentially Low-Cost Sorbents For Heavy Metals. *Journal of Water. Resources*, 33(11), 2469–2479.
- Cutillas-Barreiro, L., Ansias-Manso, L., Fernandez-Calvino, D., Arias-Estevéz, M., Novoa-Munoz, J. C., Fernandez-Sanjurjo, M. J., Núñez-Delgado, A. (2014). Pine bark as bio-adsorbent for Cd, Cu,

- Ni, Pb and Zn: Batch-type and stirred flow chamber experiments. *Journal of environmental management*, 144, 258-264.
- Das, A., Bhowal, A., & Datta, S. (2016). Biomass characterisation and adsorption mechanism of Cu (II) biosorption onto fish (*Catla catla*) scales. *International Journal of Environmental Engineering*, 8(1), 81-94.
- Eletta, A. A. O., & Ighalo, J. O. (2019). A Review of fish scales as a Source of Biosorbent for the Removal of Pollutants from Industrial Effluents. *Journal of Research Information in Civil Engineering*, 16(1), 2479-2510.
doi:10.13140/RG.2.2.20511.61604
- Garg, U. K., Kaur, M., Sud, D., & Garg, V. (2009). Removal of hexavalent chromium from aqueous solution by adsorption on treated sugarcane bagasse using response surface methodological approach. *Desalination*, 249(2), 475-479.
- Ghosh, A., Das, P., & Sinha, K. (2015). Modeling of biosorption of Cu (II) by alkali-modified spent tea leaves using response surface methodology (RSM) and artificial neural network (ANN). *Applied Water Science*, 5(2), 191-199.
- Gratisito, M. K. B., Panyathanmaporn, T., Chumnanklang, R. A., Sirinuntawittaya, N., & Dutta, A. (2008). Production of activated carbon from coconut shell: Optimization using response surface methodology. *Bioresources Technology*, 999, 4887-4895.
- Hevira, L., Munaf, E., & Zein, R. (2015). The use of *Terminalia catappa* L. fruit shell as biosorbent for the removal of Pb(II), Cd(II) and Cu(II) ion in liquid waste. *Journal of Chemical and Pharmaceutical Research*, 7(10), 78-89.
- Horsfall, M. J., Spiff, A. I., & Ai, A. A. (2004). Studies on the influence of mercaptoacetic acid (MAA) modification of cassava (*manihot sculenta* cranz) waste from biomass on the adsorption of Cu²⁺ and Cd²⁺ from aqueous solution. *Bulletin of the Korean chemical society*, 25(7), 969-976.
- Kamar, F. H., Nechifor, A. C., Nechifor, G., Al-Musawi, T. J., & Mohammed, A. H. (2017). Aqueous Phase Biosorption of Pb (II), Cu (II), and Cd (II) onto Cabbage Leaves Powder. *International Journal of Chemical Reactor Engineering*, 15(2).
- Karacan, F., Ozden, U., & Karacan, S. (2007). Optimization of manufacturing conditions for activated carbon from Turkish lignite by chemical activation using response surface methodology. *Applied Thermal Engineering*, 27, 1212-1218.
- Karthikeyan, T., Rajgopal, S., & Miranda, L. R. (2005). Chromium (VI) adsorption from aqueous solution by Hevea brasiliensis sawdust activated carbon. *Journal of Hazardous Material*, 124(3), 192-199.
- Kumar, M. S., & Phanikumar, B. (2013). Response surface modelling of Cr⁶⁺ adsorption from aqueous solution by neem bark powder: Box- Behnken experimental approach. *Environmental Science and Pollution Research*, 20(3), 1327-1343.
- Liu, X. L., & Cheng, Z. H. (2009). Removal of copper by a modified chitosan adsorptive membrane. *Frontiers of Chemical Engineering China*, 3, 102-106.
- Madala, S., Mudumala, V. N. R., Vudagandla, S., & Abburi, K. (2015). Modified leaf biomass for Pb (II) removal from aqueous solution: Application of response surface methodology. *Ecological Engineering*, 83, 218-226.
- Mandal, N., Mondal, S., Mondal, A., Mukherjee, K., & Mondal, B. (2015). Response surface modeling of Cu(II) removal from wastewater using fish scale-derived hydroxyapatite: application of Box- Behnken experimental design. *Desalination and Water Treatment*, 1-14.
- Olmez, T. (2009). The optimization of Cr (VI) reduction and removal by electrocoagulation using response surface methodology. *Journal of Hazardous Material*, 162, 1371-1378.
- Yusuff, A.S., Popoola, L.T. & Babatunde, E.O. (2019): Adsorption of cadmium ion from aqueous solutions by copper-based metal organic framework: equilibrium modeling and kinetic studies. *Applied Water Science* 9: 106. Retrieved from <http://link.springer.com/article/10.1007/s13201-019-0991-z>

THE LINEAR TRANSFORMATION OF A BLOCK HYBRID RUNGE-KUTTA TYPE METHOD FOR DIRECT INTEGRATION OF FIRST AND SECOND ORDER INITIAL VALUE PROBLEM

*Muhammad, R¹, Yahaya, Y.A.², & Abdulkareem, A.S.³

¹Mathematics Department, Federal University of Technology, PMB 65 Minna Niger State, Nigeria

²Mathematics Department, Federal University of Technology, PMB 65 Minna Niger State, Nigeria

³Chemical Engineering Department, Federal University of Technology, PMB 65 Minna Niger State, Nigeria

*Corresponding author email: r.muhd@futminna.edu.ng, +2348036128483

ABSTRACT

The Algebraic structure of a block hybrid Runge-Kutta Type Method (BHRKTM) for the solution of initial value problems was analysed. The coefficients of the first order Runge-Kutta Type Method (RKT) of the Butcher table was applied to prove to the second order RKT. The method of linear transformation and monomorphism was employed to substantiate the uniform order and error constant for the first order BHRKTM and the corresponding extended second order BHRKTM. Two equations evolved that satisfied the Runge-Kutta consistency conditions of second and first order respectively. The Algebraic structure was carefully retained during the transformation.

Keywords: Implicit, Initial Value Problems, Linear Transformation, Monomorphism., Runge-Kutta Type

1 INTRODUCTION

A linear transformation (Homomorphism) can be defined as when a function T between two vector spaces $T:V \rightarrow W$ preserves the operations of addition if v_1 and $v_2 \in V$ then

$$T(v_1 + v_2) = T(v_1) + T(v_2) \quad (1)$$

And scalar multiplication if $v \in V$ and $r \in R$, then

$$T(r \cdot v) = rT(v) \quad (2)$$

Agam (2013).

A homomorphism that is one to one or a mono is called a monomorphism.

The monomorphism Transformation preserves its algebraic structure and the order of the Domain into its Range.

Butcher and Hojjati (2005) laid another strong foundation by extending the general linear method (GLM) to the case in which second derivative as well as first derivative can be calculated. They constructed methods of third and fourth order which are A-stable, possess the Runge-Kutta stability property and have a diagonally implicit structure for efficient implementation to solve any initial value problem of ordinary differential equation. Okunuga, Sofoluwe, Ehigie and Akanbi (2012) presented a direct integration of second order ordinary differential equations using only Explicit Runge-Kutta Nystrom (RKN) method with higher derivative. They derived and tested various numerical schemes on standard problems. Due to the limitations of Explicit Runge-Kutta (ERK) in handling stiff problems,

the extension to higher order Explicit Runge-Kutta Nystrom (RKN) was considered and results obtained showed an improvement over conventional Explicit Runge-Kutta schemes. The Implicit Runge-Kutta scheme was however not considered. Yahaya and Adegboye (2013) derived an implicit 6-stage block Runge-Kutta Type Method for direct integration of second order (special or general), third order (special or general) as well as first order initial value and boundary value problems. The theory of Nystrom was adopted in the reformulation of the methods. The convergence and stability analysis of the method were conducted and the region of absolute stability plotted. The method was A-stable, possessed the Runge-Kutta stability property, had an implicit structure for efficient implementation and produced at the same time approximation to the solution of both linear and non linear initial value problems.

2 METHODOLOGY

Let T be a linear transformation which is continuously differentiable on a set of ordered three- tuple vector $\in \mathbb{R}^3$ as follows

$$V_i = (x + c_i h, y + \sum_{j=1}^s a_{ij} T(v_j), y' + \sum_{j=1}^s a_{ij} T'(v_j)) \in \mathbb{R}^3 \quad (3)$$

$$T(V_i) = h(y' + \sum_{j=1}^s a_{ij} T'(v_j)) \quad (4)$$

and

$$T'(v_i) = hf(x + c_i h, y + \sum_{j=1}^s a_{ij} T(v_j), y' + \sum_{j=1}^s a_{ij} T'(v_j)) = hm_i \quad (5)$$

That is,

$$m_i = f(x + c_i h, y + \sum_{j=1}^s a_{ij} T(v_j), y' + \sum_{j=1}^s a_{ij} T'(v_j)) \quad (6)$$

Then the Transformation $T: \mathbb{R}^3 \rightarrow \mathbb{R}$ is a well defined monomorphism:

Proof

Let $u, v \in \mathbb{R}$ defined by

$$U = (x + c_1 h, y_1 + \sum_{j=1}^s a_{1j} T(u_j), y_1' + \sum_{j=1}^s a_{1j} T'(u_j)) \quad (7)$$

$$V = (x + c_2 h, y_2 + \sum_{j=1}^s a_{2j} T(v_j), y_2' + \sum_{j=1}^s a_{2j} T'(v_j)) \quad (8)$$

$$T(U + V) = h(y_1' + y_2' + \sum_{j=1}^s a_{1j} T'(u_j) + T'(v_j)) \quad (9)$$

By the definition of T on \mathbb{R}^3

$$h(y_1' + \sum_{j=1}^s a_{1j} T'(u_j)) + h(y_2' + \sum_{j=1}^s a_{2j} T'(v_j)) = T(U + V) \quad (10)$$

$$T(U + V) = T(U) + T(V) \quad (11)$$

$$T(k \cdot U) = k \cdot T(U) \quad (12)$$

Hence T is a homomorphism

Now we show that T is 1 - 1

Let $u, v \in \mathbb{R}^3$ with

$$T(u) = T(v) \quad (13)$$

By definition of T, we have

$$h(y_1' + \sum_{j=1}^s a_{1j} T'(u_j)) = h(y_2' + \sum_{j=1}^s a_{2j} T'(v_j)) \quad (14)$$

Since

$$T(u) = T(v) \text{ then } T(u_j) = T(v_j) \text{ and } T'(u_j) = T'(v_j) \quad (15)$$

$$y_1 = y_2 \text{ and } x_1 + c_1 h = x_2 + c_1 h$$

$$\text{that is } x_1 = x_2 \quad (16)$$

$$\text{Hence } U = V \quad (17)$$

Thus T is 1 - 1 \Leftrightarrow a monomorphism from $\mathbb{R}^3 \rightarrow \mathbb{R}$

Remark: The necessity for the above proposition is to ensure that the algebraic structure and the order do not change during the transformation.

2.1 FIGURES AND TABLES

Consider the Butcher Table 1 and Table 2

Table I: Butcher Table for K=2

0	0	0	0	0
$\frac{1}{2}$	0	$\frac{8}{9}$	$-\frac{11}{24}$	$\frac{5}{72}$
2	0	$\frac{8}{9}$	$\frac{2}{3}$	$\frac{4}{9}$
1	0	$\frac{10}{9}$	$-\frac{1}{6}$	$\frac{1}{18}$
	0	$\frac{10}{9}$	$-\frac{1}{6}$	$\frac{1}{18}$

Table II: Butcher Table for second order for K=2

0	0	0	0	0	0	0	0	
$\frac{1}{2}$	0	$\frac{8}{9}$	$-\frac{11}{24}$	$\frac{5}{72}$	0	$\frac{37}{108}$	$-\frac{41}{144}$	$\frac{29}{432}$
2	0	$\frac{8}{9}$	$\frac{2}{3}$	$\frac{4}{9}$	0	$\frac{52}{57}$	$-\frac{2}{9}$	$\frac{8}{27}$
1	0	$\frac{10}{9}$	$-\frac{1}{6}$	$\frac{1}{18}$	0	$\frac{23}{27}$	$-\frac{2}{9}$	$\frac{5}{54}$
	0	$\frac{10}{9}$	$-\frac{1}{6}$	$\frac{1}{18}$	0	$\frac{23}{27}$	$-\frac{2}{9}$	$\frac{5}{54}$

3 RESULTS AND DISCUSSION

The table satisfies the Runge-Kutta conditions for solution of first order ode since

$$(i) \sum_{j=1}^s a_{ij} = c_i \quad (18)$$

$$(ii) \sum_{j=1}^s b_j = 1 \quad (19)$$

We consider the general second order differential equation in the form

$$y'' = f(x, y, y'), y(x_0) = y_0, y'(x_0) = y_0' \quad (20)$$

$$y'' = f(v), \quad v = (x, y, y') \quad (21)$$

$$T(V_i) = T(x + c_i h, y + \sum_{j=1}^s a_{ij} T(V_j), y' + \sum_{j=1}^s a_{ij} T'(V_j)) \quad (22)$$

$$= h(y' + \sum_{j=1}^s a_{ij} T'(V_j)) = h(y' + \sum_{j=1}^s a_{ij} hm_j) \quad (23)$$

$$T'(V_j) = hm_j \quad (24)$$

$$T(V_1) = 0 \quad (25)$$

$$T(V_2) = h(y' + \frac{8}{9}hm_2 - \frac{11}{24}hm_3 + \frac{5}{72}hm_4) \quad (26)$$

$$T(V_3) = h(y' + \frac{10}{9}hm_2 - \frac{1}{6}hm_3 + \frac{1}{18}hm_4) \quad (27)$$

$$T(V_4) = h(y' + \frac{8}{9}hm_2 + \frac{2}{3}hm_3 + \frac{4}{9}hm_4) \quad (28)$$

$$m_j = T'(V_j) = f(x + c_i h, y + \sum_{j=1}^s a_{ij} T(V_j), y' + \sum_{j=1}^s a_{ij} T'(V_j)) \quad (29)$$

$$m_1 = 0 \quad (30)$$

$$m_2 = f(x + \frac{1}{2}h; y + \frac{1}{2}hy' + \frac{37}{108}h^2m_2 - \frac{41}{144}h^2m_3 + \frac{29}{432}h^2m_4; y' + \frac{8}{9}hm_2 - \frac{11}{24}hm_3 + \frac{5}{72}hm_4) \quad (31)$$

$$m_3 = f(x + h; y + hy' + \frac{23}{27}h^2m_2 - \frac{4}{9}h^2m_3 + \frac{5}{54}h^2m_4; y' + \frac{10}{9}hm_2 - \frac{1}{6}hm_3 + \frac{1}{18}hm_4) \quad (32)$$

$$m_4 = f(x + 2h; y + 2hy' + \frac{52}{27}h^2m_2 - \frac{2}{9}h^2m_3 + \frac{8}{27}h^2m_4; y' + \frac{8}{9}hm_2 + \frac{2}{3}hm_3 + \frac{4}{9}hm_4) \quad (33)$$

The direct method for solving $y'' = f(x, y, y')$ is now

$$y_{n+1} = y_n + b_1T(V_1) + b_2T(V_2) + b_3T(V_3) + b_4T(V_4) \quad (34)$$

$$y_{n+1} = y_n + hy'_n + \frac{h^2}{54}(46m_2 - 24m_3 + 5m_4) \quad (35)$$

$$y'_{n+1} = y'_n + b_1T'(V_1) + b_2T'(V_2) + b_3T'(V_3) + b_4T'(V_4) \quad (36)$$

$$y'_{n+1} = y'_n + 0hm_1 + \frac{10}{9}hm_2 - \frac{1}{6}hm_3 + \frac{1}{18}hm_4 \quad (37)$$

$$y'_{n+1} = y'_n + \frac{h}{18}(20m_2 - 3m_3 + m_4) \quad (38)$$

The coefficients of the first order Runge-Kutta Type Method (RKT) of the Butcher table was applied to prove to the second order RKT. Equations (35) and (38) satisfied the Runge-Kutta consistency conditions of second and first order respectively. This further shows that it is a monomorphism.

4 CONCLUSION

This research work established the reason for the uniform order and error constant of the first order Runge-Kutta type method and the extended second order method. And also why the Linear transformation and the order of the two methods was preserved and not changed during the transformation.

5 REFERENCES

Adegboye, Z.A (2013), Construction and implementation of some reformulated block implicit linear multistep methods into Runge-Kutta type method for initial value problems of general second and third order

ordinary differential equations. Unpublished doctoral dissertation, Nigerian Defence Academy, Kaduna.

Agam, A.S (2012), A sixth order multiply implicit Runge-Kutta method for the solution of first and second order ordinary differential equations. Unpublished doctoral dissertation, Nigerian Defence Academy, Kaduna .

Butcher, J.C (2008),*Numerical methods for ordinary differential equations*. John Wiley & Sons. The Atrium, Southern Gate,Chichester, England.

Butcher, J.C & Hojjati, G. (2005). Second derivative methods with Runge-Kutta stability. *Numerical Algorithms*,40, 415-429.

Chollom J. P., Olatunbosun I.O, & Omagu S. (2012). A class of A-stable block explicit methods for the solutions of ordinary differential equations. *Research Journal of Mathematics and Statistics*,4(2),52-56.

Kendall, E. A (1989). *An introduction to numerical analysis*, (2nd ed), John Wiley & Sons. University of Iowa, Singapore 367.

Okunuga, S.A, Sofulowe, A.B, Ehigie, J.O, & Akanbi, M.A. (2012). Fifth order 2-stage explicit runge kutta nystrom (erkn) method for the direct integration of second order ode. *Scientific Research and Essays*.7(2), 134-144.

Yahaya Y.A. and Adegboye Z.A. (2013). Derivation of an implicit six-stage block Runge- Kutta type method for direct integration of boundary value problems in second order ode using the quade type multistep method. *Abacus*.40(2), 123-132.

Yahaya, Y.A. & Ajibade, M.T. (2012). A reformulation of a two-step hybrid linear multistep method (Imm) into a 3-stage Runge-KuttaType (RKT) method for solution of ordinary differential equation. *Book of Readings of the 4th Annual National Conference of the School of Science and Science Education, Federal University of Technology, Minna, Nigeria.*, 2(4), 193-198.

Yahaya, Y.A. & Badmus, A.M. (2009). A class of collocation methods for general second order ordinary differential equations. *African Journal of Mathematics and Computer Science Research* 2(4), 69-72.



Groundwater Potential Mapping in Bosso Local Government Area, Niger State, Nigeria

Abubakar, U.B^{1*} and Muhammed, M.¹

¹Department of Geography, Federal University of Technology, PMB 65 Minna Niger State, Nigeria.

*Corresponding author email: usmanaabosso@yahoo.com, +2347038310737

ABSTRACT

This study assessed groundwater potential zones in Bosso Local Government Area, Niger State. SRTM dataset was used to derive DEM, Slope, drainage network, drainage density network, convergence index and groundwater potential zones using hydrological tools and weighted overlay analysis in the ARCGIS environment. Results revealed that, groundwater potential zones were classified into three classes as High, moderate, and low zones which covered 128.54km² (8.10%), 1315.27km² (82.83%), and 144.06km² (9.07%) respectively. This groundwater potential information will be useful for effective identification of suitable locations for extraction of water. Furthermore, it is felt that the present methodology can be used as a guideline for further research.

Keywords: *Groundwater potential zones, DEM, Remote sensing and GIS*

1 INTRODUCTION

Ground water is contained in underground rocks, which contain and transmit water in economical rate generally referred to as aquifers (Hussein *et al.*, 2016). Groundwater accounts for 26% of global renewable fresh water resources. Salt water (mainly in oceans) represents about 97.2% of the global water resources with only 2.8% available as fresh water. Surface water represents about 2.2% out of the 2.8% and 0.6% as groundwater. The problem is not only to locate the groundwater, as it is often imagined, but the engineer's problem usually is to find water at such a depth, in such quantities, and of such quality that can be economically utilized. Groundwater is a term used to denote all the waters found beneath the ground surface. Groundwater aquifers are not just a source of water supply, but also a vast storage facility providing great management flexibility at relatively affordable costs (Elbeih, 2015). The amount and distribution of groundwater is a function of the amount of open space and the special extent of these rocks. The behavior of these rocks in turn is function of their formation and geological processes that shaped their status. Conventional groundwater exploration require hydro-geologic investigation to study the lithology, stratigraphy and structural aspects of a region using geologic methods to understand the factors that regulate the amount, circulation and quality of groundwater (Elbeih, 2015). These studies deliver results of various type and quality based on the scale of the study. In recent years, relatively cheap availability of remotely sensed data of higher spatial and spectral resolution and increasing availability image processing algorithms and GIS technology has enabled better

efficiency in groundwater resource potential exploration (Mohamed, 2014).

Groundwater (hydrogeological) mapping is one of the main tools for systematic and controlled development and planning of groundwater resources. These maps are used by engineers, planners and decision makers in order to allocate, develop and manage groundwater within a national water policy. Hydrogeological maps present hydrogeological data in a map form. A hydrogeological map shows the geographical distribution of aquifers, and their topographical, geological, hydrographical, hydrological and hydro chemical features. Presentation of these data in the form of maps permits the rapid evaluation of a certain area. Accordingly, hydrogeological maps assist in determining areas needing special protection (Dar *et al.*, 2012).

Many studies have revealed that groundwater potential is related with many factors, such as geological features, terrain features, hydrology features, etc. Digital Elevation Model (DEM) is the digital representations of the topography, the technological advances provided by GIS and the increasing availability and quality of DEMs have greatly expanded the potential of DEMs to applications in many fields (Tarun, 2014). Among those factors related to groundwater potential mapping, most of the information has been proved can be extracted from DEM data, and this made extracting relevant features from DEM for groundwater potential mapping is feasible (Tarun, 2014).

In Bosso Local Government Area of Niger State, groundwater exploration is gaining greater attention due to increasing demand for water supply, especially in areas with inadequate pipe-borne and surface water. The drying up of the hand dug wells in the area worsens

the problem which is becoming progressively intense with growing population. This has been attributed to poor assessment of groundwater potential zones prior to water exploration in the area.

Severe water scarcity has been one problem citizens of Bosso Local Government Area had to contend with. Of the 3.9 million people in Niger State, only those in Minna the state capital, could boast of access to potable water, though not all residents of the city have access to drinkable water (Ikegwonu, 2013). Water projects constructed in the study area are no longer capable of providing enough water for the ever-growing population. This development has subjected the people of the study area to rely on other sources of water such as; rain water and groundwater which are seasonal. Hand dug wells in the area yield little water which dries up eventually due poor construction and also lack of information on groundwater potential zone before groundwater exploration, likewise the poor yields from boreholes constructed by government agencies and other private organizations (Ikegwonu, 2013) in the study area are some of the water challenges. Several researches has been conducted with regard to groundwater potential mapping both nationally and internationally and they include Bereket (2017); Akinwumiju *et al.*, (2016); Candra *et al.*, (2010); Dar *et al.*, (2010); and Elbeih (2015). There was paucity of knowledge with regard to groundwater potential mapping in Bosso and environ which has created a gap and this study intends to fill. Therefore, the study aimed to assess groundwater potential mapping using Digital Elevation Model in Bosso and environ, Niger State, Nigeria.

2 METHODOLOGY

Several datasets were used for estimating the groundwater water potential zones over the study area. The study used Digital Elevation Model (DEM) derived from ASTER in conjunction with field Geographical Position System (GPS) Points obtained during field survey.

Drainage network, drainage density network, aspect, and slope was extracted from DEM using the spatial hydrological tools in the ArcGIS 10.5 environment. Convergence Index (CI) adopted from Kiss (2014) was used to distinguish flow convergent area from divergent area, thus could be used for groundwater potential modelling. CI was calculated based on the aspect which will be extracted from DEM. The CI was obtained by calculating the average angle between the aspect of adjacent cells and the direction to the central cell and then subtracts 90° . Positive CI values represent divergent area while negative CI values represent convergent area. Thus a lower CI value associated with groundwater accumulation and have a higher groundwater potential value. The overlay process is carried out to obtain the final map of potential groundwater zones by using weighted overlay function in

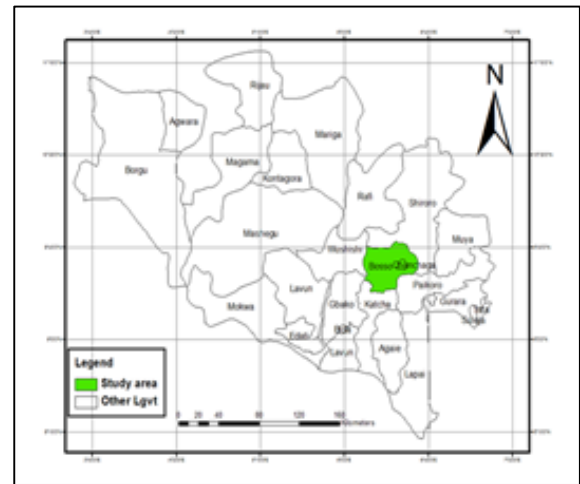


Figure 1: Location of Study Area (Bosso LGA).

the ArcGIS environment. The resulting map is classified into five different classes (High, Moderate, and Low) potential groundwater zones.

2.1 STUDY AREA

Bosso Local Government Area lies between longitude $6^{\circ} 33''$ E - longitude $6^{\circ} 37''$ E and latitude $9^{\circ} 33''$ N - latitude $9^{\circ} 38''$ N, on a geological base of undifferentiated base complex of mainly gneiss and magnetite situated at the base of prominent hills in an undulating plan. Bosso Local Government Area is situated on Niger valley. It is located in the south eastern part of Niger State with elevation in height between 100 feet (300 meters). The area geographically shares boundaries with Wushishi Local Government to the west, Chanchaga Local Government Area to the east, Shiroro Local Government Area to the north and Katcha Local Government Area to the south as indicated in Figure 1.

3 RESULTS AND DISCUSSION

3.1 DIGITAL ELEVATION MODEL

Figure 2 shows the elevations over the study area with the highest elevation of 452m located at the North eastern part of the study area and 71m as the lowest elevation found at the southwestern part respectively. The high elevation points have low potential of groundwater and low elevation has moderate and high groundwater potential in the study area.

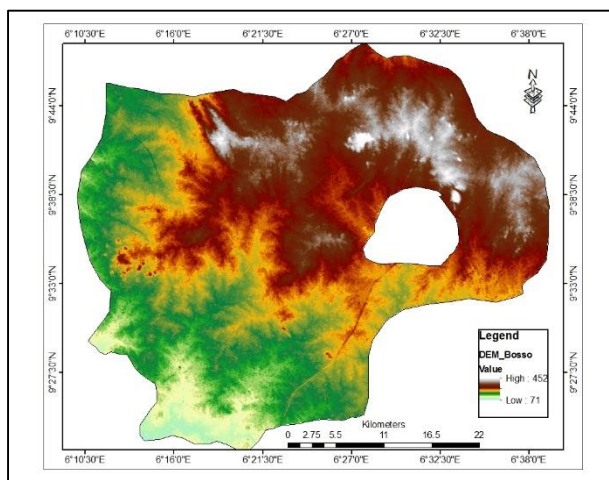


Figure 2: Digital Elevation Model over the study area

3.2 DRAINAGE NETWORKS ORDER MAP

A drainage basin is a natural unit draining runoff water to a common point. This map consists of water bodies, rivers, tributaries, perennial & ephemeral streams, ponds. The study area is fourth order basin joining the rivers, tributaries based on topography depicted in Fig.3.

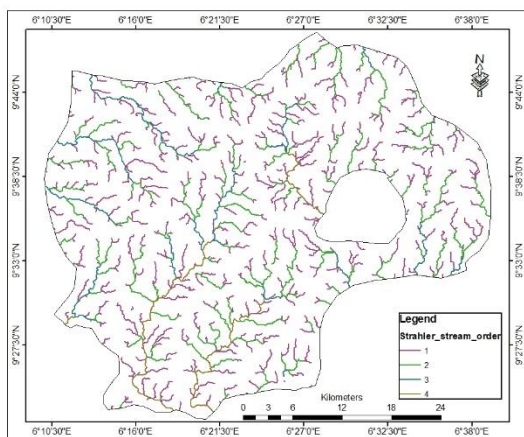


Figure 3: Drainage network order over the study area

3.3 DRAINAGE DENSITY NETWORKS MAP

A drainage basin is a natural unit draining runoff water to a common point. Drainage density is an inverse function of permeability. The less permeable a rock is, the less the infiltration of rainfall, which conversely tends to be concentrated in surface run-off. The area of very high drainage density represents more closeness of drainage lines and vice-versa. Fig.4 revealed the areas with high, moderate, and low drainage density covered 590.37km² (37.18%), 648.67km² (40.85%), and 348.83km² (21.97%)

respectively. High drainage density is the resultant of weak or impermeable subsurface material, sparse vegetation and mountainous relief. Low drainage density leads to coarse drainage texture while high drainage density leads to fine drainage texture. The drainage density characterizes the runoff in an area or in other words, the quantum of relative rainwater that could have infiltrated. Hence the lesser the drainage density, the higher is the probability of recharge or potential groundwater zone. Drainage Density is calculated using Focal statistics spatial analyst tool in ArcGIS 10.5.

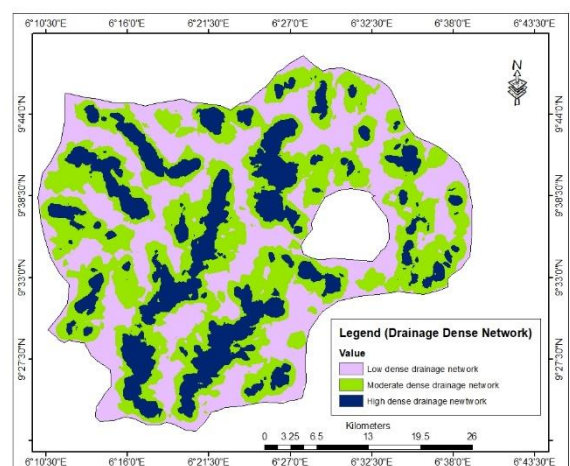


Figure 4: Drainage density network over the study area

3.4 SLOPE

Slope is an important factor in the analysis of ground water. The slope degree refers to the rate of change in elevation over distance with lower the slope value representing flatter terrain and higher values representing steeper terrain. Greater the slope, more runoff and lesser gradient tend to spread the overland flows thus favoring the infiltration and ground water prospects. Slope map was prepared with hydrological tools in the spatial analyst in ArcGIS 10.5. The study area was classified into three categories such as 0 to 2°, 2 to 5°, and above 5° based on slope measured in degrees. It is shown in Fig.5. that area with low slope (0° to 2°) covered an area 390.94km² (24.62%) and is excellent from the point of occurrence of ground water. While moderate and high slope area covered 428.95km² (27.01%) and 767.98km² (48.37%) respectively.

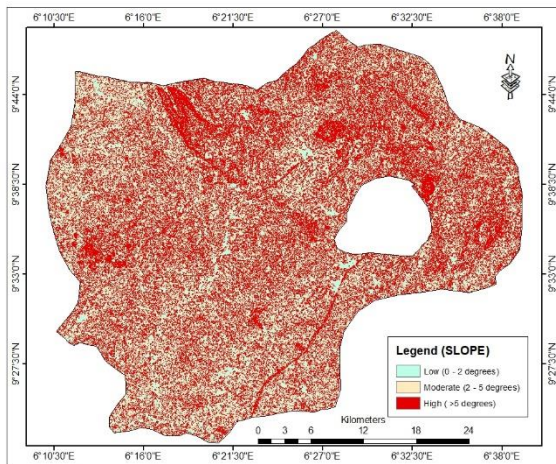


Figure 5: Slope over the study area

3.5 CONVERGENCE INDEX MAP

Figure 6 revealed the convergence index map over the study with most part of the area having low index. Areas with high convergence flow indicate high groundwater potential; areas with moderate convergence flow indicate average groundwater potential and areas with low convergence flow indicate low or no groundwater potential in the study area.

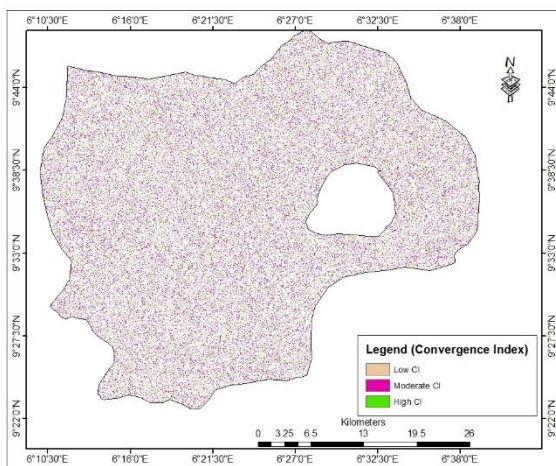


Figure 6: Convergence index over the study area

3.6 GROUNDWATER POTENTIAL MAP

Each thematic map such as drainage density, convergence index, elevation and slope provides certain clue for the occurrence of groundwater. In order to get all this information unified, it is essential to integrate these data with appropriate factor. Using weighted overlay analysis tool in ArcGIS all the thematic maps were integrated. The weightage for different layers have been assigned considering similar work carried by many researchers as

studied in literature review. A simple arithmetical model has been adopted to integrate various thematic maps by averaging the weightage. The final map has been categorized into three zones, from groundwater potential point of view High, moderate, and low which covered 128.54km² (8.10%), 1315.27km² (82.83%), and 144.06km² (9.07%) respectively as shown in Figure 7.

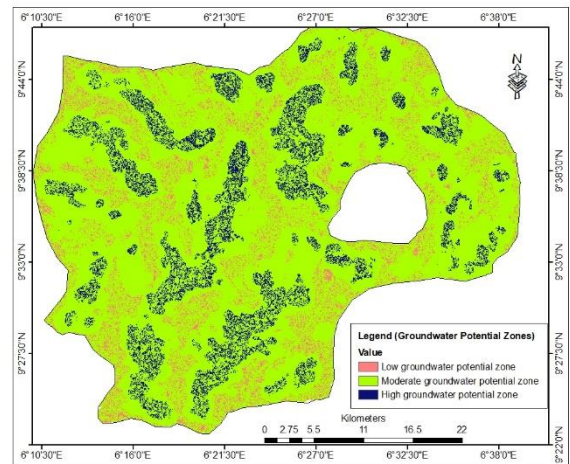


Figure 7: Groundwater potential zones over the study area

4 CONCLUSION

From the study it is concluded that based on overlaying and analysis of thematic maps in GIS three, groundwater potential zones have been delineated i.e. High, Moderate and low. Area covered by high groundwater potential zone is 8.10 km² mostly in the lower central part of the study area. Thus, integration of maps prepared from RS and GIS analytical tools proved an efficient method for delineation of groundwater in the study area. This groundwater potential information will be useful for effective identification of suitable locations for extraction of water. Furthermore, it is felt that the present methodology can be used as a guideline for further research.

ACKNOWLEDGEMENTS

This research was guided by my supervisor Dr (Mrs) M. Muhammed, for contributing excellent suggestions and support from an initial level of this research and giving me extraordinary knowledge throughout the project. I would also like to thank my family for firm support throughout in the course of carrying out this research.

REFERENCES

- Akinwumiju, A.S., Olorunfemi, M.O. and Afolabi, O. (2016). GIS-Based integrated groundwater potential assessment of Osun drainage basin, Southwestern Nigeria. *Ife Journal of Science*, 18(1), 147-168.



- Bereket, B.B. (2017). Groundwater potential mapping using remote sensing and GIS in rift valley Lakes Basin, Weito Sub Basin, Ethiopia. *International Journal of Scientific & Engineering Research*, 8(2), 43-50
- Candra, S. and Viswanadh, G.K. (2010). *Identification of Groundwater Potential Zones Using RS and GIS*. Department of Environmental Information Study and Analyses EISA Institute of Geography Hoang Quoc Viet R.D Cau Giay, Hanoi Vietnam.
- Dar, I., Sankara, K. and Dar, M. (2010). Remote Sensing Technology and Geographic Information System Modeling: An Integrated Approach towards the Mapping of Groundwater Potential Zones in Hard Rock Terrain, Mamundiyar Basin. *Journal of Hydrology*, 394, 285–295, <http://www.elsevier.com/locate/jhydrol>.
- ESRI (2011). ArcGIS Desktop: Release 10. Redlands, CA: Environmental Systems Research Institute.
- Elbeih, S. (2015). An overview of Integrated Remote Sensing and GIS for Groundwater Mapping in Egypt. *Ain Shams Engineering Journal*, 6, 1–15. <http://dx.doi.org/10.1016/j.asej.2014.08.008>
- Hussein, A., Govindu, V. and Nigusse, A.G. (2016). Evaluation of Groundwater Potential Using Geospatial Techniques, Applied Water Sciences, Print ISSN 2190-5487; Online ISSN 2190-5495, Springer Berlin Heidelberg. <http://link.springer.com/article/10.1007/s13201-016-0433-0/>
- Ikegwuonu, S. E. (2013). Geospatial assessment of groundwater potential in Jos South Local Government Area of Plateau State, Nigeria. Published Msc thesis, Department of Geography, Ahmadu Bello University Zaria, Nigeria.
- Mohamed, S. I. E. M. M. (2014). Groundwater potential modelling using remote sensing and GIS: a case study of the Al Dhaid area, United Arab Emirates. *Geocarto International*, 29(4), 433-450.
- Tarun, D. (2014). Determination of the drainage structure of a watershed using a digital elevation model and a digital river and lake network. *Journal of Hydrology*, 240(3), 225-242.



Optimization of Synthesis parameters of silica from Bentonite Clay using acid leaching

Ogwuche, A. S, Auta, M, & Kovo, A. S

Chemical Engineering Department, Federal University of Technology, PMB 65

Minna, Niger State, Nigeria.

Department of Chemical Engineering, Federal University of Technology, PMB 65

Minna Niger State, Nigeria.

Department of Chemical Engineering, Federal University of Technology, PMB 65

Minna Niger State, Nigeria

E-mail sunnychem2@yahoo.com, +2347037764582

ABSTRACT

The synthesis of silica adsorbent from natural clay obtained from Obajana, Kogi state, Nigeria was carried out using thermal and acid treatment processes. The calcined clay particles was added in 50ml of 5.00M H₂SO₄ solution and left for stirring at 100°C for 1.00hour decanted to obtain the silica reach clay. The leached clay particles were washed thoroughly with distilled water until a neutral pH was obtained. The raw clay was characterized to determine its properties using X-ray fluorescence (XRF) analysis and the effect of the thermal treatment was determined using X-ray diffraction principle. The leached clay sample using experimental design was analyzed using atomic absorption spectroscopy. The results indicated that the clay sample was rich in silica which emanated from 62.67% efficiency of leaching of alumina content present.

Keywords: Silica, Bentonite clay, Calcinations, Leaching, Acid treatment, Optimization.

1. INTRODUCTION

Silica is extensively found in nature either as a major mineral in most igneous (e.g. granite) or sedimentary (e.g. sand and sand stone) or metamorphic rocks (quartzite, gneiss) (Usama *et al.*, 2015). Silica is most commonly found in nature as quartz, as well as in various living organism. Silica particles have found applications in a variety of fields including drug delivery systems, catalysis, biomedical, biological imaging, chromatography, sensors, and liquid armors and as filler in composite materials (Usama *et al.*, 2015). Clay is a potential source of silica, which contains smectite as a main clay mineral. As alumina component is present in clays along with silica, a range of acid and alkali hydrometallurgical methods are employed to isolate them from each other (Essien *et al.*, 2011). Usually acids are used for the processing of clay rather than alkalis (Ajemba and Onukwuli, 2012) and H₂SO₄ is preferred over other acids due to the easy separation of filtrate from the residue (Usama *et al.*, 2015). For effective removal of alumina from clays, calcination is a critical step; solubility of alumina increases after thermal treatment in the temperature ranges of 500–900°C (Aghbasho *et al.*, 2012).

Previously, kaoline clay was studied for the production of aluminum sulfate and it was found that heating the clay to 700°C for 1 h followed by acid leaching with sulfuric acid (H₂SO₄) were the optimum conditions to extract alumina (Essien *et al.*, 2011). In the present study, silica particles were synthesized from bentonite clay in nanometer and micrometer size range. Alumina content in bentonite clay was lowered by a series of thermal and acid treatments.

Clays are very abundant on the earth's surface; they form rocks known as shale and are major component in nearly all sedimentary rocks. The small size of the particles and their unique crystal structures give clay materials special properties, including cation exchange capabilities,

Plastic behavior when wet, catalytic abilities, swelling behavior, and low permeabilities, (Al-Zahrani and Abdul-Majid., 2009).

This research is aimed at extracting out alumina component of the bentonite clay sample. It will involve calcination of the raw clay sample, acid leaching of the calcined clay and analysis of the leached sample.

2. METHODOLOGY

2.1 MATERIALS

The clay sample used in this research was mined from Obajana in Kogi state north central of Nigeria. The clay was analyzed to determine its chemical composition using x-ray fluorescence spectrometer (XRF). Tetraoxosulphate VI acid (H₂SO₄) was purchased from panlac and used without further purification.

2.2 PRETREATMENT OF THE CLAY SAMPLE

The clay sample was oven dried at 105°C for 12 hours, crushed and sieved to 75 mm particle sizes. The sieved samples were then calcined in a muffle furnace at temperature of 700° C for 2 hours

2.3 LEACHING OF SILICA FROM OBAJANA CLAY

About 10 g of the calcined Obajana clay was added to 250 mL conical flash containing 50 mL of predetermined concentration of H₂SO₄ solution which was stirred at a temperature of 100°C for 1.00 hour as specified by the experimental design (design experiment software) using response surface methodology application. The experimental design for the experiment is presented in Table 2. At the end of each reaction time, the undissolved materials in the suspension was allowed to settle and separated by decantation. The resulting solutions were diluted and analyzed for alumina content determination using atomic absorption spectrophotometer (AAS). The residue was also collected, washed to neutrality with distilled water, and oven dried at 105° C.

3. RESULTS AND DISCUSSION

3.1 CHARACTERIZATION OF RAW OBAJANA CLAY SAMPLE

The XRF analysis of the Obajana clay used revealed that the clay was more of a bentonite material as it had higher silica to alumina ratio (> 1:1) than the usual kaolinite. The silica content of the clay was 62.67%. The XRF characterization result of the lay is presented in Table1.

TABLE 1: XRF ANALYSIS OF OBAJANA CLAY SAMPLE

Composition	Raw clay (%)	Calcined at 700°C
SiO ₂	62.67	65.85
Al ₂ O ₃	14.91	15.99
Fe ₂ O ₃	4.90	1.47
CaO	0.13	0.07
MgO	1.77	2.10
K ₂ O	1.98	2.27
Na ₂ O	2.07	1.73
LOI	10.50	3.70

3.2 CALCINATION OF OBAJANA CLAY SAMPLE

The calcinations process was done in order to reduce the volatile matter content of the raw clay sample and to improve its susceptibility to acid leaching. The XRD analysis of the raw and calcined clay sample to determine the effect of the thermal treatment on it and the result is presented in Figure 1. The XRD patterns revealed presence of crystalline peaks of quartz on the both uncalcined and calcined clay samples. However, peaks of both kaoline and montrimorillonite were visible in the spectrum of the calcined Obajana clay (Usama et al., 2016). The XRD pattern revealed an amorphous phase between 11-14° θ . In pure bentonite, peaks of Kaoline exist in this region which disappears after thermal treatment and substituted with an amorphous band. This indicates the transformation of the kaoline content of the clay to amorphous metakaoline (Ajemba and Onukwuli, 2012). Calcination of bentonite clay causes it to dehydrate and further heating beyond 680 °C leads to dehydroxylation reaction (zymankowska et al., 2012).

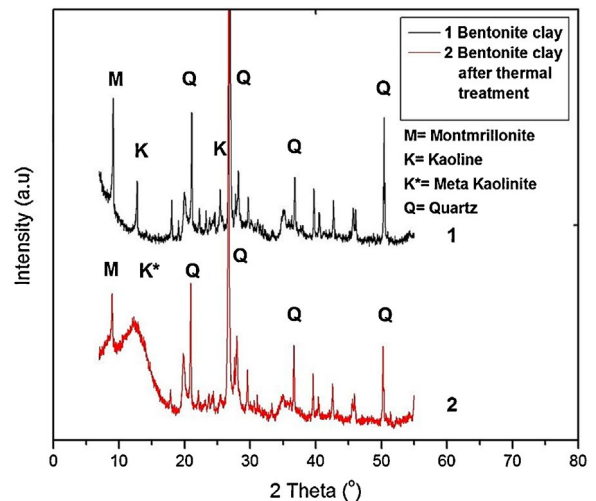


Figure 1: XRD patterns of Obajana clay before and after thermal treatment at 700°C for 1 h.

3.3 THE AAS ANALYSIS OF THE ACID LEACHED CLAY SOLUTION

The various acid leached samples using the concentration of H₂SO₄, reaction time and temperature obtained from the experimental design using RSM were analyzed using AAS to determine the alumina content. The stirring speed and dosage were kept constant in the 20 experimental runs obtained from the software (Sudamalla et al., 2012). The results of the analysis at various conditions are presented in Table II. It was observed that a non-dominated optimal response of 79.51% yield of alumina removal at 5.00 M sulphuric acid concentration, 60 min leaching time, 0.085 g/ml dosage and 214 rpm stirring speed was established as a viable route for reduced material and operating cost.

TABLE II: THE AAS ANALYSIS OF ALUMINA IN THE ACID
LEACHED CLAY SOLUTION

Run/Order	Temp (°C)	Time(min)	Conc(M)	Alumina yield(%)
1	80.00	180.00	3.50	28.60
2	80.00	21.82	3.50	26.98
3	80.00	180.00	3.50	28.60
4	100.00	60.00	2.00	30.43
5	46.36	180.00	3.50	44.22
6	100.00	60.00	5.00	79.51
7	80.00	180.00	3.50	28.60
8	80.00	180.00	0.98	29.21
9	80.00	381.82	3.50	54.36
10	80.00	180.00	6.02	22.72
11	113.64	180.00	3.50	56.795
12	60.00	300.00	5.00	33.874
13	60.00	300.00	2.00	87.63
14	80.00	180.00	3.50	28.60
15	100.00	300.00	5.00	69.37
16	80.00	180.00	3.50	28.60
17	100.00	300.00	2.00	55.98
18	80.00	180.00	3.50	55.984
19	60.00	60.00	5.00	50.719
20	60.00	60.00	2.00	26.77

were analysed in phases. The observed trends suggest that by proper adjustment of the system variables within the sampled space, a valid optimal could be attained. The results conform largely to what is already known for alumina removal processes (Ajemba and Onukwuli, 2012). Nevertheless, one noticeable unusual result may be the apparent linear (one-directional) response observed in the system response with respect to dosage ratio axis. This does not reflect a typical behavior of batch dissolution processes. Clay particle congestion which occurs at high dosage ratio in the reactor and increased turbulence associated with high stirring rate is formally expected to introduce significant nonlinearities or at least a quadratic behavior in the system response. The consistent linear behavior (in which increasing the input value leads to a corresponding increase in output with respect to dosage ratio) implies that no definite optimal solution could be obtained for the two variables. If such optimal condition exists for the present case, then it definitely lies in a range outside the sampled space. The selection of a useful optimal condition for the two variables would thus be guided strictly by a balance of compromise between their effects on system response and economic implication. The maximum removal of alumina is predicted on the optimum condition from the RSM result by the AAS analysis.

3.4 ANALYSIS OF THE RSM EXPERIMENTAL RESULT YIELDED 3D SURFACE PLOTS PRESENTED IN FIGURE 2.

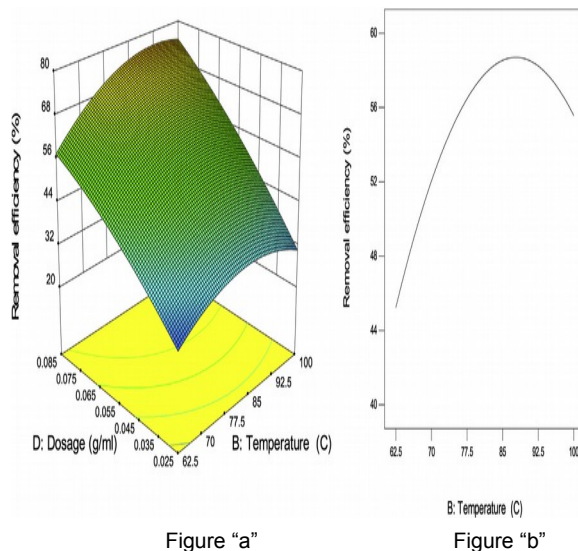


Figure 2: 3D Surface (a), and single effect (b) plot for effects of dosage ratio and reaction temperature on alumina removal from Obajana clay.

The combined effects of adjusting the process variables within the design space were monitored using 3D surface plots. Every significant interaction effects on the system response between two independent variables

4. CONCLUSIONS

Silica was synthesized from bentonite clay after sequence of acid and thermal processes. The experiment investigated the optimum condition for the extraction of alumina from obajana clay using RSM method from design expert software. The results revealed that H₂SO₄ can successfully leach alumina from clay to about 79 %.

REFERENCES

- Adekola, Folahan, A., Baba, Alafara, A., (2010). Hydrometallurgical processing of a Nigerian Sphalerite in hydrochloric acid, Characterization and dissolution kinetics. *Hydrometallurgy 101 (1)*.
- Aghbashlo, Mortaza, Mobli, Hossien, Rafiee, Shahin, Madadlou, Ashkan, (2012). The use of artificial neural network to predict exergetic performance of spray drying process: a preliminary study. *J. Comp. Electron. Agric. Arch. 88, 32-43*.
- Ajemba, R.O., Onukwuli, O.D., (2012). Determination of the optimum dissolution optimum dissolution conditions of ukpor clay in hydrochloric acid using



- response surface methodology. *Int. J. Eng. Res. Appl.* 2 (5), 732-742
- Ajemba, R.O., Onukwuli, O.D., (2012). Process optimization of sulphuric acid leaching of alumina from Nteje clay using central composite rotatable design. *Int. J. Multidiscipline. Sci. Eng.* 3(5).
- Alam, M.Z., Muyibi, S.A., Toramae, J., (2007). Statistical optimization of adsorption processes for removal of 2, 4-dichlorophenol by activated carbon derived from oil palm empty fruit bunches. *J. Environ. Sci. China* 19 (6) 674-677.
- Al-Zahrani, A., Abdul-majid, M.H., (2009): Extraction of alumina from local clays by hydrochloric acid process. *JKAU: Eng. Sci.* 20 (2), 29-41.
- Bhatti, Manpreet, Kapoor, Dhriti, Kalia, Rajeev, Reddy, Akepati, Thukral, Ashwani, (2011). RSM and ANN modeling for electro coagulation of copper from simulated wastewater: multi objective optimization using genetic algorithm approach. *Desalination* 27, 74-80, 4, 2007.
- Chen, G., Xiong, K., Peng, J., Chen, J., (2010) Optimization of combined mechanical activation roasting parameters of Titania slag using response surface methodology. *Adv. Powder Technol.* 21 (3), 331-335.
- Chen, G., Chen, J., Srinivasakannan, C., Peng, J., (2011). Application of response surface methodology for optimization of the synthesis of synthetic rutile from Titania slag. *Appl. Surf. Sci.* 258 (7). 3068-3073).
- Desai, K.M., Survase, S.A., Saudagar, P.S., Lele, S.S., Singhal, R.S., (2008). Comparison of artificial neural network (ANN) and Response surface methodology (RSM) in fermentation media optimization: case study of fermentation production of scleroglucan. *Biochem. Eng. J.* 41, 266-273
- Sudamalla, P., Saravanan, P., Matheswaran, M., (2012). Optimization of operating parameters using response surface methodology for adsorption of crystal violet by activated carbon prepared from mango kernel. *Sustain. Environ. Res.* 22(1), 1- 7
- Usama, Z., Tayyab, S., Subhani, S. & Wilayat H., (2016). Synthesis and characterization of silica nanoparticles from clay. *Journal of Asian Ceramic Societies* 4, 91-96
- Zymankowska, S.K., Hohzer, M., Olejnik, E., Bobrowski, A. (2012), Master. Sci., 18)



Chemical and Mineralogical Characterization of Locally Sourced Nigerian Clay

*Sumanu, O. M¹, Dim, P. E². & Okafor, J. O³.

¹ Engineering Department, Federal University of Technology, PMB 65, Minna, Niger State, Nigeria

² Department of Chemical Engineering, Federal University of Technology, PMB 65 Minna, Niger State, Nigeria

³ Department of Chemical Engineering, Federal University of Technology, PMB 65, Minna, Niger State, Nigeria

*Corresponding author email: olorunyomisumanu@gmail.com, +2348036781858

ABSTRACT

The application of various clay minerals is related to their structural, physical, and chemical characterization. The utilization of clay in any form is been dictated by the physical and chemical properties of the clay minerals. This study investigates the chemical and mineralogical composition of clay sample collected from Umunze, Nigeria. Some quantitative and qualitative analytical methods were employed for the purpose of chemical and mineralogical characterization. The methods include Brunauer, Emmett and Teller (BET) Analysis, Cation exchange capacity (CEC), X-ray diffraction (XRD) Scanning electron microscope (SEM) and Fourier Transform infrared spectroscopy (FTIR). The results obtained suggests that the clay is of kaolinite with traces of montmorillonite.

Keywords: *Clay, Characterization, Kaolinite, Mineralogy, XRD.*

INTRODUCTION

The study of clay and its minerals is generating new interest all over the world with an aim of providing solutions to problems of pollution eradication. The readily availability of clay in abundance which interestingly constitute a larger percentage of water in nature, justifies the need for the study. Oxygen and Silicon alone account for 75% of the mass of the earth crust and Oxygen for 90% of the total volume (Schulze, 2015). Clay, a small particle, found naturally on the surface of the earth composed mainly of silica, alumina, water and weathered rock (Uddin, 2017). Clay minerals play an important role in physico-chemical properties determination. The corresponding bulk of physico-chemical properties of certain clay distinguish clay minerals based on their different crystal structure. Kaolinite is a major mineral constituent of clay that is rich in kaolinite called Kaolin. Kaolinite is a clay mineral with chemical composition $\text{Al}_2\text{Si}_2\text{O}_5(\text{OH})_4$ with a single silica tetrahedral layer linked through Oxygen atoms to a single alumina octahedral layer (Olaremu, 2015). Kaolinite structure possesses great advantages in many processes, due to its high chemical stability, cation capacity and low expansion co-efficient (Uddin, 2017) Characterization of clay play an important role in determining the properties. The method employed to characterize the clay sample include chemical analysis, X-ray diffraction (XRD), X-ray florescence (XRF), Fourier Transform infrared spectroscopy (FTIR), Scanning electron microscopy (SEM), surface area and pore size measurement. Normally a combination of several methods are needed

for sufficient characterization of the material obtained (Khalifa *et al.*, 2016). The objectives of this study is to characterize a new locally sourced clay, to determine its physical, chemical and mineral properties.

METHODOLOGY

Clay sample collected from Umunze, Nigeria was used as raw material. It was treated by hand picking to remove the dirt and other foreign bodies and after which it was sieved with a 125 μm mesh sieve. The collected particles were sun dried.

BET surface analysis and porosity: Nitrogen adsorption/desorption isotherms in relative pressure ranging from 10⁻⁶ to 0.999 were measured at 77 K on an automatic adsorption instrument (Quantachrome Instruments, Model Nova1000e series, USA). Prior to the measurement, the given sample was crushed to powdery form to shorten the time required for reaching equilibrium in the isotherm study and degassed at 250°C under nitrogen flow for 16 hours.

The infrared spectra were obtained using a Perkin-Elmer 1720 spectrometer (the sample was diluted with potassium bromide:50mg of sample mixed with 350mg of potassium bromide). The FTIR spectra of the samples were recorded between 4000 and 450 cm^{-1} .

SEM analysis: The clay sample morphology was observed using Zeiss Auriga HRSEM. XRD analysis: The mineralogical phase characterization and estimation of the average crystallite size of the various synthesized materials were performed on a Bruker AXS D8 X-ray diffractometer system coupled with $\text{Cu-K}\alpha$ radiation of 40 kV and a current of 40 mA. The λ for

$K\alpha$ was 0.1541 nm, scanning rate was 1.5°/min, while a step width of 0.05° was used over the 2 θ range. The powder samples were placed and clipped into the rectangular aluminium sample holder. The diffractograms were recorded in the 2 θ range of 200 - 900 and the phase identification was done. The chemical analysis of the raw clay was carried out using XRF.

Cation exchange Capacity (CEC) was determined by Gillman and Sumpter method of Compulsive exchange.

RESULTS AND DISCUSSION

BET analysis

According to Babaki *et al.*, (2008) texture characteristics such as pore volume, or pore size and surface area played an extensively important role in clay mineral applications such as adsorption. The results presented in Table 1, are for pore size, pore volume and surface area of raw clay sample using BET analysis. The surface area of the raw clay from the Table is 84.233 m²/g. The result is in agreement with the findings of other work (Valenzuela Díaz and de Souza Santos, 2001), who suggested that Smectite has BET surface area varying from 16 - 97 m²/g, without any chemical treatment.

Cation exchange Capacity

Cation exchange Capacity (CEC) CEC can be described as the quantity of positively charged ions held by the negatively charged surface of clay minerals. It was determined by Gillman and Sumpter method of Compulsive exchange. The caption exchange capacity (CEC) of pure kaolinite minerals range from 3-15 Cmol/100g (Olaremu, 2015). The value as shown in Table 1 represents the determined CEC of clay sample. The CEC value of raw clay sample calculated for this work is 22.298 cmol/100g higher than the literature value for kaolinite, this is probably due to impurities and pore size (Olaremu, 2015).

Table 1: Properties of raw clay sample

Property	Pore size (nm)	Pore Volume (cc/g)	Specific Surface Area (m ² /g)	Cation Exchange capacity (CEC) cmol/100g
Value	2.115	5.266 x 10 ⁻²	84.223	22.29

XRF analysis

Table 2 shows the results of chemical analysis and loss on ignition of raw clay sample. The chemical composition of

the clay sample is in (%). The high loss of ignition (see Table 2) is associated with the dihydroxylation of the clay minerals and the oxidation of organic matter (Savazzini-Reis *et al.*, 2017).

The chemical analysis of raw clay shows that the major elements are SiO₂ and Al₂O₃ while traces of Magnesium, Chromium, Manganese, Calcium, Titanium and Zinc oxides are found in form of impurities. ZnO has the lowest percentage composition in the clay sample which may be attributed to the environmental and geographical contribution of the earth crust of an area where the Umunze clay sample was collected. Silicon (IV) oxide has been reported to constitute the highest percentage composition of kaolinite sample (Lin and Wen, 2002). The second highest constituent identified to be aluminium oxide. The ratio of alumina silica was estimated to be 1:5.4.

Table 2: Chemical analysis (wt %) and loss in ignition of raw clay sample.

Components	Percent
SiO ₂	49.752
Al ₂ O ₃	9.203
Fe ₂ O ₃	6.943
CaO	0.357
TiO	1.024
MgO	1.395
Cr ₂ O ₃	0.023
ZnO	0.009
MnO	0.105
LI	31.189

XRD analysis

The mineralogical composition of the sample was determined by the use of x-ray diffractometer studies. The sample composed majorly of Quartz (which is the non-clay mineral in clay) it is characterized by strong d-lines, Kaolinite and Montmorillonite. From Figure 1, Montmorillonite is represented by M, Kaolinite by K and quartz with Q. Kaolinite and Montmorillonite showed good absorbance for removal of toxic heavy metals as (Cd, Cr, Co, Cu, Fe, Pb, Mn, Ni, and Zn (Talaat *et al.*, 2011). Kaolinite is clay that is rarely found in a pure state, it is a

major part of the kaolin clay and is a very good type, consisting of aluminosilicate minerals (Al_2O_3 SiO_2 H_2O) (Naswir *et al.*, 2013).

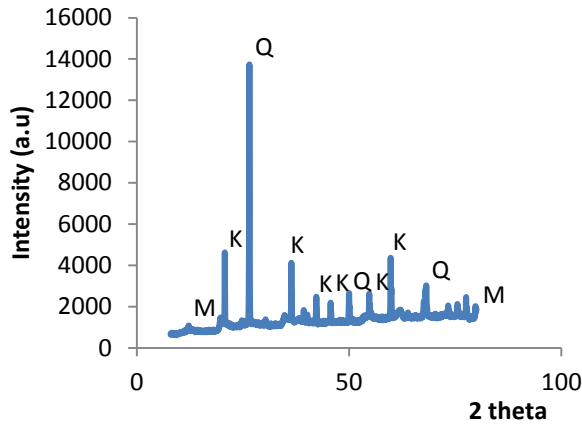


Figure 1.: Diffractogram (XRD) of raw Umunze clay.

FTIR analysis

The FT-IR spectra of the raw clay samples were carried out in the range from $400\text{-}4000\text{cm}^{-1}$ to study the effect of leaching of the clay minerals from the raw or natural sample shown in Figure 2, the inner surface OH stretching vibrations are represented at 3696 and 3623 cm^{-1} , while the absorption band at 3457 cm^{-1} represents the outer surface OH stretching vibration. These OH groups function as the active sites for the binding of positively charged cations. The absorption bands at 469.66 and 1030 cm^{-1} represented the Si-O-Si stretching vibration (Li *et al.*, 2014; Juan Yin *et al.*, 2018). The absorption band at 916 cm^{-1} represents the Al-OH bending vibration while those at 798 and 694 cm^{-1} represent the Si-O stretching vibration (Olgun *and Atar*, 2012). The (Si-O) bands are strongly evident in the infrared spectrum by adsorption band in the 1030 cm^{-1} . While those at 798.94 cm^{-1} and 694.46 cm^{-1} represent the stretching vibration (Dawodu *et al.*, 2014). The characteristic bands at 3686 cm^{-1} , 3657 cm^{-1} and 916 cm^{-1} indicated the presence of kaolinite. The presence of adsorption bands at 3623 cm^{-1} support the presence of montmorillonite. According to Spence *and Kelleher*, 2012 and Long *et al.*, 2013, Kaolinite has wave numbers peak of hydroxyl (OH) group of 3696 , 3671 and 3650 cm^{-1} and Montmorillonite with wave numbers peak of 3624 cm^{-1} (Al-OH), and 3422 cm^{-1} (water).

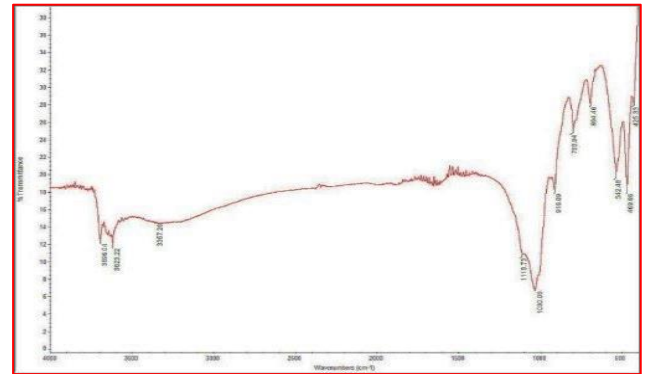


Figure 2: Infrared spectra (IR) of Umunze clay.

SEM analysis

The Scanning electron microscopy (SEM) of raw clay was carried out to assess the surface morphology of the clay. The micrograph of the natural adsorbent can be clearly observed from Figure.3 which shows the aggregate mass size made up of aggregated mass of irregularly shaped particles that appeared to have been formed by several flaky particles stacked together in form of agglomerates.

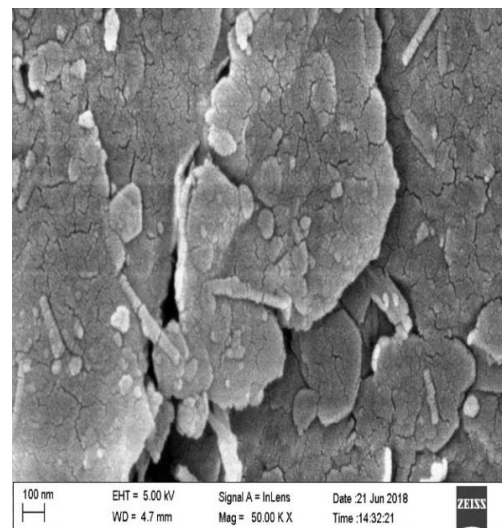


Figure 3: Scanning electron microscope of raw Umunze clay.

CONCLUSION

The study investigated the chemical and mineralogical analysis of raw clay sample. The surface area, chemical and mineralogical composition, morphological properties were studied using various techniques. It was found that raw clay has a BET surface area of $84.223\text{ m}^2/\text{g}$. The chemical analysis of the clay consists of high impurities of chemical oxides such as Fe_2O_3 , TiO_2 , MnO , MgO , Cr_2O_3 , and ZnO . Generally, quartz and iron were the major impurities present in the raw sample. The XRD results indicated that



the clay mineral is of kaolinite type with traces of montmorillonite and present of quartz, which was confirmed by the XRF results. The finding shows that clay minerals can be exploited for the removal of wastewater using low cost and environmental friendly techniques through acid activation to reduce the levels of iron, quartz and other impurities to acceptable levels.

ACKNOWLEDGEMENTS

The author acknowledges support from the Federal University of Technology, Minna for the use of departmental library and other facilities. The author would like to express utmost thanks to Dr. Tijani Oladejo, and Mr. Pius Ikokoh of SHESTCO, Sheda-Abuja for helping to conduct some of the experiments.

REFERENCE

- Babaki, H., Salem, A., and Jafarizad. (2008). "Kinetic model for the isothermal activation of Bentonite by Sulfuric acid." *J. Mat. Chem. Phy.* 108: 263-268.
- Dawodu, F.A. and Akpomie, K.G. (2014). Simultaneous adsorption of Ni(II) and Mn(II) ions from aqueous solution onto a Nigerian kaolinite. *J. Mater. Res. Technol.* 3, 129-141.
- Khalfa, L., Bagane, M., Cervera, M. L., and Najjar, S. (2016). Competitive adsorption of heavy metals onto natural and Activated clay: Equilibrium, Kinetics, and Modelling. *International Scholarly and Scientific Research & Innovation*, 10(5), 583-589.
- Lin, C. P. and Wen, S. B. (2002). *J. A. Am. Ceram. Soc.* 25, 129.
- Long, H., Wu, P., and Zhu, N. (2013). "Evaluation of Cs⁺ removal from aqueous solution by adsorption on Ethylamine-Modified Montmorillonite". *Chemical Engineering Journal* 225: 237-244.
<http://doi.org/10.1016/j.vibspec.2012.02.019>
- Naswir, M., Arita, S., Marsi, and Salmi. (2013). Characterization of Bentonite by XRD and SEM-EDS and Use to Increase PH and Colour Removal, Fe, and Organic Substances in Peat water, *Journal of Clean Energy Technologies*. 1(4),313-317.
- Olaremu, A. G., (2015). Physico-Chemical Characterization of Akoko mined Kaolin clay. *Journal of Minerals and Material Characterization and Engineering*. 3,353-361.
- Olgun, A., and Atar N. (2012). "Equilibrium, thermodynamic and kinetic studies for the adsorption of lead (II) and nickel (II) onto clay mixture containing boron impurity". *J Indust Eng Chem.* 18(5):1751-1757.
- Savazzini-Reis, A., Sagrillo, V. P. D., de Oliveira, J. N., Teixeira, P. G., and Valenzuela-Diaz, F.R. (2017). "Characterization and evaluation of Ceramic properties with spherical and prismatic samples of clay used in red ceramics". *Research material*.20(2):543-548. DOI:<http://dx.doi.org/10.1590/1980-5373-MR-2016-0915>.
- Schulze, C. D. (2015). Clay Minerals in: Hillel D.(ed) *Encyclopedia of the soils in the environment, Elsevier*,246-252.
- Spence. A., and Kelleher, B. P. (2012). " FT-IR Spectroscopic Analysis of Kaolinite-microbial interactions". *Vibrational spectroscopy*.61, 151-155.
- Talaat, H. A., El Defrawy, N.M., Abulnour, A. G., and Hani, H. A. (2011). "Evaluation of Heavy metal removals using Egyptian clays". *2nd International Conference on Environmental Science and Technology, IPCBEE*.6:37-42.
- Uddin, M. K. (2017). A review on the adsorption of heavy metals by clay minerals, with special focus on the past decade. *Chemical Engineering Journal* 308,438-462
- Valenzuela Diaz, F. R., and de Souza Santos, P. (2001). "Studies on the acid activation of Brazilian Smectite clay". *Quim. Nova*.24 (3):345-353.



Production and Optimization of Bioethanol from Watermelon Rind using *Saccharomyces Cerevisiae*

*Igbonekwu, C. A¹, Afolabi, E. A², Nwachukwu, F.O³

^{1,2}Chemical Engineering Department, Federal University of Technology, PMB 65 Minna Niger State, Nigeria

³Department of Strategic Food and Grain Reserve, Federal Ministry of Agriculture, Abuja Nigeria

*Corresponding author email: icas7742@gmail.com, +2347038658633

ABSTRACT

Bio-fuels generation from waste forms is a good solution towards the waste management and generation of energy. The utilization of fruit rinds is preferable to all the costly starchy food. Watermelon rind was used to produce the bioethanol, they were dried, ground and pretreated then saccharification was carried out by enzymatic hydrolysis by *Aspergillus Niger* followed immediately by fermentation by yeast *Saccharomyces cerevisiae*. The amount of ethanol produced after fermentation was measured by Alcohol-Meter. The factors affecting fermentation process were varied, 15 runs was experimental design matrix designed by Design Expert software by RSM (Response Surface Method). The optimization of the variables was done by ANOVA (Analysis of Variance). The optimal value was obtained at 30 °C, 48 hours and 2 g/ml of temperature, time and substrate concentration respectively at 20.3% in volume ratio. From the result, the ethanol yields achieved are too low for marketing and organisms are not robust enough for applications in industries in both cases, but as science is going on, to produce sustainable fuels in future, engineering microorganisms could help to achieve it.

Keywords: *Aspergillus Niger*, Bioethanol, Fermentation, Optimization, *Saccharomyces Cerevisiae*, Watermelon rind.

1 INTRODUCTION

Dumping of waste in the world has become a very serious issue, harm or effect to plants and animal of the systems surrounding the dumping sites. The conception of production of renewable sources of energy from the used of wastages is a solution or as alternative for fossil fuel production which is very cheap, adoptable and efficient. Bio-polymer cellulose is one of the most abundant sources of energy in the modern world, forms the most plant and algal cells walls which are the major components. The organisms responsible to produce enzyme cellulose that enhance them to hydrolyze the cellulose into constituents glucose units are such; Species of *Trichoderma*, *Aspergillus*, *Clostridium* etc. (Thiyam et Sharma, 2013).

The production of ethanol worldwide is approximately 51,000 million litres. The most efficient and low environmental degradation bio-energy sources is ethanol. Approximately 75% fuel are contained in a produced ethanol, while closely 20% and 15% beverage and industrial ethanol respectively (Sanchez et Carlos 2008).

The product of microbial fermentation is ethanol which also known as alcohol, there are some microorganisms which meets the requirement for the amount of energy to be used in conversion of carbon sources to the by-product as well, such as; carbon dioxide, lactic acid and ethanol. Since the fermentation reaction requires energy for conversion, it can be classified as an endothermic reaction. The organisms which are micro that enables the conversion of sugar to ethanol are *Saccharomyces*

Cerevisiae, *Zymomonas mobilis*, *Kluyveromyces* Species and *Schizosaccharomyces Pombe*. There are various chemical based media and agro-based feedstock that can be used for fermentation of ethanol. Wheat, sorghum, sugar-cane, and corn are the mostly common and used type of feedstock for ethanol production (Balat *et al*, 2008).

According to (Nalley and Hudson 2003, USDA 2006). The carbon sources that are highly enriched or valued products as food sources are sugar cane, sugar beet and molasses which are feasible and have been used for fermentation of ethanol.

In this research, watermelon rind is used for production of ethanol. The most excellent sources of cellulose which can be used for production of ethanol via scarification followed by fermentation are fruit rinds (Mustafa et Sanjay, 2014)

The fruit rinds can be Banana, orange, pineapple or watermelon rinds which are generally agreed that will be used in prospect as a primary source of simple hexoses. Such is watermelon rind. There are 2 main factors to be considered for possibly selecting watermelon rind as the feedstock for ethanol bio-fuel. One more or less than 20% of watermelon crop is rejected annually for fresh fruit marketing because of the spoilt appearance and which deforms the shape of the fruit, although the inside of the watermelon are sound and they are left in crop field. In 2007, the U.S farmer of watermelon lose about 360,000 tons which would have been a source of revenue of them

which occurs as a results of above reasons (Agricultural Marketing Resource Center U.S 2007).

Converting watermelon rinds to ethanol cold at all time, provide additional on a farm-fuel to the grower or in some cases, it can be sold to the market as ethanol biofuel. Two neutraceutical value of components gotten from watermelon crop or rind could be employed as a fresh substrate to extract and produce these product. The significant antioxidant carotenoid that imparts the red colour to watermelon which has been shown to be important in prostate health is lycopene (Fang *et al*, 2002).

The botanical name for watermelon is *Lanatus-Citrulline*, naturally it contains amino acid that involved in removal of toxic substances for breaking down of ammonia compound and also serve as precursor for lanatus-arginine, the amino acid generally involved in the circulatory vasodilatation production of these two neutraceuticals from watermelon yields a waste stream that contains closely 10%(weight per volume) sugar that can be fermented to ethanol directly. The composition of a watermelon is about 60% flesh, approximately 90% of flesh is juice which contain closely 7%(weight per volume) sugar. However, more than 50% of the watermelon is almost fermentable liquid. In a real sense, watermelon juice processing waste stream would be diversified into bioethanol production. Watermelon is a water based fruit ,the juice extracted from it could be serve as a diluents for concentrated fermentable sugar sources such as molasses that demands closely dilution to approximately 25%(weight per volume) sugar before fermentation. About the 7% to 10%(weight per volume) additionally are almost there to ferment sugars in watermelon(such as ; fructose, glucose and sucrose) would be additional the primary feedstock demands that are equivalent to the volume of watermelon juice to dilute the concentrated feedstock. The nitrogen supplement for yeast in the feedstocks are as a result of presence of free amino acid which is about 10 to 40 micromole per milliliters in watermelon juice such as sugar cane and molasses that have lack available nitrogen levels to stabilize the peak yeast growth and ethanol production. Investigation for optimization of parameters for watermelon rind as feedstock for fermentation has been carried in this research.(vanZyl *et Lynd* 2007).

According to (Kim *et al* 1984) reported on the factors that affects the fermentation of watermelon rind for the ultimate production of vinegar, but the optimization for maximal values of ethanol production was not only one of the it objectives. His purpose was to examine watermelon juice or rind as a whole or as a waste stream from neutral-ceuticals production, as a diluents feedstock and nitrogen supplement in production of ethanol biofuel systems.

2 METHODOLOGY

The following methods and materials used to carried the experiments were listed below:

2.1 SAMPLE COLLECTION

The watermelon rind was collected from watermelon sellers near Bosso Market, Minna Niger state. It was washed in order to remove the sand and dirt, and then it was cut into smaller sizes. After, it was sun dried for two days to reduce its water content before it was oven dried in hot air at 65^oC for 24 hours ant it was weighed to be 150grams.

2.2 Culturing of *Saccharomyces Cerevisiae*

Saccharomyces Cerevisiae yeast was separated from waste material from soil samples rich in vineyard such as overripped or unwanted grapes. Sterilized container was used to collect the sample. The sample from soil was dissolved with distilled water and allowed to Settled, the supendant was diluted by dilution and yeast extract peptone, and Dextrose (YEPD) plates were used to inoculated the samples. The plates contain the sample was incubated at 30^oC for 48 hours. The yeast grown was separated and identified as *Saccharomyces Cerevisiae* (Kregervan *et Eds*, 1984).

2.3 Culturing of *Aspergillus Niger*

Aspergillus Niger was a fungal enzyme which was cultured and screened of local paddy and groundnut crop field from different soil sample. The fungus collected was cultured and maintained on medium of potato Dextrose agar at 30^oC.The fungal growth was identified as *Aspergillus* (Barnett *et Hunter*, 1998) and (Alexopoulous *et al*, 1996).

2.4 Preparation of 1% Sodium Hydroxide solution

10 grams of sodium hydroxide pellet was measured and weighed with weighing balance into a beaker and 1000ml of distilled water was added into the beaker and stirred thoroughly to obtain a homogeneous solution.

2.5 Pretreatment

After the watermelon rind was dried in hot dry air, the sample was ground into fine powder form, and weighed and recorded as 150 grams. The sample was transferred into a container, and then the prepared 1% NaOH was added into the container and soaked for two hours. After soaking, the sample was washed thoroughly to remove the remaining impurities with distilled water and filtered. The filtrate was discarded, then the residual was oven dried, then the sample was brought out, crushed and sieve to finer structure and sample was weighed to be 90.4 grams.

2.6 Simultaneous Saccharification and Fermentation procedure

As the method implies, fermentation takes place immediately after saccharification or hydrolysis, in this experiment 15 runs was carried out according to design expert software using Box-Behnken Design RSM (Response Surface Methodology) and 27 runs according to the factorial design experiment

3 RESULTS AND DISCUSSION

The results obtained from the fermentation of the hydrolysate using *saccharomyces cerevisiae* and characterization of the bio-ethanol produced. And the effect of temperature, substrate concentration and time on the fermentation process.

Effect of Temperature on Fermentation

From the graph shown on figure 1, it was observed that temperature is very important in fermentation. The highest value of ethanol yield percentage in volume ratio is 20.3 at the temperature of 30°C. At higher temperature, the ethanol yield decreases. Therefore the ethanol yield is inversely proportional to the temperature.

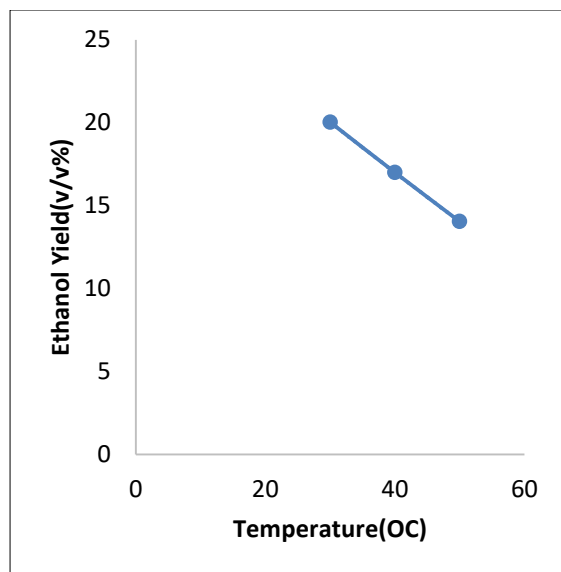


Figure 1: Graph of ethanol yield versus temperature

Effect of Substrate Concentration on Fermentation

The substrate concentration is also very important on fermentation. The highest ethanol yield on substrate concentration of 2 g/ml is 20.3 of percentage volume ratio. The above expression is shown in figure 2 below

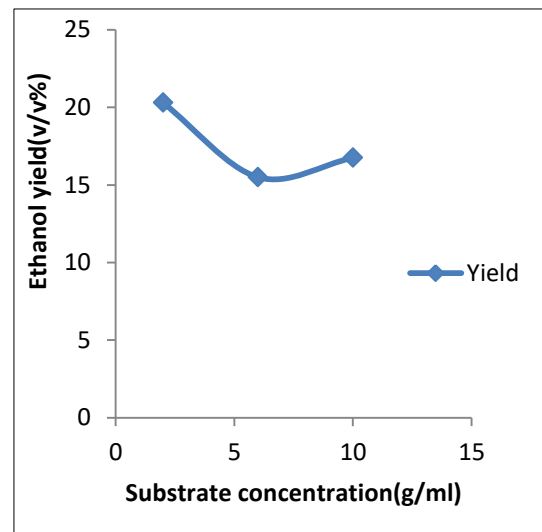


Figure2: Graph of ethanol yield versus substrate concentration

Effect of Time on Fermentation

From Figure 3 below, it was indicated that time is also important in varying the parameter for fermentation process. As the reaction time increases from 20-30 hours the ethanol yield increases. At the reaction time between 40-50 hours, the ethanol yield is highest at range 16-18 (v/v %). At the higher reaction time between 60-80 hours, the ethanol yield increases.

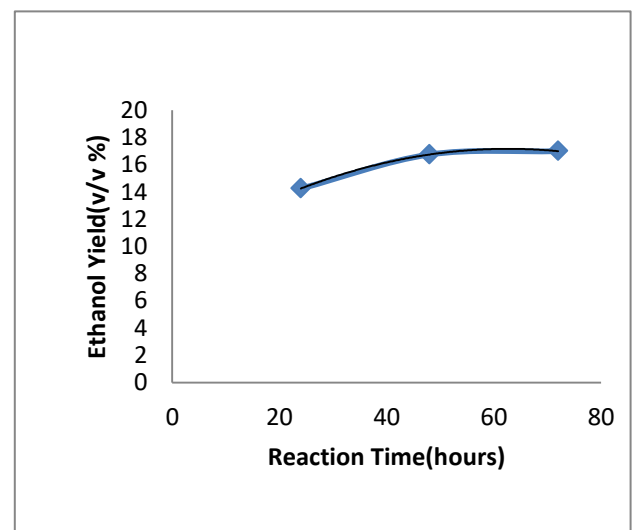


Figure 3: Graph of ethanol yield versus reaction time

3.1 EQUATIONS

ANOVA (Analysis of Variance)

ANOVA is a software used to optimise the variables to obtain the optimum (maximum and minimum) value. The optimization step was using 15-runs Box-Behnken design to identify the significant factors for fermentation process. Temperature, reaction time and substrate concentration

ANOVA for Response Surface Quadratic Model

The design and results of experiments were carried out by box-behnken design. The result obtained were submitted to analysis of variance on SASA package, with the regression model given as:

$$= 14.35 - 1.871X_1 + 1.5X_2 - 0.38X_3 + 1.19X_1X_2 + 0.70X_1X_3 - 1.06X_2X_3 + 0.00X_1^2 - 1.54X_2^2 + 1.75X_3^2 \quad (1)$$

The Equation (1) above is for coded factors.

$$Y = 27.696 - 0.52938X_1 + 0.18724X_2 - 1.576(6X_3 + 0.00494X_1X_2 + 0.01750X_1X_3 - 0.011068X_2X_3 + 0.000X_1^2 - 0.00266927X_2^2 + 0.10937X_3^2) \quad (2)$$

The equation (2) above is for actual factors.

Where Y is response value that is , ethanol yield production, and X_1, X_2 and X_3 are the coded and actual factors of temperature, time and substrate concentration respectively. The Model F-value of 4.97 implies the model is significant. There is only a 4.61% chance that a “Model F-value” this large could occur due to noise. Values of “Prob> F” less than 0.050 indicate model terms are significant. In this case X_1, X_2 and X_3 are significant model terms. Values greater indicate the model terms are not significant. If there are many insignificant model terms (not counting those required to support hierarchy), model reduction may improve your model.

The analysis of variance of the quadratic regression model demonstrated that eq.1 was a highly significant model, as was evident from the Fischer’s F-test with a very low probability value [$P_{\text{model}} > F$] = 0.0111]. The model’s goodness of fit was checked by determination coefficient (R^2). In this case, the value of the determination coefficient ($R^2 = 0.8995$) indicate that only 4.61% of the total variation were not explained by the model. The value of the adjusted determination coefficient [$\text{Adj}(R^2) = 0.7185$]. The Lack of Fit F-value of 1.81 implies the Lack of Fit is not significant relative to the pure to noise. There is 37.54% chance that Lack of Fit, a large value could occur due to noise. All the explanations are illustrated on Table I below:

3.2 TABULATION

Table 1: ANALYSIS OF VARIANCE FOR THE FITTED QUADRATIC POLYNOMIAL MODEL

Terms	Effect	SS	DF	F Ratio	P > F
X_1	-0.5293	27.9400	1	15.4500	0.0111
X_2	0.18724	18.0000	1	9.9500	0.0252
X_3	-1.5765	1.1600	1	0.6400	0.4590
X_1^2	0.0000	1	0.0000	0.0000	1.0000
X_1X_2	0.00495	1	5.6400	3.1200	0.1376
X_1X_3	0.01750	1	1.9600	1.0800	0.3455
X_2^2	0.00266	1	8.7300	4.8300	0.0794
X_2X_3	0.01106	1	4.5200	2.5000	0.1749
X_3^2	0.10937	11.3100	11.310	6.2500	0.0545
Model	-	80.9100	9	4.9700	0.0461
Error	-	2.4300	2		
Total	-		14		

Note: SS=Sum of square, DF=Degree of freedom

Effect of Temperature and Substrate Concentration and their interactive effect on Ethanol production.

From figure 4 below, from the 3-D graph, the highest ethanol yield is 18.9 (v/v%) with substrate concentration of 2g/ml and the temperature of 50°C.

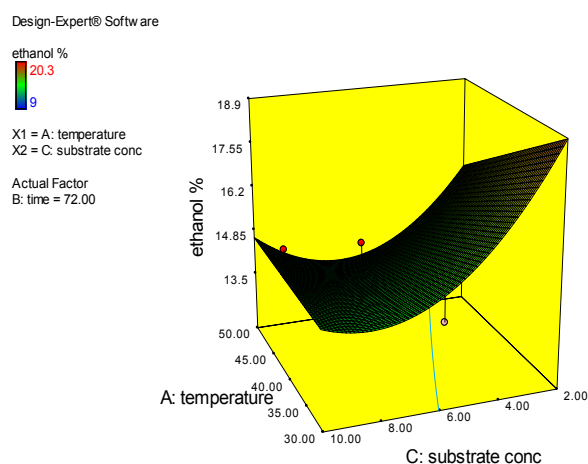


Figure 4: Response Surface plot of the interaction effect of Substrate Concentration and Temperature on the yield of ethanol.

Effect of Time and Substrate Concentration with interactive effect on Ethanol production

From the 3-D graph in figure 5 below, the highest ethanol yield is between 18.725-20.3 (v/v %) of the

substrate concentration of 2g/ml and the reaction time of 48 hours

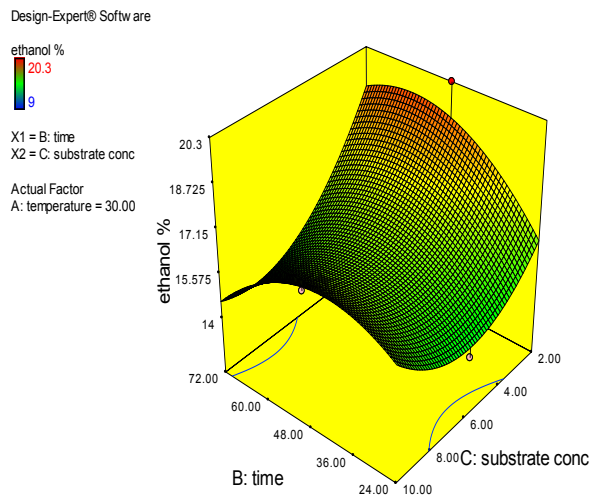


Figure 5: Response Surface plot of the effect of the interaction of the substrate concentration and time on the yield of ethanol.

Effect of Temperature and Time with their interactive Effect on Ethanol production

From the 3-D graph in figure 6 below, the ethanol yield is 14.5(v/v %) at the time of 48 hours and temperature of 30°C

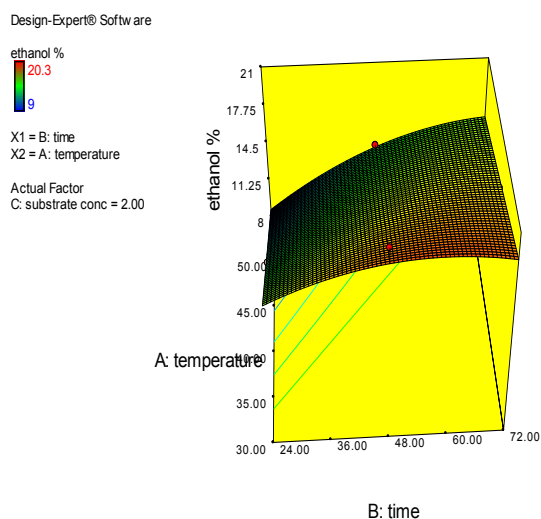


Figure 6: Response Surface plot of the effect of the interaction of the temperature and time on the yield of ethanol.

4 CONCLUSION

From the research carried out, it has been concluded that water melon rinds are suitable as a feedstock for production of bioethanol using *saccharomyces cerevisiae* as yeast the simultaneous saccharification and fermentation process and it given low cost and completion with food crops they are cost effective as raw materials even though starchy materials give a better yield. The optimum ethanol yield in volume percent of water melon rind was observed to be 20.3% at 30°C, 2g/mL for 48 hours.

The regression analysis analyzed for watermelon rind fermentation is at most fair representation of the process. The mathematical model developed for the fermentation of watermelon rind is also a very good representation of the process. The production of bioethanol from watermelon rind can provide sufficient and non-pollutant to compliment the current use of fossil and hydrocarbon based fuels. Since during the production of bioethanol from water melon rind, no odour was perceived. Then siting the plant for this will be friendly to human health and environment itself.

REFERENCES

- Alexopoulos, C. J., Charles, W., Mims, M.&Blackwell,M. *Intro-ductiry Mycology 4th edition*. Wiley, 1996
- Antoni, D.,& Zverlov, V. V. (2007)."Biofuels from microbes *Applied Microbiology and Biotechnology* 77(1): 23-35.
- Attfieid P. V. & Bell,P. J. L. (2006).Use of population genetics to derive non recombinant *Saccharomyces cerevisiae* strains that grow using xylose as a sole carbon source. *FEMS Yeast Research* 6(6): 862-868.
- Balat, M. & Balat, H (2008).Progress in bioethanol processing. *Progress in Energy and combustion. Sci.* 34; 551-573.
- Barnett, H. L. & Hunter B. B, (1998). Illustrated Genera of imperfect fungi. *Macmillian Publishing Company*, New York .U.S.A
- Cakar, Z. P., Seker, S. & U. O. (2005). "Evolutionary engineering of multiple stress resistant *Saccharomyces cerevisiae*." *FEMS Yeast Research* 5(6-7): 569-578.
- Cardona, C. A. & Sanchez, O. J. (2007). "Fuel ethanol production: Process design trends and integration opportunities. *Bioresource Technology* 98(12): 2415-2457.
- Chang, M. C. Y. (2007). Harnessing energy from plant biomass. *Current Opinion in Chemical Biology* 11(6): 677-684.
- DenHaan, R., & Rose, S. H.(2007). "Hydrolysis and fermentation of amorphous cellulose by recombinant *Saccharomyces cerevisiae*." *Metabolic Engineering* 9(1): 87-94.

- DOE. (2005). Cellulose Structure and Hydrolysis Challenges. U.S. Department of Energy office of science retrieved 09.12.2008 from <http://genomics.energy.gov/gallery/gtl/detail.np/detail.-36.html>.
- Doi, R. H. (2008). Cellulases of mesophilic microorganism Cellulosome and noncellulosome producers. *Incredible Anaerobes: From Physiology to Genomics to Fuels*. Oxford, England, Blackwell Publishing. **1125**: 267-279.
- Hahn-Hagerdal, B., & Galbe, M. et al. (2006). Bio-ethanol - the fuel of tomorrow from the residues of today. *Trends in Biotechnology* **24**(12): 549-556.
- Hill, J. (2007). Environmental costs and benefits of transportation biofuel production from food- and lignocellulose-based energy crops. A review. *Agronomy for Sustainable Development* **27**(1): 1-12. Hahn
- Himmel, M. E., & Ding, S. Y. (2007). "Biomass recalcitrance: Engineering plants and enzymes for biofuels production. *Science* **315**(5813): 804-807.
- Kregervan Rij, & Eds, N.J.W. (1984). *The Yeasts, A taxonomic study third revised and enlarged edition*. Elsevier, Amsterdam, 1004
- Lynd L.R., & Wang M.Q. (2004). A production specific framework for evaluating the potential of biomass-based products to displace fossil fuels. *J. Ind. Ecol* **7**, 17-32
- Lynd, L. R., & van Zyl, W. H. (2005). Consolidated bioprocessing of cellulosic biomass: an update. *Current Opinion in Biotechnology* **16**(5): 577-583.
- Lynd, L. R., & Weimer, P. J. (2002). "Microbial cellulose utilization: Fundamentals and biotechnology. *Microbiology and Molecular Biology Reviews* **66**(3): 506-577.
- Mustafa, V. & Sanjay, P. (2014). Bioethanol Production: Current Feedstock and Current Technologies. *Journal of Environmental Chemical Engineering* **2**(1): 573-584
- Nalley, L. & Hudson, D. (2003). The potential viability of biomass ethanol as a renewable fuel source. *A discussion in Starkville, MS* Mississippi State University-staff report 2003
- Nevoigt, E. (2008). Progress in metabolic engineering of *Saccharomyces cerevisiae*. *Microbiology and Molecular Biology Reviews* **72**(3): 379-412.
- Sanchez, O. J. & C. A. Cardona (2008). Trends in biotechnological production of fuel ethanol from different feedstocks. *Bioresource Technology* **99**(13): 5270-5295.
- Shaw, A. J., & Podkaminer, K. K. (2008). Metabolic engineering of a thermophilic bacterium to produce ethanol at high yield. *PNAS* **105**(37): 13769-13774.
- Sticklen, M. B. (2008). Plant genetic engineering for biofuel production: towards affordable cellulosic ethanol. *Nature Reviews Genetics* **9**(6): 433-443.
- Schuster, A. & Schmol, M. (2010). Biology and Biotechnology of *Trichoderma* Apple. *Microbial biotechnol* **87**: 787-799.
- Thiyam, B & Sharma G.D. (2013). post harvest diseases of fruits caused by fungi during storage in cachar district, Asam. *International Journal of Life Sciences* **1**(3): 190-192
- Teherzadeh & Karimi (2007). Bio resources- Enzyme bases ethanol pp 701.
- Tengerdy, R. P. & Szakacs G. (2003). Bioconversion of lignocellulose in solid substrate fermentation. *Biochemical Engineering Journal* **13**(2-3): 169-179.
- Van Maris, A. J. A., & Abbott, D. A. (2006). Alcoholic fermentation of carbon sources in biomass hydrolysates by *Saccharomyces cerevisiae*: current status. *Antoine Van Leeuwenhoek International Journal of General and Molecular Microbiology* **90**(4): 391-418.
- vanZyl, W. H & Lynd, L. R. (2007). consolidated bioprocessing for bioethanol production using *Saccharomyces cerevisiae*. *Biofuels*. **108**: 205-235.
- Walter, A., & Rosillo-Calle, F. (2008). Perspectives on fuel ethanol consumption and trade. *Biomass & Bioenergy* **32**(8): 730-748.
- Weng, J. K., & Li, X. (2008). "Emerging strategies of lignin engineering and degradation for cellulosic biofuel production." *Current Opinion in Biotechnology* **19**(2): 166-172.



Use of Carbide Waste as a Mineral Filler in Hot Mix Asphalt

*Murana, A. A¹ & Musa, Y²

¹Department of Civil Engineering, Faculty of Engineering, Ahmadu Bello University, Zaria, Kaduna State, Nigeria

²Department of Civil Engineering, Federal Polytechnic, Bida, Niger State, Nigeria

*Corresponding author email: fatinoyi2007@gmail.com, +2348036376697

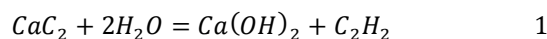
ABSTRACT

The use of mineral filler in hot mix asphalt (HMA) is intended to improve the properties of binder by reducing the binder inherent temperature susceptibility and to make the asphalt harder and stiffer. Conventional mineral filler materials that are being used in asphalt concrete are stone dust and Portland cement. The rising cost of these materials has led to use of alternative waste materials. Carbide is a waste material that can be used to improve the properties of HMA because of its high percentage of calcium oxide. This research objective is to evaluate the possibility of using carbide waste as a filler in HMA. Using Marshall Stability test and density void analysis, the optimum bitumen content for the unmodified HMA was obtained to be 5.63%. The modified HMA was prepared by partially replacing the 7% mineral filler (stone dust) with carbide waste at 10, 20, 30 40 and 50% respectively by weight. The optimum carbide waste for the modified HMA was obtained to be 27.67% of the total mineral filler. The corresponding stability, flow, void in total mix and void filled with bitumen at optimum carbide waste content were 7.60kN, 3.43 mm, 3.90% and 77.13 respectively. These values are within the specified limit in Nigerian General Specification for Roads and Bridges, 2016. It is therefore recommended to use optimum carbide waste of 27.67% by weight of mineral filler as a replacement for stone dust in HMA.

Keywords: Carbide Waste, Hot Mix Asphalt, Marshal Mix Method, Stone Dust.

1 INTRODUCTION

Construction site in urban Nigeria is growing rapidly. The cost of construction materials is high. The introduction of an alternative material for partial replacement will reduce construction cost. Carbide waste is an alternative material that can be used as filler in hot mix asphalt because of its high content of calcium oxide composition. This waste is produce from acetylene gas welding in most mechanic villages across Nigeria, which constitutes environmental pollution. Calcium carbide is widely used in industrial acetylene production for welding tools and in chemical synthesis. The chemical formula of carbide waste is CaC_2 calcium carbide, its react with water to produce ethylene gas and the by-product is calcium oxide (CaO), which is been used for this research. This gas is used around the globe for welding, lighting, fruit ripening and metal cutting. The equation for the reaction between calcium carbide (CaC_2) and water (H_2O) to form acetylene gas (C_2H_2) and calcium hydroxide [$Ca(OH)_2$] is shown in Equation 1:



Calcium carbide +Water = Hydrated Lime +Acetylene gas

This reaction is the basis for industrial manufacture of acetylene (Bogner *et al.*, 2002).

The problem of waste accumulation exists worldwide, specifically in the densely populated areas. Waste in the construction industry and the use of rejected materials is a subject of world research (Atkinson and Sakai, 1993). Highway engineers and scientist are thinking about

different research methods to meet this growing challenge.

The incorporation of alternative materials is highly significant in road construction because such materials are in great demand. According to Barišić *et al.*, (2015), alternative materials are all materials obtained as construction waste and other types of industrial waste. Based on the instruction given in the directive 2008/98/EC, minimum 50 % of household waste, and 70 % of construction and industrial waste must be recycled and reused by 2020. Asphalt is a mixture of uniformly mixed combination of asphalt cement, coarse aggregate, fine aggregate, and other materials, depending on the type of asphalt mixture (Garber and Hoel, 2009).

Asphalt surface layer plays a fundamental role among different layers of flexible pavements and it should be able to withstand varying degree of traffic loads and constantly changing environmental conditions. Due to the nature and composition of asphalt surface layer, application of solid waste in asphalt layer reduces not only environmental pollution associated with waste disposal but also the demand for virgin aggregate which will result in cost saving (Chen, *et al.*, 2011). According to Burak and Ali, (2004) who study the use of asphalt roofing shingles in hot mix asphalt, and observed that waste shingles as an additive can improve the Marshall stability and rutting resistance of the asphalt mixtures. Manasseh (2009) investigated the effect of carbide waste on the properties of rice husk ash concrete and observed that the Compressive strength and indirect tensile strength results shows that CW has effect on the strength of concrete made with RHA-cement combination.

Compressive strength test result of concrete made with RHA-cement exhibited great improvement with the addition of 10% CW after which a decline in compressive strength was observed, similar trend was also observed with indirect tensile strength of cement-RHA-CW combination. Hence the recommendation of a combination of 10%RHA and 10% CW for use in concrete production for use in rigid pavement construction, because peak compressive strength at this replacement level is comparable with result obtained with the use of only cement as binder.

1.1 MINERAL FILLER

The term mineral filler can be defined as the mineral fine particle with physical size passing the 200 mesh sieve i.e smaller than 75 micron (0.075mm square mesh). The use of mineral filler in asphalt mixtures are intended to improve the properties of binder by reducing the binder's inherent temperature susceptibility (Tunncliff, 1962). Filler play a dual role in asphalt mixtures, first; they act as a part of mineral aggregate by filling the voids between the coarser particles in the mixtures and thereby strengthening the asphalt mixture, second; when mixed with asphalt, filler form mastic, a high consistency binder or matrix that cements larger binder particles together; most likely a major portion of the filler remains suspended in the binder while a smaller portion becomes part of the load bearing framework (Harris and Stuart, 1995).

Kim *et al.*, (2003) said majority of the research on the effect of filler in asphalt is primarily based on engineering properties of the fillers such as content of the filler and gradation. Only a small number of researches have been dedicated to investigate the physicochemical properties of filler-asphalt systems. These properties are believed to have considerable influence on the performance of the asphalt mixtures.

1.2 CARBIDE WASTE

Carbide waste is a waste material generated from oxy-acetylene gas used in welding works in most automobile workshop (Chukwudebelu *et al.*, 2013). These wastes are found in abundance in our environment and many researches on it have been carried out to determine its use as a construction material in civil engineering. Nattapong *et al.*, (2010) in his research work the effects of calcium carbide residue-fly ash Binder on mechanical properties of concrete and observed that the hardened concrete produced from calcium carbide residue – fly ash mixtures had mechanical properties similar to those from normal Portland cement concrete. Carbide waste is rich in calcium oxide (CaO) which is an essential ingredient in mineral filler. The performance of asphalt is incredibly influential by this ingredient. Increase in the value of CaO, SO₃ and LOI increases the complex shear modulus and stiffness of mastic asphalt. Thus improves the rutting

resistance at high temperature, stripping to moisture attack, minimize pavement raveling, and also improve aging resistance (Osuya, 2017).

From review of literature of other researchers, calcium oxide composition of carbide waste ranges between 50 – 61% which is close to the range obtained for Portland cement.

The aim of the research is to determine the optimum carbide waste content as filler in hot mix asphalt. As part of the objectives of this paper, the properties of the constituent materials of HMA was determined; the chemical composition of the carbide waste was determined using XRF spectrum; both the optimum bitumen content of the unmodified HMA and the optimum carbide waste of the modified HMA was the determined.

2 METHODOLOGY

2.1 MATERIALS

The materials used for this research include mineral filler (carbide waste), aggregates (coarse, fine and stone dust) and a binder (bitumen). The carbide waste was obtained from the waste dumps created by automobile welders in Zaria metropolis, Nigeria. The aggregate (coarse, fine and stone dust) used are crushed rock obtained from quarry site of Mother Cat Construction Company in Zaria. The binder (bitumen) of grade 80/100 was obtained from Mother Cat Construction Company, Zaria.

2.2 METHODS

The method used in this work is outlined below.

Test of aggregates: The following tests were conducted on the aggregates. Impact and Crushing values, sieve analysis, specific gravity, flakiness and elongation index.

The Aggregate Crushing Value (ACV) gives relative measure of the resistance of an aggregate to crushing under a gradually applied compressive load. The aggregate impact value test provides a relative measure of the resistance of an aggregate to sudden shock or impact. These tests were carried out on the coarse aggregates in accordance with BS 812 (1990) at the concrete technology laboratory, Ahmadu Bello University, Zaria

Test on bitumen: The physical properties' test carried out on the bitumen are penetration, ductility, specific gravity, solubility and softening point test. These tests were carried out at the Highway and Transportation Laboratory, Department of Civil Engineering, Ahmadu Bello University, Zaria in accordance to BS standard (BS EN 12591, 2009).

Test on mineral filler: Chemical composition using X-ray fluorescence, sieve analysis and specific gravity.

Marshal stability test: Marshal Stability tests on asphalt briquettes in accordance to ASTM standard (ASTM D6926-16, 2016) was conducted to determine the optimum binder content and optimum bone ash replacement. The average of the sum of binder contents at maximum stability, maximum bulk density and 5.5% air void in total mix was used as the optimum bitumen content.

3 RESULTS AND DISCUSSION

3.1 TEST RESULT OF VIRGIN BITUMEN

From the test carried out on virgin bitumen 80/100 penetration grade as shown in Table 1. The result falls within the limits specified by the Nigerian General Specification for Road and Bridges, (NGSRB, 2016), thus, the bitumen is suitable for the HMA design.

Table 1: Test Conducted on Virgin Bitumen

Test Conducted	Unit	Result	Specification
Penetration	0.1mm	84	60 -70
Softening point	°C	49	48-56
Ductility @ 25°C	cm	77.7	100 (Min)
Specific gravity	NIL	1.042	1.01-1.06
Flash-point	°C	251	250 (Min)
Fire-point	°C	218	NIL
Solubility in C ₂ S	%	100	99 mins
Viscosity @ 60 °C	Secs	1522	NIL

3.2 PROPORTION OF AGGREGATE SIZE

From the sieve analysis conducted, Figure 1 shows the gradation of particle size distribution curve.

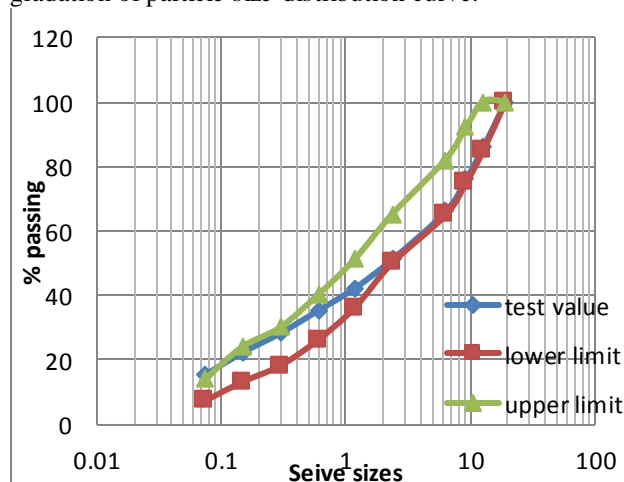


Figure 1: Gradation Curve of Aggregate

This curve shows that the mix was well graded, and maximum volume of aggregate will be achieved in the aggregate mix (Chen and Richard-liew, 2003). A dense material will be obtained when aggregate is compacted (Brennan and O'Flaherty, 2002). The gradation curve is also within the required envelop specified by NGSRB,

(2016).

3.3 TEST ON AGGREGATES

The results of the various physical properties conducted in this research are discussed and presented below: The specific gravity, aggregate crushing value and aggregate impact value test results of coarse and fine aggregates are presented in Table 2.

The values of specific gravities of coarse aggregates and fine aggregate presented in Table 2 are within the acceptable values recommended by Mageswari and Vidivelli (2009). Flakiness and Elongation index of 11.05 and 19.59 are both within the allowable limits specified by NGSRB, (2016). There will be reduction in strength of pavement if flaky and elongated aggregates are in enormous proportion as the aggregate will have low workability in the mix and then tend to break under apply load. The aggregate crushing value which is obtained to be 26.22% is within the acceptable limits of not exceeding 30% for wearing course by NGSRB, (2016). The aggregate impact value which is 28.89% is also within acceptable limits specified by the NGSRB, (2016). Aggregates with AIV greater than 30 are normally regarded as being too weak and brittle for use in pavements.

Table 2: Physical Properties of Aggregates

Properties	Test values	Standard Spec.		Remarks
		Min	Max	
Specific Gravity (Coarse)	2.637	2.6	2.9	OK
Specific Gravity (fine)	2.544			OK
Specific gravity (filler)	2.592			OK
Flakiness Index	11.05	-	35	OK
Elongation Index	19.59	-	25	OK
Aggregate Crushing value (%)	26.22	-	30	OK
Aggregate Impact value (%)	28.89	-	35	OK

3.4 TEST ON CARBIDE WASTE

Table 3 shows the Percentage of the Oxide composition of Carbide Waste. It was observed that Calcium Oxide (CaO) was 51.599%. Calcium oxide increases the complex shear and modulus of stiffness of mastic asphalt. Consequently, this in turn improves the stripping to moisture attack, rutting resistance at elevated temperature, minimize pavement raveling and improve aging resistance. Ferric oxide (Fe₂O₃) also aids in absorption of excess oil in bituminous mixture (Ahirich, 1991). This property could decrease the pavement distress behavior by the absorption of excess oil in the bituminous mixture. Aluminium oxide (Al₂O₃) helps in creep

recovery, which means better resistance to permanent deformation among the modified asphalt cements, regardless of the stress level (Mubaraki et al., 2016).

Table 3: Oxide Composition of Carbide Waste

Element	Concentration (Weight %)
Na ₂ O	0.000
MgO	1.000
Al ₂ O ₃	11.532
SiO ₂	7.879
P ₂ O ₅	5.082
SO ₃	3.286
Cl	3.082
K ₂ O	3.102
CaO	51.599
TiO ₂	2.066
Cr ₂ O ₃	0.000
Mn ₂ O ₃	0.000
Fe ₂ O ₃	10.320
ZnO	0.000
SrO	2.052

3.5 MARSHALL PROPERTIES OF THE CONTROL SAMPLES

3.5.1 STABILITY (CONTROL)

Figure 2 shows the relationship between stability and bitumen content.

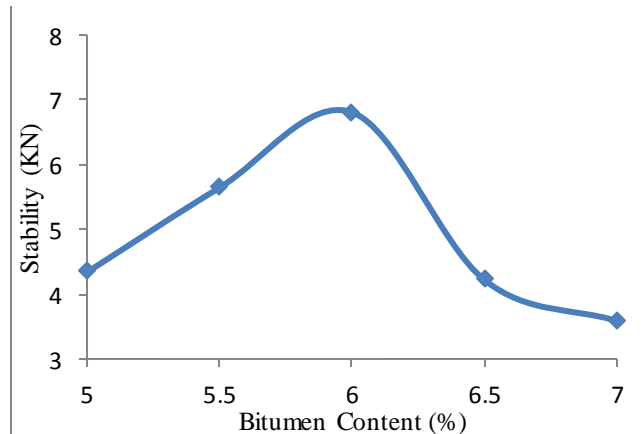


Figure 2: Relationship of Marshall Stability to Bitumen content

From Figure 2, it was observed that stability rises from 5% bitumen content up to 6% bitumen content and then it begins to drop. The observable fact is that aggregates are lubricated as bitumen content is being increased which lead to the rearrangement of the aggregate to be more densely packed together. Increase and dropping in trend of stability is due the transmitted load through the Hot-mix asphalt via hydrostatic pressure from the binder and inter-granular interaction between the aggregates particle. As

bitumen is been added at various percentages, it will cause the bitumen to fill up the voids thereby causing a drop in stability. The maximum stability of 6.9kN was obtained from the graph at 5.9% bitumen content.

3.5.2 FLOW (CONTROL)

Figure 3 shows the relationship between flow and binder content and it is observed that the flow values rises from 4.1mm to 6.0mm as the bitumen content increases which is in accordance to the range of 2mm-6mm specify by (Nigerian General Specifications for Roads and Bridges, 2016) for wearing course. The occurrence of such trend is due to an increase in flexibility of the mix as the binder content increases leading to additional displacement in the specimen, thus flow continue to increase.

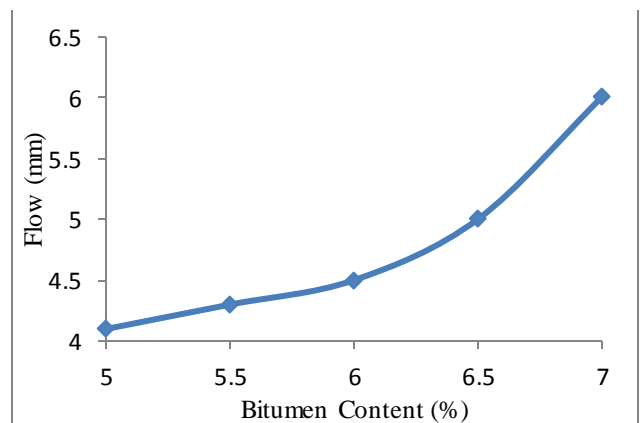


Figure 3: Relationship of Flow to bitumen content

3.5.3 BULK DENSITY (CONTROL)

Figure 4 shows the relationship between bulk density and binder content.

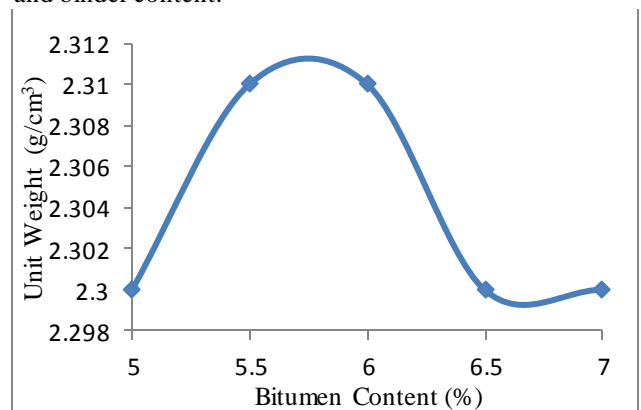


Figure 4: Relationship of Bulk Density to Bitumen content

From the figure 4, it shows that the bulk density rises and drops with the maximum bulk density achieved between 5.5 and 6% bitumen content and it is obtained to be 2.312g/cm³. The decrease is as a result of more bitumen cause the sample to be less dense than those with less bitumen.

3.5.4 VOID IN THE MIX AGGREGATE (CONTROL)

Figure 5 shows the curve of voids in the mix aggregate (VMA) it is observed from the graph that it increases as the bitumen content increases. In other words, VMA is the volume of inter-granular void space between the aggregate particles of a compacted paving mixture. It includes the air voids and the volume of bitumen not absorbed into the aggregate. VMA is expressed as a percentage of the total volume of the mix. When VMA is too low, there is not enough room in the mixture to add sufficient bitumen binder to coat adequately over the individual aggregate particles. Also, mixes with a low VMA are more sensitive to small changes in bitumen binder content. Excessive VMA will cause unacceptably low mixture stability (Roberts et al., 1996). Generally, a minimum VMA of 17% is specified.

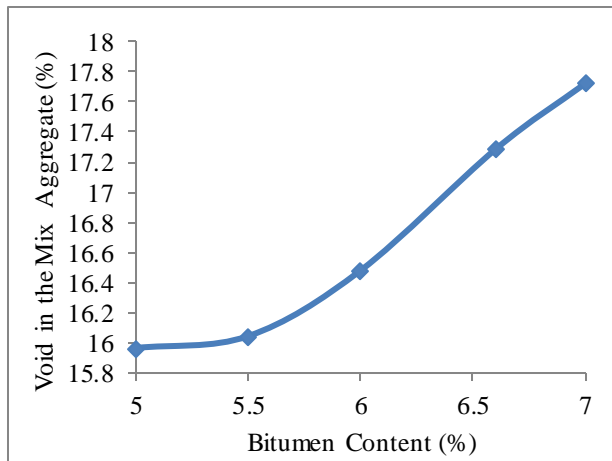


Figure 5: Relationship of Voids in the Mix Aggregate to Bitumen content

3.5.5 VOID FILLED WITH BITUMEN (CONTROL)

Figure 6 shows the relationship between void filled with bitumen and binder content. This represents the volume of the effective bitumen content. It can also be described as the percent of the volume of the VMA that is filled with bitumen. VFB is inversely related to air voids and hence as air voids decreases, the VFB increases. The decrease of VFB indicates a decrease of effective bitumen film thickness between aggregates, which will result in higher low-temperature cracking and lower durability of bitumen mixture since bitumen perform the filling and healing effects to improve the flexibility of mixture.

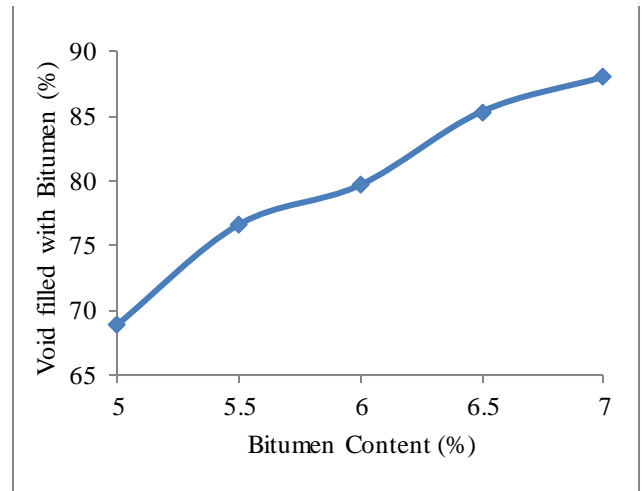


Figure 6: Relationship of Void filled with Bitumen to Bitumen content

3.5.6 PERCENT AIR VOID IN THE PAVING MIXTURE (CONTROL)

Figure 7 shows the relationship between percent air void and binder content. From this figure, it is observed that there is reduction in percent air void. This may be due networking effect within the mix as lower G_{mb} correlate to higher air voids and higher G_{mb} correlate to lower air voids. The amount of air voids in a mixture is extremely important and closely related to stability, durability and permeability. Excessive air voids in the mixture would result in cracking due to insufficient bitumen binders to coat on the aggregates, while too low air void may induce more plastic flow (rutting) and bitumen bleeding. However, the percent air void from Figure 4.7 shows that from 5-6% binder content are within the specification range of 3-5% of AASHTO standard (AASHTO T 312, 2009).

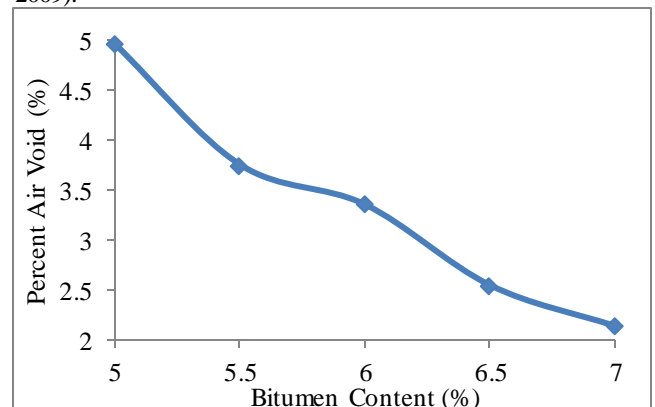


Figure 7: Relationship of Percent Air Void in the paving Mixture to Bitumen content

3.5.7 OPTIMUM BITUMEN CONTENT (OBC)

From Figures 2 – 7, the average of sum of the bitumen content for maximum stability, maximum bulk density

and percent voids within the limits specified (average of the limits) gives the Optimum Bitumen Content (OBC). From Figures 2, 4 and 7, the values of bitumen contents at maximum bulk density, maximum stability and median of air voids were 5.7%, 5.9% and 5.3% respectively. The average values of these values were obtained to be 5.63% which serves as the Optimum Bitumen Content.

The result of the comparison of Marshall Test values for the control mix at optimum bitumen content are presented in Table 5. It shows that the optimum bitumen content is within 5.0-8.0% specified standard value. Stability value is also within the range of not less 3.5kN, flow value is slightly higher than 2-4mm specified value, void in total mixture is within the range of 3-5% specified value and void filled with bitumen is also within the range of standard. The test values are within the range specified in the (Nigerian General Specifications for Roads and Bridges, 2016).

Table 5: Comparison of Marshall Test Values for the Control Mix at Optimum Bitumen Content with the (NGSRB, 2016).

Test	Result (Control)	Specification (NGSRB Wearing Course)
Optimum Bitumen Content	5.63 %	5.0-8.0%
Stability	6.9kN	Not less than 3.5kN
Flow	4.3mm	2mm-4mm
Void in Total Mixture (Pa)	3.6%	3-5%
Void Filled with Bitumen	78%	75-82%

3.6 MARSHAL STABILITY TEST FOR CARBIDE WASTE

3.6.1 STABILITY (MODIFIED SAMPLES)

Figure 8 shows the relationship between stability and carbide waste content. Its indicate that stability of the carbide waste replacement follows similar trend with that of the control mix that is, its increases initially, reaches a maximum value and then decreases with increase in carbide waste content. This behavior was equally observed by (Murana and Sani, 2015) when bagasse ash was used to partially replace cement in HMA. Consequently, stability of carbide waste replacement in hot-mix asphalt has a higher stability value of 7.60kN which is higher than that of the control hot-mix Bituminous mixture is an inconsistent, non-uniform, multi-phased composite material. Therefore, excessive carbide waste may not disperse uniformly, while coagulate together to form weak points inside the mixture.

As a result, stability decreases at high carbide waste contents. This result shows that the mixture using carbide waste as replacement result in higher performance than the control mixture.

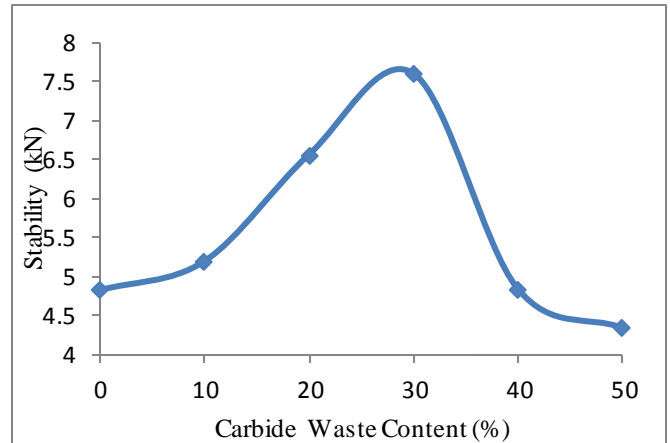


Figure 8: Relationship of Carbide Waste to Stability

3.6.2 FLOW (MODIFIED SAMPLES)

Figure 9 shows the relationship between flow and carbide waste content. The figure shows that the highest flow value was obtained at zero percent carbide waste content and the flow value decreases after adding carbide waste content to the mixture. This was equally observed by (Bindu, 2012) the influence of additives on the on the characteristic of stone matrix asphalt. This is as a result of high CaO content present in Carbide waste which tend to stiffen the asphaltic concrete, the asphaltic concrete becomes less flexible and the resistance to deformation increases resulting in a low flow value. However, these values are all within the limits specified by Nigerian General Specifications for Roads and Bridges (NGSRB, 2016) that stipulated that the flow value should lie between 2-4mm.

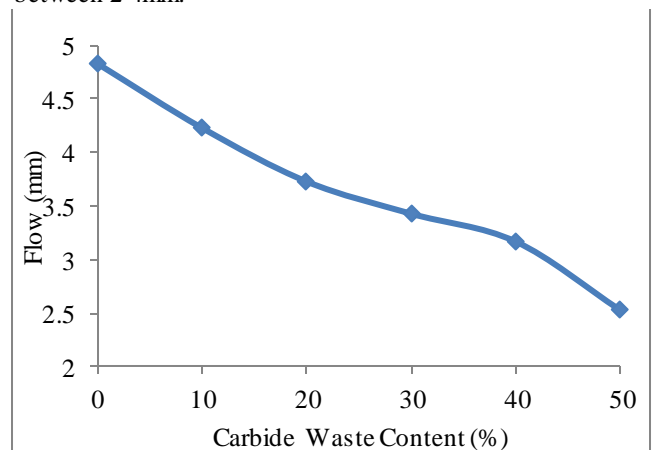


Figure 9: Relationship of Carbide Waste to Flow

3.6.3 UNIT WEIGHT (MODIFIED SAMPLES)

Figure 10 shows that the behavior of the bulk density is elastic in nature, as the CW content is increasing, there

was a corresponding increase in the values of bulk density. This trend was equally observed by (Nwaobakaba and Agwunwamba, 2014) when periwinkle shell ash was use as filler in HMA. This may be due to different specific gravities of the aggregates and a much lower specific gravity of carbide waste and they will penetrate into the aggregate and a proper coating is formed over it. Bearing in mind that better mix design is achieved with higher specific gravity. The highest value of 2.46 g/cm^3 was obtained at 30% CW content and lower values of 2.43 and 2.4 g/cm^3 were recorded at 40 and 50% CW content.

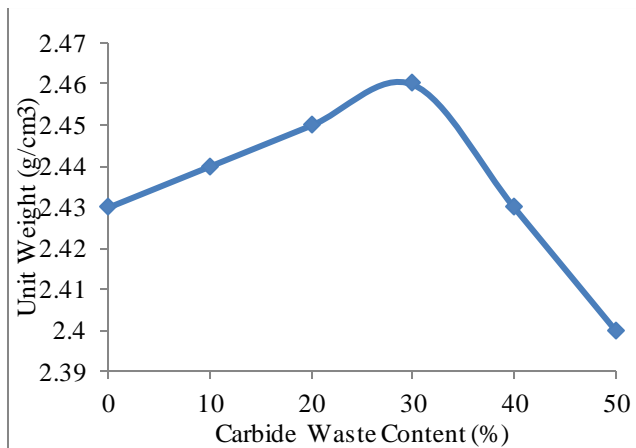


Figure 10: Relationship of Carbide Waste to Unit Weight

3.6.4 VOID IN THE MINERAL AGGREGATES (MODIFIED SAMPLES)

Figure 11 shows the relationship between void in the mineral aggregates (VMA) and carbide waste content. It can be observed from Fig. 11 that VMA decreases by the addition of carbide waste to the mixtures. This trend was equally observed by (Nwaobakaba and Agwunwamba, 2014) when periwinkle shell ash was use as filler in HMA. This may be due to the decrease of bulk specific gravity as indicated by equation for VMA. But all the results are within the specification range which also supports the use of these additives.

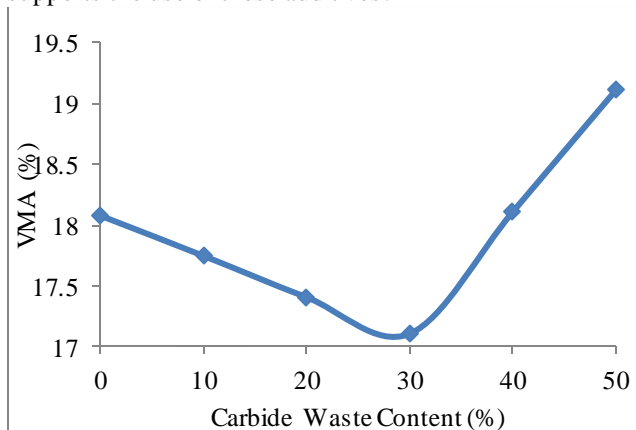


Figure 11: Relationship of Carbide Waste to Void in the Mineral Aggregates

3.6.5 VOID FILLED WITH BITUMEN (MODIFIED SAMPLES)

Figure 12 shows the relationship between void filled with bitumen (VMB) and carbide waste content. VFB of mixtures have an increase after adding carbide waste into the mixture, as shown in Fig. 12. VFB which represents the volume of the effective bitumen content in the mixture is inversely related to air voids and hence as air voids decreases, the VFB increases. This trend was equally observed by (Okobia, 2016) evaluation of sawdust ash as mineral filler in asphalt mixture.

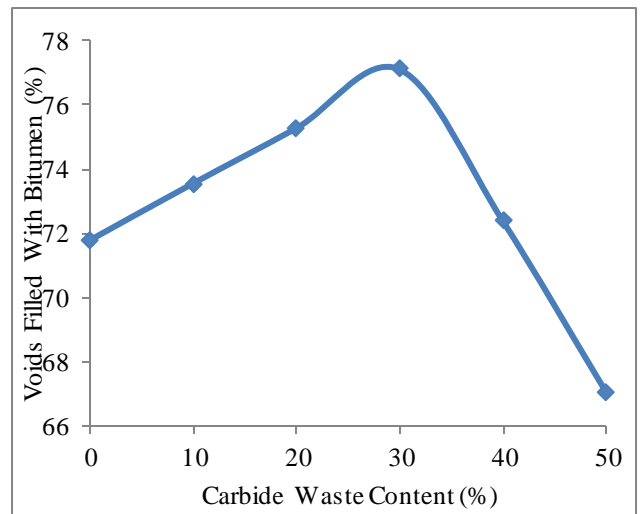


Figure 12: Relationship of Carbide Waste to Void Filled with Bitumen

3.6.6 PERCENT AIR VOID (MODIFIED SAMPLES)

Figure 13 shows the relationship between percent air void (Pa) and carbide waste content.

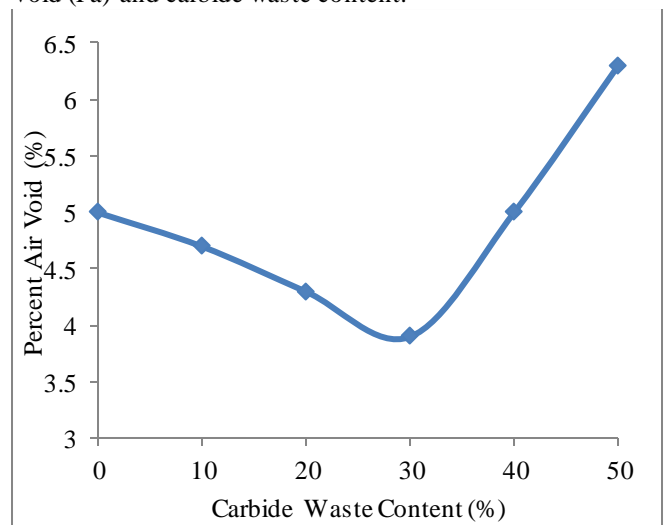


Figure 13: Relationship of Carbide Waste to Percent Air Void

It shows that as the CW content increases air void decrease at some point it begins to rise. Excessive air

voids in the mixture would result in cracking due to insufficient bitumen binders to coat on the aggregates, while too low air void may induce more plastic flow (rutting) and bitumen bleeding. Here the test results (Fig. 13) show that air void reduces after adding carbide waste into bituminous mixtures. This trend was equally observed by (Nwaobakaba and Agwunwamba, 2014) when periwinkle shell ash was used as filler in HMA. This may be due to the networking effect of the carbide waste within the mix (lower G_m correlates to higher air voids). The mixture with carbide waste has lower air void compared to the control mixtures. However, the air voids of mixtures are located within the specification range of 3% to 5% in accordance to AASHTO standard (AASHTO T 312, 2009).

From the relationships illustrated in Figures 9 – 13, it can be observed that all the Marshall Stability values for the various bone ash contents evaluated satisfy the specifications (that is, not less than 3kN) stated in the NGSRB (2016). The optimum stability value obtained was 8.76kN at 20% bone ash content. Furthermore, at 20% bone ash content, the value of flow, voids in mineral aggregate, voids in total mixture, voids filled with bitumen are given as 3.4mm, 19.17%, 6.2% and 67.65% respectively. All these are within the limits specified by the code.

Table 6 shows the comparison of Marshall properties between optimum carbide waste content and general specification. It shows that the optimum stability for carbide waste replacement is 7.6kN which is higher than that of the control mix. Flow value is lower than that of the control mixture, but is still within the 2-4mm specified value. Void in total mixture is also lower than that of the control mixture, but is still within the 3-5% specified value. Void filled with bitumen is lower than that of the control mixture, but is still within the specified value. The test values are within the range specified in the NGSRB, (2016).

Table 6: Showing the Comparison of Marshall Properties between Optimum Carbide Waste Content and General Specification

Property	Optimum Carbide Waste Content	NGSRB, (2016)	Remarks
Stability (kN)	7.60	Not less than 3.5kN	Ok
Flow (mm)	3.43	2-4	Ok
Void in Total Mix (%)	3.90	3-5	Ok
VFB	77.13	75-82	Ok

4 CONCLUSION

From this work, the following is concluded:

1. All the Marshall values for the control and investigated samples lie well within the range specified by NGSRB (2016). This indicates that the constituent materials are suitable to be used in HMA.
2. The optimum bitumen content for the control samples was obtained to be 5.63% which lie within the range specified by NGSRB (2016).
3. The chemical composition of the carbide waste shows that it has high percentage of calcium oxide (CaO) thereby making it suitable for use as mineral filler in HMA as specified by NGSRB (2016).
4. The optimum carbide waste content to partially replace stone dust in asphalt concrete mix was found to be 27.6% of the total SD. This indicates the suitability for use of carbide waste as mineral filler in HMA at an optimal value of 27.6% content by weight of SD.

ACKNOWLEDGEMENTS

The authors wish to acknowledge the assistance and contributions of the laboratory staff of Department of Civil Engineering and Department of Chemistry, Ahmadu Bello University, Zaria toward the success of this work.

REFERENCE

- AASHTO T 312 (2009). "Standard Method of Test for Preparing and Determining the Density of Hot Mix Asphalt (HMA) Specimens by Means of the Superpave Gyrotory Compactor", American Association of State Highway and Transportation Officials, Washington DC.
- ASTM D6926-16. (2016). *Standard Practice for Preparation of Asphalt Mixture Specimens Using Marshall Apparatus*. West Conshohocken, Philadelphia, PA: American Society for Testing and Materials (ASTM) International. doi:10.1520/D6926-16
- Ahirich, R.C. (1991). *The Effects of Natural Sands on Asphalt Concrete Engineering Properties*. Department of the Army, Waterways Experiment Station, Corps of Engineers. 3909 Hall Ferry Road, Vicksburg, Mississippi 39180-6199.
- Atkinson, C. J. and Sakai, E. (1993). *Ecolabeling of Building Materials and Building Products*. Building Research Establishment Information Paper. Vol.11, ser. 93.. London, UK.
- Barišić, I., Zagvozda, M., Dimter, S. (2015): *Usage of Alternative, environmentally Acceptable Materials-Experience from Eastern Croatia*, 2nd International Conference on Innovative Materials, Structures-and Technologies, IOP Conf. Series: Materials Science and Engineering 96, 2015.



- Bindu, C.S. (2012). *Influence of Additives on the Characteristic of Stone Matrix Asphalt*. Unpublished PhD Thesis, Faculty of Engineering Cochin University of Science and Technology. KOCHI – 682 022.
- BS 812: Part 112: 1990: *Methods for Determination of Aggregate Impact Value*: British Standards Institution (BSI), London, United Kingdom.
- BS 812: Part 110: 1990: *Methods for Determination of Aggregate Crushing Value (ACV)*. British Standards Institution (BSI), London, United Kingdom.
- BS EN 12591 (2009): Bitumen and bituminous binders. Specifications for paving grade bitumen: British Standards Institution (BSI), London, United Kingdom.
- Bogner, J.M., Diaz C., and Faaij A. (2002). Resources Conversion and Recycling. *Waste Management and Research Series*. 20(6): 536-540. Retrieved from <https://www.ajol.info>article>download>
- Burak, S. and Ali, T. (2004). *Use of Asphalt Roofing Shingle Waste in HMA*. *Construction and Building Materials*. 19: 337-346.
- Brennan, M.J. and O’Flaherty, C.A. (2002). *Highway Materials Used in Road Pavements*. Fourth Edition, Butterworth and Heinemann, 118-162
- Chen, M.; Lin, J. and Wu, S. (2011). Potential of Recycled Fine Aggregates Powder as Filler in Asphalt Mixture. *Article in Construction and Building Materials*. 25(10): 3909–3914. October 2011 Retrieved from <https://www.researchgate.net>
- Chen, W.L. and Richard-Liew, J.Y (2003). *The Civil Engineering Hand Book*. Second Edition, CRC. Press, LLC, 1472- 1498
- Chukwudebelu, J. A.; Igwe, C. C., Taiwo, O. E. and Tojola, O. B.. (2013). Recovery of pure slaked lime from carbide sludge: Case study of Lagos State, Nigeria. *African Journal of Environmental Science and Technology*, 7(6): 490-495.
- Garber, N.H. and Hoel, L.A. (2009). *Traffic and Highway Engineering*. University of Virginia. 4th Edition. Cengage learning Rep. in Canada by Nelson Education Ltd. P 969
- Harris, B.M. and Stuart, K.D. (1995). *Analysis of mineral fillers and mastics used in stone matrix asphalt*. *J. Assoc. Asphalt Paving Technol.*, 64: 54-95.
- Manasseh J. (2009). *Effect of Carbide Waste on the Properties of Rice Husk Ash Concrete*. *Global Journal Of Engineering Research* Vol 8, No. 1&2, 2009: 57-65 Copyright© Bachudo Science Co. Ltd Printed In Nigeria. ISSN 1596-292X www.globaljournalseries.com; Email: info@globaljournalseries.com
- Kim, Y.R., Little, D.N. and Song, I. (2003). *Effect of mineral fillers on fatigue resistance and fundamental material characteristics, mechanistic evaluation*. *Transportation Research Record* 1832, pp: 1-8. <http://144.171.11.39/view/682046>.
- Mageswari, M. and Vidivelli, B. (2009). The Use of Saw Dust Ash as Fine Aggregates Replacement in Concrete. *Journal of Environmental Research and Development, Vol. 3 No. 3*, pp. 720- 726.
- Mubaraki, M. Ali, Ismail, S.I., A. and Yusoff, N.I.M. (2016). *Rheological of Asphalt Cement Modified with ASA Polymer and Al₂O₃ Nanoparticles*. *Elsevier Journal of Advances in Transportation Geotechnics 3. The third International Conference on Transportation Geotechnics. Volume 143*, 2016, pages 1276-1284
- Murana, A.A. and Sani, L. (2015). Partial Replacement of Cement With Bagasse Ash in Hot Mix Asphalt. *Nigerian Journal of Technology (NIJOTECH) Volume 34 No. 4*, October 2017, Pp, 699-704. Retrieved from www.nijotech.com
- Nattapong, M.; Chai, J. and Thanapol, L. (2010). *Effect of Calcium Carbide Residue-Fly Ash Binder on Mechanical properties of Concrete*. *Journal of Materials in Civil Engineering*, 22(11): 1164-1170
- Okobia, E. (2016). *Evaluation of Sawdust Ash Mineral Filler in Asphalt Mixture*. Unpublished Msc. Thesis, Department of Civil Engineering Ahmadu Bello University Zaria, Kaduna. Nigeria. Pp51
- Osuya, D. O and Mohammed, H. (2017). Evaluation of Sawdust Ash as a Partial Replacement for Mineral Filler in Asphalt Concrete. *Ife Journal of Science Volume 19, No. 2*, pp. 431 – 440. <https://dx.doi.org/10.4314/ijss.v19i2.23>
- Roberts, F. L., Kandhal, P. S. and Brown, E. R. (1996), “*Hot Mix Asphalt Materials, Mixture Design and Construction*”, NAPA Research and Education Foundation, Lanham, Maryland.
- Tunncliff, D.G., (1962). *A review of mineral filler*. *Proc. Association Asphalt Paving Technology*, 31: 118-150.

REVIEW OF BIO OIL UPGRADING FROM BIOMASS PYROLYSIS

Abdullahi, M. A¹, Garba, M. U², Eterigho E. J³, & Alhassan, M⁴
Chemical Engineering Department, Federal University of Technology, PMB 65
Minna, Niger State, Nigeria.

Corresponding author email: abdulmusavespa@gmail.com, +2348035312720

Pyrolysis is a promising method of converting biomass to renewable bio-oil. However, bio-oil is crude and its use in conventional engines is restricted without efficient procedure for upgrading. A critical literature review of the current status of production and bio oil upgrading from biomass pyrolysis is presented with the aim to identify new areas for further research. The technology of thermochemical process is described. The bio-oil is characterized by undesirable properties that affect its use. These properties need to be improved upon and this aspect is considered in terms of physical, chemical and catalytic upgrading. The increasing diversity of catalytic process, particularly the current trend of dehydrogenation and deoxygenation to eliminate coke formation and increase bio-oil yield was highlighted.

Keywords: *Biomass, Catalyst, Coke, Plastic, Pyrolysis.*

1 INTRODUCTION

Growing energy depletion in the world has driven the improvement of technologies from renewable sources, such as biomass, geothermal, solar, tidal power and wind. (Brenda *et al.*, 2019). Utilisation of biomass derived fuels and chemicals would help significantly in reducing anthropogenic CO₂ emissions by providing alternatives to the consumption of traditional fossil fuels Alexander *et al.*, (2019). Renewable resources are the natural sources that can be replenished after its consumption. It can be classified into sustainable (those that can be naturally renewable) and those that can be renewable with careful planning and harvesting. The most common examples of renewable resources are solar energy, wind power, tides, hydroelectricity and geothermal power. While biomass and biofuel are examples of renewable obtained after careful planning and harvesting (Aterny *et al.*, 2011).

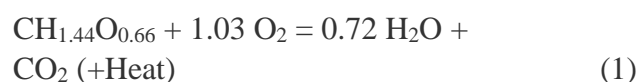
2 THERMOCHEMICAL CONVERSION PROCESSES

Thermochemical methods are more energy efficient and cost-effective (Leibbrandt *et al.*,

2011) compare to Biochemical conversions of biomass which is not cost-effective owing to the fact that the biochemical techniques can solely take advantages of cellulose and hemicellulose in lignocellulosic biomass (Anex *et al.*, 2010). These conversion technologies include torrefaction (between 200 -300 °C), pyrolysis (350-600 °C), gasification (above 800 -1200 °C) and combustion (800- 1500°C).

2.1 COMBUSTION

Combustion is a process of converting organic material such as biomass (woods, straw, bark residuals, sawdust, sawmills, switch grass and so on) by means of burning to create heat and later, to generate power through steams. The conversion can be briefly described as follows:



Note: CH_{1.44}O_{0.66} is the approximate chemical equation for the combustible portion of biomass.

Though, the amount of heat produced during combustion of biomass varies depending on species, climate, and other factors, but it is

generally about 20 Megajoules of energy per dry kilogram of biomass (Ciolkosz, 2014).

2.2. GASIFICATION

Gasification of biomass is a unique method that converts organic materials (carbon-based) in partial oxidation (not sufficient oxygen to allow for completely combustion) resulting in production of combustible gases consisting of Carbon monoxide, Hydrogen and traces of Methane. These gases when combined, producer gas or syngas is formed through different steps of thermo-chemical reactions. The gas has a low-heating value fuel with a calorific value within the range of 4.2-5.02 MJ/ Nm³ (Reed *et al.*, 1982). The gas is usually used in internal combustion engines, for direct heat applications and production of chemical such as methanol.

2.3 PYROLYSIS

Pyrolysis is thermal degradation of biomass that takes place at temperature in which the biomass material is subjected to heat in the presence of inert gas (absence of oxygen). The thermal degradation of biomass in the absence of oxygen usually occurred at 400 – 600°C (Ralph, 2002). The products include oils or tars, water, charcoal (or more correctly a carbonaceous solid), and permanent gases including methane, hydrogen, carbon monoxide, and carbon dioxide.

The process is carried out as slow or fast pyrolysis. Fast pyrolysis of biomass could obtain the highest mass yield (up to 80 wt% of dry feed) of liquid fuel and retain most energy (up to 70%) in the liquid products (Serrano *et al.*, 2011). Thus, the resultant fast pyrolysis oils have been viewed as the cheapest liquid biofuels and have attracted crucial attention at research over the past two decades. Furthermore, fast pyrolysis of biomass is on the verge of commercialization (Butler *et al.*, 2011).

2.4 BIO-OIL FROM PYROLYSIS OF BIOMASS

The products obtained from pyrolysis of biomass are char (carbonaceous solid),

condensable gas (collected as oils or tars), and non-condensable gas (methane, hydrogen, carbon monoxide, and carbon dioxide). The nature of these changes depends on the heating rate of the material, the type of material undergoing pyrolysis and the pyrolysis temperature of the material. A typical example of biomass materials includes wood, animal and plant wastes. The biomass materials are poor conductor of heat; therefore, it is important to manage the heating rate. The main biomass pyrolysis reaction is



2.4.1 SLOW PYROLYSIS

Slow pyrolysis is also known as carbonization. It is performed at temperature range of 200-300°C or above 300°C residence time of 1 hour to several hours. It is referred to as torrefaction when it carried out a temperature range of 200-300°C, so that it resulted in near complete decomposition of its hemicellulose content in such a way that the mass and energy yield of solid product is maximize. But when it is performed at higher temperature above 300°C, it produces more energy dense fuel with high energy yield. The yield of products obtained from carbonization includes 35% each of char and gas, 30% bio-oil (Bridgwater, 2012).

2.4.2 FAST PYROLYSIS

In fast pyrolysis, biomass decomposes quickly to produce more vapour, charcoal and gas. The vapour is rapidly cool and a dark brown liquid is formed. Fast pyrolysis is carried out at temperature between 400 and 600°C, high heating rate (20 °C/min) and short residence time (< 2 s) for vapours. Also, if the residence time of fast pyrolysis decreases, the liquid yield increases, and the yields of gas and char decrease. The yields of product are: 80% bio-oil, 12% char and 13% gas (Bridgwater, 2012). Pyrolysis gas can be converted into fuel gas in the presence of oxygen and steam. Fuel gas is used as a fuel in Kiln, steam boiler, internal combustion engine and gas turbine.

Intermediate pyrolysis is carried out at temperature range of 400–500°C and has vapour residence time of about 10–30s. It characterized with a low heat transfer rate which favours production of bio-oil with less tar. It is considered economical since the product is used directly as fuel engines. The yield of bio-char is 20–30%, gas 10–20%, and bio liquid of 50–60% for intermediate pyrolysis.

Figure 1 indicated the product distribution obtained from different modes of pyrolysis of woody biomass.

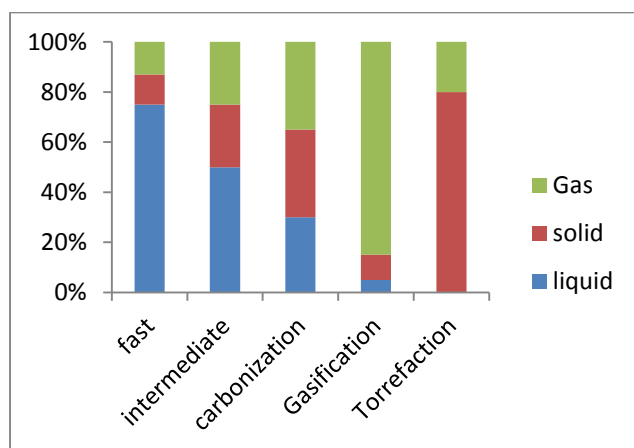


Figure 1: Mode of pyrolysis from wood biomass

2.5 PHYSICAL PROPERTIES OF PYROLYSIS OILS FROM BIOMASS

The analysis and characteristics of bio oil qualities produced from biomass for various direct applications is very significant. The quality of any bio oil depends on its physical and chemical properties as well as the suitability of the oil for a specific function. The physical properties of bio oil include: viscosity, heating value, density, water content, oxygen content, pH value, density and solid contents. While some of chemical compounds present in the bio-oil includes: various functional groups and their chemical bonding.

2.5.1 HEATING VALUE

The heating value is also known as the calorific value that ascertains the energy content present in oil (Bardalai, 2015). Calorific value can also be referred to as enthalpy of complete

combustion of a fuel where all carbon and hydrogen are converted to CO₂ and H₂O respectively (Varmuza *et al.*, 2007). As the calorific value of oil increases, the oil can become more efficient and useful for different applications. The calorific value in most of the bio-oils are basically found within the range of 15- 36 MJ/kg which is always lower than the value of 40-50 MJ/kg for conventional petroleum fuels (Pattiya *et al.*, 2009).

The calorific value of a bio-oil mainly depends on factors such as water content, oxygen content, temperature and heating rate of the pyrolysis process. Normally, the presence of oxygen in significant amount increases the water content thereby reducing the amount of hydrocarbon (Mohanty *et al.*, 2011). Consequently, calorific value become affected and will not improve even if the bio oil undergoes any of upgrading methods. For example, eucalyptus wood, rice straw and waste bamboo have calorific value within the range of 16-19 MJ/kg, this value is much lower than the value of 40-50 MJ/kg for the conventional petroleum fuels despite the fact it undergoes upgrading (Kumar *et al.*, 2010).

Hydrothermal pyrolysis is a good technique for upgrading bio oil quality, by using this technique, the calorific value increased up to 36-39 MJ/kg which is much better than other pyrolysis oil (Xiu *et al.*, 2010).

2.5.2 WATER CONTENT

The water content in oil is often refers to as the amount of moisture present in the oil. The presence of moisture in high amount in bio oil can leads to separation of water (aqueous phase) and the heavier organic phase therefore, which make the application of bio-oil more difficult. Generally, the water content present in the pyrolysed oil from most of biomasses is found in the range of 10-40 wt. % (Bardalai, 2015).

There are various methods that have been applied to reduce water content in bio oil. They include: solvent, condensation, hydro-

deoxygenating, and electrostatic precipitator (ESP). Although the addition of solvent such as methanol can improve the flow quality of the oil, the water content increases. It has been demonstrated that condensation collected at lower temperatures shows a positive improvement of bio oil, for instance condensation at -5°C contains less water content when compared to the condensation collected at 50°C (Asadullah *et al.*, 2007).

2.5.3 VISCOSITY

Viscosity of bio oil is the property that determines the characteristics of flow quality of bio liquid. The inherent bio oil viscosity obtained from biomasses does not depend largely on the type of reactor rather on other parameters. The parameters include: biomass feedstock, ageing of bio-oil, temperature, condensation, electrostatic precipitator (ESP) and water content (Bardalai *et al.*, 2015).

Viscosity also increases by condensing the vapour at very lower temperature such as -5°C , again the effect of installation of electrostatic precipitator (ESP) is to improve the quality of bio-oil in terms of calorific value, but it seriously affected the viscosity, which make the viscosity increases to a very high value (Yin *et al.*, 2013). Hydrothermal pyrolysis gives high viscosity, for example in hydrothermal pyrolysis of swine manure; the viscosity is $0.843 \text{ N}\cdot\text{s m}^{-2}$ at temperature of 50°C .

Several methods or processes can be applied to reduce the viscosity of pyrolytic oil, for instance, addition of polar solvents like methanol or acetone reduces viscosity of pyrolytic oil but at the same time, it effects on some other properties also. The effect of temperature occurred when temperature increases, the viscosity continuously reduces, for example viscosity of $0.0132 \text{ N}\cdot\text{s m}^{-2}$ measured at temperature of 40°C and continuously decreasing to $0.002 \text{ N}\cdot\text{s m}^{-2}$ when the temperature rose to 90°C .

2.5.4 ACIDITY

The acidity of bio-oils is usually determined as a numeric scale to specify oil concentration. While the pH of bio oil is hydrogen potential that measures the acidity from 0-14 as well as representation of the oil corrosiveness. The pH test method is useful for bio oil applications in which corrosive oil could cause significant damage. The bio-oils mostly contain organic acids such as acetic, carboxylic and formic acids. As the pH value of bio-oil becomes less, the oil becomes more acidic.

Because of the higher acidity, the bio-oil becomes corrosive and hence corrosion resistance material should be used in the bio-oil production and storage system. The pH value in the bio-oil depends on the type of biomass used for the bio-oil production. The pH of bio-oil is mostly within the range of 2-4 but few biomasses also have higher pH value (>4) such as rice straw, wheat straw and so on (Park *et al.*, 2004). On the other hand, some bio oil also have highly acidic properties as their pH value is found within 1.8-2.9, the typical example of the biomass is eucalyptus wood (Kumar *et al.*, 2010).

pH can be improve up to 4.5 by condensing the vapour at low temperature -5°C through the help of ice water mixed with a solution of sodium chloride (NaCl), instead of condensing at higher temperature $50-60^{\circ}\text{C}$ (Asadullah *et al.*, 2007).

2.5.5 DENSITY

The density of bio-oil always decreases with increase in temperature and increases by condensing at low temperature (Garcia *et al.*, 2002).

Unlike other bio oil properties such as acidity, pH, heating value and so on, the density of bio oil is always found to remain the-same within some definite range of value for instance, the density 1100 kg/m^3 remain same regardless of the installation of the hot vapour filter but, by using the ESP the density of the bio-oil could be increased to a higher value (Pattiya and Suttibak 2012).

Table 1: Typical properties of pyrolysis bio oil.

Physical properties	Bio oil
pH	1.8-4.0
High Heating Value (HHV) MJ/Kg	15-36
Viscosity (at 50 ⁰ C) N·s m ⁻²	40-100
Solid wt. %	0.01-0.5
Density kg/m ³	1000-1300
Water content	10-40wt%
Oxygen	10-60wt%
Ash content	0.01-0.5

2.6 USES OF BIO OIL FROM BIOMASS

Application of bio oil refers to uses or conversion of bio oil to energy in various installed system specify as a form of technology such as power, heat, engine, turbine and so on (Asadullah *et al.*, 2007).

In Europe and USA pyrolysis oil is not competitive because of the current low prices for natural gas. In contrast, countries like Brazil have high application and availability of biomass with low prices and a higher price for natural gas, pyrolysis oil seems to be competitive. In- some countries incentives are used to mandate transport system to use pyrolysis oil to replace natural gas (Muggen, 2015).

Pyrolysis oil can be used as substitutes to heavy and light fuel oils or natural gas in existing electricity plants. Substituting pyrolysis oil for fossil fuel is achievable by medium or large scale (co-) combustion with natural gas or heating oil fired boilers, furnaces and turbines to generate heat and power generation.

By direct combustion in a boiler or furnace, pyrolysis oil can be used to generate heat. This is the simplest and straight forward application of bio oil. However, various companies have been attracted for district heating to serve as substitutes for heavy fuel oil. One of the commercial companies is Red Arrow Products pyrolysis plant in wisconsin, Canada frequently uses bio oil to generate heat for over 10 years (Freel *et al.*, 1996). Biomass technology Group (BTG) has demonstrated a successful test of co-combustion of pyrolysis oil in an industrial scale with natural gas-fired at a 350 MW power plant in Harculo, the Netherlands in 2003.

Gas turbines can be used to produce electricity and heat of CHP especially at remote locations. Currently, gas turbine has been adapted to run on pyrolysis oil to generate power, for example, Hengelo change from conventional fuel to run on pyrolysis oil to provide a 2MW class system of power generation.

Another interesting application of bio oil is ship propulsion, in this field of application; pyrolysis oil is one of the little substitutes to fossil fuels that are commercially attractive. Also, pyrolysis oil has been tested successfully on stationary diesel engines.

Initially, second-generation fuels were not considered as automotive alternative fuels in transportation because of several problems such as poor volatility, high viscosity, coking, corrosiveness and high-water content. This second-generation bio oil can be derived from pyrolysis oil through different methods such as: direct upgrading, co-refining in existing oil refineries or through synthesis gas and subsequent synthesis processes such as methanol. Also Chemicals such as methanol, acetic acid, turpentine, tars, medical oil, furfural and so on can be obtained from pyrolysis of oil.

2.7 UPGRADING OF BIO-OIL

In order to upgrade the fuel quality from bio-oil, a complete deoxygenation is required. There are different methods of bio oil upgrading:

2.7.1 UPGRADING OF BIO-OIL BY PHYSICAL

The following are the physical means of upgrading bio oil

- I. Filtration: using Hot-vapour filtration can decrease the ash content of the bio oil to less than 0.01%. Also, the alkali content can decrease to less than 10 ppm (Bridgwater, 2012).
- II. Solvent addition/esterification: The addition of solvents, particularly methanol, indicated a significant effect on the oil stability (Liu, 2014).
- III. Emulsification (emulsions): Pyrolysis oils are not properly miscible with hydrocarbon fuels but with support of surfactants can be emulsified with diesel oil (Ikura, 2003).
- IV. Distillation. This process is based on the different boiling point of every single component; the bio-oil can be divided into pseudo gasoline, pseudo diesel and pseudo aviation kerosene (Czernik, 2004).

2.7.2 UPGRADING OF BIO-OIL BY CHEMICAL

Upgrading of bio-oil by chemical means is a good potential to improve the quality by separating the bio-oil into value added chemical groups. Various approaches for upgrading bio oils into value added chemical products by means of extraction include: chemicals produced from the whole bio-oil, chemicals from fractionation of bio-oil, specific chemicals.

Liquid-liquid extraction of bio oil is a technique of separating the value-added chemicals from bio oil based on their relative solubility of the oil and solvent; for example, separation of aromatics from bio oil via a water/chloroform extraction. Sugar derivatives in bio-oil can be

successfully separated from aromatics via water/chloroform extraction. Based on this separation of aromatics from bio-oil, aromatics utilization in the bio-oil will serve as a great feedstock for fine chemicals or fuels.

Chemicals produced from the Whole Bio-oil: The entire bio-oil can be converted into valuable chemicals by taking advantage of its most available functional groups: carboxyl, phenolic and carbonyl. The functional group will be subjected to reaction in such a way that the non-reacting part of bio-oil would not have to be separated from the final product. For example, phenols and carboxylic acids can certainly react with lime to form calcium salts and phenates.

2.7.3 UPGRADING OF BIO-OIL BY CATALYTIC

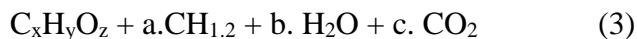
Most of the experimental studies reported in the literature employed the use of fluid catalytic cracking catalyst such as zeolite and reforming catalyst such as transition metals supported on silica-alumina (hydro-treating) for bio-oil upgrading of biomass (Suchithra, 2012).

Hydro-treating (hydrodeoxygenation) of bio-oil has been shown technically possible but has some disadvantages. Some of the disadvantages are high coking (8–25%) cause catalyst deactivation and reactor clogging, poor quality of fuels obtained and economically not achievable.

Catalytic cracking of bio oil is a process where oxygenated organics is converted into more valuable gasoline, olefinic gases, and other products oil in the presence of shape-selective catalyst such as zeolites (Bridgwater, 2011). Removal of oxygenated compounds via zeolite such as ZSM-5 occurred at atmospheric pressure and does not required hydrogen. ZSM-5 removes oxygen from bio oil as carbon dioxide and water.

Catalytic Cracking reactions of bio oil involve the separation of C-C bonds related with decarboxylation, decarbonylation and

dehydration. In cracking reaction dehydration is the main reaction as shown in Equation 2.



3 CURRENT TRENDS IN CATALYTIC CRACKING OF BIO OIL

Pyrolysis is an attractive method of converting biomass to transportation fuels (Kockar *et al.*, 2004) and (Asadullah *et al.*, 2007). Asadullah *et al.* (2007) reported that the conversion of bagasse to bio oil fuel in a fixed bed reactor at interval of 300-600°C. The analysis showed that, the yield of oil was very low (33.0wt %), low heating values of 19.91 MJ/kg, pH of 4.5. Although, Kockar *et al.* (2004) improved the yield by comparing the effect of fixed-bed of both slow and fast pyrolysis of rapeseed (*Brassica napus L.*) at 550°C, using two reactors, namely Heinze and tubular reactor. The results showed an increase in oil yields 51.7% and 68% that is (Heinze and tubular reactors) at different heating rate (30°C min⁻¹ and 300°C min⁻¹). Ala'a H. *et al.* (2016) reported that, due to strong acid activities of a catalyst with uniform pore size; pH increased, viscosity decrease and the heating value increase up to 31.65 MJ/kg against 19.91 MJ/kg reported by Asadullah *et al.* (2007).

Iliopoulou *et al.* (2012), Aysu *et al.* (2016) and Ala'a H *et al.* (2016) reported some findings on bio oil properties and upgrading as follows: Iliopoulou *et al.* (2012) in their report compare the catalytic effect of silica sand, ZSM-5 (pure) and with that of ZSM-5 modified with nickel (Ni) and cobalt (Co). The bio oil produced from their experiment for silica sand was 58.67 wt. % (with oxygen 40.68 wt. %), ZSM-5 (pure) was 34.33 wt. % (with oxygen 4.24 wt. %) less in quantity but the quality was better. Similarly, Aysu *et al.* (2016), investigated the influence of catalyst during pyrolysis of lignocellulosic biomass in tubular and fixed bed reactor in the presence of these Ca(OH)₂, Na₂CO₃, ZnCl₂, Al₂O₃. Three catalyst showed good response of bio oil quality but less response using Ca(OH)₂.

Ala'a H. *et al.* (2016) compare the upgrading of bio oil in the presence of three catalysts: HY, H-mordenite and HZSM-5 in fixed bed reactor. The amount of liquid formed was high for HZSM-5 than HY and H-mordenite. Their results showed that the quality of liquid increased, pH increased, viscosity decrease and calorific value increased up to 31.65 MJ/kg yet quantity decreases. However, low bio oil yields and high coke that is being formed when catalyst is used which create the major problems against the effectiveness of using catalytic process (French *et al.*, 2009) and (Carlson *et al.*, 2009).

Çepeliog *et al.* (2013) reported their investigation of co-pyrolysis characteristics and kinetics of biomass-plastic blends of cotton stalk, hazelnut shell, sunflower residue, and arid land plant *Euphorbia rigida*, were blended in definite ratio (1:1, w/w) by using thermogravimetric analyzer (TGA). The analysis of kinetics showed an imperative pyrolysis mechanism and the yields of bio oil increased.

Onay *et al.* (2014) made a similar observation and confirmed that the synergetic effect during the pyrolysis of waste tire and non-food biomass at 500°C in the absence and presence of catalyst. In the presence of plastic, the analysis showed that the yield of bio oil increased. However, despite the fact that, plastic increase the quantity of bio oil but coke formation is a problem.

In order to increase the quality, yield and reduce the coke, catalytic pyrolysis of biomass was co-fed with plastic or alcohol (Zhang *et al.*, 2016) and (Garba *et al.*, 2017). Zhang *et al.* (2016) studied the thermal degradation and kinetics of cellulose/ Douglas fir sawdust with plastics (LDPE) in present and absent of ZSM-5 catalyst by using thermogravimetric analyzer (TGA). The analysis of kinetics showed that addition of catalyst does not alter the mechanism of decomposition. However, the quality and yield increases, consequently the coke reduced.

Garba *et al.* (2017) made a similar approach by comparing the pyrolysis of wood fuel using two different polyethylenes: low density

polyethylene (LDPE) and high-density polyethylene (HDPE) over zeolite catalyst (ZSM-5) via a thermo-gravimetric analysis. It discovered that, the kinetics showed that the quality and yield of bio oil is increase when catalyst is co-fed with biomass and plastic.

Table () Trend of catalytic upgrading of bio oil

Name of author /year	Research Title	Finding	Gap Identify
Asadullah et al, 2007	Production of bio-oil from fixed bed pyrolysis of bagasse	Low yield (33.0wt %) low calorific values (19.91 MJ/kg) and pH of 4.5.	Low yield of bio oil and low calorific value
Iliopoulou et al, (2012)	Catalytic effect of silica sand, ZSM-5 (pure).	The bio oil produced from their silica sand was 58.67 wt. % (with oxygen 40.68 wt. %), ZSM-5 (pure) was 34.33 wt. % (with oxygen 4.24 wt. %).	Very low oxygen with less quantity and coke was formed.
Çepelioglu et al. (2013)	Thermal and kinetic behaviors of	The analysis showed an imperative pyrolysis	low quality

	biomass and plastic wastes	mechanism.	
Onay et al. (2014)	The Catalytic Co-pyrolysis of Waste Tires and Pistachio Seeds	The analysis showed that the yield of bio oil increased..	The yield increased yet coke reduced.
(Garba et al., 2017)	Thermal degradation and kinetics of wood fuel with plastics (LDPE) and HDPE in present and absent of ZSM-5 catalyst by using thermo-gravimetric analyzer (TGA).	The analysis of kinetics showed that addition of catalyst does not alter the mechanism of decomposition	The quality and yield increases, consequently the coke reduced.

4 CONCLUSIONS

This paper reviews the current trend on production and upgrading of bio-oil from biomass pyrolysis. Starting from production of bio oil from biomass, the paper shows

progression in terms of quality and quantity when biomass is pyrolyse with catalysis and /plastic admixture. This progression is testified to offer solution to the problems of less bio oil yield and the coke formation.

REFERENCES

- Anex, R. P., Aden, A., Kazi, F. A., & Fortman, j. (2010). *Fuel. energy*, 89, 529-539.
- Asadullah M., Rahman, M.A., Ali, M.M., Rahman, M.S., & Motin, M.A. (2007). Production of bio-oil from fixed bed pyrolysis of bagasse. *fuel*, 86(16): 2514-2520.
- Aterny. J. C., & Serrano-Ruiz J. (2011). Dumesic for energy Environment. *Science*, 4, 83-99.
- Alexander S., Xiaolei Z., (2019). Density functional study on the thermal stabilities of phenolic bio-oil Compounds. *Fuel* 255 (2019) 115732
- Bardalai M. (2015). A review of physical properties of biomass pyrolysis oil. *International Journal of Renewable Energy Research (IJRER)*, 5(1): 277-286.
- Brenda J. A., Stephane G. J., (2019). Physical, chemical, thermal and biological pre-treatment technologies in fast pyrolysis to maximize bio-oil quality: A critical review. *Biomass and Bioenergy* 128 105333
- Bridgwater A. V. (2012). Review of fast pyrolysis of biomass and product upgrading. *biomass and energy*, 68-90.
- Bridgwater, A. V. (2011). Review of fast pyrolysis of biomass and product upgrading. *ScienceDirect*, 80.
- Butler, E. Devlin, G., Meier D., & Mc Donnel I. (2011). Renewable Sustainable Energy Rev. *green chemistry acess*, 15, 4171-4186.
- Carlson, T. R. (2009). Aromatic Production from Catalytic Fast Pyrolysis of Biomass Derived Feedstocks. *Topics in Catalysis*, 52: p. 241 - 252.
- Cepeliog, O., & Ullar A. (2013). *Thermal and kinetic behaviors of biomass and plastic wastes*. Energy Conversion and Management.
- Ciolkosz, D. (2014). Introduction to biomass combustion. *wood energy*, 1. Retrieved from <http://articles.extension.org/pages/31758/introduction-to-biomass-combustion>.
- Czernik, S., & Bridgwater, A.V. (2004). *Overview of applications of biomass fast pyrolysis oil* (Vol. Vol.18). Energy & Fuels.
- Freel, B., & Graham (1996). Bio-Oil Production and Utilization . *Proceedings of the 2nd EU/Canada Workshop on Thermal Biomass Processing*, 23.
- Garba, M. U., Inalegwu A., & Musa, U. (2017). Thermogravimetric characteristic and kinetic of catalytic co-pyrolysis of biomass with low- and high-density polyethylenes. *Biomass Conv. Bioref*, 1, 4.8.
- García-Pèrez, M. (2002). Vacuum pyrolysis of sugarcane bagasse. *Journal of Analytical and Applied Pyrolysis*, 65(2): 111-136.

- Ikura, M., & Stanciulescu M., Hogan E. (2003). *Emulsification of pyrolysis derived bio-oil in Diesel fuel*. . Biomass Bioenergy.
- Kockar, O., Onay, O., & Mete. (2004). Fixed-bed pyrolysis of rapeseed (*Brassica napus* L.). *biomass and energy*, 291.
- Kumar, G. P. (2010). Optimization of process for the production of bio-oil from eucalyptus wood. *Journal of Fuel Chemistry and Technology*, 38(2): 162-167.
- LeibbrandtN, H., Knoetze J. H., & Görgens, J. F. (2011). Biomass Bioenergy. *energy*, 35, 2117-2126.
- Mohanty T., & Pant. (2011). Fuel production from biomass. *Indian perspective for pyrolysis oil*, 34.
- Muggen, G. (2015). Bio liquids fuel. *biomass conference*, 1. Retrieved from <https://www.btg-btl.com/en/application>.
- Onay, O. (2014). The Catalytic Co-pyrolysis of Waste Tires and Pistachio Seeds. *Energy Sources, Part A: Recovery, Utilization, and Environmental Effects*, 2.
- Park, Y., & Jeon. (2004). Bio-oil from rice straw by pyrolysis using fluidised bed and char removal system. *Prepr. Pap.-Am. Chem. Soc., Div. Fuel Chem*, 49(2): 800.
- Pattiya, A., & Titiloye J.O. (2009). Fast pyrolysis of agricultural residues from cassava plantation for bio-oil production. *Carbon*, 51: 51.59.
- Ralph, P., & Overend. (2002). THERMOCHEMICAL CONVERSION OF BIOMASS. *National Renewable Energy Laboratory, Golden, Colorado, USA*, 1-5.
- Reed, T. B., Graboski, M., & Markson, M. (1982). The SERI High Pressure Oxygen Gasifier. *Solar Energy Research Institute, Golden, Colorado*, 234-1455.
- Serrano-Ruiz, J., & Dumesic, C. A. (2011). *Energy Environ. Sci.* 4, 83-99.
- Suchithra, T. G. (2012). Bio-oil Production through Fast Pyrolysis and Upgrading to “Green” Transportation Fuels. *PhD Thesis*, 35-56.
- Varmuza, K., & Liebmann. (2007). Evaluation of the heating value of biomass fuel from elemental composition and infrared data. *energy fuel*, 123.
- Wang, H. Jonathan M., & Yong Wang (2013). *Recent Advances in Hydrotreating of Pyrolysis Bio-Oil and Its Oxygen-Containing Model Compounds*. America Chemical Society.
- Zhang, L. & Xuesong, J. (2016). *Catalytic co-pyrolysis of lignocellulosic biomass with polymers: a critical review*. *energy resources*.
- Zhu, X., Mallinson, R.G., & Resasco D.E. (2010). Role of Transalkylation Reactions in the Conversion of Anisole over HZSM-5. *Applied Catalysis A: General*, 379(1-2): p172-181.



Optimization study of Deacetylation Process in the Synthesis of Chitosan from Red Shrimp Using Response Surface Method

*Atanda, A. S¹, Jimoh, A² & Ibrahim, A.A.³

^{1,2,3} Department of Chemical Engineering, Federal university of Technology, Minna, PMB 65 Minna Niger State, Nigeria

*Corresponding author email: t33space@gmail.com, +2348032898346

ABSTRACT

Chitosan is a natural compound consisting of N-acetylglucosamine and glucosamine units, produced by deacetylation process of a chitin compound gotten from crustaceans, mollusc and insect. This study aimed at investigating the effect of process parameters on deacetylation stage during chitosan synthesis from Red Shrimp. Chemical approach was used to produce both chitin and chitosan (where deproteination and demineralization reactions were carried out to extract the chitin before deacetylation was performed to get chitosan). Design expert version 7 response surface method, central composite design methodology was used to design the deacetylation stage experiment. The four input variables considered are NaOH concentration, Chitin to Solvent ratio, Reaction temperature and Reaction time. The significant factors which affect the Deacetylation are the linear effect of the Chitin to Alkali ratio (B) and reaction temperature (C) with p-values of 0.0051 and 0.0001 respectively. Similarly, the interaction effect of NaOH concentration and reaction temperature (AC), NaOH concentration and Reaction time (AD) and Reaction temperature and Reaction time (CD) with p-values of <0.0001, 0.0385 and 0.0132 respectively. The quadratic effect of the NaOH concentration (A²) with p-value of 0.0167 and the reaction temperature (C²) with p-value of 0.0002 were also found to be significant factors in relation to the Deacetylation yield. The research observations revealed that the synthesized chitosan had molecular weight and Degree of Deacetylation of 1.14×10^5 gmol⁻¹ and 87.27% respectively. Furthermore FTIR, SEM micrograph and XRD analysis of the synthesized chitosan revealed similarities between the synthesised chitosan and chitosan reported in literature.

Keywords: Central composite design, Chemical method, Chitosan yield, optimization, Red Shrimp, Response Surface

1 INTRODUCTION

Chitosan is a natural multifunctional polysaccharide, and a polycationic copolymer, consisting of N-acetylglucosamine and glucosamine units, produced by deacetylation process of a chitin compound (Ameh, *et al.*, 2015). Sources of chitin include but are not limited to cell walls of many fungi and plants, shells of crabs, shrimps and many other crustaceans, mollusk and insects ((Das, & Ganesh, 2010; Ibrahim, *et al.*, 2018). Source materials like Shrimps have been reported to possess thinner walls that makes chitin isolation from their shells faster than other type of shells (Islem, and Marguerite, 2015)

The chitins compound found in the body structures of these crustaceans do not exist alone but are found to coexist with other pigments, proteins, lipids and calcium deposits which is responsible for the structural hardness of the outer shell of the crustacean's exoskeleton (Das and Ganesh, 2010). According to Islem and Marguerite (2015), the chitinous content of the crustaceans can be isolated through either chemical or biotechnological methods where the pigments, proteins and lipids are extracted leading to the production of chitin which is then deacetylated to give rise to chitosan. However, chemical approach that involves both the deproteination and demineralization stages have been reported to be economically viable as well as been easy to implement

unlike the biotechnological method (Thillai, *et al.*, 2017), thus, its choice for the present study.

The demineralization stage involves solubilization of the mineral by acidic treatment of the inorganic salts such as calcium carbonate found in the shells of the shrimp samples. Both organic acids (lactic, acetic, propionic and fumaric) and Inorganic acids (HCl, HNO₃, H₂SO₄) have been used (Wassila, 2013). However, a downside to the use of the inorganic acids is due to the corrosive nature of this chemicals which could lead to environmental pollution (Ibrahim, *et al.*, 2017), therefore the choice of Acetic acid (an organic acid) in the present study. Pujari and Pandharipande (2016) reported that deproteination step involves the treatment of the sample (Shrimp shell) with an alkali reagent in other to strip it of the protein pigments (deproteinate). Several alkali reagents such as Na₂CO₃, NaHCO₃, K₂CO₃, Ca(OH)₂, Na₂S, NaHSO₃, and Na₃PO₄ have also been used but sodium hydroxide still remains the most preferred due to its efficiency in deproteination (Shanta, *et al.*, 2015). The completion of both stages (demineralization and deproteination stage) results in chitin isolation. However, an optional step, decolourization, could be carried out to improve the chitins aesthetics (Pujari and Pandharipande, 2016; Ibrahim, *et al.*, 2017). Acetone and Hydrogen peroxide (H₂O₂) are two of the most widely used decolorants (Gbenebor, *et al.*, 2017).

Deacetylation of chitin is the stage that leads to the synthesis of chitosan. The deacetylation of chitin is simply the removal of the acetyl groups from the molecular chain of chitin, leaving behind a compound (chitosan) with a high degree chemical reactive amino group (-NH₂) (Wassila, 2013). The resulting chitosan possess numerous advantages over the traditional chitin in that it is soluble in most solvents and possesses a highly chemical reactive group (-NH₂), thereby enabling its wide application in numerous fields ranging from wastewater purification to medical application and even agricultural uses as a growth regulator (Islem, and Marguerite, 2015; Russell, 2013). Because of the importance of deacetylation stage, it became imperative to investigate how the major process parameters influence the process, especially the yield and quality of the chitosan, thus, the focus of this paper. Figure 1 shows the structure of chitin and chitosan.

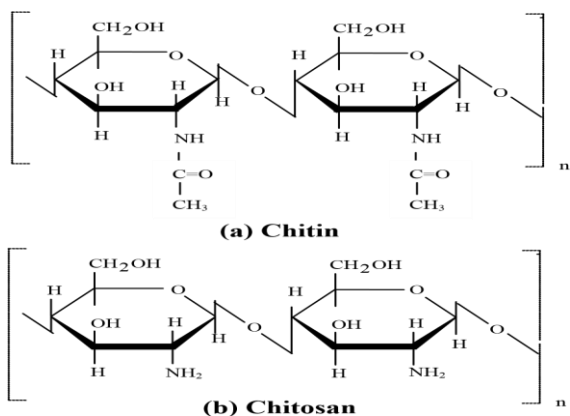


Figure 1: Structure of Chitin and Chitosan

This paper focused on the optimization of the major process parameters that play vital roles in the synthesis of chitosan (the deacetylation stage) using Response Surface Methodology (RSM). The Response surface methodology is a set of mathematical and statistical technique that's used for modeling and problem analysis (Ibrahim, et al., 2017). Its purpose is to optimize a response of interest that is dependent on several factors. Commonly employed statistical experimental designs are the full three level factorial design, Box-Behnken design and the central composite design. A major advantage in the utilization of the central composite design is that it has additional axial and star points aside the normal 3 factors level thereby bringing the design to 5 factor levels thus making the experimental design flexible (Ibrahim, et al., 2017).

2 METHODOLOGY

2.1 SAMPLE PREPARATION

Sample of the waste red shrimp shells obtained from Kure market Bosso Niger state were washed and dried at 100 ° C. It was thereafter pulverized into fine shrimp shells powder (1mm). Figure 2 is the schematic process flow diagram of chitin/chitosan production from waste shrimp shells.



Figure 2: Schematic of chitin and chitosan recovery

2.2 PROXIMATE ANALYSIS OF THE RED SHRIMP

The proximate analysis of the waste red shrimp shell was conducted using the AOAC standards (1990) to determine the moisture content, crude protein, ash content, crude fiber, nitrogen content and fat content.

2.3 CHITIN EXTRACTION

In this study the experimental procedure of deproteination and demineralization stages required to obtain chitin was carried out using the chemical approach, where NaOH was used for deproteination stage and an organic acid (Acetic acid) was used for demineralization

stage. Acetic acid was used in other to mitigate against the harmful effects posed by inorganic acids to the environment (Joshy, *et al.*, 2016).

Four parameters have been reported has having influence on the chitin extraction from crustaceans (Joshy, *et al.*, 2016). This include the reagent type used, the reagents concentration, the reaction temperature and the reaction time. Therefore, deproteination stage in this study was carried out using NaOH concentration of 4%, Shrimp sample to alkali ratio of 1:12, Reaction temperature of 76oC and reaction time of 1.1 hour Similarly, demineralization stage was carried out using Acetic acid concentration of 1 M, Shrimp sample to acid ratio of 1:30, Reaction temperature of 60oC and reaction time of 1.5 hour. The deproteination and demineralization operating conditions were obtained from previously carried out experimental work

2.4 CHITOSAN SYNTHESIS

Chitosan production is through deacetylation of chitin, thus, making optimizing the stage a very important one in the scheme of chitosan synthesis. The optimization of the deacetylation of Chitin was carried out using DESIGN EXPERT (Version 7.0.0, Stat Ease, Inc., USA) software. The process parameters considered for the deacetylation stage include the NaOH concentration, the sample to Alkali ratio, the Reaction Temperature and the Reaction time. These factors were chosen because they are the main factors that affect the molecular weight chitosan (Joshy, *et al.*, 2016). Data from literature as well as one factor at a time (OFAT) analysis was carried out in other to determine suitable process parameter values to be used in this study.

TABLE 1: PROCESS PARAMETERS UNDER INVESTIGATION

Variables	Low Value	High Value
NaOH Concentration (%)	30	60
Chitin to Solvent Ratio (w/v)	1:10	1:20
Reaction Temperature (°C)	60	100
Reaction Time (Hours)	1.5	3

Chitosan production was achieved by treatment of the chitin sample with concentrated sodium hydroxide solution at a suitable temperature and time to remove some or all of the acetyl groups from the polymer (Ameh, *et al.*, 2015). Moreover, the resulting chitosan's is then washed to neutrality in running tap water, rinsed with distilled water, filtered, and dried at 60 o C for 24 hrs. in the oven as reported by (Ameh, *et al.*, 2015).

2.4.1 CHITIN AND CHITOSAN CHARACTERIZATION

2.4.1.1 Proximate analysis

Detailed proximate analysis of the produced chitin and chitosan sample was carried out as reported by Enyeribe, *et al.*, (2017) where the moisture content, crude protein, ash content, crude fiber, nitrogen content and fat content were determined.

2.4.1.2 pH Value

The pH value of the chitin and chitosan samples were determined using a pH meter where 5 ml of distilled water is added to 20 g of the air-dried chitin and chitosan sample and stirred using a glass rod. The electrode of the digital standardized pH meter is inserted into it and the pH read off the meters display (Enyeribe, *et al.*, 2017).

2.4.1.3 Intrinsic Viscosity

The viscosity of chitin and chitosan samples was determined by using Brookfield viscometer, where the samples were dissolved in 1% of acetic acid at 1% concentration of the sample on a dried basis. The chitosan viscosity was measured in centipoises (cps) (Enyeribe, *et al.*, 2017).

2.4.1.4 Molecular Weight

The molecular weight was determined by employing Mark-Houwink equation

$$\eta = KM^a \quad (1)$$

Where η is the intrinsic viscosity, M is average molecular weight, K and a are constants, whose values depend on the polymer type and the chosen solvent as reported by Hossain and Iqbal (2014). The K and a value of $1.82 \times 10^3 \text{ cm}^3/\text{g}$ and 0.93 respectively were based on the solvent (0.1 M acetic acid and 0.2 M NaCl) used to determine the intrinsic viscosity and are not a function of the degree of deacetylation (Antonino, *et al.*, 2017; Alabaraoye, *et al.*, 2017).

The chitin and chitosan samples produced were also subjected to further characterizations like XRD (at Two-Theta settings scanning range of 4 to 75.000 degrees with a two-theta step of 0.026 at 13.7700 seconds per step) and SEM/EDS for morphological analysis, as well as FTIR for the determination of the Degree of Deacetylation.

2.4.1.5 Determination of Degree of Deacetylation (DD) by Fourier Transform Infrared Spectroscopy (FTIR)

The FTIR spectra of the chitosan was obtained by feeding the dry chitosan sample into an Impact 360 FTIR spectrometer under dry air at room temperature using KBr pellets (Yongqin, *et al.*, 2005). The DD was calculated using the formula:

$$DD = 100 \times \left(1 - \frac{A_{1655}}{1.33 A_{3450}} \right) \quad (2)$$

The A1655 and A3450 were the absorbance at 1655 cm-1 of the amide I band as a measure of the N-acetyl

group content and 3450 cm⁻¹ of the hydroxyl band as an internal standard. The factor '1.33' is the ratio of A1655/A3450 for fully N acetylated chitin (Gbenebor, *et al.*, 2017).

3 RESULTS AND DISCUSSION

3.1 PROXIMATE ANALYSIS OF THE RAW SHRIMP EXOSKELETON

The proximate analysis of the raw shrimp exoskeleton is presented in Table 2.

TABLE 2: CHARACTERIZATION OF RAW SHRIMP EXOSKELETON

S/N	Property	Unit	Values
1.	% Moisture Content	% wt	3.62
2.	Fat	% wt	10.6
3.	Crude Protein	% wt	50.91
4.	Ash Content	% wt	27.57
5.	Crude Fibre	% wt	7.3

The proximate analysis revealed a high presence of crude protein and low crude fibre content as reported by Khan & Nowsad, (2012). Similarly, a high ash content for shrimp shell was also reported by Khan & Nowsad, (2012).

3.2 PRODUCTION AND CHARACTERIZATION OF CHITIN

Chitin was obtained after carrying out a deproteinization and demineralization reaction in accordance with the work of Joshy, *et al.*, (2016). A Deproteinization (DP) yield of 30.4% was obtained while a Demineralization (DM) yield of 47.56% was obtained. The percentage yield of chitin from shrimp shell amounted to 31.03% which corresponds to similar findings as reported by Naznin, (2005) who reported a 30.6% chitin yield from shrimp shell. Table 3 shows the properties of the synthesized chitin.

TABLE 3: PROPERTIES OF PRODUCED CHITIN

Properties	Result/Value	Values from literature	Literature Reference
Colour	Brownish White	White	(Thillai, 2017)
pH	7.1	6.50	(Kaewboonruang, <i>et al.</i> , 2016)
Solubility in 1 % acetic	Insoluble	Insoluble	(Alabaraoye <i>et al.</i> , 2017)
Viscosity (cps)	3240	4500	(Alabaraoye <i>et al.</i> , 2017)
Molecular weight (gmol ⁻¹)	5.26 × 10 ⁶	7.53 × 10 ⁶	(Alabaraoye <i>et al.</i> , 2017)
Solubility in water	Insoluble	Insoluble	(Aveen, <i>et al.</i> , 2012)
Degree of Acetylation (%)	72%	-	
Moisture content (%)	8.33	9.51	(Kaewboonruang, 2016)

From Table 3 it was observed that there was a close correlation between the properties of the synthesized chitin and those of already established chitin in literature. Of major importance is the solubility of the chitin in 1% acetic solution where Joshy, *et al.*, (2016) reported that chitin is insoluble in 1% acetic acid solution.

Joshy, *et al.*, (2016) also reported that chitin has a high molecular weight and viscosity with the synthesized chitin in this study showing a high molecular weight and viscosity. Similarly, Aveen, *et al.*, (2012) reported on the insolubility of chitin in water a fact which was corroborated by the synthesized chitin. Kaewboonruang, *et al.*, (2016) reported that there was a drop in the ash content, fat content and protein content of chitin when compared to its feedstock and this can be attributed to the result of the demineralization and deproteinization of the feedstock leading to chitin formation. This trend is evident in this study as the ash content, fat content and protein content fell from 27.57%, 10.6% and 50.91% to 2.17%, 0% and 6.91% respectively as the feedstock was converted to chitin.

3.3 OPTIMIZATION OF DEACETYLATION PROCESS (CHITOSAN PRODUCTION)

Chitin deacetylation brings about the formation of Chito10010san which is a cationic, non-toxic, biodegradable biopolymer (Enyeribe, *et al.*, 2017). The DESIGN EXPERT software (Version 7.0.0, Stat Ease, Inc., USA) was used to optimize the deacetylation stage. Process parameters considered include the NaOH

concentration, the Chitin to Alkali ratio, the Reaction Temperature and the Reaction time respectively. Table 4 gives the summary of how the four major parameters investigated influenced the yield of chitosan in terms of degree of deacetylation.

TABLE 4: OPTIMIZATION OF CHITOSAN PRODUCTION FROM RED SHRIMP

Run No	A: NaOH concentration (%)	B: Chitin to Alkali ratio (w/v)	C: Reaction Temperature(°C)	D: Reaction Time (hrs)	Actual DA Yield(%)	Predicted DA Yield(%)
1	45.00	15.00	80.00	2.25	75.50	76.50
2	30.00	20.00	60.00	3.00	72.00	73.27
3	45.00	5.00	80.00	2.25	78.00	77.36
4	30.00	20.00	60.00	1.50	76.20	74.91
5	45.00	15.00	80.00	0.75	79.00	78.41
6	45.00	15.00	80.00	2.25	75.40	76.50
7	60.00	10.00	60.00	3.00	83.60	83.28
8	45.00	15.00	80.00	2.25	74.40	76.50
9	75.00	15.00	80.00	2.25	71.60	71.69
10	30.00	20.00	100.00	3.00	73.90	73.86
11	45.00	15.00	120.00	2.25	78.90	78.61
12	45.00	15.00	80.00	2.25	77.40	76.50
13	30.00	10.00	100.00	1.50	81.60	82.19
14	45.00	15.00	80.00	3.75	75.40	75.38
15	30.00	10.00	100.00	3.00	77.60	77.30
16	60.00	20.00	60.00	3.00	80.90	80.49
17	60.00	10.00	100.00	3.00	69.50	70.97
18	60.00	10.00	60.00	1.50	79.10	79.33
19	60.00	10.00	100.00	1.50	73.20	72.37
20	30.00	10.00	60.00	3.00	78.80	78.61
21	30.00	20.00	100.00	1.50	80.10	80.85
22	45.00	15.00	80.00	2.25	74.30	76.50
23	45.00	15.00	80.00	2.25	80.00	76.50
24	45.00	15.00	40.00	2.25	85.30	84.98
25	60.00	20.00	100.00	1.50	73.20	73.58

26	15.00	15.00	80.00	2.25	75.00	74.29
27	60.00	20.00	100.00	3.00	70.90	70.08
28	45.00	25.00	80.00	2.25	73.50	73.23
29	60.00	20.00	60.00	1.50	77.90	78.63
30	30.00	10.00	60.00	1.50	76.90	78.15

The results of Table 4, shows the Comparison between the experimental (actual) deacetylation yield and the predicted deacetylation yield at the different operating conditions. The close fit between the experimental and predicted data set shows conformability between the experimental work and the predicted data derived from the quadratic model used. The optimum Deacetylation yield was obtained at 69.50 % which occurred at NaOH concentration of 60%, chitin to alkali ratio of 1:10 and reaction time and temperature of 3 hours and 100 ° C.

TABLE 5: ANALYSIS OF VARIANCE (ANOVA) FOR CHITOSAN PRODUCTION

Source	Sum of Squares	Degree of Freedom	Mean Square	F Value	p-value
					Prob > F
Model	371.73	14	26.55	11.15	< 0.0001
A- NaOH Concentration	10.14	1	10.14	4.26	0.0568
B- Chitin to Alkali ratio	25.63	1	25.63	10.76	0.0051
C- Reaction Temperature	60.80	1	60.80	25.53	0.0001
D- Reaction Time	13.80	1	13.80	5.79	0.0294
AB	6.50	1	6.50	2.73	0.1192
AC	121.00	1	121.00	50.80	< 0.0001
AD	12.25	1	12.25	5.14	0.0385
BC	3.61	1	3.61	1.52	0.2372
BD	4.41	1	4.41	1.85	0.1937
CD	28.62	1	28.62	12.02	0.0035
A2	17.28	1	17.28	7.26	0.0167

B2	1.31	1	1.31	0.55	0.4694
C2	54.24	1	54.24	22.77	0.0002
D2	0.90	1	0.90	0.38	0.5477
Residual	35.73	15	3.63		
Lack of Fit	11.87	10	1.19	0.25	0.9707
Pure Error	23.85	5	4.77		
Cor Total	407.46	29			

$$R^2 = 0.9123 \text{ CV\%} = 2.01$$

The analysis of the variance (ANOVA) for the response surface quadratic model is as shown in Table 5. The model expression developed relates the DA yield and the four reactions parameters (A, B, C, D) considered (MAY be equation 5). It can be observed that the relationship is suitable because its p-value is less than 0.05. The model F-value of 11.40 obtained implies that the model is significant. The F-value is the ratio of the Model sum of squares / Residual sum of square. It shows the relative contribution of the model variance to the residual variance. The model fit was checked by the correlation factor R² which was found to be equals to 91.23%.

Analysis of the effect of significant factors from the ANOVA analysis shown that the linear effect of the Chitin to Alkali ratio (B) with a p-value of 0.0051 and that of the reaction temperature (C) with a p-value of 0.0001. The other significant factors are the interaction effect of NaOH concentration and reaction temperature (AC) with p-value of <0.0001, NaOH concentration and Reaction time (AD) with p-value of 0.0385 and that of Reaction temperature and Reaction time (CD) with p-value of 0.0132. The quadratic effect of the NaOH concentration (A²) with p-value of 0.0167 and the reaction temperature (C²) with p-value of 0.0002 were also found to be significant factors in relation to the response. The model equation that governs the deacetylation (DA) yield is represented by the coded equation numbered equation 5.

$$\begin{aligned} \text{Degree of Deacetylation (DA) yield} = & 76.17 - \\ & 0.65A - 1.03B - 1.59C - 0.76D + 0.64AB - 2.75AC + \\ & 0.88AD + 0.48BC - 0.52BD - 1.34CD - 0.79A^2 - \\ & 0.22B^2 + 1.41C^2 + 0.18D^2 \end{aligned} \quad (3)$$

The linear effect of B and C, the interaction effect of AC and CD and the quadratic effect of C² are the general determining factors of the deacetylation yield as they have the larger coefficient values of 1.03, 1.59, 2.75, 1.34 and 1.41 respectively.

3.3.1 INTERACTION EFFECT BETWEEN PROCESS PARAMETERS AND CHITOSAN YIELD

Three-dimensional response surfaces plots were generated based on the generated model equation and these were subsequently used to explain the interaction among the variables, the optimum condition of each factor for optimum deacetylation yield. Figure 3-8 are the generated plots that shows the interactions.

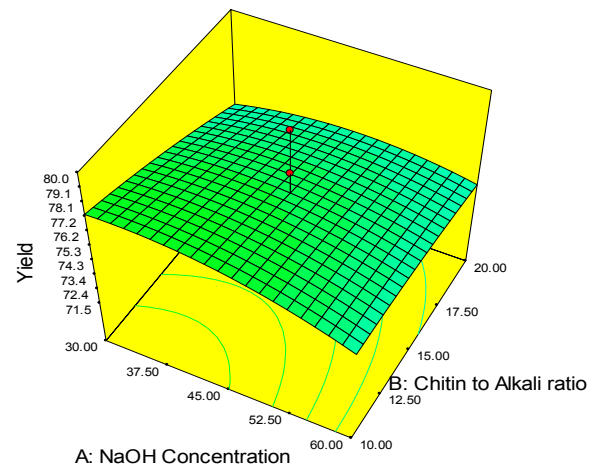


Figure 3: Response surface plot of the interaction effect of NaOH concentration and the Chitin to Alkali ratio on DA yield at a reaction temperature of 80 o C and a reaction time of 2.25 hours.

In Figure 3, it can be observed that the interaction effect of the NaOH concentration and the chitin to alkali ratio resulted in a deacetylation yield of 77.2% at NaOH concentration of 30% and chitin to alkali ratio of 1:10.

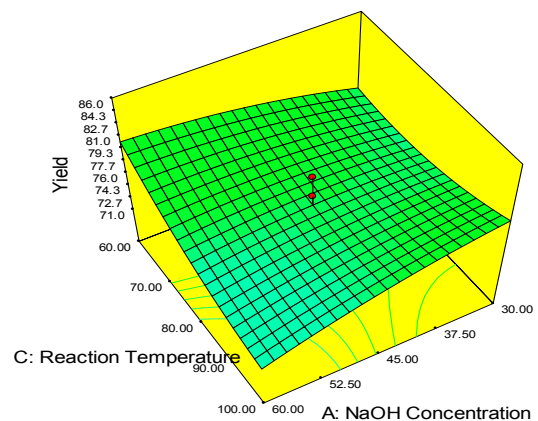


Figure 4: Response surface plot of the interaction effect of NaOH concentration and the Reaction Temperature on DA yield at a Chitin to Alkali ratio of 1:15 and a reaction time of 2.25 hours.

Figure 4 shows that the interaction effect of the NaOH concentration and the reaction temperature resulted in a deacetylation yield of 80.4% at NaOH concentration of 60% and reaction temperature of 60 °C.

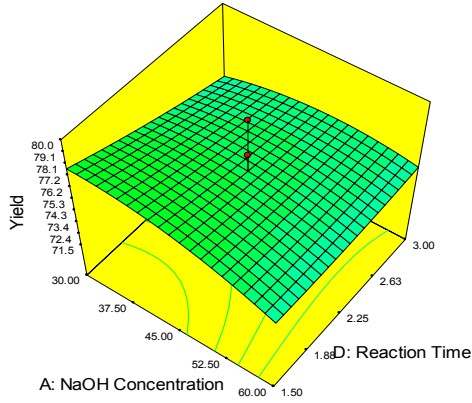


Figure 5: Response surface plot of the interaction effect of NaOH concentration and the Reaction Time on DA yield at a Chitin to Alkali ratio of 1:15 and a reaction temperature of 80 °C.

Figure 5 shows that the interaction effect of the NaOH concentration and the reaction time resulted in a deacetylation yield of 77.8% at NaOH concentration of 30% and reaction time of 1.5 hours.

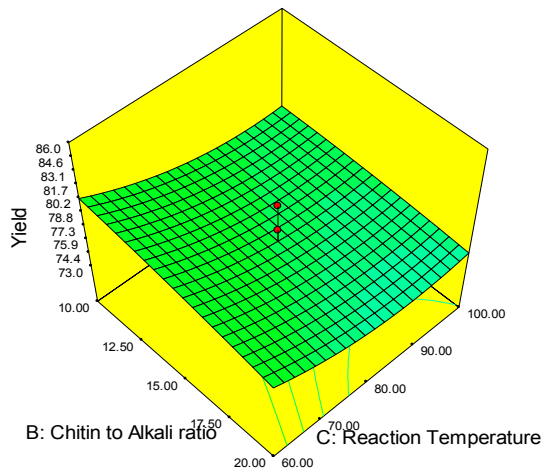


Figure 6: Response surface plot of the interaction effect of Chitin to Alkali ratio and the Reaction Temperature on DA yield at a NaOH concentration of 45% and a reaction time of 2.25 hours.

Effect of the interaction between chitin to alkali ratio and the reaction temperature are shown in Figure 6 and it can be seen that a deacetylation yield of 80.2% was obtained at chitin to alkali ratio of 1:10 and reaction temperature of 60 °C.

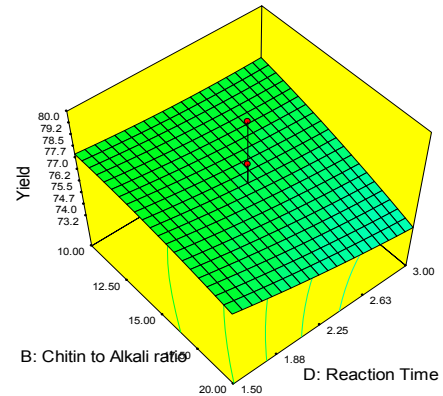


Figure 7: Response surface plot of the interaction effect of Chitin to Alkali ratio and the Reaction Time on DA yield at a NaOH concentration of 45% and a reaction temperature of 80 °C.

Figure 7 shows the interaction effect between the chitin to alkali ratio and the reaction time. A deacetylation yield of 77.39% was obtained at a chitin to alkali ratio of 1:10 and a reaction time of 1.50 hours.

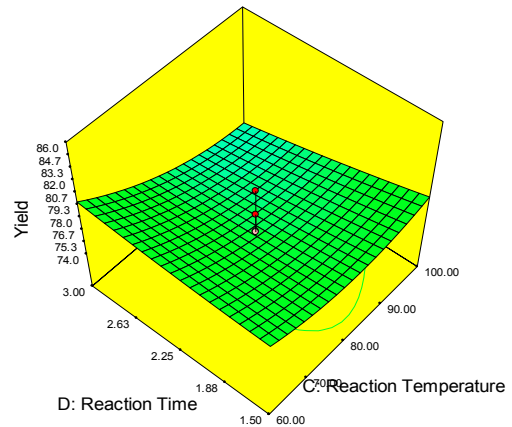


Figure 8: Response surface plot of the interaction effect of Reaction Temperature and the Reaction Time on DA yield at a NaOH concentration of 45% and a Chitin to alkali ratio of 1:15.

Figure 8 shows the interaction effect between the reaction temperature and the reaction time. A deacetylation yield of 79.3% was obtained at a reaction temperature of 60 °C and a reaction time of 3 hours.

3.3.2 STRUCTURAL ANALYSIS OF PREPARED CHITOSAN

The SEM micrograph shows the surface morphology and paints a general picture on the chitosan's surface structure.

3.1.2.1 Scanning Electron Microscopy (SEM) Analysis of Chitosan

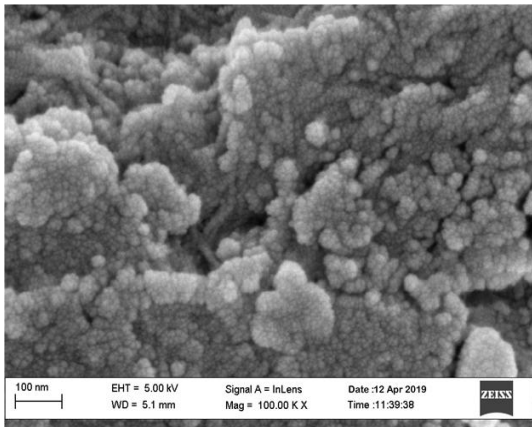
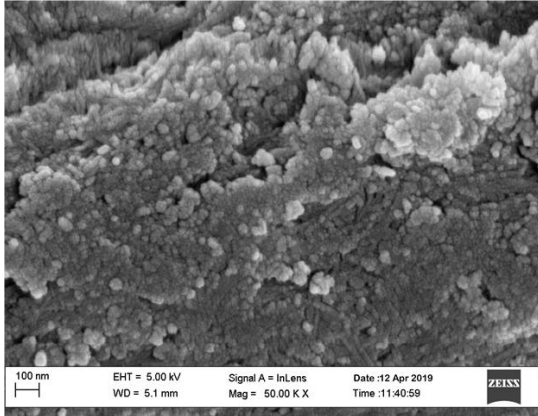


Figure 9: SEM micrographs of synthesized chitosan

The synthesized chitosan SEM micrograph showed non-homogenous and non-smooth surface with straps and shrinkage which corresponds to the SEM morphology of standard extracted chitosan (Islam, *et al.*, 2011).

3.1.2.2 Electron Dispersive Spectroscopy (EDS) Analysis of Chitosan

The EDS analysis of chitosan's shows the elemental opposition on the chitosan's surface. The EDS of the synthesized chitosan as presented in Table 4



Figure 10: EDS image for synthesized chitosan

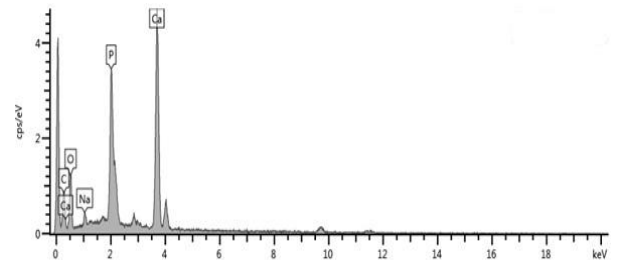


Figure 11: EDS spectrum for synthesized chitosan

TABLE 6 Elemental weight composition of synthesized chitosan

Elements	Atomic %	Wt%	Wt% sigma
Carbon	37.31	21.04	1.26
Oxygen	39.25	32.9	1.05
Sodium	2.92	2.95	0.26
Phosphorous	5.81	12.75	0.38
Calcium	14.71	30.36	0.64

According to shahidi and abuzaytoun, (2005), the presence of elements such as carbon, nitrogen and oxygen which are also found in protein makes it impossible to use eds to determine the protein content of chitosan as typical chitosan samples are made up of these elements. Similarly, Toan, (2011) reported the presence of phosphorous in chitosan derived from shrimp shells.

3.1.2.3 Fourier Transform Infrared Spectroscopy (FT – IR) Analysis of Chitosan

The FTIR plot showing the functional groups of the synthesized chitosan is presented in figure 12.

TABLE 7: WAVENUMBERS AND CHEMICAL GROUP OF FT-IR ABSORPTION BANDS FOR CHITOSAN

S/N	Standard Chitosan Wavelength in cm ⁻¹	Synthesized Chitosan Wavelength in cm ⁻¹	Group
1.	3448	3448.1	OH hydroxyl group
2.	3300-3250	3113.51	N-H group-stretching vibration
3.	2891	2850.27	C-H stretching
4.	1680-1660	1654.13	C=O stretching
5.	1560-1530	1560.13	Amide II bond amide II band
6.	1340	1363.19	Methyl C-H stretch, Amide III
7.	1153-1156	1156.12	Glycosidic linkage, C-H stretch
8.	1072	1073.64	C-O-C
9.	952	953.63	Amide III
10.	750-650	668.7	N-H

The FTIR spectra of the synthesized chitosan was compared to that of standard chitosan. The ftir spectra is used to identify the functional group present at each band. From table 7 it was observed that functional groups such as the OH hydroxyl group was present so also was the N-H and C-H stretching present as reported by Islem, and Marguerite, (2015).

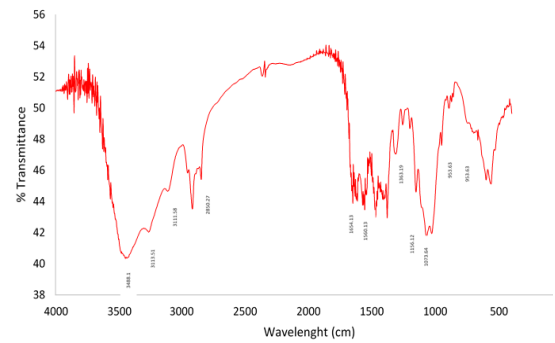


Figure 12: Fourier Transform Infrared spectrometry of the synthesized chitosan

3.1.2.3 X – ray Diffractometry (XRD) Analysis of Chitosan

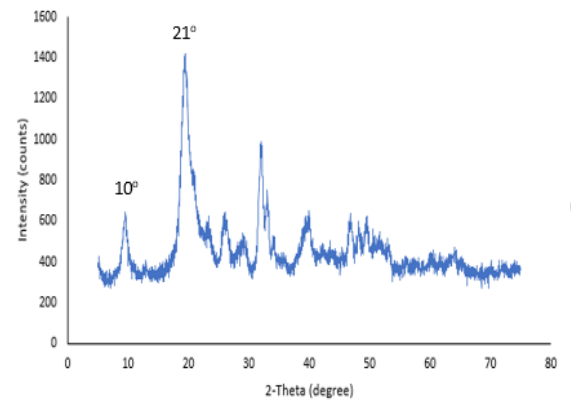


Figure 11: X – ray Diffractometry (XRD) Analysis of synthesized Chitosan

The XRD pattern of chitosan exhibits broad diffraction peaks at $2\theta = 10^\circ$ and 21° which are typical fingerprints of semi-crystalline chitosan as reported by Islam, *et al.*, (2011). The XRD analysis indicates that the synthesized chitosan has crystalline regions, which confirmed the semi-crystallinity of the chitosan as reported by Islam, *et al.*, (2011).

3.3.3 PROPERTIES OF SYNTHESIZED CHITOSAN

The properties of the synthesized chitosan are presented in Table 8. The molecular weight and the degree of deacetylation are two of the most important factors that define chitosan Islam, *et al.*, (2011). Islem, and Marguerite, (2015) reported that the degree of deacetylation of chitosan must be greater than 50% in other to obtain quality chitosan. Similarly, Kaewboonruang, *et al.*, (2016) reported that the molecular

weight of chitosan is always less than that of chitin due to the loss of the acetyl group after deacetylation giving birth to chitosan. A degree of deacetylation of 87.27% was obtained in this study while a chitosan molecular weight of 1.14×10^5 gmol⁻¹ was obtained as opposed to a higher molecular weight of 5.26×10^6 obtained for chitin. Enyeribe, et al., (2017) reported that one distinguishing factor between chitin and chitosan is the latter's ability to dissolve in 1% acetic acid solution. The synthesized chitosan in this study is soluble in 1% acetic

solution thereby showing conformity with findings by Enyeribe et al., (2017).

4 CONCLUSION

The synthesis of chitosan from red shrimp shell resulted in a percentage yield of chitin from shrimp shell amounting to 31.03% after the deproteination and demineralization was carried out. Similarly, the properties

TABLE 8: PROPERTIES OF SYNTHESIZED CHITOSAN

Property	Unit	Obtained Value	Literature Value	Reference
Colour		White	Creamy White	Abed, <i>et al.</i> , (2017)
pH		7.04	-	
Solubility in 1 % acetic		Soluble	Soluble	Enyeribe, <i>et al.</i> , (2017)
Solubility in water		Insoluble	Insoluble	Enyeribe, <i>et al.</i> , (2017)
Moisture content	%	7.81	8.07	Enyeribe, <i>et al.</i> , (2017)
Viscosity	cps	92	108.3	Enyeribe, <i>et al.</i> , (2017)
Molecular weight	gmol ⁻¹	1.14×10^5	2.32×10^5	Kumar & Ravi (2017)
Degree of Deacetylation	%	87.27	81.24	Kumar & Ravi (2017)
Ash content	%	1.13	5.88	Enyeribe, <i>et al.</i> , (2017)
Yield (per 1g of chitin)	wt.%	70.1	-	
Yield (per 100g of Shrimp shell)	%	21.24	-	

of the synthesized chitin showed conformability with established chitin from literature.

The optimization of the effect of process parameters affecting the deacetylation of chitin was carried out successfully and the synthesized chitosan was fully characterized. The statistical analysis of the four process parameters (the NaOH concentration, the Sample to Alkali ratio, the Reaction Temperature and the Reaction time) considered in the optimization study showed that the quadratic model was the best fit with an R^2 of 91.23%. Furthermore, the significant factors from the ANOVA analysis showed that the linear effect of the Chitin to Alkali ratio (B) has a p-value of 0.0051 and that of the reaction temperature (C) with p-value of 0.0001. The other significant factors are the interaction effect of NaOH concentration and reaction temperature (AC) with p-value of <0.0001, NaOH concentration and Reaction time (AD) with p-value of 0.0385 and that of Reaction temperature and Reaction time (CD) with p-value of 0.0132. The quadratic effect of the NaOH concentration (A^2) with p-value of 0.0167 and the reaction temperature (C^2) with p-value of 0.0002 were also found to be significant factors in relation to the response. The other factors have no statistically significant effect relating to the Deacetylation yield. An optimum Deacetylation yield of 70.4% at NaOH concentration of 60%, chitin to alkali ratio of 1:19.76, reaction temperature and time of 100 °C and 2.9 hours respectively.

The FTIR analysis, SEM micrograph and XRD analysis of the synthesized chitosan with molecular weight and Degree of Deacetylation of 1.14×10^5 gmol⁻¹ and 87.27% respectively showed a favorable comparison with already established parameters for chitosan.

REFERENCE

- Abed, E.H., AL Ameen, N.I., Jazaa, L.A. (2017). Extraction of Chitosan from Kentish Snail Exoskeleton Shell' s, *Monacha cantiana* (Montagu, 1803) for the Pharmaceutical Application. *International Journal of Environmental Application & Science (JIEAS)*, 12(2), 125 – 130.
- Alabaraoye, E., Achilonu, M., Hester, R. (2017). Biopolymer (Chitin) from Various Marine Seashell Wastes: Isolation and Characterization. *Journal of Environmental Polymer*, 1(1), doi: 10.1007/s10924-017-1118-y
- Antonino, R.S., Fook, B.R., Lima, V.A., Rached, R.I., Lima, E.P., Lima, R.J., Covas, C.A., & Fook, M.V. (2017). Preparation and Characterization of Chitosan Obtained from Shells of Shrimp (*Litopenaeus vannamei* Boone). *Journal of Marine Drugs*, 15(141), 1 – 12.
- Ameh, A.O., Abutu, David., Isa, M.T., Rabi, U. (2014). Kinetics of Demineralization of Shrimp Shell Using Lactic Acid. *Leonardo Electronic Journal of Practices and Technologies*, 1(24), 13 – 22.
- Das, S. & Ganesh, A. (2010). Extraction of Chitin from Trash Crabs (*Podophthalmus vigil*) by an Eccentric Method. *Current Research Journal of Biological Sciences*, 2(1), 72-75
- Enyeribe, C.C., Kogo A.A., Yakubu M.K., Obadahun, J., Agho, B.O., & Kadanga, B. (2017). Effect of Degrees Of Deacetylation On The Antimicrobial Activities Of Chitosan. *International Journal of Advanced Research and Publications*, 1(5), 55 – 61.
- Gbenebor, O.P., Akpan, E.I., Adeosun, S.O., (2017). Thermal, structural and acetylation behavior of snail and periwinkle shells chitin. *Progress in Biomaterials*, 1(1), doi: 10.1007/s40204-017-0070-1
- Hossain, M. S., and Iqbal, A. (2014). Production and characterization of chitosan from shrimp waste. *Journal of the Bangladesh Agricultural University*, 12(1), 153 – 160.
- Ibrahim, A.A., Jimoh, A., Yahaya, M.D. & Auta, M. (2017). Optimizing Deproteinization of chitin using Response Surface methodology. 1st National Conference in Chemical Technology (NCCT 2017) <http://www.narict.go.ng/ncct/>. Pp 16 – 19
- Ibrahim, A.A., Jimoh, A., Yahaya, M.D. & Auta, M. (2017). Optimizing and modelling of chitin synthesis from Fish scale using Response Surface methodology. 2nd International Engineering Conference (IEC 2017) Federal University of Technology Minna, Nigeria. Pp 254 – 261
- Ibrahim, A.A., Jimoh, A., Yahaya, M.D. & Auta, M. (2018). Proximate analysis and characterization of some Aquatic wastes as potential feedstock for chitin/chitosan production. *Nigerian Journal of Engineering and Applied Sciences (NJEAS)*, 5(1), 93 – 101
- Islam, M., Masum, S., Rahman, M., Molla, A.I., Shaikh, A.A., Roy, S.K. (2011). Preparation of Chitosan from Shrimp Shell and Investigation of its Properties. *International Journal of Basic & Applied Sciences*, 11(1), 77 – 80.
- Islem, Y., & Marguerite, R. (2015). Chitin and Chitosan Preparation from Marine Sources: Structure, Properties and Applications. *Journal of Marine Drugs*, 13(1660 – 3397), 1133 – 1174.
- Joshy, C.G., Zynudheen, A.A., George, N., Ronda, V., & Sabeena, M. (2016). Optimization of Process Parameters for the Production of Chitin from the Shell of Flower-tail Shrimp (*Metapenaeus dobsoni*). *Society of Fishery Technology India*, 53(10), 140 – 145.
- Kaewboonruang, S., Phatrabuddha, N., Sawangwong, P., & Pitaksanurat, S. (2016). Comparative Studies on the Extraction of Chitin – Chitosan from Golden



- Apple Snail Shells at the Control Field. IOSR Journal of Polymer and Textile Engineering, 3(1), 34 – 41.
- Khan, M. & Newsad, K.M.A. (2012) Development of protein enriched shrimp crackers from shrimp shell wastes. Journal of Bangladesh Agricultural University, 10(2), 367 – 374.
- Kolawole, M.Y., Aweda, J.O. and Abdulkareem, S. (2017). Archachatina marginata bio-shells as reinforcement material in metal matrix composites. International Journal of Automotive and Mechanical Engineering, 14(1), 4068 – 4079.
- Kumar, M. Y. and Ravi, A. (2017). Extraction and Characterization of Chitosan from Shrimp waste for application in the feed industry. International Journal of Science Environment and Technology, 6(4), 2548 – 2557.
- Naznin, R. (2005). Extraction of chitin and Chitosan from Shrimp shell by chemical method. Pakistan Journal of Biological Science, 8(7), 1051 – 1054.
- Oshagbemi, A.A. (2016). Adsorption Study of the Removal of chromium (vi) ion from aqueous solution using developed chitosan – zeolite composite adsorbent.
- Pujari, N. & Pandharipande, S.L. (2016). Review on Synthesis, Characterization and Bioactivity of Chitosan. International Journal of Engineering Sciences & Research Technology, 5(10), 334 – 344.
- Russell, G.S., (2013). A Review of the Applications of Chitin and Its Derivatives in Agriculture to Modify Plant-Microbial Interactions and Improve Crop Yields. Journal of Agronomy, 3(1), 757 – 793.
- Shahidi, F. & Abuzaytoun, R. (2005). Chitin, chitosan and co-products: Chemistry, production, applications and health effects. Advances in Food and Nutrition Research U.S.A., Elsevier Inc., 93-135.
- Shanta, P., Paras N.Y., Rameshwar A., (2015). Applications of Chitin and Chitosan in Industry and Medical Science: A Review. Nepal Journal of Science and Technology, 16(1), 99 – 104.
- Thillai N. S., Kalyanasundaram, N., and Ravi, S. (2017). Extraction and Characterization of Chitin and Chitosan from Achatinodes. Natural Products Chemistry & Research, 5(5), 1 – 5.
- Toan, N.V. (2011). Improved Chitin and Chitosan Production from Black Tiger Shrimp Shells Using Salicylic Acid Pre-treatment. The Open Biomaterials Journal, 3(1), 1 – 3.
- Wassila A., Leila A., Lydia A. & Abdeltif A. (2013). Chitin Extraction from Crustacean Shells Using Biological Methods – A Review. Food Technology Biotechnology, 51(1), 12 – 25.



OPTIMISATION STUDY ON THE REMOVAL Pb(II), Cd(II) and Ni(II) FROM PHARMACEUTICAL WASTEWATER USING CARBONIZED AFRICAN GIANT SNAIL SHELL (*Archachatina marginata*) AS AN ADSORBENT.

Olanipekun, O.¹, Aboje, A. A.², Auta, M.³.

^{1,2,3} Department of Chemical Engineering, Federal University of Technology, P.M.B 65, Main Campus, Gidan Kwano-Minna, Niger State, Nigeria

Corresponding author email: beautyink44@yahoo.com, +2348032474456

ABSTRACT

Rapid expansion of the pharmaceutical industry resulting to increased wastewater disposal containing heavy metals calls for concern. Therefore, carbonised *Archachatina marginata* was used in order to understand how better the Pb(ii), Cd(ii) and Ni(ii) ion in pharmaceutical wastewater can be efficiently adsorbed. A Response Surface Method (RSM) Central Composite Design (CCD) was used to study the adsorption efficiencies of these heavy metals using DESIGN EXPERT Version 7.0.0 software. This software was used for the model fitting and also to evaluate the statistical significances of models. Batch adsorption studies was then carried out at optimum conditions. Raw sample was analysed using the X-ray Fluorescence (XRF) Spectrometry to contain 54.565 % CaO, 1.35 % SiO₂ and 0.67 % Al₂O₃ among others. It was also subjected to Thermo-Gravimetric Analysis (TGA) to establish its thermal response before the production of activated carbon. Brunauer Emmet Teller (BET) analysis carried out on carbonised samples revealed an increasing surface area and pore volume with increase in temperature causing irregular pore sizing. Pharmaceutical wastewater was analysed using the Flame atomisation adsorption spectrometry (AAS) to contain 0.09 mg/l Pb(ii) 0.0439 mg/l Cd(ii) and 0.1034 mg/l Ni(ii). Percentage removal of Pb(ii) and Ni(ii) increased with increase in adsorbent dosage while that of Cd(ii) decreased. Removal of all three increased with increase in temperature and time as well. Removal efficiencies of 95.44, 90.06 and 90.89 % were recorded for Pb(ii), Ni(ii) and Cd(ii) respectively. Determination coefficient (R²) for the adsorption models of Cd, Ni and Pb are 0.9513, 0.9694 and 0.9598.

Keywords: Adsorbent dosage; Response surface methodology; Removal efficiency; Snail shell; Temperature; Time.

1 INTRODUCTION

Massive urbanization has resulted in the release of wastewater from various industrial processes into the environment which in turn pollutes the ecosystem and eventually harms living beings with their toxic nature (Hossain, et al., 2012). Process industries such as electroplating industries, hospitals, pharmaceuticals, powerplant, refineries, leather tanning, mining, dyes and pigments, steel fabrication, canning industries and inorganic chemical production plants are at the helm of affairs in the release of waste water into the environment (Radaideh, et al., 2017). The term 'heavy metal' denotes group of metals and metalloids with a density greater than 5 g/cm³ with atomic weights between 63.5 and 200.6 and a specific gravity greater than 5.0 (Chen, et al., 2018; Singh & Gupta, 2016). Chromium (Cr), Cadmium (Cd), Copper (Cu), Mercury (Hg), Nickel (Ni), Iron (Fe), Arsenic (As), Lead (Pb), Zinc (Zn) and Gold (Au) are toxic are examples of this group which has attracted attention of several researchers. Methods engaged to reduce or out rightly remove these metals are not limited to precipitation, solvent extraction, ion-exchange, reverse osmosis, oxidation/reduction, sedimentation, filtration, electrochemical techniques and cation surfactant

(Czikkely et al., 2018). In this study however, the use of low-cost adsorbent in the adsorption of Lead (Pb), Cadmium (Cd) and Nickel (Ni) from pharmaceutical water is considered. The recommended limit of Cadmium (Cd) in waste water is only 0.005 mg/L, Nickel (Ni) is 0.02 mg/L and Lead (Pb) is 0.006 mg/L (Singh & Gupta, 2016). The surge demand for pharmaceutical product stems from ground breaking research that has been made in the field of medicine. Hence, volume of wastewater from this ever-increasing industry calls for concern to bring its component within environmentally acceptable limits at minimum cost. Pharmaceutical process is water consuming therefore, the recycle of wastewater especially in the Sahara region of Africa cannot be over emphasized. African giant snail shell is abundant in the coastal region of Nigeria and can serve as a bio-sorbent subject to further studies. Therefore, this study intends to focus on the use of carbonized African giant land snail shells (*Archachatina marginata*) as a biomass-derived adsorbent for the removal of Lead (Pb), Cadmium (Cd) and Nickel (Ni) from pharmaceutical wastewater.

2 METHODOLOGY

2.1 SAMPLE PREPARATION

The Snail Shells (SnS) were washed with detergent, they were then dried in an oven and crushed to smaller particle sizes (Sunday & Magu, 2017) after which it was sieve with 1mm meshed sieve coupled to a mechanical shaker. The pulverized snail shells of 1mm particle size are placed in an airtight sample bottle and stored for further use. The chemical properties and thermal response of snail shell sample was investigated with the aid of X-ray fluorescence (XRF) and Thermo-Gravimetric Analysis (TGA) respectively. Grab sampling method was used in collecting the wastewater used in this study. Wastewater was collected in 5 L jerry can previously washed with distilled water which was then, rinsed with the wastewater. Sufficient quantities of the wastewater were collected and transported and stored under refrigerated condition. This was done to inhibit the ageing effect, biodegradation and changes in the pharmaceutical wastewater physiochemical properties (Bolade & Sangodoyin, 2018).

2.1.1 X-RAY FLUORESCENCE (XRF) SPECTROMETRY

X-rays fluorescent (XRF) analysis was conducted using PANanalytical XRF spectrometer (MiniPal 4). X-RF analysis was carried out by placing 2 g of 100 μm size of the sample on a clean stainless-steel lid which was placed in the cubicle of the spectrometer to determine its elemental composition. When the sample was irradiated by X-rays, the system software measures the individual component wavelengths of the fluorescent emission produced by atoms in the sample (Sani, et al., 2017).

2.1.2 THERMO-GRAVIMETRIC ANALYSIS (TGA)

This analysis was carried out based on the method reported by Kolawole et al., (2017) where thermal transition and decomposition of the sample was done via TGA analysis using Perkin Elmer TGA 4000 thermogravimetric Analyzer at 10 $^{\circ}\text{C}/\text{min}$ constant heating rate in nitrogen atmosphere following the ASTM D6370 standard procedure.

2.1.3 FLAME ATOMISATION ADSORPTION SPECTROMETRY (AAS)

Thermo scientific ICE 3000 AA02134104v1.30 was used to detect heavy metals present in pharmaceutical wastewater samples. Spectrometer was set to absorbance mode and a bandpass of 2 nm. It was connected to an ethylene flame flow of 0.9 L/min. calibration was then carried out at a scaling factor of 1.0 for each metal to be analysed.

2.2 ADSORBENT PREPARATION AND CHARACTERIZATION

Snail shell (SnS) sample was weighed in batches of 5 g and each was placed in a crucible and carbonised at temperatures 600, 700, 800 and 900 $^{\circ}\text{C}$ in a Gallen Kamp muffle furnace for two hours respectively after which it is exposed to free air for four hours in other to increase its surface area (Adiotomre, 2015; Odoemelum, & Eddy, 2009). Each batch of highly active calcium oxide catalyst were labeled S-600, S-700, S-800, and S-900 respectively and placed in an air tight container. Afterwards, pore volume, pore size and surface area were determined using the Brunauer Emmet Teller (BET) method (Zhang et al 2014; Adiotomre, 2015).

2.2.1 BRUNAUER EMMET TELLER (BET) ANALYSIS

Specific surface area and pore volume analysis of the adsorbent was carried out using BET surface area Nitrogen adsorption procedure. The prepared adsorbent was out gassed under vacuum condition at 300 $^{\circ}\text{C}$ for 4 hours. Out gassed carbon sample was tested for surface area (m^2/g) and pore volume (m^3/g) at 77 K using a 15-point BET NovaWin Quantachrome, 2013 version 11.03.

2.2.2 ADSORBENT RE-USABILITY

Determination of the adsorbent reusability gives an insight into the adsorbent's chemical, thermal, mechanical and physical stability of the adsorbent during consecutive rounds of adsorption – desorption. The desorption was carried out by reacting the spent adsorbent with 1M HCl. This was carried out five consecutive times (Khan & Lo, 2016).

2.3 OPTIMIZATION STUDIES

The experimental design was setup up in other to determine the optimum conditions and removal efficiency of Cd, Ni and Pb metals from the pharmaceutical wastewater. A statistical software (DESIGN EXPERT Version 7.0.0, Stat Ease, Inc., USA) was used for the model fitting and in the evaluation of the statistical significance. The Response Surface Method (RSM) Central Composite Design (CCD) was used to study the adsorption efficiencies of these metals.

Table 1. Process Parameters under Investigation for design purposes

Variables	Low Value	High Value
Adsorbent dosage (mg)	15	50
Temperature (°C)	40	60
Contact time	10	30

Table 3. Process parameters under statistical investigation

Variables	Low Value	High Value	- alpha	+ alpha
Adsorbent dosage (mg)	15	50	3.07	61.9
Temperature (°C)	40	60	33	66
Contact time	10	30	3	37

Table 2. Experimental design matrix for the adsorption of Pb, Cd and Ni

Runs	A: Adsorbent Dosage (mg)	B: Temperature (°C)	C: Contact Time (minutes)	Cd removal X_{Cd} (%)	Ni removal X_{Ni} (%)	Pb removal X_{Pb} (%)
1	15.00	60.00	30.00	50.1	57.8	61.3
2	15.00	60.00	10.00	36.2	40.9	43.1
3	32.50	50.00	20.00	70.1	82.1	75.3
4	50.00	60.00	30.00	40.2	42.2	40
5	15.00	40.00	30.00	67.1	64.3	75.1
6	32.50	50.00	20.00	79.8	76.3	78.6
7	32.50	50.00	20.00	79.5	83.6	79.8
8	32.50	50.00	20.00	77.7	75	71
9	15.00	40.00	10.00	30.1	45.4	55.1
10	32.50	50.00	20.00	78.6	76.4	80.7
11	32.50	33.18	20.00	67.3	80	92.2
12	32.50	50.00	3.18	48.1	59.1	52.2
13	50.00	60.00	10.00	31.2	33.6	48.7
14	32.50	66.82	20.00	41.4	45.2	49.6
15	61.93	50.00	20.00	56.8	62.4	65.4
16	32.50	50.00	36.82	88	92.4	80.8
17	3.07	50.00	20.00	30	37	39.6
18	50.00	40.00	30.00	91	92.7	95.5
19	50.00	40.00	10.00	86	79.8	78.1
20	32.50	50.00	20.00	86.5	77.5	76.3

2.4 BATCH ADSORPTION EXPERIMENTS

According to Abbas, et al., (2014) factors which affect the removal of heavy metals include but are not limited to the effect of temperature, contact time and adsorbent dosage. Similarly, Lakherwal, (2014) reported that adsorption parameters such as contact time, adsorbent dosage and temperature have immense effect on the removal efficiency. Each of the parameters was studied with each setup stirred continuously with the aid of a magnetic stirrer at an agitation speed of 190 rpm.

2.4.1 EFFECT OF CONTACT TIME

The effect of contact time on percentage removal was studied by transferring 50 ml of the wastewater into a 100 ml flask. The setup is left to stand on a magnetic stirrer at ambient room temperature for a suitable time at time ranges of 5, 10, 15, 20, and 30 mins at optimum adsorbent dosage and temperature (Akinoye, et al., 2016; Adewoye, et al., 2017).

2.4.2 EFFECT OF ADSORBENT DOSAGE

The effect of the adsorbent weight on the percentage removal was studied by transferring 50 ml of the wastewater into different 100ml flask. The adsorbent at different dosages (10 mg, 20 mg, 30 mg, 40 mg, 50 mg and 60 mg) was then added to the flasks and the setup was maintained at optimum conditions and left to stand on a magnetic stirrer (Akinyeye et al., 2016).

2.4.3 EFFECT OF TEMPERATURE

The adsorption process is setup in a 100 ml flask containing 50ml of the wastewater and the adsorbent. The setup is exposed to temperatures of 32, 40, 45, 50, 60 °C respectively. Data from here helps in estimation of the thermodynamic behavior of the adsorption process whereby a decrease in the adsorption rate as the temperature increase would denote an exothermic system and vice versa. The setup was left to stand on a magnetic stirrer at optimum condition (Lakherwal, 2014).

2.5 EQUILIBRIUM STUDIES

The optimum parameters determined from the batch adsorption studies was used to carry out the adsorption of the heavy metals in the pharmaceutical waste water.

2.5.1 REMOVAL EFFICIENCY DETERMINATION

The removal efficiency of the adsorbents on the metal ion adsorption was determined using equation (1)

$$\text{Removal efficiency (\%)} = \frac{(C_0 - C_e)}{C_0} \times 100 \quad (1)$$

Where C_0 and C_e are the initial and final concentrations of metal ions.

3 RESULTS AND DISCUSSION

Table 4 shows the XRF elemental analysis of African land giant snail Shell (*Achatina maginata*) this was carried out to determine the chemical composition of the snail shell. Which reveals that the bulk of the African land giant snail Shell is composed of CaO with other elements like SiO_2 , Fe_2O_3 , Al_2O_3 and ZnO occupying a minute fraction of the bulk of the African land giant snail Shell.

Table 4. XRF result showing composition of snail shell sample (*Achatina maginata*).

Composition	Weight (%)
CuO	0
NiO	0
Fe_2O_3	0.066
MnO	0
Cr_2O_3	0
TiO_2	0
CaO	54.565
Al_2O_3	0.67
MgO	0
ZnO	0.011
SiO_2	1.35
LOI	43.338

From figure 1 it was observed that at temperature ranges of 27.7 °C–320 °C there was no significant degradation of the snail shell. Hence, this implies that the snail shell is thermally stable between temperature ranges of 27.7 °C–320 °C. As the temperature approaches 525 °C, a drastic loss of weight in the snail shell is observed which can be attributed to moisture losses and loss of volatile content as well. Further down the curve as the temperature approaches 825 °C, thermal decomposition sets in indicating that the calcium carbonate in the snail shell is converted into calcium oxide. This is accompanied with the liberation of carbon (iv) dioxide. Therefore, carbonization of snail shell at a minimum reaction temperature of 600 °C is required. According to Kolawole et al., (2017) the major un-degraded constituent contains calcium oxides and carbon residues.

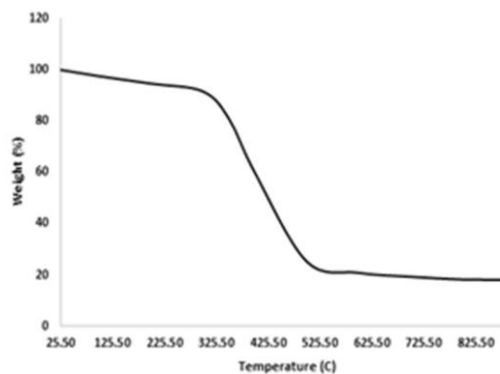


Figure 1: TGA curve for African land giant snail Shell (*Achatina maginata*) powder.

*Heating rate of 10 °C/min and 40cc/min N_2 flow rate

From table 5 below, it was observed that surface area and pore volume increased with increase in temperature while pore size reduced and increased in sinusoidal manner. This can be attributed to expansion as a response to heat treatment. Continuous expansion of the surface area and pore volume redefines pore sizes and shapes differently each time. A significant increase of 15.4271 % in surface area, 1.778 % in pore volume and a marginal decrease of 0.28 % in pore size was recorded at 600 °C. At the maximum temperature of 900 °C, 36.99 % surface area increase, 3.62 % pore volume increase and 0.468 % decrease in pore size were observed. This implied that snail shell has a shock response to heat considering changes in pore and surface structures.

Table 5. BET analysis result for African land giant snail shell (*Achatina maginata*)

Samples	Surface area (m ² /g)	Pore volume(cc/g)	Pore size (nm)
Raw Snail Shell	305.379	0.1839	2.138
S – 600	352.490	0.2166	2.132
S – 700	361.32	0.2182	2.231
S – 800	392.508	0.2111	2.100
S – 900	418.33	0.2201	2.128

Table 6,7 and 8 indicate the physiochemical, metal content and adsorption effect of adsorbent on pharmaceutical wastewater. It was observed that the adsorption process brought wastewater within standard simultaneously as heavy metals were removed. Notable among others were conductivity reduction by 76.14 %, COD reduction by 84.1 % and TDS reduction by 76.1 %. Highest removal efficiency of 95 % was recorded for Pb while Cd and nickel were removed at 90.89 and 90.06 % respectively. This shows the viability of carbonised snail shell as an adsorbent for pharmaceutical wastewater.

Table 6. Result showing physiochemical characteristics of Pharmaceutical wastewater

Parameter	Raw	Treated	NSDWQ
pH	5.83	6.87	6.5-8.5
TDS	1196.1	285.4	500
Conductivity (µS/cm)	1869	446	1000
Turbidity (NTU)	3.45	2.16	5
Total Alkalinity (mg/L)	498	20	--
Total Hardness (mg/L)	156	76	150
Dissolved Oxygen (mg/L)	8.0	7.0	--
COD (mg/L)	144.68	23.6	30
BOD (mg/L)	6.0	2.0	6.0
Chloride (mg/L)	65.66	44.1	250
Magnesium (mg/L)	13.78	1.37	2
Calcium (mg/L)	37.84	12.62	--

Table 7. AAS analysis result for pharmaceutical wastewater sample

Metal	Raw water	Standard
Cd	0.0439	0.005
Ni	0.1034	0.02
Cr	BDL	-
Pb	0.09	0.01
Fe	0.0349	-

Table 8. result showing initial and final concentration of Cd, Ni and Pb before and after adsorption process

Heavy metal	concentration (mg/l)	Removal Efficiency	MCLS (mg/l)
	Initial (C _o)	Final (C _e)	
Cd	0.0439	0.004	0.01
Ni	0.2505	0.0249	0.20
Pb	0.09	0.0041	0.006

From the surface plot depicted in figure 2, it was observed that an increment in the adsorbent dosage lead to a similar increment in the percentage removal of Cd. However, an increase in the temperature resulted to a decrement in the percentage removal of Cd. In terms of the interaction effect between the adsorbent dosage and the temperature it was observed that an optimum percentage removal of Cd of 94.5 % was observed at an adsorbent dosage of 43 mg and a temperature 41 °C.

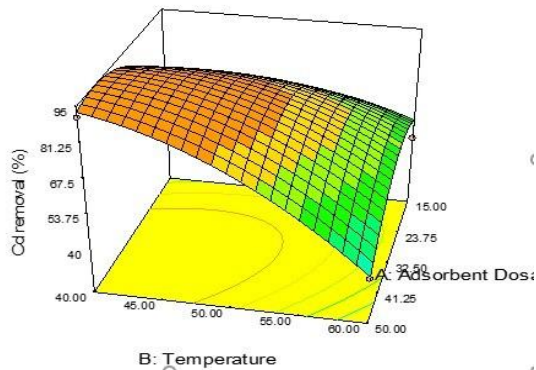


Figure 2: Response surface plot of the interaction effect of adsorbent dosage and temperature on the adsorption of Cd at a contact time of 30 minutes.

From the 3D surface plot represented in Figure 3, it was observed that an increment in the adsorbent dosage resulted in an increase in the percentage removal of Cd. Similarly, an increase in the contact time resulted in an increase in the percentage removal of Cd. However, in terms of the interaction effect of the Adsorbent dosage and contact time an optimum percentage removal of Cd of 93.2% was observed at adsorbent dosage of 50mg and contact time of 29 minutes.

From the 3D plot in Figure 4 it was observed that as the temperature dropped from 60 °C the percentage

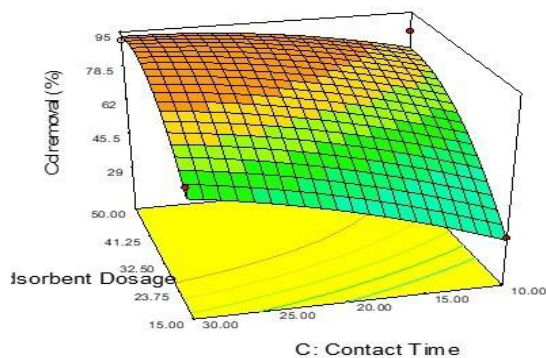


Figure 3: Response surface plot of the interaction effect of adsorbent dosage and contact time on the adsorption of Cd at a temperature of 40 °C.

removal of Cd increased simultaneously. Similarly, an increase in the contact time also resulted in an increase in the percentage removal of Cd. In terms of the interaction effect of temperature and contact time an optimum percentage removal of Cd of 92.94 % was observed at a temperature of 40 °C and a contact time of 30 minutes.

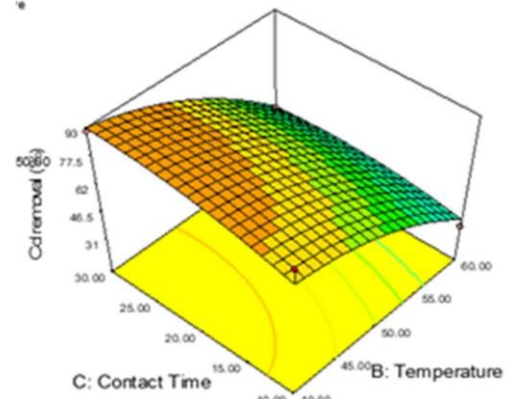


Figure 4: Response surface plot of the interaction effect of temperature and contact time on the adsorption of Cd at an adsorbent dosage of 50 mg.

From the plot represented in Figure 5 it was observed that there was an increment in the percentage removal of Ni when there was an increment in the adsorbent dosage. A similar increase in the percentage removal of Ni was observed when the reaction temperature dropped from 60 °C. The interaction effect of adsorbent dosage and temperature resulted in an optimum percentage removal of Ni of 95 % at an adsorbent dosage of 50 mg and a temperature of 40 °C.

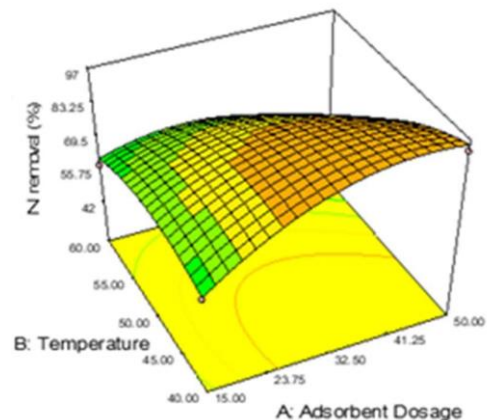


Figure 5: Response surface plot of the interaction effect of adsorbent dosage and temperature on the adsorption of Ni at a contact time of 30 minutes.

Figure 6 represents the Response surface plot of the interaction effect of Adsorbent dosage and contact time on the adsorption of Ni at a temperature of 40 °C. It was observed from the plot that an increase in the contact time brought about a similar increment in the percentage removal of Ni. A similar increment in the adsorbent dosage also led to an increment in the percentage removal of Ni. The interaction effect of the adsorbent dosage and the contact time resulted in an optimum percentage removal of Ni of 95.2 % at adsorbent dosage of 50mg and contact time of 30 minutes.

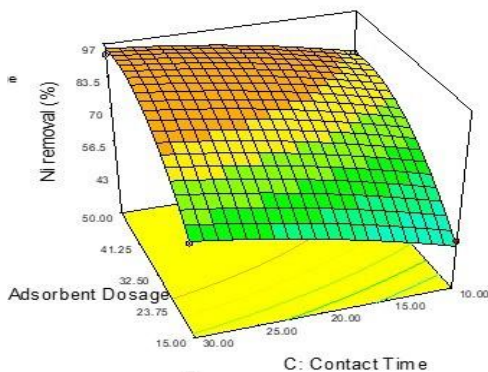


Figure 6: Response surface plot of the interaction effect of adsorbent dosage and contact time on the adsorption of Ni at a temperature of 40 °C.

The plot represented in Figure 7 represents the Response surface plot of the interaction effect of temperature and contact time on the adsorption of Cd at an adsorbent dosage of 50 mg. It was observed from the plot that an increment in the contact time resulted to an increase in the percentage removal of Ni. Similarly, a decline in the temperature from 60 °C to 40 °C resulted to an increment in the percentage removal of Ni. The effect of the temperature and the contact time resulted in an optimum percentage removal of Ni of 95 % at a temperature of 40 °C and a contact time of 30 minutes.

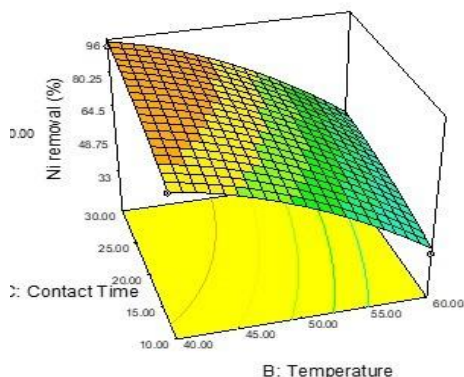


Figure 7: Response surface plot of the interaction effect of temperature and contact time on the adsorption of Ni at an adsorbent dosage of 50 mg.

From the plot represented in Figure 8 it was observed that as the adsorbent dosage increased so did the percentage removal of Pb. However, as the adsorbent dosage increased above 39 mg there was a slight dip in the percentage removal of Ni. A decrement in the temperature from 60 °C to 40 °C resulted in the increment in the percentage removal of Ni. In terms of the interaction effect of the adsorbent dosage and temperature an optimum percentage removal of Ni of 96 % was observed at an adsorbent dosage of 45 mg and a temperature of 40 °C.

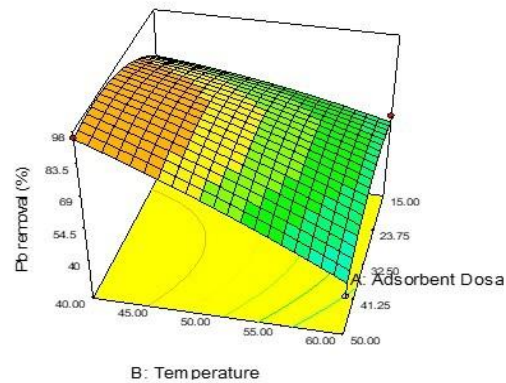


Figure 8: Response surface plot of the interaction effect of adsorbent dosage and temperature on the adsorption of Pb at a contact time of 30 minutes.

From the plot represented in Figure 9, it was observed that as the adsorbent dosage increased so did the percentage removal of Pb. Similarly, it was observed that as the contact time also increased so did the percentage removal of Pb increase. In terms of the interaction effect of the adsorbent dosage and the contact time an optimum of 95 % at an adsorbent dosage of 50 mg and a contact time of 30 minutes.

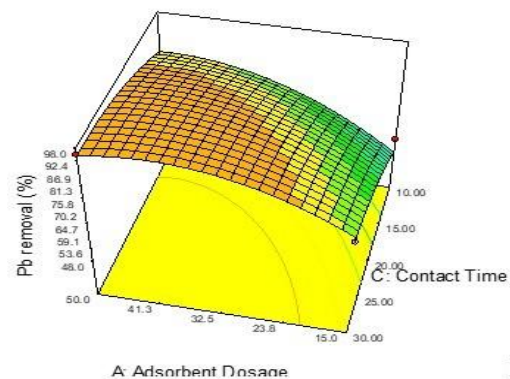


Figure 9: Response surface plot of the interaction effect of adsorbent dosage and contact time on the adsorption of Pb at a temperature of 40 °C.

The plot represented in Figure 10 represents the interaction effect of temperature and contact time on the adsorption of Pb at an adsorbent dosage of 50 mg. It was observed from the plot that a decline in the temperature resulted in an increment in the percentage removal of Pb. When the contact time is considered an increment in the contact time also resulted in an increment in the percentage removal of Pb. In terms of the interaction effect an optimum percentage removal of Pb of 94.9 % was observed at a temperature of 40 °C and a contact time of 30 minutes.

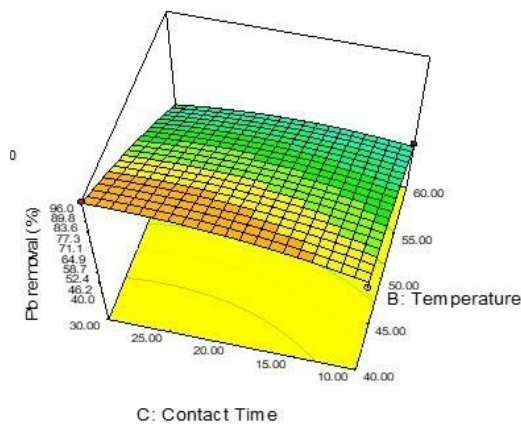


Figure 10: Response surface plot of the interaction effect of temperature and contact time on the adsorption of Pb at an adsorbent dosage of 50 mg.

From Figure 11 below, it was observed that as the adsorbent dosage increased so did the percentage removal increase. It is noteworthy that the percentage removal of cadmium, Nickel and Lead increased significantly from 67.2 to 90, 69.8 to 91.1 and 77.8 to 93.1% respectively as the adsorbent dosage was varied from 10 to 50 mg. Further increment in the adsorbent dosage resulted in a slight reduction in the removal efficiency. The reason for this may be attributed to overlapping of the adsorption sites which could lead to an overall decrease in the available binding sites (Adewoye, et al., 2017).

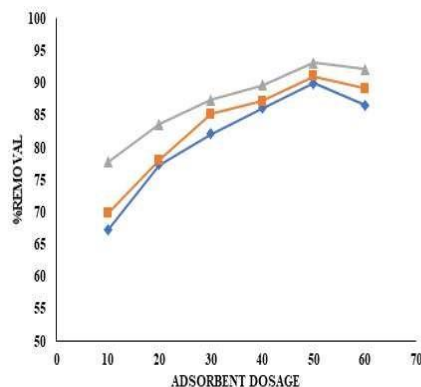


Figure 11. Effect of Adsorbent Dosage on Adsorption of Cd/Ni/Pb on Carbonized Snail shell

Figure 12 represents the plot of the effect of temperature against the adsorption of Cd/Ni/Pb on Carbonized Snail shell. It was observed that an increase in the temperature resulted in an increase in the adsorption of Ni and Pb while at the same time it resulted in a decrease in the adsorption of Cd. Further increment in the adsorption temperature above 50 °C resulted in a notable reduction in the adsorption of Cd/Ni/Pb. Optimum adsorption of Cd/Ni/Pb was observed at a temperature of 50 °C with adsorption rate of 89.4, 91.2 and 89.2 respectively.

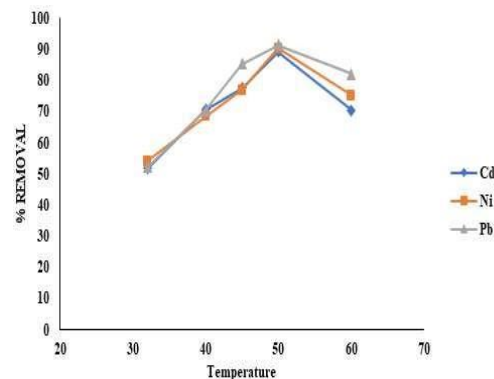


Figure 12. Effect of Temperature on Adsorption of Cd/Ni/Pb on Carbonized Snail shell

The effect of Contact Time on Adsorption of Cd/Ni/Pb on Carbonized Snail shell was studied and the data presented in Figure 13. From the graph, it was observed that an increase in the contact time resulted in a comparatively similar increment in the adsorption of Cd/Ni/Pb with the progression of time from 10 min to 40 min. Further increment in the contact time caused a decline in the adsorption rate and this was attributed to overlapping of the adsorption sites over time resulting in an overall decrease in the available binding sites (Adewoye, et al., 2017).

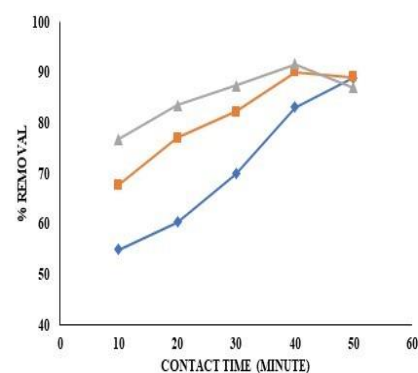


Figure 13. Effect of Contact time on Adsorption of Cd/Ni/Pb on Carbonized Snail shell

The analysis of the variance (ANOVA) for the response surface quadratic model for the adsorption of Cd, Ni and Pb was shown in Equation 2,3 and 4 respectively. The ANOVA analysis gives a model expression which relates the adsorption of Cd, Ni and Pb to the three process parameters (A, B and C). The ANOVA analysis for the adsorption of Cd and Ni shows that the significant process parameters that affect the adsorption process are A, B, C, AB, A² and B² while the ANOVA analysis of the adsorption of Pb shows that the significant process parameters that affect the adsorption of Pb are A, B, C, AB, A² and C² respectively. These terms are significant because their p-values are less than 0.05. Similarly, the quadratic model selected in the adsorption of Cd, Ni and Pb is significant because the models p-values are less than 0.05. In this study the value of the determination coefficient (R²) for the adsorption of Cd, Ni and Pb are 0.9513, 0.9694 and 0.9598 respectively imply that 95.13 %, 96.94 % and 95.98 % of the total variation can be attributed to the independent variables while 4.87 %, 3.06 % and 4.02 % of the total variation is not explained by the model in the adsorption of Cd, Ni and Pb respectively. The value of the coefficient of variation (C.V. %) gives the precision and reliability of the experiment carried out where a lower value of 10.64, 7.02 and 7.07 obtained in the adsorption of Cd, Ni and Pb respectively indicate a better precision and reliability of the experiment. Similarly, the model equation representing the adsorption of Cd, Ni and Pb respectively is presented in coded form where:

$$\begin{aligned} \text{Cd removal (\%)} = & 78.70 + 8.05A - 11.72B + 9.67C \\ & - 11.84AB - 4.61AC - 2.39BC - 12.45A^2 - 8.58B^2 - \\ & 3.74C^2 \end{aligned} \quad (2)$$

$$\begin{aligned} \text{Ni removal (\%)} = & 78.63 + 6.05A - 12.17B + 8.30C - \\ & 10.71AB - 1.79AC - 0.79BC - 11.16A^2 - 6.59B^2 - \\ & 1.94C^2 \end{aligned} \quad (3)$$

$$\begin{aligned} \text{Pb removal (\%)} = & 76.96 + 5.21A - 13.35B + 6.96C - \\ & 7.39AB - 3.69AC - 3.49BC - 8.72A^2 - 2.21B^2 - 3.77C^2 \end{aligned} \quad (4)$$

From Figure 14, 15 and 16, it was observed that there was a close correlation between the actual values obtained from the study as they lie close to the regression line as such they correlated with the predicted values generated by design expert. This close correlation is indicative of the fact that the quadratic model selected for the adsorption of Cd, Ni and Pb is suitable.

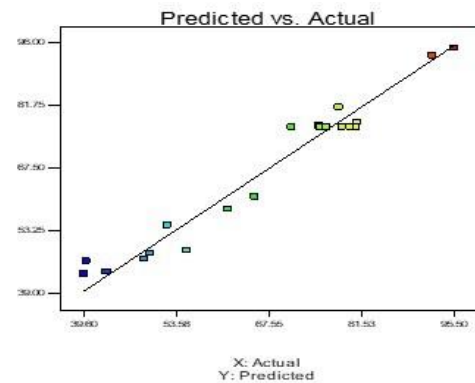


Figure 16. Parity plot of Predicted values (model) vs Actual values for the Adsorption of Pb

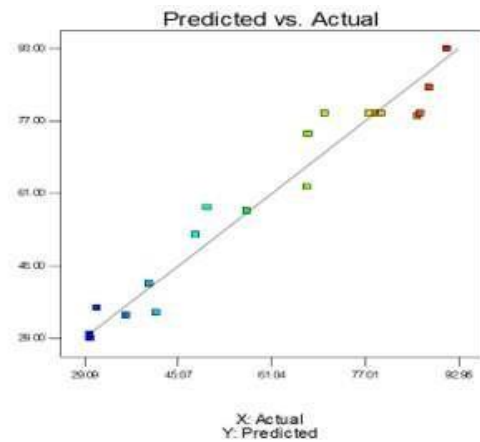


Figure 14. Parity plot of Predicted values (model) vs Actual values for the Adsorption of Ni

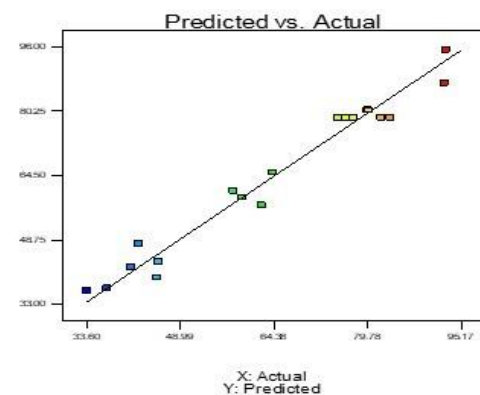


Figure 15. Parity plot of Predicted values (model) vs Actual values for the Adsorption of Ni

4 CONCLUSION

From the results obtained from the experiment, it can be concluded that African giant snail shell contains 54.565 % CaO thus, can be converted into an adsorbent with large surface area and pore volume when subjected to carbonization to burn off other components. Again, it can be concluded that temperature, time and adsorbent dosage has a significant effect on the adsorption of Pb(ii), Ni(ii) and Cd(ii) respectively using carbonised snail shell. It can also be concluded that the removal efficiency of Cadmium, Lead and Nickel were 90.89, 95.44 and 90.06 % respectively when using carbonised snail shell as an adsorbent. It can be said that the lower value of 10.64, 7.02 and 7.07 % obtained as the percentage coefficient of variation of the adsorption models of Cd(ii), Ni(ii) and Pb(ii) respectively indicate a better precision and reliability of the experiment.

ACKNOWLEDGEMENTS

Appreciations goes to Mr. Bolus and members of staff of the Water, Aquaculture and Fisheries Technology, Federal University of Technology Minna.

REFERENCE

- Abbas, S.H., Ismail, I.M., Mostafa, T.M., Sulayman, A.H. (2014). Biosorption of Heavy Metals: A Review. *Journal of Chemical Science and Technology*, 3(4), 74 – 102.
- Adewoye, L.T., Mustapha, S.I., Adeniyi, A.G., Tijani, J.O., Amoloye, M.A. & Ayinde, L.J. (2017). Optimization of nickel (ii) and chromium (iii) removal from contaminated water using sorghum bicolor. *Nigerian Journal of Technology*, 36(3), 960 – 972.
- Adiotomre, K.O. (2015). Effectiveness of Snail Shell as An Adsorbent for The Treatment of Waste Water. *International Journal of Innovative Environmental Studies Research*, 3(3), 1 – 12.
- Akinyeye, O.J., Ibigbami, T.B., Odeja, O. (2016). Effect of Chitosan Powder Prepared from Snail Shells to Remove Lead (II) Ion and Nickel (II) Ion from Aqueous Solution and Its Adsorption Isotherm Model. *American Journal of Applied Chemistry*, 4(4), 146 – 156.
- Bolade, O.O. & Sangodoyin, A.Y. (2018). Adsorption and Equilibrium Studies of Textile Effluent Treatment with Activated Snail Shell Carbon. *IOSR Journal of Environmental Science, Toxicology and Food Technology*, 12(4), 26 – 33
- Chen, H., Xie, A. & You, S. (2018). A Review: Advances on Absorption of Heavy Metals in the Waste Water by Biochar. *International Journal of Material science and Engineering*, 1(1), 1 – 5.
- Czikkely, M., Neubauer, E., Fekete, I., Ymeri, P. & Fogarassy, C. (2018). Review of Heavy Metal Adsorption Processes by Several Organic Matters from Wastewaters. *Journal of water*, 10(1), 1 – 15.
- Hossain, M.A., Hao Ngo, H., Guo, W.S. & Nguyen, T.V. (2013). Removal of Copper from Water by Adsorption onto Banana Peel as Bioadsorbent. *International Journal of GEOMATE*, 2(2), 227 – 234.
- Khan, M. & Lo, M.C. (2016). A holistic review of hydrogel applications in the adsorptive removal of aqueous pollutants: Recent progress, challenges, and perspectives. *Journal of Water Research*, 1(1), 1 – 14.
- Kolawole, M.Y., Aweda, J.O. and Abdulkareem, S. (2017). Archachatina marginata bio-shells as reinforcement material in metal matrix composites. *International Journal of Automotive and Mechanical Engineering*, 14(1), 4068 – 4079.
- Odoemelam S. A. & Eddy N. O. (2009) Studies on the Use of Oyster, Snail and Periwinkle Shells as Adsorbents for the Removal of Pb²⁺ from Aqueous Solution. *E-Journal of Chemistry*, 6(1) 213 – 222.
- Singh, N. & Gupta, S.K. (2016). Adsorption of Heavy Metals: A Review. *International Journal of Innovative Research in Science, Engineering and Technology*, 5(2), 2267 – 2281.
- Radaideh, J.A., Abdulgader, H.A. & Barjenbruch, M. (2017). Evaluation of Absorption Process for Heavy Metals Removal found in Pharmaceutical Wastewater. *Journal of Medical Toxicology and Clinical Forensic Medicine*, 3(2), 1 – 12.
- Sunday, E. A., & Magu, T. O. (2017). Determination of some metal contents in ashed and unashed snail shell powders. *World news of Natural Science*, 7(2017), 37 – 41.



Sani, J., Samir, S., Rikoto, II., Tambuwal, AD., Sanda, A., Maishanu, S.M., & Ladan, M.M. (2017) Production and Characterization of Heterogeneous Catalyst (CaO) from Snail Shell for Biodiesel Production Using Waste Cooking Oil. *Innovative Energy Research*, 6(2), 1 – 4.

Zhang, Y., Liu, S. & Wu, H. (2014). Experiment study on the decomposition properties of snail shell. *Journal of Biotechnology*, 9(8) 303 – 307.

Lakherwal, D. (2014) Adsorption of Heavy Metals: A Review. *International Journal of Environmental Research and Development*, 1, 41 – 48.

Ground Electromagnetic Prospecting for Potential Ore Mineralisation Zones in Tsohon-Gurusu Area of Minna, North-Central Nigeria

*Ogale, O. D¹, Rafiu, A. A¹, Alhassan, D. U¹, Salako K. A¹, Adetona A. A¹ & Unuevho C²

¹Department of Physics, Federal University of Technology, PMB 65 Minna Niger State, Nigeria

²Department of Geology, Federal University of Technology, PMB 65 Minna Niger State, Nigeria

*Corresponding author email: ogale.pg822219@st.futminna.edu.ng, +2347038620240

ABSTRACT

Very low electromagnetic method was used to investigate potential ore mineralisation zones in Tsohon Gurusu Area of Minna, North-Central Nigeria. A total of six (6) profiles were investigated, each with length of 500 metres, 100 metres inter-profile spacing and 20 metres inter-station distance. The VLF data were collected using Srintrex Envi VLF instrument. The acquired data sets were subjected to analysis and interpretation using MICROSOFT EXCEL, KHFFILT and OASIS MONTAJ software. The result of the study indicated a general structural trend of N-S direction with significant conductivity responses due to inferred fracturing units containing conductive minerals as indicated by the peak responses of the current distributions and the geologic features in the investigated profiles. Areas of high conductivity were observed in all the six (6) profiles corresponding to fracture zones of interest as indicated in the current density sections, with profile 5 having the highest conductivity response of 464.3 mS/m and profile 6 with the least conductivity response of -262.5 mS/m. It is generally observed that the depth of the major conductive bodies to be 80m.

Keywords: Fraser filtering, Conductivity, Cross-cutting, In-phase, Mineralisation, VLF-EM

1 INTRODUCTION

VLF-EM method is applicable in the investigation of geological conductive bodies as well as serving as a powerful tool for mapping shallow subsurface structural anomalies.

This method detects subsurface zones of anomalous electrical conductivity. Since these bodies (unlike common rock forming metals are insulators) are characterized by considerable amount of electrical conductivity distinguished by their ranges in electrical conductance, such zones of anomalous high electrical conductivity (or inversely low electrical resistivity) are potential subsurface water and conductive ore mineralisation zones (Telford et al., 2001).

Mineralisation is featured by fractured zones of dual purpose such that, it serves as channels for the mineralisation solution and a flash point for mineral deposition. General trends of geologic features are pathfinders in tracing target of interest in mineral prospecting and localized features such as contact and shear zones are responsible for the localization of ore deposit (Abubakar, 2012).

A country's ore and other mineral deposit constitute her natural wealth upon which hinges her development and prosperity (Prasad, 2012). This realization led to mining and the search for metals since the earliest times (Telford et al., 2001). Consequently, ore mineral deposits are in substantial amount embedded within the subsurface structures of the Earth, as such, systematic techniques in exploring such bodies are vital to minimize environmental degradation of the Earth's surfaces (Oluwaseun, 2013).

1.1 VLF-EM SURVEYING

VLF signal frequencies are generated by very powerful radio transmitters from Military bases in the United States of America and from other countries for the purpose of communication with their submarines and they are typically within the ranges of 15-30 kHz, transmitted for hundreds or thousands of kilometers, the curvature of the wave fronts is so slightly that they are effectively flat (Alan *et al.*, 2000). The transmitted e-m wave travels over or near the earth surface, the induced magnetic generated by the displacement current is defined by the primary magnetic field and shifts in phase when a conductive body is encountered, hence, the conductive body becomes a source of another field (secondary). As such, electrical characteristics of the subsurface can be determined by comparing the primary and secondary field.

The depth of penetrations of the transmitted electromagnetic waves depends on their frequencies and the electrical conductivity of the subsurface. This depth increases as both the frequencies and subsurface conductivity decreases (Kearey *et al.*, 1984).

$$\delta = \sqrt{\frac{\mu_0}{\sigma f}} \quad (1)$$

δ = Skin depth in meters (Depth of penetration of e-m wave passing into a conductor in which the amplitude of the wave is attenuated to $\frac{1}{e}$ of its amplitude at the surface of the conductor).

μ_0 = Magnetic permeability of free space = Henry/m.

ω = Angular frequency ($2\pi f$)

σ = Electrical conductivity of earth material (mho/m)

ρ = Electrical resistivity

f = Signal frequency.

At very large distances from a source of electromagnetic waves, attenuation of this type would control the depth of investigation. Effective depth of investigation Z_e , defines the maximum depth a body can be buried and still produce a signal recognizable above the noise. It is given as (kearey *et al.*, 1984)

$$100 \sqrt{-} \quad (2)$$

The VLF instrument detects the primary and secondary fields, and separates the secondary field into in-phase and quadrature components based on the phase lag of the secondary field. These two components of the secondary field are sometimes referred to as the tilt (in-phase) and ellipticity (quadrature), (Pirttijärvi, 2004). When the VLF-EM method is used for geophysical survey, the in-phase response is sensitive to metal or good conductive bodies (Lazarus *et al.*, 2013). The quadrature response, on the other hand, is sensitive to the variation of the earth electrical properties (Jeng *et al.* 2004).

$$n(\alpha) \quad (3)$$

$$(4)$$

The VLF electromagnetic method is a proficient tool for high grading mineralised area in preparation for competent mine development and is of significant contribution to an integrated geophysical investigative effort, Mbah *et al.* (2015).

1.2 LOCATION

Tsohon Gurusu is on the extreme south-west of Bosso Local Government area of Niger State and on latitude 9.625°N to 9.625°N and longitude 6.608°E to 9.604°E with an area extent of 250,000 square meters. The areal distance estimate is about 4.5 km from Maitumbi roundabout, Minna of which the site is about a km South-East off Minna-Gwada road and it is spanned by a well accessible road either by foot or by vehicle.

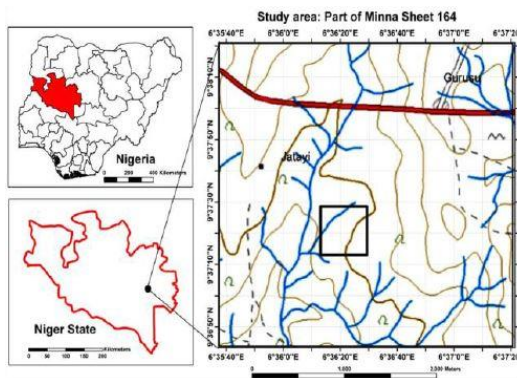


Figure 1: Part of Minna Sheet 164 Showing the (Kogbe, 1976)Location of the Study Area

1.3 GEOLOGY OF THE AREA

The study area lies within the Basement Complex of Nigeria. About half of the total area of Nigeria landmass is underlain by rocks of the Precambrian age known in the country as the Basement Complex. The remaining half is covered by Cretaceous to Quaternary sediments and volcanics. The basement complex is divided into the Western and the Eastern province. The Western Province is approximately west of longitude 8°E, typified by N-S to NNE-SSW trending schist belts separated from one another by migmatites, gneisses and granites. This trend is believed to be the result of Pan African orogeny involving collision between the West African Craton and the Pan African mobile terrain with and eastward dipping subduction zone (Ajibade *et al.*, 1979). The schist belts are differently interpreted as small ocean basins (Ajibade *et al.*, 1989), in filled rift structures (Ball, 1980) or synclinal remnants of an extensive supracrustal cover (Barley *et al.*, 1989).

The study area lies on the Kushaka schist belt. The Kushaka Schist Formation forms a number of curving schist belts, separated by domes and anticlines of gneiss (Obaje, 2009). The main rock type is semi-pelitic biotite-muscovite schist, in places containing garnet and staurolite. Other rocks are phyllites, metasiltstones and graphitic schists. Several thick units of banded garnet-grunerite iron formation are interbedded with the schists. A variety of amphibolites and amphibole, epidote, chlorite and talc-bearing schists correspond at least partly to tholeiitic basalt (Elueze, 1981). The Kushaka schist belts are invaded extensively by plutons of granite, granodiorite and syenite, which often penetrate the axial zone of the belts (Obaje, 2009).

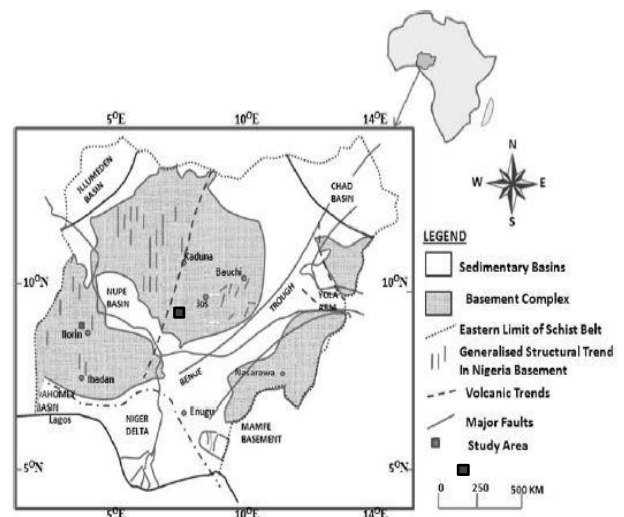


Figure 2: Geological Map of Nigeria Showing the Study Area. Source: (Kogbe, 1976).

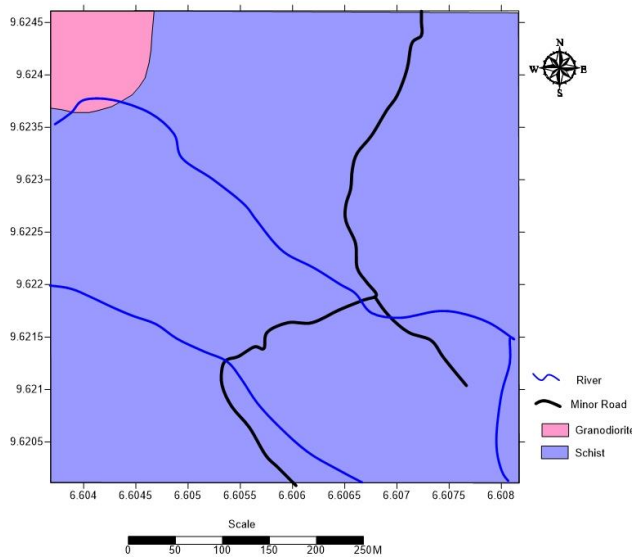


Figure 3: Geologic map of the study area

2 METHODOLOGY

The areal expanse was established by defining boundaries for investigation using a GPS and geological reconnaissance of the delineated work area was conducted to determine the regional strike of the rock foliations, established to trend in the North-South direction. Geological mapping was also carried out to generate the map indicating the different outcrops of rocks in the area.

A total of six (6) survey profiles with East-West orientations having inter-profile distances of 100 meters and inter-station spacing of 20 meters along each profile were generated across the strike formations, hence a total of 156 VLF stations were established, and from which VLF data was generated from each point of interest. This inter-profile and inter-station spacing is sufficient to give a very high density of data that will reveal high resolution subsurface geological image of the area.

The Scintrex Envi VLF Instrument was oriented along the frequency transmitter, and a frequency of 21.1kHz signal with callsign RDL from Russia having the best signal strength was selected. VLF data was then collected at the established stations which are along the dip direction (along profiles) of the rock outcrops in order to reveal the lithologic variations, (because lithologic variations occur along the dip direction and the dip direction is perpendicular to the strike).

The data acquired from the VLF survey was then interpreted using MICROSOFT EXCEL, KHFFILT and OASIS MONTAJ software.

3 RESULTS AND DISCUSSION

The VLF-EM data were analyzed and presented in profiles indicating regions of high and low conductivities, putting into cognizance the factors which gave rise to these anomalies. The data were presented in the Fraser

filtered format using KHFFILT software so as to eliminate the noise in the data caused by geologic and cultural features of less interest. Corresponding current density pseudo sections were also featured to give a 2D view of the current distributions with an average skin depth of 80 meters.

Peaks corresponding to cross cutting between the real (in-phase) and imaginary (quadrature) in the positive amplitude gave rise to interesting target locations with activities of higher current distributions and those in the negative gave lower current distributions. Conduction in earth materials are factored by the electronic, ionic and metallic conduction, with each having characteristic means of the conduction processes. Therefore, areas with high conductivity can be inferred to areas with fractures, developed pore spaces (as in sandstone) containing water, or highly mineralised zones containing conducting minerals.

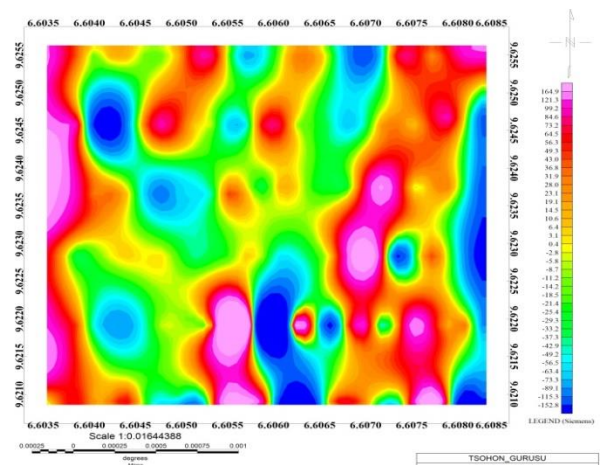


Figure 4: Filtered In-phase conductivity map

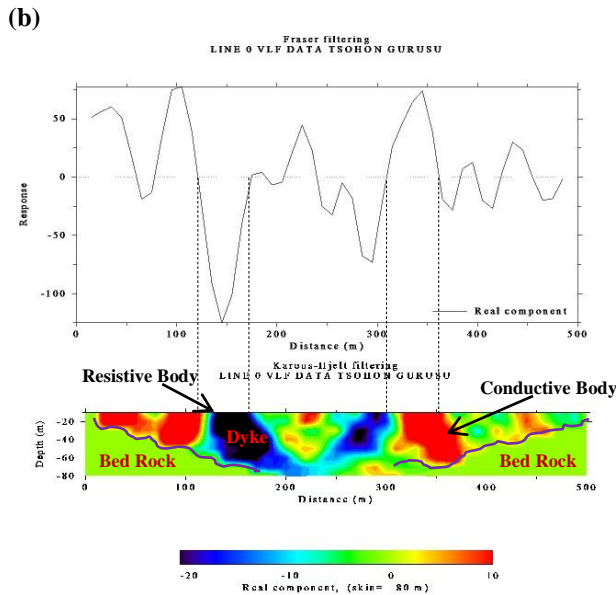
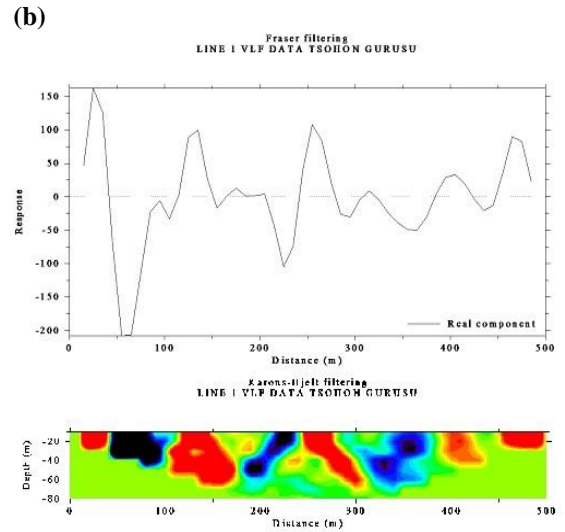
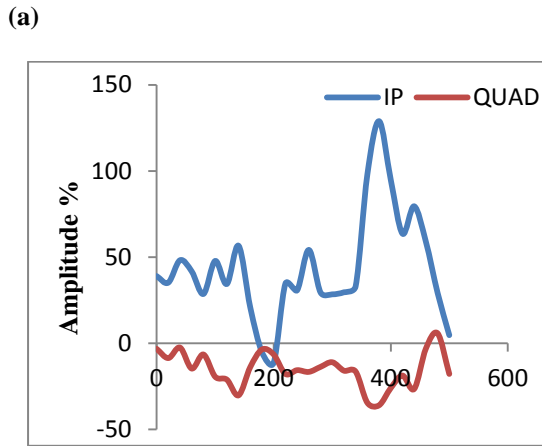


Figure 6: Profile 2; (a) unfiltered real (IP) and imaginary (Quad), **(b)** Fraser filter graph and 2D current density pseudo section.

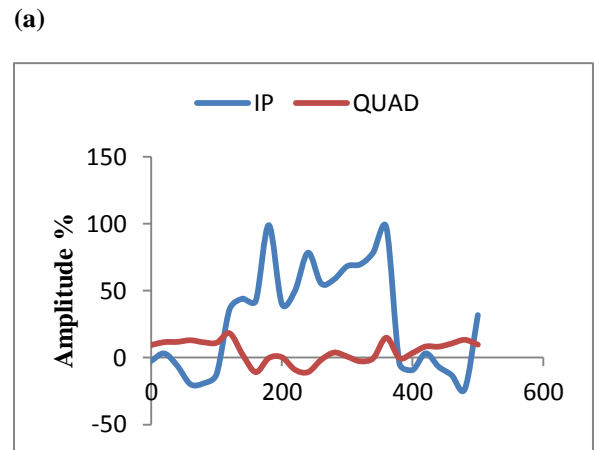
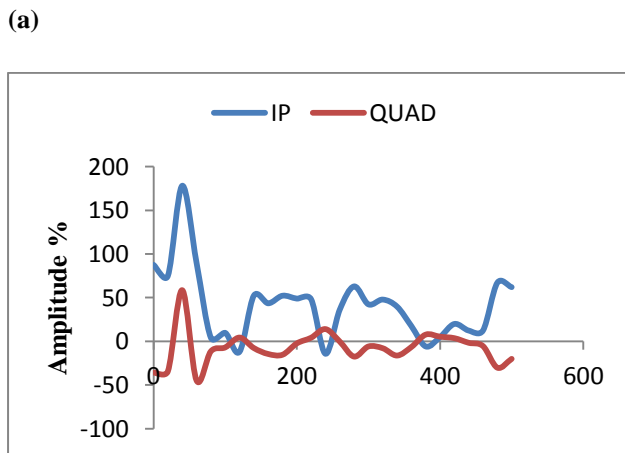


Figure 5: Profile 1; (a) unfiltered real (IP) and imaginary (Quad), **(b)** Fraser filter graph and 2D current density pseudo section.



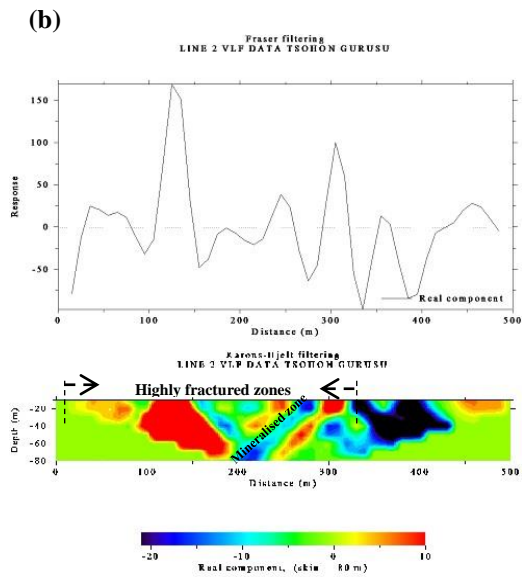


Figure 7: Profile 3; (a) unfiltered real (IP) and imaginary (Quad), **(b)** Fraser filter graph and 2D current density pseudo section.

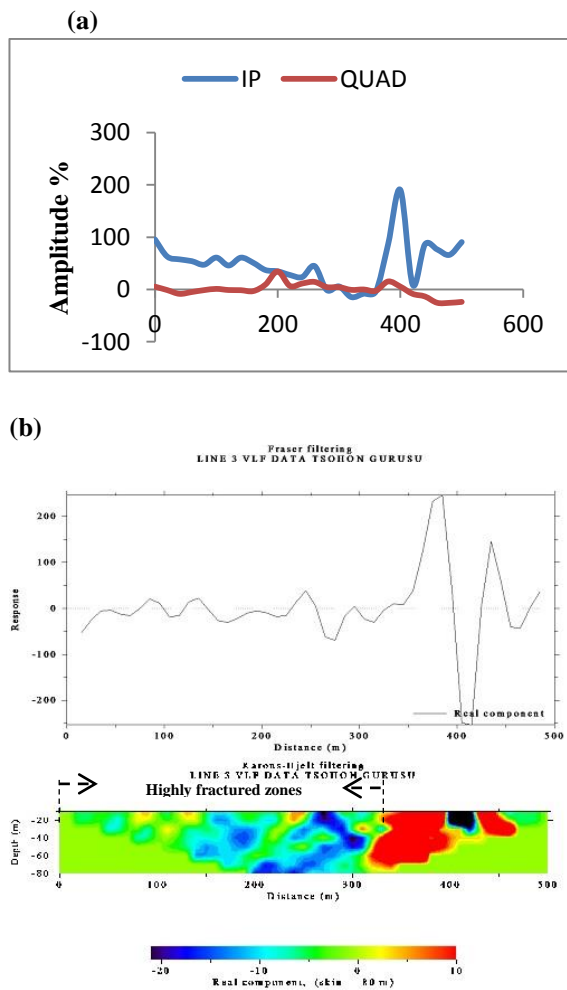


Figure 8: Profile 4; (a) unfiltered real (IP) and imaginary (Quad), **(b)** Fraser filter graph and 2D current density pseudo section.

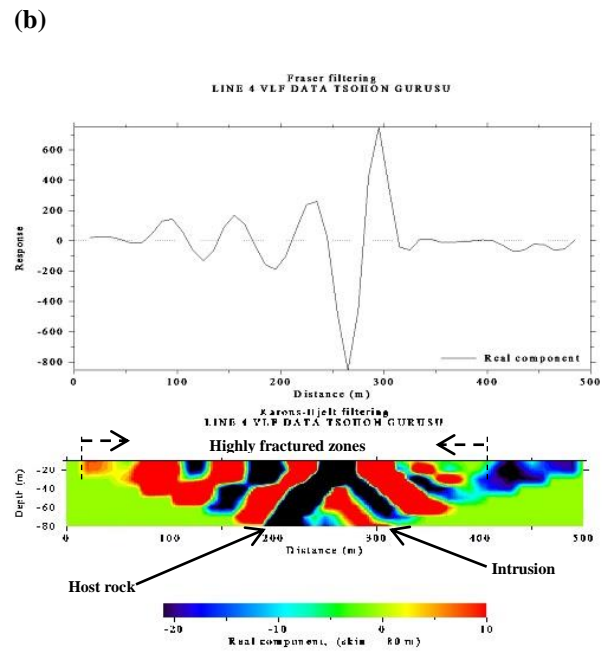
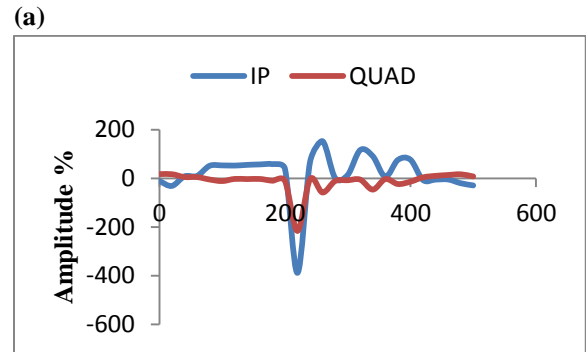
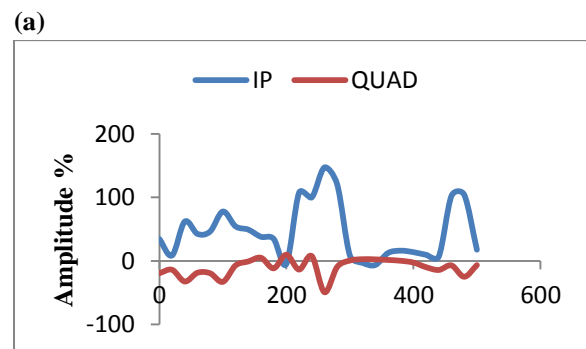


Figure 9: Profile 5; (a) unfiltered real (IP) and imaginary (Quad), **(b)** Fraser filter graph and 2D current density pseudo section.



(b)

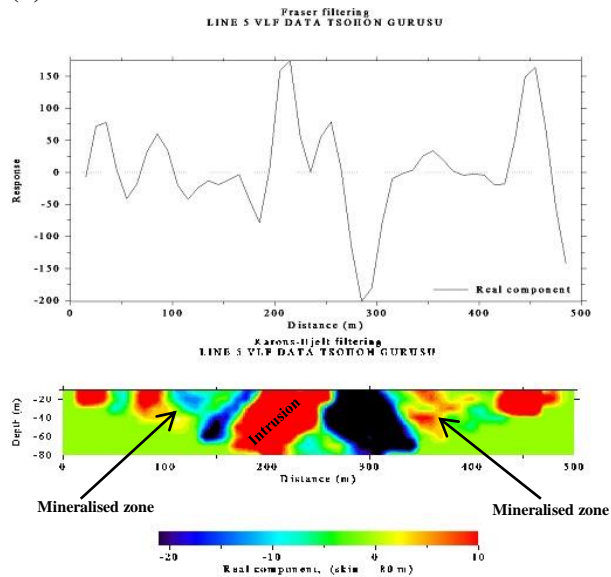


Figure 10: Profile 6; (a) unfiltered real (IP) and imaginary (Quad), (b) Fraser filter graph and 2D current density pseudo section.

Profile 1

The profile (Figure3) runs from E-W direction and lies between latitude 9.6255°N to 9.6254°N and longitude 6.6082°E to 6.6036°E indicating the highest percentage in amplitude of the in-phase response between 75m to 125m (128.9 mS/m) and 300m to 360m (56.6mS/m) with corresponding maximum response of 125% indicating a highly conductive zone which can be inferred to contain conductive minerals due to the high response.

A low conductive dyke spans from 125m to 300m, with an approximate of 80m from the surface, serving as a host to a conductive body due to fracture features.

Profile 2

The profile (Figure4) trend along the W-E direction and lies between 9.6245°N to 9.6246°N and longitude 6.6036°E to 6.6082°E with significant conductivity signatures along 10m to 40m (126.5 mS/m), 100m to 175m (98.1 mS/m), 250m to 310m (83.2 MS/m) having 110% in-phase response indicative of mineralisation and juxtaposed between low conductive bodies.

Quartzite outcrop in this profile spans from 40m to 100m with corresponding low conductive signature (-254 mS/m). There is also an outcrop of granodiorite at 200m and an outcropping dyke of quartzite with low conductivity (-76 mS/m).

Profile 3

This profile runs along the E-W direction (Figure 5) and lies between latitude 9.6237°N to 9.6236°N and longitude 6.6082°E to 6.6036°E with interesting features

of fractures and intrusions of high conductive bodies hosted by low conductive bodies, trending NW-SE and spanning from 150m to 325m.

The points of inflections of cross-cutting of the real and imaginary component gave rise to the highest conductive signature of 189.4 mS/m as the highest in this profile with in-phase response of 160% lying spanning from 100m to 150m with an estimated depth of 60m from the surface, trending along the NE-SW direction.

Profile 4

This profile (Figure6) trends along the W-E direction and lies between latitude 9.6227°N to 9.6228°N and longitude 6.6036°E to 6.6082°E having the highest conductivity from 340m to 400m (288.8 mS/m) at an approximate depth of 80m from the surface with an outcropping low conductive body between 400m to 430m serving as an intrusion.

From the start point to 300m, a body of low and intermediate high conductivities seems to dominate. As, such, suggest fracture zones susceptible to mineralisation.

Profile 5

This profile (Figure7) is along the E-W direction and lies between latitude 9.6219°N to 9.6218°N and longitude 6.6082°E to 6.6036°E. This profile registers the highest conductivity response compared to all the previous profiles as shown in the 2D section, of about 464.3 mS/m at an approximate depth of 60m from the surface with a NE-SW trend direction and spans from 280m to 320m. The general feature is that fracturing units in the profile are highly pronounced.

At distance of 262m a very low conductive response is shown by a body hosting a high conductive body which can be inferred to be an aquifer or a mineralised zone.

Profile 6

This profile (Figure8) runs on the W-E direction and lies between latitude 9.6209°N to 9.6210°N and longitude 6.6037°E to 6.6082°E. The highest conductivities response is shown at 450m (190.3 mS/m) and 200m (177.6 mS/m) on the profile with the least conductive response at 300m (-262.5 mS/m) corresponding to a geologic outcrop of quartzite which is highly resistive.

CONCLUSION

On a general scale, the area houses regions of highly fractured structures, intrusions, dykes, conductive bodies and massive resistive bodies. The highest conductivity responses on the profiles are shown on each 2D pseudo sections corresponding to profile with profile 1 having its highest conductivity response between 75m to 125m (128.9 mS/m), profile 2 records it between 10m to 40m (126.5 mS/m), profile 3 has its highest between 100m to 150m (189.4 mS/m), in profile 4, the highest conductive zone lies between 340m to 400m (288.8 mS/m), profile 5



has its highest conductivity response between 280m to 320m (464.3mS/m) which is the highest among the profiles. Profile 6, shows high conductivity response at 450m (190.3 mS/m) and an interesting relatively low conductivity at distance 300m (-262.5 mS/m) which corresponds significantly to some geologic outcrop of highly resistive quartzite body.

The fracturing units described with respect to the high conductivity patterns as indicated in the conductivity map and the 2D current density pseudo section, suggests that the average depth of the major conductive bodies is approximately 80m with significantly high conductive responses. As such, it can be inferred that zones in this area exhibiting such features are zones of mineralisation. Thus, other geophysical investigative methods such as magnetic method and geochemical analysis can be carried out on the area to ascertain the specific mineral contents, presence and extent of mineralisation.

ACKNOWLEDGEMENTS

Life itself is a school one continue to explore all forms of learning, therefore, I would like to express my sincere appreciation to God Almighty, Who gave me the opportunity to have come this far in life to learn.

My appreciation goes to my parents Mr. and Mrs. Ogale for their immense contribution towards my wellbeing. I also want to appreciate my Supervisors, lecturers, mentors and friends such as; Dr. A.A. Rafiu, Dr. Alhassan, Dr K. A. Salako, Dr. U. Christopher, Prof. E.E. Udensi, Mr Lucky Omugbe, Mr. Alao, Mr. A. Danjuma and just to mention but a few.

Thanks goes to Miss Okafor Gloria and all that are in my heart but could not mention.

REFERENCES

- Abubakar, Y. (2012, May). An Integrated Technique in Delineating Structures: A Case Study of the Kushaka Schist Belt Northwestern Nigeria. *International Journal of Applied Science and Technology*, 2(5), 164-167.
- Ajibade A.C., and Wright J.B. . (1989). The Togo-Benin-Nigeria Shield: evidence of crustal aggregation in the Pan-African belt. . *Tectonophysics*, 165, 125-129.
- Ajibade A.C., Fitches W.R, and Wright J.B. . (1979). The Zungeru Mylonites, Nigeria: recognition of a major tectonic unit. *Rev. De Geol. Phys.* 21,, 359-363.
- Alan E. Mussett and Aftab Khan. (2000). *Looking into the Earth: An Introduction to Geological Geophysics*. New York: Cambridge University Press.
- Ball, E. (1980). An example of very consistent brittle deformation over a wide intercontinental area: The late Pan-African fracture system of the Taureg and Nigeria shield. . *Tectonophysics*. 61, 363-379.
- Barley M.E., Eisenlohr B., Groves D.I., Perring C.S., and Vearncombe I.R. (1989). Late Archean convergent margin tectonics and gold mineralisation. A new look at the Norseman-Wiluna belt, western Australia. *Geology* 17, 826-829.
- Elueze, A. (1981). Petrographic Studies Of Metabasic Rocks And Meta-Utramafites in Relation to Mineralisation in Nigerian Schist Belts. *J Mining Geol*, 18:31-36.
- Jeng Y., Lin M.J., Chen C.S. (2004). *A very low frequency-electromagnetic study of the geo-environmental hazardous areas in Taiwan*. Taiwan: Environ. Geol., 46.
- Kearey P. and Brooks M. (1984). *An introduction to geophysical exploration*. Oxford: Blackwell.
- Kogbe, A. (1976). *Geology of Nigeria*. Ibadan, Nigeria.: Elizabethan Publishers.
- Lazarus G. Ndatuwong, Yadav G.S. (2013). Analysis and Interpretation of In-Phase Component of VLF-EM Data Using Hilbert Transform and the Amplitude of Analytical Signal. *Journal of Environmental and Earth Science*, 3(11), 11-24.
- Mbah Victor O, Onwumesi A. G., Aniwetalu, Emmanuel U. (2015). Exploration of Lead-Zinc (Pb-Zn) Mineralisation Using Very Low Frequency Electromagnetic (VLF-EM) in Ishaigu, Ebony State. *Journal of Geology and Geosciences*, 4(4), 1-7.
- Obaje, N. G. (2009). *Geology and Mineral Resources of Nigeria* (Vol. 772). (B. S. Bhattacharji, Ed.) Berlin: Springer.
- Oluwaseun, I. G. (2013). *Mineral Prospecting and Exploration (with special references to Nigeria)*. Ibadan: Disaster and Risk Management, Department of Geography, University of Ibadan.
- Pirttijärvi, M. (2004, February 20). Karous-Hjelt and Fraser filtering of VLF measurements. Oulu, Oulu, Finland.
- Prasad, U. (2012). Economic Geology. In U. Prasad, *Economic Geology* (pp. 318-319). New Delhi: CBS.
- Telford W. M., Geldart L. P., Sheriff R. E. (1990). *Applied Geophysics*, Second Edition. In W. M. Telford, *Applied Geophysics, Second Edition* (pp. 283-290). New York: Cambridge University Press.

MAGNETIC AND GEOELECTRICAL PROSPECTING FOR GOLD MINERALISATION WITHIN TSOHON-GURUSU AREA, PART OF SHEET 164 MINNA, NORTH-CENTRAL NIGERIA

*Omugbe, L. E¹, Salako, K. A¹, Unuevho, C.I², Rafiu, A. A¹, Alhassan, D. U¹, Ejepu, J. S², & Adetona, A. A¹

¹ Department of Physics, Federal University of Technology, PMB 65 Minna Niger State, Nigeria

² Department of Geology, Federal University of Technology, PMB 65, Minna, Niger State, Nigeria

*Corresponding author email: omugbelucky@yahoo.com, +2348136658871

ABSTRACT

Total magnetic intensity (TMI) measurements were combined with 2D electrical resistivity measurement in Tsohon Gurusu, with the objective of delineating the subsurface gold mineralisation. The TMI measurements data was acquired by the ground magnetic technique, using Geometric 876X. The traverses for the measurements were eleven, aligned North-South, 500 m long and uniformly spaced 50 m apart. The measurement stations were position East-West, across the traverses at 10 m apart in the mineral foliation direction. The acquired TMI was processed and analyzed using Euler and Analytical signal techniques. The ERT data was collected along two traverses of anomalously high TMI values (30 – 86 nT) and low TMI value. Low electrical resistivity values were found to associate with the high TMI values in an East-West pattern. This anomaly pattern confirms with the major East-West fracture pattern captured in the rose diagram of fracture and joint measurements on the outcrop. This indicates that these fractures are potential mineralization zones for conductive minerals. Local miners have been pitting all over the place in the hope of intercepting gold bearing veins, their effort has occasionally been rewarded. .

Keywords: Analytical, Electrical, Euler, Geometrics, Resistivity, Tomography

1 INTRODUCTION

The Basement Complex has been described as undifferentiated assemblage of rocks underlying the oldest stratified rock. Within the Basement Complex of Nigeria four major petro-lithological units are distinguishable, namely; Migmatite-Gneiss-Quartzite Complex, Schist Belt (metasedimentary and metavolcanic rocks), Older granites (Pan African granitoids) and the Undeformed Acid and Basic Dykes (Obaje,2009). These assemblages of rock host various minerals of economic importance for industrialization and development for which the Schist belt is of prime importance for hosting gold mineralization (Fig 1). Gold is a precious earth metal found in alluvial, eluvial placers and primary veins from several parts of schist belts in the northwest and southwest of Nigeria. The most important occurrence is found in the Anka, Bin yauri, Gurmana, Iperindo, Malele, Maru, Okolom-Dogondaji and Tsoho Birni Gwari-Kwaga. There are six world class settings for magmatic and hydrothermal gold deposits; Orogenic gold deposits, Carlin-type gold deposits, Epithermal deposits,

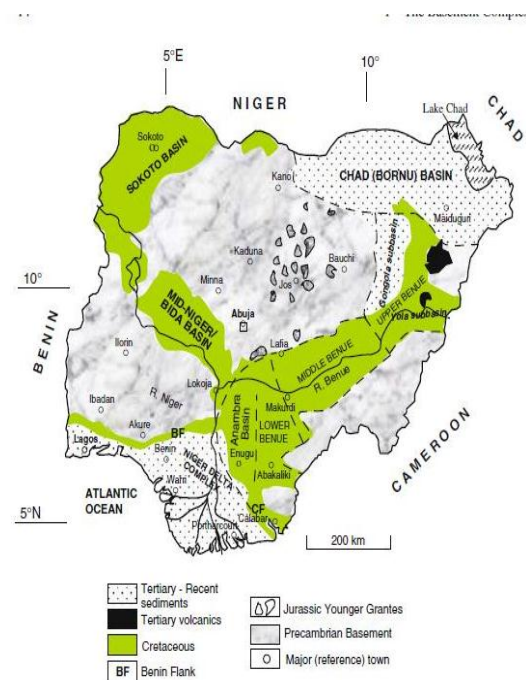


Figure 1: Geological Map of Nigeria, Showing Basement Complex. Source; Lecture Note by Obaje, 2009.

Porphyry-copper gold deposits, Iron oxide-copper gold deposits and Gold rich massive Sulphides deposits, (Encyclopedia of life systems). Thus primary gold mineralization is explored for within the neighborhood of igneous intrusions. It occurs in association with pyrrhotite, migmatite and ilmenite. These are rocks with

high magnetic susceptibility (Michael, 2009). The magnetic method is commonly deployed to delineate areas with potential for gold mineralization. Also, gold a good conductive element hence electrical resistivity is often engaged to identify areas with magnetic anomaly that are conductive, as such that most likely host gold mineralization. However, the potential revenue accruable from investment in exploration and development of gold and other mineral ores is one of the effective approaches to diversifying Nigeria mono-economy that has been hitch on petroleum for too long.

Tsoho Gurusu is a rural settlement whose major activities is basically subsistence farming (agriculture). The community is about four kilometer from Minna at the South western part of Bosso Local Government Area along Minna-Gwada road. The activities of artisanal mining as observed through pitting and trench excavated for possible minerals necessitated embarking on this research work. The general trend of the area has significant amount of quartz vein exposures and trend of mineralization gave an added impetus to the researching of gold mineralization. The study area lies on latitude $09^{\circ} 37' 28.4''N$ and $09^{\circ} 37'28.6''N$ and longitude $006^{\circ} 36' 29.4'' E$ and $006^{\circ} 36' 13.1''E$ on an area extent of $500 \times 500 m^2$ (Figure 2).

GEOLOGY OF THE STUDY AREA

Tsohon Gurusu area lies within the Kushaka Schist Formation of the north-western block of Nigeria basement complex and within the Nigeria metallogeny province, the formation has been intruded by large volumes of granitic rocks that led to extensive migmatization of metasedimentary and metavolcanic rocks carrying substantial gold mineralization (Obaje, 2009). The geology of the area under investigation is underlain by rocks that are typical of the basement complex of Nigeria, some of which shows metamorphic inprints that are quite indicative of various degree of deformation. The rocks include; granodiorite and schist. They exhibit ridge of low laying outcrop extending six to ten meters with greater exposures around stream channels that runs through the study area (Figure 3).

2. METHODOLOGY

Preliminary reconnaissance survey were first carried out to delineate the research study area using the Global Positioning System (GPS); altitude reading, observation of landscape, outcrop trending and drainage pattern. The reconnaissance survey revealed a North-South strike of the rock foliations. Geological mapping was carried out to have a detailed spatial distribution of outcrop and inherent structures (Joint and Fracture) bearings were measured.

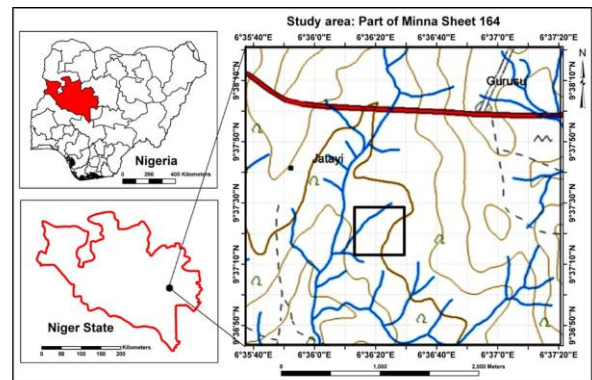


Figure 2. Map of the study area, Tsohon Gurusu.

Ground magnetic survey measurements were taken with Geometric 856AX Proton Precession Magnetometer with external GPSMAP 78sc Garmin, (Figure 4). The measurement were conducted along the dip direction of the rock outcrop in order to reveal the lithologic variation i.e perpendicular to strike direction. Eleven traverses and Fifty-one station point per profile were established comprising of 50m inter profile spacing and 10m inter station spacing. These inter profile and inter station spacing was enough to generate a high density data that is comprehensive to reveal the subsurface geology of the area. Base station method for correction of diurnal variations was used while the area selected for base station was magnetically quiet, i.e. free from moving automobiles and is not close or on top of any major outcrop neither under power line. The stored data from the instrument is downloaded on a computer system. The downloaded data is later saved in an Excel Spread-sheet for easy accessibility. All Magnetics Stations were tied to their respective coordinates. Quality Control and Quality Assurance were then applied on the raw data through visual inspection. This is useful in making sure that all survey specifications have been adhered to. Observed geology, cultural features and all possible source of noise aided the execution of Quality Control and Quality Assurance on the data.

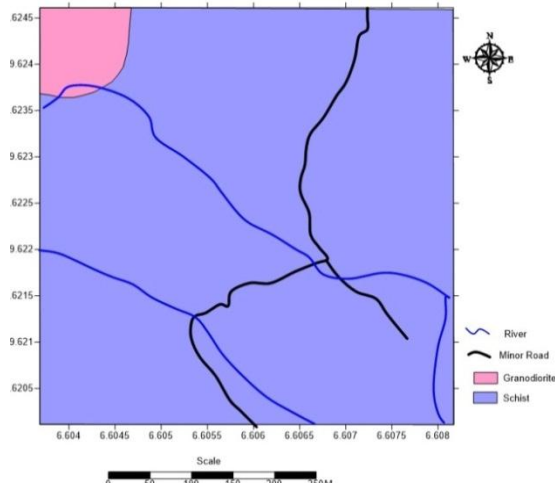


Figure 3: Geological map of the study area



Figure 4: Magnetic data acquisition

A qualitative and quantitative magnetic survey interpretation from the total magnetic intensity anomaly map comprising of high and low intensity. The high and low intensity areas delineated were further explored using 2D Electrical resistivity imaging. Such areas were based on unique Magnetic responses which are diagnostic of potential mineralization. There are many electrode arrays that are used in electrical imaging (*e.g.*, Wenner, Schlumberger, dipole-dipole etc.) depending on the application and the resolution desired. The Wenner alpha array was used for this survey. Two (2) lines of about

200m each were covered with McOHM 2115 resistivity equipment (Figure 5).



Figure 5: 2D Electrical Resistivity Data acquisition

Resistivity values were computed and saved on Excel Spread-sheet for easy access on Notepad. Res2Dinversion was used in plotting pseudo-section which resembles a cross section of the area reflecting high or low magnetic intensity of the profile. This traditional pseudo-section exaggerates the depth of the anomalous materials; therefore 2D inversion of the apparent resistivity data was carried out using finite element (Loke, 2011).

2.1 DATA PROCESSING AND INTERPRETATION

Magnetic Data Processing

The crustal field is the focus for exploration activities. Magnetic field external to the earth has great effect on magnetic measurement and must be removed during data processing. Magnetic data processing involve the removal of diurnal variations of the earth's magnetic field, which may be resolved into secular changes, solar-diurnal changes, lunar changes and changes resulting from magnetic storms, Erwan et al, 2010. At every forty minute interval revisiting of base station is achieved to correct for diurnal variation. To estimate the geometry of geologic structures and depths to magnetic source bodies, mathematical functions were applied to the total magnetic intensity grid. These are Analytical signal and Euler Deconvolution. Figures 6 show the colour-shaded map of the total magnetic intensity map of the study area.

The observed magnetic field at every point is a vector

sum of various components, such as the regional field and the local field components. The minerals found in the Earth Crust are capable of carrying both remanent and induced magnetisation. (Erwan, 2010). Remanant magnetism is the effect of the primary magnetic field at the time of rock formation. The total magnetic response is proportional to both the induced magnetism as well as remanant magnetism (Erwan, 2010)

location for electrical resistivity (Figure 9). Two points designated as magnetic high and low; South-East and North-East of the map. A traverse of 200m that runs in the East-West direction was measured to detect conductivity of mineralization (Figure 10)

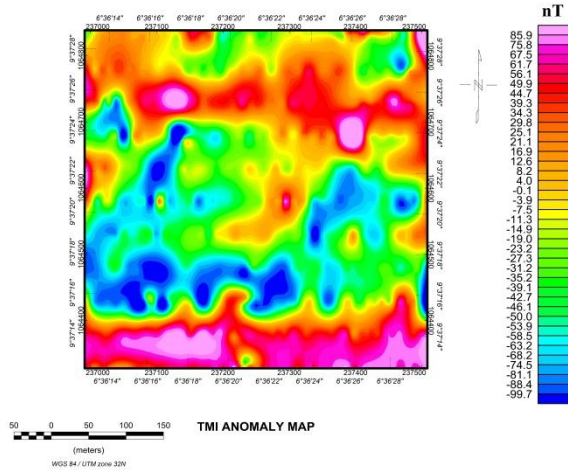


Figure 6: Total Magnetic Anomaly map

Corroborating the TMI anomaly trend and Fracture direction, the trend of structures are principally in the NorthEast-SouthWest direction and East-West inflections. Figure 7.

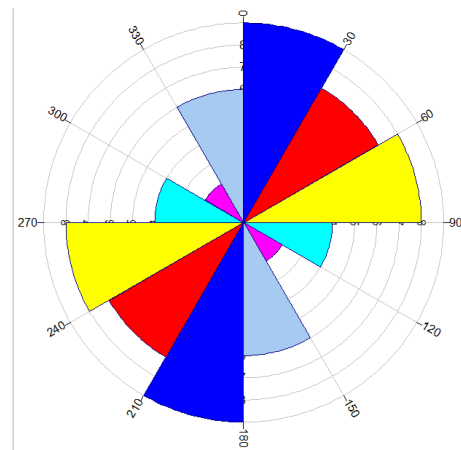


Figure 7: Rose diagram showing fracture and joint direction.

The structural trends as observed from the Rose diagram are the areas that are potential zones for mineralization. The depth of magnetic source were determined using Euler menu of the Oasis montaj, color legend range with highest source is 25m and the lowest source is 8m. Thus edge detection of magnetic body was controlled by Analytical signal which invariable inform the choice

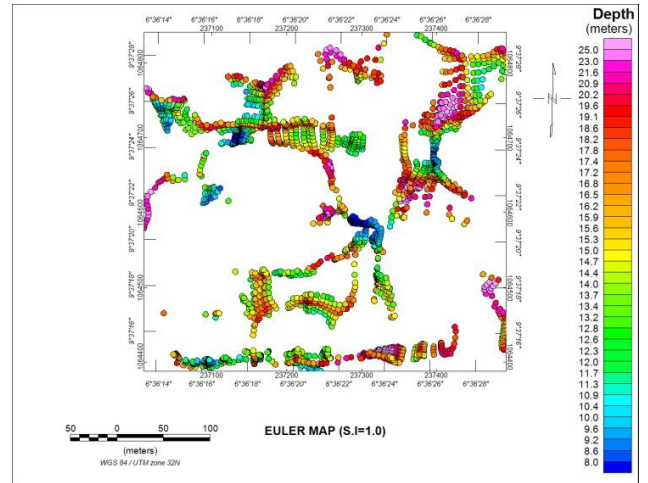


Figure 8: Euler Map for magnetic source detection

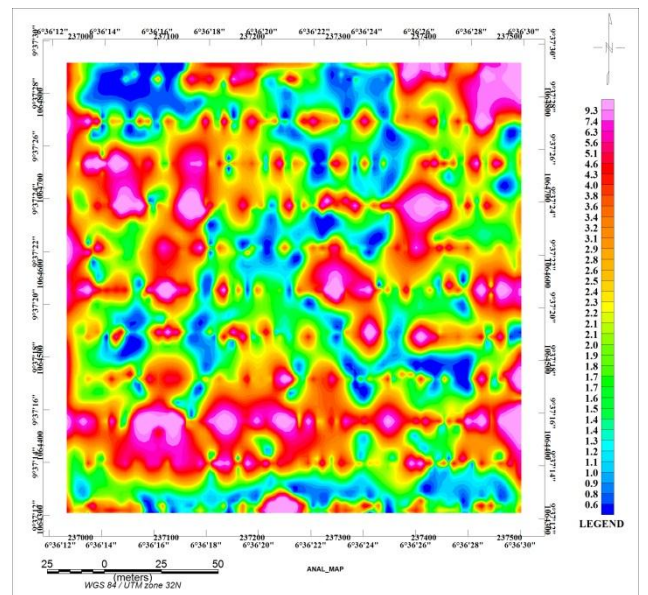


Figure 9: Analytical Signal Map

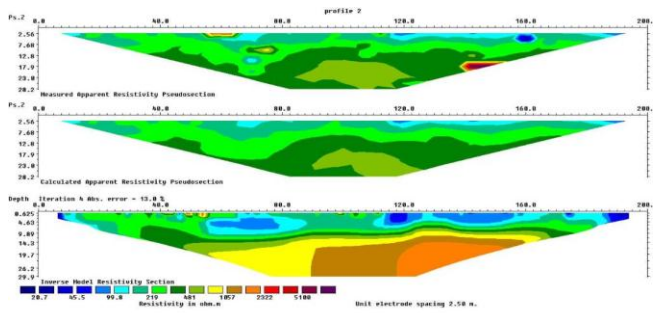


Figure 10: 2-D Resistivity profile on 9° 37' 16.0''N and 6° 36' 28.0''E

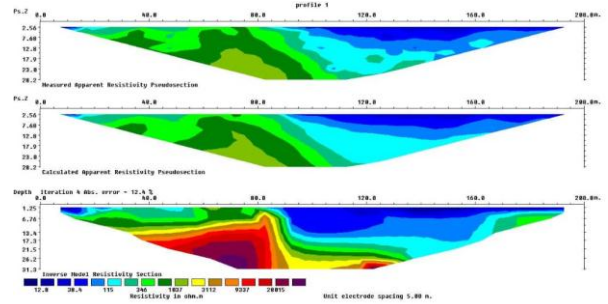


Figure 11: 2-D Electrical Resistivity on 9° 36' 28.0''N, 6° 36' 28.0''E

3. RESULT AND DISCUSSION

The total magnetic intensity map of the area (Figure 6) exhibits zonation and alteration. This indicates hydrothermal alteration which is usually associated with mineralization probably as a result of intrusion. The residual anomaly minima and maxima amplitude signature shows positive magnetic amplitude (maxima) ranging from -54 nT to 51.0 nT (Figure 12). This is quite appreciable for reasonable magnetic anomaly and it suggests that the magnetic susceptibility of the study area is contrasting, hence suitable for mineral exploration. The residual magnetic field intensity map of generally show majorly NE/SE and E/W trending anomalies with few trending in N/S (Figures 12). This shape of magnetic signature obtained in the ground magnetic survey generally suggests a step or an edge structures like dyke or intrusion, such structures are of interest may hold mineralization at certain depth. RES2DINV software was used for the 2D-inversion of the resistivity data. The revealed apparent resistivity pseudo-section of 2-D inverted resistivity show a qualitative idea of resistivity distribution in the subsurface (Figures 10 to 11) hence maximum depth penetration recorded is 39m which invariably exhaust magnetic source observed in the Euler map which ranges from minima of 8m to maxima of 25m (Figure 8). Thus, investigation reveals vertical and lateral extent of mineralization.

Primary gold occurrences in the northern Nigeria schist belts are associated with sulphide mineralization, hence low resistivity. Quartz veins are characterized by high resistivity (low conductivity). Most primary gold mineralization in the schist belts commonly occurs in quartz veins within different lithologies, therefore geophysical characteristics of the quartz veins is another important factor in mineral prospecting and delineation of gold deposit.

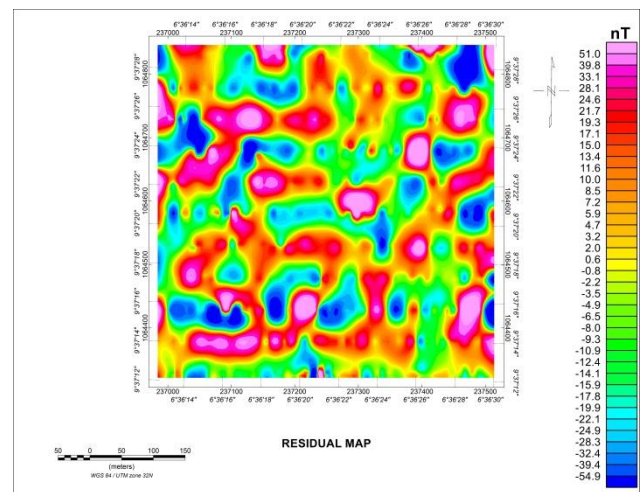


Figure 12: Residual Anomaly Map

4. Conclusion

Combining the results of geologic structures and geophysical methods reveal a wide range of linear structures suspected to be quartz veins which are believed to host ore mineralisation were identified. Careful interpretation and technical assessment of the general results, it can be inferred that some of these structures are probably mineralized veins with varying degrees of characterization. Responses to physical parameters also revealed that some of the structures delineated from the magnetic data are conductive while others are non-conductive, while some are within a resistive host and others are within a conductive host. Several of such structures trending mostly NE-SW, E-W and N-S were identified.

ACKNOWLEDGEMENTS

All praise, honor and glory to God Almighty for His favor and grace towards the success thus far. Also, my heartfelt appreciation goes to my supervisor, Dr. K. A. Salako for his immeasurable support and direction offered to the success of this



research work. No words can express my indebtedness to my co-supervisor, Dr. U.I. Christopher for providing the painstakingly in addressing all critical issues therein. Without them, I could not have completed this research.

I would like to express my profound gratitude to Professor E. E. Udensi for his advice well-spoken encouragement in his interaction in Class. To my esteemed Geophysics Lecturers; Dr. Adetona Abbas, Dr. Rafiu Abdulwaheed, Dr. Alhassan Usman and geophysics course mate. It was great having to work with Mr. Daniel Ogale for his active support and commitment. God bless you all.

REFERENCES

- JOSHUA E. O., LAYADE G. O., AKINBOBOYE V. B. AND ADEYEMI S. A. (2017, MAY 26). *GLOBAL JOURNAL OF PURE AND APPLIED SCIENCES*, 23, 301-310.
- Abdullahi, S. a. (2018, October). Geophysical Evaluation of Gold potential in Southwestern part of Kaffin Koro, Northwestern, Nigeria. *Journal of Applied Geology and Geophysics*, 6(5), 56-66.
- ANDREW J., ALKALI A., SALAKO K. A., UDENSI E.E. (2018, may). Delineating Mineralisation Zones within the Keffi-Abuja Area Using Aeromagnetic Data. *journal of geography, environment and earth science*, 15(3), 1-12.
- Austin C. Okonkwo and Chukwudi C. Ezeh. (October 2012). A Ground Integrated Geophysical Exploration for. *International Research Journal of Geology and Mining* (, 214-221,.
- Bevan, B. W. (April 2006). *Understand magnetic maps*. 272487686.
- BRUCE W. D. YARDLEY & JAMES S. CLEVERLEY. (2019, APRIL 1). <http://sp.lyellcollection.org>. Retrieved PRIL 1, 2019, from 6152
- Erwan, T., Micheal, P., Kathryn, A. W., Benoit, L., Terence, J.S. (2010). The Magnetic Field of The Earth Lithosphere. *Space Science Rev.*
- Haruna, I. (2017, FEBRUARY). Review of the Basement Geology and Mineral Belts of Nigeria. *Journal of Applied Geology and Geophysics*, 5(1), 37-45.
- J., H. C. (n.d.). GOLD DEPOSITS. *ENCYCLOPEDIA OF LIFE SUPPORT SYSTEMS*, pp. 3-4.
- Les P. Beard, Berhe Goitom and Jan Reidar. (2000). *Interpretation of low latitude magnetic anomaly*. Ethopia.
- LOKE, M. (2001). *2-D and 3-D electrical imaging surveys*.
- Martini F., Rogers E., Bennett S., Davi R., Doherty J.T., Mongan J. (2018). *Integrated Geophysical Exploration in on shore frontier Basin*. Ireland.
- Obaje, N. G. (2009). Geology and Mineral Resources of Nigeria. In P. N. Obaje, *Lecture Notes in Earth Sciences* (p. 14). Keffi, Nasarawa: Springer Dordrecht Heidelberg London New York.
- Oluwaseun S. Ogungbemi, M.Tech.1*; Olatunji O. Alu, M.Sc.2;. (2014, MAY). Integrated Geophysical Approach to Solid Mineral Exploration: A Case Study of. *The Pacific Journal of Science and Technology*, 15(1), 426-432.
- Rowland Akuzigi Ayuba*, A. N. (2019). Interpretation of High Resolution Aeromagnetic Data for Hydrocarbon Potentials over Parts of Nasarawa and Environs North Central Nigeria. *World Journal of Applied Physics*, 4(1), 1-11.
- W.J. Scott, P. P. (2014, February). *GEOPHYSICS FOR MINERAL EXPLORATION*. Newfoundland: Newfoundland and Labrador Department of Natural Resources.
- Y.I., A. (2012, MAY). An Integrated Technique in Delineating Structures: A Case Study of the Kushaka Schist Belt Northwestern Nigeria. *International Journal of Applied Science and Technology*, 2(5), 3-6.
- Zhdanov, M. S. (2009). *Methods in Geochemistry and Geophysics* (Vol. 43). Elsevier.



ROAD STABILIZATION USING COLD BITUMEN FOR LOW TRAFFIC ROAD

*KOLO S. S.¹, JIMOH, Y. A.², ALHAJI, M.M¹, OLAYEMI, J.¹ AND SHEHU, M¹

¹Civil Engineering Department, Federal University of Technology, PMB 65 Minna Niger State, Nigeria

²Civil Engineering Department, University of Ilorin, Kwara State, Nigeria

*Corresponding author email: bukysayo123@ yahoo.com

ABSTRACT

This research work is aimed at strengthening weak soil using cold bitumen for a low traffic road by stabilization method using varying percentages of cold bitumen (0%, 2%, 4% and 6%) to determine at which stabilization content is the soil strengthen for low traffic use. The lateritic soil used in this research work was collected at Kpakungu along Minna – Bida road and the cold bitumen was obtained in Minna. Standard laboratory tests were carried out on the lateritic soil. The tests carried out on the soil include particle size distribution determination, specific gravity test, Atterberg's limit test, compaction test and California bearing ratio test. The results obtained from the test showed that the optimum amount of cold bitumen in terms of effectiveness and economy was 3.5%.

Keywords: *bearing capacity, cold bitumen, stabilization, traffic and weak soil.*

1 INTRODUCTION

Bitumen can be defined as a mixture of organic liquid that are highly viscous, black, sticky, entirely soluble in carbon disulfide and composed primarily of highly condensed chemical compound or can be defined as an amorphous, black or dark colour (solid, semi-solid, or viscous) cementitious substance, composed principally of high molecular weight hydrocarbons, and soluble in carbon disulfide. Bitumen is the residual or by product obtained by fractional distillation of crude oil. It is the heaviest fraction and the one with highest boiling point. (Herbert, 2007).

Bitumen is an oil based substance. It is a semi-solid hydrocarbon product produced by removing the lighter fractions (such as liquid petroleum gas, petrol and diesel) from heavy crude oil during the refining process. As such, it is correctly known as refined bitumen. In North America, bitumen is commonly known as “asphalt cement” or “asphalt”. While elsewhere, “asphalt” is the term used for a mixture of small stones, sand, filler and bitumen, which is used as a road paving material. The asphalt mixture contains approximately 5% bitumen. At ambient temperature, bitumen is a stable, semi-solid substance.

Bitumen is any of various naturally occurring mixtures of hydrocarbons with their non metallic derivatives. Crude petroleum, asphalt and tar are bitumen which are characteristically dark brown or black and contain little Nitrogen, Oxygen, or Sulphur. Commercially, the term bitumen refers to hydrocarbon in a solid or semisolid state but in a wider sense, it refers to all natural hydrocarbons which may also occur in a liquid or gaseous state.

Bitumen is primarily used for paving roads and can also be used for stabilization where the soil is pulverized and mixed with bitumen to some percentage. In addition to this, bituminous materials and even high viscosity oil have been used for oiled earth road in which the road soil is simply sprayed on the prepared surface. Approximately, 85% of all the bitumen produced is used as a binder in asphalt for road construction. It is also used as a binder in asphalt for roads and for other paved areas such as airport, runways, car park and footways. A further 10% of global bitumen production is used in roofing applications where its water proofing qualities are in valuable. The remaining 5% of bitumen is used mainly for sealing and insulating purposes in a variety of building materials such as pipe coatings, carpet, tile backing and paints,

Also, the use of bituminous materials such as cutback, bitumen, road tars and asphalted emulsion for soil stabilization has been found satisfactory for coarse grained or granular soil, which used in plastic soil, however may be difficult (Yoder, 1957).

Stabilization refers to those techniques that reduce hazards of a waste by converting the contaminants into their least soluble, mobile or toxic form. The physical nature and handling characteristics of waste are not necessarily changed by stabilization (Fleming, 2000). Stabilization of granular materials with low percentage of slow setting binders, such as slag lime for constructing new pavement and or rehabilitation of existing granular pavements has economic and environmental benefits (Fleming, 2000).

2 MATERIALS AND METHOD

The preliminary test carried out on samples of lateritic soils collected include in-situ moisture content

determination, sieve analysis, Atterberg's limit, compaction test and California bearing ratio test administering cold bitumen as a stabilizing agent compacted according to the procedure highlighted in BS I377 (1990).

The soil sample used for this study is a natural reddish-brown lateritic soil obtained at different locations along Minna – Bida road failed portions. Minna is located at latitude 6°30'N and 9°30'N. These samples were mixed together to obtain the sample representation which was then used to carry out this research work. The lateritic material was selected based on the fact that lateritic soil are the major road and rail construction materials of universal occurrence and acceptable, as such no construction work can be executed without the use of this material as described by Muazu (2008).

According to AASHTO soil classification system, the soil was classified through the following procedures (i) Determination of natural moisture content (ii) Determining the particle size distribution (iii) Atterberg limit determination (iv) Compaction test and (v) California bearing ratio tests.

The above tests were conducted on the soil sample while varying the quantity of the stabilizing agent. The main laboratory tests carried out includes Atterberg limit, compaction test and California bearing ratio test with cold bitumen as a stabilizing agent at 0%, 2%, 4% and 6% by weight of lateritic soil.

3 RESULTS AND DISCUSSION

3.1 Determination of Natural Moisture content

According to BS EN 1377:1 (1990) which states that more than 10% of natural moisture content is required for laboratory test. Result obtained from the experiment showed that the average moisture content in the lateritic soil in its state was 13.48%. Result is shown in Table 1.

Table 1: Determination of Natural Moisture Content

Can Number	A _g	Ab
Weight of Can (g)	25.60	25.62
Mass of Can +Wet soil, M ₂ (g)	61.72	72.68
Mass of Can +Dry soil, M ₃ (g)	57.50	67.00
Mass of Dry soil, M ₄ (g)	31.88	41.40
Mass of Water, M ₅ (g)	4.22	5.68
Moisture content, ω (%)	13.24	13.72
Average Moisture Content, ω (%)	13.48	

3.2 Particle Size Distribution

Results obtained from the particle size distribution of the soil give the distribution in percentages of the various sizes present in the soil sample down to fine sand. From the result obtained, the liquid limit is 35%, plasticity index is 23.59 and the group index is 8.25. Therefore, the soil can be classified using AASHTO method as A-6. The graph of the particle size distributions shows that the soil falls below the standard recommendation and require stabilization to improve its stability.

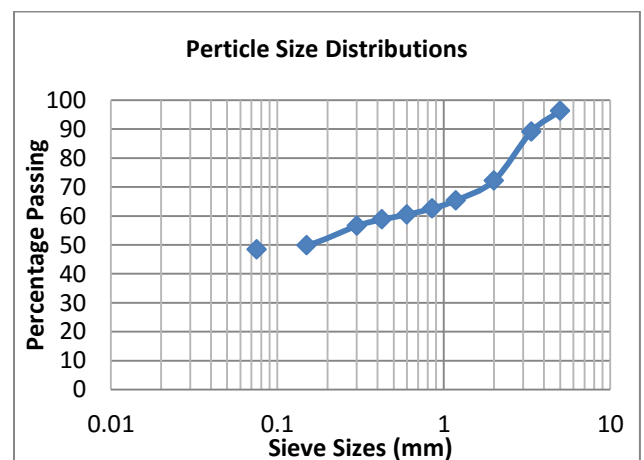


Figure 1: Particle Size Distributions

3.3 Compaction Test

Soil compaction test was carried out in order to determine the relationship between dry density and moisture content in the soil samples. The result of the compaction test carried out for the soil samples is shown in Table 2

From the graph plotted of the moisture dry density relations for the plain lateritic soil sample, it can be seen that as more water is added to the soil and then compacted, the dry density of the soil increases until it reaches maximum value, after which a further increase in the water content of the soil leads to a reduction in the dry density.

Table 2: Variation of Maximum density and Optimum Moisture Content with Cold Bitumen Content

Cold Bitumen Content	0%	2%	4%	6%
Moisture Content	9.2	10.12	11.65	13.42
MDD	1.75	1.81	1.81	1.73

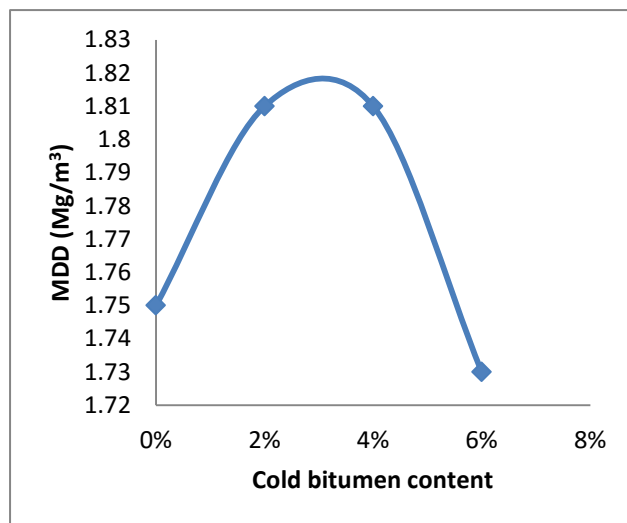


Figure 2: Variation of MDD with different cold bitumen content

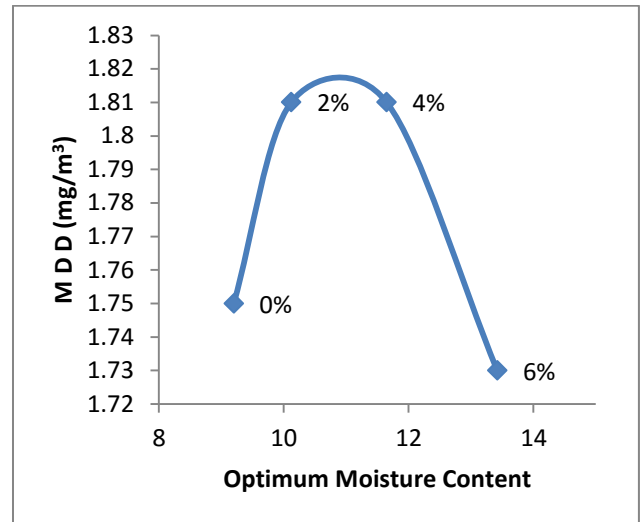


Figure 3: Variation of MDD with different Moisture content

3.4 Atterberg Limit Test

The Atterberg limit test was carried out to determine the liquid limit, plasticity index and also to determine the relationship between penetration and moisture content.

Table 3: Liquid limit test

0% Cold Bitumen		2% Cold Bitumen		4% Cold Bitumen		6% Cold Bitumen	
Moisture content	Pen	Moisture content	Pen	Moisture Content	Pen	Moisture Content	Pen
25.17	7	30.77	7.5	26.81	8.1	31.33	9.7
30.7	12	31.19	9.2	27.27	12.8	34.46	12.25
31.85	14.4	36.54	10.7	37.34	14.1	35.25	15.5
35.04	16.4	39.85	12.5	40.4	17.3	38.36	18.55
35.51	20.9	40.31	17.8	40.57	21	40.39	22.75

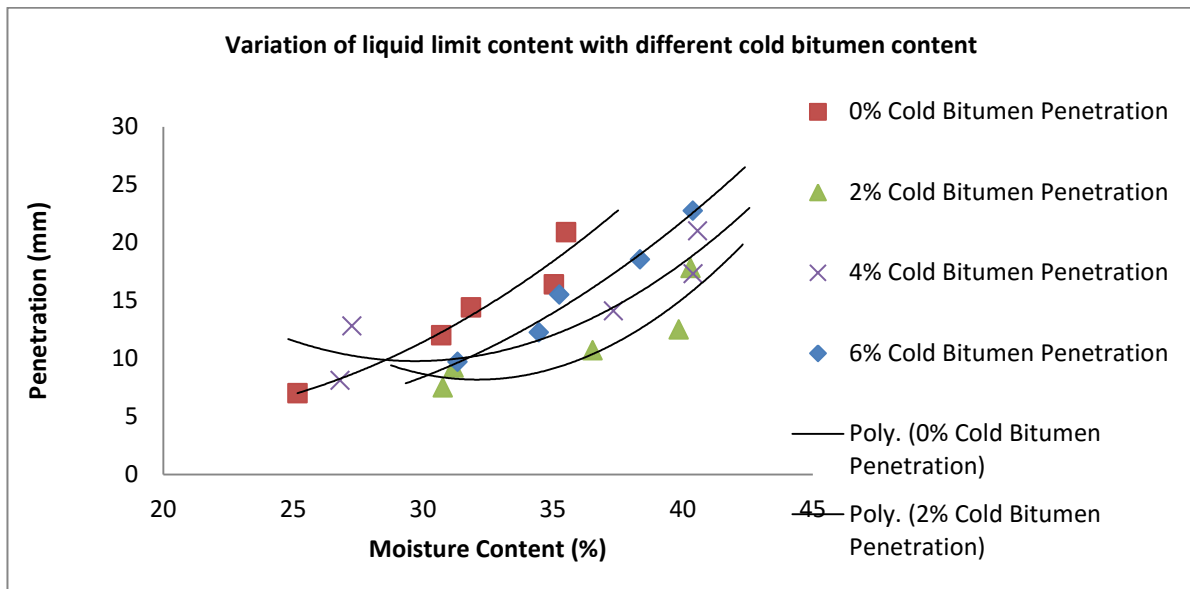


Figure 4: Variation of liquid limit content with different cold bitumen content

The trend shows that there is a corresponding decrease with increase of cold bitumen content in liquid limit, plasticity index. However, the reverse was the case for plastic limit. Liquid limit was obtained to be 42.0, 40.0, 39.0 at 2, 4, 6% respectively. While the corresponding plastic limit are 14.17, 15.04, and 15.41 for the same percentage of cold bitumen increment. The explanation consistent with complex behavior of liquid as a result of cold bitumen addition was due to decrease in void and aggregation of soil particles.

Table 4: Atterberg limit test

	0%	2%	4%	6%
Liquid Limit	35	42.5	40	39
Plastic Limit	23.59	28.33	24.96	23.59
Plasticity	11.41	14.17	15.04	15.41

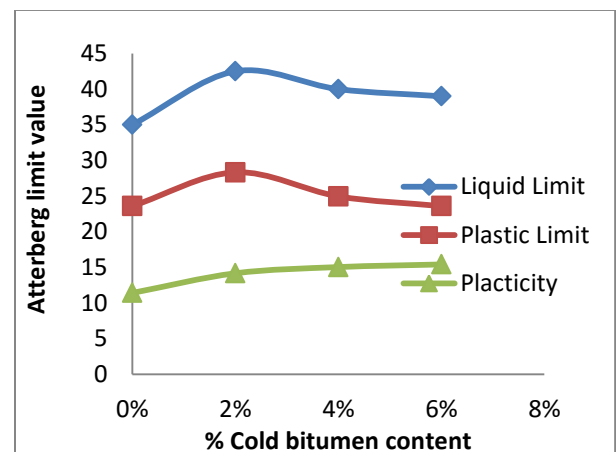


Figure 5: Variation of Atterberg limit with different cold bitumen

3.5 California Bearing Ratio

This method covers the laboratory determination of the California Bearing Ratio (CBR) of a compacted or undisturbed sample of soil. The principle is to determine the relationship between force and penetration when a cylindrical plunger of a standard cross-sectional area is made to penetrate the soil at a given rate. At certain values of penetration, the ratio of the applied force to a standard force, expressed as a percentage, is defined as the California Bearing Ratio (CBR)

The penetration increases as the corresponding load also increases also the percentage of CBR at 5.00mm penetration is having higher value than that at 2.5mm which means it is suitable for base course.

Table 5: Obtained C.B.R Values

% Cold Bitumen content	Soak	unsoak
0%	37	40.5
2%	32.5	33.3
4%	33.6	34.5
6%	35.35	35.47

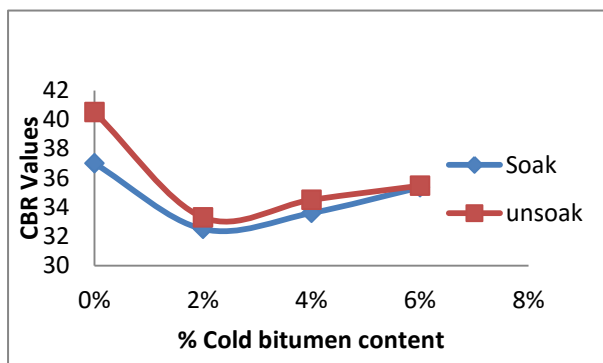


Figure 6: Comparison of CBR values of Soaked and unsoaked

4 CONCLUSION

The following conclusions were drawn from the result of the research carried out within the scope of the study.

1. The optimum effect of cold bitumen stabilization is achieved at six percent (6 %).
2. The laterite was identified to be an A-6 soil based on AASHTO (1986) classification system.
3. The maximum dry density and optimum moisture content varies with an increase in cold bitumen content.
4. The material has high liquid limit of 35% and plastic limit of 11.41%. It can conclude that it is non plastic.

RECOMMENDATIONS

1. It is recommended that cold bitumen should be widely accepted and encouraged in construction companies all over the world for better road construction.
2. Further research works should be carried out to determine the most effective and economic ratio for combined modification.

3. Index properties like liquid limit, plastic limit and plasticity index should be determined for all the admixture ratios studied to confirm the complete suitability of the mixture for engineering structures.

4. It could be recommended that the strength result obtained at optimum 3.5 % cold bitumen suggest that it is suitable as a sub-base material on road pavement.

REFERENCES

- Ola, S.A (1977). Geotechnical Properties and Behavior of some Nigeria Lateritic Soils. Manual no. 198; *Cold Base course mixes*, Public Roads Administration, NRRL, Oslo, 2000.
- Terzaghi, K. (2005). Soil Mechanics in Engineering Practices. Published by John Wiley and Son's inc United State of America.
- Bell, F.G. (1993). Engineering Treatment of Soils, E & EN SPON Publishers.
- Adeyeri, J.B. (1988). Engineering Characteristics of some Nigerian residual soils for Highway Construction Transportation, Research record. No 1492.
- AASHTO (1986). *Standard Specification for Transportation Officials*, Washington D. C, U.S.A.
- Lambe, T.W. (1962). Soil Stabilization Foundation Engineering. G. A. Leonards Ed. Mc Graw Hill Book Con New York, Chapter 4.
- BS 1377 (2016). Methods of Test for Soils for Civil Engineering Purposes- General Requirements and Sample Preparation.
- Douglas, O.A. (1986). *Evaluation of Admixture Stabilization for Laterite*.
- Anon (1998). Bronze age metalled road near oxford. British archaeology News (council for British archaeology).
- Abraham, H. (1920). Asphalts and Allied substance. D. Van Nostrand.



SAWDUST ASH STABILIZATION OF WEAK LATERITIC SOIL

Kolo S. S^{*}, Jimoh Y. A^{**}, Yusuf I. T^{**}, Adeleke O. O^{**}, Balarebe, F. and M. Shehu^{*}

^{*}Department of Civil Engineering, Federal University of Technology Minna, Niger State, Nigeria

^{**}Department of Civil Engineering, University of Ilorin, Ilorin, Kwara State, Nigeria.

^{*}Corresponding author email: s.kolo@futminna.edu.ng.

ABSTRACT

This research work investigated the improvement of the properties of weak lateritic soil using sawdust ash (SDA) as the stabilizing agent. Preliminary tests such as specific gravity, moisture content, Atterberg limits, particle size distribution, Geotechnical strength tests (compaction and unconfined compressive strength (UCS) tests) were first carried out to determine the initial properties of the weak lateritic soil without the stabilizer. Based on the results of these tests, the soil was classified according to AASHTO soil classification system as A-7-5 soil which is a poor soil. The soil was then stabilized, consistency tests and strength tests such as, compaction tests and unconfined compressive strength (UCS) were performed on the soil by the addition of 2%, 4%, 6%, 8% and 10% sawdust ash to 98%, 96%, 94%, 92% and 90% by weight of the lateritic soil respectively. The results showed that sawdust ash improved the geotechnical properties of the weak lateritic soil. The optimum improvement in the properties of weak lateritic soil by stabilization using SDA is at 4% replacement. At this percentage of stabilization, the soil was classified as an A-5 soil (fair silty soil), the liquid limit decreased by 4.96%, the plastic limit decreased by 1.50%, the plastic index decreased by 15.74%, the maximum Dry Density is seen to decrease by 3.7%, the Optimum Moisture content (OMC), increased by 11.11% and the Unconfined Compression Strength increased by 26.9%. Sawdust ash is therefore found to be an effective stabilizer for lateritic soils.

Keywords: *Sawdust Ash, Stabilization, Unconfined compressive Strength (UCS), Weak Laterite*

INTRODUCTION

Soil can be said to be any un-cemented or weakly cemented accumulation of mineral particles formed by the breaking down of rocks as part of the rock cycle, the void space between the particles containing water and/or air (Craig, 2004).

The soil that is being used for road construction is termed laterite and results from a humid tropical weathering process that is occurring or has occurred, which has the following effects of improving chemically the parent material improved with iron and aluminium oxides and hydroxides (sesquioxides). The composition of the clay mineral is largely kaolinitic and Reduced silica contents.

The process above produce yellow, brown, red or purple materials with red being the common colour. All reddish residual and non-residual tropically weathered soils which generically make up a chain of materials constituting from decomposed rock through clays to sesquioxide-rich crusts refers to laterite soil (Gidigas, 1976).

The first pedologist to discuss 'laterites' was probably Glinka (1914) and he considered 'laterite' to be characteristic of soils in the forest zone of the tropics. He had however proposed the idea that laterite is a soil which became popularized by Harrasowitz (1930).

Laterites are highly altered residual soils whose silica constituent have been leached out and have some degree of cementation. (sesquioxides, Blight, 1997).

In order for laterite to be suitable for road construction, it should be stable, incompressible, of indefinite strength and as well stable under adverse weather conditions; other properties expected of laterite is that it should be of good drainage properties and easy to compact (Edeh *et al.*, 2014).

In Nigeria, lateritic soils are used for road construction among other uses and due to the high content of clay particles present in the laterite, lateritic soils in its natural state have low bearing capacity and strength (Abdulfatah *et al.*, 2013).

Several highway pavements in Nigeria roads have failed and are still failing as a result of using weak soils with inadequate engineering strength/properties to bear the expected wheel load. In order to prevent pavement distress from occurring and to minimize damages on pavements, roadways, or any other civil engineering projects, stabilization is carried out.

Stabilization is the alteration of soils to improve their physical properties, increase the soil's shear strength and to control the shrink-swell properties of a soil, thereby improving the load bearing capacity of a sub-grade to support pavements and foundations. Therefore, the techniques of soil stabilization can be categorized into physical, chemical and mechanical stabilization.

Sawdust is an industrial waste material obtained as a by-product of timber. It occurs in large quantity in the universe as the wood is fell for human purposes especially in mills which if not properly disposed leads to

environmental hazards. In order to reduce construction costs, improve self-sufficiency and to avoid environmental pollutions it should be utilized.

The stabilizing agent concerned here is sawdust ash which is obtained by incinerating sawdust for about four to five hours is an industrial waste ash containing pozzolanic properties due to the presence of silica content which makes it a useful cementitious material and enhances the reactivity of the ash.

This research intends to solve the problem of increase in the demand for furniture in homes, offices and public places that has led to the increase in timber felling and consequently sawdust production from various wood processing industries. Sawdust is a huge source of environmental pollution when disposed in open areas and landfills. It will be most preferable to utilize it, especially for stabilizing weak soil after it must have undergone processing. This will in turn solve two major problems of limited borrow pit site by improving the physical and engineering properties of weak lateritic soil that may be available by using sawdust ash (SDA) as the stabilizing agent and environmental pollution control of sawdust disposal.

MATERIALS AND METHOD

The laterite that was used for this work was obtained at Gidan-Kwano campus of the Federal University Technology Minna, Nigeria in accordance to BS 1377:1 (2016) standard procedure for sample collection, It was then classified using BS 1377:2. The Sawdust used was also obtained from wood processing plant and at the same location, it was processed following the ASTM C618 procedure for Ash production. The ash was passed through sieve 75 μ m and was subjected to chemical test to determine its conformity with the known stabilizer and covered.

Having discovered the deficiency of the laterite to meet up the required strength, the obtained sawdust ash was added in percentages to the laterite to improve its properties. The following test were then conducted on the stabilized material to determine the effect of the sawdust ash and to determine the best percentage of addition they include Atterberg limit, Compaction, Unconfined compressive strength (UCS) to determine the basic properties of the stabilized and unstabilized laterite in accordance to the BS standard.

RESULTS AND DISCUSSION

Sawdust Ash (SDA)

The moisture content of the saw dust was observed to be 12.66%, the percentage ash content of the sawdust was also obtained as 1.62%. The chemical analysis carried out

on the sawdust ash (SDA) as shown in Table 1, revealed that SDA can be regarded as a good pozzolana since its $SiO_2 + Al_2O_3 + Fe_2O_3 = 78.81\%$ which is greater than 70%.

Table 1: Chemical Composition of the Sawdust Ash (SDA)

Element	Concentration (%)
Na ₂ O	0.663
MgO	3.822
Al ₂ O ₃	1.686
SiO ₂	75.975
P ₂ O ₅	3.610
SO ₃	1.709
Cl	1.212
K ₂ O	6.903
CaO	2.858
TiO ₂	0.181
Cr ₂ O ₃	0.002
Mn ₂ O ₃	0.059
Fe ₂ O ₃	1.156
ZnO	0.149
SrO	0.016

Preliminary Test on Unstabilized Laterite

The tests carried out on the lateritic soil sample without the additives gave its natural moisture content as 20.27% and specific gravity as 2.43. The soil was classified as a silt-clay soil since the percentage passing the sieve no. 0.075 was more than 35%. Based on its liquid limit of 48.4% and plasticity index 11.75%, the soil was further classified as an A-7-5 "fair to poor soil" which cannot be used in road construction without treatment. Hence, there is a need for stabilization. Table 2 shows a summary of the properties of the natural lateritic soil used in this study. Compaction test on the soil gave a maximum dry density (MDD) of 1.89g/cm³ with corresponding optimum moisture content (OMC) of 0.18%, while its unconfined compressive strength (UCS) was 186.86kN/m² respectively.

Table 2: Properties of the Natural (Weak) Laterite

Property	Value
Natural moisture content	20.27
Specific gravity	2.43
Liquid limit	48.4
Plastic limit	36.65
Plasticity index	11.75
AASHTO classification	A-7-5
Soil type	Silt-clay
Maximum dry density (MDD)	1.89
Optimum moisture content (OMC)	0.18
Unconfined compressive strength (UCS)	186.86kN/m ²

Atterberg Limit Test

The results and variation of the consistency limits tests on the weak lateritic soil with different percentages of sawdust ash contents are presented in Table 3 and plotted in Figure 1 respectively. The liquid limit, plastic limit and plastic index decreased linearly with increasing sawdust ash contents up to 10%. This can be considered to be as a result of the addition of saw dust ash, which has less affinity for water and yields a decrease limit of liquid.

Table 3: The Variation of Consistency Limits with the Sawdust Ash Content

Sawdust ash content (%)	Liquid limit	Plastic limit	Plastic index
0	48.40	36.65	11.75
2	47.10	36.45	10.65
4	46.00	36.10	9.90
6	45.50	35.70	9.80
8	44.00	34.70	9.30
10	33.20	30.95	2.25

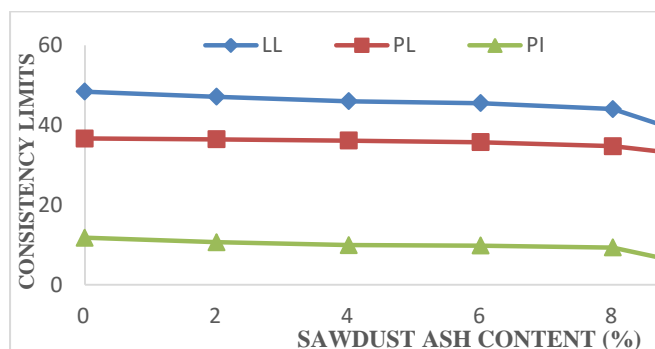


Figure 1: Effect of Sawdust Ash Content on Consistency Limits.

Compaction Parameters

The results of the compaction tests on weak lateritic soil with the addition of various percentages of ash contents are summarized in Table 4. The changes in the maximum dry density and optimum moisture content of the weak

lateritic soil with sawdust ash contents are shown in figure 2. The maximum dry density decreased from 1.89 g/cm³ at 0% sawdust ash content to 1.76 g/cm³ at 6% sawdust ash content and further increased from 1.77 g/cm³ at 8% sawdust ash content to 1.82 g/cm³ at 10% sawdust ash content while the optimum moisture content ranged between 0.18% and 0.22%.

Table 4: Compaction Properties of the Lateritic Soil Containing Sawdust Ash (SDA)

Sawdust ash content (%)	Maximum dry density (g/cm ³)	Optimum moisture content (%)
0	1.89	0.18
2	1.84	0.21
4	1.82	0.20
6	1.76	0.22
8	1.77	0.22
10	1.82	0.21

Unconfined Compressive Strength

The results of the unconfined compressive strength tests on weak lateritic soil with various percentages of sawdust ash contents are shown in Table 5. The variation in unconfined compressive strength tests of the weak lateritic soil with sawdust ash contents are presented in Figure 3. The unconfined compressive strength of the weak lateritic soil increased from 186.86 kN/m² at 0% sawdust ash content up to 237.12 kN/m² at 4% sawdust ash content. After reaching 4% sawdust ash content, the unconfined compressive strength decreases to 123.83 kN/m² at 10% sawdust ash content. The results obtained from the UCS showed that weak lateritic soil improved on addition of sawdust ash.

Table 5: UCS of the Lateritic Soil Containing Sawdust Ash (SDA)

Sawdust ash content (%)	Unconfined Compressive Strength (qu) kN/m ²	Shear Strength (qu) kN/m ²
0	186.86	93.43
2	234.97	117.49
4	237.12	118.56
6	191.92	95.96
8	154.23	77.12
10	123.83	61.92

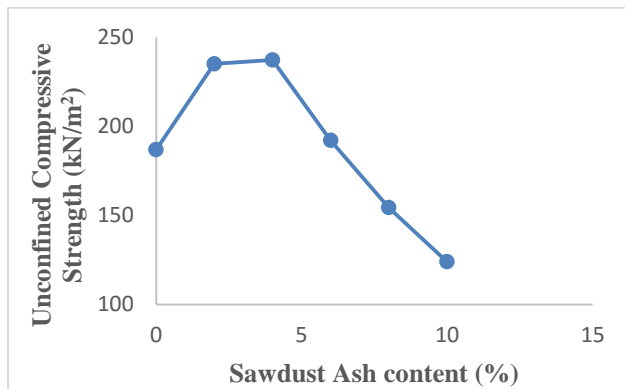


Figure 2: Variation of Unconfined Compressive Strength with Sawdust Ash Content

CONCLUSION

The results of the research work carried out shows that sawdust ash (SDA) is a suitable pozzolanic material for stabilizing weak lateritic soil. The weak lateritic soil used for this work according to AASHTO classification of soils, is an A-7-5 soil showing that it is a poor clayey soil. At 2% addition of SDA to 98% weak lateritic soil, the soil is seen to exhibit characteristics of an A-7-5 soil (poor clayey soil). On further addition of SDA at 4%, 6% and 8% to 96%, 94% and 92% weak lateritic soil respectively, the soil shows improvement in properties from an A-7-5 soil (poor clayey soil) to becoming an A-5 soil (fair silty soil). Finally, at 10% SDA addition to 90% weak lateritic soil, the sample is an A-4 soil (fair silty soil).

The unconfined compressive strength of the weak lateritic soil was 186.86kN/m², at 2% SDA addition; its strength increased by about 25.7% (243.97kN/m²) when compared to that of the weak lateritic soil, at 4% SDA addition; its strength increased by about 26.9% (237.12kN/m²) when compared to that of the weak lateritic soil, at 6% SDA addition; its strength increased by about 2.3% (191.12kN/m²) when compared to that of the weak lateritic soil, at 8% SDA addition; its strength decreased by about 17.5% (154.23kN/m²) when compared to that of the weak lateritic soil, finally at 10% addition of SDA; its strength was seen to decrease by about 33.7% (123.83kN/m²) when compared to that of the weak lateritic soil.

The optimum improvement in the properties of weak lateritic soil by stabilization using SDA is at 4% replacement. At this percentage of stabilization, the liquid limit (46.00%) decreased by 4.96% when compared to that of the un-stabilized sample (48.40%), the plastic limit (36.10%) decreased by 1.50% when compared to that of the un-stabilized sample (36.65%), the plastic index (9.90%) decreased by 15.74% when compared to that of the un-stabilized sample (11.75%), the maximum Dry

Density (1.82g/cm³) is seen to decrease by 3.7% when compared to that of the un-stabilized sample (1.89 g/cm³). The Optimum Moisture content, OMC (0.2%) is seen to increase by 11.11 when compared to that of the un-stabilized sample (0.18%). The Unconfined Compression Strength value at 4% stabilization using SDA (237.12 kN/m²) is seen to increase by 26.9% when compared to that of the un-stabilized sample (186.86kN/m²).

RECOMMENDATIONS

- The following can be recommended for further research;
1. Effect of SDA stabilization of weak lateritic soil at 1% interval from 1-5% replacement should be investigated.
 2. The strength variation of weak lateritic soil stabilized with SDA up to 10% at 1% interval should be investigated using CBR test.
 3. Long term behavior of lateritic soil stabilized using SDA should be monitored under use.

REFERENCE

- Abdulfatah, A. Y., Kiru S. G., and Adedokun T. A. (2013). Compaction Characteristics of Lateritic Soil- Stabilized Municipal Solid Waste Bottom Sediment. *International Journal of Environmental Science and Development* .4(3) DOI: 10.7763/IJESD.2013.V4.359.
- Alexander, L. T. and J. G. Cady. (1962). Genesis and hardening of laterite in soils. U.S. Department of Agriculture Tech. Bull. 1282.
- Al-Rawas, A. A., Taha, R., Nelson, J. D., Al- Shab, T. B., and Al-Siyabi, H., (2002). A Comparative Evaluation of Various Additives Used in the Stabilization of Expansive Soils,” *ASTM Geotech. Test. J.* 25(2):199–209, DOI:10.1520/GTJ11363J.
- ASTM C618 (2019). Standard Specification for Coal Flyash and Raw or Calcined Natural Pozzolan for Use in Concrete. ASTM International, PA, 19428-2959 USA.
- Blight, G. E. (1997). *Mechanics of Residual Soils*.
- BS 1377 (2016). *Methods of Test for Soils for Civil Engineering Purposes- General Requirements and Sample Preparation*.
- Buchanan, F. (1807). *A journey from Madras through the Countries of Mysore, Canara and Malabar*. East India Company, London. In three volumes.
- Craig, F. G. (2004), “*Soil Mechanics 7th Edition*”, SPON Press, London, 458.
- Edeh, J., Agbede, I., and Tyoyila, A. (2014). *Evaluation*

- of Sawdust Ash-Stabilized Lateritic Soil as Highway Pavement Material. *Journal of Materials in Civil Engineering*.
- George R. O. and Braide K. H. (2014). "Stabilization of Nigerian Deltaic Laterites with Saw Dust Ash." IJSRM volume 2 issue 8 August 2014 (www.ijstrm.in).
- Gidigas, MD. (1976). Laterite soil engineering. Pedogenesis and Engineering Principles. *Elsevier*, Amsterdam, 535.
- Harrassowitz, H. (1930). Boden des tropischen Region. Laterite and allitscher (lateritischer) Roylehm. In "Handbuch der Bodenlehre". (Blanck. E. Ed.), Vol.3, Berlin, 387-436.
- Hossain, K.M.A. and Mol, L., (2011). Some engineering properties of stabilized clayey soils incorporating natural pozzolans and industrial wastes, *Construction and Building Materials*. 25(8):34953501, DOI:10.1016/j.conbuildmat.2011.03.042.
- Hossain, K. M. A., (2011) "Stabilized Soils Incorporating Combinations of Rice Husk Ash and Cement Kiln Dust," *J. Mater. Civ. Eng.* 23(9):1320-1327, doi:10.1061/(ASCE)MT.1943-5533.0000310.
- Joseph, I. Olufemi A., and Audu T. ((2013). Evaluation of Sawdust ASH Stabilized Lateritic Soil as Highway Pavement Material. *Journal of Materials in Civil Engineering*.
- Khan S., Khan H., (2015). Improvement of Mechanical Properties by Waste Sawdust Ash Addition into Soil, *Electronic Journal of Geotechnical Engineering*, 20(7):1901-1914.
- Koteswara R. D, Anusha M., Pranav P. R.T., Venkatesh G. (2012). A Laboratory Study on the Stabilization of Marine Clay using Sawdust and Lime. *International Journal of Engineering Science and Advanced*, 2(4):851 – 862.
- Liang, Y., Li, W., and Wang, X., (2012) "Influence of Water Content on Mechanical Properties of Improved Clayey Soil Using Steel Slag," *Geotech. Geol. Eng.* 31(1):83-91, DOI:10.1007/s10706-012-9564-8.
- Moses, G. K. and Saminu, A., (2012) "Cement Kiln Dust stabilization of compacted black cotton soil, *Electron. Journal of Geotech. Eng.* 17(Bund. F):825-836.
- Ogunribido T., (2012). "Geotechnical Properties of Saw Dust Ash Stabilized Southwestern Nigeria Lateritic Soils, *Environmental Research Engineering and Management*, 2 (60), 29-33.
- Okagbue, C.O. and Yakubu, J.A., (2000) "Limestone ash waste as a substitute for lime in soil improvement for engineering construction," *Bull. Eng. Geol. Environ.* 58:107-113.
- Okagbue, C. O., (2007) "Stabilization of Clay Using Woodash," *J. Mater. Civ. Eng.* 19(1):14-18, DOI:10.1061/(ASCE)0899-1561(2007)19:1(14).
- Ola, S. A. (1978) Geotechnical Properties and Behavior of Some Stabilized Nigeria Laterite Soil *Q.T.J. Engr. Geo. London Vol.III* 144-160.
- Ramesh, H. N., Nanda, H. S., and Manoj Krishna, K. V, (2011) "Effect of Soaking on The Strength Behaviour of Shedi Soil Treated With NFA," *Procs. of Indian Geotechnical Conference*, December 15-17, Kochi, India:753-754.
- Kanaka, S. (2012). A laboratory study on the properties of sawdust on Marine Clays. Kakinada.
- Singh, B., Kumar, A., and Sharma, R. K., (2014). "Effect of Waste Materials on Strength Characteristics of Local Clay," *Int. J. Civ. Eng. Res.* 5(1):61-68.

RADIO REFRACTIVE INDEX AND REFRACTIVE INDEX GRADIENTS VARIATION IN A TROPICAL ENVIRONMENT

I.M. TUKUR, K.C. IGWE and J.O. EICHIE.
Department of Physics, Federal University of Technology, Minna.
Email: ishagmtukur@yahoo.com, +2348032075689

ABSTRACT

This paper investigates variation of radio refractivity with related weather parameters and refractivity gradient with altitude. Three years (2013-2015) upper air atmospheric data of temperature, pressure and relative humidity for Abuja were obtained from the Nigerian Meteorological Agency (NIMET). The result shows that temperature, pressure and relative humidity decreases with increasing altitude. Radio refractivity values over Abuja are observed to be decreasing with increasing altitude and values in the rainy season are higher than dry season with a maximum of 344.1 N-units recorded in August and a minimum 277.5 N-units recorded in January. The average refractivity gradient for both dry and wet months is -30.6 N-units/km and the average k-factor as 1.25 which is in agreement with the condition of Sub-refraction.

Keywords: *Refractivity, Refractivity Gradient, K-factor*

1 INTRODUCTION

Radio refractivity is the ratio of the radio wave propagation velocity in free space to its velocity in a specified medium. Radio wave propagation is determined by changes in the radio refractive index of air in the troposphere. The troposphere is the layer of the atmosphere that is most closely related to human life and it is the region of all weather on earth and also the lowest of all the layers, extending from the earth surface to an altitude of about 10km at the north poles and 17km at the equator (Hall, 1979). A change in the magnitude of radio refractive index of the troposphere causes the path of the propagating radio waves to be curved.

Electromagnetic waves propagation in the troposphere are influenced mainly by different components that make up the atmosphere due to variations of some major atmospheric weather variables such as atmospheric temperature, pressure and relative humidity in the troposphere (Ukhurebor, *et al.*, 2018; Ukhurebor and Azi, 2018; Agbo, *et al.*, 2013). Variations in these atmospheric weather variables cause the refractive index of air in the troposphere to differ from place to place (Ukhurebor, *et al.*, 2018).

Radio refractivity serves as a function in determining the quality of UHF, VHF and SHF signals for proper design of their communication station and the planning of good terrestrial radio link over a region (Chukwnike & Chinelo, 2016). Surface and elevated refractivity data are often required by radio engineers to accurately predict electromagnetic wave signals and characterization of radio channels.

In the troposphere, the vertical refractivity gradient serves as an important parameter in estimating path clearance and propagation effects such as sub-refraction, super-refraction or ducting (Adediji and Ajewole, 2008). During ducting condition, atmospheric refractive index decreases sharply with height over a large horizontal area, radio waves can be trapped and forced to follow the

earth's curvature, thus experiencing low-loss propagation over long distance, while in super-refraction, radio waves are bend towards the earth. In sub-refractive condition, refractivity increases with increasing altitude, the radio waves moves away from the earth's surface and the line of sight range and the range of propagation decreases accordingly (Akpootu and Iliyasu, 2017).

2 METHODOLOGY

Radiosonde data of daily temperature, pressure and relative humidity for three years (2013-2015) were obtained from the Nigerian Meteorological Agency (NIMET) headquarters in Abuja.

Abuja, the capital city of Nigeria, located at coordinates 9.01 N and 7.27 E in the guinea savannah of northern climate region of the country and at about 370m above mean sea level. Abuja experiences three weather conditions of a warm, humid rainy season and extremely dry weather conditions.

The daily measured upper atmospheric data of temperature, pressure, relative humidity and height were averaged to get the monthly mean data and the monthly values were also averaged to get the yearly data. These were analyzed to evaluate the monthly and yearly radio refractivity variations. Starting from the relationship between water vapour pressure and relative humidity as written in equation 1.

$$e = \frac{H es}{100} \quad (1)$$

Where

H = Relative Humidity, es = Saturated Vapour Pressure

$$e_s = a \exp\left(\frac{bt}{t+c}\right) \quad (2)$$

t: Celsius temperature (°C) and a, b, c are coefficients given as $a = 6.1121$, $b = 17.502$, $c = 240.97$ for water and $a = 6.1115$, $b = 22.452$, $c = 272.55$ for ice.

(Valid between -20° to $+50^{\circ}$, with an accuracy of $\pm 0.20\%$ for water)

(Valid between -50° to 0° , with an accuracy of $\pm 0.20\%$ for ice)

The refractivity index n , of air is measured by refractivity N in a relation given by (Agbo, *et al.*, 2013)

$$N = (n - 1)10^6 \quad (3)$$

Refractivity is a dimensionless quantity and ranges from 250 and 400N-units. As recommended by (ITU-R, 1997) N is given as:

$$N = \frac{77.6}{T} \left(P + 4810 \frac{e}{T} \right) = N_{\text{dry}} + N_{\text{wet}} \quad (4)$$

Where N_{dry} and N_{wet} according to (Hall, 1979) represent dry and wet component of refractivity and is given as

$$N_{\text{dry}} = 77.6 \frac{P}{T} \quad (5)$$

$$N_{\text{wet}} = 3.73 \times 10^5 \frac{e}{T^2} \quad (6)$$

Where T is the absolute temperature (K) and P is the atmospheric pressure (hpa).

The refractivity gradient or vertical gradient of refractive index as recommended by (ITU-R, 1997) is expressed as:

$$G = \frac{N_1 - N_2}{h_1 - h_2} \quad (7)$$

Where N_1 and N_2 are radio refractivity values at heights h_1 and h_2 respectively.

According to Adediji and Ajewole., (2008) propagation effects such as sub-refraction, super-refraction and ducting are characterize according to the following criteria.

$$\frac{dN}{dh} > -40 \quad \text{Called Sub-refraction} \quad (8)$$

$$\frac{dN}{dh} < -40 \quad \text{Called Super-refraction} \quad (9)$$

$$\frac{dN}{dh} < -157 \quad \text{Called Ducting} \quad (10)$$

Effective earth radius factor K is use to classify propagation effects such as normal refraction, sub refraction, super refraction and ducting.

$$K \approx \left[1 + \frac{\left(\frac{dN}{dh} \right)}{157} \right]^{-1} \quad (11)$$

$$\text{When, } \frac{dN}{dh} = \frac{4}{3} \quad \text{Normal refraction} \quad (12)$$

$$\frac{4}{3} > k > 0 \quad \text{Sub-refraction} \quad (13)$$

$$\infty > K > \frac{4}{3} \quad \text{Super-refraction} \quad (14)$$

3 RESULTS AND DISCUSSION

3.1 VARIATIONS OF WEATHER PARAMETERS WITH ALTITUDE

Figures 1 and 2 show variation of temperature (T), pressure (P) and relative humidity (RH) with altitude for January and August 2013. From the graphs, temperature in each of the two months period is seen to be decreasing with increasing altitude. In the two months under study, temperature inversions are observed at a height of about 18.6km which increases and continue increasing further. This corroborated the fact that temperature in the stratosphere usually increases with increasing height. From the two figures, it is also observed that January recorded the highest temperature as compared with August, with maximum of 29°C at the height of 829 m. August on the other hand recorded a temperature of 22.2°C at approximately the same height.

Air pressure also showed a decrease with increasing altitude as observed in the graphs. The result is in agreement with the facts that since most of the atmospheric molecules are held close to the earth's surface by the force of gravity, and then pressure decreases rapidly at first, then more slowly at higher levels.

Similarly, it is observed from the figures that relative humidity in both January and August shows a decrease with increasing altitude. However, an increase is observed at an altitude of about 3.2km in January and 5.9km in August which begin to decrease until it tends to zero. Due to the availability of large moisture contents expected during the raining season. August which is a rainy month, recorded the highest relative humidity with a value of 80.1% at pressure height of about 925hpa as compared with January having a value of 35%.

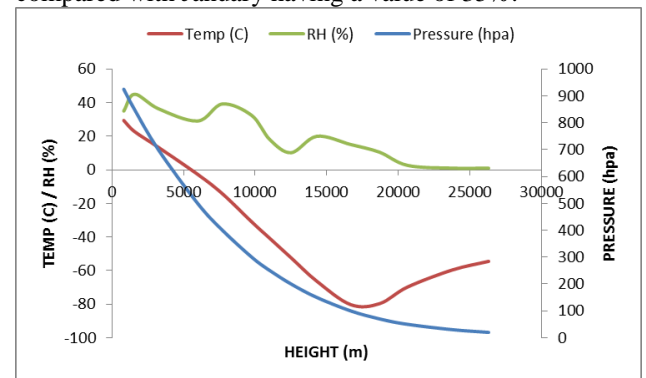


Figure 1: Variation of weather parameters with height for a typical dry month (January, 2013).

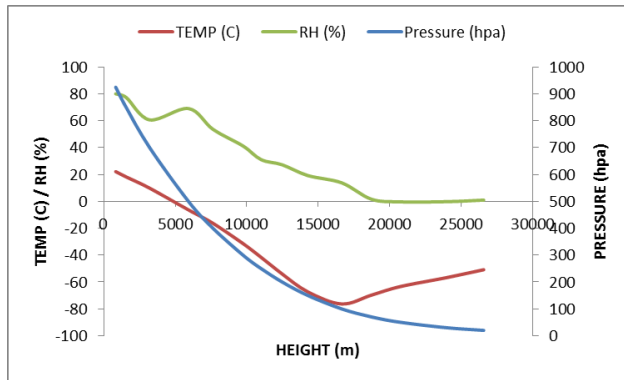


Figure 2: Variation of weather parameters with height for a typical wet month (August, 2013).

3.2 VARIATIONS OF REFRACTIVITY WITH HEIGHT

Figures 3 and 4 depict the variation of refractivity with altitude for January and August 2014. The graphs show that refractivity over Abuja in both January and August decreases with increasing altitude. Radio refractivity in August is observed to be decreasing from a maximum value of about 336.6 N-units at 830m to a minimum value of 7.0 N-units at about 26.6km, while in the month of January, it decreases from 287.9 N-units to 7.1 N-units at the heights of about 815 m and 26.3 km respectively.

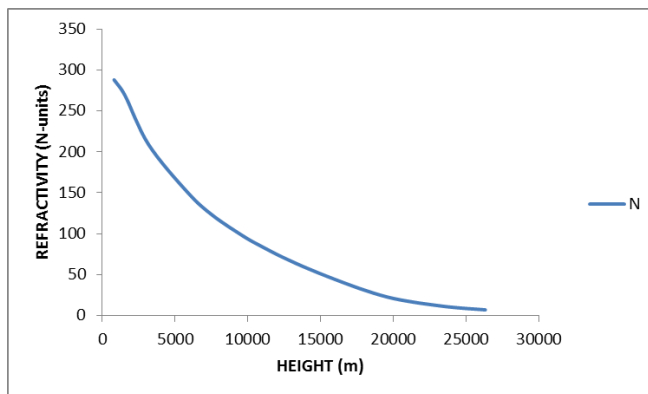


Figure 3: Variation of refractivity with height for January 2014

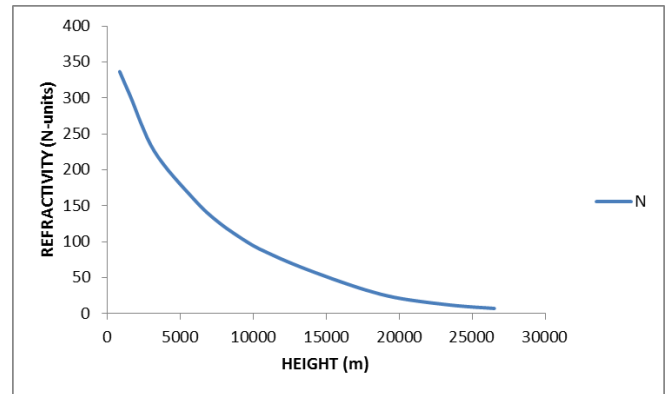


Figure 4: Variation of refractivity with height for August 2014

3.3 DRY AND WET SEASON VARIATION OF REFRACTIVITY AT A HEIGHT OF 1KM

Figures 5 and 6 show refractivity values for dry and wet season months for the year 2015. The refractivity values are seen to be lower in the dry season months (November – March) as compared to wet season months (April – October) and this is a consequence of less moisture content during the dry month period because of influx of large quantity of north easterly winds. The values are higher during the wet months due to availability of large amount of moisture content which is as a result of influx of large quantity of south westerly winds. The values in the wet months show an increase from April-October in the range of 307.9 N-units to 344.1 N-units. In the dry season months, the values are seen to increase from January-December in the range of 272.5 N-units to 306.8 N-units. In general, it is observed that refractivity values in the year 2015 ranges from the lowest value of 272.5N-units in January in the wet months to its highest value of 344.1N-units in October in the wet months. This is in agreement with the work of Igwe and Adimula (2009) on variations of surface radio refractivity and radio refractive index gradients in the Sub-Sahel.

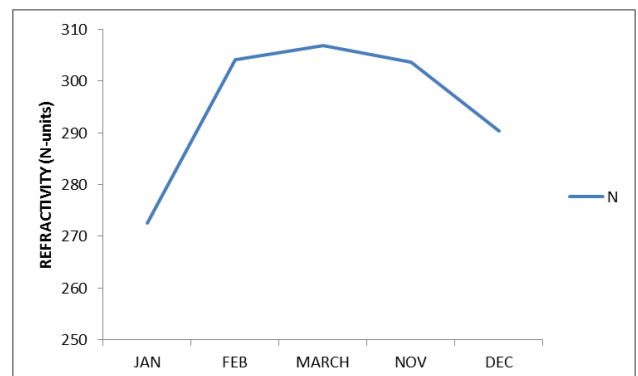


Figure 5: Dry season month's variation of refractivity at 1km for year 2015

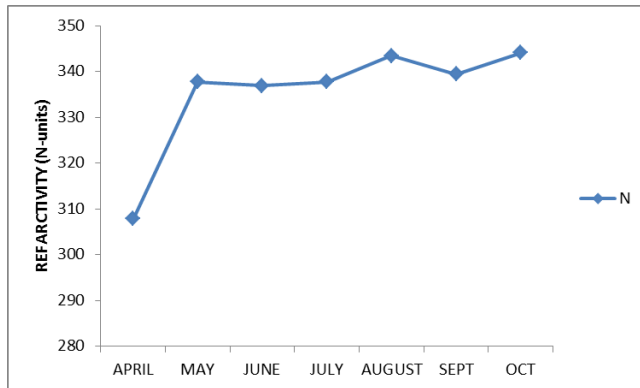


Figure 7: Dry season monthly variation of refractivity gradient at 1km for year 2015

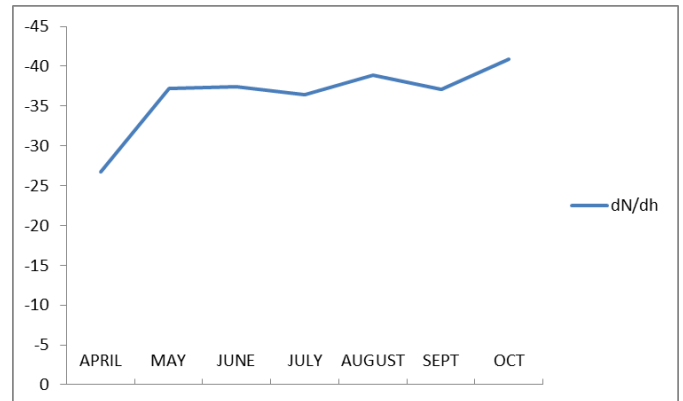


Figure 6: Wet season monthly variation of refractivity at 1km for year 2015

Figure 8: Wet season monthly variation of refractivity gradient at 1km for year 2015

3.4 DRY AND WET SEASON VARIATION OF REFRACTIVITY GRADIENT AT THE HEIGHT OF 1KM

3.5 VARIATION OF EFFECTIVE EARTH RADIUS FACTOR (K-FACTOR) FOR DRY AND WET MONTHS OF 2015

Figures 7 and 8 show dry and wet season variation of refractivity gradient at a height of 1km for the year 2015. The results show that refractivity gradient in the dry season month vary from -19.2 N-units/km in January to -22.1 N-units/km in December, while values vary from -26.7 N-units/km in April to -40.8 N-units/km in October for the wet season months. From the results obtained, it is observed that both dry and wet season months are Sub-refractive. An average value of refractivity gradient for the year 2015 at 1km is calculated to be -30.6 N-units/km. From the average value, it is observed that Abuja is generally under the sub-refractive condition which explains that radio wave are expected to move away from the earth's surface and the line of sight range.

The variation of effective earth radius factor is shown in figures 9 and 10. Values of k-factor are observed to be lower in dry months than in the wet months. The values range from about 1.20 to 1.35 in the wet months and 1.13 to 1.20 in the dry months. The values are observed to be increasing slightly both in the dry and wet months. An average value of 1.25 is obtained for both the dry and wet season months combined. From the average value, it is observed that propagation of radio waves in Abuja in the year 2015 is characterized as sub-refractive.

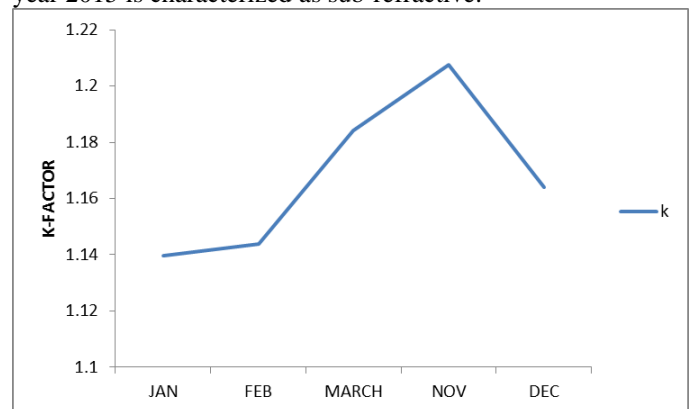
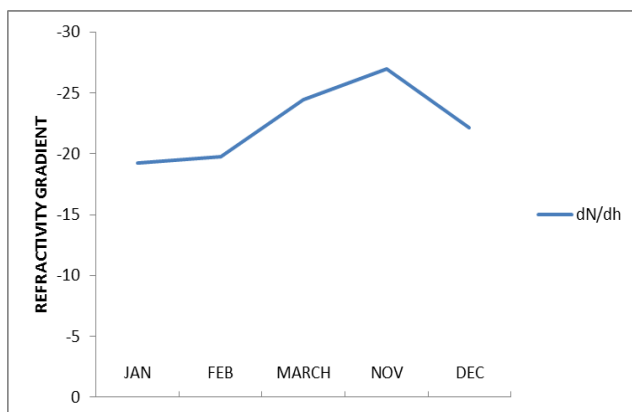


Figure 9: Variation of K-factor for the dry months of 2015

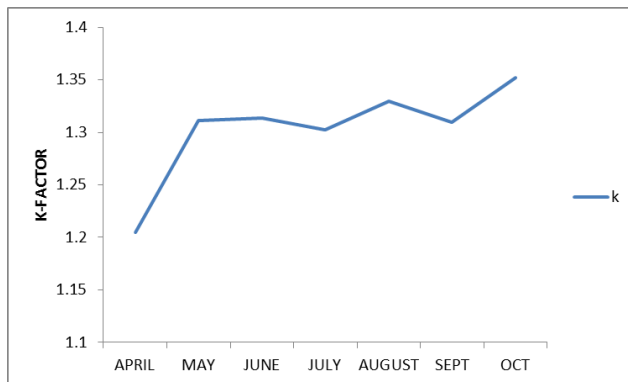


Figure 10: Variation of K-factor for the wet months of 2015

4 CONCLUSION

The radio refractive index and refractive index gradients variation in tropical environment has been investigated. It was observed from the results that, atmospheric parameters of temperature, pressure and relative humidity decreases with increasing altitude. Radio refractivity is observed to be decreasing with height, with raining season showing higher values than dry season. The average value of radio refractive index gradients and effective earth radius factor (k-factor) for 2015 were obtained as -30.6 N-units and 1.25 respectively. This implies that propagation over Abuja is sub-refractive. This explains that radio waves are expected to move away from the earth surface and the line of sight range.

ACKNOWLEDGEMENTS

The authors are grateful to the Nigerian Meteorological Agency (NIMET), Abuja for providing all the necessary data

REFERENCES

1. Adediji, A.T. and Ajewole, M.O. (2008). "Vertical Profile of Radio Refractivity gradient in Akure South-Western Nigeria", *Progress in Electromagnetic Research*, C4, 157-168
2. Agbo, G.A. and Okoro, O.N. and Amechi, A.O., (2013). "Atmospheric refractivity over Abuja, Nigeria". *International Research Journal of Pure and Applied Physics*. Vol.1, No. 1, pp.37-45
3. Akpootu, D.O and Iliyasu, M.I., (2017). "Estimation of tropospheric radio refractivity and its variation with Meteorological Parameters over Ikeja, Nigeria". *Journal of Geography, Environment and Earth Science International*. ISSN: 2454-7352
4. Chukwunike, O.C and Chinelo, I.U., (2016). "The Investigation Of The Vertical Surface Radio Refractivity Gradient In Awka, South Eastern Nigeria". *International Journal of*

Academic Research and Reflection. Vol. 4, No. 6, 2016 ISSN 2309-0405

5. Hall, M. P. M., (1979). "Effects of the troposphere on radio communication". Peter Peregrins Ltd, UK & US., P1-22
6. Igwe, K.C. and Adimula, I.A., (2009). "Variations of Surface Radio Refractivity and Radio Refractive Index Gradients In The Sub-Sahel". *Nigerian Journal of Space Research*. 135-144
7. ITU-R: (2004). *The Radio Refractive Index: Its Formula and Refractivity Data in: Recommendations ITU-R P. 453-9 – 1970-1986-1990-1992-1994-1995 19971999-2001*, 2003.
8. Ukhurebor, K.E. Azi, S.O., Abiodun, I.C. and Ojiemudia, S.E., (2018). "Influence of Weather Variables on Atmospheric Refractivity over Auchu Town, Edo State, Nigeria". *Journal of applied science environmental management*. Vol. 22 (4) 471 – 475
9. Ukhurebor, KE and Azi, SO., (2018). "Review of Methodology to Obtain Parameters for Radio Wave Propagation at Low Altitudes from Meteorological Data: New Results for Auchu Area in Edo State, Nigeria". *J. King Saud University-Sci* (doi: <https://doi.org/10.1016/j.jksus.2018.03.001>)



VOCATIONAL AND TECHNOLOGY EDUCATION: A VIABLE ENTREPREURSHIP TOOL FOR RAPID ECONOMIC GROWTH

Kareem, W.B.¹, Abubakar, H.O. (Mrs.)², Onuh, J.³, Abdulrahaman, T.S.⁴, Abdullahi S.M.⁵

¹Department of Industrial and Technology Education, Federal University of Technology, Minna, Niger State

²Department of Building Technology, Federal Polytechnic Nassarawa, Nassarawa State.

³Department of Science and Technology, Faculty of Education, University of Jos.

⁴Department of Education Technology, University of Ilorin, Ilorin

⁵Department of Technology and Vocational Education, Faculty of Science and Technology Education, Kano University of Science and Technology, Wudil. Kano State

Corresponding author e-mail: wahabami4u@futminna.edu.ng, +234 70 63751512

ABSTRACT

Vocational and technical education is an entrepreneurship skill and employment oriented type of education specially designed to train the learners needed job-skills in the society. It is an education that equipped the learners with technical knowledge, positive work attitudes and appropriate work habits required for employment in a public and private organisation. This paper discussed at length vocational technical education as a viable tool for national economic growth and development by engaging the Nigeria youth in learning the skills involved in Vocational and Technical Education. By so doing the unemployment of youth will be drastically reduced and youth will become self-reliant and self-employed in the society and these will in turn improve the economic growth of the Nation.

Keywords: *Education, Entrepreneurship, Employment, Technical, Vocational, and Youth*

1. INTRODUCTION

The word “vocation” according to the Longman Dictionary of Contemporary English means a job which a person does because he thinks he has a specific fitness or ability to give services to other people.

Vocational Education, according to United Nations Educational Scientific Cultural Organization (UNESCO, 1998) is defined as education designed to prepare skilled workers for industry, agriculture, commerce, etc. which is usually provided at the upper secondary level. Programmes of vocational education include: general studies, practical training for the development of skills required in a chosen occupation and related theory. The emphasis is usually on practical training. Vocational training programmes may be conducted full-time in schools or other educational institutions or part-time as supplementary education for apprentices or others receiving their practical training in employment. In the light of this the new National Policy on Education (NPE 2013) outlined the goals of vocational and technical education to include:

- Provide the technical knowledge and vocational skills necessary for agricultural, commercial and economic development.
- Provide trained manpower in the applied sciences, technology and business, particularly at craft, advance craft and technical levels.

- Give training and impart the necessary skills to individual who shall be self-reliant.

The above goals highlighted by National Policy on education, vocational technical education stands is a special tool for youths development in a technical skill that can make them self-reliant citizens. Technology education according to Abdullahi (1998) is a techniques or art of producing something.

Technology education are those aspects of educational process which involves in addition to general education, the study of technologies and related sciences, the acquisition of practical skills, attitude, understanding and knowledge relating to occupations in various sectors of economic growth and social life development (UNESCO,1998). Technology education is of no doubt a viable tool through which youth can be engaged in a particular skill in vocational and technical education for sustainable and self-reliance, this is to say that it is a kind of education (through skill acquisition) prepares the individual for economical growths and national development and as such it can be said that technology education is an empowerment that improves the nation’s economy, providing job opportunity, reducing rate of crime and encourage creativity and competitiveness in nation building and development (Awotunde, 2000).

In view of the synonymy of technology education with vocational and technical education, Olaitan (1991) argued that the progress of human race, vocational and



technical education has been a constant and identifiable element. VTE has been part of foundation of men's creative and progressive development and observed further that in America, for instance, development of vocational technology education is paralleled with the economic growth, which is essential for nation's technological development and self-reliance, therefore no sacrifice should be considered too great in developing it because of its demand and sustained social benefits.

Vocational and technical education (VTE) remains the most effective means for a society to develop its member's potentials to respond to the changes and demand of the future. It was on this basis Adebayo (2005) highlighted that VTE is the major area the national economic empowerment and development strategy (Needs) as currently pursued by the Federal Government could key in and give the much "sought after" industrials transformation and empowerment of the youth. In this wise vocational and technical education cannot be over emphasis as what the present and future youth need for their self-reliance especially skill trades in vocational technical education as it will go a long way to reduce rate of crime and other social vices.

Entrepreneurship in the context of this reviewed work can be said to involve innovation which can be thought of as a process of change comprising identification, evaluation and exploration of any opportunity, management and creation of value through successful exploration of new idea by an entrepreneur. An entrepreneur is any person who uses the skill acquired to improve hidden business opportunity and exploit it for a profit (Ihekwoaba 2007).

These skill include: commercial, business, agriculture, electrical/electronic, woodwork technology, metal work technology, auto-mobile technology, building technology and vocational skills.

In the same development entrepreneurs are energetic personnel who are very dynamic and always acquainted with societal needs and change along with it to establish a need business venture to meet the demand of that society. Aminu (2009) highlighted that an entrepreneur do all planning, leading and controlling the activities necessary to start the business. Therefore for an entrepreneur to be successful it required determinations, leadership quality, creativity, self-nurturing, self-discipline, energetic and future oriented. It is on this basis this paper addresses VTE as an entrepreneurship tool for rapid economic growth.

1.1 CONCEPT OF TECHNOLOGY EDUCATION

Technology Education is synonymous with vocational and technical education. Unesco (1998) defined Technology Education as the education that provide practical skills for the recipient, it also build attitudes,

understanding and knowledge relating to occupations in various sectors of nations, economic growth and development. Vocational and technical education refers to that phase of general education concerned with equipping people with saleable skills, knowledge, attitudes habits, understandings and appreciations required for entry into or hold employment in recognised occupations. Technology educations according to Nnajofor (2008) was established for the purpose of providing occupational skills (job-skills, technical knowledge, attitudes, habits and value) needed in the labour market.

Similarly, Miller (2005) define Technology Education as a systematic phenomena or process of exposing individual to the practical task for developing and producing goods and services to meet the needs and want of man. This is to say that technology education is an education that helps to identify the potentialities of every individual and develop it to the degree at which such an individual skills, knowledge and attitude required for employment in a particular occupation, group of related occupations or to function in any of economic activity including commerce, agriculture, public and private services among others. Programmes in technology education are organised and designed to equip one with work and life skill which include divisions such as trade in industrial education, vocational, business education, technical education, home economics fine and applied arts and distributive education (Adebayo 2005).

Summarily technology education is a time-honoured through which skills, knowledge and value are acquired through either formal or non-formal processes, it deals with acquisition of skills and knowledge in chosen occupation to enable an individual to earn a living and be self-reliant (Sobowale I.O., 2006)

1.2 TECHNOLOGY EDUCATION AND ECONOMIC GROWTH.

The historical experience of Nigeria with colonialism could be hanged and blamed for the poor performance to technology education in Nigeria economic development. According to Gomwalk (1992) in colonial programme, scholars were not encouraged to value any part of our native culture. Schools and the environment were pulling in opposite direction, this made Nigerians to become so spoilt and depended on all sorts of foreign technology. This attitude of colonial masters towards the nation truncated and even up till now truncating the development of the very effective indigenous technology. This has drastically affected economic growth of Nigeria.

All arms of Nigeria government are not ready to provide adequate fund needed to support vocational and technical education at all level of education. Kareem, Maaji, Abdulrahman, Onu & Nwankwo (2018) highlighted that time allocated for practical acquisition



per week is not enough, the hand tools cannot go round the students during practical. How then do we expect that these students will perform up to their expectation after graduation. This is to say in essence that Nigeria economy has been so affected, it is interested to note that adequate attention has not been paid to inherent Nigeria Indigenous technology in the areas of textiles, pottery and art design. There is no doubt about the fact that this attitudes of government has serious implication on the poor economy that eventually developed in Nigeria till date. Unfortunately it was close to the nation independence that Nigerian Scholars painfully became aware of the technological gap between the colony and the colonialist home countries.

Worst still is when Nigeria entered into partnership with other countries to have her citizens trained in various technology programmes. Beneficiaries of such training programmes acquired sound preparations only to return home into frustration by reason of lack of facilities, equipment and materials to function. In fact the equipment they were trained with are not available in Nigeria Technical Institutions. Moreso, the personnel appointed to head various technical institutions are not technically oriented, and as such they know less or nothing about VTE. Therefore, there is no how such a person can serve or defend the budget proposal for VTE at any level, because the budget will be two demanding to their thought and they will prefer to serve the interest of their own professions. So there is the urgent need to appoint a well qualify individual to head the affairs of vocational and technical education at all level of educational sectors.

It is very hard to understand that the only solution is the shift from foreign concepts to indigenous concept which the present Nigeria government has been trying to realize through the barn on importation of foreign goods and materials. Therefore, if Nigeria must grow economically well, then VTE needed to be given adequate attention.

1.3 RELEVANCE OF VOCATIONAL AND TECHNICAL EDUCATION

Vocational and technical education is a training that is design at imparting skills necessary for self-development and sustenance. Okoro (1993) was of the opinion that vocational and technical education could be described as that part of education that provides the skills, knowledge and attitude necessary for effective employment in specific occupation. The National Policy on Education (2013 edition) described Vocational and technical education as “education designed to prepare individual to acquire practical skills, basic scientific knowledge and attitude require as craftsmen and Technicians at Sub-professional level. The Important aspect of Vocational and technical education required for agricultural and technological

development and sustenance is the acquisition of practical skills.

The aim of vocational and technical education according to Olaitan (1996) are to:

- Provide trained manpower in all kinds of professional areas such as sciences, technology, commerce etc.
- Provide technical knowledge and necessary skills for agricultural, commercial and economic development.

It was in realization of the above goals that the Federal Government established school of vocational and technical education and also specifically set-up certain colleges of education for technical education only. Dawodu (2006) believe that vocational and technical education is the most reliable vehicle of self sustenance, economic prosperity and political supremacy of a nation over others. Apprasing the overall impart of vocational and technical education on the nation indicated that the nation is yet to be in the Promised Land. Efforts must be invigorated to strengthen the existing facilities and structures in these areas in order to achieve the desired goals.

1.4 THE IMPLICATION OF UNEMPLOYMENT YOUTH ON NIGERIA ECONOMIC GROWTH

Many of the Nigeria-youth are unemployed as a result of which they were roaming about Nigeria’s streets. Many are engaged in various social vices such as drug abuse, pocket picking, house burglary, smoking and drinking, thurgery and so on as a result of their idleness and without any hope of securing an occupation at the minimum level needed to survive not to talk of raising a family of their own. On this basis Salami (2011) stated that a high level of unemployment is one of the critical socioeconomic problems facing Nigeria that is inadequate unemployment of situation of youth has a number of socioeconomic, political and moral consequences which gives rise to high level of poverty in Nigeria. (Ugunde 2005) he also highlighted that Nigeria has been facing acute unemployment problems of school leavers since the last two decade. According to Somavia (2004) very many of unemployed youth who are roaming about in the big cities of Nigeria looking for job are certified schools leavers this is to say that the rate of youth unemployment is already at alarming rate as they are turned out from schools in large numbers every year. Aworanti (2000) stated that about half million of these youth are unskilled graduate on yearly bases while National Manpower board puts the current youth unemployment figure at about 3.7million or 4.2% of the Nigeria population as at 2004. Awogbenle and Iwuamadi (2010) also highlighted that the Manpower Board and the Federal Bureau of Statistics shows that Nigeria has a youth population of 80million, representing 60% of the total population of



the country, 64million of these youth are unemployed, while 1.6million are under employed because they were engaged in a job or duty which is too little to sustain them. It can be seen that this inadequate employment situation of youth has a number of socio-economic, political and moral consequences as stated earlier, the situation has also given rise to high level of poverty in Nigeria. Therefore the urgent solution to this is to allow Nigeria youth to take up training in Vocational and Technical Education.

2. TRADES IN VOCATIONAL AND TECHNICAL EDUCATION

Vocational and technical education comprises of various trades through which youth can be engaged for self reliance and development for national economic growth. This include:

AUTO-MOBILE TECHNOLOGY SKILLS

- Vulcanizing and tyre repairs
- Carburettor and electronic injection system serving and repairs.
- Car wash and painting services
- Vehicle panel beating and body works
- Vehicle electronic systems troubleshooting.
- Brake system servicing and repairs
- Vehicle alignment and wheel balancing
- Transmission maintenance works
- Engine maintenances works

BUILDING TECHNOLOGY SKILLS

- Block laying
- Concreting
- Plumbing
- Brick laying
- Building drawing and design
- Introduction to building construction
- Interlocking
- Panting and Decoration

ELECTRICAL/ELECTRONIC TECHNOLOGY SKILLS

- Electrical installation and maintenance
- Office equipment maintenance and repairs
- GSM maintenance & Repairs
- Satellite systems installation and maintenances
- Radio, Television and Maintenance works
- Refrigeration and Air conditioning works
- Electrical/Electronic part and equipment merchandising

METAL WORK TECHNOLOGY SKILLS

- Fabrication and welding

- Sheet metal works
- Forging e.g blacksmithing
- Painting & Decoration (finishing of metal work)
- Machine Skill and Maintenance

WOOD WORK TECHNOLOGY SKILLS

- Carpentry and joinery
- Cabinet making
- Pattern making
- Painting and wood finishing
- Ornamental design
- Upholstery making
- Wood machining

VOCATIONAL SKILLS

- Agriculture
- Home Economics
- Fine and Applied Arts
- Business Studies
- Textile trade
- Knitting
- Hair dressing/Barbing
- Tailoring/Fashion Designing

3. RELEVANT OF ENTREPRENEURSHIP SKILL IN VOCATIONAL TECHNICAL EDUCATION

Vocational and technical education is itself an entrepreneurial in nature as it all involves manipulation of skills in construction. Marketing and managerial skills in entrepreneurship is also of important and very relevant in VTE. It helps the recipient of whatever form of VTE to be equipped with stock taking of materials, production processes and marketing strategy for adequate profit making.

Entrepreneurial skill help the VTE recipients and professionals to possess trait like initiate such as (self-initiated individuals) perseverance that is, (strong determination, patience), need for high standard product, commitment to agreement/contract, creative problem solving, integrity, strive for growth and expansion and success achiever. Training in the Vocational Technical Education is the answer.

4. CONCLUSION

This reviewed paper has attempted to address the current issues of youth unemployment in Nigeria and its effect on economic growth. It is on this basis, the reviewers highlighted the relevant of VTE in solving this problem of youth unemployment through youth engagement in one form or the other in VTE. In support of this Awosope (2004) earmarked that the role of vocational and technical education on the living standard of an individual cannot be over-emphasized. Vocational and technical education is a base to



technological development and is the most effective means of empowering the citizens to stimulate and sustained national development, enhance employment, improve the quality of life, eliminate poverty, limit the incidence of social vices occasioned by joblessness and promote culture of peace, freedom and democracy.

5. RECOMMENDATIONS

Based on the reviews and vital discussions in this paper the following recommendations are made:

1. The Federal Government should re-awaken the National directorate for employment with adequate fund to train youth in VTE related trades. So that these youth can be useful to themselves and the societies.
2. Craft works should be re-introduce in primary education curriculum. This to some extent will gives focuses to pupils in identification of their talent in their future career.
3. Education planners should make it as a matter of pre-requisite and compulsory to offer one form of subject or the other in VTE at O'level. In this respect enough time should be earmarked for practical class so that at the end of senior secondary school the graduand should be able to carry out some repair and construction in that subject.
4. Orientation of the society and public enlightenment on vocational technical education should be organised regularly by educational stake holders particularly Federal and State Ministry of Education, so that some parents can be fully counselled on how to advice their children to study programme in VTE as against the parents usual rejection of the programme.

6. REFERENCE

- Adebayo (2005) Administration of Technical Colleges on Democratic Setting: Problems and Prospects. *Kusugu Journal of Education Kusugu Federal College of Education.*
- Abdullahi (1998). Prospect of training and management of technical teachers. Department of Education (Technical) Kaduna Polytechnic, Kaduna.
- Aminu A.A. (2009) Entrepreneurship and their Practise. Company Publishes Ltd Maiduguri.
- Awanbor, D (2005) Skill Acquisition of Technical and Vocational College: enhanced productivity for self-reliance, *A paper presented at the*

National Engineering Conference at Helel Presidential, Enugu 17th – 19th Nov, 2005.

- Awosope, C.O.A, (2004) Vocational and Technical Education as a pivot for National Economic Empowerment and Development Strategy. A graduation lecture presented at the Federal College of Education (Technical), Akoka-Lagos 15th Dec, 2004.
- Awotunde, D.O. (2000) technical and vocational education for national development. The Nigeria experiences lead paper presented at the National Conference on Science and Technology Education for National Development. Held at the Federal College of Education, Panleshin 26th – 30th Nov, 2000.
- Concept of Technical Education and Technology. P126 Pg 38-43
- Federal Republic of Nigeria (2013). National Policy on Education, Lagos: *National Educational Research Development Council Press.*
- Gomwalk U.D. (1992) Technology Education for National Development, Issues in Technology Education for National Development, Vol 1, *National Association of Teachers of Technology. NATT Pp 1-8*
- Ihekwoaba, M.E. (2008). The Entrepreneur Rothmed Publisher Ltd. Isolo
- Kareem W.B., Maaji, S.A., Abdulrahman, T.S., Onu, T. & Nwankwo, F.C. (2018) Appraisal of Woodwork Practical Skill Acquisition of Nigeria Certificate in Education (NCE) Technical Students in Niger State College of Education, Minna. *International Journal Industrial Technology, Engineering, Science and Education (IJITESD)* Pp. 87-92
- Nnajiolor, F.N. (2006) Relevance of School Industry Relationship in Improving the Quality of Graduates of Vocational Technical Education in the Current Reform Ayenda 19 Proceeding of the Annual National Conference of Nigeria Association of Teachers of Technology held at Kwara State College of Education, Uriu 6-9 2006.
- Olaitan S.O. (1996) Vocational and Technical Education in Nigeria (Issue and Analysis) Onisha, Noble Graphic Press.



3rd International Engineering Conference (IEC 2019)
Federal University of Technology, Minna, Nigeria



- Okoro, O.M. (1993). Principles and Methods in Vocational and Technical Education. Nusukska: University Trust Publishers.
- Salami, C.G.E.(2011). Entrepreneurship and youth unemployment in Nigeria: The missing link. *Global Journal of Management and Business Research*, 11(5)
- Sobowale, I.O. (2006) Consolidating and sustaining school- Industry Partnership (SIP) in Technology Education; A Key Factor for National Development, *Proceeding of 19th Annual Conference of WATT held at Kwara State College of Education, Ilorin Nov 6-9, 2006 Pp 95-102.*
- United Nations Educational Scientific Cultural Organization (Unesco 1998) Development in Technical and Vocational Education: A Comparative Study. UNESCO Monograph in education.

A 2-STEP HYBRID BLOCK BACKWARD DIFFERENTIATION FORMULA FOR THE APPROXIMATION OF INITIAL VALUE PROBLEMS OF ORDINARY DIFFERENTIAL EQUATIONS

*Akintububo, Ben.G¹, Umaru Mohammed²

¹Department of Mathematics, Federal University of Technology, PMB 65 Minna Niger State, Nigeria

²Department of Mathematics, Federal University of Technology, PMB 65 Minna Niger State, Nigeria

*Corresponding author email: ben.gakintububo@yahoo.com, +2348132832527

ABSTRACT

In this paper, a two-step hybrid backward differentiation formula, with two off-grid points incorporated at interpolation for the solution of initial value problems of ordinary differential equations is presented. The main method as well as the additional methods are obtained from the same continuous scheme formulated using interpolation and collocation methods with Legendre polynomial as the basis function. The method is seen to be of uniform order $k=4$. The stability of the proposed method is analyzed and discussed. Numerical experiments were carried out to ascertain the effectiveness of the method in comparison with the approximation produced by some existing methods.

Keywords: BDF, Continuous Collocation, IVP, Legendre polynomial.

1 INTRODUCTION

Wherever or whenever real-life problem is discussed, ordinary differential equations as a means of modelling the behavior of such reality cannot be overemphasized. Initial value problem of ordinary differential equations of the form

$$\frac{dy}{dx} = f(x), \quad y(x_0) = y_0 \quad (1)$$

occurs frequently in real life including but not limited to population dynamics, finance, engineering, to mention but a few. Over the years, several numerical methods had been adopted for the approximation of (1). One step methods (Euler methods, Runge-Kutta methods, ...), Linear multistep methods (Adams Bashforth, Adams Moulton,...) (see Burden and Faires, ninth edition) have been found to be useful in providing approximation to problem (1). But the best is yet to come and this is the reason researchers over the years have not left any stone unturned in finding a better method, one that will be close enough to the exact solutions of some existing problems, so that minds can be at rest when addressing problems to which theoretical solution do not exist. According to Imanova and Ibrahimovic, (2013), Hybrid methods were introduced in the middle twentieth century which involve joining some one step and multistep methods while preserving their best properties. Advantages of hybrid methods include high accuracy as well as extended domain of stability. Ibijola

et al (2012), Kumleng (2012), Yakusak and Adeniyi (2015), Olabode (2009) are some of the researchers who have developed hybrid methods for the solution of (1) with great success.

In this paper, we develop a two-step Hybrid Backward Differentiation Formula (2SHBDF) using interpolation and collocation techniques, incorporating two off-grid points at interpolation.

2 METHODOLOGY

It is assumed that the solution of (1) can be approximated by a polynomial of the form,

$$y(x) = \sum_{j=0}^{i+c-1} \alpha_j p_j(x), \quad (2)$$

where i and c are respectively, number of interpolation and collocation points and α_j 's are coefficient to be determined. $p_j(x)$ can be any orthogonal polynomial. In this case, Legendre polynomial is used since, on inspection, it produces exactly the same continuous form as the popularly adopted power series. Incorporating k off-grid points for every k -step method here, requires that $i + c$ equations must be satisfied. That is,

$$\left. \begin{aligned} y(x_n) &= y_n, \\ y(x_{n+j}) &= y_{n+j}, j = 0, \left(\frac{1}{2}\right), 1, \dots, k - \frac{1}{2}, \\ f(x_{n+k}) &= f_{n+k}, \end{aligned} \right\} (3)$$

where f implies the derivatives of y .

$k = 2$, $x \in [x_n, x_{n+2}]$, the continuous form of the method is as follows;

$$\varphi = \sum_{j=0}^{\frac{3}{2}} \alpha_j y_{n+j} + \beta_2 f_{n+2} \quad (4)$$

Which when evaluated in line with (3.1) produces the system of equations

$$Y_{\omega} = D\Psi_{\omega-n} \quad (5)$$

$$Y_{\omega} = (y_n, y_{n+\frac{1}{2}}, y_{n+1}, y_{n+\frac{3}{2}}, f_{n+2})^T,$$

$$\Psi_{\omega} = (\alpha_0, \alpha_{\frac{1}{2}}, \alpha_1, \alpha_{\frac{3}{2}}, \beta_2)^T \text{ and } D \text{ is a } 5 \times 5 \text{ matrix.}$$

Using matrix inversion technique with the aid of maple software, the values of the unknown coefficients α_j 's and β_2 were obtained and substituted appropriately to give the continuous form

$$\varphi = \alpha_0 y_n + \alpha_{\frac{1}{2}} y_{n+\frac{1}{2}} + \alpha_1 y_{n+1} + \alpha_{\frac{3}{2}} y_{n+\frac{3}{2}} + h\beta_2 f_{n+2} \quad (6)$$

Evaluating (3.13) at $x = x_n + 2h$ resulted in the main method

$$y_{n+2} = -\frac{3}{25}y_n + \frac{16}{25}y_{n+\frac{1}{2}} - \frac{36}{25}y_{n+1} + \frac{48}{25}y_{n+\frac{3}{2}} + \frac{6}{25}hf_{n+2} \quad (7)$$

To obtain the additional schemes that combine with the main method to form a block, the first derivative of (6) is obtained and evaluated at $x = x_{n+\frac{1}{2}}$, $x = x_{n+1}$ and $x = x_{n+\frac{3}{2}}$ which produced three other discrete schemes. Hence, the 2-step block Hybrid Differentiation Formula with 2 off-grid points is given as

$$\left. \begin{aligned} f_{n+\frac{1}{2}} &= \frac{1}{25h} \left[hf_{n+2} - 13y_n - 39y_{n+\frac{1}{2}} \right. \\ &\quad \left. + 69y_{n+1} - 17y_{n+\frac{3}{2}} \right] \\ f_{n+1} &= -\frac{1}{75h} \left[3hf_{n+2} - 14y_n + 108y_{n+\frac{1}{2}} \right. \\ &\quad \left. - 18y_{n+1} - 76y_{n+\frac{3}{2}} \right] \\ f_{n+\frac{3}{2}} &= \frac{1}{75h} \left[9hf_{n+2} - 17y_n + 99y_{n+\frac{1}{2}} \right. \\ &\quad \left. - 279y_{n+1} + 197y_{n+\frac{3}{2}} \right] \\ y_{n+2} &= -\frac{3}{25}y_n + \frac{16}{25}y_{n+\frac{1}{2}} - \frac{36}{25}y_{n+1} \\ &\quad + \frac{48}{25}y_{n+\frac{3}{2}} + \frac{6}{25}hf_{n+2} \end{aligned} \right\} \quad (8)$$

2.1 ANALYSIS OF THE METHOD

2.1.1 ORDER OF ACCURACY OF THE METHOD

In line with Endre (2014), let $y(x_{n+j})$, the solution to $y'(x_{n+j})$ be sufficiently differentiable, then $y(x_{n+j})$ and $y'(x_{n+j})$ can be expanded into a Taylor's series about point x_n to obtain

$$T_n = \frac{1}{h\sigma(1)} [C_0 y(x_n) + C_1 h y'(x_n) + C_2 h^2 y''(x_n) + \dots] \quad (9)$$

Where

$$C_0 = \sum_{j=0}^k \alpha_j,$$

$$C_1 = \sum_{j=0}^k j\alpha_j - \sum_{j=0}^k \beta_j,$$

$$\vdots$$

$$C_q = \frac{1}{q!} \sum_{j=0}^k j^q \alpha_j - \frac{1}{(q-1)!} \sum_{j=0}^k j^{q-1} \beta_j,$$

Definition 1: A Linear multistep method is said to be of order of accuracy p if $C_0 = C_1 = \dots = C_p = 0$, $C_{p+1} \neq 0$. The error constant being C_{p+1} .

In accordance with the definition 1 above, our method is of uniform order 4 with error constants in the table below.

METHOD	POINT OF EVALUATION	ORDER, P	ERROR CONSTANT, C_{p+1}
(8)	$x = x_{n+1/2}$	4	$-\frac{29}{320}$
	$x = x_{n+1}$	4	$-\frac{31}{160}$
	$x = x_{n+3/2}$	4	$-\frac{111}{320}$
	$x = x_{n+2}$	4	$-\frac{3}{40}$

2.1.2 CONSISTENCY OF THE METHOD

Definition 2: A linear multistep method is said to be consistent if

- the order of accuracy $p > 1$,
- $\sum_{j=0}^k \alpha_j = 0$,
- $\rho'(1) = \sigma(1)$ where $\rho(r)$ and $\sigma(r)$ are first and second characteristic polynomials of the method.

Conditions i and ii were taken care of in 2.1.1 since the order $p > 1$ and $C_0 = \sum_{j=0}^k \alpha_j = 0$ in all cases.

For the third condition, the first and second characteristic polynomials are obtained and evaluated as follows;

Method (8),

Evaluated at $x = x_{n+1/2}$,

$$13y_n + 39y_{n+\frac{1}{2}} - 69y_{n+1} + 17y_{n+\frac{3}{2}} = -25hf_{n+\frac{1}{2}} +$$

$$hf_{n+2}$$

$$\rho(r) = 17r^{\frac{3}{2}} - 69r^1 + 39r^{\frac{1}{2}} + 13,$$

$$\begin{aligned} \sigma(r) &= -25r^{\frac{1}{2}} + r^2 \\ \rho'(1) &= \sigma(1) = -24 \\ \text{Evaluated at } x &= x_{n+1}, \\ 14y_n - 108y_{n+\frac{1}{2}} + 18y_{n+1} + 76y_{n+\frac{3}{2}} \\ &= 75hf_{n+1} + 3hf_{n+2} \\ \rho(r) &= 76r^{\frac{3}{2}} + 18r^1 - 108r^{\frac{1}{2}} + 14, \\ \sigma(r) &= 75r^1 + 3r^2 \\ \rho'(1) &= \sigma(1) = 78 \\ \text{Evaluated at } x &= x_{n+\frac{3}{2}}, \\ 17y_n - 99y_{n+\frac{1}{2}} + 279y_{n+1} - 197y_{n+\frac{3}{2}} &= -75hf_{n+\frac{3}{2}} + \\ &9hf_{n+2} \\ \rho(r) &= -197r^{\frac{3}{2}} + 279r^1 - 99r^{\frac{1}{2}} + 17, \\ \sigma(r) &= -75r^{\frac{3}{2}} + 9r^2 \\ \rho'(1) &= \sigma(1) = -66 \\ \text{Evaluated at } x &= x_{n+2}, \\ 3y_n - 16y_{n+\frac{1}{2}} + 36y_{n+1} - 48y_{n+\frac{3}{2}} + 25y_{n+2} &= 6hf_{n+2} \\ \rho(r) &= 25r^2 - 48r^{\frac{3}{2}} + 36r^1 - 16r^{\frac{1}{2}} + 3, \\ \sigma(r) &= 6r^2 \\ \rho'(1) &= \sigma(1) = 6 \end{aligned}$$

Hence, the method is consistent.

2.13 ZERO STABILITY

The derived Hybrid Backward Differentiation Formula can be written in a block form as follows.

$$IY_{\omega+1} = AY_{\omega+1} + BY_{\omega-1} + hCF_{\omega+1}. \quad (10)$$

$$\text{Where } I = \begin{bmatrix} 1 & 0 & 0 & 0 \\ 0 & 1 & 0 & 0 \\ 0 & 0 & 1 & 0 \\ 0 & 0 & 0 & 1 \end{bmatrix},$$

$$A = \begin{bmatrix} 0 & \frac{23}{13} & -\frac{17}{39} & 0 \\ 6 & 0 & -\frac{38}{9} & 0 \\ -\frac{99}{197} & \frac{279}{197} & 0 & 0 \\ \frac{16}{25} & -\frac{36}{25} & \frac{48}{25} & 0 \end{bmatrix}, B = \begin{bmatrix} 1 & 0 & 0 & -\frac{1}{3} \\ 0 & 1 & 0 & -\frac{7}{9} \\ 0 & 0 & 1 & \frac{17}{197} \\ 0 & 0 & 0 & -\frac{3}{25} \end{bmatrix} \text{ and}$$

$$C = \begin{bmatrix} -\frac{25}{39} & 0 & 0 & \frac{1}{39} \\ 0 & \frac{25}{6} & 0 & \frac{1}{6} \\ 0 & 0 & \frac{75}{197} & -\frac{9}{197} \\ 0 & 0 & 0 & \frac{6}{25} \end{bmatrix}$$

Applying the method to the test equation,

$$y' = \lambda y \quad (11)$$

Amounts to solving the difference system,

$$[(I - zC) - A]Y_{\omega+j} - BY_{\omega-j} = 0,$$

$$z = h\lambda \quad (12)$$

whose first characteristics polynomial is given as

$$\rho(R) = \det[R(I - A) - B]. \quad (13)$$

Definition 3. (ZERO STABILITY): The block method (8) is said to be zero stable if the first characteristic polynomial $\rho(R) = \det[R(I - A) - B] = 0$ satisfies $|R_j| \leq 1, j = 1, 2, 3, \dots$ and for those roots with $|R_j| = 1$, the multiplicity must not exceed 2.

The derived method is zero stable having satisfied the required condition with the roots of its first characteristic polynomial as $R = \{0, 0, 0, 1\}$.

2.14 CONVERGENCE

Convergence of a linear multistep method requires that it be consistent and zero stable. Our 2-step Hybrid Backward Differentiation Formula is convergent.

3 NUMERICAL EXPERIMENT

The problems below were used to establish the effectiveness of the method.

Note: the following notations were used to describe the results obtained.

$y(t_n)$ is the theoretical solution, y_n is the approximation using our method and $Err(\text{Sergey})$ signifies absolute error in the method used in Sergey et al (2016).

Problem 1;

$$y' = y - t^2 + 1, 0 \leq t \leq 2, y(0) = 0.5, h = 0.1.$$

$$\text{Exact solution: } y(t) = t^2 + 2t + 1 - \frac{1}{2}e^t$$

We selected problem 1 from [1] and we compared the result with the exact solution as well as the popular fourth order Runge-Kutta method since our method is also of order 4. The results in tables 1(a) and 1(b) show that our method gives better approximation with maximum error difference of 2.96×10^{-6} .

Problem 2;

$$x'(t) = t + x(t), t \in [0,1], x(0) = 0.$$

Exact solution: $x(t) = e^t - t - 1$.

This problem was solved in Sergey et al (2016). We solved it using our method and the result was compared with the exact solution on table 2(a) which shows a reasonable approximation. The error in our method was also compared with that of Sergey et al (2016) [7] in table 2(b) with step length $h=0.1$ and our method is way better.

Table 1(a): Comparison between Our method and the theoretical solution for problem 1.

t	$y(t_n)$	y_n	Error
0.1	0.65741454096	0.65741460349	6.25E-08
0.2	0.82929862091	0.82929868816	6.73E-08
0.3	1.01507059621	1.01507074691	1.51E-07
0.4	1.21408765117	1.21408781545	1.64E-07
0.5	1.42563936464	1.42563963949	2.75E-07
0.6	1.64894059980	1.64894090078	3.01E-07
0.7	1.88312364626	1.88312409284	4.47E-07
0.8	2.12722953575	2.12723002590	4.90E-07
0.9	2.38019844442	2.38019912529	6.81E-07
1.0	2.64085908577	2.64085983410	7.48E-07
1.1	2.90791698802	2.90791798505	9.97E-07
1.2	3.17994153863	3.17994263545	1.10E-06
1.3	3.45535166619	3.45535308599	1.42E-06
1.4	3.73240001657	3.73240157952	1.56E-06
1.5	4.00915546483	4.00915744574	1.98E-06
1.6	4.28348378780	4.28348596949	2.18E-06
1.7	4.55302630413	4.55302902502	2.72E-06
1.8	4.81517626779	4.81517926561	3.00E-06
1.9	5.06705277886	5.06705647028	3.69E-06
2.0	5.30547195053	5.30547601892	4.07E-06

Table 1(b): Comparison between RK4 and the theoretical solution problem 1.

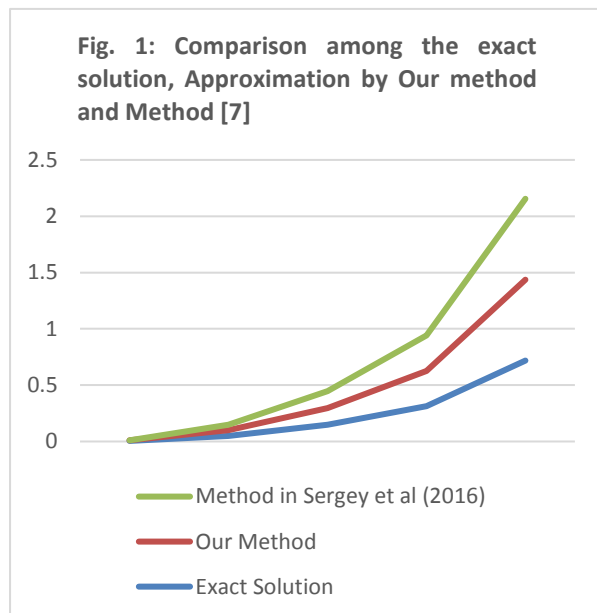
t	$y(t_n)$	y_n	0
0.1	0.65741454096	0.65741437500	1.66E-07
0.2	0.82929862091	0.82929827599	3.45E-07
0.3	1.01507059621	1.01507005843	5.38E-07
0.4	1.21408765117	1.21408690570	7.45E-07
0.5	1.42563936464	1.42563839564	9.69E-07
0.6	1.64894059980	1.64893939041	1.21E-06
0.7	1.88312364626	1.88312217855	1.47E-06
0.8	2.12722953575	2.12722779067	1.75E-06
0.9	2.38019844442	2.38019640177	2.04E-06
1.0	2.64085908577	2.64085672418	2.36E-06
1.1	2.90791698802	2.90791428491	2.70E-06
1.2	3.17994153863	3.17993847018	3.07E-06
1.3	3.45535166619	3.45534820737	3.46E-06
1.4	3.73240001657	3.73239614113	3.88E-06
1.5	4.00915546483	4.00915114530	4.32E-06
1.6	4.28348378780	4.28347899554	4.79E-06
1.7	4.55302630413	4.55302100940	5.29E-06
1.8	4.81517626779	4.81517043981	5.83E-06
1.9	5.06705277886	5.06704638594	6.39E-06
2.0	5.30547195053	5.30546496022	6.99E-06

Table 2(a): Comparison between Our method and the theoretical solution for problem 2.

t	$y(t_n)$	y_n	Error
0	0	0	0
0.1	0.00517091808	0.00517079300	1.25E-07
0.2	0.02140275816	0.02140262366	1.34E-07
0.3	0.04985880758	0.04985850617	3.01E-07
0.4	0.09182469764	0.09182436908	3.29E-07
0.5	0.14872127070	0.14872072100	5.50E-07
0.6	0.22211880039	0.22211819844	6.02E-07
0.7	0.31375270747	0.31375181431	8.93E-07
0.8	0.42554092849	0.42553994819	9.80E-07
0.9	0.55960311116	0.55960174940	1.36E-06
1.0	0.71828182846	0.71828033178	1.50E-06

Table 2(b): Comparison between absolute error in our method and that of Sergey et al (2016) for problem 2.

t	Err(Sergey)	Absolute error in Our method
0.1	5.17E-03	1.25E-07
0.3	1.89E-02	3.01E-07
0.5	3.82E-02	5.50E-07
0.7	6.51E-02	8.93E-07
1	1.25E-01	1.50E-06



3 CONCLUSION

A self-starting 2-step backward differentiation formula has been proposed and implemented for the approximation of solution of initial value problem of ordinary differential equation. The method is seen to be consistent and has a good stability property. Ongoing projects involve formation of higher steps using the same approach for the solution of certain classes of ordinary differential equations

ACKNOWLEDGEMENTS

Sincere appreciation goes to the reviewers for their sincere and constructive comments which in many ways have contributed to the preparation of the final paper.

REFERENCE

- Burden R.L and Faires J.D (2011): *Numerical Analysis, Ninth Edition*. Brooks/Cole 20 Channel Center Street Boston, MA02210 USA. Brooks/Cole, Cengage Learning
- Endre S (2014), *Numerical Solution of Ordinary Differential Equations*. Mathematical Institute, University of Oxford.
- Ibijola, I.A, Skwame Y and Kumleng G (2012) Formation of Hybrid Block Method of Higher Step-Sizes, through the Continuous Multistep. *American Journal of Scientific and Industrial Research*, ©2011, Science Hub, <http://www.scihub.org/AJSIR> ISSN: 2153-649X, doi:10.5251/ajsir.2011.2.2.161.173
- Imanova, M and Ibrahimovic V. R (2013). On a research of hybrid Methods. Retrieved from: <http://www.researchgate.net/publication/280523357>
- Kumleng G.M (2012) Formation of Hybrid Block Method of Higher Step-Sizes, through the Continuous Multistep Collocation. Retrieved from: <http://www.researchgate.net/publication/280523357>
- Mehrkanoon, S and Majid M.S (2010). A variable step implicit block multistep method for solving first order ODE's: *Journal of Computational and Applied Mathematics* 233 (2010) 2387-2394:
- Olabode, T.O, (2009) A six step Scheme for the Solution of Fourth Order Ordinary Differential Equations. Retrieved from: http://www.researchgate.net/publication/253537145_2009
- Sergey N. Dashkovskiy, et al (2016). Numerical Solution to Initial Value Problem for One Class of differential equation with maximum *International Journal of Pure and Applied Mathematics Volume 109 No. 4 2016, 1015-1027.*
- Yakusak, N.S and Adeniyi, R.B: A Four Step Hybrid Block Method for First Order Initial Value Problems in Ordinary Differential Equations. *AMSE JOURNALS-2015: Advances A; Vol. 52; No 1; pp 17-30 2014.*



SIGNIFICANT DELAY FACTORS AFFECTING COMPLETION TIME OF PUBLIC SECTOR CONSTRUCTION PROJECTS IN NIGER STATE

*Mamman, J. E¹, Abdullahi, A. H², Isah, L. M³

Department of Quantity Surveyor, The Federal Polytechnic, PMB 55
Bida, Niger state.

*Corresponding author email: ekemenajuliet@gmail.com +2348038964659

ABSTRACT

The inability to complete project on the scheduled date, low quality of work and cost overruns are the critical problems encountered by the industry in Nigeria. The study examined the significant delay factors affecting completion time of public sector construction projects in Niger state. A well structured questionnaire was administered to knowledgeable clients, consultants and contractors. 240 questionnaire were distributed and 174 questionnaire representing 72.5% were returned and analyzed using Relative Importance Index (RII). Cost information was obtained in respect of the quantitative difference between initial estimated and final completion time of 196 projects constructed. Statistical Package for Social Science (SPSS) was used to analyze the inferential statistic using Pearson moment correlation and also regression analysis. Result of percentage Time difference in project: 190 projects had time overrun with 96.94%. The result of initial estimated time and percentage time difference. Pearson moment correlation analysis revealed, that a significant relationship existed, with the p-value < 0.05, while linear regression revealed, that no significant relationship existed with the p-value >0.05. Findings from the ten top significant delays factor in construction revealed that: delay in payment, lack of fund by client, change in government, poor site management and supervision, government procedure, client interference leading to award of contract to unqualified contractor are the main causes of delays in construction projects in Nigeria. It was recommended that progress payment should be made on time to the contractor and before awarding any contract client should ensure that there is sufficient fund to complete the project.

Keywords: Completion time, Construction, Delay Factors, Estimated time, Public projects

1 INTRODUCTION

Delays in construction projects execution is one of the biggest problems faced by developing countries, as it has negative effects on projects (Pourrostan & Ismail, 2011). In Nigeria a project is considered successful if the project is completed within a specific budget or cost, getting the project into use by the stipulated date, meeting the technical specification, in addition achieving a high level of satisfaction from project participants concerning the outcome of the project (Ikechukwu *et al.* 2017). They explained further that the present state of the Nigeria construction industry falls short of meeting national and international quality standards and performance demands expected from the industry. The inability to complete project on the scheduled date, low quality of work and cost overruns are the critical problems encountered by the industry in Nigeria (Ikechukwu *et al.*, 2017). Alade *et al.*, (2016) observed that majority of the projects constructed in Nigeria experienced delays which in turn lead to

disputes, litigation, arbitration and at times total abandonment of the project.

Most of the projects constructed in Nigeria have had problems with time and cost overrun which has caused a lot of concern. Odeyinka and Yusuf (1987) surveyed construction projects in Nigeria and observed that seven out of ten projects experienced delays in their execution. A study conducted by Omoregie and Radford (2006) revealed that project had an average of 14% cost overrun and time overrun of 188%. Bajere *et al.* (2016) assessed the impact of delay factors on time for completion of public projects and discovered that 190 out of 196 projects surveyed had an average of 486.75% time overrun. A study conducted by Mamman *et al.* (2016) on predicting the final completion cost of construction projects, result revealed that 76.53% of the projects sampled had an average cost overrun of 43.26%. Saidu and Shakantu (2017) investigated cost overrun for ongoing building projects in Abuja they observed that projects with an average completion of 52.4% had an



average cost overrun of 44.46% and time overrun of 91.4%.

The problem of delays in the construction industry is a global phenomenon (Sambasivan & Soon, 2007; Owolabi *et al.*, 2014; Alade *et al.*, 2016). Several authors have highlighted the issue of poor performance in time and cost of construction projects globally. Assaf and Al-Hejji (2006) ascertain that 70% of projects constructed experienced time overrun and the average schedule overrun was between 10% and 30% of the original duration. The progress reports of 28 highway projects and 164 building projects constructed in Jordan was evaluated by Odeh and Battaineh (1999), results shows that the average ratio of actual completion time to the planned contract duration is 160.5% for highway projects and 120.3% for building projects. Frimpong, Oluwoye and Crawford (2003) conducted a survey on ground water drilling projects in Ghana and observed that out of 47 projects 33 making 70% experienced delay. Ali and Kamaruzzaman (2010) carried out a survey in Malaysia on delay practices, it was discovered that 87% of the respondent attested that they had encountered delays in their projects with time overrun of 10-40% of the contract duration. Abedi *et al* (2011) conducted a survey in the USA and observed that 845 of the kick starter top projects missed their targeted delivery dates. A survey conducted by Memon, Raham, Abdullah and Aziz (2011) in MARA large projects, result showed that an overrun with average of 23.74% of contract duration was encountered. According to Halloum and Bajracharya (2012) 90% of infrastructure projects had time overruns in Abu Dhabi.

A study by Chan and Kumaraswamy (1998) in Hong Kong on delays in projects, they observed that for projects to be considered as having been successfully delivered, they should be within budget, on time and having expected quality as specified by the client, in otherwise deficiency of any of these is regarded as a project delay. Performance demands expected from most projects executed in Nigeria industry have fallen short of meeting national and international standards due to the inability to complete project on the required date and budgeted cost. This occurrence has stimulated the authors to examine the significant delay factors affecting completion time of public sector construction projects in Niger state.

The following objectives were postulated for the study:

To identify the most significant delay factors affecting public sector construction projects and

To evaluate the impact of delays on time of completion of public sector construction projects.

2 DELAY IN CONSTRUCTION

Delay is a condition where the service provider and project client or his representative, mutually or severally, brings about to the non-completion of the undertaking within the initial or predetermined or approved contract

time (Aibinu & Jagboro, 2002). Assaf and Al-Hejji (2006) described delay in construction as the time overrun within specified finish date or time overrun within the delivery of the construction project on which every single party agreed upon. The consequences of delay are evident in the poor contractors performance, increase contract disputes, increase in cost of construction, low productivity and total project abandonment (Bajere *et al.*, 2016). When the project period is delayed, it means the project cannot be completed as originally scheduled. Aibuni and Jagboro (2002); Sambasivan and Soon (2007) and Mamman *et al.*,(2016) illustrated that time overrun; total abandonment and cost overrun are the most frequent impact regarding to delay in construction project. Delay will bring about negative effects such as interruption of work, increased time and non completion of project, cost overrun, loss of productivity, third party claim, and termination of contract or abandonment (Owolabi *et al.*, 2014; Mamman *et al.* 2016).

A contract delay has adverse effects on both the owner and the contractor either in the form of lost revenue or extra expenses and it often raises the contentious issues of delay responsibility, which may result in conflicts that frequently reach the courts (Bajere *et al.*, 2016). According to Bajere *et al.* 2016 delay means different things to people, for instance to the client, delay signifies loss of income through deficiency of manufacturing facilities in addition to rentable space or dependence on existing facilities. To the contractor, delays imply higher operating costs due to prolong work period, higher costs of materials as a result of inflation, and on account of increase in cost of labour. In contract administration time overrun is the contract period, measured by number of days, weeks, months or years (Bajere *et al.*, 2016).

3 DATA COLLECTION

Qualitative and quantitative data were utilised for the study as instruments for data collection. A self administered questionnaire was distributed to respondents that are construction practitioners (the client, contractors and consultants) from the selected agencies / ministries to obtain the qualitative (primary) data. The quantitative (secondary) data were obtained from the record of different projects executed by the selected government agencies and ministries in Niger state, which were completed within 10 (ten) years. In addition, a data collection format was designed which contained the following: type of project, initial contract sum, final completion cost, estimated duration of project, final completion duration.

The study's population was professionals from the construction industry which consist of architects, quantity surveyors, builders, structural engineers, mechanical engineers, electrical engineers and other members of the building team from governmental agencies and ministries. Research sample were randomly selected from the

registered contractors and consultants in the agencies and ministries.

A close ended type of questionnaire was adopted, to assess the perception of the knowledgeable construction practitioners on the factors causing delays in construction projects in Niger state. The questionnaire is made up of two sections. The first section requested information about the background of the respondents and the second section of the questionnaire focused on the 83 factors that contributed to delay. The respondents were asked to rank the delay factors based on a five-point Likert scale from 1 to 5, where 1= Not important, 2= slightly important, 3=moderately important, 4= Very Important, 5= Extremely important.

4 DATA PRESENTATION AND ANALYSIS

The Statistical Package for Social Science (SPSS) was used to analyse the qualitative and quantitative data. The qualitative data was analyzed using descriptive statistics which involved the use of frequencies and Relative Important Index (RII), data presentation was in form of tables. The Relative Important Index was used to obtain respondent view point and ranked from the positive ranking and the negative ranking. The ranking method is a form of statistical scale where subjects are rated in accordance to some precise measure or on operationally defined features (Morenikeji, 2006). The relative index ranges from 0 – 1. The item with the highest relative index is considered the first in the rank order.

The quantitative data was analysed using Pearson moment of correlation coefficient and linear regression analysis at 95% level of confidence. Pearson moment of correlation coefficient is a non-parametric test, which measures the strength and direction of the relationship among different variables, which can exhibit any of these relationships; +1 signifying a perfect positive correlation relationship, -1 signifying a perfect negative relationship or 0 indicating no relationship.

The simple linear regression analysis utilizes the "least squares" technique to fit a new line through observations. This study employed the following mathematical expression.

$$Y = a + b x$$

Where: Y = dependent variable, a = intercept, X = independent variable, b = coefficient of X

From the research works X is the mean of the number of projects executed by various organisation while Y is the number of recorded projects executed which were affected by delay.

5 DATA DISCUSSION

Table 1 illustrates the distribution of questionnaire. 240 questionnaires were distributed as follows: 50 to client, 70 to consultants and 120 to contractors. 174 questionnaires

were received (72.5%) as follows: 36 (20.69%) from clients, 52 (29.89%) from consultants and 86 (49.43%) from contractor's respondents.

TABLE 1: QUESTIONNAIRE DISTRIBUTION

Respondents	Number Distributed	Number Returned	Percentage Responds Rate
Client	50	36	20.69%
Consultants	70	52	29.88%
Contractors	120	86	49.43%
Total	240	174	100%

Table 2 illustrates respondent age. Result indicates that the highest number of respondents 74 (42.5%) were those within the age of 30yrs – 39yrs. About 68 (39.1%) respondents were 40yrs – 49yrs of age, while 20 (11.5%) respondents were above 50yrs of age and 12 (6.9%) number of respondents were between 20-29yrs of age.

TABLE 2: RESPONDENTS AGE

Respondents Age	Frequency	Percent
20-29	12	6.90%
30-39	74	42.5%
40-49	68	39.1%
Above 50	20	11.5%
Total	174	100

Table 3 illustrates the working experience of respondents. Result indicates that the highest number of respondents 64 (36.8%) were those with the working experience of 11yrs – 14yrs. About 46 (26.4%) respondents have 5yrs – 10yrs working experience, while 28 (16.1%) respondents have less than 5yrs working experience and 36 (20.7%) number of respondents having above 15yrs working experience.

TABLE 3: WORKING EXPERIENCE OF RESPONDENTS

Working experience	Frequency	Percent %
< 5years	28	16.10%
5-10years	46	26.40%
11-14years	64	36.80%
Above 15years	36	20.70%
Total	174	100.00%

Table 4 illustrates the top ten most important factors that contributed to delays in construction project from all

respondents view point. They include; delay in payment, first in the chart with RII of 0.89, lack of fund by client and change in government were second with RII of 0.87, poor site management and supervision, lack associated with high technological innovation mechanical tools and contractor difficulty in funding project were third with RII of 0.86, late in handling over site to contractor, shortage of equipment, government procedure were forth with RII of 0.84, client interference leading to award of contract to unqualified contractor, Not clear and insufficient sketches and Low level of equipment-operators skill were the least among the top ten most important factors that contributed to delay with RII of 0.83. Out of the ten top most important delays factors, client group had six factors (50%), equipment group had three factors (25%), contractors group had two factors (16.7%) and design group had one factor (8.3%). The result indicates that client group of delay occupied the highest degree of delay.

TABLE 4: TOP TEN MOST SIGNIFICANT DELAY FACTORS AFFECTING PROJECTS DELIVERY

Factors affecting delays	Delay group	Over all RII	Rank
Delay in progress payments	Client	0.89	1
Lack of fund by client/owner	Client	0.87	2
Change in government	Client	0.87	2
Poor management on site and supervision	Contractor	0.86	4
Lack associated with high technological innovation of mechanical tools	Equipment	0.86	4
Contractor difficulty in funding project	Contractor	0.86	4
Late in handling over site to contractor	Client	0.84	7
Equipment shortage	Equipment	0.84	7
Government procedure	Client	0.84	7
Client interference leading to award of contract to unqualified contractor	Client	0.83	10
Not clear and insufficient sketches	Design	0.83	10
Low level of equipment-operators skill	Equipment	0.83	10

Table 5: demonstrates the projects that are most frequently delayed in public sector construction projects. As revealed from the table, housing estate projects are the most frequently delayed with 47.7%. Followed by hospital projects, school, public facilities and others with 18.2%, 15.9%, 14.8%, 3.4% respectively.

TABLE 5: DATA ON PROJECTS MOST FREQUENTLY DELAYED

Most Frequently Delayed Projects	Frequency	Percent
School	28	15.9%
Public facilities	26	14.8%
Hospital	32	18.2%

Housing estate	84	47.7%
Others	4	3.4%
Total	174	100%

Table 6 illustrates Percentage Time Delay of projects. Result shows that the highest time delay of projects executed by respondent is 31.8% (54) which is 15-20% delay. 29.5 % (52) of respondent projects are delayed 21-30% delay and above 30% delay. 5.7 % (10) of respondent projects have 5-9% delay, 3.5 % (6) of respondent projects have 10-14% time delay.

TABLE 6: PERCENTAGE TIME DELAY OF PROJECTS EXECUTED BY RESPONDENTS

Percentage time delay	Frequency	Percent
5-9%	10	5.7
10-14%	6	3.5
15-20%	54	31.8
21-30%	52	29.5
Above 30%	52	29.5
Total	174	100

Table 7 illustrates the impact of delay factor on timely completion of projects. As revealed a total of 196 projects were sampled and analysed using Pearson rank correlation, projects were grouped into three categories; time under run, time completed at actual estimate (at time) and time overrun. One (1) project had time under run with -7.69% which constituted 0.51% of the sampled size. Five (5) projects were constructed at time with 0.00% which constituted 2.55 % of the sampled size. 190 projects had time overrun with 486.75% which constituted 96.94% of the sampled size.

TABLE 7: PROJECT CATEGORISATION OF PERCENTAGE DIFFERENCE BETWEEN COMPLETION TIME

Category	% time run/overrun	under	Projects in category		Total of all projects sampled
			Nr	% of sample	
Time under run	-7.69		1	0.51	196
At time	0		5	2.55	196
Time overrun	486.75		190	96.94	196

Table 8 illustrates the Pearson Moment Correlation analysis of initial estimated time and percentage time difference. As revealed, R value was negative with -0.225,

the R² value was positive 5.06% and very weak, and the P-values was lower than 0.05 (0.002 < 0.05). The deduction drawn from the result indicates that statistical significant relationship exists between the initial estimated time and percentage time difference, the null hypothesis (Ho1) was rejected.

TABLE 8: CORRELATION ANALYSIS OF INITIAL ESTIMATED TIME AND PERCENTAGE TIME DIFFERENCE

Variables		Pearson correlation (R)	R ² value (%)	P-value	Remark
X	Y				
Initial estimated time	Time difference %	-0.225	5.06%	0.002	SS

Key: SS = Statistically Significant, NS = Not Significant

Table 9: illustrates the regression analysis of initial estimated time and percentage time difference. As shown in the linear regression a positive correlation existed, with a very low R² Values of 0%. F_{cal} had a value lower than F_{tab} values (0.028 < 3.84). The P-value was 0.087 which is higher than 0.05. The deduction drawn from the result indicates that no significant relationship existed between the initial estimated time of construction and the percentage time difference, the null hypothesis (Ho2) was accepted. The R² was below 50% implying that the influence of initial estimated time of construction on the percentage time difference is real.

TABLE 9: REGRESSION ANALYSIS OF INITIAL ESTIMATED TIME AND PERCENTAGE TIME DIFFERENCE

Variables		Ty pe of Model	Observations	Inferences					
X	Y		Regression Equation	R ²	F _{cal}	F _{tab}	P _{value}	Strength of R/sh ip	Remark
Initial estimated time	Time difference %	Linear	Time diff=48.263+0.47 initial estimated time	0	0.028	3.84	0.087	very weak	NS

Key: SS = Statistically Significant, NS = Not Significant

6 CONCLUSION

The study examined the significant delay factors affecting completion time of public sector construction projects in Niger state. Findings from the result of the ten top significant factor contributing to delays in construction projects revealed that: delay in payment, lack of fund by client, change in government, poor site management and supervision, deficiency of high

technological innovation mechanical equipment, complication in funding project by contractor, late in handing over site to contractor, equipment shortage, government procedure, client interference leading to award of contract to unqualified contractor are the main causes of delays in public sector construction projects in Nigeria.

190 projects had time overrun with 486.75%. The result from Pearson Moment Correlation analysis was used to examine the initial estimated time and percentage time difference of public sector projects in Nigeria. The null hypothesis (Ho1) was rejected because the p-value was less than 0.05; significant relationship existed between initial estimated time and percentage time difference. The result from linear regression, the null hypothesis (Ho2) was accepted because the p-value was higher than 0.05, no significant relationship existed between initial estimated time and percentage time difference.

7 RECOMMENDATIONS

It was recommended that progress payment should be made on time to the contractor to strengthen the contractor's financial strength to aid in speeding the project. Before awarding any contract client should ensure that there is sufficient fund to complete the project. During the project planning period client should embark on projects that would be completed during their tenor. Before awarding contract, client should not only consider cost and time (lowest bidder) but also check for financial standing, experience and capabilities of contractors. Contractors are advised to employ qualified and experienced staff to oversee the activity on site a professional or site engineer of high experience and who is compete should be attached to the projects to help in the monitoring, managing and controlling of project activities to achieve high quality. It is anticipated that the findings from this study will awaken the consciousness of the extent to which delay can adversely affect project delivery. And also provide better ways and modalities of delivering construction projects by stakeholder by minimising the major causes of delay in project delivery.

REFERENCES

- Abedi, M., Fathi, M. S., & Mohammad, M. F. (2011). Effects of Construction Delays on Construction Project Objectives. The First Iranian Students Scientific Conference in Malaysia, 9th and 10th April 2011, UPM, Malaysia.
- Aibinu, A.A., & Jagboro, G.O. (2002). The Effects of Construction Delays on Projects Delivery in the Nigerian Construction Industry. *International Journal of Project Management*, 20, 593 – 599.



- Alade, K.T., Lawal, A.F., Omonori, A.A., & Olowokere, E.A. (2016). Causes and Effects of Delays in Construction Projects in Akure, Ondo State, Nigeria. *FUTA Journal of Management and Technology*, 29-38.
- Ali, A.S., & Kamaruzzama, S.N. (2010). Cost Performance for Building Construction Projects in Klang Valley. *Journal of Building Performance*, 1(1), 110 – 118.
- Assaf, S.A., & Al-Hejji, S. (2006). Causes of Delay in Large Construction Projects. *International Journal of Project Management*, 24(4), 349 – 357.
- Bajere, P.A., Mamman, J.E., Muazu, D.A., & Jimoh, R.A. (2016). Assessing The Impact of Delay Factors on Time For Completion of Public Projects in Niger State, Nigeria. *Journal of Environmental Technology and Science*, 7(1), 188-196.
- Chan, D.W.M., & Kumaraswamy, M.M. (1997). A Comparative Study of Causes of Time Overrun in Hong Kong Construction Projects. *International Journal of Project Management*, 15(1), 55 – 63.
- Frimpong, Y., Oluwoye, J., & Crawford, L. (2003). Causes of Delays and Cost Overruns in Construction of Ground water Projects in Developing Countries; Ghana as a case study. *International Journal of Project Management*, 21, 321 – 326.
- Halloum, M., & Bajracharya, A. (2012). Cost and Time Overrun Revisited: A Study on the Infrastructure Construction Projects in Abu Dhabi, UAE. In: Syed, (Ed.), *Third International Conference on Construction in Developing Countries*, Bangkok, Thailand, 4-6.
- Ikechukwu, A.C., Emoh, F. I., & Okorochoa, A. K. (2017). Causes and Effects of Cost Overruns in Public Building Construction Projects Delivery, In Imo State, Nigeria. *Journal of Business and Management*, 19(7), 13-20
- Mamman, E. J., Abdullahi, A.H., & Isah, L.M. (2016). A Predictive Cost Model for Building Construction Projects in Niger State. *Journal of Environmental Science and Policy Evaluation* 6 (1), 46-53.
- Memon, A.H., Abdul-Rahman, I., & Abdul-Aziz, A. (2011). Preliminary study on causative factors leading to construction cost overrun. *International Journal of Sustainable Construction Engineering and Technology*, 2(1), 57-71.
- Odeh, A., & Battaineh, H.T. (2002). Causes of Construction Delay: Traditional Contracts. *International Journal of Project Management*, 20(1), 67-73.
- Odeyinka, H.A., & Yusif, A. (1997). The Causes and Effects of Construction Delays on Completion Cost of Housing Projects in Nigeria. *Journal of Financial Management of Property and Construction*, 2(3), 31 – 44.
- Omoregie, A., & D. Radford, 2006. "Infrastructure Delays and Cost Escalation: causes and effects in Nigeria". *Proceeding of Sixth International Postgraduate Research Conference, Delft University of Technology and TNO, the Netherlands*. 3-7
- Owolabi, J. D., Amusan, L. M., Oloke, C. O., Olusanya, O., Tunji-Olayeni, P., Owolabi, D., Peter, J & Omuh, I. (2014). Causes and Effect of Delay on Project Construction Delivery Time. *International Journal of Education and Research*. 2(4) 197-208
- Pourrostan, T., & Ismail, A. (2012) Causes and Effects of Delay in Iranian Construction Projects. *IACSIT International Journal of Engineering and Technology*, 4(5) 598-601
- Sambasivan, M., & Yau, W.S. (2007). Causes and Effects of Delays in Malaysian Construction Industry. *International Journal of Project Management* 25(1), 517–526.
- Saidu, I., & Shakantu, W.M.W. 2016. A study of the Relationship between Material Waste and Cost Overrun in the Construction Industry. In: Windapo, A.O. (Ed.). *The 9th CIDB Postgraduate Conference: "Emerging Trends in Construction Organisational Practices and Project Management Knowledge Area"*, 2-4 February, Cape Town, South Africa, 124-134.



Communication Frequency and Effectiveness on Construction Sites in Abuja, Nigeria

Mamman, J.E¹, Abdullahi, A.H², Isah, M.L³ and Umesi, R.O⁴

^{1, 2, 3, 4}Quantity surveying Department Federal Polytechnic, Bida

Corresponding author email: ameenahabdullahi45@gmail.com +234-80-35975582

ABSTRACT

Communication impacts all elements of work to some extent, and is critical in the construction industry. Without effective communication among human beings, work progress might grow to be a difficult task in construction. As construction industry turns into extra multifarious, the industry organisation will become thinner, communication becomes a main difficulty and a leading component in defining actions within the industry. This study investigated the frequency of communication between parties on site at construction stage and also the effectiveness of the mode of communication between parties on site at construction stage through twenty nine (29) structured interviews conducted for 35 minutes each on construction sites in Abuja. Content analysis was then used to analyse the interviews. The interview was further analysed using the Social Network Analysis modelling software the Krackplot (KP4) to show the network of communication between parties on site. The study concluded that the Parties on site do communicate with one another on site but the frequency varies between them. During construction, the frequency changes between some parties and this is because at that stage those parties need to work hand in hand and this ensures effectiveness and reduces errors in construction since instructions are being emphasised at this stage. At the construction stage, some of the parties on site do not communicate at all because this is not necessary. The modes of communication used by these parties were also found to be effective. The study further recommended that communication during construction should be limited to parties involved in activities at a particular stage to ensure a problem free process.

Keywords: Communication, Effectiveness, Frequency, Mode

1 INTRODUCTION

In this present day, information and communication technology (ICT) is accountable for the complete construction system from information being generated, transmitted and interpreted to allowing the project to be built, maintained, reused and sooner or later recycled (Onyegiri *et al.*, 2011). Construction does, however, present a particularly complicated (and, for that matter interesting) atmosphere within which to discover communications phenomena. Due to the fact that it is project based, its groups and networks are temporary in nature and relationships and interactions usually trade to mirror the dynamic nature of the workplace (Dainty *et al.*, 2006). Wikfors and Löfgren (2007) asserted that construction tasks of today are depending on dependable and updated records through some of information communication technology (ICT) primarily based commercial business systems, communication tools and shared storage servers. To clear up issues which have arisen on-site and deal with vital construction troubles there is a need for speedy access to needed information. Jimoh (2012) set up that powerful site management calls for the balancing of formal strains of communication having to be absolutely installed from the start of a project and should be added to the attention of all the parties involved in the project. Communication impacts all

elements of work to some extent, and is critical in the construction industry. Without effective communication among human beings, work progress might grow to be an uphill task in construction (Emuze & James, 2013).

As construction industry turns into extra multifarious, the industry organisation will become thinner, communication becomes a main difficulty and a leading component in defining events within the industry. Consequently, the function of communication in the construction industry turns into a prime hassle for researchers to outline (Aiyewalehinmi, 2013). As teams develop in length, sub-teams often shape around individual elements within the system. While team members are regularly aware about with whom they have to immediately collaborate on shared works, the truth is that activities can rarely be taken into consideration in isolation (Emuze & James, 2013). As a result of this, parties on construction site tend to communicate more frequently with certain professionals and this may not be necessary at certain times. As against this backdrop, this study set out to investigate

1. The frequency of communication between parties on site at construction stage and also

2. The effectiveness of the mode of communication between parties on site at construction stage.

2 LITERATURE REVIEW

2.1 CONSTRUCTION

The construction process is carried out with labour, equipment, device, materials, machinery, methods and cash. Typically, the construction industry is fantastically fragmented as compared to other industries. The quantity of this fragmentation is unparalleled in any other sector with huge effect on productivity and performance (Akinsola *et al.*, 2000). Gaithet *et al.* (2012), affirmed that construction consists of the activities involved in the erection, installation or construction of a component or an entire project. These activities are certainly provided on the job site by the contractor, subcontractors, material providers and equipment providers.

2.2 CONSTRUCTION COMMUNICATION

According to Emmitt and Gorse (2003), communication is crucial to all creativity activities; it permits an organization, and is an essential part of the construction process. Past the argument, any improvement in communication can enhance an organization's operating effectiveness.

Construction communication, within an organizational context, is to transmit an order to steer the actions/behaviours of others, or may additionally involve an exchange of, or request for information all through a construction project. Communication inside project based environments presents unique challenges. That is particularly true in the construction industry, in which interaction tends to be characterised with the aid of unfamiliar assemblies of people coming jointly for short periods before scattering to work on other endeavours (Dainty *et al.*, 2006).

2.3 EFFECTIVE COMMUNICATION

A study by Thomas *et al.* (1998), revealed that if there is effective communication between project partakers, accurate information will be speedily transferred and consensus conclusions simply accomplished among the project team members. Consequently it will develop team work, reduce conflicts and rework and add to project success. Therefore handling project team communication and accomplishing communication effectiveness is essential for project fulfilment. It was emphasised that communication effectiveness depends no longer on the

communication among the contributors, but more importantly on the expertise among them.

2.4 TYPES OF COMMUNICATION IN THE CONSTRUCTION INDUSTRY

Various writers have written on the different types of communication. Some have labelled communication as internal and external, some as formal and informal and a few as verbal and non-verbal. Geren (2012) stated that there are two forms of communication: verbal and non-verbal. Verbal communication entails using phrases, both written and spoken, to convey a message. However, non-verbal conversation makes use of strategies that do not involve phrases, such as signals, drawings, and symbols. Contract documents make use of both techniques: specifications and notes (verbal) and drawings (nonverbal).

3 RESEARCH METHODOLOGY

The personal or face- to -face kind of interview was chosen for the purpose of this research. Face-to-face interview, in which the interviewer works directly with the respondent to ask questions and file their responses (Bhattacharjee, 2012). A total of twenty-nine structured interviews were conducted each for a minimum of 35 minutes each. Site workers (Architects, builders, quantity surveyors, artisans and engineers) working actively on construction sites were interviewed in English Language and responses were recorded in writing verbatim towards each question requested. The interview questions were then categorized and developed into common themes for content analysis. Content analysis is a systematic way of identifying all the main concepts, which arise, and then trying to categorise and develop these into common themes (Mathers *et al.*, 2002). The interview was further analysed using the Social Network Analysis modelling software the Krackplot (KP4) to show the network of communication between parties on site.

4 RESULTS AND DISCUSSION

The interviewees were asked how frequently they communicated with other parties on site during construction and the following responses were recorded.

Table 4.1 is a summary of the responses obtained from the respondents about how frequently they communicate with one another on site during construction. It can be seen that each respondent's interaction differs from project to project; it also differs, depending on the stage of construction. Some parties do not need to interact at all at some stage, and at other stages need to interact more frequently

Table 4.1 Frequency of communication between parties on site

	Client	Architects	Builders	Quantity surveyors	Contractors	Sub-contractors	Site operatives	Civil engineer	Mechanical Engineer	Electrical engineer	Total
Architects 1,2,3,4	3,5,1,3	2,0,5,4	3,5,3,5	1,1,2,4	0,2,3,4	3,3,1,3	5,5,1,3	2,5,1,2	2,4,1,2	2,2,1,2	23,32,19,32
Builders 1,2,3,4,5	5,2,4,4,5	1,1,3,5,1	0,0,3,5,0	1,2,2,4,1	5,2,2,3,5	5,4,3,3,5	5,5,3,3,5	2,5,3,5,5	2,0,4,5,1	5,0,4,5,5	31,21,31,42,33
Quantity surveyors 1,2,3,4	0,1,3,1	5,2,5,2	5,3,5,3	5,2,0,3	0,4,2,3	2,3,1,2	3,3,5,3	1,2,1,2	1,2,2,2	1,2,2,2	23,24,26,23
Iron benders 1,2	5,4	5,2	5,5	4,0	3,5	3,0	2,5	5,5	5,5	5,5	42,36
Bricklayer	0	5	5	0	3	3	0	5	5	5	31
Welder/fabricator	2	2	0	0	2	0	5	2	2	0	15
Carpenter	0	5	5	2	2	2	0	4	5	5	30
Plumber	2	1	5	1	0	5	5	5	5	5	34
Mech. engineer 1,2,3,4	0,3,3,4	5,5,3,5	1,5,3,5	1,4,3,4	4,3,4,3	5,3,4,5	1,4,3,2	1,5,3,0	5,3,2,5	5,3,2,5	28,38,30,38
Civil engineer 1,2,3,4	5,3,1,2	3,5,0,5	5,5,0,5	0,3,0,0	5,2,2,0	2,3,1,0	5,3,5,5	0,3,5,5	1,4,2,5	1,3,2,5	27,34,18,32
Electrical engineer 1,2,3	1,2,3	3,0,5	1,2,5	2,0,3	4,0,3	4,5,3	4,5,3	1,2,3	5,2,2	5,0,2	30,18,32

Key: 5 several times a day, 4 once a day, 3 several times each week, 2 once a week and 1 once in two weeks



**3rd International Engineering Conference (IEC 2019)
Federal University of Technology, Minna, Nigeria**



All parties on site do communicate with one another during construction but the frequency of communication depends on the stage of construction. This is evident from figure 5.1 (sociogram) where the interaction of the respondents were sort with other parties on site. All parties do interact but the thicker the links/lines the more frequent the communication was that is several times a day. Architect 1 communicated with all parties on site except the contractor but communication was most frequent with the artisans.

Builder 1 also communicated with all parties on site; but most frequently with the client, contractor, subcontractor, artisan and the Electrical Engineer.

Quantity surveyor 1 communicated with the parties on site but did not communicate with the client and contractor but communicated most frequently with the Architect, builder and fellow QS.

Iron Bender 1 communicated with all parties but most frequently with the client, Architect, Builder, civil Engineer, Mechanical Engineer and the Electrical Engineer.

The Bricklayer did not communicate at all with the client, the QS and other artisans but communicated most frequently with the Architect, the builder, civil engineer, mechanical engineer and the electrical engineer and less frequently with the contractor and subcontractor. This was so because the stage of work only needed the attentions of the Architect, the builder, civil Engineer, mechanical Engineer and the Electrical engineer since the work to be done was going to temper with works of other professionals.

The welder/fabricator did not communicate at all with the builder, QS, subcontractor and the Electrical Engineer, most frequently with the Artisans and less frequently with client, Architect, contractor, civil Engineer and Mechanical engineer.

The Carpenter Communicated most frequently with the Architect, the builder, the mechanical engineer, the civil engineer and the Electrical Engineer. Not at all with the client and other Artisans and less frequently with the QS, Contractor and the Subcontractor. This was so because the works to be carried out was going to temper with other professionals works so the need for communication was increased.

The plumber communicated with all the parties on site except the contractor but most frequently with the builder, subcontractor, Artisans, civil engineer, mechanical engineer and electrical engineer. This was so because the works of the plumber was going to interfere with the works of other parties so their attentions were required often.

The mechanical engineer communicated with all parties except the client, most frequently with the Architect, subcontractor, fellow mechanical engineer and Electrical engineer.

The civil engineer communicated most frequently with the client, the builder, the contractor and the artisans but not at all with the QS and less frequently with others.

The electrical engineer communicated with all parties on site; but most frequently with the mechanical and electrical engineer

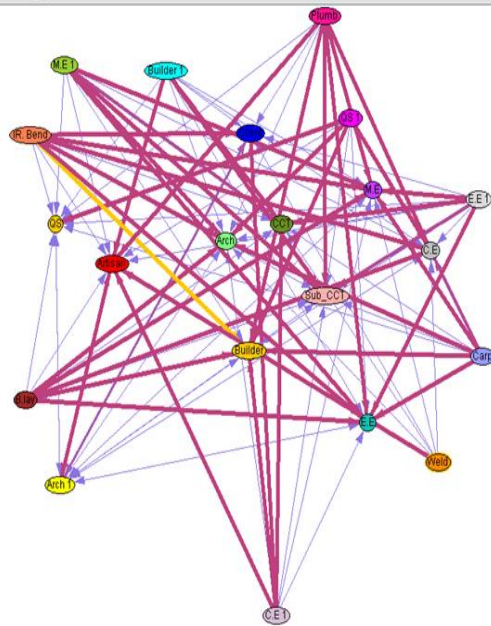


Figure 5.1 Communications Network Sociogram among parties on site during construction

Figure 5.2 shows the frequency of communication between professionals; it can be seen that all professionals on site communicate with one another. All parties on site communicate with the Architect but the frequency of communication varies at different times. It can be said that the mechanical

engineer (ME 1), QS and civil engineer communicate most frequently with the Architect.

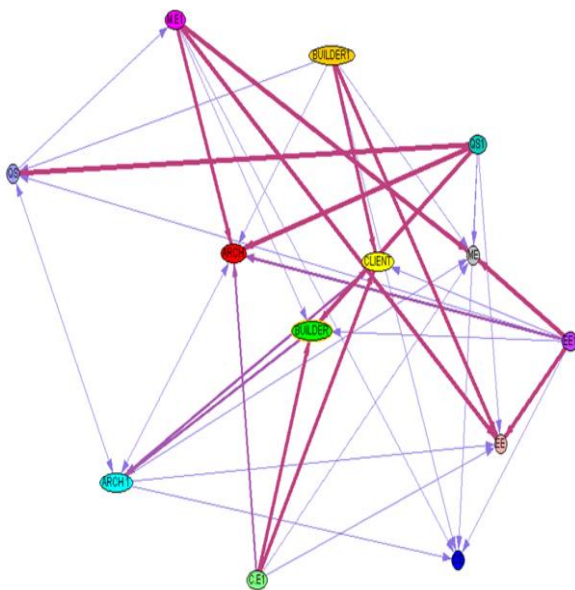


Figure 5.2 Communications between Professionals during construction



Communication effectiveness

When the question of effectiveness of mode of communication was asked the responses obtained are recorded on Table 5.2, it was established that communication modes used were very effective since both verbal and non-verbal modes of communication were employed. Even where drawings were used, they had to be interpreted with the word of

mouth (verbally). Never has effective communication been more important than it is in the modern world. Eyre and Med (in Abdullahi, 2016) argued that effective communication is essential and communication is not just the giving of information; it is the giving of understandable information and receiving and understanding the message.

Table 5.2 Communication effectiveness

Respondents	Mode	Reason
Architects	Architect's instruction	Because it keeps evidence of authority for action taken or not taken.
	Drawings	It is very easy to understand because they are detailed.
	Verbal backed up by writing	So that they can be documented.
Builders	Drawings	They are more detailed.
	Verbal	Because sometimes some people do not understand drawings so interpreting verbally helps out.
	Site meetings	Because issues are raised and thrashed immediately.
	Verbal	Because it can be understood easily.
	Verbal	Because it is the easiest.



3rd International Engineering Conference (IEC 2019)
Federal University of Technology, Minna, Nigeria



	Motivation	Because this works faster and improves output.
Quantity surveyors	Phone	It is direct and saves time.
	Drawings	because an average person can interpret it
	Written instructions	It can be documented and is formal.
	Letter	For record keeping.
Iron Bender	Verbal	For instruction purpose.
	Drawings	If drawings cannot be read, a good structure cannot be achieved.
Bricklayer	Drawings	You will see what is expected.
Welder/Fabricator	Drawings	They are more detailed.
Carpenter	Oral	You can always take your time to understand.
Plumber	Verbal	Because not all of us can interpret drawings.
Mechanical Engineers	Meetings	Since meetings are written they are more secured and are available anytime.
	Verbal	



3rd International Engineering Conference (IEC 2019)
Federal University of Technology, Minna, Nigeria



		Because it gives direct and first- hand information.
	Verbal	It leaves one with no option than to comply and comprehend.
	Phone and text messages	It is simple.
Civil Engineers	Drawings	Because the message is easily gotten.
	Verbal;	Because they can understand easily and execute work.
	Verbal	For instruction purpose.
Electrical Engineer	Drawings	They show what is expected on site and even in one's absence, they refer to it.
	Drawings	They are more understood since they can be seen
	Verbal	It provides first- hand information.



CONCLUSION

This study examined the frequency of communication between parties on site at construction stage and also established the effectiveness of communication mode used between parties on site at construction stage. The Parties on site do communicate with one another on site but the frequency varies between them. During construction, the frequency changes between some parties and this is because at that stage those parties need to work hand in hand and this ensures effectiveness and reduces errors in construction since instructions are being emphasised at this stage. At the construction stage, some of the parties on site do not communicate at all because this is not warranted. The modes of communication used by these parties was also found to be effective. For a hitch free construction, effective communication should be ensured and communication should only be down between the parties that are involved at that stage.

REFERENCES

- Abdullahi, A. H. (2016). Communication Practices on Construction Sites in Abuja, Nigeria. An unpublished MTECH thesis submitted to the postgraduate school, federal university of technology, Minna, Nigeria.
- Aiyewalehinmi, E.O. (2013). Factor Analysis of Communication in the Construction Industry. *The International Journal of Engineering and Science (IJES)*, 2(10), 49-57.
- Akinsola, A., Dawood, N. and Hobbs B (2000). Construction planning process improvement using information technology tools. Obtainable at www.academia.edu/.../construction Retrieved on 28th June, 2019.
- Bhattacharjee, A. (2012). *Social Science Research: Principles, Methods, and Practices* 2nd Edition. Tampa, Florida, USA: Published under the Creative Commons Attribution-Non-commercial-Share Alike 3.0 Unported License.
- Dainty, A., Moore, D. and Murray, M. (2006). *Communication in construction; Theory and Practice*. Oxon, United Kingdom: Taylor and Francis.
- Emmitt, S. and Gorse, C. (2003). *Construction Communication*. United Kingdom: Blackwell publisher.
- Emuze, F. and James, M. (2013). Exploring communication challenges due to Language and cultural diversity on South African Construction sites. *Acta Structilia*, 20(1), 44-65.
- Gaith, F.H., Khalim, A. R. and Amiruddin, I. (2012). Application and efficacy of information technology in construction industry. *Scientific Research and Essays*, 7(38), 3223-3242.
- Geren, R. L. (2012). Communication during Construction. Keynotes Information for the Improvement of Construction Documents No. 10. RLGA Technical services. www.specsandcodes.com Retrieved on 18th June, 2019
- Jimoh, R.A (2012). Improving site management practices in the Nigerian construction industry: the builders' perspective. *Ethiopian Journal of Environmental Studies and Management*, 5(4), 366-372.
- Mathers, N., Fox, N. and Hunn, A. (2002). Using Interviews in a Research Project. Produced by the Trent focus Group, 1998. Obtainable at www.researchgate.net/interviews/. Retrieved on 23rd June, 2018.
- Onyegiri, I., Nwachukwu, C. C. and Jamike, O. (2011). Information and communication technology in the construction industry. *American journal of scientific and industrial research*, 2(3), 461-468.
- Thomas, S.R, Tucker, R.L. and Kelly, W.R. (1998). Critical communications variables. *Journal of construction Engineering and Management*, 124(1), 58-66.
- Wikforss, Ö. and Löfgren, A. (2007) Rethinking communication in construction. *ITco*. 12, 337-345



Contribution of Quality Management Practices towards Building Collapse in Nigeria

*Yunusa, H¹, Makinde, J. K², & Oke, A. A³

¹ Project Management Department, Federal University of Technology, PMB 65 Minna Niger State, Nigeria

² Project Management Department, Federal University of Technology, PMB 65 Minna Niger State, Nigeria

³ Quantity Surveying Department, Federal University of Technology, PMB 65 Minna Niger State, Nigeria

*Corresponding author email: habibyunusa12@gmail.com, +2348060724270

ABSTRACT

Nigeria like many other countries is experiencing collapse of buildings at an alarming rate; this has become of great concern to all stakeholders in the Construction Industry. This situation is linked to the finding that the prevalent quality system on sites is the supervision of workers and work processes. Achieved levels of quality are thus totally dependent on the supervisor's expertise; this can be counterproductive where supervisors lack requisite knowledge and experience. This paper examined the quality management practices on construction sites as it affects the menace of building collapse in Nigeria. The study is exploratory in nature, and employs the use of secondary data in conjunction with primary data obtained through a questionnaire survey. Findings suggested that a cyclical trend might exist in the incidence of building collapses which may be represented by a 2-period moving average trend-line. Collapses were more prevalent in buildings employed for residential and commercial uses (a total of 72% of the entire sample). The dominant cause of building failures in the study area was structural failure (46%) and use of substandard materials (21%). Design and Material issues (Mean score = 4.62 and 3.56) had the highest influence on the quality of the construction product. Three main recommendations were offered, including the need to design and implement proactive measures such as routine testing of building integrity which could be built into an 'annual renewal of building approval' process.

Keywords: *building; collapse; ethics; integrity; quality.*

1 INTRODUCTION

Quality assurance is a planned process aimed at ensuring that products and services conform to established requirements (Leong, Zakuan and Saman, 2014; Okereke, 2003). The construction industry delivers the bulk of the fixed capital formation of any country especially in the areas of buildings and infrastructure. Quality assurance, in the building construction sector of the industry, is necessary to ensure that such huge national capital is kept durable, safe and serviceable all through their estimated life cycles. Assessments of the building construction sector in Nigeria indicate that the adoption of quality management strategies is still rudimentary. Oludare and Oluseye (2016) in their study of construction firms in Lagos, Nigeria, found that the most prevalent system in place, for construction quality, was the supervision of workers and work processes. Hence, the level of quality achieved is totally dependent on the expertise of the supervisor, a development that is usually counterproductive especially when the supervisor lacks requisite knowledge and experience. The major weaknesses of construction firms in Nigeria, according to Kado (2010) are in the areas of staff training, education and skills, objective measurement, feedback and use of total quality tools and techniques. Concerns involving quality in the Nigerian Construction Industry (NCI) are

typified by the increasing cases of collapse of buildings (Abdulkareem and Adeoti, 2010). To mitigate this, Ashokkumar (2014) opined that the management of building quality encompasses material variability, testing variability, judgment factor, contractors' variability, poorly skilled workmen and unprofessional conduct.

Similarly, Opoko, Ezema and Ediae (2014) opined that the utilisation of substandard building materials in the Nigerian context could be traced to non-existent quality management production processes. Nigeria, like many other countries (Paul and Otieno, 2018) is experiencing collapse of buildings at an alarming rate; this has become of great concern to all stakeholders in the building sector (professionals, government, private developers, clients and users). Growing concern about the increasing incidents of building failure formed the basis for this paper on the collapse of buildings in Nigeria. This paper examined the quality management practices on construction sites as it affects the menace of building collapse in Nigeria. This would be achieved by collating recent, documented incidences of building collapses, determining the quality management practices involved in building construction and relating frequency of building collapse to the level of quality management practiced on sites.

Construction projects are capital intensive, and defects / failures in constructed facilities can result in delays and

costs increases or cause personal injuries or fatalities (Sanni and Windapo, 2008). In the NCI any extra cost means huge losses to contractors and increased cost to clients (Aibinu and Odeyinka, 2006). The benefits of strict adherence by professionals like Architects, Engineers, Builders and contractors to the need for quality management has not been given the required attention in spite of a major developmental projects (Jimoh, 2012). It is significant to carry out this research in order to suggest best practices that improve quality management in building construction, which will in turn result to improved project delivery and reduced occurrence of collapsed buildings. This study focussed on the contribution of quality management practices to building collapses in Lagos state, Nigeria. The data for the study will be collected from consultants, contractors and artisans in the construction industry in Lagos State

Nigeria's striving to develop her built environment is being held back by exponential population growth. As a result, people have had to explore different approaches to housing and infrastructural development. The quality of some of these structures falls below acceptable standards; this inevitably leads to structural failures (Ede, 2010). In Nigeria the most frequent causes of building collapse are abnormal, and of a criminal shade. The cost of building failures in terms of human lives and loss of productive assets, returns on investments and livelihoods has mounted to what can only be described as significant. Also important is the dent such failures make in the reputation of construction professionals and the entire Nigerian construction industry.

Prevalence of Building Collapse

Research in Nigeria has established that collapse usually occurs in buildings having between two and five floors. A total of 33 and 22 incidents of building collapse were recorded in 2012 in Lagos and Abuja respectively. The problem of building collapse is not limited to Nigeria alone; Paul and Otieno (2018) found that in Kenya, between 2006 and 2014, an estimated 17 buildings collapsed spontaneously, causing 84 deaths and more than 290 injuries. The main immediate causes of such collapse included use of substandard building materials, poor workmanship and noncompliance to housing policy.

Oloyede, Omoogun and Akinjare (2010) found that wide variations exist in individual opinions on which of the construction professionals is most responsible for the collapse of buildings. Rising incidence of building collapse in major Nigerian cities have forced the government to enact specific rules and regulations related to safety of buildings. The problem is however in the application of such rules. Those administering Town Planning rules and regulations must be held accountable when buildings approved by them suffer collapse. However, accountability in Nigeria is generally weak (Dare, 2009)

Identified Causes of Building Collapse

Oyedele (2018) identified the causes of building collapse incidents as due to poor workmanship, substandard building materials, unsuitable sites and poor building design. Based on a case study of six collapsed buildings across Nigeria, the study traced the rampant nature of building collapse to corruption and greed of developers who reduce the quantity of cement and steel reinforcement used in concrete and refuse to employ qualified professionals. Oyedele (2018) opined that the National Building Code of 2006 is not effective due to lack of enforcement and because owners of collapsed buildings are not taken to task even where lives have been lost.

Some studies have examined the causes of building collapse from the angle of adequacy and quality of materials employed in the building process. Joshua, Olusola, Ogunde, Amusan, Ede and Tunji-olayeni (2017) investigated building collapse due to failure in reinforced concrete. Their study was limited to the production of low standard concrete, based on the premise that failure in substandard reinforced concrete is broadly based on the use of substandard materials or poor production process. The results of the study revealed that not all the test samples met the strength standards. The researchers believed that other factors as haulage, poor storage and use of expired cements might have compromised the test samples; they thus recommended that cements sold commercially should bear expiry dates. Another finding of the study was that the strength of samples of class 32.5 cement taken from sites failed to reach a marginal value of 20MPa. This led to recommendation that class 42.5 cements be used in storey structures where design concrete values greater than 20MPa are specified. A third finding of the research was that only eleven of the eighty professionals that were sampled possessed greater-than-average knowledge of cement utilization.

A study conducted by Omran, Bamidele and Baharuddin (2016) determine the remote causes of incessant building collapse in Nigeria to be mainly due to use of quacks, substandard/inadequate material, poor workmanship, non-adherence to design specifications, improper supervision, professional negligence /compromise, and corruption in governance.

Remedies to the Problem of Building Collapse

Quite a number of studies have made recommendations on how the malady of building collapse can be ameliorated, if not totally eradicated. Oloke, Oni, Ogunde, Joshua and Babalola (2017) noted that more buildings suffer collapse while in use than during construction or immediately after construction. Only 4% of a sample of 56 collapsed buildings was under construction, according to Ayedun, Durodola and Akinjare (2012). In the case of Chendo and Obi (2015), 60% of a sample of ten building collapse cases represented buildings that were already in use. In view of the high proportion of occupied buildings that suffer

collapse, Ede (2010) and Olagunju (2011) stressed the importance of carrying out periodic post-construction maintenance of buildings.

The foregoing provides a strong case for structural integrity tests during the use of any property. Oloke *et al.*, (2017) therefore investigated how post-completion management of properties could be employed to arrest the collapse of buildings in Nigeria. Their investigation was based on data from a survey of one hundred and fifty residential and seventy-five commercial properties across Lagos State, Nigeria. The findings of the research revealed that integrity assessment is rarely carried out on the properties. Ezema and Olatunji (2018) observed that building laws and regulations exist in all the 36 States of Nigeria as well as the Federal Capital Territory which can be employed to achieve effective development control. However, the inadequate government oversight of building construction activities have been attributed to unethical contract practices coupled with weak regulatory framework (Longtau, Justina, Majidadi and Makwin, 2016; Fernandez, 2014). This situation has allowed breaches of quality in the building construction industry to multiply and fester, in several cases leading ultimately to building collapse.

Quality Management in Construction

Research has revealed that poor quality performance results in increased rework, which generally has adverse effects on construction cost and schedule. Traditional methods of assuring of quality which the industry is still using depend on the inspection of work in progress. Total Quality Management (TQM) assures quality by re-engineering the entire construction process to achieve quality. In the long run this is a cheaper approach; the cost of correcting defects is around 12 percent of project cost, whereas the cost of providing TQM is between 1 to 5 percent (Xiao and Proverbs, 2002).

The problem of quality management in construction is epitomized by the case of sandcrete blocks in Nigeria. Sandcrete blocks are a very important material in building construction, which is widely used in Nigeria, Ghana, and other African countries as load bearing and non-load bearing walling units. Nine out of ten physical infrastructures in Nigeria are constructed using sandcrete blocks (Baiden and Tuuli, 2004). The Standard Organization of Nigeria (SON) prescribed the minimum requirements and uses of different kinds of sandcrete blocks in a reference document coded as NIS 87:2000 series. Anosike and Oyebade (2012) investigated whether block manufacturers meet the minimum specified standard in NIS 87:2000, which ranges between 2.5N/mm² to 3.45N/mm². Their results revealed that there was very low compliance with NIS 87:2000; compressive strength of blocks as low as 0.66N/mm² was recorded. The researchers opined that poor quality control, poor selection of constituent materials and inadequate curing period contributed to the negative results obtained.

The current situation is that the industry uses traditional methods to achieve quality, thus impeding the use of advanced quality techniques. This results in increased rework, with attendant cost and schedule implications. It has been estimated that correction of defects costs about 12% of project cost, whereas providing TQM throughout the project cycle will cost less than 6% of project cost (Xiao and Proverbs, 2002). Leonard (2010) noted that although quality management is expanding in other industries globally, the construction industry's focus is still fixated exclusively on inspection processes.

Gap Identified in Literature

This study has been able to show through a review of literature that there are quality management issues that are associated with structural failure of buildings. Some studies have documented appreciable number of cases of structural building failures. However, there is a need to begin to explore the association between how quality is managed on construction sites, and how frequently building failures occur. This represents a gap in knowledge which this study aspires to fill.

2 METHODOLOGY

This study is exploratory in nature, and employs the use of secondary data in conjunction with primary data obtained through a questionnaire survey; this is a single method quantitative research approach. Kothari (2004) defined research design as the arrangement of conditions for collection and analysis of data in a manner that serves as the blue print for the collection, measurement and analysis of data. Questionnaires were used to collect data on quality management as practiced on construction sites, while historical data provided some limited details of the various buildings that have collapsed in the study area.

The population for this study comprises consultants, contractors and artisans in the construction industry in Lagos. The artisans that were sampled were limited to Masons/Blocklayers, Iron-benders/Steel-fixers and Carpenters, because these artisans are those that actually construct the structural carcass of buildings. The professions that were sampled were limited to Architecture, Building, Civil Engineering and Quantity Surveying. These professionals are responsible for the design of buildings, and their work can influence the quality of the building structural carcass as well.

The exploratory nature of the study provided justification for the use of a sample of respondents that was not based on probability sampling. This study intends to sample at least fifteen (15) respondents from each of the 11 categories identified in Section 3.3.2. This translated to a total sample of 165 respondents, who were selected through using the snowballing technique where a sample is built up from recommendations of people who have been sampled already (Trochim, 2006).

The historical data employed in the study was derived from a variety of sources including published academic works and records maintained by the statutory agency for the control of building collapse in the study area, the Lagos State Physical Planning and Development Authority (LASPPDA). The data gathered from the respondents via the structured questionnaire was coded into Microsoft Excel as numbers representing the options selected by the respondents. Next, careful analysis of the data in relation to the stated objectives of the study was carried out. Descriptive statistical methods were employed for Objective 1 (Frequency, Percentile and cross-tabulation) and Objective 2 (Mean score and Relative Importance Index). Objective 3 employed deductive method (Simple Correlation). The analyzed data was presented using tables and charts.

3 RESULTS AND DISCUSSION

Respondents' Demographics

Quantity surveyors and Architects were most numerous in the sample followed by civil engineers and builders. The number of artisans (mason, iron-benders and carpenter) ranged between 11 and 14 per trade. Only 16% of the sample was female; this reflected a realistic picture of the NCI, where male dominance of trades and professions is highly pronounced and visible (Okoyeuzu et al., 2008). The sample was split equally between clients and contractors as employers of the sample professionals and artisans.

TABLE 1: DEMOGRAPHICS OF THE RESPONDENTS

Demographic aspect	Subcategories	Frequency	%
Type of professional	Architect	24	28.92
	Builder	16	19.28
	Civil engineer	18	21.69
	Quant. surveyor	25	30.12
Type of artisan	Mason	11	28.95
	Iron bender	13	34.21
	Carpenter	14	36.84
Gender	Female	19	16.38
	Male	97	83.62
Employer	Contractor	60	50.00
	Consultant	60	50.00

Trend Analysis of Documented Incidences of Building Collapse

The numbers of building collapses dropped between 1999 and 2000; a gradual increase however commenced in 2002, continuing up to 2007. It appeared that the trend was cyclical, spanning a number of years; a 2-period moving average trend-line was found to best fit the data, as shown in Fig. 1. This might be due to the reactive

measures usually rushed into on the heels of a series of collapse incidences. Such measures (which include testing, identification and demolition of unsafe structures) might depress the number of fresh incidents for a period of time, but owing non-sustenance of such reactive measures, the numbers of collapse incidents soon begins to increase after a few years of apparent decrease.

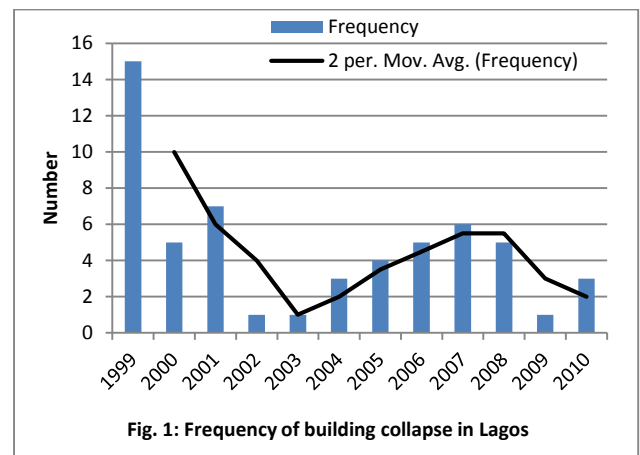


Fig. 1: Frequency of building collapse in Lagos

An instructive finding was the fact that over half of the sample of collapsed buildings consisted of buildings having not more than 3 floors as shown in Fig. 2. This finding agreed with that of Folagbade (2001), who had calculated that 76% of reported building collapses in Lagos state from 1980 to 1999 were buildings that more often than not, are constructed entirely by the informal subsector of the construction industry. Buildings having more than 3 floors are more likely to have properly drawn up plans for which statutory approval has been obtained.

The data presented in Fig. 3 revealed that collapses were more prevalent in buildings employed for residential and commercial uses (a total of 72% of the entire sample).

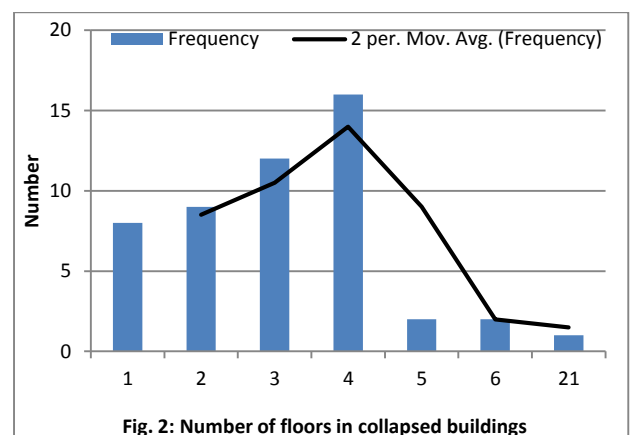


Fig. 2: Number of floors in collapsed buildings

This finding also agreed with Fagbenle and Oluwunmi (2010) who investigated the contributory role of the informal sector to building collapse incidents. They found that 70.0%, 23.3% and 6.7% of reported building collapse

cases occurred in private, public and corporate organizations respectively. It must be pointed out that commercial enterprises are usually located in privately owned buildings; in some cases such buildings have been approved for residential use only.

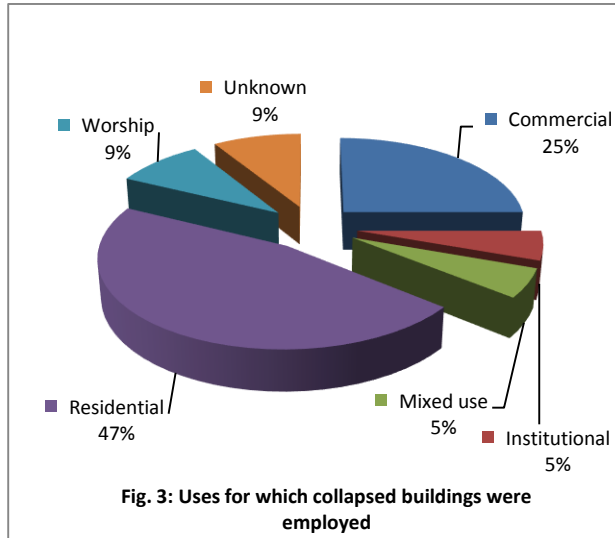


Fig. 3: Uses for which collapsed buildings were employed

Two thirds of all building failures in the study area were attributable to structural failure (46%) and substandard materials (21%). Fagbenle and Oluwunmi (2010) in their investigation of the contributory role of the informal sector to building collapse incidents had unearthed hasty construction, incompetent workmen, poor supervision and non-compliance with building regulations as causes of building collapse. It needs to be understood also that 'structural failure' is a blanket term that could cover all of the causes reported by Fagbenle and Oluwunmi (2010).

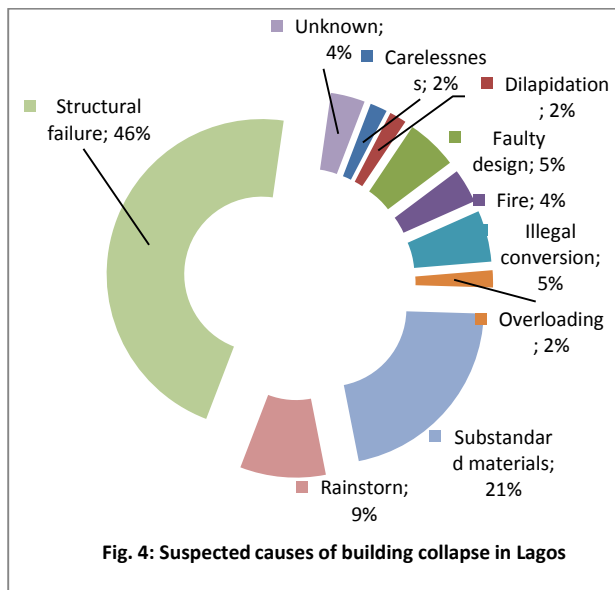


Fig. 4: Suspected causes of building collapse in Lagos

Buildings devoted to residential, commercial and worship uses had the highest casualty figures when collapse occurred in such buildings. This finding agreed with the work of Ede (2010) which used probabilistic linear regression model to establish the relationship between characteristics of collapsed buildings and number of casualties recorded. One of the findings of the research was that casualty rates in collapsed buildings were high and dynamic, dependent on building use, type and climatic season.

This paper goes further to reveal that structural failure and substandard materials are related to the highest casualty rates in collapsed buildings. Collectively, these two causes account for 64% of all casualties recorded. Therefore, focusing efforts on the mitigation of collapses due to structural failure of building frames and use of substandard materials would have a significant effect on reducing overall casualty figures.

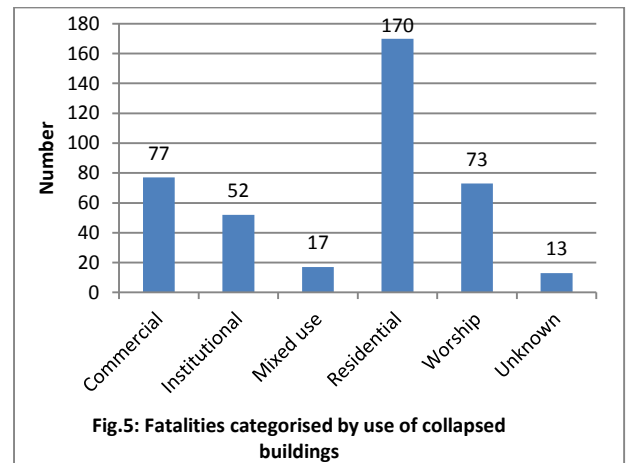


Fig. 5: Fatalities categorised by use of collapsed buildings

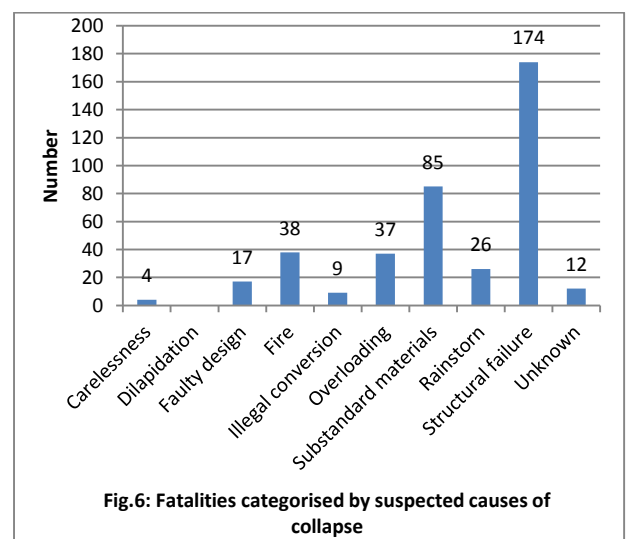


Fig. 6: Fatalities categorised by suspected causes of collapse

Quality Management Practices on Construction Sites

Design related issues were found to be most influential with respect to the quality of the final product of the

construction process. This was borne out of the fact that the derived Mean Score value of 4.62 fell within the response range (4.50 – 5.00) that was associated with the ‘Very large extent’ option in the research questionnaire. Material issues influenced construction quality ‘to a large extent’, since the Mean Score value was 3.56 which fell within the response range of 3.50 – 4.49. All other groups of issues related to construction quality (process, compliance and labour) exerted influence ‘to a moderate extent’. These findings are presented in Table 2.

TABLE 2: OVERALL PRACTICE OF SITE QUALITY MANAGEMENT

Categories of quality management practices	Mean Score	RII	Rank
Design issues	4.62	0.92	1
Material issues	3.56	0.70	2
Process issues	3.44	0.69	3
Compliance issues	3.16	0.63	4
Labour issues	3.05	0.61	5

The sole design issue explored in this paper was lack of detailed structural drawings; this was found to be the most influential issue (Mean score (MS) = 4.62) with respect to construction quality. The next three issues in descending order of influence on construction quality were ‘carry out concrete trial mixes’, ‘lack of proper supervision by professionals’, and ‘unreliable measurements’ (MS = 4.35, 4.22 and 4.01 respectively). These findings corroborate those of Ezema and Olatunji (2018) with reference to the use of concrete in construction.

TABLE 3: EXTENT OF QUALITY MANAGEMENT PRACTICES

ID	Quality management practices	Mean Score	Rank
	Design issues		
QMP01	Lack of detailed structural drawings	4.62	
	Process issues		
QMP02	Carry out concrete trial mixes	4.35	1
QMP03	Lack of Proper Supervision by Professionals	4.22	2
QMP06	Unreliable measurements - head pan is dented	4.01	3
QMP07	Use more sand than necessary	3.76	4
QMP08	Use of unqualified supervisors - Quacks	3.43	5
QMP04	Remove defective work	3.26	6
QMP05	Testing of fine aggregate for salt	2.96	7
QMP09	Vibrate wet concrete after placement	2.94	8
QMP10	Vibrator applied intermittently not uniformly	2.87	9
QMP11	Visual quality assessment instead of measurements	2.61	10
	Compliance issues		
QMP14	Non-compliance with approved drawings.	3.86	1
QMP15	Non-possession of approved drawings.	3.73	2

ID	Quality management practices	Mean Score	Rank
QMP16	Observe statutory break periods	3.73	3
QMP13	Lack of Adherence to Design Specifications	3.28	4
QMP12	Disobeying Town Planning Laws	2.82	5
QMP18	Professional present on site during concrete works	2.57	6
QMP17	Professional Negligence/Compromise	2.11	7
	Material issues		
QMP20	Outsourcing of concrete batching	3.75	1
QMP21	Use of poor quality building materials	3.68	2
QMP19	Batching locally on site	3.24	3
	Labour issues		
QMP22	All required tools provided	3.95	1
QMP24	Insist on testing new workers	3.63	2
QMP25	Poor workmanship	2.55	3
QMP23	Check worker references	2.09	4

Other notable issues that influenced the quality of construction as presented in Table 3 included ‘provision of required tools’ (MS = 3.95), ‘Non-compliance with approved drawings’ (MS = 3.86), and ‘Use of more sand than necessary in concrete’ (MS = 3.76). It is perhaps an indication of the level of awareness of ethical issues affecting the quality of construction that respondents rated issues such as ‘Professional present on site during concrete works’ and ‘Professional Negligence/Compromise’ quite low (MS = 2.57 and 2.11 respectively). It is also alarming that ‘Poor workmanship’ (MS = 2.55) was ranked as having only very moderate influence on the quality of construction works.

4 CONCLUSION

It has been proposed that a cyclical trend might exist in the numbers of building collapses which may be represented by a 2-period moving average trend-line. Collapses were more prevalent in buildings employed for residential and commercial uses (a total of 72% of the entire sample), buildings having not more than 3 floors (over half of the sample). The dominant cause of building failures in the study area were structural failure (46%) and use of substandard materials (21%). These two causes were also associated with the highest casualty rates in collapsed buildings (64% of all casualties recorded).

Design related issues were found to be most influential with respect to the quality of the final product of the construction process. Material issues influenced construction quality ‘to a large extent’ while process, compliance and labour issues exerted influence ‘to a moderate extent’. A worrisome indication of the low level of awareness of ethical issues affecting the quality of construction was provided through low rating of issues such as ‘Professional present on site during concrete works’, ‘Poor workmanship’ and ‘Professional Negligence/Compromise’ quite low (MS = 2.57, 2.55 and 2.11 respectively). Given the tone of writings on ethics in the construction industry, it would have been expected

that such practices that border on ethical conduct would be ranked highly.

This paper makes three main recommendations with respect to the improvement of construction quality in order to prevent the untimely collapse of buildings. Firstly, proactive measures to prevent building collapse need to be designed and implemented. Such measures could include routine testing of building integrity which could be built into an 'annual renewal of building approval' process. At inception, to improve their workability, such proactive measures should target residential and commercial buildings having less than 4 floors. Secondly, a vigorous, wide ranging campaign to improve the prevalence of ethical practices in the construction industry should be mounted. Such a campaign should span the entire spectrum of ethical conduct, from awareness to enforcement. Thirdly, this study should be replicated in other states of Nigeria, in order to validate some of the trends observed in building collapse incidents in Lagos state.

REFERENCE

- Abdulkareem, Y. A. and Adeoti, K. A. (2010). Quality Control Compliance in The Nigerian Construction Industry: A case Study Kwara State. Occasional paper.
- Aibinu, A. A., & Odeyinka, H. A. (2006). Construction delays and their causative factors in Nigeria. *Journal of construction engineering and management*, 132(7), 667-677.
- Anosike, M. N. and Oyebade, A. A., (2012). Sandcrete Blocks and Quality Management in Nigeria Building Industry. *Journal of Engineering, Project, and Production Management* 2012, 2(1), 37-46
- Ashokkumar, D., (2014). Study of Quality Management in Construction Industry. *International Journal of Innovative Research in Science, Engineering and Technology*. Volume 3, Special Issue 1, 36-43.
- Ayedun C.A., Durodola O.D. and Akinjare O.A. (2012). An Empirical Ascertainment of the Causes of Building Failure and Collapse in Nigeria, *Mediterranean Journal of Social Sciences* 3(1) 313 - 322
- Baiden, B. K. and Tuuli, M. (2004). Impact of quality control practices in sandcrete blocks production, *Journal of Architectural Engineering*, 10(2), 55-60.
- Chendo I.G. and Obi N.I. (2015). Building Collapse in Nigeria: The Causes, Effects, Consequences and Remedies. *International Journal of Civil Engineering, Construction and Estate Management* 3(4), 41- 49
- Dare. (2009, July16). "Narrating the Nigerian Story: The Challenge of Journalism" *The Nation Newspapers*, Retrieved from <http://www.thenationnewspapers.ng>
- Ede, A. N. (2010). Building Collapse in Nigeria: the Trend of Casualties the Last Decade (2000 -2010). *International Journal of Civil & Environmental Engineering*. 10(6). 32-38
- Ezema, I. C. & Olatunji, O., (2018). Building Collapse in Lagos State, Nigeria: Towards Quality Control in Materials, Batching and Placement of Concrete. *Covenant Journal of Research in the Built Environment*. 6(1), 25-39.
- Fagbenle, O. I. and Oluwunmi, A. O. (2010). Building Failure and Collapse in Nigeria: the Influence of the Informal Sector. *Journal of Sustainable Development* 3(4); 268-276.
- Fernandez, R. H. F. (2014), Strategies to Reduce the Risk of Building Collapse in Developing Countries, PhD Thesis, Carnegie Mellon University.
- Folagbade, S. O. (2001). Case Studies of Building Collapse In Nigeria. *Proceedings of a Workshop on Building Collapse, Causes, Prevention and Remedies*, The Nigerian Institute of Building, Ondo State Chapter, Oct 23-24.
- Jimoh, R. A. (2012). Improving Site Management Practices in The Nigerian Construction Industry, The Builders Perspective: *Ethiopian Journal of Environment Studies and Management* 5(4).
- Joshua, O., Olusola, K. O., Ogunde, A. O., Amusan, L. M., Ede, A. N. and Tunji-olayeni, P. F., (2017). Assessment of the Utilization of Different Strength Classes of Cement in Building Constructions in Lagos, Nigeria. *International Journal of Civil Engineering and Technology*, 8(9), 1221–1233.
- Kado, D. (2010). Establishing Status of Nigerian Building Design Firms based on European Construction Institute Total Quality matrix Dumas, Department of Building, Ahmadu Bello University Zaria.
- Kothari, C. R. (2004). *Research methodology: Methods and techniques*. New Delhi: New Age International.
- Leonard, D., (2010). Quality management practices in the US homebuilding industry. *The TQM Journal*.22(1), 101-110
- Leong, T.K., Zakuan, N. and Saman, M.Z.M. (2014) 'Review of quality management system research in construction industry', *Int. J. Productivity and Quality Management*, 13(1), 105–123.
- Longtau, P., Justina, A. M., Majidadi, S. T. & Makwin, G. (2016), An Assessment of the Factors Militating Against Adherence to Quality Control in Building Construction, *International Journal of Scientific & Engineering Research*, 7(4): 1211 – 1229.
- Okereke, P. A. (2003), *Construction Materials: Testing and Quality Control in Tropical Climate*. Owerri, Nigeria: Crown Publishers Ltd.
- Okoyeuzu, C. R., Obiamaka, P. E., & Onwumere, J. U. (2008). *Shaping the Nigerian Economy: The Role of Women*. Government Printer, Nigeria.
- Olagunju, R.E. (2011): Development of Mathematical Models for the Maintenance of Residential Buildings in Niger State, Nigeria, Ph.D (Architecture) Thesis, Department of Architecture, Federal University of Technology, Minna, Nigeria



- Oloke, O. C., Oni, A. S. Ogunde, A., Josuha, O. and Babalola, D. O., (2017). Incessant Building Collapse in Nigeria: A Framework for Post-Development Management Control. *Developing Country Studies*, 7(3) 114-127.
- Oloyede, S.A., Omoogun, C.B. and Akinjare, O.A. (2010). Tackling Causes of Frequent Building Collapse in Nigeria. *Journal of Sustainable Development*.3(3) 127-132.
- Oludare, O. S. & Oluseye, O. (2016), Quality Management Practices Among Construction Firms in Lagos, *PM World Journal*, V(VI): 1-13.
- Omran, A., Bamidele, O. and Baharuddin, A. H. B., (2016). Causes and Effects of Incessant Building Collapse in Nigeria. *Serbian Project Management Journal*, 6(1), 13-26.
- Opoko, A. P., Ezema, I. C. & Ediae, O. J. (2014), Implementation of Quality Management Procedures in the Production, and Utilisation of Cement Stabilised Laterite Interlocking Blocks, *Covenant Journal of Research in the Built Environment*, 1(1): 53 – 60.
- Oyedele, O. O. (2018). A study of control measures of building collapse in Lagos State, Nigeria. FIG Congress 2018 Embracing our smart world where the continents connect: enhancing the geospatial maturity of societies; Istanbul, Turkey, May 6–11.
- Paul, W., & Otieno, O. J. (2018). Prevalence, Causes and Possible Remedies to the Incessant Collapse Of Buildings In Kenya: A Strategic Discourse. *Advances in Social Sciences Research Journal*, 5(10) 413-426.
- Sanni, A. A., & Windapo, A. O. (2008, September). Evaluation of contractor's quality control practices on construction sites in nigeria. In Dainty, A.(Ed. 2008). *Proceedings of the 24th Annual ARCOM Conference* (pp. 1-3).
- Trochim, W. M. (2006). Non-probability sampling. *Research methods knowledge base*, 1(1), 1-10.
- Xiao, H. and Proverbs, D. (2002), "The performance of contractors in Japan, the UK and the USA", *International Journal of Quality & Reliability Management*, 19(6), 672-87.



Assessment of Ethical Practices at Different Stages of Public Housing Delivery in Nigeria

*Oluwadare, D. O¹ and Idiake, J. E²

¹Quantity Surveying Department, Federal University of Technology, PMB 65 Minna Niger State, Nigeria

²Quantity Surveying Department, Federal University of Technology, PMB 65 Minna Niger State, Nigeria

*Corresponding author email: dominicolagoke@yahoo.com, +2348033823328

ABSTRACT

Housing is a critical basic need, the third essential of life after food and clothing. Housing policies initiated by past successive governments in Nigeria have had low record of success due to two main reasons - lack of consistency/continuity in government policies and lack of ethical practices /corruption. This study focuses on the second reason only, and aims to examine the ethical practices in public housing delivery with the view of providing strategies to improve the prevalence of ethical performance in housing delivery. Review of construction management literature revealed that unethical practices in construction industry consist mainly of conflicts of interest, tender rigging, kickbacks and collusive pricing. Unethical practices have serious negative effects on the construction industry, manifesting mostly as reduction in the quality of finished products. Based on findings from review of methodologies employed in related literature, this study proposes to adopt a mixed methods approach that will utilise questionnaires and semi-structured interviews. This will enable the study draw conclusions as to how the industry can best tackle the occurrence of unethical practices.

Keywords: *Corruption; ethics; housing delivery; unethical practices.*

1 INTRODUCTION

Housing has been described as a critical basic need, following food and clothing. It constitutes the third essential of life (Taiwo, 2014). Housing involves the provisions of essential amenities and infrastructural facilities towards achieving a comfortable living in a built environment (Muhammad, *et al.* 2015; Festus and Amos, 2015). Almost all countries of the world were observed to have one housing problem or the other. Most African countries are faced with housing shortages; Nigeria in particular is grappling with a 17 million units housing deficit (Federal Ministry of Lands, Housing and Urban Development, 2017).

All past successive governments in Nigeria have instituted several housing policies such as the Pre-colonial period (before 1960), and the post military era (1999-to date). All of these several policies had low record of success due to several reasons; however two reasons stand out - lack of consistency and continuity in government policies and programmes as well as corruption and a lack of ethical practices (Olayiwola *et al.*, 2005; Nicholas and Patrick, 2015; Olanrewaju *et al.*, 2016). This study focuses on the second reason only.

Professional ethics is a system of moral principles or rules of behaviour which defines an occupational moral, it involves giving one's best to ensure that the client's interest are properly cared for, while the wider public interest is also adequately recognized and protected (Dalyop *et al.*, 2017). On the other hand, unethical conduct generally means the conducts that are contrary to

the accepted standards of a profession, an act involving the deliberate violation of accepted or agreed ethical standards (Johnstone, 2014). Professional ethics are applicable at all stages of the housing delivery process. Similar to general construction, three distinct stages have been identified in housing delivery by the Federal Ministry of Power, Works and Housing (FMPW&H). These are the: Stage I – Pre-contract stage; Stage II – Post-contract stage; and Stage III – Post-practical completion stage (FMW&H, 1996). The various services offered to clients by professionals in the construction industry differ among the three stages. The level of interaction among professionals, clients, contractors and statutory regulatory agencies also vary amongst the three stages.

Unethical and corrupt practices have been identified by Oyewobi *et al.* (2011) as detrimental to the development of the economy and human resources, increasing the cost of construction, and causing delays / cost overruns. The industry faces a long record of ethical challenges related to behaviour; lying, unreliable contractors, claims games (inflated claims, false claims), threats, conflicts of interest, collusion, fraud, corruption, professional negligence, gifts, bribery, kickbacking, tender theft (Al-Sweity, 2013). The construction industry has been acknowledged to be the most corrupt sector in the world (Owosu *et al.*, 2017). Corruption is found across multiple levels of the industry, where it has been accused of crippling performance (Le *et al.*, 2014). Hence a high level of ethical performance implies a high level of professional performance and hence a high level of client satisfaction (Al-Sweity, 2013).



Therefore, this research aims to examine the ethical practices in the public housing provision with the view of providing strategies to improve the prevalence of ethical performance in housing delivery. The research will focus specifically public housing provision in Nigeria, not on general construction works. Data for the study will be collected from stakeholders in public housing delivery in Abuja. The time frame for the study spans 2018 and 2019.

Ethics

Ethics has to do with studying what is right or wrong in human actions that seek to achieve man's ultimate happiness (Gichure, 1997). Ethics is the process of trying to answer the question of how we ought to live, of being true to the idea of who we are and what we stand for; and developing a well-informed conscience, (The Ethics Centre, 2015). Corruption is always a sign of deeper unethical practices, wrong doings. Some ethical theories have been developed to explain ethical behaviour. These include *Utilitarianism*, which is also known as consequentialism; this theory states that the objective of ethics is the greatest happiness for the largest number of people. As postulated by utilitarian theorists John Stuart Mill and Jeremy Bentham, the end of an action can justify the means through which such end was achieved if the benefits outweigh the costs in the service of the greater number of people (Gichure, 2008; Sinnott-Armstrong, 2014). Since corruption is mostly actuated by self-interest, utilitarianism is in opposition to corruption.

Another theory of ethics is *Deontology*, which was developed by Immanuel Kant hence its other name of Kantian Ethics. It is an ethics of formal norms which states that an action should never be carried out except it is willed that such action should become a universal law (Gomez, 1992; Beauchamp & Bowie, 2001). While people who choose not to be corrupt can adopt this maxim, it also serves those who are corrupt, who can justify their behaviour as being universally accepted. *Aristotelian ethics* (virtue theory) revolves around two concepts; that individuals are necessarily part of communities and that happiness is the sole basis for measuring success (Gomez, 1992). Ethics according to Aristotelian thesis comes about because all human beings seek happiness, which they can attain only through moral actions that preserve their dignity (Gichure, 1997). Under virtue theory human dignity is secured only through morality, which is a necessity as opposed to a luxury. Corruption and unethical behaviours find no hiding place under virtue theory; this is because the theory requires an individual to acquire virtues (by doing the right thing always) in order to attain maximum happiness.

Professional Ethics in the Construction Industry

Professional ethics have been defined by Liu *et al.* (2004) as a system of behavioural norms that guide the working relationship between experts and lay persons. Some sort of formal structuring of these behavioural norms can be observed in most professions in the form of codes of ethics (McCarthy, 2012). A profession can be

viewed as an occupation where individuals or groups of individuals apply scholarly aptitude obtained through a recognized course of learning and practice to practice autonomous judgment guided by a code of ethics (Uff, 2003).

According to Abd Rahman (2008) a professional must be capable in the specific field of work concerned by meeting some criteria which include:

- i. Highest scholastic capabilities;
- ii. Expert and specific learning in the field one is practising professionally;
- iii. Excellent manual or handy and scholarly abilities in connection to one's profession;
- iv. High quality work in manifestations, items, administrations, introductions, consultancy, essential or other research, authoritative, promoting or other work.
- v. High standard of professional ethics, conduct and work exercises while doing one's profession (as a worker, independently employed individual, endeavour, business, organization, or association).
- vi. A sensible measure of professional working knowledge in both of the above limits in fields of work one has professional capabilities.

Le *et al.* (2014) sees professional ethics as a set of moral principles that govern the conduct of professionals. Authors such as Oliver *et al.* (2006) have argued that stakeholders such as clients and the government should also be considered as a form of 'profession'. This is because clients and the government have responsibilities to be ethical in all conducts related to the construction industry.

Given the importance of professional ethics to the construction industry, a lot of effort has been made to increase ethical standards and integrity among construction professionals worldwide (Abdul-Rahman *et al.*, 2011; Ho 2011). Such efforts include improving professional ethics, streamlining the construction sector (such as the National Construction Authority in Kenya) (Republic of Kenya, 2011) and curbing corruption (through setting up anti-corruption agencies such as the Economic and Financial Crimes Commission (EFCC) of Nigeria).

The efficacy of these efforts remains doubtful. Codes of practice have contractual effect on members of most professions in the construction industry (Liu *et al.*, 2004). A shortcoming of such codes however is that they do not teach morality, ethics or values to the individuals whose personal ethics determine the ethical conduct of the industry (London & Everingham, 2006). A person's ethical behaviour is determined by individual personality and socialization, which represent his or her ethical system (Zemguliene, 2013). Without sound ethical values professionals will be easily tempted to use illicit means to achieve their goals. This is why it is important to provide

ethical training to professionals that are of a comparable calibre as the technical knowledge and skills possessed by them. Reliance on legal and financial institutions - judiciary, police and financial auditors - to enforce and strengthen public sector accountability assumes tacitly that more rules and regulations along with increased enforcement will reduce corruption. This assumption ignores the weakness of the justice system in many poor countries (Svensson, 2005). Since ethical decisions begin with the individual, this is where improvement of ethical practices ought to be focused.

The built environment makes significant contributions to the economic output of most countries. It generates employment and income for the people (Ibrahim, 2008). The industry is very important in the socio economic development of developing economies because of its unique ability to facilitate and stimulate investment and to generate employment. In Nigeria, the industry is responsible for 16% of the GDP, employs approximately eight million people, and represents approximately 25% of Nigeria's workforce and the largest in Africa (Ibrahim and Musa-Haddary, 2010).

Incidentally, the Nigerian built environment is accused of being wasteful, inefficient, unsafe, falling short of quality and quantity targets, and being late in delivery (Omole, 2000). Professionals in the built environment have severally been credited with the inability to deliver services effectively and efficiently, with the current estimated population of over 170 million and an annual growth rate of 24%, Nigeria faces colossal deficit of basic amenities required by its citizens (Ibrahim and Musa-Haddary, 2010; Usman *et al.*, 2014).

Increased project costs are usually a result of unethical misconduct in construction industry; deceptive conduct adds in the vicinity of 0.005% and 5% to construction costs. Aigbavboa *et al.* (2016) and Fan *et al.* (2001) opined that unethical practices in construction industry have one way or the other hindered development of the industry. Shakantu (2006) noted that quality of projects is reduced which affect safety and satisfaction of users. Oyewobi *et al.* (2011), Nawaz and Ikram (2013) and Inuwa *et al.* (2015) also stated that unethical practices lead to poor quality and defective structure development which results in high maintenance cost.

Related Works on Ethical Practices in the Construction Industry

This section presents the aim and findings in a selection of research works that dealt with ethical practices in the construction industry. Almost all of the studies focused on corruption or unethical behaviour of construction professionals. Quite a number of these studies were carried out in Nigeria, thus reflecting the vibrancy in efforts to interrogate the existing value system of the Nigerian Construction Industry (NCI). Adnan *et al.* (2012) posed some fundamental questions about unethical practices in the Malaysian construction industry. Their study sought to know the common unethical behaviours

evidenced by the contractors during the life cycle of construction projects. They found that the most common unethical conduct evidenced by contractors are cover pricing, bid cutting, poor documentation, late and short payments, subcontractors' lack of safety ethics, unfair treatment of contractors in tender/final account negotiations, competitors' overstatement of capacity and qualifications to secure work, competitors' falsification of experience and qualifications and bureaucratic government policy.

The findings of Abdul-Rahman *et al.* (2011) were similar to obtained in the studies presented thus far. Studying clients' perceptions of the impact that codes of professional ethics have on civil engineering works, Abdul-Rahman *et al.* (2011) identified the five worst forms of unethical conduct as "illegal award to contractor", "bribery", "breach of professional responsibility", "disclosure of project confidential baseline", and "collusive tendering". Osei-Tutu *et al.* (2010) explored the corruption practices inherent in public procurement of infrastructural projects in Ghana. They observed that conflict of interest, bribery, embezzlement, kickbacks, tender manipulation and fraud are corruption practices in the Ghanaian infrastructure projects delivery system.

Table 1: Summary of literature findings

Author(s)	Year	Location	Conclusions
Osei-Tutu, <i>et al</i>	2010	Ghana	Conflict of interest, kickbacks, fraud, and tender manipulation observed in projects.
Abdul-Rahman, <i>et al</i>	2010	Malaysia	The ethical standards among construction professional considered below average.
Abu Hassim, <i>et al</i>	2010	Malaysia	Ethical issues due to Non-transparent process and Ineffective professional ethics.
Olusegun, <i>et al</i>	2011	Nigeria	Corruption caused by poverty, indiscipline, greed, quackery, and endemic corruption in society.
Oyewobi, <i>et al</i>	2011	Nigeria	Ethical problems are evident in all the stages of building project rising from pre-tender stage to completion.
Adnan, <i>et al</i>	2012	Malaysia	Common Contractors' unethical conducts are cover pricing, bid cutting, and poor documentation.

Author(s)	Year	Location	Conclusions	Author(s)	Year	Location	Conclusions
Usman, <i>et al</i>	2012	Nigeria	Corruption thrives because of absence of punishment, non-continuity of policies, loopholes in project monitoring;	Usman, <i>et al</i>	2018	Nigeria	Ethical standards are compromised through projects without strict compliance to specifications.
Bowen, <i>et al</i>	2012	South Africa	Corruption is most prevalent during the bid evaluation and tendering phases of projects.	Otubor, <i>et al</i>	2018	Nigeria	Professionals do not adhere to professional ethics since there are no professional monitoring teams.
Nordin, <i>et al</i>	2013	Malaysia	Four significant factors are positively related to corrupt acts.	Remišová, <i>et al</i>	2018	Slovakia	Codes of ethics and related reporting and control mechanisms are most effective tools.
Adeyinka, <i>et al</i>	2013	Nigeria	The overall compliance level of construction professionals to ethical standards was 52.37%.	Kahela	2018	South Africa	Personal value, organisational culture and education are very influential factors on ethical decisions of a project manager.
Asamoah & Decardi-Nelson	2014	Ghana	All selected professionals have encountered some form of corruption, fraud, conflict of interest, tender manipulation, kickbacks, and collusion.	Shah & Alotaibi	2018	UK	Owner/client ethical practices include untimely legal action, changing project manager's responsibility, delays in payment.
Shan, <i>et al</i>	2015	China	Response strategies have not achieved a higher than acceptable level in preventing corruption vulnerabilities.	Lee & Cullen	2018	UK	Contractor's quantity surveyor more frequently witnessed unethical practices compared to consultant's quantity surveyor.
Shan, <i>et al</i>	2015	China	Modeled twenty-four items of corruption to facilitate evaluating, revealing and monitoring corruption in projects.	Akinrata, <i>et al</i>	2019	Nigeria	Clients' dissatisfaction, High maintenance cost and Poor workmanship were major results of ethical misconduct by Quantity Surveyors in the construction industry.
Shan, <i>et al</i>	2017	China	Corruption caused by flawed regulation systems, and lack of a positive industrial climate..				
Shan, <i>et al</i>	2017	China	Main collusive practices in China are loose site supervision and misrepresentation of qualification certificates.				
Dindi, <i>et al</i>	2018	Kenya	Collusion, kickbacks and supplanting are due to lack of honesty and greed is most common.				
Ogbu & Asuquo	2018	Nigeria	Bribery for access to confidential information is prevalent.				

Drivers of Unethical Practices

The causes of corruption in the public construction sector of China were the subject of a study by Shan *et al.* (2017). The results showed that causes of corruption could be categorized into two constructs, namely the flawed regulation systems, and the lack of a positive industrial climate. The most influential items under flawed regulation systems are negative role models of leadership, inadequate sanctions and the lack of rigorous supervision. Nordin *et al.* (2013) attempted to develop a Model of Corrupt Action for the Malaysian construction industry. The study found that four factors were significantly correlated with corrupt acts. These factors

included the desire to achieve a private or professional goal through corrupt action; subjective norms (SN); Perceived Behavioural Control (PBC) and attitude.

In their examination of stakeholders' views of corruption in the South African construction industry, Bowen *et al.* (2012) found that factors that facilitate corruption include a lack of transparency in the awarding of contracts and the operating environment of the industry. Stakeholders do not however report such corrupt practices because of a lack of confidence in the criminal justice system, a belief that no action will be taken, and a perception that 'whistle-blowers' are not adequately protected. Usman *et al.* (2012) examined the influence of unethical professional practices on the management of construction projects in north-eastern Nigeria. Major findings of the study included the absence of punishment for corruption; loss of money due to change in government; lack of continuity in government programmes; availability of loop holes in project monitoring.

In a study that attempted to quantitatively determine the causes of corruption in the Nigeria construction industry, Olusegun *et al.* (2011) found that the causes of corruption included: poverty; excessive love for money (greed); politics in the award of contract/godfatherism; indiscipline on the part of construction professionals; profit maximization by Contractor; quackery; fall-out of endemic societal corruption and favouritism. To reduce the incidence of corruption, Olusegun *et al.* (2011) recommended that the identified causes of corruption must be dealt with by government, contractors, individuals and construction professionals. Oyewobi *et al.* (2011) x-rayed the determinants of unethical performance in Nigerian construction industry in all the stages of building projects. They found that ethical problems are evident in all the stages of building project rising from pre-tender stage to completion and that the corruption crisis tended to have its roots in the echelons of power, whether in the public or private sector.

Abdul-Rahman *et al.* (2011) studied clients' perceptions of the impact that codes of professional ethics have on civil engineering works. They found that the three most influential causes of unethical conduct are "insufficient ethical education in schools", "economic downturn" and "insufficient ethical education from professional institution".

Strategies for Mitigating Unethical Practices

Shan *et al.* (2015) showed that the four response strategies of leadership, rules and regulations, training, and sanctions, achieved only an average level of success in preventing corruption vulnerabilities in the Chinese public construction sector. Asamoah and Decardi-Nelson (2014) revealed that all the professional associations in the construction industry have their own ethical codes of conduct; however professionals need a common understanding of ethical and professional values. Nordin *et al.* (2013) after developing their Model of Corrupt

Action for the Malaysian construction industry found that control factors such as motivations, laws, regulations and values of the individuals reduce undesirable intentions to a certain extent.

Adnan *et al.* (2012) provided detailed prescriptions for tackling unethical practices through a three-pronged approach comprising short, medium and long-term measures. Recommended Measures included (i) introducing punitive measures, penalties or even cancellation of licenses on repeated violations, and (ii) enshrining quality and ethical assurance as part of every project team. The most effective way to mitigate unethical conduct in the construction industry according to Abdul-Rahman *et al.* (2011) is "to provide training and programmes on professional ethics".

Summary of Findings from Literature Review

Many studies on unethical practices in construction industry have discovered that conflicts of interest, tender rigging, kickbacks and collusive pricing are the prevalent manifestations of corruption. Government officials (as clients) and contractors were perceived to be the parties most involved in corrupt activities (Bowen *et al.*, 2012). Corruption is most prevalent during the bid evaluation and tendering phases of projects. Studies have found that negative role models of leadership, inadequate sanctions and the lack of rigorous supervision are significant drivers of corruption in the public construction sector.

Unethical practices have serious negative effects on the construction industry, manifesting mostly in reduced quality of finished products. Various measures to mitigate the problem of unethical practices have been suggested; some of these suggestions have not been overly successful in practice. Studies have shown that curbing unethical conduct is difficult, and that all professionals need a common understanding of ethical and professional values.

2 METHODOLOGY

Following the review of literature carried out, further development of this research will be pursued on the basis of the methodology detailed in this section. Kothari (2004) defines research design to be the arrangement of conditions for collection and analysis of data. It is the conceptual structure within which the research will be conducted. The study will adopt a mixed methods approach (quantitative and qualitative research design). The quantitative aspect will encompass the use of questionnaires and past recorded data, while the qualitative aspect will use semi-structured interview.

The research population for the study has been identified as the several construction professionals in Abuja, the study area. These professionals include Architects, Quantity Surveyors, Builders and Engineers. A sample frame consists of a list of sampling units from which selection of sampling unit is drawn. The sample frame will be the lists of the professionals within the study population; that is the Architects, Quantity Surveyors,

Builders and Engineers working in the Federal Housing Authority, Federal Ministry of Works, Housing, and Power, and Federal Capital Development Authority. These lists will be obtained from the Human Resource Departments of the relevant Ministries/Agency.

The sample size for the questionnaire survey will depend on the sample frame obtained. Where the number is sufficiently small as to make it possible for the researcher to reach all of the professionals in the selected Ministries/Agency, a census of the respondents will be undertaken. Otherwise some form of purposive sampling will be carried out to select a manageable sample. Purposive sampling (Trochim, 2006) appears to be most suited for the study, if it is impossible to conduct a census.

The research instrument for quantitative data collection is being developed along the lines of a similar instrument employed by Ameyaw *et al.* (2017) and administered to identify the various ethical and unethical practices in the public housing delivery system, in order to determine the prevalence of such practices. An interview protocol is also being developed for the purpose of collecting qualitative data from selected professionals on the drivers and challenges of ethical practices on public housing delivery, which will help in creating a strategy to increase the prevalence of ethical practices. A range of statistical techniques will be applied to the data to be collected through questionnaires and interview. Descriptive methods (such as Relative Importance Index, Percentile and Mean Item Score), as well as thematic and deductive methods, which will include Pearson correlation and Simple regression, are some of the tools that will be applied.

3 CONCLUSION

Having reviewed relevant literature on ethical practices in the construction industry and drawn some findings from the review, a methodology for the research has been proposed. Further development of this study will employ the mixed research method approach to collect data and examine the opinions of professionals in the construction industry on the prevalence of ethical practices. This will enable conclusions be drawn as to how the industry can best tackle the occurrence of unethical practices.

REFERENCE

- Abd Rahman, A. (2008). Unethical conduct among professionals in the construction industry. unpublished master thesis, Universiti Teknologi Malaysia–Malaysia.
- Abdul-Rahman, H., Wang, C., & Saimon, M. A. (2011). Clients' perspectives of professional ethics for civil engineers. *Journal of the South African Institution of Civil Engineering*, 53(2), 2-6.
- Abdul-Rahman, H., Wang, C., & Yap, X. W. (2010). How professional ethics impact construction quality: Perception and evidence in a fast developing economy. *Scientific Research and Essays*, 5(23), 3742-3749.
- Abu Hassim, A., Kajewski, S. L., & Trigunarsyah, B. (2010). Factors contributing to ethical issues in project procurement planning: a case study in Malaysia. In *Proceedings of 2010 International Conference on Construction & Real Estate Management*, 1, 312-317.
- Adeyinka, B. A., Jagboro, G. O., Ojo, G. K., & Odeiran, S. J. (2013). Level of compliance of core construction professionals to ethical standards in Nigeria. *Journal of Construction Project Management and Innovation*, 3(2), 640-659.
- Adnan, H., Hashim, N., Mohd, N., & Ahmad, N. (2012). Ethical issues in the construction industry: Contractor's perspective. *Procedia-Social and Behavioral Sciences*, 35, 719-727.
- Aigbaybo, C., Oke, A. & Tyali, S., 2016, 'Unethical practices in South-African construction industry', in F. Emuze (ed.), *5th Construction Management Conference*, Port Elizabeth, South Africa, Nov 28–29, 15–22.
- Akinrata E. B., Ogunsemi D. R., and Akinradewo O. F., (2019). Outcomes of Unethical Practices by Quantity Surveyors in Nigerian Construction Industry. *International Journal of Applied Research in Social Sciences* 1(3), 84-94.
- Al-Sweity, A. (2013). Unethical conduct among professionals in construction industry. A Master thesis submitted to the department of Civil Engineering - Construction Management, The Islamic University of Gaza.
- Ameyaw, E.E., Parn, E., Chan, A.P.C., Owusu-Manu, D., Edwards, D.J. & Darko, A. (2017). Corrupt practices in the construction industry: survey of Ghanaian experience. *Journal of Management in Engineering*, 33(6), 1-11.
- Asamoah, R. O., & Decardi-Nelson, I. (2014). Promoting trust and confidence in the construction industry in Ghana through the development and enforcement of ethics. *Information and knowledge*, 3(4), 63-68.
- Bowen, P., Edwards, P., & Cattell, K. (2012). Corruption in the South African construction industry: A mixed methods study. In *Proc. of 28th Annual ARCOM Conference* (ed. Smith, S.D.) 521-531.
- Bowie, N. E., & Beauchamp, T. L. (Eds.). (2001). *Ethical theory and business*. Prentice Hall.
- Dalyop, D.J.S., Bogda, P. O., Peter, O. & Elizebeth, D. (2017). Unethical professional practices and poor craftsmanship of construction projects performance in Nigeria: Consequences and the way forward, *J Civil Eng Environ Sci* 3(1), 22-30.
- Dindi, A. M., Munala, G., Alkizim, A., Kivaa, P. & Gichure, C. (2018). Ethics as a Solution to Corruption: A Case Study of the Construction Industry in Kenya. *Africa Habitat Review Journal*, 12(2) 1339-1349.



- Fan, L., Ho, C., & Ng, V. (2001). A study of quantity surveyors' ethical behaviour. *Construction Management and Economics*, 19(1), 19-36.
- Federal Ministry of Works and Housing (FMW&H) (1996). Scale of fees for professional services in the Nigeria Construction Industry. Abuja, Nigeria: FMW&H.
- Federal Ministry of Lands, Housing and Urban Development (FMLHUD) (2017). Housing Deficit: National Housing Programme in Nigeria.
- Festus, I.A. & Amos, I.O. (2015). Housing Policy in Nigeria: An Overview. *American International Journal of Contemporary Research*, 5:2 (53-59).
- Gichure, C. W. (1997). *Basic Concepts in Ethics: With an Outline of Different Methods in Contemporary Moral Philosophy*. Nairobi: Focus Publications.
- Gichure, C. W. (2008). Ethics for Africa today: An introduction to business ethics. Nairobi:
- Gomez, R. (1992). *What's right and wrong in business? A primer on business ethics*. Manila: Sinag-tala.
- Ho, C.M.F. (2011). Ethics management for the construction industry: A review of ethical decision-making literature. *Engineering, Construction and Architectural Management*, 516-537.
- Ibrahim, A. D. & Musa - Haddary, Y. G. (2010). A Critique of the Operational Philosophy and Mechanism of the Public Concept of Value for money in Public Infrastructure Development. *Proc 3 Day International Workshop on PPP Approach to Infrastructure Development in Nigeria* July 13 - 15 Abuja: NIQS.
- Ibrahim, A. D. (2008). A Critique of the Operational Philosophy and Mechanism of Public Procurement Act: Construction Industry Perspective. In *Proc NIQS 23rd Biannual Conference* Nov 3-8, 1-7.
- Inuwa, I. I., Napoleon Daniel Usman, N. D., & Dantong, J. S. (2015). The effects of unethical professional practice on construction projects performance in Nigeria. *African Journal of Applied Research (AJAR)*, 1(1).
- Johnstone, M.J. (2014). Unethical Professional conduct. *Australian Nursing Journal*, 17:11(34)
- Kahela, T. (2018). Ethics in construction industry: project managers' case study. Master of built environment thesis, Department of Construction Management & Quantity Surveying, Faculty of Engineering and the Built Environment, Durban University Of Technology, South Africa.
- Kothari, C. R. (2004). *Research methodology: Methods and techniques*. New Delhi: New Age International.
- Le, Y., Shan, M., Chan, A. P., & Hu, Y. (2014). Overview of corruption research in construction. *Journal of management in engineering*, 30(4), 02514001.
- Lee, C. C. T. and Cullen, D. (2018). An Empirical Comparison of Ethical Perceptions among the Consultant's Quantity Surveyor and Contractor's Quantity Surveyor in the UK Construction Industry. *Proc RICS COBRA conference*.
- Liu, A.M., Fellows, R. & Ng, J. (2004). Surveyors' perspectives on ethics in organisational culture. *Engineering, Construction and Architectural Management*, (6), 438-449.
- London, K. & Everingham, P. (2006). *Ethical behaviour in the construction procurement process*. Cooperative research centre for construction innovation. Brisbane: Cooperative Research Centre for Construction innovation.
- McCarthy, S.F. (2012). Developing an Australian code of construction ethics. *Australasian Journal of Construction Economics and Building*, XII(2), 87-100.
- Muhammad, Z., Johar, F., Sabri, S. & Jonathan, Z.U. (2015). A review of housing provision and the challenges of sustainable housing delivery in the Federal Capital Territory Abuja, Nigeria. *Jurnal Teknologi (Sciences & Engineering)*, 77:14 (23-31).
- Nawaz, T., & Ikram, A. A. (2013). Unethical practices in Pakistani construction industry. *European Journal of Business and Management*, 5(4), 188-204.
- Nicholas, E.O. & Patrick, D.D. (2015). A review of governmental intervention on sustainable housing provision for urban poor in Nigeria. *International Journal of Social Science Studies*, 3:6(40-48).
- Nordin, R. M., Takim, R., & Nawawi, A. H. (2013). Behavioural factors of corruption in the construction industry. *Procedia-Social and Behavioral Sciences*, 105, 64-74.
- Nordin, R. M., Takim, R., & Nawawi, A. H. (2013). Behavioural factors of corruption in the construction industry. *Procedia-Social and Behavioral Sciences*, 105, 64-74.
- Ogbu, C.P. & Asuquo, C.F., 2018, 'A comparison of prevalence of unethical tendering practices at national and subnational levels in Nigeria', *Africa's Public Service Delivery and Performance Review* 6(1), pp1-13.
- Olanrewaju, A., Anavhe, P. & Hai, T.K. (2016). A framework for affordable housing governance for the Nigerian property market, *Procedia Engineering*, 164: 307-314.
- Olayiwola, L.M., Adeleye, O. & Ogunshakin, L. (2005). Public housing delivery in Nigeria: Problems and Challenges. *Proc World congress on housing transforming housing environments through the design*. Pretoria, South Africa.
- Oliver, J., London, K., & Everingham, P. (2006). Ethical behaviour in the construction procurement process. Occasional papers, University of Western Sydney, retrieved from researchdirect.westernsydney.edu.
- Olusegun, A. E., Benson, O. A., Esther, A. I., & Michael, A. O. (2011). Corruption in the construction industry of Nigeria: causes and solutions. *Journal of Emerging*

- Trends in Economics and Management Sciences (JETEMS)*, 2(3), 156-159.
- Olusegun, A. E., Benson, O. A., Esther, A. I., & Michael, A. O. (2011). Corruption in the construction industry of Nigeria: causes and solutions. *Journal of Emerging Trends in Economics and Management Sciences (JETEMS)*, 2(3), 156-159.
- Omole, A. O. (2000). Quality of professional service and ethics. *The Quantity Surveyor*, 33, 2-7.
- Osei-Tutu, E., Badu, E. And Owusu-Manu, D. (2010), "Exploring corruption practices in public procurement of infrastructural projects in Ghana", *International Journal of Managing Projects in Business*, 3(2) pp. 236 - 256. <http://dx.doi.org/10.1108/17538371011036563>
- Osei-Tutu, E., Badu, E. and Owusu-Manu, D., (2010), "Exploring corruption practices in public procurement of infrastructural projects in Ghana", *International Journal of Managing Projects in Business*, 3(2) pp. 236 - 256. <http://dx.doi.org/10.1108/17538371011036563>
- Otubor, C. O, Dariye, J. C. Salawu, P. O., Idris, I. R., Tsenyil, C. & Gbande, R. (2018). Assessment of professional ethics adherence for sustainable economic development in Nigeria. *International Journal of Social and Management Sciences*. 1(1), 1-13.
- Oyewobi, L. O., Ganiyu, B. O., Oke, A. A., Ola-Awo, A. W., & Shittu, A. A. (2011). Determinants of unethical performance in Nigerian construction industry. *Journal of sustainable development*, 4(4), 175.
- Remišová, A., Lašáková, A. and Kirchmayer, Z. (2018). Influence of Formal Ethics Program Components on Managerial Ethical Behaviour. *Journal of Business Ethics* 1-16.
- Republic of Kenya. (2011). National Construction Authority Act No. 41 of 2011. Nairobi: Government Printers.
- Shah, RK and Alotaibi, M (2018). A study of unethical practices in the construction industry and potential preventive measures. *Journal of Advanced College of Engineering and Management*, 3. pp. 55-77
- Shakantu, W., (2006), 'Corruption in the construction industry; Forms susceptibility and possible solutions', *Civil Engineering* 14(7), 43-47, viewed 07 August 2017, from <https://journals.co.za/content/civeng/14/7/EJC25511>
- Shan, M., Chan, A. P. C., Le, Y., Xia, B. & Hu, Y. (2015). Measuring corruption in public construction projects in China. *Journal of Professional Issues in Engineering Education and Practice*, 141(4). [https://doi.org/10.1061/\(ASCE\)EI.1943-5541.0000241](https://doi.org/10.1061/(ASCE)EI.1943-5541.0000241)
- Shan, M., Chan, A. P., Le, Y., & Hu, Y. (2015). Investigating the effectiveness of response strategies for vulnerabilities to corruption in the Chinese public construction sector. *Science and engineering ethics*, 21(3), 683-705.
- Shan, M., Chan, A. P.C., Le, Y., Hu, Y. & Xia, B. (2017). Understanding collusive practices in Chinese construction projects. *Journal of Professional Issues in Engineering Education and Practice*, 143(3). [https://doi.org/10.1061/\(ASCE\)EI.1943-5541.0000314](https://doi.org/10.1061/(ASCE)EI.1943-5541.0000314)
- Shan, M., Le, Y., Yiu, K. T., Chan, A. P., & Hu, Y. (2017). Investigating the underlying factors of corruption in the public construction sector: Evidence from China. *Science and engineering ethics*, 23(6), 1643-1666.
- Sinnott-Armstrong, W. (2014). The Stanford Encyclopaedia of Philosophy. Retrieved from Consequentialism: <http://plato.stanford.edu/archives/spr2014/entries/consequentialism/>
- Svensson, J. (2005). Questions about corruption. *Journal of Economic Perspectives*. 19(3), 19-42.
- Taiwo, A. (2014). The need for government to embrace public-private partnership initiative in housing delivery to low-income public servants in Nigeria. *Urban Design International*, 20:1 (56-65).
- The Ethics Centre. (2015). What is ethics? St James Ethics Centre. Retrieved March 26, 2015, from: <http://www.ethics.org.au/about/what-is-ethics>
- Trochim, W.M.K. (2006). *The Research Methods Knowledge Base*, 2nd Edition. Retrieved from <http://www.socialresearchmethods.net>.
- Uff, J. (2003) Duties at the legal fringe: ethics in construction law. Centre of Construction Law & Management, Available at: <http://www.scl.org.uk/> (Accessed on 22/02/2012).
- Usman, N. D., Dabs, D. Y., Shwarka, M.S., and Abubakar, H. O. (2018). Assessment Of Professionalism And Ethical Standards On Project Delivery In Nigerian Built Environment. *African Journal of Applied Research* 4(2), 216-226.
- Usman, N. D., Inuwa, I. I., Iro, A. I., & Dantong, S. (2012). The Influence of Unethical Professional Practices on The Management of Construction Projects in North Eastern States of Nigeria. *International Journal of Economic Development Research and Investment*, 3(2), 124-129.
- Usman, T., (2014). 'Nigerian govt. urges states to replicate procurement laws', *Premium Times*, 10 November, viewed 26 August 2017, from <http://www.premiumtimesng.com/business/170883-nigerian-govt-urges-states-to-replicate-procurement-laws.html>
- Zemgulienė, J. (2013). Perceived ethical leadership and job involvement in the economic-specific context. *Organisations and Markets in Emerging Economies*. 43-56.



Participation of Female Quantity Surveyors in the Nigerian Construction Industry

*Nnamoko, C. E

Quantity Surveying Department, Federal University of Technology, PMB 65 Minna Niger State, Nigeria

*Corresponding author email: chioma_nnamoko@yahoo.com, +2348142065534

ABSTRACT

The nature of the construction industry is changing; adoption of innovative technological processes and application of advanced technologies necessitate an increased emphasis on job competencies. The construction industry has been male dominated for years; women still constitute very low proportion of workers. However the last three decades after the United Nation's Decade for Women (1975-1985) have seen greater focus on gender equality, equity and empowerment of women. The Quantity Surveyor, also known as a Construction Economist or Cost Manager, is a professional adviser that estimates and monitors construction costs from the feasibility to completion of projects. The aim of this paper is to examine female Quantity Surveyors participation in the construction industry with the view of identifying strategies that can be applied in improving the level of female quantity surveyors' participation. Through a review of related literature, this paper has brought to the fore the perception that the current image of the construction industry presents a strong barrier to the attraction of women into the industry in significant numbers. The paper proposes to employ a sequential mixed methods research design as a vehicle for delivery of the fieldwork phase of the research. It is expected that further development of this research through fieldwork and subsequent analysis of data will lead to the development of strategies that, if implemented, will help in improving the participation of women quantity surveyors in the Nigeria construction industry.

Keywords: *Construction; female; gender; Nigeria; quantity surveyor.*

1 INTRODUCTION

In Nigeria, the construction industry is the second largest employer of labor after agriculture, and it provides jobs for skilled, unskilled and semi-skilled workers (Odubiyi, 2018). The changing nature of the construction industry, as evidenced by adoption of innovative technological processes, training of highly focused professionals, and application of advanced technologies necessitates an increased emphasis on job competencies (Lenard, 2000). Nigeria is attempting to accelerate the delivery of tangible dividends of democratic system of government (re-commenced in 1999) to her teeming populace. Achieving this will only be possible with improved output of the construction industry, which provides the entire needed basic infrastructure for the country's socio-economic development such as hospitals, schools, townships, highways, roads and telecommunication systems.

Since the launching of the United Nation's Decade for Women (1975-1985), the last three decades have seen greater focus on gender equality, equity and empowerment of women as means of increasing productivity and enhancing the socioeconomic status of a nation. The need for unbiased utilization of human resources has given research impetus to gender participation in various economic endeavors in both the developed and the developing countries (Adeyemi, 2015). Women face uniquely daunting challenges at work which

are rooted in the process of socialization right from childhood. Socialization received early in life almost always predisposes a person to choose a specific career path. Stereotyping teaches girls, directly or indirectly, to steer clear of studies and jobs considered to be for males. Such stereotyping is reinforced by comments received from childhood and eventually inadvertently results into barriers (Adogbo *et al.*, 2015). Most of the barriers stem from negative perceptions that the construction industry is dirty, dangerous and difficult, with no guarantee of long-term employment.

The construction industry has been male dominated for years, and on many jobsites female construction workers are not welcome. In recent times however, there has been rising global consciousness, both at the grassroots and policy levels, regarding the impact of gender issues on education and national development (Aguale and Agwagah, 2007). There is also the growing realization that women constitute more than half of the world's population. In most developed countries, female representation in the workplace has significantly increased in recent decades and the number of women entering traditionally male-dominated jobs is increasing because of organizational changes in worksite settings and other economic reasons (Jaafar *et al.*, 2014). However, women still constitute very low proportion of workers in construction (Adogbo *et al.*, 2015).

The construction industry consists of various professionals of which Quantity Surveyors are an



important part. The Quantity Surveyor, also known as a Construction Economist, or Cost Manager, is a professional adviser that estimates and monitors construction costs, from the feasibility stage of a project through to the completion of the construction period. After construction they may be involved with tax depreciation schedules, replacement cost estimation for insurance purposes and, if necessary, mediation and arbitration. Women participation in Quantity surveying and Nigerian construction industry is an important area for research, as evidenced by the number of studies carried out by researchers. These include Jaafar *et al.* (2016) who worked on investigating the level of duties and competencies of female quantity surveyors in the Malaysian construction industry. Another study by Tunji-Olayeni *et al.* (2018) focused on assessing job satisfaction of female construction professionals (Architects, Builders, Quantity Surveyors and Engineers) in male dominated fields specifically the construction industry. Still yet, other studies that are relevant are Jimoh *et al.* (2016) and Odubiyi (2018) who worked on overcoming barriers of female students' choice of built environment courses (Architecture, Building, Civil engineering, Quantity surveying and surveying and geo-informatics) and identifying the new noticeable trend among female construction workers of taking up vocational occupations outside the construction industry respectively. The study of women participation in the Nigerian Construction Industry is important because of several reasons. These include the fact that women make up at least 49.19% of the population of Nigeria, yet according to Oyewobi and Adeneye (2016), only 6.10% of workers in the Nigerian Construction Industry are women. The figures for Quantity surveyors are either unavailable or apply only to small sections or segments of the Nigerian Construction Industry, mostly on a geographical basis. This means that some areas have not been covered in any level of detail.

A careful study of works related to women participation in the construction industry such as carried out by Jimoh *et al.* (2016) and Adeyemi *et al.* (2006), reveals that no study was found that addressed women Quantity surveyors' participation in the Nigerian Construction Industry specifically in the Abuja FCT area. Therefore, it is impossible to address or tackle this industry problem without an in-depth study of current participation level of female professionals specifically in Quantity surveying. This gap in knowledge is what this paper intends to fill. The aim of this paper is to examine female Quantity Surveyors participation in the construction industry with the view of identifying strategies that can be applied in improving the level of female quantity surveyors' participation.

The Quantity Surveying Profession

The history and origins of quantity surveyors according to Timothy and Olaleke (2016) have been traced back to the ancient Egyptian civilization that used dedicated personnel to carry out estimates and costing for

their magnificent structures and buildings. It became an occupation during the 17th-century restoration of London after the Great Fire. In 1836, the profession entered its new age when the new Houses of Parliament of Great Britain, designed by Sir Charles Barry, became the first major public contract to be fully measured and tendered using detailed bills of quantities for financial accountability (Royal Institute of Chartered Surveyors (RICS), 2005).

The quantity surveying profession has gained international recognition through construction professional organizations such as RICS and Quantity Surveyors International (QSI) (Joel, 2016). In Nigeria the activities of Quantity Surveyors are regulated by the Nigerian Institute of Quantity Surveyors (NIQS), which was founded in 1969 by a group of Nigerians who trained, qualified and practiced in the United Kingdom. The Regulated and other Professions (Miscellaneous Provisions) Act of 1978 recognised Quantity Surveying profession as one of the scheduled Professions while the Decree No.31 of 1986 gave legal backing and recognition to the Quantity Surveying profession and set up the Quantity Surveyors Registration Board of Nigeria (QSRBN) to regulate the Profession. The Quantity Surveying profession is thus practiced in Nigeria along the same pattern as in the United Kingdom and other Commonwealth countries. In non-Commonwealth countries quantity surveying functions are still performed but described by various names. Since the late 90s, the Nigerian Institute of Quantity Surveyors (NIQS) has been a member of the International Cost Engineering Council (ICEC). Thus, the role is universal.

Quantity Surveyors' Skill and Competence

According to Hay (2015) studies have revealed that women are considered to have special skills to contribute to the construction industry and that women are interested in and capable of tackling a range of jobs that occur on and off the construction site (e.g. administration, offsite production and project management on site). From research carried out by Gurjao (2006) and Aja-Okorie (2013), it was observed that women remain disadvantaged gender-wise; such gender unfairness spans exclusion from policy making to labour market discriminations (Anugwom, 2009). The rating of Nigeria in the 2012 Gender Equality Index as 118th out of 134 countries considered reveals the extent of existing disparities.

Jaafar *et al.* (2016) investigated the level of duties and competencies of female Qs in the Malaysian construction industry and discovered that many studies have focused on women who are employed in the construction industry; however only a limited number of these studies have specifically investigated the actual involvement of women. In the construction industry, the issue of competencies expected from quantity surveyors (Qs) remains on the research agenda (Dada & Jagboro, 2012). Findings from Jaafar *et al.* (2016) indicated that

female QSs are fairly competent in six mandatory competencies as well as six core competencies.

Table 1: Competency level of female QSs

S/Nr	Type of Competencies	Competency level
Mandatory		
1	Conduct rules, ethics and professional practice	Fair
2	Client Care	Fair
3	Communication and negotiation	Fair
4	Health and safety	
5	Accounting principles and procedures	
6	Business planning	
7	Conflict avoidance, management and dispute resolution procedures	Fair
8	Data management	Fair
9	Sustainability	
10	Team working	Fair
Core		
11	Commercial management of construction or Design economics and cost planning	Fair
12	Contract practice	Fair
13	Construction technology and environmental services	Fair
14	Procurement and tendering	Fair
15	Project financial control and reporting	Fair
16	Quantification and costing of construction works	Fair
Optional		
17	Building information modelling (BIM) management	
18	Capital allowances	
19	Commercial management of construction or Design economics and cost planning	Generally more than 'basic' level but below 'expert' level
20	Contract administration	
21	Corporate recovery and insolvency	
22	Due diligence	
23	Insurance	
24	Programming and planning	
25	Project evaluation	
26	Risk management	
27	Conflict avoidance, management and dispute resolution procedures or Sustainability	

Sources: RICS (2015); Jaafar *et al.* (2016)

Note: Blank spaces in third column indicate 'below average competency levels'

When optional competencies are considered, female QSs are advanced in performing traditional QS activities and are also deemed experts in documentation, particularly in drafting bills of quantities and measurements. Female QSs also have more than a basic knowledge in performing evolved activities but not to the point of experts. Transformative industry trends like BIM and integrated project delivery require quantity surveyors to draw upon different skills than just the traditional ones (Wu and Issa, 2013).

Challenges faced by practicing female Quantity Surveyors

The Royal Institute of Chartered Surveyors (RICS) noted that of their 100,000 Chartered surveyors worldwide, only 10 per cent are female (Ellison, 2003). The under representation of women in construction is not confined to Nigeria; globally, women face a variety of barriers in the labour market such as societal perceptions, work-life balance issues, glass ceiling and a low skill set. Much of the literature on gender discrimination in the labour market focuses on the lack of education, societal perceptions, the glass ceiling, the queen bee syndrome and work-life balance issues, especially for women aspiring to positions of leadership (Mathur-Helm, 2011; English and LeJeune, 2012). The results obtained from a study of industry stakeholders by Madikizela and Haupt (2010) revealed that most of the few women employed by construction firms each year were assigned secretarial and administrative roles.

The perceived male-dominated nature of the construction industry and family commitments such as marriage and childbirth are responsible for the underrepresentation of females. The findings from some nine selected studies on female participation in the Nigeria construction industry are summarized in Table 2. Overall, the studies show that the gender unfairness situation in Nigeria is similar to what obtains in other parts of the world, most especially the developing world.

Table 2: FINDINGS ON FEMALE PARTICIPATION IN NIGERIA

Authors	Year	Summary of findings
Odubiyi	2018	Vocational jobbing by professional female construction workers might pose a threat to female population in the construction industry.
Afolabi <i>et al.</i>	2018	Identified barriers can guide policies on attracting, retaining and exploring the capabilities of women in green jobs.
Tunji-Olayeni <i>et al.</i>	2017	Suggested adequate career counseling and exposure to female role models to give females opportunity to demonstrate their skill and aptitude.

Authors	Year	Summary of findings
Jimoh <i>et al.</i>	2016	The barriers/constraints that prevent women's entry into the construction industry are of high impact.
Adogbo <i>et al.</i>	2015	family responsibility posed the greatest barrier to female participation in the construction industry.
Obamiro and Obasan	2013	Low participation in construction by women begins with choice of course, education and continues throughout recruitment process.
Adogbo <i>et al.</i>	2013	Marriage, societal culture and religious affiliations influence the choice of whether to continue in construction professions.
Dada	2011	Relative to men, women enrolment in construction disciplines over a ten year period was extremely low.
Adeyemi <i>et al.</i>	2004	Only 16.3% of the construction industry workforce is female. Approximately 50% of these women are employed as laborers, 37.5% as administrative staff, 10% as management staff and 2.5% as craftsmen.

According to Dada (2017), who worked on factors affecting women's enrolment in construction education in Nigeria, in his study rated the "lack of female role model to emulate", as the highest rating factor affecting women's enrolment in construction education. This revelation is not surprising as previous researchers have established that fewer than 5 per cent of Nigerian women are managers. Another important factor is the perception that construction is not suitable for women and is invariably meant for men. This finding agrees with Loosemore and Galea (2008) study which viewed the construction industry as a male-dominated and threatening environment, with an ingrained culture characterized by masculinity, conflict and crisis. However Mohammaden (2013) established that there exists equal opportunity for both male and female genders in the industry because 66% of construction organizations that were surveyed accord women equal chance as men in office work, 48% allow women the same opportunities as men in tasks on site, 22% provide separate facilities to women, 48% of organizations have a distinct and clear policy on non-discrimination when hiring, training and gathering information on the basis of gender, 96% of organizations give females opportunities to get promoted within the structure of the company's organization.

Future prospects of female Quantity Surveyors

Professions must evolve in response to the ever-increasing changes in the global business environment; quantity surveying is no exception. It requires urgent and far-reaching strategic transformation if it is to survive and remain relevant (Frei and Mbachu, 2009). In providing best value to project owners, quantity surveyors (QS) determine cost estimates of projects and ensure that construction activities are executed in a manner that satisfy the project owner's needs (Joel, 2016). The advancement of females in the quantity surveying profession will depend on their ability to respond to the variations in the international construction business environment. QSs, including female QSs will need to make adjustments in areas such as professional ethics, practices, and overall level of expertise (Frei & Mbachu, 2010). There is no doubt that quantity surveyors' jobs will change in the coming years owing to arrival of new innovations; technological advances will however not lessen the demand for quantity surveyors. Rather it will create more room for quantity surveyors to expand their skills.

2 METHODOLOGY

This study is concerned with the participation of women quantity surveyors (WQS) in the Nigerian construction Industry (NCI). From anecdotal as well as documentary evidence (for example Oyewobi and Adeneye, 2016), WQS are in a very noticeable minority in the industry. To understand why this is so, it will be necessary to seek out members of this very noticeable minority to collect information that can help in answering the research questions.

While a questionnaire survey will provide a wider reach at relatively low cost in terms of time and effort, employing a mixed methods research design, which will pursue the research objectives using both questionnaire survey and interview will be more advantageous.

This is because the interview phase of the study will permit the researcher to tap the deeper contextual issues that underlie the minority status of WQS in the NCI in a way that questionnaires cannot. A sequential mixed methods research design will allow further analysis of findings obtained from analysis of questionnaire survey data. A visual representation of the research design proposed for this study is presented in Figure 1. Mixed method research designs help to offset the weaknesses inherent in single method designs made up of either qualitative or quantitative method (Dunning *et al.*, 2008).

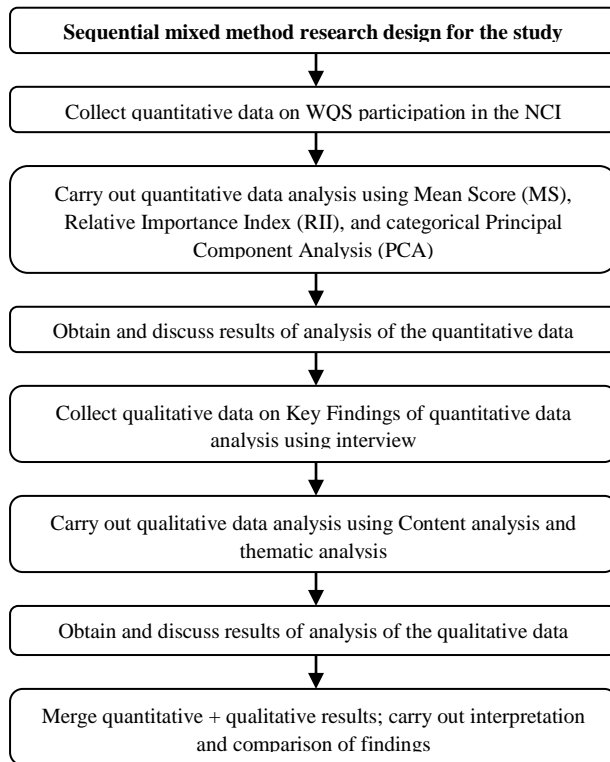


Figure 1: Proposed sequential mixed methods research design for the study

3 CONCLUSION

Through a review of related literature, this paper has brought to the fore the perception that the current image of the construction industry presents a strong barrier to the attraction of women into the industry in significant numbers. There is a need to change the image to focus on the good features of the industry. Although the general image of the industry is equated with site work and physical labour, it is a complex industry with many sub-sectors such as consultancy, design, manufacturing and supply (Gurgao, 2006). There is little realization that the industry is becoming high-tech, no longer simply requiring physical strength; it is more about mental strength, commitment and the determination to succeed (Ginige *et al.*, 2007).

It is expected that further development of this research through fieldwork and subsequent analysis of data will lead to the development of strategies that, if implemented, will help in improving the participation of women quantity surveyors in the Nigeria construction industry. It is proposed to employ a sequential mixed methods research design as a vehicle for delivery of the fieldwork phase of the research.

REFERENCE

Adeyemi, A. Y., Ojo, S. O., Aina, O. O., & Olanipekun, E. A. (2006). Empirical evidence of women under-

representation in the construction industry in Nigeria. *Women in Management Review*, 21(7), 567-577.

- Adogbo, K. J, Ibrahim, A. D. & Ibrahim, Y. M. (2013). Perceptions of final-year female undergraduates on their propensity to participate in construction practice In: Laryea, S. and Agyepong, S. (Eds) *Procs 5th West Africa Built Environment Research (WABER) Conference*, 12-14 August 2013, Accra, Ghana, 843-855.
- Adogbo, K. J., Ibrahim, A. D., & Ibrahim, Y. M. (2015). Development of a framework for attracting and retaining women in construction practice. *Journal of construction in Developing Countries*, 20(1), 99.
- Afolabi, A. O., Ojelabi, R. A., Tunji-Olayeni, P. F., Fagbenle, O. I. & Mosaku, T. O. (2018). Survey datasets on women participation in green jobs in the construction industry. *Data in Brief* 17 856–862
- Afolabi, A.O., Tunji Olayeni, P.F., Oyeyipo, O.O., & Ojelabi, R.A. (2018). The Socio-Economics of Women Inclusion in Green Construction. *Construction Economics and Building*, 17(1).
- Aguele, L. I., & Agwagah, U. N. (2007). Female participation in science, technology and mathematics (STM) education in Nigeria and national development. *Journal of social sciences*, 15(2), 121-126.
- Aja-Okorie, U. (2013). Women education in Nigeria: Problems and implications for family role and stability. *European Scientific Journal*, 9(28).
- Anugwom, E. E. (2009). Women, education and work in Nigeria. *Educational Research and Reviews*, 4(4), 127-134.
- Dada, J. O., & Jagboro, G. O. (2012). Core skills requirement and competencies expected of quantity surveyors: perspectives from quantity surveyors, allied professionals and clients in Nigeria. *Construction Economics and Building*, 12(4), 78-90.
- Dada, J.O (2017). factors affecting women’s enrolment in construction education in Nigeria. *Journal of Construction Project Management and Innovation* 7(1), 1893-1907.
- Dada, J.O. (2011) Factors affecting women enrolment in construction education in Nigeria. In: Laryea, S., Leiringer, R. and Hughes, W. (Eds) *Procs West Africa Built Environment Research (WABER) Conference*, 19-21 July 2011, Accra, Ghana, 453-464.
- Dunning, H., Williams, A., Abonyi, S., & Crooks, V. (2008). A mixed method approach to quality of life research: A case study approach. *Social indicators research*, 85(1), 145-158.
- Ellison, L. (2003), Raising the ratio: the surveying profession as a career, Report for the RICS Raising the Ratio Committee, Kingston University, Upon Thames.
- English, J. and Le Jeune, K. (2012), Do professional women and tradeswomen in the South African construction industry share common employment



- barriers, despite progressive government legislation?", *Journal of Professional Issues in Engineering Education and Practise*, 38(2), 145-191.
- Fadason, R.T., Chitumu, D.Z., & Buba, S.G. (2017) Repositioning the Nigerian Quantity Surveyor for global competitiveness in infrastructure development. Paper presented at Quantity Surveyors Registration Board Of Nigeria (QSRBN) 7th Building And Construction Economic Roundtable (Bcert7)
- Frei, M., & Mbachu, J. (2009). The future of quantity surveying in New Zealand: Likely changes, threats and opportunities. In *13th Pacific Association of Quantity Surveyors Congress*.
- Frei, M., & Mbachu, J. (2010). Toward a Strategic Framework for Australasian Construction Cost Management Organizations. In *7th International Cost Engineering Council World Congress and the 14th Pacific Association of Quantity Surveyors Congress*.
- Frei, M., Mbachu, J., & Phipps, R. (2013). Critical success factors, opportunities and threats of the cost management profession: the case of Australasian quantity surveying firms. *International Journal of Project Organization and Management* 7, 5(1-2), 4-24.
- Ginige, K N, Amaratunga, R D G & Haigh, R (2007). Improving construction industry image to enhance women representation in the industry workforce. In: Boyd, D (Ed) *Procs 23rd Built Environment Education Conference*
- Gurjao, S. (2006), *Inclusivity: The Changing Role of Women in the Construction Workforce*. The Chartered Institute of Building (CIOB), London.
- Hay, J. E. P., (2015). "Black South African women in construction: cues for success", *Journal of Engineering, Design and Technology*, 13(1), 144 – 164.
- Jaafar, M., Jalali, A., & Sini, N. M. (2016). Assessing the duties and competencies of female quantity surveyors. *Asian Social Science*, 12(1), 129.
- Jaafar, M., Puteri Yazrin, M. Y., Nuruddin, A. R., & Jalali, A. (2014). How women quantity surveyors perceive job satisfaction and turnover intention. *International Journal of business and entrepreneurship*, 4(1), 1-19.
- Jimoh, R. A., Oyewobi, L. O., Adamu, A. N., & Bajere, P. A. (2016). Women professionals' participation in the Nigerian construction industry: finding voice for the voiceless. *Organization, technology & management in construction: an international journal*, 8(1), 1429-1436.
- Joel, O.W., (2016). Predicting the future of quantity surveying profession in the construction industry. *Journal of Construction Project Management and Innovation* (1), 1363-1374.
- Kamaruddeen, A.M, Khalid, K.N, & Wahi, W.(undated). Factors influencing females' work in the construction companies. *Journal of social sciences and humanity*. 16(3) 1-9.
- Lenard, D. (2000). Future Challenges in Cost Engineering: Creating Cultural Change Through the Development of Core Competencies. In R. H. Harbuck (Ed.), 2000 AACE International transactions: 44th annual meeting of AACE international. Morgantown, West Virginia, USA: AACE international.
- Loosemore, M., & Galea, N. (2008). Genderlect and conflict in the Australian construction industry. *Construction management and economics*, 26(2), 125-135.
- Mohd Shafiei, M.W. & Said, I. (2008). The Competency Requirements for Quantity Surveyors: Enhancing Continuous Professional Development. *Sri Lankan Journal of Human Resource Management*. 2(1)
- Madikizela, K. & Haupt, T. (2010). "Influences on women's choices of careers in construction: a South African study", *Australasian Journal of Construction Economics and Building*, 10(1), 1-15.
- Mathur-Helm, B. (2011). "Women in management in South Africa", in Davidson, M.J. and Burke, R.J. (Eds), *Women in Management Worldwide: Progress and Prospects*, 2nd ed., Gower Applied Business Research, London, 339-358.
- Mohammaden, A. H. (2013). Factors affecting women career choice: comparison between civil engineering and other engineering disciplines. Ph.D. Thesis, The Islamic University, Gaza
- Obamiro, J. K. O. & Obasan K. O. (2013). Glass ceiling and women career advancement: Evidence from Nigerian construction industry. *Iranian Journal of Management Studies*, 6(1), 77-97.
- Odubiyi, T. B. (2018). Nigerian Professional Female Construction Workers in Vocational Occupations: Diversification or Deviation? *Organization, Technology and Management in Construction*; 10: 1696–1703
- Oyewobi, L. O. and Adeneye, T. D. (2016). Work-Life Balance Among Women Construction Workers: A Conceptual Approach. *Procs of School of Environmental Technology Conference, SETIC 2016*, Minna, Nigeria.
- Royal Institute of Chartered Surveyors (RICS) (2005). Website, <http://www.rics.org> [Accessed on the 5th of October 2006].
- Royal Institution of Chartered Surveyors (2015). Assessment of Professional Competence - Quantity Surveying and Construction. Website, <http://www.rics.org> [Accessed on the 5th of July 2016]
- Timothy O. O and Olaleke A. A (2016). Are Quantity Surveyors competent to value for civil engineering works? Evaluating QSs' competencies and militating factors. *Journal of Education and Practice* 7(16), 2016.



- Tunji-Olayeni, P.F, Owolabi. J. D, Amusan, L. M, and Nduka, D.O (2018). Job satisfaction of female construction professionals in male dominated fields. *International Journal of Mechanical Engineering and Technology (IJMET)*. 9(1). 732–738.
- Tunji-Olayeni, P. F., Afolabi, A. O., Omuh, I. O., Ojelabi, R. A., Amusan, L. M. and Ogundipe, K. E. (2017). Attracting and retaining female students in construction related programs. *Turkish Online Journal of Educational Technology*; Special Issue for INTE 2017; 425-430.
- Wu, W., & Issa, R. R. (2013). Impacts of BIM on talent acquisition in the construction industry. In *Proc., 29th Annual ARCOM Conference*. 35-45.



Performance Evaluation of WUPA Wastewater Treatment Plant Idu-Industrial Area, Abuja

Saidu, M¹, *Adesiji, A. R¹, Asogwa, E.O¹, Jiya, A.M¹ and Haruna, S.I²

¹Department of Civil Engineering, Federal University of Technology, PMB 65, Minna Niger State, Nigeria

²Department of Water Resources and Environmental Engineering Ahmadu Bello University Zaria.

*Corresponding Author: email: adrichard01@yahoo.co.uk Phone: +2348060913106.

ABSTRACT

This paper evaluates the performance efficiency of WUPA waste water treatment plant. Wastewater samples were collected and monitored in the raw influents, primary effluents and final treated effluents at three different locations of WUPA waste water treatment plant using standard methods for physiochemical characteristic analysis. The results revealed that the average concentrations of DO, BOD₅²⁰, COD, TSS, TDS, NH₄^{-N}, NO₃^{-N} and PO₄^{-P} in the final effluent of WUPA WWTP were 6.7, 22, 50, 13.1, 20, 3.8, 2.73, and 2.4 mg/L respectively and that of electrical conductivity, temperature and pH are 271 μ s (cm), 25.1% and 7.42 respectively which fell within the standard recommended by WHO for effluent discharged into water bodies. Values of TDS and NO₃^{-N} however increase from the raw influent to the final treated effluent instead of decreasing which shows the inefficiencies of the system to effectively reduce the concentration of these parameters. The average removal efficiencies of BOD₅²⁰, COD, TSS and NH₄^{-N} were found to be 87.28%, 85.88%, 91.44% and 38.71% respectively. The effect of the final treated effluent on the water quality of WUPA river was also determined by analyzing the physiochemical characteristic of the surface water sample collected at two sampling locations 30m away upstream from the discharge point before the effluent meets the river water (S₄) and 30m away downstream from the exist point after the effluent meets the river water (S₅). Though there were slight increases in the concentrations of the most parameters downstream after the effluent meets the WUPA River, the study has revealed that there was no adverse effect on the physiochemical characteristics of the receiving water.

Keywords: *Effluent, influent, river water, wastewater, water treatment plant*

1 INTRODUCTION

Fresh accessible water is a scarce and unevenly distributed resource, not matching patterns of human development. Because it plays a vital role in the sustenance of all life, water is a source of economic and political power (Narasimhan, 2008). However, it is not right to discharge contaminated water back into the environment which can be a source of pollution to the water at the downstream (Ado et al., 2015; Proia et al., 2016; Eunice et al., 2017). As water travels through the hydrological system from the upstream to the sea, the activities of human society capture, divert and extract, treat and reuse water to sustain communities and economies throughout the watershed (industrial, agricultural and municipal) (Izah et al., 2016; Oribhabor, 2016; Seiyaboh & Izah, 2017). These activities however, do not return the water they extract in the same condition. Unmanaged waste water can be a source of pollution, a hazard for the health of human populations and the environment like (Fattoruso et al., 2015; Onifade et al., 2015; Ogunjuyigbe et al., 2017). Wastewater can be contaminated with a myriad of different compounds pathogens, organic compounds, synthetic chemicals nutrients, organic matter and heavy metals (Naveen et al., 2017). They are either in solution or particulate matter and are carried along in the water from different source and affect water quality. These components can have bio-

cumulative and persistence characteristics affecting ecosystem human health and food production. Harder et al. (2019) defined wastewater as a combination of one or more domestic effluent consisting of black water (excreta, urine and fecal sludge) and grey water (kitchen and bathing waste water). Wastewater is also defined as the spent or used water of a community or industry which contains dissolved and suspended matter (Rana et al., 2017). Even though nature has an amazing ability to cope with certain amount of contaminants, there is a necessity to treat the billion gallons of wastewater and sewage generated daily by homes, business establishments and industries before releasing back to the environment.

The effluent discharged into the receiving water bodies which serves as a source of water to some communities downstream is used for variety of purposes. The need to know the quality of the effluent discharged through the appraisal of the waste water treatment plant informed this study. This study therefore, is undertaken to evaluate performance efficiency of a waste water treatment plant located at WUPA, Idu-industrial district, Abuja-Nigeria, operating on biological treatment method (activated sludge process). The objective is to analyze the effluent collected from three sampling locations and compare the final treated effluents with WHO standards. The second objective is to analyze the physiochemical parameters of the water sample

collected from upstream and downstream and compare to WHO standards.

2 METHODOLOGY

2.1 DESCRIPTION OF STUDY AREA

The study area is WUPA sewage treatment plant, located in Idu-industrial layout, Abuja-Nigeria it covers an area of 297,960 square meters and is designed to meet the requirements of 700,000 population's equivalent meaning that the plant can accommodate an annual dry weather inflow of 5,500 cubic meters per day. It lies between longitude 7°8'20.33 and latitude 9°2'14.46'' respectively the WUPA sewage treatment plant Abuja is designed for F.C.T to handle waste water generated by 700,000 populations equivalent and expandable to 1,000,000 populations equivalent on an average domestic waste water of 230 l/c/d.

2.2 DATA COLLECTION AND SAMPLING

According to Kumar et al. (2010), there is no truer sign of civilization and culture than good sanitation. The entire treatment process can be divided into mechanical and biological phases. WUPA sewage treatment plant performs its two main operations in the treatment process as follows unit operations; which involves the raw sewage (influent) undergoing physical treatment from the intake structure to the screen and grease chambers. The practically treated sewage then goes to the distribution well for transport to next stage of operation, and unit process; which involves the biological treatment of the pre-treated sewage by ensuring an unlimited supply of oxygen to facilitate aerobic microbial biodegrading activity. This microbial activity takes place in the aeration tank after which the sewage is transported to the clarifiers (sedimentation tank) where the effluent would be ready for disinfection before final discharge to the stream. Sludge formed at the clarifiers is then collected and transported to the dewatering house from where it is concentrated and later sent to the drying beds before it is used as manure. Part of the sludge in the clarifier would be recycled to the aeration tank in order to maintain adequate food to micro organisms

Sampling design and data collections were carried out once in a week from WUPA waste water treatment plant for 4 weeks at the three different sampling points. This involves collection of samples in a well labeled clean plastic container that was rinsed with distilled water prior to collection.

The samples, were analyzed to determine parameters like; pH, BOD₅, COD, TDS, TSS, NH₄-N, NO₃-N, and PO₄P, according to the procedure outlined in standards methods for examination of water and waste water APHA (1998).

The three different sampling locations or units of the treatment plant where waste water samples were collected are as below;

- influent to the plant S₁
- effluent to aerobic tank S₂ and
- final effluent from secondary clarifiers (S₃)

The overall efficiency of the plant was estimated from the formula:

$$\text{Removal efficiency} = \frac{\text{Influent}(mg/l) - \text{Effluent}(mg/l)}{\text{Influent}(mg/l)} \times 100 \quad (1)$$

Sampling water at WUPA River was conducted to establish short-term relationship between the physiochemical characteristics of the river and the final treated effluent from the WWTP. Samples were collected from WUPA River at two different sampling locations which are as follows;

- The upstream point (stream before meeting the effluent) S₄
- and downstream at the point (effluent and stream at the point of use) S₅

2.3 PHYSIOCHEMICAL ANALYSIS

The total suspended solids, total dissolved solids, and biochemical oxygen demand, were calculated thus;

$$TSS = \left(\frac{A-B}{\text{Sample volume}} \right) \times 1000 \left(\frac{mg}{l} \right) \quad (2)$$

where

A = weight of filter paper and solids(mg),

B=weight of cooled filter paper(mg), V=volume(ml).

$$TDS = \left(\frac{B-A}{\text{sample volume}} \right) \times 1000 \left(\frac{mg}{l} \right) \quad (3)$$

where

A=the weight of the evaporating dish only,

B= the weight of the evaporating dish and solids.

$$BOD(5) = \left(\frac{D_1-D_2}{P} \right) \left(\frac{mg}{l} \right) \quad (4)$$

where

D₁ = dissolved oxygen of sample immediately after preparation,

D₂ = dissolved oxygen of sample after 5days at 20°C,

P = decimal volumetric fraction of sample used.

The pH was calculated by conducting a test on site using a multi-purpose meter. A calibrated pH meter Probe was submerged in a sample of the effluent and was stirred gently for a few moments and the pH meter gave a stable pH reading. The concentration of the chemical oxygen

demand (COD) was measured in a photometer. The determination of phosphate (PO_4^{P}) was carried out using calorimetric method and was determined using photometer (palintest photometer 7100). This same method was used in the determination of ammonium as nitrogen (NH_4^{N}) and nitrate (NO_3^{N}).

3 RESULTS AND DISCUSSION

The results obtained from physiochemical analysis of effluents from three different sampling locations are summarized in Table 1. The pH of the water samples ranged from 6.99 in S_2 to 7.49 in S_1 as shown in Table 1. Both COD and BOD_5 were reduced to meet the WHO Standards as the analysis made on S_3 gave a reduced value compared to the analysis on S_1 and S_2 . This showed the efficiency of the treatment plant. Same pattern was recorded on other parameters like Temperature, Total Suspended Solids, TSS, Total Dissolved Solids, TDS, Ammonium ions, Potassium ions, with the exception of Nitrate ions, Dissolved Oxygen, and Electrical Conductivity

TABLE1: AVERAGE PARAMETERS CHARACTERIZED AT DIFFERENT SAMPLING LOCATION COMPARED WITH PERMISSIBLE LIMIT OF WHO

PARAMETERS	SAMPLING LOCATION			
	(S ₁)	(S ₂)	(S ₃)	WHO Value
pH	7.49	6.99	7.42	6.0-9.0
COD (mg/l)	354	317	50	100
BOD ₅ (mg/l)	173	158	22	30
TSS (mg/l)	153	141	13.1	30
TDS (mg/l)	193	198	201	500
NH ₄ (mg/l)	6.2	5.9	3.8	10
NO ₃ (mg/l)	1.69	1.67	2.73	2.0
PO ₄ (mg/l)	3.3	3.1	2.4	5
DO	2.0	4.7	7.7	7.0-10.0
EC	263	273	271	1250
TEMP	26.9	25.5	25.1	< 40 °C

S_1 = RAW INFLUENT; S_2 = PRIMARY INFLUENT; S_3 = FINAL TREATED EFFLUENT

3.1 ASSESSMENT OF WATER SAMPLES FROM WUPA RIVER

The physiochemical parameters (pH, conductivity temperature, total suspended solids total dissolved solids, COD, $\text{NO}_3\text{-N}$, $\text{NH}_4\text{-N}$ $\text{PO}_4\text{-P}$, dissolved oxygen (DO) and BOD_5) were analyzed. The result indicated that all the parameters at the downstream and upstream point showed conformity with the WHO standards as shown in the Table 2.

TABLE 2: PARAMETERS CHARACTERIZED AT UPSTREAM AND DOWNSTREAM OF THE WUPA RIVER WITH WHO STANDARDS

PARAMETER	UPSTREAM	DOWNST REAM	W.H.O MAXIMUM PERMISSIBL E LIMIT
TDS (mg/l)	152	155	560
Temperature o	30.7	30.9	Less than 40 °C.
Conductivity (μs/cm)	227	232	1250
Dissolved Oxygen (mg/l)	6.23	5.70	700-10.0
Suspended Solid (mg/l)	3	6	30
BOD ₅ (mg/l)	0	1	30
COD (mg/l)	0	3	100
Nitrogen (mg/l)	1.63	1.67	20
Phosphate (mg/l)	0.45	0.68	5
Ammonia as Nitrogen (mg/l)	0.67	0.69	10
pH	7.38	7.41	6.5-8.5

3.2 REMOVAL EFFICIENCY

The performance of WUPA WWTP in terms of removal efficiency (%) in the pollution parameters is given in Table 3. The removal efficiencies of different units in terms of average TSS, COD, BOD_5 , and $\text{NH}_4\text{-N}$ were determined. The reduction in COD (85.88%), BOD_5 (87.28%) and TSS (91.44%) which is within the required range of 85-100% confirms the efficiency of the secondary clarifiers. But the reduction in $\text{NH}_4\text{-N}$ (38.71%) dropped below the normal limit.

TABLE 3: REMOVAL EFFICIENCY OF THE DIFFERENT SAMPLING LOCATION OF WUPA WWTP

	BOD (%)	COD (%)	TSS (%)	NH ₄ ^N
(S ₁ -S ₂)	8.67	10.45	7.84	4.84
(S ₂ -S ₃)	86.08	84.23	90.71	35.59
(S ₁ -S ₃)	87.28	85.88	91.44	38.71

4 CONCLUSION

Performance evaluation of WUPA waste water treatment plant in Idu Industrial area in Abuja, FCT has been studied. That WUPA WWTP achieved higher percentages in terms of removal efficiencies for most parameters and the overall efficiency is in the order $\text{NH}_4\text{-N} < \text{COD} < \text{BOD}_5 < \text{TSS}$. The effluent qualities met the



acceptable standards outlined by WHO for effluents to be discharged into water bodies which are critical to the provision of clean and safe water. The analysis revealed that parameters such as BOD₅²⁰, COD, TSS, NH₄-N, PO₄-P, E.C, PH, temperature and DO in the final treated effluent when compared with the standards were found mostly within the limits set by world health organization. TDS and NO₃-N in the final treated effluent also fell within the standard but their values increase from raw influent to final treated effluent instead of decreasing which shows the inefficiency of the system to effectively reduce the concentration of these parameters. The final treated effluent can be safely discharged in the receiving water bodies.

Downstream concentration of the physiochemical parameters increases slightly when compared with the upstream values after the final treated effluent was discharged into the river from the exits point, but the values are still within the standards recommended by WHO for drinking water. Therefore, it can be concluded that waste water effluents from WUPA WWTP have no much effect on the water qualities of WUPA River.

REFERENCES

- Ado, A., Tukur, A. I., Ladan, M., Gumel, S. M., Muhammad, A. A., Habibu, S., & Koki, I. B. (2015). A Review on Industrial Effluents as Major Sources of Water Pollution in Nigeria. *Chemistry Journal*, 1(5), 159-164.
- American Public Health Association (APHA), 1998. Standard methods for the examination of water and wastewater, 20th ed. APHA AWWA WPCF, Washington, DC.
- Eunice, O. E., Frank, O., Voke, U., & Godwin, A. (2017). Assessment of the impacts of refinery effluent on the physicochemical properties of Ubeji Creek, Delta State, Nigeria. *J Environ Anal Toxicol*, 7(428), 2161-0525.
- Fattoruso, G., Tebano, C., Agresta, A., Buonanno, A., De Rosa, L., De Vito, S., & Di Francia, G. (2015). Applying the SWE framework in smart water Utilities domain. In *Sensors* (pp. 321-325). Springer, Cham.
- Harder, R., Wielemaker, R., Larsen, T. A., Zeeman, G., & Öberg, G. (2019). Recycling nutrients contained in human excreta to agriculture: Pathways, processes, and products. *Critical Reviews in Environmental Science and Technology*, 49(8), 695-743.
- Izah, S. C., Chakrabarty, N., & Srivastav, A. L. (2016). A review on heavy metal concentration in potable water sources in Nigeria: Human health effects and mitigating measures. *Exposure and Health*, 8(2), 285-304.
- Onifade, T., Adeniran, K., & Ojo, O. (2015). Assessment of cassava waste effluent effect on some water sources in Ilorin, Nigeria. *Afr. J. Eng. Res*, 3, 56-68.
- Ogunjuyigbe, A. S. O., Ayodele, T. R., & Alao, M. A. (2017). Electricity generation from municipal solid waste in some selected cities of Nigeria: An assessment of feasibility, potential and technologies. *Renewable and Sustainable Energy Reviews*, 80, 149-162.
- Naveen, B. P., Mahapatra, D. M., Sitharam, T. G., Sivapullaiah, P. V., & Ramachandra, T. V. (2017). Physico-chemical and biological characterization of urban municipal landfill leachate. *Environmental Pollution*, 220, 1-12.
- Oribhabor, B. J. (2016). Impact of human activities on biodiversity in Nigerian aquatic ecosystems. *Science International*, 4(1), 12-20.
- Proia, L., von Schiller, D., Sánchez-Melsió, A., Sabater, S., Borrego, C. M., Rodríguez-Mozaz, S., & Balcázar, J. L. (2016). Occurrence and persistence of antibiotic resistance genes in river biofilms after wastewater inputs in small rivers. *Environmental pollution*, 210, 121-128.
- Rana, R. S., Singh, P., Kandari, V., Singh, R., Dobhal, R., & Gupta, S. (2017). A review on characterization and bioremediation of pharmaceutical industries' wastewater: an Indian perspective. *Applied Water Science*, 7(1), 1-12.
- Narasimhan, T. N. (2008). Water, law, science. *Journal of hydrology*, 349(1-2), 125-138.
- Kumar, K. S., Kumar, P. S., & Babu, M. R. (2010). Performance evaluation of Waste water treatment plant. *International Journal of Engineering Science and Technology*, 2(12), 7785-7796.
- Seyiboh, E. I., & Izah, S. C. (2017). Review of impact of anthropogenic activities in surface water resources in the Niger Delta region of Nigeria: a case of Bayelsa State. *International Journal of Ecotoxicology and Ecobiology*, 2(2), 61-73.



Evaluation of Strength Characteristics of Compacted Deltaic *Chikoko* Clay Stabilized with Rice Husk Ash

T.W.E. Adejumo* and B. B. Olanipekun

Department of Civil Engineering, Federal University of Technology, Minna. Niger State, Nigeria.

* Corresponding author email: adejumo.taiye@futminna.edu.ng +2349033795541

ABSTRACT

One of the key parameters usually considered in soil improvement techniques is strength gain. *Chikoko* clay is a muddy weak clay soil commonly found along the coastal shelf Rivers, Bayelsa, Delta and other coastal states of Nigeria. Deltaic *chikoko* clay is a weak soil with low bearing capacity that requires some forms of stabilization and strength enhancement. *Chikoko* clay obtained from Eagle Island in Port Harcourt, Nigeria was stabilized with 2, 4, 6 and 8% of Rice Husk Ash. The engineering characteristics of Reduced British Light (RBL) compacted Deltaic *Chikoko* clay were assessed. Unconfined Compressive Strength (UCS) was taken after 7, 14 and 28 days curing. The UCS values decreased with increase in water content relative to optimum for the compactive efforts. Addition of Rice husk Ash from 4 – 6% increased the UCS of the compacted stabilized *chikoko* soil by 14.7%. However, further increase to 8% reduced the UCS by 8.5%. The UCS also decreased by 4.6% after 21 days curing. A maximum unconfined compressive strength (UCS) value of 152 kPa at 6% RHA corresponding to 17.8% increment was recorded. Optimal stabilization of Deltaic marine *chikoko* clay was achieved at 6% RHA. Stabilization of *chikoko* clay improved its unsoaked CBR value from 8.6% to 17.4%, thereby making the stabilized soil suitable for sub-grade application.

Keywords: *Chikoko soil, Compaction, Deltaic clay, Lateritic soil, Rice husk ash, Stabilization.*

1 INTRODUCTION

The quest for sustainable soil improvement methods has led researchers to the discovery of novel and innovative methods. Another emerging innovative method called microbial induced calcite precipitation (MICP), a multi-disciplinary studies that involve civil engineering, microbiology, chemical engineering and chemistry has found application in soil stabilization (Achal and Pan 2014; Dawoud *et al.*, 2014; Feng and Montoya, 2016; Hamdan *et al.*, 2011; 2016; Ijimdiya, 2017; Mujah *et al.*, 2019; Osinubi *et al.*, 2017; 2018; 2019). Research is still on going on modern soil improvement and stabilization and enhancements.

When building on soil with inadequate strength properties, the need to stabilize soil and enhance its properties becomes a necessity (Ogunsanwo, 1985). Working in marine and especially difficult terrain, right from the onset of planning any construction work, the necessity to enhance soil properties readily comes to mind. Lateritic soil is one of the most widely used filled or backfill material. Proper understanding of the geotechnical properties of this lateritic soil is therefore paramount in evaluating their performance when used as construction material (Atolagboye and Talabia, 2014).

Soil stabilization becomes an option when soil encountered is vast, and/or the process of replacement is uneconomical. In general, a stabilized soil is a composite material produced from combination and optimization of properties in individual constituent material (Basha *et al.*,

2005). The enhanced engineering properties of various soils, resulting from the usefulness of by-products including Agricultural wastes, bring about environmental and economic importance (Walid & Hariahan, 2010). It is way of converting what is presently being considered as waste into a productive use.

Several works have been done on the suitability or otherwise of Rice husk ash for soil stabilization. Alhassan & Mustapha (2007) examined cement stabilized lateritic soil; Alhassan (2008) studied potential of rice husk ash for soil stabilization; Otoko & Aitsebaomo, (2009); Otoko (2014); Otoko & Karibo (2014); Otoko & Onuoha (2015) studied the physical properties and engineering characteristics of Nigerian Deltaic clay (*Chikoko*) soil.

Rice husk, an agricultural waste is generated in a large quantity as rice crop is frequently produced and processed in a large scale in Ebonyi state and other parts of Nigeria. One of the common ways of improving such materials is by burning them to produce ash. This study is focused on the use of Rice husk ash to enhance the engineering properties of compacted stabilized Deltaic *Chikoko* clay soil.

2 MATERIALS AND METHODS

2.1 MATERIALS

Soil: The soil used in this study was collected using the disturbed sampling technique at depths of between 0.5 m and 2.0 metres from three clusters A, B and C from the

Eagle Island River behind the Rivers State University campus, Port Harcourt, Nigeria. It is a lateritic soil classified as CL and CH or A – 6, and A – 7 – 6 according to USC and AASHTO soil classification systems respectively.

Rice husk ash: The rice husk ash used in this research was sourced from Ebonyi State Mill, Abakaliki, Nigeria. The Rice husk were burnt to ashes and then sieved through sieve No 200 of the BS sieve to get very fine grain ash. It was thereafter stored in air tight containers to prevent moisture loss/gain and any form of contamination plate I.



Plate I: Rice Husk Ash Preparation

2.2 METHODS

Index properties: Natural moisture content, specific gravities, particle size analysis and Atterberg limits tests were conducted in accordance with tests procedures specified in BS 1377: 1990.

Compaction characteristics: Compaction of stabilized RHA-Chikoko clay specimens was conducted in accordance with the guidelines specified in BS 1377 (1990) to compute the required parameters. The reduced British Standard light (RBSL) compactive effort was used. The RBSL compaction is the energy resulting from 2.5 kg rammer falling through a height of 30 cm onto three layers, each receiving 15 blows.

Unconfined compressive strength (UCS): The UCS test was conducted in accordance with the procedure specified in BS, 1377: (1990). The treated specimens were prepared with RHA of 2, 4, 6 and 8 % relative to OMC and compacted with RBSL compactive energy. The compacted specimens were cured for 24 hours in the moulds before extrusion and trimming as well as further cured for another 7, 14, 21 and 28 days in the laboratory at temperature of $24 \pm 2^\circ\text{C}$. The average of six (6) crushed specimens was recorded and used for the computation of the unconfined compressive strength.

California bearing ratio (CBR): The unsoaked CBR of stabilized RHA-Chikoko clay specimens was conducted in accordance with the guidelines specified in BS 1377

(1990) to compute the required parameters as shown in Plate II. 6 kg of pulverized mixed samples divided to five parts were poured into CBR mould and rammed with 4.5 kg rammer into five layers, each receiving 62 blows. The attached upper and lower dial gauges measures the upper and lower penetrations of the plunger.



Plate II: California Bearing Ratio test of samples

3 RESULTS AND DISCUSSION

Index properties of the natural and treated soil:

The index properties of the natural and RHA-treated Chikoko clay soil are shown in Figure 1 and Table 1. The fraction passing No 200 sieve is 53.1%. The soil is classified as CL and CH or A – 6, A – 7 – 6 according to USC and AASHTO soil classification systems respectively (AASHTO, 1986; ASTM, 1992). The oxide composition of the soil is summarized in Table 2 indicates that the soil is lateritic with silica - sesquioxide ratio value {that is $\text{SiO}_2 / (\text{Al}_2\text{O}_3 + \text{Fe}_2\text{O}_3)$ } of 1.54 which is within the 1.33 – 2.00 threshold recommended for lateritic soils by Bell, (1993). X-Ray Diffraction (XRD) analysis of the sample shows that the dominant clay minerals are orthoclase, anorthite, anorthoclase and montmorillonite which are indicated in Table 3 and Figure 2.

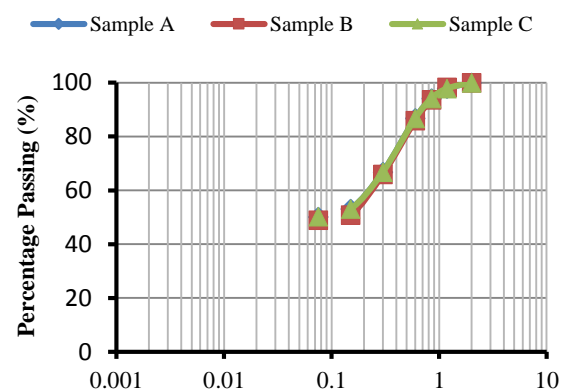


Figure 1: Sieve size analysis of deltaic chikoko clay

TABLE 1: PROPERTIES OF NATURAL DELTAIC CHIKOKO CLAY

Properties (Average)	Sample A	Sample B	Sample C
Specific gravity of soil	2.74	2.65	2.68
Natural moisture content (%)	29.0	29.6	30.6
Atterberg Limits			
Liquid limit (%)	37.5	32.8	44.5
Plastic limit (%)	25.7	20.5	26.13
Shrinkage limit (%)	9.64	9.21	10.0
Plasticity index	11.8	12.3	18.37
% Passing BS No. 200 sieve	51.9	52.7	54.7
Classification			
USCS	CL	CH	CH
AASHTO	A-6	A-6	A-7-6

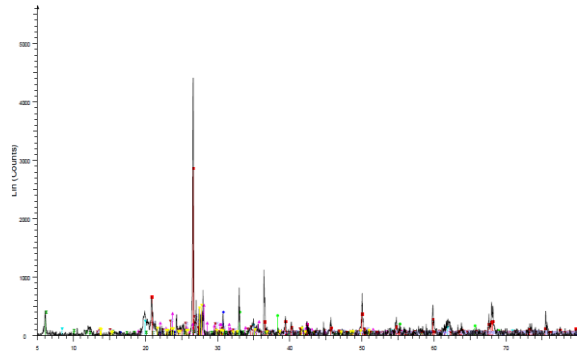


Figure 2: X-ray Diffraction of deltaic chikoko clay

TABLE 2: OXIDE COMPOSITION OF DELTAIC CHIKOKO CLAY

Chemical Constituent	Percentage Composition (%)
SiO ₂	31.6
Al ₂ O ₃	8.8
Fe ₂ O ₃	11.7
CaO	13.3
MgO	6.4
SO ₃	1.6
Na ₂ O	1.4
K ₂ O	1.1
TiO ₂	1.0
P ₂ O ₅	1.0

TABLE 3: MINERALOGICAL COMPOSITION OF DELTAIC CHIKOKO CLAY

Description	Quantity
Quartz (%)	50.00
Anorthite (%)	8.35
Calcium Silicide (%)	6.25
Montmorillonite (%)	8.23
Ankerite (%)	6.25
Sodium Aluminium/ Silicate Hydrate	6.25
Anothoclase	8.33
Orthoclase	10.07

Effect of curing age on UCS of *Chikoko* clay

The effect of curing age on unconfined compressive strength (UCS) of *chikoko* clay was investigated. It was observed that the unconfined compressive strength increased by 1.6% from 14 to 21 days curing age, and 2.3% from 21 to 28 days curing for specimens compacted at the reduced British Standard light (RBSL) energy level as shown in Figures 3 – 5. Also, it was noted that unconfined compressive strength increases with curing age.

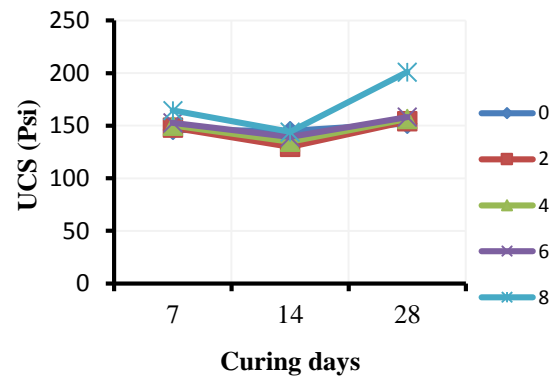


Figure 3: Variation of UCS values with curing days for Location A Samples

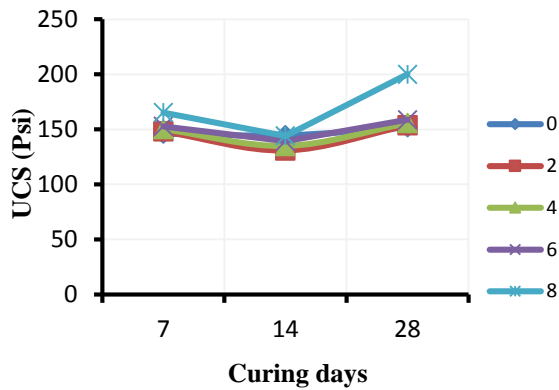


Figure 4: Variation of UCS values with curing days for Location B Samples

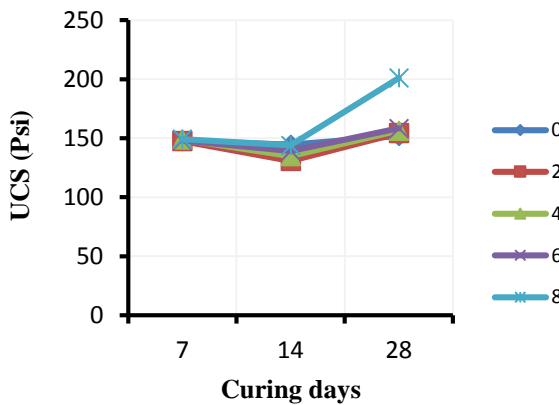


Figure 5: Variation of UCS values with curing days for Location C Samples

Effect of RHA addition on Compaction Characteristics of Chikoko clay

An increase in OMC of compacted stabilized *chikoko* clay was observed. This was due to the additional water required for wetting the large surface area of the fine rice husk ash particles Figures 6 - 10. The increase in OMC is also probably due 'to the additional water held within the flocculent soil structure due to excess water absorbed as a result of the porous property of rice husk ash. The decrease in MDD of all treated *chikoko* clay was due to the partial replacement of relatively heavy soils with light weight rice husk ash (with Specific gravity of 1.36). This decrease in density could also be influenced by increase in porosity of all compacted soil samples due to addition of rice husk ash. In addition, the decrease can also resulted from the flocculation and agglomeration of clay particles, caused by the cation exchange reaction, leading

corresponding increase in volume and decrease in dry' density as advanced by Lees *et al.*, (1982) and corroborated by the findings of Basha *et al.*, (2005).

Effect of RHA addition on UCS of Chikoko clay

The UCS values decreased with increase in water content relative to optimum for the compactive efforts. Addition of Rice husk Ash from 4 – 6% increased the UCS of the compacted stabilized *chikoko* soil by 14.7%. However, further increase to 8% reduced the UCS by 8.5%. The UCS also decreased by 4.6% after 21 days curing. A maximum unconfined compressive strength (UCS) value of 152 kPa at 6% RHA corresponding to 17.8% increment was recorded. Optimal stabilization of Deltaic marine clay was achieved at 6% RHA. Stabilization of *chikoko* clay improved its unsoaked CBR value from 8.6% to 17.4%.

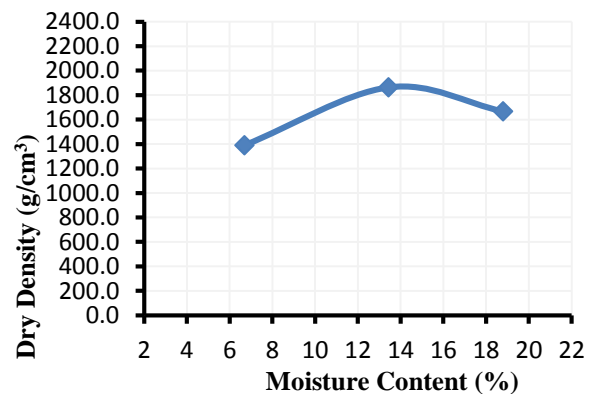


Figure 6: Compaction characteristics of stabilized *chikoko* clay 0% RHA

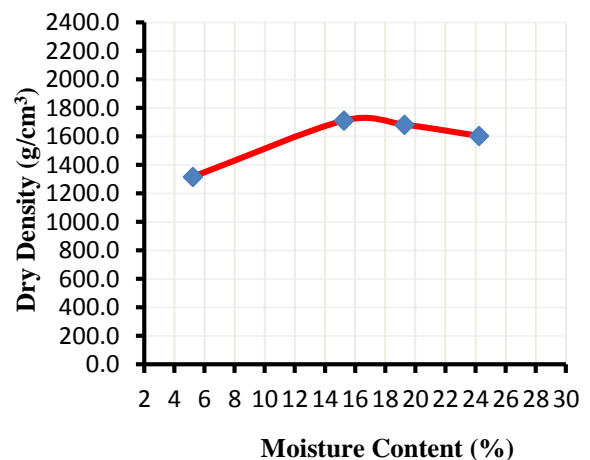


Figure 7: Compaction characteristics of stabilized *chikoko* clay 2% RHA

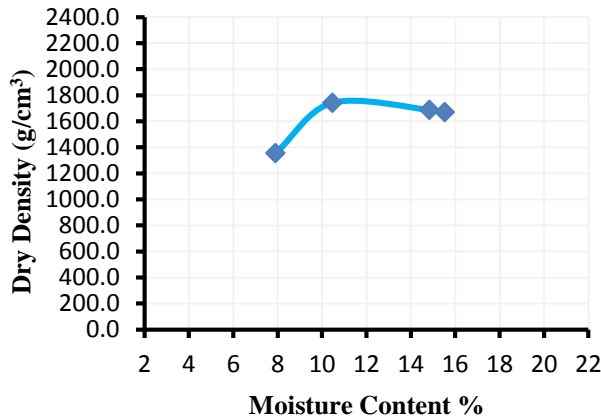


Figure 8: Compaction characteristics of stabilized *chikoko* clay with 4% RHA

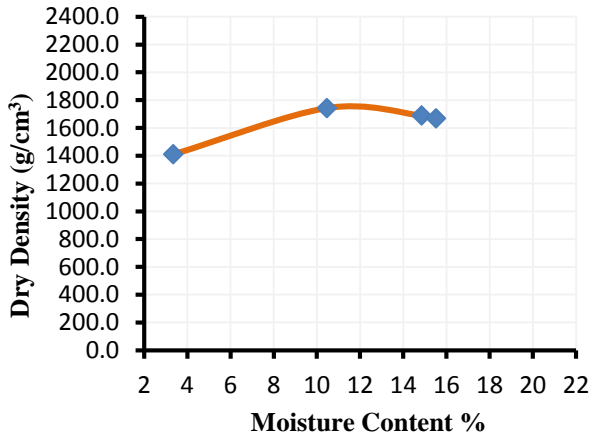


Figure 9: Compaction characteristics of stabilized *chikoko* soil with 6% RHA

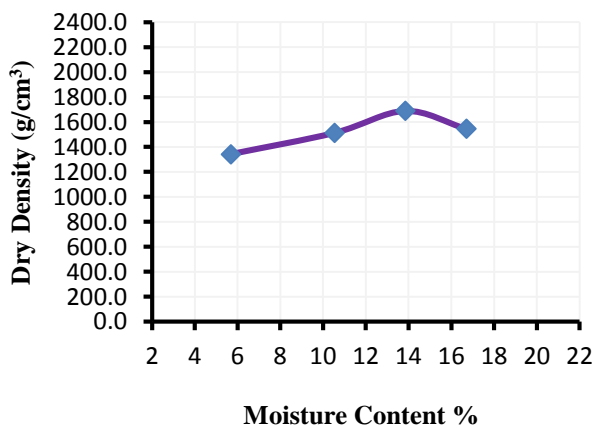


Figure 10: Compaction characteristics of stabilized *chikoko* soil with 8% RHA

Effect of RHA addition on CBR of *Chikoko* clay

Generally, a slight increase in CBR was observed for the RHA-stabilized *chikoko* clay specimens compacted at Reduced Standard Proctor energy steadily up to 6% after which it reduced. The effect of soaking on CBR values of the specimens can be seen in Figures 11 – 12. Soaking produced reduction and divergence in the CBR values of stabilized *chikoko* clay.

While unsoaked CBR of stabilized compacted *chikoko* soil from different locations exhibited similar pattern, soaking produced reduction and divergence in the CBR values of stabilized *chikoko* clay from the same locations. The unsoaked and soaked CBR values of all the soil samples increased considerably on stabilization with rice husk ash. This shows that the load bearing capacity of the soil increased with the stabilization mix. The increase in both the soaked and unsoaked CBR may be due to the availability of calcium from the ash for the cementations reaction with the silica and iron oxide from the *Chikoko* clay.

Optimal stabilization of Deltaic marine *chikoko* clay was achieved at 6% RHA. Stabilization of compacted *chikoko* clay improved its unsoaked CBR value from 8.6% to 17.4%, thereby making the stabilized soil suitable for sub-grade application.

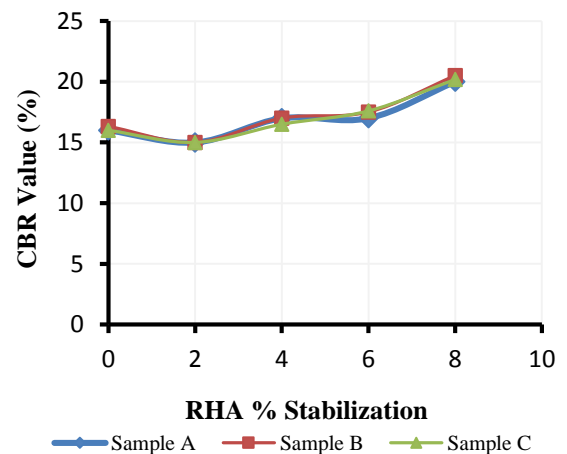


Figure 11: Variation of unsoaked C.B.R values for *Chikoko* clay Sample

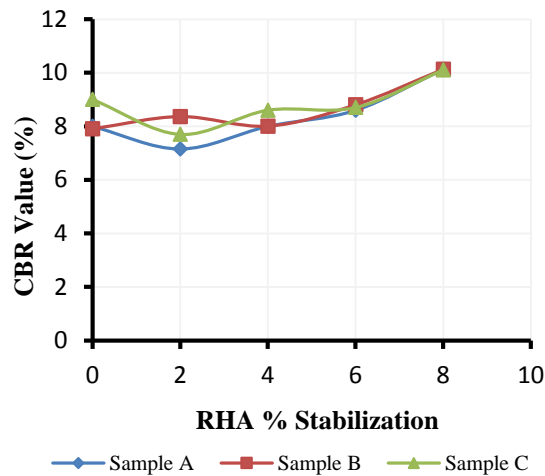


Figure 12: Variation of soaked CBR values for Stabilized *Chikoko* Clay Samples

4 CONCLUSION

Unconfined compressive strength of *chikoko* clay increased with curing age. A maximum unconfined compressive strength (UCS) value of 152 kPa at 6% RHA corresponding to 17.8% increment was recorded. The unconfined compressive strength increased by 1.6% from 14 to 21 days curing age, and 2.3% from 21 to 28 days curing for specimens compacted at the reduced standard proctor energy level. Soaking produced reduction and divergence in the CBR values of stabilized *chikoko* clay from the same locations. Optimal stabilization of Deltaic marine *chikoko* clay was achieved at 6% RHA. Stabilization of compacted *chikoko* clay improved its unsoaked CBR value from 8.6% to 17.4%, thereby making the stabilized soil suitable for sub-grade application.

ACKNOWLEDGEMENTS

The authors wish to acknowledge the contributions of colleagues and technologists in Federal University of Technology, Minna and River State University of Science and Technology, Port Harcourt.

REFERENCES

AASHTO (1986). American Association of State Highway and Transport Officials. Standard Specifications for Transport Materials and Methods of Sampling and Testing. 14th Edition, AASHTO, Washington, D.C.

Achal, V. & Pan, X. (2014). Influence of calcium sources on microbial induced calcite precipitation calcite precipitation by bacillus sp. CR2. *Appl Biochem*

Biotechnol. **173**:307–317. DOI: 10.1007/s12010-014-0842-

Alhassan, M. & Mustapha, A.M (2007). Effect of rice husk ash on cement stabilized laterite. *Leonardo Electronic J. practice and technology.* **6**(11); 47-58.

Alhassan, M. 2008, potential of rice husk ash for soil stabilization. *AUJ.T.* **11**(4); 246-250.

ASTM, D 4208 (1992). American Standards Testing Methods. Annual book of ASTM standards, Vol. 04.08, 1992. Philadelphia.

Atolagboye, L.O. & Talabia, A. O, (2014). Geotechnical properties of lateritic soil. *Construction and Building Materials*, **1**, 1 – 13.

Basha, E.A., Hashim, R. Mahmud, H.B. & Muntohar. A.S. (2005) Stabilization of residual soil with rice husk ash and cement, *Construction and Building Materials*, **19**, 448- 453.

Bell, F.G. (1993). Engineering Geology, *Blackwell Scientific Publications*, London.

BS 1377 (1990). Method of Testing Soils for Civil Engineering Purposes. *British Standard Institute*, BSI, London.

Dawoud, O., Chen, C. Y., & Soga, K., (2014). Microbial induced calcite precipitation for geotechnical and environmental applications. *Pro. New frontiers in geotechnical engineering. Technical Papers, ASCE, Geotechnical Special Publication.* **234**, 11-18.

Feng, K., & Montoya, B. M., (2016). Influence of confinement and cementation level on the behaviour of microbial-induced calcite precipitated sands under monotonic drained loading. *ASCE, Journal of Geotechnical and Geoenvironmental Engineering.* **142** (1), 040150571–9. DOI:10.1061/(ASCE)GT.1943-5606. 0001379.

Hamdan. N., Kavazanjian, J., Rittman, B.E., & Karatas I. (2011). Carbonate Mineral Precipitation for Soil Improvement through Microbial Denitrification. *Pro. GeoFrontiers 2011: Advances in Geotechnical Engineering, Dallas TX, ASCE, Geotechnical Special Publication.* **211**, 3925-3934.



- Hamdan, N., Kavazanjian Jr. E., Rittmann, B.E. & Karatas, I. (2016). Carbonate Mineral Precipitation for Soil Improvement through Microbial Denitrification, *Geomicrobiology Journal*, DOI: 10.1080/01490451.2016.1154117
- Ijimdiya, T. S. (2017). Bioremediation of oil contaminated soils using NPK as nutrient for use in Road Subgrade. *Nigerian Society of Engineers Technical Transactions*. Jan. - March. **51** (1): 56–63.
- Mujah, D., Cheng, L. & Shahin, M.A. (2019) Microstructural and Geo-Mechanical Study on Bio-cemented Sand for Optimization of MICP Process. *ASCE Journal of Materials in Civil Engineering*, **31**(4): 04019025-10. DOI: 10.1061/(ASCE)MT.1943-5533.0002660.
- Ogunsanwo, O., (1985). Variability in the geotechnical properties, mineralogy and microstructure of an arnphibolites-derived laterites soil. *Bulletin of Interl. Ass. Engineering Geology*, **33**, 1-25.
- Osinubi, K.J., A.O. Eberemu, T.S. Ijimdiya, S.E. Yakubu, J.E. & Sani, J.E. (2017). Potential Use of *B. pumilus* in Microbial-Induced Calcite Precipitation Improvement of Lateritic soil. *Proceedings of the 2nd Symposium on Coupled Phenomena in Environmental Geotechnics (CPEG2)*, Leeds, United Kingdom, 6-8 September, 2017.
- Osinubi, K.J. Eberemu, A.O. Ijimdiya, T.S. Gadzama, E.W. & Yakubu, S. E. (2018). Improvement of the Strength of Lateritic Soil Treated with *Sporosarcina pasteurii*-Induced Precipitate. *Nigerian Building and Road Research Institute International Conference*. Theme: Sustainable Development Goals (SDGs) and the Nigerian Construction Industry – Challenges and the Way Forward. 12 – 14 June, Abuja, Nigeria.
- Osinubi, K. J., Gadzama, E. W., Eberemu, A. O., Ijimdiya, T. S. & Yakubu, S. E. (2019). Evaluation of the strength of compacted lateritic soil treated with *Sporosarcina pasteurii*. *Proceedings of the 8th International Congress on Environmental Geotechnics (ICEG 2018)*, Edited by Liangtong Zhan, Yunmin Chen and Abdelmalek Bouazza, 28th October – 1st November, Hangzhou, China, © Springer Nature Singapore Pte Ltd., Vol. 3, pp. 419–428, On-line: https://doi.org/10.1007/978-981-13-2227-3_52.
- Otoko G.R and Karibo P. (2014), Stabilization of Nigeria deltaic clay with groundnut shell ash. *International journal of engineering technology research*, volume 2, No.6, 1-11.
- Otoko, G.R. & Aitsebaomo, F.O (2009). Geotechnical characteristics of Deltaic marine clay of the Niger Delta state, Nigeria. *Journal of Engineering Research Vol. 14*(3): 84-100.
- Otoko, G.R. & Onuoha, S.I. (2015), Lime stabilization of Deltaic soil. *Electronic Journal of Geotechnical Engineering, EJGE* 20(24): 12039-12043.
- Otoko G.R (2014) Cement and lime stabilization of Nigeria Deltaic marine clay. *European International Journal of science and Technology*, 3(4): 53-60.
- Walid, Z. & Hariahance, K., (2010). Effect of Lime and Natural Pozzolana on Dredged Sludge Engineering Properties. *Electronic Journal of Geotechnical Engineering*, 18, 589-600.



EMPIRICAL IMPACT EVALUATION OF SALES PROMOTIONAL MIX ON SACHET-WATER PRODUCT DISTRIBUTION ON ENTERPRISE PERFORMANCE: A SURVEY OF SELECTED SACHET-WATER OUTFITS IN NIGER STATE

Dr. Adima Julius Osaremen

The Federal Polytechnic Bida, Dept of Business & Management, Niger State, Nigeria.

juliusadimaosas@yahoo.com GSM:08036040931

ABSTRACT

Extant studies bear, no significant empirical research effort as to the potency of sales promotional mix on enterprise performance and its profitability. The marketing communication mix element has become essential players in the life of any business be it small size, medium or large scale; Sales promotional-mix has been perceived to have a link with the contraction and expansion of start-up and new venture creations, though not yet empirically supported. It is the anchor of this study to investigate the direct impact of sales promotional mix on enterprise performance and its profitability, using a well-developed measurement and structural models to explore this inherent literature gap. Using a scientific approach, adopt primary and secondary data, formulate hypotheses, literature review, and adopted questionnaire, 208 sample size, stratified random sampling, PLS-SEM analytical methods. The study revealed that Advertising sales promotion, Personal selling sales promotion, Pricing sales promotion . and Publicity sales are positively, and significantly related to enterprise performance and profitability. And the researcher recommends that the five sales promotional mix be adopted in the national strategic policy of the nation to secure and sustain individual and national economic advantage in a competitive production enterprise environment.

Keywords: *Sales promotional-mix, Enterprise-performance, Profitability, and Sachet-Water.*

1 INTRODUCTION

Promotion activation has contributed greatly to the creation of an affluent society. In promotional activities, there are ways of promoting a particular product which the management commonly use as the five aspects of the promotional mix, which are advertising usual process personal selling direct marketing public relation and pricing. Advertising is the process whereas to any paid form of nonpersonal presentation and promotion of ideas, goods, or services by an unidentified sponsor are made.

Personal selling is an oral presentation that takes place as a result of a conversation between one or more prospective buyers to make sales. Publicity/public relation; this refers to giving out information to the public or relating with one another about something to attract the attention of the public. Sales promotion is identified as those marketing activities other than personal selling advertisement and publicity.

Sales promotion are essential features of the final consumers; the success of every enterprise depends on the sales promotion received by the public. Creative sales promotion is the process of persuading potential customers to buy the product which has brought us changes and motivation in our marketing place, and both our producers and consumers also changed. Both are

more sophisticated and intelligent in the marketplace. There is close communication linkage between the two parties (buyers and sellers relationship).preparation and effectiveness of sales promotion procedures, which include giving out premium as branding and packaging of produce.

Even though reasonable research efforts have been made to understand the symbiotic relationship between promotional mix on organization,s profitability, scanty studies near to none is in the existing database focusing on the impacts of Sales Promotional mix on Sachet-Water Product Distribution. As Syda Nazish Zohra Rizui and Sadaq Malik, (2011) examine promotion on organization profitability and consumer's perception in Pakistan. Stephen Pembri, Aliyu Umaru Fudamu and Ibrahim Adam (2017) carried out research on sales promotional strategies organizational performance Oye Dapo Williams O; Akinlabi Babatunde and Sufian Jeleel B (2012), examines sales promotion or organization effectiveness in the Nigerian manufacturing industry, B. Nweie Laghi Michael and E. Ogwo (2013) investigate sales promotion and marking performance. Abajo Bolanle Odumami and Amos Ogunsiyi (2011) examine sales promotion as a tool for organizational performance.

Sales promotional mix has both positive and negative effects on the society, consumers, the competitors, the entrepreneurs invested capital, the growth, and



development sustenance of the enterprise itself, which can manifest as stunted growth, inability to meet up with its financial obligations, bankruptcy, recession, liquidation and folding up of the enterprise entity. Therefore, the research oversights by various investigators constitute gaps that require urgent attention in the enterprise landscape business practice.

2 STATEMENT OF PROBLEM

Recent economic depression no doubt has a significant effect on most enterprises economic activities, among which a decrease in the sale (i.e., sales drop) stands out.

In some cases, there are no sales for an extended period of time, which leads to closure or liquidation of such companies, since customers are unaware of the organizations product offering, or have developed a stable habitual behavior on the use of a particular product, thereby leading to the death of close substitute in the marketplace, where the significance of sales promotion is unavailable.

In the face of all the strategies being used by enterprise/organization to achieve its goal and objectives, as they do not operate in a vacuum, they function in an environment which has its effect on the performance of these organizations.

However, the study intends to Empirically Evaluate the impacts of Sales Promotional Mix on Sachet-Water Product Distribution on enterprise performance and profitability. And to unravel

the reasons why some firm is selling faster than the others. What is the significant relationship between advertising sales promotion on sachet table-water product distribution and enterprise performance and its profitability?

The postulated hypotheses of this investigation include:

H1: There will be a substantial positive relationship between advertising sales promotion on table water and enterprise performance and its profitability

H2: There is a significant correlation between personal selling sales promotion on table water and enterprise performance and its profitability

H3: There exists a significant favorable relationship between direct marketing sales promotion on table water and enterprise performance and its profitability

H4: The relationship between publicity/public relation sales promotion on table water and enterprise performance and its profitability expressed positive significance.

H5: There is a positive significant impact relationship between pricing sales promotion on table water and enterprise performance and its profitability

3 REVIEW OF RELATED LITERATURE

Organizational have to communicate with their existing and prospective customer about the new product/service development in their organization. This indeed is a phenomenal task in Nigeria market environment due to their characteristics in nature which is further sum up by the nation of Nigeria economic, demographic, social, political, legal, religious, cultural and environmental forces. Marketing communication is very significant and at the same time challenging in the organization. The marketing communication mix element have become important players in the life of any business be it minor, medium or major; they help in moving market offerings (goods, services, and ideas) from producers/relationships with customers and build and maintain relationship with a customer with customers prospect and other stakeholders of the company.

3.1 CONCEPTUALIZATION OF VARIABLES (IV AND DV)

Sharia (2013) reviewed that sales promotion brand royalty, Rotimosho (2013) reported that sales promotion encourage the purchase of large size unit such as premium product warranty.

Advertising: this refers to as any paid form of non-personal presentation and promotion of ideas, goods, and services by an unidentified sponsor. The message channel of advertising is not person to person, and it is not as specifically targeted to a set of the audience as another form of promotion such as personal selling which involves face to face interaction between the buyer and the seller. Most advertising is intended to be persuasive, i.e., to win a buyer for a product or service. Advertising reaches the audience through mass media such as radio, television, newspaper magazines, direct mail, outdoor billboards, and transit media such as posters in and outside the moving object.

Publicity: Is a non-personal stimulation of demand for a product service or business unit but by planting

commercially, significant news about it published medium or obtained a favorable presentation of upon broadcasting television or stage that is not funded by the sponsor. It is also referred to any message or information about an enterprise, or its products that are transferred via the mass media but is not paid by an organization and the organization and the organization is not identified as the source of the message or information.

Personal selling: Is described as a face to face communication and presentation of goods, services, ideas, activities, and emotions between buyers and sellers and is usually done in a persuasive model. It is a way of persuading a prospective buyer to buy a product or service or to act favorably upon an idea that is of commercial value or significance to the seller.

4 RESEARCH METHODOLOGY

Research Design: The research design adopted by this research is the descriptive and quantitative research design in nature and operationalized as data would be in a quantitative presentation and empirically analyzed.

The population of the study: The research work was carried out on all the workers in bida poly water consult, EED Centre, and some other selected table water outfit in Bida metropolis. With a staff strength of (Federal poly consult Table water: 16, Entrepreneurship Development Centre (EED) FPB 105, Other selected Table water outfits in Bida Metropolis 90, amounting to 201 total population).

Sampling Method: The stratified random sampling approach was adopted by this investigation as stratified into CEO/Owners 25, Technical staff permanent and casual 79, Operational staff/marketer permanent and casual 97= 201 valid respondents. The instrument used in gathering relevant data for this research work is the questionnaire, on primary and extensive literature review on the secondary sources of information, especially in the related literature.

Research Instrument /measurement Adopted /Adapted

The measurement of this study was adopted from Oyedepo William O, Akinlabi Babatude H and Sfian Jeheel B(2012) and Abajo Bolanle Odunlami Amos Ogunsiji (2011)

The data gotten from this research study would be analyzed using the Partial Least Square Structural Equation Modeling, supplemented with chi-square and descriptive, analytical methods.

4.1: Structural Framework

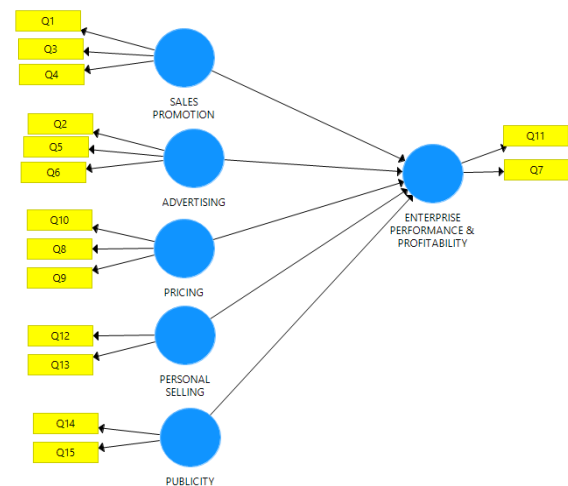


Figure 1: Structural Framework of the study

SOURCE: Researcher's design (field Data), Using PLS-SEM 3.0 Version

Ascertaining the validity and reliability of the two models in every scientific investigation (measurement and structural models) is strongly recommended using the following variables: the convergent validity was use through factor loadings, composite reliability (CR) and average variance extracted (AVE) (Hair et al. 2010) Hulland, (1999) Discriminant validity, Hypothesis testing using Path coefficient(Gefen, Straub, and Boudreau, 2000). Bootstrapping approach (Bakshi and Krishna, 2009, Chin, 2010) the Variance explained, the Effect size and the predictive relevance of the models, which this study strictly complied with to ensure adequate validity and reliability of result findings. (See appendix I, and as reported in Table iii)

Using the Discriminant Validity tool assessment to evaluate the level to which the used measures reflect some other concerned variables used in the study, manifesting in the varied level of correlation between the measured interest and another construct measure in the study. (Fornell and Larcker, 1981, the use of AVE with a score of 0.50 or more, and the square root of Average Variance Extracted should be greater than the correlations among latent constructs. (See appendix I,

and as reported in Table iii, and table I, as reported in this study)

Table i: DISCRIMINANT VALIDITY

	ADVERTIS	ENTERPRISE	PERSONAL	PRICING	PUBLICITY	SALES PRC
ADVERTISING	0.806					
ENTERPRISE PERFORMANCE	0.591	0.781				
PERSONAL SELLING	0.313	0.595	0.934			
PRICING	0.536	0.659	0.365	0.755		
PUBLICITY	0.425	0.632	0.677	0.411	0.963	
SALES PROMOTION	0.721	0.369	0.161	0.384	0.293	0.866

Note: “Squared correlations; AVEs in the diagonal is greater than correlated.”

SOURCE: Researcher’s field Data, Using PLS-SEM 3.0 Version

Using the outer loading to evaluate, the single item reliability of this research study on the individual elements construct, Duarte & Raposo, 2010; Hair et al., 2014; Hair et al., 2012; Hulland, 1999). Maintained that retainment of items with loadings between 0.40 and 0.70 after Bootstrapping (Hair et al., 2014), Adherence to this rule by this study resulted to, out of 15 items, four were deleted because they presented loadings below the threshold of 0.40. Thus, in the whole model, only 11 items were retained as they had loadings between 0.644 and 0.964 (see table ii, as reported in this investigation)

Table ii: OUTER LOADING

	ADVERTISING
Q1	0.799
Q10	0.785
Q11	0.893
Q12	0.922
Q13	0.945
Q14	0.964
Q15	0.961
Q2	0.73
Q3	0.939
Q4	0.856
Q5	0.876
Q6	0.805
Q7	0.651
Q8	0.644
Q9	0.825

SOURCE: Researcher’s field Data, Using PLS-SEM 3.0 Version

Composite Reliability

Using Composite Reliability tool to evaluate the study Internal consistency reliability refers to the extent to which all items in a particular (sub) scale are measuring the same concept (Bijttebier et al., 2000; Sun et al., 2007). Although two estimators exist, composite reliability stand out against Cronbach’s alpha approach due fact that composite reliability coefficient provides a much less biased estimate of reliability than Cronbach’s alpha coefficient because the latter assumes all items contribute equally to its construct without considering the actual contribution of individual loadings (Barclay, Higgins, & Thompson, 1995; Gotz, Liehr-Gobbers, & Krafft, 2010). Secondly, Cronbach’s alpha may over or under-estimate the scale reliability.

The composite reliability takes into account that all indicators have different loadings and an internal consistency reliability value above 0.70 is regarded as satisfactory for an adequate model, yet, the figure as a value that falls below 0.60 represents a lack of reliability). Nevertheless, Bagozzi and Yi (1988) as well as Hair et al. (2011), who suggest that the CV (composite reliability) coefficient should be at least 0.70 or more (see appendix I, as reported in table iii of this study)

Average Variance Extracted

Using the Average Variance Extracted Estimator to evaluate the Convergent study validity refers to the

extent to which the study items truly represent the intended latent construct and indeed correlate with other measures of the same latent construct (Hair et al., 2006). To achieve adequate convergent validity, Chin (1998) recommends that the AVE of each latent construct should be 0.50 or more.

While the multicollinearity issue was assessed using Variance Inflated Factor in adherence to the threshold of

Hair, Ringle, and Sarstedt (2011) that variance inflated factor only constitute an issue when its assessment index exceeds 5. There, reporting VIF value ranging from 1.313 – 2.632 among the latent constructs (See appendix ii, as reported in table iii) indicates adequate and acceptable variance inflated factor as lack of multicollinearity issue in the study.

Table iii: REPORTING PATH COEFFICIENTS, HYPOTHESES TESTING, VIF, C.R, AVE, R² Q², AND F², OF THE STUDY.

Hypothesis	Relationship	Beta	Std Err	T-value	Decision	Composite Reliability	Average Variance Extracted (AVE)	R-Square	F.Square	SSO	SSE	Q ² (=1SSE/SSO)	VIF
H1	ADVERTISING -> ENTERPRISE PERFORMANCE & PROFITABILITY	0.285	0.085	3.343	Supported	0.847	0.65		0.091	603	603		2.623
H2	PERSONAL SELLING -> ENTERPRISE PERFORMANCE & PROFITABILITY	0.233	0.07	3.319	Supported	0.931	0.871		0.084	402	402		1.903
H3	PRICING -> ENTERPRISE PERFORMANCE & PROFITABILITY	0.357	0.061	5.888	Supported	0.798	0.571		0.246	603	603		1.513
H4	PUBLICITY -> ENTERPRISE PERFORMANCE & PROFITABILITY	0.229	0.059	3.869	Supported	0.962	0.927		0.074	402	402		2.069
H5	SALES PROMOTION -> ENTERPRISE PERFORMANCE & PROFITABILITY	-0.078	0.059	1.317	NOT Supported	0.900	0.751		0.008	603	603		2.109
	Enterprise Performance & Profitability					0.754	0.61	0.659		402	257.718	0.359	

SOURCE: Researcher's field Data, Using PLS-SEM 3.0 Version

The results in Table 4 indicated that, Advertising sales promotion, Personal selling sales promotion, Pricing sales promotion . and Publicity sales promotion (B=0.285, t-value=3.343), (B=0.233, t-value=3.319) (B=0.357, t-value=5.888), and (B=0.229, t-value=3.869 are positively, and significantly related to enterprise

performance and profitability meaning that advertising promotional mix have significant positive direct relationship with enterprise performance and profitability. And, while the relationship between Sales promotion and enterprise performance and profitability was not positively correlated with enterprise



performance and profitability ($B=-0.078$, $t\text{-value}=1.317$) but negatively related to enterprise performance and profitability. In the same vein, the exogenous study constructs, Advertising sales promotion, Personal selling sales promotion, Pricing sales promotion, Publicity sales promotion and Sales promotion, bear variance inflated factor index values as. 2.623, 1.903, 1.513, 2.069 and 2.109, respectively, indicating lack of linear and multicollinearity issues with and among the study and the variables explaining 65.9% (R^2), at a moderate predictive relevance of 0.359 (Q^2) and lastly, the effect size of the five endogenous constructs (F^2) = Advertising promotional mix = 0.091, Personal selling promotional mix = 0.084, Pricing promotional mix = 0.246, Promotional mix = 0.074, Publicity and Sales promotional mix = 0.008. An indication that the study designed models, i.e., both measurement and the structural models are dependable instruments for assessing promotional mix on enterprise performance and profitability in any economy.

Summary of findings

- 1: Significant positive relationship exists between advertising sales promotion on table water's enterprise performance and its profitability
- 2: There is a significant correlation between personal selling sales promotion on table water's enterprise performance and its profitability
- 3: There exists a substantial favorable relationship between direct marketing sales promotion on table water's enterprise performance and its profitability
- 4: The relationship between publicity/public relation sales promotion on table water's enterprise performance and its profitability expressed positive significance.
- 5: There is no significant impact relationship between pricing sales promotion on table water's enterprise performance and its profitability

5.0 DISCUSSION OF RESULTS

The milestone research investigation of this study revealed that Significant positive relationship exists between advertising sales promotion on table water's enterprise performance and its profitability. This result is consistent, regular, and stable with the work of Rotimosho (2013) who reported that advertising sales promotion encourage the purchase of large size unit such as premium product warranty. The second reported finding of this study shows that there is a significant correlation between personal selling sales promotion on table water's enterprise performance and its

profitability. In a related development, this result is also consistent with the effort of Pauwels et al. (2002) who find out the permanent impact of personal selling sales promotion on accumulative annual sales form the two product categories, which storable and perishable product. The third and fourth findings of this investigation show that: There exists a significant favorable relationship between direct marketing sales promotion on table water's enterprise performance and its profitability, and The relationship between publicity/public relation sales promotion on table water's enterprise performance and its profitability expressed positive significance respectively. While from existing studies, the investigations of Ailawad and Neslin (1998) revealed that direct sales promotions motivate consumers to make immediate purchases and positively impacts consumption volume. And Pauwels Silva-Risso and Janssens (2003) depicts the effect of public relation sales promotion on firms revenue, respectively. Lastly, this study reported in its finding that, There is no significant impact relationship between pricing sales promotion on table water's enterprise performance and its profitability. And this was also found to be similar finding with the work of Dekimpe et al. (1999) show that there is rarely any permanent effect of Price sales promotion on the volume of sales, Together with the work of Aware et al. (2008) who supported that, price sales promotion (price promotion hurt the profitability of the Niger state transport Authority.

5.1: The implication of the Study

5.1.1: Practical Implication

With this very investigation into the economic and economic contractual relationship between sales promotional mix and the enterprise performance and its profitability, practical statements are made that Advertising sales promotion, Personal selling sales promotion, Pricing sales promotion . and Publicity sales promotion are reliable tools to turn around the fortune enterprise performance and its profitability. By demonstrating its efficacy of increasing the sales volume sachet water in our economy through positive motivation and persuasion of consumers to make immediate purchases and granting and dissemination of relevant knowledge of the contents of the product as well as encouragement to present and potential consumers towards large size units purchase as a premium product.



5.1.2: Theoretical implication

This study has theorized the symbiotic relationship existing between sales promotions variables and two dependent variables, i.e., enterprise performance and profitability. Advertising sales promotion, Personal selling sales promotion, Pricing sales promotion . and Publicity sales promotion are positively and significantly related to enterprise performance and its profitability. Indicating that any individual, group of entrepreneurs, community and the country who is in dire need of significant and favorable enterprise performance and enhancement of economic empowerment through investment proceeds as profits, dividends, enterprise rewards or rent for capital, should focus on the sales promotional mix theory synergy with sachet water enterprise performance.

5.1.3: Methodological implication

This study has novelty attended to methodological gaps in the analysis. Analytically this research has attended to the science needed investigation with the use of SPSS, and Partial least square-SEM design and structure research framework, that require an assessment of both the measurement and structural models, which have revealed the psychometric properties of the study as individual item reliability, average variance explained and composite reliability.

The purification of the adopted measurement/instrument with the application of scientific-analytical approach Partial Least Square Structural Equation Model (Bootstrapping) quality measurement/instrument was secured and guaranteed the validity and reliability of results from this investigation.

5.2: Limitation and Future Research Direction

Replication of this study is needed in other states, possibly with collaboration as this investigation geographical scope is limited to Bida-Niger state, which does not permit the generalization of the result. Expounding the scope of coverage is recommended with a scientific analytical approach on more ventures and start-ups instead of limiting it to Sachet-water only.

5.3: Conclusion and Recommendation

An investigation into the efficacy of conscious design and established a contractual relationship, between five selected sales promotional mix. As independent variables and two dependent variables in a clean water product production industry in Niger state. Which scientifically and sequentially showcased that, advertising sales promotion, Personal selling sales promotion, Pricing sales promotion . and Publicity sales promotion are positively and significantly catalysts to

enhance and motivate enterprise performance and its profitability for individual and national development. And given this research findings, the researcher recommends that the five sales promotional mix be adopted in the national strategic policy of the nation to secure and sustain individual and national economic advantage in a competitive production enterprise environment.

REFERENCES

- Ailawad and Neslin (1998) Sales Position in an Organization. *Journal of Marketing*
- Aware et al. (2008) Impact of Sales promotion and Organizational profitability.
- Bagozzi, R., & Yi, Y. (1988). On the evaluation of structural equation models. *Journal of the Academy of Marketing Science*, 16, 74-94. DOI: 10.1007/bf02723327
- Barclay, D., Higgins, S., & Thompson, R. (1995). The partial least squares approach to causal modeling: Personal computer adoption and use as an illustration — *technology Studies*(2), 285–374.
- Bijttebier, P., Delva, D., Vanoost, S., Bobbaers, H., Lauwers, P., & Vertommen, H. (2000). Reliability and Validity of the Critical Care Family Needs Inventory in a Dutch-speaking Belgian sample. *Heart & Lung: The Journal of Acute and Critical Care*, 29, 278-286. DOI: p
- Bolanle Odunlami & Amos Ogunsiji (2011) Effect of sales promotion as a tool on organizational performance. *Journal of Emerging Trends in economics and management science (JETEMS)* 2(1):9-13
- Chin, W. (2010). How to write up and report PLS analyses. In V. Esposito Vinzi, W. W. Chin, J. Henseler & H. Wang (Eds.), *Handbook of Partial Least Squares* (pp. 655-690): Springer Berlin Heidelberg.
- Chin, W. W. (1998). The partial least squares approach to structural equation modeling. In G. A. Marcoulides (Ed.), *Modern Methods for*



- Business Research (pp. 295-336). Mahwah, New Jersey: Laurence Erlbaum Associates.
- Dekimpe et al. (1999) Management of Sales and its Impact on Business. Hand Book of Management. 6th Ed. Pp. 105 - 133.
- Duarte, P., & Raposo, M. (2010). A PLS model to study brand preference: An application to the mobile phone market. In V. Esposito Vinzi, W. W. Chin, J. Henseler & H. Wang (Eds.), Handbook of Partial Least Squares (pp. 449-485): Springer Berlin Heidelberg.
- Fornell, C., & Larcker, D. F. (1981). Evaluating Structural Equation Models with unobservable variables and measurement error. Journal of Marketing Research 18, 39-50.
- Gefen, D. and D. Straub (2000) "The Relative Importance of Perceived Ease-of-use in IS Adoption: A Study of e-Commerce Adoption," JAIS (forthcoming).
- Gotz, O., Liehr-Gobbers, K., & Krafft, M. (2010). Evaluation of Structural Equation Models using the Partial Least Squares (PLS) Approach. In V. E. Vinzi, W. W. Chin, J. Henseler & H. Wang (Eds.), Handbook of Partial Least Squares: Concepts, Methods, and Applications (pp. 691-711). Heidelberg: Springer.
- Hair, J. F., Black, W. C., Babin, B. J., & Anderson, R. E. (2010). Multivariate data analysis (7th ed.). Upper Saddle River, New Jersey: Prentice-Hall.
- Hair, J. F., Hult, G. T. M., Ringle, C. M., & Sarstedt, M. (2014). A primer on partial least squares structural equation modeling (PLS-SEM). Thousand Oaks: Sage Publications
- Hair, J. F., Ringle, C. M., & Sarstedt, M. (2011). PLS-SEM: Indeed, a Silver Bullet. Journal of Marketing Theory and Practice, 18, 139-152.
- Hair, J. F., Ringle, C. M., & Sarstedt, M. (2013). Partial least squares structural equation modeling: Rigorous applications, better results, and higher acceptance. Long Range Planning, 46(1-2), 1-12. DOI: <http://dx.doi.org/10.1016/j.lrp.2013.01.001>
- Hair, J. F., Sarstedt, M., Ringle, C. M., & Mena, J. A. (2012). An assessment of the use of partial least squares structural equation modeling in marketing research. Journal of the Academy of Marketing Science, 40, 414-433.
- Hulland, J. (1999). Use of partial least squares (PLS) in strategic management research: a review of four recent studies. Strategic Management Journal, 20, 195-204. DOI: 10.1002/(sic)1097-0266(199902)20:2<195::aid-smj13>3.0.co;2-7
- Nazish zebra Rizvi & Sadia Malik (2011) Impact of sales promotion on organization profitability and consumer's perception in Pakistan Interdisciplinary journal of contemporary research in business vol. 3, No. 5
- Nwielaghi M.B. & Ogwo E. (2013) Trade sales promotion strategies and marketing performance in the soft drink industries in Nigeria international journal of marketing studies, vol. 5, No. 4Ijbojo
- Oyedapo Williams O. Akinlabi Babatunde H. & Sufian Jaleel B. (2012) the impact of sales promotion on organization effectiveness in Nigeria manufacturing industry. Universal Journal of marketing and business research (ISSN: 2315-5000) vol. 1(4) pp. 123-131.Syeda
- Pauwels et al. (2002) Promotion and Improvement of an Organizational Sales and Productivity. Journal of Business.
- Rotimosho (2013) The Impact of Sales Promotion on Organization Effectiveness in Nigerian Manufacturing Industry. Journal of Marketing and Business Research.
- Schindler (1998) Organization and Management of its Sales and Promotion.
- Sharia (2013) Sales and Sales Promotion, a Way to Effectiveness and Efficiency Productivity in an Organization.
- Stephen membi, Ph.D. students, Aliyu Umaru Fudamu, Ph.D. & Ibrahim Adamu (2017) Impact of sales promotion strategies on organizational



performance in Nigeria. European journal of research and reflection in management science Vol. 4 ISSN 2056-5992

Sun, W., Chou, C.-P., Stacy, A., Ma, H., Unger, J., & Gallaher, P. (2007). SAS and SPSS macros to calculate standardized Cronbach's alpha using the upper bound of the phi coefficient for

dichotomous items. Behavior Research Methods, 39(1), 71-81. DOI: 10.3758/bf03192845

Syeda N.Z. (2011) Impact of Sales Promotion on Organization's Profitability and Consumers Perception in Pakistan. Journal of Contemporary Research in Business.

Appendix i

	Cronbach's Alpha	Composite Reliability	Average Variance Extracted (AVE)
ADVERTISING	0.731	0.847	0.65
ENTERPRISE PERFORMANCE & PROFITABILITY	0.386	0.754	0.61
PERSONAL SELLING	0.853	0.931	0.871
PRICING	0.615	0.798	0.571
PUBLICITY	0.921	0.962	0.927
SALES PROMOTION	0.833	0.9	0.751

Appendix ii: Collinearity Statistics (VIF)

	ENTERPRISE PERFORMANCE & PROFITABILITY
ADVERTISING	2.623
PERSONAL SELLING	1.903
PRICING	1.513
PUBLICITY	2.069
SALES PROMOTION	2.109



ASSESSING THE LEVEL OF READINESS TO ADOPT BUILDING INFORMATION MODELLING (BIM) AMONGST BUILT ENVIRONMENT PROFESSIONALS IN SELECTED NORTHERN NIGERIAN STATES

Abubakar, I. T¹ and Oyewobi, L. O²

¹Department of Quantity Surveying, Federal University of Technology, PMB 65 Minna, Niger State, Nigeria
Email: ibrahimtanko79@gmail.com, +234 8033598685

ABSTRACT

Globally, the adoption of BIM by building professionals has tremendously increased over the last decade owing to the many benefits it provides in construction projects such as improved productivity, reduction of rework, reduction of conflict amongst building professionals and saving of funds. In spite of these benefits, in the Nigerian context, the adoption of BIM amongst built environment professional is still very low. Thus, this study assesses the level of readiness of building professionals in using BIM by exploring the factors guiding the acceptance of new technologies; awareness, performance expectancy, effort expectancy, social influence and facilitating conditions with the view to encourage BIM adoption. The objective of the study was achieved by conducting in-depth interviews with 36 building professionals in Niger state, Abuja and Kaduna. This study discovered that the Nigerian building professionals are nowhere near ready to adopting Building Information Modelling (BIM) and there is a dire need for Nigerian buildings professionals to restore their good name and regain their sense of professional pride in providing the highest quality buildings and structures.

Keywords: *Built environment, Building Information Modelling, Building Professional, Effectiveness, Efficiency*

1 INTRODUCTION

Shelter is considered a fundamental human right for the over six billion human beings living in the world today (Franz *et al.*, 2015; Mukhtar *et al.*, 2016; Seneviratne *et al.*, 2017). Building professionals have the honour and privilege of participating directly in the provision of this great societal need, as well as other vital building infrastructure such as hospitals, schools, and office complexes (Chou *et al.*, 2015; Jallow *et al.*, 2017). Unfortunately as of 2015, over 1.6 billion people worldwide did not possess adequate housing (Homeless World Cup Foundation, 2019), which means that building professionals have a lot of work to do in fulfilling their crucial mandate.

Leeds (2016) argued that there are two major challenges hampering the ability of the global construction industry to provide quality and much-needed housing and infrastructure projects: project performance and sustainability concerns. Project performance refers to the seeming inability of construction firms to finish projects on time and within budget, with an Accenture study showing that only 30% of large projects are completed within

budget, and only 15% are completed on time (Leeds, 2016). Additionally, a 2015 KPMG survey revealed that half of all construction firms globally reported at least one underperforming project in the previous year (Leeds, 2016). As for the issue of sustainability, the global construction industry is responsible for about 40% of carbon emissions yearly, and this is dangerous for the environment (Leeds, 2016). It is thus incumbent for the global construction industry to become more efficient and effective in the way it estimates and uses needed building materials (Leeds, 2016).

Based on this backdrop, it is reasonable to assume that any innovation that can improve the effectiveness and efficiency through which buildings are designed and constructed would be welcomed with all interest by building professionals (Fedoruk *et al.*, 2015; Hossain, 2017). This is where the concept of Building Information Modelling (BIM) comes into play.

There are over thirty definitions of BIM that have been propounded in the construction literature (Matejka & Tomek, 2017; Zhang *et al.*, 2017). However, a critical examination of these definitions revealed that BIM has been conceptualized as one of three categories; a

technology, a method or a methodology (Matejka & Tomek, 2017). For the purpose of this study, BIM is considered a digital technology following the example of The National Building Information Model Standard Project Committee in the USA who defined BIM as “a digital representation of the physical and functional characteristics of a facility. It is a shared knowledge resource for information about a facility, forming a reliable basis for decisions during its life cycle; defined as existing from earliest conception to demolition” (Zhang *et al.*, 2017).

Building professionals and experts around the globe who have utilized BIM have proclaimed several benefits it has provided regarding increased efficiencies and effectiveness: It reduces rework (Li *et al.*, 2017; Teo Ai Lin *et al.*, 2017); It improves productivity (Atazadeh *et al.*, 2017; Nguyen & Hadikusumo, 2017); It reduces conflict amongst the building professionals (Chen & Luo, 2014; Forsythe *et al.*, 2015), and it saves time and money (Gheisari & Irizarry, 2016; Chong *et al.*, 2017). It is in recognition of these benefits that countries like Australia (Bridge & Carnemolla, 2014), Denmark (Kim & Kim, 2009), Finland (Tulenheimo, 2015), Russia (Chernykh & Yakushev, 2014), the autonomous territory of Hong Kong (Pan *et al.*, 2017), Singapore (Ho & Rajabifard, 2016), South Korea (Won *et al.*, 2016), Sweden (Hooper, 2015), the UAE (Mehran, 2016), the UK (Gledson & Greenwood, 2016) and the US (Shelbourn *et al.*, 2017) have mandated the adoption of BIM by building professionals for public sector construction.

According to the Unified Theory of Acceptance and Use of Technology (UTAUT), the adoption of any new technology by a professional is dependent on four factors: The degree to which the professional believes the new technology will improve his or her performance (performance expectancy), how easy the professional feels the technology will be to use (effort expectancy), other experts' opinions about the importance of using the technology (social influence), and the degree to which the professional believes that the necessary infrastructure exists to support the use of the new technology (facilitating conditions) (Urpelainen & Yoon, 2017; Aklin *et al.*, 2018; Tanner *et al.*, 2018). However, an important pre-requisite to these four factors is that the professional first be aware of the existence of the new technology (Elmustapha *et al.*, 2018). There are thus five factors that need to be in place before a professional will adopt a new technology: Awareness; Performance expectancy; Effort expectancy; Social influence, and Facilitating conditions.

With the above critical factors in place and favorable, the building professionals' chances of BIM adoption may likely increase. As it relates to BIM adoption by building professionals, for those countries described in an earlier paragraph where BIM has been mandated for public sector construction, it is no surprise to see that the adoption of

BIM by building professionals has significantly increased over the last few years. For example, the percentage of building companies in North America that adopted BIM in 2007 was 28%; this more than doubled to 49% in 2009 and then leapt to 71% in 2012 (Quirk, 2012). A contributing factor for this rapid increase in BIM adoption by building professionals in these countries is the fact that BIM adoption has been mandated (Succar & Kassem, 2015). For building professionals in these countries interested in partaking in lucrative public sector construction contracts, the adoption and effective utilisation of BIM becomes a necessity (Arunkumar *et al.*, 2018; Liao & Ai Lin Teo, 2018). Additionally, once these professionals have taken the time, effort and resources to integrate BIM into their processes, it becomes logical that they will transfer this technology into their private construction projects as well (Jung & Lee, 2015; Singh & Holmstrom, 2015; Howard *et al.*, 2017).

However for countries like Nigeria where BIM adoption has not been mandated, there is no extrinsic factor to encourage building professionals to invest the time and resources necessary to effectively adopt BIM. In order for Nigerian construction professionals and other building professionals in other countries where BIM adoption is not mandated to reap the many benefits of BIM usage in construction projects, the motivation to adopt must be intrinsic; each professional must be aware, willing and able to integrate BIM into existing building strategies (Chang & Howard, 2014; Juan *et al.*, 2017). There can be no denying that widespread BIM adoption by Nigerian building professionals would dramatically improve the efficiency and effectiveness of the building construction processes (Wang *et al.*, 2015; Ezeokoli *et al.*, 2016). It thus becomes important that Nigerian building professionals' level of readiness to adopt BIM be ascertained in order to improve the efficiency of the industry and reduce or eliminate most of the challenges confronting the industry, and that is the ultimate aim of this study.

2. Literature Review

The National Building Information Model Standard Project Committee in the USA defines BIM as “a digital representation of the physical and functional characteristics of a facility. It is a shared knowledge resource for information about a facility forming a reliable basis for decisions during its life cycle; defined as existing from earliest conception to demolition” (Zhang *et al.*, 2017). Over the last decade, several studies have explored the BIM adoption process in various contexts (Gu & London, 2010; Mom *et al.*, 2014; Chen *et al.*, 2017), from three major perspectives: the micro level; the meso level, and; the macro level. This review describes these three conceptualizations of BIM adoption, and discusses how BIM adoption is conceptualized in this study given the Nigerian context.

Studies that conceptualized BIM adoption from a macro perspective sought to determine to what extent BIM had been adopted by a specific building industry (Hossein *et al.*, 2015; Kim *et al.*, 2016; Gokuc & Arditi, 2017), by an entire country across several industries (Chen *et al.*, 2017; Herr & Fisher, 2017; Hore *et al.*, 2017) or across several countries (Jung & Lee, 2015; Chong *et al.*, 2016; Kassem & Succar, 2017). The objective of these studies was to provide a holistic assessment of how much BIM usage had diffused across the building industry and beyond (Walasek & Barszcz, 2017).

As for studies that adopted a meso perspective of BIM adoption, their objective was to understand BIM adoption from an organizational point of view (Gledson, 2016; Gurevich *et al.*, 2017; Monko *et al.*, 2017). Simply put, they adopted case studies of specific firms (Linderoth, 2010; Arayici *et al.*, 2011; Ahuja *et al.*, 2016) or surveyed a number of organizations from the same industry (Rogers *et al.*, 2015; Edirisinghe *et al.*, 2016; Khodeir & Ness, 2017) in order to understand the various factors affecting BIM adoption in those firms.

Finally, representing the distinct minority of studies reviewed, were those that conceptualized BIM adoption from a micro perspective by attempting to understand BIM adoption from the point of view of individual building professionals (Ding *et al.*, 2015; Singh & Holmstrom, 2015; Addy *et al.*, 2017). It is no surprise that the vast majority of studies reviewed either adopted a macro or meso perspective to understanding BIM adoption. This is because most of these studies were carried out in developed nations such as the US (Gokuc & Arditi, 2017), UK (Gledson & Greenwood, 2017) and Australia (Chong *et al.*, 2016) where BIM is no longer a new phenomenon. There is thus no need to understand BIM adoption from an individual building professional's perspective because it has already become a standard part of building practice (Loveday *et al.*, 2016). This is further buttressed by the fact that BIM adoption is mandated for a lot of public construction in these countries (Chen *et al.*, 2017).

However, for developing countries like Nigeria, where this current study took place, BIM is not a widespread phenomenon (Wang *et al.*, 2015; Ezeokoli *et al.*, 2016). BIM use is not mandated nor has it diffused sufficiently amongst Nigerian building professionals to warrant conceptualizing BIM adoption from a macro or meso perspective. It is for these reasons that this study conceptualized BIM adoption from the point of view of the individual Nigerian building professional. It is only once the readiness of these individual building professionals to adopt BIM are ascertained, and the obstacles hindering their adoption of BIM are identified and resolved that diffusion of BIM can really take place. It is hoped that the findings of this study will be an important first step towards

widespread diffusion of BIM usage amongst building professionals in Nigeria, which hopefully will lead to dramatic improvements in how buildings are built and maintained in this country.

3. Theoretical Framework

The Unified Theory of Acceptance and Use of Technology (UTAUT) was developed in 2003 by American-based scholars, Viswanath Venkatesh, Michael Morris, Gordon Davis and Fred Davis. The theory states that there are four key constructs that influence new technology adoption: 1) Performance expectancy, 2) Effort expectancy, 3) Social influence, and 4) Facilitating conditions. Addy *et al.* (2017) utilized the constructs of UTAUT to study the factors that facilitated BIM adoption amongst quantity surveyors in Ghana.

Ten theories were discussed that served as the 'population' of theories from which one would be selected. As BIM was defined as a technology in this study, only theories that specifically addressed new technology adoption were considered appropriate for this study, rather than theories that addressed general behavioural concepts. This led to the elimination of six of the ten theories as potential theories for this study (TRA, TPB, ANT, CLT, CST and MHN). This left four theories as contenders for adoption by this study (TAM, TOE theory, UTAUT and DOI).

In order to select the most suitable theory from the four remaining theories, the Japanese management concept of "kaizen" was adopted (Cannas *et al.*, 2018). "Kaizen" means continuous improvement, and the concept was utilized in selecting a theory for this study by considering which of the four theories had made the most improvements after learning from the criticisms of prior technology-adoption theories. DOI was developed in 1962, TAM was developed in 1989, while TOE theory was developed in 1990. On the other hand, UTAUT was developed much later in 2003 and critically considered the drawbacks of the other three earlier theories (Li *et al.*, 2018). UTAUT could thus be considered the latest and 'most improved' theory of technology adoption, and thus UTAUT was selected as the most appropriate theory for this study.

UTAUT served as the foundation for this study's theoretical framework. To reiterate, UTAUT posits that technology adoption is influenced by four factors: 1) Performance expectancy, 2) Effort expectancy, 3) Social influence, and 4) Facilitating conditions (Addy *et al.*, 2017).

A critical examination of these four factors reveals that UTAUT makes an assumption that the individual is “aware” that the technology exists. This is because awareness of the technology is an obvious pre-requisite before an individual can have any perception as to how effective and easy the technology can potentially be (Elmustapha *et al.*, 2018). As alluded to by Wang *et al.* (2015), this assumption of awareness cannot be taken for granted as regards BIM adoption amongst Nigerian building professionals. For this reason, this study adds “awareness” as a fifth factor in exploring the level of readiness to adopt BIM amongst building professionals in Niger State, Abuja and Kaduna State. Therefore a modified version of the unified theory of acceptance and use of technology (UTAUT) was adopted to understand the factors that would help the researcher investigate how ready building professionals in Niger state, Abuja and Kaduna state are to adopt BIM. These factors were: 1) Awareness of BIM, 2) Performance expectancy, 3) Effort expectancy, 4) Social influence, and 5) Facilitating conditions. Interview questions had to be developed to measure each factor, and for this reason a semi-structured interview approach was adopted guided by these five factors. The following subsections describe the question-development process and the pilot-test procedure to reinforce the validity and reliability of the questions developed.

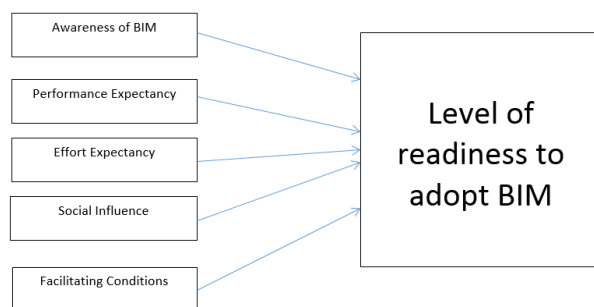


Figure 1: Theoretical Framework to explore BIM adoption amongst building professionals in Niger state, Kaduna state and Abuja.

4. Research Methodology

This study adopted an exploratory and qualitative research design rather than a confirmatory research design due to the fact that as far as the researchers are aware, this was the first study to investigate BIM readiness amongst Nigerian building professionals in Niger state, Abuja and Kaduna state. The researchers thus had no expectations which the study could confirm, rather the objective was to explore

and discover how ready building professionals in Niger state, Abuja and Kaduna state were to adopt BIM.

Similarly, a qualitative research paradigm was adopted rather than a quantitative approach because the use of semi-structured interviews enabled the researchers to dig deep into the mind-set of the selected building professionals as to their awareness of BIM, their performance and effort expectancies towards BIM usage, as well as their perception regarding whether or not the facilitating conditions existed in this region for BIM to be fully implemented (La Marca, 2011; Trott, 2012).

The population for this study were represented by quantity surveyors, architects, builders and civil engineers registered with their respective professional bodies practicing in Niger state, Abuja and Kaduna. Being registered with a professional body was important because this accreditation serves as stamp of approval regarding the credibility and competence of the building professional. Getting the exact number of registered building professionals in these three regions proved abortive as the professional bodies informed the researcher that membership was not categorized by location. Additionally, there was reluctance on the part of these bodies to reveal the entire number of registered building professionals in the entire country. These two reasons prevented the researcher from obtaining the actual population size for this study. This serves as a limitation of this study.

Marshal *et al.* (2013) stated that when it comes to determining an ideal sample size of the population to study, there is a distinct difference between quantitative and qualitative studies. Elliot *et al.*, (2018) reiterated that for quantitative studies, the main concern is ensuring that the sample is representative of the entire population. For qualitative studies like this current study however, the main concern is achieving saturation (Buckley, 2018).

Because of the in-depth interviews utilized in this current study, saturation is reached when interviewing one more building professional will not provide any additional information to the study (Guest *et al.*, 2017). Further, this helps answers the question, ‘What is the ideal number of in-depth interviews to conduct?’ (Guest *et al.*, 2017). Although according to Bolkvadze (2017), there is no scholarly consensus on what this ideal number of interviews, Wong-Parodi and De Bruin (2017), Kosonen and Kim (2018) and Weller *et al.* (2018) however reported that majority of scholars suggest between 10-15 interviews is usually ideal. In this study, there are four categories of building professionals represented: quantity surveyors, architects, builders and civil engineers. The professionals are spread across three regions: Niger state, Abuja and Kaduna state. For this reason, the researchers’ objective was to ensure that each professional category was equally

represented in each of the three regions whilst making sure that the upper saturation limit of 15 interviews (Weller *et al.*, 2018) was at least attained. The table below shows how these two objectives were achieved.

Table 1: Building professionals interviewed by region

Building Professional	Location		
	Niger State	Abuja	Kaduna State
Quantity surveyor	3	3	3
Architect	3	3	3
Builder	3	3	3
Civil Engineer	3	3	3
Sub-Total	12	12	12
Total		36	

In order to mitigate the problem of interviewees giving socially-desirable answers regarding their awareness of BIM, the researchers decided to follow the suggestion of Tucker and Parker (2018) by using audio-visual aids to measure awareness rather than asking the interviewees directly. Specifically for this study, a short three-minute video introducing and showcasing the uses of BIM was downloaded. The table below shows the final set of interview questions used for the actual study to determine how ready BIM professionals in Abuja, Niger state and Kaduna state are to adopt BIM. It also depicts the interview administration process:

Table 2: Final interview questions and administration process

S/N	Factor	Interview Questions
1.	Awareness	<ol style="list-style-type: none"> Are you aware of BIM? [If yes]: Can you explain your understanding of it? Show video after answer. [if no]: Show video immediately
	Filler question to aid interview flow	<ol style="list-style-type: none"> What do you think of the video you have just seen?
2.	Performance expectancy	<ol style="list-style-type: none"> How has BIM improved your effectiveness and efficiency? (those already using BIM) How do you think BIM could improve your effectiveness and efficiency? (those not using BIM)
3.	Effort expectancy	<ol style="list-style-type: none"> How easy was it to implement BIM? (those who have already implemented) How easy do you think it will be to implement BIM? (those who have yet to implement BIM)
4.	Social Influence	<ol style="list-style-type: none"> Does your professional body encourage the use of BIM? [if yes], how?
5.	Facilitating conditions	<ol style="list-style-type: none"> Do you have the necessary resources (expertise, technology, funding) to effectively implement BIM?

5. Results and Discussions

5.1 Demographic characteristics of participants

The table below presents the demographic characteristics of the 36 building professionals interviewed for this study. It includes their gender, age groups, level of professional experience, academic qualifications and the professional bodies they belong to.

Table 3: Demographic characteristics of participants

Demographics		Niger state n = 12					Abuja n = 12					Kaduna state n = 12					Overall Total N = 36
		A	B	C	Q	T	A	B	C	Q	T	A	B	C	Q	T	
Gender	Male	3	3	3	3	12	2	3	2	3	10	2	3	3	3	11	33 (92%)
	Female	0	0	0	0	0	1	0	1	0	2	1	0	0	0	1	3 (8%)
Age	20-29	0	0	0	0	0	0	0	1	0	1	1	0	2	0	3	4 (11%)
	30-39	2	1	2	0	5	2	2	1	1	6	2	2	1	3	8	19 (53%)
	40-49	1	2	1	3	7	1	0	1	2	4	0	1	0	0	1	12 (33%)
	>=50	0	0	0	0	0	0	1	0	0	1	0	0	0	0	0	1 (3%)
Experience	<5year	0	0	0	0	0	0	1	1	0	2	2	1	2	0	5	7 (19%)
	5-10 years	2	0	2	1	5	2	1	0	1	4	0	1	0	3	4	13 (36%)
	11-20 years	1	2	1	2	6	1	0	1	2	4	1	0	1	0	2	12 (33%)
	>20 years	0	1	0	0	1	0	1	1	0	2	0	1	0	0	1	4 (12%)
Acad. Quals.	HND/Diploma	0	0	0	0	0	1	0	0	0	1	0	0	0	0	0	1 (3%)
	First Degree	0	3	1	0	4	1	3	1	3	8	0	2	2	0	4	16 (44%)
	Masters	3	0	2	3	8	1	0	2	0	3	3	1	1	3	8	19 (53%)
	PhD	0	0	0	0	0	0	0	0	0	0	0	0	0	0	0	0 (0%)
Prof. Body	NIA	2	0	0	0	2	2	0	0	0	2	2	0	0	0	2	6
	ARCON	1	0	0	0	1	1	0	0	0	1	1	0	0	0	1	3
	NIQS	0	0	0	2	2	0	0	0	2	2	0	0	0	3	3	7
	QSRBN	0	0	0	1	1	0	0	0	1	1	0	0	0	0	0	2
	COREN	0	0	3	0	3	0	0	0	0	0	0	0	2	0	2	5
	CORBON	0	3	0	0	3	0	3	0	0	3	0	1	0	0	1	7
	NSE	0	0	0	0	0	0	0	3	0	3	0	0	1	0	1	4
	NIB	0	0	0	0	0	0	0	0	0	0	0	2	0	0	2	2

5.2 BIM Awareness

The table below shows the level of BIM awareness amongst the 36 building professionals interviewed for this study. Other subsections of the study discussed BIM awareness by location, BIM awareness by profession, and overall BIM awareness as well as all the other factors explored guiding the acceptance of new technologies; performance expectancy, effort expectancy, social influence and facilitating conditions

Table 4: BIM awareness amongst building professionals in Niger state, Abuja and Kaduna state.

	Niger State		Abuja		Kaduna State		Total	
	Aware	Not aware	Aware	Not aware	Aware	Not aware	Aware	Not aware
Architects	3	0	2	1	2	1	7 (78%)	2 (22%)
Builders	1	2	1	2	0	3	2 (22%)	7 (78%)
Civil Engineers	1	2	0	3	1	2	2 (22%)	7 (78%)
Quantity Surveyors	0	3	1	2	3	0	4 (44%)	5 (56%)
Total	5 (42%)	7 (58%)	4 (33%)	8 (67%)	6 (50%)	6 (50%)	15 (42%)	21 (58%)

5.3 Summary of Findings

Table 5: Summary of the study

S/N	Objective	Findings
1.	BIM Awareness	Only 42% of building professionals were aware of BIM.
2.	BIM Performance Expectancy	100% of building professionals felt adopting BIM would enhance their efficiency and effectiveness.
3.	BIM Effort expectancy	Only 44% of building professionals felt that integrating BIM into their existing practices would be easy.
4.	BIM Social Influence	Only 42% of building professionals felt that their professional bodies encouraged the use of BIM.
5.	BIM Facilitating Conditions	Only 19% of building professionals believed their organizations had the necessary resources to successfully implement BIM.
Conclusion		Building professionals in Niger state, Abuja and Kaduna state are not close to being ready to adopt BIM in the foreseeable future.



4. Conclusion and Recommendations

4.1 Conclusion

The Nigerian building professionals need to be willing and able to adopt new technologies like BIM in order to drastically harmonize and improve performance as well as project delivery of construction works in the country. There is a dire need for Nigerian building professionals to restore their good name and regain their sense of professional pride in providing the highest quality buildings and structures that will keep people and property safe. An important first step in restoring their standing as the providers of the fundamental human right of shelter is to embrace technologies like BIM that will enhance their effectiveness and efficiency. It is hoped that this study will help galvanize the Nigerian building profession to seek greatness once again.

4.2 Recommendations

There is a need for the building professionals in Nigeria to be more aware of technologies that can help propel the practice of the building profession such as Building Information Modelling (BIM) amongst other important issues. As it relates to the curriculum developers, junior and secondary schools in Nigeria should be a point of focus by targeting subjects that are baseline subjects to courses of Engineering/Environmental technology. One of such subjects in focus should be “construction technology”. Identified subjects such as construction technology should be taught digitally rather than through the traditional use of the drawing board. This will afford the students to better understand the concept of BIM early on. Curriculum developers at states and federal levels should set up at least one (1) standard computer lab with no less than ten (10) computers, a power back-up system (inverter) with solar panels in all government owned junior and secondary schools through Universal Basic Education (UBE) funding with counterpart support funding from the state

government. Secondary schools teachers, who are to teach the identified subjects digitally, should be trained and retrained by the government through UBE or other sources as deemed appropriate by states governments. At the tertiary institution level, courses that are crucial for the adoption of BIM in the construction industry such as construction technology, engineering design and architectural courses should be pre-requisites taught with relevant software at different levels in the universities or tertiary institutions in construction related disciplines. This will help the students see the existing linkages and relevance of the use of BIM and collaborating with other construction professionals in the construction industry.

As it relates to the professional bodies for building professionals, the study's results showed that many of the building professionals felt that these organizations did not do enough to encourage the adoption of such innovations and technologies like BIM. Besides merely discussing in seminars and workshops, professional bodies such as ARCON, NIA, NIQS, RQSBN, COREN, ESTABORN etc. should enforce the use of BIM through regulations of their members and memberships in the industry. If admission into these bodies is dependent on BIM implementation, it will ensure that building professionals are strongly encouraged to adopt such new technologies which will improve the efficiency and effectiveness of the entire industry. An additional step these professional bodies can take is to draft a bill for the national assembly seeking a law mandating the adoption and use of BIM by the construction industry professionals from the design stage through implementation and handover of a construction project of a defined magnitude or complexity.

Finally, NIA had done a good job establishing an agreement with AutoDesk whereby their members can purchase BIM related software at a discounted rate. Other professional bodies can follow their examples and establish similar partnerships with manufacturers of BIM software. These partnerships can be expanded to include BIM trainings and even internships for Nigerian building professionals.

A crucial stakeholder for the advancement of the Nigerian building industry through the adoption of innovative technologies like BIM is the Nigerian government. The reality is that for BIM to be effectively integrated and utilized by building professionals, there are certain basic infrastructure such as stable electricity and high-speed internet that are a must-have. Until and unless the government is able to establish such basic, but crucially important, infrastructure, widespread BIM adoption in the Nigerian building industry might remain an unattainable dream. Other policies the government can enact include the encouragement of the development of innovative building software by local Nigerian software developers and making it mandatory for Nigerian building professionals to utilize such locally-developed software when bidding for government building projects.

REFERENCES

- Abanda, F. H., Vidalakis, C., Oti, A. H., & Tah, J. H. (2015). A critical analysis of Building Information Modelling systems used in construction projects. *Advances in Engineering Software*, 90, 183-201.
- Addy, M., Adinyira, E., & Ayarkwa, J. (2017). Antecedents of building information modelling adoption among quantity surveyors in Ghana: an

- application of a technology acceptance model. *Journal of Engineering, Design and Technology*, (just-accepted), 00-00.
- Adjei, J. M.P. (2014). An Evaluation of the Approaches Used by Graduates in Job Search, Ghana. *Journal of Finance and Economics*, 2(1), 36-43.
- Afify, M. (2018). E-learning content design standards based on interactive digital concepts maps in light of meaningful learning theory and constructivist learning theory. *Journal of Technology and Science Education*, 8(1), 5-16.
- Ahuja, R., Jain, M., Sawhney, A., & Arif, M. (2016). Adoption of BIM by architectural firms in India: technology–organization–environment perspective. *Architectural Engineering and Design Management*, 12(4), 311-330.
- Aibinu, A., & Venkatesh, S. (2013). Status of BIM adoption and the BIM experience of cost consultants in Australia. *Journal of Professional Issues in Engineering Education and Practice*, 140(3), 04013021.
- Aklin, M., Cheng, C. Y., & Urpelainen, J. (2018). Geography, community, household: Adoption of distributed solar power across India. *Energy for Sustainable Development*, 42, 54-63.
- Alazmeh, N. I. D. A. A., Underwood, J. A. S. O. N., & Coates, S. P. (2017). Implementing a BIM collaborative workflow in the UK construction market. *International Journal of Sustainable Development and Planning*, 13(1), 24-35.
- Alfonso, M. L., Colquitt, G. T., Walker, A. D., & Gupta, A. (2016). Adapting a physical activity intervention for youth in a rural area: A case study. *Journal of the Georgia Public Health Association*, 5(3), 204-211.
- Ali, M., Raza, S. A., & Puah, C. H. (2017). Factors affecting to select Islamic credit cards in Pakistan: the TRA model. *Journal of Islamic Marketing*, 8(3), 330-344.
- Arayici, Y., & Coates, S. P. (2013). Operational knowledge for BIM adoption and implementation for lean efficiency gains. *Journal of Entrepreneurship and Innovation Management*, 1(2), 1-21.
- Arayici, Y., Coates, P., Koskela, L., Kagioglou, M., Usher, C., & O'reilly, K. (2011a). BIM adoption and implementation for architectural practices. *Structural survey*, 29(1), 7-25.
- Arayici, Y., Coates, P., Koskela, L., Kagioglou, M., Usher, C., & O'reilly, K. (2011b). Technology adoption in the BIM implementation for lean architectural practice. *Automation in construction*, 20(2), 189-195.
- Ashagidigbi, W. M., Amos, T. T., & Azeez, F. (2018). Contribution of Fluted Pumpkin Leaf Production by Women to Household Income in the Tropics. *International Journal of Vegetable Science*, 24(3), 205-211.
- Atazadeh, B., Kalantari, M., Rajabifard, A., Ho, S., & Champion, T. (2017). Extending a BIM-based data model to support 3D digital management of complex ownership spaces. *International Journal of Geographical Information Science*, 31(3), 499-522.
- Babatunde, S. O., & Perera, S. (2017). Barriers to bond financing for public-private partnership infrastructure projects in emerging markets: A case of Nigeria. *Journal of Financial Management of Property and Construction*, 22(1), 2-19.
- Barton, P. T. (2018). A level-set based Eulerian method for simulating problems involving high strain-rate fracture and fragmentation. *International Journal of Impact Engineering*, 117, 75-84.
- Bates, S., & Saint-Pierre, P. (2018). Adaptive Policy Framework through the Lens of the Viability Theory: A Theoretical Contribution to Sustainability in the Anthropocene Era. *Ecological Economics*, 145, 244-262.
- Bavorova, M., Traikova, D., & Doms, J. (2018). Who are the farm shop buyers? A case study in Naumburg, Germany. *British Food Journal*, 120(2), 255-268.
- Bhattacharjee, A., Davis, C. J., Connolly, A. J., & Hikmet, N. (2018). User response to mandatory it use: A coping theory perspective. *European Journal of Information Systems*, 1-20.
- Bin Zakaria, Z., Mohamed Ali, N., Tarmizi Haron, A., Marshall-Ponting, A. J., & Abd Hamid, Z. (2013). Exploring the adoption of Building Information Modelling (BIM) in the Malaysian construction industry: A qualitative approach. *International Journal of Research in Engineering and Technology*, 2(8), 384-395.
- Bolkvadze, K. (2017). Hitting the saturation point: unpacking the politics of bureaucratic reforms in



- hybrid regimes. *Democratization*, 24(4), 751-769.
- Brand, R., & Ekkekakis, P. (2018). Affective–Reflective Theory of physical inactivity and exercise. *German Journal of Exercise and Sport Research*, 48(1), 48-58.
- Bredella, N., & Höfler, C. (2017). Processes and practices in computational design. *arq: Architectural Research Quarterly*, 21(1), 5-9.
- Chong, H. Y., Lopez, R., Wang, J., Wang, X., & Zhao, Z. (2016). Comparative analysis on the adoption and use of BIM in road infrastructure projects. *Journal of Management in Engineering*, 32(6), 05016021.
- Cordero, R., Mascareño, A., & Chernilo, D. (2017). On the reflexivity of crises: Lessons from critical theory and systems theory. *European Journal of Social Theory*, 20(4), 511-530.
- Dawson, J., & Jöns, H. (2018). Unravelling legacy: a triadic actor-network theory approach to understanding the outcomes of mega events. *Journal of Sport & Tourism*, 22(1), 43-65.
- Devi, W. P., & Kumar, H. (2018). Frugal Innovations and Actor–Network Theory: A Case of Bamboo Shoots Processing in Manipur, India. *The European Journal of Development Research*, 1-18.
- Ding, Z., Zuo, J., Wu, J., & Wang, J. Y. (2015). Key factors for the BIM adoption by architects: A China study. *Engineering, Construction and Architectural Management*, 22(6), 732-748.
- Doumbouya, L., Gao, G., & Guan, C. (2016). Adoption of the Building Information Modeling (BIM) for construction project effectiveness: The review of BIM benefits. *American Journal of Civil Engineering and Architecture*, 4(3), 74-79.
- Du, Y., Roberts, P., & Xu, Q. (2017). The effects of tai chi practice with asynchronous music on compliance and fall-related risk factors in middle-aged and older women: a pilot study. *Journal of Holistic Nursing*, 35(2), 142-150.
- Eadie, R., Browne, M., Odeyinka, H., McKeown, C., & McNiff, S. (2015). A survey of current status of and perceived changes required for BIM adoption in the UK. *Built Environment Project and Asset Management*, 5(1), 4-21.
- Edirisinghe, R., Kalutara, P., & London, K. (2016). An investigation of BIM adoption of owners and facility managers in Australia: Institutional case study. Retrieved from <http://researchbank.rmit.edu.au/view/rmit:38270/n2006066771.pdf>
- Elliott, H., Parsons, S., Brannen, J., Elliott, J., & Phoenix, A. (2018). Narratives of fathering young children in Britain: linking quantitative and qualitative analyses. *Community, Work & Family*, 21(1), 70-86.
- Elmelund-Præstekær, C., Hopmann, D. N., & Pedersen, R. T. (2017). Survey Methods, Traditional, Public Opinion Polling. *The International Encyclopedia of Communication Research Methods*, 1-5.
- Elmustapha, H., Hoppe, T., & Bressers, H. (2018). Consumer renewable energy technology adoption decision-making; comparing models on perceived attributes and attitudinal constructs in the case of solar water heaters in Lebanon. *Journal of Cleaner Production*, 172, 347-357.
- Loveday, J., Kouider, T., & Scott, J. (2016). The Big BIM battle: BIM adoption in the UK for large and small companies. Retrieved from <http://rua.ua.es/dspace/handle/10045/55250>
- Mahalingam, A., Yadav, A. K., & Varaprasad, J. (2015). Investigating the role of lean practices in enabling BIM adoption: Evidence from two Indian cases. *Journal of Construction Engineering and Management*, 141(7), 05015006.
- Malik, K., Chand, P. K., Marimuthu, P., & Suman, L. N. (2018). Awareness and beliefs about alcohol use among women in India. *International Journal of Culture and Mental Health*, 11(3), 311-320.
- Mamun, A. A. (2018). Diffusion of innovation among Malaysian manufacturing SMEs. *European Journal of Innovation Management*, 21(1), 113-141.
- Marcus, B., Weigelt, O., Hergert, J., Gurt, J., & Gelléri, P. (2017). The use of snowball sampling for multi source organizational research: Some cause for concern. *Personnel Psychology*, 70(3), 635-673.
- Marshall, B., Cardon, P., Poddar, A., & Fontenot, R. (2013). Does sample size matter in qualitative research?: A review of qualitative interviews in



IS research. *Journal of Computer Information Systems*, 54(1), 11-22.

- Masood, R., Kharal, M. K. N., & Nasir, A. R. (2014). Is BIM adoption advantageous for construction industry of Pakistan?. *Procedia Engineering*, 77, 229-238.
- Mehran, D. (2016). Exploring the Adoption of BIM in the UAE Construction Industry for AEC Firms. *Procedia Engineering*, 145, 1110-1118.
- Mills, F. (2016). What is 4D BIM? Retrieved from <https://www.theb1m.com/video/what-is-4d-bim>
- Moberg, E. (2018). Exploring the relational efforts making up a curriculum concept—an Actor-network theory analysis of the curriculum concept of children's interests. *Journal of Curriculum Studies*, 50(1), 113-125.
- Mom, M., Tsai, M. H., & Hsieh, S. H. (2014). Developing critical success factors for the assessment of BIM technology adoption: Part II. Analysis and results. *Journal of the Chinese Institute of Engineers*, 37(7), 859-868.
- Monko, R. J., Berryman, C. W., & Friedland, C. J. (2017). Critical Factors for Interorganizational Collaboration and Systemic Change in BIM Adoption. *International Journal of Construction Engineering and Management*, 6(4), 111-132.
- Ngooi, B. X., Packer, T. L., Warner, G., Kephart, G., Koh, K. W. L., Wong, R. C. C., & Lim, S. P. (2018). How adults with cardiac conditions in Singapore understand the Patient Activation Measure (PAM-13) items: a cognitive interviewing study. *Disability and rehabilitation*, 40(5), 587-596.



Design and Implementation of an SMS-based dynamic matrix LED Display Board

*Habibu, H.¹, Chukwu, E. C.², Latifa, Y.³, Haris, M. Y.⁴ & Okosun, O. E.⁵

^{1,3,4,5}Electrical and Electronics Engineering Department, Federal University of Technology, PMB 65
Minna Niger State, Nigeria

²Electrical and Electronics Engineering Department, Nile University of Nigeria, Plot 681
Abuja, FCT, Nigeria

*Corresponding author email: habufarid@futminna.edu.ng, +2348066544604

ABSTRACT

This research work involves the development and implementation of an SMS-based dynamic matrix LED display board. It is a model for displaying messages at strategic positions on campus that requires real-time noticing at various locations such as lecture halls, health care center, Bus-park, cafeteria and so on. The device is developed based on Microcontroller control over GSM technology. The administrator (user) sends a message in the form of SMS via Mobile phone. The GSM/GPRS module in the device receives the sent message and sends it directly to the Master unit (Microcontroller). The Microcontroller performs a password check on the strings it received. If there is a password match, it displays the message on the arrays of the fast switching Light Emitting Diodes (LEDs) else the message is discarded, after which it displays current date time as default message. The SMS is stored in the Module's SIM card after each message has been displayed repeatedly for five times, thereby giving room for the next SMS to be displayed. When the queue is filled, then any new message received would replace the oldest in the memory. This device will eliminate the inconveniences of physically going to the display board to manually input information or messages. This device will find application in our educational institutions.

Keywords: Global System for Mobile Communication (GSM), Light Emitting Diode (LED), Short Message Service (SMS).

1 INTRODUCTION

The need for information dissemination in our educational institutions cannot be overemphasized due to its importance in conveying important information from an individual to another. The application of Global System for Mobile Communications (GSM) and General Packet Radio Service (GPRS) based designs, has developed an innovative and public utility product used for mass communication (Kenneth, 2007). The visual impact is the most effective mode of influencing human minds, which is the main purpose of advertisements and communication. A display device serves this purpose. A display device is a device used for the presentation of information for visual reception. This device is an SMS (Short Message Service) based dynamic matrix LED (Light Emitting Diode) scrolling (moving) message display. It displays the message received via Short Message Service (SMS) or General Packet Radio Service (GPRS) packets.

The message to be displayed is sent via Short Message Service (SMS) by an authorized user in a unique format containing the appropriate password followed by the message to be displayed. When this message is sent, the Global System for Mobile Communication (GSM) Module incorporated in the device receives the text and

sends the strings to the Master unit (Microcontroller) over UART (Universal Asynchronous Receiver/Transmitter). The Microcontroller then compares the first four characters with a predefined password. If there is a password match with the programmed password, the message will be displayed. This electronic device consists of a matrix of LEDs (Light Emitting Diodes) arranged in a rectangular configuration such that by switching ON or OFF selected lights, texts or graphics can be displayed. This electronic device can be kept in a lecture theatre and can be managed by an administrator. The administrator can also change the password of this device anytime it is compromised. Class representatives', Lecturers', examination officers' and any other authorized user can send flash information from their mobile phones to this device for instant viewing irrespective of their distance from the device, which makes the device completely wireless. As a result of the current advancement in technology, wireless communication has announced its arrival on the big stage since the world is now going mobile (Mazidi and Mazidi, 2016). This device is built with the aid of an embedded system. The use of embedded systems in sharing information has given rise to many interesting applications that ensures comfort and safety to human life (Vijay, 2007).

The purpose of this research work is to design and develop an electronic system that can adequately receive Short Message Service (SMS) and effectively display the sent information on an array of Light Emitting Diodes (LEDs). Due to the versatility of this device, it can be used in banks to show the current value of trading on the stock exchange market, currency exchange rate and interest rate. It can also be used in a shopping mall to notify customers' of the prices of goods and other commercial information. Research works similar to this can be found in (Bollen and Hoppe, 2004), (Kurdthongmee, 2005), (Gaurav et al, 2017), (Ketkar et al, 2013), (Kumar et al, 2018), (Kumar et al, 2012), (Ryan, 2019), (Maha, Bhuiyan, & Masduzzaman, 2019), and (Singh, et al., 2019). The uniqueness about this work is in the provision of an alternative way of sending a message via the use of a keyboard connected to the display system in a situation of GSM network unavailability.

2 MATERIALS AND METHOD

The method adopted in carrying out this work is the principle of serial communication in collaboration with an embedded system. The display device was built by arranging Light Emitting Diodes (LEDs) in the form of a [7x5] matrix in ten (10) places, turning them ON and OFF at a very high speed. The user of this device is expected to send a Short Message Service (SMS) in a unique format containing the appropriate password followed by the message to be displayed. The use of a password was incorporated into the system to eliminate unauthorized access to the device. The Module (SIM 300) in the device receives a text and then sends the strings to the Microcontroller over Universal Asynchronous Receiver and Transmitter (UART). The Microcontroller compares the first four (4) characters with the predefined password, if there is a match, the message received will be scrolled for a programmed time, and else the message is discarded. The device beeps through a buzzer which was interfaced with the Microcontroller for at least three (3) times to alert the audience that a new message is about to be displayed. After the message must have been displayed, it returns back to display the current date and time as the default message. A 230V AC power supply Mains was stepped down, rectified, filtered and regulated to obtain the desired operational output voltage of 5V. An extra battery bank of 6V was also incorporated in the device. It serves as a back-up power supply to the device during a power outage.

The methods used in developing this device consist of two sections viz: the Hardware and the Software section. The use of breadboard was adopted in the hardware

section for building and testing of the circuit components. The software section is sub-divided into two parts. The first part involves the writing of the program codes with the aid of software called "Mickro C". The second part of the software section is a circuit simulation. The simulated design of the hardware was tested and analyzed before the actual circuit was built. The software used for the schematic capture and circuit simulation is known as "Proteus Professional".

The idea behind the research was to ease access to information in our educational institutions, putting into extinction the old practice or method of disseminating information. Figure 1 shows the block diagram design of the various stages that makes up the display device.

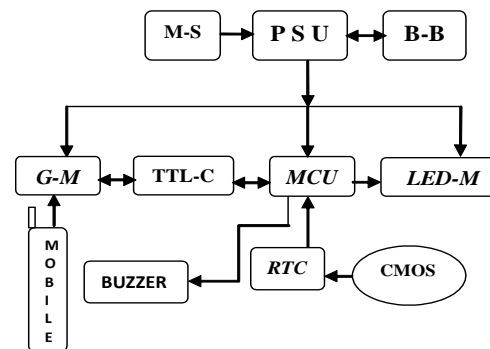


Figure 1. System Block Diagram

The various units (modules) that make up the system are discussed in the following subsections:

2.1 POWER SUPPLY UNIT

This unit consists of a 230V/12V, 1.5A transformer which stepped down the 230V AC mains to 12V AC. This voltage was then fed into a full-wave bridge rectifier (KBL406) which was used to convert the oscillating AC voltage into a unidirectional DC voltage. The DC voltage was then fed into the two 1000 μ F electrolytic capacitors which filter out the voltage ripples of about ± 2 V. The filtered DC voltage was then fed into a 7809 voltage regulator which maintains the voltage level at a fixed output of 9V followed by a 7805 regulator which further limits the voltage level to a constant voltage of 5V required to drive the whole circuit. A 10 μ F capacitor was placed after each voltage regulator to suppress any possible ripples and also to enhance the stability of the voltage regulators.

The output DC voltage and filter capacitor used is thus calculated using equations (1) and (2) (Gupta, 2009).

$$V_{L(DC)} = \frac{2 \times V_s(max)}{\pi} \quad (1)$$

$$= \frac{2 \times \sqrt{2} \times v_{rms}}{\pi}$$

therefore: $V_{L(DC)} = \frac{2 \times \sqrt{2} \times 12V}{\pi} = 10.80V.$

Hence, the output DC voltage is approximately 11V DC. The filter capacitor used was as:

$$C = \frac{1}{(4V\gamma F\sqrt{3})} \quad (2)$$

Where V is the supply voltage, γ =Ripple factor and F is the system frequency. Hence,

$$C = \frac{1}{(4 \times 12 \times 0.12 \times 50 \times \sqrt{3})} = 0.002005F = 2005\mu F.$$

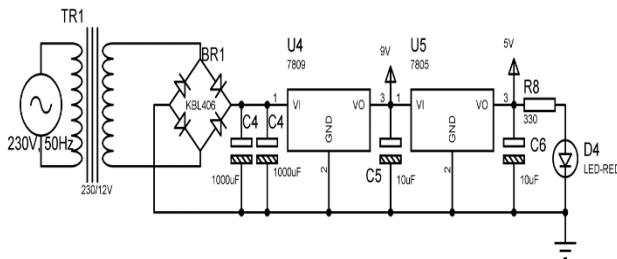


Figure 2. Circuit diagram of the power supply Unit

The 12V AC transformer was used because 12V is the maximum voltage required by the components in this circuit i.e. the buzzer, 1.5A is just sufficient to meet the brightest current requirement of the whole 350 LED's. (KBL406) bridge rectifier was chosen because it can rectify up to 100V. Two 1000µF capacitors were used because the resultant capacitance of the two capacitors in parallel is the sum of the two capacitors and the voltage handling capacity is just more than required. Two (2) voltage regulators (7809 and 7805) were chosen and used so as to avoid excessive heat loss on a single regulator.

2.2 CONTROL UNIT

This unit consists of the Microcontroller and seven 74HC595 shift registers as shown in Figure 3. All the ICs stake 5V from the power supply unit. The DS pin (pin14) of the first shift register was connected to PB0 (pin1) of the Microcontroller while the rest are cascaded by connecting the Q7 pin of the current shift register to the DS pin of the subsequent shift registers. The SH_CP pin (pin11) was connected to PB1 (pin2) of the Microcontroller and the ST_CP (pin12) to PB2 (pin3) of the Microcontroller. Whenever a row is set to logic 1, the corresponding data bits of each character to be displayed

is extracted and arranged serially in the shift registers through the DATA pin. This is done in 50 SH_CP clock cycles after which the ST_CP is pulsed once to latch the arranged data bits. The output is used to trigger the ULN2003A in the display section immediately since the enable pin is always HIGH. The same process is repeated for the other rows.

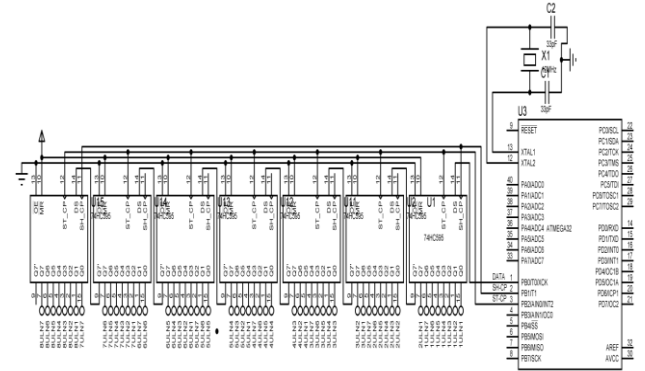


Figure 3. Circuit diagram of the control unit

The AT-mega 32 was used because it has enough memory to manage this data. It has 3 timers and they were used to generate clock pulse at overflow interrupt and many GPIO pins out of which three (3) were used to control the shift register. 74HC595 shift registers were chosen because they are fast, low power consumption and easy to control.

2.3 DISPLAY UNIT

This unit is an important part of this research because it displays the message sent to the device. It consists of three hundred and fifty (350) LEDs arranged in matrix form, forming 7 rows and 50 columns as shown in Figure 4. All the anodes were wired together to form the rows, while the cathodes were also joined together to form the columns. This was carried out to minimize the number of pins needed to drive each LED. The rows were connected to PORT A of the ATmega32 Microcontroller. ULN2003A was used to drive the columns, the 16 pin IC contain seven (7) in-built Darlington NPN transistors, having a maximum collector-emitter voltage of 50V. Each channel is capable of sinking 500mA and can withstand peak current of 600mA. Eight (8) ULN2003A were used to achieve this project. Each output pins of the ULN2003A were connected to a column of the LED matrix.

The Microcontroller was used to drive the rows directly because it can source up to 40mA DC current at any

GPIO. ULN2003A was chosen because it is cheap, robust and has a very high gain. Ultra-bright LED's were used because they glow with a sparkling brightness, they can take as low as 1.8V and 25mA.

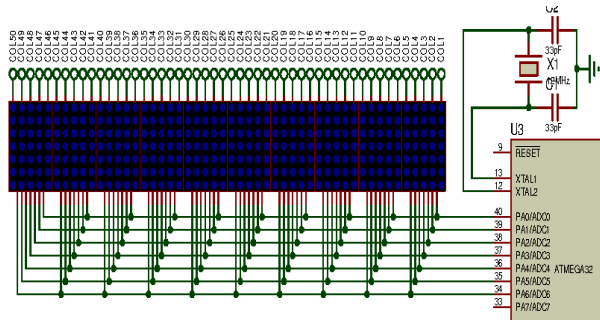


Figure 4. Circuit diagram of the display unit

2.4 COMMUNICATION UNIT

The communication unit comprises of the GSM/GPRS module (SIM300) and a microcontroller as shown in Figure 4. The GSM module communicates with the Microcontroller over UART. The Microcontroller controls the module using the standard AT Commands (Attention Command). The Microcontroller receives the message to be displayed from the GSM module in form of strings at a baud rate of 9600 Bps. It processes the data after which it extracts the message to be displayed or the time/date setting information.

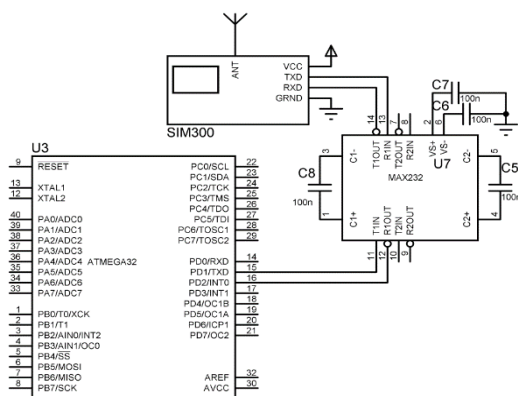


Figure 5. Circuit diagram of the communication unit

The SIM300 was used because it can be programmable via AT command. The Microcontroller was chosen because it has the UART feature which is needed to interface both devices.

2.5 REAL-TIME UNIT

The real-time unit comprises of the Microcontroller, DS1307 real-time clock (RTC), and two pull-up resistors as shown in Fig. 6. The serial clock input (SCL) and the serial data input/output (SDA) pins of the DS1307 real-time clock were connected to pins PC0/SCL and PC1/SDA respectively of the Microcontroller. It serves as the communication line between the Microcontroller and the DS1307 clock. A 32.768 kHz crystal oscillator was used to clock the DS1307. The two pull-up resistors as shown in Fig.3.6 were used to pull up the communication line. A 3V CMOS (Complimentary Metallic Oxide Semiconductor) battery was used as a back-up battery to keep the time/date counting during a power outage.

The AT-mega 32 Microcontroller was used because it has I²C and TWI interface. DS1307 was chosen because it consumes low power and provides seconds, minutes, hours, day, date, month, and year information. The CMOS battery was used because it is resistant to corrosion.

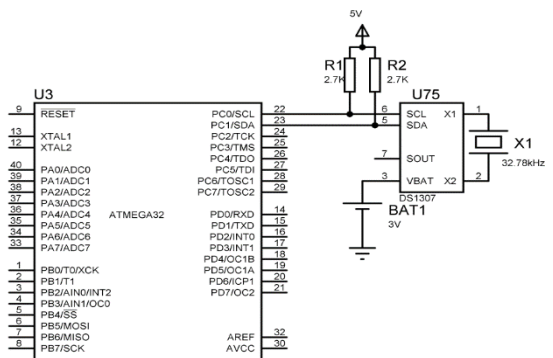


Figure 6. Circuit diagram of the real-time unit

3 TESTS CARRIED OUT

It is a common practice that when a project is designed and constructed, it is expedient that the test should be conducted on it so as to ascertain results in comparison to a standard. Tests were conducted on the overall system. The results obtained were compared with the design specification using a test instrument such as Digital multimeter.

3.1 TEST ON POWER SUPPLY UNIT

A digital Multimeter was used in testing the power supply unit at various outputs such as the transformer, rectifier, 7809 and 7805 voltage regulators, shift register and the LED. The results obtained are shown in Table 1.

TABLE 1. TEST ON POWER SUPPLY UNIT

COMPONENTS	VOLTAGE OUTPUTS (Volts)
Transformer	12.00
Rectifier	10.80
7809 Voltage Regulator	8.95
7805 Voltage Regulator	4.96
Microcontroller	4.85
Shift Register	4.89
LED Connected in Shunt	1.93

3.2 TEST ON LED-MATRIX DISPLAY BOARD

Testing of the LED-Matrix Display board was carried out by sending some Short Message Service (SMS) with the four (4) digit predefined password, using a Mobile-phone to the GSM module incorporated in the device and the results thus obtained are as shown in Table 2.

4 RESULTS AND DISCUSSION

The overall system/device was tested to meet the design requirement and functionality specifications of each component that makes up the entire circuit.

From Table 1, a test carried out at various outputs of the components used for this research such as; transformer, rectifier, voltage regulators, shift register, and Microcontroller, showed conformity to standard because the measured values were approximate that of the original manufacturer's value.

From Table 2, tests carried on the LED Matrix display board showed that after sending a message with the appropriate password, the message displayed on the board is exactly that of the originally sent message.

5 CONCLUSION

This design work was implemented and found to be functioning in compliance with the model specifications as expected. The device was developed based on Microcontroller control over GSM technology thereby eliminating the inconveniences of physically going to the display board to manually input information or messages.

TABLE 2. LED-MATRIX DISPLAY BOARD RESULTS

MESSAGE SENT	MESSAGE DISPLAYED ON BOARD
1989DISP Please submit your project work.	Please submit your project work.
1989DISP EEE 522 Lecture holds by 11.00am.	EEE 522 Lecture holds by 11.00am.
1989DISP Happy birthday to Mr. Haruna Ali.	Happy birthday to Mr. Haruna Ali.
1989DISP Submit your course form to Jack.	Submit your course form to Jack.
1989DISP I will be with you In 30minutes time.	I will be with you In 30minutes time.
1989DISP Am on my way to Dubai. Lectures continue when I return. Thank you.	Am on my way to Dubai. Lectures continue when I return. Thank you.



Figure 7. Result of the Implemented Research Work

This device can be used our educational institutions and other establishments that want to do away with the use of papers for displaying messages. The device is easy to use.



The developed model can be improved upon to display multiple lines of messages at a time.

Big Data Analytics for Smart Generation (pp. 105-133). Springer, Cham.

REFERENCE

- Bollen, L., Eimler, S., & Hoppe, H. U. (2004). SMS-based discussions-technology enhanced collaboration for a literature course. In *The 2nd IEEE International Workshop on Wireless and Mobile Technologies in Education, 2004. Proceedings.* (pp. 209-210). IEEE.
- Gaurav, S., Rushabh, T., Vaidehi, K., Rupesh, S., & Manish, K. S. (2017). A Past, Present and New Features of Digital Notice Board. *International Journal of Scientific and Research Publications*, 594-601.
- Gupta, J. B. (2009). *Electronic Devices and circuits.* Seagull Books Pvt Ltd.
- Kenneth, A. J. (2007). The 8051 Microcontroller. *Johnson Press, New York, USA*, 23-42.
- Ketkar, P. U., Tayade, K. P., Kulkarni, A. P., & Tugnayat, R. M. (2013). GSM mobile phone based led scrolling message display system. *International Journal of Scientific Engineering and Technology*, 2(3), 149-155.
- Kumar, K., Ritu, K., Singh, M., & Patil, M. V. (2018). Wireless Display using GSM and Arduino.
- Kumar, P., Bhrdwaj, V., Pal, K., Rathor, N. S., & Mishra, A. (2012). GSM based e-Notice Board: wireless communication. *International Journal of Soft Computing and Engineering*, 2(3), 601-605.
- Kurdthongmee, W. (2005). Design and implementation of an FPGA-based multiple-colour LED display board. *Microprocessors and Microsystems*, 29(7), 327-336.
- Maha, M. M., Bhuiyan, S., & Masduzzaman, M. (2019). Smart Board for Precision Farming Using Wireless Sensor Network. *2019 International Conference on Robotics, Electrical and Signal Processing Techniques (ICREST)* (pp. 445-450). IEEE.
- Mazidi, M. A., & Mazidi, J. G. (2016). The 8051 microcontroller and embedded systems. *Instructor*.
- Ryan, T. (2019). Variable Frame Rate Display for Cinematic Presentations. *SMPTE Motion Imaging Journal*, 10-14.
- Singh, R., Anita, G., Capoor, S., Rana, G., Sharma, R., & Agarwal, S. (2019). Internet of Things Enabled Robot Based Smart Room Automation and Localization System. *Internet of Things and*



AN IMPROVED USER PAIRING, SUBCHANNELING, AND POWER ALLOCATION ALGORITHM FOR 5G NOMA SYSTEM.

* Muhammad Z.Z¹, Tekanyi A.M.S², Abubilal K.A³, Usman A. D⁴, Abdulkareem H. A⁵ * and Kassim A. Y⁶

^{1,2,3,4,5&6} Department of Communications Engineering, Ahmadu Bello University, Zaria- Nigeria.

*Corresponding Author Email address: zzmuhammad38@gmail.com

Due to increasing demand on telecommunications services, wireless network suffers low speed and high latency. These seriously impact on the performance of the networks because there is a big burden on the existing multiplexing techniques such as Orthogonal Multiple Access (OMA) to deliver high speed data rates. Hence, the ever increasing demand for high speed and low latency data communications by mobile users define future features of networks. To ease the burden on the existing multiple access techniques and also offer high data rates in 5G networks, Non Orthogonal Multiple Access (NOMA) is used to multiplex multiple users over the same channel at the same time and frequency. The high speed sum rate of data in this kind of multiple access is another problem because it depends on efficient user pairing, subchanneling, and power allocation techniques used to avoid high rate of interference and decoding errors. These important conditions are difficult to meet because techniques are not perfects. These techniques used by previous researchers to resolve low speed and high latency introduced some problems such as multi user and inter user interference, hence the need to improve these techniques. In this research work, an improved user pairing, subchanneling, and power allocation algorithm that used the differences in channel conditions (that is, channel gain) of users and sub channeling to mitigate the effect of multi-user and inter user interferences in 5G NOMA systems to improve data sum rate, coverage probability, and Energy Efficiency was developed. A multiple users' downlink NOMA system with N subchannels and 32 users that were uniformly distributed in a circle of 300 meters diameter was considered.

Keywords: OFDMA, NOMA, Power Allocation, Sum rate, Coverage probability, Energy Efficiency, SIC.

1. INTRODUCTION

Every generation of wireless communications systems comes with additional features and also increases the speed at which communication is done. 1G gives the first cellphone, 2G allows users to text for the first time, 3G connects users to the internet and 4G allow users to enjoy the internet speed of today. The exponential increase in the number of mobile subscribers and the emergence of various technologies such as; Virtual Reality, Augmented Reality, Artificial Intelligence (AI), Three-Dimensional (3D) media, Ultra-high Definition Transmission Video (UDTV), Internet of Things (IoT), Intelligence Transport Systems (ITS), etc. in the society have created a significant increase in the demand for high data rate in wireless networks (Xiao et al., 2017). It is predicted that there will be over 100 billion subscribers by the year 2025 and more than 7.6 percent of the mobile subscribers would use their devices to download and upload information (Wei et al., 2017). Network operators using LTE platform and running the network on this platform will not be able to cope with the rate of the data increment (Chen et al., 2018). In order to withstand strict and harsh conditions, handle more data, pursuit higher sum rate, increase capacity, spectral and energy efficiency at a considerable cost in 5G, Non Orthogonal Multiple

Access (NOMA) is considered due to its ability to handle multiple users in same channel at same time and frequency without any separation between them (Ding et al., 2017). In a NOMA system, resource is assigned to multiple users unlike Orthogonal Multiple Access (OMA), where single radio resource (i.e. frequency or time) can only be allocated to one user (Wei et al., 2017). Current researches have verified that NOMA can increase the overall sum rate of macro cell significantly in the downlink scenario.

This technique requires a combination of serial interference cancellation or maximum probability of demodulation to achieve the ultimate capacity limit of the system. Its difficulty is in the design and implementation of a low complex and effective transmitter and receiver algorithm, which is the hottest research area worldwide. NOMA as a new technique, that incorporates some 3G and 4G techniques and ideas. For example, subchannels and carriers were employed in 4G and Successive Interference Cancellation (SIC) was used in 3G. NOMA uses orthogonal transmission between subchannels, so the near-far problem in 3G is reduced and multiple access interference problem is also mitigated. NOMA allows one subchannel to be shared by multiple users under the

same transmit rate which enhances the spectrum efficiency. NOMA is used in 5G not because it can satisfy the mobile service speed demand but also it enhances spectrum efficiency. For effective utilization of NOMA, user pairing, subchanneling and power allocation procedure is developed to avoid high rate of interference, error during decoding, and power wastage during transmission. User pairing is the process of pairing users based on the difference that exists between them which could be received power level, channel correlation, or proportional fairness (Tsai & Wei, 2018). Subchannel allocation is the process of allocating users to subchannels based on their data and power requirements (Ding et al., 2015). Also power allocation is the process of allocating power to users and subchanneling is based on the channel condition requirement of each user (He et al., 2016).

2. RELATED WORKS

Liu et al., (2015) developed a User Pairing and Power Allocation (UPPA) technique for two user NOMA systems. The technique used optimal closed form solution for Power Allocation (PA) and Proportional Fairness (PF) equations to derive a PA equation with proportional fairness objective. The derived equation was then used to develop UPPA technique that allocated power to user pairs without unnecessary comparison between them. The performance of the technique was compared with OFDMA and Tree based Transmit Power Allocation (TTPA) and showed a significant improvement in terms of user fairness and system efficiency over OFDMA and achieved higher gain with low complexity over TTPA. The number of users in the algorithm was limited and fixed at two, which restrained the application of NOMA as a multiple access technique and did not give significance to network energy usage. This is a serious limitation of their system.

Al-Abbasi & So, (2015) proposed a power allocation algorithm for maximization of sum rate in NOMA systems based on total transmit power and minimum rate constraint. The algorithm used Lagrangian function to obtain an optimal closed form power solution function in which two sub-optimal approaches with low complexity were used to provide solution to the closed form solution function. The first approach allocated power equally to each subcarrier, which was in turn allocated to user within it based on their service requirement, while the other used average channel gain to allocate power to each user. The performances of the two algorithms were compared with OFDMA and other existing sub-optimal and optimal algorithms and showed better performance with similar behavior as the optimal one. The two approaches were also compared with one another, the first approach outperformed the later at the expense of slightly higher complexity. Similar limitations were encountered, in that, the number of users in these

algorithms were limited and fixed at two, which restrained the application of NOMA as a multiple access technique and energy usage of the network was not accounted for.

Liu et al., (2016) developed a tree searching-based User Set Selection (USS) technique on the closed form solution of Power Allocation (PA) with a proportional fairness objective to derive a set selection theorem which classified users into singular user and non-singular user sequence based on optimal PA. The technique achieved a significant complexity reduction compared to exhaustive searching techniques and a close performance as the optimal technique in terms of user fairness. The technique omitted candidate users' sets with similar or identical optimal PA from the USS and considered only cell centered users in a uniformly distributed manner, which was a setback on the algorithm because it restrained the diversity of NOMA as a multiple user access technique.

Al-Abbasi & So, (2016) proposed a sub-optimal hierarchical (proportional and uniform distribution) power sharing algorithm with vertical user pairing concept to share transmit power between multiple users in a NOMA system. The algorithm used closed form power sharing solution to estimate the power requirement of each user and group them into two, based on their channel condition and power requirements. The groups were further divided into two sub-groups and the sub-groups were also divided further into sub-sub groups. The division, pairing, and sharing continued until two closet users were paired and supplied with the required transmit power. The algorithm achieved a significant improvement in terms of sum rate and pairing as concepts of NOMA with reduced complexity when compared to other sub-optimal pairing techniques. The algorithm grouped users with similar power requirement together, which led to high multi-user and inter-user interference. These reduced the users sum rate and the overall sum rate of the system, which was a serious drawback of their system.

Marcano & Christiansen, (2017) analyzed the performance of NOMA in millimeter wave (mmwave) cells using Orthogonal Multiple Access (OMA) as a reference standard. The analysis was carried out in mmwave cell operating at 73GHz with two users within its coverage Area. One user was placed at a fixed position at the edge of the cell while the other was positioned dynamically within the cell center to achieve the desired Signal-to-Interference plus Noise Ratio (SINR). The analysis compared NOMA and OMA in terms of channel capacity and the required SINR to achieve the desired block error rate. The analysis showed that NOMA had a significant improvement in terms of channel capacity and spectral efficiency with a SINR tradeoff of about 12dB over OMA. The number of users used in the analyses was limited to two which restrained the application of NOMA

as a multiple access technique and no consideration was given to energy efficiency as a fundamental requirement for 5G green communication, which was a serious oversight and this might have affected the accuracy of their results.

Tsai & Wei, (2018) developed a quality-balanced user clustering and PA algorithm for NOMA system with Minimum Service Rate (MSR) and Dynamic Service Rate (DSR) constraints. The algorithm used water filling concept to assign level set to user based on its received Signal-to-Noise Ratio (SNR). Users with high SNR were assigned high power among the leading user level in MSR constraint algorithm. The strongest user of the leading user level was paired with strongest user of each non leading level and vice versa to form a cluster. For DSR constraint, the strongest user of the leading user level was paired with the weakest user of each non leading level and vice versa to form a cluster. The algorithms showed significant improvement in terms of sum capacity per users with low computational complexity when compared to the Quality Based User Clustering (QBUC), Random Clustering for Non-Leading (RC-NL) user, Greedy Clustering for Non-Leading (GC-NL) user, and dynamic user clustering with PA. Comparing the two techniques with each other, MSR showed better performance over DSR. Both algorithms were complex and no significance consideration was given to power requirement of the system, which was a setback.

Hou et al., (2018) studied the behavior of Fixed PA NOMA (F-NOMA) in the downlink scenario over Nakagami-m fading channel, where fading parameters for NOMA users differ. A new closed form expression for the outage behavior of user and system was derived with a diversity order at a high Signal to Noise Ratio (SNR) condition. The study showed that for F- NOMA, the data rate of the user with higher channel gain increased dramatically at the expense of the poorer channel gain user, whose data rate decreased to less than that of OFDMA user. Also, the outage probability of the higher channel user decreased dramatically with the existence of Line of Sight (LoS) while that of the poorer channel gain user slightly decreased. These proved that the diversity order of the system depended on both users in Nakagami-m fading channel unlike the Rayleigh fading channel which depended on the high channel gain user only. The number of users used in the analysis was limited and fixed at two, which restrained the application of this NOMA technique as a multiple access technique. Furthermore, to this limitation, consideration was not also given to the energy efficiency as a fundamental requirement for 5G green communication.

3. MATERIALS AND METHOD

3.1 System Model

Considering a single cell downlink NOMA system with U users, grouping the users into S pairs based on their channel gain, the channel gain of users with better condition is denoted as $|h_{H,S}|^2$ while that of worst condition is given as $|h_{L,S}|^2$.

Suppose a given Base Station (BS) is transmitting a signal $X_{i,S}$ to U -th users ($U = \{1, 2, \dots, u\}$ and $i = \{H, L\}$) with transmit power $P_{i,S}^u$, the received signal, $Y_{i,S}^u$ by the user U at a pair S is given as:

$$Y_{i,S}^u = \sum_{U=1}^U \sqrt{(P_{i,S}^u h_{i,S}^u X_{i,S}^u + N_{i,S}^u)} \quad (1)$$

where:

$h_{i,S}^u$ represent the channel gain between the BS and the user.

$N_{i,S}^u$ represent the additive white Gaussian noise.

In this model, user pairs are allocated to subchannels so as to mitigate the effect of multi-users interference, which occurs as a result of multiplexing large number of users in the same channel. This reduce complexity in receiver design, users with dissimilar channel condition (that is strong and weak user) are paired and assign to a subchannel so as to reduce the effect of inter user interference, which occurs as a result of pairing users with similar channel condition. Energy efficiency was also incorporated in the developed model to cater for the needs of green communication in 5G networks. The modified model equations for the multiple users and subchannels are as follows:

$$R_{sys} = \sum_{n=1}^N R_n \quad (2)$$

where:

R_{sys} is the total sum rate of the system.

R_n is the total sum rate of a subchannel n .

N is the total number of subchannels in a system.

R_n is given as follows:

$$R_n = B \log_2((1 + \gamma_{L,S}) + (1 + \gamma_{H,S})) \quad (3)$$

where:

B is the bandwidth of a sub-channel n .

$\gamma_{H,S}$ and $\gamma_{L,S}$ are the SINR of the strong and weak user in a pair S .

B is given as:

$$B = \frac{W_T}{N} \quad (4)$$

where:

W_T is the total bandwidth of the system.

N is the total number of subchannels in a system.

$\gamma_{H,S}$ and $\gamma_{L,S}$ are given as:

$$\gamma_{L,S} = \frac{P_{L,S} |h_{L,S}|^2}{P_{H,S} |h_{L,S}|^2 + BN_0} \quad (5)$$

where:

B is the bandwidth of a sub-channel.

N_0 is noise power spectral density.

$P_{H,S}$ and $P_{L,S}$ are allocated power of the stronger and weak users which are given as:

$$P_{H,S} = \frac{-\left(BN_0(|h_{H,S}|^2 + |h_{L,S}|^2) \right)}{2|h_{H,S}|^2|h_{L,S}|^2} + \frac{\sqrt{4|h_{H,S}|^2|h_{L,S}|^2 BN_0(|h_{H,S}|^2 P_s) + ((N_0 B)^2) (|h_{H,S}|^2 + |h_{L,S}|^2)^2}}{2|h_{H,S}|^2|h_{L,S}|^2} \quad (6)$$

$$P_{L,S} = \frac{BN_0(|h_{H,S}|^2 + |h_{L,S}|^2) + 2P_s|h_{H,S}|^2|h_{L,S}|^2}{2|h_{H,S}|^2|h_{L,S}|^2} - \frac{\sqrt{4|h_{H,S}|^2|h_{L,S}|^2 BN_0(|h_{H,S}|^2 P_s) + ((N_0 B)^2) (|h_{H,S}|^2 + |h_{L,S}|^2)^2}}{2|h_{H,S}|^2|h_{L,S}|^2} \quad (7)$$

$|h_{H,S}|^2$ and $|h_{L,S}|^2$ are the channel gains of the strong and the weak users in a pair.

$$|h_{L,S}|^2 = |h_{H,S}|^2 = \xi |h_{U,S}|^2 d^{-\nu} \quad (8)$$

where:

$|h_{U,S}|^2$ is Rayleigh fading factor.

ξ is log-normal shadowing factor.

$d^{-\nu}$ is distance between user and the base station.

ν is the path loss exponent.

U is number of users.

The power allocation given in equation (9) is:

$$P_n = \frac{G_{g,n} P_t}{\sum_{n=1}^N G_{g,n}} \quad (9)$$

where:

$G_{g,n}$ is the sum of channel gains of users in a subchannel n.

P_t is the total power of the system.

$$P_n = \frac{P_t}{N} \quad (10)$$

where:

P_c is circuit power of the transmitter.

P_n is power allocated to a subchannel n.

P_t is the total power of the system.

N is the number of subcarriers.

The Energy Efficiency (EE) of subchannel n is given in equation (11) as:

$$EE_n = \frac{\text{Total Sum rate of subchannel n}}{\text{Total power allocated}} = \frac{R_n}{P_n} \quad (11)$$

where, R_n is the total sum rate of subchannel n.

3.2 Development of User pairing, Subchanneling, and power Allocation Algorithm.

The improved algorithm adopts subchannel allocation to reduce the effect of multi-user interference and receiver design complexity. It pairs users with dissimilar channel conditions (that is, strong and weak users) to mitigate the effect of inter-user interference and also allocates the pairs to a subchannels to mitigate the effects multi user interference. Energy efficiency is also incorporated to cater for the needs of green communications in 5G networks. For proper illustration of the procedure, four users are considered and the process of pairing, subchanneling, and power allocation is shown in Figure 1.

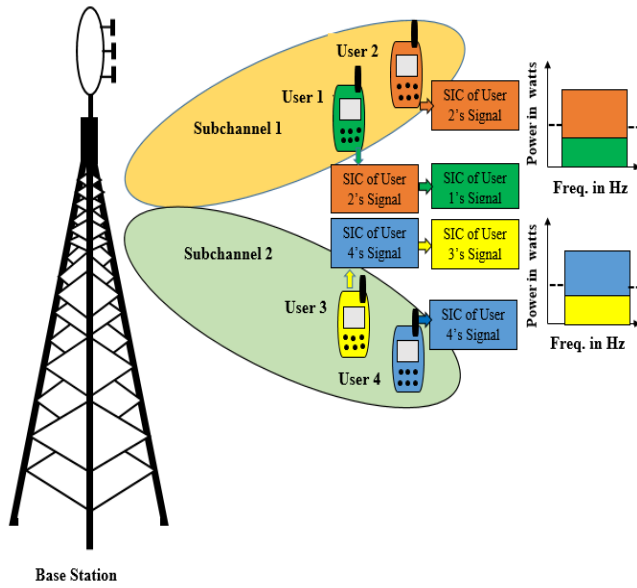


Figure 1. Pairing, Subchanneling, and Power Allocation Procedure for Four Users.

The operational flowchart of the algorithm is described in Figure 2. The developed algorithm is made up of two main phases which are: the pairing and subchannel allocation phases, and power allocation and energy efficiency evaluation phase. In pairing and subchannel allocation phase, the channel gains of registered users are evaluated. Users with dissimilar channel gains are paired and allocated to an empty subchannel so as to mitigate the effect of multi-user and inter user interferences. While in the power allocation and energy efficiency evaluation phase, the power required by the subchannel based on its user pair is estimated and then allocated so as to reduce energy wastage. The energy efficiency of the subchannel is also determined in this phase to ensure conformity with the requirement for green communications in 5G networks. The pseudo-code for the developed algorithm is presented below.

```
function parameter_declaration
U=32; %Number of Users
Pt=30; % Total Transmission Power
Wt=5e6; % Total Bandwidth
Nsc=512; % Number of subcarriers
ssd=8; % Shadowing standard deviation
No=-176; % Noise Power Density
D=300; % Cell Diameter
v=3; % Pathloss exponent
phiv_min=0.6e5; % Minimum rate requirement
ki=linspace(0.2,1,U);
% end
function user_pair_gain
s=1:32;
s1=i+s;
Pt=30;
Sj(s,s1)=Gg(s,s1);
```

```
Ps=(Ggs.*Pt)/Sj;
function pairing_schedule and power allocation
Pmax = 30;
P1min = 0;
P1max = Pmax;
B = 5e6;
N = 512;
rho = 0:1:32;
h1=(1/sqrt(2))*(randn(N,1)+1i*randn(N,1));
h2=(1/sqrt(2))*(randn(N,1)+1i*randn(N,1));
for aa = 1:length(rho);
while (abs(P1max - P1min)) >= 1;
P1 = (P1min+P1max)/2;
P2 = Pmax - P1;
C2=vpa(B.*log2(1+min((P2.*rho.*abs(h2).^2)/(1+rho.*P1.*abs(h2).^2),(rho.*P2.*abs(h1).^2)/(1+rho.*P1.*abs(h1).^2)))));
if (C2 < 1)
P1max = P1;
else
P1min = P1;
break
end
end
```

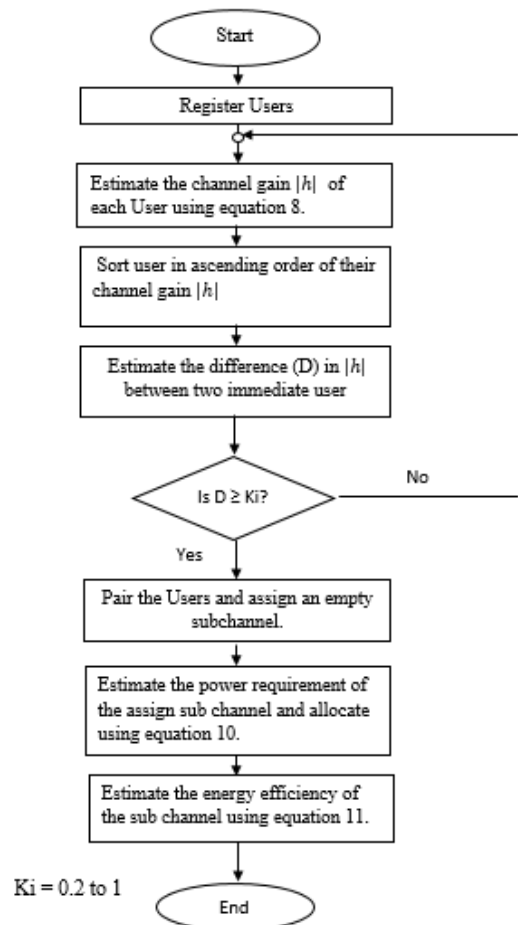


Figure 2. Flowchart of the Developed Algorithm Operation.

4. RESULTS AND DISCUSSION

In this section, the results obtained from simulation are presented to evaluate the performance of the developed user pairing, subchanneling, and power allocation scheme for 5G NOMA system. In the simulation, a single Base Station (BS) with 32 users uniformly distributed in a cell range of 300 meters at random locations are considered. The minimum distance between a user and the BS is 30 meters, the bandwidth and the carrier frequency of the system are 5MHz and 512Hz, respectively. To reduce the demodulating and decoding complexity of the SIC receiver, each subchannel is allocated with one matched pair (that is, two users) in this NOMA system. OFDM scheme compared to this developed scheme can only be allocated by one user in a subchannel. Also, for the power allocation and energy efficiency evaluation, the developed scheme is compared with the work of Al-Abbasi & So (2016) and optimal power allocation scheme for validation.

The scheme was developed in MATLAB simulation environment, using MATLAB R2017a version. The parameters used for the simulation are presented in Table 1.

Table 1: Simulation Parameter Values of the Developed Scheme.

Parameter	Value
Number of Users (U)	32
Total Transmission Power (P_T)	30 dBm
Total Bandwidth (W_T)	5 MHz
Number of Subscribers (N_{sc})	512
Shadowing Standard Deviation	8 dB
Noise Power Density (N_o)	-174 dBm /Hz
Cell Diameter (D)	300m
Link space (ki)	0.2 to 1
Path Loss Exponent (ν)	3
Minimum rate requirement ($\Phi_{u,min}$)	0.6×10^5 bps

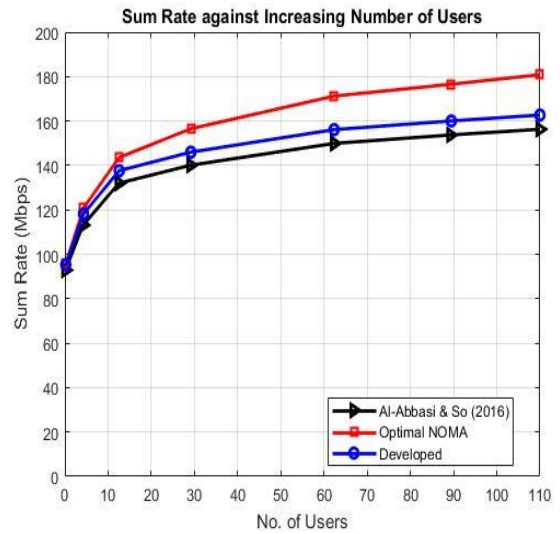


Figure 3. Sum Rate of the System versus Different Number of Users.

In Figure 3, the performance of the total system sum rate is evaluated with the number of users U (where U varies from 0 to 110). A tolerance, k_i of 0.2 and the maximum bandwidth limit of 5MHz are set. It is observed that the sum rate increases as the number of users grows which is due to the multi users' diversity gain. As the number of users grows higher, the sum rate keeps on increasing, but the increase become smaller as the number of users grows higher, as expected from Shannon's formula of sum rate calculation. It is also observed that the performance of the developed scheme is better than the Hierarchical Pairing and Power Allocation (HPPA) scheme of Al-Abbasi & So (2016) and the schemes exhibit similar behavior as the optimal one which is the desirable. For example, when the number of users is 30, the sum rate of the developed scheme is 6.4% more than that of the HPPA scheme of Al-Abbasi & So (2016). This is because the inter user and multi user interferences are mitigated by the developed scheme.

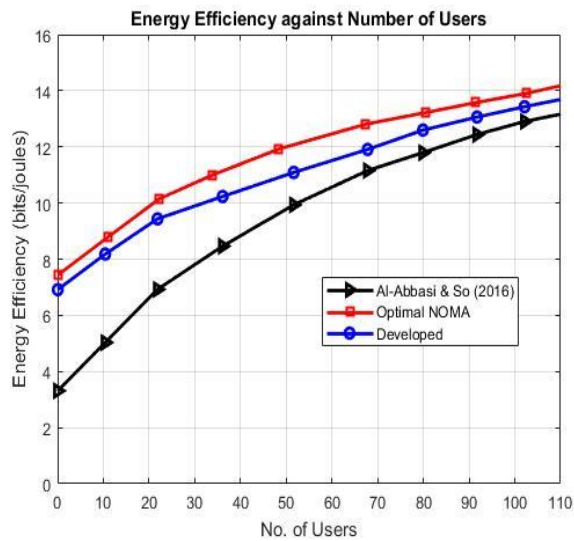


Figure 4. Energy Efficiency of the System versus Different Number of Users.

Figure 4, shows the energy efficiency of the system versus number of users with the same constraint as Figure 3. It is observed that the energy efficiency of the system also increases as the number of users grows. The trend of the curve is similar to the sum rate curve due to the dependence of energy efficiency on sum rate which is shown in equation 11, From the Figure 4, the developed scheme shows better performance than the HPPA scheme of Al-Abbasi & So (2016) and the schemes exhibit similar behavior as the optimal one which is the desirable. When the number of users is 30, the developed scheme is 27% more energy efficient than the HPPA scheme of Al-Abbasi & So (2016).

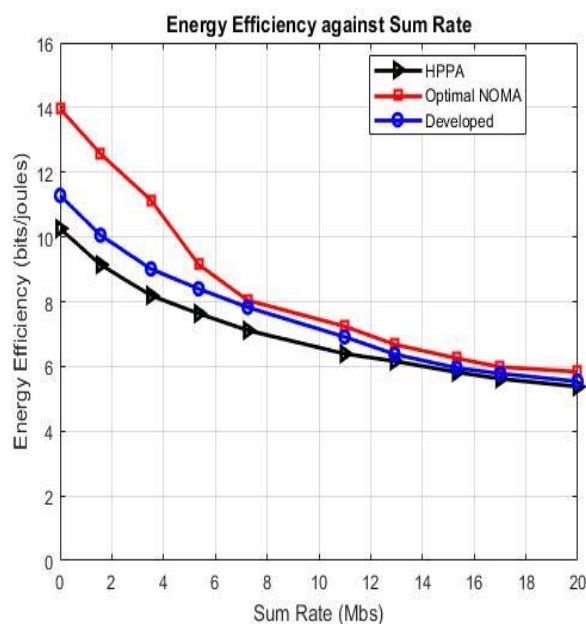


Figure 5. Energy Efficiency of the System versus overall System Sum Rate.

Figure 5, shows the energy efficiency of the system versus the overall system sum rate with the same constraint as Figure 3. It is observed that the energy efficiency of the system decreases as the overall system sum rate increases this is due to the direct dependency of system sum rate on transmit power.

5. CONCLUSION

From these results, it can be concluded that the developed user pairing, subchanneling and power allocation scheme performs better than the existing multi user pairing and power allocation schemes in terms of sum rate, coverage probability, and energy efficiency. This is attributed to the fact that, unlike the existing schemes which pair similar users or random users and allocate power, this developed scheme pairs dissimilar user, allocate them to a subchannel then evaluate the power requirement of the subchannel before allocation. This reduces multi user interference, inter user interference and energy wastage in the system. These made it possible for the sum rate, coverage probability, and energy efficiency of the system to improve.

REFERENCES

- Al-Abbasi, Z. Q., & So, D. K. (2015). Power allocation for sum rate maximization in non-orthogonal multiple access system. Paper presented at the Personal, Indoor, and Mobile Radio Communications (PIMRC), 2015 IEEE 26th Annual International Symposium on, aug 2015, [Available online:<https://www.escwholar.manchester.ac.uk/uk-ac-man-scw:266841>]
- Al-Abbasi, Z. Q., & So, D. K. (2016). User-pairing based non-orthogonal multiple access (NOMA) system. Paper presented at the Vehicular Technology Conference (VTC Spring), 2016IEEE 83rd, May 2016, P.3(Chapter3). [Availableonline:https://www.research.manchester.ac.uk/portal/files/78710042/FULL_TEXT.PDF]
- Chen, X., Zhang, Z., Zhong, C., & Ng, D., W., K. (2018). NOMA in Downlink SDMA with Limited Feed back; Performance Analysis and Optimisation. IEEE Journal on Selected Areas in Communications SI in Non-Orthogonal Multiple Access for 5G system, 35(10),2281-2294.
- Ding, Z., Peng, M., & Poor, H. V. (2015). Cooperative non-orthogonal multiple access in 5G systems.



IEEE Communications Letters, 19(8), 1462-1465.

Ding, Z., Liu, J. Choi, Sun, M. ElKashlan, & Poor, H.,V. (2017). Application of non-orthogonal multiple access in LTE and 5G networks. IEEE Communication magazine, 55(2) 185-191.

Fang, F., Zhang, H., Cheng, J., & Leung, V. C. (2016). Energy-efficient resource allocation for downlink non-orthogonal multiple access network. IEEE Transactions on Communications, 64(9), 3722-3732.

He, J., Tang Z. & Che, Z. (2016). Fast and efficient user pairing and power Allocation Algorithm for non-orthogonal multiple access in cellular networks. Electronics Letters 52(25), 2065-2067.

Hou, T., Sun, X., & Song, Z. (2018). Outage Performance for Non-Orthogonal Multiple Access With Fixed Power Allocation Over Nakagami-m Fading Channels. IEEE Communications Letters, 22(4), 744-747.

Marcano, A. S., & Christiansen, H. L. (2017). Performance of Non-Orthogonal Multiple Access (NOMA) in mmWave wireless communications for 5G networks. Paper presented at the Computing, Networking and Communications (ICNC), 2017 International Conference on (pp. 969-974).IEEE



3rd International Engineering Conference (IEC 2019)
Federal University of Technology, Minna, Nigeria



AUTOMATION OF AGRICULTURAL MACHINERY OPERATION SYSTEMS; AN IMPERATIVE FOR SUSTAINABLE DEVELOPMENT

Bala Ibrahim
Department of Agricultural Technology,
Hassan Usman Katsina Polytechnic, P.M.B.2052,
Katsina state, Nigeria.
balaibrahim58@gmail.com

ABSTRACT

The demand for automation and mechanization in the field of agriculture is in the response for the demand of high quality agricultural products, likewise the shifting of the economies towards the industrial society have force people to move from rural agricultural areas resulting in population becoming more concentrated in the urban cities, producers were forced into producing more food using less labour to feed ever increasing populace in the urban areas, which resulted to the emergence of agricultural mechanization with development and use of steam engines for threshing and the development of prototype fully-autonomous farm machinery today. The development of mobile hydraulics, electronics and steam engines have enables the technology for automation of agricultural operations like threshing formerly done by hands, also farmers as mechanical by nature, invented attachments and machinery driven by tractor to automate tasks previously done by hand. To overcome inefficiencies associated with operator's poor judgment of distance and fatigue, many hours operating machinery in the farm for tilling, planting, cultivation, spraying and harvesting operations, machine veered from correct path production losses will occur due to crop damage or harvest losses. Guidance system for agricultural machinery operation provide a better solution in increasing field efficiency and field capacity by 5% to 10%. It is possible to say that mechanization of agriculture bears undisputed truth in improving food security, productivity, creating employment and reducing loss and promoting economic growth and development.

Keywords: *Automation, Agricultural systems, Efficiency, Machinery.*

1 INTRODUCTION

One of the major problems of Nigeria for the last four decades is the inability of its agricultural population base to produce enough food to feed the teeming population or the inability of its other sectors of the economy to grow and derive income for the majority to access food from anywhere else. This problem has proportionally aggravated up-till today with a high number of food insecure population increasing in size and proportion). Nigeria is well endowed with a fertile soil, abundant water resources, populace and good climatic conditions. What needs careful analysis is why Nigerian farmers continue to practice essentially the same farming methods with very little management and technical improvement for many years. The low productivity level of Nigerian farmers even compared to African standards could largely be

traced to low technical efficiency along with the decreasing soil fertility. Agricultural Mechanisation (AM) is the application of tractorization technology in the field of agriculture production in order to improve agricultural output, also a deliberate and conscious departure from the peasant as well as the subsistence agriculture into a commercial based agriculture. The process also involves the management and development of machines for crop production, water control, material handling and post-harvest operations (Rahman and Lawal, 2003). In another words, AM could be defined as the application of the most locally appropriate tools, machines, implements, and approaches to make for the most sustainable beneficial decisions. If AM is implemented rightly, it will have a considerable effect on agricultural productivity. It will optimize inputs costs. Initial application of AM was tractor entrance to the land. But during last century or



**3rd International Engineering Conference (IEC 2019)
Federal University of Technology, Minna, Nigeria**



so, AM has found several interpretations; and the description was changed from tractorization to precision farming. This procedure gives evidence of AM maturity. In many parts of the world, AM has made a significant contribution to agricultural and rural development. Levels of production have increased, soil and water conservation measures were constructed, the profitability of farming improved, the quality of rural life enhanced, and development in the industrial and service sectors was stimulated (Bishop, 1997). To some, agricultural mechanisation is synonymous with tractorization while others take it to mean increase in production per farmer per hectare of land cultivated. Inns (1995) opined that AM development depends on the farmers' satisfaction and capability to identify opportunities for achieving sustainable benefits by improved or increased usage of power and machinery, selecting the most worthwhile opportunity and carrying it through to successful implementation. Because of its obvious contribution, mechanical aspect of AM has been presented till now. But it was a progression of technological innovation that influenced all of society throughout the twentieth century (Foulke et al, 2000). Fernandes et al (2008) mentioned that even in high crowded populations, it can be difficult to attract or retain labourers to work in farm operations. Much of the stimulus for AM has come from laborer shortages in the more economically advanced countries. They described mechanization as tractorization. Mechanization reduces agricultural required labour and can reduce or remove the costs in countries which energy is cheap. But for poorer countries, mechanization forces Engine powered agricultural mechanization was introduced in the early sixties through the farm settlement schemes in Nigeria. The technology include the use of a wheel range tractor sizes as mobile power for field operations engines or motors to power such machines as threshers, mills, irrigation pumps, air craft for spraying chemicals and self-propelled machine for production harvesting and handling of wide variety of crops. According to Kepner et al (1978), the increased production that has been achieved during the past century resulted from the growing of better crop varieties, the more effective use of fertilizers, improved cultural practices, and, more importantly, the increased utilization of (i) more appropriate non-human energy and (ii) employing functionally-appropriate machines and implements. The energy consumption at any stage of agricultural practices is

gross for human compare to machine. Stout et al, 1979, reported specific human energy consumption for bush clearing as 1680MJ, and 19.4 man-days were required to prepare a hectare of land, where as for the same task, the machine required as little as 0.88MJ energy utilization and 0.019 machine-days per hectare. According to the same source, energy utilization for manual weeding was 1320MJ and 2.29 MJ for machine field operation: 32.6 man-day/ha and 0.015 MJ machine efforts were reported. Energy related data from a number of tropical cultivation systems and products for which cassava was one of them have been averaged by Leach 1976 as 0.749 MJ for manual labour and 0.0487MJ when using machine power (Adams, 2007).

The development of the steam engine in the late nineteen so also at early of twentieth centuries was an enabling technology for the development of agricultural automation, because the steam engines are relatively portable power source. During the 1920's and 1930's years, smaller tractors with internal combustion engines powered by gasoline were mass produced at relatively lower cost, which more farmers could afford. This in turns led to increased farm machinery automation, because farmers are mechanical in nature they invented attachments and machinery that are driven by tractor to automate jobs previously done using hands. The development of hydraulic and electronic allowed large forces to be generated using hydraulic cylinders, remote power of hydraulic motors without the need of a mechanical driveline. Electronic Control Units (ECUs) can control and regulates the flow of hydraulic fluids to actuators, use information from sensors to control the operation of systems on tractors, such as transmission, hitch, power-take-off (PTO), brake and steering systems (Dagninet and Wolelaw,2016).

Autonomous tractor guidance system development is a current state of the art in mechanization of agricultural operations, because since in the late nineteenth centuries farmers have device methods of making tractor to follow plow furrow using feeler, later in the twentieth century the combination of hydraulics and electronics have fade way for more sophisticated guidance strategies such as low force feeler that guide the tractor or implement based on rows or position of the tractor based on Global Positioning System (GPS). On the farm, technology is changing the way farmers manage farmland and farm



animals – such as the use of satellite driven geo-positioning systems and sensors that detect nutrients and water in soil. This technology is enabling tractors, harvesters and planters to make decisions about what to plant, when to fertilize, and how much to irrigate. Many experts are looking forward to a future where the Internet of Things (IOT) (where physical objects such as vehicles, buildings and devices are connected to collect and exchange data) is applied to food and farming connected to advanced sensors embedded in fields, waterways, irrigation systems and tractors to combine with machine-learning systems, genome-identifying devices and data dashboards to give rise to a generation of smart farming technology that will have the capacity to sense and respond to its environment in a way that maximizes production while minimizing negative impact. In year 1995 “thing to thing” was coined by Bill Gates, while EPC global came up with IOT (internet of things) in 1999 that interconnects human to thing, thing to thing and also human to human (Sreekantha and Kavva, 2017). Another break through is the introduction of a component by Nguyen and Kha, 2015 that improve the accuracy in the monitoring of environmental conditions and reducing human power through the collection, analyses and data presentation on a graphical user interface (GUI).

Modernization of Agricultural sector is progressing smoothly with the successful implementation of agricultural mechanization. The modernization of agriculture can be defined as applying of the up-to-date technologies to agricultural production activities. Mechanization, automation and emerging technologies are the key factors in modernizing agricultural production. The objective of this paper is to report on the development of mechanization and automation of agricultural production.

1.1 GLOBAL CHALLENGES

With the global population increasing tremendously. The UN experts have forecasted that the world’s population to hit 8.5 billion by 2030, rising to 9.7 billion by 2050. In order to produce enough food for the 2050 population, the World Bank has forecast that we’ll need to produce 50 per cent more food. With climate change and a skills shortage limiting crop yields, Thus, agricultural mechanization in Nigeria can be divided into three levels of technology; hand tools technology, draught-animal technology and

engine powered technology (Oudman, 1993). As at 1996 Nigeria has an estimated 32,474,000 ha of land under cultivation, 11,900 tractors and 2,729 ha of land cultivated per tractor. This mechanization level is grossly low compare to Niger whose land area under cultivation was 11,097,000 ha, with total tractor owned as 180 and about 61,650 ha was cultivated per tractor (FAO, 1998). Engine powered agricultural mechanization was introduced in the early sixties through the farm settlement schemes in Nigeria. The technology include the use of a wheel range tractor sizes as mobile power for field operations engines or motors to power such machines as threshers, mills, irrigation pumps, air craft for spraying chemicals and self-propelled machine for production harvesting and handling of wide variety of crops.

1.2 DEVELOPMENT PLAN OF AGRICULTURAL MACHINERY

Mechanization means the application of machines in the field crop production operations or in the post-harvest processing activities. Human and animal power, as well as mechanical and engine power have played important roles in agricultural mechanization. Power machinery, for example, a tractor which multiplies human power a thousand times (from 0.07 kw to 70 kw), can increase output several hundred times over what a farmer can produce yearly. Agricultural machinery has transformed from the utilization of hand-tools to automation technology. This evolution can be divided into the following stages (Rijk, 1999).

- i. Improved hand-tool technology
- ii. Draft animal power
- iii. Stationary power substitution
- iv. Motive power substitution
- v. Human-control substitution
- vi. Adaptation of cropping practices
- vii. Farming-system adaptation
- viii. Plant adaptation
- x. Automation of agricultural production

The application of Geographical Information System (GIS) and Global Positioning System (GPS) have opened a frontier for the automation of machinery used in precision agriculture. Automation in agriculture can best be introduced by an optimized combination of computer-controlled technologies and mechanized agricultural production. The ten-year taskforce was aimed for the promotion of agricultural



**3rd International Engineering Conference (IEC 2019)
Federal University of Technology, Minna, Nigeria**



automation in crops, fisheries, livestock production, and services was initiated in 1991 in Taiwan. Their aim was to use economic, social, and environmental factors to increase farmers' income; to develop special agricultural zones; to fully utilize land and water resources; to solve the manpower shortage and the aging problem in the villages; to provide nutritious, sanitary and fresh high-quality agricultural products; to improve shipping and distribution system services for agricultural products; to improve the working environment and increase farming safety; to handle farm waste disposal and minimize environmental pollution; and to increase the effective use of energy resources (Lee 1997, Fon 1998, Lu 2001). Automation techniques have increasingly been applied to agricultural sectors. Automated crop production focuses on several areas such as pesticide application, post-harvest processing, vegetable seedling production, planting and transplanting, greenhouse engineering, and field machinery. Vegetable and flower production in plant factory systems equipped with modern facilities have proven successful in increasing microclimatic control and production efficiency, thereby providing economic benefits. Besides improvements in hardware, farming operations can also benefit from greater use of information technology. E-farmer, which promotes the sale of farm products on the internet, is one of these new resources. Many networking platforms now sell high quality products, such as packed rice, processed foods, and fish goods over the internet. All of these new technologies add another dimension in agricultural modernization efforts.

1.3 MECHANIZATION-EMERGING TECHNOLOGY DEVELOPMENT

Precision agriculture has been introduced by using satellite positioning systems and geographical information for farm management. Farmers, using ample data can easily determine the most productive fields for farming and the best suited machinery to be used. Studies on precision spraying systems for boom sprayers, software integration of a GPS/GIS system for agricultural applications, near infrared measurements of rice canopy, and yield monitoring systems for rice crop production in Taiwan were conducted successfully. Recently, nondestructive means and RFID have also been utilized in evaluating

and monitoring the quality of agricultural products. Hands Free Hectare (HFH) is a company based in the United Kingdom that was set-up to develop automated agriculture starting from the planting and monitoring, upto maintenance and eventual harvesting. The group has accomplished their aim using two harvests, one of winter wheat and one of barley, proving autonomous vehicles and drones can handle the farming process without a single person stepping out onto the field.

1.4 NIGERIAN'S MECHANIZATION-AUTOMATION DEVELOPMENT.

Automation in agriculture sector can best be introduced through the optimized combination of computer-controlled technologies as well as the mechanized agricultural production processes. The taskforce for promoting agricultural automation in fisheries, crops and livestock production was to use social, economic and environmental factors to increase farmers' income; to fully utilize land and water resources; to solve the manpower shortage and the aging problem in the villages; to handle farm waste disposal and minimize environmental pollution; and to increase the effective use of energy resources; to develop special agricultural zones; to provide nutritious, sanitary and fresh high-quality agricultural products; to improve shipping and distribution system services for agricultural products; to improve the working environment and increase farming safety; (Lee 1997, Fon 1998, Lu 2001). From human history, increasing agricultural production has been a function of either adding more labourers or finding more efficient tools to do the job. Modern agriculture is no different. In the face of labour shortages, farmers are turning to technology to make farms more efficient and automate the crop production cycle. These startups are addressing every aspect of the agriculture value chain. Some place remote sensors in the field to collect hyper-local data about growing conditions. Others create software to manage seed, soil, fertilizer, and irrigation, and make predictions about timing and yield. Some startups use drones to monitor conditions remotely and even apply fertilizers, pesticides and other treatments from above.



Figure 1: Aerial spraying of chemicals using drone.

On the farm, technology is changing the way farmers manage farmland and farm animals such as the use of satellite driven geo-positioning systems and sensors that detect nutrients and water in soil. This technology is enabling tractors, harvesters and planters to make decisions about what to plant, when to fertilize, and how much to irrigate. As this technology progresses, equipment will ultimately be able to tailor decisions on a meter-by-meter basis. In advancing the existing technology, the tractor, is undergoing a technological makeover. Manufacturers including John Deere, CNH Industrial and AGCO are developing driverless tractors. The new machines will be satellite driven, using geo-positioning to avoid collisions and make planting decisions.



Figure 2: Automated tractor.

2 CONCLUSION

The man with hoe will still remain an apt description of the Nigerian farmer upto today. The Nigerian agricultural industry, populated as it is by an aged and ageing peasants, has progressively developed into a world of drudgery for losers, shunned and despised by the Nigerian youths. In spite of decades of immense investments and expenditures into agriculture sector, in terms of men, money and materials, by national and international governments and agencies, an average Nigerian farmer remains an indigent serf, regarded by today's youths as a dreadful anachronism. The major instrument for agricultural growth remains the transfer and adoption of technology and the knowledge systems that underpin it, which will, itself contributes to the transformation of rural society. The stagnant features of African agriculture and particularly Nigeria; a consequence of non-mechanization and adoption of improved farming methods, have negatively robbed off African development. However, the Nigerian's agricultural operations do not easily lend itself to the total mechanization of all operations as a result of inherent problems in our farming systems. Mechanization, which involves employment of machine technology in the process of development; in this case powering agricultural operations do not work in isolation. It requires conducive, environment in terms of variety traits, appropriate cropping systems, crop arrangement, land area under cultivation, constant and affordable power etc. various studies shows that tractorization simply displaced bullock labour, but its impact on man power was much less, indeed mechanization opens up new avenues for human employment such as management and supervisory jobs, servicing, maintenance and repair of the machines (Dagninet and Wolelaw, 2016). In conclusion, the author strongly believes that successful mechanization of Nigerian agriculture will continue to be a day-dream unless thoughts and 'blue-prints' similar to those expressed in this paper form the basis of any mechanization scheme in Nigeria. Instead of hoping for adequate rains, farmers' concept is to adopt a mechanization strategies so flexible that it can be changed even at short notice to suit the pattern of rainfall available, crops, soils, because the failure of mechanization has had negative multiplier effects on farmers' economy.



RECOMMENDATIONS.

After, reviewing the researcher recommends the adoption of Agricultural mechanization and Automation that follow simple and clear stages the local peasant farmers can experience from low to high for better productivity as well as food security, strengthening the capacity of farmers to develop agricultural implements that could be modified, delivering mechanization based extension services to farmers and undertaking intensive land use and sustainable activities and the implementation of supportive policies and programmes.

REFERENCES

- Adams, T. B. (2007). Farm Machinery Automation for Tillage, Planting, Cultivation and Harvesting, Myer Kutz (ed.) Hand book of Farm Dairy and Food Machinery. Pp. 73-91.
- Bishop, C. (1997): A Guide to Preparing an Agricultural Mechanization Strategy. Food and Agriculture Organization of United Nations, Rome, Italy pp. 37.
- Charles, I. O. (2016): Failure of Agricultural Mechanization in Nigeria: The Multiple Cropping System Factor.
<https://www.researchgate.net/publication/295688512>
- Dagninet, A. and Wolelaw, E. (2016). Agricultural Mechanization: Assessment of Mechanization Impact Experiences on the Rural Population and The Implications for Smallholders, *Engineering and Applied Sciences*, Vol. 2, 2016 pp. 39-48
- FAO (1998): Motorized Soil Tillage in West Africa, A Survey on the Use and Consequences of Tillage done With Engine-driven Machinery, Food and Agriculture Organization of the United Nations FAO Regional Office for Africa Accra, Ghana Agricultural Engineering Branch, Agricultural Support Systems Division, FAO, Rome, Italy.
- Fernandes, E., Pell, A. and Uphoff, N. (2008): Rethinking Agriculture for New Opportunities. In: Pretty J. Sustainable Agriculture and Food. Volume I: History of Agriculture and Food. Pp. 403-422. Earthscan Publication. UK.
- Fon, D. S. (1998): Evaluation of Agricultural Automation In the Crops, Fisheries, Livestock Production and Services. Council of Agriculture, R.O.C.
- Foulke, T., Coupal, R. and Taylor, D. (2000): Trends in Wyoming Agriculture, University of Wyoming, Cooperative Extension Service, US.
- Inns, F. M. (1995): Selection, Testing and Evaluation of Agricultural Machines and Equipment Theory. FAO Agricultural Services Bulletin (FAO) No. 115.
- Kepner, R. A., Bainer, R. and Baeger, E. L. (1978): Principles of Farm Machineries (3rd edition) AVI Publishing Company Inc. Connecticut, USA.
- Lee, K. W. (1997): Agricultural Mechanization and Automation in the Republic of China on Taiwan In *Proceeding of International Symposium on Agricultural Mechanization and Automation*, eds S.M. Chen and Chon, C.Y. Volume I, pp. 31-49, Tapei, Taiwan, National University.
- Lu, F. M. (2001): Automation and Precision Agriculture *Journal of Rural Development* 34 (1) pp. 19-36.
- Nguyen, T. K. D, Nguyen, D. T. H. S and Luong, H. D. K. (2015) "Automated Monitoring and Control System for Shrimp Farms Based on Embedded System and Wireless Sensor Network". Electrical, Computer and Communication Technologies (ICECCT), 2015, IEEE International Conference.
- Oudman, L. (1993): The Animal Draught Power Development Project in the Department of Agricultural Engineering' in C. L.
- Rahman, S. A. and Lawal, A. B. (2003): Economic Analysis of Maize-based Cropping System in Giwa Local Government Area of Kaduna State, Nigeria. *An International journal of Agricultural Sciences, Science, Environment and Technology*, 3:139-148.
- Rijk, A. G. (1999): Agricultural Mechanization Strategy In CIGR Handbook of Agricultural Engineering, Plant Production Engineering edition, B. A. Stout, 536-553 St. Joseph MI. ASAE.
- Sreekantha, D. K, and Kavya, A. M. (2017). Agricultural Crop Monitoring Using IOT. 11th International Conference on Intelligent Systems and Control (ISCO). IEEE International Conference.

Electricity Generation using Locust Bean Waste and Coal in a Molten Carbonate Direct Carbon Fuel Cell

Yakubu E.,* Adeniyi, O.D., Alhassan M., Adeniyi, M.I., Uthman H., and Usman A.A.
Chemical Engineering Department, Federal University of Technology, Minna, Nigeria

*Corresponding author Email: o.adeniyi@futminna.edu.ng.

ABSTRACT

The quest for a sustainable source of energy has made researchers turn towards direct carbon fuel cell (DCFC). It is a device that directly converts the chemical energy of a biomass or fossil fuel into electrical energy. The combination of the coal and a renewable biomass Locust bean waste (LBW)(*Parkia Biglobosa*) can enhance the electrochemical performance of the DCFC. Pyrolysis pre-treatment process was initially carried out at heating rate of 10°C/min. This was done for each of the sample and their combination. The pyrolyzed biomass for both of them was then used to determine the electrochemical performance of DCFC using molten carbonate salt as electrolyte and using five different resistor loads (1Ω, 2Ω, 3Ω, 4Ω & 5Ω). Performance of coal in the DCFC was observed to be better than *Parkia Biglobosa*. However upon combination of both solid fuels, an enhanced performance was observed. At a temperature of 800°C and resistance of 1Ω, the combined fuel showed an open circuit voltage of 1.16 V, current density of 43.2 mA/cm², power density of 2.91 mW/cm² with 73% efficiency. The SEM result of the carbon fuels was obtained using Nova NanoSEM 200 FEI, Netherlands. The SEM results of the combined fuel were observed to be better. The phase composition of each fuel was determined using Siemens D500 XRD System. The highest peak for the LBW, Coal and the combined fuel was at an angle of 25.988°, 26.24°, 26.637° respectively and the corresponding inter-planar spacing of 3.42Å for LBW fuel and 3.34Å for coal and the other fuel.

Keywords: Biomass, carbon fuel, direct fuel cell, locust bean waste, coal, Pyrolysis.

1 INTRODUCTION

Energy is very important to perform the day to day activities of mankind and different alternative energy sources have been the research focus globally. The alternatives from non-renewable forms of energy have been the subject of scientific researches with the aim of addressing the emission challenges of harmful gases released to the atmosphere thus reducing the greenhouse gas effect of climate change and global warming. For developing country like Nigeria, the electrical energy supply is grossly inadequate for the growing population. Thus there is a need to look inward for more sustainable and renewable energy sources from biomass and its blend with other energy sources. Most developing economies will adopt renewable energy, since fossil fuels are limited in supply and will eventually run out of supply. The combination of biomass and fossil fuel (like coal) will be a good blend for sustainable electrical energy generation. These when properly developed will alleviate the effects of climate change and global warming using the direct carbon fuel cell (DCFC) technology (Dudek *et.al.*, 2018; Adeniyi *et.al.*, 2014; Adeniyi & Ewan, 2012; Jain *et.al.*, 2009,2007).

A sustainable modern industrial economy can only be achieved through electrical power generation. The direct

carbon fuel cell (DCFC) technology offer a viable technique that can practically produce electricity that is safe, relatively simple, cost effective, remarkably efficient, reliable, environment friendly and a more effective way to improve conventional power generation. Coal is a fossil fuel which is abundant in nature and is responsible for more than 30% of the world primary energy generation. It has been estimated that this forecast will slightly increase or remain steady until 2030 showing that coal will still be relevant for the future. The conventional method of power generation from coal has contributed to global warming and climate change and thus the DCFC technology offer an efficient and environmentally benign way of utilizing the energy stored in coal (Kacprzak *et.al.*, 2019; Cooper & Berner, 2005; Munnings *et.al.*, 2014; Arenillas *et.al.*, 2013; Li *et.al.*, 2010).

A direct carbon fuel cell is an electrochemical device that efficiently converts the chemical energy of a carbon rich fuel directly to electrical energy without burning the fuel. The DCFC gives off a pure stream of carbon dioxide that can be captured without incurring additional costs of collection and can be used in other industrial requirements such as in the oil and gas industry. In the DCFC technology, solid carbonaceous fuels are used and directly oxidized at the anode surface. Different carbon fuels, such as coal, biomass, or blends of these are exposed to high temperature conversion, the fuel is electro-oxidized to CO₂ at anode compartment creating electricity. A conversion efficiency rate of 80% is achievable depending

on the type of carbon fuel applied; it could reduce carbon emissions by 50% and off-gas volume by 10 times when compared to conventional coal-fired power stations of about 35% efficiency. This increased efficiency results in a beneficial pay off for DCFC development. Fuel produced from waste offers many benefits (Giddey *et al.*, 2012; Jia *et al.*, 2010; Declaux *et al.*, 2010; Cooper & Cherepy, 2008; Cao *et al.*, 2007; Dicks, 2006; Cherepy *et al.*, 2005; Zecevic *et al.*, 2004; Larminie & Dicks, 2003; Hoogers, 2003).

The direct carbon fuel cell offers a higher efficiency and lower emissions in the production of electricity; it is portable and easy to construct. The direct carbon fuel cell use of biomass materials as its fuel source makes it economically viable for waste management and reduction of greenhouse effect. Nigeria as a country is challenged with the lack of adequate electricity to power its economy, which is a major factor affecting the development of most third world countries like: Nigeria, Burkina Faso, Burundi, Niger, Tanzania and others. This paper investigate the use of biomass (locust bean waste (LBW)), coal and the blend to generate electricity using the DCFC technology.

2 METHODOLOGY

Two types of samples were selected for investigation; Locust bean waste (LBW) and Bituminous coal (Figures 1 and 2). Locust bean waste was obtained from Niger State and carefully sorted, sun dried and then reduced in size. This sample was subjected to pyrolysis at 500°C at Badeggi Research Centre Bida, Niger State and the char obtained was ground to fine particles. The same process was carried out for the coal sample obtained from Kogi state and the combination of the two sample simultaneously. A portion of the char was appropriated for proximate and ultimate analysis (Ash content, Volatile matter, Fixed carbon, Moisture content). The proximate analysis was carried out using an ELTRA CHS-580 Analyser (Netherlands). The phase compositions of the carbon samples thus obtained were evaluated using X-ray diffraction analysis (XRD, Netherland) and the Scanning Electron Microscopy (Nova NanoSEM 200 FEI, Netherlands). An EDS system (EDAX, Netherlands) was also used to characterise the morphology and chemical composition of carbon particles used as solid fuel.

The fuel cell experimental set-up was developed for the electrochemical operation of the molten carbonate direct carbon fuel cell (MCDCFC). The electrolyte consisted of sodium carbonate and potassium carbonate, both saturated to a wire mesh to hold it together and subjected to different temperature of 500°C to 800°C. 38 mol% of Na₂CO₃ and 62 mol% of K₂CO₃ were measured, mixed and transferred to a stainless steel plate. The mixture was subjected to high temperature using the

blacksmith fire and was stirred continuously to obtain homogeneous mixture.



Figure 1: Locust bean waste (LBW)



Figure 2: Bituminous coal

At a temperature of 1159°C - 1310°C the carbonate salt mixture changed to molten state, the mesh wire was saturated in the molten mixture so that upon cooling, the molten carbonate stuck to the mesh (Adeniyi *et al.*, 2014; Cooper & Berner, 2005). The carbon fuel is mixed with carbonate salts (sodium and potassium carbonate) as 15 wt.% of carbon fuel, 46.6 wt.% of Na₂CO₃ and 53.4 wt.% of K₂CO₃. The sodium carbonate and potassium carbonate were mixed with individual weight of 13.98 g and 16.02 g, and mixed with 45 g of the carbon fuel (Adeniyi and Ewan, 2012; Cooper and Cherepy, 2008).

3 RESULTS AND DISCUSSION

Tables 1 and 2 give the type of analysis that was carried out on the locust bean waste (LBW), coal and their blend after pyrolysis. The proximate and ultimate analysis was conducted at the National Cereal Research Institute, Badeggi in Niger state where the moisture content, volatile matter, fixed carbon and ash content and as well as the carbon (C), nitrogen (N), hydrogen (H), sulphur (S), oxygen (O) content and the calorific values were obtained.

Table 1: Proximate analysis of LBW, coal and blend

Sample	Moisture Content	Ash Content	Volatile Matter	Fixed Carbon
LBW	3.0	8.0	67.0	22.0
Coal	2.4	6.9	68.8	21.9
LBW and Coal	1.82	8.0	64.18	26.0

Table 2: Ultimate analysis of LBW, coal and blend

Sample	C wt. %	H wt. %	O wt. %	N wt. %	S wt. %	Calorific Value MJ/Kg
LBW	3.92	4.8	36.4	0.4	0.2	21.6
Coal	6.43	8.2	27.24	0.08	0.18	21.9
LBW and Coal	5.84	6.8	33.8	0.8	0.2	21.4

3.1 LBW CARBONFUEL

The carbon fuel in the molten carbonate direct carbon fuel cell (MCDCFC) performance at temperatures of 500°C, 600°C, 700°C and 800°C are shown in Figures 3 and 4. These include the SEM and XRD pattern for the locust bean waste fuel pyrolyzed at 500°C. Figure 3 shows the XRD of locust bean waste carbon sample used in the DCFC. The highest peak is at an angle of 25.988°(2θ-axis), with corresponding d-spacing of 3.42Å and a relative intensity of 100%. The peak value suggests a disordered form of carbon and this is a favourable criteria for application in the direct carbon fuel cell (Dudek *et al.*, 2018; Adeniyi *et al.*, 2014; Cooper & Berner, 2005). Figure 4 shows the SEM micrograph for the biochar from the LBW. This shows the size distribution and structure of the pyrolyzed carbon sample. This contains a combination of large particles with smaller ones which shows the interaction of the carbon particles.

Figure 5 presents the MCDCFC performance of the carbon sample used in the direct carbon fuel cell. The voltage increased with increase in the temperature, reaches a maximum, and finally falls at higher current densities.

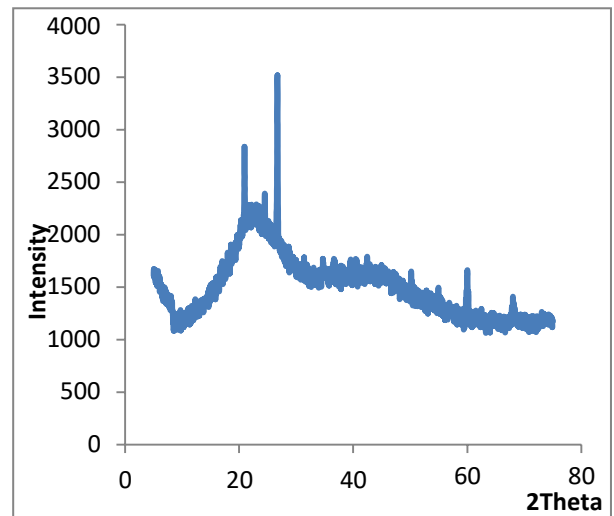


Figure 3: XRD pattern for pyrolyzed LBW at 500°C

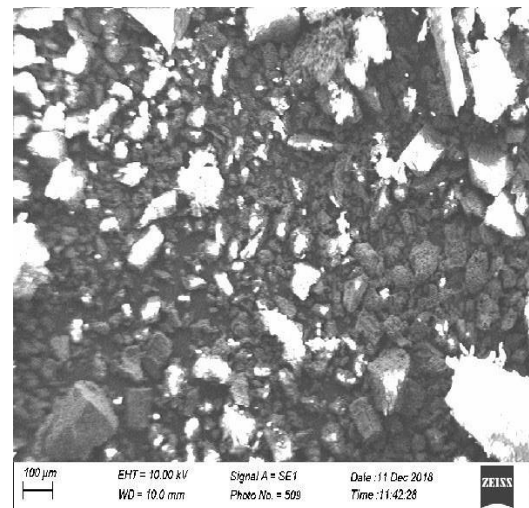


Figure 4: SEM of locust bean waste fuel

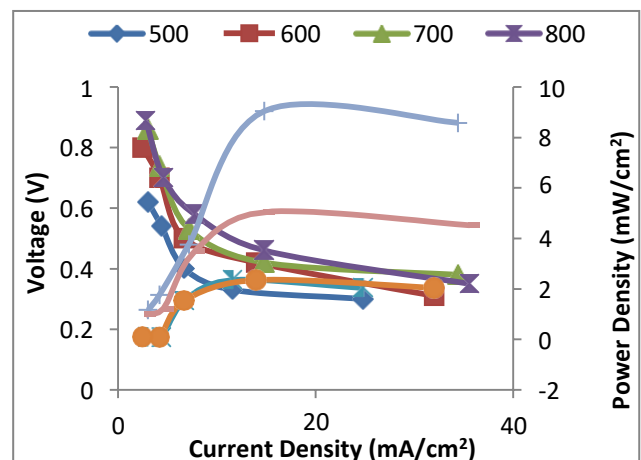


Figure 5: DCFC performance for Locust bean waste fuel

The current density and power density have high values at 800°C. At this temperature, the carbon fuel is consumed at the anode side of the fuel cell and a porous surface created on the electrolyte leading to a sharp rise in the current density. It was also observed from Figure 4 that the carbon particle have finer grain size and more homogeneous microstructure, and the surface morphology enhances the current density (Munnings *et al.*, 2014; Jia *et al.*, 2010; Jain *et al.*, 2009).

3.2 COAL CARBONFUEL

There was a slight difference in the DCFC performance of carbon fuel from coal as compared with that in Figures 3 to 5 at temperature 500-800°C. Figures 6 to 8 shows that the carbon fuel from coal gave a better performance than what was obtained from LBW carbon fuel. Figure 6 displays the X-ray diffraction pattern of the coal carbon fuel pyrolyzed at 500°C. The result obtained showed the degree of disordered graphite content and the sharp peaks indicates the presence of silica, oxygen and other impurities identified by the STOE Databank spectra. It was also observed that the presence of non-crystallites increases the surface area and thus produced improved current density. The peak at 26.24° corresponds to quartz (crystalline SiO₂). The inter-planar spacing of the carbon particle is 3.34Å, which indicates the presence of larger reactive sites units. These are indications of the suitability of the coal carbon fuel in the application of DCFC (Arenillas *et al.*, 2018; Kacprzak *et al.*, 2017).

Figure 7 represents the SEM micrograph of the coal carbon fuel sample. The fuel showed larger particle sizes, irregular shapes and fine grain sized particles. It was observed that the higher the current density the finer the surface morphology of the sample. However it could be deduced that the carbon fuel from coal is a better fuel when used in the direct carbon fuel cell because it possess higher calorific value. From Figure 8, it was noticed that the voltage increased with corresponding increase in the temperature, up to a point where there was a slight drop in the voltage reading. The coal carbon fuels also display higher current density at higher temperature (Li *et al.*, 2010; Jain *et al.*, 2009).

3.3 COMBINED CARBONFUEL

Figures 9 to 11 represents the electrochemical performance of the combined carbon fuels used in the fuel cell. The X-ray diffraction pattern for the combined carbon particle is represented in Figure 9. The presence of non-crystallites increases the surface area and thus producing improved current density.

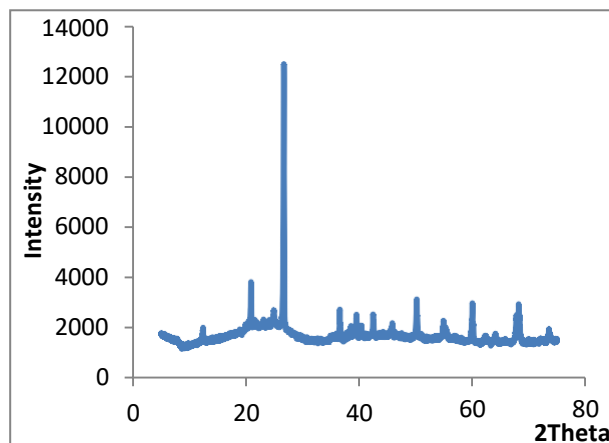


Figure 6: XRD pattern for coal pyrolyzed at 500°C

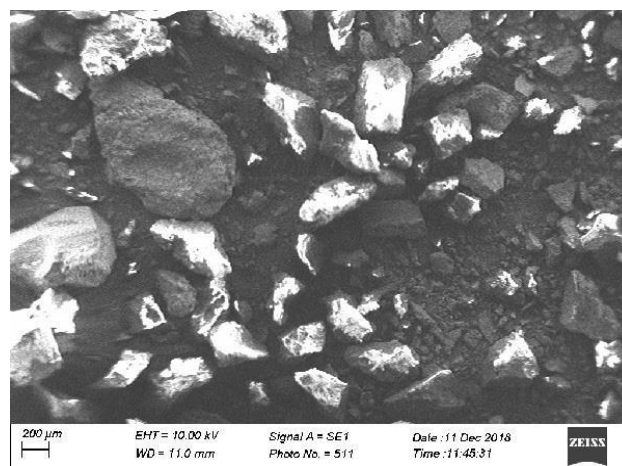


Figure 7: SEM pattern for coal carbon fuel

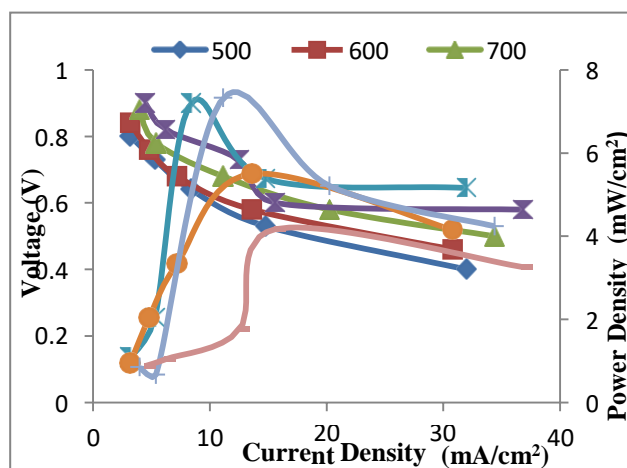


Figure 8: DCFC performance for coal fuel

The highest peak is at an angle 26.637° with corresponding d-spacing of 3.34Å on a relative intensity of 100%, which is the same with what was obtained for

the coal carbon fuel. The result obtained shows the degree of disordered graphite content and the sharp peaks indicates the presence of silica, oxygen and other impurities identified by the STOE Databank spectra. The disordered carbon particle is an important property in the operation of DCFC. Pyrolysis is vital to the disorderliness of the carbon particles (Cooper & Cherepy, 2008; Zecevic *et al.*, 2004). Figure 10 represents the SEM micrograph of the combined fuel and it shows larger particle sizes, irregular shapes and fine grain particles with slightly homogenous microstructure. The finer the particle surface morphology of the sample the higher it influences on the value of the current density. Figure 11 reveals the overall electrochemical performance of the combined carbon fuel and it interprets that a higher current density of 43.2 mA/cm² was obtained at 800°C alongside the power density. 8.10 mW/cm² was also obtained as the peak power density value. The performance of the DCFC is enhanced when coal is blended with LBW, which could lead to a lower CO₂ emission from the operation. This itself will have significant effect on the reduction of climate change and global warming when compared to the conventional burning of coal.

Figures 5, 8 and 11 shows the characteristics of power, current and voltage curves for a molten carbonate direct carbon fuel cell (MCDCFC). Some electrochemical parameters are presented in Table 3. The combined fuel (LBW and Coal) has the highest power efficiency of 73% at 800°C while LBW (locust bean waste) had the lowest at 54°C at same operating temperature. The open circuit voltage, peak power density, current density at 73% voltage efficiency proved to be the best result amidst the carbon fuel samples.

Table 3: MCDCFC performance at 800°C

MCDCFC Parameter	LBW	Coal	Combined Fuel (LBW & Coal)
Open circuit voltage (V)	0.90	1.012	1.16
Maximum power density (mW/cm ²)	9.05	7.32	8.10
Maximum current density (mA/cm ²)	35.6	36.8	43.2
Voltage at peak power (V)	0.89	0.90	1.08
Efficiency at peak power (%)	54	61	73

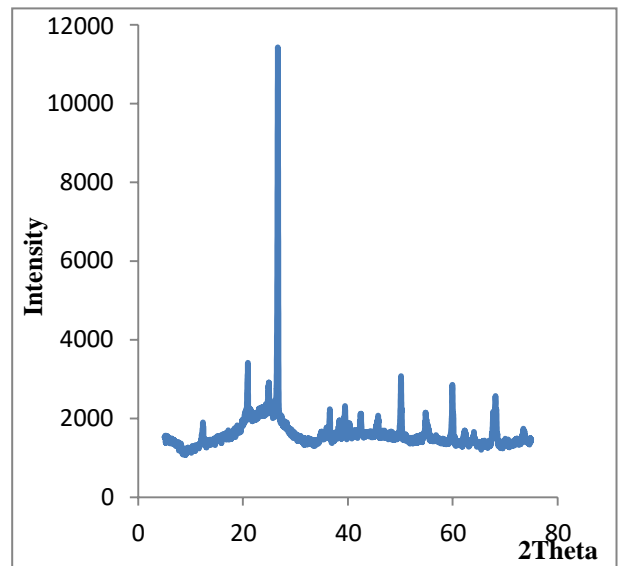


Figure 9: XRD for combined fuel (LBW and Coal)

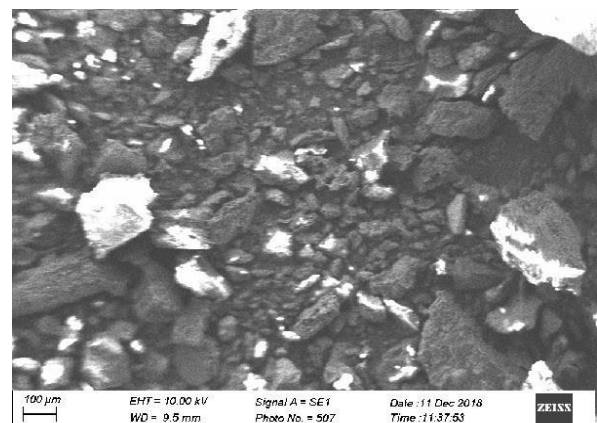


Figure 10: SEM for combined fuel (LBW and Coal)

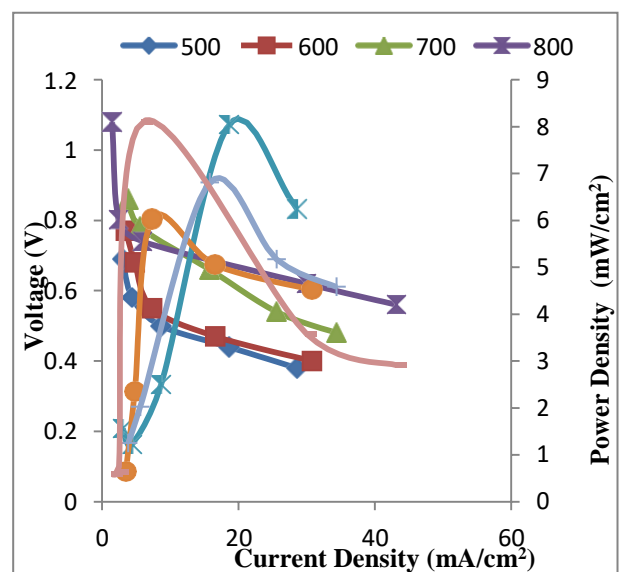


Figure 11: DCFC performance for combined fuel.

4 CONCLUSION

The investigation of the molten carbonate direct fuel cell showing the electrochemical performance of locust bean waste, coal and the combined fuel were carried out. The performance for the combined fuel was higher than that obtained from coal and locust bean waste. The open circuit voltage of the combined fuel is 1.16 V and is higher than 0.90 V of locust bean waste and 1.012 V for coal. The optimum peak power density recorded for the combined fuel (LBW & Coal) is 8.10 mW/cm², maximum current density of 43.2 mA/cm² with a resistance of 1 Ω. An efficiency of 73% was obtained from the combined carbon fuel which gave it a better performance in the direct carbon fuel cell operations. The scanning electron micrograph and X-ray diffraction reveals that the combined carbon fuels contain large sized particles with the highest peak of 26.637° with corresponding d-spacing of 3.42 Å similar to the coal carbon fuel. It was observed that finer particle morphology led to high current density and the presence of non-crystallites improved the current and power densities achievable with the fuel cell.

REFERENCES

- Adeniyi, O.D. & Ewan, B.C.R. (2012). Electrochemical conversion of switchgrass and poplar in molten carbonate direct carbon fuel cell. *International Journal of Ambient Energy*, 33:4, 204-208.
- Adeniyi, O.D., Ewan, B.C.R., Adeniyi, M.I. & Abdulkadir, M. (2014). The behaviour of biomass char in two direct carbon fuel cell designs, *Journal of Energy Challenges & Mechanics*, 1(4) 6, 1-6.
- Arenillas, A., Menéndez, J.A., Marnellos, G.E., Konsolakis, M., Kyriakou, V., Kammer, K., Jiang, C., Chien, A. & Irvine, J.T.S. (2013). Direct coal fuel cells (DCFC). The ultimate approach for a sustainable coal energy generation. *Bol. Grupo Español Carbón*, 29, 8-11.
- Cao, D., Sun, Y., Wang, G. (2007). Direct carbon fuel cell: Fundamentals and recent developments. *Journal of Power Sources*, 167(2), 250-257.
- Cherepy, N.J., Krueger, R., Fiet, K.J., Jankowski, A.F. & Cooper, J.F. (2005). Direct conversion of carbon fuels in a molten carbonate fuel cell. *Journal of the Electrochemical Society*, 152(1) A80-A87.
- Cooper, J.F., & Berner, K. (2005). The carbon/air fuel cell, conversion of coal-derived carbons” in: *The Carbon fuel Cell Seminar*, Palm Spring, CA, Nov. 14th, UCRL-PRES-216953, 1-16.
- Cooper, J.F., & Cherepy, N. (2008). Carbon fuel particles used in direct carbon conversion fuel cells. *US Patent Publication*, No. US 2008/0274382 A1.
- Desclaux, P., Nürnberger, S., & Stimming, U. (2010). Direct carbon fuel cells”, in R. Steinberger-Wilckens, W. Lehnert (eds.) *Innovations in Fuel Cell Technologies*, RSC Energy and Environment Series No. 2, Royal Society of Chemistry, Cambridge, 190-210.
- Dicks, A.L. (2006). The role of carbon in fuel cells. *Journal of Power Sources*, 156, 128-141.
- Dudek, M., Adamczyk, B., Sitarz, M., Sliwa, M., Lach, R., Skrzykiewicz, M., Raźniak, A., Ziąbka, M., Zuwała, J. & Grzywacz (2018). The usefulness of walnut shells as waste biomass fuels in direct carbon solid oxide fuel cells, *Biomass and Bioenergy*, 119, 144–154.
- Giddey, S., Badawal, S.P.S., Kulkarni, A. & Munnings, C. (2012). A Comprehensive Review of Direct Carbon Fuel Cell Technology. *Progress in Energy and Combustion Science*, 38, 360 – 399.
- Hoogers, G. (2003). Fuel Cell Technology Handbook. *CRC Press LLC*, Florida.
- Jain, S.L., Lakeman, J.B., Pointon, K.D. & Irvine, J.T.S. (2007). A novel direct carbon fuel cell concept. *Fuel Cell Science & Technology*. 4, 280-282.
- Jain, S.L., Lakeman, J.B., Pointon, K.D., Marshall, R. & Irvine, J.T.S. (2009). Electrochemical performance of a hybrid direct carbon fuel cell powered by pyrolysed MDF. *Energy Environ. Sci.* 2,687-693.
- Jia, L., Tian, Y., Liu, Q., Xia, C., Yu, J., Wang, Z., Zhao, Y., & Li, Y., (2010). A direct carbon fuel cell with (molten carbonate)/(doped ceria) composite electrolyte. *J. Power Sources*, 195:5581-5586.
- Kacprzak, A., Kobyłcki, R. & Bis, Z. (2017). The effect of coal thermal pretreatment on the electrochemical performance of molten hydroxide direct carbon fuel cell. *Journal of Power Technologies* 97 (5) (2017) 382–387.
- Larminie, J. & Dicks, A. (2003). Fuel cell systems explained. 2nd edition, John Wiley & Sons Ltd., England.
- Li, X., Zhu, Z.H., de Marco, R., Bradley, J. & Dicks, A. (2010). Evaluation of Raw Coals as Fuels for Direct Carbon Fuel Cells. *Journal of Power Sources*, 195 (13): 4051 – 4058.
- Munnings, C., Kulkarni, A., Giddey, S., & Badwal, S.P.S. (2014). Biomass to power conversion in a direct carbon fuel cell. *International Journal of Hydrogen Energy*, 39, 12377-12385.
- Zecevic, S., Patton, E.M., & Parhami, P. (2004). Carbon-air fuel cell without a reforming process. *Carbon*, 42, 1983-1993.



DESIGN OF A PROGRAMMABLE SOLID STATE CIRCUIT BREAKER

Ajagun, A. S.,¹ Abubakar, I. N.,² Yusuf, L.,³ & Udochukwu P. C.⁴

^{1,2,3,4} Department of Electrical and Electronics Engineering Federal University of Technology, Minna
Corresponding author's email: bimbo.ajagun@futminna.edu.ng

ABSTRACT

The use of a circuit breaker in the power system cannot be over emphasized. When fault is detected in a power system, the power system is disconnected from the power supply due to the presence of the circuit breaker which prevents the fault from damaging the power system. In this design, a simple and reliable programmable solid-state circuit breaker for power systems is presented so as to achieve the basic objectives of power system protection. The design includes the utilization of numerous modules/units such as the current sensing module (RF module), a microcontroller, and a solid-state relay. From the results obtained; it was observed that when the power of the system connected to the circuit breaker reaches the set threshold value programmed, the system goes off and the Liquid Crystal Display (LCD) displays a statement "overload detected". A new threshold value of power can be re-programmed using reset buttons on the system.

Keywords: *Circuit Breaker, programmable, power system protection, SSR*

1 INTRODUCTION

In electric transmission and distribution systems, industrial fields and consumer homes, sensitive equipment must be protected from long-period overload and instant short circuit conditions. (Bin *et al.*, 2015). There are different form of protection schemes and devices for various fault condition. (Chunyang *et al.*, 2017). Among all protection devices, the circuit breaker is the most efficient. Circuit breakers are designed using electronic components to eradicate the time wastefully spent in getting circuit breaker for specific loads. (young *et al.*, 2018) With the rapid growth of the capacity of electric systems, the occurrence of faults especially short circuit faults has become more frequent than at any time in the past. It does require even higher ultimate short circuit breaking capacity, ultra-fast breaking capability circuit breakers to avoid interruption of faults in both alternating and direct current systems. (Elavarasan *et al.*, 2017). This aids in preventing cables or terminal equipment from damages caused by transient or prolong fault currents. Circuit breaker facilitates the protection of the consumer's house from overloading of the circuit and short circuits (Alan, 2017). Well-protected houses usually reflect the level of expertise of electrician/electrical engineering in charge of its design. Therefore, protection level can be used as an evaluation tool (Journal, 2017). A good protection scheme provides a better way to serve both the electrician and the consumer. (Huaren *et al.*, 2015). Every consumer of electricity must include the following specific information during circuit breaker installation: consumer's identity which includes the consumer's input voltage level, manual or automatic mode of switching

back to connection, and so forth. It must also include the appropriate amount of load to operate on the circuit breaker. (Gregory *et al.*, 2012). In recent times, power semiconductor devices have been applied expansively in circuit breakers as they are practically controlled switches. Solid state circuit breaker is the circuit breaker with pure semiconductor devices. (McBride *et al.*, 2011). They offer switching speed of up to hundreds of microseconds Furthermore, as there are no mechanical components or parts; contact erosion, electric arc and strong mechanical shake do not exist. (Naser *et al.*, 2013). On the other hand, they have several disadvantages. Firstly, the semiconductors are sensitive to transit over voltage and heat causing over currents, which makes them a natural weakness of the whole electric system and need more self-protection technology. Secondly, bidirectional semiconductor devices are needed for bidirectional appliances (States, 2017). And lastly, the on state resistance which cannot be ignored means significant power loss, which could cause critical heat and lower system efficiency (Kempkes *et al.*, 2004). The installation of circuit breaker will go a long way in ensuring protecting the consumer and devices. A solid state circuit breaker is able to switch as fast as voltage or current sensing devices can respond to the faulty signal that is fast fault interruption, its design is also reliability and has good performance and cooling therefore it will be used in this project (Meyer *et al.*, 2004).

This paper presents a programmable low voltage solid state circuit breaker. This is designed to implement a protection scheme in order to solve the problems associated with extensibility. The existing system has

been studied and hence a power electronics based application would be provided to replace this method. In this paper, a circuit breaker is designed using electronics to eradicate the time and resources it takes to provide different circuit breaker for specific loads. The device is connected to a power source. The electronics based system monitors and measures the circuit current as the power source supply the load. This work generally looks for a more accurate, reliable and efficient method with respect to the present day technology to facilitate protection so as to ensure efficient outcome that will lessen time consumption and stress.

2 REVIEW OF RELATED WORKS

Alan, 2017 reviews the current status for solid-state circuit breakers (SSCBs) as well as hybrid circuit breakers (HCBs) with semiconductor power devices. A few novel SSCB and HCB concepts are described in this paper, including advantage and limitation discussions of wide-band-gap (WBG) devices in basic SSCB/HCB configuration by simulation and 360 V/150 A experimental verification. Novel SSCB/HCB configurations combining ultra-fast switching and high efficiency at normal operation are proposed. Different types of power devices are installed in these circuit breakers to achieve adequate performance. Challenges and future trends of semiconductor power devices in SSCB/HCB with different voltage/power levels and special performance requirements are clarified.

Kempkes *et al.*, 2004 described the architecture of a solid state circuit breaker for medium voltage DC power and highlighted its performance and faults.

Meyer *et al.*, 2004 compared different semiconductors considering the requirements of a solid-state switch integrated into a 20-kV medium-voltage grid. Based on these semiconductor characteristics, various switch topologies are developed, which are compared under technical and economic aspects. It is shown that solid-state circuit breakers offer significant advantages when compared to present solutions and can be used in today's medium-voltage power systems.

However, in this paper, a circuit breaker is designed using electronics to handle various specific loads through the programmable switch of the system. The system allows the circuit breaker to cut off at the threshold value set at any point in time.

3 METHODOLOGY

The block diagram in Figure 1 gives a pictorial view of the whole system design.

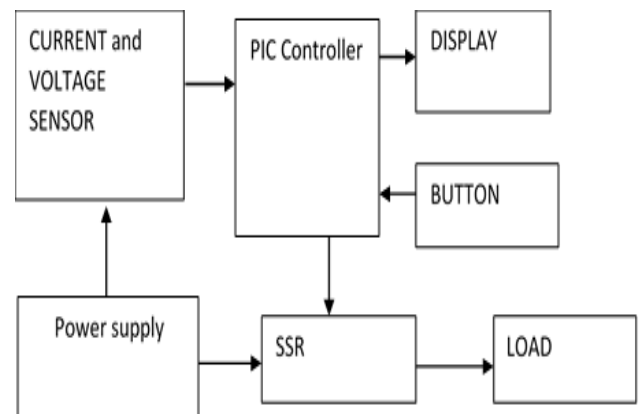


Figure 1: Block diagram of the system.

3.1.1 POWER SUPPLY UNIT

A transformer is needed to reduce the voltage level from 220V AC to 12V AC. The 12V AC is then converted to DC via the use of a bridge rectifier. However, the DC produced by the bridge rectifier still has ripples which are filtered off via the use of a capacitor as shown in figure 3. Afterwards, 5V is achieved via the use of 7805. The LED is used as power indicator and must be connected with a resistor in series. The resistor is to limit the current flowing through the LED. Figure 2 shows the power supply circuit.

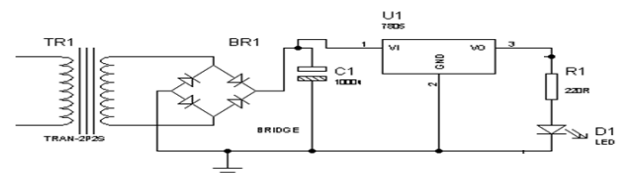


Figure 2: Circuit diagram of the power circuit

3.1.2 PIC Controller Unit

The PIC controller used in the study is PIC16F877. The justification for using the controller is that it has internal EEPROM which will help to reduce the number of components needed for the work. The controllers pin 11 and 32 is connected to the 5volt supply while pin 12 and 31 is connected to the ground so as to power the chip. For the chip to be able to access codes from within its program memory pin 1 which is the master reset will be connected to 5V supply. This also helps to start the performance of instruction from the beginning of the code. In other word it helps the system to properly boot up. Figure 3, Shows the controller connected to the power supply.

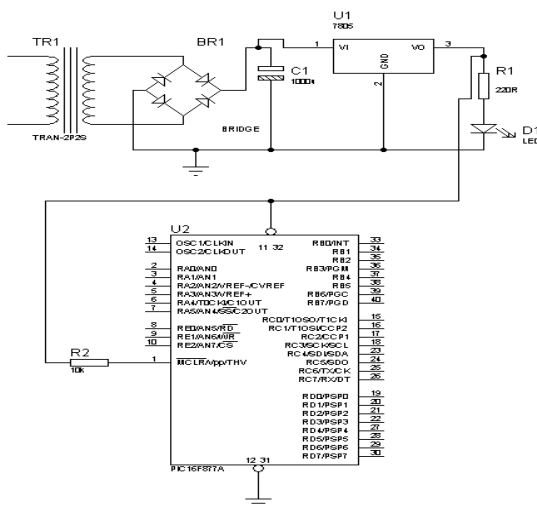


Figure 3: Circuit diagram of the controller connected to power supply

3.1.3 DISPLAY UNIT

The display unit used is a 16 by 2 alpha numeric liquid crystal display. The device is used to make the work user friendly and interactive. The 16 pins device has 8 bits for communication but one nibble was used for this work. Pin1 and 2 connected to 5V supply and ground are used to power the device. Also, pin 16 and 15 is used to power the back light of the device which makes the display visible. Pin 4 also called register select helps to specify if the code or data sent to the LCD is an instruction or a data to be displayed. Pin 6 also called the enable pin of the LCD must be clocked from high to low logic so as to enable the LCD treat the data sent to it either as data to be displayed or as an instruction. Pin 3 is used to adjust the contrast of the display. That is why a variable resistor is connected between the pin and ground. pin 7 to pin 14 is the data pins through which data sent to the LCD from the controller flows.

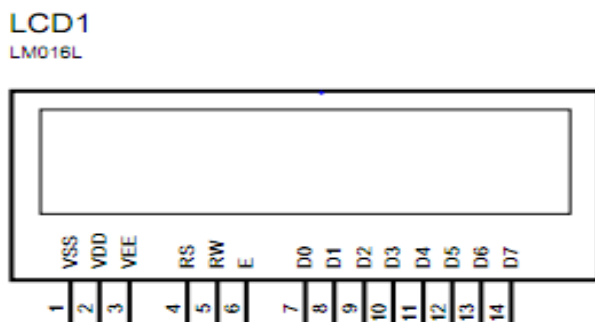


Figure 4: Symbolic Representation of the LCD (Abubakar *et al.*, 2017).

3.1.4 CURRENT SENSOR UNIT

The current sensor used in the work is ACS712 module which can be in 5A scale, 20A scale and 30A scale. However, for the purpose of this study, 20A scale was used. The sensor was used to measure the current that

flows to the load. The reason for the choice is because the maximum current sensed in this paper is 10A. The circuit in Figure 6 shows how the current sensor is interfaced with the pin 2 of the controller.

3.1.5 VOLTAGE SENSING UNIT

To be able to monitor load properly, the power used by the load is given by the equation

$$P = VI \quad (1)$$

$P =$ power used, $V =$ voltage supplied, $I =$ current demand by the load

To achieve the measuring of the voltage, a variable resistor is connected across the unregulated part of the power supply. The variable resistor is then set to give 2.5V at 220V. Therefore, the maximum voltage it can read at 5V will be 440V. The voltage output of this resistor is then connected to the analog to digital converter pin 3 of the controller.

3.1.6 PRESET BUTTON UNIT

These are momentary switches used to set the load desired for the circuit breaker to allow. The switches are pulled up with 1kΩ resistor as shown in Figure 8. The point 'X' on the circuit outputs 5V when the switch is opened and 0V when the switch is closed. Also, the switch is interfaced with the controller. Five switches were used for the design for the purpose of incrementing load, decrementing load, save and hold value switch and ON switch.

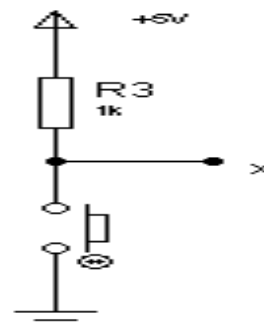


Figure 5: Circuit diagram of momentary switch

4 RESULTS

The design was tested and the following results were obtained as shown in Table 4.1, Plate I, Plate II and Plate III. Table 4.1 shows the experimental result of the phase selected and output of phase(s) available upon selection

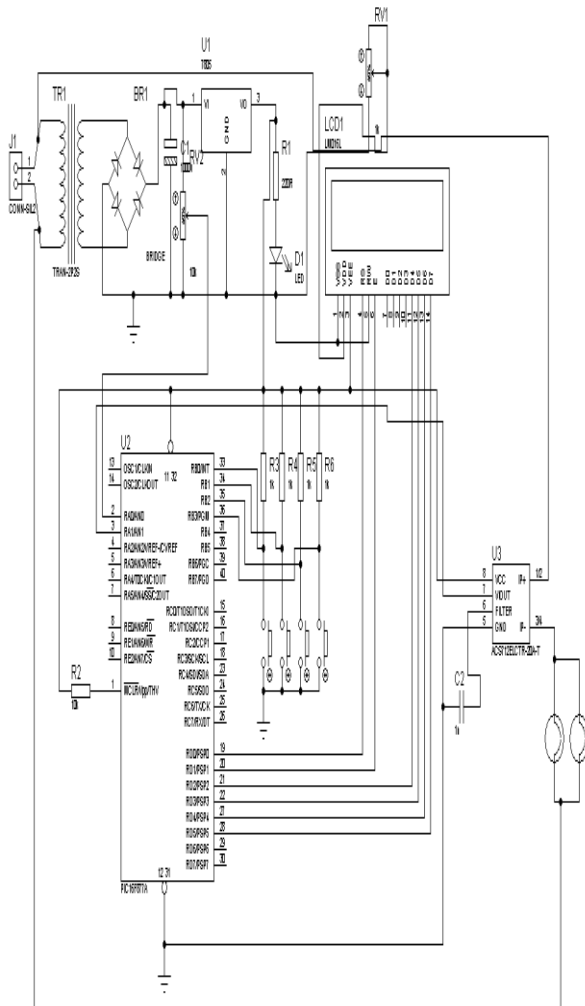


Figure 6: Complete circuit diagram

TABLE 4.1: SHOWS THE READINGS OBTAINED DURING THE TESTING OF THE POWER SUPPLY UNIT

S/N	MEASURED QUANTITIES	READING (VOLTS)
1	Input Voltage into the regulator	12.00
2	Output voltage from the regulator	5.00
3	Voltage supplied to the microcontroller	5.00
4	Voltage supplied to the LCD	5.00



PLATE I: PROJECT CASING AND LCD RESULT SHOWING OVER LOAD DETECTED DUE TO EXCESS CURRENT



PLATE II: RESULT SHOWING THE CIRCUIT BREAKER READY TO BE PROGRAMMED TO DESIRED VALUES AND THE TWO BUTTONS USED TO PROGRAM IT.



PLATE III: PROJECT SHOWING CIRCUIT BREAKER WITH MAX VALUE OF POWER ALLOWED AND CURRENT POWER CONNECTED.

4.1 DISCUSSION OF RESULTS

From the results obtained; it was observed that when the power of the system connected to the circuit breaker reaches the set threshold value programmed, the system goes off and the LCD displays a statement "overload detected". This was shown in Plate 1.

Plate II shows how a new threshold value of power can be re-programmed using reset buttons on the system.

In Plate III, the maximum value of power the circuit breaker can withstand is displayed with the present value of power connected to the system.

5 CONCLUSION AND FUTURE WORK

The results obtained showed that the Programmable Solid State Circuit Breaker is capable of not only disconnecting power system when faults occur but also capable of being programmed to ensure flexibility. For future research

purposes, the following recommendations should be put into consideration:

1. A more accurate current sensor should be used;
2. More intelligence features should be incorporated in the system.

REFERENCES

- Abubakar, I. N., Jacob, T., & Mustapha, B. M. (2017). Enhancement of Electrical Energy Transaction Through the Development of a Prepaid Energy Meter using GSM Technology. *International Journal of Research Studies in Electrical and Electronics Engineering (IJRSEEE)*, 3(4), 10-18. DOI:- <http://dx.doi.org/10.20431/2454-9436.0304003>.
- Alan, J. (2017). Semiconductor Devices in Solid-State/Hybrid Circuit Breakers: *Current Status and Future Trends*, 10. <https://doi.org/10.3390/en10040495>
- Bin, X., Zhiyuan, L., Yingsan, G., Yanabu, S. (2015). DC Circuit Breaker Using Superconductor for Current Limiting. *IEEE Trans. Appl. Supercond.*, 25, 1–7.
- Chunyang, G., Pat, W., Alberto, C., Alan J. W., & Francis E. (2017). Semiconductor Devices in Solid-State/Hybrid Circuit Breakers: Current Status and Future Trends. *Energy journal of Engineering*, 12 (3) 1-25
- Elavarasan, T., Chandrasekar. S., & Mathiyazhagan. R., (2017). Designing and Simulation of Power Electronic Solid State Circuit Breaker for Medium Voltage Transmission Line. *journal of Electrical Engineering*. 11 (8), 457-464
- Huaren, W., Ling, Y., Lin, S., Xiaohui, L. (2015). Modeling of Current-Limiting Circuit Breakers for the Calculation of Short-Circuit Current. *IEEE Trans. Power Deliv.*, 30, 652–656.
- Gregory, G.D., Hall, W.M. (2012). Predicting molded-case circuit breaker let-through characteristics in an electrical system under short-circuit conditions. *IEEE Trans. Ind. Appl.*, 29, 548–556.
- Journal, O. A. (2017). Designing and Simulation of Power Electronic Solid State Circuit Breaker for Medium Voltage Transmission Line. *International Journal of Electrical and Electronics Engineering (IJEEE)*, 2(1), 109-121.
- Kempkes, M., Roth, I., & Gaudreau, M. (2004). "Solid-State Circuit Breakers For Medium Voltage DC Power": S.Chand, 2004. pp. 25-28.
- McBride, J.W., Weaver, P.M. (2011). Review of arcing phenomena in low voltage current limiting circuit breakers. *IEE Proc. Sci. Meas. Technol.*, 148, 1–7.
- Meyer, C., Member, S., Schröder, S., & Doncker, R. W. De. (2004). *Solid-State Circuit Breakers and Current Limiters for Medium-Voltage Systems Having Distributed Power Systems*.
- Naser, E. R., Amor, A., Massoud, N., & Ben B. L. (2013). Smart low voltage ac solid state circuit breakers for smart grids. *Global Journal of Advanced Engineering Technologies*, 3 (2), 2277-6370
- States, U. (2017). Solid State Circuit Breaker. *Patent Application Publication (10) Pub. No.: US 2017/0029152 A1*, 1(19)
- Young, S. K. (2018). Analysis of electric field for solid-state isolated multi-circuit breaker according to switching mode. *International Journal of Pure and Applied Mathematics*, 118 (19), 1573-1586

DESIGN OF AN ARDUINO BASED RFID LINE SWITCHING USING SOLID STATE RELAY WITH INDIVIDUAL PHASE SELECTION

Ajagun, A. S.,¹ Yusuf, L.,² Abubakar, I. N.,³ & Yusuff, S. D.⁴

^{1,2,3,4} Department of Electrical and Electronics Engineering Federal University of Technology, Minna
Corresponding author's email: bimbo.ajagun@futminna.edu.ng

ABSTRACT

The use of line switching in the power system cannot be over emphasized. When fault is detected on a distribution line, the line is disconnected/isolated due to the presence of this fault and switched over to another distribution line by a line switching system. In this paper, a simple and reliable line switching system for distribution lines is presented so as to achieve the basic objectives of power system protection which are continuity of power supply and safety of personnel and equipment. The design includes the utilization of numerous modules/units such as the radio frequency module (RF module), a microcontroller, and a Radio Frequency Identifier (RFID) reader. The RFID card is swiped across the sensor and the experimental result shows the phase selected and the output of phase(s) available upon selection.

Keywords: *Line switching, distribution line, power system protection, RFID, SSR*

1 INTRODUCTION

Line switching is used to connect and disconnect distribution substations to and from a distribution grid. At the cradle of technology, several faults were associated with line switching, which were achieved using manual switches or fuses. It has endangered lives due to its exposure leading to electrocution during maintenance, thereby compromising the objective of power system protection. With advancement in technology and for realization of the objectives of power system protection, that is, continuity of supply and safety of both personnel and equipment; (Gupta *et al.*, 2009) the need to avert these faults was of paramount importance. This brought about the development of automated line switching using relays and contactors. As time progresses, the relays and contactors begin to fail due to damage encountered (wearing of contacts) as a result of arcing and under voltage. In electrical power system, prior to the load in substations are the feeder pillars. Feeder pillars; which are distribution transformer cabinet boards, are used by the power authority for supplying 3-phase and single-phase loads to feed residential and some small scale commercial consumers. This is done at distribution level of 415 V and 240 V respectively which is a safe, economical and convenient way for operational and maintenance purposes. The use of fuses within the system is of paramount importance. To avoid overloading and ensuring the safety of lives and equipment from faults such as short circuit (arcing); fuses, which are overcurrent protective devices with a circuit opening fusible part are used. These fuses can become heated and severed by the passage of large amount of current through it. Before the advent of modern technologies; when faults occur, fuses are disconnected using insulated pliers so as to create a safe ground for repairs or maintenance. Also, electricity

consumer may experience intentionally engineered rolling black out due to fault or maintenance. Even with that, this method still exposes the operator or technologist to the risk of being electrocuted (Michael *et al.*, 2010).

In recent technologies, automated switching of lines using Radio Frequency Identification (RFID) and Solid State Relays (SSR) have been introduced (Ahmed *et al.*, 2009). In this design, an Arduino Based Radio Frequency Identification (RFID) Line Switching using Solid State Relay (SSR) with Individual Phase Selection is presented. This paper is focused on achieving the objectives of power system protection by ensuring safety of lives and continuity of power supply through selection of phases and the use of SSR.

2 REVIEW OF RELATED WORKS

(Filipovic-Grcic *et al.*, 2017). Presented the application of controlled switching techniques for limitation of switching over voltages (SOVs) and transient currents on 400 kV transmission line with capacitive voltage transformers installed at both ends. The work shows that the controlled switching significantly reduces SOVs, current transients and energy stress of station surge arrestors. The controlled switching is a method for eliminating harmful transients via time-controlled switching operations. Consequently, the controlled switching reduces the mechanical and electromagnetic stresses of the high voltage equipment and also prevents the unwanted operation of relay operation. This work has to do with clearing of transient faults for improving continuity of power supply. It is thus limited to high voltages and applicable to transmission lines. (Huang *et al.*, 2014). Investigates the stability issues that might arise when incorporating transmission line switching into smart grid planning and operation. To demonstrate the

feasibility of line switching, scenarios and dynamic simulations were used to demonstrate system security margin and online stability issues. Results shows that proper line switching can resolve system energy and boost system security margin, even though less transmission lines were used. It also reveals that small signal instability can be triggered by line switching. This work was employed in transmission lines for system stability. The author did not consider line switching in distribution system. (Tada & Kitamori, 1996) introduces an object of the present invention to provide a line switching system for switching lines by using Automatic Protection Switch (APS) byte. It entails line disconnection between the nodes when a fault is found in the transmission devices of the nodes to switch one transmission path to the other transmission path. With this system, there is no need to be conscious of the state for setting the lines of the entire system. Thus, it becomes possible to reduce the time required for switching and the amount of managing data. (Michael *et al.*, 2010). presents Arduino based Radio Frequency Identification (RFID) Line Switching using Solid State Relay (SSR). In this work, no individual phase selection. Intentionally engineering rolling black out is encouraged as the healthy phase(s) is not separated from the faulty phase (s), instead all lines are either switched to logic 0V (off) or to logic high (5V). During maintenance or clearing of faults, all phases are taken out of supply irrespective of whether faulty or not, hence the objective of power system protection cannot be realized as continuity of power supply is compromised. The application of RFID in power system by different researchers can also be seen in works presented by (Ralph and Mackenzie, 2014, Yerlan and Alex, 2014)

3 METHODOLOGY

Line switching is used to connect and disconnect distribution substations to and from a distribution grid. This section of the paper contains the processes involved to get the system working. This section mainly deals with the designed aspect of the hardware and the analysis of individual unit that made up the device. Figure 1 shows a block representation of an Arduino Based RFID Line Switching Using Solid State Relay with Individual Phase Selection.

3.1.1 AC TO DC CONVERTER UNIT

This is achieved via the use of a 12V step down transformer TR1 as shown in Figure 2. The main supply is step down from 220V to 12VAC. This is then converted to DC via the bridge rectifier BR1. The DC power produced still has some elements of AC which is then filtered off via the use of capacitor C1. Afterwards, voltage regulators of 9V and 5V are used since 9V is used

to power the Arduino board while the 89C52 is powered with 5V.

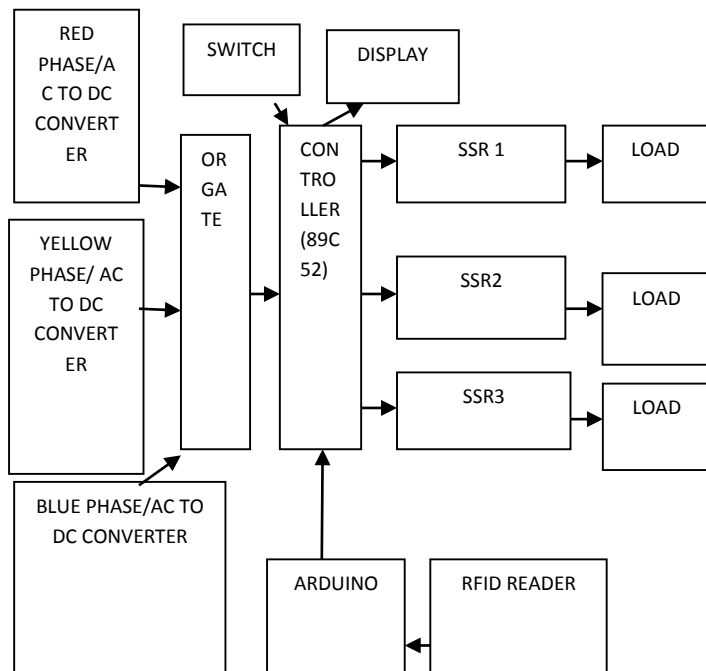


Figure 1: Block diagram of the system

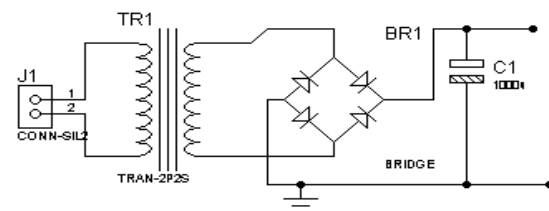


Figure 2: Circuit diagram of the power circuit

3.1.2 OR Gate Unit

The use of the OR Gate is to ensure that power is supplied to the controller whenever power is detected either before or after the fuses. To achieve this, diodes D1, D2 and D3 was used as shown in the Figure 3. Figure 4 Shows the three phase AC to DC converter with voltage regulators.

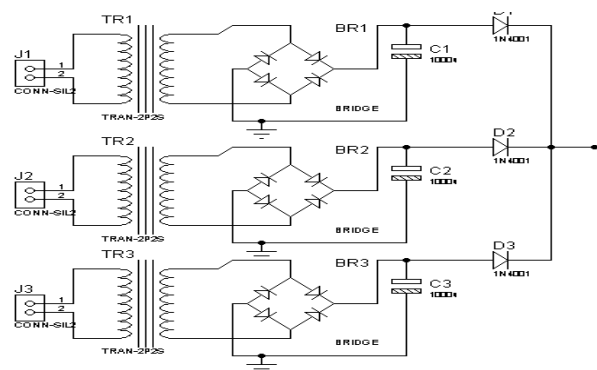


Figure 3: The circuit diagram of AC to DC Converter with Diodes as OR gate.

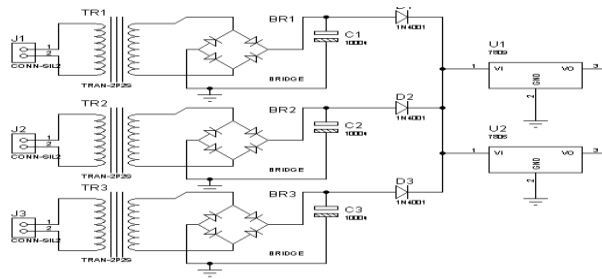


Figure 4: Circuit diagram of the three-phase supply with voltage regulator.

3.1.3 Controller Unit

The controller used for selection of the phases is 89C52. The controller was clocked with 12MHz crystal at pin 18 and 19. Also, pin 40 and pin 31 are connected to 5V while pin 20 is grounded. This will aid the system to be powered and enabled so as to fetch instructions from within its memory. Pin 9 is connected to 5V supply via a 1µf capacitor. The circuit is shown in Figure 5.

3.1.4 Display Unit

This section was achieved by the use of a liquid crystal display (LCD). Instructions from the datasheet are employed in interfacing the LCD with the controller. The different control signals that could initialize the system were specified. All these instructions were adhered to for success in the prototype made (Abubakar *et al*, 2018). The symbolic representation of the device is shown in Figure 6.

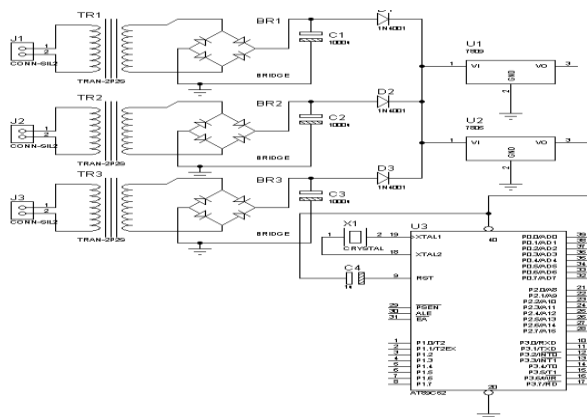


Figure 5: Circuit diagram of the controller connected to the power supply

LCD1
LM016L

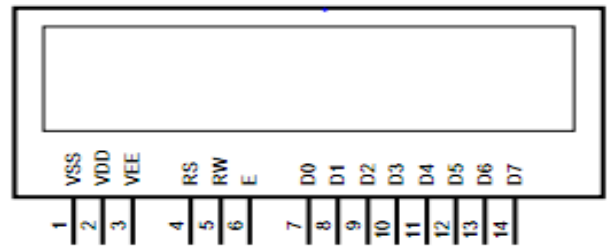


Figure 6: Symbolic Representation of the LCD (Abubakar *et al.*, 2017)

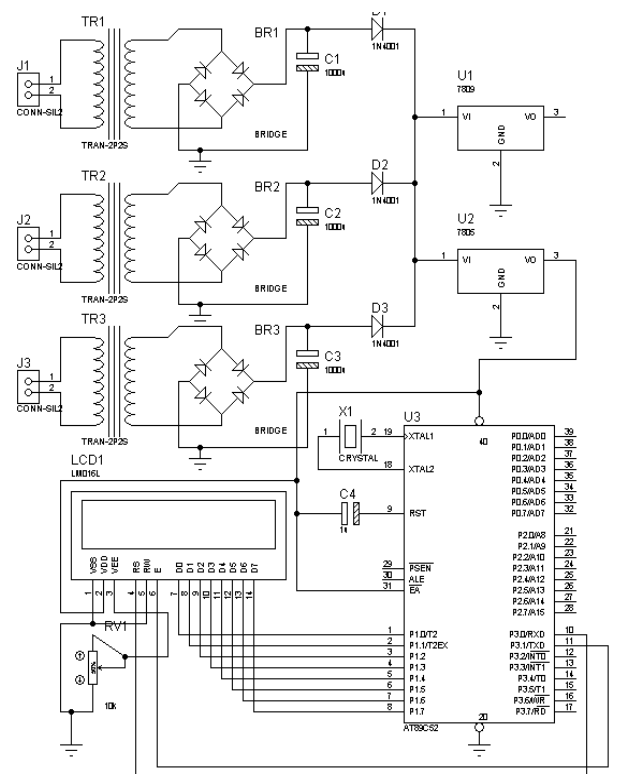


Figure 7: Circuit diagram of the LCD interfaced with the circuit.

3.1.5 Switches Unit

The button was introduced to ensure the selection of active lines. The momentary switches called buttons are connected in series with 1kohms resistor as shown in the Figure 8. Closing the switch will aid the output of 0V which is logic low while if opened it outputs logic high.

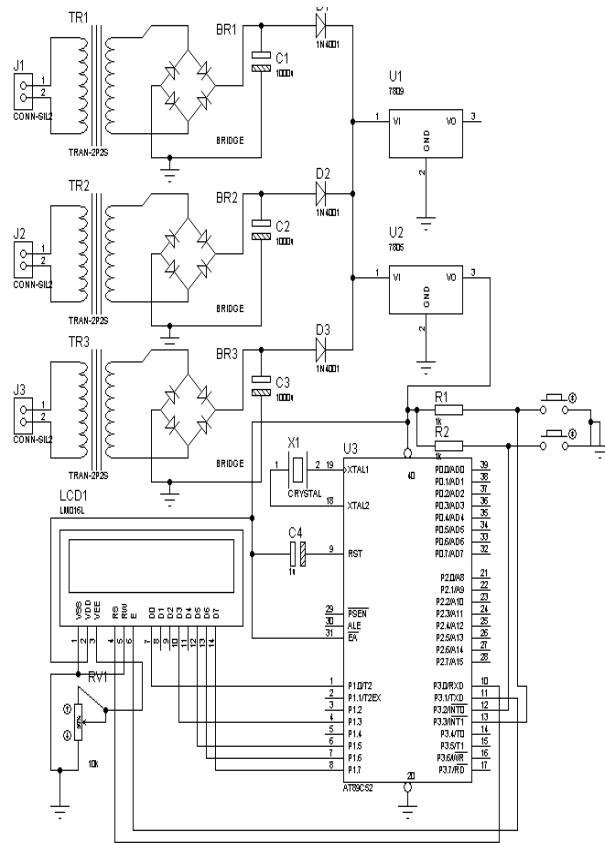


Figure 8: Circuit description of the system and buttons added.

3.1.6 Arduino Unit

The Arduino used as shown in Figure 9 is Arduino Uno R3. The micro controller board is made with ATMEGA328 which has 14 digital input and output pins, 6 analog inputs, 16MHz ceramic resonator, USB connector and many more. However, because of the different modules within it, this controller was chosen to reduce cost and time of design. The controller serves as the central processing unit of the whole design. It is interfaced RFID Reader and the 89C52. Figure 11 shows the device in the whole circuit.

3.1.7 RFID Sensor Unit

The sensor as shown in Figure 1., used in this work is a Mafare product MFRC522. The 3V driven sensor comes with a card (RFID tag). This card is embedded with some information which is picked up by the sensor at proximity and then interpreted by the controller.



Figure 9: Pictorial view of Arduino Uno R3



Figure 10: Pictorial view of the RFID sensor

3.1.8 Solid State Relay Unit

This is an opto-coupler made up of a light emitting diode and a photo triac. For the triac to allow AC power to flow through, the LED has to be ON. This is achieved when the controller sends Logic 1 (5V) to a resistor R1 connected in series with the LED. However, in this project, three SSR were used for switching the three phases.

The circuit diagram in Figure 11 shows the connection of the different circuit of the entire design.

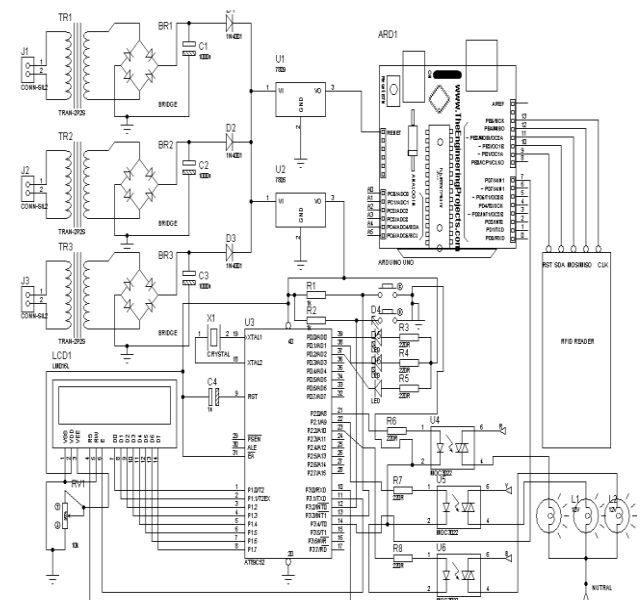


Figure 11: Complete circuit diagram

4 RESULTS

The design was tested and the following results were obtained as shown in tables 4.1,4.2 and 4.3. Table 4.1 shows the experimental result of the phase selected and output of phase(s) available upon selection. Table 4.3 shows the lamp that comes on which is in phase with the line selected from the output obtained in Table 4.2. The lamps come on only after swiping the RFID card on the sensor.

TABLE 4.1: EXPERIMENTAL RESULT OF THE POWER CIRCUIT

S/N	Power IN Red Phase	Power IN Yellow Phase	Power IN Blue Phase	Power OUT
1.	0	0	0	0
2.	0	0	1	1
3.	0	1	0	1
4.	0	1	1	1
5.	1	0	0	1
6.	1	0	1	1
7.	1	1	0	1
8.	1	1	1	0

Key; Power Out=1 when 12V is measured and Power Out=0 when 0V is measured.

4.1 DISCUSSION OF RESULTS

Table 4.1 shows that the main circuit is powered whenever any of the phases is available by giving an output voltage of 12 V for phase availability and 0 V for non-availability of phase; The OR Gate is used to ensure that power is supplied to the controller whenever power is detected in any of the phases. Table 4.2 shows the phase(s) available upon selection by giving a numeric value 1 when the phase is selected and 0 when the phase is non selected. Table 4.3 shows the effect of the phase(s) selected on the lamp(s) when the RFID Card was swiped across the sensor. The lamp(s) turns on when it corresponds with the phase(s) selected and the lamp(s)

turns off when the phase(s) is/are not selected only after the RFID Card has being swiped on the sensor by giving numeric value 0 when the lamp is off and 1 when the lamp is on.

5 CONCLUSION AND FUTURE WORK

The results obtained showed that the Arduino Based RFID line Switching Using SSR with Individual Phase Selection is capable of not only connecting and disconnecting distribution lines to and from a distribution substation but also capable of selecting the phase(s) at which to connect or disconnect. For future research purposes, the following recommendations should be put into consideration:

1. A database should be built with the system so as capture the identity of the operating personnel;
2. More intelligence features should be incorporated in the system.

TABLE 4.2: EXPERIMENTAL RESULT OF PHASE SELECTION AND OUTPUT

S/N	Red Phase	Yellow Phase	Blue Phase	OUT
1.	0	0	0	NIL
2.	0	0	1	Blue Phase
3.	0	1	0	Yellow Phase
4.	0	1	1	Yellow & Blue Phase
5.	1	0	0	Red Phase
6.	1	0	1	Red & Blue Phase
7.	1	1	0	Red & Yellow Phase
8.	1	1	1	ALL

Key: 1=Selected 0=Not selected



Plate I: Result showing connection to power supply



Plate II: Result showing initialization

TABLE 4.3: EXPERIMENTAL CONTROL OF THE RFID CONTROL OF THE PHASES

S/N	L1	L2	L3	OUT
1.	0	0	0	NIL
2.	0	0	1	Blue Phase
3.	0	1	0	Yellow Phase
4.	0	1	1	Yellow & Blue Phase
5.	1	0	0	Red Phase
6.	1	0	1	Red & Blue Phase
7.	1	1	0	Red & Yellow Phase
8.	1	1	1	ALL

Key: L1=Lamp 1, L2=Lamp 2, L3=Lamp 3
0= When lamp comes off
1= When lamp comes on.

REFERENCES

- Abubakar, I. N., Jacob, T., & Mustapha, B. M. (2017). Enhancement of Electrical Energy Transaction Through the Development of a Prepaid Energy Meter using GSM Technology. *International Journal of Research Studies in Electrical and Electronics Engineering (IJRSEEE)*, 3(4), 10-18. DOI:- <http://dx.doi.org/10.20431/2454-9436.0304003>.
- Ahmed, J., & Tau, S. R., (2009). The Impact of Emerging RFID Technology In The Wireless Environment For Automatic Identification Data Collection And Dedicated Short Range Communication. *Journal of Theoretical and Applied Information Technology*, 5(4), 2004-2009.
- Filipovic-Grcic, B., Uglesic, I., Bojic, S., and Zupan A. (2017). Application of Controlled Switching For Limitation of Switching Overvoltages on 400kV Transmission Line," *Paper submitted to the International Conference on Power Systems Transients (IPST2017)*, in Seoul, Republic of Korea 117-119.
- Gupta, J. B. (2014). A textbook on Switchgear and Protection. 7th Edition, Published by S.K Kataria and Sons, publishers of Engineering and computer Books, New Delhi pp. 8
- Huang, G. M., Wang, W., & An, J. (2014). Stability Issues of Smart Grid Transmission Line Switching, *Proceedings of The 19th World Congress, The International federation of Automatic Control*, Cape Town, South Africa, 20-25.
- Michael, E., Isah, Y., Bako, H., Hassan, O. F. & Ezika, V.



C. (2010). Arduino Based RFID Line Switching Using SSR. *The International Journal Of Scientific and Technological Research*, 6(10), 19-25.

Ralph, T., & Mackenzie, K. (2014). RFID Door Lock. Senior Project Electrical Engineering Department California Polytechnic State University San Luis Obispo.

Tada, K., & Kitamori, K. (1996). Line Switching System. United States Patent. Jul. 2, 1996.

Yerlan, B., & Alex, P. J. (2014). RFID-Cloud Smart Cart System. Department of Electrical and Electronic Engineering School of Engineering, Nazarbayev University Astana, Kazakhstan.



DEVELOPMENT OF AN IMPROVED ADAPTIVE HYBRID TECHNIQUE TO MITIGATE CROSS-TIER INTERFERENCE IN A FEMTO-MACRO HETEROGENEOUS NETWORK

*Kassim, A. Y¹, Tekanyi, A. M. S², Sani, S. M³, Usman, A. D⁴, Abdulkareem, H. A⁵ & Muhammad, Z. Z⁶

^{1,2,3,4,5&6} Department of Communications Engineering, Ahmadu Bello University, Zaria- Nigeria.

*Corresponding author email: jalaluddeen91@gmail.com; +2348167688890

ABSTRACT

The deployment of femtocells presents an attractive solution for the improvement of mobile network services, providing better data rates and coverage to indoor users. Since the deployment of femtocells results to a heterogeneous network, where two layers utilize the available spectrum, issues of interference arise. The interference mitigation in literature made use of a single or hybrid enhanced inter-cell interference coordination techniques to reduce interference in heterogeneous networks. These techniques mitigate interference at the expense of reduced capacity or coverage of the interfering cell as well as the network as whole and also cause underutilization of the spectrum resources. A method used in this research to address this challenge investigated the positions of the user equipment and the installed femto base stations. The developed improved adaptive hybrid technique that combined Time domain technique using reduced power ABS and Power control technique was then used to mitigate the cross-tier interference between the femto base station and the macro-user in the vicinity of the femtocell. This was done in order to achieve optimal and fair overall performance of the network.

Keywords: *Heterogeneous Networks, Femtocell, Reduced-power ABS, Zero-power ABS, Interference, Closed Subscriber Group.*

1 INTRODUCTION

Heterogeneous Networks (HetNets) promises to address the technical challenges of high demand for mobile data traffic on cellular networks in terms of data throughput and network capacity (Ali, 2015). There are unprecedented trends in the growth of mobile data traffic in recent years and that will continue globally for years to come. According to Ericsson, (2013), voice traffic was surpassed by mobile data traffic in 2009 and it is anticipated to continue consistently. It is anticipated that there will be annual growth in mobile video traffic by 45 percent through 2023 which will account for 73 percent of all mobile data traffic. Also, it is anticipated over the next 6 years that data traffic from social networking applications will grow steadily by 31 percent annually (Ericsson, 2018).

To accommodate this exponential growth in demand for high mobile data, the telecommunications industry is faced with the urgent needs of expanding the mobile access network capacity by 1000 times. Today, customers want to communicate with one another anytime, anywhere, and through any available media, including instant messages, video conferencing, email, voice, and video calls (Afolalu *et al.*, 2016). The growth in mobile data traffic is driven by the increasing number of smartphone subscriptions and increasing average data volume per subscription, primarily propelled by more viewing of video content at higher resolutions (Ericsson, 2018).

This makes it vital for the network operators to devise new means of enhancing the indoor coverage by reducing transmit-receive distance by bringing the transmitter and receiver closer to each other. The users' expectations on demand for mobile broadband services is met by improving the overall performance at hotspots and cell edges. In order to achieve this, efficient use of the available resources is required as well as new techniques of securing, deploying, utilizing, managing, and optimizing these resources. Telecommunications services providers make use of various methods to meet customers' expectations which includes: improving the coverage and capacity of the existing network by densifying the current macrocells through the addition of small cells (Bhosale and Jadhav, 2015).

The concept of heterogeneity and dense deployment of small cells as a paradigm shift in cellular networks has become an attractive solution recently in meeting future demands for high data rates, reduced latency, and enhanced coverage (Hossain *et al.*, 2014; Kaddour *et al.*, 2015). HetNets can be defined as a collection of low power Base Stations (BS) distributed across a macrocellular network in order to improve the capacity and enhance the coverage of the network. These low power BS includes femtocells, microcells, relays, picocells, and remote radio heads, which are deployed at hotspots, enterprise environment, homes, and low geometry locations (Saad *et al.*, 2013).

Femtocells provide high spectral efficiency, low cost of both deployment and maintenance which made it to gain

enormous attention in the wireless industry (Bouras *et al.*, 2013). Studies have shown that 50 percent of the total voice traffic and 70 percent of the total data traffic are generated indoors and for the mobile operators to provide better Quality of Service (QoS) to these indoor users, femtocells deployment is considered a promising solution (Cao & Fan, 2013). The deployed femtocell makes use of the same or different carrier frequencies with the existing macrocell network. Using different carrier frequencies prevents inter-cell interference between macrocell and femtocell, but requires more radio resources. From the fact that licensed spectrum is scarce and expensive, network operators make use of the same carrier frequency (co-channel) in order to reduce large spectrum requirement (Bartoli *et al.*, 2014). Although, the same carrier frequency deployment ensures efficient spectrum utilization and larger bandwidth for both macrocell and femtocell, but also results to cross-tier interference, which may prevent the macro users within the vicinity of the femto eNodeB from having good Signal-to-Interference-Plus-Noise Ratio (SINR) (Kurda *et al.*, 2015). Typically, femtocells are deployed in a closed access mode, where the network is only accessed by users enlisted in the Closed Subscriber Group (CSG). In the downlink transmission, femtocells operating in CSG mode tend to subject macro users in its vicinity to severe cross-tier interference (Wang & Pedersen, 2011).

Hence, it is necessary and important to mitigate this interference that comes along with femtocell deployment within macrocell in order to fully utilize its advantages. The Third Generation Partnership Project (3GPP) LTE-A release 10 standards in its enhanced Inter-Cell Interference Coordination (eICIC) introduced techniques for interference mitigation. These techniques (Lopez-Perez *et al.*, 2011) include Power Control (PC), Time Domain (TD), and Frequency Domain (FD). The literatures consulted used either FD, TD, PC or a hybrid of the techniques to mitigate interference in a femto-macro HetNet.

RELATED WORKS

Nasri *et al.*, (2015) proposed a new algorithm that integrated interference avoidance and interference cancellation to mitigate the effect of interference in the downlink channel of a macro-femto HetNet. The scheme implemented interference avoidance at the transmitter and interference cancellation at the receiver. At the transmitter, Low Power Almost Blank Subframe (LP-ABS) was used to minimize the effect of interference by transmitting signals with low power during the ABS instead of muting the frames completely. The downlink interference cancellation scheme reduced the effect of interference on users by optimizing their received Signal-to-Interference plus Noise Ratio (SINR) at the receiver. System level simulation results showed an enhancement

in network performance and user experience in terms of total throughput and received SINR. There was high computational burden at the receiver due to optimization processes. There is still room for improvement on the capacity of the network by using suitable adaptive LP-ABS such that the interfering cell can transmit on both the normal and ABS.

Koutlia *et al.*, (2015) developed a new enhanced Inter-Cell Interference Coordination (eICIC) technique for managing ABS subframes. The algorithm exploited jointly power, frequency and time dimensions in order to balance the tradeoff between capacity degradation of macro users and interference mitigation in small cells. This is aimed at providing efficient utilization of the available spectrum resources. Simulation results presented higher capacity gains without subjecting the victim users to severe interference. Limitation of the work was that interference experienced by small cell users that were not in the Cell Range Expansion (CRE) region was not mitigated.

Kurda *et al.*, (2015) studied a scheme that mitigate the effect of interference on interfered macro users and at the same time preventing throughput degradation of the femtocell. The scheme used power control technique with the objective of adjusting the transmit power of the interfering femtocell. Selective Power Adjustment (SPA) and Global Power Adjustment (GPA) were the two adaptive power control schemes used, with the objective to mitigate the interference on interfered macro users and at the same time implementing two degrees of awareness of femtocell users' throughput degradation. Simulation results showed the average throughput of the femtocell and macrocell was improved at different data. The solutions obtained were sub-optimal because there were situations where the femtocell users were placed in outage and the main objective of densification was not achieved.

Saha and Aswakul, (2017) addressed the major problem of reusing spectrum resources in deploying femtocells using Almost Blank Subframe (ABS) based enhanced Inter-Cell Interference Coordination (eICIC) technique. The simulation environment considered dense deployment of femtocells in multi-floor buildings in an urban area. Using ABS-based eICIC, the optimum number of ABS (OPNA) and femtocell clustering are the two major challenges. The ABS-based time-domain technique mitigates the cross-tier interference between the femtocell tier and macrocell-plus-picocell-tier. Frequency-domain eICIC was used to mitigate the co-tier interference of user equipment in any tiers by allocating resource blocks orthogonally. System level simulation results showed that the capacity of the adaptive scheme outperformed the non-adaptive OPNA scheme. The limitation of this work was that the capacity of the macrocell was degraded due

to high inter-cell interference from various small cells.

Magaji *et al.*, (2017) developed an adaptive hybrid technique to mitigate cross-tier interference in a femto-macro HetNet. Depending on the position of the victim macro user, the technique uses power control or Zero-power ABS based time domain techniques to mitigate the effect of interference simultaneously. A target Signal-to-Interference-plus-Noise Ratio ($SINR_{tar}$) and a threshold distance D_{min} was set for all users. Macro users at the cell edge, meaning users that were at distances greater than D_{min} , the scheme implemented power control technique by adaptively changing the transmit power of the femto base station. The scheme implemented Zero-power ABS time domain technique for macro users at distances less than D_{min} . Simulation results showed that the hybrid scheme performed better in terms of SINR and throughput when compared to implementing only power control or time domain technique. The limitations of this work is that time domain technique using zero power ABS limits the capacity of the femtocell which in turn degrades the throughput of the femtocell users and also leads to spectrum underutilization. This left room for modification or enhancement in the ABS scheme in order to provide better SINR, higher throughput and enhanced spectral efficiency.

2 METHODOLOGY

2.1 SYSTEM MODEL

The femtocells deployed in a macrocell network introduce cross-tier Interference to the network. Severe interference scenario could be caused in both downlink and uplink of nearby macro UE due to the operation of femtocell in closed access mode (Lopez-Perez *et al.*, 2011). It is difficult for the operators to supervise, manage and optimize the network due to the ad hoc deployment of femtocells (Palanisamy & Nirmala, 2013). The femtocells proper operations strongly depend on their sensing, self-optimizing features, and continuous monitoring of the radio environment in order to mitigate interference adaptively (Claussen *et al.*, 2008).

For macro users at the edge of a femtocell operating in a CSG, the macro eNodeB tries to initiate a handover request which fails due to the fact that it is not in the CSG list (Zhenwei *et al.*, 2011). This makes the macro UE to experience a severe cross-tier interference in the downlink, which results to a decrease in the SINR of the user and this interference is a major technical challenge in HetNet. Figure 1 shows the cross-tier interference scenario in a femto-macro HetNet. This deployment scenario was adopted during the course of this research.

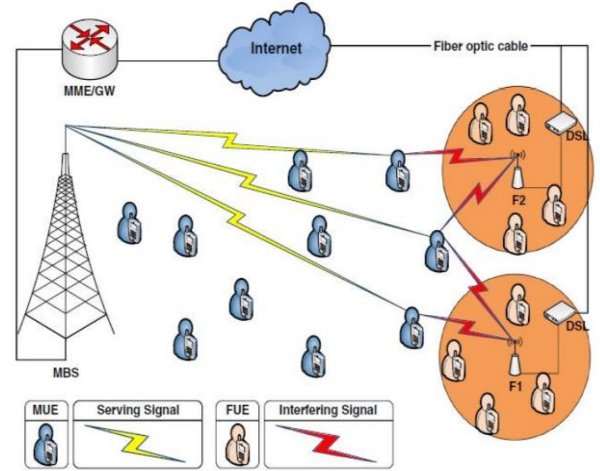


Figure 1: Cross-Tier Interference Scenario in a Femto-Macro HetNet (Kurda *et al.*, 2015)

2.1.1 Path Loss Model

The path loss heavily depends on the technology used and environment in which the network is deployed. The path loss between the UE and their corresponding macrocell or femtocell is determined in the following ways (Bouras *et al.*, 2012):

The path loss between a femto UE and a femtocell in the same apartment is given by (Bouras *et al.*, 2012):

$$PL(\text{dB}) = 38.46 + 20 \log_{10} R + 0.7d_{2D \text{ indoor}} + 18.3n \left(\frac{(n+2)}{(n+1)-0.46} \right) + q * L_{iw} \quad (1.1)$$

Considering the case of a femto user associated to a femtocell but not in the same apartment. When outdoor loss is also considered in this case, the path loss between the user and the femtocell is given as (R1-104414, 2010):

$$PL(\text{dB}) = \max(15.3 + 37.6 \log_{10} R, 38.46 + 20 \log_{10} R) + 0.7d_{2D \text{ indoor}} + 18.3n \left(\frac{(n+2)}{(n+1)-0.46} \right) + q * L_{iw} + L_{ow} \quad (1.2)$$

When the femto user equipment and femtocell is inside a different room but in the same building. The path loss can be obtain as follows (R1-104414, 2010):

$$PL(\text{dB}) = \max(15.3 + 37.6 \log_{10} R, 38.46 + 20 \log_{10} R) + 0.7d_{2D \text{ indoor}} + 18.3n \left(\frac{(n+2)}{(n+1)-0.46} \right) + q * L_{iw} + L_{ow1} + L_{ow2} \quad (1.3)$$

where:

R and $0.7d_{2D indoor}$ are respective transmit-receive distance and penetration loss due to walls inside the apartment respectively.

n is number of penetrated floors.

q is number of walls separating apartments between UE and femtocell.

L_{iw} is penetration loss of the wall separating apartments.

L_{ow1} and L_{ow2} are the penetration loss of outdoor walls 1 and 2, respectively.

Channel Gain (G) is a function of path loss and differs depending on the path loss model, whether it is indoor or outdoor. In order to determine G , the calculation of path loss is required according to the following expression (Bouras *et al.*, 2013):

$$G = 10^{\frac{-PL}{10}} \quad (1.4)$$

Where, PL is path loss between the UE and the eNodeB.

2.1.2 Signal-to-Interference-plus-Noise Ratio Model

The estimation of the received Signal-to-Interference-plus-Noise Ratio (SINR) for a femto user, f on sub-carrier, k associated with a femtocell, F when it is interfered by all neighboring femtocell, F' and macrocell, M , the SINR can be obtained as follows (Bouras *et al.*, 2012):

$$SINR_{f,k} = \frac{P_{F,k}G_{f,F,k}}{N_0\Delta f + \sum_M P_{M,k}G_{f,M,k} + \sum_{F'} P_{F',k}G_{f,F',k}} \quad (1.5)$$

where:

$P_{F,k}$ and $P_{F',k}$ are the respective transmit power of serving and neighboring femtocell on subcarrier respectively.

$G_{f,F,k}$ is the channel gain between femto user, and serving femtocell on subcarrier.

$G_{f,F',k}$ is the channel gain from neighboring femtocell.

$P_{M,k}$ is the transmit power of neighboring macrocell on subcarrier.

$G_{f,M,k}$ is the channel gain between femto user, and neighboring macrocell on subcarrier.

N_0 is the white noise power spectral density

Δf is subcarrier spacing.

2.1.3 Throughput Model

The throughput is determined after determining the path loss and the SINR of a user depending on its environment. The capacity of the macro user, m , and femto user, f , on a sub-carrier k , is given by Bouras *et al.*, (2012):

$$C_{m,k} = \Delta f \cdot \log_2(1 + \alpha SINR_{m,k}) \quad (1.6)$$

$$C_{f,k} = \Delta f \cdot \log_2(1 + \alpha SINR_{f,k}) \quad (1.7)$$

$$\alpha = \frac{-1.5}{\ln(5BER)} \quad (1.8)$$

where:

$C_{m,k}$ is macro user capacity on a sub-carrier k .

$C_{f,k}$ is femto user capacity on sub-carrier k .

Δf is bandwidth of operation.

$SINR_{m,k}$ is macro SINR on subcarrier k .

$SINR_{f,k}$ is femto SINR on subcarrier k .

α is a constant for target bit error rate
BER is bit error rate which is set to 10^{-6}

2.1.4 Spectral Efficiency

Increasing the profitability of the available radio spectrum is one of the major objectives of telecommunication operators. Let R_k be the mean throughput achieved by UE k . The spectral efficiency is therefore defined as follows (Yassin *et al.* 2017):

$$S.E = \frac{\sum_{k=1}^k R_k [\text{bit/s}]}{\text{Total spectrum [Hz]}} \quad (1.9)$$

Table 1.1: System Level Simulation Parameters

PARAMETERS	VALUE/DESCRIPTION
Cellular layout	Single macrocell
Number of Macrocell	1
Macrocell radius	250m
Macro eNodeB TX power	46dBm
Carrier frequency	2GHz
Femto eNodeB max TX power	20dBm
Femto eNodeB default TX power	11dBm
D_{min}	75% Femto range (0-50m)

Exterior wall loss	15dBm
Interior wall loss (low)	7dBm
Bandwidth	20MHz
Modulation Type	64QAM
Subcarrier spacing	15KHz
Number of Femtocell Users	5
Number of Femtocells	2
Number of macro users	5

The flowchart of the work is shown in figure 3. The procedures and conditions of implementing the two techniques simultaneously are shown on the flowchart.

2.2 IMPLEMENTATION

The implementation of the Zero-power ABS scheme makes the throughput of the macro users in the vicinity of the femtocell to significantly improve due to the reduction in interference seen by these users. Conversely, this leads to the decrease in throughput of the femtocells because femtocells are only allowed to transmit in the normal subframes.

With respect to this, a mechanism was developed for the efficient utilization of the spectrum resources. The developed mechanism allows data transmission of the femtocell users in the ABS subframes under special conditions, which also reduces interference generation to the macro users. The conditions are stated in terms of the maximum allowed transmit power and the allowed RBs in the frequency domain.

Equation for separating the resource blocks into reserved and non-reserved blocks in this strategy is given as follows:

$$\varepsilon = \min([\alpha \cdot \text{numMU}], \text{numRB}) \quad (1.10)$$

where:

ε is number of reserved resource blocks

numMU is number of macro users in the vicinity of the femtocell

α is the average number of reserved resource block per subframe

numRB is the number of resource blocks

Instead of devoting all the RBs to the macro users in the vicinity of the femtocell in the ABS subframes as in the Zero power ABS scheme, the data transmission was separated into two by splitting the frequency domain. This was achieved by allocating RBs to femtocell and macro users respectively as shown in figure 2.

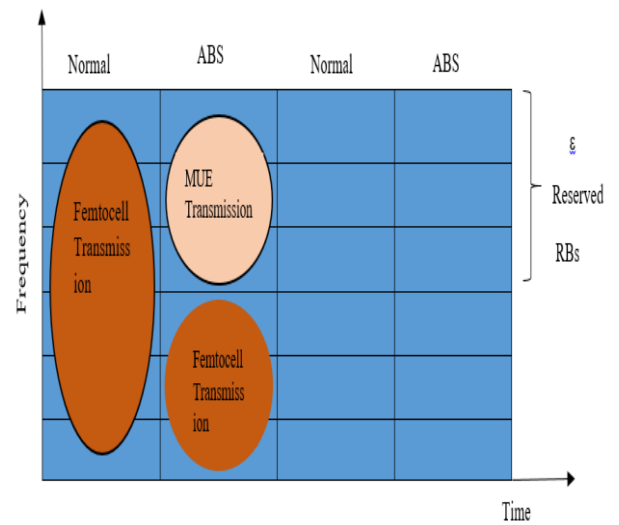


Figure 2: Developed User Allocation Principles.

The macro users, being the victim users in the vicinity of the femtocell are allocated the reserved RBs. Meaning only macro user data transmissions are permitted during these ε RBs. Femtocell data transmissions takes place in both the non-reserved RBs ($\text{numRB} - \varepsilon$) with the restriction of low transmit power and the normal subframes with high transmit power in the ABS subframes. By this, the interference experienced by macro users is reduced to low level. Also, the non-silencing of the ABS subframe results to an increase in the femto user capacity.

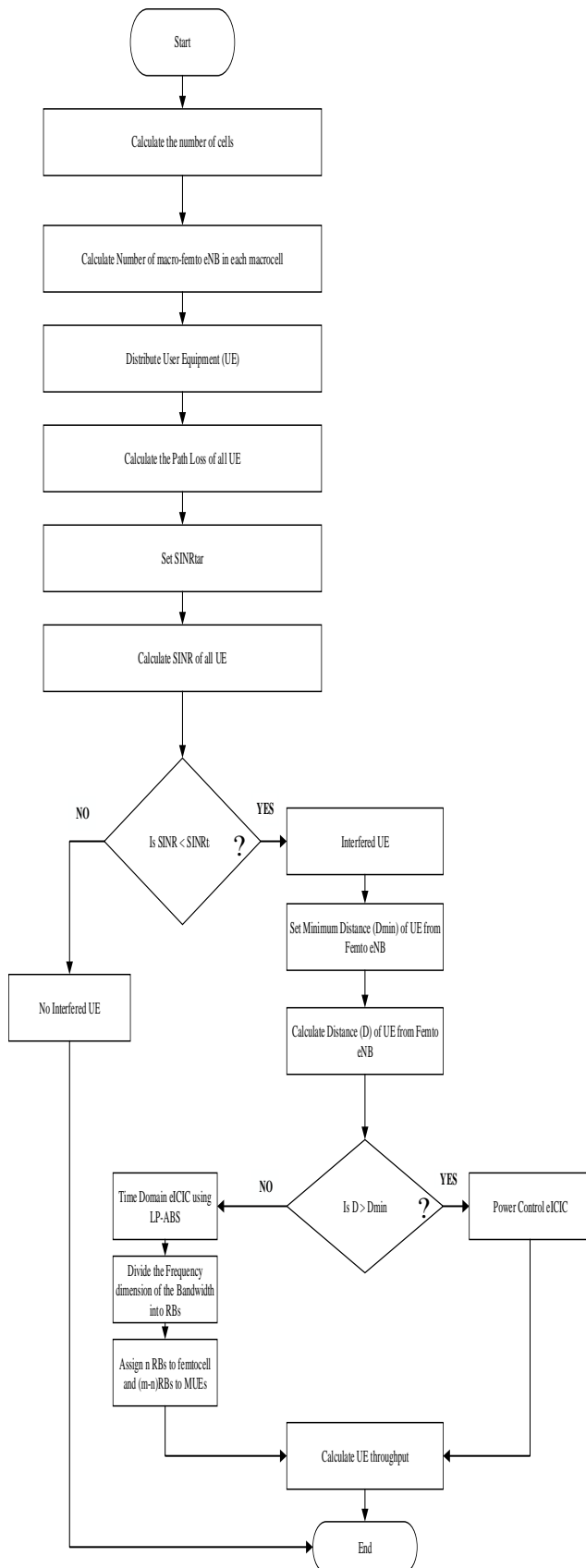


Figure 3: Flowchart of the Developed Improved Adaptive Hybrid Technique.

3 RESULTS AND DISCUSSION

The SINR of the femtocell users using 0.5 muting ratios is shown in Figures 4. The plots were obtained by first determining the path loss of the user from equation (1.1), the path loss depends on the distance of the user from the serving eNodeB. Gain between the femto user and femto eNodeB was obtained by inputting the path loss value into equation (1.4). SINR was obtained by inputting the gain in the equation (1.6). Figure 4 shows the graph of SINR against distance, It is observed that the maximum SINR achieved was 8.2dB for both the Zero power and Reduced power schemes at 0m distance up to about 30m away from femtocell. At 40m away from the femtocell, the improved scheme has a SINR of 2.9dB as against the adaptive scheme that has SINR of 2.6dB at 0.5 muting ratio which depicts a better quality of signal reception and thus a better quality of service for users of improved scheme.

The throughput of the femtocell users using 0.5 muting ratios is shown in Figures 5. The plots were obtained by first determining the path loss of the user from equation (1.1), the path loss depends on the distance of the user from the serving eNodeB. Gain between the femto user and femto eNodeB was obtained by inputting the path loss value into equation (1.4). SINR was obtained by inputting the gain in the equation (1.6) and finally the throughput was obtained from equation (1.8) and plotted against distance from femtocell. Figure 5 shows the graph of throughput against distance. It is observed that the maximum throughput achieved was 24Mbps for both the Zero power and Reduced power schemes at 0m distance up to about 35m away from femtocell. At 40m away from the femtocell, the improved adaptive scheme has a throughput of 19.2Mbps as against the adaptive scheme that has throughput of 13.5Mbps at 0 muting ratio which depicts a better quality of signal reception and thus a better quality of service for users of improved adaptive scheme.

The spectral efficiency of the femtocell is show on figure 6. Using 0.5 muting ratio, the developed improved scheme presented better spectral efficiency of 2.4 bit/s/Hz as against the zero power scheme that has 1.6 bit/s/Hz.

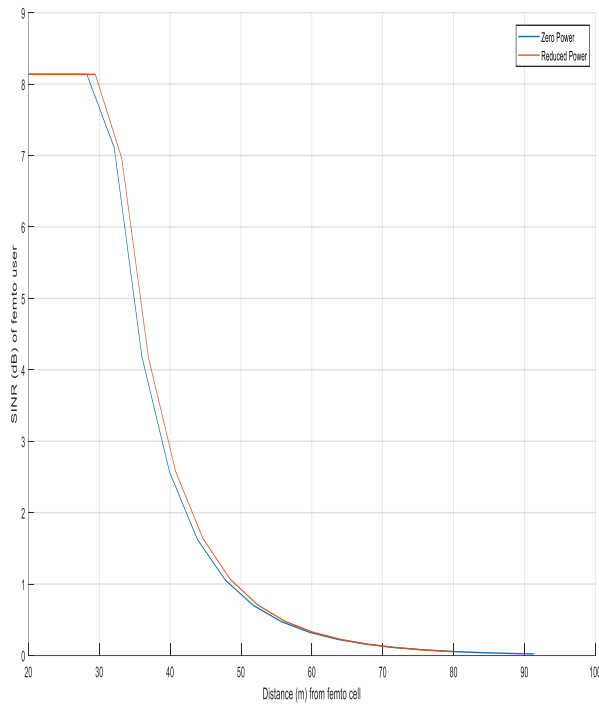


Figure 4: SINR of a Femto User using ABS with 0.5 Muting Ratio

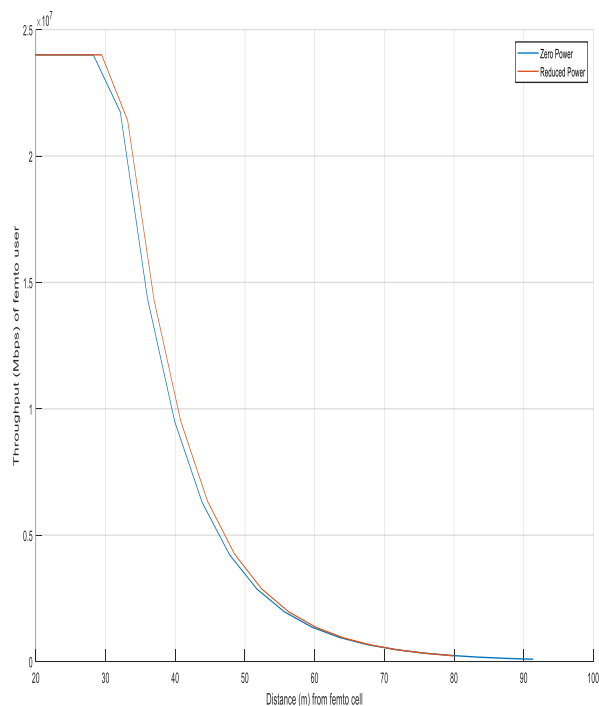


Figure 5: Throughput of a Femto User using ABS with 0.5 Muting Ratio.

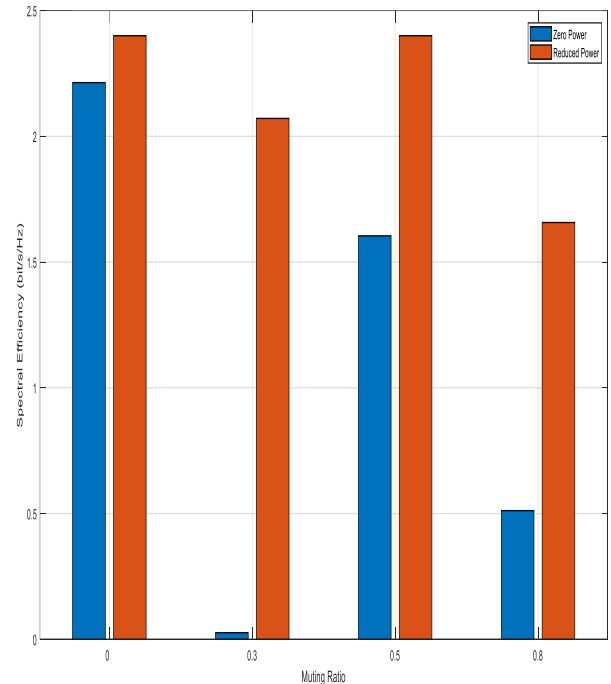


Figure 6: Spectral Efficiency of the Femtocell.

4 CONCLUSION

One of the major technical challenges of HetNet deployment is cross-tier interference which limits the potentials of HetNet in improving total network capacity. Most researches conducted focused on using the Zero-power ABS to mitigate interference in a femto-macro HetNet scenario which presents some drawbacks when it comes to the femtocell user capacity. This research work has developed an improved adaptive hybrid scheme that mitigated cross-tier interference in femto-macro HetNet. Using an ABS muting ratio of 0.5, the significant contributions of the developed improved adaptive hybrid technique when compared with the adaptive technique that used Zero power scheme are that the:

Throughput of the femtocell users was improved by 15.2%. SINR of the femtocell users was increased by 11.5%. Spectral efficiency of the femtocell was enhanced by 50%.

REFERENCE

- Afaz, U. A., Mohammad, T. I., & Mahamod, I. (2014). Dynamic resource allocation in hybrid access femtocell network. Paper presented at the *Scientific World Journal*, 539-720.
- Ali, M. S. (2015). An Overview on Interference Management in 3GPP LTE-Advanced Heterogeneous Networks. *International Journal of Future Generation Communication and Networking*, 8(1), 55-68.

- Afolalu O.F, Petinrin J.O and Ayoade M.A (2016). A Survey of Interference Challenges and Mitigation Techniques in 5G Heterogeneous Cellular Networks. *International Conference of Sciences, Engineering & Environmental Technology (ICONSEET)*, 1(2): 8-14.
- Bartoli, G., Fantacci, R., Marabissi, D., & Pucci, M. (2014). Adaptive muting ratio in enhanced Inter-Cell Interference Coordination for LTE-A systems. Paper presented at the *International Wireless Communications and Mobile Computing Conference (IWCMC)*, pp. 990-995.
- Bhosale, D. V. & Jadhav, V. D. (2015). A review of enhanced inter-cell interference coordination in long term evolution heterogeneous network. *International Journal of Innovative Science, Engineering & Technology*, Vol. 2 (2). pp. 6-10.
- Bouras, C., Kokkinos, V., Kontodimas, K., & Papazois, A. (2012). A simulation framework for LTE-A systems with femtocell overlays. *Proceedings of the 7th ACM workshop on Performance monitoring and measurement of heterogeneous wireless and wired Networks*.
- Bouras, C., Kokkinos, G, Diles, V., Kontodimas, K., & Papazois, A. (2013). *A simulation Framework for evaluating interference mitigation techniques in heterogeneous cellular Environment*. Springer, New York. DOI 10.1007/s11277-013-1562-5
- Cao, F., & Fan, Z. (2013). Downlink power control for femtocell networks. Paper presented at the *IEEE 77th Vehicular Technology Conference (VTC Spring)*, pp. 1-5.
- Claussen, H., Ho, L. T., & Samuel, L. G. (2008). An overview of the femtocell concept. *Bell Labs Technical Journal*, 13(1), 221-245.
- Deb, S., Monogioudis, P., Miernik, J., & Seymour, J. P. (2014). Algorithms for enhanced inter-cell interference coordination (eICIC) in LTE HetNets. *IEEE/ACM Transactions on Networking (TON)*, 22(1), 137-150.
- Ericsson mobility Report (2013)
- Ericsson mobility Report (2018)
- Hossain, E., Rasti, M., Tabassum, H., & Abdelnasser, A. (2014). Evolution toward 5G multi-tier cellular wireless networks: An interference management perspective. *IEEE Wireless communications*, 21(3), pp. 118–127.
- Kaddour, F. Z., Denis, B., & Ktenas, D. (2015). Downlink interference analytical predictions under shadowing within irregular multi-cell deployments. In *Communications (ICC), 2015 IEEE International Conference*. pp. 1649–1654.
- Koutlia, K., Perez-Romero, J., & Agustí, R. (2015). On Enhancing Almost Blank Subframes Management for Efficient eICIC in HetNets. Paper presented at the *IEEE 81st Vehicular Technology Conference (VTC Spring)*, pp. 1-5.
- Kshatriya, S. N. S., Kaimalettu, S., Yerrapareddy, S. R., Milleth, K., & Akhtar, N. (2013). On interference management based on sub frame blanking in heterogeneous LTE networks. Paper presented at the *Fifth International Conference on Communication Systems and Networks (COMSNETS)*, pp. 1-7.
- Kurda, R., Boukhatem, L., & Kaneko, M. (2015). Femto-cell power control methods based on Users' context information in two-tier heterogeneous networks. *EURASIP Journal on Wireless Communications and Networking*, pp. 1-17.
- Lee, S., Yoon, J., Lee, S., & Shin, J. (2010). Interference management in OFDMA femtocell Systems using fractional frequency reuse. Paper presented at the *International Conference on Communications, Circuits and Systems (ICCCAS)*, pp. 176-180.
- Lopez-Perez, D., Güvenç, S., De la Roche, G., Kountouris, M., Quek, T. Q., & Zhang, J. (2011). Enhanced intercell interference coordination challenges in heterogeneous networks. *IEEE Wireless Communications*, 18(3), pp. 22-30.
- Magaji S., Sani S. M. and Tekanyi A. M. S. (2017). Development of an Adaptive Hybrid Technique to Mitigate Cross-Tier Interference in a Femto-Macro Heterogeneous Network. *International Journal of Computer Applications*. 168(12), pp. 21-29.
- Yassin M., Mohamed Aboulhassan, Samer Lahoud, Marc Ibrahim, Dany Mezher, Bernard Cousin, Essam Sourour.(2017) Survey of ICIC Techniques in LTE Networks under Various Mobile Environment Parameters. *Wireless Networks*, Springer Verlag, 23 (2), pp.403-418.
- Palanisamy, P., & Nirmala, S. (2013). Downlink interference management in femtocell networks-a comprehensive study and survey. Paper presented at the *2013 International Conference on Information Communication and Embedded Systems (ICICES)*, pp. 747-754.
- R1-104414. (2010). Home enhanced NodeB Power Setting Specifications (TSG RAN WG1 R1-104414). *3rd Generation Partnership Project Spain*.
- Saad, S. A., Ismail, M., & Nordin, R. (2013). A Survey on Power Control Techniques in Femtocell Networks. *Journal of Communications*, 8(12), 845-854.
- Saha R. K. & Aswakul C. (2017). A Novel Frequency Reuse Technique for In-Building Small Cells in Dense Heterogeneous Networks. *IEEJ Transactions on Electrical and Electronic Engineering*. John Wiley & Sons, Inc.
- Wang, Y., & Pedersen, K. I. (2011). Time and power domain interference management for LTE networks with macro-cells and HeNBs. Paper presented at the *IEEE Vehicular Technology Conference (VTC Fall), 2011*, pp. 1-6.
- Zhenwei, W., Xiong, W., Dong, C., Wang, J., & Li, S. (2011). A novel downlink power control scheme in LTE heterogeneous network. Paper presented at the *2011 International Conference on Computational Problem-Solving (ICCP)*, pp. 241-245.
- Nasri, R., Affes, S., & Stephene, A. (2015). Combined Interference Cancellation and Avoidance over the Downlink of Spectrum-Sharing LTE HetNet. Paper



3rd International Engineering Conference (IEC 2019)
Federal University of Technology, Minna, Nigeria



presented at the *IEEE International Conference on Ubiquitous Wireless Broadband (ICUWB), 2015*, pp. 1-6.

THE LEVEL OF AWARENESS OF ELECTRICAL SAFETY AMONG ENERGY USERS IN SOKOTO STATE

Umar, A.,¹ Abubakar, I. N.,² Yusuf, H. M.³ & Okosun, O. E.⁴

¹Department of Electrical and Electronics Engineering Umar Ali Shinkafi Polytechnic.

^{2,3,4}Department of Electrical and Electronics Engineering Federal University of Technology, Minna.

Corresponding author's email: is.abubakar@futminna.edu.ng

ABSTRACT

Electricity hazards and safety measure awareness of energy user's is very important in the sense that it enhances the safety of people's lives and their properties. Consequently, the study assessed the level of electrical hazards and safety measures awareness among electricity users in Sokoto State. Two research questions and two hypotheses were formulated and tested at 0.30 level of significant. Questionnaire was the sole instrument used for the study, distributed to 200 industrial and 100 Domestic users in 5 places namely Sokoto North Local government area, Sokoto South Local Government Area, Wamakko Local Government Area, Cement Company of Northern Nigeria PLC, Sokoto and Kaduna Electricity Distribution Company of sokoto state metropolis using purposively sampling techniques. Mean, standard deviation and t-test was used to analyze research questions and hypotheses. One of the findings that emerged among other; energy users are aware of lack of proper electrical installation which in turn destroy electrical/electronic gadgets and equipment's.

Keywords: *Electrical Safety, Energy, Population, Domestic Energy, Industrial Energy, Questionnaire*

1 INTRODUCTION

Safety should be defined as the reduction of risk to a level that is as low as reasonable and as practicable. It is a state of mind and environment that must become an integral part of each working procedure. (Manik, *et al.*, 2015). Energy is an essential ingredient for socio-economic development and economic growth. The objective of energy system is to provide energy services. (Abalaka, 1998). Energy services are the desired and useful products process or indeed services that result from the use of energy such as lighting, provision of air conditions indoor climate, refrigerated storage, transportation, appropriate temperature and others. (Doherty, 2011). The energy chain to deliver these cited services begins with the collection or extraction of primary energy, which is then converted into energy carriers suitable for various end-uses. (Doughty *et al.*, 1991). It is clear that energy is an essential input to all aspects of modern life. It is indeed the life wire of industrial production, the fuel for transportation and as well for the generation of electricity, in conventional thermal plant. (Croft *et al.*, 1953) Currently, a high proportion of the world's total energy output is generated from fossils such as oil and coal. The unit of energy is Joules or ergs; energy can take a wide variety of forms, such as potential, chemical, electrical, kinetic, heat, magnetic, light and sound energy. (Becker, 2010). This paper focuses on Electrical Energy. Electrical Energy is the energy made by the flow of electric charge through a conductor. It is used to describe energy absorbed or delivered by an electrical circuit (for example, one produced by an electric power), once electrical energy has been converted from potential

energy, it can always be described as another type of energy heat, light, motion and others.

Electricity is virtually important in our daily lives, as long as the electricity is available; no one think much about it. The importance is realized when the power goes out. If for any reason there was no electricity in the world chaos and disorder will immediately take hold. Despite the fact, that electricity plays an important role to national development, and aid us to be comfortable. It is also regarded as a bad servant when it is used wrongly or when the users have shallow knowledge of it; thereby there is need for electrical safety awareness among energy users. It is also important for us to know that risk in electrical work is more than any other job. (Roberts, 2014).

Safety is a practical certainty that injury will not result from the use of electrical substance or agents, equipment's, (Williams, 2008). machines, under specified condition or quality and manner of use. (Kumbhar *et al.*, 2012).

The need for the general public to be aware of the revised electrical regulations to ensure that electrical installations and wiring are done in compliance with the IEE regulations. It has been discovered that 98% of electrical fatalities occurred from all causes and are due to lack of awareness of electrical safety rules and regulation. Electricity exists as a hazardous condition and has long been recognized as a serious hazard. It is present in the form of overhead and underground power lines, temporary and permanent power supplies. No matter what

the source or form of electricity, it exists as a hazard to those who use/work around it. Every year lives are lost or injured due to electrical related accidents that could have been prevented with proper training and awareness of electrical hazards. Electrical safety hazards are the cause of about a quarter of all deaths within the domestic and industrial energy users. As we all know electricity is a good slave but a bad master (Usifo, 2010). It is also important to know that the result of electric shocks ranges from stopping of the heartbeat, bleeding, neurological imbalance and ventricular fibrillation. Electrical Energy always follows the shortest path of a circuit of lower resistance. Electricity can pass through the human body to the ground if there is any provision for it to. (Cadick and Neitzel, 2006) the effects of electric shocks are severe and the table below presents the amount of current and its effect on the body.

Table 1: The amount of current and its effect on the body.

Current in milliamperes	Effects
1 or less	No sensation, probably no effect
1 to 3	noticed
3 to 10	Mild sensation not painful
10 to 30	Painful shock
30 to 75	Muscular control could be lost or
75mA to 4	muscle clamping
amps	Respiratory paralysis
Over 4 amps	Ventricular fibrillation
	Tissue begins to burns. Heart muscles clamp and heart stops beating.

(Cadick and Neitzel, 2006)

1.1 PURPOSE OF THE STUDY

The main purpose of this study is to assess the level of electrical hazards and safety measures awareness among electricity users in Sokoto State of Nigeria; specifically, the study will determine:

1. The level of electrical hazards awareness among electricity users in Sokoto State of Nigeria.
2. The level of safety measures awareness among electricity users in Sokoto State of Nigeria.

1.2 RESEARCH QUESTIONS

In order to achieve the objective of the study, the following research questions were formulated to guide the study:

1. What is the level of electrical hazards awareness among electricity users in Sokoto State of Nigeria?
2. What is the level of safety measures awareness among electricity users in Sokoto State of Nigeria?

1.3 HYPOTHESES

The following null hypotheses was stated and tested at $P < 0.03$ level of significance in order to guide the study:

H₀₁: There is no statistical significant difference between the mean responses of industrial electricity users and Domestic electricity users with respect to their perceptions on level of electrical hazards awareness among electricity users in Sokoto State of Nigeria.

H₀₂: There is no statistical significant difference between the mean responses of industrial electricity users and Domestic electricity users with respect to their perceptions on level of safety measures awareness among electricity users in Sokoto State of Nigeria.

2 METHODOLOGY

The research design used in carrying out this study was the survey method. Survey research is defined as a procedure in which a group of people or items is studied by collecting and analyzing data from only a few people or items considered to be representative of the entire group to determine the level of electrical hazards and safety measures awareness among electricity user's in Sokoto State. The study utilized electricity user's as the population. Purposive sampling was adopted as the populations of the electricity users were not known. 200 industrial electricity users and 100 Domestic electricity users were used in five (5) local Government Area of Sokoto.

The questionnaire was the sole instrument developed by the researcher for the collection of data and was validated by Lecturers in Electrical and Electronics Engineering and Industrial and Technology Education Department, Federal University of Technology Minna. The analysis of data for the research questions and hypotheses were accomplished using frequency counts, mean, standard deviation and t-test at 0.03 level of significant. The mean value of 2.50 was used as a decision point at four (4) point rating scale and any item that has it mean rating of 2.50 and above was considered aware or knowledgeable and any item that has the mean item below 2.50 was considered not aware and not knowledgeable.

Table 2 shows the target population of domestic and industrial energy users in Sokoto State.

TABLE 2: SHOWS THE TARGET POPULATION OF DOMESTIC AND INDUSTRIAL ENERGY USERS IN SOKOTO STATE

S/N	Name of Places	Industrial energy user	Domestic energy user
1	Sokoto North Local government area	70	-
2	Sokoto South Local Government Area	70	-
3	Wamakko Local Government Area	60	-
4	Kaduna Electricity Distribution Company	-	55
5	Cement Company of Northern Nigeria, Sokoto	-	45
	Total	200	100

2.1 Research Question 1.

What is the level of electrical hazards awareness among electricity users in Sokoto State?

Table 1. Show the level of electrical hazards awareness among electricity users in Sokoto State. This indicated that people are aware of certain electrical hazards and also they are still ignorant of some hazards despite long time of electricity usage. The results indicated that industrial

2.2 Research Question 2.

What is the level of safety measures among electricity users in Sokoto State?

Table 3: Mean Responses of Industrial energy users and Domestic energy users on the level of electrical hazards awareness among electricity users in Sokoto State. $N_1 = 200, N_2 = 100$

S/N	ITEM	X_1	X_2	X_t	Remarks
1	Defective parts	2.00	2.00	2.00	Not Aware
2	Inadequate electrical protection of installation	3.00	3.00	3.00	Aware
3	Ground faults in equipment	2.60	2.40	2.50	Aware
4	Use of tools or equipment too close to energized parts	2.40	2.40	2.40	Not Aware
5	Improper insulation	2.30	2.30	2.30	Not Aware
6	High voltage bulb on lower lighting fitting	3.70	3.30	3.50	Aware
7	Loose connections	2.95	2.55	2.75	Aware
8	Covered ventilation holes in electrical equipment	2.31	2.31	2.31	Not Aware
9	Placing socket outlet in wet ground	1.79	1.79	1.79	Not Aware

$N_1 =$ Industrial energy users $N_2 =$ Domestic energy users
 $\bar{X}_1 =$ Mean responses of Industrial energy user's $\bar{X}_2 =$ Mean responses of Domestic energy user's $\bar{X}_t =$ Average Mean responses of Industrial energy user's and Domestic energy user's. Table 3 shows that Industrial energy users were more aware of hazards while using electricity compare to Domestic Energy users.

Table 4: Mean Responses of Industrial energy users and Domestic energy users on the level of safety among electricity users in Sokoto State. $N_1=200, N_2=100$

S/N	ITEM	X_1	X_2	X_t	Remarks
1	Labeling of defective equipment	3.70	3.30	3.50	Aware 2.2
2	Pull out the plug from socket by the plug	3.00	3.00	3.00	Aware
3	Placing of socket outlet on dry ground	2.10	1.90	2.00	Not Aware
4	Proper electrical insulation	2.30	2.30	2.30	Not Aware
5	Uncovered slots of electrical machine and equipment	3.60	3.00	3.30	Aware

Table 4 revealed the level of safety measures knowledge among electricity users in Sokoto State, shows that many people have no Knowledge of safety measures when using electricity. The results indicated that industrial users were more knowledgeable in safety measures compare to Domestic users

2.1 HYPOTHESIS ONE

There is no statistical significant difference between the mean responses of Industrial electricity users and Domestic electricity users with respect to their perceptions on level of electrical hazards awareness among electricity users in Sokoto State

Table 5: t-test Analysis of industrial electricity users and Domestic electricity users with respect to their perceptions on level of safety measures awareness among electricity users in Sokoto State

Respondent	N	Me	SD	df	P	tCal	tcri
Industrial	250	2.8	0.23	234	.03	3.33	1.96
Domestic	210	2.6	0.16				

N =Number of Respondents, $S.D$ =Standard Deviation, $d.f$ =Degree of Freedom, P = Probability of Testing, Me = Mean

The result of t-test presented in Table 5 shows that t-cal was 3.33. This implies that there is significant difference

($P > .03$) in the mean responses of industrial electricity users and Domestic electricity users with respect to their perceptions on level of electrical hazards awareness among electricity users in Sokoto State.

2.2 HYPOTHESIS TWO

There is no statistical significant difference between the mean responses of industrial electricity users and Domestic electricity users with respect to their perceptions on level of safety measures among electricity users in Sokoto State

Table 6: t-test Analysis of industrial electricity users and Domestic electricity users with respect to their perceptions on level of safety measures awareness among electricity users in Sokoto State

Respondent	N	Me	SD	df	P	tCal	tcri
Industrial	250	2.8	0.23	234	.03	3.33	1.96
Domestic	210	2.6	0.16				

N =Number of Respondents, $S.D$ =Standard Deviation, $d.f$ =Degree of Freedom, P = Probability of Testing, Me = Mean

The result of t-test presented in Table 6 shows that t-cal was 3.33. This implies that there is significant difference ($P > .03$) in the mean responses of industrial electricity users and Domestic electricity users with respect to their perceptions on level of on level of safety measures among electricity users in Sokoto State

3 FINDINGS

The electricity users are aware of the followings as electrical Hazards.

1. Defective parts
2. Ground faults in equipment
3. High voltage bulb on lower lighting fitting
4. Loose connections

The electricity users are not aware of the followings as electrical Hazards

1. Inadequate electrical protection of installation.
2. Use of tools or equipment too close to energized parts
3. Improper insulation
4. Placing socket outlet in wet ground

The safety measures awareness among electricity users.

1. Labeling of defective equipment
2. Pull out the plug from socket by the plug
3. Uncovered slots of electrical machine and equipment

The safety measures not awareness among electricity users.

1. Placing of socket outlet on dry ground
2. Proper electrical insulation.

4 DISCUSSION OF FINDINGS

Ensuring safety and raising awareness among individual is very important as knowledge is wealth/health. Electrical hazard posed a significant risk of death and injuries to individual therefore, attention to safety is the necessary as first step in any environmental set up. The findings from Table 3 agreed with the work of (Kolok., 2007, Saba, *et al.*, 2014) which said electric shock occurs if the body contacts with electric circuit. This may cause serious burns, muscle damage and may kill victim by stopping the heart or breathing. In support of this (Smith., 2006) opined that when the body is in contact with live wire or any live components of an energized electrical device and also in contact with grounded object will receive a shock. The risk of receiving electrical shock is greater if one stands in a wet floor or touch live wire with wet body. If someone comes in contact with live electrical source, do not touch the victim with your bare hand. The person must be free either by switching off supply or with the use of insulating materials such as dry wood, clothing, rubber and when people are ignorant of hazards of using electricity they often become a victim of electrical shock or electrocution and related hazards (MacKinnon, 2010)

5 CONCLUSION AND RECOMMENDATION

Base on the findings of the study, it was analyzed that there is need for Domestic and Industrial consumers to be well equipped with Electrical Safety knowledge through various methods of electrical safety awareness for effective safety. The use of standard products, wiring accessories should also be done. Houses should be adequately equipped with electrical control devices such as electrical circuit breaker, switches, fuses and earth leakage circuit breaker. Correct fuse rating should be used and never overload electrical circuit. Do not touch electricity with metal, in wet hand condition and all the industries should be well installed with firefighting devices e.g. fire extinguisher etc.

1. The federal and state government should partake in the effort to improve status of electrical safety awareness through television (jingles, news, and advertisement), and also electricity distribution companies can do the work by sensitizing energy users as they move and distribute bills.

2. The state Government, Electricity Distribution companies and other cooperate bodies should give more information on safety practices to Domestic and Industrial Energy users.
3. The Sokoto state government should involve companies in the state that would supervise new building electrical installation so as to reduce the hazards of fire outbreak, electrocution, loss of lives and valuable properties in the state.

The effectiveness of the result will provide answer to the need of Domestic and Industrial Energy Users of the accident prevention (one who work safely, live to work another day).

REFERENCES

- Abalaka, A. F. (1998). Health and Safety Management Efforts correlates of performance in Nigeria. *Journal of Electrical Engineering and Management*. 14(4), 277-285.
- Becker, T. (2010). Measuring performance of your electrical safety program. *Proceedings of the Industry Conference on audit and petroleum (pic 2010)*, 1-10.
- Cardick, J., & Neitzel, D. K., (2006). Electrical safety handbook. New York MC Graw-Hill Companies, Inc
- Croft, E., Summers, W. & Hartwell F. P. (1953). Electrical Safety in the workshop 4th Ed, McGraw-Hill, New York, pp. 51 – 70
- Doherty, M. (2011). Workplace Electrical Safety Standard, CSA Z462-08, Electrical Safety workplace (ESW 2011), 1-4.
- Doughty, R. L., Epperly, R. A. & Jones, R. A. (1991). Maintaining Electrical Work Practices in a Competitive Environment. *Proceedings of the Annual Conference on safety (pacs 1991)*, 3-7.
- Kolak, J. (2007). Electrical Safety: Elements of an effective program. *Professional Safety*. 52(2):18-24.
- Kumbhar, N. R. & Dobhi, R. R. (2012). An industrial Energy Auditing. *International Journal of Modern Engineering Research* 2(1), 313-315.
- MacKinnon, J.T (2010). Important electrical and fire safety tips for families. Publication of Plymouth Utilities



- Manik, C. G., Raju, B., Avik, G. Writwik, B. & Ayan, B. (2015). An article on Electrical safety. *International Journal for Scientific Research and Development*. 3(10), 2321-2342.
- Roberts, D. T. (2014). Integrating OHMS, Risk Management & Safety. *Journal of Electrical Engineering and Management*. 1(4), 2177-2185.
- Saba, T. M., Tsado, J., Raymond, E., & Adamu, M. J. (2014). The Level of Awareness on Electrical Hazards and Safety Measures among Residential Electricity User's in Minna Metropolis of Niger State. *IOSR Journal of Electrical and Electronics Engineering (IOSR-JEEE)*. 9 (5), 1-6
- Smith, A.M., (2006). Assessment of the injured athlete. In J. Crossman (ed) *Coping with sports injuries: Psychological strategies for rehabilitation*. New York: Oxford University Press.
- Usifo, O. (2010). *A Text Book of Electrical Installation*.
- Williams, J. H. (2008). Employee engagement: Improving participation in safety. *Professional safety*, 53(12), 40-45



Phytoremediation of Soil Contaminated with Brewery and Beverage Effluents using *Cynodon dactylon*

*Mustapha, H. I¹, Ehichoya, C. S¹, & Musa, J. J¹

¹Agricultural and Bioresources Engineering Department, Federal University of Technology, PMB 65
Minna Niger State, Nigeria

*Corresponding author email: h.i.mustapha@futminna.edu.ng, +2348037011315

ABSTRACT

Phytoremediation is a natural treatment process that involves the use of green plants and microorganisms to degrade, accumulate, or eliminate various types of contaminants and pollutants in soil and water through physical, chemical and biological processes. Thus, this study evaluated the effects of green plant (*Cynodon dactylon* L.) in phytoremediation of soil contaminated with brewery and beverage wastewater (BBW). Four microcosm plots were used to conduct this experiment, the plots were irrigated with BBW and tap water (control). The results indicated that BBW is characterized with high organic contents [BOD₅ (270.25 mg/L), COD (591.50 mg/L)], suspended solids [total suspended solids (372.75mg/L), total solids (74.75 mg/L)], and nutrients [phosphate (20.83 mg/L)], no significant change in the soil texture was observed, however, there was increase in pH, electrical conductivity and chlorine content of the soil. The phytoremediation of the polluted soil decreased the concentrations of Cu by 25% after 49 days of the experimentation with about 75% of the heavy metal retained in the soil. However, future studies should focus on decrease of the build-up of salts (electrical conductivity) in the soil which could negatively affect crop yield as well as the determination of sodium adsorption ratio of the brewery and beverage wastewater to ascertain its suitability for irrigation purpose.

Keywords: *Beverage wastewater, Contaminated soils, Cynodon dactylon, Phytoremediation, Threshold limits.*

1 INTRODUCTION

Brewery and beverage industries are both water consuming and waste generation industries. According to Fillaudeau et al. (2006), beer is the fifth most consumed beverage in the world behind tea, carbonates, milk and coffee with an average consumption of 23 litres/person per year. For instance, an average of 2 - 8 hectolitres (hl) of water/hl of beer is consumed in the production of beer (Fillaudeau et al., 2006; Simate, 2015; Jaiyeola & Bwapwa, 2016; Srivastava et al., 2016) consequently, large volumes of effluent are produced (Fillaudeau et al., 2006; Simate, 2015; Jaiyeola & Bwapwa, 2016), approximately 10 - 20 times the beer produced according to Fillaudeau et al. (2006) and Jaiyeola & Bwapwa (2016). These effluents are discharged into drains or waterways (Simate, 2015) or soils which can lead to death of crops or reduction in crop yields, cause death or reproductive failure in fish, shellfish and wildlife, contamination of drinking water supplies, as well as accumulation and dissemination of toxic chemicals in sediments, that may further endanger the ecosystems and threaten public health (Simate, 2015; Srivastava et al., 2016). Though, the effluent vary in their composition (Simate, 2015), it is required to treat the effluent before discharge into the environment or for reuse purposes.

1.1 CHARACTERISTICS OF BREWERY WASTEWATER

The composition of brewery wastewater is highly variable, it has a characteristic that differ from time to time and from location to location due to the numerous different processes in the production of beer (Simate, 2015; Srivastava et al., 2016). The effluent is characterized by high levels of organic matter [biological oxygen demand (BOD) and chemical oxygen demand (COD)], nutrients (nitrogen, ammonia content, phosphates), solids [total suspended solids (TSS), total dissolved solids (TDS) and total solids (TS)], chloride salts and heavy metals (Simate 2015; Jaiyeola & Bwapwa, 2016; Srivastava et al., 2016). However, organic materials are the main concern of brewery wastewater, as well as suspended solids and pathogenic (Adelegan & Agbede, 2011). Accordingly, Simate (2015) reported 1200 – 3600 mg BOD/L and 2000 – 6000 mg COD/L and 2901 – 3000 mg TSS/L as well as 25 – 80 mg N/L and 10 – 50 mgPO₄-P/L in brewery wastewater. Jaiyeola & Bwapwa (2016) also reported the same quantity of BOD, COD, nitrogen and phosphorus though with lower range of TSS (200 – 1000 mg/L). Both Simate (2015) and Jaiyeola & Bwapwa (2016) reported low concentration of heavy metals in brewery wastewater.

1.2 PHYTOREMEDIATION OF POLLUTED SOILS AND WASTEWATER

Phytoremediation is a natural treatment process that involves the use of green plants and microorganisms to



degrade, accumulate, or eliminate various types of contaminants and pollutants in soil and water through physical, chemical and biological processes (Jing et al., 2007; Peng et al., 2009; Samer, 2015; Mustapha & Lens, 2018). Its processes include constructed wetlands, rhizofiltration, rhizodegradation, phytodegradation, phytoaccumulation, phytotransformation and hyperaccumulators (Jing et al., 2007; Singh et al., 2012; Oh et al., 2014; Samer, 2015).

Phytoremediation is used for the treatment of organic pollutants (Mustapha et al., 2015; Mustapha et al., 2018), heavy metals (Md. Nizam et al., 2016; Mustapha et al., 2018) and radionuclides (Shawai et al., 2017). This natural treatment system is a promising alternative in reducing sludge production, has low operation and maintenance cost as well as efficient and effective wastewater treatment system (Mudgal et al., 2010; Mustapha et al., 2015). Thus, this paper describes the phytoremediation of soil contaminated with brewery and beverage effluents using *Cynodon dactylon*.

2 METHODOLOGY

2.1 DESCRIPTION OF THE STUDY SITE

The study site is located at Gidan Kwano Campus, Federal University of Technology, Minna, between Lat. 09° 32' 27.01''N and Long. 06° 28' 31.59''E (Galadima, 2014), in the sub-humid tropics with two distinct climatic seasons; wet/rainy and dry/harmattan seasons. The mean annual air temperature is about 27.2°C with the highest and lowest occurring in the month of March and December respectively. The relative humidity falls between 50 to 70% annually with total annual mean value of about 65% (Mustapha et al., 2015).

2.2 EXPERIMENTAL PROCEDURE

Insert Four replicate plots of size of 30 cm x 25 cm x 20 cm (length x breadth x height) were used for the phytoremediation of brewery and beverage contaminated soils. Plot A (two duplicates) was irrigated with brewery and beverage wastewater and plot B (two duplicates) was irrigated with tap water, which served as the control plot to enable the assessment of the phytoremediation potential of *C. dactylon*. To maintain soil moisture, daily watering/irrigation of the plots were done twice daily morning and evening hours for four weeks with about 1L of water each to avoid leaching of the water from the bottom of the pots. The plots were then sown with ten seeds of *C. dactylon* each, raking it lightly to cover about 1/8 inch with soil material. To achieve even distribution of water and no disturbance of the sown seeds, fine spray was used and the soil was continuously kept moist. Weeding were also done as needed.

2.3 WASTEWATER ANALYSIS

The wastewater was collected from the effluent discharge point of the International Brewery and Beverage Industry (IBBI) Kaduna. The samples were analyzed onsite for pH and temperature (using a handheld instrument) and electrical conductivity (EC) using a portable HACH conductivity meter. The samples were conveyed to the laboratory for further analyses according to the procedures described in the Standard methods for the examination of Water and Wastewater (APHA, 2002); total dissolved solids (TDS) and total suspended solids (TSS) using gravimetric method, dissolved oxygen (DO) using Winkler's modification method, biological oxygen demand (BOD) determined by incubation method at 20 °C for 5 days, chemical oxygen demand (COD) using open reflux titration method, spectrophotometric analysis for phosphate and nitrate-N and for the metals using a Buck 210 Atomic Absorption Spectrophotometer.

2.4 SOIL ANALYSIS

The soils used were collected from the experimental site (Campus premises, Gidan Kwanu). There are two experimental plots replicated, A and B. Plot A was used for the contaminated soil and plot B for the reference (uncontaminated) soil. The soils were sieved through a 4.0 mm sieve and thoroughly mixed to ensure homogeneity. The sieved soils were analyzed for textural class and physical and chemical characteristics (pH, EC, alkalinity) according to standard analytical methods for soil analysis. Post-harvest soil samples were collected from each plot for analyses. The pH and EC values of the soil samples were measured electrometrically in a 1:2.5 and 1:5 suspension of soil and water, respectively as described by Md. Nizam et al. (2016). The soil samples taken at different interval of time from each experimental plot were air dried, crushed and passed through a 0.2 mm sieve were analyzed for heavy metal using a Buck 210 Atomic Absorption Spectrophotometer.

2.5 PLANT ANALYSIS

The choice of plants for phytoremediation is very crucial, thus the selection criteria should include geographical distribution, climate and habitat conditions, wastewater composition, availability of the plants, long term maintenance and agronomic management costs, project aims (Leto et al., 2013) and as well as biomass production (Ebrahimi et al., 2013), thus, *Cynodon dactylon* is a good candidate species for the phytoremediation of brewery and beverage wastewater. Additionally, *C. dactylon* is also known for its high adaptability to stress environment and heavy metal accumulation (Mustapha et al., 2018b).

To determine the phytoremediation ability of *C. dactylon*, the plants were harvested at the end of the experiment from each plot. The plant samples were thoroughly washed under running tap water and then rinsed with deionized water to remove any soil particles attached to it. The plant height was measured using a metre rule. Plant samples were oven-dried and finely ground and digested with HNO₃ and H₂O₂ following the procedure described by Md. Nizam et al. (2016). Zn, Mn, Fe, Mn, Cl and Cu concentrations were determined from the extract using a Buck 210 Atomic Absorption Spectrophotometer.

2.6 REMOVAL EFFICIENCY (%)

The ability of *C. dactylon* to reduce heavy metal concentrations in the experimental plots was estimated by calculating the removal efficiency of *C. dactylon* by subtracting the initial concentration of heavy metals in the polluted soil at the startup of the experiment from the concentration at the end of the experiment. This is expressed in Mustapha & Lens, 2017 as:

Removal efficiency (%) =

$$\frac{\text{Concentrations}_{\text{Initial}} - \text{Concentrations}_{\text{final}}}{\text{Concentrations}_{\text{Initial}}} \quad (2.1)$$

3 RESULTS AND DISCUSSION

All Figures and Tables inserted should be properly referenced in the discussion of the results. Results and discussion entails the use of words to describe the implication of the results expected/obtained. Often, Figures, Tables and Plates are powerful means for proper technical result reporting and discussion. Examples of Figures and Tables are given in Figure 1 and Table 1.

The results of the analysis of brewery and beverage wastewater revealed a high concentrations of BOD₅ and COD (270 and 592 mg/L), this high BOD₅ and COD concentrations is similar to concentrations reported by Adelegan & Agbede (2011); Simate (2015); Srivastava et al. (2016) for brewery and beverage wastewater. Consequently, the discharge of wastewater with high levels of organic compounds can deplete dissolved oxygen for aquatic species survival (Simate, 2015). Wastewater with high concentrations of organic matter is synonymous to high amount of suspended solids (Simate, 2015). Accordingly, this present study contained large amount of suspended solids that ranged from 331 to 435 mg/L of TDS and 72 to 78 mg/L of TSS above the permissible limits for wastewater discharge (Table 4.1). These results are similar to results obtained in Simate (2015) and Jaiyeola & Bwapwa (2016). High suspended solids in discharged wastewater can result into low light accessibility for

photosynthetic organisms (Simate, 2015). Simate (2015) and Jaiyeola & Bwapwa (2016) also reported low concentrations of heavy metals in discharged brewery and beverage wastewater as reported in this present study.

3.1 CHARACTERIZED BREWERY AND BEVERAGE WASTEWATER

The characteristics of brewery and beverage wastewater collected at the effluent discharged point of IBBI is presented in Table 4.1. The table is a descriptive statistics that includes values of mean, minimum, maximum, range, standard error, standard deviation and variance using the SPSS Statistics 16.0 for Windows (SPSS Inc., Chicago, IL, USA; version 16.0). The wastewater consists of concentrations higher than the Federal Ministry of Environment (FME), Nigeria threshold limit for the discharge into river bodies for food processing industry (Adelegan and Agbede, 2011). The wastewater had values ranging from 8.14 to 8.19 for pH, 28 to 34°C for temperature, this relative high temperature may be due to discharge of hot liquor and steam condensates from the brewery and beverage operation as reported by Belay and Sahile, (2013), 2.0 to 2.5 mg DO/L, 253 to 295 mg BOD₅/L, 570 to 619 mg COD/L, with lower concentrations of heavy metals below the threshold limits (Table 4.1). The BBW contained low levels of dissolved oxygen (DO), due to high concentrations of BOD₅ and COD in the BBW. This can make water unsuitable for drinking, irrigation or any other uses if this effluent is discharged into waterbodies or the environment (Olajumoke et al., 2010). However, the wastewater had mean suspended solids and organic contents concentration higher than the threshold limits according to standards given for food processing industry by FME (Nigeria).

3.2 SOIL QUALITY

The soils of the experimental plots was sandy clay loam soils (10% clay, 10 - 15% silt and 70 - 80% sand) classified according Md. Nizam et al. (2016). Soil pH was alkaline in nature. The soil chemistry were affected based on the sources of the water types used for irrigation, soils irrigated with BBW had a higher pH than soils irrigated with tap water (Table 4.2). Also, soils irrigated with BBW had higher conductivity (1581 $\mu\text{S}/\text{cm}^2$) than the tap water irrigated soils (Table 4.2). This is an indication of the accumulation of salts due to the irrigation with BBW wastewater.

Taylor et al. (2018) reported a similar observation in their study with higher pH and conductivity in the soils irrigated with brewery wastewater. Soil irrigated with BBW was characterized with high conductivity and pH, these qualities are known to negatively affect the growth and health of plants (Taylor et al., 2018).

TABLE 1: CHARACTERISTICS OF DISCHARGED BREWERY AND BEVERAGE WASTEWATER

Parameter	Mean	Minimum	Maximum	Range	Std. Error	Std. Deviation	Variance	*Threshold limit
pH	8.17	8.14	8.19	0.06	0.025	0.03536	0.001	6.5-7.5
Temp	30.50	28.00	34.00	6.00	1.3229	2.64575	7.000	30-36
Alkalinity	103.25	98.00	110.00	12.00	2.5617	5.12348	26.250	200 ^a
Hardness	144.25	124.00	160.00	36.00	8.2298	16.45955	270.917	500 ^a
EC	1097	990	1200	210	42.8836	85.76713	7356	1000
DO	2.20	2.00	2.50	0.50	0.1080	0.21602	0.047	<0.2
TDS	372.75	331.00	435.00	104.00	22.1524	44.30482	1963	2000
TSS	74.75	72.00	78.00	6.00	1.2500	2.50000	6.250	30
BOD	270.25	253.00	295.00	42.00	9.2320	18.46393	340.917	30
COD	591.50	570.00	619.00	49.00	10.3963	20.79263	432.333	80
Nitrate	2.65	2.26	3.00	0.74	0.1605	0.32104	0.103	20
Phosphate	20.83	18.80	22.50	3.70	0.7793	1.55858	2.429	5
Cl	19.83	17.80	22.30	4.50	1.0896	2.17926	4.749	600
Zn	0.55	0.47	0.63	0.16	0.0375	0.07500	0.006	<1
Mn	0.18	0.13	0.22	0.09	0.0193	0.03862	0.001	20
Cu	0.40	0.31	0.50	0.19	0.0417	0.08347	0.007	1
Fe	0.54	0.43	0.62	0.19	0.0413	0.08261	0.007	20

however, *C. dactylon* grew healthy. This may be related to *C. dactylon* being a salt tolerant plant.

TABLE 2. CHARACTERISTICS OF BREWERY AND BEVERAGE CONTAMINATED SOILS

Characteristics	Uncontaminated soil	Contaminated soil	Post Treated Soil
Sand	78.24	78.80	-
Silt	13.50	12.00	-
Clay	8.26	8.20	-
Textural Class	Sandy clay loam	Sandy clay loam	Sandy clay loam
pH	7.89	9.07	8.08
Electrical conductivity, $\mu\text{s}/\text{cm}^2$	890	1581	1022

3.3. PLANT: GROWTH AND DENSITY OF *C. DACTYLON*

In order to assess the phytoremediation potential of *C. dactylon* on soil contaminated with brewery and beverage wastewater, *C. dactylon* was planted in the contaminated soil, plant stem height (Fig. 1) and plant density (Fig. 2) were measured and recorded. Post hoc (Bonferroni) test was used to determine the effect of wastewater and tap water on the growth of *C. dactylon* (Table 4.3). The results indicate that from day 7 to day 14, there were no significant

difference on the type of water that was used. However, with increased exposure of wastewater and tap water over time, plant growth (Fig. 1) and density (Fig. 2) was higher in the plot irrigated with wastewater than the tap water. Also, there was a higher positive effect of the wastewater on the growth of *C. dactylon* each week than tap water (Fig. 1 and Fig. 2). Indicating that the constituents in the water types (BBW and tap water) and soils may have affected the growth and health of *C. dactylon*.

Sufficient concentrations of macro- and micro-nutrients are required for healthy plant growth (Taylor et al., 2018). Meanwhile, tap water contain low concentration of nutrients, this is observed in Fig. 1, accordingly, higher plant growth and health in the plants irrigated with brewery and beverage wastewater was recorded. Thus, *C. dactylon* utilized the nutrients in the brewery and beverage wastewater that was used to irrigate it. In addition, the water pH and air temperature were appropriate for the growth of *C. dactylon*.

The salinity of wastewater is of utmost importance when it comes to irrigation, this is because sodic soils are unsuitable for the cultivation of most vegetable crops, it can lead to low yield, cause extreme flocculation and decrease in infiltration rates (Taylor et al., 2018). The BBW wastewater used in this present study contained low salinity with a concentration that ranged from 990-1200 $\mu\text{s}/\text{cm}^2$. Figs. 2a, b and c shows the growth and density of *C. dactylon* from the time of sowing the seeds to

establishment. After 5 days of sowing, young *C. dactylon* began to sprout and by day 30, the seed bed was well established. *C. dactylon* grew and spread rapidly by rhizomes and stolons over the period of experimentation (Fig. 2). It indicate that *C. dactylon* has a good endurance to contaminants in brewery and beverage wastewater (Fig. 2).

The rapid growth of *C. dactylon* implies that it has high biomass productivity and uptake capacity which is an important feature for phytoremediation (Md. Nizam et al., 2016).

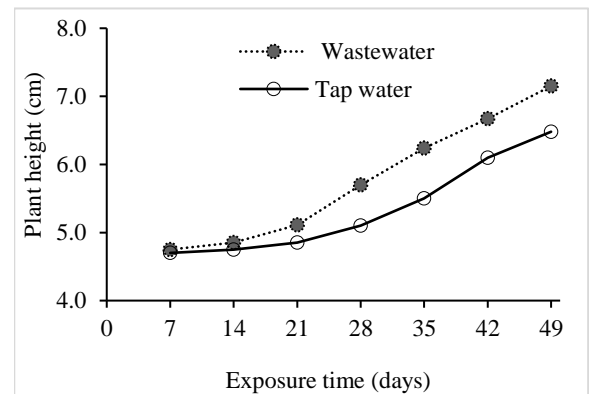


Figure 1: *C. dactylon* growth rate over time

TABLE 3: EFFECTS OF WASTEWATER AND TAP WATER ON PLANT GROWTH RATE (CM)

Exposure time	Wastewater			Tap water		
	Mean*	Min	Max	Mean	Min	Max
07	4.74 ^a ±0.01	4.73	4.75	4.71 ^a ±0.01	4.70	4.72
14	4.83 ^b ±0.04	4.80	4.85	4.78 ^b ±0.04	4.75	4.80
21	5.11 ^c ±0.01	5.10	5.11	4.84 ^c ±0.01	4.83	4.85
28	5.69 ^d ±0.02	5.67	5.70	5.09 ^d ±0.02	5.07	5.10
35	6.22 ^e ±0.03	6.20	6.24	5.54 ^e ±0.02	5.52	5.55
42	6.69 ^f ±0.02	6.67	6.70	6.09 ^f ±0.01	6.08	6.10
49	7.17 ^g ±0.02	7.15	7.18	6.27 ^g ±0.02	6.25	6.28

*Values are means of two duplicates (n = 2), mean±standard deviation. Values on the same column with different superscript are significantly different (P≤0.05) while those with the same superscript are not significantly different (P ≥ 0.05) as assessed by LSD, Tukey (HSD) and Duncan's Multiple Range Test.



Fig. 2. Plant density: (a). Emergence of *C. dactylon* 5 days after sowing; (b). 14 days after sowing and (c). 28 days after sowing

3.4. HEAVY METAL CONTENT OF SOIL AND *C. DACTYLON*

To determine the phytoremediation potential of *C. dactylon* for brewery and beverage contaminated soil, the pre-

planting and post-harvest soils were analyzed for heavy metal concentration (Table 4.4). The heavy metal concentrations in the pre-planting soil ranged from 0.61 to 10.22 mg/L while post-harvest concentrations ranged from 0.60 to 10.18 mg/L. The results showed a lower concentrations in the post-harvest soil. This is an indication of the phytoremediation potential of *C. dactylon* (Mustapha

et al., 2018b). The results revealed a low concentrations of heavy metals in the contaminated soils. This low metal concentrations is most likely due to the low concentrations of heavy metals in brewery and beverage wastewater. The observation is in agreement with reports of Simate (2015) and Jaiyeola & Bwapwa (2016). Although, metals are more soluble in acidic soil than alkaline soils, the heavy metal concentrations in the soil were found to be within acceptable levels.

TABLE 4. HEAVY METAL CONTENTS IN THE EXPERIMENTAL SOILS

Heavy metal (mg/g)	Initial soil content (before sowing the seeds)	Post-harvest content from wastewater plot	Post-harvest content from tap water plot
Zn	14.21	14.08	13.71
Mn	0.61	0.60	0.61
Fe	10.22	10.18	10.25
Cu	6.88	5.22	6.87
Pb	Bdl	Bdl	Bdl

Plants are known to take up heavy metals and other pollutants into their tissues as reported in literatures (Mudgal et al., 2010; Ali et al., 2012; Md. Nizam et al., 2016; Mustapha et al., 2018b). These values were within the threshold limits, nevertheless, the plants were able to take up the some heavy metals into their tissues.

C. dactylon is an ideal plant species for phyto extraction of heavy metals, from the results of this present study, the plant grew rapidly, produce high biomass and accumulated metals into its shoots. *C. dactylon* was observed to accumulate some quantity of heavy metals into it parts (Table 4.5) with Zn being the most accumulated and Mn as the least accumulated.

Zn is an essential element to plants that is easily taken up by roots (Mustapha et al., 2018b). In a study conducted by Mustapha et al. (2018b), demonstrating the bioaccumulation and translocation ability of *C. dactylon* of Zn from petroleum wastewater, *C. dactylon* accumulated 184 mg/kg and 407 mg/kg of Zn into its shoots and roots, respectively with a translocation factor of 0.5. This is an indication of the exclusion strategy of Zn in *C. dactylon* (Bragato et al., 2006).

TABLE 5. PLANT ANALYSIS BEFORE AND AFTER PLANTING FOR *C. DACTYLON* IRRIGATED WITH BREWERY AND BEVERAGE WASTEWATER

Parameter (ug/g)	Concentrations (initial) @ day 14 after sowing	Concentrations (final) wastewater @ day harvest (day 30)	Concentrations (final) tap water @ day harvest (day 30)
Zn	1.24	3.45	2.96
Mn	0.65	0.82	0.77
Fe	0.34	1.22	1.13
Cl	0.96	1.05	1.08
pb	bdl	bdl	bdl

3.5. PERFORMANCE EVALUATION: HEAVY METAL RETENTION

This study showed a low removal efficiency of the studied heavy metals. This may be attributed to many factors such as (1). The BBW was characterized with low levels of Zn, Mn, Fe and Cu; thus, the metals were non-available; (2). Substrate medium is the primary sink for heavy metals present in the aquatic environment (Mustapha & Lens, 2017). Fine textured substrate was used, they are known to accumulate metals if they contain high amount of organic matter, hence, a higher retention of the studied heavy metals were observed with a corresponding lower removal of the heavy metals (Fig. 3); and (3). The short experimental period (49 days), a longer experimentation may result into higher removal efficiencies as reported in literature (Mustapha et al., 2018b).

In addition, of the four (4) heavy metals studied, Cu had the highest removal and the least retained in the substrate medium while Fe was the most retained and lowest removal performance. Nutrient can enhance phytoremediation processes, however, the BBW contained low concentrations of nitrate and a higher concentrations of phosphate (Table 4.1), and nitrate are more easily assessable by plants and microorganisms. This may also have contributed to the low performance of this system.

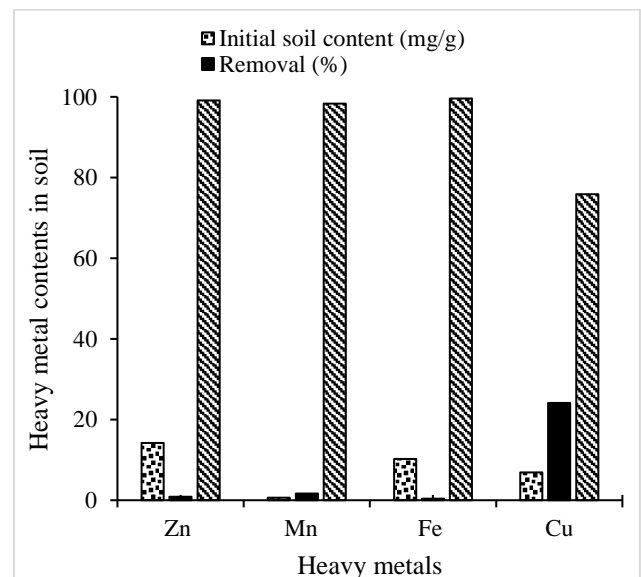


Fig. 3. Removal and retention of heavy metals

4 CONCLUSION

The characterized discharged brewery and beverage wastewater contained high levels of organic contents and suspended solids above the threshold limits for food processing industry. Thus, to prevent environmental pollution and protect public health, phytoremediation is



recommended as a tertiary/advance wastewater treatment system for brewery and beverage industry to thoroughly treat its effluent before its discharge into the environment. The brewery and beverage wastewater was characterized with low concentrations of heavy metals that were within the threshold limits for wastewater discharge.

C. dactylon was observed to accumulate some quantity of heavy metals into its parts with Zn being the most accumulated and Mn as the least accumulated.

Also, further studies will be required to analyze the soil structural porosity and bulk density in order to make proper conclusion on the effectiveness of phytoremediation of *C. dactylon* for treatment of brewery and beverage contaminated soil. Furthermore, sodium adsorption ratio of the brewery and beverage wastewater should be determined to ascertain its suitability for irrigation purposes. It is also recommended that the experiment should be ran for longer period of time.

5 REFERENCE

- Adelegan, J. A., & Agbede, O. A. (2011). Wetland system: a cheaper and efficient treatment option for food processing waste in Africa. *35th WEDC International Conference*, (pp. 1-8). Loughborough.
- Ali, H., Naseer, M., & Sajad, M. A. (2012). Phytoremediation of heavy metals by *Trifolium alexandrinum*. *International Journal of Environmental Sciences*, 2(3), 1459-1469.
- APHA. (2002). *Standard methods for the examination of water and wastewater* (20th ed.). Baltimore, Maryland, USA, Maryland, USA: American Public Health Association.
- Belay, A., & Sahile, S. (2013). The Effects of Dashen Brewery Wastewater Treatment Effluent on the Bacteriological and Physicochemical Quality of Shinta River in Gondar, North West Ethiopia. *World Environment*, 3(1), 29-36. doi:10.5923/j.env.20130301.04
- Bragato, C., Brix, H., & Malagoli, M. (2006). Accumulation of nutrients and heavy metals in *Phragmites australis* (Cav.) Trin. ex Steudel and *Bolboschoenus maritimus* (L.) Palla in a constructed wetland of the Venice lagoon watershed. *Environmental Pollution*, 144(3), 967-976. doi:10.1016/j.envpol.2006.01.046
- Ebrahimi, A., Taheri, E., Ehrampoush, M. H., Nasiri, S., Jalali, F., Soltani, R., & Fatehizadeh, A. (2013). Efficiency of Constructed Wetland Vegetated with *Cyperus alternifolius* Applied for Municipal Wastewater Treatment. *Journal of Environmental and Public Health*, 2013, 1-5. Retrieved from <http://dx.doi.org/10.1155/2013/815962>
- Fillaudeau, L., Blanpain-Avet, P., & Daufin, G. (2006). Water, wastewater and waste management in brewing industries. *Journal of Cleaner Production*, 14, 463-471. doi:10.1016/j.jclepro.2005.01.002
- Galadima, I. M. (2014). *An analysis of growth trends in Gidan Kwano and its impact on agriculture*. Federal University of Technology Minna, department of urban and regional planning. Minna: School of Environmental Technology.
- Jaiyeola, A. T., & Bwapwa, J. K. (2016). Treatment technology for brewery wastewater in a water-scarce country: A review. *South African Journal of Science*, 112(3/4), 1-8. Retrieved from <http://dx.doi.org/10.17159/sajs.2016/20150069>
- Jing, Y.-d., He, Z.-l., & Yang, X.-e. (2007). Role of soil rhizobacteria in phytoremediation of heavy metal contaminated soils. *Journal of Zhejiang University SCIENCE B*, 8(3), 192-207. Retrieved from www.zju.edu.cn/jzus; www.springerlink.com
- Leto, C., Tuttolomondo, T., LaBella, S., Leone, R., & Licata, M. (2013). Effects of plant species in a horizontal subsurface flow constructed wetland – phytoremediation of treated urban wastewater with *Cyperus alternifolius* L. and *Typha latifolia* L. in the West of Sicily (Italy). *Ecological Engineering*, 61, 282–291. doi:10.1016/j.ecoleng.2013.09.014
- Md. Nizam, U., Wahid-Uz-Zaman, M., Md. Mokhlesur, R., Md. Shariful, I., & Md. Shahidul, I. (2016). Phytoremediation Potentiality of Lead from Contaminated Soils by Fibrous Crop Varieties. *American Journal of Applied Scientific Research*, 2(5), 22-28. doi:10.11648/j.ajasr.20160205.11
- Mudgal, V., Madaan, N., & Mudgal, A. (2010). Heavy metals in plants: phytoremediation: Plants used to remediate heavy metal pollution. *agriculture and*



- Biology Journal of North America*, 1(1), 40-46. Retrieved from <http://www.scihub.org/abjna>
- Mustapha, H. I., & Lens, P. (2018). Constructed wetlands to treat petroleum wastewater. In R. Prasad, E. Aranda, & R. P. Aranda (Ed.), *Approaches in Bioremediation, the New Era of Environmental Microbiology and Nanobiotechnology* (1 ed., pp. 1-403). Switzerland AG: Springer Nature. Retrieved from https://doi.org/10.1007/978-3-030-02369-0_10
- Mustapha, H. I., & Lens, P. N. (2017). Treatment of Secondary Refinery Wastewater by *Cynodon dactylon* planted Horizontal Subsurface Flow Constructed Wetland Systems. *Journal of Engineering and Technology*, Vol. 3. No.1 (2017), 3 (1), 5-9.
- Mustapha, H. I., van Bruggen, H. J., & Lens, P. N. (2018a). Vertical subsurface flow constructed wetlands for the removal of petroleum contaminants from secondary refinery effluent at the Kaduna refining plant (Kaduna, Nigeria). *Environmental Science and Pollution Research*, 25(30), 30451-30462. doi:10.1007/s11356-018-2996-9
- Mustapha, H. I., van Bruggen, J. J., & Lens, P. N. (2015). Vertical subsurface flow constructed wetlands for polishing secondary Kaduna refinery wastewater in Nigeria. *Ecological Engineering*, 84, 588-595. doi:10.1016/j.ecoleng.2015.09.060
- Mustapha, H. I., van Bruggen, J. J., & Lens, P. N. (2018b). Fate of heavy metals in vertical subsurface flow constructed wetlands treating secondary treated petroleum refinery wastewater in Kaduna, Nigeria. *International Journal of Phytoremediation*, 20(1), 44-56. doi:10.1080/15226514.2017.1337062
- Oh, K., Cao, T., Li, T., & Cheng, H. (2014). Study on Application of Phytoremediation Technology in Management and Remediation of Contaminated Soils. *Journal of Clean Energy Technologies*, 2(3), 216-220. doi:10.7763/JOCT.2014.V2.126
- Olajumoke, A., Oluwatosin, A., Olumuyiwa, O., & Abimbola, F. (2010). Impact assessment of brewery effluent on water quality in Majawe, Ibadan, Southwestern Nigeria. *Researcher*, 2(5), 21-28. Retrieved from <http://www.sciencepub.net/researcher>
- Peng, S., Zhou, Q., Cai, Z., & Zhang, Z. (2009). Phytoremediation of petroleum contaminated soils by *Mirabilis Jalapa L.* in a greenhouse plot experiment. *Journal of Hazardous Materials*, 168, 1490-1496. doi:10.1016/j.jhazmat.2009.03.036
- Samer, M. (2015). Biological and Chemical Wastewater Treatment Processes. In *Wastewater Treatment Engineering* (pp. 1-51). Cairo, Egypt: INTECH open science. Retrieved from <http://dx.doi.org/10.5772/61250>
- Shawai, S. A., Muktar, H. I., Bataiya, A. G., Abdullahi, I. I., Shamsuddin, I. M., Yahaya, A. S., & Suleiman, M. (2017). A Review on Heavy Metals Contamination in Water and Soil: Effects, Sources and Phytoremediation Techniques. *International Journal of Mineral Processing and Extractive Metallurgy*, 2(2), 21-27. doi:10.11648/j.ijmpem.20170202.12
- Simate, G. (2015). Water treatment and reuse in breweries. In *Brewing Microbiology* (pp. 425-456). Retrieved from <http://dx.doi.org/10.1016/B978-1-78242-331-7.00020-4>
- Singh, D., Tiwari, A., & Gupta, R. (2012). Phytoremediation of lead from wastewater using aquatic plants. *Journal of Agricultural Technology*, 8(1), 1-11. Retrieved from <http://www.ijat-aatsea.com>
- Srivastava, A. K., Gupta, A. K., Mehrotra, T., Choudhury, R., & Singh, R. (2016). Physicochemical, Biochemical and Statistical Analysis of Beverages Industry Effluent. *Research J. Pharm. and Tech.*, 9(7), 887-892. doi:10.5958/0974-360X.2016.00169.4
- Taylor, R. P., Jones, C. L., Laing, M., & Dames, J. (2018). The potential use of treated brewery effluent as a water and nutrient source in irrigated crop production. *Water Resources and Industry*, 19, 47-60. doi:10.1016/j.wri.2018.02.001
- WHO. (2008). *Guidelines for drinking water quality* (3rd ed.). Geneva: Health Criteria and Supporting Information.



APPLICATION OF DREYFUS MODEL OF SKILLS ACQUISITION IN CURBING YOUTH UNEMPLOYMENT AMONG THE MOTOR VEHICLE MECHANIC STUDENTS' IN NIGERIA

*Aliyu Mustapha¹., Abdulkadir Mohammed¹., Abubakar Mohammed Idris¹., Benjamin Oke Ujevbe²., Uchechukwu Chikodili Oguguo² and Abdulrahman Musa Ewugi³

¹Industrial and Technology Education Department, Federal University of Technology, PMB 65 Minna Niger State, Nigeria

²Industrial and Technical Education Department, University of Nigeria, Nsukka, Enugu State, Nigeria

³Department of Automobile Technology, Niger State College of Education Minna, Nigeria

*Corresponding author email: al.mustapha@futminna.edu.ng, +2348038786082

ABSTRACT

Unemployment has become a leading problem that causes anxiety in the lives of youths resulting in increased antisocial behaviours such as kidnappings and restiveness. Youth unemployment is devastating to both the individual and the society as a whole, psychologically and economically. The paper examines the issue of youth unemployment and looks at potential interventions such as the application of the Dreyfus model of skills acquisition in curbing youth unemployment among motor vehicle mechanic students in Nigeria. This placed a substantial hope in the power and potential of the Dreyfus model of skill acquisition to transform the relationship between the educational system and the labour market. In view of this, the paper reviews the concepts and causes of youth unemployment; Technical, Vocational Educational Education and Training (TVET); Motor Vehicle Mechanic (MVM) programme in Technical Colleges; Dreyfus model of skills acquisition; approaches of learning a skill; training implications of Dreyfus model of Skill acquisition to MVM students and applying the Dreyfus model for skills acquisition in curbing youth unemployment and to changing demands. In view of the conclusion reached, there should be a regular and systematic evaluation of teaching curricula, taking into account the industrial and employers' requirements.

Keywords: *Dreyfus model, Motor Vehicle Mechanic Students', Skills acquisition and Youth unemployment.*

1 INTRODUCTION

Unemployment is a precarious situation has left the youths in a vicious cycle of poverty that daily crumble their self-confidence and bright future in Nigeria. It is the lack of job opportunities for people typically aged 15–24 years old. According to Gary (2009), this age range is determined by the period when mandatory schooling ends through the age of 24 years. In order to qualify as unemployed for official and statistical measurement, the individual must be without employment, willing and able to work, of the officially designated 'working age' and actively searching for a position (Andy 2012). However, from the extract of statistics obtained from the National Manpower Board and Federal Bureau of Statistics showed that Nigeria has a youth population of 80,000,000 which corresponds to 60% of the total population of the country. The extract revealed that 64,000,000 of them are unemployed while 1,600,000 are underemployed. In effects resulting in social vices, including armed robbery, destitution, prostitution, political thuggery, kidnapping and generally reduces national output and aggregate income and with resultant effects on the economic growth. Alas, about 4.5 million people go into the labour market annually without any hope of getting employment for life sustenance and workforce development (Musari, 2009). This burning issue of workforce development in Nigeria is to ascertain that human resources are developed to such an extent that the achievement of the desired rate of technological changes will not be impeded by lack of

personnel with sustainable skills in the automobile industry.

The automobile industry is a service industry that sustains the transport sector of a nation's economy. The people behind this industry are the Motor Vehicle Mechanic (MVM). The MVM are set of technicians who apply technical knowledge and skills to repair, service and maintain all types of automobiles. These technicians make use tools to adjust, test, diagnose service and completely repair any fault on the motor vehicle for safe and reliable operation according to the manufacturer's specification (Mustapha et al., 2017). In large shops, they specialize in repairing, rebuilding and servicing specific sections of the vehicles such as the braking system, steering and suspension system. In smaller shops, they work on a wider variety of repairs jobs. In order to carry out this operation, good analytical and troubleshooting skills are important to isolate problems with assemblies, components and parts. The skills of an MVM vary greatly; some develop the skills to work on all parts of a vehicle, while others choose to specialize in a particular aspect of the motor vehicle such as automobile electrical/electronics, motor vehicle body building and repair works.

In the automobile industry, there have been complex changes in the systems and components of automobiles that are imported or assembled in Nigeria. The new development has greatly brought about changes in the skills required of MVM for employment in the automobile and related industry. However, the consequences of MVM



has also inhibited the growth of rural-urban migration which escalates the rate of unemployment causing many unemployed people even reject job offers in rural areas and move to cities thereby worsening the situation. Notwithstanding, this study establishes the application of the Dreyfus model of skills acquisition towards curbing unemployment among the graduates of the MVM in Nigeria.

2 THE CONCEPT AND CAUSES OF YOUTH UNEMPLOYMENT

Youths occupy a prominent place in any society. The Federal Government of Nigeria (2014) asserts that the youth are the foundation of a society; their energies, inventiveness, character and orientation define the pattern of development and security of a nation. Mahmud, Mustapha and Saba (2014) defines youth as people aged between 18 and 35. Nigeria's unemployment rate is projected at over 11 per cent compared to the average rate of 9.5 per cent in sub-Saharan Africa. According to the National Bureau of Statistics, young people aged between 15 and 24 years, account for 52.9 per cent of unemployed people while those aged between 25 and 44 years accounted for 41.1 per cent. Therefore, those in the age bracket of 15 and 44 years, account for 94 per cent of the total unemployed persons in Nigeria (Osibanjo, 2006).

Youth's unemployment in Nigeria is a consequence of several factors. Nigeria has continued to experience a high rate of population growth. This increasing population growth has produced an overwhelming increase in the youth population thereby resulting in an increase in the size of the working age population. In Nigeria, youth migrate to the cities more than other migrants and in the cities, job opportunities are very limited. Thus, the rate of urbanization of the youth has continued to create unemployment (Oladele, Akeke & Oladunjoye, 2011). Lack of employable skills due to inappropriate school curricula is another factor contributing to rising youth unemployment. Analysts have argued that in Nigeria generally, many graduates in Nigeria are deficient in Technical Vocational Educational Education and Training (TVET) skills to facilitate self-employment.

3 MVM PROGRAMME IN TECHNICAL COLLEGES

Technical, Vocational Education and Training (TVET) is an umbrella term that covers two inseparable concepts, that is, the Vocational Education (VE) and the Technical Education (TE). According to Fitzgerald (2014), these concepts wrap up all "those aspects of the educational process involving, in addition to general education, the study of technologies and related sciences and the acquisition of practical skills, attitudes, understanding and knowledge relating to occupation in various sectors of economic life". As such, Okolie and Yasin, (2017)

defined the terms VE and TE respectively as 'any form of education whose primary purpose is to prepare persons for employment in recognized occupations' while the latter is "seen as the formal training of persons to become technicians in different occupations" such as the Motor Vehicle Mechanic (MVM) in the Technical Colleges (TC).

MVM deals with scientific concepts appertained in the construction and design of a motor vehicle. It is one of the mechanical trades offered as a motor vehicle mechanics' work trade in the Technical Colleges (TC) in Nigeria. According to Okoro (2006), the standpoint for the vocational institution in Nigeria is the TC and the training in MVM is carried out from TC I to TC III at the technical colleges and AT at the tertiary institutions. At the technical college level, the programme is schemed to give birth to the auto mechanic that is competent to carry out preventive maintenance, general repairs and overhauling of various automobile units and components (National Board for Technical Education (NBTE), 2009). At the completion of these programmes, the graduates according to the Federal Republic of Nigeria (FRN) (2013) are opened to be employers of labour, pursue further education in the colleges of education (technical) polytechnics and universities and secure employment either after completing one or more modules of employment skills or at the end of the whole course.

In the quest for the above points, the FRN (2014) further justified that the key components of the curricular activities for technical colleges are mapped out in foundation and trade modules consisting of general education with 30% theory and trade-related courses with 40% workshop practices with 25% and Students Industrial Work Experience Scheme (SIWES) 5% of the total requirement to complete the programme (FRN, 2013).

In line with the above policy, the revised National Technical Certificate (NTC) modular curriculum programme was published in 2001 for automobile mechanics' work and other vocational courses in technical colleges by the NBTE to guide the programmes. The publication was sponsored by the United Education, Scientific and Cultural Organization (UNESCO)-Nigeria project in support of the revitalization of Technical and Vocational Education (TVE) in Nigeria. It is a detailed curriculum in a modular form for trade and practice theory modules (Mustapha, 2018). Furthermore, Nwagbo (2010) stated that lack of interest, low achievement and retention rate in science and technical students to the teaching methods adopted by teachers to teach the students. The negative attributes associated with the conventional teaching methods pose a challenge in the teaching and learning process in MVM course. Udogu and Njeleta (2010) confirmed that innovative instruction approaches have proven effective for students to learn Science Technology Mathematics and Education (STEM).

Furthermore, Idris (2012) also stressed that this challenge necessitates a shift from the instructional approaches (from conventional teaching methods to acquiring a skill by means of instruction and experience).

4 DREYFUS MODEL OF SKILLS ACQUISITION

The model was propounded by Stuart Dreyfus and Hubert Dreyfus in 1980. The model was first published as a five-stage model of the mental activities involved in directed skill acquisition. Dreyfus and Dreyfus (1980) stated that in acquiring a skill by means of instruction and experience, the student normally progresses through five developmental stages designated as a novice, advanced beginner, competence, proficient and expertise. As a student becomes skilled, there is less dependency on abstract education and learns more about the factual experience. At each stage of training, the appropriate issues involved in facilitating skill acquisition are addressed.

4.1 APPROACHES TO LEARNING A SKILL BY THE DREYFUS MODEL IN THE AUTOMOBILE INDUSTRY

There are two divergent approaches to learning a skill; this includes learning through imitation or trial and error or through an instructor and instruction manual. The latter approach is adopted by the Dreyfus model because of its efficiency as demonstrated in aircraft skills of flying as a learning process by students. The approaches to learning a skill by the Dreyfus model in the automobile industry are categorized based on these stages:

STAGE 1: NOVICE (STARTING WITH CONTEXT FREE RULES)

At this stage, the work environment of the automobile student is divided into features and rules. The feature is the context-free environment which the student can autonomously recognize without the benefit of experience as non-situational. The students are then given rules for determining action on the basis of these features. Dreyfus' model helps us understand the role of such checklists plays for novices who need rules to guide their actions. Rules prevent novices from becoming overwhelmed by the complicated details of real-world information contexts. To improve on this stage, the automobile student needs monitoring either by self-observation or instructional feedback as to bring his behaviour closer to the rule (Dreyfus & Dreyfus, 1988).

4.1.2 STAGE 2: ADVANCE BEGINNER (DISCOVERING MAXIMS AND RULES OF THUMB IN CONTEXT)

As novices acquire more experience in the domain, they begin to be capable of moving from responding by rote to predefined, context-free features of the domain of practice to acting according to rules, either given to them or derived by themselves, grounded in situational aspects of the domain. Aspects, again, are those parts of a situation that come to light only through repeated experience of the domain of practice in which skills are performed (trial and error) or the presentation of "choice examples" by instructors (Dreyfus, 2002). They have perceived characteristics of situations that reveal themselves to be important in some way to the practice of the skill. The example Dreyfus gives of an aspect in driving is the situational engine sound that indicates that it's time to shift gears. While the beginner is limited to following rules such as shift when the speedometer hits 10, the advanced beginner is able to sense that there is a situational aspect connected with shifting as well. Rather than continue to follow an a priori rule, she develops or is given a different kind of rule, an "instructional maxim," to inform her behaviour during skill practice. In the case of driving, she "learns the maxim: Shift up when the motor sounds like it is racing and down when it sounds like it's straining" (Dreyfus, 2002). Clearly, rules covering this sort of situated practice cannot be given to the learner of skill outside the context of practice. But they can be made clear through independent practice and through examples given by a teacher along with the instructional maxims that correspond to them.

STAGE 3: COMPETENCE (ENCOURAGING ENGAGEMENT AND EMOTIONAL INVOLVEMENT)

This third stage in Dreyfus' developmental model therefore marks the point in the student's development when mechanical rule following should productively begin to reveal its limitations, for it is in this phase of development that students begin to choose their own perspectives on situations and act according to the rules and maxims they've acquired as best they can. In the sphere of driving, the driver must soon move beyond abstract rule-following, which in practice can lead to mechanical performance and, in this domain, potentially dangerous accidents. Following Dreyfus' example, the competent driver going dangerously fast down an off-ramp does not yet have the perceptual background to feel that he/she is in a dangerous situation, nor is there a general rule she can follow to tell her what to do once she determines the nature of her situation. As noted, the competent driver has to "spend ...time considering the speed, angle of bank, and felt gravitational forces" that is



to say determine the salient aspects of a situation and also “decide whether the car’s speed is excessive” (Dreyfus, 2002). In other words, the driver must make two decisions in this phase versus the single decision within the controlled learning environment proper to the advanced beginner phase. After deliberating about the circumstances in which the action is to be performed, and the action itself, the driver makes a choice about whether or how much to brake or let off of the gas and “is relieved if they get through the curve without being honked at, and shaken if they begin to go into a skid” (Dreyfus, 2004). In the process of experiencing joy and relief at successfully navigating the ramp, or fear and shakiness if things go awry, learners begin to associate the variety of perceived sensations of leaving an off-ramp with the joy or disconcertedness that results from the outcome of their chosen actions. Restated, they begin to acquire an emotionally charged perceptual repertoire in this stage, repertoire students need in order to move in later stages of development towards more intuitive forms of action characteristic of expertise.

STAGE 4: PROFICIENT (FACILITATING “WORLD IMMERSION”)

At this period of time, the automobile student needed some sort of analytical principles, in the form of rules, guidelines or maxims to connect his experience of general situation to a specific action. This is the trial stage in the step-wise improvement of mental processing as the experience situation is so vast that normally each specific situation immediately dictates an intuitively appropriate action. As the automobile students almost master the skills, he/she becomes capable of supervising others and developing his own rules. Drivers who reach proficiency begin to have a visceral sense of the road and their relationship to it. As Dreyfus notes, “The proficient driver, approaching a curve on a rainy day, may feel in the seat of his pants that he is going dangerously fast” (Dreyfus & Dreyfus, 2005). By the phrase “feel in the seat of his pants,” Dreyfus means that emotion or feeling is intuitively evoked in the driver by virtue of having felt similar emotions in like circumstances. But even though the driver perspective may be intuitive at this point, the driver still does not have the accumulated background experience to intuitively know what to do to adjust his driving.

STAGE 5: EXPERTISE

The mastery stage is achieved when the learner no longer needs principle, the automobile students can stop to pay conscious attention to his performance and can let all the mental energy previously used in monitoring his performance go into almost instantaneously, the appropriate perspective and associated actions (Dreyfus & Dreyfus, 2005). Dreyfus notes that “the expert driver,

generally without any awareness, not only feels when slowing down on an off-ramp is required, he or she knows how to perform the appropriate action without calculating and comparing alternatives.

5 TRAINING IMPLICATIONS OF THE DREYFUS MODEL OF SKILL ACQUISITION TO MVM STUDENTS

The training implications of the stages of the model include the fact that it facilitates advancement to the next stage, and help to avoid the temptation of introducing intricate and sophisticated aids. Besides, it does not impede advancement to a higher level and prevents regression to a lower level. These stages of Dreyfus model are related to this study in the sense that at Novice stage, the MVM as a newcomer learns the tools, equipment and machines used in automobiles while at Advance Beginner stage, the MVM becomes acquainted with the factors used in the automobiles skills acquisition centre. At the Competence stage, the MVM goes further to see that all actions or procedures are directed towards a goal when learning the procedures and techniques used in mechatronics. As the MVM advance to the Proficient stage, the MVM becomes familiar with practical processes and applications of the tools, equipment and machines used in mechatronics and can even train other MVM at the end. The individual can develop rules and regulations based on circumstance. Finally, at the Expertise stage, the MVM can make available a systematic approach to common engine faults and malfunctions in relation to the manufacturers’ specification (Dreyfus & Dreyfus, 2005).

6 APPLYING THE DREYFUS MODEL FOR SKILLS ACQUISITION IN CURBING YOUTH UNEMPLOYMENT

Dreyfus illustrates this model with a number of practical examples in various domains of skill acquisition. Driving, piloting an aircraft, chess playing, the complex skill sets that comprise decision-making in business management, and language acquisition are just some of the domains of practice that Dreyfus uses to illustrate the stages of skill acquisition he advances (Dreyfus & Dreyfus, 1980; Dreyfus & Dreyfus, 1988). The perspectives on learning posited by Dreyfus suggest that MVM is a profession that an individual enters through graduate automobile technology education. As a novice, an individual becomes a member of the community of practice and assumes personal responsibility for learning and mastering technical skills and competencies through experience, mentoring professional development, and continued actions (or tasks) comprising activities situated in automobile and related industry.



The actions that makeup works as an automobile technician are consciously undertaken and targeted at specific goals that may or may not be explicitly directed toward the object of the activity but are nonetheless directed and guided by it. These actions have operational aspects that are determined by the conditions under which they are carried out. Considering that part of the beginner and advanced-beginner stages of the Dreyfus Model of Skill Acquisition, routine tasks for MVM are the unconscious abilities that emerge as a result of practice and experience, and if conditions change to where the normal execution of an operation is impeded, conscious attention is necessary and the operation becomes an action. MVM can use observations and experiments to identify and describe qualitative differences between the processes of experienced workers and those of novices. Understanding how experienced MVM use knowledge to get around in the automobile and related industry and how and what knowledge was acquired in the course of getting around illustrates the ways in which an individual gains mastery over technical skills, increases proficiencies and competencies and progresses professionally.

7 APPLYING THE DREYFUS MODEL FOR SKILLS ACQUISITION TO CHANGING DEMANDS

Today, the automobiles are getting intricate and the need for professional care is becoming imperative as the development of new technologies and mechanisms that have been taking place in the automobile and related industry (Idris et al, 2018). The twenty-first-century automobile workshop is a vibrant place of change, discovery, learning and experimentation. Relying on the workshop as a place where a range of technology services, tutoring and learning services, advising and other services aimed at meeting the needs of students and scholars. These differentiated skills can be seen in the work of proficient MVM in the workshop and academic environment.

Training and learning throughout a professional career are not routine or repetitive. Professional development opportunities focus on specific forums for personal growth in support of the organizational change. Updating position descriptions enables managers to incorporate expectations that staff grow and develop professionally so that increasingly sophisticated user demands can be met. Position descriptions are generally prepared by workshop managers in consultation with human resources officers. While the goal is to craft a position description that meets an organizational need, they work within the constraints of previous descriptions and legally acceptable language. Writing job descriptions does not lend itself to the recognition of nuanced levels of skills development or the relationship between tacit understanding and ability. The

focus is on the cognitive abilities and explicit skills needed to do the work. Position descriptions use verbs reflecting levels of skill tied to educational preparation, years of experience and salary. Aligning skill levels with career ladders enables both the employee and the manager to identify the development of competencies that parallel advancements through positions from entry-level to mastery to expert.

8 CONCLUSION

It is pertinent at this point to note that the situation as it pertains to youth unemployment in Nigeria is a vivid menace to social, economic and political development. This paper has placed substantial hope in the power and potential of the Dreyfus model of skill acquisition to transform the relationship between the educational system and the labour market. It is strongly believed that the application of the Dreyfus model of skill acquisition can be therapeutic for curbing the escalating rate of youth unemployment with Technical, Vocational Education and Training (TVET) being on the front burner. This will in-turn, strengthen the possibility of tapping the rich proceeds of TVET, eradicating forms of poverty and promote lasting sustainable development.

9 RECOMMENDATIONS

In view of the conclusion reached, the following recommendations are hereby offered.

1. There should be a review of the MVM training programmes to ensure that the youths are competent and employable in the automobile and related industries.
2. Given the evolution of industrial and labour laws, there should be a regular and systematic evaluation of teaching curricula, taking into account the industrial and employers' requirements.
3. The roles, responsibilities, and ethical obligations of employees in the industry should be adequately communicated to the students during training by focusing on career guidance and counselling, support and introduction of entrepreneurship education into the school curriculum.
4. More attention should be placed on orientating the psyche of beginners at entry level into TVET programmes, to strengthen career adaptability and academic major satisfaction of the potential graduates. If this is done correctly, dropout rate will plummet, consequently, youth unemployment in the country.



REFERENCES

- Andy, F. (2012). *Youth Studies: An Introduction*. New York, N.Y.: Routledge.
- Dreyfus, H. L., & Dreyfus, S. E. (2005). Expertise in real-world contexts. *Organization Studies*, 26(5), 779-792.
- Dreyfus, H. L. (2002). Intelligence without representation—Merleau-Ponty's critique of mental representation the relevance of phenomenology to scientific explanation. *Phenomenology and the Cognitive Sciences*, 1(4), 367-383.
- Dreyfus, H. L., & Dreyfus, S. E. (1988). *Mind over machine: The power of human intuition and expertise in the era of the computer*. New York: Free Press.
- Dreyfus, S. E., & Dreyfus, H. L. (1980). *A five-stage model of the mental activities involved in directed skill acquisition*. Berkeley: Operations Research Center, University of California, Berkeley.
- Federal Government of Nigeria (FGN, 2013). Technical and vocational education development in Nigeria, The way forward, *Report of the adversary panel of Inquiry on TVE in Nigeria*. Abuja: Federal Government Press.
- Federal Republic of Nigeria (FRN, 2013). National Policy of Education. 6th Edition. *Nigerian Education Research and Development Council (NERDC) Press*, Yaba- Lagos Nigeria.
- Fitzgerald, T. (2014). *Advancing knowledge in higher education: Universities in Turbulent Times*. USA: IGI Global.
- Gary, M. (2009). "A portrait of the youth labour market in 13 countries, 1980-2007". *Monthly Labor Review*: 3–21.
- Idris, A. M., Mustapha, A., Abdulkadir, M & Ekhalia, B. J. (2018). Alternative sources of fuels used in automobiles towards zero carbon emission. *Proceedings of the Technology Education Practitioners Association of Nigeria (TEPAN) (Formally NATT) on 15th- 19th October 2018*
- Idris, A. M. (2012). Effect of cognitive apprenticeship instructional method on auto-mechanics students. *AU Journal of Technology*. 16(2), 89-98
- Musari, A. (2009). Youth and the National Youth Employment Action Plan, Abuja, *Guardian Newspapers*, March 19
- Mustapha, A. (2018). Effects of e-content on students' achievement, interest and retention in learning automobile lighting system in technical colleges in Niger State. Unpublished MTech thesis, Federal University of Technology Minna.
- Mustapha, A. Idris, A. M., Musa, A. E., Ajah, A. O., Gabriel, G. A. & Kolo, A. A. (2017). The Impact of Referral Marketing Strategy on Micro, Small and Medium Scale Motor Vehicle Mechanic. *Proceedings of the 2nd International Engineering Conference (IEC 2017) Federal University of Technology, Minna, Nigeria on 17th- 19th October 2017*. Pp. 383-388
- Mustapha, A., Umar, I. Y. & Igwe, C. O. (2018). *Effects of e-content in teaching and learning of automobile lighting system in technical colleges in Niger State. Proceedings of the 2nd Annual National Conference of the Centre for Technical Vocational Education, Training and Research (CETVETAR), University of Nigeria, Nsukka. 20th -23rd June 2018*
- National Board for Technical Education (NBTE) (2009). *National vocational certificate (NVC). Curriculum and module specification in motor vehicle mechanics work*. NBTE, Kaduna Government Press.
- Nwagbo, C. (2010). Effects of constructivist instructional model on student interest, achievement and retention in Basic Ecological Concepts in Biology in Anambra State, Nigeria. *Journal of Science Teacher Association of Nigeria*. 45(2), 26-35.
- Okolie, U. C. & Yasin, A. M. (2017). *Technical Education and Vocational Training in developing nations*. USA: IGI Global.
- Okoro, C. O. & Ekpo, E. E. (2016). Effects of Information and Communication Technology (ICT) Application on Academic Achievement of Students in Christian Religious Studies in Cross River State. *International Journal of Interdisciplinary Research Methods* 3 (2), 14-24.
- Oladele, P. O., Akeke, N. I. & Oladunjoye, O. (2011). Entrepreneurship Development: A Panacea for Unemployment Reduction in Nigeria. *Journal of Emerging Trends in Economics and Management Sciences* 2(4), 251 – 256.
- Osibanjo, O. (2006). The concept of Entrepreneurship: A paper presented at the workshop on entrepreneurship and innovation for 200 level student at the University of Ibadan, Ibadan.
- Udogu, M. E. & Njeleta, C. B (2010). Effect of constructivist-based instructional models on students conceptual change and retention in Chemistry. *African Research review. International Multi-Disciplinary Journal. Ethiopia* 4(2), 219-229.



A NUMERICAL ANALYSIS OF CONVECTIVE HEAT TRANSFER RATE FROM A WAVY FIN PROJECTING HORIZONTALLY FROM A RECTANGULAR BASE

Okon, J. O

Department of Mechanical Engineering, Federal University of Technology,
PMB 65 Minna Niger State, Nigeria

Corresponding Author email: joshuaoyosuhuokon@gmail.com. +2348067928206

ABSTRACT

In a bid to develop an effective rate of heat dissipation from any system with limited space and size, a study has been carried out on twelve configuration of wavy fin array protruding from a horizontal base with different space and height configuration. A free convection steady state heat analysis was carried out using solidworks flow simulation, version 2018, which is based on Computational fluid dynamics (CFD) finite volume analysis. The result found showed that the heat transfer rate in wavy fin array increases with increase in the fin height, Base-to-ambient temperature, as well as decrease in fin spacing.

Keywords: Heat transfer, wavy fin, Simulation, Temperature, fin height.

1 INTRODUCTION

A common occurrence in engineering system is the generation of heat due to its operations, and sometimes leads to overheating of the system (May & Almubarak, 2017). The end effects of this overheating if not effectively dissipated out of the system may give rise to malfunctioning of the system and sometimes total damage of the system. Therefore in order to transfer the generated heat from the surface of the system at a low cost, and fast rate, and reduced dimension an extended surface is most times incorporated into the system to increase the surface area of the system over which the convective heat transfer takes place. This is because according to Newton's law of cooling, the rate of heat transfer is a function of the convective heat transfer coefficient, the surface area of the system and the temperature gradient between the solid temperature and the environmental temperature. See equation below.

$$Q = hA (t_s - t_f) \quad (1)$$

several researchers have studied the problem of optimizing the shape of the finned surfaces in order to increase heat transfer effectiveness and decrease the dimensions as a function of limited space, and the weight of heat sinks and exchangers and as such several experimental and numerical investigations have been conducted for various kinds of shape of the fin; such as straight, plate, wavy fin and others.

When calculating the heat transfer rate from an extended surfaces the following assumptions need to be made such as; steady state heat transfer, the properties of

the material are constant (independent of temperature), there is no internal heat generation. The heat conduction happens in one dimension only. The material has uniform cross-sectional area. Convection occurs uniformly across the surface area. Example of application of extended surfaces (fins) are in the radiator of cars, refrigerators, power transformers and electronic boards

The heat transfer from an extended or finned surfaces to the ambient atmosphere occurs by convection and radiation. But as a result of relatively low values of emissivity of the fin materials such as aluminum, duralumin and steel alloys, the effect of radiation on the heat transfer may be neglected (Yardi, Karguppikar, Tanksale, & Sharma, 2017). Convection heat transfer is therefore the mode of energy transfer between a solid and it adjacent fluid in motion. The faster the motion of the fluid, the greater the convection heat transfer from the surface.

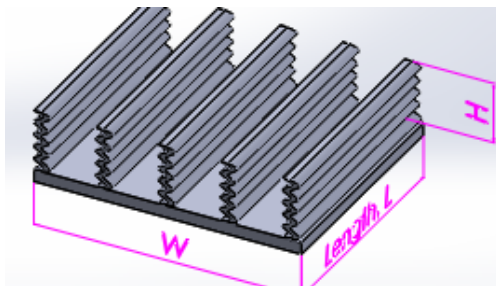
Convection can take place in two forms; Natural convection and forced convection. The former takes place as a result of the fluid flow that is caused by density difference, otherwise known as Buoyancy forces. While in the later (forced convection) fluid is forced to flow over the surface by the use of external means such as fan, pump, compressors etc. The wavy fin surface is popular because it can increase the length of the airflow in the heat exchanger by improving or enhancing the air flow mixing and increasing heat transfer performance (Moorthy, Nicholas, & Oumer, 2018). The wavy fin is one of the most popular fin types in plate fin heat exchangers, particularly where superior heat transfer performance is demanded

under tight pressure drop allowance (Nikam, Pharate, & Tingare, 2015)

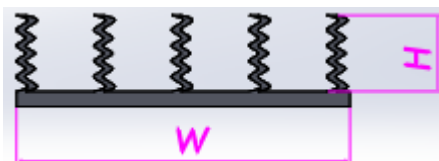
2 METHODOLOGY

2.1 DESIGN OF THE FIN SAMPLE

The fin array model was designed into twelve (12) different configurations using Solidworks 2018 version. The base length (L), base width and the base thickness, fin wavelength (λ) and fin thickness (t) was taken generally to be 110 mm, 95 mm, 5 mm, 7 mm, and 3 mm throughout the whole configurations. The fin height (H) ranges from 15 mm to 35 mm while the fin spacing (S) ranges from 7.3 mm to 22.6 mm. The fins were designed to protrude horizontally from a rectangular base. See some of the different fin array configurations in the figures 1 through 5 below.



a. Isometric fin array view



b. Fin array Front view

Figure 1. Fin Configuration geometry

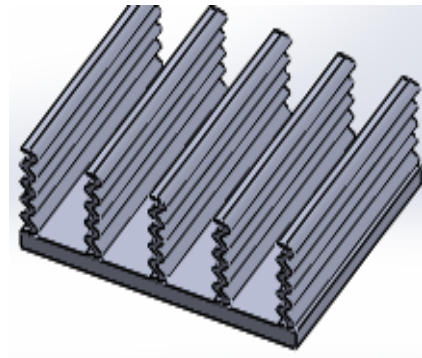


Figure 2. H = 35 mm, s = 22.6 mm

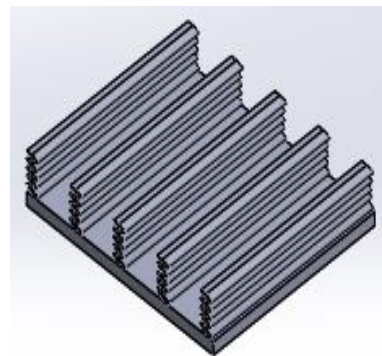


Figure 3. H = 15 mm, s = 22.6 mm

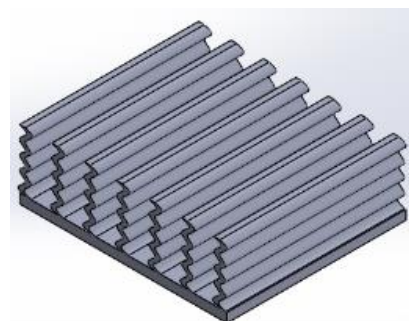


Figure 4. H = 25 mm, s = 14.2 mm

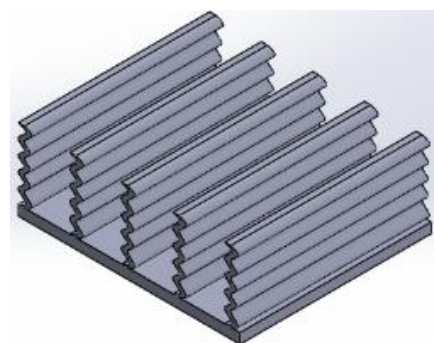


Figure 5. H = 25 mm, s = 22.6 mm

2.2. Simulation Procedures

A steady state numerical simulation analysis for each of the configuration was carried out using solidworks flow simulation, version 2018. The material selected was aluminum metal because of it high thermal conductivity and strength and low emissivity. The simulation was carried out at four different base temperature; 45^oC, 60^oC, 90^oC and 120^oC respectively. The simulation procedures are; modelling of the fin array configurations, selection of material, selection of boundary conditions, creating Meshing on the model, running the study and display/processing of results. See the initial and boundary conditions summary used below.

Analysis Type:	External
Flow Characteristics:	Laminar and turbulent
Convective Fluid:	Air
Convective heat transfer coefficient (h):	20W/m ² K
Initial solid temperature:	27 ^o C
Environmental pressure:	101325Pa
Wall Condition:	Real wall
Wall Temperature (T _w):	45 ^o C – 120 ^o C
Ambient Temperature (T _a):	27 ^o C
Material of solid	Aluminum metal

The boundary conditions were chosen such that; the fin and base plate was assigned as solid domain and the enclosure (that is the computational domain) automatically becomes the fluid domain. The back surface of the base plate was taken as real wall 1 with temperature value assigned to it. The remaining surfaces of the fin and base plate assembly were taken as real wall 2 with a convective heat transfer coefficient and air duct temperature assigned to it. Solidworks flow simulation automatically assigns the inlet and outlet pressure, the surrounding fin temperature and the adiabatic condition to the walls of the computational domain.

3 RESULTS AND DISCUSSION

A numerical analysis was carried out on various configuration of wavy fin array to find out the heat transfer rate based on different geometry of the fin array and the results are presented in the figures 6 through 15 below and discussed as follows.

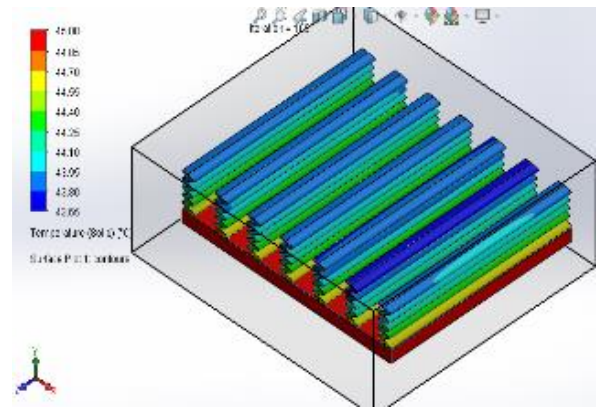


Figure 6. Surface plot of configurations at H = 25 mm, s = 9.9 mm at 45^oC wall temperature.

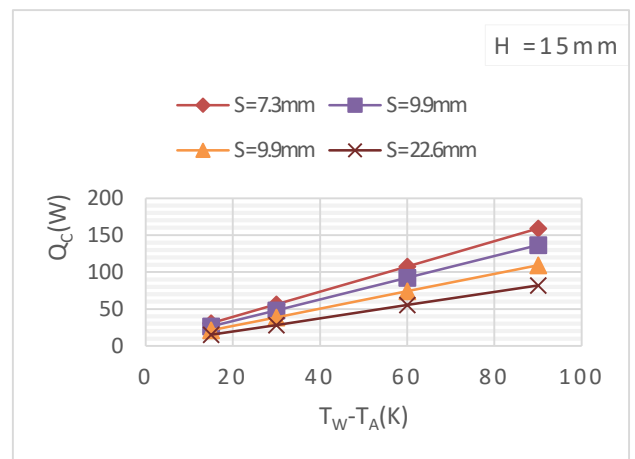


Figure 7. Variation of Convection Heat Transfer Rate with Fin spacing at a Fin Height of H = 15mm and at a Fin Length of L = 95mm

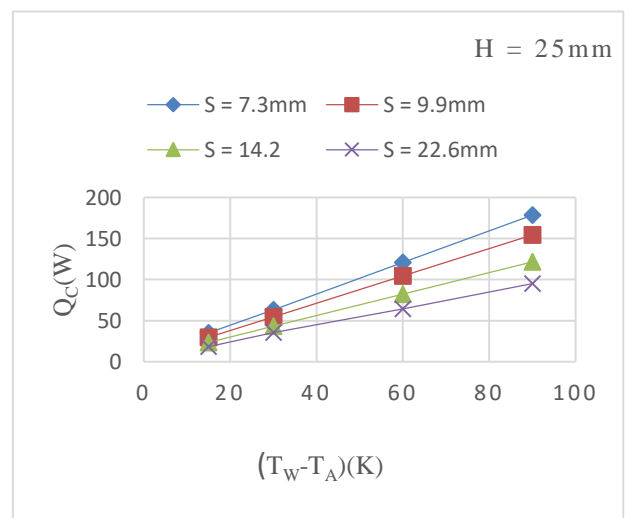


Figure 8. Variation of Convection Heat Transfer Rate with Fin spacing at a Fin Height of $H = 25$ mm and at a Fin Length of $L = 95$ mm

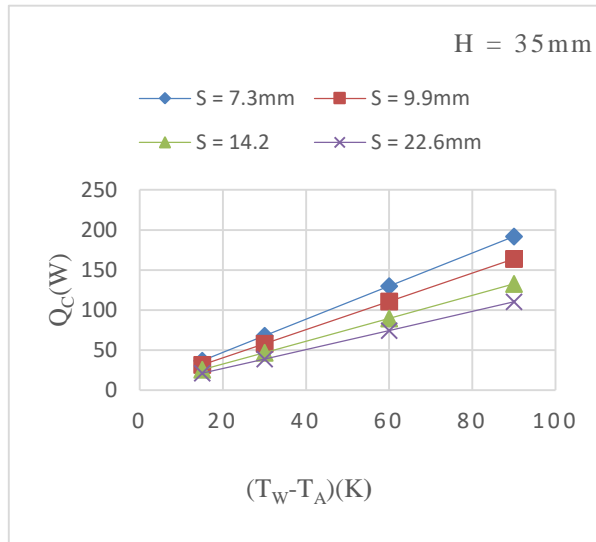


Figure 9. Variation of Convection Heat Transfer Rate with Fin spacing at a Fin Height of $H = 35$ mm and at a Fin Length of $L = 95$ mm

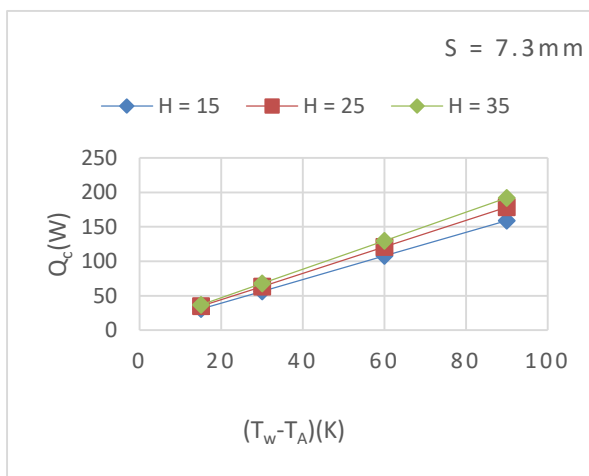


Figure 10. Variation of Convection Heat Transfer Rate with Fin Height at a Fin Spacing of $s = 7.3$ mm and at a Fin Length of $L = 95$ mm

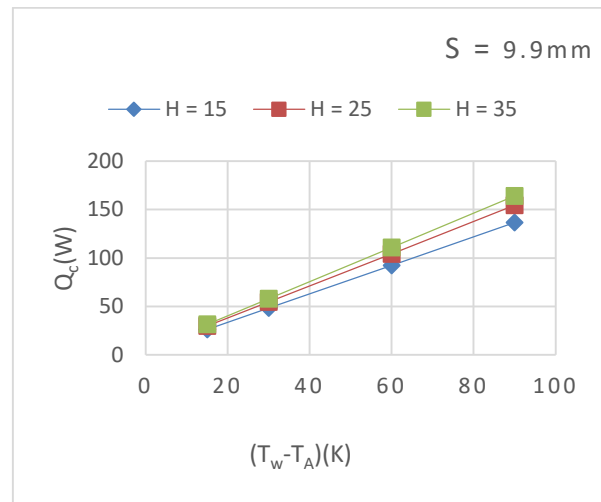


Figure 11. Variation of Convection Heat Transfer Rate with Fin Height at a Fin Spacing of $s = 9.9$ mm and at a Fin Length of $L = 95$ mm

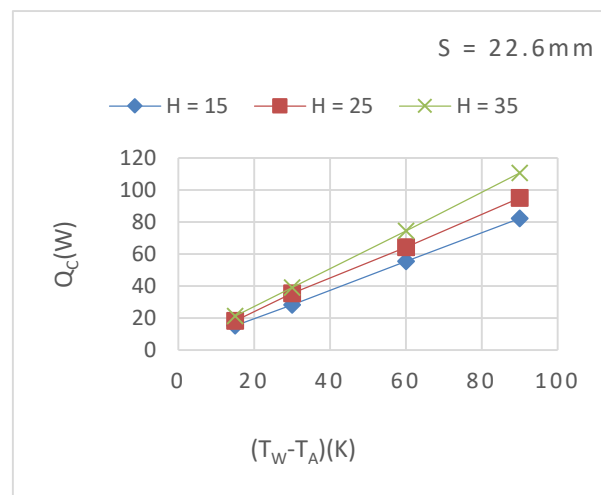


Figure 12. Variation of Convection Heat Transfer Rate with Fin Height at a Fin Spacing of $s = 14.2$ mm and at a Fin Length of $L = 95$ mm

As observed in Figures 6 to 12, the convection heat transfer rate from the fin arrays depends on fin height, fin length, fin spacing and base-to-ambient temperature difference. It is seen that the convective heat transfer rates from the fin arrays increases with fin height and base-to-ambient temperature difference.

When the curves in Figures 9 to 11 are considered altogether, it can be concluded that at low base to ambient temperature difference inputs, the convection heat transfer rate from fins are closer than those at high base-to-ambient temperature difference, inconsequent of the variation in fin spacing and fin height. In all of these three figures, the convection heat transfer rate from fin arrays for fin spacing values, $s = 7.3$ mm is greater than those of remaining fin

spacing, for any given base-to-ambient temperature difference and fin height.

In Figures 13 through 14, the effect of base-to-ambient temperature difference on convection heat transfer rate can be clearly seen in these figures. Convection heat transfer rates are plotted as a function of fin spacing. From this Figures, it can be inferred that the convection heat transfer rate from an array increases with fin spacing, fin length and base-to-ambient temperature difference.

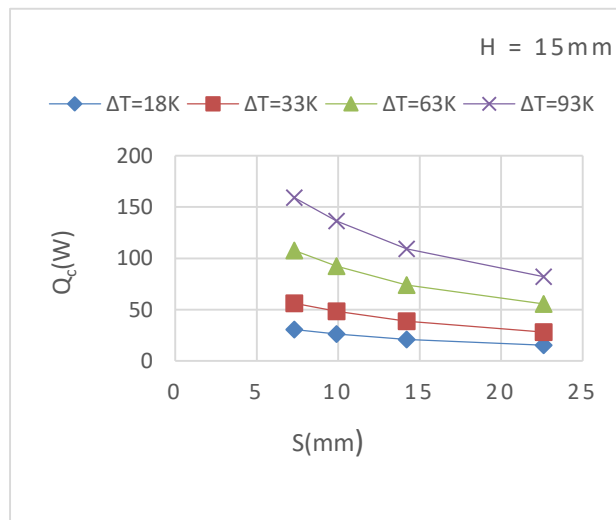


Figure 13. Variation of Convection Heat Transfer Rate with Base-to-Ambient Temperature Difference at a Fin Height of H=15 mm and a Fin Length of L=95 mm

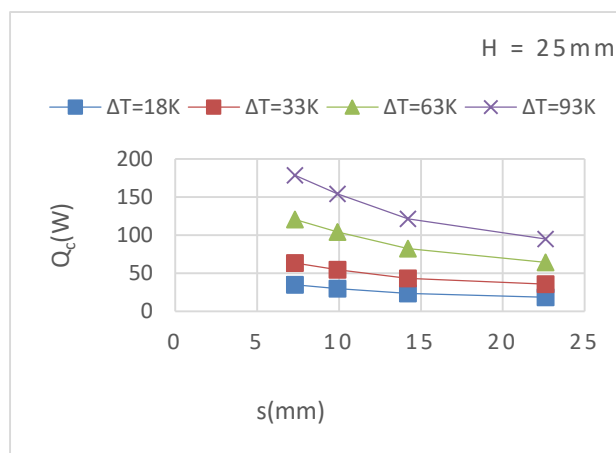


Figure 14: Variation of Convection Heat Transfer Rate with Base-to-Ambient Temperature Difference at a Fin Height of H=25 mm and a Fin Length of L=95 mm

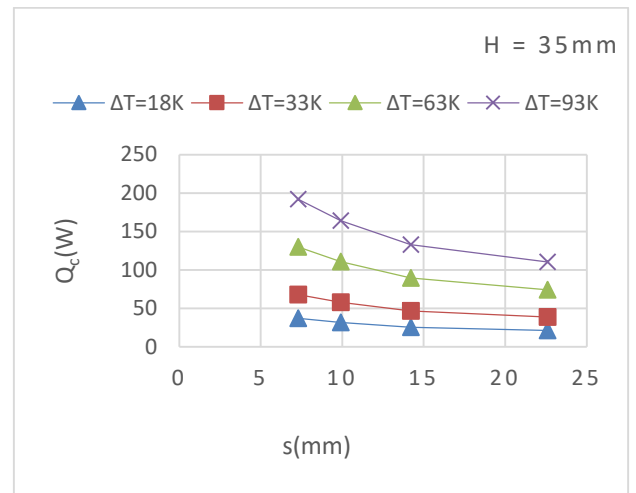


Figure 15: Variation of Convection Heat Transfer Rate with Base-to-Ambient Temperature Difference at a Fin Height of H=35 mm and a Fin Length of L=95 mm.

4 CONCLUSION

A numerical analysis was carried out on a wavy fin array of about twelve different configuration based on space and height. From the plots of the simulation results shown in the figures above. The following conclusions were made as follow;

The convective heat transfer rate is much effective and increases with increase in fin height at any fin spacing. It also increases with decrease in the fin spacing of the array at all height of fin. And lastly it is concluded that the convective heat transfer rate is affected by the difference in base-to-ambient temperature of the fin array. It could be further concluded that a wavy fin array can be suitably used as heat sink in effective heat dissipation if space and weight management must be taken into consideration in thermal system design.

REFERENCES

- Dong, J., Zhang, Y., Li, G., & Xu, W. (2013). Fin optimization in heat sinks and Heat exchangers. *Journal of Thermal Energy Generation , Transport, Storage and Conversion*, 26(4), 384–396.
- Eastop, T. D., & McConkey, A. (2006). *Applied Thermodynamics for Engineering Technologies* (5th ed.). Pearson Education.
- Incropera, F., Dewitt, D., Theodore, B., & Adrienne, L. (2007). *Fundamentals of Heat And mass Transfer* (6th ed.). United States of America: John Wiley & Sons, Inc. Retrieved from <http://www.wiley.com/go/permissions.%0Ato>



-
- Long, C., & Sayma, N. (2009). *Heat Transfer* (1st ed.). Retrieved from bookboon.com
- May, P., & Almubarak, A. A. (2017). The Effects of Heat on Electronic Components, 7(5), 52–57. <https://doi.org/10.9790/9622-0705055257>
- Moorthy, P., Nicholas, N., & Oumer, A. N. (2018). Experimental Investigation on Effect of Fin Shape on the Thermal-Hydraulic Performance of Compact Fin-and-Tube Heat Exchangers. In *IOP Conference Series: Materials Science and Engineering PAPER*. <https://doi.org/10.1088/1757-899X/318/1/012070>
- Naidu, S. V, Rao, V. D., Rao, B. G., Sombabu, A., & Sreenivasulu, B. (2010). Natural Convection Heat Transfer From Fin Arrays- Experimental And Theoreticalal Study On Effect Of Inclination Of Base On Heat Transfer, 5(9), 7–15.
- Nikam, N. R., Pharate, G. M., & Tingare, S. V. (2015). Review on Heat Transfer Enhancement Using the Wavy Fin, 49–53.
- Ranjan, S., & Mishra, D. P. (2018). Heat transfer analysis through horizontal rectangular inverted notched fin array using natural convection by experimental method, (July 2013).
- Theses, M., & Miller, G. E. (1967). Optimum fin spacing for heat transfer per unit length of heat exchange section.
- Wais, P. (2016). Correlation and numerical study of heat transfer for single row cross-flow heat exchangers with different fin thickness. *Procedia Engineering*, 157, 177–184. <https://doi.org/10.1016/j.proeng.2016.08.354>
- Yardi, A., Karguppikar, A., Tanksale, G., & Sharma, K. (2017). Optimization of Fin spacing by analyzing the heat transfer through rectangular fin array configurations (Natural convection). *International Research Journal of Engineering and Technology (IRJET)*, 4(09 september-2017), 985. Retrieved from www.irjet.com

TOWARDS A HYBRID MQTT-COAP PROTOCOL FOR DATA COMMUNICATIONS IN WIRELESS SENSOR NETWORKS

*Nwankwo, E. I¹, Onwuka, E. N² & Michael, D³

^{1,2,3}Department of Telecommunications Engineering, School of Electrical Engineering and Technology, Federal University of Technology, Minna, Niger State, Nigeria.

*Corresponding author email: emmanueln_nike@hotmail.com, +2347035448942

ABSTRACT

Wireless Sensor Networks (WSNs) consist of sensor nodes and gateways which are resource constrained devices. Lightweight communication protocols for WSNs are emerging for Machine to Machine (M2M) communications and thus there is always going to be a possible conflict of interest on which protocol is best suited for any particular application. The architecture of these emerging protocols is mainly categorized into the publish-subscribe architecture and the request-response architecture. Although there are other protocols for data communication in WSNs, the two protocols of interest in this study are the Message Queuing Telemetry Transport (MQTT) protocol based on the publish-subscribe architecture and the Constrained Application protocol (CoAP) based on the request-response architecture. Studies have shown that the performance of these different protocols are dependent on different network conditions and they have complimentary advantages and disadvantages. MQTT messages experience lower delays than CoAP for lower packet loss and higher delays than CoAP for higher packet loss. MQTT is also considered very scalable since message subscribers do not need to know about the publishers and vice-versa as opposed to CoAP where the client has to explicitly know the server address to be able to make requests. In this paper we propose a hybrid MQTT-CoAP protocol technique for data communication in wireless sensor networks that harnesses the advantages of both MQTT and CoAP protocol.

Keywords: *CoAP, Hybrid protocol, Machine to Machine Communication, MQTT, Wireless Sensor Network*

1 INTRODUCTION

In recent years, introduction of smart sensors in the market place has given rise to considerable advancements in the development of wireless sensor networks (WSNs). Smart sensor nodes are low power devices equipped with one or more sensors, possibly with an actuator, a processor unit, memory/storage unit, a power supply and a wireless communication radio (Akyildiz, Weilian Su, Sankarasubramaniam, & Cayirci, 2002).

As the Internet of Things (IoT) expands to numerous applications through the increasing minimization of hardware, availability of versatile sensors, and “smart objects” (Giusto, Iera, Morabito, & Atzori, 2010), many potential protocols are emerging for M2M communications thus, the question of which protocol to use for the Internet of Things becomes a topic of high interest. From an end-to-end perspective, a WSN can be viewed as comprising of two subnets; a subnet connecting sensor nodes and one or more gateway nodes in which sensor nodes route data until it reaches one of the gateways using WSN protocols (e.g., Collection Tree Protocol (Gnawali, Fonseca, Jamieson, Moss, & Levis, 2009)), and another subnet connecting the gateway and a back-end server or broker. The typical communication architecture for WSNs is shown in Figure 1 below. Sensor data generated by sensor nodes are delivered to the server through the gateway. Meanwhile, clients that are interested to receive sensor data connect to the server to obtain the data. To transfer all the sensor data collected by a gateway node to a server, the former requires

a protocol that is bandwidth-efficient, energy-efficient and capable of working with limited hardware resources. As a result, protocols such as Message Queue Telemetry Transport (MQTT) (MQTT, 2014) and Constrained Application Protocol (CoAP) (Shelby, 2013) have been proposed to specifically address the difficult requirements of real-world WSN deployment scenarios.

One way for wireless sensor networks to transfer data from a gateway to clients is the “request-response” also known as “client-server” architecture which is supported by CoAP. In the client-server architecture, request messages initiate a transaction with a server, which may send a response to the client with a matching transaction ID and this is based on a polling method (Davis, Calveras, & Demirkol, 2013). Another way is the “publish-subscribe” architecture (Eugster, Felber, Guerraoui, & Kermarrec, 2003). In this architecture, a client needing data (known as subscriber) registers its interests with a server (also known as broker). The client producing data (known as publisher) sends the data to a server and this server forwards the fresh data to the subscriber. One of the major advantages of this architecture is the decoupling of the clients needing data and the clients sending data. This decoupling enables the architecture to be highly scalable (Eugster et al., 2003). The “publish-subscribe” architecture is supported by MQTT and CoAP (Davis et al., 2013; Thangavel, Ma, Valera, Tan, & Tan, 2014). The publish-subscribe architecture, emerged out of the need to provide a distributed, asynchronous, loosely coupled communication between data generators and destinations. The solution appears today in the form of numerous publish-subscribe Message-Oriented

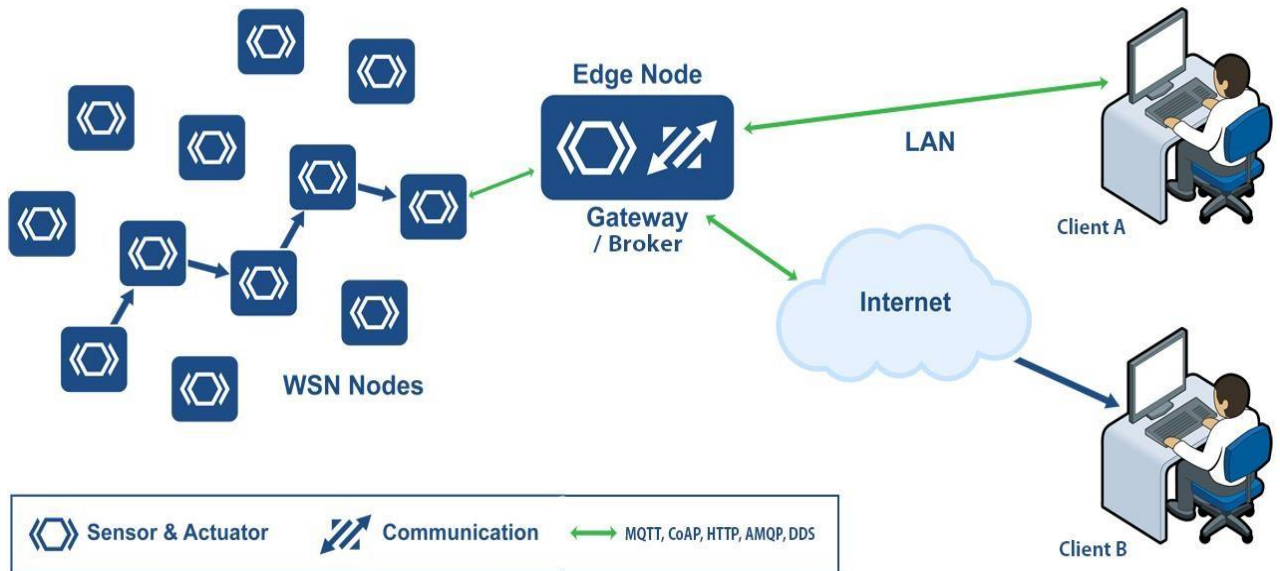


Figure 1: Typical Wireless Sensor Networks (WSNs) communication architecture

Middleware (MoM) (Jia, Bodanese, Phillips, Bigam, & Tao, 2014) and recently has been a subject of numerous research efforts (Chelloug & El-Zawawy, 2018; Hakiri et al., 2017; Veeramanikandan & Sankaranarayanan, 2017). Experimental studies as will be highlighted in this paper have shown that when CoAP is compared with MQTT, some of the disadvantages offered by one protocol is complemented by the other protocol and vice-versa, this study proposes a hybrid MQTT-CoAP protocol technique that brings the advantages of both protocols to be utilized in data communication.

2 MESSAGE QUEUE TELEMETRY TRANSPORT (MQTT) PROTOCOL

MQTT is a lightweight messaging protocol released by IBM that is based on the publish-subscribe paradigm. This makes it suitable for resource constrained devices and for non-ideal network connectivity conditions, such as with low bandwidth and high latency. The latest version used for IoT by the OASIS (Cohn, R., & Coppen, 2014) is MQTT v3.1. Because of its simplicity, and a very small message header compared with other messaging protocols, it is often recommended as the communication solution of choice in IoT. MQTT runs on top of the TCP transport protocol, which ensures its reliability. In comparison with other reliable protocols, such as HTTP, and thanks to its lighter header, MQTT comes with much lower power requirements, making it one of the most prominent protocol solutions in constrained environments. As illustrated in Figure 2 below, there are two communication parties in MQTT architecture that usually take the roles of publishers and subscribers, clients and servers/brokers. Clients are the devices that can publish messages, subscribe to receive messages, or both. The client must know about the broker

that it connects to, and for its subscriber role it has to know the subject it is subscribing to. A client subscribes to a specific topic, in order to receive corresponding messages. However, other clients can also subscribe to the same topic and get the updates from the broker with the arrival of new messages. Broker serves as a central component that accepts messages published by clients and with the help of the topic and filtering delivers them to the subscribed clients. For a device to have a role of the broker, it is necessary to install MQTT broker library, for example Mosquitto broker (Eclipse, 2019), which is one of best-known open source MQTT brokers. It should be noted that there are various other MQTT protocol brokers that are open for use, which differ by way of implementation of the MQTT protocol. The clients are realized by installing MQTT client libraries. Topics in MQTT are treated as a hierarchy, with strings separated by slashes that indicate the topic level (Tantitharanukul, Osathanunkul, Hantrakul, Pramokchon, & Khoenkaw, 2017). One MQTT publisher can publish messages to defined set of topics. In this case client will publish the topic: topic/1. This information will be published to the broker which can temporarily store it in a local database. The subscriber interested in this topic sends a subscribe message to a broker, specifying the same topic.

An important feature MQTT offers is the possibility to store some messages for new subscribers by setting a 'retain' flag in published messages. Brokers usually discard messages if there is nobody interested in a topic on which the publisher sends the updates. By setting a 'retain' flag to value: true, the broker is informed that it should store the published message, so it could be delivered to new subscribers. MQTT uses TCP which is quite critical for constrained devices and this has led to a proposed MQTT for Sensor Networks (MQTT-SN) which is an MQTT version that uses UDP and supports topic name indexing

(Govindan & Azad, 2015; Stanford-Clark & Truong, 2013). MQTT-SN added a feature which is the reduced size of the payloads by using numeric topic IDs rather than long topic names. At the moment MQTT-SN is only supported by a few platforms. There is a free broker implementation called Really Small Message Broker (Xu, Mahendran, Guo, & Radhakrishnan, 2017) and also EMQTT MQTT-Broker which supports MQTT-SN through a plugin (EMQTT, 2013). Since it was designed to be lightweight, MQTT does not provide encryption, and instead, data is exchanged as plain-text, which is clearly an issue from the security standpoint. Therefore, encryption needs to be implemented as a separate feature, for instance via TLS, which on the other hand increases overhead. Authentication is implemented by many MQTT brokers, through one of the MQTTs control type message packets, called CONNECT. Brokers require from clients, that when sending the CONNECT message, they should define username/password combination before validating the connection, or refusing it in case the authentication was unsuccessful. Overall, security is an ongoing research effort for MQTT (Lesjak et al., 2015).

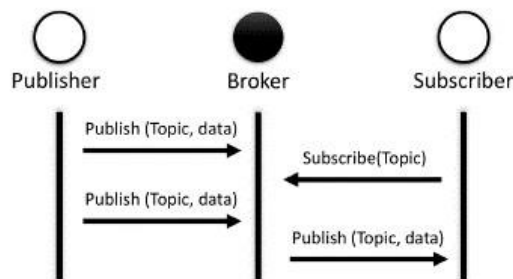


Figure 2: Publish subscribe architecture of MQTT

3 CONSTRAINED APPLICATION PROTOCOL (CoAP)

This protocol was designed for use in constrained devices with limited processing capability by the Constrained RESTful Environments (CoRE) working group of IETF (Shelby, 2013). Similar to HTTP it is based on the request/response architecture and one of its most defining characteristics is its use of tested and well accepted REST architecture. CoAP is considered a lightweight protocol, so the headers, methods and status codes are all binary encoded, thus reducing the protocol overhead in comparison with many protocols. It also runs over less complex UDP transport protocol instead of TCP, further reducing the overhead. When a CoAP client sends one or multiple CoAP requests to the server and gets the response, this response is not sent over a previously established connection, but exchanged asynchronously over CoAP messages. The Figure 3 below shows the request response architecture of CoAP. The price paid for this reduction is reliability. Since UDP features reduced reliability, IETF has recently created an additional standard document,

opening up the possibility of CoAP running over TCP (Bormann, Lemay, Tschofenig, Hartke, & Silverajan, 2018). CoAP relies on a structure that is logically divided into two layers, the request/response layer and the message layer. The request/response layer, implements RESTful architecture and allows for CoAP clients to use methods like GET, PUT, POST or DELETE when sending requests to specific URI. (Nguyen & Iacono, 2015). The request and responses are matched through a token; a token in the response has to be the same as the one defined in the request. It is also possible for a client to push data, for example updated sensor data, to a device by using method POST to its URL. As we can see, in this layer CoAP uses the same methods as REST HTTP. What makes CoAP different from HTTP is the second layer. CoAP uses its second layer known as message layer for reliability by retransmitting lost packets since UDP does not ensure reliable connection. The message layer defines four types of messages: CON (Confirmable), NON (non-confirmable), ACK (Acknowledgement), and RST (reset). The CON messages demand an ACK message as reply from the receiver while the NON messages don't request any reply. CoAP has an optional feature that allows clients to continue receiving changes on a requested resource from the server (Correia, Sacramento, & Schutz, 2016). This is achieved by adding an observe option to a GET request. The server then adds the client to the list of observers for the specific resource which allows the client to receive the notifications when resource state changes. This feature which is considered a variant of the publish-subscribe architecture, eliminates the need to poll the server repeatedly for a specific resource trying to get the changed resource state. In an attempt to get even closer to publish/subscribe paradigm, IETF has recently released the draft of Publish-Subscribe Broker that extends the capabilities of CoAP for supporting nodes with long interruptions in connectivity and/or up-time (Koster, SmartThings, Keranen, Jimenez, & Ericsson, 2019). As a security mechanism CoAP uses DTLS (Rescorla & Modadugu, 2012) on top of its UDP transport protocol based on TLS protocol with necessary changes to run over an unreliable connection giving a secure CoAPS protocol version. Most of the modifications in comparison to TLS include features that stop connection termination in case of lost or out of order packets. As an example, there is a possibility to retransmit handshake messages. Handshaking process is very similar to the one in TLS, with the exchange of client and server 'hello' messages, but with the additional possibility for a server to send a verification query to making sure that the client was sending its 'hello' message from the authentic source address. This mechanism helps prevent Denial-of-Service attacks. Through these messages, client and server also exchange supported cipher suits and keys, and agree on the ones both sides support, which will further be used for data exchange protection during the communication. Since DTLS was not originally designed for IoT and constrained devices, new

versions optimized for the lightweight devices have emerged recently (Panwar & Kumar, 2015; Raza, Shafagh, Hewage, Hummen, & Voigt, 2013). Some of the DTLS optimization mechanisms with a goal of making it more lightweight include IPv6 over Low-power Wireless Personal Area Network (6LoWPAN) header compression mechanisms to compress DTLS header (Raza, Trabalza, & Voigt, 2012). Due to the limitations of DTLS, its optimization is an open and ongoing research issue (Granjal, Monteiro, & Sa Silva, 2015; Lakkundi & Singh, 2014).

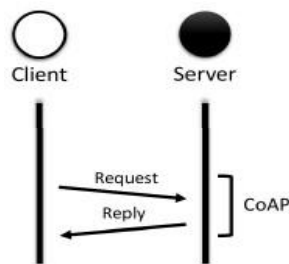


Figure 3: Request-response architecture of CoAP

4 RELATIVE ANALYSIS AND COMPARISON OF MQTT AND CoAP PROTOCOLS

This section presents a comparative analysis of the two protocols in terms of message size and overhead, power consumption and resource requirement, bandwidth and latency, reliability/QoS and Interoperability, security and provisioning, IoT usage and standardization.

4.1 Message size and overhead

In terms of both message size and message overhead, studies have shown that CoAP has the lowest compared to MQTT (Bandyopadhyay & Bhattacharyya, 2013; De Caro, Colitti, Steenhaut, Mangino, & Reali, 2013; Ngo Manh Khoi, Saguna, Mitra, & Ahlund, 2015; Thangavel et al., 2014). This is due to the fact that MQTT runs on TCP unlike CoAP which runs on UDP, thereby incurring a higher message size and message overhead for MQTT with a header size of 2-bytes per message (Naik, 2017).

4.2 Power consumption and Resource requirement

When comparing MQTT and CoAP in terms of normal power consumption and resource requirement, studies have shown that CoAP requires the lowest power and resource compared to MQTT. Various experimental studies found that CoAP consumes slightly less power and resources in similar circumstances: unreliable scenario (MQTT QoS 0 vs. CoAP NON), and reliable scenario (MQTT QoS 1 or 2 vs. CoAP CON), while assuming that no packet losses happened (Bandyopadhyay & Bhattacharyya, 2013;

Colitti, Steenhaut, & Caro, 2011; De Caro et al., 2013; Ngo Manh Khoi et al., 2015; Thangavel et al., 2014).

4.3 Bandwidth and Latency

Experimental studies have shown that CoAP has the lowest bandwidth consumption and latency compared to MQTT when transferring the same payload under the same network condition (MQTT QoS 1 or 2 vs. CoAP CON) (Bandyopadhyay & Bhattacharyya, 2013; Colitti et al., 2011; De Caro et al., 2013; Ngo Manh Khoi et al., 2015; Thangavel et al., 2014). TCP is a major factor as to why MQTT consumes more bandwidth and has more latency because the technique employed by TCP during congestion is for the TCP sender to open the congestion window and double the number of packets in each round-trip time (RTT). In CoAP, a UDP transaction requires only two UDP datagrams, one in each direction; this reduces the network load response times (Naik, 2017). Experimental studies have also shown that MQTT messages experienced lower delays than CoAP for lower packet loss and higher delays than CoAP for higher packet loss. Moreover, when the message size is small and the loss rate is equal to or less than 25%, CoAP generates less extra traffic than MQTT to ensure reliable transmission (Chen & Kunz, 2016; Thangavel et al., 2014).

4.4 Reliability/QoS and Interoperability

CoAP protocol does not explicitly define a QoS whereas MQTT defines three QoS levels: 0- at most once (only TCP guarantee), 1- at least once (MQTT guarantee with confirmation), 2- exactly once (MQTT guarantee with handshake) (Bandyopadhyay & Bhattacharyya, 2013). The use of TCP in MQTT ensures higher reliability compared to CoAP. In terms of interoperability, CoAP is a HTTP-based RESTful protocol and thus offers higher interoperability compared to MQTT because all that is needed to support message exchange is in the HTTP stack (Naik, Jenkins, Davies, & Newell, 2016).

4.5 Security and provisioning

Studies have shown that MQTT is a messaging protocol with the lowest level of security compared to CoAP. MQTT has minimal authentication features aside TLS/SSL and relies only on simple username and password. CoAP on the other hand uses DTLS and IPsec for authentication, integrity and encryption (Naik, 2017).

4.6 IoT Usage and Standardization

MQTT has been employed by a larger number of organizations without yet becoming a global standard while CoAP has been less used by organizations but its technique being much closer to HTTP is considered to be of higher standardization (Naik, 2017). MQTT is an established M2M protocol and has been used and supported by the large number of organizations such as IBM, Facebook, Eurotech, Cisco, Red Hat, M2Mi, Amazon Web

Services (AWS), InduSoft and Fiorano (Bandyopadhyay & Bhattacharyya, 2013; De Caro et al., 2013; Thangavel et al., 2014).

5 RELATED WORK AND JUSTIFICATION

Dizdarevic et al (2019) in their paper on a survey of communication protocols for internet of things and related challenges of fog and cloud computing integration, discussed multiple protocol solutions for IoT to Fog computing and then to Cloud computing. In their study they proposed a HTTP-CoAP solution or an MQTT-AMQP solution but the technique used involved having for example, the CoAP protocol functioning between IoT devices and the Gateway and the HTTP protocol functioning between the gateway and the Cloud. Also, their multiple protocol solution involved protocols of similar architecture.

Thangavel et al (2014) conducted an experimental study on the performance evaluation of MQTT and CoAP using a common middleware. They designed a common middleware on the gateway using a common API capable of interfacing with CoAP, MQTT and any other lightweight protocol that they care to attach. Their multiprotocol implementation was limited to gateway/broker to client/end user and did not offer solutions for working with nodes. This work is an extension of the work done by Thangavel et al with an improvement of implementing the hybrid technique in the nodes as well and not just on the gateway.

A hybrid of MQTT-CoAP protocol is necessary because for WSNs that use only the MQTT protocol, communicating or requesting a resource from the node directly cannot be done without going through the broker which increases the latency and bandwidth consumption. On the other hand, WSNs that use only the CoAP protocol are not as scalable because of the coupling between clients and servers and also since there is no inherent capability in the CoAP protocol to retain messages from nodes.

WSN design is application specific and the application layer protocol is always a factor to consider both for sensor nodes and for gateways. Although the application specific nature of WSN design means that either of the protocols is best suited for any application, there is often need to reprogram the device when network conditions change or device application change for optimal utilization of the system resources. The hybrid MQTT-CoAP protocol system will eliminate the need for this reprogramming and also significantly reduce the time taken to decide which protocol best suits the application and network conditions. Therefore, having a hybrid protocol technique will be invaluable to an engineer looking to optimize data communication in the network.

6 PROPOSED TECHNIQUE FOR HYBRID MQTT-COAP PROTOCOL

CoAP and MQTT differ in architecture and also as discussed in the comparison in section 4 above they have complimentary advantages and disadvantages thus the need for a technique to combine both protocols.

The flow chart in Figure 4 shows the proposed hybrid technique. The technique requires the designer to make resources of their choice available via the CoAP protocol and other or similar resources available via the MQTT protocol so the node publishes topics to a broker using the MQTT protocol and also receives requests and processes these requests using the CoAP protocol. In this protocol technique, the observe feature of the CoAP protocol will be optionally replaced or handled by the MQTT protocol so as to make the hybrid solution scalable.

Since studies have shown that at lower packet loss rates and higher delay, MQTT messages have lower delay than CoAP, a decision algorithm could be developed in the gateway to instruct nodes to communicate with either of the protocols depending on the observed network condition and this is only possible because the hybrid system would make it possible for both protocols to be used simultaneously in the node.

7 CONCLUSION

In this study we briefly overviewed the MQTT and CoAP protocols and made a brief comparison between both protocols in terms of message size and overhead, power consumption and resource requirement, bandwidth and latency, reliability/QoS and Interoperability, security and provisioning, IoT usage and standardization. This is in effort to expose the limitations and strong points of the protocols with a view to hybridizing the complementing strong points of the protocols. It is anticipated that this hybrid will produce a better performing protocol system. We propose a hybrid MQTT-CoAP protocol technique for data communication not only between gateway and server/cloud/end user but also between nodes and between a node and the gateway.

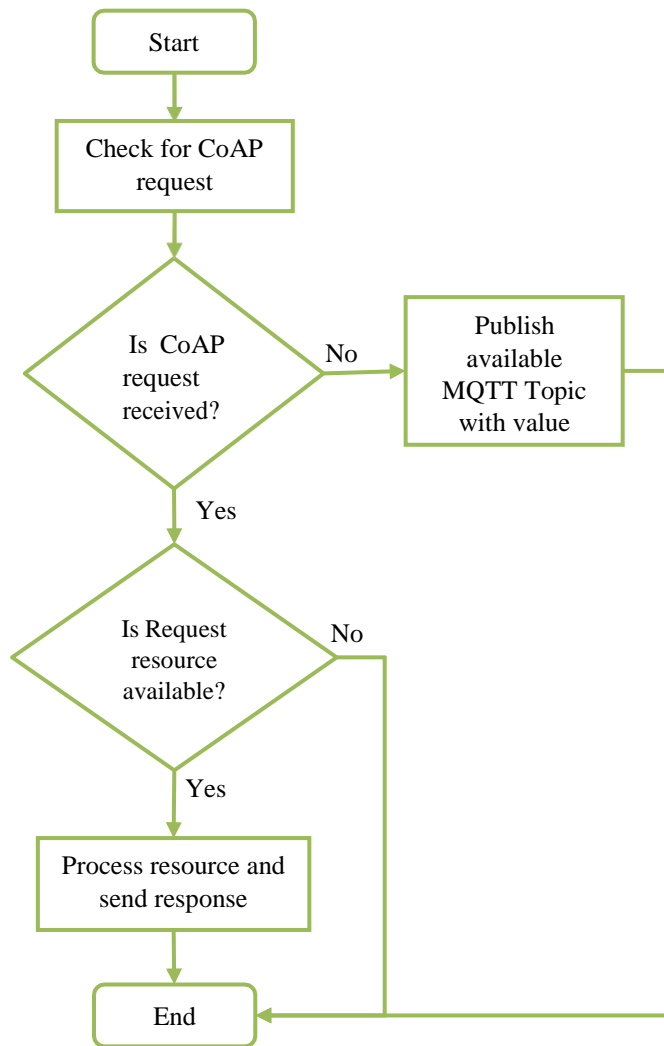


Figure 4: Algorithm for hybrid MQTT-CoAP Protocol technique

REFERENCES

- Akyildiz, I. F., Weilian Su, Sankarasubramaniam, Y., & Cayirci, E. (2002). A survey on sensor networks. *IEEE Communications Magazine*, 40(8), 102–114. <https://doi.org/10.1109/MCOM.2002.1024422>
- Bandyopadhyay, S., & Bhattacharyya, A. (2013). Lightweight Internet protocols for web enablement of sensors using constrained gateway devices. *2013 International Conference on Computing, Networking and Communications (ICNC)*, 334–340. <https://doi.org/10.1109/ICCNC.2013.6504105>
- Bormann, C., Lemay, S., Tschofenig, H., Hartke, K., & Silverajan, B. (2018). *CoAP (Constrained Application Protocol) over TCP, TLS, and WebSockets* (B. Raymor, Ed.). <https://doi.org/10.17487/RFC8323>
- Chelloug, S. A., & El-Zawawy, M. A. (2018). Middleware for Internet of Things: Survey and Challenges. *Intelligent Automation and Soft Computing*, 24(2), 309–318. <https://doi.org/10.1080/10798587.2017.1290328>
- Chen, Y., & Kunz, T. (2016). Performance evaluation of IoT protocols under a constrained wireless access network. *2016 International Conference on Selected Topics in Mobile and Wireless Networking, MoWNeT 2016*. <https://doi.org/10.1109/MoWNeT.2016.7496622>
- Cohn, R., & Coppen, R. (2014). MQTT Version 3.1.1. In *OASIS Standard*. <https://doi.org/10.1073/pnas.1201805109>
- Colitti, W., Steenhaut, K., & Caro, N. De. (2011). Integrating Wireless Sensor Networks with the Web. *Extending the Internet to Low Power and Lossy Networks (IP+ SN 2011)*, 2–6.
- Correia, N., Sacramento, D., & Schutz, G. (2016). Dynamic Aggregation and Scheduling in CoAP/Observe-Based Wireless Sensor Networks. *IEEE Internet of Things Journal*, 3(6), 923–936. <https://doi.org/10.1109/JIOT.2016.2517120>
- Davis, E. G., Calveras, A., & Demirkol, I. (2013). Improving packet delivery performance of publish/subscribe protocols in wireless sensor networks. *Sensors (Switzerland)*, 13(1), 648–680. <https://doi.org/10.3390/s130100648>
- De Caro, N., Colitti, W., Steenhaut, K., Mangino, G., & Reali, G. (2013). Comparison of two lightweight protocols for smartphone-based sensing. *2013 IEEE 20th Symposium on Communications and Vehicular Technology in the Benelux (SCVT)*, 1–6. <https://doi.org/10.1109/SCVT.2013.6735994>
- Dizdarevic, J., Carpio, F., Jukan, A., & Masip-Bruin, X. (2019). *Survey of Communication Protocols for Internet-of-Things and Related Challenges of Fog and Cloud Computing Integration*. 1(1), 1–30. <https://doi.org/10.1145/3292674>
- Eclipse. (2019). Eclipse Mosquitto. Retrieved from Mosquitto.Org website: <https://mosquitto.org/>
- EMQTT. (2013). EMQ - The Massively Scalable Open Source MQTT Broker. Retrieved June 13, 2019, from <http://emqtt.io/>
- Eugster, P. T., Felber, P. A., Guerraoui, R., & Kermarrec, A.-M. (2003). The many faces of publish/subscribe. *ACM Computing Surveys*, 35(2), 114–131. <https://doi.org/10.1145/857076.857078>
- Giusto, D., Iera, A., Morabito, G., & Atzori, L. (Eds.). (2010). *The Internet of Things*. <https://doi.org/10.1007/978-1-4419-1674-7>
- Gnawali, O., Fonseca, R., Jamieson, K., Moss, D., & Levis, P. (2009). Collection tree protocol. *Proceedings of the 7th ACM Conference on Embedded Networked Sensor Systems - SenSys '09*, 1. <https://doi.org/10.1145/1644038.1644040>
- Govindan, K., & Azad, A. P. (2015). End-to-end service assurance in IoT MQTT-SN. *2015 12th Annual IEEE Consumer Communications and Networking Conference (CCNC)*, 290–296.

- <https://doi.org/10.1109/CCNC.2015.7157991>
Granjal, J., Monteiro, E., & Sa Silva, J. (2015). Security for the Internet of Things: A Survey of Existing Protocols and Open Research Issues. *IEEE Communications Surveys & Tutorials*, 17(3), 1294–1312.
- <https://doi.org/10.1109/COMST.2015.2388550>
Hakiri, A., Berthou, P., Gokhale, A., Abdellatif, S., Hakiri, A., Berthou, P., ... Gokhale, A. (2017). *Publish / subscribe-enabled software defined networking for efficient and scalable IoT communications To cite this version : HAL Id : hal-01633323 Publish / Subscribe-enabled Software Defined Networking for Efficient and Scalable IoT Communications.*
- Jia, Y., Bodanese, E., Phillips, C., Bigham, J., & Tao, R. (2014). Improved reliability of large scale publish/subscribe based MOMs using model checking. *2014 IEEE Network Operations and Management Symposium (NOMS)*, 1–8.
<https://doi.org/10.1109/NOMS.2014.6838311>
- Koster, M., SmartThings, Keranen, A., Jimenez, J., & Ericsson. (2019). *Publish-Subscribe Broker for the Constrained Application Protocol CoAP*. Retrieved from <http://datatracker.ietf.org/drafts/current/>.
- Lakkundi, V., & Singh, K. (2014). Lightweight DTLS implementation in CoAP-based Internet of Things. *2014 20th Annual International Conference on Advanced Computing and Communications, ADCOM 2014 - Proceedings*, 7–11.
<https://doi.org/10.1109/ADCOM.2014.7103240>
- Lesjak, C., Hein, D., Hofmann, M., Maritsch, M., Aldrian, A., Priller, P., ... Pregartner, G. (2015). Securing smart maintenance services: Hardware-security and TLS for MQTT. *2015 IEEE 13th International Conference on Industrial Informatics (INDIN)*, 1243–1250.
<https://doi.org/10.1109/INDIN.2015.7281913>
- MQTT. (2014). MQ Telemetry Transport. Retrieved May 9, 2019, from <https://mqtt.org>
- Naik, N. (2017). Choice of effective messaging protocols for IoT systems: MQTT, CoAP, AMQP and HTTP. *2017 IEEE International Symposium on Systems Engineering, ISSE 2017 - Proceedings*, 1–7.
<https://doi.org/10.1109/SysEng.2017.8088251>
- Naik, N., Jenkins, P., Davies, P., & Newell, D. (2016). Native Web Communication Protocols and Their Effects on the Performance of Web Services and Systems. *2016 IEEE International Conference on Computer and Information Technology (CIT)*, 219–225. <https://doi.org/10.1109/CIT.2016.100>
- Ngo Manh Khoi, Saguna, S., Mitra, K., & Ahlund, C. (2015). IReHMo: An efficient IoT-based remote health monitoring system for smart regions. *2015 17th International Conference on E-Health Networking, Application & Services (HealthCom)*, 563–568.
- <https://doi.org/10.1109/HealthCom.2015.7454565>
Nguyen, H. V., & Iacono, L. Lo. (2015). REST-ful CoAP Message Authentication. *2015 International Workshop on Secure Internet of Things (SIoT)*, 35–43. <https://doi.org/10.1109/SIoT.2015.8>
- Panwar, M., & Kumar, A. (2015). Security for IoT: An effective DTLS with public certificates. *2015 International Conference on Advances in Computer Engineering and Applications*, 163–166.
<https://doi.org/10.1109/ICACEA.2015.7164688>
- Raza, S., Shafagh, H., Hewage, K., Hummen, R., & Voigt, T. (2013). Lite: Lightweight Secure CoAP for the Internet of Things. *IEEE Sensors Journal*, 13(10), 3711–3720.
<https://doi.org/10.1109/JSEN.2013.2277656>
- Raza, S., Tralbalza, D., & Voigt, T. (2012). 6LoWPAN Compressed DTLS for CoAP. *2012 IEEE 8th International Conference on Distributed Computing in Sensor Systems*, 287–289.
<https://doi.org/10.1109/DCOSS.2012.55>
- Rescorla, E., & Modadugu, N. (2012). *Datagram Transport Layer Security Version 1.2*.
<https://doi.org/10.17487/rfc6347>
- Shelby, Z. (2013). Constrained Application Protocol (CoAP) draft-ietf-core-coap-17. Retrieved from <http://tools.ietf.org/html/draft-ietf-core-coap-17>
- Stanford-Clark, A., & Truong, H. L. (2013). MQTT for sensor networks (MQTT-SN) protocol specification. In *Ibm*. Retrieved from http://mqtt.org/new/wp-content/uploads/2009/06/MQTT-SN_spec_v1.2.pdf
- Tantitharanukul, N., Osathanunkul, K., Hantrakul, K., Pramokchon, P., & Khoenkaw, P. (2017). MQTT-Topics Management System for sharing of Open Data. *2017 International Conference on Digital Arts, Media and Technology (ICDAMT)*, 62–65.
<https://doi.org/10.1109/ICDAMT.2017.7904935>
- Thangavel, D., Ma, X., Valera, A., Tan, H. X., & Tan, C. K. Y. (2014). Performance evaluation of MQTT and CoAP via a common middleware. *IEEE ISSNIP 2014 - 2014 IEEE 9th International Conference on Intelligent Sensors, Sensor Networks and Information Processing, Conference Proceedings*, (April), 21–24.
<https://doi.org/10.1109/ISSNIP.2014.6827678>
- Veeramanikandan, M., & Sankaranarayanan, S. (2017). Publish/subscribe broker based architecture for fog computing. *2017 International Conference on Energy, Communication, Data Analytics and Soft Computing (ICECDS)*, 1024–1026.
<https://doi.org/10.1109/ICECDS.2017.8389592>
- Xu, Y., Mahendran, V., Guo, W., & Radhakrishnan, S. (2017). Fairness in fog networks: Achieving fair throughput performance in MQTT-based IoTs. *2017 14th IEEE Annual Consumer Communications & Networking Conference (CCNC)*, 191–196.
<https://doi.org/10.1109/CCNC.2017.7983104>



TOWARD A HYBRID TECHNIQUE FOR FRIENDS RECOMMENDATION SYSTEM IN SOCIAL TAGGING

Usman Bukar Usman

Faculty of Computer Science and Information Technology
Bayero University Kano, Nigeria
ubu1700016.msc@buk.edu.ng

Kabir Umar

Faculty of Computer Science and Information Technology
Bayero University Kano, Nigeria
ukabir.cs.@buk.edu.ng

ABSTRACT

Due to Web2.0's acceptance, social tagging systems became an interesting research topic. Recommenders are the best solution for reducing the problem of information overloading, cold starting and Existing social networking site recommending friends to users based on their social graphs or choosing a friend as friend of friend. In the past, the performance of friend's recommendation system in the social networking site received little attention as a subject of research. Social tagging systems allow Internet resources to be classified, discovered and organized by a user. We proposed a novel hybrid technique based on FP-Growth and ant colony optimization algorithm in this paper to enhance the recommendation of friends in the social tagging system. The experimental results will be on Delicious dataset.

Keywords: Ant Colony Optimization; FP-Growth Algorithm; Friend Recommendation; Social Tagging

1 INTRODUCTION

Over the past few years, individuals have assisted in the online social networking site's continuous growth, both in terms of services and size. The social relationship is an emerging topic with the social networking site's significant development. Presently Social tagging systems have become a hot and interesting research topic due to the acceptance of Web2.0. social tagging systems allow a user to, classify, discover and organize Internet resources. users can control their resources simply and explain them with their keywords called tags and categorize content and share them with other people. People tag resources for future retrieval and sharing. Tags can convey information about the content and creation of a resource. Tags explain about the resource and the characteristics of a resource. Tagging is a new way to create user preference. (Wu et al., 2015, and hu et al., 2013). Online social tagging platforms such as Amazon, Facebook, Twitter, WeChat, Flickr, delicious.com are web-based sites that store keywords called tags, provide individuals with good support for tagging resources, such as videos and images, as well as communicating with friends. Carullo et al., (2014) stated that the Services of Social Networks (SNSs) are making great efforts to increase their importance and popularity. Although the method is based on as-yet-unrevealed algorithms, some of them provide utility services to recommend friends. The human factors behind how a user comes into contact with others, however, follow complex mechanisms due to significant development of information technology and the gives rise to Internet resources and e-commerce. the total number of information in the network environment is increasing dramatically. However, internet

users are faced with the dimension disaster problem while enjoying the abundant information resources. Considering the redundant and disordered features of massive data, it has become increasingly difficult for people to quickly and efficiently mine useful content from the large data (Peng et al., 2018). There is a constant increase in the number of users using social sites. Friend Recommendation is one of the most important aspects of Social networking sites. Recommender system has become an effective method to solve information overloading and helps users to make decisions (Ren et al., 2018). According to Kavin et al., (2017). The day to day activities of a social networking use can help determine the lifestyle of the users, father more user will have different lifestyle when compared with others. It is difficult to know the lifestyle of the users at ease. But it is easy in life to determine a person's lifestyle on his daily activities. The activities of the user will be acquired during the registration of the user. After determining the user's lifestyle, the similarity should be found to find the real connection between the users. Literature investigation Shehu (2017) reveal that the major problem of finding friends on social networking sites is caused by overloading which is a problem that occurs due to rapid increase in size and services experienced by social networking sites on daily bases, several researchers made. Hybridizations of ACO with Other Metaheuristics is the most straightforward hybridization and improvement methods (Dorigo & Stützle 2019).

2. LITERATURE REVIEW

In this section, our main focus is on investigating the friend's recommendation system. Before reviewing existing work about friend recommendation, we firstly, introduce the general background of recommender

systems, including the goals, formulations and types, the friend's recommender system in social network and Finally, we describe the existing technique for friend's recommender system Specific related work.

A. RECOMMENDER SYSTEM

Recommendation systems for social networking site is a modern area of research as social peoples are more interested in online social networking sites, like Facebook, Twitter, Flickr, LinkedIn, etc. (Hasan, *et al.*, 2015). the recommender system is a system that accurately predicts the users' tastes as well as expands their horizon about the available products (Dhruv *et al.*, 2019). Recommender systems are widely used in our life for automatically recommending items related to our preference. The main goal of the recommender system is to filter the unwanted information based on users' preference that helps users to find interested items (Wang *et al.*, 2016). Chai *et al.*, (2019) Stated that the recommendation system plays a vital role in helping people to get information effectively from mass data. Lots of items provided by the electronic retailers and content providers to meet user's interested needs and tastes. How can we get what we want? This emphasizes the importance of the recommendation system, which predicts personalized products that suit a user's preferences. the recommendation system is a subset of information filtering system that seeks to predict the "preference" or "rating" a user would give to an item (Hassannia *et al.*, 2019 & Park *et al.*, 2012) Recommendation systems are algorithms which are used to make perfect predictions based off user preferences or needs (Fessahaye *et al.*, 2019) Recommender systems are widely categorized as content-based filtering, collaborative filtering (CF), hybrid approach, and knowledge-based recommender systems (Dhruv *et al.*, 2019). According to Chai *et al.*, (2019) the content-based methods based on information analysis of items and users. (Hassannia *et al.*, 2019) stated that the main disadvantage of the CB system is no suitable prediction, i.e., the analyzed content does not have enough information to differentiate between items the user would like or not like. The problem with content-based filtering is overspecialization. Overspecialization is taking into account only those items that more similar to each other and giving minimum advantage to the interests of the users (Dhruv *et al.*, 2019). Collaborative filtering (CF) recommender system is a filtering method that utilizes an information filtering technique based on the user previous evaluations (Koren 2009). CF is the approach that providing automatic filtering or prediction interest of a user by collecting preference information from other users collaborating (Sheugh, & Alizadeh 2015). The hybrid system uses information from the contents of purchased items and previous user-item history (Dhruv *et al.*, 2019). the hybrid recommendation system is based on the combination of two different techniques. For instance, a hybrid system combining techniques of CB and CF tries to use the advantages of CB to fix the disadvantages of CF. CF methods suffer from recommending new-item problems, i.e., they cannot predict items that have no

ratings. This does not limit content-based approaches since the prediction for new items is based on their previous history (features) that are typically easily available (Ricci *et al.*, 2011). Burke (2000) sees the knowledge-based recommendation system is one that uses knowledge about users and items to pursue a knowledge-based approach to generating a prediction, reasoning about what item meets the user's requirements or need. Knowledge-based systems recommend items based on particular domain knowledge about how certain item features meet users' preferences ultimately, how that item is important for the user (Ricci *et al.*, 2011).

B. FRIEND'S RECOMMENDER SYSTEM IN SOCIAL NETWORK

With the rapid development of online community, increasing demand of modern technology and advancement in social networking sites such as Facebook, twitter and G+ the modern technology they have increased the advancement of making friends. (Hassannia *et al.*, 2019). Existing social networking site recommend friends to users based on their social graphs or pick the friend applicant like friend of friend, for instant Facebook are suggest friends based on mutual friends or common friends shared and social relationship which may not be the most appropriate to return a user's preferences on friend selection in real life (Parvathy & Ratheesh 2017). Wu *et al.*, (2015) sees Friend recommendation in social networking site can be categorized into two different classifications: predicting friends based on social graphs, like friends of friends; or suggesting based on the interest of users which is built with the text information in recommendation systems. Following friends of friends on social graphs can mostly recommend people you may know already. Thus, it is practical significance to friend recommendation based on interest which can predict the users with strong similarities of interest as potential friends. The table 1 below shows summary of existing technique for friend recommendation with their references. with their references.

table 1: summary of existing technique

REF.	SUMMARY OF PROPOSED SOLUTION
(Peda & sharma 2015)	A PbTR calculation is made which takes as info labels apportioned to a specific asset by the objective client and different clients. The objective client might be a present client who has effectively offered labels to the asset or a new client who has not allocated labels to the asset, the objective client for whom companions are proposed and the aggregate trust diagram of all clients is taken as criticism by the FR

	calculation and utilized in suggest companions.		learning calculation for paired class dependent on data hypothesis.
(Manca et al., 2014)	In the social bookmarking space, article presents a companion suggest plot. The plan prompts clients with tantamount interests by mining the objective client's substance. Our recommender framework utilizes the open information specifically and does not consider the chart.	(Huang, et al., 2015)	Start by finding the arrangement of two systems. In the article adjust particular systems by picking noteworthy attributes that catch the similarity between unmistakable systems. Taking the tag and contact arranges as an occasion, we by and large judge a person who may be our forthcoming companion with only a couple of expressions
(Wang et al., 2016).	In the wake of playing out our TROIA calculation, we can get the reproduced rank – (2,5,4,4) estimate tensor X. the yield of our calculation for the model is fascinating, on the grounds that new relationship among clients and gatherings are uncovered. These new affiliations are somewhere in the range of U1 and G3 just as U2 and G1, Our TROIA calculation can catch the inactive relationship among clients and gatherings.	(cheng et al., 2018)	The report proposed a safe and productive suggestion framework for companion's dependent on a security protecting convention. Target clients send the application for companions to Center Authority (CA), CA picks companion candidates from all clients in the plan with label coordinating dependent on protection safeguarding convention. Target clients pick companions among CA sifted companion candidates.
(Dhawan, et al., 2017)	In the proposed activity, the attachment of at least two qualities is utilized to make the proposal decision, a companion proposal framework called a union based suggestion framework is recommended in which a new companion is recommended situated on some trust worth determined on the grounds of couple of current parameters.	(Zhang et al., 2015)	The up-and-comer's attributes, for example, sexual orientation, age, spot, intrigue and number of regular neighbors, could possibly be self-ruling. Youngsters may show incredible enthusiasm for games, for example, so sexual orientation and age will adequately affect the characteristic of intrigue.
(Wu et al., 2015)	Propose a User Similarity Graph (FRUG) Friend Recommendation calculation for social labeling plans. FRUG proposes a similar diagram dependent on significance to planned partners for clients with equivalent intrigue.	(Wei et al., 2018)	A coordinating computation can be performed based on the asset model and client model. The asset model and client model are altogether founded on the model of vector space and sound in structure in this record. The client model can be considered as an exceptional asset model from a specific view.
(Yang et al., 2018)	Subsequent to completing the determination of qualities, we get crisp information with supportive attributes and bring it into a preparation classifier model where we pick the choice tree calculation, ID3 calculation, a directed		

3. PROPOSED MODEL

In this section, we introduce our proposed model and the description of the five various steps

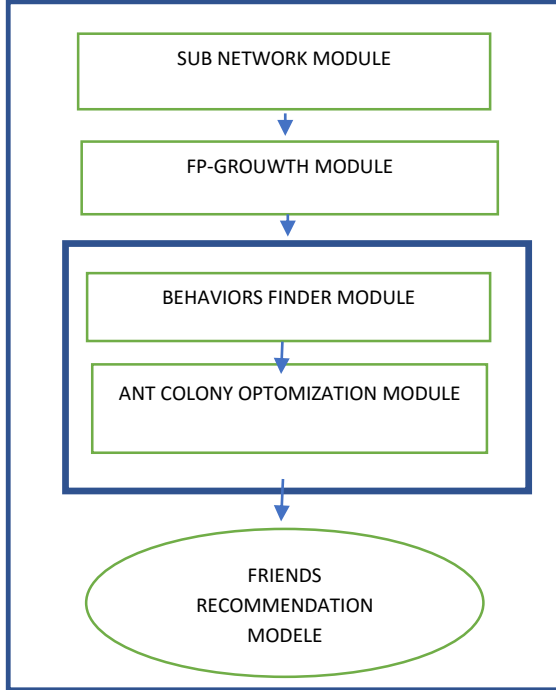


Fig.1: Proposed Model

A. SUB NETWORK MODULE

These days, Social Networking destinations are huge element with its administrations and size are winding up increasingly mainstream. Consistently the size and administrations of the system are expanding quickly and as the individuals are joining, there is tremendous number of data over-burdening occurs on the two administrations and destinations. our proposed framework, we separate the entire system of an individual discretionarily After getting the entire system of a customer for who will suggest companions, we remove the subnetwork from the system of 'x' individuals from the envisioned chart.

B. FP-GROWTH MODULE

Since in (Hasan, *et al.*, 2015) authors highlight that the behavior of the users is reflected in their tagging activities. There are a huge number of activities on SNS's nowadays and increasing every day because of the advancement of technology and user's involvement from different domain of life. A social network is controlled by communities of organizations or an individual that are connected by a common goal or interest. The behavior of a social networking user depends on the type of activities user perform on the SNS. User activities are the main base of social networking sites. in our proposed model we can

consider a different set of user activities like types of post user tagged, types of videos user where tagged, etc. From all the activities we will obtain then we will find out the entity with the highest frequency. We make the network scanned by using this frequency with the maximum frequency related activities are there. all activities come down to the number of activities, where every classified activity contains one activity with the highest frequency. Finally, only the activities with maximum frequencies will be chosen.

C. BEHAVIORS FINDER MODULE

To see the ideal conduct of client (normal and remarkable) we will utilize FP-Growth calculation in our adjusted dataset. FP-Growth works in separation and overcomes way. FP-Growth calculation gives us an example from the dataset. Among this example, the ideal conduct will be found. It needs two outputs on our database model. FP-Growth calculation initially figures a rundown of regular things arranged by recurrence in sliding request (F-List) during its first database filter. In its subsequent output, the database is packed into an FP-tree. At that point, FP-Growth begins to dig the FP-tree for everything.

D. ANT COLONY OPTIMIZATION MODULE

In this another significance steps we will take the aftereffects of the FP-Growth as the contribution of subterranean insect settlement improvement, and afterward figure the ideal companion prescribed request through cycle. At first we will get a Path, In the Tth cycle, for insect k which is situated in hub I, it chooses the following hub as indicated by the accompanying course likelihood.

$$p_{ij}^k(t) = \frac{[\tau_{ij}(t)] \cdot [\eta_{ij}]^\beta}{\sum_{l \in N_i^k} [\tau_{il}(t)] \cdot [\eta_{il}]^\beta}, \quad \text{if } j \in N_i^k \quad (1)$$

Where β is a parameter which decides the overall impact of the pheromone trail and the heuristic data n_i^k speaks to the open however ever passed neighbor hubs for subterranean insect k which touches base at hub i. $\tau_{ij}(t)$ speaks to the pheromone of the edge ij in Tth iteration.

At that point Pheromone update it includes two viewpoints, one is pheromone dissipation, the other is refreshing which is the impression of ants' inquiry experience. Lastly, Solve the ideal arrangement Compare the length of spared M way: minL1, minL2,...,minLn, and locate the base worth minL, which is the worldwide ideal, and the relating hub request is the ideal suggested request.

E. FRIENDS RECOMMENDATION MODULE

In this last step our proposed system will recommend the friends with the by FP-Growth and combined with ACO apply in previous steps.

3. EXPERIMENT AND RESULT

In this section, we describe our experiment and result of our proposed system, it contains four different components.

A. DATASET

We evaluate the proposed recommendation algorithm on Delicious dataset which is a popular social tagging resource. hetrec2011-delicious-2k is a Delicious dataset which is published at the workshop of HetRec2011 (Cantador et al., 2011). and it's available can be downloaded from the website of group lens. The dataset contains 1867 total number of users, 53388 tags and 69226 resources. There are 437593 times of user annotation and; averaged 234.383 tags annotated by a user and averaged 6.321 annotated tags per resource

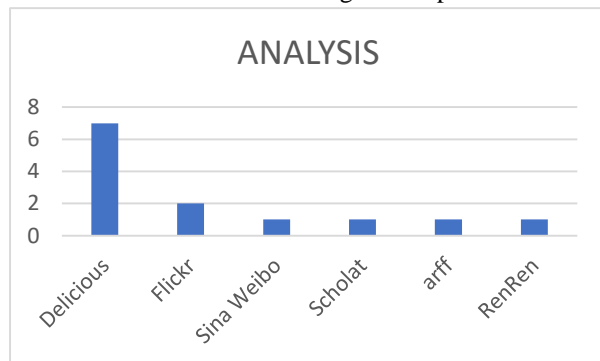


Fig 2: Dataset

Delicious dataset is the most popular dataset in used for Most of the researchers are basically make used of precision, recall and F-measure to evaluate the performance of their proposed method, Peda and sharma (2015), (Manca et al., 2014), (Wu et al., 2015, and hu et al., 2013), (Yang et al., 2018), (Huang, et al., 2015), (cheng et al., 2018) and (Puglisi et al., 2015) based on the above analysis we will used first three most used evaluation

B. PERFORMANCE MATRIX

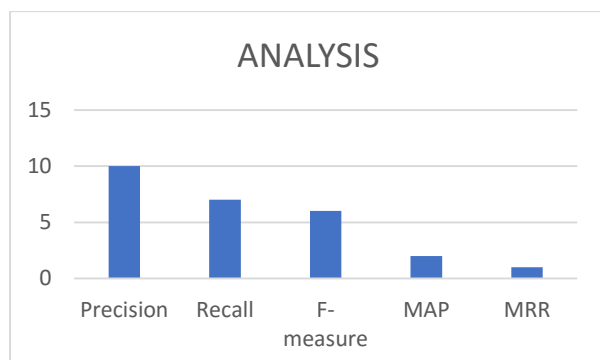


Fig 3: Performance Matrix

Most of the researchers are basically make used of precision, recall and F-measure to evaluate the performance of their proposed method (Peda & sharma 2015), (Manca et al., 2014), (Wu et al., 2015, and hu et al., 2013), (Yang et al., 2018), (Huang, et al., 2015), (cheng et al., 2018), and (Puglisi et al., 2015) based on the above analysis we will used first three most used evaluation

C. EXPERIMENTAL DESIGN

In our experimental design intended to perform two different experiments which are normally divided in test and training set. We will compare our proposed approach with FP-Growth based and ant colony optimization-based technique, enables the comparison between those approaches applied to the same delicious dataset. We have to evaluate the performance of a system to evaluate the recommendations, by measuring the precision, recall, and F-measure of the system. we will get the following main conclusion: The comparison of the value of P, R, and F1.

4. CONCLUSION

Continue an increase in the number of users using social sites rapidly. Friend Recommender system most important aspects of the Social networking sites and has become an effective method to solve information overloading and helps users to make decisions by providing an interested friend to the user. In our paper, we proposed a novel Hybrid technique-based FP-Growth and ant colony optimization algorithm friend's recommendation system in a social tagging system. Combining ideas of traditional ranking algorithms such as FP-Growth and ACO. for our experiments we will use 1867 users from delicious to verify the proposed methodology. We do hope our new framework of friend's recommendation system will improve the quality of friend prediction and will help the user to social networking sites. Our future work is to work with different data mining algorithms and large-scale datasets from Facebook, Twitter, and U-Tube, etc.

REFERENCES

- Wu, B. X., Xiao, J., & Chen, J. M. (2015, August). Friend recommendation by user similarity graph based on interest in social tagging systems. In *International Conference on Intelligent Computing* (pp. 375-386). Springer, Cham.
- Hu, W., Zhang, Y., Zhou, Y., & Deng, K. (2013, December). Tagpref: User Preference Modeling by Social Tagging. In *2013 IEEE 10th International Conference on Ubiquitous Intelligence and Computing and 2013 IEEE 10th*



- International Conference on Autonomic and Trusted Computing (pp. 111-118). IEEE.
- Carullo, G., Castiglione, A., & De Santis, A. (2014, September). Friendship recommendations in online social networks. In *2014 International Conference on Intelligent Networking and Collaborative Systems* (pp. 42-48). IEEE.
- Peng, H., Ying, C., Tan, S., Hu, B., & Sun, Z. (2018). An Improved Feature Selection Algorithm Based on Ant Colony Optimization. R. Nicole, "Title of paper with only first word capitalized," J. Name Stand. Abbrev., in press.
- Kavin K., Ponvimal M., Nithya L., Vishnu Priya B., & Boopathi Rajan P. (2017, February). A Life Style Based Friend Recommendation System. *International Journal for Research in Applied Science & Engineering Technology (IJRASET)*. Volume 5 Issue II, ISSN: 2321-9653
- Bedi, P., & Sharma, R. (2015). Ant-based friends recommendation in social tagging systems. *International Journal of Swarm Intelligence*, 1(4), 321-343.
- Shehu, S. (2017) ACohesion Based Friend Recommendation System. *International Journal of Computer Science, Engineering and Information Technology (IJCSEIT)*, 7,(5).
- Hasan, M. M., Shaon, N. H., Al Marouf, A., Hasan, M. K., Mahmud, H., & Khan, M. M. (2015, December). Friend recommendation framework for social networking sites using user's online behavior. In *2015 18th International Conference on Computer and Information Technology (ICCIT)* (pp. 539-543). IEEE.
- Cantador, I., Brusilovsky, P., and Kuflik, T. (2011). Second workshop on information heterogeneity and fusion in recommender systems (hetrec2011). In *Proceedings of the 2011 ACM Conference on Recommender Systems, RecSys 2011*, pages 387–388. ACM.
- Ning, I. J., & Duan, H. Y. (2014). an algorithm for friend-recommendation of social networking sites based on simrank and ant colony optimization. *the journal of china universities of posts and telecommunications*, 21, 79-87.
- Delicious dataset forms the website Grouplens. <http://grouplens.org/datasets/hetrec-2011/>
- Dhruv, A., Kamath, A., Powar, A., & Gaikwad, K. (2019). Artist Recommendation System Using Hybrid Method: A Novel Approach. In *Emerging Research in Computing, Information, Communication and Applications* (pp. 527-542). Springer, Singapore.
- Chai, Z. Y., Li, Y. L., Han, Y. M., & Zhu, S. F. (2019). Recommendation System Based on Singular Value Decomposition and Multi-Objective Immune Optimization. *IEEE Access*, 7, 6060-6071.
- Wang, K., Xu, L., Huang, L., Wang, C. D., & Lai, J. H. (2019). SDDRS: Stacked Discriminative Denoising Auto-Encoder based Recommender System. *Cognitive Systems Research*, 55, 164-174.
- Hassannia, R., Vatankhah Barenji, A., Li, Z., & Alipour, H. (2019). Web-Based Recommendation System for Smart Tourism: Multiagent Technology. *Sustainability*, 11(2), 323
- Park, D. H., Kim, H. K., Choi, I. Y., & Kim, J. K. (2012). A literature review and classification of recommender systems research. *Expert systems with applications*, 39(11), 10059-10072.
- Fessahaye, F., Perez, L., Zhan, T., Zhang, R., Fossier, C., Markarian, R., ... & Oh, P. (2019, January). T-RECSYS: A Novel Music Recommendation System Using Deep Learning. In *2019 IEEE International Conference on Consumer Electronics (ICCE)* (pp. 1-6). IEEE.
- Koren, Y. (2009, June). Collaborative filtering with temporal dynamics. In *Proceedings of the 15th ACM SIGKDD international conference on Knowledge discovery and data mining* (pp. 447-456). ACM.
- Sheugh, L., & Alizadeh, S. H. (2015, April). A note on pearson correlation coefficient as a metric of similarity in recommender system. In *2015 AI & Robotics (IRANOPEN)* (pp. 1-6). IEEE.
- Ricci, F., Rokach, L., & Shapira, B. (2011). *Introduction to recommender systems handbook*. In *Recommender systems handbook* (pp. 1-35). Springer, Boston, MA.
- Burke, R. (2000). Knowledge-based recommender systems. *Encyclopedia of library and information systems*, 69(Supplement 32), 175-186.
- Burke, R. (2000). Knowledge-based recommender systems. *Encyclopedia of library and information systems*, 69(Supplement 32), 175-186.



Snehal C., Rucha A., Vaibhavi G., Priyanka S., & Anisaara N. (2015). A Friend Recommendation System for Social Networks. *Global Journal of Advanced Engineering Technologies*. ISSN (Online): 2277-6370 & ISSN (Print):2394-0921.

Parvathy, V. S., & Ratheesh, T. K. (2017, April). Friend recommendation system for online social networks: a survey. In *2017 International conference of Electronics, Communication and Aerospace Technology (ICECA)* (Vol. 2, pp. 359-365). IEEE.

Manca, M., Boratto, L., & Carta, S. (2014, August). Mining User Behavior in a Social Bookmarking System-A Delicious Friend Recommender System. In *DATA* (pp. 331-338).

Wang, X., Zhao, X., Zhou, J., & Xu, M. (2016, August). Group recommendation in social tagging systems by consistent utilization of items and tags information. In *2016 3rd International Conference on Informative and Cybernetics for Computational Social Systems (ICCSS)* (pp. 261-266). IEEE.

Dhawan, S., Singh, K., & Jain, A. (2017, September). An assessment of feature selection based mechanism to recommend friends in online social networks. In *2017 6th International Conference on Reliability, Infocom Technologies and Optimization (Trends and Future Directions)(ICRITO)* (pp. 678-682). IEEE.

Wu, B. X., Xiao, J., & Chen, J. M. (2015, August). Friend recommendation by user similarity graph based on interest in social tagging systems. In *International Conference on Intelligent Computing* (pp. 375-386). Springer, Cham.

Yang, Z., Li, D., Lin, R., Tang, Y., Li, W., & Liu, H. (2018, October). An Academic Social Network Friend Recommendation Algorithm Based on Decision Tree. In *2018 IEEE SmartWorld, Ubiquitous Intelligence & Computing, Advanced & Trusted Computing, Scalable Computing & Communications, Cloud & Big Data Computing, Internet of People and Smart City Innovation (SmartWorld/SCALCOM/UIC/ATC/CBDCOM/IO P/SCI)* (pp. 1311-1316). IEEE.

Huang, S., Zhang, J., Wang, L., & Hua, X. S. (2015). Social friend recommendation based on multiple network correlation. *IEEE transactions on multimedia*, 18(2), 287-299.

Cheng, H., Qian, M., Li, Q., Zhou, Y., & Chen, T. (2018). An Efficient Privacy-Preserving Friend Recommendation Scheme for Social Network. *IEEE Access*, 6, 56018-56028.

Zhang, Z., Liu, Y., Ding, W., Huang, W. W., Su, Q., & Chen, P. (2015). Proposing a new friend recommendation method, FRUTAI, to enhance social media providers' performance. *Decision support systems*, 79, 46-54.

Wei, J., Meng, F., & Arunkumar, N. (2018). A personalized authoritative user-based recommendation for social tagging. *Future Generation Computer Systems*, 86, 355-361.

Manca, M., Boratto, L., & Carta, S. (2014, August). Using Behavioral Data Mining to Produce Friend Recommendations in a Social Bookmarking System. In *International Conference on Data Management Technologies and Applications* (pp. 99-116). Springer, Cham.

Balasubramaniam, T., Nayak, R., & Yuen, C. (2018). People to people recommendation using coupled nonnegative Boolean matrix factorization.

Puglisi, S., Parra-Arnau, J., Forné, J., & Rebollo-Monedero, D. (2015). On content-based recommendation and user privacy in social-tagging systems. *Computer Standards & Interfaces*, 41, 17-27.

I Ren, Y., & Chi, C. (2018, May). Research on Recommender System based on Social Trust. In *2018 8th International Conference on Social science and Education Research (SSEER 2018)*. Atlantis Press. *IEEE Access*, 6, 69203-69209. M. Young, *The Technical Writer's Handbook*. Mill Valley, CA: University Science, 1989.

Dorigo, M., & Stützle, T. (2019). Ant colony optimization: overview and recent advances. In *Handbook of metaheuristics* (pp. 311-351). Springer, Cham.



TOWARDS A MODEL FOR ASPECT BASED SENTIMENT ANALYSIS OF ONLINE PRODUCT REVIEW

Abdulganiyu, O. H.¹ & Kabiru, U.².

¹Faculty of Computer Science and Information Technology, Bayero University, Kano, Gwarzo Road, Kano State, Nigeria.

²Faculty of Computer Science and Information Technology, Bayero University, Kano, Gwarzo Road, Kano State, Nigeria.

email: Sege50@yahoo.com, ukabir.cs@buk.edu.ng

ABSTRACT

With the rapid growth in ecommerce, reviews for popular products on the web have grown rapidly. When an individual wants to make a decision about buying a product or using a service, or when an organization wants to benefit by obtaining the public opinion or to market its products, identify new opportunities, predict sales trends, or manage its reputation, they have access to a huge number of user reviews but reading and analyzing all of them is a tedious task. If someone reads only few numbers of reviews and come to a decision then the decision could be biased. Because of these reasons having a better data mining technique to mine these product reviews which are in semi structured format is very important. Therefore, there is a growing need to analyze and summarize a large collection of reviews automatically to overcome subjective biases and mental limitations. With sentiment analysis techniques, it is possible to analyze a large amount of available data, and extract opinions from them that may help both customers and organization to make decision. However incorporation of emoticon in sentiment analysis of online product review has received little attention, there has also been the problem of misspelled words and emoticon has a different idea with its associated text in a review. In this paper, aspect based sentiment analysis model that incorporate emoticon is proposed because incorporation of emoticon in sentiment analysis is likely to give complete and accurate result. The proposed model will be evaluated using dataset of 2582 mobile review downloaded from Amazon website. Emoticon Lexicon Technique and Naïve Bayes Classifier were used for the successful implementation of the Model. The result of this study shows that the usage of emoticons improves the performance of the model with accuracy of 91.69%, Precision of 89.23% and recall value of 88.93% as compared to when emoticon is not considered which gives an accuracy value of 83.72%, Precision value of 78.12% and a recall value of 76.12%.

Keywords: Opinion mining, aspect and emoticon based approach, data mining.

1 INTRODUCTION

Product reviews can be of great benefit for both consumers and producers. Numbers of reviews could be ranging from hundreds to thousands and containing various opinions, this makes the process of analyzing and extracting information on existing reviews become increasingly difficult. Product reviews are demanded for both consumers and producers to know market response. However, consumers face the problem of making decision on what product to buy because they have access to a huge number of user reviews, but reading and analyzing all of them is a tedious task, likewise, when a producer or an organization wants to benefit by obtaining the public opinion or to market its products, even identify new opportunities, predict sales trends, or manage its reputation, it needs to deal with an overwhelming number of available customer comments, If someone reads only few numbers of reviews and come to a decision then the decision could be biased. Because of these reasons having a better data mining technique to mine these product reviews which are in semi structured format is very

important. Hence, the need to analyze and summarize a large collection of reviews automatically to overcome subjective biases and mental limitations arises. Opinion mining techniques can help to alleviate the problem of information overload in online reviews by analyzing, summarizing and presenting people's opinions (5). With sentiment analysis techniques, it is possible to analyze a large amount of available data, and extract opinions from them that may help both consumers/customers and producers/organization in taking decisions to achieve their goals.

When a customer review talks about a product, the user might want to discuss multiple aspects or features related to the product being discussed. For example, in an online product review, while the customer might have good things to say about the phone quality, the user might as well be disappointed with some features of the phone like camera or battery. So a general sentiment analyzer that determines the overall sentiment towards the product might not be able to capture the full essence of the review. Hence the need for Aspect-based Sentiment Analysis, for better and more fine-grained analysis of user feedback,

which would enable service providers and product manufacturers to identify those business aspects that needs improvement. In this regard, several studies has been conducted within the aspect/feature based sentiment analysis as seen in the work carried out by (15) (14) (13). Opinion Mining of Customer Reviews: Feature and Smiley Based Approach (1). However, literature reviewed shows that previous and recent study conducted on sentiment analysis of online product review rarely consider emoticon into sentiment analysis of product reviews. According to literature investigation by incorporation of emoticon into sentiment analysis, it leads to a more accurate and complete result. Despite the importance of emoticon, there seems to be very little research being done on sentiment analysis of product reviews with the incorporation of emoticon as seen in the work of (1) carried out on “Opinion Mining of Customer Reviews: Feature and Smiley Based Approach” which revealed that the algorithm used gives better precision values for all the datasets in every test, although recall values were not improved in feature extraction. Their work also revealed that the developed algorithm could not identify infrequent features. By introducing infrequent feature identification component to the algorithm, the recall values could be improved. There work did not address some issues, for instance polarity of opinions were identified only as positive or negative, hence like neutral opinion could help in giving a better performance. Secondly, there wasn’t attempt for corrections of misspelled words in the review which will be helpful in extracting features and adjectives correctly and relevantly. The work did not as well address issues where emoticons are put which have an opposite idea to the text. Therefore, this research proposes an aspect and emoticon based sentiment analysis model that is expected to yield a better performance and address the problem stated.

2 LITERATURE REVIEW

In this section we review literatures on sentiment analysis of online product review, aspect based sentiment analysis and sentiment analysis with emoticons

2.1 SENTIMENT ANALYSIS OF ONLINE PRODUCTS

According to (5), opinion mining has been investigated mainly at three levels: Document Level, Sentence Level and Entity Aspect Level. The task at document level is to classify whether a whole opinion document expresses a positive or negative sentiment. This level of analysis assumes that each document expresses opinions on a single entity (e.g., a single product). Thus, it is not applicable to documents which evaluate or compare multiple entities. The task at sentence level goes to the sentences and determines whether each sentence expressed a positive, negative, or neutral opinion. Neutral

usually means no opinion. Both the document level and the sentence level analyses do not discover what exactly people liked and did not like. Aspect level performs finer-grained analysis. Aspect level is also called feature level (feature-based opinion mining and summarization) (6). Instead of looking at language constructs (documents, paragraphs, sentences, clauses or phrases), aspect level directly looks at the opinion itself. It is based on the idea that an opinion consists of a sentiment (positive or negative) and a target (of opinion). An opinion without its target being identified is of limited use. Realizing the importance of opinion targets also helps us understand the sentiment analysis problem better. Opinion targets are the product features.

Opinion mining is a vast field of interest (7) and with increasing popularity in recent times of technological and analytical advancements it has been extensively studied in various research areas such as text mining (Lia and Wu, 2010), data processing (16) natural language processing (10) and many other fields. In this generation of tweets and stories on Instagram and twitter and shares and likes in Facebook, social media is a very crucial and important platform to showoff various aspects of numerous matters and products. This has been utilized for marketing various products and also became a medium of mass communication since a single share or tweet can reach worldwide population easily and immediately. Hence modern experts are studying and implementing various opinion mining techniques to predict and understand sentiment towards various trends (12).

Sentiment analysis is very often applied in twitter to get summarised opinion of any political decision or any breaking headlines or any huge manifestations (8). In the work of (8) a case study on ‘the digital India’ initiative of Indian government was performed. All tweets having the trending hashtag of “#digitalindia” or related were mined and the aggregate sentiment classification was performed. Dictionary based approach is used to analyze the sentiments of various users. Then the polarity classification of this data is done; they are classified into 3 categories: Positive, Negative or Neutral. Features such as term frequency, term co- occurrence, parts of speech tags were extracted and using predefined dictionary of positive and negative words; the final review collected are classified depending upon the emotions expressed as positive, negative or neutral. Also, many travel-related sites or forums promote reviews and ratings on different hotels, their service, etc. In (5) these hotel reviews and ratings are taken into consideration. The comment data and related features are extracted and a mathematical model is constructed and a clustering algorithm is created to extract the final opinions.

In a study conducted by (4) a novel technique was proposed “to recommend online products to the customer after comparing products with each other from large Ecommerce database. Natural Language Processing (NLP) technique was used to obtain the polarity of the

reviews and AdaBoost classifier is used for review processing from different E-commerce sites”. Similarly, in the work of (2) a system has been proposed in which Support Vector Machine (SVM) using for mining. The study conducted by (11) have developed a system in which by using tools and python code customer reviews extracted and processed based on that product recommended. In the study of (9), various feature extraction techniques under various scenarios are mentioned for online product reviews. It also discusses about various relations and was a great help to us during the mapping of the mined reviews with crawled features of the product.

2.2 ASPECT BASED SENTIMENT ANALYSIS OF ONLINE PRODUCTS

(17) conducted a study on Aspect-based sentiment analysis to review products using Naïve Bayes, they used a training set of 3618 reviews that are divided into five aspects, These are food, service, price, ambience, and miscellaneous. Each aspect may have one of four sentiments, such as positive, negative, neutral, or conflict. Performance was also calculated on aspect classification and sentiment polarity classification measuring accuracy, precision, recall and F1 measure. The findings of the study revealed that Naïve Bayes classifier performed well for aspectbased sentiment analysis with the best F1-Measure of 78.12%. The best F1-Measure for aspect classification is 88.13%, and the best F1-Measure for sentiment classification is 75%. The study also concluded that the POS tagging approach and the Chi Square method can be involved for features selection which are further used for classification process in Naïve Bayes classifier. The Chi Square also has been proven to speed up the computation time in the classification process of Naïve Bayes although it degraded the system performance.

Solainayagi and Ponnusamy (2018) conducted a study on “To Improve Feature Extraction and Opinion Classification Issues in Customer Product Reviews Utilizing an Efficient Feature Extraction and Classification (EFEC) Algorithm” in which a proposed technique extracts features in product reviews. The nouns and noun phrases are extracted from every product review. An Efficient Feature Extraction and Classification (EFEC) methodology was utilized in the study to find all various features for the provided product review and also to recognize whether the sentence is positive or negative opinion and also recognize the amount of positive and negative opinion of every extracted feature. The amount of positive and negative opinions in a product review was calculated. An opinion word provides the classification accuracy. An EFEC strategy enhances the feature extraction and classification accuracy 15.05%, precision 13.7%, recall 15.59% and F-measure 15.07%. The study however declares the proposed EFEC algorithm is best in all several aspects.

In a study conducted by (15) on Aspect Based Sentiment Analysis Of Amazon Product Reviews, Naïve Bayes classifier was used for sentiment classification. The user review was analyzed and each feature wise score rating of the product is determined. The reviews were preprocessed to eliminate noises using various tools and methods such as stop word removal, stemming, etc. The extracted words are classified into positive and negative through unigrams using naïve Bayesian classifier. Machine learning based lexicon tool called SentiWordNet was used. Its mechanism is based on the bag of words generated from applying machine learning techniques to learn the significant Senti-word as a sentiment word lexicon. n-gram and multinomial Naïve Bayesian classification was used to analyze the opinion of the customers. The heavy weight bigrams were used for training to include phrases like “not bad” in the output bag of words. The study stated the need to improve the User Interface and further improve the efficiency and address humor-based analogy in reviews for better understanding the sentiment.

(14) conducted a study on Feature Based Sentiment Analysis of Product Reviews Using Deep Learning Methods. Python version 3.6 was used for examination as well as its parameter. The Amazon reviews database was used for sentiment analysis. The applied method was CNN and RNN. The parameter used is accuracy of both the algorithms. The performance was based on their classification. The result was based on product review taken from Amazon review database which has a total number of 55740 reviews about the mp3 player which has been sold by Amazon. Then deep learning methods were applied on the dataset that is CNN and RNN and the accuracy, precision, recall, and f1 score of the methods was computed. With CNN having an accuracy of 88.03%, Precision score of 0.86, Recall of 0.91 and F1score of 0.88 while RNN has Accuracy of 85.45%, Precision score of 0.87, Recall score of 0.84 and F1 score of 0.85. The study concluded that deep learning concepts work better than machine learning approach.

2.3 SENTIMENT ANALYSIS WITH EMOTICON

(1) conducted a study on “Opinion Mining of Customer Reviews: Feature and Smiley Based Approach” develop a more accurate data mining algorithm for opinion mining of customer reviews on the web. The research was conducted as an experimental study. A new algorithm was developed which enables feature and smiley based approach for opinion mining in customer reviews on the web. Product feature extraction, opinion word identification, opinion orientation identification of opinion words, smiley extraction, smiley orientation identification and opinion summary generation were the main components of the developed algorithm. Stanford POS tagging and SentiWordNet were used for tagging

sentences and meaning identification of opinion words respectively. Findings of the study revealed that the algorithm gives better precision values for all the datasets in every test. Although recall values were not improved in the feature extraction, when considering the ultimate objective, opinion orientation identification recall values are improved by the new algorithm. It was also revealed that for opinion identification the new algorithm was better than the existing algorithm for all the datasets tested with smiley.

3 PROPOSED MODEL

This Paper proposes a model for aspect based sentiment analysis that incorporates emoticons. The model used Emoticon Lexicon Technique (ELT) and Naïve Bayes Classifier (NBC)

3.1 ARCHITECTURE OF THE PROPOSED MODEL

The architecture of the proposed model can be seen in Figure 1.

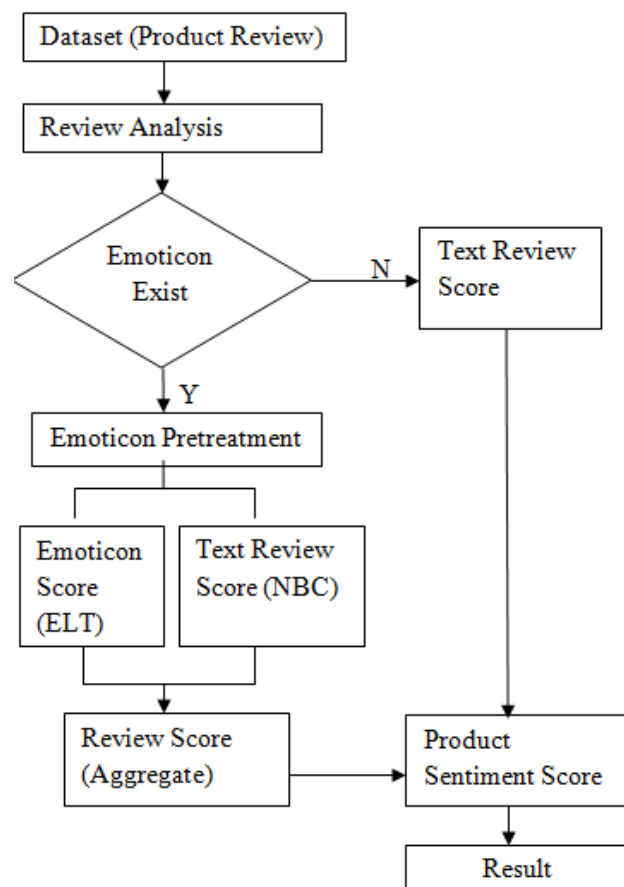


Figure 1: Emoticon Aware Aspect Based Sentiment Analysis Model

The work flow of the model is as follows;

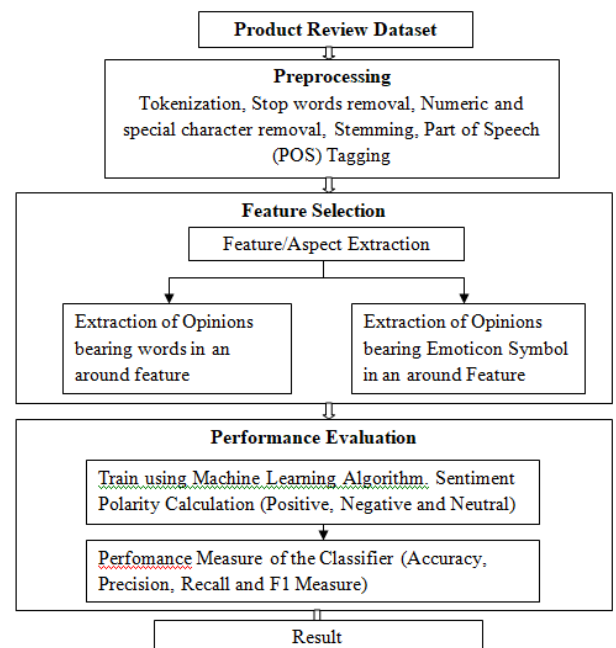
1st Step: The download dataset of product review serves as input to the model.

2nd Step: Preprocessing and Analysis is performed on the dataset, misspelled words are identified and corrected here, stop words are removed and other necessary preprocessing is done here.

3rd Step: The Model verify the existence of Emoticon in each review, if emoticon exist then it goes to emoticon pretreatment where Emoticon Lexicon Technique is being applied to give score, otherwise Naïve Bayes Classifier gives score to the text review only. The model address situations where emoticon has different idea with text by giving them different score.

4th Step: Total Score to give final Result

3.2 NAÏVE BAYES CLASSIFIER



Preprocessing: the dataset of the product review serve as an input to the preprocessing component. The preprocessing phase eliminates the incomplete, noisy and inconsistent data and stop words. This phase consist of Tokenization, Stop words removal, Numeric and special character removal, Stemming, Part of Speech (POS) Tagging and also corrects misspelled words

Feature Selection: The preprocessed data generated by the first component serve as input to this component. At this stage, extraction will take two forms: extraction of opinions bearing words in an around feature and extraction of Opinions bearing Emoticon symbol in an

around Feature. Two bag-of words will be created. The first one is for a group of words that contain aspects, and the second one is for a group of words that contain tendency of sentiment polarity. The words in each group will be selected based on the results of POS tagging.

Performance Evaluation: Sentiment polarities calculation will be performed on the data generated from the reviews of previous phase, the review will be divided into positive, negative and neutral. Performance evaluation will be done on the classification to include recall, precision and accuracy.

Naive Bayes Classifier (NBC) Workflow for the proposed model

In this paper, we use a Aspect Based sentiment-aware tokenizer combined with a Naïve Bayes model as our basic classifier. Refer to the Stanford Classifier, here is the basic idea for the Naive Bayes:

We assume that:

n is the number of words appeared in training set T ,

n_{cj} is the number of feature which belong to class j (cj in training set T (j can be positive or negative),

n_{fi} is the number of times feature i appeared in training set T ,

n_{fi_ci} is the number of times feature i appeared in class j .

Then, we use the following equations to compute the probabilities p_{cj} and p_{fi_cj} :

$$P_{cj} = \frac{n_{cj} + \epsilon}{n + |classes| \times \epsilon} \quad (1)$$

$$P_{fi_cj} = \frac{n_{fi_cj} + \sigma}{n_{fi} + |classes| \times \sigma} \quad (2)$$

While we have two classes (positive and negative), so $|classes| = 2$.

In (1) (2), the parameters ϵ and σ are smoothing parameters to avoid assigning zero weight to unseen feature. In our experiment, we choose $\epsilon = 10^{-30}$ and $\sigma = 1.0$ (Laplacian smoothing). With (1) (2), we can compute negative weight and positive weight of every feature:

$$W_{i,j} = \text{Log} \left(\frac{p_{fi_cj}}{P_{cj}} \right) \quad (3)$$

After get weights of all features, we can compute the weights of sentences according to Naïve Bayes assumption. Assuming that review t consists of n features, then the weights of the tweet t will be:

$$W_{_sentence_t,j} = \sum_{i=1}^n W_{i,j} \quad (4)$$

Finally, we will compute the possibilities of the sentence belonging to negative class and positive class:

$$P(t|neg) = \frac{e^{W_{t,neg}}}{e^{W_{t,neg}} + e^{W_{t,pos}}} \quad (5)$$

$$P(t|pos) = \frac{e^{W_{t,pos}}}{e^{W_{t,neg}} + e^{W_{t,pos}}} \quad (6)$$

Finally, we propose a method based on emoticon aware aspect based weight lexicon and introduce a strategy to integrate emoticon aware aspect based weight lexicon method with naive Bayes method.

For every emoticon, we give a polarity value which can be negative or positive, a specific translation and a weight. This lexicon is showed in Table 1. We will use this emoticon lexicon in subsequent parts.

3.3 EMOTICON LEXICON TECHNIQUE (ELT) WORKFLOW FOR THE PROPOSED MODEL

In this emoticon pre-processing method, we just delete all the emoticons defined in emoticon lexicon in TABLE 1 from the training data.

Emoticon	Value	Translation	Weight
:) :D :-) :)	Positive	Happy	1
XD :]) (: ;)			
) =D =] :D			
^_^ (8 :o)			
(=o 8)			
:o) (= [:8D :]			
:o :O o:	Positive	Surprise	1
=P :P :P =P	Positive	Playful	1
:D :]	Positive	Wink	1
\m/	Positive	Salute	1
:(D: :((:)	Negative	Sad	-1
:[:(=[
=/ :/ \ :/ :/	Negative	Annoyed	-1
=\			
:(Negative	Crying	-1
:@	Negative	Angry	-1

This emoticon pre-processing method is pretty simple and straightforward. We give all the emoticons a 2-valued label: NEGATIVE or POSITIVE. We give a label of NEGATIVE to those emoticons with negative meanings and give a label of POSITIVE to those emoticons with positive meanings. This kind of translation is not so close to natural language, but it is more intuitive and robust

because it could avoid some translation errors. For both training data and test data, when we find any emoticon defined in emoticon lexicon, we replace it with its 2-valued labels in pre-processing.

From both training data and testing data, when we find any emoticon defined in emoticon lexicon, we replace it with its translation in pre-processing. For example, a review “This phone camera is so bright!! :)” are translated into “This phone camera is so bright!! happy” after pre-processing.

In polarity classification, we place a text into negative or positive class. Similarly, we use a polar weight to define an emoticon which is a character sequences. For an emoticon with positive meaning, we give it the value 1, otherwise, we give it the value -1. The format of an emoticon-weight lexicon is (emoticon, weight), for example, (:), 1), (:(-, -1).

When classifying a text, we consider both emoticons and verbal cues that speak on the aspect of the product, and combine the two factors to get an integrated assessment to the text review. The framework is as below [Figure 1]: Firstly, we load a set of reviews for analysing sentiment. Then, the classifier split it into different parts.

For each review, we check if this review contains emoticon.

We compare each word in the review with the emoticon lexicon entries. If there exist emoticons which match the emoticons in lexicon, we compute the emoticon score of this review and combine this score with words score. Otherwise, we just use the words score which is given by the NB classifier. When the review i contains emoticon, $ei = 1$, otherwise $ei = 0$. i.e.

$$e_i = \begin{cases} 0, \text{ no emoticon in review } i \\ 1, \text{ exist emoticon in review } i \end{cases} \quad (7)$$

For every review, the NB classifier gives us two probabilities $piw(neg)$ and $piw(pos)$ for classifying verbal cues. If $piw(neg) > piw(pos)$, the NB classifier places the review into negative class. Otherwise, the review is placed into positive class. When $ei = 1$, the emoticon score of ith review s_{ie} equals the sum of weights of each emoticon. Assuming that the number of emoticons in ith review is Ni ($Ni > 0$), and the weight of jth emoticon is W_{emoj} , we have:

$$S_{ie} = \sum_{j=1}^{ni} W_{emoj} \quad (8)$$

The emoticon-weight lexicon helps us to deal with only emoticons. The NB classifier deals with verbal cues. Hence, we need a combination strategy to combine

EWLM with NB classifier, to get a final classification result.

As above, s_{ie} is the sum of weight of emoticons in review i , which is not in the range of (0, 1). We use the Sigmoid function to convert the range of s_{ie} into a new range which is between 0 and 1, because we need to combine this value with a probability value which is between 0 and 1 given by the NB classifier. With Sigmoid function, we can compute P_{EWLM} :

$$P_{EWLM}(t|pos) = Sigmoid(S_{ie}) \quad (9)$$

$$P_{EWLM}(t|neg) = 1 - Sigmoid(S_{ie}) \quad (10)$$

The sentiment of both emoticons and verbal cues can be computed as a probability of being negative or positive. We use α as a factor, which decides the importance of the emoticon in a review, to integrate these two probabilities and get the final probabilities. $pi(pos)$ is the probability of the ith review being positive, and $pi(neg)$ is the probability of the ith review being negative. If $\alpha \geq 0.5$, verbal cues play a more important role. Otherwise, the emoticon occupies a greater proportion on analysing sentiment.

$$P_i(neg) = \alpha \times P_{NB(neg)} + (1 - \alpha) \times P_{EWLM}(neg) \quad (11)$$

$$P_i(pos) = \alpha \times P_{NB(pos)} + (1 - \alpha) \times P_{EWLM}(pos) \quad (12)$$

The classification ci of ith review is defined as a function of its final probabilities $pi(neg)$ and $pi(pos)$:

$$C_i = \begin{cases} \text{Positive,} & \text{if } P_i(pos) \geq P_i(neg) \\ \text{Negative,} & \text{if } P_i(pos) < P_i(neg) \end{cases} \quad (13)$$

4 RESULTS AND DISCUSSION

4.1 DATASET

The dataset for this paper is on Amazons Mobile review dataset which is a popular e-commerce site. The dataset is published on the Amazon website and it's available and can be downloaded from the website of Amazons. The dataset contains 2582 reviews with 35 emoticons of mobile reviews on Samsung S5.

4.2 EXPERIMENTAL DESIGN

The proposed model will use two techniques: Emoticon Lexicon Technique and Naïve Bayes Technique. The former will be used on the emoticons while the latter will be used on the text review. The sentiment polarity of the aspect is evaluated as positive and negative and neutral while the performance metrics will be evaluated on the

sentiment polarity by measuring the Accuracy, precision and recall.

4.3 EXPERIMENTAL RESULT

The experimental results clearly show the data distribution of aspect based on the sentiment polarity as positive, negative and neutral, it also shows the classification performance on the aspects measured in accuracy, precision and recall.

Table 2: Data Distribution of Sentiment Polarity on Aspects without Emoticon

Aspect	Positive	Negative	Neutral	Total
Camera	622	299	216	1,137
Battery	513	359	150	1,022
Memory	173	29	12	214
Sensor	149	51	9	209

Table 3: Data Distribution of Sentiment Polarity on Aspects with Emoticon

Aspect	Positive	Negative	Neutral	Total
Camera	719	269	149	1,137
Battery	699	259	64	1,022
Memory	187	19	8	214
Sensor	164	41	4	209

Table 4: Performance measure of the Aspects

Polarity	Accuracy	Precision	Recall
Without Emoticon	83.72%	78.12%	76.12%
With Emoticon	91.69%	89.23%	88.93%

5 CONCLUSION

This paper was able to propose a model for aspect based sentiment analysis with the incorporation of emoticons. After successful implementation of the model, this research was able to address some issues like misspelled words in reviews, consider neutral opinions and finally address issues where emoticon has a different idea with the text review it's associated with. The result of this study shows that the usage of emoticons improves the performance of the model with accuracy of 91.69%, Precision of 89.23% and recall value of 88.93% as compared to when emoticon is not considered which gives an accuracy value of 83.72%, Precision value of 78.12%

and a recall value of 76.12%. This paper only considers Accuracy, Precision and Recall; future paper can consider F1 measure. Future paper can as well consider conflict opinion in reviews and also make use of more dataset that contains more emoticons.

6 REFERENCES

- Jayasekara, I.R. and Wijayanayake, J.I (2016) Opinion Mining of Customer Reviews: Feature and Smiley Based Approach *International Journal of Data Mining & Knowledge Management Process (IJDMP)* Vol.6, No.1, January 2016 DOI : 10.5121/ijdkp.2016.6101
- Khairnar, J., and Kinikar, M. (2013) "Machine Learning Algorithms for Opinion Mining and Sentiment Classification", *International Journal of Scientific and Research Publications*, 2013.
- Kumar, A.D and Wala, T (2015) A Review Paper on Data Mining Techniques and Algorithms *International Journal of Advanced Research in Computer Engineering & Technology (IJARCET) Volume 4 Issue 5, May 2015* 1976 ISSN: 2278 – 1323.
- Kushwaha, L. and Rathod, S.D. (2016) "Opinion Mining of Customer Reviews based on their Score using Machine Learning Techniques", *International Research Journal of Engineering and Technology*, Volume: 03 Issue: 06, June 2016.
- Li, H., Peng, Q., and Guan, X. (2016) "Sentence level opinion mining of hotel comments", *The 11th International Conference for Internet Technology and Secured Transactions*, 2016.
- Lia, N. and Wu, D.D. (2010) "Using text mining and sentiment analysis for online forums hotspot detection and forecast", *Scientometrics*, Volume 85 Issue 3, December 2010, Pages 803-820, Springer-Verlag New York, Inc. Secaucus, NJ, USA.
- Medhat, W., Hassan, A. and Korashy, H. (2014) "Sentiment analysis algorithms and applications: A survey," *Ain Shams Engineering Journal.*, vol.5, no. 4, pp. 1093–1113, 2014.
- Mishra, P., Rajnish, R., and Kumar, P. (2016) "Sentiment analysis of Twitter data: Case study on digital India", *International conference on Information Technology (InCITe)- The Next Generation IT Summit*, 2016.
- Mukherjee, S. and Bhattacharyya, P. (2015) "Feature Specific Sentiment Analysis for Product Reviews", *International Conference on Intelligent Text Processing and Computational Linguistics*, pp 475-487.
- Nasukawa, T. and Yi, J. (2003) "Sentiment analysis: capturing favourability using natural language processing", *Proceedings of the 2nd international*



- conference on Knowledge capture, Pages 70-77, Sanibel Island, FL, USA — October 23 - 25, 2003.
- Rajeev P.V, Rekha V.S (2015) Recommending products to customers using opinion mining of online product and features. ICCPCT 2015 IEEE.
- Sobkowicz, P., Kascheskya, M., and Bouchardb, G. (2012) "Opinion mining in social media: Modeling, simulating, and forecasting political opinions in the web", Government Information Quarterly, pages 470-479, January 2012.
- Solainayagi, P. and Ponnusamy, R. (2018) To Improve Feature Extraction and Opinion Classification Issues in Customer Product Reviews Utilizing an Efficient Feature Extraction and Classification (EFEC) Algorithm *Indonesian Journal of Electrical Engineering and Computer Science* Vol. 10, No. 2, May 2018, pp. 587~595.
- Soni, S., Dubey, S., Tiwari, R., and Dixit, M. (2018) Feature Based Sentiment Analysis of Product Reviews Using Deep Learning Methods *International Journal of Advanced Technology & Engineering Research (IJATER)* www.ijater.com Volume 8, Issue 3, May 2018.
- Sindhu, C., Deo, S.N., Mukati, Y., Sravanthi, G., and Malhotra, S. (2018) Aspect Based Sentiment Analysis Of Amazon Product Reviews. *International Journal of Pure and Applied Mathematics*, Volume 118 No. 22 2018, 151-157.
- Wang, H., Can, D., Kazemzadeh, A., Bar, F. and Narayanan, S. (2012) "A system for realtime Twitter sentiment analysis of 2012 U.S. presidential election cycle", Proceedings of the 50th Annual Meeting of the Association for Computational Linguistics, pages 115–120, Jeju, Republic of Korea, July 2012.
- Mubarok, Adiwijaya, and Aldhi (2017) Aspect-based Sentiment Analysis to Review Products Using Naïve Bayes AIP Conference Proceedings 1867, 020060 (2017); doi: 10.1063/1.4994463

Parametric Oscillations in Electric Oscillatory System

*Enesi A.Y¹, Ejiogu. E. C²

¹Electrical Engineering Department, Federal University of Technology, PMB 65 Minna Niger State, Nigeria

²Electrical Engineering Department, University of Nigeria, Nsukka

*Corresponding author email: enesi.asizehi@futminna.edu.ng, +2348035671462

ABSTRACT

The paper presents the parametric oscillations generated in an electric oscillatory system. Parametric oscillations are oscillations that are periodically modulated with time. The modulation depth and the carrier frequency are investigated by MATLAB/Simulink Model developed from Mathieu's equation. With this Model, parametric oscillations are generated. The maximum and minimum amplitudes of oscillations for each characteristic number, a and the characteristic parameter, q is determined. The time taken for one oscillation (which is the period) for each characteristic number and characteristic parameter is determined. The relationship between the carrier frequency, the modulation depth and the characteristic number are established through graphical illustrations. These are approximate results of the solutions of Mathieu equation in electric oscillatory system.

Keywords: Carrier frequency, characteristic number, characteristic parameter, Mathieu's equation, modulation depth, parametric oscillations.

1 INTRODUCTION

The second order differential homogeneous equation or alternatively known as Mathieu's equation in canonical form (Figueroa & Torrentí, 2017) is applied in this paper for the purpose of explaining the parametric oscillation in electric oscillatory circuit. This equation is necessary for the description of the vibrating or oscillatory body. The Hill equation describes the vibration or the oscillation of electrical system or mechanical system. The generation of parametric oscillations in three-phase autonomous reluctance generator is discussed (Rabinovici, 2001). An autonomous induction generator generates self-oscillations (Hail, 1999). Electromechanical device develops parametric oscillatory motion (Russel, and Pickup, 1978) and parametric transformer (Tez & Smith, 1984) have the potential of generating parametric oscillations when excited. In this paper, the modulation depth and the carrier frequency are investigated by MATLAB/Simulink Model. In electrical system whose electric circuit consists of energy-storing elements such as the capacitor, inductor and the resistor, the component elements can be periodically modulated with time resulting in parametric oscillations using Mathieu's equation. Parametric oscillation is a stable phenomenon and they appear first before the appearance of the parametric resonance (the unstable phenomenon). The excitations of parametric oscillations generate the steady growth of amplitude of the oscillations with time resulting into unstable phenomenon known as parametric resonance. At natural frequency of a system, the system oscillates or vibrates as it maintains its stable condition. A system becomes unstable if it operates twice its fundamental natural frequency (Mclachian, 1951).

2 METHODOLOGY

The Mathieu's equation in canonical form is expressed as:

$$\frac{d^2 y}{dz^2} + (a + 2q \cos 2z)y = 0 \quad (1)$$

Equation (1) is in MATLAB/Simulink shown in Figure 1

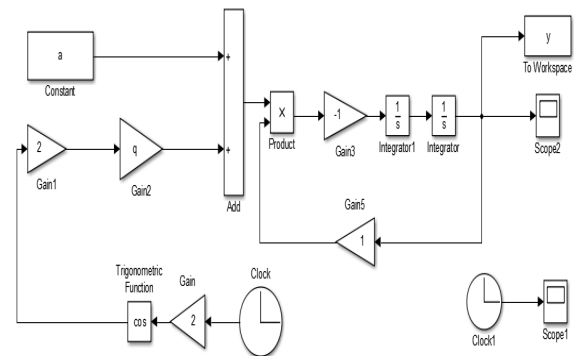


Figure 1: MATLAB/Simulink Model of Mathieu's equation

The time taken for one oscillation is called the period (in seconds). The period T is shown in Figure 2 when $a=0.1$ and $q=0.1$ and it is simulated for a 100 seconds. H_{\max} and H_{\min} are the maximum and the minimum amplitude of the oscillations generated. The difference between

H_{max} and H_{min} is the H_{diff} while the sum of H_{max} and H_{min} is denoted by H_{sum} . The parametric oscillations generated using Mathieu equation are investigated in Figure 3, 4, 5, 6, 7, 8 and Figure 9.

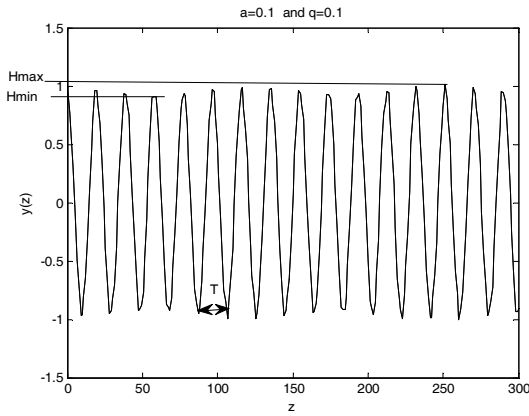


Figure 2: $a=0.1$ and $q=0.1$

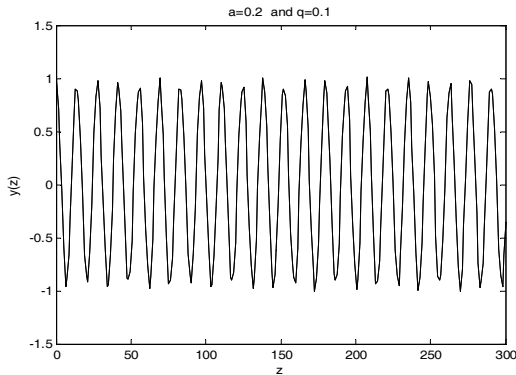


Figure 3: $a=0.2$ and $q=0.1$

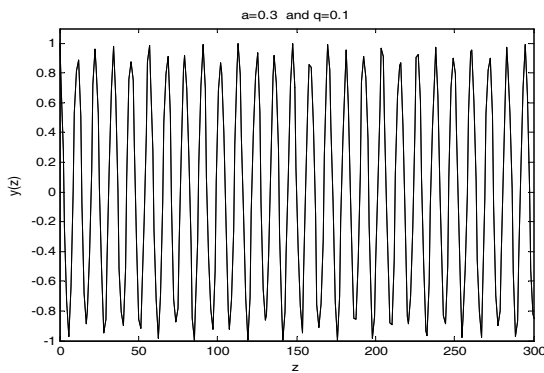


Figure 4: $a=0.3$ and $q=0.1$

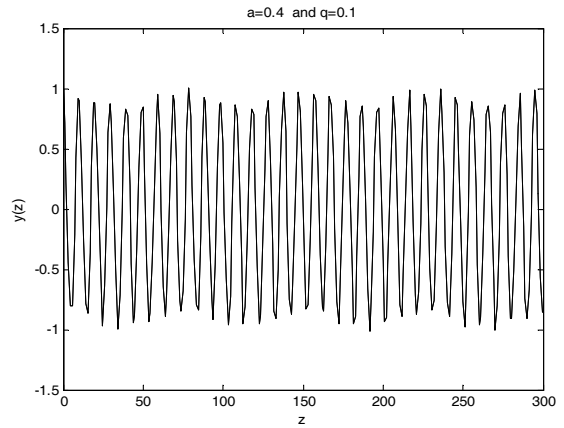


Figure 5: $a=0.4$ and $q=0.1$

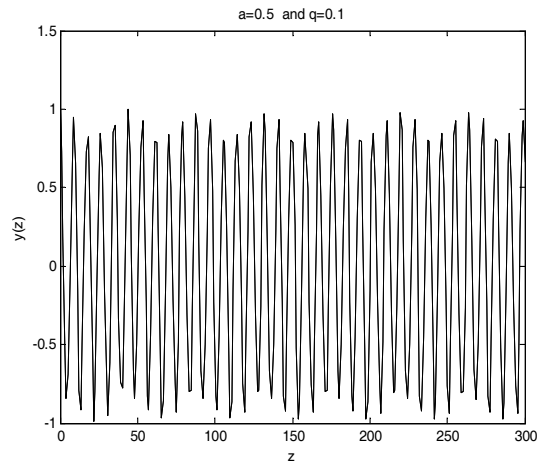


Figure 6: $a=0.5$ and $q=0.1$

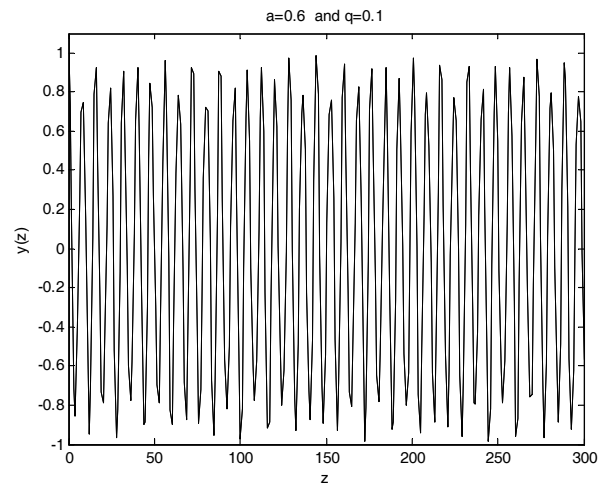


Figure 7: $a=0.4$ and $q=0.1$

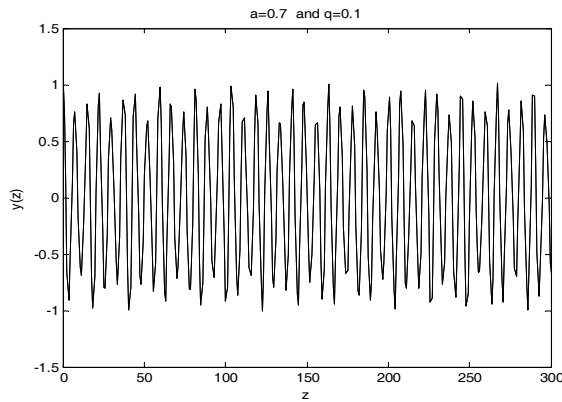


Figure 8: $a=0.7$ and $q=0.1$

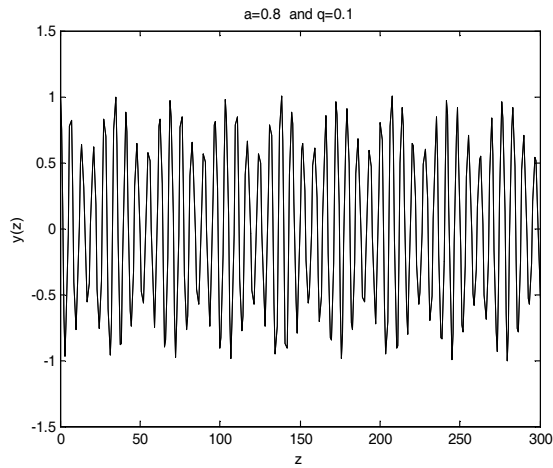


Figure 9: $a=0.8$ and $q=0.1$

2.1 RESULTS AND DISCUSSION

The results of the investigation are shown in Table 1

Table 1: Characteristic number and Modulation depth

a	H_{\max}	H_{\min}	H_{diff}	H_{sum}	$m = \frac{H_{\text{diff}}}{H_{\text{sum}}}$
0.1	1.017	0.9088	0.1082	1.9258	0.0562
0.2	1.011	0.8967	0.1143	1.9077	0.0599
0.3	0.998	0.8552	0.1428	1.8532	0.0771

0.4	1.003	0.8309	0.1721	1.8339	0.0938
0.5	1.002	0.7873	0.2147	1.7893	0.1200
0.6	0.9884	0.7482	0.2402	1.7366	0.1383
0.7	1.016	0.6538	0.3622	1.6698	0.2169
0.8	1.004	0.5377	0.4663	1.5417	0.3025

Table 2 shows the output data of period and carrier frequency

Table 2: Characteristic number, period and the carrier frequency

a	T_1 (sec)	T_2 (sec)	T (sec)	$w = \frac{2\pi}{T}$ (rad/s)
0.1	87.21	106.6	19.3900	0.3240
0.2	90.53	103.3	12.7700	0.4920
0.3	96.85	107.7	10.8500	0.5791
0.4	93.98	103.1	9.1200	0.6889
0.5	172.3	180.3	8.00	0.7854
0.6	140.9	148.4	7.5000	0.8378
0.7	181.4	188.8	7.4000	0.8491
0.8	99.99	106.9	6.9100	0.9093

Table 3 shows the characteristic number and the number of oscillations generated

Table 3: Characteristic number and the number of oscillations

a	Number of oscillations, (Nso)
0.1	16
0.2	22
0.3	27
0.4	31
0.5	34
0.6	38
0.7	41
0.8	44

Figure 10 shows the characteristic number versus the period of parametric oscillations. The characteristic number increases with the decrease in the period of oscillations.

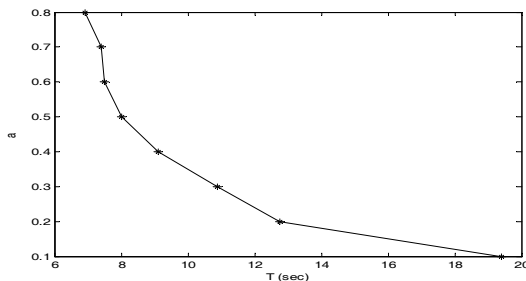


Figure 10: Characteristic number (a) versus period (T)

Figure 11 shows the modulation depth versus the carrier frequency. The carrier frequency increases as the modulation depth decreases.

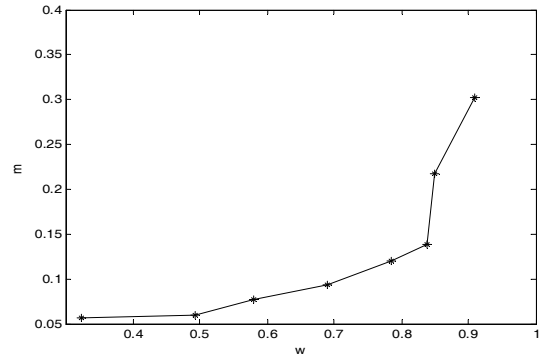


Figure 11: Modulation depth versus carrier frequency

Figure 12 shows the characteristic of the characteristic number versus the modulation depth and the carrier frequency. In Figure 12 (a), the modulation depth increases as the characteristic number increases. The carrier frequency in Figure 12 (b) increases gradually with the characteristic number.

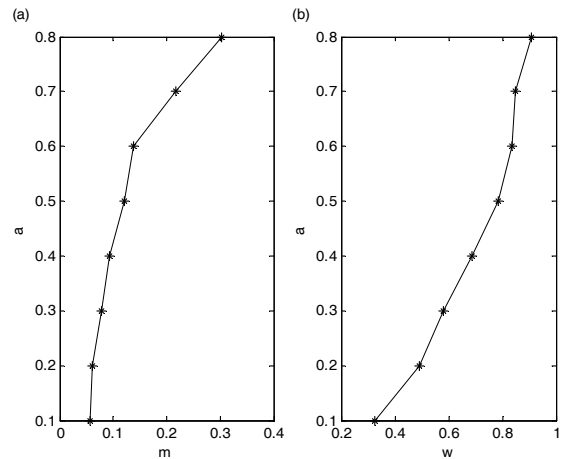


Figure 12: Characteristic number versus modulation depth and carrier frequency

CONCLUSION

The solutions to Mathieu equation in electric oscillatory system are in the form of amplitude modulated oscillations. MATLAB/Simulink is developed for the generation of parametric oscillations. The modulation depth and carrier frequency are computed experimentally. The characteristic number versus period, modulation depth versus the carrier frequency are plotted graphically for various combinations of the coefficient of a and q . The graphical results show the



approximate solution of Mathieu equation in electric oscillatory circuit using energy conversion system.

REFERENCES

- Figueroa, D. G., & Torrentí, F. (2017). Parametric resonance in the early Universe - A fitting analysis, *Journal of Cosmol. Astropart Phys*, 2(1), 1–41
- Hail, B. (1999) Starting Oscillations of an Autonomous Induction Generator, *IEEE Trans. Magn.* 35(5), 3562–3564.
- Mclachian, N. W. (1951). *Theory and Application of Mathieu Functions*, Oxford Univ. Press. Amen House, London. 1–423
- Rabinovici, R. (2001) Three-phase autonomous reluctance generator, *IEE Proceedings*, 148(5), 438–442
- Russel, A. P., & Pickup, I. E.D. (1978). Parametric oscillatory motion in electromechanical devices, *Proc. IEE*, 124(4), 269–277.
- Tez, E. S., & Smith, R. (1984). The Parametric Transformer: A Power Conversion Device Demonstrating the Principles of Parametric Excitation, *IEEE Trans. Education*, 2(2), 56–65.



Fenestration Effect on the Adequacy of Classroom UDD

* Azodo, A.P.¹, Onwubalili, C², & Mezue T.C.³

¹Department of Mechanical Engineering, Federal University of Agriculture, P. M. B. 2240, Abeokuta, Ogun state

^{2,3}Department of Electrical and Electronic Engineering, Federal Polytechnic Oko, P. M. B 021, Anambra State

*Corresponding author email: azodopat@gmail.com, +2348139513021

ABSTRACT

The design properties of any building which describes the space characteristics include the openings, orientation, and location. These determine among other things the illuminance and daylight distribution of the indoor space. This study evaluated the effect of building fenestration on students' work plane daylight illuminance distribution. Point to point illuminance measurements was carried out on the students' work plane using a Sunche digital luxmeter of model HS1010 on an hourly basis from 8:00 am – 5:00 pm and clear sky conditions. Analysis of the illuminance data obtained showed that the range of useful daylight illuminance (UDI) distribution in the one-sided and two adjacent-sided window oriented classroom were unevenly distributed as more UDI 'fell-short' (< 100 lux) and UDI autonomous (> 300 and < 3000 lux) were respectively experienced towards the windowless and window side of the classrooms. The two opposite-sided window oriented classrooms observed comparatively efficient illuminance distribution but more UDI 'fell-short' in the middle column. The independent t-test between the daylight factor of the one-side and the two-sided window classrooms irrespective of the orientation at a confidence level of $p < 0.05$ were invariably significant. It was also invariably significant between the two opposite-sided (north-south) and two adjacent-sided (west-south) window oriented classrooms. However, it was not significant between the two north-south window oriented classrooms. The illuminance and light distribution variation in the three building fenestration categories is an indication of its effect on the classroom space usable potential and visual safety.

Keywords: *Illuminance, grid, orientation, positioning, opening.*

1 INTRODUCTION

Daylighting system represents the predominant source of illuminance for visual concerned academic need purposes in classroom buildings in Nigeria. The daylight is basically the utilization of sunlight illumination which naturally enters into space through the structural design openings; windows, doors, and skylights (Pulay, 2010). This according to Yacan (2014) is mostly preferred during the day time hours due to the quality of light and sustainability it offers in schools. Other advantages daylighting system offers include aversion of artificial lighting installation expenses and operational cost, reduction of energy consumption and environmental problems associated with the use of fossil fuels for artificial lighting of buildings (Lim et al., 2012; İnan, 2013; Drosou et al., 2016). On the part of the occupants and the indoor visual activities, daylighting provides full-spectrum of light most appropriate for the visual stimulus and response, facilitates environmentally friendliness of an indoor space, the health, safety, work performance and productivity of the occupants (Galasiu and Veitch, 2006; Cheung and Chung, 2008; Kim et al., 2012; Dianat et al., 2013). Where the lighting system is inadequate it can cause discomfort to the occupants which affects not only performances of visual concern task but also the general indoor work

(Parsons 2000). This explains the important effect of building fenestration on the light admittance and maximum daylighting illumination and performance of an indoor space (Li, 2010 and Azodo, 2017). The maximization of daylighting system for safe and convenient visual academic work on the student's work plane requires that the openings and their positioning be characteristically considered at the design stage of the building. The impact of inappropriate consideration of the illuminance source in the design plan of a building is disposed to illumination challenges of eventual source decided on. Illuminance recommendation in classrooms is specific with the work task involved for the characteristics regulatory usefulness potentials. The recommended adequate level of illuminance for indoor spaces such as offices, classrooms and library, where the occupants spend at least one-third of the day is 300 lux (IESNA, 2011). Daylight illuminances at 300 to 3000 lux range technically referred to as UDI autonomous is a level where additional lighting supplement (artificial lighting) will most likely not be needed (Mardaljevic et al., 2012). Light distribution in the workspace through the provision of good lighting as stated by Ibañez et al. (2017) guarantees a good view of the tasks as such allows the tasks to be carried out easily and comfortably. The daylight performance evaluation is contingent on the illuminance levels under several sky conditions. Effectual daylighting



and maximization of the natural illumination level is estimated by point to point calculation using indoor and exterior illuminance described based on the daylight factor (DF) (Inan, 2013). Reinhart and Weissman (2012) stated that DF is an established parameter for indoor daylight analysis for benefits certainty of interior illuminating from daylight. This is usually obtained from the information on the amount of daylight available outside the building. The significant criterion for health and safety establishment of daylighting in a space is illuminance distribution. Studies in this area of research focused on the climate-based daylighting factors, illuminance evaluation using the grid measurement points technique with specifics on the use of DF measurement (Nabil and Mardaljevic, 2005; Reinhart et al., 2006; Barret and Zhang, 2009; Mardaljevic et al., 2009; IESNA, 2011; Mardaljevic et al., 2012; Inan, 2013; Yükses et al., 2015; Paraskeva and Vakouli, 2016; Azodo, 2017). However, there is no studies found in literature that considered comparisons of students' work plane illuminance for the established the certainty benefits of interior illumination from daylight in classrooms as a result of building fenestration. It is on the basis of this background knowledge that this study was conducted to evaluate the effect of building fenestration on students' work plane daylight illuminance distribution and visual safety.

2 METHODOLOGY

This illuminance survey which evaluated the impact of the classroom building openings orientation on students' work plane illuminance level and daylight distribution was conducted in four selected classrooms in Federal University Wukari, Taraba state, Nigeria. The geographical coordinates of Wukari town is on latitude 7°51'N to 7°85'N and longitude 9°46'E to 9°78'E and at an altitude of 189 meters. The geographical location of Wukari is within Southern Guinea Savannah vegetation zones with dry season experienced from November to

are 28 - 35 °C and 90 - 1400 mm respectively (Azodo, 2018).

The instrumentation designs for this study were as follows:

- i. A Garmin GPS 72H high-sensitivity handheld floatable global positioning system (Garmin Ltd. Kansas, United States). This was used to take the respective coordinates of the study site location (classrooms).
- ii. Sunche model HS1010 digital luxmeter with a sampling frequency of 2 times per sec and a high precision wide measurement range of 1 - 1200,000 lux (Shanghai Industrial Co., Ltd, Shanghai) was used for point to point illuminance measurement performed at the top of the students' desk (work plane).
- iii. Generic 5m retractable measuring tape rule (Generic Manufacturing Corporation, Temecula California, USA) was used for grid point (point to point) measurement distances on the students work plane, height of the desks and window dimensions.
- iv. Delectable marker pen (Ningbo Becol Stationery & Gifts Co., Ltd. Zhejiang, China), this was used to indicate grid point (point to point) measurement distances for measurement point consistency.
- v. A digital professional handheld LCD stopwatch (Shenzhen super deal Co. Ltd, China) was used for timing of the measurement intervals at each grid point.

The specifications of the classrooms such as location (geographical coordinates), seat capacity, classroom dimensions, window positioning and orientations were noted and presented in table 1. The daylight admittance factors in the classrooms which were the glazing areas (doors and window openings) are presented in table 2. Details of the number of illuminance measurement grids considered in each of the four classrooms assessed is presented in table 3. The general specification shared among the three classrooms assessed were three columns arrangement of the students' desk, approximate desk and window seat heights of 0.85 m and 0.92 m respectively.

TABLE 1. THE SPECIFICATIONS OF THE CLASSROOMS

Classrooms	GPS Locations		Capacity		Window	
	Lat.	Long.	Dimension (m ³)	Seat	Characteristics	Orientation
MPB LR 001	7.8440636	9.7752578	278.00	103	Two-sided	West-South
MPB LR 002	7.8440661	9.7751708	279.76	103	One-sided	West
Block A LR 2	7.8437213	9.7764955	253.90	91	Two-sided	North-South
Block A LR 3	7.8437254	9.7763212	262.30	91	Two-sided	North-South

March and the wet season from April through to October. The mean annual temperature and annual rainfall ranges

TABLE 2. DAYLIGHT ADMITTANCE FACTORS OF THE CLASSROOMS

Classrooms	No of doors	No of windows		Per door (m2)	Per Window (m2)	Glazing area (m2)	Wall area (m2)
MPB LR 001	2	5 West	3 South	1.6	1.32	15.16	51.87
MPB LR 002	2	5 West	-	2.3	1.32	11.20	53.48
Block A LR 2	2	2 South	2 North	2.3	1.32	8.48	117.12
Block A LR 3	2	2 South	2 North	2.3	1.32	8.48	186.50

TABLE 3. NUMBER OF ILLUMINANCE MEASUREMENT GRIDS

Classrooms	Number of measurement grid			
	Column 1	Column 2	Column 3	Total
MPB LR 001	31	36	36	103
MPB LR 002	31	36	26	103
Block A LR 2	28	35	28	91
Block A LR 3	28	35	28	91

The grid points for the illuminance measurement were 0.26 m from the edges of the desk and 0.53 m between the grids. The gaps between the desks along the rows are approximately 0.86 m and 0.55 m from the wall. However in MPB LRs 001 and 002 the desks along the window sides are aligned to the wall. For each of the measurements taken along the rows inside the classrooms, an outside measurement was also taken. The outside measurements were aligned to the rows of the classroom desks and on a stole positioned at the commensurate height (0.85 m) with the desks. The measurements were carried out on hourly basis in the classroom on the grids and outside the classrooms (along the corridors) from 8:00 am – 5:00 pm on clear sky condition. The illuminance measurements were conducted during the students' vacation to avoid human shadow effect.

The useful daylight illuminance (UDI) scheme was applied on the data collected at each grid for the evaluation of the occurrence of daylight levels. Table 4 shows the useful daylight illuminance subdivision in the UDI scheme for the various ranges of experienced illuminance levels used for the analysis of useful daylight illuminance data obtained from the illuminance survey data obtained in this study.

TABLE 4. USEFUL DAYLIGHT ILLUMINANCE (UDI) SCHEME FOR A RANGE OF EXPERIENCED LEVELS

Illuminance subdivided range	UDI interpretation	Abbreviation
< 100 lux	UDI 'fell-short'	UDI-f
> 100 and < 300 lux	UDI supplementary	UDI-s
> 300 and < 3000 lux	UDI autonomous	UDI-a
> 3000 lux	UDI exceeded	UDI-e

Mardaljevic et al. (2012)

The daylight factor is a parameter which helps to establish the benefits interior illumination certainty from daylight as a result of building fenestration was calculated using Eq. (1) (Vincenc and Mitas, 2017) on the data obtained for illuminance inside and outside of the classrooms as follows

$$D = \frac{E}{E_h} \quad (1)$$

Where

D = daylight factor (%),

E_h = inside illuminance (lux),

E = outside illuminance (lux).

With the use of SPSS version 16.0 and Microsoft Excel version 2007 software, the analysis in this study was carried out. Multiple independent-sample t-test analyses were used on the daylight factor variables obtained at each grid for illuminance comparisons between a) the two adjacent-sided (West-South) window oriented classroom and the two opposite-sided (North-South) window oriented classroom b) the two adjacent-sided (West-South) window oriented classroom and the one-side (West) window oriented classroom c) the one-side (West) window oriented classroom and the two opposite-sided (North-South) window oriented classroom and d) between the two opposite-sided (North-South) window oriented classroom, The level of significance was set at $p < 0.05$.

3 RESULTS AND DISCUSSION

The descriptive statistics of the illuminance data obtained using the digital luxmeter from the four classrooms assessed presented in table 5 includes the minimum, maximum, mean and std. deviation. The fenestration of Block A LR 2 and 3, two opposite-sided window oriented classrooms (see figure 3), allow sunlight entrance in the classrooms from the two sides. These observed higher illuminance at the window side columns in the classrooms (columns 1 and 3) compared to the middle columns (column 2) (Table 5). In MPB 002 (West window oriented classroom) and MPB 001 (West-South window oriented classroom), it was observed that the illuminance of the windowless side column 1, was comparatively lower compared to that of columns 2 and 3 (Table 5)

TABLE 5. THE DESCRIPTIVE STATISTICS OF THE ILLUMINANCE OF THE CLASSROOMS ASSESSED

Classrooms	Column	N	Minimum	Maximum	Mean	Std. Deviation
MPB 001	1	341	50.00	740.00	191.79	137.43
	2	396	61.00	1331.00	329.26	216.76
	3	396	56.00	12940.00	872.04	1292.78
MPB002	1	341	52.00	559.00	117.09	60.21
	2	396	52.00	7140.00	340.59	798.69
	3	396	52.00	26100.00	1068.9	2099.22
Block A LR 2	1	280	85.00	1988.00	532.89	357.75
	2	350	87.00	414.00	202.93	49.82
	3	280	109.00	532.00	245.32	63.43
Block A LR 3	1	280	85.00	1988.00	535.61	360.26
	2	350	84.00	415.00	203.59	50.82
	3	280	111.00	543.00	243.97	65.5

Analysis of the data obtained on a range of experienced levels of useful daylight illuminance (UDI) scheme (see table 4) in the classrooms assessed it was found that MPB 002 classroom which is a one-side window oriented classroom recorded the maximum number of UDI “fell short” of useful daylights especially at the windowless side (column 1) (Table 6). The UDI “fell short” drops from the windowless side to the windowed side while the UDI autonomous illuminance drops from the window side to the windowless side. Similar observation was found in Azodo (2017). This observation agreed with Li (2010) study that in a one-sided window room, the daylight is likely to be more nearly proportional to the amount of daylight falling on the window, compared to the external horizontal daylight illuminance. With reference to table 4 specifics, the UDI “fell short” is within the range of < 100 lux. Illuminance of this range according to Mardaljevic et al. (2012) is generally considered insufficient to serve as sole source of illumination nor contribute significantly to artificial lighting. Insufficiency of illuminance observed in the one-side windowed classroom in study falls within the bound of Figueiro et al. (2004) study who noted that the use of daylight from side windows as the primary source of illumination of a space reduces the usable potential of the classroom space as the illuminance level at the windowless side is not safe to visual need in the classroom. This same observation was made in MPB 001 classroom which was a West-South window oriented classroom with proportion of 24.6% of the illuminance along the windowless column (column 1) (Table 6). Whereas the Block A LRs 2 and 3, UDI “fell short” was high and UDI autonomous illuminances low in the middle column compared to window side columns (columns 2 & 3). This implies that when the illumination from the sunlight is low, it results to

low illuminance in the middle row for Block A LRs 2 and 3 and the windowless side of MPB 001 and 002 LRs but improves when it is high. Across the table, for the experienced illuminance range of > 100 and < 300 lux, MPB 001 and MPB 002 recorded higher UDI supplementary illuminance compared to the two-sided classrooms, Block A LRs 2 and 3. However, Block A LRs 2 and 3 have higher autonomous range of experienced levels of useful daylight illuminance. Applying the specific useful daylight illuminance (UDI) scheme and the associated interpretation (see table 4) that UDI range of > 100 and < 300 lux is useful, it cannot serve as sole source of illumination as such requires additional artificial lighting to supplement the daylight for safe academic need purposes particularly reading. There was no case of UDI exceeded in Block A LRs 2 and 3. However, the range of experienced levels of UDI exceeded was recorded in MPB 001 and MPB 002 classrooms predominantly at the column 3. This can be attributed to the higher number of windows on the west window side of the classrooms and sunset effect. The UDI exceeded range experienced is most likely to produce either visual and/or thermal discomfort to the space occupants. The overall analysis of the range of experienced levels of useful daylight illuminance scheme in the classrooms showed the UDI ‘fell-short’ are more towards the windowless side of the classrooms whereas the UDI autonomous proportion are towards the window side in MPB 001 and MPB 002 classrooms. The distribution seemed better in Block A LRs 2 and 3 with less UDI autonomous and high UDI supplementary proportion for the middle column. This agrees with Inan (2013) that the fenestration of a building affects the distribution of daylight into the building.

TABLE 6. ANALYSIS OF THE ILLUMINANCE DATA ON THE UDI RANGE OF EXPERIENCED LEVELS SCHEME

Illuminance analysis	Columns in the classrooms											
	Block A Rm 2 (n (%))			MPB 001 (n (%))			MPB 002 (n (%))			Block A Rm 3 (n (%))		
	1	2	3	1	2	3	1	2	3	1	2	3
UDI-f	29(9.4)	44(11.4)	26(8.4)	84(24.6)	20(5.1)	5(1.3)	152(44.6)	3(0.8)	3(0.8)	29(9.4)	47(12.2)	28(9.1)
UDI-s	60(19.5)	336(87.3)	230(74.7)	191(56.0)	211(53.3)	52(13.1)	181(53.1)	299(75.5)	56(14.1)	62(20.1)	334(86.8)	231(75.0)
UDI-a	219(71.1)	5(1.3)	52(16.9)	66(19.4)	165(41.7)	306(77.3)	8(2.3)	88(22.2)	321(81.1)	217(70.5)	4(1.0)	49(15.9)
UDI-e	0.0(0.0)	0.0(0.0)	0.0(0.0)	0.0(0.0)	0.0(0.0)	33(8.3)	0.0(0.0)	6(1.5)	16(4.0)	0.0(0.0)	0.0(0.0)	0.0(0.0)
Total	308(100)	385(100)	308(100)	341(100)	396(100)	396(100)	341(100)	396(100)	396(100)	308(100)	385(100)	308(100)

Considering building daylight illuminance and light distribution as a factor of building fenestration, the certainty of interior illuminating from the daylight source was determined by independent-sample t-test using the daylight factor analysis and comparing the illuminance data obtained in the classrooms assessed. Simple comparisons made between the MPB 001 and 002 LRs to see whether the means of two groups are statistically

different from each other at 95% confidence level, has p-value = 0.00 which is less than 0.05, meaning that there is statistical significant difference between the means of MPB 001 and MPB 002 classrooms. This may be attributed to illuminance distribution variation on the students work plane in the classrooms as a result of the one-sided window property of MPB 002 classroom and two-sided window property of MPB 001.

TABLE 7. INDEPENDENT SAMPLE T-TEST FOR ILLUMINANCE BETWEEN MPB 001 AND MPB 002

Descriptive statistics					t-test for equality of means		
Classrooms	N	Mean	Std. Deviation	Std. Error Mean	t	df	P-value (Sig. (2-tailed))
MPB 001	90	19.58	12.86	1.36	-4.22	96.72	0.00
MPB 002	90	47.62	61.71	6.50			

In table 8, the daylight factor mean score for MPB 002 is 47.62 and 14.19 in Block A LR 2 classrooms, From the standard deviations it was observed that there is variation in the daylight factor computed from the illuminance data is a wider for MPB 002 classroom (SD = 6.50) than the

relationship Block A LR 2 (SD = 0.50). An independent t-test between MPB 002 and Block A LR 2 was found to be significant, $t(158) = 4.52$, $p < 0.05$. This suggests that there is significant difference between daylight factor for the certainty of interior illuminating from daylight of the two classrooms.

TABLE 8. INDEPENDENT SAMPLE T-TEST FOR ILLUMINANCE BETWEEN MPB 002 AND BLOCK A LR 2

Descriptive statistics					t-test for equality of means		
Classrooms	N	Mean	Std. Deviation	Std. Error Mean	t	df	P-value (Sig. (2-tailed))
MPB 002	90	47.62	61.71	6.50	5.13	90.04	0.00
Block A LR 2	70	14.19	4.16	0.50			

The independent t-test results between MPB 001 and Block A LR 2 classrooms showed that the daylight factor of Block A LR 2 classroom had lower daylight factor value (M = 14.19, SD= 4.16) than the daylight factor value of MPB 001 classroom (M = 19.58, SD = 12.86) (Table 9) at p-value = 0.00. Since $p < 0.05$ is less than the considered significance level $\alpha = 0.05$, the mean daylight factor for the certainty of interior illuminating from daylight between MPB 002 and Block A LR 2 is significantly different.

The independent t-test used to determine whether the certainty of classroom space illuminance from daylight in the MPB 001 classroom was statistically different from that of Block A LR 3 classroom showed that MPB 001 classroom (mean = 19.58 ± 12.86 , SEM = 1.36) had statistically higher mean values (mean = 14.56 ± 4.57 , SEM = 0.55) compared to Block A LR 3 classroom which was significant at confidence level of $p < 0.05$ (Table 10).

of building structure. The overall anSAFEalysis of the

TABLE 9. INDEPENDENT SAMPLE T-TEST FOR ILLUMINANCE BETWEEN MPB 001 AND BLOCK A LR 2

Descriptive statistics					t-test for Equality of Means		
Classrooms	N	Mean	Std. Deviation	Std. Error Mean	t	df	P-value (Sig. (2-tailed))
MPB 001	90	19.58	12.86	1.36	3.73	111.99	0.00
Block A LR 2	70	14.19	4.16	0.50			

TABLE 10. INDEPENDENT SAMPLE T-TEST FOR ILLUMINANCE BETWEEN MPB 001 AND BLOCK A LR 2

Descriptive statistics					t-test for Equality of Means		
Classrooms	N	Mean	Std. Deviation	Std. Error Mean	t	df	P-value (Sig. (2-tailed))
MPB 001	90	19.58	12.86	1.36	3.43	116.28	.001
Block A LR 3	70	14.56	4.57	0.55			

In table 11, the illuminance mean score for MPB 002 is 47.62 and 14.56 in Block A LR 3, From the standard deviations it was observed that there is variation in the illuminance data is a wider for MPB 002 classroom (SD = 61.71) than the relationship Block A LR 2 (SD = 4.57).

An independent t-test between MPB 002 and Block A LR 3 was significant, $t(90.25) = 5.07$, $p < 0.05$. This suggests that there is significant difference between daylight factor for the certainty of classroom space illuminance from daylight of the two classrooms.

TABLE 11. INDEPENDENT SAMPLE T-TEST FOR ILLUMINANCE BETWEEN MPB 002 AND BLOCK A LR 2

Descriptive statistics					t-test for equality of means		
Classrooms	N	Mean	Std. Deviation	Std. Error Mean	T	Df	P-value (Sig. (2-tailed))
MPB 002	90	47.62	61.71	6.50	5.07	90.25	0.00
Block A LR 3	70	14.56	4.57	0.55			

The independent t-test used for the comparisons between the Block A LR 2 and 3 classroom whether the means of two groups, or conditions to see if they are statistically different from one other at 95% confidence level, has p -value = 0.62 which is greater than 0.05,

meaning that there is statistical significant difference between the means of Block A LR 2 and 3 (Table 12). This suggest that illuminance distribution on the students work plane in the classrooms as a result of the two-sided window property of Block A LR 2 and 3 classroom

TABLE 12. INDEPENDENT SAMPLE T-TEST FOR ILLUMINANCE BETWEEN BLOCK A LR 2 AND 3 CLASSROOM

Descriptive statistics					t-test for equality of means		
Classrooms	N	Mean	Std. Deviation	Std. Error Mean	t	Df	P-value (Sig. (2-tailed))
Block A LR 2	70	14.19	4.16	.50	-.50	136.83	0.62
Block A LR 3	70	14.56	4.57	.55			

4 CONCLUSION

The point to point illuminance quality and daylight distribution assessment carried out using a digital luxmeter on an hourly basis from 8:00 am – 5:00 pm under clear sky conditions basis on the students' classroom work plane in this study was compared among three different categories

the range of experienced levels of useful daylight illuminance scheme in the classrooms showed the UDI 'fell-short' are more towards the windowless side of the classrooms whereas the UDI autonomous proportion are towards the window side in one side window oriented classroom (MPB 001) and two-side adjacent windowed classroom (MPB 002). The illuminance distribution is



better in Block A LRs 2 and 3 but with less deficient illuminance distribution in the middle column. This study concluded that fenestration of the building has effect on the illuminance level of the classroom environment as the two opposite-sided window oriented classrooms provided better illuminance level and light distribution potentially usable for classroom space which can serve as sole source of illumination in a classroom. It is recommended that further studies be carried out that will have representation of at least two buildings on each of the fenestration category.

REFERENCES

- Azodo, A. P. (2017). Illuminance and daylight distribution assessment for learners' comfort and safety in one-side-window oriented classroom building. *Arid Zone Journal of Engineering, Technology and Environment*, 13(5), 567-576.
- Azodo A. P., Ismaila S. O., Nwonodi, R. I. Owoeye, F. T. & Jibatswen, T. Y. (2018). Object-based approach in the assessment of thermal sensation and physiological stress through the eye of eco-city design and land cover type: the case of Wukari, Taraba state. Proceedings of the National Engineering Conference 2018, Faculty of Engineering, Ahmadu Bello University, Zaria,
- Barrett, P. & Zhang Y. (2009). Optimal Learning Spaces Design Implications for Primary Schools. Salford Centre for Research and Innovation in the built and human environment SCRI, England: Design and Print Group, University of Salford, Maxwell 100, Salford, M14 5WT.
- Cheung, H. D., & Chung, T. M. (2008). A study on subjective preference to daylit residential indoor environment using conjoint analysis. *Building and Environment*, 43(12), 2101-2111.
- Dianat, I., Sedghi, A., Bagherzade, J., Jafarabadi, M. A., & Stedmon, A. W. (2013). Objective and subjective assessments of lighting in a hospital setting: implications for health, safety and performance. *Ergonomics*, 56(10), 1535-1545.
- Drosou, N., Brembilla, E., Mardaljevic, J., & Haines, V. (2016). Reality bites: measuring actual daylighting performance in classrooms. In: PLEA 2016: 32nd International Conference on Passive and Low Energy Architecture Los Angeles. Los Angeles, 2016.
- Galasiu, A. D., & Veitch, J. A. (2006). Occupant preferences and satisfaction with the luminous environment and control systems in daylit offices: a literature review. *Energy and Buildings*, 38(7), 728-742.
- Ibañez, C. A., Zafra, J. C. G., & Sacht, H. M. (2017). Natural and Artificial Lighting Analysis in a Classroom of Technical Drawing: Measurements and HDR Images Use. *Procedia engineering*, 196, 964-971.
- Illuminating Engineering Society of North America (IESNA) (2011), Lighting Measurement e Spatial Daylight Autonomy, Illuminating Engineering Society of North America, New York, NY.
- İnan, T. (2013). An investigation on daylighting performance in educational institutions. *Structural Survey*, 31(2), 121-138.
- Kim, G., Lim, H. S., Lim, T. S., Schaefer, L., & Kim, J. T. (2012). Comparative advantage of an exterior shading device in thermal performance for residential buildings. *Energy and buildings*, 46, 105-111.
- Li, D. H. (2010). A review of daylight illuminance determinations and energy implications. *Applied Energy*, 87(7), 2109-2118.
- Lim, Y. W., Kandar, M. Z., Ahmad, M. H., Ossen, D. R., & Abdullah, A. M. (2012). Building façade design for daylighting quality in typical government office building. *Building and Environment*, 57, 194-204.
- Mardaljevic, J., Andersen, M., Roy, N., & Christoffersen, J. (2012). Daylighting metrics: is there a relation between useful daylight illuminance and daylight glare probability? In *Proceedings of the building simulation and optimization conference BSO12* (No. CONF).
- Mardaljevic, J., Heschong, L., & Lee, E. (2009). Daylight metrics and energy savings. *Lighting Research & Technology*, 41(3), 261-283.
- Musa, Y. N., Reuben, J., Sa'adu, M., & Makinta, U. (2014) Assessment of the effect of chemical crop protection techniques adoption on the income of maize farmers in Wukari Local Government Area of Taraba State, Nigeria. *Dutse Journal of Agriculture and Food Security*, 1(1), 36-41.
- Nabil, A., & Mardaljevic, J. (2005). Useful daylight illuminance: a new paradigm for assessing daylight in buildings. *Lighting Research & Technology*, 37(1), 41-57.
- Paraskeva, P. & Vakouli, V. (2016). Skylights in classrooms, optimal design for a cold climate through daylighting and energy simulations. Master thesis in Energy-efficient and Environmental Buildings, Faculty of Engineering, Lund University.
- Parsons, K. C. (2000). Environmental ergonomics: a review of principles, methods and models. *Applied ergonomics*, 31(6), 581-594.
- Pulay, A. S. (2010). Awareness of daylighting on student learning in an educational facility. University of Nebraska - Lincoln, Lincoln.



3rd International Engineering Conference (IEC 2019)
Federal University of Technology, Minna, Nigeria



-
- Reinhart, C. F., Mardaljevic, J., & Rogers, Z. (2006). Dynamic daylight performance metrics for sustainable building design. *Leukos*, 3(1), 7-31.
- Reinhart, C. F., & Weissman, D. A. (2012). The daylit area—Correlating architectural student assessments with current and emerging daylight availability metrics. *Building and Environment*, 50, 155-164.
- Vincenec, J. & Mitas, M. (2017). The effect of blinds on workplace illuminance. *MATEC Web of Conferences* 125, 02024, 1-4.
- Yacan, S. D. (2014). *Impacts of daylighting on preschool students' social and cognitive skills*. Masters Dissertation the Graduate College at the University of Nebraska.
- Yüksek, I., Görgülü, S., Kocabey, S., Tuna, M. & Dursun, B. (2015). Assessment of daylight performances of classrooms: a case study in Kırklareli University, Turkey. *Light and Engineering*, 23(1), 15 - 24.



Prediction of Upper Limb Functional Ability in Post-Traumatic Patients Using Machine Learning.

Zaiyanu Nuhu¹, Yeong Che Fai², Elijah David Kure³, Ibrahim B. Shehu¹, Mahmoud Mustapha¹,
Rabiu Al-Tanko¹, Khor Kang Xiang⁴

¹Department of Electrical/Electronic Engineering, Nuhu Bamalli Polytechnic Zaria, Kaduna State

²Control and Mechatronics Engineering Department, Universiti Teknologi Malaysia

³Department of Computer Engineering, Nuhu Bamalli Polytechnic Zaria, Kaduna State

⁴Techcare Innovation Sdn Bhd, Johor, Malaysia

Corresponding Author: ¹zayyan3168@gmail.com

ABSTRACT

Rehabilitation robots have become increasingly popular for stroke rehabilitation. However, the high cost of robots hampers their implementation on a large scale. The various types of wrist rehabilitation robots available are mostly tailored for post-stroke patients although there are other patients with similar physiotherapy needs who suffered from different muscular-skeleton ailments such as Parkinson's disease, Tennis Elbow and Trigger Finger. Hence the need to establish whether a single robot can be used in the treatment and rehabilitation of such ailments, thereby cutting cost and manpower, enhancing the efficiency of rehabilitation activities, improving Turn-Around-Time (TAT) and providing accurate data for comparison and analysis. This paper provided a machine learning-based assessment for the prediction of the upper limb functional ability in such patients, to assist caregivers to determine the extent of rehabilitation level required for respective patients and investigate the effectiveness of Compact Rehabilitation Robot (CR2-Haptic) in the rehabilitation of such patients. Six patients were assessed at the Universiti Teknologi Malaysia Clinic (PKU) over a period of time and their corresponding relative upper limb functional ability determined and six healthy subjects were also assessed as a basis for comparison. The availability of the therapy also increased the frequency of clinical therapy, indicating an improvement in TAT. The recovery of the post-traumatic patients was evaluated based on the pre and post-therapy prediction results of the Machine learning model. The availability of Machine Learning model also eliminated subjective assessment by humans. An accuracy of 89% - 91% of the models was achieved.

Keywords: Prediction, Rehabilitation, Post-traumatic, Patient, Machine learning.

1 INTRODUCTION

Rehabilitation robots are becoming increasingly popular for stroke rehabilitation because they can quantify and further enhance the rehabilitation training [1], [2]. A robot can optimize the use of therapists' time for more complicated treatment [3], as it is able to provide patients with a large number of repetitive therapies under minimal supervision. High-intensity repetition of training movement is important in motor retraining following stroke [4]. The robot is also able to aid and challenges based on the recovery rate of the patient, these movements can be made with the robot either providing a variety of force intensity to assist or resist the limb movement. Rehabilitation robots also have the capability to simulate real-world situations through haptic interfaces and virtual reality technologies [5]. Interactive virtual reality games in robot-assisted therapy can also provide motivation and biofeedback for patients to perform more training.

The goal of robotic rehabilitation is to provide a high dose of repetitive training to increase the recovery rate as well as objective assessment [6]. Robotic therapy brings many advantages in terms of objective clinical and biomechanical measurement compared to conventional therapy [7]. Accurate sensors from robot-assisted rehabilitation devices can continuously monitor and obtain various information related to the patient's movement. Examples of commercial rehabilitation robots include Armeo Power, ReoGo Robotic Therapy and in Motion Arm [8]. All of these robots provide a virtual reality environment for patients to train their arm movements and they are proven to help the arm in reaching movement based on several clinical studies conducted with stroke patients [9]. However, the existing robots are generally expensive [10], therefore most of the rehabilitation centres and hospitals could not afford them. In Malaysia, only the larger hospitals and rehabilitation centres possess 2 robotic rehabilitation equipment, such as UM Medical Centre, Hospital Rehabilitasi Cheras, Ara

Damansara Medical Centre, Sau Seng Lum and Pusat Rehabilitasi PERKESO.

There are various types of patients with similar physiotherapy needs who suffered from different ailments. This research is to investigate the effectiveness of Compact Rehabilitation Robot (CR2-Haptic) in the rehabilitation of such patients, assessing the results and comparing with healthy subjects.

2 METHODOLOGY

This Section discusses the steps taken to achieve the established research objectives. These steps include the configuration of the robot, assessing the patients, conducting the therapeutic exercises, recruiting healthy subjects, data collation and analysis, and development of the predictive model.

2.1 THE SUBJECTS

Six subjects (four men, two women) satisfied the inclusion criteria and volunteered to participate in this study. They are adults and there was no segregation due to paucity of patients. All the subjects possessed a certain level of active movements; this made them suitable for resistive exercises. The subjects did not experience any pain or discomfort during or after the study. The subjects were able to conveniently perform exercises with the CR2-Haptic and rest comfortably during set-up. The subjects gave their written consent to participate in this study and signed the patient's consent form accordingly.

The inclusion criteria are listed below:

- (a) Post-traumatic patients aged 18 years and above with upper limb neurology or muscular-skeletal impaired forearm and wrist movement
- (b) Have sufficient cognitive and language abilities to understand the training instructions.

There was however no patient excluded from the study due to the paucity of the patients. Six additional subjects (all men), healthy and fully active were also recruited for the comparison and validation process.

2.2 SUBJECTS PROFILING AND SETUP

The robot software has a personalized training module. Each subject's data is protected by a username and password as shown in Figure 1. Each account is created by the therapist in the clinic and each account can create hundreds of patients' records, consisting of the training data and progress. The number of records is only limited by the data storage capacity of the computer. The therapist created the new patient account in the portal and recorded each of the subject's demographic data

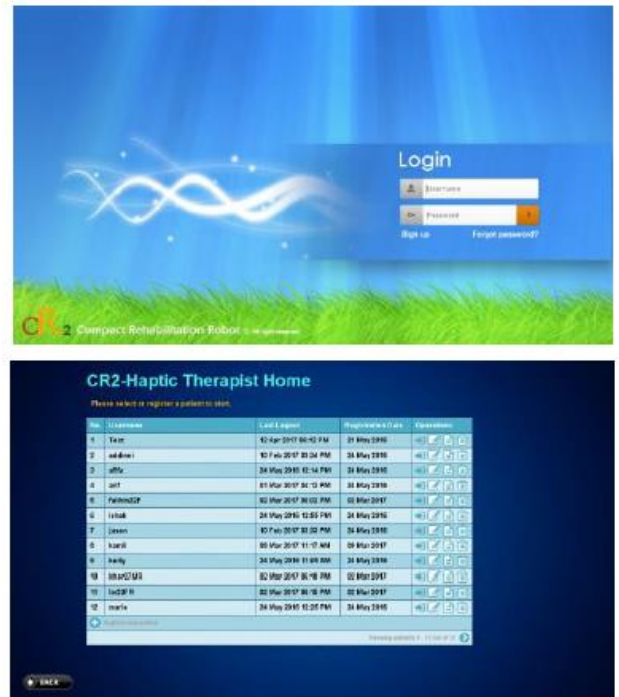


Figure 1: Software interface: Login page of CR2 software (top) and therapist portal with subject registration list (bottom)

Figure 2 shows the main menu interface that enables the user to select the option for setup, assessment, therapy and report. In the setup menu, the user will set up their training side, whether left or right and type of training movement or robot configuration as shown in Figure 3. The assessment menu is used for user performance assessment on a range of movement, strength and movement quality otherwise referred to as match assessment. The therapy menu is used for the user to select the type of robot-assisted training therapy exercises. Report menu is used as a progress review tool for the therapist and the subject to review the performance throughout the training.

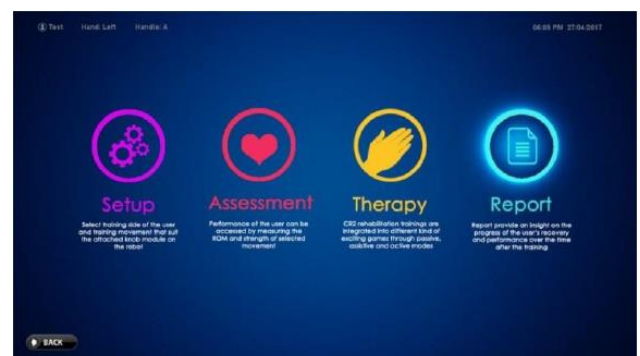


Figure 2: Main menu interface, which includes the setup, assessment, therapy and report option for the user to select



Figure 3: Subject training and assessment setup interface: Training side (left) and training configuration (right)

2.3 THE PROTOCOL

This section describes the apparatus used while conducting the experiment. Before the robotic therapy, the subjects were given instructions on how to train with the robot and the correct way to interact with the robot. Subjects received resistive training for forearm pronation-supination configuration of the CR2-Haptic. The Match Assessment, which records the active range of motion (AROM), passive range of motion (PROM), the strength and the coordination was conducted on each subject and the robot recorded the data and use it automatically for setting up the range of the obstacles for the therapy games. The passive mode was used to guide patients along a predefined set path or to train a movement pattern before starting an active exercise. In the passive mode, the robot performs the movement without any account of the patient's activity. In resistive training, the training range was set within the passive range based on the performance of the patient as obtained from the match assessment. The subject can at any time stop the training if exhausted or encountered any other personal issues.

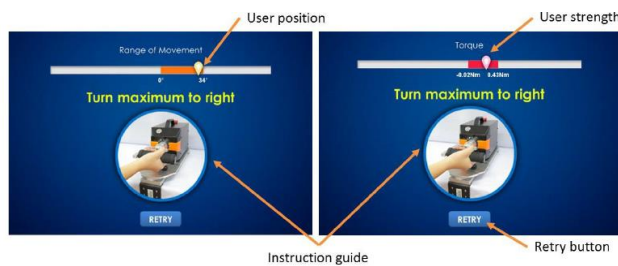


Figure 4: Match Assessment program interface: ROM assessment (left) and strength assessment (right)

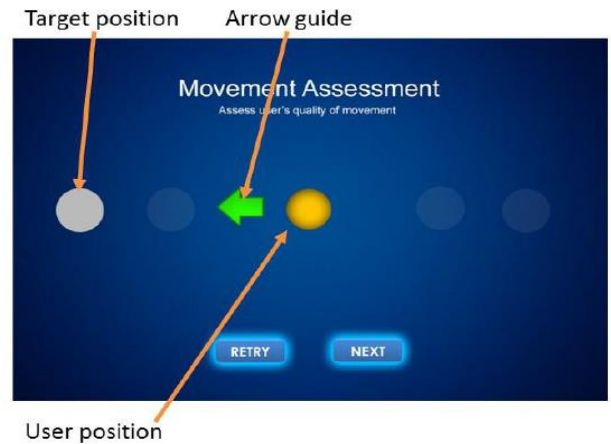


Figure 5: Match Assessment program interface: Movement coordination assessment module

Figure 6 shows the control panel interface, which enables the therapist to customize the training range and strength based on each patient's condition. The therapist can drag the arrow to determine the training range of movement for two directions. The patient's strength, active and passive range of movements are shown in the interface to give the reference for the therapist during the adjustment. The range of training movement can be adjusted from 0° to 90° and the strength is from level 1 to level 3 in both directions.



Figure 6: Adjustment panel: Training range adjustment panel (top) and strength adjustment panel (bottom)

During the training, the subjects sitting posture was upright with shoulder placed between 30° to 60° and elbow arched between 90° to 120°, supported by an armrest with strap. The subjects placed their forearm on arm support. The height of the chair was adjusted to ensure a comfortable sitting posture of the subject while interacting with the device. Possible compensatory trunk movement was avoided by applying body strap to subject, if less stable, and monitored by the onsite physiotherapist. The robot was fixed on a table in front of the subject with a display monitor for visual feedback during the exercise.



Figure 7: Some of the subjects during the therapy session

2.4 THE PROTOCOL

The training therapy program is designed to be patient-tailored, where the therapist is able to adjust the program based on every patient's requirement. The therapist is able to create a series of training programs for different patients in the therapy program control panel page, as shown in Figure 8. Figure 9 shows the software's *CR2 Game Store* which provides a variety of virtual reality games with different training modes for the users to choose. By using the therapy control panel, each training program type, repetition, game, level of difficulty, range of movement and strength can be customized.



Figure 8: Therapy program control panel, which enables the therapist to customize the therapy based on each patient's requirements. The option includes the training program, range of movement, strength, level of difficulties, repetition and sequence.



Figure 9: CR2 Games Store includes a variety of virtual reality games, with different training modes for the users to choose

The games available are: -

- 1) Water drop
- 2) Water drop 2
- 3) Heli explorer
- 4) Space venture
- 5) Traffic on the go, and
- 6) Candy castle

For this study, all the six different games were played for one minute each and for two different difficulty levels.

2.5 RESISTIVE MODE

Resistive exercise is a therapeutic strategy of providing resistance to the subject's hemiparetic limb movements during exercise [2]. In the resistive mode, different levels of resistance intensity will be applied during training to oppose the patient's movement in both directions (pronation-supination and flexion-extension), with the aim to strengthen their muscles [2]. The resistive force is generated by the controller based on the current position of the end effector. The resistance will only be applied when the user actively turns away from the neutral position (0°). The resistance would increase gradually, whereby the greater range they turn, the higher the

resistance applied to oppose their movement. The robot will exert a different level of resistance to strengthen the muscle strength of the patients by adjusting the speed of the motor depends on the recovery rate of the patient.

The haptic simulation was used for resistive training in the active mode. The advantages of this approach compared to training in physical reality are the different interactive environments making training more interesting, realistic and flexible compared to typical rehabilitation clinic [2].

So, for this study, the therapy was set at resistive mode.

2.6 PERFORMANCE SCORE

The training performance of virtual reality game is important to be known, it indicates the performance of the users and motivates them to do better. Thus, at the end of each game, an accuracy percentage is displayed for the user.

Initially, the total percentage is 100, however, as the targets are missed, the score drops until the end of the time. The users may also select the “report” option, Figure 2 to have an overview of their performance



Figure 10: Stars and points will be rewarded at the end of the game according to patients' performance



Figure 11: Performance report display

2.7 ANALYSIS

The performance results were obtained in two forms:

- Robotics interface for user tracking and analysis (as displayed in Figure 11)
- Scientific data sets recorded in excel sheets format at the background, in 2 categories –
 - The Match assessment, and
 - The therapeutic games data

The scientific data is used for this study and it is discussed in the next section.

3 RESULTS AND DISCUSSION

Data analysis on the prediction of a certain disease and recovery management is of great significance to both the patients and the physiotherapists. Machine learning is one of the popular tools that are able to visualize the hidden relationship between the collected data. It is an algorithm that gives the system the ability to learn or search for something without any specific human's programming.

In this chapter, the data collected at the background of the robot interface is presented, analyzed and used to develop a machine learning model for the prediction of each particular health condition.

The data is presented in excel files format and contains vital information about the subjects, obtained from both the match assessment and the therapy exercise. Each registered subject has a folder named after his registered name and sub-folders for match assessment and the respective games.

3.1 THE DATA

The data is presented in excel files format and contains vital information about the subjects, obtained from both the match assessment and the therapy exercise. Each registered subject has a folder named after his registered name and sub-folders for match assessment and the respective games.

3.2 THE MATCH ASSESSMENT

The match assessment shows the date and time of the assessment, whether right or left hand, the Active Range of Motion (ROM), the Passive Range of Motion and the strength of the subject. Figure 12 shows the two different patients have a deficiency in ROM (less than $\pm 90^\circ$) and strength (much less than $\pm 1\text{Nm}$), in contrast to Figure 13 where the healthy subject possessed full ROM and strength almost $\pm 1\text{Nm}$, which is the maximum. All such information is automatically replicated in the therapy games files.

#Program: Match Assessment	#Program: Match Assessment
#Type: Resistive	#Type: Resistive
#Start tim Wed Nov 07 12:24:12 2018	#Start tim Wed Nov 07 11:44:25 2018
#Patient Assessment:	#Patient Assessment:
# Hand: Right	# Hand: Right
# Handle: A	# Handle: A
# ROM: -90° to 83°	# ROM: -56° to 42°
# Passive -90° to 90°	# Passive -90° to 90°
# Strength -0.60Nm and 0.47Nm	# Strength 0.00Nm and 0.01Nm

Figure 12: Sample Match Assessment of some of the patients

#Program: Match Assessment	Salim Match	#Program: Match Assessment
#Type: Resistive		#Type: Resistive
#Start tim Sun Mar 17 13:40:18 2019		#Start tim Sun Mar 17 00:34:32 2019
#Patient Assessment:		#Patient Assessment:
# Hand: Right		# Hand: Right
# Handle: A		# Handle: A
# ROM: -90° to 90°		# ROM: -90° to 90°
# Passive -90° to 90°		# Passive -90° to 90°
# Strength -0.87Nm and 0.93Nm		# Strength -0.87Nm and 0.88Nm

Figure 13: Sample match Assessment of some of the healthy subjects

3.3 THERAPY GAMES

The six games available are classified into target-based (Water Drop and Water Drop 2): where the subjects strive to collect targeted virtual water drops in a virtual cup, Fig 4.3; and obstacle-based (the remaining 4 games): where the subjects virtually moved and avoid virtual obstacles in the game environment



Figure 14: Virtual reality game interface showing target (water drop) and position (cup)

There are majorly five different indices describing a subject at any time within the game period: Time, Target (°), Position (°), Torque (Nm) and Output PWM (%). However, as explained above, only two games have readings for target, others use the remaining four indices.

25	##Time	Target (°)	Position (°)	Torque (Nm)	Output PWM
26	0.007	1.#QNAN	0.54	-0.01002	-0.29
27	0.017	22.32	0.45	-0.00668	-0.24
28	0.029	22.32	0.36	-0.0167	-0.19
29	0.037	22.32	0.36	-0.00835	-0.19
30	0.047	22.32	0.27	-0.00835	-0.14
31	0.057	22.32	0.27	-0.00501	-0.14
32	0.067	22.32	0.18	-0.01837	-0.09
33	0.077	22.32	0.18	-0.01336	-0.09
34	0.087	22.32	0.18	-0.00668	-0.09
35	0.097	22.32	0.09	-0.00167	-0.04
36	0.107	22.32	0	-0.00668	0
37	0.117	22.32	0	-0.01002	0
38	0.127	22.32	-0.09	-0.01837	0.04
39	0.137	22.32	-0.09	-0.00501	0.04

Figure 15: Cross-section of data series for water drop game

The “Target” column for the obstacle-based games read “0” all through

3.4 RESISTIVE MODE

In order to determine how fast a subject move to reach a target or avoid an obstacle, the velocity of movement is calculated and tabulated as an additional index

$$Velocity, v = \frac{\text{Change in Position}}{\text{Change in Time}} = \frac{\Delta P}{\Delta T} \quad (1)$$

25	##Time	Target (°)	Position (°)	Velocity	Torque (Nm)	Output PWM (%)
26	0.004	1.#QNAN	4.23	0.00658	0.00658	-2.3
27	0.013	1.#QNAN	4.23	0	0.01837	-2.3
28	0.024	53.55	4.14	-0.16364	0.02505	-2.25
29	0.033	53.55	4.05	-0.2	0.01837	-2.2
30	0.044	53.55	3.96	-0.16364	0.01837	-2.15
31	0.058	53.55	3.87	-0.12857	0.02572	-2.1
32	0.064	53.55	3.87	0	0.01336	-2.1
33	0.073	53.55	3.87	0	0.01336	-2.1
34	0.083	53.55	3.96	0.18	0.01837	-2.15
35	0.093	53.55	3.96	0	0.0167	-2.15
36	0.105	53.55	3.96	0	0.01002	-2.15

Figure 16: Cross-section of data series for water drop game showing velocity index

The data series for both patients and healthy subjects were plotted using MATLAB for analysis.

3.5 MATLAB PLOTS

MATLAB software was used to plot the data so as to analyze it. The plots are analyzed below.

3.6 WATER DROP

The water drop and water drop 2 are similar in their context, hence only one is plotted below, using MATLAB for analysis and comparison.

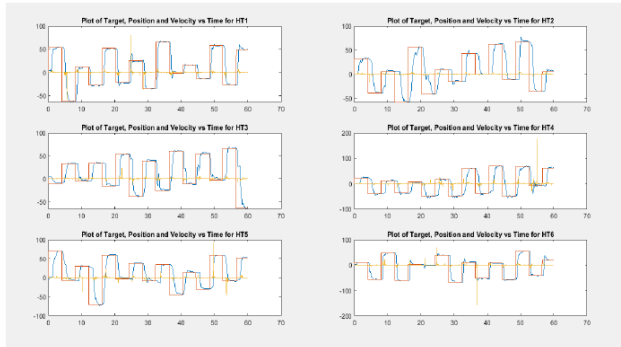


Figure 17: Plots of Target (red), Position (blue) and Velocity against Time for Water drop therapy for healthy subjects (HT1 – HT6)

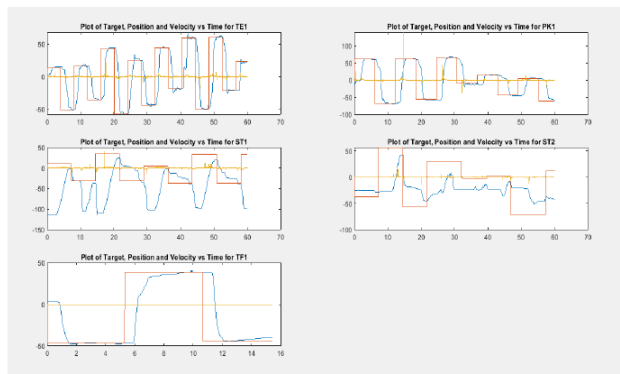


Figure 18: Plots of Target (red), Position (blue) and Velocity against Time for Water drop therapy for patients (Tennis Elbow: TE, Parkinson's: PK, Stroke: ST and Trigger Finger: TF)

Only four out of the six patients successfully played the water drop therapy game, hence the other two were analysed along with others, in the subsequent games to be discussed.

Numerical analysis of the above plots was conducted by calculating the total area between the target and position curves, as a measure of closeness (for healthy) or otherwise (for non-healthy). It was established that the areas for the six healthy subjects range between 67,717 to 135,662 degrees-minute while for the Parkinson's it was 179,152; and for the two Stroke patients, 221,792 and 321,149 degrees-minute. This is an indication that healthy subjects have a relatively lower area between the position and target. However, for Tennis Elbow, the area is 69,186 degrees-minute, which falls within the healthy range and as such makes the numerical analysis not suitable for this type of patient.

Another challenge for the numerical analysis is that it can only be applied in the target-based therapy games but not in the obstacle-based as can be seen below.

3.7 HELI-EXPLORER

The Heli-explorer have similar navigation pattern with all the other three obstacle-based games. There is no target hence only smoothness of the navigation can be observed from the plots. While it might be crystal clear for some patients, there might not be any numerical relation to depict a particular health condition.

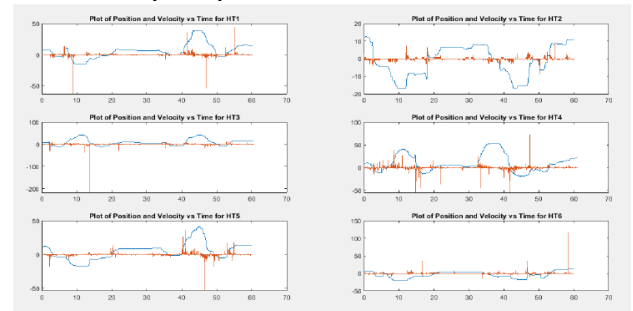


Figure 19: Plots of Position (blue) and Velocity against Time for Heli-explorer therapy for healthy

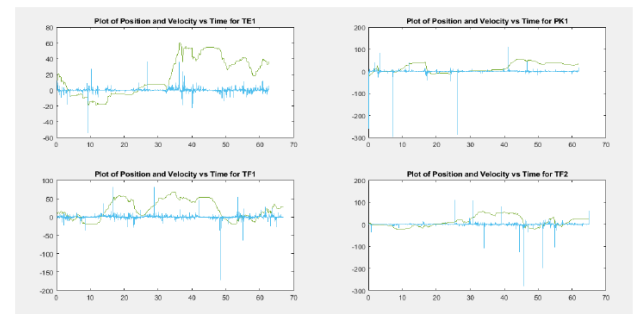


Figure 20: Plots of Position (green) and Velocity against Time for Heli-explorer therapy for patients (Tennis Elbow: TE, Parkinson's: PK and Trigger Finger: TF)

From the above, it is noted that the two Stroke patients could not play the Heli-explorer game, but that was not a problem as they can be properly analysed using the water drop game.

3.8 MACHINE LEARNING

In order to overcome the shortfall of the numerical analysis and the MATLAB plots observation, a Machine Learning model was developed using the WEKA software through the Explorer application of the WEKA.

The indices extracted as discussed above were used as the input to the system and the classification of the health condition as the output, together, they are referred to as attributes in the WEKA. The indices were treated as numeric attributes while creating the data file executable by the WEKA. A separate file was created for each game and the subjects' data indices compiled therein and saved as ".arff" data file (WEKA executable file extension).

In the WEKA Explorer, the data files were uploaded one at a time for pre-processing, this detects if

there were any missing values and outliers in each of the indices in addition to the provision of statistical analysis such as minimum, maximum, mean and standard deviation. The classifier was set to functions, then multilayer perceptron. Other classifiers were tried but the multilayer perceptron yielded the optimal output hence it is used for this analysis.

In machine learning, model validation is a process to evaluate the trained model with a testing dataset. Two different test options for the model validation were considered: The standard cross-validation and the percentage split. A different number of folds and splits were tried until the optimal values were obtained for 10-folds and the 70/30 percentage split for training and testing.

The summary of four of the models is presented in the Figures 21 – 24.

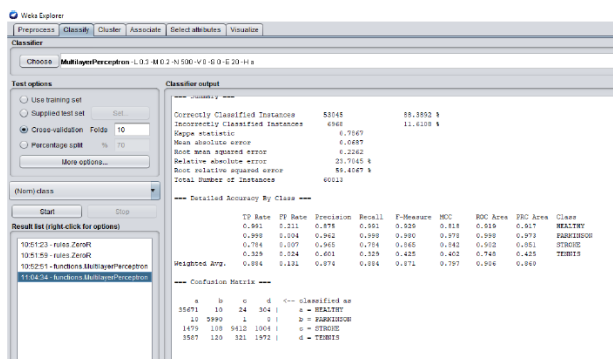


Figure 21: WEKA Explorer Machine Learning model for water drop game (10 folds cross-validation)

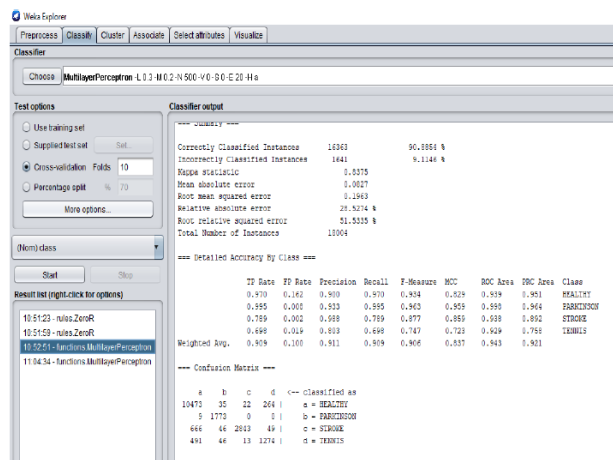


Figure 22: WEKA Explorer Machine Learning model for water drop (70/30% split)

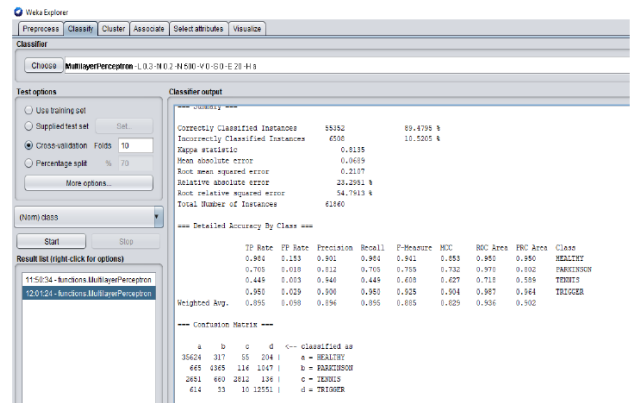


Figure 23: WEKA Explorer Machine Learning model for Heli-explorer (10 folds cross-validation)

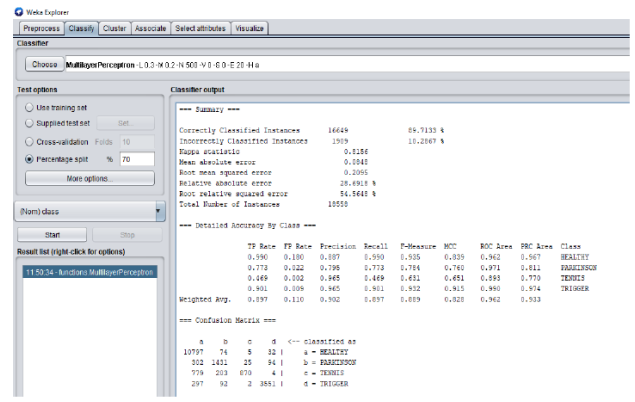


Figure 24: WEKA Explorer Machine Learning model for Heli-explorer (70/30% split)

From the above figures, it is observed that both the standard cross-validation and the percentage split yield similar accuracy results with percentage split having a bit higher accuracy.

3.9 DISCUSSION OF RESULTS

An accuracy of 88% in standard cross-validation and 91% in 70/30% split for the water drop prediction model is achieved. For the Recall, it was 99.1% and 97.0% for Healthy, 99.8% and 99.5% for Parkinson's, 78.4% and 78.9% for Stroke but 32.9% and 69.8% for Tennis Elbow respectively. It was also seen that the Tennis Elbow has a high rate of True-Negative instances in the confusion matrix, mostly classified as healthy.

Also, the accuracy of 89% in standard cross-validation and 90% in 70/30% split for the Heli-explorer prediction model achieved. For the Recall, it was 98.4% and 99.0% for Healthy, 70.5% and 77.3% for Parkinson's, 95.0% and 90.1% for Trigger Finger but 44.9% and 46.9% for Tennis Elbow respectively. It was also seen that the Tennis Elbow has a high rate of True-Negative instances in the confusion matrix, mostly classified as healthy.

The True Positive (TP) rate, False Positive (FP) rate and the Precision are all displayed along with other accuracy details for each health condition in the Detailed Accuracy by Class section.

4 CONCLUSION

All the subjects have full range PROM and most of them have full AROM pre-therapy. Their strength levels and coordination vary hence the robot showed the tendency to improving such. The availability of the therapy also increased the frequency of clinical therapy, indicating an improvement in TAT. It has also been established that numerical analysis is not suitable for some health conditions. An accuracy of 89% - 91% of the models was achieved.

REFERENCES

- [1] N. Nordin, S. Q. Xie, and B. Wünsche, "Assesment of movement quality," 2014.
- [2] P. Poli, G. Morone, G. Rosati, and S. Masiero, "Robotic Technologies and Rehabilitation: New Tools for Stroke Patients' Therapy," *Biomed Res. Int.*, vol. 2013, pp. 1–8, 2013.
- [3] N. Norouzi-Gheidari, P. S. Archambault, and J. Fung, "Effects of robot-assisted therapy on stroke rehabilitation in upper limbs: systematic review and meta-analysis of the literature.," *J. Rehabil. Res. Dev.*, vol. 49, no. 4, pp. 479–96, 2012.
- [4] K. Kawahira, M. Shimodozono, S. Etoh, K. Kamada, T. Noma, and N. Tanaka, "Effects of intensive repetition of a new facilitation technique on motor functional recovery of the hemiplegic upper limb and hand," *Brain Inj.*, vol. 24, no. 10, pp. 1202–1213, 2010.
- [5] L. Marchal-Crespo and D. J. Reinkensmeyer, "Review of control strategies for robotic movement training after neurologic injury.," *J. Neuroeng. Rehabil.*, vol. 6, p. 20, 2009.
- [6] K. Laver, S. George, S. Thomas, J. E. Deutsch, and M. Crotty, "Cochrane review: Virtual reality for stroke rehabilitation," *Eur. J. Phys. Rehabil. Med.*, vol. 48, no. 3, pp. 523–530, 2012.
- [7] L. E. Kahn, P. S. Lum, W. Z. Rymer, and D. J. Reinkensmeyer, "Robot-assisted movement training for the stroke-impaired arm: Does it matter what the robot does?," *J. Rehabil. Res. Dev.*, vol. 43, no. 5, pp. 619–30, 2006.
- [8] B. A., A. F., N. S.M., B. J.H., P. G.B., and S. A.H.A., "Training modalities in robot-mediated upper limb rehabilitation in stroke: A framework for classification based on a systematic review," *J. Neuroeng. Rehabil.*, vol. 11, no. 1, pp. 1–15, 2014.
- [9] J. Hidler, D. Nichols, M. Pelliccio, and K. Brady, "Top Stroke Rehabil," *Top Stroke Rehabil*, vol. 12, no. 2, pp. 22–35, 2005.
- [10] D. J. Reinkensmeyer and M. L. Boninger, "Technologies and combination therapies for enhancing movement training for people with a disability," *J. Neuroeng. Rehabil.*, vol. 9, no. 1, pp. 1–10, 2012.
- [11] T. Platz, "Evidenzbasierte Armrehabilitation," *Nervenarzt*, vol. 74, no. 10, pp. 841–849, 2004.
- [12] R. C. V. Loureiro, W. S. Harwin, K. Nagai, and M. Johnson, "Advances in upper limb stroke rehabilitation: A technology push," *Med. Biol. Eng. Comput.*, vol. 49, no. 10, pp. 1103–1118, 2011.
- [13] D. Lynch, M. Ferraro, J. Krol, C. M. Trudell, P. Christos, and B. T. Volpe, "Continuous passive motion improves shoulder joint integrity following stroke," *Clin. Rehabil.*, vol. 19, no. 6, pp. 594–599, 2005.
- [14] T. Nef, M. Mihelj, and R. Riener, "ARMin: A robot for patient-cooperative arm therapy," *Med. Biol. Eng. Comput.*, vol. 45, no. 9, pp. 887–900, 2007.
- [15] J. M. Veerbeek, A. C. Langbroek-Amersfoort, E. E. H. Van Wegen, C. G. M. Meskers, and G. Kwakkel, "Effects of Robot-Assisted Therapy for the Upper Limb after Stroke," *Neurorehabil. Neural Repair*, vol. 31, no. 2, pp. 107–121, 2017.
- [16] F. Mcdowell and T. Bruce, "Training Recovery," 2012.
- [17] G. Kwakkel, B. J. Kollen, and H. I. Krebs, "Effects of robot-assisted therapy on upper limb recovery after stroke: A systematic review," *Neurorehabil. Neural Repair*, vol. 22, no. 2, pp. 111–121, 2008.
- [18] G. B. Prange, M. J. A. Jannink, C. G. M. Groothuis-Oudshoorn, H. J. Hermens, and M. J. Ijzerman, "Systematic review of the effect of robot-aided therapy on recovery of the hemiparetic arm after stroke.," *J. Rehabil. Res. Dev.*, vol. 43, no. 2, pp. 171–84, 2006.
- [19] N. Hogan *et al.*, "Motions or muscles? Some behavioral factors underlying robotic assistance of motor recovery.," *J. Rehabil. Res. Dev.*, vol. 43, no. 5, pp. 605–18, 2006.
- [20] W. W. Liao, C. Y. Wu, Y. W. Hsieh, K. C. Lin, and W. Y. Chang, "Effects of robot-assisted upper limb rehabilitation on daily function and real-world arm activity in patients with chronic stroke: A randomized controlled trial," *Clin. Rehabil.*, vol. 26, no. 2, pp. 111–120, 2012.
- [21] R. Colombo *et al.*, "Design strategies to improve patient motivation during robot-aided rehabilitation," *J. Neuroeng. Rehabil.*, vol. 4, pp. 1–12, 2007.
- [22] N. D., N. A., K. U., and R. R., "Increasing motivation in robot-aided arm rehabilitation with competitive and cooperative gameplay," *J. Neuroeng. Rehabil.*, vol. 11, no. 1, pp. 1–15, 2014.
- [23] M. Mihelj, D. Novak, M. Milavec, J. Zihlerl, A. Olenšek, and M. Munih, "Virtual rehabilitation environment using principles of intrinsic motivation and



game design,” *Presence Teleoperators Virtual Environ.*, vol. 21, no. 1, pp. 1–15, 2012.

[24] S. Balasubramanian, R. Colombo, I. Sterpi, V. Sanguineti, and E. Burdet, “Robotic assessment of upper limb motor function after stroke,” *Am. J. Phys. Med. Rehabil.*, vol. 91, no. 11 SUPPL.3, pp. 255–269, 2012.

[25] M. J.-C. *et al.*, “Assessment-driven selection and adaptation of exercise difficulty in robot-assisted therapy: A pilot study with a hand rehabilitation robot,” *J. Neuroeng. Rehabil.*, vol. 11, no. 1, p. 154, 2014.

[26] R. Sigrist, G. Rauter, R. Riener, and P. Wolf, “Augmented visual, auditory, haptic, and multimodal feedback in motor learning: A review,” *Psychon. Bull. Rev.*, vol. 20, no. 1, pp. 21–53, 2013.

[27] N. Jafari, K. D. Adams, and M. Tavakoli, “Haptics to improve task performance in people with disabilities: A review of previous studies and a guide to future research with children with disabilities,” *J. Rehabil. Assist. Technol. Eng.*, vol. 3, p. 205566831666814, 2016.



ARDUINO BASED AUTOMATIC IRRIGATION SYSTEM

¹Ibrahim Bashir Shehu ²Zayyan Nuhu ³Rbiu Altanko Ummaisha

^{1,2,3}Department of Electrical/Electronic Engineering Technology Nuhu Bamalli Polytechnic Zaria
ibrahimbshehu@yahoo.com

ABSTRACT

The importance of water in all agricultural activities cannot be over emphasized. Watering system ease the burden of getting water to a particular farmland/plant whenever the need arises. To know the amount of water is required by plants and when it is required is very important. To make life easier for both the farmer and the plants, an automatic irrigation system is developed. This project uses Arduino based system which is programmed in such a way that water is supplied automatically by sensing the level of soil moisture. The system consists of ATmega328 Microcontroller. the system can be employed for all aspect of irrigation system and can also be extended to other type of system that requires automatic supply of water based on the moisture level of a substance.

Keywords: *Automatic irrigation System, Arduino-board*

INTRODUCTION

Irrigation is the artificial application of water to the land or soil. It is used to assist in the growing of agricultural crops, maintenance of landscapes, and re vegetation of disturbed soils in dry areas and during periods of inadequate rainfall. When a zone comes on, the water flows through the lateral lines and ultimately ends up at the irrigation emitter (drip) or sprinkler heads.

Many sprinklers have pipe thread inlets on the bottom of them which allows a fitting and the pipe to be attached to them. The sprinklers are usually installed with the top of the head flush with the ground surface. When the water is pressurized, the head will pop up out of the ground and water the desired area until the valve closes and shuts off that zone. Once there is no more water pressure in the lateral line, the sprinkler head will retract back into the ground. Emitters are generally laid on the soil surface or buried a few inches to reduce evaporation losses.

Healthy plants can transpire a lot of water, resulting in an increase in the humidity of the greenhouse air. A high relative humidity (above 80-85%) should be

avoided because it can increase the incidence of disease and reduce plant transpiration. Sufficient venting or successive heating and venting can prevent condensation on plants surfaces and the greenhouse structure. The use of cooling systems during the warmer summer months increases the greenhouse air humidity.

During periods with warm and humid outdoor conditions, humidity control inside the greenhouse can be a challenge.

Since the relative humidity alone does not tell us anything about the absolute water holding capacity of air, a different measurement is sometime used to describe the absolute moisture status of the soil. The vapor pressure deficit is a measure of the difference between the amount of moisture the air contains at a given moment and the amount of moisture it can hold at that temperature when the air would be saturated. Pressure deficit measurement can tell us how easy it is for plants to transpire: higher values stimulate transpiration (but too high can cause wilting), and lower values inhibit transpiration and can lead to condensation on leaf and greenhouse surfaces.

BLOCK DIAGRAM

There are two functional components in this project. They are the moisture sensors and the motor/water pump. Thus the Arduino Board is programmed using the Arduino IDE software. The function of the moisture sensor is to sense the level of moisture in the soil. The motor/water pump supplies water to the plants.

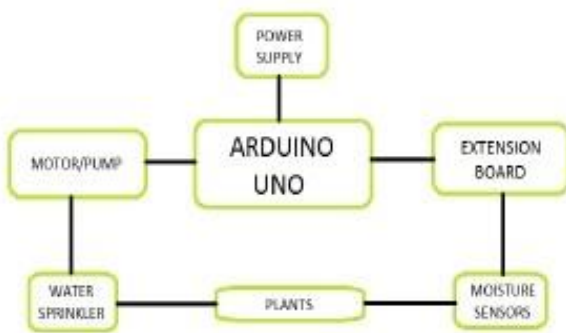


Figure 2.1 Automatic Plant Watering Block Diagram

This project uses Arduino Uno to controls the motor. Follow the schematic to connect the Arduino to the motor driver, and the driver to the water pump. The motor can be driven by a 9 volt battery, and current measurements show us that battery life. The Arduino Board is programmed using the Arduino IDE software. The moisture sensor measures the level of moisture in the soil and sends the signal to the Arduino if watering is required. The motor/water pump supplies water to the plants until the desired moisture level is reached.

2.1 ARDUINO UNO:

The Arduino Uno is a microcontroller board based on the ATmega328. It has 14 digital input/output pins (of which 6 can be used as PWM outputs), 6 analog inputs, a 16 MHz ceramic resonator, a USB

connection, a power jack, an ICSP header, and a reset button. It contains everything needed to support the microcontroller; simply connect it to a computer with a USB cable or power it with a AC-to-DC adapter or battery to get started.



Fig 2.1.1 Arduino Uno

The Uno differs from all preceding boards in that it does not use the FTDI USB-to-serial driver chip. Instead, it features the Atmega16U2 (Atmega8U2 up to version R2) programmed as a USB-to-serial converter

FEATURE	SPECIFICATION
Microcontroller	ATmega328
Operating Voltage	5V
Input Voltage (recommended)	7-12V
Input Voltage (limits)	6-20V
Digital I/O Pins	14 (of which 6 provide PWM output)
Analog Input Pins	6
DC Current per I/O Pin	40 mA
DC Current for 3.3V Pin	50 mA
Flash Memory	32 KB (ATmega328) of which 0.5 KB used by boot loader
SRAM	2 KB (ATmega328)
EEPROM	1 KB (ATmega328)
Clock Speed	16 MHz

Table 2.1.1 Arduino Specifications

The Arduino Uno can be powered via the USB connection or with an external power supply. The power source is selected automatically. External (non-USB) power can come either from an AC-to-DC adapter (wall-wart) or battery. The adapter can be connected by plugging a 2.1mm center- positive plug into the board's power jack.

Leads from a battery can be inserted in the Gnd and Vin pin headers of the POWER connector. The board can operate on an external supply of 6 to 20 volts. If supplied with less than 7V, however, the 5V pin may supply less than five volts and the board may be unstable. If using more than 12V, the voltage regulator may overheat and damage the board. The recommended range is 7 to 12 volts

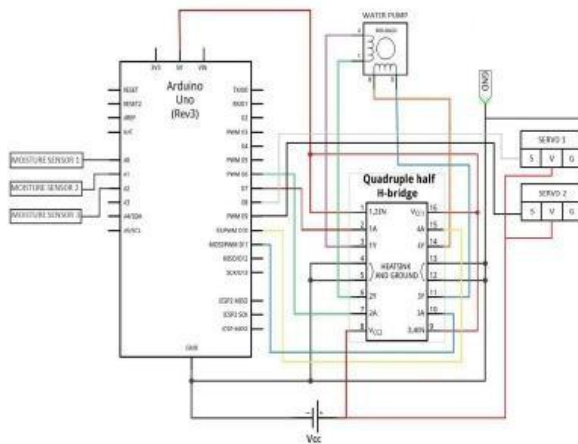


Figure 2.2 Automatic Plant Watering Schematic diagram

2.2 PROGRAMMING:

The Arduino Uno can be programmed with the Arduino software. Select "Arduino Uno" from the Tools > Board menu (according to the microcontroller on your board). For details, see the reference and tutorials.

The ATmega328 on the Arduino Uno comes preburned with a boot loader that allows you to upload new code to it without the use of an external hardware programmer. It communicates using the original STK500 protocol (reference, C header files). We can also bypass the boot loader and program the microcontroller through the ICSP (In-Circuit Serial Programming) header; see these instructions for details.

The ATmega16U2 (or 8U2 in the rev1 and rev2 boards) firmware source code is available. The ATmega16U2/8U2 is loaded with a DFU boot loader, which can be activated by:

- On Rev1 boards: connecting the solder jumper on the back of the board (near the map of Italy) and then resetting the 80U2

- On Rev2 or later boards: there is a resistor that pulling the 8U2/16U2 HWB line to ground, making it easier to put into DFU mode

The Arduino Uno has a number of facilities for communicating with a computer, another Arduino, or other microcontrollers. The ATmega328 provides UART TTL (5V) serial communication, which is available on digital pins 0 (RX) and 1 (TX). An ATmega16U2 on the board channels this serial communication over USB and appears as a virtual com port to software on the computer. The '16U2 firmware uses the standard USB COM drivers, and no external driver is needed. However, on Windows, a .inf file is required. The Arduino software includes a serial monitor which allows simple textual data to be sent to and from the Arduino board. The RX and TX LEDs on the board will flash when data is being transmitted via the USB-to-serial chip and USB connection to the computer (but not for serial communication on pins 0 and 1). A Software Serial library allows for serial communication on any of the Uno's digital pins.

The ATmega328 also supports I2C (TWI) and SPI communication. The Arduino software includes a Wire library to simplify use of the I2C bus.

2.3. PHYSICAL CHARACTERISTICS:

The maximum length and width of the Uno PCB are 2.7 and 2.1 inches respectively, with the USB connector and power jack extending beyond the former dimension.

Four screw holes allow the board to be attached to

a surface or case. Note that the distance between digital pins 7 and 8 is 160 mil (0.16"), not an even multiple of the 100 mil spacing of the other pins

2.4. MOISTURE SENSOR:

Soil moisture sensors measure the water content in soil. A soil moisture probe is made up of multiple soil moisture sensors. In this particular project, we will use the moisture sensors which can be inserted in the soil in order to measure the moisture content of the soil.

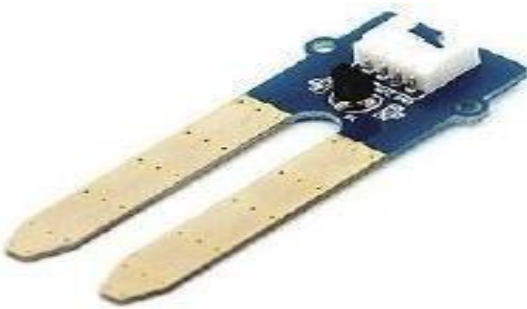


Fig 2.4.1 Moisture Sensor

Soil electrical conductivity is simply measured using two metal conductors spaced apart in the soil except that dissolved salts greatly alter the water conductivity and can confound the measurements. An inexpensive fix is to embed conductors in a porous gypsum block which releases calcium and sulphate ions to swamp the soil background level of ions. The water absorbed by the block is correlated with soil water potential over the range -60 to -600 kPa providing a tertiary indicator for use in medium to heavy soils. Non-dissolving granular matrix sensors are now available with a more exacting specification for the range 0 to -200 kPa and use internal calibration methods to offset variations due to solutes and temperature.

Methods for exploiting soil dielectric properties actually measure proxy variables that more or less include a component due to the soil electrical conductivity and are thus inherently sensitive to variations in soil salinity and temperature as well as water.

Measurements are also affected by soil bulk density and the proportion of bound and free water determined by the soil type.

Nevertheless, good accuracy and precision can be achieved under specific conditions and some sensor types have become widely adopted for scientific work.

Soil dielectric measurement is the method of choice for most research studies where expertise is available for calibration, installation and interpretation, but scope for cost reduction through sensor multiplexing is limited due to the possibility of stray capacitances. A lower manufacturing cost is possible through development of application specific integrated circuits (ASICs), though this requires a high level of investment.

Multiple sensors are required to provide a depth profile and cover a representative area, but this cost can be minimized through use of a computer model to extend the measurements in a predictive way. Thus, by using the moisture sensors, the overriding factor will be reliable, cost-effective sensors and electronic systems for accessing and interpreting the data.

2.5. WATER PUMP:

The water pump is used to artificially supply water for a particular task. It can be electronically controlled by interfacing it to a microcontroller. It can be triggered ON/OFF by sending signals as required. The process of artificial supplying water is known as pumping. There are many varieties of water pumps used. This project employs the use of a small water pump which is connected to a H-Bridge.



Fig 2.5.1 Water Pump

The pumping of water is a basic and practical technique, far more practical than scooping it up with one's hands or lifting it in a hand-held bucket. This is true whether the water is drawn from a fresh source, moved to a needed location, purified, or used for irrigation, washing, or sewage treatment, or for evacuating water from an undesirable location. Regardless of the outcome, the energy required to pump water is an extremely demanding component of water consumption. All other processes depend or benefit either from water descending from a higher elevation or some pressurized plumbing system.

DESCRIPTION OF ATMEGA 328P MICRO CONTROLLER:

The ATmega48PA/88PA/168PA/328P is a low-power CMOS 8-bit microcontroller based on the AVR enhanced RISC architecture. By executing powerful instructions in a single clock cycle, the ATmega48PA/88PA/168PA/328P achieves throughputs approaching 1 MIPS per MHz allowing the system designed to optimize power consumption versus processing speed. The ATmega48PA/88PA/168PA/328P provides the following features: 4K/8K bytes of In-System Programmable Flash with Read-While-Write

capabilities, 256/512/512/1K bytes EEPROM, 512/1K/1K/2K bytes SRAM, 23 general purpose I/O lines, 32 general purpose working registers, three flexible Timer/Counters with compare modes, internal and external interrupts, a serial programmable USART, a byte-oriented 2-wire Serial Interface, an SPI serial port, a 6-channel 10-bit ADC (8 channels in TQFP and QFN/MLF packages), a programmable Watchdog Timer with internal Oscillator, and five software selectable power saving modes. The Idle mode stops the CPU while allowing the SRAM, Timer/Counters, USART, 2-wire Serial Interface, SPI port, and interrupt system to continue functioning. The Power-down mode saves the register contents but freezes the Oscillator, disabling all other chip functions until the next interrupt or hardware reset. In Power-save mode, the asynchronous timer continues to run, allowing the user to maintain a timer base while the rest of the device is sleeping. The ADC Noise Reduction mode stops the CPU and all I/O modules except asynchronous timer and ADC, to minimize switching noise during ADC conversions. In Standby mode, the crystal/resonator Oscillator is running while the rest of the device is sleeping. This allows very fast start-up combined with low power consumption. The AVR core combines a rich instruction set with 32 general purpose working registers. All the 32 registers are directly connected to the Arithmetic Logic Unit (ALU), allowing two independent registers to be accessed in one single instruction executed in one clock cycle. The Boot program can use any interface to download the application program in the Application Flash memory. This allows very fast start-up combined with low power consumption.



Fig 3.1. ATMEGA 328

In the ATMEGA variant, the working register file is not mapped into the data address space; as such, it is not possible to treat any of the ATMEGA's working registers as though they were SRAM. Instead, the I/O registers are mapped into the data address space starting at the very beginning of the address space.

Additionally, the amount of data address space dedicated to I/O registers has grown substantially to 4096 bytes (000016–0FFF16). As with previous generations, however, the fast I/O manipulation instructions can only reach the first 64 I/O register locations (the first 32 locations for bitwise instructions).

ARDUINO IDE TOOL

The open-source Arduino environment makes it easy to write code and upload it to the i/o board. It runs on Windows, Mac OS X, and Linux. The environment is written in Java and based on Processing, avr-gcc, and other open source software

STEPS FOR USING ARDUINO IDE:

Step 1: Get an Arduino board and USB cable

In this tutorial, we assume you're using an Arduino Uno You also need a standard USB cable (A plug to B plug): the kind you would connect to a USB

printer, for example.

1 STEP 2 : DOWNLOAD THE ARDUINO ENVIRONMENT

Get the latest version from the download page. When the download finishes, unzip the downloaded file. Make sure to preserve the folder structure. Double-click the folder to open it. There should be a few files and sub- folders inside.

STEP 3 : CONNECT THE BOARD

The Arduino Uno, Mega, Duemilanove and Arduino Nano automatically draw power from either the USB connection to the computer or an external power supply. If you're using an Arduino Diecimila, you'll need to make sure that the board is configured to draw power from the USB connection. The power source is selected with a jumper, a small piece of plastic that fits onto two of the three pins between the USB and power jacks. Check that it's on the two pins closest to the USB port. Connect the Arduino board to your computer using the USB cable. The green power LED (labelled PWR) should go on.

STEP 4 : INSTALL THE DRIVERS

Installing drivers for the Arduino Uno or Arduino Mega 2560 with Windows7, Vista, or XP

Step 5: Launch the Arduino application Double-click the Arduino application. (Note: if the Arduino software loads in the wrong language, you can change it in the preferences dialog. See the environment page for details.)

STEP 6: OPEN THE BLINK EXAMPLE

Open the LED blink example sketch: File > Examples > 1.Basics > Blink.

STEP 7: SELECT YOUR BOARD

You'll need to select the entry in the Tools > Board menu that corresponds to your Arduino.



STEP 8: SELECT YOUR SERIAL PORT

Select the serial device of the Arduino board from the Tools | Serial Port menu. This is likely to be COM3 or higher (COM1 and COM2 are usually reserved for hardware serial ports). To find out, you can disconnect your Arduino board and re-open the menu; the entry that disappears should be the Arduino board. Reconnect the board and select that serial port.

STEP 9 : UPLOAD THE PROGRAM

Now, simply click the "Upload" button in the environment. Wait a few seconds - you should see the RX and TX leds on the board flashing. If the upload is successful, the message "Done uploading." will appear in the status bar.

CONCLUSION

Thus the “ARDUINO BASED AUTOMATIC PLANT WATERING

SYSTEM” has been designed and tested successfully. It has been developed by integrated features of all the hardware components used. Presence of every module has been reasoned out and placed carefully, thus contributing to the best working of the unit. Thus, the Arduino Based Automatic Plant Watering System has been designed and tested successfully. The system has been tested to function automatically. The moisture sensors measure the moisture level (water content) of the different plants. If the moisture level is found to be below the desired level, the moisture sensor sends the signal to the Arduino board which triggers the Water Pump to turn ON and supply the water to respective plant using the Rotating Platform/Sprinkler. When the desired moisture level is reached, the system halts on its own and the Water Pump is turned OFF. Thus, the functionality of the entire system has been tested

thoroughly and it is said to function successfully.

REFERENCES

- The 8051 Micro controller and Embedded Systems, by Muhammad Ali Mazidi
- Design and construction of automatic power changeover system, by Jonathan Gana Kolo
- Embedded system, by Raj Kamal
- Micro processor Architecture, Programming & Applications, by Ramesh S. Gaonkar
- Fundamentals Of Micro processors and Micro computers, by B.Ram



PRODUCTION AND APPLICATION POTENTIALS OF SUGARCANE BAGASSE REINFORCED POLYMER COMPOSITES FOR ACOUSTIC CONTROL

¹Engr Sanda Askira Damboama, Department of Mechanical Engineering, Federal University of Technology Minna. Email: damboama@gmail.com

²Prof. R.N. Muriana, Department of Mechanical Engineering, Federal University of Technology Minna. Email; mrraremu@futminna.edu.ng

ABSTRACT

Acoustic isolation is one of the major problems in areas where noise control is critical. Selection of the right acoustic materials for effective absorption or reflection of such sounds is even more challenging. A material that exhibits perfect absorptivity is rated as 1.0; a perfect reflector of sound would have a coefficient of sound absorption of 0.0. The use of natural plant fibres, combinations of natural and synthetic fibers, and wood furnish as reinforcement in polyester matrix for making low cost engineering materials has generated much interest recently. Corresponding researches have also gained considerable attention to find natural, sustainable and low cost materials as alternative sound absorbers. This paper investigated the application potentials of sugarcane bagasse reinforced polymer composites for acoustic control. Sound absorber samples were produced from sugarcane bagasse and polymers of Unsaturated polyester, Polyurethane and Urea-formaldehyde respectively using compositions of filler and matrix of 50/50, 55/45, 60/40, 65/35 and 70/30 respectively and their acoustic properties investigated. The method used for measuring the acoustic properties is the impedance tube method. Sound absorption coefficients were determined at selected frequencies in accordance with ASTM 1050 – 08 standards. Acceptable sound performance and absorption coefficient of >0.75 was achieved on all tested samples at frequency of 1000Hz. This is found to be comparable with some of Branded acoustic boards.

Keywords: *Acoustic, Absorption coefficient, Polyurethane, Urea-formaldehyde, Unsaturated polyester*

1 INTRODUCTION

Acoustics is the interdisciplinary science that deals with the study of all mechanical waves in gases, liquids, and solids including vibration, sound, ultrasound and infrasound. The application of acoustics is present in almost all aspects of modern society with the most obvious being the audio and noise control industries. Acoustic isolation is one of the major problems in areas where noise control is critical. Selection of the right acoustic materials for effective absorption or reflection of such sounds is even more challenging. Sound absorbing acoustical panels and soundproofing materials are used to eliminate sound reflections, echoes and resonance reverberation. Such materials include open cell polyurethane foam, cellular melamine, fiberglass, fluffy fabrics and other porous materials. A wide variety of materials in thickness and shape are applied to walls and ceilings depending on application and environment to achieve different absorption ratings depending on the specific sound requirements. Sound diffusers reduce the intensity of sound by scattering it over an expanded area rather than eliminating the sound as an absorber would. Noise barriers block the transmission of airborne sound to devices and compounds used to isolate structures from one another and reduce impact noise. However, these acoustic materials are synthetic in nature and continuous

usage goes against the global realization of “green environment”.

Several works have been done concerning the ability of natural fibres to be employed as sound absorbers (Koizumi *et al.*, 2002). Sugarcane Bagasse being one of such natural fibres with such properties as bio-degradable, sustainable, abundant and less health risk has attracted interest in this regard (Azman *et al.*, 2013). Bagasse, the residual dry fiber of the cane after cane juice has been extracted, is used as fuel for the boilers and kilns and as raw materials for production of chemicals. It is commonly used as a substitute for wood in many tropical and subtropical countries such as India, China, Colombia, Iran, Thailand, and Argentina, for the production of pulp, paper, boards, boxes and newspaper production (Rainey *et al.*, 2016).

Polymer has wide range of applications due to its resistance to water, weather conditions and variety of chemicals. It has minimal shrinkage in comparison with other industrial fibers and is relatively cheap. The use of natural fibres, combination of natural and synthetic fibres, and wood finish as reinforcement in polyester matrix for making lowcost engineering materials have generated much interest recently (Sayester and Smith, 2015). This research work “Production and application potentials of sugarcane bagasse reinforced polymer composites for acoustic control” aims at exploring the sound absorption

properties of sugarcane bagasse composites to be used for acoustic control.

This study therefore focuses on obtaining a wideband type sound absorption materials by developing a composite materials based on sugarcane bagasse and polymers from unsaturated polyester, Polyurethane and Urea-formaldehyde respectively that meet product standards.

The intent of this research work is to explore the acoustical absorption properties of Sugarcane bagasse composites of polymers. Production and application potentials of sugarcane bagasse reinforced polymer composites for acoustic control is therefore considered as an alternative acoustic material.

2 METHODOLOGY

2.1 Materials and Equipment

The major materials used are sugarcane bagasse, unsaturated polyester, Polyurethane and Urea-formaldehyde, methyl ethyl ketone peroxide, Formaldehyde Naphthalene Cobalt, Polyurethane (Polyol), Urea, Toluene di-isocyanate (TDI), Methylene Chloride (MC), Amine, Silicon oil, Stannous octane, Concentrated sulphuric acid, Hydrogen Chloride HCL, Distilled water and Ammonium Chloride.

The equipment used are mixer, steel mould, beaker, set of sieves, electronic balance, hydraulic press machine, funnel and impedance tube.

2.2 Method

2.2.1 Production of bagasse/Unsaturated polyester composite

The major materials used in the production of the bagasse/unsaturated polyester composite were unsaturated polyester and sugarcane residual, bagasse. Also, Methyl ethyl ketone peroxide was used as the activator and Naphthalene Cobalt as accelerator.

2.3 Mixing of composite materials

Weighing of the materials in grams was done using electronic balance. Compositions by mass of sugarcane bagasse and unsaturated polyester were mixed in a glass mixer using ratios of 50/50, 60/40, 65/35 and 70/30 by mass respectively. 2mls of Methyl ethyl ketone catalyst was first introduced to the unsaturated polyester and manually stirred using a steel rod for 2 minutes. 2mls of the accelerator, Nathaline Cobalt was then brought and further mixed for further 2 minutes. Bagasse was then slowly introduced into the polyester mixture and manually stirred for 3 minutes until homogenous mix is achieved.

TABLE 1: FORMULATION FOR BAGASSE-UNSATURATED POLYMER

Sample	Bagasse	Unsaturated polyester
A	50g	50g
B	60g	40g
C	65g	35g
D	70g	30g

The mixtures were filled into the 69mm x 25.4mm round steel moulds and placed on the compression moulding machine (Carver Hydraulic Press No 4533.4D10B00). A pressure of 3bars for duration of 5 minutes was used. The samples were then transferred into a cool platen for cooling for at least 2 minutes.

2.3.1 Production of Bagasse/polyurethane composite

The major materials used in the production of the bagasse polyurethane composite were sugarcane bagasse and polyurethane.

The materials were weighed using electronic balance and charged into a stainless bowl (reactor) according to the order of arrangement and quantities in table 3.4 with exception of Toluene diisocyanate (TDI) which is based on compositions as indicated in table 3.5. At every stage of addition of each material, the mixture is thoroughly using the stirring rod rod. The milky liquor was stored for further use.

TABLE 2: FORMULATION FOR BAGASSE POLYURETHANE

Sample	Sugarcane Bagasse	Polyurethane	Toluene diisocyanate (TDI)
A	50g	50g	25g
B	60g	40g	30g
C	65g	35g	32.5g
D	70g	30g	35g

The samples were produced as indicated in the table 3.5. The quantity of the Toluene diisocyanate (TDI) was calculated based on the composition of polyurethane in each sample in relation to the typical formulation in table 3.5. The polyurethane was mixed thoroughly with the bagasse before charged into the prepared cyclic steel mould of internal diameter 69mm. The mixture was compressed on the hydraulic compression moulding machine (Carver Hydraulic press No 4533.4DIOBOO) at pressure of 3bar for 5 minutes to allow the sample to cure.

The samples were then transferred into a cool platen for cooling for at least 2 minutes.

2.3.2 Production of Bagasse/Urea-formaldehyde composite (UF)

The major materials used in the production of the bagasse urea-formaldehyde composite were sugarcane bagasse and Urea-formaldehyde.

TABLE 3: FORMULATION FOR BAGGASSE/UF COMPOSITES

Sample	Sugarcane Bagasse	Urea-formaldehyde (UF)
A	50g	50g
B	60g	40g
C	65g	35g
D	70g	30g

Urea-formaldehyde liquor was measured into a stainless container (reactor). 2grams of Ammonium Chloride was added as curing agent and mixed using glass rod. Bagasse was measured and charged into the urea – formaldehyde liquor in the reactor. The mixture was mixed thoroughly until almost homogeneity was achieved.

The mixture was filled into the prepared cyclic steel mould of inner diameter 69mm and compressed on the hydraulic compression machine (Carver Hydraulic press No 4533.4DIOBOO) at temperature and pressure of 150°C and 3bar respectively for 5minutes.



Plate I: Sample of bagasse/polymer composite

2.4 Test Procedure

2.4.1 Sound Absorption Test

Different techniques can be used to quantify the sound absorbing behavior of porous materials. In general one of the following properties is usually of interest: sound absorption coefficient (α), reflection coefficient (R), or surface impedance (Z).

Takahashi *et al.*, (2005) enumerated that measurement techniques used to characterize the sound absorptive properties of a material are

1. Reverberant Field Methods
2. Impedance Tube Methods

The acoustical properties of fabrics and webs were measured using the impedance tube method according to ASTM E 1050-08 Standard Test Method for Impedance and Absorption of Acoustical Materials; using a tube, microphone and Digital Frequency Analysis. In this method; broadband signal from a noise source plane waves are generated in the tube. A stationary sound wave pattern is formed in the tube. This sound wave pattern includes the incident sound and the fraction of the sound that has been reflected back and not absorbed by the specimen.

2.4.2 Measurement of Sound Absorption Coefficient

The acoustics material testing is done using the impedance tube B400.

The following procedures and parameters are used in calculating the absorption coefficient.

- i. The composite sample is fit into the sample holder and placed into the open end of the tube.
- ii. The function generator is adjusted to the desired frequency (250Hz).
- iii. The Cathode Ray Oscilloscope (CRO) is adjusted to show the function generator output, ensuring a pure sine wave is produced.
- iv. A signal from the function generator through the amplifier of the impedance tube is incidence on the sample. At this point both absorbed and reflected signals are captured.
- v. The Signal microscope signal level is adjusted to approximately the mid position of the screen. By adjusting the position of the microphone the maximum signal (V1)

and minimum signal (V2) registered on the CRO.

- vi. Procedures (ii) to (v) above are repeated for frequencies 500Hz, 1000Hz and 2000Hz respectively.

The Absorption coefficient is calculated below;

F (Hz) – Frequency

V1 – maximum voltage (mv)

V2 – minimum voltage (mv)

$B = V_1/V_2$ – ratio of maximum to minimum voltage (signal)

$$\alpha = \text{absorption coefficient} = 4B / (B+1)^2$$

3.0 RESULTS AND DISCUSSION

3.1 Results for Bagasse/unsaturated polyester composites

TABLE 4: BAGASSE/UNSATURATED POLYESTER COMPOSITES – 50/50

S/N	Frequency	Sound absorption
1	250Hz	0.785
2	500Hz	0.422
3	1000Hz	0.960
4.	2000Hz	0.725

TABLE 5: BAGASSE/UNSATURATED POLYESTER COMPOSITES – 60/40

S/N	Frequency	Sound absorption
1	250Hz	0.725
2	500Hz	0.274
3	1000Hz	0.888
4	2000Hz	0.750

TABLE 6: BAGASSE/UNSATURATED POLYESTER COMPOSITES – 65/35

S/N	Frequency	Sound absorption
1	250Hz	0.691
2	500Hz	0.504
3	1000Hz	0.987
4	2000Hz	0.750

TABLE 7: BAGASSE/UNSATURATED POLYESTER COMPOSITES – 70/30

S/N	Frequency	Sound absorption
1	250Hz	0.750
2	500Hz	0.691
3	1000Hz	0.960
4	2000Hz	0.816

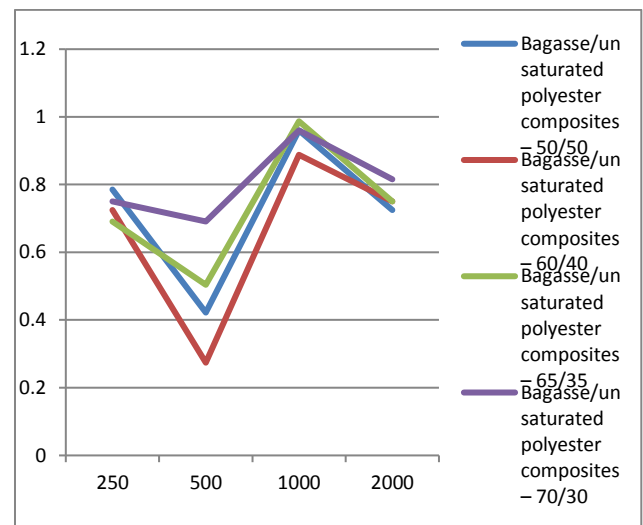


Figure 3.1: Bagasse/unsaturated polyester composites

Tables 4, Table 5, Table 6, Table 7 and Figure 3.1 show the acoustic absorption of sugarcane bagasse of four different compositions using unsaturated polyester as the binder. In Figure 3.1, the influence of the binder on the sound absorption coefficient can be observed. There is no appreciable absorption coefficient at frequency less than 600Hz. The absorption coefficients for all compositions decrease between frequencies 250Hz and 500Hz. It was observed that for frequencies above 500Hz, the absorption coefficient rose steadily for frequency up to 1000Hz and then began to decline again towards 2000Hz. For all compositions, the highest absorption coefficient of 0.987 was represented at frequency of 1000Hz for a composition of 65/35.

3.2 Results for Bagasse/Polyurethane composites

TABLE 8: BAGASSE/POLYURETHANE COMPOSITES – 50/50

S/N	Frequency	Sound absorption
1	250Hz	0.555
2	500Hz	0.349
3	1000Hz	0.888
4	2000Hz	0.816

TABLE 9: BAGASSE/POLYURETHANE COMPOSITES – 60/40

S/N	Frequency	Sound absorption
1	250Hz	0.640
2	500Hz	0.349
3	1000Hz	0.888
4	2000Hz	0.856

TABLE 10: BAGASSE/POLYURETHANE COMPOSITES – 65/35

S/N	Frequency	Sound absorption
1	250Hz	0.750
2	500Hz	0.426
3	1000Hz	0.750
4	2000Hz	0.888

TABLE 11: BAGASSE/POLYURETHANE COMPOSITES – 70/30

S/N	Frequency	Sound absorption
1	250Hz	0.640
2	500Hz	0.505
3	1000Hz	0.937
4	2000Hz	0.640

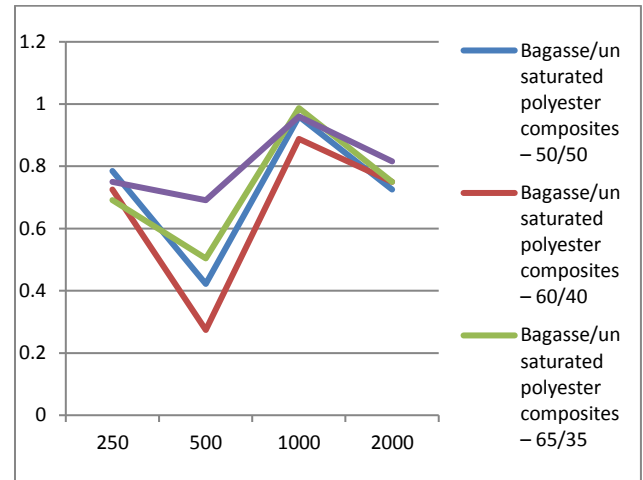


Figure 3.2: Bagasse/Polyurethane composites

Tables 8, Table 9, Table 10, Table 11 and Figure 3.2 show four different compositions of bagasse using polyurethane as the binder. In Figure 3.2, it can be seen that there is no appreciable absorption coefficient at frequency less than 600Hz. The absorption coefficients for all compositions decrease between frequencies 250Hz and 500Hz and then steadily rose for frequency up to 1000Hz and then began to decline again towards 2000Hz. For all compositions, the highest absorption coefficient of 0.937 was represented at frequency of 1000Hz for a composition of 70/30.

3.3 Results for Bagasse/Urea-formaldehyde composites

TABLE 12: BAGASSE/UREA-FORMALDEHYDE COMPOSITES – 50/50

S/N	Frequency	Sound absorption
1	250Hz	0.640
2	500Hz	0.357
3	1000Hz	0.888
4	2000Hz	0.640

TABLE 13: BAGASSE/UREA-FORMALDEHYDE – 60/40

S/N	Frequency	Sound absorption
1	250Hz	0.395
2	500Hz	0.453
3	1000Hz	0.888
4	2000Hz	0.960

TABLE 14: BAGASSE/UREA-FORMALDEHYDE – 65/35

S/N	Frequency	Sound absorption
1	250Hz	0.489
2	500Hz	0.555
3	1000Hz	0.960
4	2000Hz	0.888

TABLE 15: BAGASSE/UREA-FORMALDEHYDE – 70/30

S/N	Frequency	Sound absorption
1	250Hz	0.691
2	500Hz	0.555
3	1000Hz	0.949
4	2000Hz	0.856

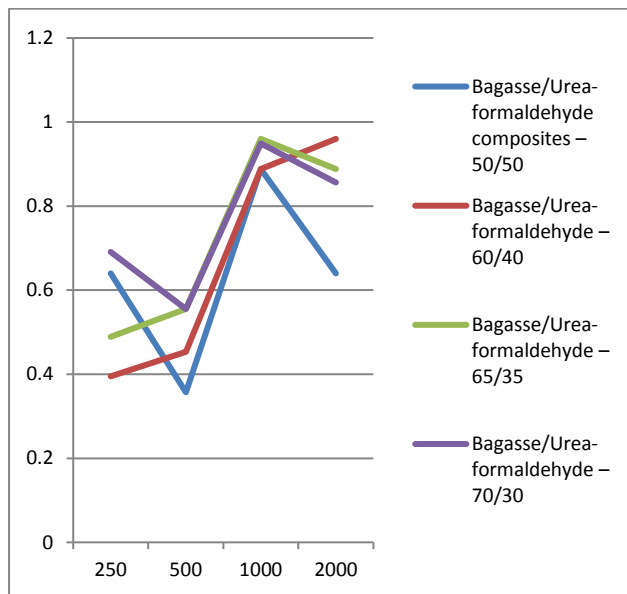


Figure 3.3: Bagasse/Urea-formaldehyde

Tables 12, Table 13, Table 14, Table 15 and Figure 3.3 show compositions of 50/50, 60/40, 65/35, 70/30 grams of bagasse and urea-formaldehyde as the binder respectively. Figure 4.3 shows no appreciable absorption coefficient at frequencies less than 600Hz. The absorption coefficients for all compositions decrease between frequencies 250Hz and 500Hz and then steadily rose for frequency up to 1000Hz and then began to decline again towards 2000Hz. For all compositions, the highest absorption coefficient of

0.960 was represented at frequency of 1000Hz for a composition of 65/35.

3.4 Comparing Absorption Coefficients of Composites with Branded Acoustic Board



Plate II: OEM acoustic board

TABLE 16: BAGASSE/UNSATURATED POLYESTER COMPOSITES – 70/30

S/N	Frequency	Sound absorption
1	250Hz	0.750
2	500Hz	0.691
3	1000Hz	0.960
4	2000Hz	0.816

TABLE 17: BAGASSE/POLYURETHANE COMPOSITES – 70/30

S/N	Frequency	Sound absorption
1	250Hz	0.640
2	500Hz	0.505
3	1000Hz	0.937
4	2000Hz	0.640

TABLE 18: BAGASSE/UREA-FORMALDEHYDE – 70/30

S/N	Frequency	Sound absorption
1	250Hz	0.691
2	500Hz	0.555

3	1000Hz	0.949
4	2000Hz	0.856

TABLE 19: CERTAINTEED OEM ACOUSTICAL BOARD

S/N	Frequency	Sound absorption
1	250Hz	0.280
2	500Hz	0.710
3	1000Hz	0.900
4	2000Hz	0.930

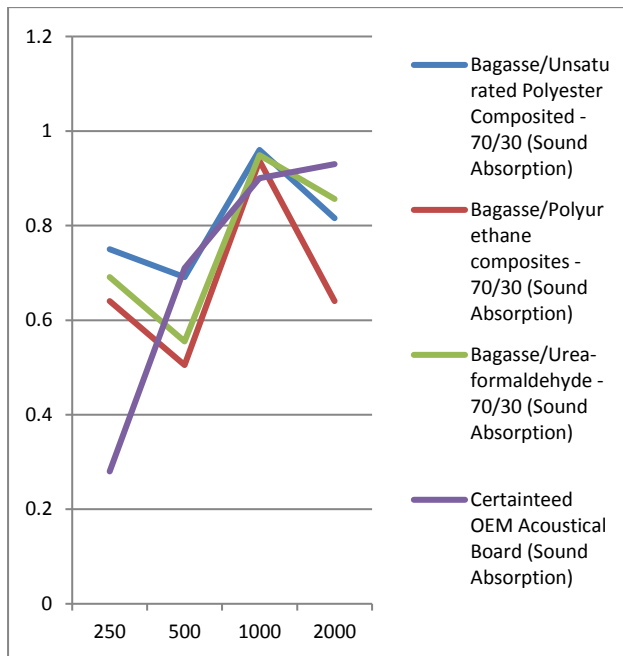


Figure 3.4: Comparing Absorption Coefficients of Composites with Branded Acoustic Board

Figure 3.4 compares compositions of 70/30 grams of bagasse/unsaturated polyester, bagasse/Polyurethane, bagasse/urea-formaldehyde and Certainteed OEM Acoustical Board respectively. The absorption coefficients for all composites decrease between frequencies 250Hz and 500Hz and then steadily rose for frequency up to 1000Hz and then began to decline again towards 2000Hz. For the OEM Acoustical Board, there is steady rise from 250Hz up to 2000Hz. However, the absorption coefficient of the OEM board is lower than those for the composite samples at frequency of 1000Hz. It is also indicated from the figure that the absorption coefficients of all the four samples is >0.90 at 1000Hz.

4 CONCLUSION

To achieve the overall aim of this study, the following objectives are highlighted:

1. To investigate the effect of polymers on the sound absorption properties of the sugarcane bagasse.
2. To have a precise understanding of the composite's acoustic characteristics, such as its performance at certain frequencies.
3. To investigate the composite's absorption coefficient and determine its suitable areas of applications.
4. To broaden the scope on the applications of polymer for acoustic use.

The results show that the polymer binders have effects on the acoustic performance of the composites. The thickness is maintained at 25.4mm while bagasse/binders are altered proportionately. It has been noticed that the lesser the densities of the binders the better the absorption coefficients of the corresponding composites. It is however observed that there is no significant difference on the affect of the individual binders on the acoustic characteristics of the composites. However, no consistent trend is shown from the results.

The results show no appreciable absorption coefficient at frequencies less than 600Hz. The absorption coefficients for all compositions decrease between frequencies 250Hz and 500Hz and then steadily rose for frequency up to 1000Hz and then began to decline again towards 2000Hz. However for bagasse/PU composition of 65/35 and bagasse/UF composition of 60/40 there is steady raise from 1000Hz. This decrease and increase was due to the specific characteristic of Lignocellulosic fibers reflecting sound at 1300 Hz but absorbing sound in the middle and high frequency ranges (E. Jayamani et al, 2014). It is seen that for frequency at 1000Hz, the absorption coefficient for all composites is > 0.75 .

This research was achieved for low and medium noise frequencies of up to 2000Hz. For such frequencies, the composites would be ideal for use on office furniture, acoustical panels, baffles, architectural panels and ceiling panels.

ACKNOWLEDGEMENTS

I wish to express my profound gratitude to my project supervisor Prof. R. A. Muriana, Dr. S.A Lawal all the staff of Mechanical Engineering Department, Federal University of Technology Minna for his support, guidance and patience in seeing to the success of the research work. I am ever indebted to my parents, family and friends. I also express my thanks to the staff of the Nigerian Institute of Leather and Science Technology, Samaru, Zaria the Department of Physics, University of Jos for



assisting in production of composite samples and test on Sound absorption respectively.

REFERENCE

- Abdullah Y., Putra A., Effendy H., Farid W.M., and Ayob M.R. (2011). *Investigation on natural fibers from dried paddy straw as a sustainable acoustic absorber*. Proceedings of IEEE 1st Conference on Clean energy and Technology (CET), Malaysia.
- Azma Putra, Yaseer Abdullahi, Hady Efendy, Wan Mohd Farid, Md Razali Ayob, Muhammad Sajidin Py (2013). *Utilizing sugarcane waste fibres as a sustainable Acoustic absorber*. Procedia Engineering 53, 632 – 638.
- Chemistry, 2012, Wiley-VCH, Weinheim. doi:10.1002/14356007.a02_115.pub2
- Dunkey, M. (1997) *Urea-Formaldehyde (UF) Adhesive Resins for Wood*. International Journal of Adhesion and Adhesives, 18, 95-107.
- Dunky, M. (1998), *Urea-formaldehyde (UF) adhesive resins for wood*," International Journal of Adhesion and Adhesives, 1998. (18:2).
- Environmental Protection Agency (2005). United States.
- Harris C.M. (1991). *Handbook of Acoustic measurement and Noise control*. (R.R. Donnelly & Sons Company) USA.
- Hoda S. Seddeg (1990). Factors Influencing Acoustic performance of sound Absorptive materials. *Australian Journal of Basic and Applied Sciences*, 3(4); 4610 – 4617, 2009 ISSN 1991-8178.
- Husseinsyah, S. and Mostapha, M. (2011), "The effect of filler content on properties of coconut shell filled polyester composites", *Malaysian Polymer Journal*, Vol.6, No.1, pp. 87-97.
- Koizumi T, Tsujiuchi N, Adachi A. (2002). *The development of sound absorbing materials using natural bamboo fibres*. In: Brebbia CA, De Wilde WP, editors. High performance structures and composites for high performance structures and materials. Witpress; p.157–66. 7.
- Lewis, H., Bell. (1994). *Industrial noise control, Fundamentals and applications*. (2nd) edition, New York: M. Dekker.
- Rainey, Thomas J, & Covey, Geoff (2016). *Pulp and paper production from sugarcane bagasse*. In O'Hara, Ian M. & Mundree, Sagadevan (Eds.) *Sugarcane-based Biofuels and Bioproducts*. John Wiley & Sons Inc, Hoboken, New Jersey, pp. 259-280.
- Saadatnia M., Ebrahimi G., and Tajvidi M. (2008). *Comparing sound absorption characteristics of acoustic boards made of Aspen particles and different percentage of wheat and barley straws*. Proceedings of 17th World Conference on Nondestructive Testing, China.
- Sachin Yadav, Gourav Gupta, Ravi Bhatnagar (2015). *A Review on Composition and Properties of Bagasse Fibers*, *International Journal of Scientific & Engineering Research*, Volume 6, Issue 5, May-2015 ISSN 2229-5518,
- Salman Zafar, (2018). *Energy Potential of Bagasse*, BioEnergy Consult
- Sayester Haghdan, Gregory D. Smith, (2015). *Natural fiber reinforced polyester composites*, *Journal of reinforced plastics and composites* Volume: 34 issue: 14, page(s): 1179-1190 Article first published online: May 29, 2015; Issue published: July 1, 2015
- Stacy E.F. (1959). *Sound Insulation in Buildings*. *Building Research station, Department of Scientific and Industrial Research*. *Journal of Royal Society for the promotion of Health*; 78, 789.



Electromagnetic Field analysis of a Single-phase Induction Motor based on Finite Element Method

Omokhafa J. Tola¹, Edwin A. Umoh², Enesi A. Yahaya³, Chika Idoko⁴, Ayo Imoru⁵

^{1,3,5}Electrical Engineering Department, Federal University of Technology, PMB 65 Minna, Niger State, Nigeria

²Electrical Engineering Technology Department, Federal Polytechnic Kaura Namoda, Nigeria

⁴Department of Electrical Engineering, University of Nigeria, Nsukka

*Corresponding author email: enesi.asizehi@futminna.edu.ng, +2348035671462

ABSTRACT

Electric motors are critical components of Electric drives systems, and their performance efficiency has consequences for the fidelity of Electric drives and control. This paper presents an analysis of the electromagnetic field of a single-phase induction motor based on two-dimensional finite element method. The developed model of the machine was used to study its performance characteristics at different speed conditions, a view to affirm the accuracy of the specifications of the motor. The motor losses were analysed and the transient results revealed the losses and a start-up time of 0.07 second with low pulsation at steady state. This implies the specifications are accurate. Therefore, the developed model has possibilities of applications in power system generating systems and industrial plants.

Keywords: Electromagnetic field analysis, finite element analysis, single-phase induction motor, transient analysis.

1 INTRODUCTION

With the recent advances in finite element analysis (FEA), it has become numerically possible to apply finite element method (FEM) to computation of magnetic fields of electrical motors, which is a numerical technique used to determine the distribution of electric or magnetic fields inside a motor, using the solutions of Maxwell's equations.

Single-phase induction motors are generally built in fractional kilowatt size and extensively used in the manufacturing industries for producing power systems and home appliances which rely on electrical rotor actions for their functionalities such as electric fans, refrigerators, vacuum cleaner, air conditioners, pumps, compressors and other types of appliances that may require fractional horsepower (Olarinoye & Oricha, 2013).

Due to the mutual coupling of the two windings (main and auxiliary) and the elliptic electromagnetic field due to the rotor winding in single-phase induction motor air gap, the electromagnetic analysis always poses challenging to designers. Special attention is paid to the machine geometry in the FEA model, by considering the outer and inner diameters of the stator and rotor as well as the air gap length. Compared to analytical method, FEM enables a designer to solve problems that are difficult to consider

with analytical method. Since analytical model of any electrical machine cannot represent complex electromagnetic phenomena such as magnetic saturation and skin effect, the use of FEA models take care of these drawbacks. In this paper, the analysis of a single-phase induction motor based on the numerical FEA model is presented. The model was developed with the Electromagnetic Suite (ANSYS MAXWELL), and used to study the performance of the motor. FEA enables a designer to compute the performance characteristics of the motor without the need to physically construct a prototype. The governing mathematical equations are developed to describe the behaviour of the motor. Electromagnetic field occupies a favourable position in engineering sciences and is one of the foundations of electrical engineering. Unlike Finite difference method (FDM), compared to methods such as Boundary element method (BEM) and Moments method (MM), FEM has gained acceptance for solving linear and nonlinear problems without geometrical restrictions (Ramón Bargallo, 2006). Several researchers have applied FEA to analyzed the electromagnetic performance of induction motor (Hong & Hwang, 1991; Williamson, Lim, & Robinson, 1990; Yahiaoui & Bouillault, 1994). In (Belmans et al., 1992), the authors applied FEA to analyzed the magnetic fields of the iron loss in an induction motor. Petkovska and Cvetkovski (Petkovska & Cvetkovski, 2010) used FEM to

analysed the starting characteristics of single phase induction motor by sizing the start-up capacitor.

2 OVERVIEW OF ANSYS MAXWELL'S SIMULATION ENVIRONMENT

ANSYS Maxwell handles low-frequency electromagnetic field simulation. It consists of different solvers, namely electrostatic, magneto-static and transient among others (Tola & Umoh, n.d.). It can be applied to modelling and analysis of electromagnetic and electromechanical devices such as transformers, motors, actuators amongst others. ANSYS uses FEM of solving the Maxwell's equations, and is therefore suitable for a variety of analysis (Maxwell, 2013). The starting point for deriving partial differential equation models for electromagnetic field computations is the application of Maxwell's equations, which relate six sets of vector and scalar: electric field intensity E (V/m), magnetic field intensity H (A/m), electric flux density D (coulomb/m²), magnetic flux density B (T), electric current density J (A/m²) and electric charge density ρ (coulomb/m³) respectively. Therefore, the static reference frame of Maxwell's equations in differential form which governs the equation of the motor are written as follows (D, n.d.):

$$\begin{cases} \nabla \times E = -\frac{\partial B}{\partial t} \\ \nabla \times H = J + \frac{\partial D}{\partial t} \\ \nabla \cdot D = \rho \\ \nabla \cdot B = 0 \end{cases} \quad (1)$$

where, E is electric field intensity, D is electric flux density, H is magnetic field intensity, J is electric current density, ρ is electric charge density, B is magnetic field density.

The electric field strength is further related by the relationship:

$$J = \sigma E \quad (2)$$

The electromagnetic prodigies defined by Maxwell's equation in static and moving reference frame are expressed as:

$$\begin{cases} B^* = B \\ E^* = E + v \times B \\ H^* = H \\ J^* = J \end{cases} \quad (3)$$

Where the quantities on the right-hand side described the moving reference frame, and the electric field vector E is only quantity modified. The divergence of the magnetic field density is given by:

$$\nabla \cdot B^* = 0 \quad (4)$$

The magnetic vector potential satisfies the following expressions:

$$\nabla \cdot (v \nabla A) = -J \quad (5)$$

$$J = \sigma E^* = \sigma (E + v \times B) \quad (6)$$

Where H is the magnetic field strength, A is magnetic vector potential, J is the current density, v is the moving velocity, σ is the conductivity of the material.

3 MODEL EQUATIONS OF THE MOTOR

The voltage equation of the (stator) phase winding and rotor bars of the machine are expressed as (Sami Kanerva & Slavomir Seman, n.d.):

$$V_p = \frac{d\psi}{dt} + R_c i + L_e \frac{di}{dt} \quad (7)$$

Where R_c is the resistance of the coils, V_p is the phase voltage and L_e is the coil inductance. The flux linkage of the coils is determined by the relationship:

$$\psi = \sum_{k=1}^{n_c} \beta_k l_k A_k^{ave} \quad (8)$$

Where

β_k is a multiplier l_k is the length of the coil side, A_k^{ave} is the average vector potential.

The currents and the magnetic vector potential are obtained from the field solution (8) where the applied voltages are

source of field to the phase windings in the stator and the rotor.

The electromagnetic torque of the machine expressed as:

$$T_e = l_a \frac{d}{d\theta_r} \int_{\Omega} \int_0^H B \cdot dH d\Omega \quad (9)$$

Where l_a is the machine axial length, Ω is the cross-sectional area of the air gap and θ_r is the rotor position. The equations governing the movement of the motor are given by:

$$J_m \frac{d\omega}{dt} + B\omega = T_e - T_f \quad (10)$$

$$\frac{d\theta_r}{dt} = \omega \quad (11)$$

Where J_m is the moment of mechanical inertia, B is the damping coefficient, which is very small and can be neglected, ω is the rotational speed, T_e is electromagnetic torque and T_f is the load torque applied externally. FEA analyzes the transient conditions of the motor using two-dimensional vector potential formulation and voltage equations of the windings. Therefore, the field solution is used to determine the magnetic flux density and the magnetic field strength respectively.

Second-order differential equations are used to define the boundary value of two-dimensional finite element analysis. As a result, the magnetic field of the FEM model in two-dimensional plane is analytically expressed as:

$$\frac{\partial A}{\partial x} \left(\frac{1}{\mu} \frac{\partial A}{\partial x} \right) + \frac{\partial A}{\partial y} \left(\frac{1}{\mu} \frac{\partial A}{\partial y} \right) = J - j\omega\sigma A \quad (12)$$

Where ω is the angular frequency of the magnetic field. The development of the FEA model of the single-phase induction motor is based on the procedure established in (Tola & Umoh, n.d.). The geometry dimension, and other parameters used are tabulated in Table I. Based on Eq. (4) to (11), the magnetic vector potential and current density are computed by finite element method using ANSYS Maxwell software.

Table I: Single-phase induction motor parameters.

Parameter	Value
Rated Output Power (kW)	0.37
Number of the stator slot	24
Stator outer diameter (mm)	95
Stator inner diameter (mm)	55.25
Air gap (mm)	0.25
Number of the rotor slot	18
Rotor inner diameter (mm)	16
Stator core length (mm)	65
Rated speed (rpm)	3750

The results obtained and portrayed by Fig. 1 to Fig. 4 showed the performance characteristics of the proposed single-phase induction motor design using ANSYS Maxwell. These results meet the required specifications for the design of the motor.

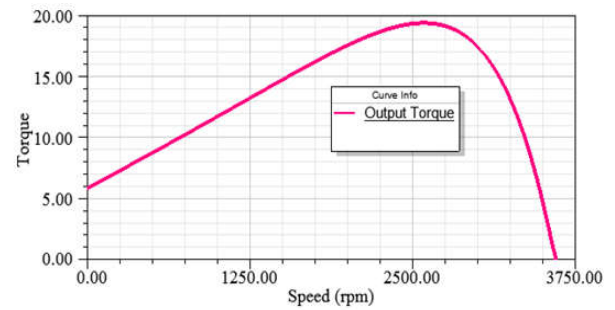


Fig. 1. Torque versus rotor speed

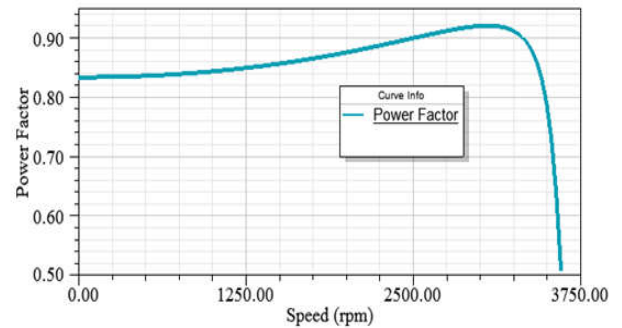


Fig. 2. Power factor versus rotor speed

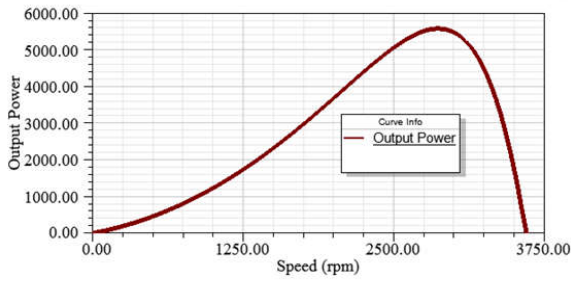


Fig. 3. Output power versus rotor speed

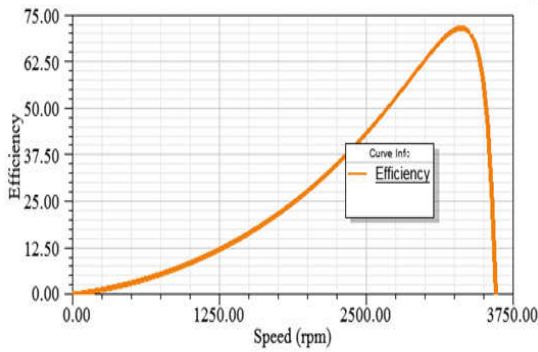


Fig. 4. Efficiency versus rotor speed

A. Meshing

The cross-section of the motor is divided into some two-dimensional elements which determines the accuracy of the magnetic vector potential A . Triangular elements are typically used for 2-D models and each element is related by several nodes by the relationship:

$$\phi^e(x, y) = \sum_{j=1}^3 N_j^e(x, y) \phi_j^e \quad (13)$$

Where $N_j^e(x, y)$ are expansion functions which are expressed by the relationship:

$$N_j^e(x, y) = \frac{1}{2\Delta^e} (a_j^e + b_j^e x + c_j^e y) \phi_j^e \quad (14)$$

Where Δ^e is the area of the e^{th} element. Fig. 5 shows the mesh generation of the model, and its spread over the whole cross-section of the motor. Fig. 6 shows the equivalent circuit of the motor.

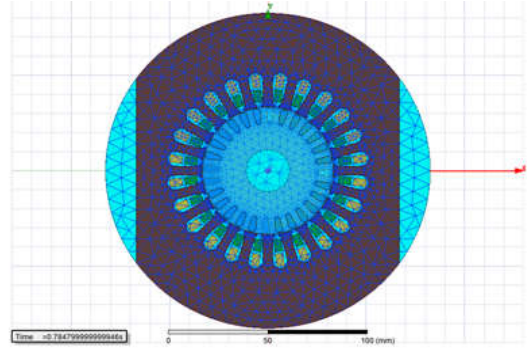


Fig. 5. 2-D mesh of the motor



Fig. 6. The equivalent circuit of the motor

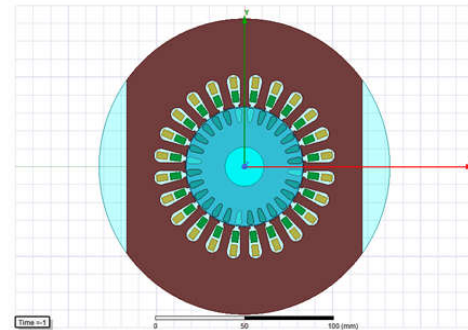


Fig. 7. 2-D model of the motor

3.1 SIMULATION OF RESULTS

The dynamic operation of the induction motor with 100mF capacitor, 230V supply at 50 Hz are analyzed and presented. The dynamic characteristics used in (Krzysztof MAKOWSKI & Marcin J. WILK, 2011) were also used in this study. The transient behavior of the machine was simulated under no-load condition, with stopping time of

2s at 0.002 steps. The starting waveforms of the motor are depicted in Fig. 8 – Fig. 11.

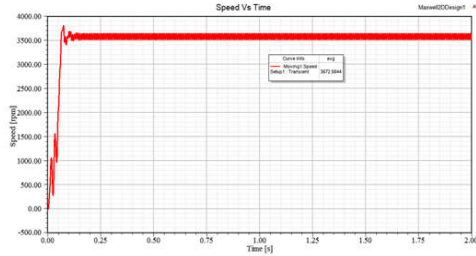


Fig. 8. Rotor speed

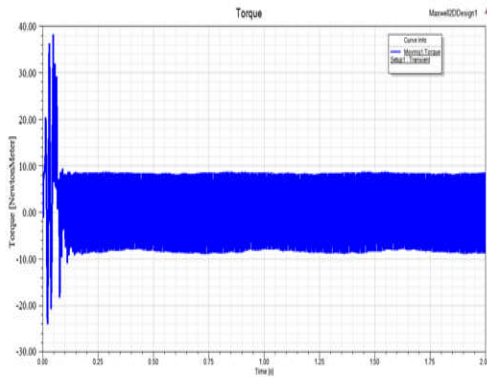


Fig. 9. Electromagnetic Torque

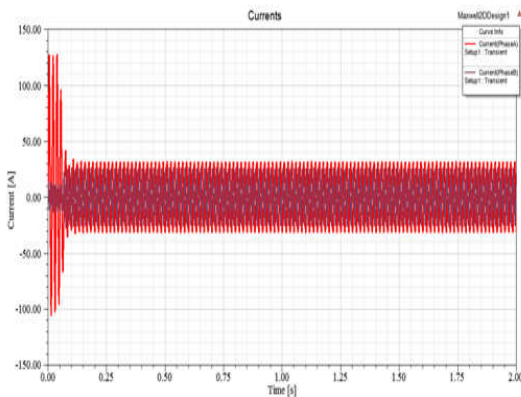


Fig. 10. Stator currents

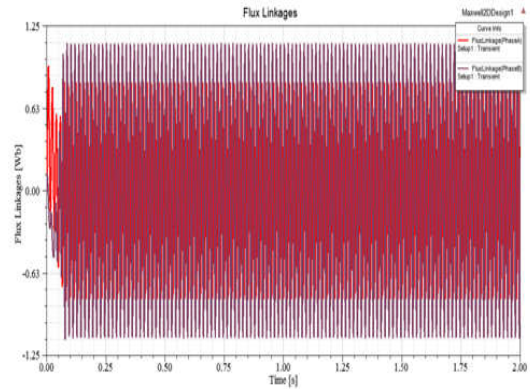


Fig. 11. Flux Linkages

The motor starts and reaches synchronous speed in 0.07 seconds. The elliptical rotational field in the air gap due to the asymmetry of the stator windings leads to non-uniform running of the rotor. It was observed that the capacitor placed on the auxiliary winding increases the start-up of the motor and a phase shift increase.

3.2 ANALYSIS OF LOSSES

The efficiency of a single-phase induction motor can be used to gauge its performance. Electrical engineers have continued to optimize electric motors with the aim of improving their efficiencies. However, a universal challenge during optimization of motor efficiency relates to losses in the magnetic circuit of the motor. Motor losses may be broadly classified as stator copper loss, core losses, rotor eddy current losses and windage loss (Huynh, Zheng, & Acharya, 2009)(Engineering, Ko, Jang, Park, & Lee, 2010). Copper loss includes I^2R loss. Core losses occur when the magnetic material is exposed to a time-varying magnetic flux, and is made up of two major components-hysteresis loss and eddy current loss, and are measured based on sinusoidal flux density of fluctuating magnitude and frequency. It can be expressed as (Gordon, R. Slemon, 1990)(Smith, 1995):

$$P_{Core} = K_h f B_{max}^\alpha + K_e f^2 B_{max}^2 \quad (15)$$

Where f is frequency, B_{max} is the peak flux density in Tesla,

K_h , K_e and α are constants for the core material.

SOLID LOSS

The stranded loss which is the ohmic loss of multi-turn coils or stranded type coil. it can be determined by the expression (Tikhonova, Malygin, Beraya, Sokolov, & Plastun, n.d.):

$$P = \frac{1}{\sigma_V} \int J^2 dV \quad (16)$$

Where V is the volume. In research, core loss, solid loss and stranded loss are a major concern. However, hysteresis and eddy-current loss are often neglected in the performance analysis of electrical machines due to the difficulty in the classical formula caused by the distribution of magnetic field strength and flux density. Fig. 12 depicts results associated with the motor. However, with proper selection of the magnetic material, the core loss will be negligible. Fig. 13 and Fig. 14 portrayed the distribution of magnetic line and magnetic flux density on of the 2-D module machine. The presence of high magnetic flux density distribution in the stator and rotor can be lowered by implementing a high-quality material at the critical point of motor construction.

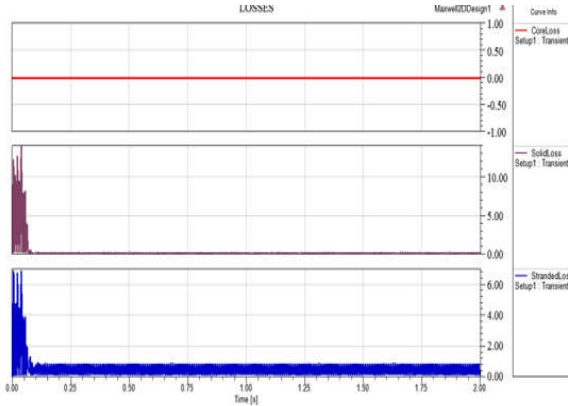


Fig. 12: Losses associated with the motor

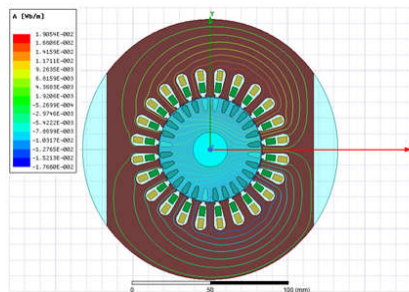


Fig. 13. Magnetic line of flux of the 2-D model motor

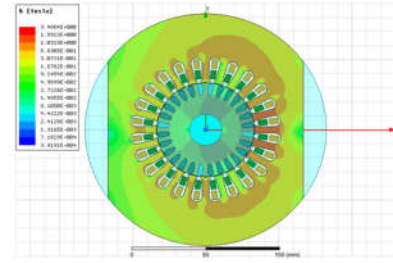


Fig. 14. The magnetic flux density of the 2-D model motor

The divergence div of the magnetic flux density, B given in (4) was computed using the ANSYS program. The computed value was $div B = 4.14E-017$ which is approximately equal to zero.

4 CONCLUSION

An analysis of the electromagnetic field of a single-phase induction motor using ANSYS Maxwell was presented. The analysis of the dynamic performance characteristics of the motor shows a good starting torque and a minimal pulsating of the rotor speed. The motor has a short start-up time of 0.07s, but the pulsation at steady state that generates the elliptic rotational field in the air gap due to the asymmetry of the main and auxiliary winding. The losses associated with the motor were clearly shown from the results presented. These results indicate that the modeled motor is a good candidate for industrial applications.

REFERENCE

- Belmans, R., Verdyck, D., Geysen, W., Findlay, R. D., Szabados, B., Spenser, S., & Lie, S. (1992). Magnetic Field Analysis in Squirrel Cage Induction Motor. *IEEE Transaction on Magnetic*, 28(2), 1367–1370.
- Ko, K., Jang, S., Park, J., & Lee, S. (2010). *Electromagnetic losses calculation of 5kW class high-speed permanent magnet synchronous motor considering current waveform*. 39(3), 7062.
- Gordon, R. Slemon, X. . (1990). Core Losses in Permanent magnet motors. *IEEE Transactions on Magnetics*, 26(5).
- Hong, C. H., & Hwang, G. J. (1991). *Non Linear Finite Element Modeling for Electrical Energy Applications Lecture Notes for ET4375*.



- Belmans, R., Verdyck, D., Geysen, W., Findlay, R. D., Szabados, B., Spenser, S., & Lie, S. (1992). Magnetic Field Analysis in Squirrel Cage Induction Motor. *IEEE Transaction on Magnetic*, 28(2), 1367–1370.
- Ko, K., Jang, S., Park, J., & Lee, S. (2010). *Electromagnetic losses calculation of 5kW class high-speed permanent magnet synchronous motor considering current waveform*. 39(3), 7062.
- Gordon, R. Slemon, X. . (1990). Core Losses in Permanent magnet motors. *IEEE Transactions on Magnetics*, 26(5).
- Hong, C. H., & Hwang, G. J. (1991). Non Linear Complex Finite Element Analysis of Squirrel Cage Induction Motor Performance. *Electrical Power Application Institute of Electrical Engineering Proceeding*, 277–284.
- Huynh, C., Zheng, L., & Acharya, D. (2009). *Losses in High Speed Permanent*. 131(March), 2–7. <https://doi.org/10.1115/1.2982151>
- Krzysztof MAKOWSKI, & Marcin J. WILK. (2011). Determination of dynamic characteristics of the single-phase capacitor induction motor. *Electrotechnical Review Vol 87, No. 5*, 231–237.
- Maxwell, A. (2013). *ANSYS Maxwell V16*. 1–31.
- Olarinoye, G. A., & Oricha, J. Y. (2013). *A Method for Solving the Voltage and Torque Equations of the Split-Phase Induction Machines*. 10(1), 1–6.
- Petkovska, L., & Cvetkovski, G. (2010). *FEM based assessment of capacitor sizing on starting characteristics of a single-phase induction motor*. (12), 113–116.
- Ramón Bargallo. (2006). *Finite Element for Electrical Engineer*. UNIVERSITAT POLITÈCNICA DE CATALUNYA, ELECTRICAL ENGINEERING DEPARTMENT.
- Sami Kanerva, & Slavomir Seman. (n.d.). Inductance Model for Coupling Finite Element Analysis With Circuit Simulation. *IEEE Transaction on Magnetic*, 41(5), 1620–1623.
- Smith, K. E. (1995). Influence of manufacturing Processes on Iron losses A.C. *IEEE Conference on Electrical Machine Drive*, (412).
- Tikhonova, O., Malygin, I., Beraya, R., Sokolov, N., & Plastun, A. (n.d.). *LOSS CALCULATION OF INDUCTION MOTOR WITH RING WINDINGS BY "ANSYS MAXWELL."* 5(11), 63–66.
- Tola, O. J., & Umoh, E. A. (n.d.). MODELING AND ANALYSIS OF A PERMANENT MAGNET SYNCHRONOUS GENERATOR DEDICATED TO WIND ENERGY CONVERSION. *2nd International Engineering Conference (IEC 2017) Federal University of Technology, Minna, Nigeria*, 216– 223



PARAMETER INVESTIGATION AND ANALYSIS FOR ELITE OPPOSITION BACTERIAL FORAGING OPTIMIZATION ALGORITHM

*Maliki, D¹, Muazu, M. B², Kolo, J.G³, & Olaniyi, O. M⁴

^{1,4}Department of Computer Engineering, Federal University of Technology, PMB 65 Minna Niger State, Nigeria

²Department of Computer Engineering, Ahmadu Bello University Zaria Kaduna State, Nigeria

³Department of Electrical and Electronics, Federal University of Technology, PMB 65 Minna Niger State, Nigeria

*Corresponding author email: danlami.maliki@futminna.edu.ng, +2348062502102

ABSTRACT

The investigation and analysis of algorithm parameters is an important task in most of the global optimization techniques. However, finding the best set of parameter value for the optimum performance of an algorithm still remain a challenging task in a modified Bacteria Foraging Optimization Algorithm (BFOA) since most of the existing research focuses on the application of the algorithm and likewise it benchmarking with the global test function. The Elite Opposition Bacterial Foraging Optimization Algorithm (EOBFOA) is a modified nature inspired optimization algorithm from BFOA which focuses on the generation of an elite solution from the opposition solution for an optimization process. This research is focused on the investigation of such parameters population size, probability of elimination dispersal, step size and number of chemotaxis so as to determine the extent to which they affect the optimal solution from the EOBFOA with respect to global minimum or least minimum standard deviation. From the results obtained, it was observed that the global minimum in EOBFOA depend on the exploitation ability of the bacteria in the search space.

Keywords: BFOA, EOBFOA, elite solution, opposition solution, parameters.

1 INTRODUCTION

Every organism in life is faced with the problem of survival needs. The needs for survival ranges from the availability of water, food, minerals, sunlight and even oxygen for sufficient movement and growth. These resources are been acquired using different strategies, the behavioural process of using different strategies for survival is refer to as foraging (Hai, 2014). In optimization process foraging activities are relevant in providing inspiration for the design of different algorithms. The search for nutrient, the quality and quantity of the nutrient with the characteristics of the forager must also be taken into consideration during the algorithm development (Murugan, 2015). In the foraging search process, the ability of exploring the entire search space also depends on the elite individual participating in the foraging process (Naresh, 2011).

Some algorithms developed were obtained from biological processes which mimic the behaviour of some particular organisms (plants and/or animals). For example, Particle Swarm Optimization (PSO) proposed by Eberhart and Kennedy from the Social behaviour of bird and fish schooling, Genetic Algorithm (GA) proposed by Holand from genetics and Darwinian evolution theory, and the Ant

Colony Optimization (ACO) developed by Dorigo based on the foraging behaviour of ants (Hanning, 2011). Nature inspired algorithms can be grouped into either population or trajectory-based. The population-based algorithms involve the use of agents that perform the search process so as to arrive or converge to a better solution. Whereas, the trajectory-based uses a single agent that moves through the design space (Mouayad, 2018).

The performance of nature inspired algorithms revolves around the exploration and exploitation abilities of the search agent during the search process in finding a good solution. The exploration process searches the entire search space so as to determine the possible region(s) of the best solution(s) while exploitation is a local search process that uses ideas from problem of interest to obtain a best possible solution from the outcome of exploration (Yang, 2014). In nature inspired algorithms, population size is one of the important parameters in the optimization process. In addition, it favours more of the exploration during the search process. The relationship between population size and dimension of the optimization problem is of great important. Varying the population size or selecting the right population can enhance the performance of the algorithm (Li, 2010).



The BFOA inspired by the *E.Coli* foraging strategy can be simulated based on different processes of chemotaxis, swarming, reproduction, elimination and dispersal (xiaohual, 2016). The chemotaxis is a search behaviour of the bacteria that implements the method of optimization in which the bacteria try to move up to a nutrient concentration level by avoiding harmful substances by finding its way into acidic or alkaline free environment. The bacteria when in a favourable medium swim for a long time by releasing a chemical substance during swarming to attract its fellow bacteria and when in an acidic region turns to move away to find an environment that favours its survival (Nachammai, 2017).

Furthermore, after swarming process, the bacteria extend to another stage of elimination and dispersal. In this stage, the bacteria with the lowest value of cost function will survive and also split into two making the population of the bacteria remains constant (Vipul, 2012). The elimination dispersal event greatly influences the performance of chemotaxis. This process can also result in the death of some bacteria due to increase in temperature as well as other factors that can disperse the bacteria such as water (Heng, 2018). The value of step size is one of the most sensitive parameters in BFOA when solving constraint optimization problems. The right choice of step size can make the algorithm to converge to a better result (Betania, 2014).

This research is focused on the variation of population size, probability of elimination-dispersal, step size and number of chemotaxis as an optimization parameter value in EOBFOA. The population size provides how small or large the search space will be during the exploration activities of the bacteria. In foraging process of the bacteria, there are possibilities that certain bacteria will be eliminated by the process of probability of elimination-dispersal so that the algorithm will not be trapped in a local optima search. The step size and number of chemotaxis step are important to the performance of the algorithm since the bacteria will try to avoid noxious substance and tend to concentrate in a region of better nutrient for best performance.

2 ELITE OPPOSITION BACTERIA FORAGING PROCESS

The process is shown using the following relevant equations

$$V_i^t = [v_{i1}^t, v_{i2}^t \dots v_{iD}^t] \quad (1)$$

represent the *i*th solution in the current population at generation *t*. its elite opposition-based solution is represented in equation (2).

$$EP_i^t = [ep_{i1}^t, ep_{i2}^t, \dots, ep_{iD}^t] \quad (2)$$

is given by

$$ep_{i1}^t = k \cdot (F_j^t + G_j^t) - x_{i1}^t \quad (3)$$

$$EF_j^t = \min(ex_{mj}^t),$$

$$EG_j^t = \max(ex_{mj}^t),$$

$$ep_{i1}^t = rand(EF_j^t, EG_j^t),$$

$$\text{if } ep_{i1}^t < LG_i \parallel ep_{i1}^t > UG_i$$

$$i = 1, 2, \dots, SN; j = 1, 2, \dots, D;$$

$$m = 1, 2, \dots, ER; k = rand(0, 1)$$

Where

$$EV_m^t = [ex_{m1}^t, ex_{m2}^t, \dots, ex_{m,D}^t] \quad (4)$$

$m = 1, 2, \dots, ER$ are the chosen elite solutions

Where ep_{ij}^t is the elite opposition-based value of x_{ij}^t , ER is the size of the selected elite solution.

Where EF_j^t and EG_j^t are the minimum and maximum value of the *j*th dimension of the selected elite solutions (Guo, 2015).

[1] Initialize parameters $p, S, N_c, N_s, N_{re}, N_{ed}, P_{ed}, C(i), (i = 1, 2, \dots, S), \theta^i$.

[2] Elimination-dispersal loop: $l = l + 1$

[3] Reproduction loop: $k = k + 1$

[4] Chemotaxis loop: $j = j + 1$

(a) for $i = 1, 2, \dots, S$

Chose the ER elite solutions from the current population

Calculate the lower and upper boundary of the chosen elite solution

$$\text{for } i = 1 \text{ to } SN$$

$$k = rand(0, 1)$$



<p>Create the elite opposition solution and evaluate EP_i^t</p> <p>Chose the top best SN solution from population and the elite opposition population</p> <p style="padding-left: 40px;">else</p> <p>compute the normal procedure of the traditional BFOA</p> <p>Perform a chemotactic step for bacterium i as follows</p> <p>(b) Compute fitness function, $J(i, j, k, l)$.</p> <p>Let, $J(i, j, k, l) = J(i, j, k, l) + J_{cc}(\theta^i(i, j, k, l), P(i, j, k, l))$</p> <p>(c) Let $J_{last} = J(i, j, k, l)$</p> <p>(d) Tumble by generating a random vector $\Delta(i) \in \mathfrak{R}^p$ with each element $\Delta_m(i)$, $m = 1, 2, \dots, p$ a random number on $[-1, 1]$</p> <p>(e) Move: Let $\theta^i(j + 1, k, l) = \theta^i(j, k, l) + C(i) \frac{\Delta(i)}{\sqrt{\Delta^T \Delta(i)}}$</p> <p>There will be a step size $C(i)$ in the direction of tumble for bacterium i</p> <p>(f) Compute $J(i, j + 1, k, l)$ and let</p> $J(i, j + 1, k, l) = J(i, j, k, l) + J_{cc}(\theta^i(j + 1, k, l), P(i, j + 1, k, l))$ <p>(g) Swim</p> <p>Let $m = 0$ (counter for swim length)</p> <p>While ($m < N_s$). Do</p> <p style="padding-left: 40px;">Let $m = m + 1$.</p> <p style="padding-left: 40px;">If $J(i, j + 1, k, l) < J_{last}$ (if doing better) then</p> <p style="padding-left: 80px;">Let $J_{last} = J(i, j + 1, k, l)$ and let</p> $\theta^i(j + 1, k, l) = \theta^i(j, k, l) + C(i) \frac{\Delta(i)}{\sqrt{\Delta^T \Delta(i)}}$ <p style="padding-left: 40px;">And use this $\theta^i(j + 1, k, l)$ to compute the new $J(i, j + 1, k, l)$ as in (f)</p> <p style="padding-left: 40px;">Else</p> <p style="padding-left: 80px;">let $m = N_s$</p>	<p>end if</p> <p>end while</p> <p>(h) Move to the next bacterium ($i + 1$) if $i \neq S$ (i.e move to [b] and process the next bacterium)</p> <p>[5] IF $j < N_c$, the life of the bacteria is not over move to step 4.</p> <p>[6] Reproduction:</p> <p>(a) for each $i = 1, 2, \dots, S$, and for given k and l,</p> <p>Let $J_{health}^i = \sum_{j=1}^{N_c+1} J(i, j, k, l)$</p> <p>and sort the bacteria in ascending order of J_{health}</p> <p>(b) The bacteria with the highest J_{health} die and the one with lowest J_{health} survive and split into two.</p> <p>[7] If $k < N_{re}$, move to step 3. Since the maximum number of N_{re} is not attain.</p> <p>[8] Elimination-dispersal loop.</p> <p>for $i = 1, 2 \dots S$ with P_{ed} do</p> <p>eliminate and disperse each bacterium.</p> <p>if $k < N_{ed}$ then</p> <p style="padding-left: 40px;">Go to step 2.</p> <p>else</p> <p style="padding-left: 40px;">end</p> <p style="padding-left: 40px;">end if</p> <p>end for</p> <p>3 RESULTS AND DISCUSSION</p> <p>The parameter investigation and analysis of EOBFOA is perform using zakrov function for the unimodal test with the range of [-5 10] as shown in figure 1 and Goldstein and price function for multimodal test with the range of [-2 2] as shown in figure 2. The objection function for zakrove function with Goldstein and price function are given in equation (5) and equation (6).</p>
--	---

$$f_1(x) = \sum_{i=1}^n x_i^2 + \left(\frac{1}{2} \sum_{i=1}^n ix_i\right)^2 + \left(\frac{1}{2} \sum_{i=1}^n ix_i\right)^4 \quad (5)$$

$$f_2 = [1 + (x_1 + x_2 + 1)^2(19 - 14x_1 + 3x_1^2 - 14x_2 + 6x_1x_2 + 3x_2^2)] \times [30 + (2x_1 - 3x_2)^2(18 - 32x_1 + 12x_1^2 - 48x_2 + 36x_1x_2 + 27x_2^2)] \quad (6)$$

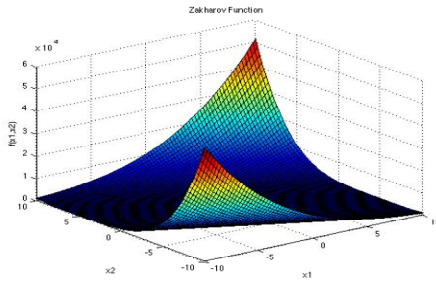


Figure 1: Zakrov function

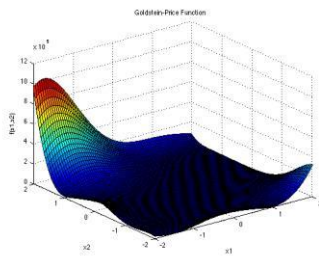


Figure 2: Goldstein and price function

The EOBFSA is run ten times for twenty iteration, for each chosen value of S , P_{ed} , $C(i)$, and N_c . The best minimum convergence value, worst convergence value, mean value and standard deviation value were calculated. Where M1 = Mean Value for unimodal test function, B1= Best convergence value for unimodal test function, W1 = Worst Value for unimodal test function Std1 = Standard deviation value for unimodal test function, M2 = Mean Value for multimodal test function, B2= Best convergence value for multimodal test function, W2 = Worst Value for multimodal test function, Std2 = Standard deviation value for multimodal test function.

3.1 EFFECT OF POPULATION SIZE (S) on EOBFSA

The chosen population size (S) for EOBFSA is shown in table 1.1. The test for each population size is perform using unimodal and multimodal benchmark test function. The best global minimum (B1= 0.000 and B2= 3.1284) as shown in figure 3 and figure 4, and the least standard deviation (std1 = 0.0012 and std2 =0.5206) are obtain at population size of 20. The population size of 30 and 40 also obtain exact the global minimum but with standard deviation of std1 of 0.0047 and 0.0014, and std2 of 1.5724 and 0.5732 higher than that of population size of 20. Increasing the population size of the EOBFSA will favour more exploration of the bacteria in search space which will directly increase the complexity of the algorithm.

TABLE 1.1: POPULATION SIZE (S) ON EOBFSA

S	UNIMODAL TEST FUNCTION				MULTIMODAL TEST FUNCTION			
	M1	B1	W1	Std1	M2	B2	W2	Std2
20	0.0038	0.0000	0.0072	0.0012	3.4233	3.1284	4.3477	0.5206
30	0.0011	0.0004	0.0018	0.0047	4.3319	3.2032	6.9831	1.5724
40	0.0016	0.0065	0.0029	0.0014	3.8229	3.2436	4.4873	0.5732
50	0.0024	0.0083	0.0059	0.0022	3.8896	3.2689	5.6636	1.0502

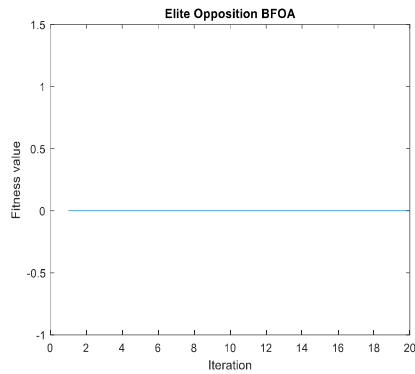


Figure 3: Unimodal test for best population size

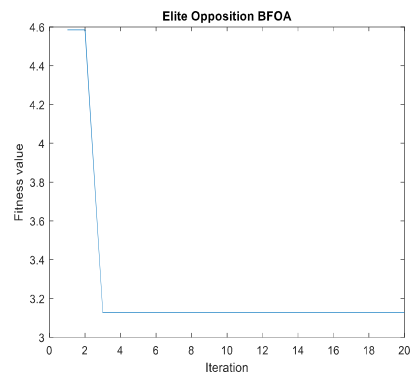


Figure 4: Multimodal test for best population size

3.2 EFFECT OF PROBABILITY OF ELIMINATION-DISPERSAL (P_{ed}) on EOBFOA

The results in table 1.2 shows the different range of P_{ed} values and its effect on EOBFOA. The global minimum (B1= 0.004 and B2 = 3.0147) is shown in figure 5 and figure 6. The least standard deviation (std1 = 0.0006 and std2 = 0.5303) is obtained at the P_{ed} value of 0.5. Increasing the value of P_{ed} above 0.5 affects the chance of getting to the global minimum. From the results obtained, if the P_{ed} value is large, the EOBFOA can degrade to a random exhaustive search. If a smaller value of P_{ed} is chosen appropriately, it will help the algorithm to escape from local minima and move to the global minimum.

TABLE 1.2: PROBABILITY OF ELIMINATION-DISPERSAL (P_{ed}) ON EOBFOA

P_{ed}	UNIMODAL TEST FUNCTION				MULTIMODAL TEST FUNCTION			
	M1	B1	W1	Std1	M2	B2	W2	Std2
0.1	0.0011	0.0004	0.0021	0.0007	3.9249	3.2671	5.0101	0.6485
0.5	0.0007	0.0000	0.0015	0.0006	3.5103	3.0417	4.4100	0.5303
0.9	0.0018	0.0005	0.0041	0.0017	3.9942	3.0537	4.0647	1.5358
1.3	0.0034	0.0006	0.0106	0.0041	5.0580	3.2206	9.9413	2.7841

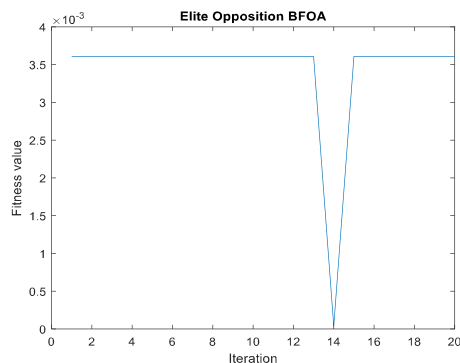


Figure 5: Unimodal test for best Ped Value

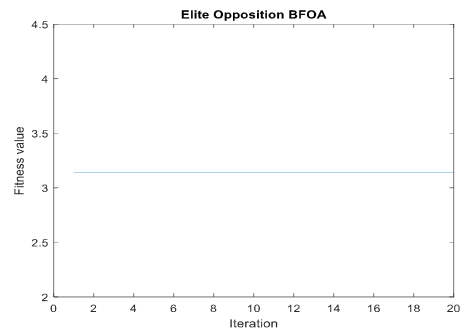


Figure 6: Multimodal test for best Ped Value

3.3 EFFECT OF STEP SIZE $C(i)$ on EOBFOA

The step size value ($C(i)$) is an important parameter with greater influence on the convergence behaviour of the EOBFAO. The best performance of EOBFAO is at $C(i)$ value of 0.01 of B1= 0.0002 and B2=3.0778 as shown in figure 7 and figure 8. The least standard deviation value of std1 = 0.0012 and std2 = 1.0535 on both unimodal and

multimodal benchmark test function is also shown in table 1.3. A higher value of $C(i)$ above 0.01 will promote exploration of the search space by the bacteria and reducing the step size value will promote the exploitation by the bacteria in the search space.

TABLE 1.3: STEP SIZE $C(i)$ ON EOBFOA

$C(i)$	UNIMODAL TEST FUNCTION				MULTIMODAL TEST FUNCTION			
	M1	B1	W1	Std1	M2	B2	W2	Std2
0.01	0.0030	0.0002	0.0043	0.0012	4.1957	3.0778	4.7561	1.0535
0.05	0.0143	0.0017	0.0163	0.0104	31.5270	5.6320	74.8100	30.0859
0.09	0.0538	0.0114	0.1823	0.0723	26.4181	3.1323	57.2976	21.4121
0.13	0.0117	0.0024	0.0276	0.0101	38.1482	12.9209	114.5691	43.1189

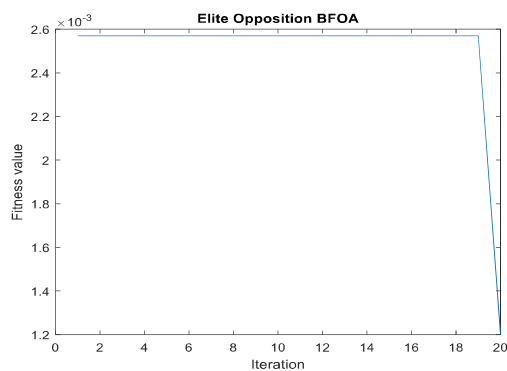


Figure 7: Unimodal test for best Cvalue

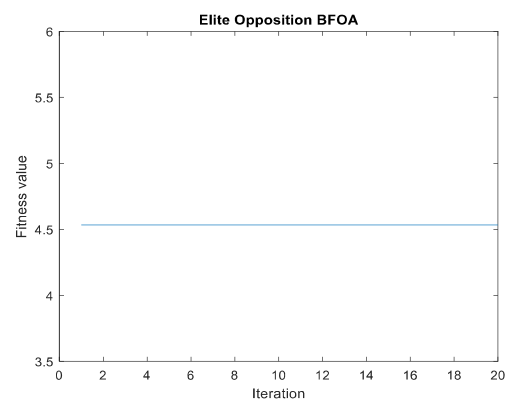


Figure 8: Multimodal test for best Cvalue

3.4 EFFECT OF NUMBER CHEMOTAXIS (N_c) on EOBFOA

The number of chemotaxis indicate the how meaningful movement the bacteria make from one location to another. From table 1.4, at $N_c = 20$, the EOBFAO performs better by arriving at the global minimum of B1 = 0.000 and B2 = 3.0811 as shown in figure 9 and figure 10. The least standard deviation is a obtain at std1 =0.0003 and std2 =

0.3715. increasing the value N_c above 20, will enable EOBFAO to move away from bad region during the optimization search process while decreasing the value of N_c below 20 will reduce the active participation of the bacteria in the search space.

TABLE 1.4: NUMBER OF CHEMOTAXIS (N_c) ON EOBFOA

N_c	UNIMODAL TEST FUNCTION				MULTIMODAL TEST FUNCTION			
	M1	B1	W1	Std1	M2	B2	W2	Std2
10	0.0006	0.0004	0.0005	0.0004	3.6178	3.1396	4.9483	0.7558
20	0.0007	0.0000	0.0018	0.0003	3.6794	3.0811	4.1247	0.3715
30	0.0032	0.0006	0.0085	0.0033	4.6853	3.3650	5.3604	1.3017
40	0.0035	0.0022	0.0041	0.0009	4.5466	3.5275	5.5310	0.8866

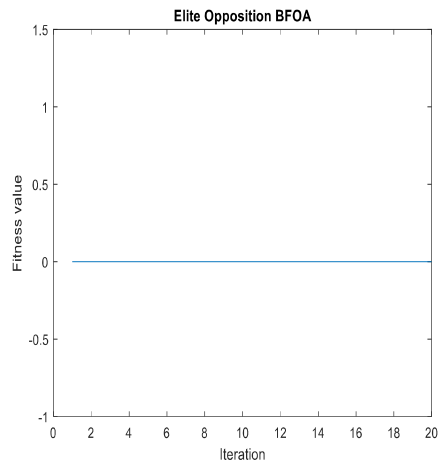


Figure 9: Unimodal test for best Nc value

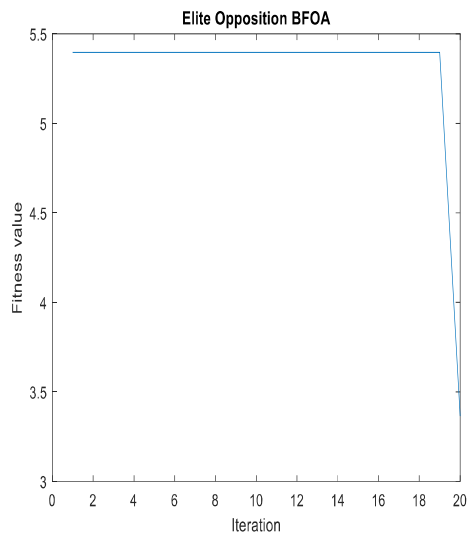


Figure 10: Multimodal test for best Nc value

4 CONCLUSION

In this research paper, an investigation and analysis of some parameters value has been performed on EOBFOA base on convergence to a better solution or the least standard deviation. From the performance analysis, it has been observed that the EOBFOA had its best performance at the population size of 20, probability of elimination of dispersal of 0.5, step size value of 0.01 and number of chemotaxis of 20. Furthermore, increasing the size of some parameter values like population will also increase the complexity or running time of the algorithm since the agent will take more time during the exploration process. Further research will focus on performance evaluation of BFOA and EOBFOA on statistical test function and

another optimization application in the field of image processing.

REFERENCES

- Betania, H., Ma D.P.P., & Efren, M. M. (2014). Step Size Control on the Modified Bacterial Foraging Algorithm for Constrained Numerical Optimization. *GECCO '14 Proceedings of the 2014 Annual Conference on Genetic and Evolutionary Computation*. Pp 25-32.
- Guo, Z., Wang, S., Yue, D., & Jian, K. L. (2015). Elite Opposition-based Artificial Bee Colony Algorithm for Global Optimization. *IJE Transactions C: Aspect* Vol.28, No. 9, Pp 1268-1275.
- Hai, S., & Yunlong, Z. (2014). Adaptive Bacterial Foraging Optimization Algorithm Based on Social Foraging Strategy. *Journal of Networks*. Pp 799-806.
- Heng, L., Wayan, I. M., Noor, A. S. (2018). Discrete Bacterial Foraging Optimization for Resource Allocation in Macrocell Femtocell Networks. *Wiley ETRI Journal*. Pp 726-735.
- Li, M.S., Ji, T.Y., Tang, W.J., Wu, Q.H., & Saunders. (2010). Bacterial Foraging Algorithm with Varying Population. *Elsevier Journal of Bio System*. Pp 185-197.
- Murugan, P., Karthikeyan, R., & Pandiaraj, K. (2015). Implementation of Bacterial Foraging Optimization Algorithm in Leaf Spring Cutting Stock Problem. *International Journal of Advanced Technology in Engineering and Science*. Pp 381-391.
- Nachammai, N., & kayalvizhi, R. (2017). Performance Analysis of Fuzzy Logic Controller Using Bacterial Foraging Optimization Algorithm. *Journal of Engineering Technologies and Innovative Research (JETIR)*. Vol. 4, Issue 12. Pp 177-182.
- Naresh, G., Ramalinga, M., & Nasasimham, S.V.L. (2011). Bacterial Foraging Algorithm for the Robust Design of Multi Machine Power System Stabilizer. *International Conference on Signal, Image Processing and Applications*. Pp 181-187.
- Sankalap, A., & Satvir, S. (2013). The Firefly Optimization Algorithm: Convergence Analysis and Parameter



3rd International Engineering Conference (IEC 2019)
Federal University of Technology, Minna, Nigeria



-
- Selection. *International Journal of Computer Applications*. Vol. 69, No. 3. Pp 48-52.
- Vipul, S., Pattnaik, S.S, & Tanuj, G. (2012). A Review of Bacterial Foraging Optimization and Its Applications. National Conference of Future Aspect of Artificial Intelligence in Industrial Automation. *International Journal of Computer Application*. Pp 9-12.
- Xiaohul, F., Yuyao, H., Honghi, Y., & Yu, J. (2016). Self-Adaptive Bacterial Foraging Optimization Algorithm Based on Evolution Strategies. *Rev. T c. Ing. Univ. Zulia*. Vol. 39, No. 8. Pp 350-358.
- Yang, X.S. (2014). Nature Inspired Optimization Algorithms. *Elsevier Journal*. Pp 1-20.



Multi-Access Edge Computing Deployments for 5G Networks

*Mosudi, I. O¹, Abolarinwa, J¹, & Zubair, S¹

¹Telecommunication Engineering Department, Federal University of Technology, PMB 65 Minna Niger State, Nigeria

*Corresponding author email: mosudi.pg7331@st.futminna.edu.ng +2348053673498

ABSTRACT

The growth of the telecommunication industry is fast-paced with ground-breaking engineering achievements. Notwithstanding the technological advancement in the industry, it had continued to cope with the phenomenon of resource constraint in portable mobile telecommunication devices compared to fixed and tethered devices. Portable mobile handheld devices have very low computational, storage and energy carrying capacity occasioned by the needs to satisfy portability, very small form factor, ergonomics, style and trends. Solutions such as cloudlets, cyber foraging, mobile cloud computing (MCC), and more recently but most applicable, multi-access edge computing (MEC) have been proffered with different application methodologies including computational offloading, distributed computing, thin clients, middleware, mobile environment cloning as well as representational state transfer. There is a need to satisfy requirements of new and emerging use cases, especially the deployments of 5G coming up with applications such as virtual reality (VR), augmented reality (AR), intelligent transport systems (ITS), connected autonomous vehicle (CAV), smart hospitals, ultra high definition multi-feed live streaming, etc. The usage patterns of most of these different applications, though not always, is ephemeral and on-demand, except that the demand will be numerous, huge, asymmetric and highly latency-sensitive in terms of needs for computation, storage and analytics while at the fringe of the network where data are being generated and results being applied. In this research, we evaluated 5G end-to-end transport for vantage location of MEC server to achieve low user plane latency.

Keywords: 5G, control plane latency, functional decomposition, Multi-access edge computing, radio access network, resource constraint, user plane latency.

1 INTRODUCTION

There are several constraints on mobile devices as well as other portable 5G user equipment (UE) devices. Computational resources, memory limitation, storage, network and energy carrying capacity are some of the constraints of cellular mobile communication UEs and these have a significant effect on the type of application software available and for how long battery can hold a charge to support such applications. The major constraints include computational power, charge holding time, storage and memory limitations, especially for complex processes [1]. Several latency critical services which need to be supported by 5G include: factory automation, intelligent transportation systems, robotics and telepresence, virtual reality (VR), augmented reality (AR), health care, serious gaming, smart grid, education and culture [2]. Moreover, the demand for high definition images and multi-feed super high definition quality live video streaming for mobile users is constantly being escalated over the recent decade. 5G is projected to provide services that will support communication, computing, control and content delivery (4C) [10] for high-intensity network traffic. There will be an enormous increase in the number of mobile devices, expectedly

about 50 billion devices, but this number will be completely dwarfed by the exponential growth in the volume of data generated by powerful applications and feature-rich multimedia applications, and these will create hype for mobile data traffic and compute requirements [11]. The advent of so much anticipated 5G technologies, newly emerging mobile applications such as augmented reality (AR), virtual reality (VR)[32], face detection and identification surveillance, connected autonomous vehicles(CAV), intelligent transportation systems (ITS) and highway traffic management systems, ultra high definition multi-feed live streaming, etc. are anticipated to be among the most demanding applications over cellular wireless networks. In particular, the newly emerging mobile Augmented Reality and Virtual Reality (AR/VR) applications are anticipated to be among the most demanding applications over cellular wireless networks [12].

To resolve challenges posed by these constraints, the computational requirements of mobile applications were offloaded [22] to be processed on tethered external infrastructures with adequate resources. These external infrastructures are usually commercial off-the-shelf or customized standardized IT infrastructures configured to



process and return results for applications. Different interventions have been proposed, including cyber foraging, cloudlet, mobile cloud computing (MCC) and multi-access edge computing (MEC).

A cloudlet is a trusted, resource-rich computer or cluster of computers that is well-connected to the Internet and is available for use by nearby mobile devices [3]. Cyber foraging dynamically augments the computing resources of mobile devices by opportunistically exploiting computing of tethered infrastructure in the surrounding environment [4], Cyber foraging provided the ability of infrastructure to seamlessly migrate computation from one node to another [5]. Cloud computing (CC) is the abstraction of computing resources e.g. processor, RAM, storage and network services from separate hardware units while presenting as a pool of reusable on-demand shared computing infrastructure that can be rapidly provisioned and released programmatically or manually with minimal management effort while creating cost benefits and flexibility. MCC is the integration of CC to serve cloud-based web apps over the Internet for smartphones, tablets, and other portable devices. Cloud computing in mobile cellular networks, like every other technology, has come with its fair share of challenges and solutions as cellular mobile communication technologies mature from 1G, 2G, 3G to 4G and looking forward to 5G. Ordinarily, cloud computing should provide enough resources for offloading [22] of computational demands. Despite all the potentials of cloud computing, it has failed in fulfilling latency requirements due to long response times, due, in turn, to the centralized cloud architecture model resulting into high signal propagation delay, affecting the end-user quality of experience (QoE) [1]. Other concerns presented by the use of cloud computing included security and privacy, addressing, interoperability, latency and bandwidth [6].

2 LITERATURE REVIEW

Prominent among the research efforts is the offloading of computation tasks based on the .NET framework to overcome the energy limitations of handhelds by leveraging nearby computing infrastructure, Mobile Assistance Using Infrastructure (MAUI) [13]. MAUI proposed a system that enabled energy-aware offload of mobile code to the connected infrastructure but could not support for multi-threaded applications but only applicable to Microsoft .NET Common Language

Runtime (CLR) based applications. M. Satyanarayanan et al, 2009, proposed hybrid solution making mobile devices function as thin clients, all significant computation performed by VM in a nearby “cloudlet”, mobile devices gracefully degrade to a fallback mode whereby significant computation occurring at a distant cloud, or, in the worst case, solely its own resources [3]. Xinwen Zhang et al (2010) proposed a cloud computing model of a distributed framework that elastically extends application between mobile UE and the cloud [14]. In [15] CloneCloud proposed the seamless transformation of mobile device computation into a distributed execution on the mobile device and cloud virtual machine (VM). Kosta S. et al, 2012, proposed ThinkAir providing an efficient way to perform on-demand resource allocation and parallelism by dynamically creating, resuming, and destroying VMs in the cloud when needed supporting on-demand resource allocation critical to the management of asymmetric mobile users computational requirements[16]. Hyrax was proposed in [36], overlaying MapReduce[71] on a cluster of mobile phones to provide infrastructure for mobile computing. Exploring the now discontinued, Android Dalvik Virtual Machine, a distributed runtime environment aimed at offloading workload from smartphones, Code Offload by Migrating Execution Transparently (COMET) [37] was proposed. Likewise, Cloudlet Aided Cooperative Terminals Service Environment for Mobile Proximity Content Delivery (CACTSE) was proposed in [70] by leveraging cooperating terminals to provide mobile internet content delivery service at the edge of the network but this relied on resource-constrained mobile devices thereby challenging its scalability. A secure service-oriented mobile ad hoc networks (MANETs) communication framework named MobiCloud was proposed in [72] providing a platform for the cloned image of UE as a virtualized component.

To the best of my knowledge, every suggested solution has been geared toward edge computing. Edge computing is the technology that brings together IT and computing into radio access network (RAN), providing rapid computation while saving costs in terms of mobile device power consumption and a lot of data traffic between network edges and the core network. This paper explores the drawbacks of previous research works as well as limitations posed by pre 5G wireless technologies and seeks to demonstrate the importance of multi-access edge computing in meeting 5G enhance mobile

broadband(eMBB) and ultra-reliable low latency communications (URLLC) specification of International Telecommunication Union (ITU) [7][8],[9].

“Edge computing is a distributed, open IT architecture that features decentralised processing power, enabling mobile computing and Internet of Things (IoT) technologies. In edge computing, data is processed by the device itself or by a local computer or server, rather than being transmitted to a data centre. “ - Hewlett Packard [28]. Multi-access edge computing, formerly mobile edge computing, is defined by European Telecommunications Standard Institute (ETSI) as a platform that provides IT and cloud computing capabilities within the radio access network (RAN) in close proximity to mobile cellular and non-cellular subscribers - It is network functionality that offers connected compute and storage resources at the fringe of network providing dramatic improvement of mobile network UE experience through near wireline latency[21]

3 METHODOLOGY

We designed prototypes for MEC deployment scenarios for 5G network and evaluated the 5G network 3GPP and non-3GPP components specifications for us to be able to compare MEC application end to end transport latency in 5G deployment with 4G as well as deployments in previous mobile wireless technologies. This took into considerations; CUPS, lower layer splits and higher layer splits. The end-to-end transport latency has a significant effect on determining the value of the user plane (UP) latency which in combination with control plane latency determines the effective end-to-end latency.

The estimated UP latency values were compared with benchmark values of known low latency use case requirements [34]:

- Virtual Reality & Augmented Reality: **7-12ms**.
- Tactile Internet (e.g. Remote Surgery, Remote Diagnosis, Remote Sales): **< 10ms**.
- Vehicle-to-Vehicle (Co-operative Driving, Platooning, Collision Avoidance): **< 10ms**.
- Manufacturing & Robotic Control/Safety Systems: **1-10ms**.

3.1 TRANSPORT NETWORK

This paper focuses on 3GPP 5G service-based architecture (SBA) as presented in Figure 8.1 instead of the standard representation in reference point architecture as we bring MEC into the RAN, specifically at the packet layer convergence protocol (PDCP) layer. In SBA, 5G network functions interact directly if required [17] by

employing RESTful API principle over hypertext transfer protocol version 2 (HTTP/2) [25] using JavaScript Object Notation (JSON) as a data format and OpenAPI as the interface definition language [26]. 3GPP 5G SBA core network functions (NF) interactions occur over a common computer platform (CCP) [34]. CCP, mostly represented as a data bus, can be fully distributed permitting localization of virtualized network functions (VNFs) in different parts of the network to manage different capabilities.

5G software entities of concern to this research work are the network exposure function (NEF) and network repository function (NRF). NEF allows access to shared data layer for MEC. It provides support for event exposure, packet flow description (PFD) s management, provisioning information for an external party which can be used for the UE in 5GS, device triggering, and negotiation about the transfer policies for the future background data transfer. Also, provide the ability to influence traffic routing [17]. The network repository function (NRF) offers discovery functions allowing for software entities in the control plane, for example, can identify others and connect directly whenever there is a need to interact.

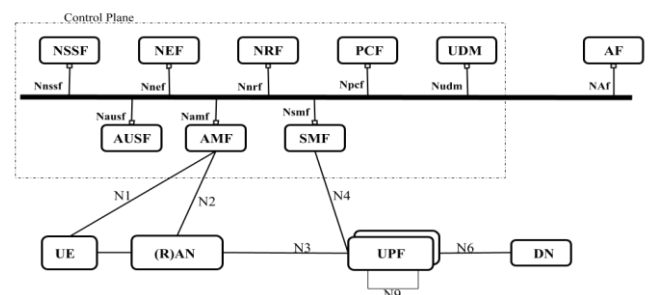


Figure 2.1: 3GPP 5G System Service-Based Architecture [17]

It provides support for register, deregister and update services to NF, NF services and consumers with notifications of newly registered NF along with its NF services. NRF provides capability which allows a particular NF service consumer to discover a set of NF instances with specific service or a target NF type. Also enables one NF service to discover a specific NF service [17] while the services available will be indexed via network exposure function (NEF) in the control plane (CP)

3.2 NG-RAN Decomposition

Considering the functional decomposition of NG-RAN achieved with Next-generation Node B Centralised Unit (gNB-CU) - gNB-Distributed Unit (gNB-DU) split connected together over F1 logical interface [19],[20]. F1 interface provides means for interconnecting a gNB-CU

and a gNB-DU of a gNB within an NG-RAN, or for interconnecting a gNB-CU and a gNB-DU of an en-gNB within an E-UTRAN [35]. While F2(eCPRI/CPRI/NGFI) is non-3GPP specified interface[24][31][33] connects gNB-DU with active antenna unit(AAU), radio unit(RU) or remote radio unit(RRU) when deployed over distance, NG logical interface connect a set of gNBs interconnected via Xn logical interface within an NG-RAN to the 5G core network (5GC)[20]. F1, F2 and NG interfaces constituting midhaul, fronthaul and backhaul networks, respectively [20].

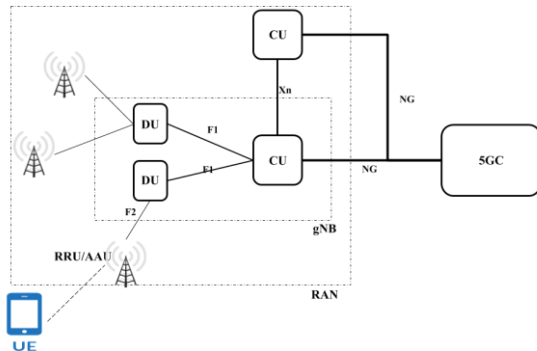


Figure 2.2: Functional Decomposition of NG RAN.

Considering eCPRI, this functional decomposition of RAN will permit the location of MEC server close to the CU sending and receiving UP packet data traffic over F1 and eCPRI providing high bandwidth capacity at very low latency capable of supporting eMBB and URLLC use cases [7], [8]. Decomposition of RAN permits distance separations between CU, DU and RRU/AAU [20] while allowing for C (cloud, cooperative and centralized) - RAN configurations [27], [28], [29] [30].

The functional decomposition of RAN may not be as simple as depicted in Figure 2.2 but it depends on the level of applicable split options as available in Figure 8.6 as this will determine the level of coordination capabilities that can be delivered by a C-RAN.

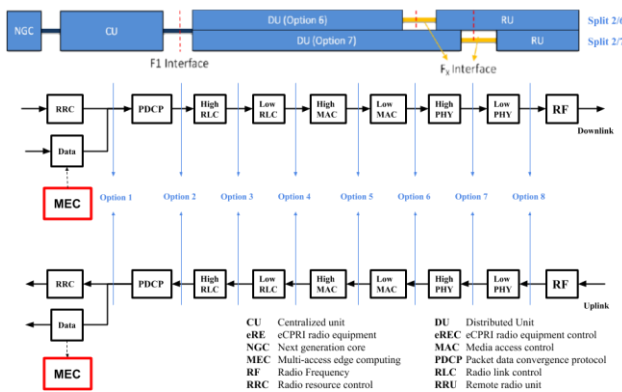
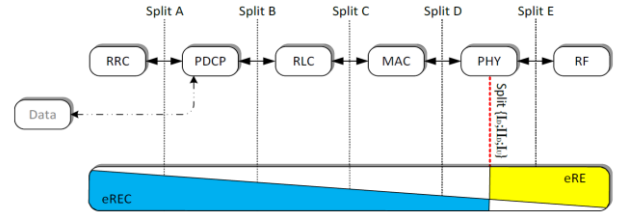


Figure 2.3(a): RAN protocol split [21], [23] with addition of MEC



2.3(b): eCPRI Functional decomposition on RAN layer level [24]

3.3 5G MEC Deployment Prototypes

Higher layer functional split (HLFS) option 2 for the midhaul [20], and lower layer functional split (LLFS) option 7 for fronthaul [24] were considered permitting four RAN deployment scenarios [20] and as a result four MEC deployment scenarios:

1. Independent RRU, DU and CU/MEC locations;
2. DU and CU/MEC co-located with distance separated RRU;
3. RRU and DU co-located with distance separated CU/MEC;
4. RRU, DU and CU/MEC integration within a single co-location.

3.4 Latency

Latency varies from one MEC deployment scenario to another and might be difficult quantifying all the parameters due to differences in performance of equipment along the way, e.g. from DU to CU [31], and all the way to MEC, etc. However, we assumed 1-way latency range between 5 ~ 8ms between CU and DU, and in essence, 8ms network latency between CU and DU eases the co-location of the CU with the Serving Gateway and other application platforms [31], but in this case, with MEC

The total one-way user plane latency becomes:

$$T = T_{NR} + T_{DU} + T_{CU} + T_{Transport} \quad (1)$$

Where:

- T_{NR} is the one-way packet propagation delay over new radio (NR) i.e delay between UE and DU, including packet processing time within the UE.
- T_{DU} is the one-way packet propagation delay between DU and CU, including processing delay within the DU.
- T_{CU} is the one-way packet propagation delay between CU and 5GC, including processing delay within the CU.
- $T_{Transport}$ is the one-way packet propagation between the 5GC and data network (DN). This might include propagation delay to the Internet if service requested by the UE is not within an operator network and has to be sourced from the Internet.

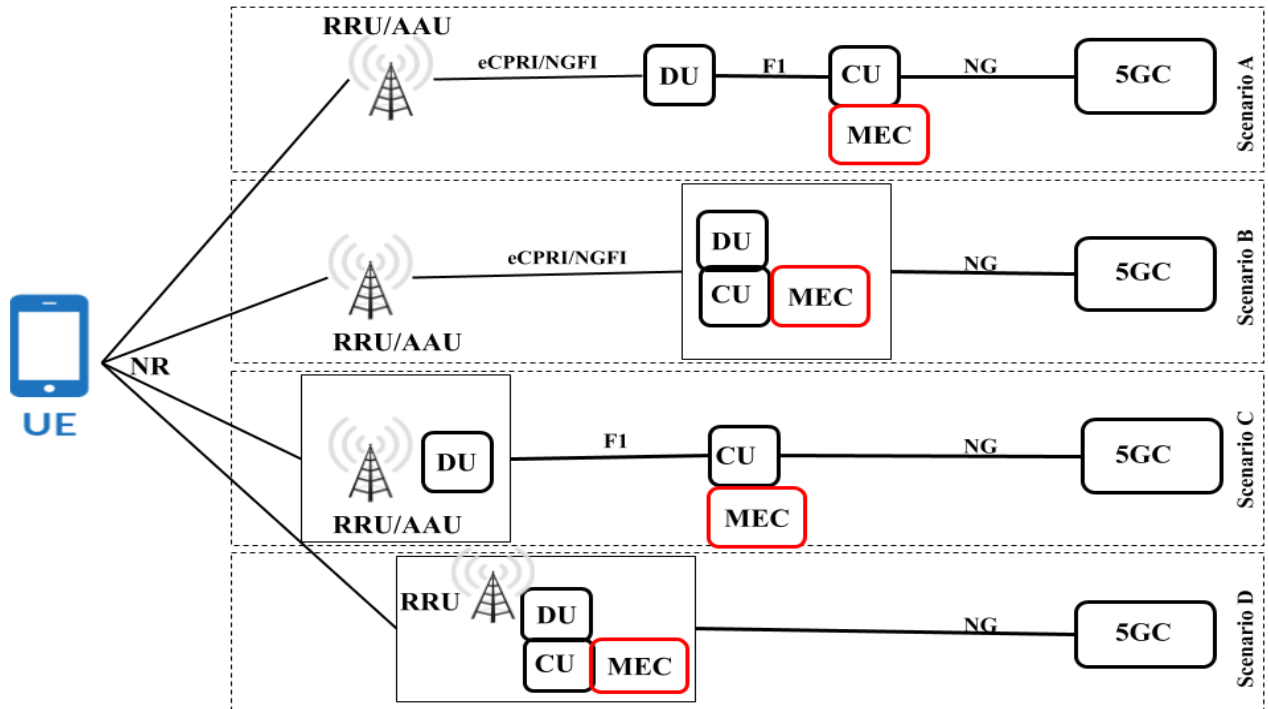


Figure 2.4: 5G MEC deployment prototypes

Deployment of MEC in all the four scenarios in the proposed prototypes above provided the options for a direct connection between MEC and the CU. The total one-way UP latency became:

$$T = T_{NR} + T_{DU} + T_{CU} \quad (2)$$

4 RESULTS AND DISCUSSION

This is a work in progress, our efforts to simulate 5G network transport latency to determine UP latency is being challenged by the fact that 5G next-generation (NG) core and RAN technologies are, to a large extent, still on white papers but enough specifications have been defined and written about it. Therefore, 3GPP and non-3GPP specifications were the major sources of our data for the evaluation of UP latency for our proposed MEC deployment.

TABLE I: 5G INTERFACES SPECIFICATIONS [20]

Network	Reach distance	Latency (1-way)	Capacity requirements
New radio(NR)		4 ms eMBB 2 ms URLLC	
Fronthaul(eCPRI)	1 ~ 20 km	< 100 μ sec	10Gb/s-825Gb/s
Midhaul(F1)	20 ~ 40 km	1.5 ~10 msec	25Gb/s-800Gb/s
Backhaul(NG)	5-80km (Aggregation) 20~300km (Core)		CU: 10Gb/s-25Gb/s CN: 100+Gb/s

Evaluating (2) for eMBB for the proposed four deployment scenarios by applying 5G specification values in Table I:

$$T = T_{NR} + T_{DU} + T_{CU} \quad (2)$$



4.1 RESULTS

SCENARIO A

$$\begin{aligned} T &= 4000 + 100 + 1500 \mu\text{sec} \\ &= 5600 \mu\text{sec} \\ &= 5.6 \text{ ms} \end{aligned}$$

Or

$$\begin{aligned} T &= 4000 + 100 + 10000 \mu\text{sec} \\ &= 14100 \mu\text{sec} \\ &= 14.1 \text{ ms} \end{aligned}$$

SCENARIO B

$$\begin{aligned} T &= 4000 + 100 \mu\text{sec} \\ &= 4100 \mu\text{sec} \\ &= 4.1 \text{ ms} \end{aligned}$$

SCENARIO C

$$\begin{aligned} T &= 4000 + 1500 \mu\text{sec} \\ &= 5500 \mu\text{sec} \\ &= 5.5 \text{ ms} \end{aligned}$$

Or

$$\begin{aligned} T &= 4000 + 10000 \mu\text{sec} \\ &= 14000 \mu\text{sec} \\ &= 14 \text{ ms} \end{aligned}$$

SCENARIO D

$$\begin{aligned} T &= 4000 \mu\text{sec} \\ &= 4000 \mu\text{sec} \\ &= 4 \text{ ms} \end{aligned}$$

4.2 DISCUSSION OF RESULTS

Scenario A features dual functional splits in the RAN. The RRU/AAU at the cell site, DU at the aggregation site while CU and MEC deployed at the edge site. Every interface interconnecting all 5G functional split contributed to the UP latency, optimally this prototype deployment produced an estimated round trip time (RTT) value of **11.2ms**. Considering scenario B, this is a centralized RAN MEC deployment which employed only the lower layer functional split having DU, CU and MEC co-located at the edge site while RRU/AAU connected via eCPRI interface is deployed at a remote cell site. Optimally, the RTT is **8.2ms**. Scenario C features only 3GPP upper layer single functional split between DU deployed with RRU at the cell site and CU with MEC at the edge site with optimal RTT **11ms**. Scenario D is monolithic RAN. This setup is most applicable to 5G MEC

deployment for femtocells with RRT of **8ms**. The RTT values from the mentioned prototype MEC deployment are all with the latency requirements for Virtual Reality & Augmented Reality of 7-12ms, Tactile Internet < 10ms, Vehicle-to-Vehicle < 10ms and Manufacturing & Robotic Control/Safety Systems: 1-10ms.

5 CONCLUSION

So far, several research efforts have been carried out to augment for the mobile wireless device computational power and energy carrying capacity deficiencies, but the ultimate solutions lie in the optimization of MEC capacities to cater for asymmetric UE applications by improving the latency figures. Co-locating MEC server close to gNB-CU assures low user plane latency to support emerging 5G applications

ACKNOWLEDGEMENTS

A short acknowledgement section can be written between the conclusion and the references. Authors may wish to acknowledge the sponsors of the research and others in brief. Acknowledging the contributions of other colleagues who are not included in the authorship of this paper is also added in this section. If no acknowledgement is necessary, this section should not appear in the paper.

REFERENCE

1. Taleb, T., Samdanis, K., Mada, B., Flinck, H., Dutta, S., & Sabella, D. (2017). On Multi-Access Edge Computing: A Survey of the Emerging 5G Network Edge Cloud Architecture and Orchestration. *IEEE Communications Surveys & Tutorials*, 19(3), 1657-1681. doi:10.1109/comst.2017.2705720
2. Parvez, I., Rahmati, A., Guvenc, I., Sarwat, A. I., & Dai, H. (2018). A Survey on Low Latency Towards 5G: RAN, Core Network and Caching Solutions. *IEEE Communications Surveys & Tutorials*, 20(4), 3098-3130. doi:10.1109/comst.2018.2841349
3. Satyanarayanan, M., Bahl, V., Caceres, R., & Davies, N. (2011). The Case for VM-based Cloudlets in Mobile Computing. *IEEE Pervasive Computing*. doi:10.1109/mprv.2009.64
4. Satyanarayanan, M. (2001). Pervasive computing: vision and challenges. *IEEE Personal Communications*, 8(4), 10-17. doi:10.1109/98.943998
5. Patil, P., Hakiri, A., & Gokhale, A. (2016). Cyber Foraging and Offloading Framework for Internet of Things. 2016 IEEE 40th Annual Computer Software and Applications Conference (COMPSAC). doi:10.1109/compsac.2016.88



6. Díaz, M., Martín, C., & Rubio, B. (2016). State-of-the-art, challenges, and open issues in the integration of Internet of things and cloud computing. *Journal of Network and Computer Applications*, 67, 99-117. doi:10.1016/j.jnca.2016.01.010
7. International Telecommunication Union, "IMT Vision – Framework and overall objectives of the future development of IMT for 2020 and beyond." Recommendation ITU-R M.2083-0 (09/2015)
8. Eiman Mohyeldin, "IMT Vision – Minimum technical performance requirements form IMT-2020 radio interface(s)." ITU -R Workshop on IMT-2020 terrestrial radio interface(s) (2016)
9. International Telecommunication Union, "Minimum requirements related to technical performance for IMT-2020 radio interface(s)." DRAFT NEW REPORT ITU-R M.[IMT-2020.TECH PERF REQ] (02/2017)
10. Mao, Y., You, C., Zhang, J., Huang, K., & Letaief, K. B. (2017). A Survey on Mobile Edge Computing: The Communication Perspective. *IEEE Communications Surveys & Tutorials*, 19(4), 2322-2358. doi:10.1109/comst.2017.2745201
11. Mark Skarpness. "Beyond The Cloud: Edge Computing, Embedded Linux Conference Europe." Retrieved from : <https://www.youtube.com/watch?v=SQipnBNVjv0> , Oct. 22 – 24, 2018[Dec. 18, 2018]
12. Erol-Kantarci, M., & Sukhmani, S. (2018). Caching and Computing at the Edge for Mobile Augmented Reality and Virtual Reality (AR/VR) in 5G. *Ad Hoc Networks*, 169-177. doi:10.1007/978-3-319-74439-1_15
13. Cuervo, E., Balasubramanian, A., Cho, D., Wolman, A., Saroiu, S., Chandra, R., & Bahl, P. (2010). MAUI. Proceedings of the 8th international conference on Mobile systems, applications, and services - MobiSys '10. doi:10.1145/1814433.1814441
14. Zhang, X., Jeong, S., Kunjithapatham, A., & Gibbs, S. (2010). Towards an Elastic Application Model for Augmenting Computing Capabilities of Mobile Platforms. *Lecture Notes of the Institute for Computer Sciences, Social Informatics and Telecommunications Engineering*, 161-174. doi:10.1007/978-3-642-17758-3_12
15. Chun, B., Ihm, S., Maniatis, P., Naik, M., & Patti, A. (2011). CloneCloud. Proceedings of the sixth conference on Computer systems - EuroSys '11. doi:10.1145/1966445.1966473
16. Kosta, S., Aucinas, A., Pan Hui, Mortier, R., & Xinwen Zhang. (2012). ThinkAir: Dynamic resource allocation and parallel execution in the cloud for mobile code offloading. 2012 Proceedings IEEE INFOCOM. doi:10.1109/infcom.2012.6195845
17. ETSI. "System Architecture for the 5G System. " 3GPP TS 23.501 version 15.2.0 Release 15- ETSI TS 123 501 V15.2.0 (2018-06).
18. Hewlett Packard Enterprise. "What is Edge Computing." Retrieved from: <https://www.hpe.com/dk/en/what-is/edge-computing.html>[Sept. 3, 2018]
19. Sutton, A. (2018). 5G Network Architecture. *The ITP (Institute of Telecommunications Professionals) Journal*, 12(1), 9–15.
20. International Telecommunications Union. "ITU-T Technical Report." GSTR-TN5G Transport network support of IMT-2020/5G (2018-10).
21. ETSI, Mobile-edge Computing Introductory Technical White Paper, White Paper, Mobile-edge Computing Industry Initiative, 2014.
22. Mach, P., & Becvar, Z. (2017). Mobile Edge Computing: A Survey on Architecture and Computation Offloading. *IEEE Communications Surveys & Tutorials*, 19(3), 1628-1656. doi:10.1109/comst.2017.2682318
23. 3GPP TR 38.801, "Technical Specification Group Radio Access Network; Study on new radio access technology: Radio access architecture and interfaces", March 2017.
24. eCPRI Specification V2.0 (2019-05-10), "Common Public Radio Interface:eCPRI Interface Specification".
25. Belshe, M., & Peon, R. (2015). Hypertext Transfer Protocol Version 2 (HTTP/2). doi:10.17487/rfc7540
26. ETSI. "5G System; Technical Realization of Service Based Architecture. " Stage 3 (3GPP TS 29.500 version 15.0.0 Release 15)- ETSI TS 129 500 V15.0.0 (2018-07)
27. Kevin Murphy. "Centralized RAN and Fronthaul," Ericsson Inc.(May 2015) Retrieved from : https://www.isemag.com/wp-content/uploads/2016/01/C-RAN_and_Fronthaul_White_Paper.pdf. [Mar. 30, 2019]
28. Checko, A., Berger, M. S., Kardaras, G., Dittmann, L., & Christiansen, H. L. (2016). Cloud radio access network architecture. Towards 5G mobile networks. Technical University of Denmark.
29. Hassan Halabian, "Front-haul networking for 5G: An analysis of technologies and standardization," Huawei technologies co., ltd.(nov. 2017). Retrieved from : https://mpls.jp/2017/presentations/MPLS_Japan2017_Fronthaul_Solution_V1_3.pdf [May 16, 2019]
30. Kitindi, E. J., Fu, S., Jia, Y., Kabir, A., & Wang, Y. (2017). Wireless Network Virtualization With SDN and C-RAN for 5G Networks: Requirements, Opportunities, and Challenges. *IEEE Access*, 5, 19099-19115. doi:10.1109/access.2017.2744672
31. NGMN White Paper, "NGMN Overview on 5G RAN Functional Decomposition," v1.0, Feb. 2018.



3rd International Engineering Conference (IEC 2019)
Federal University of Technology, Minna, Nigeria



32. Westphal, C. (2017). Challenges in networking to support augmented reality and virtual reality. IEEE ICNC.
33. Knopp, R., Nikaein, N., Bonnet, C., Kaltenberger, F., Ksentini, A., & Gupta, R. (2017). Prototyping of next generation fronthaul interfaces (NGFI) using OpenAirInterface. White Paper, EURECOM.
34. Sutton, A. N. D. Y. (2018). 5G network architecture. J. Inst. Telecommun. Professionals, 12(1), 9-15.
35. ETSI TS 123 501, "5G;NG-RAN;F1 Application Protocol (F1AP)," V15.2.0 Release 15 (2018-7)
36. Marinelli, E. E. (2009). *Hyrax: cloud computing on mobile devices using MapReduce* (No. CMU-CS-09-164). Carnegie-mellon univ Pittsburgh PA school of computer science.
37. Gordon, M. S., Jamshidi, D. A., Mahlke, S., Mao, Z. M., & Chen, X. (2012). {COMET}: Code Offload by Migrating Execution Transparently. In Presented as part of the 10th {USENIX} Symposium on Operating Systems Design and Implementation ({OSDI} 12) (pp. 93-106).



Suitable Propagation Models for 2.4 GHz Wireless Networks: Case Study of Gidan Kwano Campus, FUT MINNA.

*Ogunjide, S. B¹, Usman, A. U², & Henry, O. O³

¹Electrical and Electronics Engineering Department, Federal University of Technology,
PMB 65 Minna Niger State, Nigeria

² Department of Telecommunication Engineering, Federal University of Technology,
PMB 65 Minna Niger State, Nigeria

³ Electrical and Electronics Engineering Department, Federal University of Technology,
PMB 65 Minna Niger State, Nigeria

*Corresponding author email: favouredben78@gmail.com, +2348069561603

ABSTRACT

In the last few decades, the use of Wireless Local Area Network (WLAN) popularly referred to as Wi-Fi (Wireless Fidelity) in communication system has been on the increase with the exponential usage of handheld cell phones, laptops, and palm-tops to mention but a few. However, WLAN faces a peculiar propagation issue which lies in its changing propagation environment and this affects the quality of service. Poor quality of service is experienced on WLAN of Gidan Kwano campus of Federal University of Technology (FUT), Minna, due to signal propagation impairment caused by the terrain and the structures within the campus. In this work, Received Signal Strength (RSS) measurement was conducted at varying radial distances away from the selected Access Points (APs) both in Line of Sight (LOS) and Non-Line of Sight (NLOS) situations. The path loss exponent (n) and standard deviation (σ) were estimated for the environment. For LOS and NLOS scenarios, the obtained path loss exponents were 2.31 dB and 3.2 dB respectively. The developed models were contrasted with the existing standard models and found to perform better based on the quantitative measures taken in the study area. This shows that the developed models can be utilised for accurate access point deployment within the Gidan Kwano Campus, FUT Minna and other environment with similar features.

Keywords: *Wireless Local Area Network (WLAN), Path loss Model, Path Loss exponent, Path loss impairment, Access Points (APs).*

1 INTRODUCTION

The Gidan Kwano campus of Federal University of Technology (F.U.T) Minna is a moderately sized campus located in Minna, the Niger state capital. The campus lies on Longitude 6.5°E and Latitude 9.7°N. The aerial view of the campus as captured from the Google Earth is shown in Plate I.

Wireless Local Area Networks (WLANs) have recently gained prominence in various walks of life, including medical centres, retail, assembling, warehousing, and academic environment (Abhayawardhana *et al.*, 2012). These sectors have benefitted immensely by utilising hand-held gadgets and notebook computers for real time data transmission (Aye and Myo, 2016).

Wireless communication offers clients and associations numerous advantages, for example, compactness and adaptability, increased profitability, and lower cost of installation when compared to the wire line communication systems (Alyaa *et al.*, 2015). WLAN gadgets enable clients to move their cell phones from place to place without the requirement for wires. Less wiring implies more noteworthy adaptability and increased proficiency. Handheld gadgets, such as, Personal Digital Assistants (PDA) and mobile phones permit remote clients to synchronize individual databases

and give access to network services, for example, remote email, web browsing, and other web administrations (Aremu, 2016 and Bartz, 2009).

However, as wireless signals move from a transmitter to a receiver, they get diffracted, scattered, and absorbed by the territory, trees, building, vehicles and individuals which constitute the environment of propagation (Anderson *et al.*, 2005, Deygout, 2013, Ogbulezie, 2013, Oyetunji, 2013 and Zachaeus *et al.*, 2016). The nearness of obstacles along the path of wireless signal may cause great signal attenuation more noteworthy than it would under free space condition (Carrasco and Johnson, 2012, Eibert and Kuhlman, 2015, Graham *et al.*, 2014). Radio signal attenuation and path losses are greatly due to the terrain of propagation (Daniel, 2016, Hanchinal, 2016, Idim and Anyasi, 2014, Llorete *et al.*, 2015). Poor network planning is a factor responsible for WLAN poor quality of service (Mukesh *et al.*, 2015, Nwalozie and Gerald, 2014, Ogbulezie, 2013 and Yuvraj, 2012). For accurate network planning, a good knowledge of propagation characteristics is of great importance (Pathlaven, 2014 and Zhang, 2012). In the literature, empirical propagation models are most prevalently used for handling network planning issues. However, due to changes in the environment of propagation, the empirical models are not globally applicable (Aye and Myo, 2016). Accordingly, it is important to determine the particular

radio propagation characteristics that will be ideal for the environment under study while carrying out network planning (Zachaeus, 2016). The Gidan Kwano campus of FUT, Minna often times encounter poor quality of service arising from the signal propagation impairment. The accurate prediction of well-known propagation models is not suitable to evaluate the propagation characteristic of this campus due to the peculiarity of its terrain. This paper is geared toward developing a propagation model for the campus using received signal strength measurements from a selected access points within the campus.

2 METHODOLOGY

Many techniques and materials have been utilised in taking information from an access point (or a base station) (Llorete *et al.*, 2015, Pathlaven and Kishnamur, 2014). These techniques include radio frequency (RF) overview and drive test among others (Mukesh, 2015, Bidgoli, 2013 and Alyaa *et al.*, 2015). For this work, the technique for RF overview was utilised and this section describes the materials and strategies used to achieve this investigation. Figure 1 shows the summary of the methodology deployed.

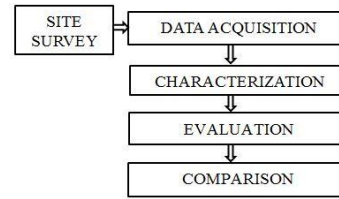


Figure 1: Summary of the methodology

A. Study area description

The Gidan Kwano campus of Federal University of Technology (F.U.T) Minna is situated in Minna, the Niger state capital, Nigeria. It lies on Longitude 6.5⁰E and Latitude 9.7⁰N. The campus is moderately sized with complex terrain because of the presence of tall structures, classrooms and trees within it. The attenuation of the Wi-Fi signal within the campus is attributed to numerous reflections, absorption and diffractions off rooftops, trees, cars and so on. Plate I is the aerial view of the campus as captured from the Google Earth, showing the locations of the access points and the measurement routes.



Plate I: Google Earth view of F.U.T Minna, Gidan Kwano campus showing the buildings on which the Access Points were mounted and the measurement routes.

The access points (APs) utilised for this work are referenced with respect to the campus building they were mounted on, in particular, ITS Wi-Fi, LIB. Wi-Fi, SEM Wi-Fi, SEET2 Wi-Fi, PTDF Wi-Fi, AGRIC-AP, CON-Wi-Fi, SICT Wi-Fi, ABE Wi-Fi, and SET Wi-Fi. These APs were picked as a result of accessibility of their hardware specifications and configuration.

B. Radio Frequency Site Survey

An RF site survey is the initial phase in the deployment of a wireless network and the most important development to guarantee wanted operation. A site study is a step-by-step process by which the surveyor thinks about the facility to understand the RF behaviour, finds RF coverage areas and decides the appropriate placement of wireless devices. RF site survey was led utilising apparatus that enables data to be gathered from an access point, example of such data is the received signal strength indicator.

C. Surveying Tools

In carrying out the site survey, Air Check Wi-Fi Tester 2.4GHz and 5.0GHz was utilised to capture wireless packets from an ad-hoc or infrastructure network setup utilising an access point. The specifications of the software and hardware equipment utilised for this study are given below.

1) Software specifications:

- i. Inssider software
- ii. Matlab version R2014a
- iii. Microsoft window 8 Pro.

2) Hardware specifications:

a: Air Check Wi-Fi Tester 2.4GHz and 5.0GHz

b: Laptop

- i. Vendor Hp
- ii. Model: Note book 15
- iii. CPU Speed: 2.7GHz
- iv. Memory: 2GHz
- v. Wireless Card: Intel PRO/Wireless 2200BG

c: IEEE 802.11b/g Access Point

- i. Vendor: Mikrotik RB Metal G52SHPacn
- ii. Range: $\approx 183m = 600ft$
- iii. Transmitter reference Power: $1W$
- iv. Bands: $2.4GHz$ to $2.4835GHz$
- v. Transmission speed-Wi-Fi 2.4GHz: $150Mb/s$

d: Global Positioning System (GPS)

- i. Vendor: Magellan
- ii. Model: Explorist 500

e: 25-foot measuring tape.

D. Data Collection Methods

An Hp laptop with a Network Interface Card (NIC) installed and running on Microsoft Windows 8 Pro with Inssider software was utilised to obtain RSSI information at varying radial distance from the chosen APs on the campus. The following privacy guidelines were observed during data collection:

- 1) The Inssider software did not attempt gaining access to the network.
- 2) The Inssider software sees all the access points publicly communicating their Service Set Identifier (SSID).

Ten (10) APs were chosen on the Campus at distinctive areas. The chosen APs were from a similar vendor and with similar specifications utilising IEEE 802.11 b/g standard. At each AP, straight ways were stamped out at various bearings from the AP to the laptop. On every one of these ways, test points were physically estimated at a 10m interval utilizing a measuring tape estimating to a 100m stamp from the AP.

1) Line of Sight (LOS) data collection procedure scenario:

In a LOS environment, the receiving antenna is detectable to the transmitting antenna with an exceptionally minimal obstacle. The origins of attenuations are essentially from the movement of individuals and vehicles over the path of signal transmission. This is so since the human body is made of around 70 percent water, hence, it ingests some amount of signal accordingly causing loss of strength of the signal being transmitted. Signal information with relating separations from the APs were measured, and at each measured separation, a few estimation of RSSI were gathered. The APs in a LOS environment situation are: FUT Wi-Fi (ITS), FUTLIB. WiFi, SEM MBB Wi-Fi, SEET2-Wi-Fi and GOOGLE Wi-Fi (PTDF).

2) Non-Line of Sight (NLOS) data collection procedure scenario:

For NLOS condition, there were no visual observable pathway between the receiving and the transmitting antennas. The radio transmission way is mostly or completely impeded by the nearness of physical obstructions, for example, tall structures, trees, slopes, individuals, vehicles and so on. These interference bodies weaken the signal strength by method of absorption, reflection, scattering and diffraction. RSSI values were

gathered from five (5) APs on the campus at estimated separations from the APs in a NLOS domain situation. The APs in a NLOS situation are: FUTAGRIC-AP, CON-FUT Wi-Fi, GOOGLE Wi-Fi (SICT), ABE-Wi-Fi and GOOGLE WIFI (SET).

Data were gathered between the hours of 10 am and 12 pm and between 2 pm and 4 pm from Monday through Friday. The movement of individuals and vehicles is reduced at these hours of the day being the lecture hours. This is aimed at reducing the attenuation caused by individuals and car movement. There is an interior antenna situated behind the laptop screen, so the laptop screen was directed toward the apex sky keeping in mind the end goal to improve the probability that the direct beams signal path falls on the beam width of the antenna.

3 RESULTS, DISCUSSION AND ANALYSIS

In the study of wireless data communication networks, the path loss exponent is the principal parameter of interest (Alyaa et al., 2015). The path loss exponent relies greatly upon the environment of propagation. High path loss exponent symbolizes how quick the signal strength drops with respect to the distance between the transmitter and the receiver (Nwalozie and Gerald, 2014, Oyetunji, 2013). Therefore, in carrying out signal propagation modelling for a given study area, the path loss exponent for such study area has to be determined. This section shows results, discussion and analysis of information gathered on RSSI from the environment of propagation.

A. Presentation of results

The ranges of the signal strength measurements and the corresponding signal quality from Insider software is presented in Table I based on the standard (Mukesh et al., 2015). The measurement surveyed signal strength obtained for some of the APs in LOS and NLOS are presented in Tables II and III respectively.

TABLE I
Standard definition of signal quality in terms of RSSI
(Alyaa et al., 2015)

Received Signal Strength in dBm	Signal quality
-60 < RSSI ≤ -20	Excellent signal
-75 < RSSI ≤ -60	Good signals
-85 < RSSI ≤ -75	Low signal
-90 < RSSI ≤ -85	Very Low signal
-108 < RSSI ≤ -90	No signal

TABLE II
MEAN RSSI FOR LOS ENVIRONMENT SCENARIO

d(m)	Mean RSSI FUT Wi-Fi (ITS)	Mean RSSI FUT_LI B. Wi-Fi	Mean RSSI SEM MBB Wi-Fi	Mean RSSI SEET2-Wi-Fi (ITS)	Mean RSSI GOOGLE Wi-Fi(PTDF)
1	-14.03	-14.03	-14.03	-14.03	-14.03
10	-41.65	-42.70	-43.45	-42.35	-42.75
20	-42.35	-44.45	-45.85	-46.40	-43.90
30	-43.25	-42.65	-46.75	-44.35	-45.80
40	-42.85	-44.35	-47.50	-47.10	-48.65
50	-48.05	-47.40	-45.90	-54.90	-47.55
60	-53.75	-51.30	-53.05	-57.85	-53.65
70	-52.90	-52.85	-56.95	-56.75	-62.25
80	-56.55	-54.70	-54.85	-62.50	-52.60
90	-61.80	-52.40	-65.75	-65.00	-65.40
100	-67.85	-60.25	-63.55	-66.75	-69.40

TABLE III
MEAN RSSI FOR NLOS ENVIRONMENT SCENARIO

d(m)	Mean RSSI FUTAGRIC-AP	Mean RSSI CON-FUT Wi-Fi	Mean RSSI GOOGLE Wi-Fi (SICT)	Mean RSSI ABE-WIFI	Mean RSSI GOOGLE WIFI (SET)
1	-14.03	-14.03	-14.03	-14.03	-14.03
10	-54.10	-52.60	-48.85	-50.80	-48.35
20	-57.15	-57.85	-52.50	-55.40	-54.50
30	-62.25	-56.80	-55.75	-59.65	-57.20
40	-68.60	-58.50	-62.90	-61.50	-56.95
50	-65.65	-66.20	-70.25	-59.05	-59.95
60	-67.75	-62.35	-67.30	-63.20	-66.45
70	-74.20	-83.85	-66.60	-71.10	-70.45
80	-73.30	-81.40	-74.85	-69.00	-75.85
90	-86.25	-85.70	-81.90	-79.15	-79.85
100	-84.90	-87.80	-79.85	-84.05	-78.95

B. Computation of path loss exponent using Log distance path loss propagation model.

$$P_L(d)[dB] = P_L(d_0)[dB] + 10n \log(d/d_0) \quad (1)$$

$$P_L(d)[dB] = P_T - RSSI(dBm) \quad (2)$$

$$P_T = 10 * \text{Log}(P_t / W_m) \quad (3)$$

Where $P_L(d)$ is the Path Loss at distance d , $P_L(d_0)$ is the Path Loss at reference distance 1m, P_T is the transmitter power in dBm, P_t is the reference transmitter power of 1W and W_m equals 10^{-3} W. RSSI are the measured data against distance at the various locations.

With reference to (3) for P_t equals one Watt and W_m equals 10^{-3} Watt,

$$P_T = 10 * \text{Log}(1 / 10^{-3})$$

$$P_T = 30 \text{ dBm}$$

Substituting $P_T = 30$ in equation (2) gives,

$$P_L(d)[dB] = 30 - RSSI(dBm) \quad (4)$$

With reference to (4) at reference distance of 1m away from the access point, RSSI is -14.03dBm. From which $P_L(d_0)$ is solved to be 44.03dB. Hence (1) becomes,

$$P_L(d)[dB] = 44.03 + 10n \log(d) \quad (5)$$

The path loss exponent for both LOS and NLOS were obtained using (5). The standard deviation (σ) and Sum of Square Error (SSE) of the developed models from the established standard model were computed by applying (6) and (7) utilizing MATLAB tool.

$$\sigma = \sqrt{\sum_{i=1}^M (y_i - \bar{y})^2} / M \quad (6)$$

$$SSE = \sqrt{\sum_{i=1}^M (y_i - \bar{y})^2} \quad (7)$$

Where y_i is the measured path loss at a particular interval, \bar{y} is the developed model path loss and M is the data length. Table IV and V show the mean path loss exponents for LOS and NLOS scenarios respectively.

TABLE IV
THE MEAN PATH LOSS EXPONENTS FOR LOS

Location	Mean Path Loss Exponent(n)
FUT Wi-Fi(ITS)	2.24
FUT_LIB Wi-Fi	2.16
SEM MBB Wi-Fi	2.34
SEET2 Wi-Fi	2.44
GOOGLE Wi-Fi(PTDF)	2.36

TABLE V
THE MEAN PATH LOSS EXPONENTS FOR NLOS

Location	Mean Path Loss Exponent(n)
FUTAGRIC-AP	3.36
CON-FUT Wi-Fi	3.34
GOOGLE Wi-Fi(SICT)	3.14
ABE Wi-Fi	3.11
GOOGLE Wi-Fi (SET)	3.07

Table VI gives the summary of the path loss exponents for both LOS and NLOS scenarios.

TABLE VI
SUMMARY OF THE PATH LOSS EXPONENTS FOR BOTH LOS AND NLOS SCENARIOS.

Environment	Mean Path Loss exponent (n)
LOS	2.31
NLOS	3.20

(8) and (9) are the derived mean path loss models for LOS and NLOS scenarios.

$$P_L(d)_{(LOS)}[dB] = 44.03 + 23.1 \log(d/d_o) \quad (8)$$

$$P_L(d)_{(NLOS)}[dB] = 44.03 + 32 \log(d/d_o) \quad (9)$$

C. Discussion of results

Path loss exponent is the most imperative model parameter obtained from the analysis. This parameter gives noteworthy knowledge into how wireless signals attenuate with respect to the distance between the access point and the mobile users. In the analysis, it was gathered that the path loss exponent for NLOS scenario was higher when compared to that of the LOS environment. This shows that the signal strength for NLOS scenario decreases faster due to the presence of obstructions along the path of propagation than for LOS scenario.

D. Comparison with existing standard models

Propagation path loss exponents gotten from the empirical measurements were contrasted with that of the free space, Hata and COST-231 model (refer Table VII and Table VIII and depicted in Figure 2 and 3). Obviously, the path loss exponents from the empirical measurements as contrasted with the free space loss appeared to be higher, and this was seen to be caused by extra losses from environment of propagation which attenuates the signal quicker than in free space. The standard deviation (σ) and Sum of Squared Error (SSE) of the developed models from the field measurements and established models were the parameters used to evaluate the models quality. In this analysis (refer Table IX AND X), the standard deviation of the measured LOS path loss and the developed model LOS path loss was 2.81 dB as opposed to 5.60 dB of the measured LOS path loss and Free Space Loss. Also, the standard deviation of the measured NLOS path loss and the developed NLOS model was 3.23 dB while that of Hata model and the measured NLOS path loss was 7.04 dB. The SSE of the measured LOS path loss and the developed model LOS path loss was 8.87 dB while that of the free space model and the measured LOS path loss was 17.71 dB. The measured NLOS path loss and the developed model NLOS SSE was 10.20 dB while that of Hata model and the measured NLOS path loss was 22.26 dB.

TABLE VII
COMPARISON BETWEEN MEASURED DATA, DEVELOPED MODEL AND FREE SPACE LOSS

d (m)	Measured data [PL _{LOS}]	PL (d) [LOS] For n=2.31	PL (d) [FSL] For n=2.0
10	71.95	67.13	64.03
20	75.90	74.08	70.05
30	73.80	78.15	73.57
40	75.95	81.03	76.07
50	83.30	83.27	78.01
60	86.25	85.11	79.60
70	84.40	86.65	80.93
80	88.50	87.99	82.09
90	89.80	89.17	83.11
100	90.85	90.23	84.03

TABLE VIII
COMPARISON BETWEEN MEASURED DATA, DEVELOPED MODEL, HATA MODEL AND COST-231 MODEL

d (m)	Measured data [PL _{NLOS}]	PL (dB) [NLOS] For n=3.20	PL(dB) Hata Model	COST-231 MODEL
10	83.60	76.03	72.46	59.83
20	89.10	85.66	81.44	68.81
30	92.25	91.30	86.69	74.06
40	98.45	95.29	90.42	77.79
50	97.70	98.39	93.31	80.68
60	98.25	100.93	95.67	83.04
70	105.30	103.07	97.67	85.04
80	103.15	104.93	99.40	86.77
90	108.75	106.57	100.92	88.29
100	109.90	108.03	102.29	89.65

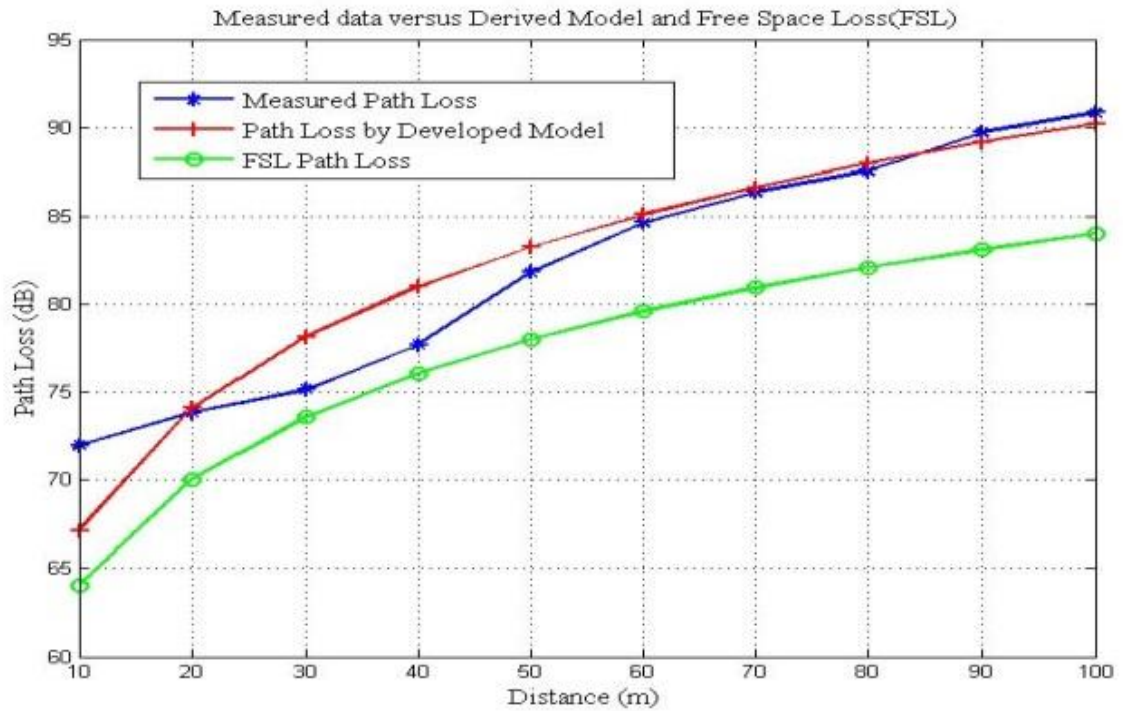


Figure 2: Comparison of the measured data with the derived model and Free Space Loss (FSL).

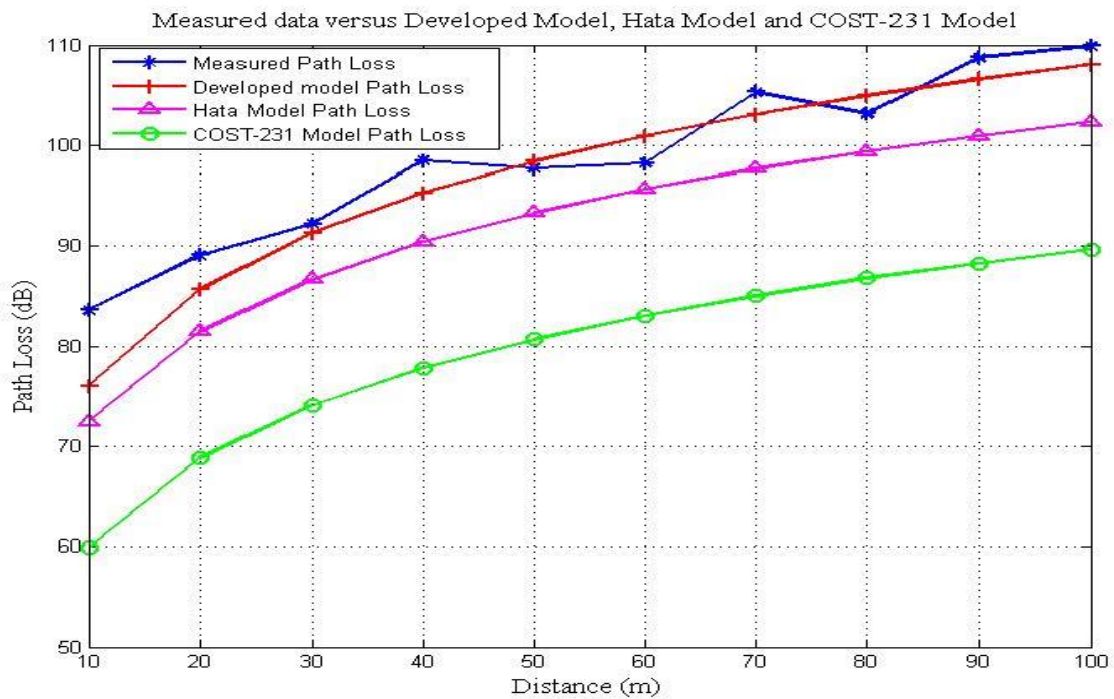


Figure 3: Comparison of the measured data with the derived model, Hata Model and COST-231 Model.

TABLE IX
LOS Model validation

Measured LOS Path Loss versus Developed model LOS Path Loss standard deviation	Measured LOS Path Loss versus FSL model standard deviation	Measured LOS Path Loss versus Developed model LOS Sum of square error	Measured LOS Path Loss versus FSL Sum of square error
2.81 dB	5.60 dB	8.87 dB	17.71 dB

TABLE X
NLOS Model validation

Measured NLOS Path Loss versus Developed model NLOS Path Loss standard deviation	Measured NLOS Path Loss versus Hata model standard deviation	Measured NLOS Path Loss versus Developed model NLOS Sum of square error	Measured NLOS Path Loss versus Hata model Sum of square error
3.23 dB	7.04 dB	10.20 dB	22.26 dB

4. CONCLUSION

The fundamental target of this work was to develop suitable propagation models capable of enhancing the quality of services rendered by WLAN networks of Gidan Kwano campus, FUT Minna. This was actualised by taking in succession the Received Signal Strength (RSS) measurements of some selected access points both in LOS and NLOS scenarios within the campus. It was seen in the cause of this work that the nearness of obstacles along radio transmission path influences the quality of the transmitted signal. The RSS fluctuates fundamentally at the various locations of measurement due to these obstructions resulting in the attenuation of the received signal. It is exceptionally essential to determine RSS at various locations where WLAN network is to be deployed. Diverse estimations of RSS for each area indicate whether such area receives good signal strength or not. Propagation path loss exponents were obtained for the selected access point both in LOS and NLOS showing the extent to which the signal strength attenuates with distance. The NLOS path loss exponents were seen to be higher than those acquired for LOS condition. This perception demonstrates that the nearness of obstructions

along the transmitting antenna truly has effect on the quality of radio frequency signal resulting in multipath effect which weakens the signal strength in NLOS condition. In view of the empirical data gathered, propagation models were developed for both NLOS and LOS conditions. As contribution to knowledge, the developed models were contrasted with the established standard models from which a standard deviation of 2.81 dB was obtained comparing the measured LOS Path Loss and the developed model LOS as opposed to 5.60 dB of the measured LOS Path Loss and the Free Space model. Also, the measured NLOS Path Loss and the developed model NLOS standard deviation gives 3.23 dB as opposed to 7.04 dB of the measured NLOS Path Loss and Hata model. This demonstrates that the developed models can effectively be utilised for proper access point deployment at Gidan Kwano campus, FUT Minna to accomplish maximum network coverage and excellent quality of service.

REFERENCES

- [1] Abhayawardhana, V. S., Wessel, I. J., Crosby, D., Sellars, M. P., & Brown, M. G. (2012). Comparison of Empirical Propagation Path Loss Model for Five Wireless Access Systems. *Vehicular Technology Conference, IEEE*, 1, 73–77.
- [2] Alyaa, S. A., Mohammad, R. K., & Muzammil, J. (2015). Transparent antenna for WiFi application: RSSI and throughput performances at ISM 2.4GHz. *Telecommunication systems, modelling, analysis, design and management Conference*, 8, 4.
- [3] Anderson, J. B., Rappaport, T. S., & Yoshid, A. S. (2005). Propagation measurements and models for wireless communication channel. *International multi conference of Engineers and computer scientists*, 33, 42-46.
- [4] Aremu, O. A. (2016). Experimental study of variation of Path Loss with respect to Heights at GSM frequency band. *International Journal of Scientific Research in Science, Engineering and Technology (IJSRSET)*, 2, 347-351.
- [5] Aye, A., & Myo, M. (2016). Comparison of Signal Strength Prediction Models for Indoorto-Outdoor and Outdoor-to-Indoor Wireless Communications. *American Scientific Research Journal for Engineering, Technology and Sciences (ASRJETS)*, 25, 181-191.
- [6] Bartz, J. R. (2009). Certified Wireless Technology Specialist. *International Journal of Next generation networks*, 2, 16-19.
- [7] Bidgoli, H. (2013). An Investigation on propagation path loss in Urban Environments for various models transmitter Antenna height and different Receiver Antenna height. *International Journal of Receiver and reviews in Computer Science*, 3, 66-71.
- [8] Carrasco, R. A., & Johnson, M. (2012). Non-Binary Error Control coding for wireless Communication and Data Storage. *International Journal of Soft Computing*, 14, 88-92.
- [9] Chen, A., & Kobayshi, H. (2014). Signal Strength based indoor geo location. *IEEE journal on selected areas in communications*, 20, 3.



- [10] Daniel, K. (2016). A Study on Path Loss Analysis for KNUST Campus WLAN, Ghana. *International Journal of Innovation and Scientific Research*, 27, 257-263. Daniel, K. (2016). A Study on Path Loss Analysis for KNUST Campus WLAN, Ghana. *International Journal of Innovation and Scientific Research*, 27, 257-263.
- [11] Deygout, J. (2013). Multiple Knife-Edge Diffraction of Microwaves. *IEEE Transaction on Antenna and Propagation*, 39, 1256-1258.
- [12] Eibert, T. F., & Kuhlman, P. (2015). Notes on Semi empirical wave propagation modelling for microcellular environments comparison with measurements. *Journal of Microwaves and Optoelectronics application*, 10, 1-4.
- [13] Goransson, P., & Greenlaw, R. (2013). Secure Roaming in 802.11 Networks. *International Journal of computers and communications*, 35,102-106.
- [14] Graham, A. W., Kirkmann, N. C., & Paul, P. M. (2014). Mobile radio network design in the VHF and UHF bands: A practical approach. *Turk Journal of Physics*, 50, 91-96.
- [15] Hanchinal, C. S., & Muralidhara, K. N. (2016). A Survey on the Atmospheric effects on Radio Path Loss in Cellular Mobile Communication System. *International Journal of Computer Science and Information technology*, 80, 1124-1128.
- [16] Idim, A. I., & Anyasi, F. I. (2014). Determination of building penetration loss of GSM signals using selected buildings in Orhuwhorun, Delta state, Nigeria as a case study. *Journal of Electronics and Mechatronics Engineering*, 19, 01-05.
- [17] Llorete, J., Lopez, J. J., Turro, C., & Flores, S. (2015). A fast design model for outdoor and indoor radio coverage in the 2.4GHz wireless LAN. *International symposium on Wireless Communications Systems, Maeritus*, 21, 408-412.
- [18] Mukesh, K., Vijay, K., & Suchika, M. (2015). Performance and analysis of propagation models for predicting RSS for efficient Handoff. *International Journal of Advanced Scientific and Technical Research*, 55, 32-36.
- [19] Nwalozie, D., & Gerald, V.N. (2014). Path loss prediction for GSM mobile networks for Urban region of ABA, South - East, Nigeria. 2, *International journal of computer science and mobile computing*, 3, 267-281.
- [20] Ogbulezie, J.C. (2013). Site specific measurements and propagation models for GSM in three cities in Northern Nigeria. *American Journal of Scientific and Industrial Research*, 3, 40-41.
- [21] Oyetunji, S.A. (2013). Determination of Propagation Path Loss and Contour Map for FUTA FM Radio Federal University of Technology, Akure. *Journal of Electronics and Communication Engineering*, 6, 4-9.
- [22] Pathlaven, K., & Kishnamur, P. (2014). Estimating the location of maximum exposure to Electromagnetic fields associated with a radio-communication station. *Journal of Microwaves, Optoelectronics and Electromagnetic Applications*, 16, 152-154.
- [23] Zachaeus, K., Owolabi, K., & Akinyinka, O. (2016). Genetic Algorithm Based Path Loss Optimization for Long Term Evolution in Lagos, Nigeria. *International Journal of Applied Science and Technology*, 6, 2.
- [24] Yuvraj, S. (2012). Comparison of Okumura, Hata and COST-231 Models on the Basis of Path Loss and Signal Strength. *International Journal of Computer Applications*, 59, 11.
- [25] Zhang, W. (2012). Fast two-dimensional different modelling for site-specific propagation prediction in urban microcellular environment. *International Journal of Techno-research*, 49, 428-436.



A Survey on Mobile Edge Computing: Focus on MEC Deployment, Site Selection Problems and Application Scenarios.

*Atolagbe, M. I¹, Osanaiye, O².

¹ Department of Telecommunication Engineering, Federal University of Technology, PMB 65 Minna Niger State, Nigeria

² Department of Telecommunication Engineering, Federal University of Technology, PMB 65 Minna Niger State, Nigeria

* Email¹: atolagbe.pg7509@st.futminna.edu.ng, +2348035884108

Email²: okeyemi177@futminna.edu.ng, +2348059879284

ABSTRACT

In recent years, the increasing rate of mobile traffic and increasing rate of operational costs have driven the telecommunication operators into implementing several changes in order to generate more revenue, maintain quality of service (QoE), optimizing their network operations and providing optimum utilization of resources. This has resulted in a new technology which provides low latency, network and context awareness, high bandwidth, increased flexibility with usage of network function virtualization (NFV), software defined networks (SDN), thereby providing increase in (QoE) to end users and making network operations more cost effective and very competitive. Mobile edge computing (MEC) is a forthcoming technology providing edge computing, brings data storage closer to end users, and network resources within the edge of the Radio Access Network.

Keywords: *Cellular Network, Edge deployment, Mobile Edge Computing (MEC) and Quality of Experience (QoE).*

1 INTRODUCTION

In the past few years, due to our increased love for business, entertainment, education, social networking, health care, etc. we are exposed to abundance of mobile applications used for our daily activities named above. furthermore, mobile data traffic and bandwidth demands is predicted to continue doubling each year (Ericsson, 2013). The internet of things (IoT) is furthering congesting the network with more utilization of the network resources which is one of the distinctive challenges of network providers, applications and content providers are faced with latency of network during connectivity to the cloud. Mobile network traffic majorly today is caused by data traffic because many mobile applications are dependent on data and services hosted in a centralized location which causes latency, due to high load of network being up-downloaded from a centralized location connected to the internet. Recently, Mobile Edge Computing (MEC) was proposed as a likely technology to overcome this problem in some certain scenarios. MEC aims at reducing traffic congestion, access to content, application responsiveness

can be increased and network stress can be minimized by moving computational efforts from the Internet to mobile edge.

To keep up with these enormous demands, mobile network operators have to improve users' experience, upgrade the currently existing technology, provide more viable options for sharing of network resources while at the same time keep a healthy revenue growth and a competitive market. Telecommunication network operators and information technology (IT) are converging, bringing a new natural development in the evolution of base stations providing opportunities and capabilities that can be deployed into the network, which is based on virtualized platform. The vast change brought has been the ability to run IT servers at mobile network edge nearby the mobile subscriber applying cloud computing methods, which is known as MEC. MEC speeds up content, providing a distributed computing environment used for mobile applications and service hosting, with various ability to store, process the content nearer to cellular networks subscribers for faster response time and augmenting

reactivity from the edge. Laying the ground for MEC in internet of things (IoT) applications including smart home and smart cities, eHealth, smart energies, self-driving cars, augmented reality, autonomous vehicle, enhanced mobile broadband and many other applications.

MEC is technology recognized by European 5G PPP (5G infrastructure Public Private Infrastructure Partnership) research body as a key technology for 5G networks based on its virtualized platform together with key emerging technologies, such as Software Defined Networks (SDN) and Network Functions Virtualization (NFV) (ESTI, 2015). MEC represents a key emerging technology and architectural concepts that has enhanced the directional change to 5G network as it helps in solving the demanding requirements of 5G in terms of scalability, latency, throughput, automation, bandwidth, creating exposure to real time radio network and metamorphosing mobile broadband into a computing and programmable world.

Furthermore, mobile devices deployed at the edge of the network are used for mobile access points while base station helps in forwarding traffic with both not actively involved in analyzing or responding to user's requests. MEC servers are implemented or installed at places or regions with lots of computational demands, such as commercial areas, relatively dense populated areas or co-located with existing infrastructure to save cost. Examples of these include (i) macro base stations (LTE) (ii) aggregation points which may be the edge of the network (iii) Multi-Radio Access Technology cell aggregation site and (iv) Radio Network Controller (RNC) sites, allowing applications execution at close proximity to mobile subscribers. Additionally, with this position, MEC provides various improvements such as : (i) optimization of network and service operation, mobile resources by running computer-intensive applications at the edge of the network, requesting, responding and adopting changing network conditions thereby providing knowledge of real time radio network and context awareness information to improve quality of experience (QoE), better utilization of network resources, creating efficient way of handling increased amounts of traffic. (ii) segregating large volume of data and pre-processing at network edge before sending those with large computational requirements (or some extracted features) to the cloud, and (iii) context aware services such as user location, cell load and allocated bandwidth with help of RAN (ESTI, 2015). MEC introduces new network elements at the edge, providing

computing, storage capabilities and IT services environment at the edge of cellular network. In addition, new devices are co-hosted and deployed at the base station towers. These devices deployed are being referred to as MEC servers.

Figure 1, which shows the MEC network topology with the integration of MEC servers. There are few main custodians involved in MEC, these includes (i) mobile users or subscribers using the User Equipment(UE), as illustrated in Figure 2, are the service requesters and content requesters (ii) base stations serving as the mobile access points and MEC servers (iii) internet infrastructure providers (iv) application service providers.

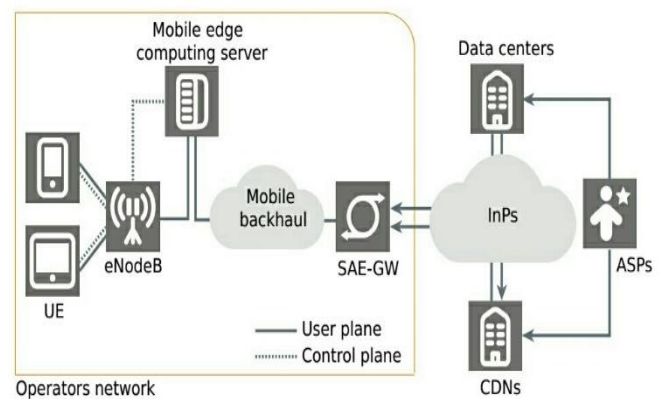


Figure 1: Mobile Edge Topology (M. Beck, et al, 2014.)

As seen from Figure 1, MEC servers are small scale data centers deployed by mobile operators next to base stations, co-located with access points (APs) and linked to the base stations. MEC servers are usually equipped with hardware, i.e. usual server CPUs, memory for storage, and communication interfaces. The APs do not only introduce wireless interfaces for MEC servers but also creates access to remote data centers through backhaul links. Communication in the MEC server are majorly between access points, mobile devices and base stations, with a possible usage of device to device (D2D) communication while application deployment rely on cloud technology and virtualization. Therefore, mobile devices having difficulty communicating directly with MEC servers because of limited wireless interfaces can make use of D2D communication with devices in close proximity to it, thereby translating same to MEC server by the new device.

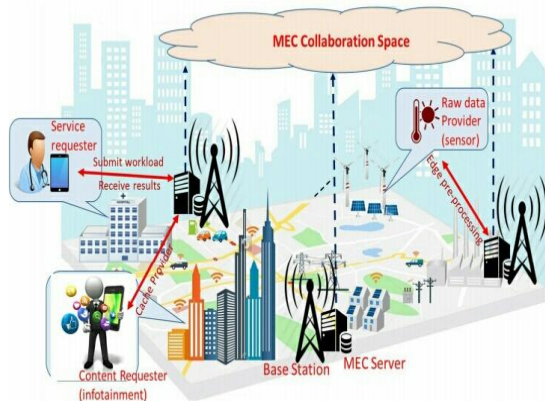


Figure. 2: Illustration of mobile edge computing network. (D. Pompili, X. Tran et al, 2017)

User equipment (UE), as seen is connected to the macro base station which overset radio signals and route them through the core networks. MEC servers are integrated at RAN which provides computing, storage, connectivity and are accessible for RAN information, therefore, they are solely deployed in close proximity to the macro base station, basically attaching it there and fastening the traffic through the MEC server for further processing of data. Furthermore, to deploy MEC solutions effectively, cellular operators are permitted to open their RAN to authorized third parties which can be a content provider or an application developer. The MEC server has the ability to handle both the user traffic and control traffic.

Furthermore, when the UE (content requesters or applications requesters) sends a request, the MEC servers are capable of handling those requests as laid down by the MEC services on how to handle or manage specific user request directly at the network edge and not forward all traffic to the remote internet service or cloud, as the computation may require. MEC servers sends requests which requires loads of computation to the remote data centers and content distribution networks (CDN). When the request is being directly handled by MEC services hosted on MEC servers, these requests will not need to be forwarded through the core infrastructure to either the CDN, data centers nor cloud. Furthermore, all data traffic is assigned through the core of the network passing through the base station to deliver the content or solution to mobile devices.

MEC servers takes control of some or even all of the tasks initially being performed by Internet services or

cloud. Being in close proximity to base stations, computing and storage resources of MEC servers are closely available to the mobile users, therefore eliminating the need of passing these data through the core of the network. MEC is seen as the future, with promising approach to increase quality of experience (QoE) in cellular networks, reducing the volume of data that must be moved and consequently decreasing the traffic congestion in the network. This paper provides an analysis and limitations of MEC by identifying, discussing, and classifying various applications, deployment issues of MEC servers, its reference architecture and application types, for the deployment at the mobile edge.

2 FIRST MOBILE COMPUTING PLATFORM.

MEC was defined originally by the Nokia, Siemens and IBM as a computing system within a mobile base station. Regarding to its standardization, in December 2014, European Telecommunication Standard Institute (ETSI) launched an Industry Specification Group (ISG) (i.e. ISG MEC) saddled with the responsibility of producing documents for series of specifications for MEC framework and pinpointed that MEC can provide a new ecosystem that can migrate demanding computing tasks of Mobile users to nearby servers. MEC, as defined by ETSI, is capable of providing *... "IT services environment and cloud computing capabilities at the edge of the mobile network to reduce latency, ensure highly efficient network operation and service delivery, and offer improved user experience"*. With this definition being applied to multiple communication technologies, MEC is being referred to as Multiple-access Edge Computing. An open platform called Open-RAN (Saguna, 2016) was introduced by Saguna. Open-RAN is fully equipped with a virtualized MEC platform that provides an environment for third parties to run their applications. Radio Application Cloud Server (RACS) create a virtual machine (VM) hypervisor (software or firmware system providing a VM that allows operation directly underneath the hardware) for the deployment of VM photos or videos running some MEC applications. Radio Application Cloud Server (RACS) create a virtual machine (VM) hypervisor (software or firmware system providing a VM that allows operation directly underneath the hardware) for the deployment of VM photos or videos running some MEC applications. The RACS from IBM is fully integrated by Networks Flexi Multi-radio base station with special features to access real-time network data.



Emerging key technologies, such as the software defined network (SDN) and the network function virtualization (NFV) are solutions to simplify network management by enabling flexibility and easy management. The network function virtualization is the proposed network architecture that allows virtualization technologies to be used by a single device, providing multiple services for multiple devices through creation of multiplied virtual machines (VM) for performing simultaneous tasks or different functions. SDN is a computing network architecture that performs the function of dividing functions attributed to the control plane and user/data plane integrated at the macro base station, which helps to improve the performance and monitoring of the network.

3 DEPLOYMENT OF MEC SYSTEM AND EDGE LOCATION TRADEOFFS.

The major reason for MEC is to move or shift the cloud computing capability to the network edge to provide low latency caused by traffic congestion and propagation delay due to distance; provide better flexibility, agility, usage of virtualization in the core network. After all, there is no official definition of the supposed location of the MEC server and how MEC server should be specified. This makes the MEC server site selection entirely different from base station site selection problems, as the optimum performance has to be put into consideration. Computational tasks and resource sharing also needs to be considered as well as deployment budget.

Nevertheless, efficiency of MEC system is based on the architecture, which should account for the various problems that needs to be solved, such as the workload intensity, communication cost between different tiers, workload distribution strategies and communication rates statistic. In addition, we would be discussing some research problems related to MEC deployment, including MEC architecture, server density and site selection for MEC servers. As it is important to determine server density, accounting for computation demand statics, combination of different edge servers for optimum performance, the infrastructure deployment cost and market generalship is equally important.

- A. **Site Selection for MEC Servers:** In building a MEC system, the first basic step is selecting site for MEC server. The mobile operator or system planner should consider the most cost effective deployment options and at the same time sites with higher computational demands, which could

be a crowded area, business regions, commercial areas and markets. Proximity to existing infrastructure to save cost, and budget friendly rental sites should also be considered. Telecom networks or operators already have their infrastructure installed, which provides option of installing the MEC servers co-located with macro base stations, therefore, providing attractive MEC markets for telecom network operators interested in MEC.

Notwithstanding, certain problems are encountered due to increase in computational demands, ever present smart devices with frequents requests may affect the user quality of experience (QoE) because of poor quality signals and congestion in the macro cells. Other options include: installing the MEC servers at the aggregation points (may be the edge of the network) because some application requires computational capability in close proximity to the end users. This can be accomplished by administering some resources at small cell base stations which are specifically low cost and small size base station. For such, the computational capability is less than those at the macro base station which causes delay and latency when handling computational intensive tasks. It may be an easy target for attackers causing security problems because it is easier to reach, vulnerable to external attacks, which reduce resilience level or level of reliability. Furthermore, sites with higher computational results may have communication problem, due to non-availability of communication infrastructure, either at the small size base stations or the macro base station which requires deployment of edge servers with wireless transceivers by choosing new sites.

- B. **MEC Network Architecture:** The future of MEC is to build MEC servers with heterogeneous computation and communication capabilities consisting of multiple tiers of MEC system (3 layers) as shown in the Fig. 3 below (i.e. cloud, edge and the service subscriber layer). While the first layer (cloud) has been in existence for long, there are still few problems in designing the edge layer. The multiple tiers have different communication and computational capabilities, with such hierarchical MEC structures enabling efficient transmission by distributing computational tasks or workload to different tiers

according to their abilities solving congestion, latency and related problems.

Furthermore, there are problems associated with Het-Nets which remain unsolved such as communication costs across multiple tiers, workload intensity and distribution generalship. More also, for mobile subscribers or users served by a Het-MEC system, it is critical to determine when designing the destination of computation offloading problems (i.e. either the mobile edge or the central cloud which leads to resource management in MEC system). As a single user MEC system, there are three task models used for offloading computational tasks. These are (i) deterministic task model with binary offloading (ii) deterministic task model with partial offloading and (iii) stochastic task model.

Multi-user MEC system comprising of multiple mobile devices with one single edge server and one central cloud server, can make use of total successful offloading probability using heuristic scheduling algorithm as (a) joint radio and computational resource allocation which could be (i) centralized resource allocation with low computation latency arising from abundant resources at central cloud server (ii) distributed resource allocation with low computational latency due to closeness to MEC server (b) MEC server scheduling (stochastically) which could as well be asynchronous arrival by delivering and solving tasks according to arrival time. This, however, causes delay, or synchronous arrival by scheduling according to their priorities.

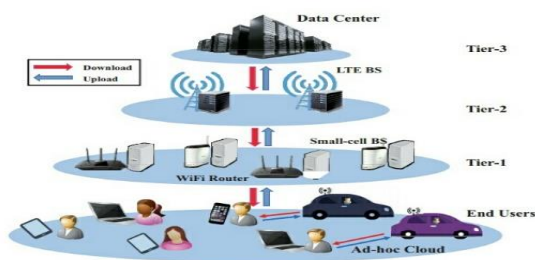


Figure 3. A 3-tier Heterogeneous MEC system (Y. Mao, C. You et al, 2017.)

C. Server Density Planning: MEC infrastructure combines different types of edge servers, which in turn provides variability in the computational tasks of each server and deployment cost of each

varies. Based on the deployment budget available, it is important to determine the number of edge nodes and different types of servers to match the computational demands. Numerical simulation can be used to address this problem but it is time consuming and has poor scalability. Furthermore, stochastic geometry theory has been developed recently and applied successfully in the performance analysis of wireless network, as well as similarity between Het-Net and Het-MEC system (Haenggi, 2011), (Haenggi et al, 2009). Conducting such performance analysis on MEC system should address some concerns including, the computational demands which could be clustered or non-uniformly distributed, computational offloading policies and timescale of computation.

3.1. EDGE LOCATION TRADEOFF.

Table 1. Impact of location on MEC Performance

Limiting Parameters	MEC Location (Closer To UE)	Closer To Centralized Cloud
Cost	Low	High
Distance	Low	High
Latency	Low	High
Processing capability	Limited	High
Storage capacity	Low	High
Area covered (Size)	Limited	High

4. APPLICATION OF MEC AND USE CASES.

In this section, we will review the application of MEC. The introduction of MEC platforms into the cellular network makes various applications to be executed at the edge of the network, thereby reducing the cost operation of the network, improving user QoE and providing IoT scalability for time-sensitive applications. In addition,

when the notion of MEC was introduced, the major question that cropped up was *what are the applications that can benefit from the deployment of MEC at the edge?* (Ansari, Sun, 2018) proposed a Mobile Edge Internet of Things (MECIoT) architecture that brings many resources (i.e. storage and computing resources) in close proximity to the IoT devices while (Taleb et al, 2017) proposed a concept to improve video streaming in smart cities. The application scenarios of MEC is discussed below.

4.1.1 Local content and Video caching.

Data traffic caused by mobile streaming of videos is foretold to be responsible for 72% of the total mobile data traffic by 2019, creating loads of pressure on network operators. (White Paper c11-520862, Cisco index, 2014-2019). In order to solve this problem, edge caching has been introduced as a likely solution by caching the popular content (i.e. videos) at the base station or access points. Any request from mobile users for the same content can be easily fetched without transmitting the requests to remote servers or causing duplication. Figure 4. shows how mobile subscribers at a particular time and location tends to view continuously a narrow set of content causing rapid growth of traffic, at the same location justifying content storage and processing at the edge. This concept helps in the reduction of content access delay, latency and backhaul and usage.

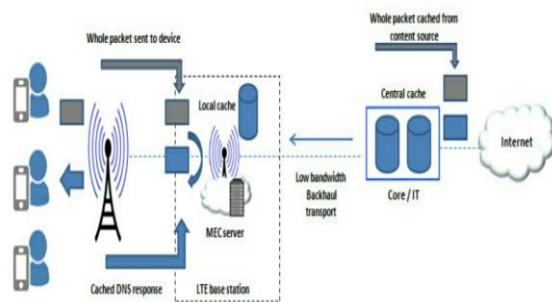


Figure 4: Local Content Caching (A. Belghol & I. Abdellah, 2017)

4.1.2 Intelligent Video Acceleration.

The use of radio network resources and quality of experience by the mobile users can be enhanced by the use of intelligent video acceleration. Most download or streaming of videos, internet files and media are done by use of Hypertext Transmission Protocol (HTTP) over the

Transmission Control Protocol (TCP). Due to changes in the radio channel conditions caused by device egression or ingression, available resources and capacities continues to vary in order of seconds or microseconds leading to under-utilization of radio resources because it is difficult for TCP to adapt to rapid varying conditions of the radio access network (RAN). Figure 5 depicts an example of radio analytic application scenario with an attempt to solve the problems reported above. This application is embedded in the MEC server, providing the video server with an indication on the throughput estimation available at the radio downlink interface.

This particular information can be used in assisting TCP decisions on congestion control, ensuring that the application level coding correspond to the estimated capacity at the radio downlink and enabling enhanced video quality and throughput. It also provides a way of using data in network conditions (particularly the RAN conditions) and radio access network load in generating intelligence for content and application providers on how best to manage and control traffic exchanged with the mobile subscriber. When there is enough capacity in the network, the providers can decide to share content at the highest quality available. However, when there is congestion in the network, content and TCP transmission are adapted to provide mobile users with the best experience possible, given the real-time availability of network resources.

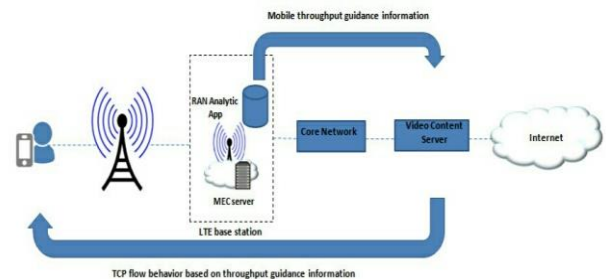


Figure 5: Intelligent Video Acceleration (ESTI, 2016)

4.1.3 Connected Cars

The number of cars connected are becoming increasingly much and will continue growing in the coming years. Existing cloud services are expanded into the highly distributed environment of mobile base station, and leveraging on the existing LTE connectivity (Belghol & Abdellah, 2017). The communication of cars and the

sensors located on the roadside which operates as a roadside unit for vehicle-to-infrastructure (V2I) are meant for efficiency, to increase road safety and limit road hazards, leading to effective, efficient and convenience use of road transportation system. In the case of road hazards (i.e. accident on the road) this can be spotted and warnings can be sent to nearby cars with extremely low latency which enables a nearby vehicle to receive data in a matter of seconds (as shown in Figure 6), and this helps the driver to react instantly.

MEC applications are able to run MEC servers which can also be deployed at LTE base stations providing the roadside functionality. This can speed up the deployment of connected cars communications and also helps latency requirements of connected cars communication. The roadside application sends local messages to the connected vehicles cloud server for continuous centralized processing and reporting.

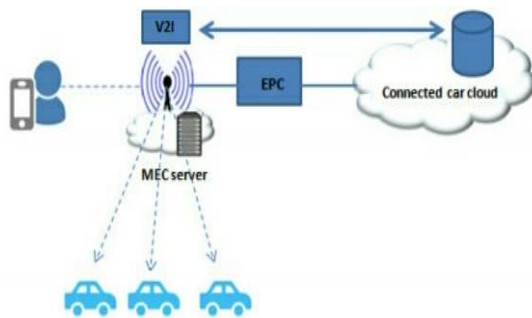


Figure 6: Connected Cars (A. Belghol & I. Abdellah, 2017)

4.1.4 Augmented Reality

New applications and services are made possible when mobile network supports deployments of low latency computation, high data rates and increased flexibility, which are all provided by the MEC system. Augmented reality is an example of such application as shown in (Figure 7). It combines the view of real world environment with computer generated sensory data (i.e. video, sound, GPS, graphics data). A typical application of Augmented Reality is the enhancement of user's visitation to a Museum, monumental centers such as city monument, art gallery, music or sport events, pointing and holding their devices concentrating it to their particular point of interest. This MEC application analyses the output from a device's

camera and the precise location related to their visit activated (i.e. the museum application). The users position and direction been faced are noted through camera view or positioning techniques.

Objects viewed from the user's device camera are overlaid with local augmented reality content and it displays additional information related to what the visitor is viewing or experiencing. It is advantageous to host this application on MEC platform instead of cloud as point of interest is often irrelevant beyond point of interest, and additional information as regarding point of interest is localized. Further processing may be required as there may be need to update information fast, depending on the movement of users and the AR context used.

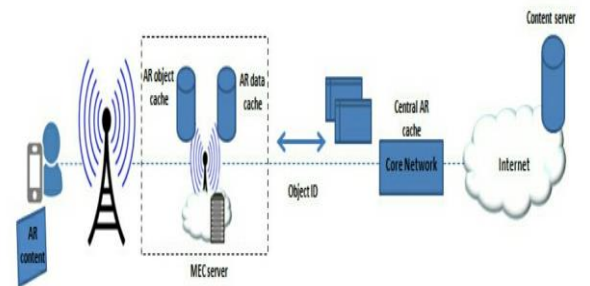


Figure 7: Augmented Reality ((ESTI, 2016)

5. CONCLUSION

This paper discussed several applications of mobile edge computing, deployment at the mobile edge with the problems faced in selection of MEC location and edge tradeoffs. We have also highlighted content, applications and services in MEC are accelerated by way of increasing responsiveness from the edge. These tradeoffs were evaluated based on the key parameters such as power consumption, delay, cost, latency, bandwidth usage, and scalability. In addition, in most deployment scenarios, mobile end subscribers and internet network providers benefit from reduced network delay, and, thus, offering faster services.



REFERENCES

- [1] Ericsson, "Ericsson Mobility Report – June 2013 mobile." <http://www.ericsson.com/res/docs/2013/ericsson-mobility-report-june-2013.pdf>.
- [2] Cisco VNI Mobile, "Cisco Visual Networking Index: Global Mobile Data Traffic Forecast Update, 2016-2021," <http://www.cisco.com>: White paper, February 2017, pp.1-28
- [3] IBM Corporation, "Smarter wireless networks; add intelligence to the mobile network edge." <http://www.researcher.watson.ibm.com>
- [4] Saguna and Intel, "Using mobile edge computing to improve mobile network performance and profitability," White paper, 2016. <http://www.saguna.net/saguna-white-paper>.
- [5] M. Chen, Y. Zhang, L. Hu, T. Taleb, and Z. Sheng, "Cloud based wireless network: Virtualized, reconfigurable, smart wireless network to enable 5g technologies," *Mobile Networks and Applications*, vol. 20, no. 6, pp. 704–712, 2015.
- [6] H. Bhelgol, A. Idrissi, "A survey on concept, use cases and location tradeoffs, MEC towards 5G, 2017." *Society for science and education United Kingdom* 5(4) 440-445. DOI: 10.14738/tmlai.54.3215
- [7] X. Tran, A. Hajisami, P. Pandey, D. Pompili, "Collaborative Mobile Edge Computing in 5G Networks: New Paradigms, Scenarios, and Challenges, 2016." <http://arxiv.org/pdf/1612.03184.pdf>.
- [8] M. Beck, M. Werner, S. Feld "Mobile Edge Computing: A Taxonomy". *The Sixth International Conference on Advances in Future Internet. AFIN Lisbon, Portugal, Nov 2014*, pp 48-54.
- [9] M. Haenggi, J. Andrews, F. Bacelli, O. Dousse, and M. Francetti, "Stochastic geometry and random graphs for the analysis and design of wireless networks". *IEEE J. Sel. Areas Communication.*, vol. 27, no. 7, pp. 1029–1046, Sep. 2009.
- [10] A. Ahmed and E. Ahmed, "A survey on mobile edge computing," in Proc. *IEEE International Conference in Intell. Syst. Control (ISCO)*, Coimbatore, India, Jan. 2016, pp. 1–8.
- [11] X. Wang, M. Chen, T. Taleb, A. Ksentini, and V. Leung, "Cache in the air: Exploiting content caching and delivery techniques for 5G," 2014. *IEEE Comm. Mag.*, vol. 52, no. 2, pp. 131–139, Feb. 2014
- [12] Y. Mao, C. You, J. Zhang, K. Hung, and K. Letaief "Mobile Edge Computing: survey and Research Outlook" Jan, 2017. [http://arXiv:1701.01090v1\[cs:IT\]](http://arXiv:1701.01090v1[cs:IT])
- [13] ESTI GS MEC_IEG 005; "Mobile Edge Computing (MEC); Proof of Concept Framework" 2016. http://portal.esti.org/portal/otbpages/mec/docs/MEC_IEG_005.
- [14] K. Peng, V. Leung, X. Zheng, X. Xu, J. Weng, Q. Huang. "A Survey on Mobile Edge Computing: Focusing on Service Adoption and Provision" 2018. *Wireless and communication mobile computing*, Wiley. 8267838,1-16. doi.org/10.1155/2018/8267838
- [15] ESTI Portal, "Mobile-edge computing-introductory technical white paper," 2014. <http://portal.esti.org>
- [16] M. Satyanarayanan, "Mobile computing: the next decade," ACM SIGMOBILE. *Mobile Computing and Communications Review*, vol. 15, no. 2 pp. 2-10, Apr. 2011.
- [17] O. Salman, I. Elhajj, A. Kayssi, and A. Chehab, "Edge computing enabling the internet of things," in Internet of Things (WF-IoT), 2015. *IEEE 2nd World Forum on. IEEE*, 2015, pp. 603–608.
- [18] M. Patel, J. Joubert, J. Ramos, N. Sprecher, S. Abeta, A. Neal, "Mobile Edge Computing – Introductory Technical White Paper," <https://portal.etsi.org/WhitePaper>, September 2014
- [19] D. Sabella, N. Sprecher, M. Patel, V. Young, Y. Chao Hu "Mobile Edge Computing a key technology towards 5G," Whitepaper, Sep 2015 <http://www.etsi.org/>.
- [20] D. Sabella, A. Vaillant, P. Kuure, U. Rauschenbach, and F. Giust, "Mobile-edge computing architecture: The role of MEC in the Internet of Things." *IEEE Consum. Electron. Mag.*, vol. 5, no. 4, pp. 84–91, Oct. 2016
- [21] H. T. Dinh, C. Lee, D. Niyato, and P. Wang, "A survey of mobile cloud computing: architecture, applications, and approaches: A survey of mobile cloud computing," *Wireless Communications and Mobile Computing*, vol. 13, pp. 1587–1611, Dec. 2013.



Influence of Processing Techniques and Packaging Materials on Anti-Nutritional Properties of Soybean Flour

* Orhevba, B. A¹, Anehi, A² & Obasa, P. A³

^{1, 2 & 3} Agricultural and Bioresources Engineering Department, Federal University of Technology, PMB 65 Minna Niger State, Nigeria

*Corresponding author email: bosedo.orhevba@futminna.edu.ng, +2348061688880

ABSTRACT

This study investigated the anti-nutritional properties of soya bean flour produced from steeping and gelatinization techniques and stored in different packaging materials. The freshly harvested soya bean seeds used for the study were cleaned and soaked for five different durations (6, 9, 12, 15, and 18 hours); cooked at five different cooking times (20, 25, 30, 35 and 40 mins); packaged in five different materials (paper bag, low density polythene bag, composite bag, high density polythene bag and plastic) and stored for five different periods (20, 40, 60, 80 and 100 days). A Central Composite Orthogonal Design was used. The samples of flour were then subjected to anti-nutritional analysis. All experiments were carried out in triplicates. Data obtained was analyzed using Design Expert 9.0; the Analysis of Variance (ANOVA) was conducted and empirical models developed. Statistical analysis shows that steeping duration had significant effect ($P \leq 0.05$) on the cyanide, tannin and phytic acid contents of the flour. The gelatinization duration, storage duration and packaging materials had no significant effect ($P \leq 0.05$) on the cyanide content, tannin content, saponin content and oxalate content of the flour samples.

Keywords: Cyanide content, oxalate content, soya beans, steeping, tannin content.

1 INTRODUCTION

Soybean (*Glycine max*) is a legume that originated from Eastern Asia (www.fao.org), it was introduced into Nigeria in 1908 (Omotayo *et al.*, 2007). According to Ajayi *et al.*, (2011), soya bean is being acknowledged as a viable and essentially nutritious crop with numerous health benefits. The crop has also been identified as a major raw material for many domestic and industrial products. Soybean has a great demand due to its versatility; it has found many applications in the formulation of both human and animal foods, pharmaceutical and confectionery industries and other industrial uses (Omotayo *et al.*, 2007). It is utilized in many forms like bean, meal, cake and oil. The industrial demand and domestic supply level for soybean was estimated to be about 634,000 metric tons and 386,864 metric tons respectively (Omotayo *et al.*, 2007). According to Soetan and Oyewole (2009), soybeans contain anti-nutritional factors such as tannin which must be inactivated by heat during processing before usage.

Soybean flours can be obtained by grinding full-fat dehulled soybeans or defatted flakes made from dehulled soybeans; they are then allowed to pass through a 100-mesh standard screen (www.fao.org). Steeping and gelatinization techniques are used in the processing of soybean to flour so as to minimise the anti-nutritional properties (Bibianalbabul and Sule, 2013).

Packaging has become part of our daily lives. Packaged products are found all over the world. The global packaging market is currently valued at \$597 billion and is estimated to reach \$820 billion by 2016 (Silayoi and Speece, 2004). Consumers are increasingly demanding higher quality packaging for products which has in turn increased the role

of packaging in the sale of goods and services (Institute of Packaging Ghana, IOPG, 2014). Packages come in such forms as packaged foods, canned drinks, and bottled water.

W Packaging helps consumers know the contents of products, and serve as instruction guides. Manufacturing and expiry dates, warning symbols, net weight, country of origin, recyclable symbol, company's address and nutritional facts are all very essential facts that, through packaging are provided to the consumers. Best packaging material for soybean flour, gives aesthetic delight and satisfaction, and also tactile pleasure (Soroka, 2002).

The objective of storage is to preserve the properties of the flour present after it has been processed, thereby making it possible to obtain and market sub-products with satisfactory quality. Vitality of the product can be preserved and the grinding quality and nutritive properties of the food can be maintained (Brooker *et al.*, 1992).

Most soya products are made out of soya flour, thus there is a high demand for the flour in commercial quantity. The knowledge of a suitable processing technique and packaging material for soybean flour will go a long way to meeting this demand.

The use of other types of flour from locally available root, tubers, legumes and cereal crops in production will reduce the cost of wheat importation in Nigeria. This will help save the dwindling foreign reserves. The losses incurred in soybean can be reduced by processing it into flour. This will also increase the earning of farmers of this crop. The use of better packaging materials for soybean flour will reduce losses during transportation and storage.

This research finds relevance in the establishment of the best packaging materials and storage conditions for

soybean flour that will serve as baseline for confectionary industries.

2 METHODOLOGY

2.1 MATERIALS

Freshly harvested soybean (*Glycine max*) seeds that were used in producing the flour were obtained from a farmer in Lapai, Niger State, Nigeria. The chemicals and reagents that were used were obtained from the Food Science Laboratory, School of Agricultural Technology, Federal University of Technology Minna, Niger State, Nigeria.

2.2 METHODS

2.2.2 SAMPLE PREPARATION

The flour was prepared according to the method described by Bibianalgbabul and Sule (2013). The grains were manually cleaned by separating all foreign materials, such as sticks, dirt, husk, chaff and other extraneous materials from the soybeans. The soybeans were washed in clean water and soaked for 6 hrs. This method was repeated for soaking times of 9, 12, 15 and 18 hrs. The soaked soybeans were poured in boiling water, and boiled for 20, 25, 30, 35 and 40 mins. The soybeans were washed and the coats removed and separated from the beans in cold water. The beans were dried at 65°C, grinded into flour, sieved, packaged and stored for 100 days. The experimental design employed in this study is the Central Composite Orthogonal Design giving twenty-five runs as shown in Table 1.

Table 1: Central Composite Orthogonal Design

Run	Sample	X ₁ (mins)	X ₂ (hrs)	X ₃ (days)	X ₄ (materials)
1	A	-1(9)	-1(25)	-1(40)	-1(LDPE)
2	B	+1(15)	-1(25)	-1(40)	-1(LDPE)
3	C	-1(9)	+1(35)	-1(40)	-1(LDPE)
4	D	+1(15)	+1(35)	-1(40)	-1(LDPE)
5	E	-1(9)	-1(25)	+1(80)	-1(LDPE)
6	F	+1(15)	-1(25)	+1(80)	-1(LDPE)
7	G	-1(9)	+1(35)	+1(80)	-1(LDPE)
8	H	+1(15)	+1(35)	+1(80)	-1(LDPE)
9	I	-1(9)	-1(25)	-1(40)	+1(HDPE)
10	J	+1(15)	-1(25)	-1(40)	+1(HDPE)
11	K	-1(9)	+1(35)	-1(40)	+1(HDPE)
12	L	+1(15)	+1(35)	-1(40)	+1(HDPE)
13	M	-1(9)	-1(25)	+1(80)	+1(HDPE)
14	N	+1(15)	-1(25)	+1(80)	+1(HDPE)
15	O	-1(9)	+1(35)	+1(80)	+1(HDPE)
16	P	+1(15)	+1(35)	+1(80)	+1(HDPE)
17	Q	-α(6)	0(30)	0(60)	0(Composite)
18	R	+α(18)	0(30)	0(60)	0(Composite)
19	S	0(12)	-α(20)	0(60)	0(Composite)
20	T	0(12)	+α(40)	0(60)	0(Composite)
21	U	0(12)	0(30)	-α(20)	0(Composite)
22	V	0(12)	0(30)	+α(100)	0(Composite)
23	W	0(12)	0(30)	0(60)	-α(Paper)
24	X	0(12)	0(30)	0(60)	+α(Plastic)
25	Y	0(12)	0(30)	0(60)	0(Composite)

X₁= Steeping duration, X₂= Gelatinization duration, X₃= Storage duration,
X₄= Packaging materials

PACKAGING

Electronic weighing balance was used to measure 200 grams of the flour and packaged in paper bag, low density polythene bag, composite (mixed), high density polythene bag and plastic as shown in Plate I.



Paper bag



Low density polythene bag



Composite



High density polythene bag



Plastic

Plate I: Soybeans flour in different packaging materials.

2.2.3 Storage

The packaged soybean flour was stored for a period of 100 days. The anti-nutritional properties were determined every 20 days so as to assess the effect of the packaging materials on them during storage.

2.2.4 Analysis of Anti-nutritional properties

The anti-nutritional contents determined are cyanide, tannin, saponin, oxalate and phytic acid. The Cyanide content was determined by the alkaline picrate method according to the method used by Onwuka, (2005).

Tannin was determined according to Association of Official Analytical Chemist, AOAC (2002). Saponin was determined according to the method described by Kim and Wampler, (2009).

Oxalate in the sample was determined by the permanganate titrimetric method as described by Liener, (1994). The phytic acid content was determined using a modified indirect colorimetric method reported by Wheeler and Ferrel (1971).

2.3 Statistical Analysis

All experiments were carried out in triplicates. Data obtained were analysed using Design Expert 9.0; Analysis of Variance (ANOVA) was conducted and empirical models were developed.

3 RESULTS AND DISCUSSION

3.1 Results

The mean of the replicated results obtained for the anti-nutritional properties are presented in Table 2.

Table 2: Anti-Nutritional Content of Soybean Flour

Run	Sample	Cyanide (g/100g)	Tannin (g/100g)	Saponin (g/100g)	Oxalate (g/100g)	Phytate (g/100g)
1	A	0.0554	0.8309	0.5496	0.0119	0.9429
2	B	0.0335	0.6938	0.5062	0.0119	0.9803
3	C	0.0526	0.8300	0.5570	0.0119	0.9429
4	D	0.0335	0.7143	0.5062	0.0119	0.9803
5	E	0.0554	0.8309	0.5496	0.0119	0.9429
6	F	0.0335	0.6938	0.5062	0.0119	0.9808
7	G	0.0526	0.8300	0.5570	0.0119	0.9429
8	H	0.0333	0.7143	0.5062	0.0119	0.9808
9	I	0.0554	0.8309	0.5496	0.0119	0.9429
10	J	0.0335	0.6938	0.5062	0.0119	0.9803
11	K	0.0526	0.8300	0.5570	0.0119	0.9429
12	L	0.0333	0.7143	0.5062	0.0119	0.9803
13	M	0.0554	0.8309	0.5496	0.0119	0.9429
14	N	0.0335	0.6938	0.5062	0.0119	0.9803
15	O	0.0526	0.8300	0.5570	0.0119	0.9429
16	P	0.0333	0.7143	0.5062	0.0119	0.9803
17	Q	0.0824	0.8329	0.6253	0.0119	0.9832
18	R	0.0333	0.8056	0.5451	0.0103	0.9738
19	S	0.0529	0.6234	0.5210	0.0127	0.9554
20	T	0.0463	0.6490	0.5316	0.0128	0.9614
21	U	0.0463	0.6144	0.5154	0.0129	0.9554
22	V	0.0463	0.6144	0.5154	0.0129	0.9554
23	W	0.0463	0.6144	0.5154	0.0129	0.9554
24	X	0.0463	0.6144	0.5154	0.0129	0.9554
25	Y	0.0463	0.6144	0.5154	0.0129	0.9554

X₁=Steeping duration, X₂=Gelatination duration, X₃=Storage duration, X₄= Packaging Material

3.2 DISCUSSION

3.2.1 The impact of processing parameters on the anti-nutritional properties of soybean flour

3.2.1.1 Cyanide Content

The ANOVA result (Table 3) indicated that the linear model is significant. The linear term of the model indicated that an increase in steeping and gelatinization duration reduces the cyanide content of the flour.

Statistical analysis shows that steeping duration had significant effect ($P \leq 0.05$) on the cyanide content while the gelatinization duration, storage duration and packaging materials had no significant effect on the cyanide properties of soybean flour as their values were higher than 0.05. Only the interaction between the steeping duration and gelatinization duration had positive effect on the cyanide content as shown in the model equation (1). The 3D plots showing the effect of variables on cyanide content is shown in Figures 1 and 2.

Table 3: ANOVA of the Cyanide Properties of Soybean Flour

Source	Sum of Squares	Df	Mean Square	F Value	p-value
Model	0.002911	10	0.000291	9.801546	< 0.0001
X ₁ -Steeping Duration	0.002878	1	0.002878	96.90154	< 0.0001
X ₂ -Gel. Duration	2.6E-05	1	2.6E-05	0.87692	0.3649
X ₃ -Storage Duration	1.67E-09	1	1.67E-09	5.61E-05	0.9941
X ₄ -Package Material	1.67E-09	1	1.67E-09	5.61E-05	0.9941
X ₁ X ₂	7.02E-06	1	7.02E-06	0.236474	0.6343
X ₁ X ₃	2.5E-09	1	2.5E-09	8.42E-05	0.9928
X ₁ X ₄	2.5E-09	1	2.5E-09	8.42E-05	0.9928
X ₂ X ₃	2.5E-09	1	2.5E-09	8.42E-05	0.9928
X ₂ X ₄	2.5E-09	1	2.5E-09	8.42E-05	0.9928
X ₃ X ₄	2.5E-09	1	2.5E-09	8.42E-05	0.9928
Residual	0.000416	14	2.97E-05		
Cor Total	0.003326	24			

* Values of "Prob > F" less than 0.05 indicate model terms are significant
X₁ = Steeping duration, X₂ = Gelatinization duration, X₃ = Storage duration,

Final equation in terms of coded factors

$$\text{Cyanide} = 0.045832 - 0.0219X_1 - 0.00208X_2 - 1.7E - 05X_3 - 1.7E - 05X_4 + 0.002651X_1X_2 - 5E - 05X_1X_3 - 5E - 05X_1X_4 - 5E - 05X_2X_3 - 5E - 05X_2X_4 - 0.00005X_3X_4$$

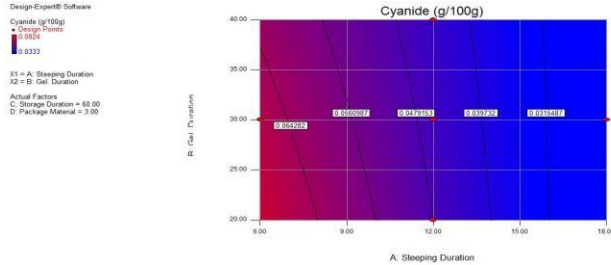


Fig. 1: Effect of Steeping Duration and Gelatinization Duration on the Cyanide Content of Soybean Flour.

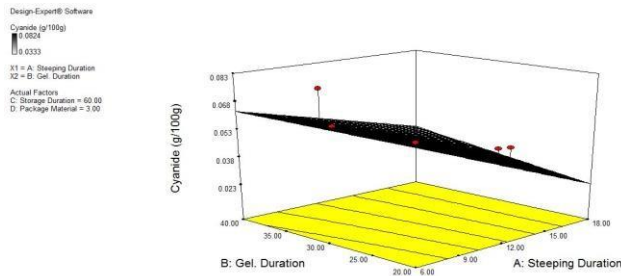


Fig. 2: Three-Dimensional Surface Plot of Cyanide Content Mode

3.2.1.2 Tannin Content

The ANOVA result (Table 4) showed that linear model is not significant. However, steeping duration is seen to have significant effect on tannin content of the flour while the gelatinization duration, storage duration and packaging materials had no significant effect on the tannin content of the flour as presented in Table 4. Only the interaction between the steeping duration and gelatinization duration had positive effect on the tannin content as shown in the model equation (2). The plot of the tannin content of the flour is shown in Figures 3 and 4.

Table 4: ANOVA of the Tannin Content of Soybean Flour

Source	Sum of Squares	Df	Mean Square	F	p-value
Model	0.048488	10	0.004849	0.486603	0.8722
X ₁ -Steeping Duration	0.04733	1	0.04733	4.749844	0.0469
X ₂ -Gel. Duration	0.0007	1	0.0007	0.070232	0.7949
X ₃ -Storage Duration	0	1	0	0	1.0000
X ₄ -Package Material	0	1	0	0	1.0000
X ₁ X ₂	0.000458	1	0.000458	0.045959	0.8333
X ₁ X ₃	0	1	0	0	1.0000
X ₁ X ₄	0	1	0	0	1.0000
X ₂ X ₃	0	1	0	0	1.0000
X ₂ X ₄	0	1	0	0	1.0000
X ₃ X ₄	0	1	0	0	1.0000
Residual	0.139505	14	0.009965		
Cor Total	0.187993	24			

* Values of "Prob > F" less than 0.05 indicate model terms are significant
X₁ = Steeping duration, X₂ = Gelatinization duration, X₃ = Storage duration, X₄ = Packaging Material

Final equation in terms of coded factors

$$\text{Tannin} = 0.730356 - 0.08882X_1 + 0.0214X_1 X_2$$

2

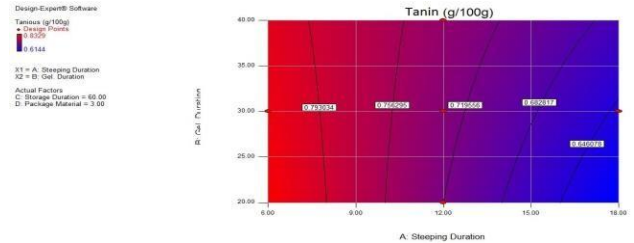


Fig 3: Effect of Steeping Duration and Gelatinization Duration on the Tannin Content of Soybeans Flour.

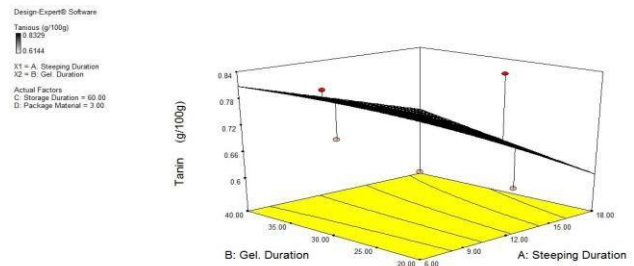


Fig. 4: Three-Dimensional Surface Plot of Tannin Content Model

3.2.1.3 Saponin Content

The statistical analysis shows that there was no significant effect (P≤0.05) on the saponin content of the flour samples. The model (linear) also had no significant influence on the saponin content of the flour as its above 0.05 (Table 5). Steeping duration, gelatinization duration and storage duration all had positive effect on the saponin content of the flour. The interactions between the steeping

duration and gelatinization duration; steeping duration and storage duration; gelatinization duration and storage duration also had positive effect on the saponin content as shown in the model equation (3). The 3D plots showing the effect of variables on saponin content are shown in Figures 5 and 6.

Table 5: The ANOVA of the Saponin Properties of Soybean Flour

Source	Sum of Squares	Df	Mean Square	F Value	p-value Prob > F
Model	13876583	10	1387658	1.812724	0.1499
X ₁ -Steeping Duration	1067220	1	1067220	1.39413	0.2574
X ₂ -Gel. Duration	1067468	1	1067468	1.394454	0.2573
X ₃ -Storage Duration	1067447	1	1067447	1.394426	0.2573
X ₄ -Package Material	1067447	1	1067447	1.394426	0.2573
X ₁ X ₂	1601151	1	1601151	2.091614	0.1701
X ₁ X ₃	1601170	1	1601170	2.091639	0.1701
X ₁ X ₄	1601170	1	1601170	2.091639	0.1701
X ₂ X ₃	1601170	1	1601170	2.091639	0.1701
X ₂ X ₄	1601170	1	1601170	2.091639	0.1701
X ₃ X ₄	1601170	1	1601170	2.091639	0.1701
Residual	10717137	14	765509.8		
Cor Total	24593719	24			

* Values of "Prob > F" less than 0.05 indicate model terms are significant X₁ = Steeping duration, X₂ = Gelatinization duration, X₃ = Storage duration, X₄ = Packaging Material

Final equation in terms of coded factors

$$\text{Saponin} = 202.9908 + 421.7464X_1 + 421.7954X_2 + 421.7912X_3 - 421.791X_4 + 1265.366X_1X_2 + 1265.373X_1X_3 - 1265.37X_1X_4 + 1265.373X_2X_3 - 1265.37X_2X_4 - 1265.37X_3X_4$$

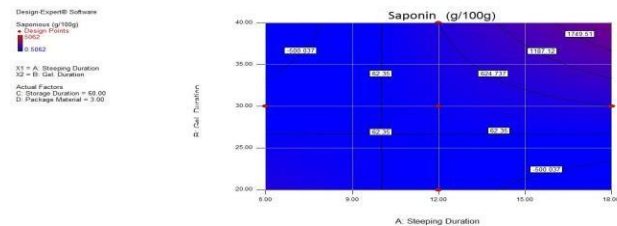


Fig. 5: Effect of Steeping Duration and Gelatinization Duration on the Saponin Content of Soybeans Flour.

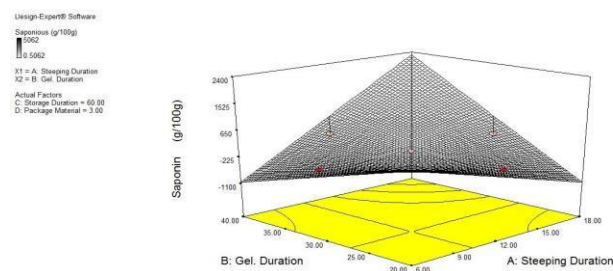


Fig. 6: Three-Dimensional Surface Plot of Saponin Content Model

3.2.1.4 Oxalate Content

Statistical analysis showed that the processing parameters have no significant effect ($P \leq 0.05$) on the oxalate content of soybean flour samples; the developed model was also found to be statistically insignificant as shown in Table 6. The 3D plots showing the effect of variables on oxalate content of soybean flour is shown in Figures 7 and 8.

Table 6: The ANOVA of the Oxalate Properties of Soybean Flour

Source	Sum of Squares	Df	Mean Square	F Value	p-value Prob > F
Model	4.28E-07	10	4.28E-08	0.079518	0.9998
X ₁ -Steeping Duration	4.27E-07	1	4.27E-07	0.792086	0.3885
X ₂ -Gel. Duration	1.67E-09	1	1.67E-09	0.003094	0.9564
X ₃ -Storage Duration	0	1	0	0	1.0000
X ₄ -Package Material	0	1	0	0	1.0000
X ₁ X ₂	0	1	0	0	1.0000
X ₁ X ₃	0	1	0	0	1.0000
X ₁ X ₄	0	1	0	0	1.0000
X ₂ X ₃	0	1	0	0	1.0000
X ₂ X ₄	0	1	0	0	1.0000
X ₃ X ₄	0	1	0	0	1.0000
Residual	7.54E-06	14	5.39E-07		
Cor Total	7.97E-06	24			

* Values of "Prob > F" less than 0.05 indicate model terms are significant X₁ = Steeping duration, X₂ = Gelatinization duration, X₃ = Storage duration, X₄ = Packaging Material

Final equation in terms of coded factors

$$\text{Oxalate} = 0.012104 - 0.00027X_1 + 1.6E - 05X_2$$

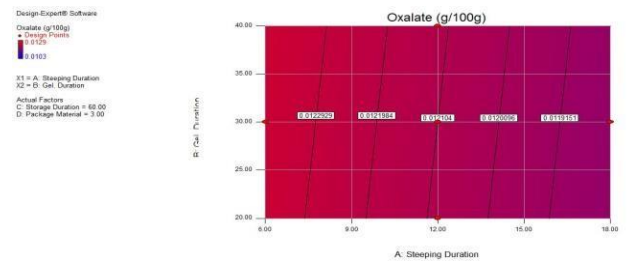


Fig. 7: Effect of Steeping Duration and Gelatinization Duration on the Oxalate Content of Soybeans Flour.

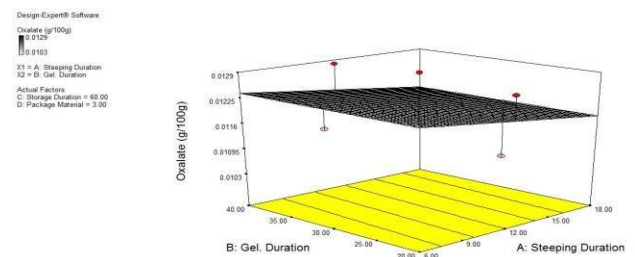


Fig. 8: Three-Dimensional Surface Plot of Oxalate Content Model

3.2.1.5 Phytic Acid Content

The linear model was insignificant in the ANOVA result but has a significant effect ($P \leq 0.05$) on the steeping duration as presented in Table 7. The steeping duration, gelatinization duration and interaction between the steeping duration and storage duration all had positive effect on the phytic content of the flour as shown in the model equation (5). The 3D plots showing the effect of variables on phytic acid is shown in Figures 9 and 10.

Table 7: The ANOVA of the Phytic Properties of Soybean Flour

Source	Sum of Squares	Df	Mean Square	F Value	p-value Prob > F
Model	0.003306	10	0.000331	1.458515	0.2518
X ₁ -Steeping Duration	0.003299	1	0.003299	14.55748	0.0019
X ₂ -Gel. Duration	6E-06	1	6E-06	0.026473	0.8731
X ₃ -Storage Duration	4.17E-08	1	4.17E-08	0.000184	0.9894
X ₄ -Package Material	4.17E-08	1	4.17E-08	0.000184	0.9894
X ₁ X ₂	0	1	0	0	1.0000
X ₁ X ₃	6.25E-08	1	6.25E-08	0.000276	0.9870
X ₁ X ₄	6.25E-08	1	6.25E-08	0.000276	0.9870
X ₂ X ₃	0	1	0	0	1.0000
X ₂ X ₄	0	1	0	0	1.0000
X ₃ X ₄	6.25E-08	1	6.25E-08	0.000276	0.9870
Residual	0.003173	14	0.000227		
Cor Total	0.006479	24			

* Values of "Prob > F" less than 0.05 indicate model terms are significant
X₁=Steeping duration, X₂=Gelatinization duration, X₃=Storage duration,
X₄= Packaging Material

Final equation in terms of coded factors

$$\text{Phytic} = 0.961496 + 0.02345X_1 + 0.001X_2 + 8.33E-05X_3 - 8.3E-05X_4 + 0.00025X_1X_3 - 0.00025X_1X_4 - 0.00025X_3X_4$$

5

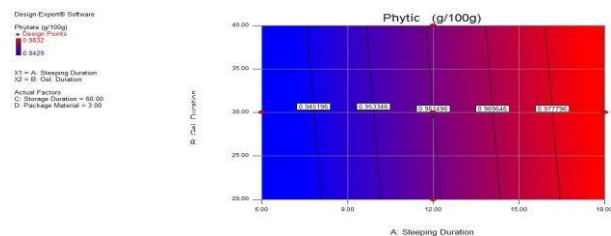


Fig. 9: Effect of Steeping Duration and Gelatinization Duration on the Phytic Content of Soybeans Flour.

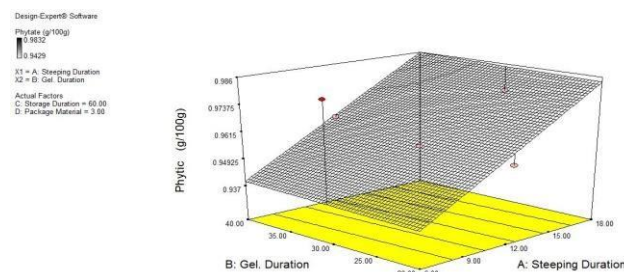


Fig. 10: Three-Dimensional Surface Plot of Phytic Content Model

4 CONCLUSIONS

In evaluating the impact of processing parameters and packaging materials on the anti-nutritional properties of soybean flour, the following conclusions were drawn:

Statistical analysis shows that steeping duration had significant effect ($P \leq 0.05$) on the cyanide content while the gelatinization duration, storage duration and packaging materials had no significant effect on the cyanide properties of soybean flour.

Steeping duration is seen to have significant effect on tannin content of the flour while the gelatinization duration, storage duration and packaging materials had no significant effect on the tannin content. Processing parameters and packaging materials had no significant effect ($P \leq 0.05$) on the saponin content of the flour samples.

The processing parameters and packaging materials have no significant effect ($P \leq 0.05$) on the oxalate content of soybean flour samples; the developed model was also found to be statistically insignificant. Only the steeping duration had significant effect ($P \leq 0.05$) on the phytic acid content of the flour.

REFERENCES

- Ajayi, I. A, Ajibade, O, Oderinde, R. A. (2011). Preliminary Phytochemical Analysis of some Plant Seeds. *Res. J. Chem. Sci.* 1(3):58-62.
- AOAC. (2002). Official Methods of Analysis, 15th edition; Association of Official Analytical Chemists: Washington DC.
- Bibianalgbabul, D. A. and Sule, S. (2013). Proximate composition, functions and sensory properties of Banbara nut (*Voandzeia Subterranean*), Cassava (*Manihot esculentus*) and soybean (*Glycine max*) flour blends for Akpekpa production. Department of Food Science and Technology, University of Agriculture Markurdi, Nigeria.
- Brooker, D.B.; Bakker-Arkema, F.W. and Hall, C.W. (1992). *Drying and storage of grains and oilseeds*, Springer. ISBN 0442205155, New York, United States
- IOPG (2014). Ghana. Institute of Packaging Ghana, Situational Analysis Report, January.
- Kim, Y and Wampler, D. J. (2009). Determination of Saponin and Various Chemical Compounds in Camellia Sinensis and Genus Ilex. Sensus Technical Note (SEN-TN-0027); Pp1-5.
- Liener, I.E. (1994). Implications of anti-nutritional components in soya bean foods. *Criteria Reverse Food Science Nutrition*; 34, 31-67.
- Omotayo, A. M., Olowe, V. I. O, Fabusoro, E, Babajide, J.M, Ojo, D. K and Adebite, D. A. (2007). Commercial Demand for Soybean in Nigeria. Report of a Survey Commissioned by Propcom (Promoting Pro-Poor Opportunities in the Commodity and Service Market). Monograph Series # 29.



Onwuka, G.I. (2005). Food Analysis and Instrumentation: Theory and Practice. Naphtali Prints, Nigeria; 95-96.

Silayoi, P. and Speece, M. (2004). Packaging and Purchase Decisions, *British Food Journal*; 106(8): 607-628

Soetan, K. O. and Oyewole, O.E. (2009). The need for adequate processing to reduce the anti-nutritional factors in plants used as human foods and animal feeds: A review. *African Journal of food science*, 223-232.

Soroka, W. (2002). Fundamentals of Packaging Technology, Institute of Packaging Professionals, Naperville, Illinois, USA.

Wheeler, E.L., and Ferrel, R.E. (1971). A method for phytic acid determinations in wheat and wheat fractions. *Cereal Chemistry*; 48 (3), 312-320.

FAO (1992). www.fao.org. Technology of Production of Edible Flours and Protein Products from Soybeans, FAO AGRICULTURAL SERVICES BULLETIN No. 97.



PROSPECTS AND CHALLENGES OF OFF-GRID POWER GENERATION FOR RURAL COMMUNITIES IN NIGERIA – THEORETICAL PERSPECTIVE

*¹Dangana Audu & ²Ikechuku A. Diugwu

^{1,2}Department of Mechanical Engineering. Federal University of Technology Minna. Niger State. Nigeria.

*Corresponding Author Email address: danganaaudu@@gmail.com

ABSTRACT

Rural area electrification in developing countries is vital for socio-economic growth. However, these small settlements also face erratic, and in worst scenarios no supply of power; just like in some urban cities. Only about 29% of rural communities have access to electricity as against 77% in urban settlement. These figures are relatively low as compared to developed countries and some other African countries. A lasting solution to these protracted problems could be the adoption and design of off-grid power generation for remote areas facing difficulties of on-grid extension reach. This paper therefore seeks to explore the prospects and challenges of adopting off-grid power generation for rural communities in Nigeria. Efforts made by the government to deploy off-grid power generation as an alternative source has been faced with challenges. Amongst these include; planning, gap in existing technology, operational issues, and political instability. The study recommends that; all tiers of government be duty-bound to implement off-grid projects to make the country attain its long-term plans of sustainable power supply, collaboration with the World Bank, United Nations (UN), NGOs and other institution to develop the power sector.

Keywords: *Generation, Power, Nigeria Off-grid, Renewable Energy*

1 INTRODUCTION

Generally, electricity is considered as a vital component and instrument for development. Nigeria being among the world's largest electricity access deficit account for about 77 Million people without access (The World Bank, 2017). The role of electricity in our everyday lives is enormous and the derivable benefits are countless. Adequate power supply is a mandatory precondition to any nation's development. Energy access policies are steadily yielding significant progress, as the number of people without access to electricity fell below 1 billion in 2017 (IEA, 2017). According to a recent report shown in table 1 below, North African countries are able to achieve 99% electricity access for rural communities, while China has a 100% access for both urban and rural settlements.

However, despite significant steps forward in Kenya, Ethiopia, Tanzania and Nigeria, rural communities still have very low access. In Nigeria, only about 29% of rural communities have access to electricity as shown in table 2 below (IEA, 2018). A significant amount of the economy is powered largely by small-scale generators, and about 50% of the population have limited or no access to the grid. As a result Nigerians and their businesses spend almost \$14 billion (₦ 5 trillion) annually on inefficient generation that

is expensive, of poor quality, noisy, and polluting (REA, 2017)

Table 1: Electricity Access, summary by region

	Electricity Access, Summary by Region						
	Rate of access						Population without access (million)
	2000	2005	2010	2017	2017	2017	
WORLD	73%	76%	80%	87%	95%	76%	992
Developing Countries	64%	69%	74%	83%	93%	73%	992
Africa	35%	39%	43%	52%	74%	36%	603
North Africa	90%	96%	99%	100%	100%	99%	<1
Sub-Saharan Africa	23%	28%	32%	43%	67%	28%	602
Developing Asia	67%	74%	79%	91%	98%	85%	351
China	99%	99%	99%	100%	100%	100%	-
India	43%	58%	66%	87%	98%	82%	168
Indonesia	53%	56%	67%	95%	100%	89%	14
Other Southeast Asia	68%	76%	84%	88%	97%	82%	44
Other Developing Asia	38%	45%	58%	76%	88%	68%	125
Central and South America	86%	90%	94%	96%	98%	86%	20
Middle East	91%	80%	91%	92%	98%	78%	18

Source: IEA, World Energy Outlook-2018

Table 2: Electricity Access, in West Africa

	Electricity Access in Africa						
	Rate of access						Population without
	National			Urban	Rural		
	2000	2005	2010	2017	2017	2017	2017
West Africa	33%	37%	42%	51%	77%	29%	182
Nigeria	40%	47%	50%	60%	80%	40%	77
Benin	22%	23%	27%	30%	54%	9%	8
Cote d'Ivoire	50%	49%	59%	60%	88%	31%	10
Ghana	45%	51%	61%	84%	97%	69%	5
Senegal	30%	35%	54%	65%	90%	43%	6
Togo	9%	18%	28%	36%	64%	16%	5
Burkina Faso	13%	9%	15%	18%	58%	1%	16
Cape Verde	59%	65%	70%	96%	100%	89%	<1
Gambia	18%	27%	35%	45%	66%	13%	1
Guinea	16%	18%	20%	17%	46%	1%	11
Guinea-Bissau	10%	11%	12%	10%	14%	8%	2
Liberia	0%	1%	2%	10%	16%	3%	4
Mali	12%	14%	17%	38%	83%	6%	11
Mauritania	15%	17%	19%	30%	56%	1%	3
Niger	7%	8%	9%	12%	68%	1%	19
Sao Tome and Principe	53%	55%	57%	68%	87%	22%	<1
Sierra Leone	9%	11%	12%	20%	19%	20%	6

Source: IEA, World Energy Outlook-2018

Events have shown that access to electricity through the grid can no longer sustain increasing population, especially in developing economies of the world. For instance, in a study by Perez (2006), an estimated 1.7 Billion people live off- grid worldwide.

Off grid technologies can generally be explained as an affordable decentralized energy designed for homes, villages, dispersed settlements islets; which can be made up of solar home systems, wind systems, biogas digesters, biogas gasifiers, micro-hydro power plants, etc. Alliance for Rural Electrification (2013). In addition, off-grid systems are able to support the incorporation of decentralized renewable power generation into the grid and provide power reliability and stability.

Thus, major objectives of this study are to;

1. Explore prospects and challenges of off-grid power generation
2. Recommend policies for increased adoption of the system.

The system of off-grid power generation will go a long way to address the recurring issues facing the Nigerian Power sector over the years. This sustainable and renewable system has been fully implemented in some countries and is yielding excellent results. Subsequent sections of the paper further discourses power generation; off-grid power generation and will further address issues of prospects and challenges hindering full adoption of this system.

2 LITERATURE REVIEW

2.1 POWER GENERATION IN NIGERIA

According to Claudius (2014), the history of electricity generation in Nigeria can be dated back to the end of the 19th century, when the first generating power plant was installed in Lagos in 1898, fifteen years after its introduction in England. The total capacity of the generators used then was 60Kw due to the low demand then

(Onochie *et al.*, 2015). In 1946, the public works department ceased to have control over the operation of the electricity generating plants and distribution system in the country. As a result of this, the Nigeria Government Electricity Undertaking (NGEU) was established under the jurisdiction of the Public Works Department (PWD) to take over the responsibility of electricity supply in Lagos state. Five years later, a central body was established to take over all the various electricity supply outlets within the country.

The body is referred to Electricity Corporation of Nigeria (ECN), and was established by act of parliament in 1951 (Olugbenga *et al.*, 2013). With the increase in demand for electricity, some projects were carried out in Ijora, Oji River, Kano, and Ibadan power stations to further compliment the availability and quality of power delivery in the country (Claudius, 2014).

In 1962, a decade after the establishment of ECN, Niger Dams Authority (NDA) was set up, which was responsible for dam construction after discovering the countless benefits that would generate from the dam. This led to the construction of Kainji Dam in 1962 and was completed in 1968 (Claudius, 2014).

The electricity produced by NDA was sold to ECN for distribution and sales at utility voltages. However, a merger of the two was made in 1972 to National Electricity Power Authority (NEPA). According to Olugbenga *et al.* (2013), electric power demand increasingly overshoots available supply as population increases and this resulted in a decline in electricity generation capacity. As a result of the Government effort to revitalize power sector, NEPA was renamed to Power holding company of Nigeria (PHCN) by electricity power sector reform (EPSR) Act of 2005. In addition, the study stated that by the act, NEPA was translated into the newly corporated PHCN plc comprising of 18 separate successor companies that took over the assets, liabilities and employees of NEPA, and responsibilities for the generation (6 companies), transmission (1 company) and distribution (11 companies). Sambo *et al.*(2010) states that electricity generation in Nigeria over the last 40 years varied from gas –fired, oil – fired, hydroelectric power stations to coal-fired with hydroelectric power system and gas – fired system taking precedence.

The study further posits that Nigeria has 14 generating plant (of the which, 3 are hydro and 11 are thermal (gas/steam)) supplying electricity to the National Grid. The national grid is made up of 4,889.2km of 330kV line, 6,319.33km of 132kV line, 6,098MVA transformer capacity at 330/132kV and 8,090MVA transformer capacity at 132/33kV.

2.2 OFF-GRID POWER GENERATION

Over the past few years, the Nigerian government had expanded its focus on exploring other sources of power generation through off-grid to reduce pressure on grid supply due to the recurrent problems facing the sector. Apart from irregular and unreliable supply, high cost of connection, recurrent vandalism of the transmission lines, pressure on the national grid has led to constant system collapses; all these necessitates the provision of electric power through off-grid option. Furthermore, these problems have led to; those who play in the industrial sector and a number of residential power consumers to solely disconnect from grid supply to rely on self-generated power for their operations (Ugwuanyi, 2018). Off-grid generation can be described as stand-alone power generation systems or mini-grids, which typically provide smaller communities with electricity through independent electricity distribution network systems (Financial Nigeria, 2016). Off-grid supply is power supply that does not go through the national grid. They are usually low capacity generations.

The broad difference between off-grid and centralized grids is the latter is larger in size, produces several hundred megawatts (MW) or thousands of gigawatts (GW) that can cover larger area and rely on centralized power stations to meet electricity demand. While the former is smaller in size, producing lesser, and has a (semi)-autonomous capability to satisfy electricity demand through local power generation. According to Elusakin, Ajide, and Diji (2014), off-grid technologies are majorly linked with renewable technologies such as solar and hydro.

According to the IEA (2017), annual per capita electricity consumption was 140 kWh in 2015, or roughly 12 kWh per capita per month. An online publication by Punchng (2015) shows that the total off-grid generation capacity as approved by the Nigerian Electricity Regulatory Commission (NERC) is still less than 500MW. There is need for significant investments in off-grid power generation; considering Nigeria's plans to increase power generation capacity in the coming years. Off-grid supply meant for solar home systems (SHS) and comes in small systems of between 10W and 500W and mainly for rural communities while SHS of larger systems of between 500W and 15KW for urban and semi-urban. Off-grid systems for SMEs and businesses are between 500KW and 1MW and perfectly runs the rural electrification agency (REA) energizing economy, while mini grids can range from 15KW to 10MW for industries, estates, educational institutions and markets, solar agriculture, solar irrigation (Ugwuanyi, 2018). For instance, the figure below shows a schematic diagram of an off-grid PV system. Here, the solar panels become generates the needed energy by one's home or any energy dependent system. There may be no option other than to go with an off-grid solar system.

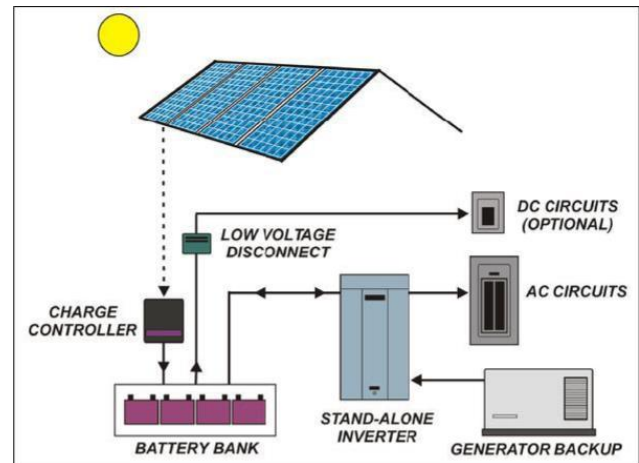


Figure 1: Off-grid PV System Schematic
Source: Ammar & Noor (2018)

2.3 OFF-GRID POWER GENERATION IN RURAL COMMUNITIES

The government through the ministry of power, works and housing in partnership with the private sector operator, has been developing solar and wind projects to feed the population that does not have access to grid supply. The rural electrification agency (REA) is another major vehicle the government is using to drive the off-grid generation project in the rural areas of the country (Ugwuanyi, 2018).

The Nigerian Rural Electrification Agency (REA) was created by the Electric Power Sector Reform Act in 2005 to facilitate the provision of affordable power supply for residential, commercial, industrial, and social activities in the rural areas. The agency is dedicated to supporting off-grid development to enable people function without the support of remote grid infrastructure. According to a report by Source: Ben *et al*, 2015, about 31 million people may be living in an area where electricity is available, yet do not have access. Nearly three-quarter (72%) of under-the-grid Nigerians live in rural communities, and just about 30% live within 10Km of a high voltage transmission line- as shown in the figure below.

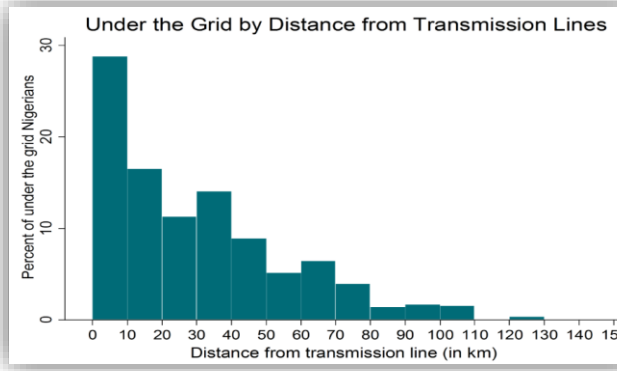


Figure 2: "Under the Grid" population distance from Transmission line (Km)

Source: Ben *et al*, 2015

According to (ARE, 2015; IRENA 2015), there are majorly two approaches to conduct rural power generation in an effective way; one of the approach is mini-grid or isolated grid which generates between 10KW – 10MW to serve limited number of consumers (rural communities, institutional buildings and commercial/industrial plants and buildings).

The other approach is through stand-alone system which provides electricity to individual appliances, homes or a small business. For instance, Bangladesh is one of the world's most densely populated countries with a population of over one hundred and fifty eight million and has made a success story from implementing off-grid power solutions. The government of Bangladesh initiated the solar home system (SHS) based rural electrification programme in 2003 through development company limited under a microcredit scheme. In 2002, only 7000 Bangladeshi households used solar panels, but as of today, the programme has installed about 2 million SHS in the country (Financial Nigeria, 2016).

3.0 PROSPECTS OF OFF-GRID POWER GENERATION

According to the Minister for Power, Works and Housing in Nigeria, Mr. Babatunde Fashola (2016), Elusakin, Ajide, and Diji (2014) the following are some of the prospects for off-grid power generation in the country:

Potential to grow industrial clusters and small cottage industries

Most industrial groups and some small businesses require uninterrupted power supply to function optimally. This could be generated through fully off-grid power plants or embedded within distribution networks. This could potentially transform the economy of these areas; increase profitability for the existing businesses; create jobs; and

breed a crop of customers who are willing to pay for electricity supplied.

Opportunity to expand and refurbish distribution networks of the DISCOs

In line with the NERC Regulation for Independent Electricity Distribution Networks (IEDNs), 2012, off-grid generation plants require Independent Electricity Distribution Networks (IEDNs) to supply electricity to end users, except for eligible customers upon declaration by the Minister of Power, who can be supplied to directly. This creates opportunities for investors who may wish to create off-grid projects with their own IEDN. This could potentially be a win-win situation for DISCOs who could either collaborate with developers to expand or refurbish their network; add to their number of paying customers; or acquire the developer assets given the right regulatory framework.

Access to other fuel alternatives

Most of the power plants in Nigeria are gas fired thermal plants. Given the current constraints with gas, off-grid power plants could be an alternative, taking advantage of diverse and hybrid fuel sources like renewables (solar, wind, biomass). This would be particularly more useful in areas where there is limited gas supply, e.g. the northern part of Nigeria where solar, wind, and hydro sources are prevalent.

Opportunity for rural electrification

Off-grid solutions are also useful in the area of topographical or geographical challenges in rural areas which have made it uneconomical to extend the grid to such areas. Rural electrification in Nigeria is currently in a weak and ramshackle state; hence there is a dire need for investments in the area.

Technology development

Positive passion for improved technological development on the side of the government will go a long way to foster the development of this system. Government should invest more in science and technology as well as creating enabling environment for foreign technology companies to train and develop our engineering graduates.

4.0 CHALLENGES OF OFF-GRID POWER GENERATION IN RURAL COMMUNITIES

Technology gap

Due to the fact that many of the off-grid equipment are sophisticated and advanced, there is need to develop the



adequate technological know-how for installation, operation and maintenance. It is common to find that many solar PVs (photovoltaic) installed fail shortly after installation. Also, renewables such as wind and biomass have not been fully explored in Nigeria, and would require adequate know-how. The country needs to strive hard to close these gaps in technology for improved practices.

Objections from existing Monopolies.

There are possibilities that there would be objections to the granting of off-grid licenses from electricity distribution companies (DISCOs) over the areas where their DISCO licenses currently cover. NERC also maintains a balance to ensure that the DISCO's market share will not be destroyed by the grant of an off-grid license (Financial Nigeria, 2016).

Improper planning

Inadequate planning is an impediment to the success of off-grid development in Nigeria. Off-grid projects are not well planned such that the viability of the projects are not being considered in each location before the implementation. Planning and design proceed any sustainable off/grid power project which is the beyond the challenges of technology type and availability (Elusakin, Ajide, and Diji, 2014)

Lack of monitoring the implementation of off-grid projects

Off-grid projects when awarded to contractors are not effectively monitored. Due to corruption in the REA, project fund are also misappropriated which leads to non-implementation of off-grid projects (Alao and Awodele, 2018).

Political Instability

Another major challenge hindering the full implementation of off-grid power generation in rural communities is the frequent political instability faced in the country, as well as change in government policies

5.0 CONCLUSION

There is the urgent need to strategically increase the rate of electrification for rural communities to promote socio-economic development in the country. The main aim of this study was to examine the prospects and challenges facing the adoption of off-grid power generation in rural communities. This was achieved through theoretical review of relevant literature. One of the constraints encountered in the course of this study is the limited

literature in the area of off-grid system in Nigeria. Hence, as a recommendation, further research should be done to breach the existing gap between Nigeria and other countries.

5.1 RECOMMENDATION

- To encourage further investments in off-grid solutions, it is important that the government ensures that the environment is welcoming enough to elicit tax support from the government in terms of tax reforms
- Projects for rural electrification should be adequately funded as well as strategy to ensure sustainable growth in the projects
- Collaboration with the World Bank, United Nations (UN), NGOs and other institution to develop the power sector.
- All tiers of government be duty-bound to implement off-grid projects to make the country attain its long-term plans of sustainable power supply.

REFERENCES

- Alao O. and Awodele K. (2018) 'An overview of the power sector, the challenges of its National grid and off-grid development as a proposed solution', *Institute of electrical electronics engineer power and energy society*, Conference paper, pp. 178-183.
- Alliance for Rural Electrification (ARE) (2015), retrieved from [http://www.ruralelec.org/17.0.html] on August 20, 2019).
- Ammar A, and Noor, H. A (2018). Design of an Off-Grid Solar PV System for a Rural Shelter. Masters' Thesis. German Jordanian University
- Ben, L; Jared K; and Robert M. (2015). Living "Under the Grid" in Nigeria – New Estimates. Available online (<http://www.cgdev.org/blog/living-under-grid-nigeria-new-estimates>) accessed; 23-8-2018
- Claudius A. A. (2014) 'Nigeria electricity industry: issues, challenges and solutions', Public lecture series 3(2), covenant university.
- EATON (2013), "Blackout Tracker Annual Report 2013" Available online:



- (www.eaton.com/Eaton/OurCompany/NewsEvents/NewsReleases/PCT_1044447)
- Elusakin, J. E; Ajide, O. O; and Diji, J. C (2014). Challenges of Sustaining Off-Grid Power Generation in Nigeria Rural Communities. *African Journal of Engineering Research*, pp51-57
- IEA (2017) International Energy Agency *Electricity Access Database*. Available online (<https://www.iea.org/sdg/electricity/>) (Assessed on: 20/8/2019)
- IEA (2018) International Energy Agency *Electricity Access Database*. Available online (<https://www.iea.org/sdg/electricity/>) (Assessed on: 20/8/2019)
- International Energy Agency (IEA) and the World Bank. Sustainable Energy for All 2017 Global Tracking
- IRENA, (2015), Off-Grid Renewable Energy Systems: Status and Methodological Issues
- Nigerian Minister of Power, Works and Housing, Fashola B. (2016) ‘Opportunities for off-grid solutions in Nigeria Power sector’, Available at: <http://www.financialnigeria.com> [Accessed 20th August, 2019].
- Olugbenga T. K., Jumah A. and Philips D. A. (2013) ‘The current and future challenges of electricity market in the face of deregulation process’, *African journal of engineering research*, 1(2), pp. 33-39.
- Onochie U. P., Egware H. O. and Eyakwanoer T. O (2015) ‘The Nigeria electric power sector (opportunities and challenges)’, *Journal of multidisciplinary engineering and technology*, 2(4), pp. 494-502.
- Perez R, (2006). USA Today, Home Power Magazine. Available online (http://archive.org/stream/Home_Power_Magazine_Issue_111_2006-02-03/) (Retrieved: August 20, 2019).
- Punch Nigeria Newspaper (2015) Available at: <http://www.punchng.com>
- Rural Electrification Agency (RAE) (2017). The Off-Grid Opportunity in Nigeria Upscaling minigrids for least cost and timely access to electricity Action Learning Event.
- Rural Electrification Agency (RAE). <http://rea.gov.ng>
- Sambo, A. S; Garba, B Zarma, I. H; and Gaji, M. M. (2010). Electricity Generation and the Present Challenges in the Nigerian Power Sector
- The World Bank, (2017). State of Electricity Access
- Ugwuanyi E. (2018) ‘Off-grid power supply will bridge Nigeria’s energy deficit’, Available at: <http://www.rea.gov.ng/> [Accessed 20th August, 2019].



Spectrum Occupancy Measurement in the VHF Band- Results and Evaluation in the Context of Cognitive Radio

*Ajiboye, J.A¹, Adegboye, B.A², Aibinu, A.M³, Kolo, J.G⁴

^{1,2,4}Department of Electrical and Electronics Engineering, School of Electrical Engineering and Technology (SEET), Federal University of Technology, P.M.B 65, Minna, Nigeria.

³Department of Mechatronics Engineering, School of Electrical Engineering and Technology (SEET), Federal University of Technology, P.M.B 65, Minna, Nigeria.

*Corresponding author email: ajiboye2003@yahoo.com, +2348035532375

ABSTRACT

In this paper the results of spectrum occupancy survey in the context of Cognitive Radio was presented. In Cognitive Radio, secondary unlicensed users are allowed to opportunistically use the primary licensed users' bands with the understanding that there will be no interference i.e Secondary Users (SU) quits at the arrival of Primary Users (PU). A 24-hour measurement survey was carried out at the centre of Minna metropolis in Niger State, Nigeria covering a frequency range of VHF (30-300MHz). Aeronia HF 6065 V4 spectrum analyzer was used for data collection. Results show that the band allocated for Aeronautical Navigation has the highest spectral occupancy of 39.83% followed by the FM band with occupancy of 12.90% while the frequency band meant for Aeronautical Mobile and Space Operation has occupancy of 4.73% and TV Broadcasting 0.09%. The average occupancy of the VHF band is 14.39%.

Keywords: *Cognitive Radio, FM, Primary Users, Secondary Users, VHF*

1 INTRODUCTION

The rise in the demand for wireless devices and wireless communication technology has resulted to the scarcity of the finite radio spectrum. Several wireless services and applications like satellite radio broadband, Wi-Fi internet connections and Bluetooth devices have contributed to the heavy demand of the spectrum. Several regulatory bodies worldwide including the Federal Communications Commission (FCC) of the United States of America (USA) have discovered that lots of frequency bands in the radio frequency spectrum is currently under-utilized. Therefore, the implication is that most spectrum that are allocated are not fully utilized (Barau *et al.*, 2013). This has led to inefficient use of this natural resource (Weiss and Jondral 2004). In the current policy, unlicensed users are disallowed from accessing the spectrum even when they are not utilised by the primary users (Saladhine *et al.*, 2017). Cognitive Radio is envisioned to solve the problem of spectrum scarcity by gaining an understanding of the dynamism of the spectrum occupancy of the frequency band (Barnes *et al.*, 2013; Barnes and Maharaj, 2011).

According to Mitola and Maguire (1999) Cognitive Radio is a radio that senses the environment and adapt its operating parameters to changes in the environment. The essence of Cognitive Radio is to assess the free frequency bands so as to improve on the usage of spectrum opportunistically. It has been generally accepted as a standard solution to spectrum scarcity and under-utilization due to the ineffective way of spectrum allocation to

Primary User (PU). To effectively deploy Cognitive Radio, there is the need to have correct and accurate understanding of the allocated spectrum.

Several spectrum occupancy measurement campaigns have been conducted all over the world (Juarez *et al.*, 2016 and Wiles *et al.*, 2016). The study reveals heavy underutilization of spectrum. Few of the campaigns focused on some specific frequency bands while others focused on power received in dBm or percentage of spectrum utilization such as duty cycle (Lima and Mello 2013). Spectrum measurement campaigns is important so that spectrum occupancy samples on pre-selected frequency bands can be obtained such as in cellular bands or TV bands (Eltom *et al.*, 2018).

However, there is still a general lack of the understanding of the spectrum occupancy in Africa and in particular in Nigeria. According to Kliks *et al.*, (2013), spectrum occupancy measurement information for a particular location is not applicable for other locations. Therefore, this work presents results of an outdoor spectrum occupancy measurement in Minna metropolis, Niger State, Nigeria with focus on the Very High Frequency (VHF) band of 30-300MHz).

2 METHODOLOGY

The description of the measurement location and the equipment used are described in the following sub-sections.

2.1 MEASUREMENT LOCATION

A careful choice of a measurement location is essential for a good spectrum measurement campaign. The location site chosen has an impact on the spectrum occupancy measurement. In general, according to Sanders (1998), a site for spectrum measurement demands that:

1. Transmitters around the measurement location are minimal to avoid intermodulation and saturation challenges.
2. Minimal impulsive noise due to vehicular movements and electrical machines which can increase the signals received.

Bearing in mind these conditions, the spectrum occupancy measurement site for this work was chosen to be the Abuja Electricity Distribution Company (AEDC) office located at the centre of Minna town in Niger State, Nigeria. The google map of the site is shown in Fig. 1 while the Geographical Coordinates are shown in Figure 2.

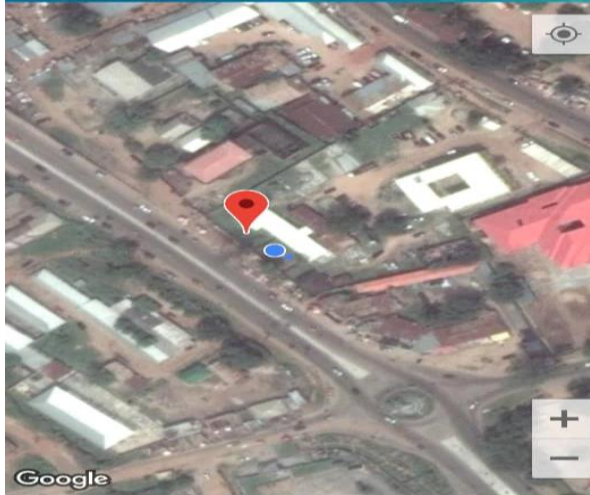


Figure 1: Google Map of Measurement Location


Current Pos	
Longitude:	6.55070667
Altitude:	257.90m. above ellipso
Altitude:	257.90m. above M.S.L.
Accuracy:	1.80m.
PDOP=	0.93
HDOP=	0.56
VDOP=	0.74
Satellites:	18/22
Auto <input type="checkbox"/> Start accurate positioning 	
Accurate Position	
Latitude:	9.61195620
Longitude:	6.55071664
Altitude:	248.08m. above ellipso
Altitude:	248.08m. above M.S.L.
Accuracy:	0.32m.
PDOP=	0.35
HDOP=	0.12
VDOP=	0.16
Readings:	H=97/V=97

Figure 2: Geographical Coordinates of the Site

2.2 MEASUREMENT EQUIPMENT

The setup of equipment used for measurement in this work includes a calibrated Aaronia Spectran HF-6065 V4 spectrum analyzer. The range of the spectrum analyzer is 10MHz to 6GHz and an Omni directional antennae with a range of 10MHz to 3GHz and a laptop connected via USB cable to the spectrum analyzer and an MCS software designed specifically to run on Aaronia Spectrum Analyzer. The equipment was powered with an 850VA inverter. The setup is as shown in Figure 3.



Figure 3: Equipment Setup

The full frequency measurement range of the study is 30-300MHz and was observed for 24 hours before band to band telecommunications spectrum occupancy analysis was carried out. As a result of the analysis, the occupied telecommunication bands were identified and the duty cycle and occupancy was measured. The parameter configuration of the spectrum analyzer is shown in Table 1.

TABLE 1: PARAMETER CONFIGURATIONS OF SPECTRUM ANALYZER

Parameter	Value
Frequency Range of the Analyzer	10MHz-6GHz
Frequency Range of the Antennae	10MHz-3GHz
Frequency Range for the Study	30-300MHz
Resolution Bandwidth (RBW)	100KHz
Video Bandwidth (VBW)	100KHz
Sample Time	1ms
Detection Type	RMS
Sample Points	5401
Attenuation Factor	Auto

2.3 DATA COLLECTION AND PROCESSING

The outdoor measurement was taken for 24 hours in the location. All raw data was collected by the spectrum analyzer in a matrix form as shown in Table 2 with P_{ij}

being the elements of the received signal powers in dBm while the rows and the columns records the time slots and the frequency respectively. A total of Thirty Million Eight Hundred and Fifty Thousand Five Hundred and Twelve (30,850,512) data elements was recorded by the spectrum analyzer and saved file using .csv extension. Processing of the measurement samples was done with the aim of getting necessary parameters in order to measure spectrum occupancy.

TABLE 2: Matrix for the Power Spectrum Measurement

Time/Frequency	1	→	5,401
1	$P_{1,1}$	→	$P_{1,5401}$
↓	↓	↘	↓
5,712	$P_{5712,1}$	→	$P_{5712,5401}$

The duty cycle is the same as the frequency occupancy rate and describes or quantifies how a particular frequency band is occupied by signal. According to Mehdawi (2013) and Paulson *et al.* (2018), the duty cycle shows how frequent signals are seen on a particular channel during a sample period and is obtained as shown in (1):

$$Duty\ Cycle = \frac{DD_{Tslot}}{N_{Tslot}} * 100\% \quad (1)$$

where DD_{Tslot} is the number of time slots where received signal power is equal to or greater than the decision threshold and,

N_{Tslot} is the entire time slot.

Spectrum power measurements was done by the Spectrum Analyzer at intervals of 50 kHz for the entire range of the 30 MHz to 300 MHz spectra span giving rise to 5401 trace points. Trace points determines the resolution. The higher it is the better the resolution.

In Energy detection, the determination of the decision threshold is very crucial. When the decision threshold is set too high, the entire spectrum is underestimated and many signals are missed. However, when the threshold is set too low, the spectrum is overestimated and even noise is seen as signals.

The noise levels are taken into consideration when the Energy Detection (ED) method is used to compute the proportion of the presence of signal in a particular band of

interest. The decision threshold is taken as 10 dBm power above the average noise level. The ED method therefore does a comparison between the signals received in a particular frequency band of interest to a predefined threshold values. In a situation when the signal is lower than the threshold then the band is assumed to be idle and hence is available for use by Cognitive Radio.

3 RESULTS AND DISCUSSION

Analysis of the spectrum for some particular bands dedicated for specific services was done as shown in Table 3. The plot of Power Received (dBm) against Frequency (MHz) for the entire range of frequency measurement (30-300MHz) is shown in Figure 4.

TABLE 3: SERVICES ALLOCATED TO SPECIFIC FREQUENCY BANDS

Services	Frequency Range (MHz)
FM Radio	87.5-108
Aeronautical Navigation	108.05-137.95
Aeronautical Mobile & Space Operation	138-144
TV Broadcasting	174-230



Figure 4: Power Spectral Density Plot for 30-300MHz Frequency Range

Decision threshold plays a major role in determining the actual spectral occupancy in the frequency band under investigation. Whereas a high thresholds leads to underestimation of the spectrum a low threshold results in spectrum overestimation. When thresholds are extremely high signals in the occupied bands are missed. Likewise, very low thresholds are affected by noise hence assuming the frequency channel as not available. These scenario are shown in Figure 5. The Average duty cycle of 100% corresponds to a low decision threshold of -75 dBm for FM Radio, -81 dBm for Aeronautical Navigation, -81 dBm for Aeronautical Mobile and Space Operation and -87 dBm for TV Broadcasting. Also the Average duty cycle of 0%

corresponds to a high decision threshold of -57 dBm for FM Radio, -73 dBm for Aeronautical Navigation, -73 dBm for Aeronautical Mobile and Space Operation and -75 dBm for TV Broadcasting.

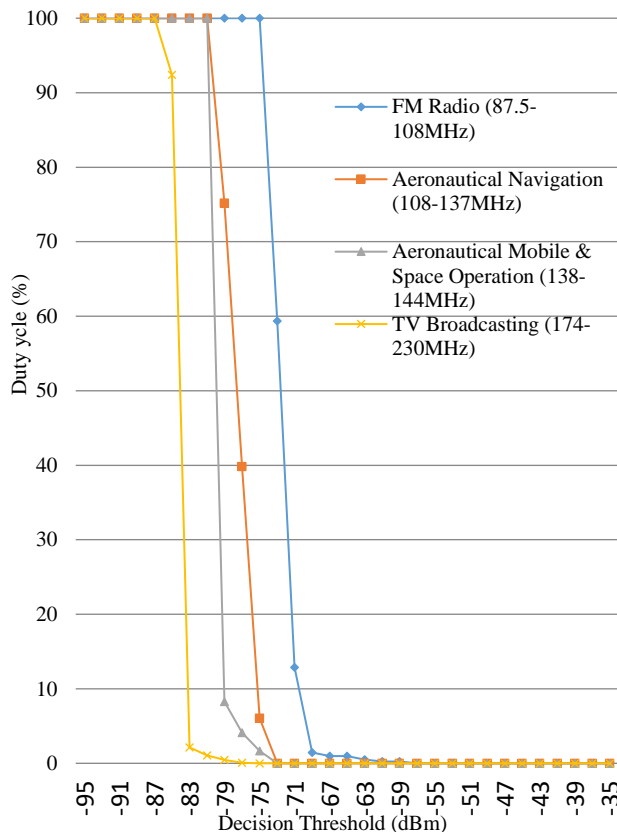


Figure 5: Average Duty Cycle as a Function of Decision Threshold

TABLE 2: AVERAGE DUTY CYCLE FOR SPECIFIED BANDS

Services	Frequency range (MHz)	Bandwidth (MHz)	No. of trace points in bandwidth	Average Duty Cycle (%)
FM Radio	87.5 – 108	20.5	411	12.90
Aeronautical Navigation	108.05 – 137	28.95	580	39.83
Aeronautical Mobile & Space Operation	138 – 144	6	121	4.73
TV Broadcasting	174 – 230	56	1121	0.09

Figure 6 to Figure 9 show the Power Spectral Density (PSD) Plots for FM Radio, Aeronautical Navigation, Aeronautical Mobile and Space Operation and TV

Broadcasting which is averaged for the 24 hours measurement period. Figure 6 shows that there are some activities within the FM band with only about two broadcasting stations active and with a threshold of -71 dBm. Figure 7 reveals significant activities with a threshold value of -77 dBm within the band allocated for Aeronautical Navigation while Figure 8 shows minor activities with a threshold of -69 dBm within the band allocated for Aeronautical Mobile and Space Navigation. Figure 9 shows no significant activities within the TV Broadcasting band with a threshold of -61 dBm.

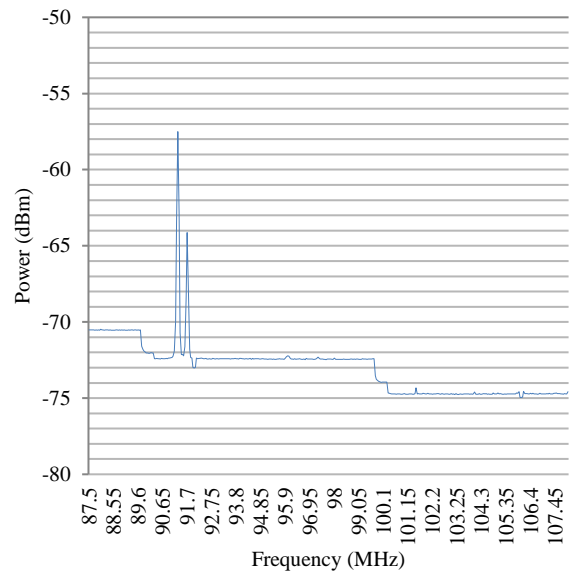


Figure 6: Power Spectral density Plot for FM Band

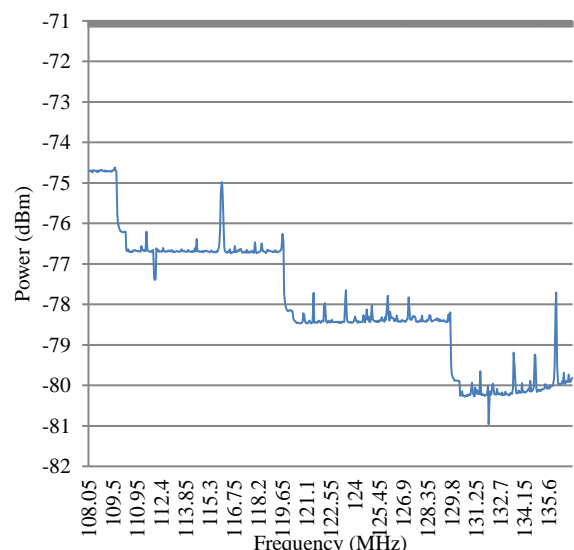


Figure 7: Power Spectral density Plot for Aeronautical Navigation

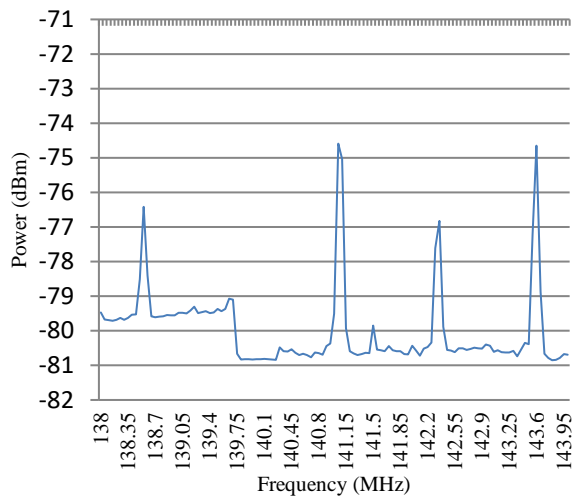


Figure 8: Power Spectral density Plot for Aeronautical Mobile & Space Operation

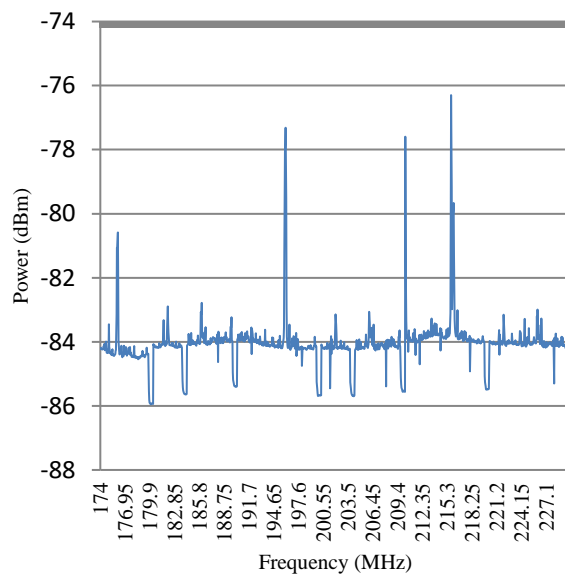


Figure 9: Power Spectral density Plot TV Broadcasting

4 CONCLUSION

Although several measurement campaigns have been done in many parts of the world, most of the campaigns focused on a wide band of frequency. This work focused on the narrow part of the VHF in the TV spectrum band. Spectrum Occupancy results show a very low occupancy particularly in the TV broadcasting sub band making the band appropriate for Cognitive Radio deployment.

REFERENCES

- Barnes S.D., Jansen van Vuuren P.A. & Maharaj B.T. (2013). Spectrum Occupancy Investigation: Measurements in South Africa. *Measurement Journal*, 2013, 46(9), 3098-3112.
- Barnes S. D. and Maharaj B. T. (2011). Performance of a Hidden Markov Channel Occupancy Model for Cognitive Radio. *Proceedings of IEEE AFRICON Conference*, Livingstone, Zambia. 1–6.
- Eltom H., Kandeepan S., Evans R. J., Liang Y. C. & Ristic B. (2018). Statistical Spectrum Occupancy Prediction for Dynamic Spectrum Access: A Classification. *EURASIP Journal on Wireless Communications and Networking*.
- Juarez-Cardenas M., Diaz-Ibarra A., Pineda-Rico U., Arce A. and Stevens-Navarro E. (2016). On Spectrum Occupancy Measurements at 2.4 GHz ISM Band for Cognitive Radio Applications. *Proceedings of International Conference on Electronics, Communications and Computers*, 25–31.
- Kliks A., Kryszkiewicz P., Perez-Romero J., Umberto A., and Casadevall F. (2013). Spectrum Occupancy in Big Cities—Comparative Study—Measurement Campaigns in Barcelona and Poznan. *Proceedings of the 10th International Symposium on Wireless Communication Systems (ISWCS '13)*, 1–5.
- Mehdawi, M., Riley, N., Paulson, K., Fanan, A., & Ammar, M. (2013). Spectrum Occupancy Survey in HULL-UK for Cognitive Radio Applications: Measurement & Analysis. *International Journal of Scientific & Technology Research*, 2(4), 231–236.
- Mitola J., and Maguire G. Q. (1999). Cognitive Radio: Making Software Radios more Personal, *IEEE Communications*. 6(4), 13–18.
- Paulson E. N., Dauda U. S., Salawu N., Alias M., Kamaludin M. Y., Adip S. and Rozeha A. R. (2018). Interference Temperature Measurements and Spectrum Occupancy Evaluation in the Context of Cognitive Radio. *Indonesian Journal of Electrical Engineering and Computer Science*. 10(3).
- Salahdine F., Kaabouch N., El. Ghazi H. (2017). Techniques for Dealing with Uncertainty in Cognitive Radio Network. *7th IEEE Annual Computer Communication Workshop Conference*, 1-6.
- Sanders F. H. (1998). Broadband Spectrum Surveys in Denver, CO, San Diego, CA, and Los Angeles, CA: Methodology, Analysis and Comparative Results. *IEEE International Symposium on Electromagnetic Compatibility*, 988-993.
- Weiss T. A. and Jondral F. K. (2004). Spectrum Pooling: An Innovative Strategy for the Enhancement of Spectrum Efficiency, *IEEE Communications*. 42(3), 8–14.
- Wiles E., Hill B., da Silva F.A. and Negus K. (2016). Measurement and Analysis of Spectrum Occupancy from 140 to 1000 MHz in Rural Western Montana. *Proceedings of European Conference on Networks and Communications (EuCNC)*, 1-5.

Modelling and Simulation of Adaptive Fuzzy-PID Controller for Speed Control of DC Motor

*Timothy Onyechokwa, Adegboye B. A. & A.S. Mohammed

¹Electrical Electronic Engineering Department, Federal University of Technology, PMB 65 Minna Niger State, Nigeria

*Corresponding author email: chekwason@yahoo.com, +2348033035354

ABSTRACT

DC motors have long been use as a primary means of electrical traction. It has find wide area of applications ranging from industrial applications to basic home appliances. In most recent DC motor applications, there is need for precise speed control to give the desired performance. Thus, this paper presents a method for speed control of DC motor using adaptive fuzzy-PID controller algorithm. An adaptive fuzzy-PID controller was modelled and simulated using MATLAB control toolbox. The performance of the proposed model was measured using parameters such as rise time, peak overshoot, and settling time. Obtained results show the advantage of a combined fuzzy-PID over classical PI, PD, and PID controller.

Keywords: *DC Motor; Fuzzy-PID; Fuzzy Logic Controller (FLC); PID Controller.*

1 INTRODUCTION

DC motors have long been the primary means of electrical traction. Direct current (DC) motors have been widely used in many industrial applications such as electric vehicles, electric cranes and steel rolling mills due to precise, wide, simple and continuous control characteristics. The development of high-performance motor drives is very important in industrial as well as in other application.

The development of high-performance motor drives is very important in industrial as well as other general purpose applications such as steel rolling mills, electric trains and robotics. Generally, a high-performance motor drive system must have good dynamic speed command tracking and load regulating response to perform task. DC drives, because of their simplicity, ease of application, high reliabilities, flexibilities and favourable cost have long been a backbone of industrial applications, robot manipulators and home appliances where speed and position control of motor are required (Bansal Umesh Kumar, 2013).

There are mainly two types of dc motors used in industry. The first one is the conventional dc motor where the flux is produced by the current through the field coil of the stationary pole structure. The second type is the brushless dc motor where the permanent magnet provides the necessary air gap flux instead of the wire-wound field poles. BLDC motor is conventionally defined as a permanent magnet synchronous motor with a trapezoidal Back EMF waveform shape. As the name implies, BLDC motors do not use brushes for commutation; instead, they are electronically commutated. Recently, high performance BLDC motor drives are widely used for variable speed drive systems of the industrial applications and electric vehicles (Kandiban & Arulmozhiyal, 2012).

DC drives are less complex with a single power conversion from AC to DC. Again, the speed torque characteristics of DC motors are much more superior to that of AC motors. A DC motors provide excellent control of speed for acceleration and deceleration. DC drives are normally less expensive for most horsepower ratings. They have long tradition of use as adjustable speed machines and a wide range of options have evolved for this purpose. In these applications, the motor should be precisely controlled to give the desired performance. The controllers of the speed that are conceived for goal to control the speed of DC motor to execute one variety of tasks, is of several conventional and numeric controller types, the controllers can be: proportional integral (PI), proportional integral derivative (PID) Fuzzy Logic Controller (FLC) or the combination between them: Fuzzy-Neural Networks, Fuzzy Genetic Algorithm, Fuzzy-Ants Colony, Fuzzy-Swarm. The proportional – integral – derivative (PID) controller operates the majority of the control system in the world. It has been reported that more than 95% of the controllers in the industrial process control applications are of PID type as no other controller match the simplicity, clear functionality, applicability and ease of use offered by the PID controller. PID controllers provide robust and reliable performance for most systems if the PID parameters are tuned properly (Bansal Umesh Kumar, 2013).

The major problems in applying a conventional control algorithm (PI, PD, PID) in a speed controller are the effects of non-linearity in a DC motor. The nonlinear characteristics of a DC motor such as saturation and friction could degrade the performance of conventional controllers (Chalmers, 1992; Johnson & Lorenz, 1992). Generally, an accurate nonlinear model of an actual DC motor is difficult to find and parameter obtained from systems identification may be only approximated values. The field of Fuzzy control has been making rapid progress in recent years.

Fuzzy logic control (FLC) is one of the most successful applications of fuzzy set theory, introduced by L.A Zadeh in 1973 and applied (Mamdani 1974) in an attempt to control system that are structurally difficult to model. Since then, FLC has been an extremely active and fruitful research area with many industrial applications reported (Li & Tso, 2000). In the last three decades, FLC has evolved as an alternative or complementary to the conventional control strategies in various engineering areas. Fuzzy control theory usually provides non-linear controllers that are capable of performing different complex non-linear control action, even for uncertain nonlinear Systems. Unlike conventional control, designing a FLC does not require precise knowledge of the system model such as the poles and zeroes of the system

It is well known that the mathematical model is very crucial for a control system design. For a DC motor, there are many models to represent the machine behaviour with a good accuracy. However, the parameters of the model are also important because the mathematical model cannot provide a correct behaviour without correct parameters in the model. Fuzzy rule-based models are easy to comprehend because it uses linguistic terms and the structure of if-then rules. In this study, the characteristics of PID controllers and fuzzy logic controllers and their application to an industrial DC motor at steps including structure, characteristics and the mathematical model and simulation of stability response for speed control of DC motor will be discussed. The study involves the modelling and simulation studies used to demonstrate the basic theoretical feasibility of the system used by fuzzy and PID control to achieve better response by less noise and less overshoot.

Various researchers have explored this area. The study by Al-Maliki & Iqbal, (2018) addressed a PID controller tuning for sensor-less speed control of DC motor based on FLC. A Proportional-Integral-Derivative (PID) type speed controller with Kalman Filter (KF) estimator was used and Integral of Absolute Error (IAE), peak overshoot and settling time were chosen as performance indices. The work examined the sensor-less speed control of a DC motor in a noisy environment simulating actual working conditions. The Kalman Filter used in the work can only be used in linear state transitions. Aside the noise that was reduced by KF, the PID controller gains tuned via MATLAB resulted in large peak overshoot and IAE with a relatively long settling time. When compared, a Fuzzy Logic Controller (FLC) based PID (FLC-PID) tuned using genetic algorithms (GA), reduced the settling times by 75.98%, the IAE and the maximum overshoot by 56.2% and 97.89% respectively. Compared to the conventional PID without KF, the FLC-PID radically improved the reference command speed tracking and sudden load changes disturbance rejection for the dc motor model. Therefore, this work has a great application in a linear transition.

A comparative study of fuzzy and PID controllers as regards to the DC Motor's speed control was done by Mohammed & Ali, (2014). PID and Fuzzy controllers were tested and compared using MATLAB/SIMULINK program for speed under load and no-load conditions. The work is an extensive study that revealed the differences between the fuzzy logic controller and the PID controller. Nonetheless, the mathematical model of DC motor used was based on trial and error method. The results showed that the overshoot, settling time and control performance had been improved greatly by using Fuzzy Logic controller making it to have a better performance than the PID controller.

Rajkumar, Ranjhitha, Pradeep, Mohammad Fasil, & Kumar, (2017) proposed a fuzzy logic controller (FLC) for speed control of a BLDC motor. The fuzzy logic technique used was to estimate the speed of the brushless DC motor (BLDC) motor under variable and fixed condition of the back-EMF. More so, the speed was controlled using Proportional-Integral (PID) Controller with the help of fuzzy based estimation of the speed and rotor position. The DC-AC conversion with current resonance was achieved with a resonant inverter. The inverter was used to regulate voltage and fed into the BLDC motor through a motor driver circuit. This was then simulated on MATLAB/Simulink. Even though, fuzzy based system is always associated with tuning issues, the work provided a system for the speed control of a BLDC fed inverter with the electric vehicle. It has better noise rejection capabilities and is more robust. The simulation results showed variation of different parameters of BLDC motor including total output electrical torque, rotor speed, rotor angle, three phase stator currents, and three phase back EMF's with respect to time.

Sahputro, Fadilah, Wicaksono, & Yusivar, (2017) described the design and implementation of adaptive PID control strategy for controlling the angular velocity of DC motor. The adaptive PID controller is designed to calculate the control parameters which are timed adaptively to give control performances even if the parameters of DC motors are changed. To achieve effective performance in matching the output speed with the input speed, proportional, integral and derivative (PID) controller is commonly used for DC motor speed control. The determination of PID constants depends on the characteristics of the DC motor that are being used, which is different in each motor and sometimes change throughout the time. To find the optimal PID constants, most people use trial and error which requires a lot of time. The paper furthered shows how the PID constants can be achieved even when parameters changes. In the simulation result, controller constants can be adjusted automatically while the parameters of DC motor changed and send control signal to the DC motor. The experiment also proves the same result as in simulation. The algorithm can adjust DC motor parameters and update the controller constants.

Achanta, (2017), emphasized on the speed of DC motor which plays a major role in control industries. Traditional tuning techniques for classical PID controller suffer from many disadvantages like non-customized performance measure and insufficient process information. In this paper, the author used the Jaya optimization algorithm (JOA) for better performance in speed control and time response of the system. Experimental results are presented to study the performance of JOA based PID controller in comparison with particle swarm optimization (PSO) based PID controller. The performance of the PID controller is based on the tuning of parameters, which are proportional gain (k_p), integral gain (k_i), derivative gain (k_d). The proportional gain (k_p) will reduce the rise time and also reduce the steady state error. An integral gain (k_i) will reduce or eliminate the steady state error but it makes transient response worse. A derivative gain (k_d) will have the effect of increasing stability of system.

Sharma & Palwalia, (2018) presented simulation of a complete system of adaptive fuzzy PID controller along with DC motor model using MATLAB/SIMULINK. The writer showed comparison of conventional PID with adaptive fuzzy PID controller; hence, the results shows adaptive fuzzy tuned PID controller provides better dynamic behaviour of DC motor with low rise time, low settling time, minimum overshoot and low steady state error in speed. PID controllers are commonly exploited in conventional speed control loops. Some of the shortcomings of conventional PID controllers are undesirable overshoot and stagnant response due to sudden change in load torque and sensitivity to controller gains. To achieve better results an adaptive fuzzy logic based PID controller designed is thus proposed herewith.

2 METHODOLOGY

The methodology to be adopted in the proposed study involves the modelling and simulation of fuzzy PID controller for DC motor speed control.

2.1 MODELLING OF DC MOTOR

For modelling, the DC motor analysis becomes essential. DC motors are most suitable for wide range speed control and are there for many adjustable speed drives. Intentional speed variation carried out manually or automatically to control the speed of DC motors.

$$\frac{\alpha(V_a - I_a R_a)}{\Phi} = \frac{(V_a - I_a R_a)}{K_a \Phi} \quad (1)$$

Where Φ = Field flux per pole

$$K_a = \frac{PZ}{2\pi a} \quad (2)$$

Where P = Number of poles, Z = Total number of armature conductor, a = Number of parallel path.

From equation (1), it is clear that DC motors have basically three methods of speed control. They are: variation of resistance in armature circuit, variation of field flux, and variation of armature terminal voltage. The armature voltage equation is given by:

$$V_a = E_b + I_a R_a + L_a \left(\frac{dI_a}{dt} \right) \quad (3)$$

The torque balance equation which varies with the armature current is given by

$$T_m = K I_a \quad (4)$$

K is the torque Constant, where back emf of the motor is given as

$$E_b = K_b \omega \quad (5)$$

K_b is the back emf constant, thus, taking the Laplace transform of (3) gives

$$V_a(s) = (R_a + L_a s) I_a(s) + E_b(s) \quad (6)$$

$$V_a(s) = (R_a + L_a s) I_a(s) + K_b s \quad (7)$$

Now, taking equation (4) into consideration, the equation of torque can also be written as:

$$T_m = J \frac{d\omega}{dt} + B\omega \quad (8)$$

And taking the Laplace transform of (8) gives

$$T_m(s) = sJ\omega(s) + B\omega(s) \quad (9)$$

$$\frac{\omega(s)}{T_m(s)} = \frac{1}{Js + B} \quad (10)$$

Using (7) and (10), the transfer function of the model is obtained as:

$$\frac{\omega(s)}{V_a(s)} = \frac{K}{L_a J s^2 + (BL_a + R_a J)s + R_a B + KK_b} \quad (20)$$

The parameters of the DC motor under consideration are given in Table 1. A 3hp, 2400V, 1500 rpm separately excited DC motor will be considered in this study.

TABLE 1: PARAMETERS OF THE DESIGN

Description of the Parameter	Parameter Value
Armature resistance, R_a	0.5 Ω
Armature inductance, L_a	0.02H
Armature voltage, V_a	200V
Mechanical inertia, J	0.1 Kg.m ²
Friction coefficient, B	0.008 N.m/rad/sec
Back emf constant, K_b	1.25 V/rad/sec
Rated speed	1500 r.p.m
Motor torque constant, K	1 N.m/A

From the parameters in Table 1, the model for the speed control of the DC motor is obtained as:

$$\frac{\omega(s)}{V_a(s)} = \frac{1}{0.002s^2 + 0.0502s + 1.254} \quad (21)$$

2.2 PID CONTROLLER DESIGN

In a PID system, the best features of each of PI and PD are utilized. The system function of a PID system is given as in (22).

$$G_c(s) = K_p + K_D s + \frac{K_i}{s} \quad (22)$$

PID controllers have advantage of simple structure, robust performance, and easy to understand. The model in (22) can be represented in cascaded format as:

$$G_c(s) = (1 + K_{D1})(K_{P2} + \frac{K_{I2}}{s}) \quad (23)$$

Equations (22) and (23) are related by:

$$K_p = K_{P2} + K_{D1}K_{I2}$$

$$K_D = K_{D1}K_{P2} \quad (24)$$

$$K_I = K_{I2}$$

Where K_p, K_D, K_I are the proportional, differential and integral gain respectively. The cascade approach allows modular design and tuning of the PID system. Taking the Laplace transform of the armature voltage V_a , and applying the PID model of (23) on the speed control model of (21), the speed control model becomes:

$$\omega(s) = \frac{200[(K_{P2} + K_{D1}K_{P2})s + K_{I2} + K_{D1}K_{I2}]}{0.002s^4 + 0.0502s^3 + 1.254s^2} \quad (25)$$

2.3 ADAPTIVE FUZZY PID CONTROLLER

The heart of a fuzzy system is a knowledge base

consisting of the so-called If-Then rules. A fuzzy If-Then statement may have some words characterized by continuous membership functions. After defining the fuzzy sets and assigning their membership functions, rules must be written to describe the action to be taken for each combination of control variables. These rules will relate the input variables to the output variable using If-Then statements which allow decisions to be made. In this paper, the simulation of motor speed control with adaptive fuzzy PID controller was carried out using MATLAB/SIMULINK. Parallel structure of fuzzy PI and PD controllers will be used as speed control circuit. The switching action takes place according to the error signal. The output of the controller was fed to a controlled voltage source which feeds the inverter. Fuzzy logic and control toolboxes in MATLAB were used for the simulation.

Fuzzy logic involves fuzzification and defuzzification; The success of a fuzzy logic system depends on how good this stage is conducted. The first step in designing a fuzzy controller is to decide which state variables represent the system dynamic performance and this must be taken as an input signal to the controller. Fuzzy logic uses linguistic variables instead of numerical variables. The process of converting a numerical variable (real number or crisp variables) into linguistic variables (fuzzy number) is called fuzzification. Defuzzification is the reverse process. This is achieved with different types of fuzzifiers. There are generally three types of fuzzifiers which are used for the fuzzification process; they are singleton fuzzifier, Gaussian fuzzifier and trapezoidal or triangular fuzzifier. Fuzzification converts input data to degree of membership function. In this process, data is matched with condition of rules. Thus a degree of membership function is developed.

The speed error e and the change in speed error ce serve as input to the fuzzy logic system. The membership functions associated to the control variables have been chosen with Gaussian shapes. The universe of discourse of all the input and output variables were established and a suitable scaling factors will be chosen to bring the input and output variables to this universe of discourse. Each universe of discourse is divided into seven overlapping fuzzy sets: NL (Negative Large), NM (Negative Medium), NS (Negative Small), ZE (Zero), PS (Positive Small), PM (positive Medium), and PL (Positive Large).

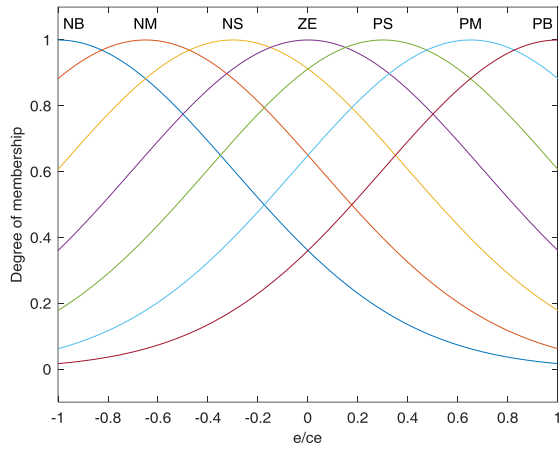


Figure 1: Gaussian membership function for inputs ce and e

Each fuzzy variable is a member of the subsets with a degree of membership μ varying between 0 (non-member) and 1 (full-member). All the membership functions have asymmetrical shape with more crowding near the origin (steady state). This permits higher precision at steady state. The reverse of fuzzification is called defuzzification. It converts resulting fuzzy set into a number that is sent to the system and this number is actually the control signal. There are many defuzzification methods but the most commonly methods are as follow; centre of gravity (COG), bisector of area (BOA) and means of maximum (MOM).

In adaptive fuzzy PID, the initial PID gains are continuously updated according to the output of the fuzzy logic controller which takes the speed error and the change in speed error as input. The final tuned parameter is obtained by multiplying the initial gain with the output from the fuzzy logic controller. The block diagram of the Fuzzy-PID is as shown in Figure 2.

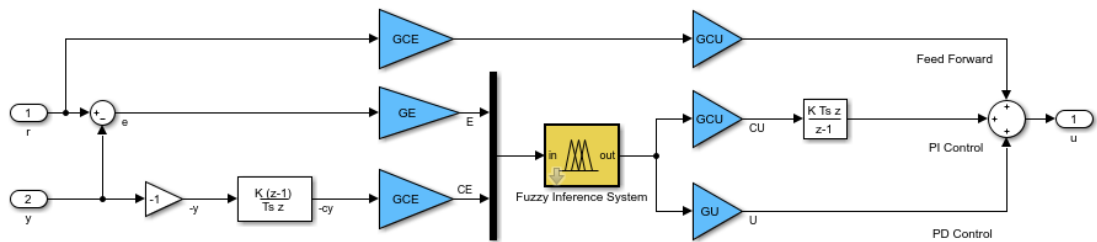


Figure 2: Block diagram of the Fuzzy-PID system

3 RESULTS AND DISCUSSION

The proposed model was simulated using MATLAB control and fuzzy logic toolbox. Obtained results are thus presented in this section. Results presented in this paper include that of traditional PID controller and fuzzy PID controller. Our future work will compare the performance of adaptive fuzzy-PID to the two aforementioned model. The obtained response for traditional PID is as shown in Figure 3, while the response of the fuzzy-PID is as shown in Figure 4.

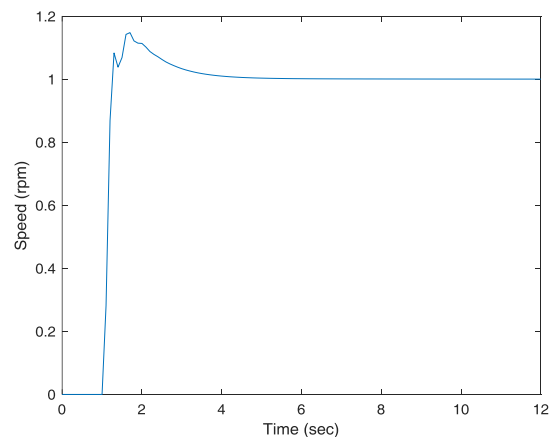


Figure 3: output response of traditional PID

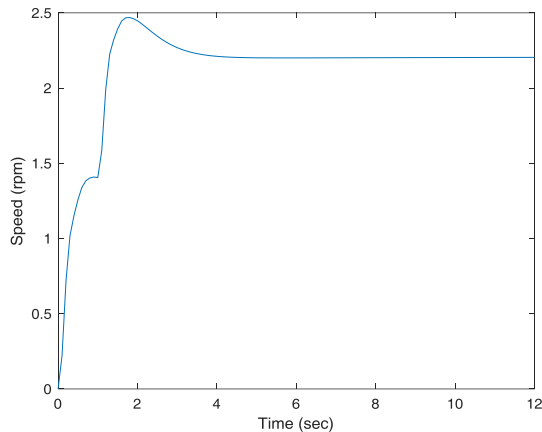


Figure 4: Output response of the fuzzy-PID controller

Though the Fuzzy-PID approach has a longer rise time, it however outperforms the other approaches in terms of settling time and percentage overshoot. Obtained results are summarized in Table 2.

TABLE 2: SUMMARY OF SYSTEM PERFORMANCE

Evaluation Metrics	PI	PD	PID	Fuzzy-PID
Rise time (s)	0.46	0.21	0.28	1.10
Settling time (s)	5.29	3.38	3.49	3.20
Overshoot (%)	29.9	14.8	16.4	12.0

4 CONCLUSION

In this paper, an adaptive fuzzy-PID controller for DC motor speed control was presented. The model was simulated using MATLAB/Simulink. Adaptive fuzzy PID provides a continuous change in the PID gains according to speed error and change in speed error. Obtained results showed that the fuzzy-PID has a faster settling time than the traditional PID though with higher overshoot. Future work will explore means of reducing the rise time while maintaining faster settling time and reduced percentage overshoot.

ACKNOWLEDGEMENTS

The authors will like to acknowledge the department of Electrical Electronics Engineering, Federal University of Technology, Minna, Nigeria

REFERENCES

Achanta, R. K. (2017). DC Motor Speed Control using PID Controller Tuned by Jaya Optimization Algorithm University College of Engineering

Kakinada. 2017 IEEE International Conference on Power, Control, Signals and Instrumentation Engineering (ICPCSI), 983–987.

Al-Maliki, A. Y., & Iqbal, K. (2018). FLC-based PID controller tuning for sensorless speed control of DC motor. *Proceedings of the IEEE International Conference on Industrial Technology, 2018–Febru*, 169–174.

<https://doi.org/10.1109/ICIT.2018.8352171>

Bansal Umesh Kumar, N. R. (2013). Speed Control of DC Motor Using Fuzzy PID Control. *Advance in Electronic and Electric Engineering*, 1209–1220.

Chalmers, B. (1992). Influence of saturation in brushless permanent magnet drives. In *IEE proc. B, Elect. Power Appl.*

Johnson, C. T., & Lorenz, R. D. (1992). Experimental identification of friction and its compensation in precise, position controlled mechanism. *IEEE Trans. Ind. Applicant*, 28(6).

Kandiban, R., & Arulmozhiyal, R. (2012). Design of Adaptive Fuzzy PID Controller for Speed control of BLDC Motor. *International Journal of Soft Computing and Engineering (IJSCE)*, 2(1), 2231–2307.

Li, H. X., & Tso, S. K. (2000). Quantitative design and analysis of Fuzzy ProportionalIntegral-Derivative Control- aStep towards Auto tuning. *International Journal of System Science*, 31(5), 545–553.

Mohammed, O. O. A., & Ali, A. T. (2014). Comparative Study of PID and Fuzzy Controllers for Speed Control of DC Motor. *International Journal of Innovative Research in Science, Engineering and Technology*, 3(9), 16104–16110.

Rajkumar, M. V., Ranjhitha, G., Pradeep, M., Mohammad Fasil, P., & Kumar, R. S. (2017). Fuzzy based Speed Control of Brushless DC Motor fed Electric Vehicle. *International Journal of Innovative Studies in Sciences and Engineering Technology (IJISSET)*, 3(3), 12–17.

Sahputro, S. D., Fadilah, F., Wicaksono, N. A., & Yusivar, F. (2017). Design and Implementation of Adaptive PID Controller for Speed Control of DC Motor, (1), 179–183.

Sharma, K., & Palwalia, D. K. (2017). A modified PID control with adaptive fuzzy controller applied to DC motor. In *IEEE, International conference on Information, Communication, Instrumentation and Control (ICICIC-2017)* (pp. 1–6). IEEE.



Implementation of Remote Patient Monitoring System using GSM/GPS Technology

*Umar Abdullahi, Salihu Aliyu Oladimeji, Waheed Moses Audu, Muslim Saidu, Manasseh Wayo
Telecommunication Engineering Department, Federal University of Technology, PMB 65 Minna Niger
State, Nigeria

*Corresponding author email: umarabdullahi@futminna.edu.ng,+2348035328592

ABSTRACT

Remote patient monitoring (RPM) is a technology that enables the continuous monitoring of patients from remote locations. This usually involves the monitoring of patient's vital signs (e.g., heart rate, blood pressure, temperature etc.) and other health information (e.g. disease signs and symptoms) from a remote location using RPM devices. This data is collected by monitoring devices, placed on the patient's body or in the patient's residence. This data is transferred electronically to a remote location where it is stored, and analyzed by care givers in order to detect early disease onset, improvements or deterioration in patient conditions. This work proposes an implementation of Remote Patient Monitoring System using GSM/GPS Technology. The system monitors heart rate and body temperature of patient and display information on an LCD Display. The measured data and GPS location coordinates is continuously uploaded to a remote database on a web server. An SMS alert is sent to a preregistered phone number when the measured values fall below or go above the set threshold. The system was tested and worked as expected.

Keywords: GSM, GPS modules; Heart Rate, RPM; Temperature sensor

1 INTRODUCTION

Remote patient monitoring (RPM) is a technology that enables the continuous monitoring of patients from remote locations. This usually involves the monitoring of patient's vital signs (e.g., heart rate, blood pressure, temperature etc.) and other health information (e.g. disease signs and symptoms) from a remote location using RPM devices. This data is collected by monitoring devices, placed on the patient's body or in the patient's residence. This data is transferred electronically to a remote location where it is stored, and analyzed by care givers in order to detect early disease onset, improvements or deterioration in patient conditions. Using remote monitoring allows the patient to send in vital signs on a regular basis to a health care manager without the need for hospital visitation. One of the most common uses of RPM is in chronic disease management. There is significant confirmation that RPM can enhance healthcare and wellbeing, and also reduce costs from emergency hospital visits, unnecessary hospital admissions and length of stays (Priyanka, Tripathi, & Kitipawang, 2015). The differing applications of RPM lead to different architectural designs of RPM devices. On the other hand, most RPM enabled devices take after a general architectural design that consists of four functional sub units.

- Biomedical sensors that measure patients' vital signs.
- Local storage systems at the patient's site that interfaces between sensors and the remote data storage systems.
- Remote data storage system, to store data sent from sensors and other relevant sources.

- Diagnostic software that trigger intervention alerts and develop treatment recommendations based on the analysis of the collected data.

Depending upon the ailment and the vital signs that are monitored, diverse blends of measuring devices and software may be deployed (Malasingle, Ramzan, & Dahal, 2017)

Patient vitals, for example, heart rate, temperature, and other patient health information are gathered by sensors on measuring devices. Some examples of these devices include: pulse oximeter, and glucometer etc. The data gathered by these measuring devices is transmitted to health care providers or other concerned third party by means of communication devices and networks. This information is assessed for potential issues by a health care professional or by means of clinical decision support systems, and care givers and other concerned parties are quickly alerted if a problem is detected (Saleem, Muhammad, & Martine-Emrique, 2010). The major goals of RPM are to improve access to health care and reduce health care delivery costs. These goals are facilitated by delivering health care straight to the home (Pantelopoulos & Bourbakis, 2010). Monitoring of patient vitals is one of the most precise methods for detecting early disease onset, improvements, and deterioration (Patil & Khadelwal, 2013). Currently, patient monitoring is carried out manually and can be a costly process when continuous monitoring is required. Therefore, the need to automate this process and enable continuous monitoring of patients cannot be overemphasized. In this work, we hope to tackle this problem by developing a system that will enable the continuous monitoring of patients' heart rate and body temperature from any location.

The developed system will be able to provide the following services:

- To continuously measure heart rate and body temperature of patients.
- To upload measured data to a remote database server.
- To enable device and patient location tracking by acquiring GPS coordinates and sending to remote server.
- To send SMS alerts to care giver's phone when an anomaly is detected in the measured data.

The scope of this work includes the design of an RPM system equipped with temperature and heart rate measuring devices, a GPS receiver, and a GSM/GPRS module. This work leveraged on the fact that substantial research and development has been done in the area of biomedical sensors design, GPS, and GSM/GPRS. Therefore, our main focus in this project was the integration of the component hardware modules and the development of the software required to implement the system functionality specified.

2 LITERATURE REVIEW

In order to gain sufficient understanding and information about RPM device design and development, and other related information relevant to this work, it is necessary to review existing projects, research papers and the base technologies that support or have a relationship with this subject area. There are several academic projects and research papers about Remote Patient Monitoring devices, but we have chosen to review the most notable literatures that have a direct relationship or are very similar to this project work.

Remote Patient Monitoring projects and papers are based on the one fundamental problem of "building a device that will efficiently and effectively enable remote and continuous monitoring of vital signs from patients". Therefore, these projects often include an extensive study of the problem domain and a system specification and design that is expected to serve as an optimal solution.

A Heart beat monitoring and alert system using GSM Technology was proposed in (Ufoaroah, Oranugo, & Uchechuku, 2015). The paper showed the development of a system that was able to measure heart rate and send SMS alerts to a medical expert only when a set heart rate threshold value was exceeded. The system was made up of the heart rate measuring device, an LCD display, Arduino Uno board for data processing and signal conditioning, and a Quectel GSM Modem for sending alerts via SMS. One of the limitations of this system was that the data measured was not stored either locally or remotely for record and trend analysis but only served as an alert system.

An Implementation of a GSM Based Heart rate and Temperature Monitoring system was proposed by (Subhani, Sateesh, Chaitanya, & Prakash, 2013). The major components of the system were a Heart rate

monitor circuit, LM35 temperature sensor, an AT89S52 Microcontroller and a GSM Modem. The system was able to measure temperature and heart rate and send the data via SMS to a predefined phone number programmed in the system.

(Krishna, Rokibul, & Maruf, 2014) developed a portable GSM-Based Patient Monitoring System. The system was able to measure four vital signs from a patient and send the data to the health care manager's phone via SMS. Four vital signs measuring devices were used, and the system could measure heart rate, blood pressure, temperature, and blood glucose level. The system used an ARM7 Microcontroller for data processing, signal conditioning and storage, and a SIMCOM SIM300 GSM modem for sending the measured data via SMS. One of their main targets was to build a low cost system which, if adopted, would be able to improve access to health care especially for the deprived masses. However, the system does not have GPS tracking system and cannot provide World Wide Web service.

A GSM Based Patient Monitoring System using biomedical sensors was proposed by (Atiya & Madhuri, 2016). The main theme of the paper is to continuously monitor the patient health parameters.

2.1 GSM

GSM which stands for Global System for Mobile Communications is a digital mobile telephony system that was developed by the European Telecommunications Standards Institute (ETSI). It is the most widely mobile communications system in the world. GSM uses a variation of time division multiple access (TDMA) and cellular technology to provide high capacity and extensive coverage. GSM digitizes and compresses data, then sends it down a channel with two other streams of user data, each in its own time slot. GSM operates in the 900 MHz and 1800 MHz frequency band (Haq, Rahman, Ali, & Faisal, 2017). Some of the services offered by GSM include DTMF, Voicemail, Short Messaging Service (SMS) etc.

2.2 GPRS

The General Packet Radio Service (GPRS) packet based data communication system for mobile devices that enables data to be sent and received across a mobile telephone network. GPRS is a packet switching network that is deployed on the existing circuit switched GSM network infrastructure. It enables services such as internet access for mobile devices connected to the GSM network (Haq, Rahman, Ali, & Faisal, 2017).

2.3 GPS

The Global Positioning System (GPS) is a space-based navigation system that provides location and time information anywhere on the Earth surface. The GPS

system was developed by the United States Government for the Military, although access to the system has been made available to civilians also. GPS generates specially coded satellite signals that are processed in a GPS receiver, enabling the receiver to compute position, velocity and time. Signals from four GPS satellites are used to compute positions in three dimensions and the time offset in the receiver clock. The GPS system consists of three segments namely:

- The Space Segment: This consists of Satellite constellations.
- The Control Segment: Ground Stations that monitor and control the GPS satellites.
- The User Segment: This consists of GPS receivers and the users.

3 DESIGN AND METHODOLOGY

In this section, the design process and methodology adopted in other to achieve the set goals for this work are stated and explained in detail. The design processes carried out here were mainly influenced by the literature reviewed in the previous section. Some of the system improvement recommendations gotten from the literature review were also taken into consideration in the system design process.

In the development of this system, the Modular Design approach was adopted. Modular Design is a system design approach that breaks down a system into smaller self-contained parts called modules. The modules have well defined interfaces and are reusable.

3.1 SYSTEM SOFTWARE ARCHITECTURE

The system's software was developed using Object Oriented Analysis and Design (OOAD) techniques. Shown below is the software architecture model, showing the software classes and object relationships. The system software architecture is shown in figure 1.

3.2 HARDWARE REQUIREMENT

The following hardware modules were used to achieve the desired system functionality:

- Arduino Mega2560
- SIMCOM SIM900A GSM/GPRS Module
- U-BLOX Neo-5M GPS Module
- Photoplethysmograph (Pulse Sensor device)
- LM35 Precision Centigrade Temperature Sensor

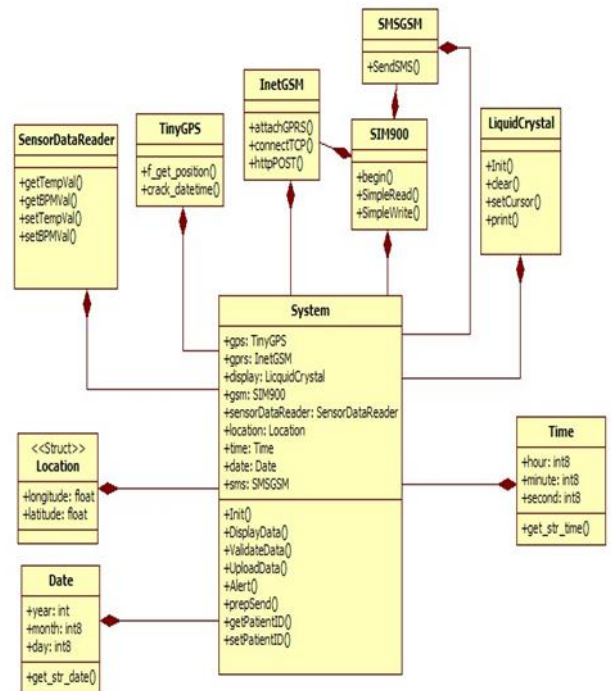


Figure 1: System Software Architecture

The Mega 2560 is a microcontroller board based on the ATmega2560. It has 54 digital input/output pins (of which 15 can be used as PWM outputs), 16 analog inputs, 4 UARTs (hardware serial ports), a 16 MHz crystal oscillator, a USB connection, a power jack, an ICSP header, and a reset button. It contains everything needed to support the microcontroller.

The Pulse Sensor Amped is a photoplethysmograph, which is a device that uses light to measure the changes in blood volume due to the heart movement. The signal produced by this device is used to determine heart rate.

The SIM900A is a complete Dual-band GSM/GPRS module which is designed specifically for small form factor and cost-effective solutions. Featuring an industry-standard interface, the SIM900A delivers GSM/GPRS 900/1800MHz performance for voice, SMS, Data, and Fax in a small form factor and with low power consumption. The LM35 temperature sensor is a precision integrated-circuit temperature device with an output voltage that is linearly-proportional to the Centigrade temperature. The LM35 sensor does not require any external calibration to provide typical accuracies of $\pm 1/4^{\circ}\text{C}$ at room temperature and $\pm 3/4^{\circ}\text{C}$ over a full -55°C to 150°C temperature range.

3.3 SYSTEM PROCESS FLOW

The system interfaces with the patients via the sensors, a sensor data reader object reads the data measured by the sensors and a sensor data analyzer object analyzes this data in order to validate the data and the data uploading system gets this data and uses the services provided by the

GPRS interface to upload this data to a remote server. The uploading system also acquires GPS coordinates from the GPS receiver device and uploads them to the server. The sensor data analyzer also calls an alert function whenever measured values go above or below some set thresholds. This alert functions sends an SMS message using the services provided by the GSM interface, to a preregistered phone number programmed in the system. The integrated system process flow is shown in the flowchart diagram of figure 2.

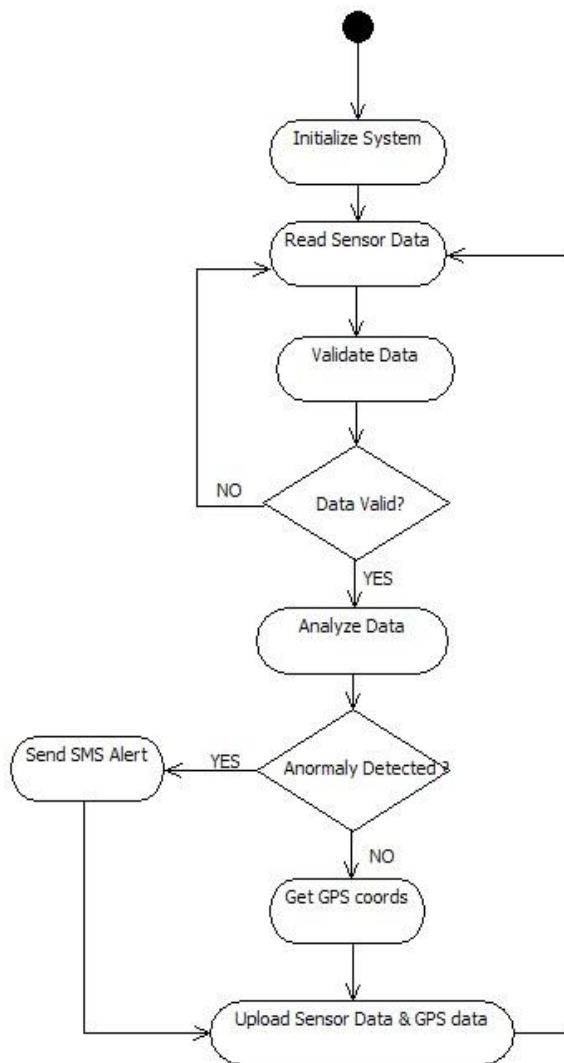


Figure 2: System Process Flow Chart

4 TEST AND RESULT DISCUSSION

This section shows the tests carried out and the respective results that were obtained. The developed system measures the heart rate and body temperature of a patient attached to it, and transmits this data to a remote server for storage in a database and for further processing.

This measured data is also monitored so that it does not go above or below some clinical set values for normal conditions. Incase these measured values go above or below this set thresholds, an SMS alert is sent to a preregistered detail (phone contact) programmed in the system. The system also displays all these measured data on an LCD display. Also all the functional units used in this project to achieve the desired functionality were individually tested and their respective results recorded. A general system integration test was carried out and all the results were recorded.

4.1 PULSE SENSOR TEST AND RESULT

The pulse sensor used in this work uses optical signals to detect the variations in blood volume that occur during a heartbeat cycle. This data is converted into an analog electrical signal and processed with a microcontroller in order to determine the heart rate. We were able to accomplish that in this work, and the following results of heart rate measurements were captured at intervals of 1s for an observation period of 10 seconds. The result obtained for the measurement of the heart rate at an interval of 1 second is shown in table 1. It can be observed that the heart beat rate varies at different time.

TABLE 1: HEART RATE VALUES MEASURED BY THE SENSOR

Interval	Measured Heart Rate
1	120
2	92
3	90
4	87
5	81
6	76
7	78
8	80
9	75
10	70

4.2 LM35 TEMPERATURE SENSOR TEST & RESULTS

The LM35 is a precision centigrade grade (Celsius) temperature sensor with an accuracy of ± 0.5 and linear scale of 10mV/oC rise in temperature. It was used in this

project as the device for measuring body temperature. The test for this device was carried out in two stages. In stage one, the devices was left to measure the environmental temperature and the values were read at intervals of one (1) second for an observation period of 10s and the results were recorded in a table. In the second stage, we placed the device in the armpit area of the body the values were read for the same interval and observation period and the results were also recorded to produce the table 2.

TABLE 2: TABLE OF MEASURED TEMPERATURE VALUES

Interval	Measured Environmental Temperature	Measured Body Temperature
1	31.25	33.69
2	30.76	34.18
3	31.25	35.15
4	30.76	34.67
5	31.25	35.64
6	31.25	36.13
7	31.25	36.13
8	30.76	35.64
9	30.76	36.13
10	31.25	36.13

4.3 GSM MODULE TEST & RESULTS

The GSM/GPRS module is used in this system for connecting the system to the internet, and for sending SMS alerts to a phone number programmed in the system. The GSM/GPRS module is controlled using AT commands, and it was tested for registration to the GSM network, and for connecting to the GPRS network and acquiring an IP address. The module was connected to the ArduinoMega2560 board via the UART Serial1 interface, and the responses to the commands sent to the module were displayed on the Arduino IDE's Serial monitor interface as shown in the images in figure 3.

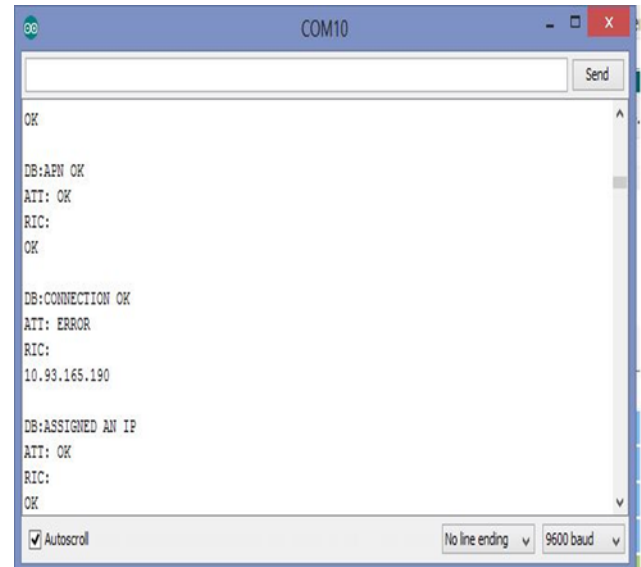


Figure 3: GSM/GPRS Configuration Results via Serial Monitor

4.4 GPS MODULE TEST & RESULTS

The GPS module in this device is a GPS receiver that outputs GPS information from satellites in NMEA format. The output information from this module is processed with the microcontroller in order to extract location information, date, and time. The following image in figure4 is a capture of the data output by the GPS Module in NMEA format from the Arduino IDE's Serial monitor interface.

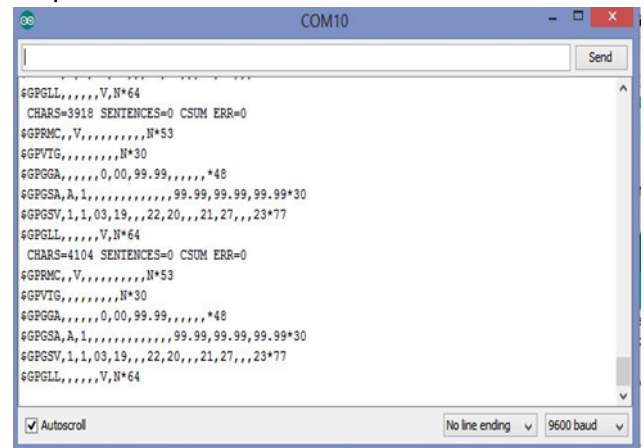


Figure 4: Received GPS information from module in NMEA format

4.5 SYSTEM INTEGRATION TEST & RESULTS

The components mentioned in the sub-sections above are connected together in order to achieve some desired set functionalities. In the final general system integration test, test cases were generated for all the functions the system was expected to carry out. The system monitors heart rate and body temperature of patient and display information on an LCD Display. The measured data and GPS location coordinates is continuously uploaded to a

remote database on a web server. An SMS alert is sent to a preregistered phone number when the measured values fall below or go above the set threshold.

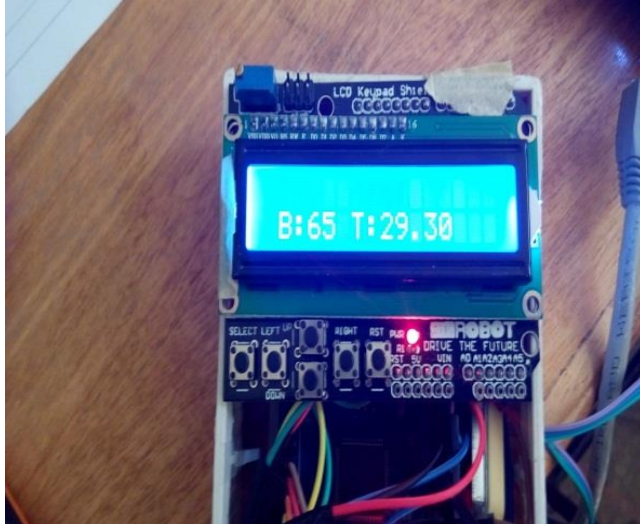


Figure 5: System Displaying Heart Rate and Environmental Temperature

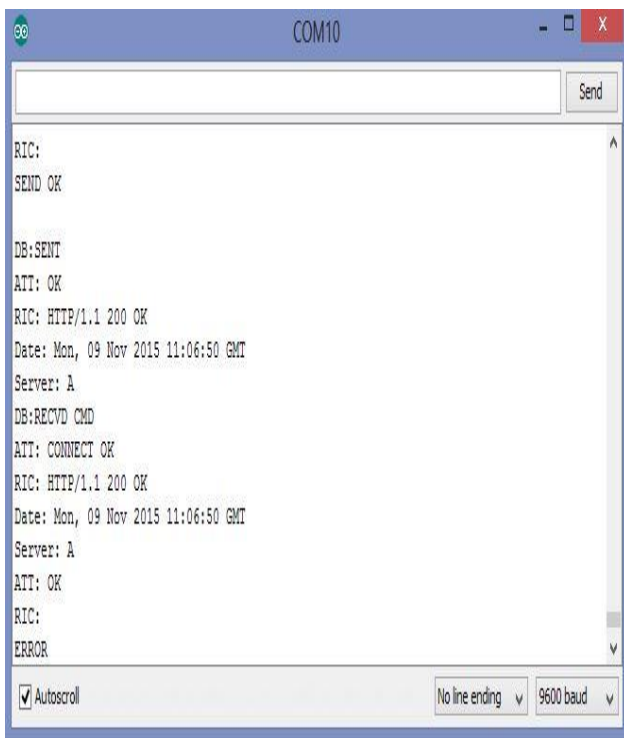


Figure 6: HTTP Response from server after data sent

+ Options		Date	Time	Heart_rate	Temperature	Latitude	Longitude
<input type="checkbox"/>	Edit Inline Edit Copy Delete	2015-11-09	11:04:13	112	30.27	0	1000
<input type="checkbox"/>	Edit Inline Edit Copy Delete	2015-11-09	11:04:34	82	30.27	0	1000
<input type="checkbox"/>	Edit Inline Edit Copy Delete	2015-11-09	11:04:54	77	30.27	0	1000
<input type="checkbox"/>	Edit Inline Edit Copy Delete	2015-11-09	11:05:08	103	29.79	0	1000
<input type="checkbox"/>	Edit Inline Edit Copy Delete	2015-11-09	11:05:30	135	29.79	0	1000
<input type="checkbox"/>	Edit Inline Edit Copy Delete	2015-11-09	11:05:54	88	29.79	0	1000
<input type="checkbox"/>	Edit Inline Edit Copy Delete	2015-11-09	11:06:16	102	30.27	0	1000
<input type="checkbox"/>	Edit Inline Edit Copy Delete	2015-11-09	11:06:50	177	30.27	0	1000

Figure 7: Snapshot of Data Received and Stored in database by Server

5 CONCLUSION

In this project we set out to develop a low cost remote patient monitoring system that could monitor the heart rate and body temperature of a patient. The results show that the system was able to monitor the body temperature and heart rate of a person. The result data was then uploaded to the server. The SMS Alert functionality also worked as expected. For future work, the system can be equipped with more sensors so that it can be able to monitor more vital signs. A web application can also be developed to display the plots of the data stored in the database for visualization and trend analysis. The GPS coordinates can also be connected to the Google Maps API and the location of the device & patient can be displayed on Google Maps.

REFERENCES

- Atiya, U. S., & Madhuri, S. K. (2016). GSM Based Patient Monitoring System using biomedical sensors . Internal Journal of Computer Engineering in Research Trends, 620-624.
- Haq, I. U., Rahman, Z. U., Ali, S., & Faisal, M. (2017). GSM Technology: Architecture, Security and Future Challenges. International of Science Engineering and Advance Technology.
- Krishna, C. R., Rokibul, H. R., & Maruf, H. S. (2014). Development of a portable GSM-Based Patient Monitoring System for Healthcare Applications. Global Journal of Computer Science and Technology.
- Malasingle, L., Ramzan, N., & Dahal, K. P. (2017). Remote Patient Monitoring: A Comprehensive Study. Journal of Ambeient Intelligence and Humanized Computing, 13-.
- Pantelopoulos, A., & Bourbakis, N. G. (2010). A Survey on Wearable Sensor-Based Systems for Healthcare Monitoring and Prognosis. IEEE Transactions on Systems, Man and Cybernetics-PARTC-Applications and Review (pp. 1-12). IEEE .



Patil, M. M., & Khadelwal, C. S. (2013). Implementation of Patient Monitoring System using GSM Technology. *International Journal of Electronics and Communications Engineering & Technology*, 18-24.

Priyanka, K., Tripathi, N. K., & Kitipawang, P. (2015). A real-time Monitoring system for remote cardiac patients using smart phone and wearable sensors. *International Journal of Telemedicine and Applications*.

Saleem, R. M., Muhammad, A., & Martine-Emrique, A. M. (2010). Remote Patient Monitoring and Healthcare Management using Multi-Agent Based Architecture. *Mexican international Conference on Artificial Intelligence*. Pachua, Mexico: IEEE.

Subhani, S. M., Sateesh, G. V., Chaitanya, C., & Prakash, B. G. (2013). Implementation of GSM Based Heart Rate and Temperature Monitoring System. *Research Journal of Engineering Sciences*, 43-45.

Ufoaroah, S. M., Oranugo, C. O., & Uchechuku, M. E. (2015). Heartbeat Monitoring and alert system using GSM Technology. *International Journal of Engineering Research and general sciences*, 20-34.



COMPARISON OF ADAPTIVE NEURO FUZZY INFERENCE SYSTEM AND SUPPORT VECTOR MACHINE FOR THE PREDICTION OF IMMUNOTHERAPY WARTS DISEASE

*Abisoye, B.O¹, Abisoye, O.A², Kehinde Lawal³, Ogunwede Emmanuel⁴

¹Computer Engineering Department, SEET, Federal University of Technology, PMB 65 Minna Niger State, Nigeria

²Computer Science Department, SICT, Federal University of Technology, PMB 65 Minna Niger State, Nigeria

³Computer Science Department, SICT, Federal University of Technology, PMB 65 Minna Niger State, Nigeria

⁴Computer Science Department, SICT, Federal University of Technology, PMB 65 Minna Niger State, Nigeria

*Corresponding author email: b.abisoye@futminna.edu.ng, +23463096254

ABSTRACT

Warts diseases are caused by virus within the Human Papilloma Virus Family (HPV). HPV are the cause of some types of cancer. Due to social stigma and the fact that warts never develop any symptoms until its full manifestation many patients seek medical treatment; The fast spread of warts disease due to skin-to-skin contact; Treatment are not cheap and simple, low number of treatment sessions and a lot of complications that do arise during the treatment seasons of warts disease; Lack of enough medical personals to treat warts disease cases and expert system to help the medical practitioners. To reduce the aforementioned problems, a machine learning approach of Adaptive Neuro Fuzzy Inference System (ANFIS) And Support Vector Machine (SVM) is proposed to predict Immunotherapy Warts Disease occurrence of before it gets out of hand. Performance comparison of ANFIS and SVM to the response of immunotherapy treatment of warts disease was conducted to get a good model. Selected features like age, type of warts, diameter of the warts, surface area of warts and the number of warts were considered as input variables. The accuracy of ANFIS and SVM models gave 69.697% and 96.29% respectively, the SVM model was considered to perform better than ANFIS in response to immunotherapy treatment of warts disease.

Keywords: immunotherapy, warts, ANFIS, Support Vector Machine, Prediction, Classification.

1 INTRODUCTION

Warts are the infection of the upper layer of the skin by a virus known as the human papilloma virus HPV. This type of virus attacks the outer layer of the skin that has a cut or has been damaged. When an individual come in contact with warts virus it takes months for the wart diseases to manifest in relation to the type of the skin warts, a popular saying goes by "people gets warts from other people with warts" the very common way people gets warts are direct skin-skin contact, hands shaking, objects like towels, typing on a keyboard, turning doorknobs, from shaving, biting fingernails (Gerend & Magloire, 2008). Human papilloma virus HPV attacks and infect the mucous membrane of the outer skin, study have uncovered that there are over 60 different types of HPV within the HPV family that causes warts each affecting a different and distinct location of the body for instance the type of HPV that cause warts on the inside of the mouth is different from

the HPV that cause warts on the genitals or rectal areas of the body (Khozeimeh, et al., 2017).

Treatment is the positive response to patient's biological, physical and mental status and condition over a session of pharmacological dosage prescription. Response to Treatment can be evaluated as in terms of a scale or with sequence of measurement as a score rating and be classified as responding or non-responding, its largely assume that a patients syndrome or symptoms should be modified after some set of treatment sessions and the rating scale also changed. In the case of non-response to treatment it may not mean that the drug administered is ineffective it can be because of some factors that can cut across the patient's commitment to treatment, changes in the illness/infection/disease, drug metabolism and drug to food interaction. There are other physical and environmental factors such as nursing and hospital care, clinical standard and charisma, and how severe the disease or disorder



appears to be. A patient may experience 'optimistic bias' which is a clinic sincere care to a patients. It's a fact that people tolerate success than failure, as a result of this scientific research have consider blind trial to drugs as a source of treatment (Gelernter & Uhde, 1991).

Immunotherapy is a treatment that stimulates the immune system of a patient to fight against disease and infections. This type of treatment is targeted to boost the body's natural abilities that will protect the body system from disease that are within or outside the body (Parham, 2014). Immunotherapy uses substance like biological response modifiers (BRMS) that is found in the body and also it can be manufactured from the laboratory in large quantities so as to treat disease. Due to the manufactures BRMS produced from the laboratory helps to predict the treatment of immunotherapy. The prediction identifies patients with similar clinical parameters and then applies a suitable treatment which helps to give prior knowledge whether the patient is a treatment respondent or not (Talmadge, Fidler, & Oldham, 2012). The treatment features can be biological or clinical parameters that serves as the baseline for evaluating the degree of patient's response. The history of patient's response to drugs can be a good medical record or information that can be used to predict the response of treatment of a patient across a period of time in consideration to the baseline parameter that is use in evaluating. The rate of response to treatment that be compared and measured using biological features or clinical parameters that could be obtain or gotten from a patient historic medical record before and after the disease infection or disorder. Collection of relevant data is of great significance to comparing and predicting the treatment of any patient in relation to any type of disease (Fayers & Machin, 2013).

Adaptive neuro fuzzy inference system (ANFIS) is a hybrid learning algorithm with the capabilities of supervised learning, supervised learning is a technique of machine learning which is use to achieve certain precise targeted knowledge from the collection of relevant data. This tool is very useful in modern medicine especially in medical diagnosis, it's also use in profit prediction, crime detection, risk assessment, construction and reengineering of business process. ANFIS uses a hybrid learning algorithms to analyze data in order to uncover the patterns in a very large collection of dataset. This technique is applied by big industries to reduce cost, enhance research outcomes and standards of research, increase product sales and the accuracy of predicting business situations (Taher, 2010).

Support Vector Machine (SVM) is a new and promising method for both linear and nonlinear classification data. SVM is basically the concept of decision planes which specify the boundaries for decision. The decision plane focus on separating a set of objects with different class Memberships, where SVM algorithms share the n dimensional space representation of data into two regions with the help of a hyper plane. The hyper plane usually maximizes the margin in between the two separate regions or classes. This margin is usually defined by the longest distance in between the two class's examples; the margin is computed based on the distance between the instance that is close to both classes to the margin that are referred to as supporting vectors.

2 STRENGTH AND WEAKNESSES OF EXISTING MODELS

A study Conducted on 180 patients, with plantar and common warts, who were divided into two groups, where 90 patients were treated using cryotherapy method with liquid nitrogen and 90 patients with immunotherapy method. A fuzzy logic rule-based system was proposed and implemented to predict the responses to the treatment method. It was observed that the prediction accuracy of immunotherapy and cryotherapy methods was 83.33% and 80.7%, respectively. According to the results obtained, the benefits of this expert system are multifold: assisting physicians in selecting the best treatment method, saving time for patients, reducing the treatment cost, and improving the quality of treatment (Khozeimeh, et al., 2017).

A paper presented a developed hybrid machine learning system using Support Vector Machines (SVM) and Adaptive Neuro-Fuzzy Inference System (ANFIS) alongside domain knowledge to provide a solution to the problem of prediction. The two-stage proposed Domain Knowledge based Fuzzy Information System (DKFIS) worked on improving the accuracy of ANFIS prediction model alone. The framework used a noisy dataset that is incomplete and oil saturation was predicted from four distinct well logs. Stage one of the research used SVM to classify the input vector into two distinct classes (i.e. Class 0 and 1) that was based on zero, near zero or non-zero level of oil saturation. The research further fine-tuned the classified results by applying expert knowledge that depended on the relationship that exist among prediction variables. Stage two used a designed ANFIS that predict a non-zero (Class 1) values of oil saturation. The experimental results reveals the intervention of expert knowledge with qualitative inference at every stage of the



work that has made the prediction feasible with realistic ranges. Performance analysis of the model of the prediction reveals that DKFIS based on SVM and ANFIS is a useful model for characterization of oil saturation level in a reservoir (Chaki, Routray, Mohanty, & Jenamani, 2015).

A study proposed a method using multi-SVM (Support Vector Machine) over 45 digital images that were obtained from MIT BMI unit which consists of warts, benign skin cancer and malignant skin cancer image and also normal skin images. These images were rendered to various pre-processing techniques such as RGB to LAB conversion, resizing and contrast enhancement. Then image segmentation using c-means and watershed algorithms were conducted on the individual images. They performed Feature extraction using Grey Level Co-occurrence Matrix (GLCM) and used Image Quality Assessment (IQA) methods to determine the texture which reveals the statistical parameters of each algorithm individually. These features were combined to obtain a better classification efficiency. The research work used different types of skin diseases that are commonly classified as Benign Skin Cancer, Malignant Skin Cancer and Warts using multi-SVM (Support Vector Machine). Support Vector Machines (SVM) as a machine learning model with associated algorithms was used to analyze images within the database and classify them. In terms of feature selection and extraction the diagnosis system involves two stages of process such as training and testing. Features values of the training data set are compared to the testing data set of each type. C-means algorithm provides better segmentation and feature extraction compared to watershed algorithm (Manerkar, et al., 2016)

A paper proposes a very relevant feature selection for image segmentation of skin lesion, a new unsupervised dictionary learning Theoretic Dictionary Learning (UITDL) method was proposed and it involves two stages in the first stage a feature dictionary was constructed using textual variation of images and are represented non-negative matrix factorization (NMF). The stage two performs feature dictionary selection from adaptive number of dictionary atoms. The result reveals that the model can provide accurate segmentation of skin lesions which can positively affect the diagnosis provided to patients (Polat & Güneş, 2007).

A study proposed Computerized image analysis model for dermoscopy that are of great benefit and interest, as significant information about lesion are provided. A

required image processing algorithms that describes mathematical the suspected regions used on diagnostic Computer-based system, the Computer-based technique was used in each of the following steps dermoscopic image pre-processing, segmentation, extraction and selection of peculiar features, and relegation of skin lesions. The paper also presents reasonable judgment to every methodology utilized and in addition to every corresponding results obtained (Pathan, Prabhu, & Siddalingaswamy, 2018).

R. S. Gound et al, January 2018 proposed a system that capture skin image through smart-phone camera. Preprocess them and segment each image. Feature extraction was performed on every skin lesion, in predicting application model Feature Extraction is important. The process of capturing, processing, indexing and retrieval of visual content of images is known as Feature extraction. After feature extraction, then feature classification which compares the image that have been captured to the stored training dataset with image processing techniques that judges using decision tree whether a skin is infected with a disease or not. The system gives medical advice when there is a disease through an android application.

3.0 Machine Learning Models

Machine learning, deals with the development of algorithms and software based on the machine's past experiences. A program capable of machine learning is able to perform a certain task or improve how it performs a task through previous runs and without any additional changes in the software. It involves the extraction of knowledge from data. Machine learning is split into three primary categories: supervised learning, unsupervised learning, and reinforcement learning. The machine learning models attempt to adopt principles based on how humans naturally learn and involve building systems that can 'think' and adapt themselves. One of the primary applications to healthcare for machine learning involves patient diagnosis and treatment. It is important not only in emergency medical situations, but also in general primary care and in specialized physicians as well. (Gupta, 2017)

3.1 Adaptive Neuro-Fuzzy Inference System

ANFIS combines the principle of fuzzy logic and neural networks, The advantage of fuzzy logic is smoothness and the advantage of neural network is adaptability which is built on the processing of partial truth ANFIS allows the translation of the final intelligent system into a set of expert if-then rules, the fuzzy logic model can be viewed as neural

network structure as the name implies is a network that consist of nodes and directional links, the input-output structural behavior is determined by collected values of parameters that can be modified through the inter connected nodes. The adaptive network system uses hybrid learning algorithm for parameter identification of Sugeno fuzzy inference systems. It combines the least-square method with back-propagation method for training fuzzy membership function to evaluate a given dataset. There are two learning phase of ANFIS, the forward phase identifies the least square estimate and the backward phase deals with error signals, The learning and training phase of the adaptive network determines the parameters of sufficiently fitted valued for training data. The main advantage of this hybrid model is that it converges faster because it reduces the space in search dimension of back propagation method in neural network, ANFIS are the fuzzy inference model put in framework of the adaptive system which serves in model building and validation of developed model to facilitate training and adaptation (Walia, Singh, & Sharma, 2015).

Fig 3: Basic architecture of ANFIS

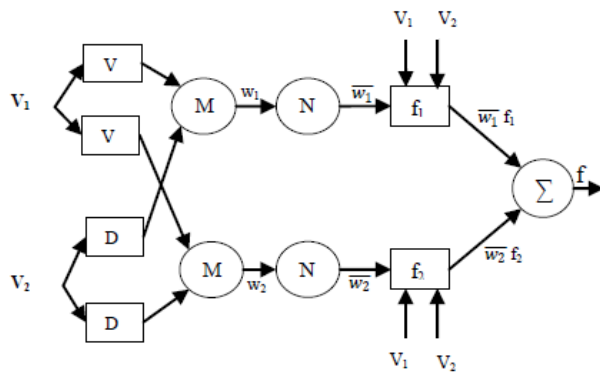


Fig 3: Basic architecture of ANFIS

3.2.3 Learning Algorithm of ANFIS

Neuro-adaptive learning techniques endow with a method for the fuzzy modeling procedure to learn information about a data set. It computes the membership function parameters that best allow the associated fuzzy inference system to track the given input/output data. In order to more efficiently cope with real world problems, the task of the learning algorithm for this architecture is to tune all the modifiable parameters, to formulate the ANFIS output match the training data. To improve the rate of convergence, the hybrid network can be trained by a hybrid learning algorithm combining least square method and gradient descent method can be used. The least squares

method can be used to identify the optimal values of the consequent parameter on the layer 4 with premise parameter fixed. The hybrid algorithm is composed of a forward pass (LSM) and a backward pass (GDM). Once the optimal consequent parameters are found, backward pass starts. In the backward pass, errors are propagated backward and the premise parameters corresponding to the fuzzy sets in the input domain updated by gradient descent method (Polat & Güneş, 2007). ANFIS uses a combination of least squares estimation and back-propagation for membership function parameter estimation. Two passes in the hybrid learning algorithm for ANFIS shown in table 1

Table 1: Passes of Hybrid learning algorithm

Table 1: Passes of Hybrid learning algorithm

	Forward pass	Backward pass
Premise parameters	Fixed	Gradient descent
Consequent parameters	Least square	Fixed
Signals	Node outputs	Error signals

The output error is used to adapt the premise parameters by means of a standard back-propagation algorithm to minimize the mean square error function defined by Eq. (12). It has been proven that this hybrid algorithm highly efficient in training the ANFIS (Gerend & Magloire, 2008)

$$E(\theta) = (z_i - a_i T \theta)^2 = e T e = m_i = 1 (z - A \theta) T z - A \theta \dots\dots\dots(1)$$

Where $e = z - A\theta$ is the error vector produced by a specific choice of θ . In Eq. (12) the squared error is minimized and is called the least squares estimator (LSE) (Taher, 2010). Therefore, the hybrid learning algorithm can be applied directly. More specifically, the error signals proliferate backward and the premise parameters are updated by Gradient Descent (GD) and node outputs go forward until layer 3 and the consequent parameters are identified by the Least Squares (LS) method. This hybrid learning is structured as by defining, linear and nonlinear parameters are illustrious each iteration (epoch) of GD update the nonlinear parameters, LS follows to identify the linear parameters.

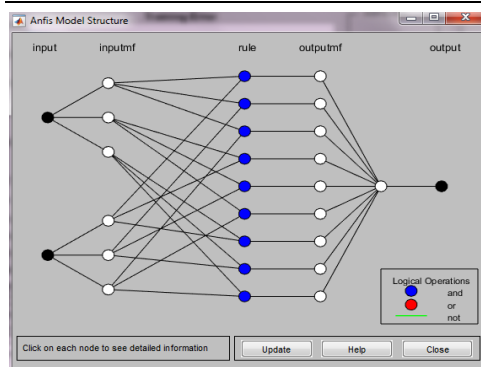


Fig. 3.4 ANFIS Structure

The structure of the model created for immunotherapy dataset was shown in Fig. 3.4 where MinMax normalized data was used consisting of two inputs, three (3) input membership functions at every input making a total of six (6) input membership functions, nine (9) generated fuzzy rules and nine corresponding output membership functions.

3.3 SUPPORT VECTOR MACHINE (SVM)

Support vector machine is a machine learning algorithm that generates support vectors. It is mainly used in activity that cuts across pattern recognition, predicting, classification and regression analysis. Severally, SVM has been proved and its application shows superior performance compared to prior developed methodologies such as neural networks and other conventional statistical applications (Polat & Güneş, 2007)

SVM application spans through a variety of fields such as computing, hydrology, medicine and environmental researches (Walia, Singh, & Sharma, 2015).

3.4 SVM CLASSIFICATION

Support vector machine classifies binary class problems without loss of generality but also classifies multiclass problems by adapting a unique algorithm, its primary goal is to separate the two classes by a function induced from available examples by a classifier called optimal separation hyperplane. This optimal classifier separates the data by finding the maximum margin among the two classes of data.

An SVM training algorithm builds a model that predicts whether a new data point mapped and fitted in a category or the other learned from historical examples. SVM models take a set of input data and predict for each instance the possible output which makes them non-probabilistic binary linear class. The operation of SVM algorithm is based on finding the hyperplane that gives the highest minimum distance to

the training examples. Therefore the optimal separating hyperplane maximizes the margin of the dataset.

3.5 Data Collection

The records of patients with warts disease were collected from the dermatology clinic of Ghaem Hospital from 2013 January to 2015 February in Mashhad. The datasets collected are for patients with plantar and common warts, that were referred to the Mashhad dermatology clinic. For the purpose of this research the records were obtained from the UCI dataset repository.

3.5.2 Data Description

The dataset consists of eight features for immunotherapy method. Table 3.1 presents these features. The attribute *Response to Treatment* is the target feature.

Table 3.1 Immunotherapy dataset description

Attribute	Description	Range
Sex	Male=1 Female=2	41 Man 49 Woman
Age	How old the patients	year 15–56
Time	The month taking for the administration of treatment	month 0–12
Number of warts disease	The number of warts an individual has on his/her body	1–19
Types of warts	Which type of warts is the individual suffering from	1– Common (47), 2– Plantar (22), 3– Both (21)
Surface area of warts	The length and width of warts on the skin	Discrete (mm ²) 6–900
Induration of diameter of warts	How deep the immunotherapy treatment administered	Discrete (mm) 5–70
Response to treatment (target)	Response to immunotherapy treatment of warts disease	0 for not treated 1 for treated

3.5 Data Normalization

Data normalization can provide a better modeling and avoid numerical problems. Several normalization algorithms have been developed that can be used to normalize datasets. These algorithms scale a given data in the same range of values for each input feature in order to minimize bias within the network for one feature to another. Data normalization also help to speed up training time by starting the training process for each feature within the same scale. There are many types of data normalization that can be used during modelling of systems.

3.5.1 Min-max Normalization

Min-max normalization algorithm is a linear scaling algorithm. It transforms the original input range into a new data range (typically 0-1). It is given as

$$Y_{old} = \frac{y_{old} - \min_1}{\max_1 - \min_1} (\max_2 - \min_2) + \min_2 \text{ equ. 4}$$

Where y_{old} is the old value, y_{new} is the new value, \min_1 and \max_1 are the minimum and maximum of the original data range, and \min_2 and \max_2 are the minimum and maximum of the new data range.

Since the min-max normalization is a linear transformation, it can preserve all relationships of the data values exactly.

3.5.2 Zscore Normalization

Zscore normalization algorithm converts an input variable data into zero mean and unit variance. The mean and standard deviation of the input data are calculated first. The algorithm is shown below

$$Y_{new} = \frac{y_{old} - \text{mean}}{\text{std}} \text{ equation 5}$$

Where y_{old} is the original value, y_{new} is the new value, and mean and std are the mean and standard deviation of the original data range, respectively.

3.6 NETWORK TRAINING

The preprocessed data where divided into two 70 percent for training which consist of 63 instances of data. The data served as input for training ANFIS and SVM models.

3.7 NETWORK TESTING

The data instances used for testing was 30 of the dataset respectively. 27 instance of immunotherapy dataset where used for testing the developed ANFIS and SVM models. The models where tested to ascertain the instances that where accurately predicted when compared to the target response to treatment.

Table 3.2: sample of data used

1	sex	age	Time	Number_of Type	Area	induration	Result_of Tr	
2	1	22	2.25	14	3	51	50	1
3	1	15	3	2	3	900	70	1
4	1	16	10.5	2	1	100	25	1
5	1	27	4.5	9	3	80	30	1
6	1	20	8	6	1	45	8	1
7	1	15	5	3	3	84	7	1
8	1	35	9.75	2	2	8	6	1
9	2	28	7.5	4	1	9	2	1
10	2	19	6	2	1	225	8	1
11	2	32	12	6	3	35	5	0
12	2	33	6.25	2	1	30	3	1
13	2	17	5.75	12	3	25	7	1
14	2	15	1.75	1	2	49	7	0
15	2	15	5.5	12	1	48	7	1
16	2	16	10	7	1	143	6	1
17	2	33	9.25	2	2	150	8	1
18	2	26	7.75	6	2	6	5	1
19	2	23	7.5	10	2	43	3	1
20	2	15	6.5	19	1	56	7	1

4.0 RESULTS

ANFIS model was developed for three different data processes namely; raw data, Minmax and Zscore normalized data. The following results where obtain

Table 4.1: ANFIS Confusion matrix for the raw data

TP = 11	FN = 2	P = 13
FP = 8	TN = 6	N = 14
		P + N = 27

The confusion metric in Table 4.1 reveals that eleven (11) instances out of 27 instances used for testing were predicted to be the positive instances that were correctly predicted while two (2) instances where the negative instances that were correctly predicted .

Table 4.2: ANFIS Confusion matrix for MinMax

TP = 19	FN = 0	P = 19
FP = 4	TN = 4	N = 8
		P + N = 27

The confusion metric in Table 4.2 reveals that nineteen (19) instances out of 27 instances used for testing were predicted to be the positive instances that were correctly predicted while no instances were predicted as negative instances.

Table 4.3: ANFIS Confusion matrix for Zscore

TP = 10	FN = 0	P = 10
FP = 12	TN = 5	N = 17
		P + N = 27

The confusion metric in Table 4.3 reveals that ten (10) instances out of 27 instances used for testing were predicted to be the positive instances that were correctly predicted while no instances were predicted as negative instances.

Table 4.4: ANFIS result

Data normalization method	Error	Accuracy	Specificity	Sensitivity
Raw data (without preprocessing)	0.50622	0.49378	0.40741	0.22222
Minmax normalization	0.30303	0.69697	0.14801	0.70370
Zscore normalization	0.6339	0.3661	0.018518	0.33333

In the above results it was observed that Minmax data performed better than the normal data and Zscore data with minimal error of 0.30303, accuracy of 0.69697.

4.3 SVM Result

SVM model was developed for three different data processes namely; raw data, Minmax and Zscore normalized data. The following results were obtained

Table 4.5: SVM Confusion matrix for MinMax

TP = 15	FN = 4	P = 19
FP = 3	TN = 5	N = 8
		P + N = 27

An SVM code was used with polynomial “Pol” as activation function, Fig. 4.1 shows the matlab worksheet environment for MinMAX data it captures the performance measure in the workspace at the left corner of the fig. The confusion metric in Table 4.5 reveals that fifteen (15) instances out of 27 instances used for testing were predicted to be the positive instances that were correctly predicted while four (4) instances were predicted as negative instances that are actually negative.

Table 4.6: SVM Confusion matrix for Zscore

TP = 20	FN = 4	P = 24
FP = 3	TN = 0	N = 3
		P + N = 27

An SVM code was used with linear “linear” as activation function, Fig. 4.2 shows the matlab worksheet environment for Zscore data it captures the performance measure in the workspace at the left corner of the fig. The confusion metric in Table 4.6 reveals that twenty (20) instances out of 27 instances used for testing were predicted to be the positive instances that were correctly predicted while four (4) instances were predicted as negative instances that are actually negative.

Table 4.7: SVM Confusion matrix for raw data

TP = 23	FN = 0	P = 23
FP = 1	TN = 2	N = 4
		P + N = 27

An SVM code was used with Radio Biases function “Rbf” as activation function. The confusion matrix in Table 4.7 reveals that twenty three (23) instances out of 27 instances used for testing were predicted to be the positive instances that were correctly predicted while no instances were predicted as negative instances.

Table 4.8: SVM result

Normali zation method	Activat ion fu nction	Error	Accura cy	Specifi city	Sensiti vity
Raw data	Rbf	0.0385	0.9787	0.6667	1
Minmax Zscore	Pol Linear	0.0371 0.1835	0.9629 0.8165	0.4286 0	0.7500 1

From the result above it was observed that Minmax data with ‘pol’ activation function produces the best result with an error rate of 0.0371, accuracy of 0.9629, specificity of 0.4286 and Sensitivity of 0.7500

4.4 Discussion of Result

The Comparison of the proposed models ANFIS and SVM values for error, accuracy, sensitivity and specificity are discussed thus.

Table 4.9: ANFIS and SVM result compared

	Error	Accuracy	Specificity	Sensitivity
ANFIS	0.30303	0.69697	0.29629	0.70370
SVM	0.0371	0.9629	0.4286	0.7500

This study, analyze ANFIS and SVM model that were design to predict the response to immunotherapy treatment of warts disease. The accuracy of ANFIS and SVM values of the model are ANFIS 0.69697 and SVM 0.9629, respectively, based on their results SVM model performed best in response to immunotherapy treatment of warts disease.

5.0 CONCLUSION

This study has described the architecture and structure of adaptive neuro-fuzzy inference systems alongside its reasoning mechanisms. ANFIS model can improve the generation of relevant if-then fuzzy rules for the prediction of warts disease based on knowledge obtained from human experts which will describe the relevant input and output behavior of warts disease. The set of if-then fuzzy rules can give a desired approximate output. Support vector machine model has the potential of combining human heuristic into computer assisted decision. SVM training algorithm described a model that predicts if an input data of warts disease can fit into response or non-response category based on historic patterns. SVM algorithm operated based on finding the hyper-plane within the warts disease dataset that gives the highest distance to the training pattern, the optimal separation hyper-plane maximizes the margin of the dataset. In this research work, used machine learning techniques to classify and predict immunotherapy treatment of warts disease. ANFIS and SVM models were used to analyze immunotherapy treatment of warts disease dataset, the performance and accuracy of the models compared. This intelligent system will provide a simple way to arrive at a definite conclusion from ambiguous medical data. This will help individuals, medical professionals, world health organizations and government agencies to take appropriate actions. Contributions and suggestions are welcome at this stage of the research.



REFERENCES

- Chaki, S., Routray, A., Mohanty, W. K., & Jenamani, M. (2015). Development of a hybrid learning system based on SVM, ANFIS and domain knowledge: DKFIS. *In India Conference (INDICON)* (pp. 1 - 6). India: IEEE.
- Fayers, P. M., & Machin, D. (2013). *Quality of life: the assessment, analysis and interpretation of patient-reported outcomes*. John Wiley & Sons.
- Flores, E., & Scharcanski, J. (2016). Segmentation of melanocytic skin lesions using feature learning and dictionaries., 56, 300-309. *Expert Systems with Applications*, 56, 300 - 309.
- Gelernter, C., & Uhde, M. (1991). Cognitive-Behavioral and Pharmacological Treatments. *Arch Gen Psychiatry*, 48, 938-945.
- Gerend, M. A., & Magloire, Z. F. (2008). Awareness, knowledge and beliefs about human papilloma virus in a racially diverse sample of young adults. *Journal of Adolescent Health*, 43(3), 237 - 242.
- Gupta, P. (2017). Machine Learning: The Future of Healthcare.
- Khozeimeh, F., Alizadehsani, R., Roshanzamir, M., Khosravi, A., Layegh, P., & Nahavandi, S. (2017). An expert system for selecting wart treatment method., 81, . *Computers in biology and medicine*, 81, 167-175.
- Manerkar, M. S., Harsh, S., Saxena, J., Sarma, S. P., Snehalatha, U., & Anburajan, M. (2016). CLASSIFICATION OF SKIN DISEASE USING MULTI SVM CLASSIFIER. *In 3rd International Conference on Electrical, Electronics,*
- Engineering Trends, Communication, Optimization and Science*, (pp. 362 - 368).
- Parham, P. (2014). (2014). *The immune system*. Garland Science.
- Pathan, S., Prabhu, K. G., & Siddalingaswamy, P. C. (2018). Techniques and algorithms for computer aided diagnosis of pigmented skin lesions—A review. I, 39, 237-262. *Biomedical Signal Processing and Control*, 39, 237 - 262.
- Polat, K., & Güneş, S. (2007). An expert system approach based on principal component analysis and adaptive neuro-fuzzy inference system to diagnosis of diabetes disease. , 17(4),. *Digital Signal Processing*, 17(4), 702 - 710.
- Taher, A. (2010). Adaptive neuro-fuzzy systems. In *Fuzzy systems*. InTech.
- Talmadge, J. E., Fidler, I. J., & Oldham, R. K. (2012). Screening for biological response modifiers: methods and rationale. *Springer Science & Business Media*, 29.
- Walia, N., Singh, H., & Sharma, A. (2015). ANFIS: Adaptive neuro-fuzzy inference system-a survey. *International Journal of Computer Applications*, 13, 123.



Prediction of Epileptic Seizure using Support Vector Machine and Genetic Algorithm

* Abisoye, O. A¹, Abisoye, B.O², Ekundayo Ayobami.³, &Ogunwede Emmanuel.⁴

¹ Computer Science Department, SICT, Federal University of Technology, PMB 65 Minna Niger State, Nigeria

² Computer Engineering Department, SEET, Federal University of Technology, PMB 65 Minna Niger State, Nigeria

³ Computer Science Department, SICT, Federal University of Technology, PMB 65 Minna Niger State, Nigeria

⁴ Computer Science Department, SICT, Federal University of Technology, PMB 65 Minna Niger State, Nigeria

*Corresponding author email: o.abisoye@futminna.edu.ng, +23460546074

ABSTRACT

Epilepsy is a condition defined by the occurrence of epileptic seizures. An epileptic seizure is a brief episode of symptoms caused by abnormal electrical activities in the brain. A common way to treat epileptic seizure is the use of medication. When medication fails, surgery is usually the proposed but surgeries have been found to fail in numerous cases leaving victims with no option than to manage their condition. This scenario, prompt the prediction of epileptic seizures earlier before its invasion so that appropriate precautions can be observed. This research proposes machine learning algorithm; support vector machine and genetic algorithm for the prediction of epileptic seizures. Genetic algorithm was adapted for feature selection while support vector machine was used in classifying EEG signals as seizure or non-seizure signals. The developed model generated accuracy 97.73%, sensitivity 97% and specificity 97%.

Keywords: classification, epileptic seizure, genetic algorithm, prediction, support vector machine.

1 INTRODUCTION

A study defined epilepsy as a diverse family of disorders having in common an abnormally increased predisposition to seizures (Fisher, et al., 2005). Generally epilepsy is first treated with medications but if the medications fail to treat the condition, doctors usually propose surgery or other type of treatment like therapies such as valgus nerve simulation and ketogenic diet. In determining the type of seizure a patient suffers from, a neurological exam to test behaviour and mental function is usually carried out (Betts & Boden, 1992).

Computational methods are usually employed in the detection of epileptic seizures. These techniques have been derived from both non-linear and linear analysis, morphological analysis, model based analysis and recently, there is a notion of selecting and combining the most robust features from various techniques and using them to reveal more striking features from the techniques for revealing various signal characteristics and making more reliable

assumptions. After the feature extraction, intelligent classifiers are then used to distinguish epileptic state from normal states. Some example of such classifiers is Bayesian networks, decision tree, support vector machine, and artificial neural network (Hosseini, Mohammed-Reza, & Mohammed-Bagher, 2013).

A study proposed a machine learning approach to patient-specific classifiers for detecting the onset of an epileptic seizure (Shoeb & Gutttag, 2010). A data set of continuous scalp EEG sampled at 256khz which was recorded over 916 hours of pediatric patients. It was recorded that 173 events occurred during the recordings which were considered to be clinical seizures by medical experts. The data set was then divided into two classes; records containing a seizure and records without a seizure. A high performance machine learning algorithm (a support vector machine) was designed and when trained on 2 or more seizures per patients and tested on 916 hours long recording of



continuous EEG from 24 patients the algorithm was found to have had an accuracy of 96% (Hosseini, Akbarzadeh-T, & Naghibi-Sistani, 2013). Evaluated chaos dynamics for EEG signals of epileptic patients and applied non-linear analysis in understanding the role of chaos in the brain. This approach was found to be 98.6% accurate and they were able to prove that non-linear analysis could be used as an efficient tool in the detection of relative changes in complex brain dynamics. A study presented an overview of various methods for feature selection for seizure detection and prediction placing emphasis on information theory (Giannakakis, Sakkalis, Padiaditis, & Tsiknakis, 2014). Each method was subjected to an evaluation of performance; its ability to automatically detect/predict seizures was also assessed. A combination of various methods was employed in order to exploit efficiently the most robust features. The authors argued that when using support vector machines as a classifier, the selected features played a major role in the efficiency of the classifiers ability to accurately classify. Various results from various authors using the reviewed techniques were compared. A combination of genetic programming and K-nearest neighbours was found to be 99.2% accurate while a combination of PCA-FFT and AIRS classifier and ApEn with Elman network both returned an accuracy of 100%. The models were limited to small data sets and hence provided accurate results and there was no standard guidelines with reliable standardized data (Giannakakis, Sakkalis, Padiaditis, & Tsiknakis, 2014).

2 STATEMENT OF THE PROBLEM

Most people affected by epilepsy live in less developed of developing countries. Early diagnosis is quite useful better treatment of victims. When seizures cannot be predicted the activities of a victim is limited for the sake of safety. Surgery and medication are the common ways to treat seizures but surgeries have been found to fail in helping patients control seizures and medications may not always help patients manage their conditions, being able to predict seizures before occurrence becomes the best way of managing the condition when treatments fail. Due to varying experiences not all patients experience physical symptoms of the pre-ictal phase of a seizure hence the need for intelligent systems that could predict seizures

without a patient being admitted and examined for long hours. Previous works have been found to produce good accuracies, using a powerful optimization technique such as genetic algorithm can reduce the feature vector and hence increase prediction speed and also accuracy. This study examines the power of genetic algorithm and compares result to already existing methods.

3 SUPPORT VECTOR MACHINE

The support vector machine was invented in 1995 by Vapnik and Cortes for binary classification. It is a supervised learning model and although it has undergone many modification in its basic form the support vector machine classifies labelled data into two classes. Using separating hyperplane. The hyperplane is such that it is the farthest away from both classes of data to be classified.

Support vector machine is used for both classification and regression problem. The support vector machine is usually trained using a learning algorithm. The most common used algorithms include sequential minimal optimization and coordinate descent. Because of the success of support vector machines in classification, various derivation of the model that employ the same logic for other type of problems has emerged some of them include least square support vector machine(LS-SVM) used for classification and regression and support vector clustering used to perform cluster analysis.

A book by (Russell & Norvig, 2016) describes three characteristics that makes the Support vector machine attractive:

1. It constructs a decision boundary with the largest possible distance to example points (maximum margin separator) which helps it generalize well.
2. The possess the ability to embed data into a higher-dimensional space using something called the kernel trick
3. They combine the advantages of parametric and non-parametric models and thus have flexibility to represent complex functions.



4 GENETIC ALGORITHM

Genetic algorithm is a search optimization technique that is based on Darwinian principle of evolution and natural selection. A solution generated by genetic algorithm is called a chromosome, while collection of chromosome is referred as a population (Hermawanto, 2013). The chromosome is made up of genes whose value can either be numerical, binary, symbols or characters. The algorithm usually starts by generating a random population of parent chromosomes and defining a fitness function which is used to measure the fitness of each parent. The fit parents are usually selected to be members of the next generation of chromosomes. A new generation of chromosome is created by a process of selection mutation and cross over. The genetic algorithm will be used in feature extraction and Support vector machine will be trained to carry out binary classification of the data.

A description of the genetic algorithm as described by (Hermawanto, 2013) is as follows:

Step 1: Determine the number of chromosomes, generation, and mutation rate and crossover rate value

Step 2: Generate chromosome-chromosome number of the population, and the initialization value of the genes chromosome-chromosome with a random value

Step 3: Process steps 4-7 until the number of generations is met

Step 4: Evaluation of fitness value of chromosomes by calculating objective function

Step 5: Chromosomes selection

Step 6: Crossover

Step 7: Mutation

Step 8: Solution (Best Chromosomes)

5 METHODOLOGY

The process of detecting the epileptic seizure using the support vector machine classifier is broken down into phases of pre-processing, feature selection and classification of input vectors. Figure 2.1 shows a block diagram of the methodology



Figure 2.1: block diagram of proposed model

SVMs usually employ a learning algorithm for classification; our approach to classifying our dataset will involve the use of genetic algorithm for the selection of robust features for the SVM classifier. Our data set was obtained from UCI online data repository and consists of 5 classes of data subjects such that class 2-5 are subjects who did not have epileptic seizure and only subjects in class 1 have epileptic seizure. A binary classification of class 1 against the other classes will be performed. 2/3 of the data will be used in training the SVM and the remaining 1/3 of the data will be used to test the SVM classifier the result will then subjected to sensitivity specificity and accuracy test.

The parameters of the genetic algorithm are summarized in table 2.1 below.

parameter	Parameter value
Probability of crossover	The probability that two population members will exchange gene
Probability of mutation	The probability that a gene will be flipped
Population size	The number of individuals in each generation
Number of generations	The maximum number of generations created by the algorithm

Table 2.1: summary of parameters of Genetic algorithm

The population size is the total number of individuals in each generation. Each member is called a chromosome and each chromosome is made up of genes. The gene is represented using a binary number



of 0 or 1. The total number of gene in each chromosome equals to the total number of features in the feature vector. The number of generation is the maximum number of times the algorithm will generate a population to find the best individual. The probability of a crossover is the probability that two members of the population will exchange genes. If the probability is set to zero then there is no exchange of genes and hence crossover will not occur. The probability of mutation defines the possibility of random elements of chromosomes will be flipped, i.e. the probability that a gene with a current value of 1 will be flipped to 0 and vice versa.

The algorithm was implemented in weka (wekai to environment) version 3.5 and a correlation based feature selection attribute evaluator was used to evaluate the subset of attributes. The objective function was therefore a measure of the correlation of each attribute to the target class and the attributes with higher correlation to the class labels and low correlation with other attributes was selected as fit by the algorithm.

After using genetic algorithm to select a subset of most fit features, SVM will then be used to classify the instances. The classifier's efficiency will be evaluated based on some performance metrics as summarized in table 2.2

Performance metric	Brief description
Accuracy	Ratio of instances correctly classified by the classifier
Sensitivity	The ratio of positive instances classified as positive by the classifier. Also called the true positive rate
Specificity	The ratio of negative instances classified as negative by the classifier also called the true negative rate.

Table 2.2: summary of performance metrics used in the research

6 RESULTS AND DISCUSSIONS

Missing values were not found in the dataset hence for preprocessing the data, Z-score normalization was carried out. The preprocessed data was then passed to the genetic algorithm. The values of the genetic algorithm parameters are shown in Table 3.0

Table 3.0: Genetic algorithm parameter values

parameter	Parameter value
Crossover Probability	0.6
Mutation Probability	0.033
Population size	100
Number of generations	100

The algorithm selected 100 out of the 178 original features, reducing the feature vector by 78 features. The features were then passed to the SVM classifier for classification. The hyper-parameters used in our SVM model are described in table 3.1 below

Hyperparameter	Value
Kernel	Gaussian kernel also known as the radial basis function(RBF)
Regularization parameter, C	1000
Gamma	0.001

Table 3.1: Support Vector Machine hyper-parameters

The classifier achieved an accuracy of 97.39%. the performance of the classifier is summarized in table 3.2 below.



Performance metric	Value
Accuracy	97.73%
Sensitivity	97%
Specificity	97%

Table 3.2: SVM classifier performance result

It is also noteworthy to know that most classifiers performance can be affected by many factors some of which are unique to the classifier, the quality of data or preprocessing techniques employed. It is therefore safe to say that feature selection employed in this research has pointed us in the right direction towards an improved prediction of epileptic seizures.

Figure 3.1 below shows the confusion matrix of the SVM classifier. A total of 3450 instances made up the test set. 2760 of them were labelled negative by the classifier, 2718 of them were correctly classified (true negative) while 42 was misclassified (false positive). 690 of them were classified as positive by the classifier, 642 were correctly classified (true positive) and 48 were misclassified (false) positive.

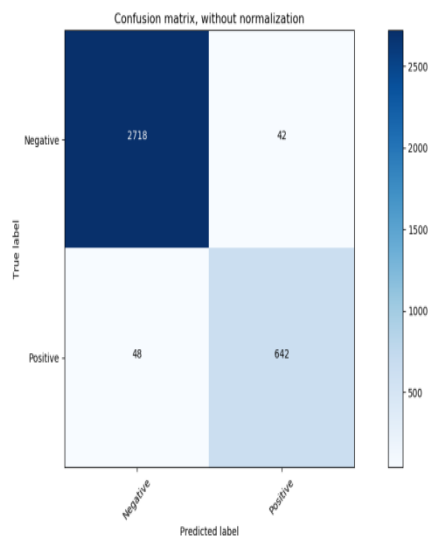


Figure 3.1: confusion matrix without normalization

7 CONCLUSION

From our research genetic algorithm was found to improve the classification accuracy by 0.36% and also improves the SVM sensitivity by 8.11% with respect to the existing models. We can therefore conclude that performing feature selection improved the classifier accuracy.

8 REFERENCES

- Betts, T., & Boden, S. (1992). Diagnosis, management and prognosis of a group of 128 patients with non-epileptic attack disorder. Part I. Seizure., *1*(1), 19-26.
- Fisher, R. S., Boas, W. V., Blume, W., Elger, C., Genton, P., Lee, P., & Engel, J. (2005). Epileptic seizures and epilepsy: definitions proposed by the International League Against Epilepsy (ILAE) and the International Bureau for Epilepsy (IBE). *46*(4), 470-472.
- Giannakakis, G., Sakkalis, V., Pedititis, M., & Tsiknakis, M. (2014). *Methods for seizure detection and prediction: an overview*. New York, NY: Humana Press.
- Hermawanto, D. (2013). Genetic algorithm for solving simple mathematical equality problem. arXiv preprint arXiv:1305.0001.
- Hosseini, S. A., Akbarzadeh-T, M. R., & Naghibi-Sistani, M. B. (2013). Qualitative and quantitative evaluation of eeg signals in epileptic seizure recognition. , *5*(6), 41. *International Journal of Intelligent Systems and Applications*, *5*(6), 41.
- Hosseini, S. A., Mohammed-Reza, A.-T., & Mohammed-Bagher, N.-S. (2013). Methodology for epilepsy and epileptic seizure recognition using chaos analysis of brain signals. *Computational Intelligence in Multi-Agent Systems: Theory and Practice*, (pp. 20 - 36).



3rd International Engineering Conference (IEC 2019)
Federal University of Technology, Minna, Nigeria



-
- Russell, S. J., & Norvig, P. (2016). *Artificial intelligence: a modern approach*. Malaysia: Pearson Education Limited.
- Shoeb, A. H., & Guttag, J. V. (2010). Application of machine learning to epileptic seizure detection. In Proceedings of the (pp. 975-982). *27th International Conference on Machine Learning (ICML-10)* (pp. 975 - 982). Proceeding.
- Zhang, T., & Oles, F. J. (2001). Text categorization based on regularized linear classification methods. *Information Retrieval*, 4(1), 5 - 31.



THE PREDICTION OF CERVICAL CANCER OCCURENCE USING GENECTIC ALGORITHM AND SUPPORT VECTOR MACHINE

* Abisoye, O. A¹, Abisoye, B.O², Ekundayo Ayobami³ & Kehinde Lawal⁴

¹ Computer Science Department, SICT, Federal University of Technology, PMB 65 Minna Niger State, Nigeria

² Computer Engineering Department, SEET, Federal University of Technology, PMB 65 Minna Niger State, Nigeria

³ Computer Science Department, SICT, Federal University of Technology, PMB 65 Minna Niger State, Nigeria

⁴ Computer Science Department, SICT, Federal University of Technology, PMB 65 Minna Niger State, Nigeria

*Corresponding author email: o.abisoye@futminna.edu.ng, +23460546074

ABSTRACT

Cervical cancer is a malignant neoplasm arising from cells originating in the cervical uteri. Cervical cancer can be treated using Human Papilloma virus vaccine and carrying out regular pap test. The manual system contains large amount of errors by virtue of human decision, the visual screening is very demanding, tedious, and expensive in terms of labor requirements. This paper proposed machine learning algorithm; Support Vector and Genetic algorithm to predict the occurrence of cervical cancer. Evaluation results show the effectiveness of the proposed approach with the overall Precision, Recall, F1 score, Sensibility, Sensitivity, Accuracy values 96%, 95%, 95%, 89%, 96% and 95% respectively for Biopsy and 97%, 96%, 96%, 50%, 97% and 96% for Hinselmann. In this study cervical cancer was predicted with Support vector machine classifier and Genetic algorithm optimization tool. The prediction was found to have acceptable performance measures which will reduce future incidence of the outbreak in the world and aid timely response of medical experts.

Key Words: Cancer, Classification, Extraction, Human papillomavirus, Prediction,

1 INTRODUCTION

Human papillomavirus is a virus responsible for the cause of Cervical cancer. Symptoms of cervical cancer can include painful sex, vaginal bleeding, and discharge (CDC, 2016). A Cervical cancer risk factor is any means that changes the possibility of contacting cervical cancer. **Cervical cancer** is a type of cancer that develops from the cervix. Other types of cancer includes breast cancer, lungs cancer, sarcoma cancer, leukaemia cancer, liver cancer (Idikio, 2011). It is due to the abnormal growth of cells that have the ability to spread to other parts of the cervix. Early on, typically no symptoms are seen. Some of the symptoms that precede later in the growth of abnormal cells include vaginal discharge of blood, pelvic pain. In as much as bleeding after sex is not really considered a symptom of cancer because it can be caused by several diseases, it can also indicate the presence of cervical cancer (Zhang & Liu, 2004).

This cancer is preventable by screening for premalignant lesions but this is rarely provided and hardly utilized. Considering the main risk of cervical cancer result from human papillomavirus, the vaccine for this virus is required to prevent against it. People with weak immune system are at risk of developing some types of cancer. Weak immune systems include system that have had organs transplant, HIV, have consistently take drugs Unlike the developed countries other screening methods can be explored in countries with low resources (Roy & Mukherjee, 2014).

The diagnosis of cervical cancer using an artificial intelligent system with statistics by (Chandraprabha & Singh, 2016) reveals that the percentage of cervical cancer rising in developing countries is 70%. It is the major cause of death in low-income countries. The considered techniques in this research work are image processing and classification techniques. The research work reviewed various algorithms required for the diagnosis of primary features required for

classification of cervical cancer (Chandraprabha & Singh, 2016).

2 RELATED WORKS

The research work by (Athinarayanan, Srinath, & Kavitha, 2016) uses a screening method which is the pap smear test and several classification techniques for detecting cervical cancer like support vector machine (SVM), fuzzy based techniques and texture classification to differentiate the benign and cancerous cells. This research reveals an expert system designed for predicting cervical cancer using data mining techniques. It explains the different methods of controls and prevention of cervical cancer which includes Pap smear, Human Papilloma virus screening and vaccination against Human Papilloma virus, liquid-based cytology. With data processing and manipulation of data taking the lead in our system as a result of large volume of data, data mining techniques are emerging. The data mining techniques used include features selection and classification (Benazir & Nagarajan, 2018).

A paper reviewed the classification of cervical cancer using artificial neural networks. It uses artificial neural network to detect cervical cancers by classifying the cells either as normal or abnormal cells in the cervix area. This classification produces an accurate result compared to Pap smear test which is a manual screening method. Analysis was made using all the network architecture which includes single neural network, deep and shallow neural network (Devi, Ravi, Vaishnavi, & S, 2016).

A research work reviewed the manual method of screening cervical cancer using Pap smear test, the need for carrying out feature selection and the classification of the features. The classification are done using K-NN and Artificial neural network. The analysis shows that the classification accuracy for K-NN was 88.04% and 54% for artificial neural network (Malli & Nandyal, 2017).

2.1 STATEMENT OF THE PROBLEM

There is a general understanding by the public that precise tool called pap smear is responsible for cancer detection has led many to believe that cancer after a normal Pap smear must imply malpractice. This understanding is a costly assumption hence pervasive. The limited number of experts and the large

number of patients resulted in a long queue for the screening process. The manual system contains large amount of errors by virtue of human decision. The visual screening is very demanding, tedious, and expensive in terms of labour requirements.

3.0 PROPOSED METHODOLOGY

Several papers have revealed the need for early detection of cervical cancer owing to the fact that it is one of the deadliest cancer in the world. This paper discusses how cervical cancer data is pre-processed to eliminate noise, selected suitable features from the data collected and prepare the data for classification, and how SVM is used in training the system using the prepared data in classifying cervical cancer.

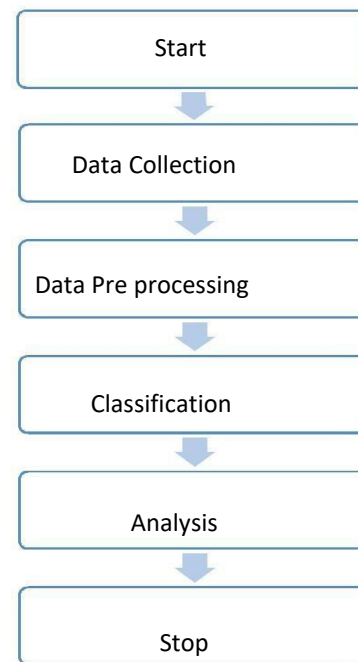


Figure 1: Block diagram for cervical cancer prediction

3.1 Data Collection

Data collection refers to the process of gathering data on a particular area of interest that are measurable and can be statically fashioned. The main goal of data collection is to capture data that is of high quality and its analysis would lead to the formation of answers that are convincing and credible. Figure 1 explains the methodology required for the predicting cervical cancer which includes data collection, preprocessing, classification and analysis.



The data collected for this research was gotten from UCI Machine Learning Repository. UCI Machine Learning Repository is a database or data generator that collects and store data relevant to the machine learning and statistics. The attributes of the cervical cancer data set can be viewed in the table 1.

Table 1: Attributes of the Cervical Cancer data set

S/N	Attributes	Description/ Data types
1	Age	Integer value
2	Number of sex Partners	Integer value
3	First sexual Intercourse	Integer value
4	Number of Pregnancies	Integer value
5	Smokes	Integer value
6	Smokes(year)	Integer value
7	Smokes(packs/year)	Integer value
8	Hormonal Contraceptives	Boolean value
9	Hormonal Contraceptives (years)	Boolean value
10	Condylomatosis	Boolean value
11	Cervical Condylomatosis	Boolean value
12	Vaginal Condylomatosis	Boolean value
13	Vulvo- Perineal Condylomatosis	Boolean value
14	Syphilis	Boolean value
15	Pelvic Inflammatory Disease	Boolean value
16	Genital herpes	Boolean value
17	Molluscum Contagiosum	Boolean value
18	AIDS	Boolean value
19	HIV	Boolean value
20	Hepatitis B	Boolean value
21	Number Of Diagnosis	Integer value
22	Time since first Diagnosis	Integer value
23	Time since last Diagnosis	Integer value
24	Dx:CIN	Boolean value
25	Dx:HPV	Boolean value

26	Dx	Boolean value
27	Dx:Cancer	Boolean value
28	bool) IUD	Boolean value
29	IUD (years)	Integer value
30	STDs (number)	Integer value
31	Dx:Cancer	Boolean value
32	HPV	Boolean value
33	Hinselmann	Boolean value
34	Schiller	Boolean value
35	Cytology	Boolean value
36	Biopsy	Boolean value

3.2 Data Pre-processing

Data pre-processing is a technique which involves the transformation of raw data into a more understandable and correct format. Data processing in a broad sense prepares the raw data for further processing. It aims to remove inconsistencies, missing values and error which are all contained in various real world data (El-Halees, 2008).

Data pre-processing is a very important in data mining because the value of the data rest on the feature decision.to improve the feature of medical diagnosis it is very important we improve the medical database.to check the accuracy of the diagnosis, it is required to check the attributes because the computation time is dependent on the number of attributes (Khare & Burse, 2016).

3.3 Feature selection

The data acquired from the data collection process is subjected to an optimization techniques called Genetic Algorithm to select the best fit for the classification process. Feature selection is a key tool to a successful data mining.

Genetic algorithm is a prominent example of evolutionary computation techniques. The evolutionary systems use optimization tool like evolution to solve engineering problems (Singh, 2013). This algorithm is a random search technique that is guided by genetics in natural evolution.

3.4 (Data Scaling)

Data normalization provides a better model and avoids numerical problems. Any statement problem required for pre-processing cannot eliminate the normalization stage because the data are manipulated or scaled before considered for the next stage. In this pre-processing stage, we can use the existing range to find the new range (Patro & Sahu, 2015). The normalization technique used was this research Min-Max normalization other types of normalization techniques includes, Z-score normalization, Decimal scaling normalization and Integer normalization. In this study a total number of thirty-six (36) attributes were collected with 858 instances.

3.5 GENETIC ALGORITHM

Genetic algorithm is a search optimization technique that is based on Darwinian principle of evolution and natural selection solution generated by genetic algorithm is called a chromosome, while collection of chromosome is referred as a population The chromosome is made up of genes whose value can either be numerical, binary, symbols or characters. The processes in genetic algorithm includes; population initialization, selection, two-point cross over, mutation, modification etc. as viewed in Figure 2

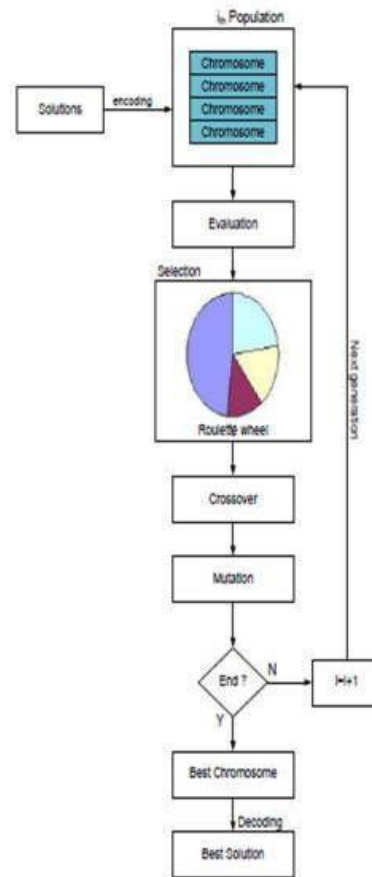


Figure 2: Genetic algorithm flowchart

In the genetic search the configurations were in Table 2 were put into considerations to select best features needed for good prediction.

Table 2: Genetic Search Features

Search Method: Genetic search.
Population size
Number of generations
Probability of crossover
Probability of mutation
Report frequency
Random number seed
Attribute Subset Evaluator

3.4 Training and Testing the Model.

Table 2 shows the attributes of cervical cancer that was selected from the genetic algorithm process. The selected features were used at the training and testing phase. SVM (Support Vector Machine) was used to create a model that will classify a trained dataset as either cancerous or non-cancerous.

Table 3: The Attributes of Cervical Cancer data set

S/n	Attributes	Data Types
1.	Hormonal Contraceptives	Boolean
2.	STDs: vaginal condylomatosis	Boolean
3.	STDs: genital herpes	Boolean
4.	STDs: molluscum contagiosum	Boolean
5.	STDs:Hepatitis B	Boolean
6.	STDs:HPV	Boolean
7.	STDs: Number of diagnosis	Boolean
8.	Dx:Cancer	Boolean
9.	Dx	Boolean
10.	Biopsy:	target
11.	Cytology:	target
12.	Schiller:	target

Table 3 is a list of some of the attributes in the cervical data set with its values. The IDE (Integrated Development Environment) used for the Genetic Search Attribute Subset Evaluator in WEKA. Out of existing 36 features, 12 features were selected as the best features for prediction.

3.7 SUPPORT VECTOR MACHINE

The support vector machine was invented in 1995 by Vapnik and Cortes for binary classification. It is a supervised learning model and although it has undergone many modification in its basic form the support vector machine classifies labelled data into two classes. Using separating hyper plane. The hyper plane is such that it is the farthest away from both classes of data to be classified. (Russell S & P, 2010) describes three characteristics that the Support vector machine attractive:

1. It constructs a decision boundary with the largest possible distance to example points (maximum margin separator) which helps it generalize well.

2. They possess the ability to embed data into a higher-dimensional space using something called the kernel trick
3. They combine the advantages of parametric and non-parametric models and have flexibility to represent complex functions.

Support vector machine is used for both classification and regression problem. The support vector machine is usually trained using a learning algorithm.

SVMs usually employ a learning algorithm for classification; our approach to classifying our dataset will involve the use of genetic algorithm for the extraction and selection of robust features for the SVM classifier

4.0 Results and Analysis

4.11 Genetic search Result for Biopsy

Search Method: Genetic search.

Population size: 20

Number of generations: 20

Probability of crossover: 0.6

Probability of mutation: 0.033

Report frequency: 20

Random number seed: 1

Attribute Subset Evaluator (supervised, Class (numeric): 36 Biopsy): CFS Subset Evaluator Selected attributes for Biopsy:

- Hormonal Contraceptives (years)
- STDs:vaginal condylomatosis
- STDs:genital herpes
- STDs:molluscum contagiosum
- STDs:Hepatitis B
- STDs:HPV
- STDs: Number of diagnosis
- Dx:Cancer
- Dx
- Hinselmann
- Schiller
- Citology

4.2 Result for Biopsy from Classification

This section presents the result when the model was tested to classify a total of 223 instances.

Table 4: The confusion matrix of the SVM for Biopsy

	Predicted class	
	Non-Cancerous	Cancerous
Non-Cancerous	195	9
Cancerous	2	17

Table 4 shows the confusion matrix from the SVM classification on the Biopsy test, with 195 true negative classifications, 17 true positive classifications, 9 false positive calculations and 2 false negative calculations.

Table 5: The performance metrics of the classification for the Cancerous and Non- Cancerous class

Metrics	Non-Cancerous	Cancerous	Average
Precision	0.650	0.99	0.96
Recall	0.890	0.960	0.950
F1-score	0.760	0.97	0.95

Classification has a high precision, recall and F-score for the Cancerous class compared to the Non-Cancerous class.

Table 6 The sensitivity, specificity and accuracy.

Metrics	Cancerous
Sensitivity	0.890
Specificity	0.960
Accuracy	0.950

The sensitivity in Table 6 shows that the model recognizes 89% of the Cancerous instances in the test dataset. Specificity 96 % on the other hand shows how the model was able to differentiate among Cancerous and Non-Cancerous instances in the entire test Dataset. The total accuracy of the model is 95% which is moderately acceptable for the imbalanced dataset.

4.3 Genetic search Result for Hinselmann

Search Method: Genetic search.
Population size: 20

Number of generations: 20
Probability of crossover: 0.6
Probability of mutation: 0.033
Report frequency: 20
Random number seed: 1
Attribute Subset Evaluator (supervised, Class (numeric): 33
Hinselmann): CFS Subset Evaluator

Including locally predictive attributes Selected attributes: 2, 24, 34, 36: 4

- ❖ Number of sexual partners
- ❖ STDs: Hepatitis B
- ❖ Schiller
- ❖ Biopsy

4.4 Result for Hinselmann

This section presents the result when the model was tested to classify a total of 220 instances.

Table 6: The confusion matrix of the SVM for Hinselmann

	Predicted class	
	Non-Cancerous	Cancerous
Non-Cancerous	208	6
Cancerous	3	3

Table 6 above shows the confusion matrix from the SVM classification on the Hinselmann test, with 208 true negative classifications, 6 true positive classifications, false positive calculation and 3 false negative calculations.

Table 7: The performance metrics of the classification for the Cancerous and Non-Cancerous class

Metrics	Non-Cancerous	Cancerous	Average
Precision	0.330	0.99	0.970
Recall	0.500	0.970	0.960
F1-score	0.400	0.980	0.960

Classification has a high precision, recall and F-score for the Cancerous class compared to the Non-Cancerous class.



Table 8: The sensitivity, specificity and accuracy.

Metrics	Cancerous
Sensitivity	0.500
Specificity	0.970
Accuracy	0.960

The sensitivity 50% shows that the model could detect only averagely cancerous cases in the entire dataset. Specificity 97% on the other hand shows how the model was able to differentiate among Cancerous and Non-Cancerous instances in the entire test Dataset. The total accuracy of the model is 96% which is not acceptable for the imbalanced dataset.

5.0 Conclusion

Machine Learning techniques have proven to be of great tools in various sectors, there has been quite a number of research works in cervical cancer owing to the fact that it is one of the deadliest cancer diseases in the world that have taken hold of rural areas and developing countries particularly. In this study cervical cancer was predicted with Support vector machine classifier and Genetic algorithm optimization tool. The prediction was found to have acceptable performance measures which will reduce future incidence of the outbreak in the world and aid timely response of medical experts.

REFERENCES

- Athinarayanan, S., Srinath, M. V., & Kavitha, R. (2016). Detection and Classification of Cervical Cancer in Pap Smear Images using EETCM, EEETCM & CFE methods based Texture features and Various Classification Techniques, 2(5), 533 - 549.
- Benazir, B., & Nagarajan, A. (2018). An Expert System for Predicting the Cervical Cancer using Data Mining Techniques, 118(20), 1971–1987. 118(20), 1971–1987.
- CDC. (2016, January 2). www.Cdc.Gov/Cancer/Knowledge 800-CDC-INFO,.
- Chandraprabha, R., & Singh, S. (2016). Artificial Intelligent System for Diagnosis of Cervical Cancer: a Brief Review and Future Outline. 38-41.
- Devi, M. A., Ravi, S., Vaishnavi, J., & S, P. (2016). Classification of Cervical Cancer using Artificial Neural Networks. 465-472. doi:https://doi.org/10.1016/j.procs.2016.06.105
- El-Halees, A. (2008, February). Mining Students Data to Analyze Learning Behavior: a Case Study Educational Systems. Work. doi:https://doi.org/10.1504/IJTEL.2012.051816
- Idikio, H. A. (2011). Human cancer classification: A systems biology-based model integrating morphology, cancer stem cells, proteomics, and genomics. *Journal of Cancer*, 2(1), 107 - 115. doi:https://doi.org/10.7150/jca.2.107
- Khare, P., & Burse, K. (2016). Feature Selection Using Genetic Algorithm and Classification using Weka for Ovarian Cancer. *International Journal of Computer Science and Information Technologies (IJCSIT)*, 7(1), 194–196.
- Malli, P. K., & Nandyal, S. (2017). Machine learning Technique for detection of Cervical Cancer using k-NN and Artificial Neural Network. 6(4).
- Patro, S. G., & Sahu, K. K. (2015). Normalization, A preprocessing stage. *Iarjset*, 20-22. doi:https://doi.org/10.1017/SO269888900007
- Singh, S. R. (2013). Genetic Algorithms for Staging Cervical Cancer.3(Ii), 39–43. 39-43.
- Roy, M., & Mukherjee, S. (2014). Reversal of resistance towards cisplatin by curcumin in cervical cancer cells. *Asian Pac J Cancer Prev*, 15(3), 1403-10.
- Zhang, J., & Liu, Y. (2004). Cervical Cancer Detection Using SVM Based . 2, 873– 880.



PERFORMANCE EVALUATION OF ANT LION OPTIMIZATION AND PARTICLE SWARM OPTIMIZATION FOR UNCAPACITATED FACILITY LOCATION PROBLEM (UFLP)

*Shehu Hussaina¹, & Morufu Olalere²

¹ Department of Computer Science, Federal Polytechnic, PMB 55 Bida, Niger State, Nigeria

²Department of Cyber Security Science, Federal University of Technology, PMB 65 Minna Niger State, Nigeria

*Corresponding author email: mamakausar2015@gmail.com, +2348065633807

ABSTRACT

The Uncapacitated Facility Location Problem (UFLP) is one of the widely studied discrete optimization problem due to its application in modelling and solving various real life problems. In UFLP, the minimum cost of connecting a facility with some demand points is being sought. Due to its NP-hard (nondeterministic polynomial time) nature and increasing complexity of the problem as the dimension increases, metaheuristic optimization algorithms have been proposed in solving them. In this paper, the performance of two successful and recent metaheuristic optimization algorithms (the Ant Lion Optimizer (ALO) and Particle Swarm Optimization (PSO)) which were applied to solving UFLP were evaluated and compared. The data set used for the experiments were obtained from OR-library (Operational Research Library) and the results shows that the algorithms were efficient in obtaining a minimum cost and minimize distance of travel to yield a better facility location. The performance of ALO algorithm when compared to PSO show much better results in terms of obtaining the minimum city-facility connection cost. In all the test problems, the results indicate that ALO can get better best fitness results, showing better convergence speed. ALO is also more stable and robust compared with PSO, from the results ALO appear to converge faster and had better accuracy.

Keywords: *Ant lion optimizer (ALO), Facility location, Particle Swarm Optimization (PSO), Un-capacitated Facility Location Problem (UFLP).*

1 INTRODUCTION

Facility Location is a branch of Operation Research (Ghosh, 2003, Kole *et al.*, 2014) that deals with mathematical modeling and solving issues related to optimal placement of facilities in order to minimize the costs. In order to provide certain services to clients, multiple facilities of the same type are situated within an area. In this situation, service providers must select the location of the facility with reference to the cost and the customer convenience. The facility location problem (FLP) is a combinatorial problem that integrates basic issues related to such selection of a facility location (Hiroaki, *et al.*, 2011). A Facility Location Problem (FLP) consists in positioning a set of structures (facilities) in a given space in order to satisfy the demand (actual or potential) expressed by a set of customers. The facility location problem is a central problem in operational research. In this problem, there are set of clients and a set of facilities, and here each client is connected to a facility in a way that minimizes the sum of fixed costs for opening facilities and the total cost for servicing the clients. This problem comprises two main

stages of decision making: at the upper level, when a set of facilities to be opened is chosen and at the lower level, where the clients are assigned to these facilities by taken into consideration the clients preferences (Hajiagh, *et al.*, 2003, Maric, *et al.*, 2015). There are two kinds of FLP, depending on the presence of limitations on the amount of service provided by every facility. If each facility has a limit on the number of customers it can serve, it becomes a capacitated facility location problem (CFLP). On the other hand if an arbitrary number of customers can be connected to a facility, the problem is called uncapacitated facility location problem (UFLP) (Ling, *et al.*, 2006) Both CFLP and UFLP are NP-hard and have been extensively studied. Also, lots of algorithms, exact and heuristics have been developed. In this study, solution to UFLP using ALO and PSO is been proposed. UFLP is one of the most widely studied discrete location problem. It is a problem of finding facility locations and assigning facilities among customers so as to minimize the total costs of opening a facility and connection costs (Hiroaki, *et al.*, 2011, Hajiagh, *et al.*, 2003, & Ling, *et al.*, 2006).

1.2 RELATED WORK

Vasilyev and Klimentova, (2010). Provided a new BLUFLP formulation based on a family of valid inequalities linked to the problem of a pair of matrices and the problem of set packing. To calculate the corresponding lower boundaries, a cutting plane technique is introduced. The proposed cutting plane algorithm was further incorporated in two versions of a branch-and-cut method in order to find an optimal solution. The simulated annealing method is proposed for obtaining the upper bounds of the optimal solution used in the proposed branch-and-cut methods. Numerical experiments are conducted on the same benchmark set as in (Canovas, *et al.*, 2007), including test instances of relatively small dimensions ($M \leq 75$, $N \leq 100$). Computational results from (Vasilyev and Klimentova, (2010)) approve the efficiency of the implemented branch-and-cut methods when solving the considered BLUFLP test instances.

Another popular metaheuristic, tabu search algorithm, is applied by (Al-Sultan and Al-Fawzan, 1999). Their application produces good solutions, but takes significant computing time and limits the applicability of the algorithm. (Michel and Van Hentenryck, 2004) also applied tabu search and their proposed algorithm generate more robust solutions. There are artificial neural network approaches to solve UFL problems in (Gen *et al.* 1996). Finally there are Particle Swarm Optimization approach applied by (Guner1 & Sevkli, 2008) and Modified Particle Swarm Optimization by (Saha, *et al.*, 2011).

Kole *et al.*, (2014) in his work uses Ant colony optimization (ALO) to solve Uncapacitated facility location problem UFLP: The problem was solved using another meta-heuristic method Particle Swarm Optimization technique. Comparing results with PSO technique gave almost same results for same data set using ACO. In this work modification such as in the value of the heuristics, the range of the initial weight of the nodes, and the greedy method can be used to get initial solution.

(Nevena *et al.*, 2010), described a new approach to solving the UFLP using message passing algorithms. The approach demonstrates that LP relaxation based message passing algorithms such a max-product linear programming (MPLP) can be used to construct approximations for NP hard problems in a manner similar to primal-dual methods. Relating such algorithms to standard dual LPs and approximation algorithms is a good direction of future work.

A fast Algorithm for facility location problem was investigated by Wenhao.,(2013). Here, Facility location problem has been proved NP-hard. Algorithm with running time of $O(m \log m)$, was used in achieving approximation guarantee of 2 by the dual fitting technique. The distinguishing feature of the algorithm compared with that in Jain *et al.*, (2002) is the lower running time.

In (Guner and Sevkli, 2008), Discrete version of particle swarm optimization DPSO is applied to solve UFL bench mark problems. The results of DSPO are compared

with results of a The results are compared with a continuous particle swarm optimization (CPSO) algorithm and two other metaheuristics approaches show s that DSPO is slightly better.

(Mesa *et al.*, 2018), Used, Cuckoo search via levy flight (CS-LF) to solve facility location problem. Results showed that applying CS-LF for the problem produced better facility locations. When compared to the existing facility locations from the data and from the PSO program,though suggest further work on the on the work.

2 PROBLEM FORMATION

Un-Capacitated Facility Location Problem (UFLP), also called warehouse location problem is a classical problem (that is NP-hard in nature) that is studied in operational research from which several other variants of location problems are derived (Shu, 2013). In UFLP, the objective function is to find the minimum cost of connecting a city to an opened facility. Given a set of clients Q which are required to be serviced by a subset of facilities F , such that each facility i has an opening cost f_i . The cost of facility i serving Client ($j: j \in Q$) is $Q_{i,j}$. Equation 1 shows the Objective Function of the UFLP.

$$OF = \min \sum_{i,j} Q_{ij} X_{ij} + \sum_i f_i Y_i \quad (1)$$

Subject to;

$$j \in Q: \sum_{j=1} X_{ij} = 1 \quad (2)$$

$$Y_i - X_{ij} \geq 0 \quad (3)$$

$$Y_i \in \{0, 1\} \text{ and } X_{ij} \in \{0, 1\} \quad (4)$$

Where, X_{ij} is a variable that shows if client j is connected to facility i , while Y_i shows if facility i is open or not. Equation 2 ensures that every client is connected to one facility while Equation 3 ensures that the facility Y must be opened.

3 THE ANT LION OPTIMIZATION

ALO is a novel nature-inspired algorithm developed in 2015 (Mirjalili, 2015). This algorithm consists of exploration by random walk and random selection of agents. The exploitation is done with traps. The ALO algorithm imitates the real-life hunting mechanism of ant lions which employs five main steps of hunting i.e. random walk of agents, building traps, entrapment of ants in trap, catching prey and rebuilding traps. The roulette wheel and random walks of ants in ALO optimizer can eliminate local optima. Mathematical modeling of ALO algorithm is presented.

The lifecycle of ant lions includes two main phases: larvae and adult. An ant lion larva digs a cone shaped pit in sand by moving along a circular path and throwing out sands with its massive jaw. After digging the trap, the larva hides underneath the bottom of the cone and waits for insects to be trapped in the pit. The edge of the cone is sharp enough for insects to fall to the bottom of the trap easily. Once the ant lion realizes that a prey is in the trap, it tries to catch it. Then, it is pulled under the soil and consumed. After consuming the prey, ant lions throw the leftovers outside the pit and prepare the pit for the next hunt (Mehta & Nischal, 2015) (Ali, Elazim, & Abdelaziz, 2017).

Algorithm 1: ALO Algorithm

```

Initialize the first population of ants and ant lions randomly
Calculate the fitness of ants and ant lions
Find the best ant lions and assume it as the elite
(determined optimum)
while the end criterion is not satisfied
    for every ant
        Select an ant lion using Roulette wheel
        Update c and d using equations  $c^t = \frac{c^t}{I}$  and
 $d^t = \frac{d^t}{I}$  Create a random walk and normalize it
using Equations  $X(t) = [0, cumsum(2r(t_1) - 1), cumsum(2r(t_2) - 1), \dots, cumsum(2r(t_n) - 1)$  and  $X_i^t = \frac{(X_i^t - a_i) \times (d_i^t - c_i^t)}{(b_i - a_i)} + c_i^t$ 
Update the position of ant using equation  $Ant_i^t = \frac{R^t + R^t}{2} E$ 
    end for
Calculate the fitness of all ants
Replace an ant lion with its corresponding ant if it
becomes fitter  $Antlion_j^t = Ant_i^t$  if  $f(Ant_i^t) > f(Antlion_j^t)$ 
Update elite if an ant lion becomes fitter than
the elite
end while
Return elite

```

Figure 1: ALO Algorithm

3.1 PARTICLE SWARM OPTIMIZATION (PSO)

PSO was originally conceived as a representation of organisms in a bird flow or fish school. Later it was simplified and was used for solving optimization problems. PSO uses a bunch of particles called the swarm. These particles are allowed to move around and explore the

search-space. These particles move in a direction which is guided by;

1. The particle's own previous velocity (Inertia)
2. Distance from the individual particles' best known position (Cognitive Force)
3. Distance from the swarms best known position (Social Force) (Thiyagaraj, 2018)

PSO is a computational method that optimizes a problem by iteratively trying to improve a candidate solution with regard to a given measure of quality. It solves a problem by having a population of candidate solutions, here dubbed particles, and moving these particles around in the search-space according to simple mathematical formulae over the particle's position and velocity. Each particle's movement is influenced by its local best known position, but is also guided toward the best known positions in the search-space, which are updated as better positions are found by other particles. This is expected to move the swarm toward the best solutions (Wikipedia, 2019).

Algorithm 2: PSO Algorithm

```

for each particle i = 1, ..., S do
    Initialize the particle's position with a uniformly distributed
    random vector:  $x_i \sim U(b_{lo}, b_{up})$ 
    Initialize the particle's best known position to its initial
    position:  $p_i \leftarrow x_i$ 
    if  $f(p_i) < f(g)$  then
        update the swarm's best known position:  $g \leftarrow p_i$ 
    Initialize the particle's velocity:  $v_i \sim U(-|b_{up} - b_{lo}|, |b_{up} - b_{lo}|)$ 
    while a termination criterion is not met do
        for each particle i = 1, ..., S do
            for each dimension d = 1, ..., n do
                Pick random numbers:  $r_p, r_g \sim U(0,1)$ 
                Update the particle's velocity:  $v_{i,d} \leftarrow \omega v_{i,d} + \phi_p r_p (p_{i,d} - x_{i,d}) + \phi_g r_g (g_{d,d} - x_{i,d})$ 
                Update the particle's position:  $x_i \leftarrow x_i + v_i$ 
                if  $f(x_i) < f(p_i)$  then
                    Update the particle's best known position:  $p_i \leftarrow x_i$ 
                if  $f(p_i) < f(g)$  then
                    Update the swarm's best known position:  $g \leftarrow p_i$ 

```

Figure 2: PSO Algorithm

The values b_{lo} and b_{up} represents the lower and upper boundaries of the search-space. The termination criterion can be the number of iterations performed, or a solution where the adequate objective function value is found. The parameters ω , ϕ_p , and ϕ_g are selected by the practitioner and control the behaviour and efficacy of the PSO method. (Wikipedia, 2019)

4 EXPERIMENT

Data collection and Description

The data was taken from OR-library and used by Shu (Shu, 2013), where a set of facilities F consisting of five facilities and the set of cities Q consisting of seven cities. We first evaluate the algorithms on the Uncapacitated Facility Location Data (UFLD) provided by the OR-library and used as in Shu, (2013) to find the optimal location of five facilities required to service some clients in some cities. The data consist of five facilities and seven cities. The facilities cost f_i (for $i = 1, 2, 3, 4, 5$) and facility-city connection cost Q_{ij} (for $j = 1, 2, 3, 4, 5, 6, 7$) is given in figure 3 as follows (Shu, 2013). Figure 4 shows the facility-city connectivity for UFLD. The source nodes are the facilities while the destination nodes are the cities and while the cost of connecting a facility-city are the values on the edges between nodes. The problem is to minimize this graph such that all cities must be connected to at least one facility at a minimum cost.

UFLD: FIVE FACILITIES AND SEVEN CITIES

$$f_4 = 5, f_1 = 6, f_5 = 8, f_2 = 10, f_3 = 12$$

$$Q_{12} = 2, Q_{11} = 4, Q_{13} = 5, Q_{15} = 6, Q_{14} = 8$$

$$Q_{22} = 2, Q_{21} = 3, Q_{23} = 6, Q_{24} = 7, Q_{25} = 9$$

$$Q_{33} = 1, Q_{34} = 4, Q_{31} = 6, Q_{35} = 7, Q_{32} = 8$$

$$Q_{43} = 2, Q_{44} = 3, Q_{45} = 4, Q_{41} = 5, Q_{42} = 7$$

$$Q_{55} = 3, Q_{52} = 4, Q_{51} = 7, Q_{54} = 9, Q_{53} = 10$$

$$Q_{61} = 1, Q_{64} = 3, Q_{65} = 6, Q_{63} = 8, Q_{62} = 9$$

$$Q_{74} = 3, Q_{72} = 5, Q_{75} = 7, Q_{73} = 8, Q_{71} = 12$$

Figure 3: Datasets

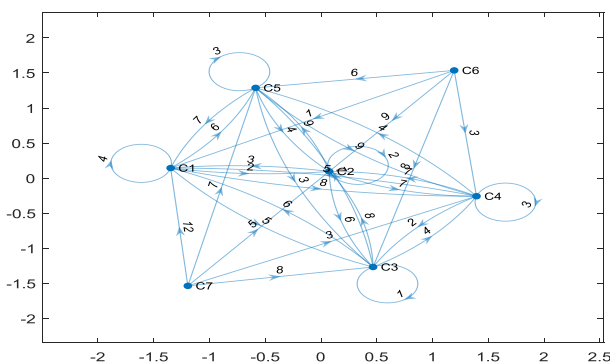


Figure 4: Facility-city graph for UFLD

TABLE 1: ALO AND PSO PARAMETERS

S/N	Parameter	Value
1	Ant lion population (n)	20-40
2	Ant population	20-40
3	Maximum Iteration	50
4	Number of values	5
5	Number of particles	55
6	Number of iteration	1000

PERFORMANCE EVALUATION

The performance of the model was evaluated using the average cost value obtained after 10 independent runs. The solution with the minimum cost is preferred with no constraint violation and the result will be compared with that obtained by (Shu, 2013).

5 RESULTS AND DISCUSSION

In this section, the result obtained by ALO is compared with PSO. First, the results obtained by ALO is presented and the results are validated with the results obtained using Particle Swarm Optimization (PSO) algorithm. From the trend of the performance, ALO obtained better solutions compared to PSO

5.1 ALO RESULTS

Figure 5, 7 and 8. Shows the convergence plot for ALO applied to data 1, Data 2 and Data 3. The plot is a plot of elite ant lion (average minimum cost of allocating cities to facilities) on the Y-axis and number of iterations on the X-axis. For all the cases, 1000 iterations were performed and repeated five independent runs. From the plot, the minimum cost obtained by ALO for Data 1 is 55 at 90th iteration, Data 2 is 80 at 80th iteration and Data 3 is 114 at 100th iteration. Similarly, Figure 6, Figure 9 and Figure . Shows the minimized Facility-City connectivity graph for Data 1, Data 2 and Data 3. The source nodes 1 to 5 indicate the facility and the destination indicates the cities. The result show that the algorithm is efficient in obtaining a minimum cost and minimized connectivity graph for the problem.

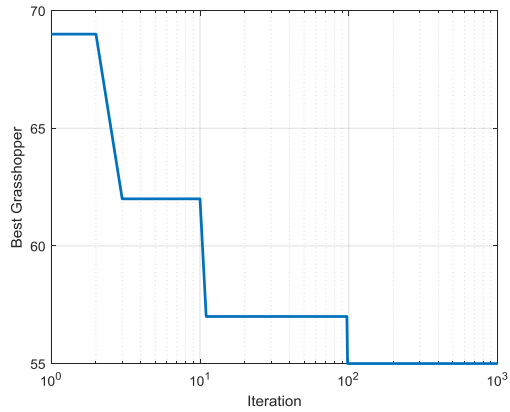


Figure 5: ALO Convergence curve

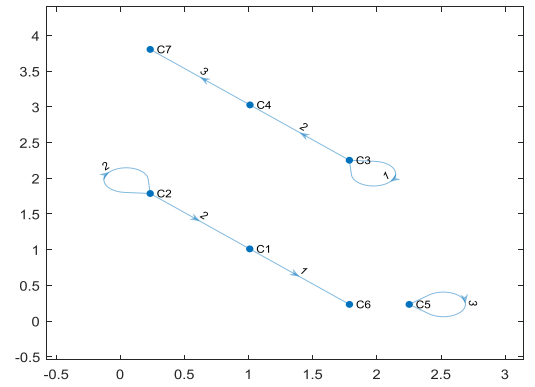


Figure 6: ALO Graph For Data 1

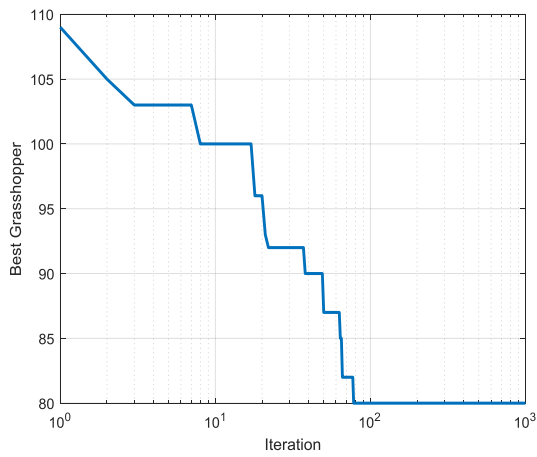


Figure 7: ALO Convergence curve

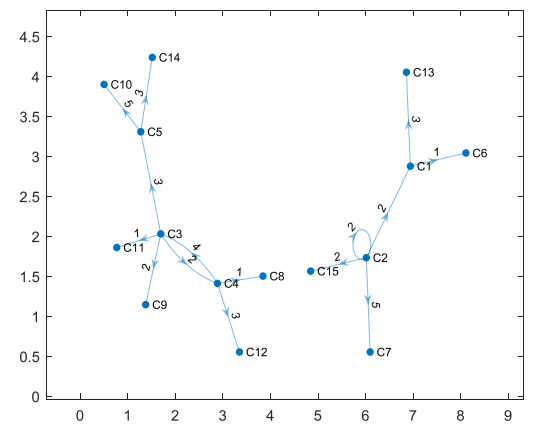


Figure 9: ALO graph for data 2

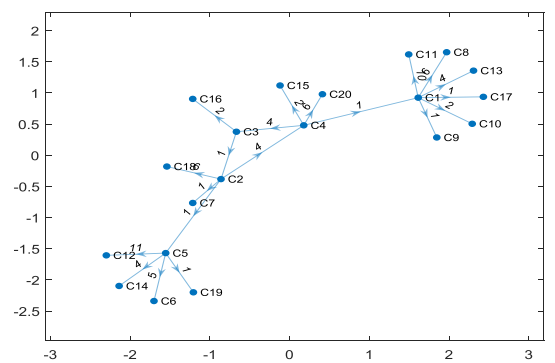
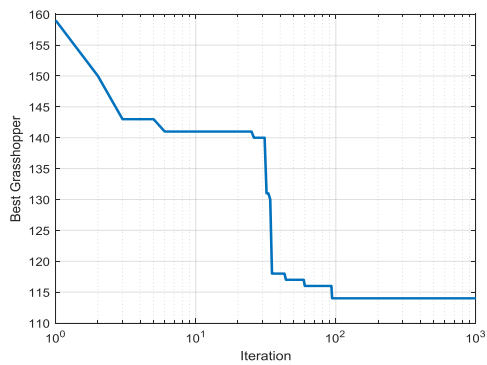


Figure 10: ALO graph for data 3

5.2 PSO Results

Figure 11, 12 and 14 shows the convergence plot for PSO applied to data 1,2,and 3. The plot is a plot of elite ant lion (average minimum cost of allocating cities to facilities) on the Y-axis and number of iterations on the X-axis. For all the cases, 1000 iterations were performed and repeated five independent runs. From the plot, the minimum cost obtained by PSO for Data 1 is 55 at 200th iteration, Data 2 is 83 at 310th iteration and Data 3 is 121 at 440th iteration. Similarly, Figure 12, 15 and 16 shows the minimized Facility-City connectivity graph for Data 1,2 and 3. The source nodes 1 to 5 indicate the facility and the destination indicates the cities. The result show that the algorithm is efficient in obtaining a minimum cost and minimized connectivity graph for the problem.

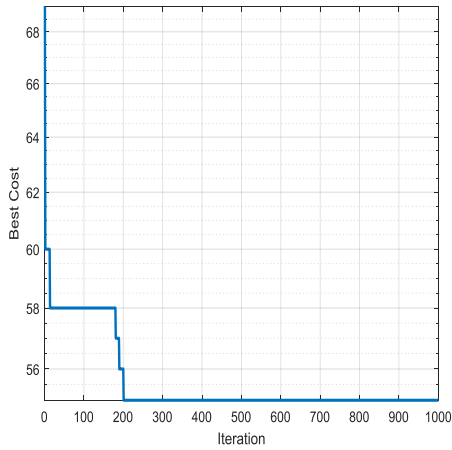


Figure 11: PSO Convergence curve

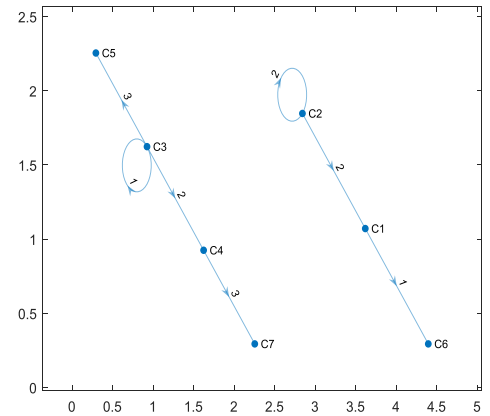


Figure 12: PSO graph for data 1

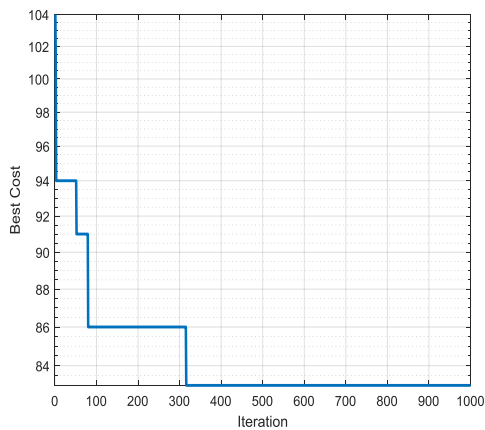


Figure 13: PSO Convergence curve

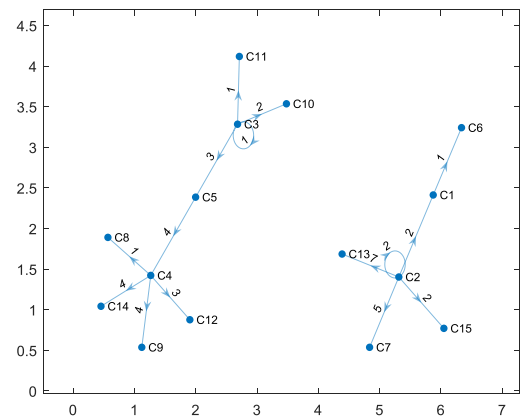


Figure 15: PSO graph for data 2

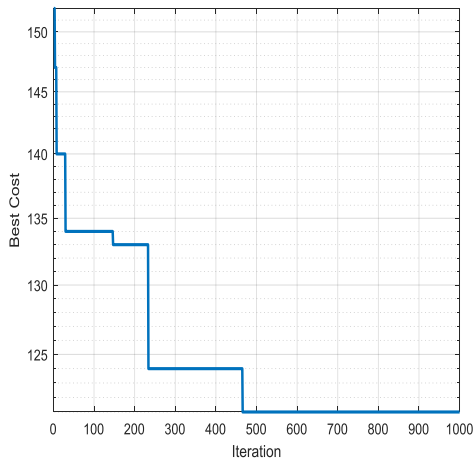


Figure 14: PSO Convergence curve

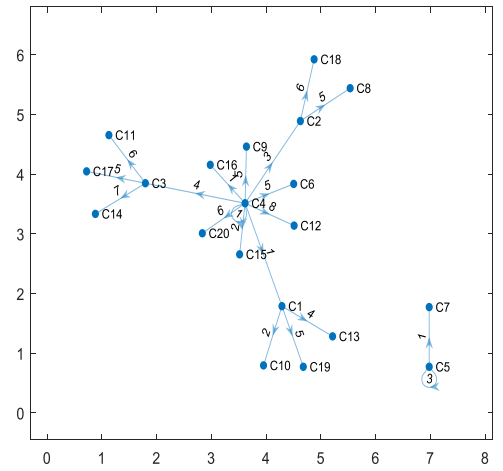


Figure 16: PSO graph for data 3

5.3 PERFORMANCE EVALUATION AND VALIDATION OF ALO AND PSO FOR UFLP

In this section, the performance of ALO and PSO are compared in order to ascertain the effectiveness of the proposed ALO on the three Data problems. The results were also validated with the results obtained by Shu, (2013) for data 1. Table 3 shows the summary of convergence cost obtained for UFLP. From the table, ALO obtained 55, 80 and 114 for Data 1, Data 2 and Data 3 respectively. PSO

however, obtained 55, 83 and 121 for Data 1, Data 2 and data 3 respectively. This is an indication of the robustness of ALO as the data size increases as shown in Figure 16. Similarly, when compared with Shu, (2013), ALO also performs better. It is clear from the table that ALO produces much better results compared to PSO.

TABLE 2 : MINIMUM COST AND NUMBER OF ITERATION OBTAINED FROM THE ALO AND PSO OPTIMIZERS

Dataset	Minimum Cost		No. Of Iteration	
	ALO	PSO	ALO	PSO
Data 1	55	55	90th	200th
Data 2	80	83	80th	310th
Data 3	114	121	100th	

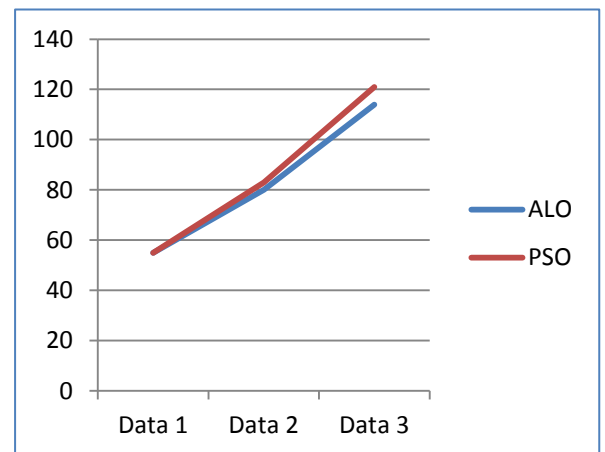


Figure 16: ALO vs PSO performance

6 CONCLUSION

This paper presents an Uncapacitated facility location problem using Ant lion optimizer and Particle swarm optimization. The performance of ALO and PSO are compared in order to ascertain the effectiveness of the ALO on Un-capacitated facility location problem, indicating more accurate results and takes less time. The results obtained show the robustness of ALO for problems over other algorithm compared with for UFLP, also obtained the minimum cost values for the three Data sets experimented upon. In all the test problems, the results indicate that ALO can get better optimum fitness results, showing better convergence speed. ALO is also more stable and robust compared with PSO, from the results LO appear to converge faster and had better accuracy. The main advantage of ALO algorithm over PSO is the good ability of finding the solution.

REFERENCE

1. Ali, R. G., Mehmet, S. (2008). A discrete particle swarm optimization algorithm for uncapacitated facility location problem. *Journal of artificial evolution and applications, Volume 2008, Article ID 861512*, P9.
2. Al-sultan, K. and Al-Fawzan, M. (1999). A tabu search approach to the uncapacitated facility location. *Annals of Operations Research, vol. 86*, pp. 91–103,.
3. Anovas, C´ L., Garc´ia, S., Labb´e, M., and Mar´in, A. (2007). A Strengthened Formulation for the Simple Plant Location Problem with Order. *Operations Research Letters, 35 (2007)*, 141-150.
4. Armacheska, M.,Kris, C., Cinmayi, G. M., and Vicente, C. (2018). Cuckoo search via levy flights applied to uncapacitated facility location problem. *J Ind Eng Int (2018), 14*, 585-592.
5. Arnab, K., Parichay, C., and Somnath B. (2014). An ant colony optimization algorithm for uncapacitated facility location problem. *Artificial intelligence and applications, Vol 1,Number 1, 2014*.
6. Gen, M., Tsujimura, Y., and. Ishizaki, S. (1996). Optimal design of a star-lan using neural networks. *Computers & industrial engineering, vol. 31, no. 3-4*, pp. 855–859.
7. Ghosh, D. (2003). Neighborhood search heuristics for the uncapacitated facility location problem. *European Journal of Operational Research, vol. 150, no. 1*, pp. 150–162, 2003.
8. Guner, A. R., and Sevcli, M. (2008). A discrete particle swarm optimization algorithm for uncapacitated facility location problem. *Journal of Artificial Evolution and Applications, vol. 2008*, p. 10, 2008.
9. Hiroaki, T., Kenichi, I., and Jun, M. (2011). A genetic algorithm for the uncapacitated facility location problem. *electronics and communication in japan, Vol. 94 No. 5 2011*, p 628-635.
10. Ling-Yun, W., Xiang-sun, z., and Ju-Ling, Z. (2006). Capacitated facility location problem with general setup cost. *Computer and operations research, 33(2006)*, 1226-1241.
11. Maric, M., Stanimirovic, Z., Milenkovic, N., and Djenic A. (2015). Metaheuristic approaches to solving largr-scle bilevel uncapacitated facility location problem with clients' preferences. *yugoslav journal of operation research, 25 (2015) NO.3*, p 365-378 Doi 10.2298/YJOR130702032M.
12. Michel, L. and Van Hentenryck, P. (2004). A simple tabu search for warehouse location. *European Journal of operational research, vol. 157, no. 3*, pp. 576–591, 2004.
13. Neven, L., Brenda, J. F., and Parham, A. (2010). Solving the Uncapacitated Facility Location Problem Using Message Passing Algorithms. *Appearing in Proceedings of the 13th International Conference on Artificial Intelligence and statistics chia laguna resort, Vol 9 of JMLR. Sardinia, Italy*.
14. Vaithyanathan, S., Burke, L. I., and Magent M. A. (1996). Massively parallel analog tabu search using neural networks applied to simple plant location problems. *European Journal of Operational Researchvol. 93, no. 2, pp. 317–330, 1996., vol. 93, no. 2*, pp. 317–330.



15. Vasilev, I.L., and Klimentova, K.B. (2010). The Branch and Cut Method for the Facility Location Problem with Clients' Preferences. *Journal of Applied and Industrial Mathematics*, 4 (2010) , 441–454.
16. Wenhao, S. (2013). A fast algorithm for facility location problem. 2013 Academy Publisher, p 2360-2366



Potential, Barriers and Prospects of Biogas Production in North-Central Nigeria

¹Ahonle Jennifer Eferi & ²Adeoye Peter Aderemi

^{1,2}Department of Agricultural and Bioresources Engineering,
Federal University of Technology, Minna.

*Corresponding author email: peter.adeoye@futminna.edu.ng, +2348035868053

ABSTRACT

Despite research work and implementation of biogas having started as early as in the 1980s, Nigeria is lagged behind in the adoption and use of biogas in the sub-Saharan Africa. The study established that there is a theoretical biogas potential of 76PJ per annum from animal manure and crop residues. This is sufficient to provide energy for cooking and lighting in more than 16 million households. Lack of funding, lack of policy, regulatory framework and strategies on biogas, unfavorable investor monetary policy, inadequate expertise, lack of awareness of the benefits of biogas technology among leaders, financial institutions and locals, resistance to change due cultural and traditions of the locals, high installation and maintenance costs of biogas digesters, inadequate research and development, improper management and lack of monitoring of installed digesters, complexity of the carbon market, lack of incentives and social equity are among the challenges that have derailed the adoption and sustainable implementation of domestic biogas production in Nigeria. Unless these are addressed, it is unlikely that the biogas sector in Nigeria will flourish.

Keywords: *Biogas, Digester, Implementation, Installation, Research.*

1 INTRODUCTION

Biogas technology is an alternative source of energy that utilizes various organic wastes in order to produce biogas. Some countries that lack natural abundance or inadequate distribution of energy supply have over the years adapted biogas generating equipment to meet rural energy needs. In the 1970s when renewable energy became recognized as an entity. A conference was held at Imperial College, University of London where researchers agreed on the great potential for biogas technology in many countries of the world, focusing more on the developing countries. Biogas has provided an economically viable and sustainable means of meeting the thermal energy needs of China (7.5 million), India (3 million) and Nepal where over 37,000 biogas digesters were installed from 1992 to 1998 (Deolle, 1998). The rapid development of biogas technology in most European countries could be linked to various strategies employed by the respective countries, and most especially by the Renewable Energy Directive (RES) proposed by the European Union, which sets a

binding target for all Member States to reach a 20% share of renewable energies in the total energy consumption by 2020. Biogas is a gaseous fuel, which is produced by the fermentation of organic material. The main component of biogas is methane gas and other gases like hydrogen sulphides, carbon dioxide, siloxanes and moisture also

form a part of biogas. Biogas is generally produced in a closed container where anaerobic digestion takes place efficiently and the closed container is called biogas digester. It is called so since the digestion of organic matter takes place in the presence of bacteria. The bacteria present in the digester need to be fed everyday with food waste and water.

2.0 Biogas Production and Composition

There are four stages in which the decomposition of bio-waste takes place: Hydrolysis, Acidogenesis, Acetogenesis and Methanogenesis. The first step of the digestion process is bacterial hydrolysis (of the input materials). This is done in order to degrade the organic polymers which are insoluble in nature, for example, carbohydrates. The next step is to convert amino acids and sugars into ammonia, carbon dioxide, hydrogen and organic acids

Table 1. Specific Composition of Biogas

Compound	Formula	percentage
Methane	CH ₄	50-75
Carbon Dioxide	CO ₂	25-50
Nitrogen	N ₂	0-10
Hydrogen	H ₂	0-1
Hydrogen Sulphide	H ₂ S	0-3
Oxygen	O ₂	0-0.5

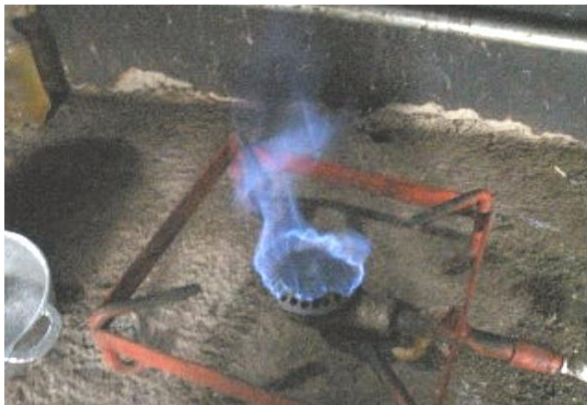


Figure 1: A typical stove burning with Biogas.

The process of anaerobic digestion for the production of biogas is usually made to take place in a cylindrical tank that is air tight. These air tight cylindrical tanks are called anaerobic digesters. Concrete bricks or cement or steel are used to build up the digester, which is usually built underground. The mixing tank has an inlet attached to it, this is for feeding in the cow dung. A gas outlet is also present. The slurry or the used cow dung is made to come out of an outlet present in the digester. This slurry which comes out of the digester can be used as manure. When cow dung is used as a substrate, the process takes around 2-3 week.

3.0 Different Solid Wastes from which Biogas can be Generated

A few solid wastes from which biogas can be generated are:

3.1. Food wastes or green wastes:

Food that is discarded or left uneaten are called food wastes, basically the wastes that are produced by food items are called food wastes. Food waste, decomposable organic matter and kitchen waste which consist of a little amount of carbon dioxide and of methane, are used to produce biogas, which is then used as an alternative for cooking gas or LPG. Also, the waste materials can be

disposed of efficiently without leaving behind any odour or flies. The slurry or the digested slurry obtained can then be used as organic manure in gardens.

4.0 PROSPECTS OF BIOGAS TECHNOLOGY IN NIGERIA.

With a stable climate and easy availability of plant materials and wastes (cow dung, poultry droppings, pig excreta among others) coupled with the current positive shift in agricultural policies of government, Nigeria is in a good position for adopting and popularizing biogas. At present, much of dung produced by about millions of herds of cattle in is either wasting or burnt away as wasteful cooking fuel. Biogas is not widely known in Nigeria much of the materials available in Nigeria are reports of scientific researchers into the technical aspects and basic factors for biogas production, especially on raw materials (Garba and Ojukwu,1998, Zuru et al,1998). However, The Federal government in 2001 established the National Biotechnological Development Agency (NABDA) that is mandated among others to develop conservation strategies to promote sustainable utilization of Nigeria's enormous biological resources and to facilitate the speedy evaluation and utilization of the processes and products of biotechnology while ensuring environment stewardship (Omaliko, 2006).

In Nigeria, some biogas projects have been executed, including construction of biogas plants at Zaria prison in Kaduna, Ojokoro in Lagos, Mayflower School Ikene in Ogun State, and a biogas plant at Usman Danfodiyo University in Sokoto with capacity of the digesters ranges between 10 and 20m³ (Abubakar However, the biogas projects are yet to be commercialized, since most of them are either non-operational or still at the research stage.

4.1 Biogas Production from Crop Waste

Agricultural crop wastes are potential sources of biogas energy, especially in Nigerian rural areas where nearly everyone practices farming. Nigeria produces a wide range of agricultural crops in large quantities for consumption and exportation, and consequently huge amount of residues are generated from the crops after harvest. Agricultural crop wastes comprise of rotten crops due to inadequate storage facilities, Infected crops due to diseases and also residues produced from crop processing after harvest. As regards animal fodder, the most commonly fed crop residues include cassava and yam peels, cowpea husk, and groundnut husks, brans, oilcakes, maize, millet, and sorghum stovers (DE-Leew 1997; Onwuka et al. 1997; Singh et al. 2011). Leguminous crop residues are often preferred to cereal residues as animal fodder due to their higher nutritive value, digestibility, crude protein content, and minerals (Owen 1994). This greatly affect the quantity of crop residues available for biogas production. Taking the crop residues used for other purposes into consideration,



the quantity of available crop residues for biogas production was estimated at approximately 52 million tonnes, from which 21 billion cubic metres of methane gas could be generated at 35^oc.

5.0 HARNESSING BIOGAS OPPORTUNITIES IN NORTH CENTRAL STATES OF NIGERIA

5.1 Plateau State.

The government of Plateau, the twelfth largest state in Nigeria, located circa in the center of the country, has developed and signed off a new policy to advance the development and deployment of renewable sources of energy to its residents. The three policies – State Policy and Strategy on Renewable Energy, Plateau State Rural Electrification Plan, and the Public Private Partnership (PPP) Guidelines for Solar Mini-Grids, was recently launched by the state at the third edition of the annual National Council on Power (NACOP) hosted in its capital, Jos, with the state asking the Rural Electrification Agency (REA) to now look its way for more projects. Going by this adoption of renewable energy in Plateau state is still at planning level.

5.2 Benue State

The Nigerian National Petroleum Corporation (NNPC) is set to conclude on the choice of a core investor for the proposed Bio-fuel plant in Agasha Guma area of Benue State. The NNPC said upon completion, the plant was projected to generate about one million direct and indirect jobs for the populace noting that the project would help link the energy sector with the agric. sector through the commercial production of biofuels from selected energy crops. Other components of the project include a sugar cane feedstock plantation of about 20,000 hectares; a cane mill and raw/refined sugar plant capable of producing 126,000 tonnes annually as well as a fuel-ethanol processing plant with production capacity of 84 million litres annually. The bio-fuels projects will also help to establish the Bio-gas cogeneration power plant which will generate 64 MW; a carbon dioxide recovery and bottling plant that will produce 2, 000 tonnes annually as well as an animal feed plant that will produce 63, 000 tons annually. This also shows that Benue state is yet to start using biogas as a fuel at commercial scale.

5.3 Kwara State

The home biogas units are also said to be simple to operate, and require minimal annual maintenance, and although the biogas can be burned on a regular stove, at least one burner does need to be converted to use the fuel. The Department of Agricultural and Biosystems Engineering, University of Ilorin, Kwara State has conducted series of local researches on biogas, organic fertiliser and biofuel development. With

the efforts so far, Kwara state is confident that the technology with the lowest capital and operating costs that would allow more Nigerians generate fuel from organic waste.

5.4 Nassarawa State

FCT Administration Sets up Biogas plant at Abattoirs in Karu Nasarawa state. Poor sanitary condition of abattoirs in the Federal Capital Territory has been a challenge to the government, residents and other stakeholders, who depend on the slaughter houses for their daily meat needs. The poor environmental condition of most abattoirs is said to have contributed to the spread of diseases, which help in endangering human health. In a bid to address the challenges, the government had made several efforts but the conditions have persisted, creating anxieties in the minds of residents. Secretary of Agriculture and Rural Development Secretariat, Federal Capital Territory, Stanley Nzekwe, said that when he assumed office, the condition of abattoirs in FCT was so poor, that he had to start work towards evacuating animal dung that was allowed to pile up everywhere in these abattoirs. Recently, the sanitary condition of the abattoirs attracted the attention of an International Environmental Organization, African Environment Action Network(EANet-Africa). The organization has taken some steps to provide a biogas plant said to have the capacity of addressing the challenges of evacuation of animal waste in these slaughter houses.

5.5 Niger State

Niger State (Nigeria) was selected as a case study of renewable, affordable and user friendly clean energy provision in remote areas of developing countries. Niger state has 80% of its 4.5 million population living in rural agrarian areas with low literacy rates, there is a lack of wind thus eliminating wind as widely available potential power source. Based on the assessment of the local large insolation, the type of agricultural, biomass and husbandry resources, this study selected the design of anaerobic digestion units processing mostly animal and human waste, and whose heating and power requirement would be entirely provided by solar photovoltaic/thermal to maintain optimum efficiency of the biogas production. The designs were carried out at the scale of up to 15 household demand (community scale), Volume and therefore the production of biogas maybe increased or decreased in the design considered, and local, low cost resilient material were proposed. The proposed system was costed for a community of 24 people, demonstrating the potential for clean and renewable gas production economically. This also shows that in Niger state adoption of biogas as a commercial source of energy is still at proposal stage.



5.6 Kogi State

The Nigerian National Petroleum Corporation (NNPC) and the Kogi State Government have signed a Memorandum of Understanding (MoU) for the development of a sugarcane-based fuel ethanol processing plant that would produce 84 million litres of biofuel per annum. The MoU was signed in Abuja on February 27 between Dr Maikanti Baru, Group Managing Director of the Nigerian National Petroleum Corporation (NNPC) said that the MoU was “another milestone in the history of the state.” According to Dr Baru, the signing of the MoU would lead to the formation of a Special Purpose Vehicle (SPV) to steer the future activities of the proposed Kogi Biofuels Project in Kaba/Bunu. The sugarcane feedstock would require 19 000 hectares and Dr Baru stated that discussions had been held with the various parties and stakeholders on the Kogi Biofuels Project on the modality for the implementation, adding that agreements had been reached on the first stage of the project. In addition, the Alape Staple Crop Processing Zone (SCPZ) in Kogi State, provides suitable agronomics for the cultivation of sugarcane, cassava and oil palm.

6.0 CHALLENGES OF SUSTAINABLE BIOGAS USE IN NIGERIA

6.1 Policy and strategy

Biogas technology transfer requires good fiscal policies which provide incentives. There are no such fiscal policies to encourage investment in biogas technology in most sub-Saharan African Countries Energy policies and strategies put in place by governments are not focused and thereby fail to achieve their intended goals of attracting both domestic and foreign investments in biogas production.

6.2 Inadequate expertise and training

Lack of skilled and experienced masons to undertake the construction and maintenance of biogas plants is a constrain hindering the fully dissemination and adoption of biogas production in Nigeria. Universities in Nigeria have not designed and implemented appropriate programs to teach and train students in biogas technology.

6.3 Research and development

Presently, the research institutes are not adequately equipped as far as renewable energy research and development is concerned. Research funds are often not adequate or are misapplied. There has not been enough research in higher learning institutions on biogas technology due to non -support from responsible government ministries

6.4 Feedstock availability and other technical issues

Though technically available, feedstock maybe

practically inadequate due to a number of reasons, such as grazing patterns of animals, location of fields, farming practices. Where one kind of feedstock is inadequate, co-digestion may just be the answer. Information is required on how to pretreat the manure before adding it to the digester and how much water should be used.

6.5 Lack of political will

Suberu et al. (2013) argue that political will is among the most important factors that have a significant impact on determining the amount of renewable energy in the national energy mix. In Nigeria political will in renewable energy has lagged behind as compared to other developing countries elsewhere across the globe

6.6 Resistance to change

Inertia to change from use of primitive energy forms to modern energy such as biogas has been attributed to customs and traditions in some communities. The perceived unreliability of biogas also has contributed to resistance to change in some instances. A study conducted in Nasarawa state and results showed that there is a tendency among urban dwellers, especially those in the peri-urban areas, to continue using charcoal or firewood because they feel it is cheaper even when their homes are connected to the grid

6.7 Financing

Financial institutions often perceive the bioenergy sector as high risk, making it very challenging for investors to obtain funds. Inadequate funds to finance power generation, transmission and distribution coupled with low rates of returns due to high operating costs and low consumption are some of the challenges faced by some North central states in Nigeria.

7.0 CONCLUSION

The future is green energy, sustainability and renewable energy. To make life possible without a hitch, alternative sources of energy should be used. Utilization of biogas reduces global warming and also prevents harmful diseases. The availability of feedstock for biogas production in Zambia is adequate. Cow dung being and maize cobs are the major feedstock sources among the animal waste and crop residues respectively. There are many technical and socioeconomic constraints that have hindered full adoption and sustainability of biogas production in Zambia. Lack of mobilization of external and local funds, the complexity of the carbon market, lack of policy, strategy and regulations in biogas production, high capital and maintenance costs, lack of trade and investment incentives, resistance to change among the beneficiaries, lack of co-operation between implementers of biogas projects and researchers, inadequate research and



development due to insufficient funding, low levels of full time equivalent researchers who are qualified at PhD level, inadequate expertise and training in biogas production and unfair equity are some of the major constraints hindering adoption and implementation of biogas projects in Nigeria. Developing and implementing renewable energy systems will increase security of national energy supply and reduce dependency on energy from fossils, it will also protect the environment in terms of climate change, as a result, of their uncontrolled emission into the atmosphere.

7.0 REFERENCE

- Abila, N. (2012). Biofuels development and adoption in Nigeria: Synthesis of drivers, incentives and enablers. *Energy Policy* 43: 387-395.
- Abubakar, M. (1990). Biogas generation from animal wastes. *Nigeria Journal of Renewable Energy* 1(1), 69-73.
- Adewunmi, I. K., Ogedengbe, M. O., Adepetu, J. A., and Fabiyi, Y. L. (2005). Planning Organic fertilizer industries for municipal solid wastes management. *Journal of Applied Sciences Research* 1(3): 285-291.
- Agbo, K.E., and Eze, J.I. (2011). *Anaerobic digestion of municipal solid waste for generation of energy: prospects and challenges in Nigeria*. Nigeria Journal of Solar Energy, 22: 130-137
- Akpan, U.S.' and Ishak, S.R. (2012). Electricity Access in Nigeria: is off-grid electrification using solar photovoltaic panels economically viable? A sustainability, Policy, and Innovative Development Research (SPIDER) Solutions Nigeria Project. (Interim Report).
- Amori, A. A., Fatile, B. O., Ihuoma, S. O., and Omoregbee, H. O. (2013). Waste generation and management practices in residential areas of Nigerian tertiary institutions. *Journal of Educational and Social Research* 3(4):664 – 670.
- Arthur, M., Zahran, S., and Bucini, G. (2010). On the adoption of electricity as a domestic source by Mozambican households. *Energy Policy* 38: 7235-7249.
- Atuanya, E. I., and Aigbirior, M. (2002). Mesophilic biomethanation and treatment of poultry wastewater using a pilot scale UASB reactor. *Environmental Monitoring and Assessment*. 77:139-147.
- Babayemi, J. O., and Dauda, K. T. (2009). Evaluation of solid waste generation categories and disposal options in developing countries: A case study of Nigeria. *Journal of Applied Science and Environmental Management*. 13, 83-88.
- Blight, G. E., and Mbande, C. M. (1996). Some problems of waste management in developing countries. *Journal of Solid Waste Technology Management*. 23(1):19-27.
- Bond, T., and Templeton, M. R. (2011). History and future of domestic biogas plants in the developing world. *Energy for Sustainable Development* 15: 347-354
- Chaggu, E. J., Mashauri, A., VanBuren, J., Sanders, W., and Lettinga, J. (2002). Profile: Excreta disposal in Dar es Salaam. *Journal of Environmental Management*. 30(5): 609-620.
- Chen, Y., Yang, G., Sweeney, S., and Feng, Y. (2010). Household biogas use in rural China: a study of opportunities and constraints. *Renewable and Sustainable Energy Reviews* 14(1):545-549.
- Dangogo, S. M., and Fernando, C. E. C. (1986). A simple biogas plant with additional gas storage system. *Nigerian Journal of Solar Energy*. 5:138-141.
- Davis, M. (1998). Rural household energy consumption: The effects of access to electricity-evidence from South Africa. *Energy Policy* 26: 207-217.
- Federal Ministry of Environment (2005): *policy guideline on solid waste management*, Federal Republic of Nigeria.
- Gerardo, B., Et al (2001): Solid Waste Characterisation Study in Guadalajara Metropolitan Zone, Mexico. *Waste Management and Research*. 14 (6): 338 – 346.
- Igbinomwanhia, D.I (2010): Characterization Residential Solid Waste In Benin Metropolis, Nigeria. *International Journal of Engineering*, 4(4): 479-486.
- Igbinomwanhia, D.I. and E.N Ohwovorirole (2011) A Study of the Solid Waste Chain in Benin Metropolis, Nigeria. *Journal of Applied*



Sciences and Environmental Management, 15
(4): 589 – 593.

- Igoni, A.H., Abowei, M.F, Ayotamuno, M.J., and Eze, C.L. (2008). Effect of total solids concentration of municipal solid waste on the biogas produced in an anaerobic continuous digester. *Agricultural Engineering International: The CIGR E journal*. 8(6):11 – 22.
- Ikelegbe, O.O and Ogeah, F.N. (2003). Perception and response to the challenges of environmental sanitation problems in Benin City and its environs. *Benin Journal of Social Science*, 12(2), 189 -200.
- Ogweleka, T.C. (2003). Analysis urban solid waste in Nsuka , Nigeria. *The journal of Solid Waste technology and Management, Department of Civil Engineering Widener University, Chester, U.S.A*, 29(4):668 – 690.
- Sadjere, E.G and Ariavie, G.O (2012). Determination of electrical energy equivalent of a typical household in the Niger Delta region of Nigeria. *International Journal of Academic Research*, 4(3): 180 – 196.



DESIGN ANALYSIS OF MANUALLY OPERATED MACHINE FOR ON-ROW TRANSPLANTING OF PADDY RICE

*Ibrahim, T. M., Ndagi, A., Katun. I. M. & Anurika, U. A.

Department of Agricultural & Bioenvironmental Engineering, The Federal Polytechnic, Bida Niger State.

*Corresponding Author: timprimes45@gmail.com +2347061690150

ABSTRACT

Manual transplanting of paddy rice seedlings exposes small scale rice farmers to musculoskeletal disorders as well as back problems resulting from repetitive bending and awkward postures involved. This research is focused on the design analysis of a simple but durable manually operated machine for on-row transplanting of paddy rice. A simple manual rice transplanter was developed consisting of the following basic components: seedling tray, chassis, picking fork/fingers, wheels assembly, transmission drives, pulling mechanism, and float board. Some of the design parameters of considered includes mean forward speed 1.4 m/s, plant spacing 250 mm and assumed loose physical state of rice seedlings. The designed machine theoretically weighting 163.84 N is to be operated by a single operator, and has a planting rate of 777 plants in a minute at the mean forward speed. The component analysis was conducted and power requirement for the machine is 41.3 W well below the power of average man which is 76 W.

Keywords: *Drudgery, seedling, picking fingers, musculoskeletal, float board*

1 INTRODUCTION

Rice (*Oryza sativa*) is a staple food in many countries of Africa and other parts of the world. This is the most important staple food for about half of the human race (Imolehim and Wada, 2000). Saka and Lawal (2009) classified rice as the most important food depended upon by over 50 percent of the World population for about 80 percent of their food need. Due to the growing importance of the crop, Food and Agricultural Organization (FAO, 2003) estimated that annual rice production should be increased from 586 million metric tons in 2001 to meet the projected global demand of about 756 million metric tons by 2030. Statistically, Nigeria is the highest importer of rice globally and the largest producer in West Africa.

Rice cultivation mainly depends on the following factor (i) age of the variety (ii) availability of moisture (iii) climatic conditions (iv) availability of inputs and labour (IRRI, 2017). Among these reasons, availability of inputs and labour play a huge role on deciding the method of production of rice. Several attempts have been made to mechanize paddy transplanting operation by introducing various transplanters and research is under progress to reduce the cost of production with less fatigue. Traditional method of rice transplanting requires frequent bending down and straightening up for transplanting process where as mechanical transplanter requires energy for pulling the transplanter in a puddled field.

In Nigeria, rice is grown by broadcasting of seeds and manual transplanting of seedlings. In practicing this method however, framers are exposed to musculoskeletal disorders as well as back problem due to repetitive bent posture needed in performing the task. Therefore the development of manually operated rice transplanter is considered a promising option as it would saves time,

labor, and ensure timely planting optimum plant density that well contribute to high productivity.

2 METHODOLOGY

2.1 DESIGN CONSIDERATIONS

The following factors were considered in the design specifications of the machine.

- Engineering properties of rice seedlings
- Availability of materials
- Strength
- Ease of operation.
- Ease of maintenance
- Material Cost.

2.2 DESCRIPTION OF THE MACHINE

The designed rice transplanter consists of the following major component parts: chassis, pulling assembly, seed tray, picking arm, chain drive, base board, ground wheel and central shaft. The rice seedling is loaded on two-sided seed trays which allows easy picking two seedlings each by the picking mechanism that is operated through the help of the ground wheel and four bar linkage. The two seedlings are planted by the oscillation of the picking arm.

2.3 WORKING PRINCIPLE

As the process is manual, the worker has to provide the initial motion. When the rice transplanter move forward the ground wheels rotate and there by generate torque to power chain drives through the central shaft. The wheels are provided with the fins so that they can

travel easily in the mud. The ground wheels are used to maintain constant distance between the two successive plants. The larger sprocket is provided on the same shaft with the ground wheels while the smaller one placed on the same shaft with the planting mechanism.

As the power will get transmitted to the smaller sprocket, it will rotate and oscillate the 4 bar linkage that forms planting mechanism. As the mechanism oscillates, the planting fingers pick the rice seedlings from the carefully positioned seedling trays and plant them in the mud. The planting finger is designed in such a way that rice plant should be easy to pick and only during the downward motion.

2.4 COMPONENT DESIGN ANALYSIS

2.4.1 GROUND WHEEL DESIGN

Assuming Diameter of the ground wheel $d = 260$ mm
The perimeter or circumference of ground wheel was calculated using the equation from Khurmi and Gupta (2005).

$$\text{Circumference of the ground wheel} = 2\pi r \quad (1)$$

$$\text{Radius} = \frac{d}{2} = \frac{260}{2} = 130 \text{ mm}$$

Standard spacing for rice plant = 25cm = 250mm

$$\begin{aligned} \text{Circumference of the ground wheel} &= 2 \times \pi \times 130 \\ &= 817 \text{ mm} \end{aligned}$$

Number of plants to be planted per ground wheel rotation

$$\begin{aligned} \frac{\text{Wheel circumference}}{\text{plant spacing}} & \quad (2) \\ &= \frac{817}{250} = 3.268 \text{ Plants} \end{aligned}$$

Note: This for single picking finger

Therefore for the two picking fingers
 $= 3.268 \times 2 = 6.536$

Therefore the number of plants that will be planted per each revolution of the wheel will be 6 plants.

Angular Speed of the Wheel

From Rajib *et.al.*, (2016)

$$\omega = \frac{v}{r} \quad (3)$$

$$N = \frac{60\omega}{2\pi} \quad (4)$$

Where:

ω = angular speed of the wheel in rad/seconds

v = Average walking speed of a man in m/s

r = radius of the wheel

N = revolution of the wheel in a minute

Adopted walking speed of a man $v = 1.4$ m/s

Assumed radius of the ground wheel $r = 130$ mm = 0.13m

$$\omega = \frac{1.4}{0.13} = 10.769 \text{ rad/sec}$$

$$N = 60 \times \frac{10.769}{2\pi} \times \pi = 102.839 \text{ rpm}$$

The revolution of wheel in a minute = 102.839

2.4.2 ANALYSIS OF CHAIN DRIVE

All the power transmission will be achieved by wheel, sprocket and chain mechanism.

Sprocket velocity ratio is given by $S_R = \frac{S_1}{S_2}$ (5)

Where,

S_1 is the number of teeth on the driving sprocket

S_2 is the number of teeth on the driven sprocket

Assuming

$$S_1 = 34$$

$$S_2 = 9$$

$$S_R = \frac{34}{9} = 3.78$$

Driving Sprocket N_1

Speed of driving sprocket is equivalent to speed of ground wheel rotation = 102.84 rpm

Driven sprocket N_2

$$\text{From } N_1 \times S_1 = N_2 \times S_2 \quad (6)$$

Where:

N_1 = speed of driving sprocket

N_2 = speed of driven sprocket

S_1 = No of teeth on the driving sprocket

S_2 = No of teeth on driven sprocket

$$N_1 = 102.84 \text{ rpm}$$

$$S_1 = 34$$

$$S_2 = 9$$

$$N_2 = 102.84 \times 3.78$$

$$N_2 = 388.4 \text{ rpm}$$

2.4.3 ANALYSIS OF PLANTING FINGERS

Rate of Oscillation of the Planting Fingers

The rate of oscillation of the planting fingers or mechanism is equivalent to the rotational speed of the driven sprocket powering it.

$$i.e. N_p = N_2 \quad (7)$$

Where

N_p = rate of oscillation of planting fingers, rpm

N_2 = speed of the driven sprocket in rpm

$$\therefore N_p = 388.4 \text{ rpm or } 388.4 \text{ cpm}$$

Number of Seedlings Transplanted in a Minute

Since in each cycle of oscillation, a hole is planted by each finger; therefore, number of seedlings transplanted in a minute of planting is determined using the relationship:

$$\dot{s} = n_f \times N_p \quad (8)$$

Where

\dot{s} = number of seedlings transplanted in a minute

n_f = number of planting fingers

N_p = rate of oscillation of the planting mechanism

$$\dot{s} = 2 \times 388.4$$

$$= 777 \text{ plants}$$

2.4.4 DETERMINATION OF WEIGHT

The total weight of a machine is calculated considering the length, geometric sections and mass per unit length of individual component materials used and the weight of various metals used was computed from Artizon (2017).

Weight of Chassis

The Chassis is made up of two different materials that is the angle Iron (25 x 25 x 3) and a hollow square pipe (30mm).

Length of Angle Iron selected

$$L = (147 \times 2) + (200 \times 2) + (395 \times 2) = 194 + 400 + 790 = 1384 \text{ mm} = 1.384 \text{ m}$$

Cross Sectional Area of Angle Iron

$$= (W_0 - W_i) \quad (9)$$

$$= (25 \times 25) - (22 \times 22) = 625 - 484 = 141 \text{ mm}^2$$

$$\text{Mass of Angle Iron} = \text{Volume } (v) \times \text{Density } (\delta) \quad (10)$$

$$D(\delta) = \text{Density of mild steel} = 7850 \text{ kg/m}^3$$

$$V = \text{Volume of Angle Iron} = 1.95 \times 10^{-4} \text{ m}^3$$

$$m = 0.000195 \text{ m}^3 \times 7850 \text{ kg/m}^3$$

$$m = 1.53075 \text{ kg}$$

$$\text{Weight of Angle Iron} = \text{Mass} \times \text{gravity} \quad (11)$$

$$m = 1.53075 \text{ kg}$$

$$g = 9.81 \text{ m/s}^2$$

$$1.53075 \times 9.81 \text{ m/s}^2$$

$$W = 15.016657 \text{ N} = 15.02 \text{ N}$$

Length of Square pipe.

$$L = 150 + (141 \times 2) + (147 + 2) + (80 \times 3) + (210 \times 2) + (134 \times 4)$$

$$L = 150 + 284 + 294 + 240 + 420 + 536$$

$$L = 1922 \text{ mm} = 1.922 \text{ m}$$

$$L = 1.922 \text{ m}$$

$$\text{Cross sectional Area of Square hollow pipe} = (W_0^2 - W_1^2) \quad (12)$$

W_0 = Outer width of the pipe

W_1 = Inner width of the pipe

$$W_0 = 30 \text{ mm} = 0.03 \text{ m}$$

$$W_1 = 26 \text{ mm} = 0.026 \text{ m} = (0.03^2 - 0.026^2)$$

$$\text{Cross Sectional area} = (0.03^2 - 0.026^2)$$

$$\text{C.S.A} = 0.0009 - 0.00068 = 0.0002 \text{ m}^2$$

$$\text{Volume of the square pipe} = \text{cross sectional area} \times \text{length} \quad (13)$$

$$\text{C.S.A} = 2.2 \times 10^{-4} \text{ m}^2$$

$$L = 1.922 \text{ m}$$

$$\text{Mass of pipe} = \text{Volume} \times \text{Density} \quad (14)$$

$$\text{Volume } (v) = 4.38 \times 10^{-4} \text{ m}^3$$

$$\text{Density} = 7850 \text{ kg/m}^3$$

$$m = 4.38 \times 10^{-4} \times 7850 \text{ kg/m}^3 = 3.437 \text{ kg}$$

$$\text{Weight of the pipe} = \text{Mass} \times \text{gravity} \quad (15)$$

$$m = 3.437 \text{ kg}$$

$$g = 9.81 \text{ m/s}^2$$

$$w = 3.437 \times 9.81 = 33.71 \text{ N}$$

$$\text{Total weight of Chassis, } w_c =$$

$$\text{Weight of Angle Iron} + \text{Weight of pipe} \quad (16)$$

$$w_c = 15.02 + 33.71 \times 10^{-4} = 48.73 \text{ N}$$

Weight of seed Tray.

Seed Tray is made of 2 mm thick mild steel sheet.

$$\text{Length of metal sheet used} = 720 \text{ mm} = 0.72 \text{ m}$$

$$\text{Width} = 160 \text{ mm} = 0.16 \text{ m}$$

$$\text{Thickness} = 2 \text{ mm} = 0.002 \text{ m}$$

$$\text{Density} = 7850 \text{ kg/m}^3$$

Substituting from equation 9

$$\text{Volume} = l \times w \times t \quad (17)$$

$$V = 0.72 \times 0.16 \times 0.002 \text{ m}$$

$$V = 0.002304 \text{ m}^3$$

$$V = 2.000234 \times 10^{-4} \text{ m}^3$$

$$\therefore \text{Mass} = v \times \delta$$

$$m = 2.304 \times 10^{-4} \text{ m}^3 \times 7850 \text{ kg/m}^3$$

$$m = 1.8086 \text{ kg}$$

Substituting from equation 8

$$\text{Weight} = m \times g$$

$$W = 1.8086 \times 9.81$$

$$w_t = 17.7424\text{N}$$

Weight of Seed Tray Support, w_{ts}

Seed tray Support is made of 50 mm by 5 mm mild steel flat bar.

$$\text{Weight of the flat bar used} = \text{Width (mm)} \times \text{Thickness (mm)} \times \text{length (m)} \times \text{density} \quad (18)$$

$$\text{Width (w)} = 50 \text{ mm} = 0.05 \text{ m}$$

$$\text{Length (L)} = 200 \text{ mm} = 0.2 \text{ m}$$

$$T = 5 \text{ mm} = 0.005 \text{ m}$$

$$\text{Density } (\delta) = 7850 \text{ kg/m}^3$$

$$m = 0.05 \times 0.2 \times 0.005 \times 7850 = 3.925 \text{ kg}$$

$$\text{Weight of seed tray support} = 38.504 \text{ N.}$$

Total weight of Seed tray = weight of tray mild sheet + weight of tray support (19)

$$w_{ts} = 17.742 + 38.054 = 56.246 \text{ N}$$

Weight of Wheels Assembly, w_w

Wheels are made from 8mm thick M.S Plates and 50mm by 3mm flat bar. Figure 1 below presents the ground wheel assembly.

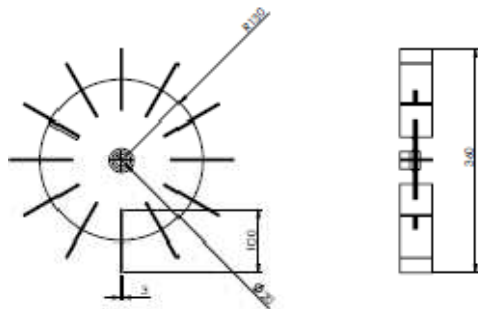


Figure 1 Ground wheel

$$\text{Disc diameter, } D = 260 \text{ mm} = 0.26 \text{ m}$$

$$r = 130 \text{ mm} = 0.13 \text{ m}$$

$$\pi = 3.142$$

$$\text{Area of a circle} = \pi r^2 \quad (20)$$

$$A = 3.142 \times 130^2$$

$$A = 53099.8 \text{ mm}^2$$

$$A = 0.05309 \text{ m}^2 = 5.3 \times 10^{-2} \text{ m}^2$$

Area of the open spaces on the wheel disc

$$A = 50 \times 3$$

$$A = 150 \text{ mm}^2 = 1.5 \times 10^{-4} \text{ m}^2$$

For 12 spaces

$$A = 1.5 \times 10^{-4} \text{ m}^2 \times 12 = 1.8 \times 10^{-3} \text{ m}^2$$

$$\text{Actual Area of the wheel disc} = 5.3 \times 10^{-2} - 1.8 \times 10^{-3}$$

$$A = 5.13 \times 10^{-2} \text{ m}^2$$

Substituting.

$$\text{Volume (v)} = \text{Area (A)} \times \text{Thickness (t)}$$

$$A = 5.13 \times 10^{-2} \text{ m}^2$$

$$t = 0.003 \text{ m}$$

$$v = 5.13 \times 10^{-2} \text{ m}^2 \times 0.003 \text{ m}$$

$$v = 1.54 \times 10^{-4} \text{ m}^3$$

Substituting

$$\text{Mass (m)} = \text{Volume (v)} \times \text{Density } (\delta)$$

$$v = 1.54 \times 10^{-4} \text{ m}^3$$

$$\delta = 7850 \text{ kg/m}^3$$

$$m = 1.54 \times 10^{-4} \times 7850 = 1.21 \text{ kg}$$

Substituted from equation 8

$$\text{Weight (W)} = \text{Mass (m)} \times \text{gravity (g)}$$

$$m = 1.21 \text{ kg}$$

$$g = 9.81 \text{ m/s}^2$$

$$W_t = 1.21 \times 9.81 = 11.870 \text{ N}$$

The weight of wheel blades.

The blades are made of 50mm by 5mm flat bars

$$\text{Area of the blades} = \text{Length (L)} \times \text{width (w)} \quad (21)$$

$$L = 50 \text{ mm} = 0.05 \text{ m}$$

$$W = 5 \text{ mm} = 0.005 \text{ m}$$

$$A = 0.05 \times 0.005 = 0.00025 \text{ m}^2 = 2.5 \times 10^{-4} \text{ m}^2$$

For 12 pieces

$$2.5 \times 10^{-4} \times 12 = 0.003 \text{ m}^2$$

Substituting

$$\text{Volume} = \text{Area (A)} \times \text{Thickness (t)} \quad (22)$$

$$A = 3.0 \times 10^{-3} \text{ m}^2$$

$$t = 0.003 \text{ m} = 3.0 \times 10^{-3} \text{ m}$$

$$= 3.0 \times 10^{-3} \times 3.0 \times 10^{-3}$$

$$v = 9.0 \times 10^{-6} \text{ m}^3$$

Substituting

$$\text{Mass} = \text{Volume (v)} \times \text{Density } (\delta)$$

$$v = 9.0 \times 10^{-6} \text{ m}^3$$

$$\delta = 7850 \text{kg/m}^3$$

$$m = 9.0 \times 10^{-6} \times 7850$$

$$m = 0.07065 \text{kg}$$

$$m = 7.065 \times 10^{-2} \text{ kg}$$

$$\text{Weight} = \text{mass} \times \text{gravity}$$

$$m = 7.065 \times 10^{-2}$$

$$g = 9.81 \text{m/s}^2.$$

$$\text{Weight of blades} = 7.065 \times 10^{-2} \times 9.81 = 0.693 \text{N}$$

$$\text{Total weight of wheels} = \text{Weight of wheel disc} + \text{Weight of blades} \quad (23)$$

$$= 11.870 \text{N} + 0.693 \text{N}$$

$$= 12.563 \text{N}.$$

$$\text{For the two wheels, total weight} = 2 \times 12.563$$

$$w_{wa} = 25.13 \text{ N}$$

Weight of Pulling Mechanism, w_p

Pulling Mechanism is made from a square pipe of 30mm.

Weight of square pipe

$$= \text{Volume} (v) \times \text{Density} (\delta) \times \text{gravity} (g) \quad (24)$$

$$L = 120 \text{mm} = 0.12 \text{m}$$

$$Wt = 30 \text{mm} = 0.03 \text{m}$$

Area of the square pipe.

$$A = (30^2 - 26^2)$$

$$= 900 - 676$$

$$= 224 \text{ mm}^2$$

$$A = 2.24 \times 10^{-4} \text{m}^2$$

$$\text{Volume} = \text{Cross Sectional Area} \times \text{Length} \quad (25)$$

$$A = 2.24 \times 10^{-4} \text{m}^2$$

$$L = 0.12 \text{m}$$

$$v = 2.24 \times 10^{-4} \times 0.12$$

$$v = 2.69 \times 10^{-5} \text{m}^3$$

Mass of pipe = Volume \times Density

$$v = 2.69 \times 10^{-5} \text{m}^3$$

$$\delta = 7850 \text{kg/m}^3.$$

$$m = 2.69 \times 10^{-5} \text{m}^3 \times 7850 \text{kg/m}^3$$

$$m = 0.221 \text{kg}$$

Weight = Mass \times Gravity

$$m = 0.221 \text{kg}$$

$$g = 9.81 \text{m/s}^2$$

$$W_p = 0.221 \text{kg} \times 9.81 \text{m/s}^2$$

$$= 2.072 \text{N}.$$

Weight of Wooden Board.

Wooden board: The type of wood selected is Madrone. Weight of the board determined by first evaluating its volume and then using the following the relationship:

$$\text{Weight wt} = \text{Mass} (m) \times \text{Gravity} (g)$$

Dividing the board into two segments to evaluate its surface area

$$\text{Area } A_1 = \text{Length} \times \text{Breath} (L \times B)$$

Substituting

$$A_1 = 496 \times 300$$

$$= 148800 \text{mm}^2 = 1.49 \times 10^{-1} \text{ m}^2$$

$$A_2 = 418 \times 200 = 83600 \text{ mm}^2 = 8.36 \times 10^{-2} \text{ m}^2$$

$$\text{Volume} = (A_1 + A_2) t$$

Substituting

$$t = 25 \text{mm} = 0.025 \text{m}$$

$$A_1 = 1.49 \times 10^{-1} \text{ m}^2$$

$$v = (1.49 \times 10^{-1} + 8.36 \times 10^{-2}) 0.025$$

$$v = 5.82 \times 10^{-3} \text{m}^3$$

$$\text{Mass} = \text{Volume} (v) \times \text{Density} (g)$$

Substituting

$$v = 5.82 \times 10^{-3} \text{m}^3$$

$$D (g) = 7850 \text{kg/m}^3$$

$$\therefore m = 5.82 \times 10^{-3} \times 7850 = 4.31 \text{kg}$$

$$\text{Weight, } Wt = 4.31 \times 9.81 = 42.28 \text{N}$$

Measurement Weight of Accessories

$$\text{Total Weight of Accessories} = 1.95$$

$$\begin{aligned} \text{Total Weight} &= (\text{Weight of chassis}) \\ &+ (\text{wt of seed tray}) \\ &+ \text{Weight of wheel assembly} \end{aligned}$$

$$\begin{aligned} &+ \text{Weight of (wooden board)} + \\ &\text{Weight (Pulling) Mechanism} + \\ &\text{Weight of Accessories).} \end{aligned} \quad (26)$$

$$\text{Weight of Chassis} = 48.73 \text{N}$$

$$\text{Weight of seed tray} = 56.246 \text{N}$$

$$\text{Weight of wheel Assembly} = 12.563 \text{N}$$

$$\text{Weight of wooden board} = 42.28 \text{N}$$

$$\text{Weight of Pulling Mechanism} = 2.072 \text{N}$$

$$\text{Weight of Accessories} = 1.95 \text{N}$$

$$48.73 + 56.25N + 12.5631N + 42.28N + 2.07N + 1.95 \\ = 163.84N$$

3.3.5 DETERMINATION OF DRAFT OF THE RICE TRANSPLANTER

The draft of the transplanter is going to be of two components which are from the weight of transplanter and functional losses on the bearings and transplanting mechanism. The following relation is used

$$D = D_r + F \quad (27)$$

Where;

D = Total Draft

D_r = Rolling Resistance of the wetted soil

F = Frictional Losses

$$D_r = W_t \times R \quad (28)$$

$$W_t = 163.84N$$

$$R = 0.03$$

$$D_r = 163.84N \times 0.03$$

$$D_r = 4.92N$$

If 15% of weight is F (frictional losses)

$$F_f = 0.15 \times 163.84$$

$$= 24.58N.$$

$$D = D_r + F \quad (29)$$

$$D_r = 4.92N$$

$$F = 24.58N$$

$$D = 4.921 + 24.58 = 29.5 N$$

2.4.5 POWER REQUIREMENT

The machine will be powered manually by pulling force of the farmer. The following relationship was used

$$P = D \times S \quad (30)$$

Where P = Power in Watts

D = Total drafts of the transplanter in Newton

S = Forward speed of the transplanter

$$D = 29.5N$$

$$S = 1.4m/s$$

$$P = 29.5N \times 1.4 = 41.3 W$$

The power required is 41.31 which is less than the average power of a human being which is 76 W; therefore, the machine can be operated without much drudgery.

2.4.6 DESIGN OF THE MAIN SHAFT

The shaft is used to transmit torque from the ground wheel to four bar linkage system via chain drive.

Therefore the load acting on the shaft is simply the force

required to drive the four bar linkage. which has computed as losses in 3.5.5 above and calculated from the equations given by Khurmi and Gupta (2005)

$$\tau = \frac{16T}{\pi d^3} \quad (31)$$

Where,

τ = Allowable shear stress

T = Torque

d = Shaft diameter

$$T = \frac{60P}{2\pi N} \quad (32)$$

$$P = 41.3W$$

$$N = 102.84 \text{ rpm}$$

$$T = \frac{60 \times 41.3}{2 \times 3.142 \times 102.84}$$

$$= \frac{2478}{646.162}$$

$$= 3.834Nm$$

$$\text{From } \tau = \frac{16T}{\pi d^3}$$

$$\therefore d^3 = \frac{16T}{\pi \tau} \quad (33)$$

$$d = \sqrt[3]{\frac{16T}{\pi \tau}} \quad (34)$$

$$d = \sqrt[3]{\frac{16 \times 3.834}{3.142 \times 0.5}}$$

$$d = 3.421 \text{ mm}$$

A mild steel commercial shaft of 12 mm is chosen.

3 RESULTS AND DISCUSSION

The results of the design computation and analysis are presented in the Table 1 below.

TABLE 1: PARAMETERS OF THE DESIGN

Parameter	Description	Value
ω	Angular speed of the ground wheel	10.769 rad/sec
N	Revolution of the ground wheel in a minute	102.839 rpm
S_R	Speed ratio of the chain drive	3.78
N_1	Revolution speed of the driving sprocket	102.84 rpm
N_2	Revolution speed of the driven sprocket	388.4 rpm
N_p	Rate of oscillation of the planting fingers	388.4 rpm
\dot{s}	Number of seedling transplanted in a minute	777 plants
w_c	Weight of chassis	48.73 N
w_{ts}	Total Weight of seedling tray	56.246 N
w_{wa}	Weight of the ground wheel assembly	25.13 N
w_p	Weight of pulling mechanism	2.072 N
w_b	Weight of wooden board	42.28 N
w_a	Weight of accessories	1.95 N
w_T	Total weight of the transplanter	163.84 N
D_r	Rolling resistance of the wetted rice field	4.92 N
F_f	Frictional losses on mechanisms	24.58 N
D	Draft of the transplanter	29.5 N
P	Power requirement of the rice transplanter	41.3 W
d	Diameter of the central shaft	12 mm

Figure 2 below presents the isometric drawings of the designed manual rice transplanting machine.



Figure 2: Isometric Drawing of the Designed Manually Operated Rice Transplanter

4 CONCLUSION

The design analysis of a simple and durable manually operated machine for on-row transplanting of paddy rice was successfully undertaken. A simple manual rice transplanter was developed consisting of other following basic components, seedling tray, chassis, picking fork, wheels assemble pulling mechanism. The power requirement for the machine is 41.3 W well below the average power of a man which is 76 W; designed planting rate being 777 plants in a minute at a mean forward speed of 1.4 m/s. The design upon implementation would contribute immensely to mechanization of rice production in Nigeria; as it could make available to small scale rice farmers a simple yet affordable mechanical transplanter replacing manual transplanting, eliminating drudgery, and thereby increasing their production capacity and more revenue.

REFERENCES

- Artazono (2017) Theoretical metal weight calculator. Theoretical metal weight calculation formula . 30 types of metals. Retrived November 2018.
- FAO, Food and Agriculture Organization (2003). Sustainable Rice Based Production and People's Livelihood, International Rice Commission Newsletter (Special Edition): vol. 52, International Rice Commission, FAO, Rome.
- Imolehim E.D and Wada A.C (2000). Meeting the rice production and consumption demand of Nigeria with improved Technologies. National Cereal Research institute, Badeggi, Niger State pp1-11
- Khurmi R.S. and Gupta J.K. (2005). A Textbook on Machine Design (S.I UNITS).. Eurasia Publishing House, New Delhi. pp205-215
- Longtau S.R (2003). Multiagency Partnerships in West Africa Agriculture. A Review and Description of rice



production systems in Nigeria. Document prepared by the overseas Development institute, London.

Rajib B. A. Sharma H. K. Jabin S. Jeuna G. (2016). Design and Fabrication of paddy transplanter. *An International Journal of Engineering Science and Technology*. Vol.6 No 4, ISSN: 2250-3498.

International Rice Research Institute IRRI (2017). Rice Knowledge Bank.

Saka J. O. and Lawal B. O. Ajijola S. (2019). Determinants of Adoption and Productivity of Improved Varieties in Southwestern Nigeria. *World Journal of Agricultural Sciences among small holder farmers*.1(1). 42-49.



Investigation of Vulnerability of Oil and Gas Critical Infrastructures and Developing a Tracking Algorithm to track Malicious Attacks on the Streams

*Isah, A.O¹, Alhassan, J.K², Idris, I³, Adebayo, O.S⁴, Onuja, A. M⁵

1, 2, 3, 4. Cyber Security Science Department, Federal University of Technology, PMB 65

Minna Niger State, Nigeria

⁵. Computer Science Department, Federal University of Technology, PMB 65

Minna Niger State, Nigeria

*Corresponding author email: ao.isah@futminna.edu.ng

ABSTRACT

This paper is a presentation of part of the preliminary achievements of an ongoing research work by the authors. The said research work is on tracking and locating cyber-attacks in general. This very paper seeks to propose a solution to the security challenges of oil and gas ICT infrastructures. Oil and gas industry is no doubt one of the most lucrative industries and high income generator for almost all oil and gas producing countries of the world. Since most of the operations of oil and gas industry is Information Technology driven, the accompanying cyber security challenges of the Information Technologies are mostly targeted at the upstream, the midstream and the downstream sector of the oil and gas industry. The methodology employed is a system design of a developed algorithm of data and server application tracking. The methodology and implementation trials of the ongoing research work so far, proved that the final result could be implemented to solve a wide range of cyber security problems especially, in the area of tracking and locating instantaneous malicious attacks on data files or software applications on the cyber space.

Keywords: *Vulnerability, Critical Infrastructures, Inter-streams, tracking, malicious attacks, agents, Encryption.*

1 INTRODUCTION

Developing country like Nigeria faces more cybercrime threats in its oil and gas industry, this is due to the low level of preparedness in the fight to combating cybercrime. This research seeks to solve this problem by investigating the cyber security vulnerability of the oil and gas systems, Isah et al., (2016) by developing an implementable model of inter-stream systems encryption and artificial agent to counter malicious attacks on critical systems of oil and gas.

The benefits of digitalization in the oil and gas industry are profound, but they are also causing cyber risks to emerge, Maurice Smith, (2017). The Ponemon Institute LLC reported in February that almost 68 per cent of oil and gas companies were affected by at least one significant cyber incident in 2016, and many attacks are assumed to be undetected or unpublished. And according to the Ponemon Institute, 59 per cent of oil and gas companies surveyed believe there is greater risk in the operational technology (OT) than the information technology (IT) environment.

Critical network segments in production sites, which used to be kept isolated, are now connected to networks, making the OT more vulnerable.

When considering the issue of cyber security and its impact on business continuity, several types of threats come into play. Philippe Carle (2017). The first is the exposure of employees to outside emails. Over 400 businesses every day are exposed to email “spear-phishing” schemes draining three billion dollars from businesses over the last three years. The percentage of emails that contain potential business disrupting malware today stands at one in 131, the highest rate in five years.

A second issue involves attacks by organized groups on critical infrastructure. Oil & gas facilities are increasingly considered critical national infrastructure. As such they are targeted not only by malevolent individuals but also by organizations that use cyber-attacks as weapons to be used to weaken nation states and other global institutions.

A third element to consider when formulating a cyber-security strategy is the proliferation of mobile devices. Cell phones, tablets, laptops and thumb drives in the hands of practically every oil & gas industry employee worldwide creates a need for the development of more modern and robust security policies. The added connectivity of these devices makes it easy for outsiders who guess or steal passwords to penetrate the control environment.

1.1 THE THREE MAJOR SECTORS OF OIL AND GAS UNDER CONSIDERATION.

Source: ERP scan RSA Conference 2016

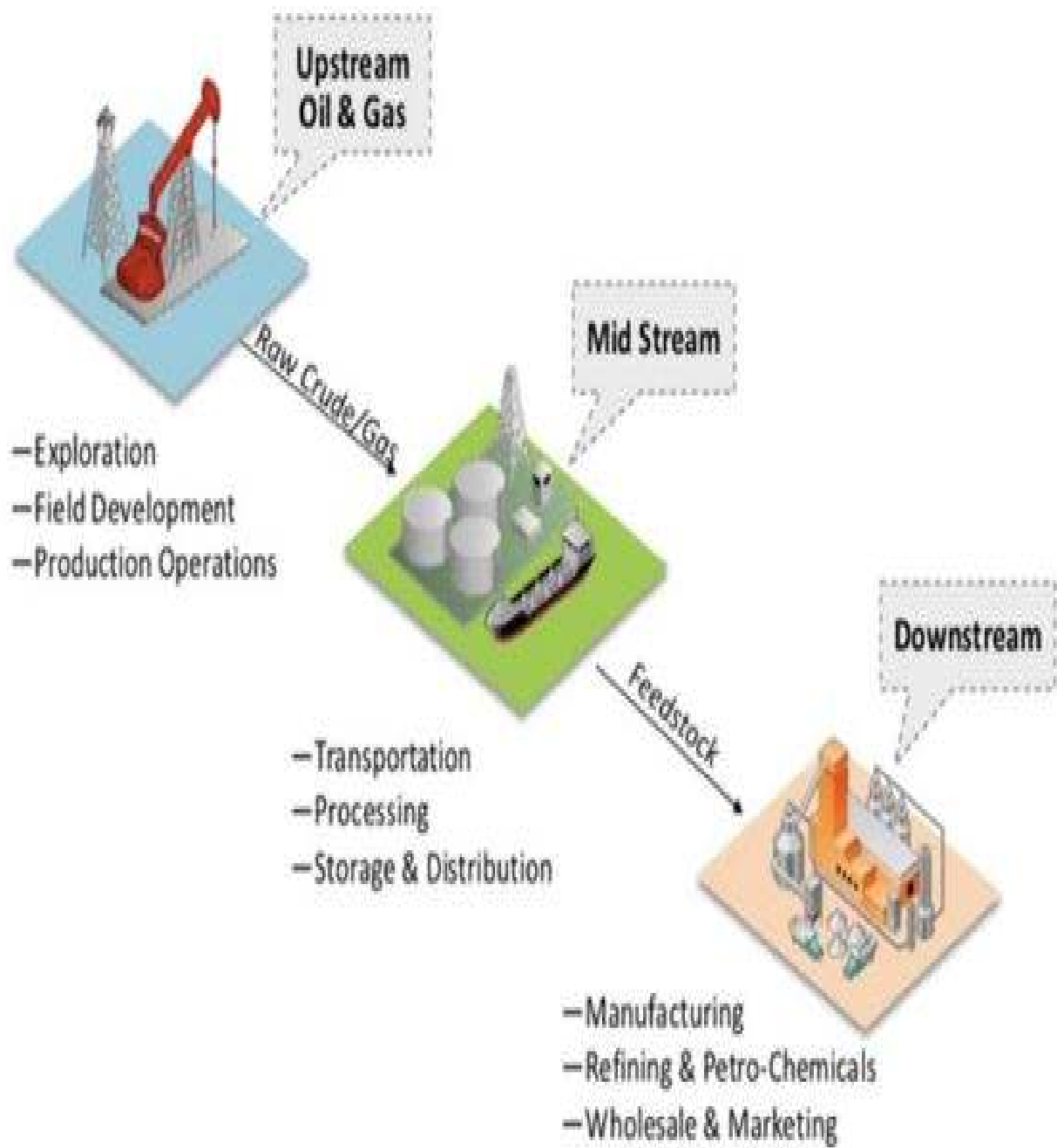


Figure 1: Streams of oil and gas



1. **The Upstream sector:** This comprise of Exploration and production

The critical infrastructure Systems of interest under this sector includes

- Exploratory rigs systems
- Drilling rigs system
- Remotely data acquisition system,
- Industrial control systems,
- Drilling control system,
- Data conversion,
- Remote camera network
- Access control sensors
- Processors.

2. **The Midstream sector:** This includes logistics and transportation operations of products

The critical infrastructure systems includes,

- Pipeline control system,
- Storage systems,
- Pumping stations control system,
- Depots loading systems.

3. **The Downstream sector:** This incudes majorly of product refining, manufacturing and sales

The critical infrastructure systems includes,

- Refining control software systems
- Manufacturing software applications
- Sales and data information files.

1.1 AIM AND OBJECTIVES

The aim of this research proposal is to investigate the vulnerability of oil and gas critical Infrastructures and to develop a tracking algorithm to track malicious attacks on the streams.

This aim will be achieved by the following objectives;

To employ cyber security tools to test critical infrastructure systems.

To design system of a developed algorithm of data and server applications tracking.

1.2 THE CYBER SECURITY ISSUES ON OIL AND GAS INTER-STREAM SECTORS

The operations of the main sectors of the oil and gas as mentioned above are almost fully automated now for ease and efficient control, maintenance, monitoring and tracking of essential activities. The streams are the Up-stream, Mid-stream and the Down-stream. Two systems Udofia, O. O., & Joel, O. F. (2012) are chiefly employed in this areas; they are the Computerized Maintenance Management Systems (CMMS) and Supervisory Control and Data Acquisition (SCADA) system.

The SCADA

The SCADA is a centralized control system architecture using computers and communication networked with monitoring sensors and other signal devices Gligor, A., & Turc, T. (2012). It's a software embedded system that allows data and signal controls to be displayed by the Graphical User Interfaces (GUI) of the system for administrators to monitors.

The CMMS

The CMMS are computer oriented system that controls processes and infrastructural facilities, these facilities could be hardware and even some software based resources. For instance, the Power and water utilities as well as the channels and network of pipelines of the oil and gas products. Monitoring, control and faults tracing activities of these quantities are no longer by the legacy methods of physical tracing and physical incidence reports. They are remotely being done.

For all these system to work effectively, they have to be on the network within the cyberspace, hence this give rise to the cyber security issues of the whole system.

Research has shown that these systems themselves are being attacked. Therefore tracking and detecting attacks location for real-time countermeasure is an important solution.

1.3 STATEMENTS OF THE PROBLEM

The current nature of oil & gas operations that is digital and industrially ICT driven. As much as it's benefits, it has greatly increased the cyber-attack risks.

According to Philippe Carle (2017), Cyber-attacks cost companies worldwide an estimated \$300-400 billion each year in unanticipated downtime and still counting. Some large industrial organizations estimate their cost of downtime in the millions of dollars per hour. When a plant shuts down unexpectedly, it takes 3 to 4 days to get everything started up again. These are sobering business continuity-related lost revenue numbers.

Emmanuel Elebeke (2018) in a report dated January 31 2018 in Vanguard newspaper and titled Cyber-attacks: Banks, health sector, MDAs major target in 2018, the National Information Technology Development Agency (NITDA) raised alarm over impending cyber-attacks in 2018 that many Nigerian companies are at risk unless they begin to put proper protection measures in place. Some of the previous works reviewed were able to provide some solutions to some cyber security challenges in the oil and gas economy, but many were not able to track attackers' on-the-act with their solutions.



1.4 REVIEW OF SOME RELATED WORKS

Christina Nikolova (2019), affirmed that cyber security is of very high priority in organized oil and gas businesses due the commercially sensitive data and other automated infrastructures. This was also collaborated by Trond Winther (2015) in the executive summary of Lysne Committee study, the author observed that the Industrial automation, control and safety systems used in the oil and gas sector are now digitalized and as such, their operations are dependent on technology and digital systems. This has accordingly, exposed the oil and gas sector to digital vulnerability.

One of the more serious cyber-attacks on data and software applications on the cyber space, especially on oil and gas systems are the Denial-of-Service (DoS) attack and Distributed Denial-of-Service (DDoS). Lo, C. C., Huang, C. C., & Ku, J. (2010, September), presents a cooperative intrusion detection system framework for cloud computing networks. They proposed a solution on how to reduce the impact of DoS attack or DDoS in cloud computing environment. The method implemented is to allow IDSs in cloud computing region to exchange alert with each other, whereas each IDSs has a cooperative agent used to compute and determine whether to accept or deny an alert from other IDSs. Thus the occurrence of same type of attack is avoided. This method is efficient in intrusion detection. The paper neither considers how to prevent new type of attacks nor did it detail on locating the attacks.

In assessing the security risk of oil and gas industries, Srivastava, A., & Gupta, J. P. (2010) worked on some new methodologies. The authors discussed a number of security risks, but of more interest is the treats vulnerability of the industry (oil and gas) which is also the focus of this paper. The authors employed the Security Risk Factor Table (SRFT) and the Stepped Matrix Procedure (SMP Matrix) model to assess the security risks. The authors proffers some safety barriers of which isolation of critical systems from the internet and network top the safety barrier. However, isolation of these critical systems could also cause temporary halt to system operations. Hence the focus of this paper is to identify and remedy attacks while system continue operations.

In the comparative study of intrusion detection system and its recovery mechanism, Khan, N. Y., Rauf, B., & Ahmed, K. (2010), analyzed intrusion detection systems (IDS) ability to detect the intrusions in computer systems after a thorough comparative theoretical study. The authors thoroughly discusses IDS highlighting its different characteristics, suggests the usage of Host Based IDS in the organizations to provide complete protection. The authors showed that damaged data can be recovered by the IDS using the recovery mechanism. The study was able to

detect intrusion and also able to recover damaged data. The security system can neither prevent an intrusion nor can it locate the intruders' position.

Khan, et al., (2017), carried out an appreciable research on solving some of the problems facing the oil and gas industries. The authors observed that critical processes are involved in oil and gas industries in the area of exploration, refining and others. These processes are to be secured. Wireless sensor network (WSN) solution was discussed by the authors highlighting its various uses in the upstream, midstream and the downstream. WSN aids data transmission and other sensitive information exchange between the terminals. As much as the WSN it poses the challenge of being targeted because of its vulnerabilities to cyber attackers which this author were not able tackle in their work. Tracking and locating these attacks is the focus of this paper.

Prabakar, M. A., Karthikeyan, M., & Marimuthu, K. (2013), presented an efficient technique for preventing SQL injection attack using a pattern matching algorithm. The research work used pattern matching technique to identify or detect any anomaly packet from a sequential action. The authors defined Injection attack as a method of injecting any kind of malicious string or anomaly string on the original string. To be able to detect and prevent SQL injection attack (SQLIA) in a string, they presented Aho-Corasick pattern matching algorithm. After the evaluation of the algorithm, the algorithms proved efficient to all kind of SQL attack but unable to deals with the issue of attacker's location.

Ullah, I., Khan, N., & Aboalsamh, H. A. (2013), did survey on BOTNET: its architecture, detection, prevention and mitigation, describing Robot network as the biggest network security threats faced by home users, organizations, and governments. The authors presented several ways of detecting it based on the existing methods of detection. BOTNET, a large network of compromised computers used to attack other computer systems for malicious intent, is the most significant current issue in computer network security. It was analyzed in the research, structured based detection and behavioural based detection as method of detecting BOTNET. Unfortunately, the work was unable to come out with prevention and mitigation measure for BOTNET.

Singh et al., (2011) presented a paper titled detection and prevention of phishing attack using dynamic watermarking. This method caters for phishing attacks that are increasing at a burgeoning rate which is highly problematic for social and financial websites. Since many existing methods suffer from one or more deficiency, the authors proposed an approach for prevention of phishing attack based on dynamic position watermarking technique. The approach is divided in to three modules, namely; Registration process, Login verification process and Web site closing process. Conclusively, the research was able to conveniently and securely prevent phishing attack. The



limitation of this approach is that it does not look into the location of the phisher.

2 METHODOLOGY

This research proposal seeks to investigate how vulnerable are these oil and gas critical infrastructures in the cyber environment since they are being driven by Information and Communication Technology in today's world. The methodology for this proposal shall be in two broad parts. The first part is to employ some cyber security tools for hybrid vulnerability investigation techniques broadly under:

- I. *Credentialed Vulnerability investigation technique*: this will be conducted at;
 - a. Lockdown condition comprising of administrative vulnerability, configuration vulnerability and patch management vulnerability
- II. *Non-Credentialed Vulnerability investigation technique*: this will be conducted at;
 - b. Ethical penetration condition comprising of port vulnerability, network service detection vulnerability, manual and automatic scan vulnerability.

The result of these investigations are subjected to mathematical analysis and evaluated. The second part is to develop the model for mitigation and counter measures to be recommended for implementation as policy by operators, regulators and companies in oil and gas business.

2.1 Mathematical and logical considerations

From figure 2, Attacker (a), can strike at any point on the interconnected stream systems: Upstream (u_s), Midstream (m_s) and Downstream (d_s)

The linear expressions of the model is thus;

$$a(u_s + m_s + d_s) = et \dots \dots (1)$$

But,

$$et = c(u_s + m_s + d_s) \dots \dots (2)$$

Where

$$a = \text{attack,}$$

$$et = \text{encryption and tracking algorithm}$$

$$c = \text{control access}$$

$$u_s = \text{upstream systems}$$

$$m_s = \text{midstream systems}$$

$$d_s = \text{downstream systems}$$

According to a research by the Worldwide Broadband Speed League, 2018 and reported by Cable, Singapore has the fastest internet speed of 60.388459245Mbps and Yemen has slowest of 0.3085728996Mbps; these are approximately 60.39Mbps and 0.31Mbps respectively.

We shall use these two countries as reference to set the threshold broadband internet speed by which possible attackers could strike.

In this mathematical expressions, conversions of bandwidth units were employed in speed Mb/s (Megabits per second) or Kb/s (Kilobits per second) into Megabytes (MB) as the case may be.

A "bit" is the least unit of storage in discrete values of a '0' or '1', 8 bits = byte.

A reasonable internet speed ranges from 3 to 5 Mbps to a maximum of 100Mbps, but for the purpose of maximum security and the sensitivity index required for the proposed system to respond to attack, the authors set the internet speed threshold to 100Mbps higher than the fastest country's value as mentioned above.

Then, attacks intruding the oil and gas data and applications' systems is:

$$\text{For the threshold, } \frac{100}{8} = 12.5s \dots \dots (3)$$

$$\text{For the fastest location, } \frac{60.39}{8} = 7.54875s \dots \dots (4)$$

$$\text{For the slowest location, } \frac{0.31}{8} = 0.03875s \dots \dots (5)$$

Now, for 1 Megabyte ($1e^{-6}$ byte) data to be compromised, we have;

$$\text{For the threshold, } 1e^{-6}/12.5 = 8e^{-8} \dots \dots (6)$$

$$\text{For the fastest location, } 1e^{-6}/7.54875 = 1.324722e^{-7} \dots \dots (7)$$

$$\text{For the slowest location, } 1e^{-6}/0.03875 = 2.5806452e^{-5} \dots \dots (8)$$

2.2 The proposed model

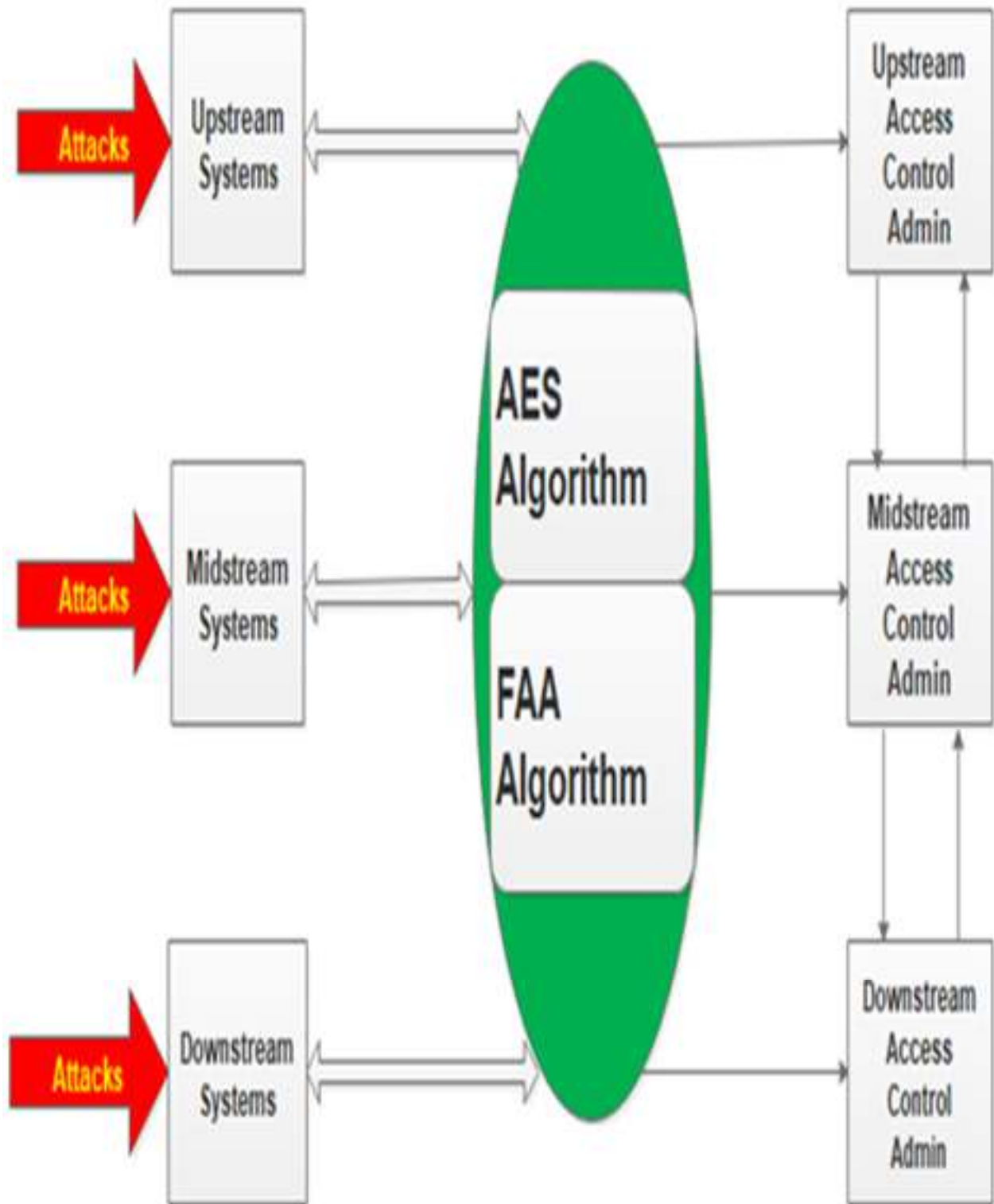


Figure 2: Model of oil and gas inter-streams Encryption and Tracking Agent Algorithm.



Figure 2 is the proposed model of inter-streams Encryption and the tracking agent algorithm. The cyber attackers mainly targets the application software, data files or folders containing vital information of the critical systems of any of the streams mentioned above.

The green area of figure 1, comprise the tracking algorithm that will counter the attack in two ways; the Advance Encryption Standard (AES) encrypts all the application software and data on the server. The Feedback Artificial Agent (FAA) is tracking and automatically sending malicious attempts to the Access Control Admin via the Access Control interfaces. Since the sectors' access control and administration are interconnected, any attacks at one point is detected and countered at all other points of the sector.

2.3 Algorithm pseudo-code for the Inter-streams Encryption and Tracking Agents

```
START
SELECT TARGET FILE/APPLICATION FOR ATTACK
ATTEMPT DECRYPTION ATTACK CODES
INPUT DECRYPTION ATTACK CODES
IF DECRYPTION CODES INCORRECT
FAA SEND UNSUCCESSFUL AND LOCATION OF
ATTACKS SMS/EMAIL TO STREAM CONTROL
ADMIN
ELSE IF DECRYPTION CODE CORRECT
FAA SEND SUCCESSFUL SMS/EMAIL TO STREAM
CONTROL ADMIN
DECRYPT AND ACCESS FILE/APPLICATION
END
```

The algorithm as stated above, shall represents the expected complex codes that shall be written in java language

3 RESULTS AND DISCUSSION

Equation (1) and (2) explains the summary of operation of the model. In (1), for any possible attack 'a', it must be targeted at either the upstream system 'u_s' or the midstream system 'm_s' or the downstream system 'd_s' or the all at the same time. The encryption and tracking algorithm 'et' acting as an agent, will be automatically activated to start up the tracking of the malicious attack at the instant.

In (2), all malicious actions being tracked from by 'et' is in turn sent to all the streams' access control 'c' which is also interacting with u_s, m_s and d_s.

Equation (3) to (8) explains the sensitivity of the model in tracking the attacks. It could be observed from (7), that any attack coming from a location with the fastest internet speed could take $1.324722e^{-7}$ seconds to cause any breach, this is slower than the threshold time of the model $8e^{-8}$ seconds in (6). From (8), any attack coming from a location with slowest internet speed, will even be much slower before it can cause any breach when we compare the time $2.5806452e^{-5}$ seconds in (8) to the threshold of $8e^{-8}$ seconds in (6).

The host system otherwise known as the Industrial server, that host the data files of oil and gas, the tracking agent and access control admin systems are all in communication with the cyberspace. Although the malicious systems used by cybercriminals to access the oil and gas streams' system is not normally in direct communication with the streams' systems, they also have access to the cyber space from any location across the globe, this makes all oil and gas industries' systems accessible to the malicious system. In the proposed solution, malicious attempt on the data file and software applications are instantly being tracked and located.

4 CONCLUSION

All the three sectors of the oil and gas are linked together for cyber security information sharing and system administration. Encryption and Tracking agent is embedded in critical system servers to track and report malicious cyber-attacks on oil and gas facilities.

The result of the critical system vulnerability investigation is utilized in the proposed system development and also kept as data base for use by other researchers working on oil and gas cyber security.

REFERENCE

- Isah, A. O., Alhassan, J. K., Misra, S., Idris, I., Crawford, B., & Soto, R. (2016). Network System Design for Combating Cybercrime in Nigeria. In International Conference on Computational Science and Its Applications (pp. 497-512). Springer, Cham.
- Maurice Smith (2017). Oil and gas steps up fight against cyber-attacks targeting operational technology. Retrieved from <http://www.jwnenergy.com/article/2017/9/og-industry-steps-fight-against-cyber-attacks-targeting-operational-technology/>



- Udofia, O. O., & Joel, O. F. (2012). Pipeline vandalism in Nigeria: Recommended best practice of checking the menace. In Nigeria Annual International Conference and Exhibition. Society of Petroleum Engineers.
- Gligor, A., & Turc, T. (2012). Development of a service oriented SCADA system. *Procedia Economics and Finance*, 3, 256-261.
- Philippe Carle (2017). 3 Steps for Countering Oil & Gas Cyber security-related Business Continuity Threats retrieved from <https://blog.schneider-electric.com/power-management-metering-monitoring-power-quality/2017/11/09/oil-gas-cybersecurity-business-continuity-threats/>
- Emmanuel Elebeke. (2018). Cyber-attacks: Banks, health sector, MDAs major target in 2018 retrieved from <https://www.thisdaylive.com/index.php/2017/08/17/global-hunt-for-nigerian-cyber-criminal-spreading-malware/>
- Christina Nikolova. (2019) Operational Technology Cyber Security Risks Rising for Oil, Gas https://www.rigzone.com/news/operational_technology_cyber_security_risks_rising_for_oil_gas-22-apr-2019-158651-article/
- Trond Winther, (2015) Lysne Committee study Cyber security vulnerabilities for the oil and gas industry <https://www.dnvgl.com/oilgas/download/lysne-committee-study.html>. Retrieved 13th July, 2019.
- Lo, C. C., Huang, C. C., & Ku, J. (2010). A cooperative intrusion detection system framework for cloud computing networks. In 2010 39th International Conference on Parallel Processing Workshops (pp. 280-284). IEEE.
- Srivastava, A., & Gupta, J. P. (2010). New methodologies for security risk assessment of oil and gas industry. *Process Safety and Environmental Protection*, 88(6), 407-412.
- Khan, N. Y., Rauf, B., & Ahmed, K. (2010). Comparative study of intrusion detection system and its Recovery mechanism. In 2010 The 2nd International Conference on Computer and Automation Engineering (ICCAE) (Vol. 5, pp. 627-631). IEEE.
- Khan, W. Z., Aalsalem, M. Y., Khan, M. K., Hossain, M. S., & Atiquzzaman, M. (2017). A reliable Internet of Things based architecture for oil and gas industry. In 2017 19th International conference on advanced communication Technology (ICACT) (pp. 705-710). IEEE.
- Prabakar, M. A., Karthikeyan, M., & Marimuthu, K. (2013). An efficient technique for preventing SQL injection attack using pattern matching algorithm. In 2013 IEEE International Conference ON Emerging Trends in Computing, Communication and Nanotechnology (ICECCN) (pp. 503-506). IEEE.
- Ullah, I., Khan, N., & Aboalsamh, H. A. (2013, April). Survey on botnet: Its architecture, detection, prevention and mitigation. In 2013 10th IEEE International Conference on Networking, Sensing and Control (ICNSC) (pp. 660-665). IEEE.
- Singh, A. P., Kumar, V., Sengar, S. S., & Wairiya, M. (2011). Detection and prevention of phishing attack using dynamic watermarking. In International Conference on Advances in Information Technology and Mobile Communication (pp. 132-137). Springer, Berlin, Heidelberg.



Optimization of Process Variables in Bio-Waste Based Activated Carbon Preparation Using Response Surface Methodology.

*Onuoha, D. C¹, Egbe, E. A. P², Abdulrahman, A. S³ & Abdulkareem, A. S⁴

¹PhD Student, Mechanical Engineering Department, Federal University of Technology, PMB 65 Minna Niger State, Nigeria

²Mechanical Engineering Department, Federal University of Technology, PMB 65 Minna Niger State, Nigeria

³Materials and Metallurgical Engineering, Federal University of Technology, PMB 65 Minna, Niger State, Nigeria

⁴Chemical Engineering Department, Federal University of Technology, PMB 65 Minna Niger State, Nigeria

*Corresponding author email: chikansel6@gmail.com +2348035404855

ABSTRACT

Cost and environmental issues associated with conventional precursors for the preparation of commercial activated carbon and the desire for highest product yield have continued to drive investigations into alternative sources of activated carbon and optimization of its production parameters. In this investigation therefore, activated carbon was prepared from groundnut (*Arachis Hypogaea*) shell in a chemical activation process using zinc chloride (ZnCl₂) and the process variables optimized using the central composite design of response surface methodology. The effects of activation temperature, activation time and impregnation ratio on carbon yield were investigated. A quadratic model for carbon yield was developed to correlate the preparation variables to the response of yield. From the analysis of variance (ANOVA), the most significant factor on the yield was identified as the activation temperature. Optimization of process variables was undertaken using the Design Expert software where the targeted response of yield was set at maximum and the three process variables of activation temperature, activation time and impregnation ratio were set at either maximum or minimum, depending on their corresponding synergic and antagonistic influence. Activation temperature, activation time and impregnation ratio of 600°C, 1.32 hour and 3 respectively were found to be the optimum production conditions. A carbon yield of 50.04% was obtained at the optimum conditions. Result from validation experiment agreed with the predicted result obtained from the designed experiment with a percentage error of 0.58%.

Keywords: *Activated Carbon, Groundnut Shell, Optimization, Response Surface Methodology, Yield*

1. INTRODUCTION

Yahya *et al* (2015); Subhashree (2011); Eric (2010) Al-Qodah and Shawabkah (2016) defined the term activated carbon as carbonaceous materials with high porosity, high physicochemical stability, high adsorptive capacity, high mechanical strength, high degree of surface reactivity, with immense surface area which can be differentiated from elemental carbon by the oxidation of the carbon atoms found at the outer and inner surfaces. These materials are characterized by their extraordinary large specific surface areas, well-developed porosity and tunable surface-containing functional groups. McDougall (1991) submitted that the volume of pores in activated carbons is generally defined as being greater than 0.2ml/g and the internal surface area is generally larger than 400m²/g as measured by the nitrogen BET method. Malik *et al* (2006); Yahya *et al* (2015) have opined that environmental concerns, renewability and high cost of

commercial activated carbons (which are traditionally sourced from coal, petroleum residues, peat and lignite) are the major reasons for the search for alternative sources of the material. Therefore, Nasehir *et al* (2010) have made case for the production of activated carbon with high adsorption performance from alternative material that is cheaper and readily available. Sugumaran *et al* (2012); Busari *et al* (2012) have reported that in recent years researchers have been focusing on production of activated carbon from agricultural bio-wastes and lignocellulosic materials which are effective and inexpensive. This option is particularly attractive since Nigeria is an agro-based nation with yearly harvesting and processing of various agricultural crops resulting in considerable quantities of agricultural by-products such as groundnut shell. The use of such eco-friendly starting materials will reduce solid waste pollution, while reducing the cost of the raw material for the production of activated carbon.

2. METHODOLOGY

2.1 CARBONIZATION OF GROUNDNUT SHELL ASH (GSA).

The groundnut shell (GS) was washed three (3) times in tap water and dried under sunlight for two weeks to remove moisture. The groundnut was dried in the oven at 100°C for 24 hours and ground locally. Then the particle size analysis of the resulting char was carried out in accordance with ASTM E11-Seive Designation. 600g of the char was placed into a set of sieves arranged in descending order of fineness and shaken for 15 minutes which is the recommended time to achieve complete classification. The groundnut shell ash (GSA) used in the carbonization process were those that passed through the 45µm sieve, therefore the particle size of the char used was < 45µm. The dried particles of groundnut shell (precursor) were loaded into a stainless steel vertical tubular reactor placed in a furnace. The temperature was increased gradually from room temperature to 200°C under nitrogen (99.99%) flow at flow rate of 150ml/min; this temperature was kept constant for 3 hours to produce char. The char was cooled down to room temperature and under nitrogen flow and then stored in air-tight containers for analysis. SEM analysis was carried out on the carbonized groundnut shall char sample as can be seen in Figure 1.

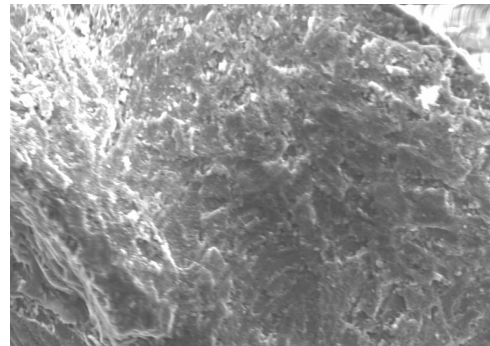


Figure 1: SEM micrograph of carbonized GSA

2.2 DESIGN OF EXPERIMENT

A standard response surface methodology (RSM) design called central composite design (CCD) was applied to verify the influences of individual process variables and their interactive influences on the response of yield in preparing activated carbon from GS. Kwager and Ibrahim (2013) elucidated that response surface methodology is a collection of mathematical and statistical technique that is useful for modeling and analysis of problems in which a response of interest is influenced by several variables. Replicates at the center points have been used to estimate residual error and the reproducibility of the data. The axial points are located at (0, 0, ± α), (0, ± α, 0) and (± α, 0); where, according to Yahaya *et al* (2010) and Montgomery (2001), α represents the distance of the axial point from the center and makes the design rotatable. In this study, the α value was calculated to be 1.682 (rotatable). The number, N of experiments (20) was obtained using equation (1).

$$N = 2n + 2n + nc \quad (1)$$

Where N denotes the total number of experiments n is the number of independent variables and nc is the number of center runs used in the experiment.

For the purpose of this investigation 6 center runs as used by Yahaya *et al* (2010) and Chowdhury *et al* (2012) will be adopted. Therefore, we have:

$$N = 2n + 2n + nc = 23 + 2(3) + 6 = 20 \text{ experiments.}$$

The percentage yield experiments were conducted using the design parameters provided by response surface methodology as presented in Table 1 (design of experiment table showing coded and actual levels).

The response function representing the percentage groundnut shell carbon yield is expressed as:

$$Y = f(A, B, C) \quad (2)$$

Where Y is the percentage carbon yield while A, B and C are the process variables of activation temperature, activation time and impregnation ratio respectively.

The model quadratic equation used to represent the carbon yield is given by:

$$Y = b_0 + \sum_{i=1}^n b_i x_i + (\sum_{i=1}^n b_{ii} x_i^2) + \sum_{i=1}^{n-1} \sum_{j=i+1}^n b_{ij} x_i x_j \quad (3)$$

Where Y represents the predicted response, b₀ is the constant coefficient, b_i denotes the linear coefficient, b_{ij} is the interaction coefficient, b_{ii} is the quadratic coefficient and x_i, x_j are the coded values of the activated carbon production variables in line with the positions of Myers and Montgomery (2002), Zainudin *et al* (2005).

2.3 PREPARATION OF GROUNDNUT SHELL BASED ACTIVATED CARBON

The method used by Yahaya *et al* (2010); Chowdhury *et al* (2012) was adopted in preparing the activated carbon from groundnut shell char. As submitted by Sumathi *et al* (2009), the sequence of the experiment was randomized to minimize the effects of uncontrolled factors. Prior to mixing with groundnut shell char, 250ml of de-ionized water was used to dissolve measured gram weight of ZnCl₂ pellets. The activation procedure was done using similar reactor as in carbonization process. The activation

TABLE I: DESIGN OF EXPERIMENT TABLE SHOWING CODED AND ACTUAL LEVELS

Run	Type	Coded Factors			Actual Factors		
		A(°C)	B(hr)	C	Temp	Time	Ratio
1	Fact	-1	-1	-1	600	1	1
2	Fact	+1	-1	-1	800	1	1
3	Fact	-1	+1	-1	600	3	1
4	Fact	+1	+1	-1	800	3	1
5	Fact	-1	-1	+1	600	1	3
6	Fact	+1	-1	+1	800	1	3
7	Fact	-1	+1	+1	600	3	3
8	Fact	+1	+1	+1	800	3	3
9	Axial	-1.682	0	0	531.82	2	2
10	Axial	+1.682	0	0	868.18	2	2
11	Axial	0	-1.682	0	700	0.32	2
12	Axial	0	+1.682	0	700	3.68	2
13	Axial	0	0	-1.682	700	2	0.32
14	Axial	0	0	+1.682	700	2	3.68
15	Center	0	0	0	700	2	2
16	Center	0	0	0	700	2	2
17	Center	0	0	0	700	2	2
18	Center	0	0	0	700	2	2
19	Center	0	0	0	700	2	2
20	Center	0	0	0	700	2	2

TABLE II: EXPERIMENTAL DESIGN TABLE FOR PREPARATION OF GSAC

Run	Temp. (°C)	Time (hr)	Ratio	GSAC Yield (%)
1	700.00	2.00	0.32	29.38
2	600.00	3.00	1.00	37.72
3	800.00	1.00	1.00	20.53
4	800.00	1.00	3.00	28.12
5	868.18	2.00	2.00	18.64
6	531.82	2.00	2.00	51.60
7	600.00	1.00	3.00	49.94
8	700.00	2.00	2.00	34.09
9	700.00	2.00	2.00	34.45
10	600.00	3.00	3.00	47.56
11	600.00	1.00	1.00	37.94
12	800.00	3.00	3.00	25.16
13	700.00	2.00	3.68	41.14
14	700.00	2.00	2.00	34.68
15	700.00	2.00	2.00	35.29
16	700.00	2.00	2.00	34.25
17	700.00	2.00	2.00	34.87
18	800.00	3.00	1.00	19.91
19	700.00	3.68	2.00	30.95
20	700.00	0.32	2.00	33.52

parameters of activation temperature, activation time and impregnation ratio from the design of experiment table were strictly adhered to for each sample loaded into the furnace. The char produced was mixed with $ZnCl_2$ pellets at different impregnation ratio (IR). At the end of each procedure, the activated product was cooled to room temperature under nitrogen flow and the impregnation ratio was calculated using equation (4).

$$\text{Impregnation ratio (IR)} = \frac{W_{ZnCl_2}}{W_{Char}} \quad (4)$$

Where W_{ZnCl_2} is the dry weight of Zinc chloride pellets and W_{char} is dry weight of char.

The actual results from the activation process are shown in Table II.

TABLE III: ANOVA FOR RESPONSE SURFACE QUADRATIC MODEL FOR GSAC YIELD

Source	Sum of Squares	Deg. of freed	Mean Square	F Value	p-value Prob > F	
Model	1585.08	9	176.12	319.19	< 0.0001	Sig.
A- Temp.	1331.98	1	1331.98	2413.99	< 0.0001	
B- Time	8.06	1	8.06	14.60	0.0034	
C- Ratio	217.08	1	217.08	393.43	< 0.0001	
AB	0.1203	1	0.1203	0.2181	0.6505	
AC	10.11	1	10.11	18.33	0.0016	
BC	2.52	1	2.52	4.57	0.0583	
A²	0.0014	1	0.0014	0.0025	0.9612	
B²	14.71	1	14.71	26.65	0.0004	
C²	0.0477	1	0.0477	0.0864	0.7748	
Residual	5.52	10	0.5518			
Lack of Fit	4.56	5	0.9115	4.75	0.0563	Not Sig.
Pure Error	0.9603	5	0.1921			
Cor Total	1590.60	19				

The analysis of variance (ANOVA) of the regression model demonstrates that the model is highly significant as evident from the calculated F-value and a very low

probability value. According to Sahu *et al* (2010), if the value of Prob. > F less than 0.05, the model terms are considered as significant. The ANOVA for the quadratic model for GSAC yield is shown in Table III. The model F-value of 319.19 and Prob. > F less than 0.0001 implies that this model was significant. However, A, B, C, AC and B² were significant model terms whereas AB, BC, A² and C² were insignificant to the GSAC response of yield. Also from Table III, it was observed that activation temperature (A), the activation time (B) and impregnation ratio (C), were significant on the response of GSAC yield. However, the activation temperature imposed the greatest influence on the response of GSAC yield and therefore was the most significant factor.

TABLE IV: REGRESSION COEFFICIENTS FOR FITTING EMPIRICAL EQUATION OF PERCENTAGE YIELD.

Factor	Reg. Coeff. (Coded)	Reg. Coeff. (Actual)	Std. Err
Yield			
Intercept	34.63	74.29	0.3030
A-Temp.	-9.88	-0.07	0.2010
B-Time	-0.77	5.25	0.2010
C-Ratio	3.99	12.75	0.2010
AB	-0.12	-0.01	0.2626
AC	-1.12	-0.01	0.2626
BC	-0.56	-0.56	0.2626
A ²	0.01	9.76×10^{-7}	0.1957
B ²	-1.01	-1.01	0.1957
C ²	0.06	0.06	0.1957

Therefore, the final empirical model in terms of the coded factors for the response of yield is represented by the following equation:

$$Y(\%) = 34.63 - 9.88A - 0.77B + 3.99C + 0.01A^2 - 1.01B^2 + 0.06C^2 - 0.12AB - 1.12AC - 0.56BC \quad (5)$$

The coefficients with one variable of temperature (A), time (B) and Impregnation ratio (C) represent the effect of that particular factor on the response of yield (Y). The coefficients which are multiples of two variables and

others with second order terms demonstrate the interaction of the multiples of the two variables and quadratic effect respectively. A positive sign in front of the terms indicates a synergistic effect whereas a negative sign implies an antagonistic behavior.

4. PROCESS OPTIMIZATION

Chowdhury *et al* (2012) stated that high adsorption efficiency with adequate product yield is expected in the production of commercial activated carbon. Azargohar and Dalai (2005); Wu and Tseng (2006) posited that the highest possible yield can be increased by optimizing the production variables of activation temperature, activation time and impregnation ratio. Therefore, the main focus of this investigation is to optimize the experimental parameters for optimum GSAC yield. To achieve this, the *numerical* optimization menu was selected on the Design-Expert software version 11.0 (STAT-EASE Inc Minneapolis, LTS). Yield which is the targeted response was set at maximum while the values of the three variables of activation temperature, activation time and impregnation ratio were set in the ranges being studied. After model simulation, the process variables were suggested by the software and the experimental conditions with the highest desirability were selected. The process variables selected were the activation temperature, activation time and impregnation ratio of 600°C, 1.32hr and 3 respectively with optimum groundnut shell activated carbon yield of 50.04%.

3. RESULTS AND DISCUSSION

The quality of the model developed can be evaluated by the correlation coefficient, R^2 and standard deviation values. According to Myers and Montgomery (2002) R^2 indicates the ratio of sum of the squares (SSR) to total sum of the squares (SST) and signifies how well the model approximates experimental data points. Ahmad *et al* (2009) posited that the model developed seems to be the best at low standard deviation and high R^2 statistics. In this experiment, the R^2 value for equation (5) was given as 0.9965 for the carbon yield (Table V). This implies that 99.65% of the total variation in GSAC yield was attributed to the experimental variables studied. The value of 'Adequate Precision' which measures the signal to noise ratio was obtained as 63.2426. The ratio indicated that the developed model can be used to navigate the design space as posited by Chowdhury *et al* (2012).

The performance of the model can also be visualized by observing the plots of the predicted against the experimental percentage yield in figure 2. As can be observed, the predicted value for the percentage yield was close to their experimental values, reflecting suitability of the model represented in equation (5). This might not be unconnected with the high R^2 value for equation (5), which in the opinion of Nasehir Khan *et al* (2010) indicates that the predicted value for GSAC yield would be more accurate and closer to its actual value.

Figure 3 shows studentized residuals and predicted plot for percentage carbon yield. The data points in the plot are randomly scattered, showing that the variance of experimental observations were between ± 3.00 , which implies that no response transformation was needed for the experimental design of this study as suggested by Myers and Montgomery (2002).

From the outlier t plot in figure 4, it was observed that all the standard residuals fell within the interval of ± 3.0 . This implies that the data approximation for the fitted model (Equation 5) to the response surface was good and reflected no data recording error.

As shown in the 3-Dimension response surface plot in Figure 5, the carbon yield was found to decrease with increase in activation temperature and activation time, with impregnation ratio (IR) fixed at mid point (IR =2.0).

The carbon yield was found to increase with increase in impregnation ratio as seen in the 3-D response surface plot in Figure 6. The highest yield was obtained at the maximum point of impregnation ratio within the range under investigation. Yorgun and Yaldiz (2015) observed that the presence activating agent promotes the depolymerization, dehydration and redistribution of constituent biopolymers and also favours the conversion of aliphatic to aromatic compounds, thus increasing yield.

The SEM micrograph in Figure 7 shows well-developed porous network which resulted due to chemical activation with $ZnCl_2$. The presence of pores in the activated sample is in clear contrast with the SEM micrograph (Figure 1) of carbonized sample which showed no visible pores.

The FTIR spectra as seen in Figure 8 recorded functional groups typical of any cellulose material. A stretching wave number range at about 3300 – 3400 cm^{-1} point to the existence of O- H functional group and a bending wave number range at about 2900 – 2800 cm^{-1} reveals the existence of C- H functional group.

The XRD pattern (Figure 9) obtained revealed that the major diffraction peaks are at 25.80, 26.78, 31.78, 34.25 and 35.51° and their inter-planar distance are 3.45, 3.32,

2.81, 2.62 and 2.52Å and phases at the peaks as silicon oxide (SiO₂), iron oxide (Fe₂O₃) and zinc oxide (ZnO).

The TGA graph in Figure 10 represents the decomposition behaviour of the activated carbon prepared from groundnut shell. It was observed that weight loss occurred in two different stages. In the first stage of weight loss which could be attributed to loss of water of crystallization at temperature of less than 100°C and the second stage of weight loss which could be as a result of further decomposition of lignin and hemicellulose occurred in the temperature range of 550 - 800°C. The material showed good thermal efficiency with weight loss of about 10%

TABLE V: FIT STATISTICS

Std. Dev.	0.7428	R ²	0.9965
Mean	33.99	Adjusted R ²	0.9934
C.V. %	2.19	Predicted R ²	0.9774
		Adeq Precision	63.2426

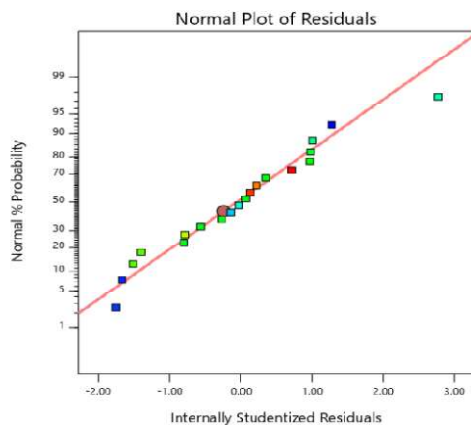


Figure 2: Plot of predicted against actual values of production yield of GS carbon yield.

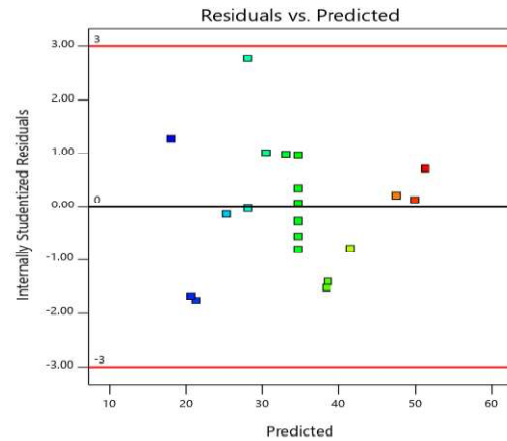


Figure 3: Predicted studentized residual and predicted plot for production yield (%) of GS carbon yield

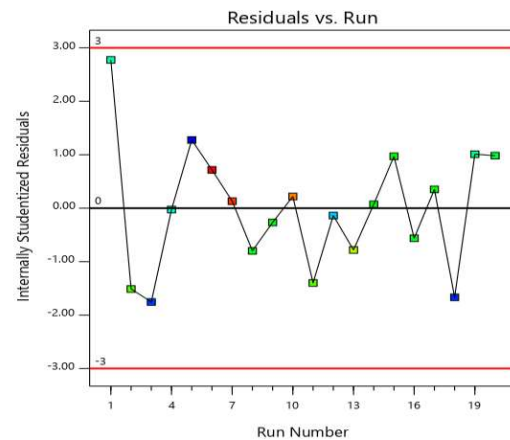


Figure 4: Outlier *t* plot for production yield (%) of GS carbon yield.

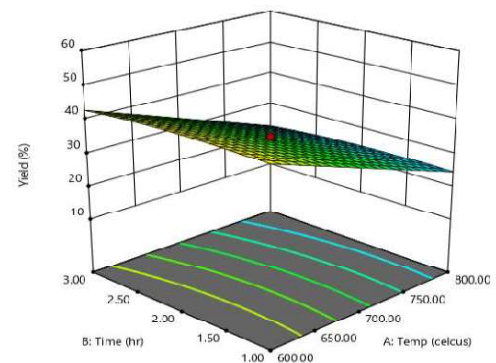


Figure 5: 3- Dimension Response Surface Plot of Effect of Activation Temperature and Activation Time on GS carbon yield

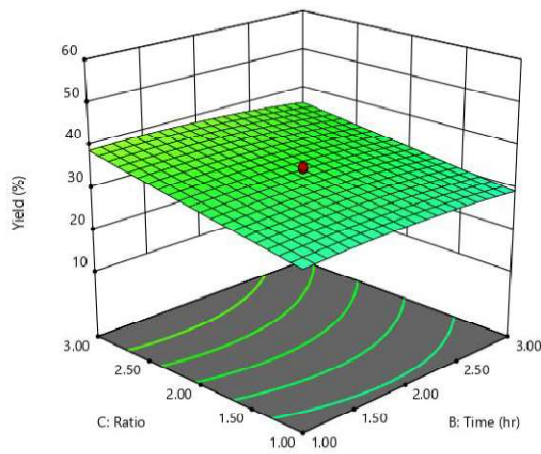


Figure 6: 3- Dimension response surface plot of effect of impregnation ratio and activation time on GS carbon yield

5. MATERIAL CHARACTERIZATION

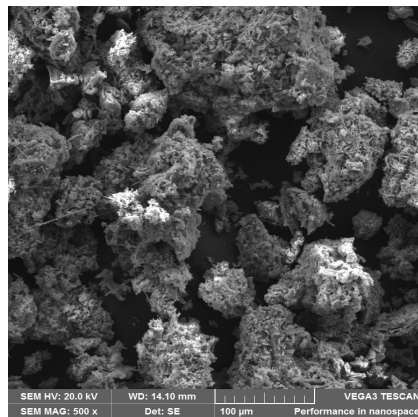


Figure 7: SEM micrograph of groundnut shell activated carbon at optimum conditions.

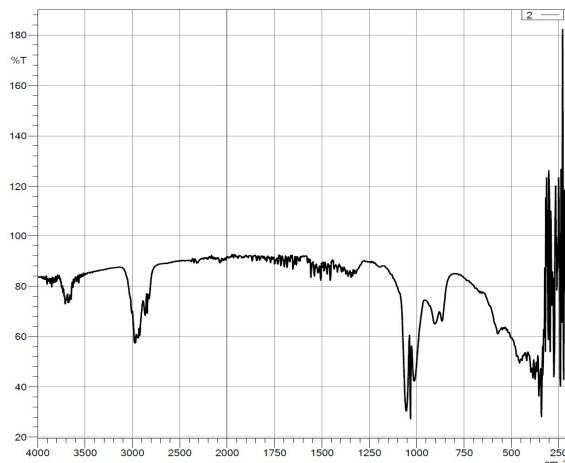


Figure 8: FTIR spectra of groundnut shell activated carbon at optimum conditions

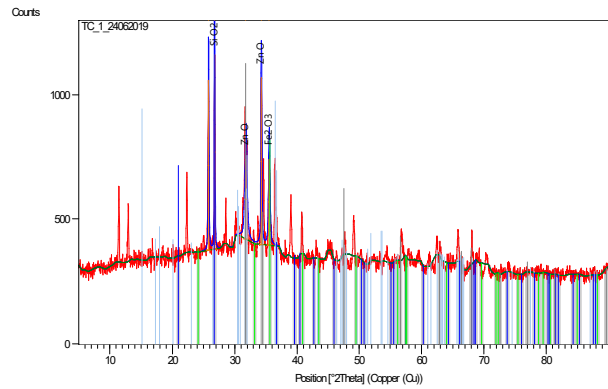


Figure 9: XRD pattern of groundnut shell activated carbon at optimum conditions

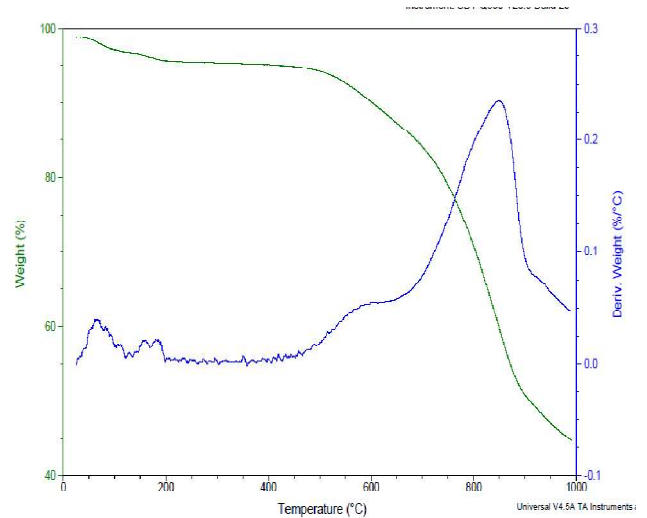


Figure 10: TGA curve for groundnut shell activated carbon at optimum conditions

6. MODEL VALIDATION

Upon validation, the experimental value for percentage yield was close to the value predicted from the model as shown in Table VI, with relatively small error of 0.58% between the predicted and the actual values.

TABLE VI: VALIDATION RESULT

TEMP. TIME RATIO A (°C) B (HR) C			GSAC YIELD (%)		
			PREDICTED	ACTUAL	ERROR (%)
60	1.3	3	50.04	49.75	0.58

6. CONCLUSION

Groundnut shell (GS) is a good precursor for preparing activated carbon and the GSAC prepared showed high surface area and well developed porosity. The RSM was successfully used to study the influence of process parameters on GSAC percentage yield. A quadratic model was developed to correlate the preparation parameters to the carbon yield response. Activation temperature was found to have the most significant effect on the yield. The optimum GSAC yield was obtained by using activation temperature, activation time and impregnation ratios of 600°C, 1.32 hour and 3 respectively, resulting in 50.04% carbon yield.

7. REFERENCES

- Ahmad, A. A., Hameed, B. H. and Ahmad, A. L. (2009). Removal of Disperse Dye from Aqueous Solution Using Waste- Derived Activated Carbon; Optimization Study. *J. Hazard Mater*, 170, 2009, 612-619
- Al-Qodah, Z. Shawabkah, R., and Eliseo A. G., (2016). "Production and Characterization of Granular Activated Carbon from Activated Sludge" *Chemical Engineering Transactions*, vol. 50, 2016 , Vol. 26, No. 01, pp. 127 - 136, January - March, 2009
- Azargohar, R. and Dalai, A. K. (2005). Production of Activated Carbon from Luscar Char: Experimental and Modelling Studies. *Micropor Mesopor Mater* 85, 219-225
- Busari, A. Chaikut, N., Loryuenyong V., Rodklum, C., Chaikwan, T., Kumphan, N., Jadee, K., Klinklom, P. and Wittayarounayut, W. (2012). Transesterification of Waste Frying Oil for Synthesizing Biodiesel by KOH Supported on Coconut Shell Activated Carbon in Packed Bed Reactor. *Sc Asia* 2012; 38: 283-53
- Chowdhury, Z. Z. Zain, S. M., Khan, A. R., Arami-Niya, A. and Khalid, K. (2012). Process Variables Optimization for Preparation and Characterization of Novel Adsorbent from Lignocellulosic Waste. *BioResources* 7(3), 3732-3754.
- Eric, P. L. (2010). Production, Characterization, and Applications of Activated Carbon. *Masters Thesis, University of Missouri* (2010)
- Kwagher, A., and Ibrahim, J. S. (2013). Optimization of Conditions for the Preparation of Activated Carbon from Mango Nuts Using HCl. *American Journal of Engineering Research (AJER)* 2013; vol. 02. Issue 07, pp 74-85
- Malik, R., Ramteke, D. S. and Wate, S. R. (2006). Physico- Chemical and Surface Characterization of Adsorbent Prepared from Groundnut Shell by ZnCl₂ Activation and its Ability to Adsorb Colour, *Indian Journal of Chemical Technology*, vol. 13, July 2006, pp 319-328
- McDougall, G. J. (1991). The Physical Nature and Manufacture of Activated Carbon, *Journal of the South African Institute of Mining and Metallurgy* vol. 91, no. 4. Apr. 1991. pp. 109-120.
- Montgomery, D. C. (2001). Design and Analysis of Experiments, 5th Ed., John Wiley and Sons Inc. USA.
- Myer, R. H., and Montgomery, D. C. (2002). Response Surface Methodology: Process and Product Optimization Using Designed Experiment, 2nd Ed., John Wiley and Sons., USA 2002
- Nasehir-Khan, E. M., Muhamad, F. P. M. L., Ismail, A. and Mohd, A. A. (2010). Effects of Preparation Conditions of Activated Carbon Prepared from Rice Husk by ZnCl₂ Activation for Removal of Cu(II) from Aqueous Solution. *International Journal of Engineering & Technology IJET-IJENS* 2010; vol: 10 No. 6
- Sahu, J. N., Acharya, J. and Meikap, B. C. (2010). Optimization of Production Conditions for Activated Carbons from Tamarind Wood by Zinc Chloride Using Response Surface Methodology. *Bioresour Technol* 2010; 101: 1974 – 82
- Subhashree, P. (2011). Production and Characterization of Activated Carbon Produced from a Suitable Industrial Sludge, *A Report Submitted in partial fulfillment of the requirements for the degree of Bachelor of Technology (Chemical Engineering), National Institute of Technology, Rourkela.* 2011
- Sugumaran, P., Susan, V. P., Ravichandran, P. and Seshadri, S. (2012). Production and Characterization of Activated Carbon from Banana Empty Fruit Bunch and Delonix Regia Fruit Pod. *J. Sustain Energy Environ* 2012; 3: 125-32



Sumathi, S., Bhatia, S., Lee, K. T. and Mohamed, A. R. (2009). Optimization of Microporous Palm Shell activated Carbon Production for Flue Gas Desulfurization: Experimental and Statistical Studies, *Bioresour Technol.* 100, 1614-1621

Wu, F. C. and Tseng, R. L. (2006). Preparation of Highly Porous Carbon from Fire Wood by KOH Etching and CO₂ Gasification for Adsorption of DYES and Phenols from Water. *J Colloid Interface Sci* 294-, 21-30

Yahaya, N. K. E. M., Latiff, M. F. P. M., Abustan, I. and Ahmad, M. A. (2010). Effects of Preparatory Conditions of Activated Carbon from Rice Husk by ZnCl₂ Activation for Removal of Cu(II) from Aqueous Solution. *Int J. Eng Technol* 2010 ;(6):27-31

Yahya, M. A., Al-Qodahb, Z. and Zanariah Ngaha, C. W. (2015). Agricultural bio-waste materials as potential sustainable precursors used for activated carbon production: A Review Renewable and Sustainable *Energy Reviews* 46 (2015) 218-235

Yorgun, S. and Yildiz, D. (2015). Preparation and Characterization of Activated Carbon from Paulownia Wood by Chemical Activation with H₃PO₄. *Journal of the Taiwan Institute of Chemical Engineers* 53 (2015) 122 – 131

Zainudin, N. F., Lee, K. T., Kamaruddin, K. T., Bhatia, S. and Mohamed, A. R. (2005). Study of Adsorbent Prepared from Oil Palm Ash (OPA) for Flue Gas Desulfurization. *Sep. Purf. Technol.* 45, 50 – 60.



Development of a Petroleum Pipeline Monitoring System for Detection, Location and Characterization of Damages in Pipes

*Aba, E. N¹, Olugboji, O. A¹, Nasir, A¹, Oyewole, A¹, & Olutoye, M. A²

¹Department of Mechanical Engineering, Federal University of Technology, PMB 65 Minna Niger State, Nigeria

²Department of Chemical Engineering, Federal University of Technology, PMB 65 Minna Niger State, Nigeria

*Corresponding author email: emmaaba22@yahoo.com, +2348067104205

ABSTRACT

Significant damage to the environment and huge economic losses are potential problems caused by leakage from petroleum pipelines. Even though petroleum pipelines are designed and constructed to maintain very high integrity, the occurrence of a leakage in a pipeline throughout its lifetime is very difficult to prevent. To minimize environmental damage and high economic losses, an efficient pipeline monitoring system is required to carry out accurate damage detection, location and characterization thereby enhancing quick response. A lot of research has been carried out on pipeline monitoring with several damage detection techniques proposed. Some of these damage detection methods like air surveillance have the disadvantage of being very expensive with very slow response time while other methods like the hydraulic leak detection have the advantage of a faster response time and also being less expensive. This paper surveys various damage detection methods that are employed in pipeline monitoring. The strengths and weaknesses of several methods and their application for different pipeline systems are highlighted. This work focuses mainly on a damage detection technique based on the principle of vibration that is able to characterize damage scenarios on a pipe with pressure pulses propagating through, thereby being able to determine the actual cause or nature of the damage. The Fourier transform method in particular, a signal processing tool is discussed in detail.

Keywords: *characterization, damage-detection, Fourier transform, pipeline-monitoring.*

1 INTRODUCTION

Major pipelines across the world transport large quantities of crude oil, natural gas, and petroleum products. These pipelines play an important role in modern societies and are crucial in providing needed fuels for sustaining vital functions such as power generation, heating supply, and transportation. In light of the hazardous properties of the products being transmitted through these pipelines, a ruptured pipeline has the potential to do serious environmental damage. Ruptured pipelines also cause huge economic as well as humanitarian losses. The risk associated with pipeline in terms of safety of people, damage to the environment and loss of income has been a major concern to pipeline integrity managers. Factors, such as external impacts, environmental corrosion, internal erosion, material initial defects, ground surface movements, improper maintenance and human reasons (vandalization, etc) may lead to pipeline leakage. Very important is early detection of pipeline leakage and this is becoming a very important application field for structural health monitoring (SHM) technologies (Shi *et al.*, 2018).

Pipeline inspection technologies using sensor networks have drawn significant attention, for example, in the applications of natural gas pipeline inspection and monitoring by acoustic sensors (Park *et al.*, 2007) (Agrawal, 2008). This study intends to use sensor networks to detect damages in pipeline systems using

pressure guided waves or pulses, and a signal processing techniques based on the principle of vibration in pipes.

In general, pipeline defects can occur in the manufacture, construction, and operation processes. In this study, focus is on the operational defects that encompass fatigue, third party damage, denting and buckling. To ensure the continued safe operation of the transmission pipelines, continuous monitoring or periodic assessment of the integrity of the pipelines is necessary. In pipeline monitoring and inspection, the ultimate objective is to identify the locations that have defects, and obtain an accurate measurement and assessment of the defects so that human operators can take appropriate actions to prevent further damage. The goal of this study is to develop a continuous, remote, and real-time monitoring and inspection system using wire/wireless sensors that can provide early detection for pipeline systems.

A pipeline monitoring and inspection system has a long list of tasks to accomplish ranging from detection of damage to determining structural defects in pipes. To achieve these goals, various actuators and sensors are relied upon. There are many types of sensors that have been studied and tested for pipeline inspections including acoustic sensors, fiber optic sensors, and magnetostrictive sensors. Each type of sensors has its unique feature and operational condition. In this study, piezoelectric sensors were used.

Vibration-based approaches have been developed in the past and have been proven to be relatively successful in detecting damage in pipes (Razi *et al.*, 2013). For a long period of development, vibration-based and guided waves-based damage detection technologies have produced a good number of research results. Some of the noteworthy ones are briefly presented here. Olugboji (2011) developed and tested mathematical techniques for locating an impulsive event on a pipeline using the pressure pulse caused by it from measurements made remotely. His experimental work was carried out using an experimental test rig comprising a flexible hose pipe with four pressure sensors distributed along the pipe and connected to a data acquisition system. The experiments were tested using static air in the pipe, and were found to give good results. Junxiao *et al.*, (2017) carried out damage detection in a gas pipeline making use of the negative pressure wave (NPW), a stress wave generated by leakage in the pipeline which propagates along the pipeline from the leakage point to both ends, and the hoop strain variation along the pipe wall. Guofeng *et al.*, (2017) developed a wavelet packet-based damage index matrix to identify the crack damage in pipeline structure using a stress wave propagation approach with piezo-ceramic transducers. In their work, four cracks were artificially cut on the specimen, and each crack had six damage cases corresponding to different crack depths. This aided them to simulate cracks at different locations with different damage degrees. In each damage case, they used one piezo-ceramic transducer as an actuator to generate a stress wave to propagate along the pipeline specimen, and the other piezo-ceramic transducers were used as sensors to detect the wave responses. Golmohamadi (2015) used wavelet transform for processing signals to recognize damage and leak location in a hardware-based technique which used ultrasonic wave emission. Changhanget *al.*, (2017) used a low-power piezo-ceramic transducer as the actuator of vibrothermography and explored its ability to detect multiple surface cracks in a metal part. They employed the Fourier Transform signal processing technique in their work and their results showed that all cracks can be detected conveniently and simultaneously by using the proposed low-power vibrothermography. Enrique *et al.*,(2016) combined the guided waves and electro-mechanical impedance techniques based on smart sensing to define a new and integrated damage detection procedure. This combination of techniques was studied by them and they proposed a new integrated damage indicator based on Electro-Mechanical Power Dissipation (EMPD). They tested the applicability of their proposed technique through different experimental tests, with both lab-scale and real-scale structures. Kia *et al.*,(2018) proposed a new approach to damage detection of a concrete column structure subjected to blast loads using embedded piezo-ceramic smart aggregates (SAs). They proposed active-sensing based approach in which the

embedded SAs act as actuators and sensors that can respectively generate and detect stress waves.

Pipeline inspection technologies using sensor networks have drawn significant attention around the world. This study intends to use sensor networks to detect, localize, and characterize bursts, leaks and other anomalies (damages) in general pipeline systems using pressure pulses and signal processing techniques based on the principle of vibration in pipes. The competitive advantage of this research work and its contribution to knowledge lies in its ability to perform real-time damage characterization through the use of a combination of wave propagation, an active sensor network and suitable digital processing technique. This would make the interpretation of the cause of damage on pipes possible and would enhance faster response to damage by technicians. It would also assist the technicians in knowing what kind of repair work to do before arrival at the scene of the event and be armed with the requisite tools when signalled with a pipeline leak or rupture alarm. The early adopters for this technology would be petroleum companies; innovative pipeline maintenance companies, and government with obligation to maintain uninterrupted petroleum products supply.

2 DAMAGE DETECTION AND LOCATION TECHNIQUES

These techniques are basically the techniques used in oil and gas industries, and those based on transient methods used for detecting existing leaks.

2.1 TRANSIENT MODELING

A real-time transient flow simulator can be an effective tool for monitoring abnormalities in pipelines. Several methods based on a fluid transient model are found in literature. Most of them are applied in oil and gas industry. Two different approaches are described – a pressure discrepancy method and a dynamic volume balance method. Both approaches use the analysis of discrepancies between simulated and measured data. The pressure discrepancy method compares pressure values at a number of points throughout the system. In the dynamic volume balance method, two flow discrepancies are computed at the inlet and outlet. This method uses the fault sensitive approach – the pipeline is assumed to be intact in the calculations. The real-time pressure and flow measurements at both ends of the pipeline are collected with a sampling interval of 15-30s. The measured pressure and flow are used as boundary conditions in a transient model. When the leak occurs, it is manifested in the measurements. Thus, the simulated flow and pressure values diverge from the measured ones. The average response time of the method is expected to be less than one hour.

2.2 ACOUSTIC METHODS

As an alternative to the model-based techniques described above, acoustic measurements can be used to detect and locate leaks. An acoustic signal generated by the escaping leak mass propagates through the flowing fluid or through the pipeline wall. The complexity of acoustic systems varies from manual checks using geophones to permanent continuous monitoring systems (Rajtar and Muthiah, 1997). Acoustic leak detection systems have been successfully applied to detect and locate defects in nuclear power plants, petroleum and chemical systems and water distribution systems. However, according to the review of leak detection methods presented in Wang et al. (2001), there are several disadvantages of acoustic methods. Factors that affect the performance of acoustic leak detection and location are: (1) unwanted interference noise (traffic, wind, etc.), (2) varying sound propagation conditions from one pipeline section to another, (3) characteristics of the leak (i.e. large pipe burst surrounded by the water that has escaped the pipe produces weak signal), (4) multiple leaks tend to give incorrect leak locations and (5) strong acoustic damping in plastic pipes.

2.3 TRANSIENT ANALYSIS

The occurrence of a sudden leak in a pipeline causes a pressure decrease which is followed by a transient wave or pressure pulse travelling upstream and downstream along the pipeline. The analysis of this burst-induced wave or pulse can be used for leak detection and location. The main objective of all transient leak detection methods is the same – extract the information about the presence of the leak from the measured transient trace or pressure pulse. For the generation of a transient event or damage event, system elements (i.e. inline valves and pumps) or special devices (such as solenoid side discharge valves or pulse generators) are used. The fact that the transient wave speed can be over 1000 m/s means that a high sampling frequency of pressure measurements is required. The choice of measurement position and the characteristics of generated transients depend on the method that is used for further analysis.

The leak reflection method (Brunone and Ferrante, 2001) is probably the most straightforward and simple application of transient analysis for leakage detection. A transient wave travelling along the pipeline is partially reflected at the leak. If the reflected wave can be identified in a measured pressure trace, the location of the burst can be found using simple calculations. This method is based on the principle of time domain reflectometry (TDR). The inverse method (Olugboji and Yisa, 2012) uses least squares regression between modeled and measured transient pressure traces. The leak is modeled at discrete positions (usually nodes) in the network and the minimization of the deviation between the measured and calculated pressures produces a solution of leak location

and size. In addition to leak detection, inverse method can be used for any system parameter calibration, given enough measurement data. The transient damping method (Wang et al.; 2002) uses the damping rate of the transient trace to detect a leak. The decay of the transient wave is caused by pipe friction and leaks. Leaks can be detected by comparing the measured pressure containing the leak-induced damping to the simulated results for the same pipeline without a leak. The possibility of applying this method in pipe networks has not been investigated. The frequency response method (Ferrante and Brunone; 2003, Lee et al., 2003, Olugboji, 2011) uses the analysis of transient response in the frequency domain. Fourier transforms are used to transform time-domain data into the frequency domain. By comparing the dominant frequencies of no-leak and leaking pipelines, the leak location can be obtained.

2.4 METHODS OF PIPELINE MONITORING

2.4.1 TIME DELAY BETWEEN PULSE ARRIVALS AT SENSORS (CROSS CORRELATION METHOD)

To locate an event such as an impact or explosion along a pipeline, the use of sensors along the pipeline on opposite sides of the event is required. This method determines this from the knowledge of the pulse arrival times and sensor positions. As an advantage, it does not require measurements of the time of arrivals of the pulse signals at the sensors in order to calculate the time delay, but rather gives the delay directly. Also even with the addition of noise to the pulse, performing a correlation between the pulse signals still gives a good estimate of the measured time delay in arrivals of the pulse signals since the correlation method acts as an integrator which averages the random noise present in the pulse signals. A disadvantage is that there is some error using this method, though not as much as the uncertainty involved in using the peak detection and threshold crossing methods. The magnitude of the cross correlated peak is lower as compared to peak detection and threshold crossing methods due to the poorer fit, and the size of the error will depend on the size and form of the distortion in each application.

2.4.2 ACOUSTIC MONITORING

Leak transients are associated to “rarefaction waves”, and any interaction with the pipe generates pressure (acoustic) waves that are guided within the fluid for long distances, carrying information on the source event. Acoustic monitoring technology makes use of hydrophone sensors placed at discrete distances along pipelines in order to detect third party interference (TPI) and leaks. Acoustic leak correlators, which are equipped with microprocessors or portable computers, can be used to improve the

accuracy of leak location. The disadvantages of this method include various unwanted interference noise such as those from traffic, wind, use of water and air craft; varying pressure conditions in the pipes especially varying pipe materials, thus changing sound propagation conditions from one pipeline section to another. Small holes with high pressure produce clearer and stronger noises, and are easier to locate than a large pipe burst surrounded by the escaped water or ground water with weak noise. Also, multiple leaks tend to give incorrect leak location, and they are strong acoustic damping in plastic pipes.

2.4.3 WAVELET BASED ANALYSIS

When a transient travelling in a pipeline reaches a leak, the transient is partially reflected and partially transmitted. If the reflected wave (normally the first reflected one) can be identified from the measured transient, the location of the leak can be determined. Its advantage is that the concept of this method is simple and is easy to apply with the condition that initiating time of the transient must be smaller than the reflection time between the leak and measurement location. It can also be used on a real-time base for monitoring of pipeline rupture. The downside of this method is that some pipeline elements such as elbows, changed pipe diameter, or partially closed valves can also cause transient reflections. It may result in leak induced transient reflection not being identified in some situations depending on the location of the transient measurement.

2.4.4 INVERSE LEAST SQUARE METHODS

This method uses regression between modeled and measured transient pressure traces. The leak is modeled at discrete positions (usually nodes) in the network and the minimization of the deviation between the measured and calculated pressures produces a solution of leak location and size. Its advantage is that it can be used for any system parameter calibration, given enough measurement data. Experiences from real tests indicate that the challenge for applying inverse least square method is that of accurate modelling of the transients and boundary conditions in a pipe network. This is a major disadvantage of this method.

2.4.5 INVERSE METHODS

An Inverse problem is one where there is a relationship between the model parameters and the data. This relationship is referred to as the model and that the model usually takes the form of one or more formulas that the model parameters and data are anticipated to follow. Inverse method preserves monotonicity and correlation which helps in variance reduction methods, generating truncated distributions and order statistics.

2.5 SIGNAL PROCESSING

The leak detection and location techniques used in transient analysis make use of different signal processing techniques for the computing and analysis of the transient waves or pressure pulses generated when a damage event occurs on a pipe. Signal processing is carried out for various reasons. Some of the objectives of signal processing include information gathering for signal analysis: determination of system state; detection: detection of abnormality by comparison to reference/normal values; monitoring: obtaining continuous or periodic information, identifying relative changes to the state of the system; remedy and control: intervention based on measurements; evaluation. This is illustrated in Figure 1.

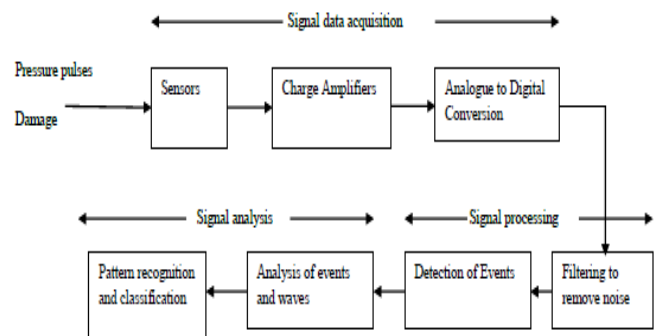


Figure 1: Computer-aided detection and classification based on pressure pulse signal analysis

2.5.1 SIGNAL PROCESSING METHODS

A wide variety of integral transforms and methods exist that can be applied in discrete form to digital signals for their analysis and processing. Many of these transforms and methods yield properties that are better or worse in terms of doing 'something useful' with the signal. Some of these important methods are listed below:

- Fourier Transform
- Wavelet Transform
- Digital Filtering (convolution-type filters; Fourier based filters)
- Fast Fourier Transform
- Convolution and Correlation

2.5.2 SAMPLING SIGNALS (SAMPLING THEOREM)

Digital signals are often obtained from analogue signals by converting them into a sequence of numbers (a digital signal) so that digital computers can be used to process them. This conversion is called digitization (Blackledge, 2006). When conversion takes place, it is a naturally common requirement that all the information in the

original analogue signal is retained in digital form. To do this, the analogue signal must be sampled at the correct rate. The correct rate to sample a signal is given by the sampling theorem. The sampling theorem states that if a continuous function $f(t)$ is bandlimited and has a complex spectrum $F(\omega)$, $|\omega| \leq \omega_c$, then it is fully specified by values spaced at regular intervals

$$\delta t \leq \frac{\pi}{\omega_c} \quad (1)$$

(Blackedge, 2006)

The parameter ω_c/π is known as the ‘Nyquist frequency’. When sampling an analogue signal the sampling frequency must be greater than twice the highest frequency component of the analogue signal to be able to reconstruct the original signal from the sampled version. To convert an analogue signal into a digital signal with no loss of information, one must choose a sampling rate that is at least equal to the Nyquist frequency of the signal. If this criterion is not adhered to, a distortive effect known as “aliasing” will occur causing the replicated spectrum to overlap. A digital signal that has been sampled according to the condition:

$$\delta t = \frac{\pi}{\omega_c} \quad (2)$$

is called a Nyquist sampled signal where ω_c/π is the Nyquist frequency (equal to twice the frequency bandwidth of the signal). This is the optimum sampling interval required to avoid aliasing and to recover the information of an analogue signal in digital form. It is the fundamental result used in all A-to-D (Analogue-to-Digital) conversion schemes.

2.5.3 SIGNAL RECONSTRUCTION

In digital signal processing, the term “reconstruct” has a special meaning. It is related to converting a signal from its discrete form to a continuous form using a Digital-to-Analog Converter (DAC) and an ideal reconstruction low-pass filter.

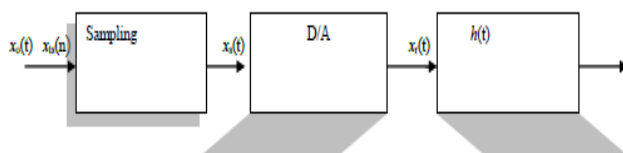


Figure 2: An ideal sampling and reconstruction process

$x_o(t)$ = original signal
 $x_o(n)$ = sampled signal or time-discrete sequence
 $h(t)$ = ideal reconstruction low-pass filter
 $x_t(t)$ = reconstructed signal

Figure 2 shows an ideal sampling and reconstruction system based on the results of the sampling theorem. This consists of a sampling device which produces a time-discrete sequence $x_o(n)$. $h(t)$, an ideal reconstruction low-pass filter is an analog sinc filter, with

$$h(t) = (t/T_s) \quad (3)$$

This analog filter cannot be applied directly to the time-discrete signal. The delta function is used to solve this challenge by turning the sequence into an analog signal $x_s(t)$. This is expressed as in the equation below:

$$x_s(t) = \sum_{n=-\infty}^{\infty} x_o(n) \delta(t - nT) \quad (4)$$

According to the sampling theorem, this system will only produce an output or reconstructed signal ‘ $x_r(t) = x_o(t)$ ’ when the sampling frequency f_s is at least twice the highest frequency of the original signal $f_o(t)$. To achieve a practical reconstruction system, only finite length pulses must be inputted into the reconstruction filter. This is achieved by the use of an operation known as the “Hold” operation.

2.5.4 DIGITAL SIGNAL PROCESSING FOR CHARACTERIZATION OF DAMAGES IN PIPES

Every “real world” signal produced by an event/occurrence/source be it Pressure (Speech, Music, Sonar, Drilling, Explosion); Bio-Electric (EEG, ECG); Electromagnetic (Radio, Radar); Images (Camera, MRI) or others (Seismic) has its own special characteristics. As a result of the special characteristics each of these signals possesses, the appearance of each signal’s wave spectra is completely different from the other. In other words, the wave spectra of a signal caused by pressure from an explosion will be completely different from the wave spectra of a radio signal caused by an electromagnetic event. This is the whole idea behind the characterization of damages in pipes using digital signal processing. Digital signal processing methods would be applied to a pipe that has undergone a damage causing impulsive event to process these signals from their analogue states to their digital states. Filtering of these signals would also be done to remove unwanted frequencies like those caused by noise and then generate the wave spectra of these signals.

These DSP methods in order to fully characterize damages in pipes would be able to carry out Pattern Recognition through:

- Abnormal signals (with event introduced) versus the normal signals (with no event)
- Using an average of several outputted normal waveforms as the template

- Detection of new waveforms, segmentation and comparison to the normal template

3 PROPOSED DAMAGE DETECTION AND CHARACTERIZATION METHODS

A pressure pulse is generated when a pipe is damaged and this pressure pulse propagates in both directions away from the location of the damage. Both pressure pulses are eventually reflected when they reach the boundaries of the pipelines. This work looks at the location of an event on a pipeline considering a situation with fluid (water) flowing through the pipe. This would require the use of sensors on opposite sides of the event. Using a pressure measurement sampled at a high frequency at several points along the pipe, the travel times of the pressure pulses can be found.

3.1 DAMAGE LOCATION BASED ON PRESSURE PULSE ANALYSIS

The pulse arrival times in a pipe and the sensor positions along the pipe can be used to determine the location of an event along a pipe. These events could either be caused by drilling, impact, explosion, etc. In Figure 3, the schematic representation of a pipeline with four sensors placed along it is shown. These sensors are denoted by 1, 2, 3, 4 and are at distances $x_1, x_2, x_3,$ and x_4 from some boundary. The arrival times of some generated pulses caused by a damage-inducing impulsive event occurring at an unknown location is recorded as $t_1, t_2, t_3,$ and t_4 by the four sensors.

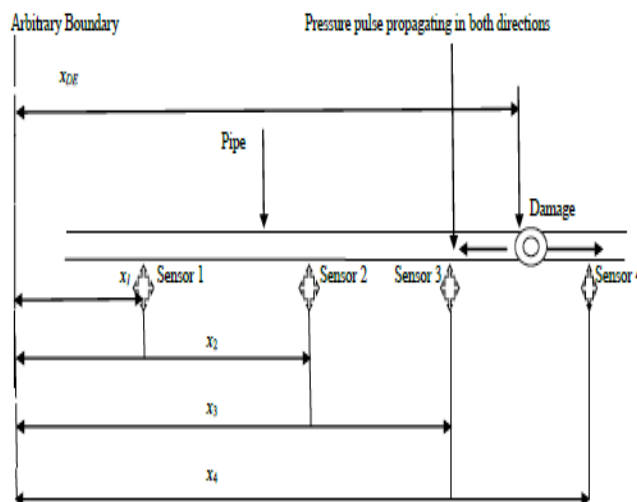


Figure 3: Schematic representation of sensors on a pipeline.

Sensor 3 or 4 maybe used to determine the location of the event on the pipe shown in Figure 3. The occurrence of a damage event on a pipe leads to a change in pressure within the pipe which eventually leads to the generation

of pressure pulses. Every increase or decrease in pressure travels at a velocity c_p in the form of a pressure pulse through the fluid filled pipe in both directions. The pressure pulse propagation velocity in a fluid filled pipe depends on fluid elastic properties as well as on pipe geometry and material. The velocity of a pressure pulse in an elastic fluid inside an elastic pipe is given as:

$$C_p = \sqrt{\frac{1}{\rho \left(\frac{1}{E_v} + \frac{ID}{W_t E} \right)}} \quad (5)$$

(Finnemore and Franzini, 2002; Záruba, 1993)

Where ρ = density of water (kg/m^3)
 E_v = bulk modulus of water (N/m^2)
 ID = inner pipe diameter (mm)
 W_t = wall thickness (mm)
 E = Elasticity modulus of pipe (N/m^2)

Also this pulse propagation velocity can be measured from the arrival of pulses at the same side of the event which are sensors 3 and 2, or sensors 2 and 1 as in the case shown in Figure 3. Thus, the exact location of the event from sensor 3 is calculated by:

$$x_{DE3} = \frac{t_{34} C_p + x_{DE3}}{2} \quad (6)$$

or from sensor 4,

$$x_{DE4} = \frac{x_{43} - C_p t_{34}}{2} \quad (7)$$

3.2 CHARACTERIZATION OF DAMAGE EVENTS IN PIPES

Pipelines are considered as one of the safest means of transporting petroleum products. These pipelines are damaged from time to time as a result of natural events (erosion, earthquakes, etc) or due to third party activities (explosions, drilling activities, vehicular movement, etc). A great challenge that pipeline operators has faced in the past even in situations where it had been known that damage has occurred along pipelines is the difficulty in pin-pointing the exact cause of the damage.

Most times, damages caused by impulsive events generate a pressure pulse that propagates in both directions through the fluid in the pipe. Detection and measurement of these pressure pulses can be carried out at points remote from the event. These measured pulses contain information about the event and can be used to characterize what must have caused the damage. The information about damage-causing impulsive event contained in these measured pressure pulses can be outputted through proper analysis of the pressure pulses (signals). Therefore, to achieve the characterization of damage events in pipes, proper signal analysis of measured pressure pulses is carried out.

3.3 NUMERICAL SIMULATION AND MODELING OF PRESSURE PULSE PROPAGATION FOR CHARACTERIZATION

In this work, emphasis is based more on outputting, analyzing and categorizing the wave spectra obtainable from different impulsive or damage causing events. In terms of linking the characteristics of a signal to the 'physics' of the system that produces it, particularly with regard to the interactions of wave fields with matter and the design of sensors to record such interactions, the Fourier transform has and continues to reign supreme. This is because it provides the most general and comprehensive solution to physical systems described by differential equations and most of the laws of physics can be expressed in the form of differential equations (Blackledge, 2006).

3.4 MATHEMATICAL MODEL FOR SAMPLING

For this work, the Fourier Transform is employed as the basis to develop the mathematical model needed for the reconstruction of the signals arising from various impulsive events.

The following notations were adopted in the course of this work:

$x_o(t)$ = original analog signal

$x_r(t)$ = reconstructed signal (where $x_r(t) = x_o(t)$)

$x_{ts}(n)$ = time-discrete signal or sampled signal

where $x_{ts}(n) = x(nT_s)$ (8)

f_s = sampling frequency (samples/second)

T_s = sampling interval (seconds/sample)

where $T_s = \frac{1}{f_s}$ (9)

$\dot{\varphi}$ = real angular frequency (radians/second)

ω = digital angular frequency (radians/second)

where $\omega = \varphi T_s$ (10)

t = continuous time variable

n = discrete integer variable

The inverse Fourier transform of a time discrete signal $x_{ts}(n)$ obtained from sampling $x_o(t)$ every T_s second is given by:

$$x_{ts}(n) = \frac{1}{2\pi} \int_{-\pi}^{\pi} X_{ts}(e^{i\omega}) e^{i\omega n} d\omega \quad (11)$$

In simplifying the above, the equation is expressed in terms of real angular frequency, φ . This gives:

$$x_{ts}(n) = \frac{T_s}{2\pi} \int_{-\frac{\pi}{T_s}}^{\frac{\pi}{T_s}} X_{ts}(e^{i\varphi T_s}) e^{i\varphi T_s n} d\varphi \quad (12)$$

For a continuous signal, the inverse Fourier transform given by:

$$x_o(t) = \frac{1}{2\pi} \int_{-\infty}^{\infty} X_o(i\varphi) e^{i\varphi t} d\varphi \quad (13)$$

Replacing t with nT_s in the above equation, we obtain

$$x(nT_s) = \frac{1}{2\pi} \int_{-\infty}^{\infty} X_o(i\varphi) e^{i\varphi nT_s} d\varphi \quad (14)$$

Splitting the integration in (14) into sub-intervals of length $\frac{2\pi}{T_s}$ and taking the sum over the resulting integrals to obtain the complete area, we have:

$$x(nT_s) = \frac{1}{2\pi} \sum_{k=-\infty}^{\infty} \int_{\frac{(2k-1)\pi}{T_s}}^{\frac{(2k+1)\pi}{T_s}} X_o(i\varphi) e^{i\varphi nT_s} d\varphi \quad (15)$$

Changing the integration variable by setting

$\varphi = \alpha + \frac{2*\pi k}{T_s}$, we obtain:

$$x(nT_s) = \frac{1}{2\pi} \sum_{k=-\infty}^{\infty} \int_{-\frac{\pi}{T_s}}^{\frac{\pi}{T_s}} X_o\left(i\left(\alpha + \frac{2*\pi k}{T_s}\right)\right) e^{i\left(\alpha + \frac{2*\pi k}{T_s}\right)nT_s} d\alpha \quad (16)$$

Multiplying (15) all through by $\frac{T_s}{T_s}$, with ' $\alpha = \pi r^2$ ', and noting that $e^{i2*\pi kn}$, we obtain:

$$x(nT_s) = \frac{T_s}{2\pi} \int_{-\frac{\pi}{T_s}}^{\frac{\pi}{T_s}} \sum_{k=-\infty}^{\infty} \frac{1}{T_s} X_o\left(i\left(\varphi + \frac{2*\pi k}{T_s}\right)\right) e^{i\varphi nT_s} d\varphi \quad (17)$$

In order for $x_{ts}(n)$ to be equal to $x(nT_s)$ for all values of the integer n , (12) and (17) must agree as given below:

$$X_{ts}(e^{i\varphi T_s}) = \frac{1}{T_s} \left(i\left(\varphi + \frac{2\pi k}{T_s}\right) \right) \quad (18)$$

The above is the mathematical model for sampling of signals to obtain their digital spectrum.

3.5 MATHEMATICAL MODEL FOR SIGNAL RECONSTRUCTION

The inverse Fourier transform for a bandlimited signal is given by:

$$x_o(t) = \frac{1}{2\pi} \int_{-\frac{\pi}{T_s}}^{\frac{\pi}{T_s}} X(i\varphi) e^{i\varphi n} d\varphi \quad (19)$$

' $X_{ts}(e^{i\varphi T_s}) = \frac{X(i\varphi)}{T_s}$, for the interval being integrated and when this is substituted into (19), we obtain:

$$x_o(t) = \frac{T_s}{2\pi} X_{ts}(e^{i\varphi T_s}) e^{i\varphi t} d\varphi \quad (20)$$

When the DTFT expression for $X_{ts}(e^{i\varphi T_s})$ is applied, we obtain:

$$x_o(t) = \frac{T_s}{2\pi} \int_{-\frac{\pi}{T_s}}^{\frac{\pi}{T_s}} \sum_{k=-\infty}^{\infty} x_{ts}(n) e^{(-i\varphi n T_s)} e^{i\varphi t} d\varphi \quad (21)$$

With summation and integration interchanged, we obtain:

$$x_o(t) = \frac{T_s}{2\pi} \sum_{k=-\infty}^{\infty} x_{ts}(n) \int_{-\frac{\pi}{T_s}}^{\frac{\pi}{T_s}} e^{i\varphi(t-nT_s)} d\varphi \quad (22)$$

Integrating, we obtain:

$$x_o(t) = \sum_{k=-\infty}^{\infty} x_{ts}(n) \frac{\sin\left(\frac{\pi}{T_s}(t-nT_s)\right)}{\frac{\pi}{T_s}(t-nT_s)} \quad (23)$$

The above is the reconstruction model that was used to recover the original signal $x_o(t)$ from the time-discrete sequence or sampled signal $x_{ts}(n)$.

4 SIMULATION OF MATHEMATICAL MODEL

The simulation of these mathematical models developed for both the sampling and reconstruction of signals obtained from pressure pulses' propagating within a pipe was carried out using the MatLab software. This was done to ascertain the workability of the model and its ability to perform proper event reconstruction. The results of the simulation were good.

4.1 EXPERIMENTATION FOR VALIDATION OF SIMULATION

For the validation of the proposed models for damage location and characterization in pipes, three different experiments were carried out. These three experiments were carried out to mimic damage events in pipes caused by Explosion, Drilling and Vehicular movement respectively. The set-up consisted of a PVC (Polyvinyl Chloride) pipe of total length 25m and internal diameter of 20mm along which pressure pulses would propagate. Five sensors were located at different positions along the PVC pipe and connected to a single data instrumentation system to capture and record the propagation of the pulses. The set up is shown in Figure 4.

4.1.1 EXPERIMENTATION TO MIMIC DAMAGE EVENT CAUSED BY EXPLOSION

A pulse generator was used to mimic an explosion in the pipe. Sensors connected to a single USB data logging were placed at known points along the pipe and an instrumentation system was used to capture the propagation of the pressure pulses and saved in a tab delimited data file. Analysis of the captured data was done offline using a program written in the MatLab programming language.

4.1.2 EXPERIMENTATION TO MIMIC DAMAGE EVENT CAUSED BY DRILLING

The experimental setup was basically the same with that explosion. To mimic a drilling operation, sharp fronted pressure pulses were generated into the pvc pipe by using a hand drill to drill a hole at a point along the surface of the pipe. The signals from the sensors were recorded using the data acquisition model and saved. The saved data was analyzed using a program written in the MatLab programming language.

4.1.3 EXPERIMENTATION TO MIMIC A POTENTIAL DAMAGE EVENT OR A FALSE ALARM CAUSED BY VEHICULAR MOVEMENT

With a similar experimental setup as that of explosion and drilling, this experiment was carried out by placing a mass on the pvc pipe with sensors attached to it. The signals from the sensors (accelerometers) were recorded using the data acquisition device and saved. The saved data will then be analyzed using a program written in the MatLab programming language.



Figure 4: Experimental Test Rig

5 CONCLUSION

In a pipe-damage scenario, pulses are generated and these pulses contain information about the event and can be used to characterize what must have caused the damage. The information about damage-causing impulsive event contained in these measured pressure pulses can be outputted through proper analysis of the pressure pulses (signals). The digital signal processing techniques through

sampling and event reconstruction is used to generate the wave spectra of the various damage sources to be considered and then characterize the damage by carrying out Pattern Recognition.

For this work, the Fourier Transform was employed as the basis for developing the mathematical model needed for the reconstruction of the signals arising from various impulsive events. The following have so far been established in the course of this research work:

- Mathematical techniques for the location, detection and characterization of damages along petroleum pipelines
- Simulation of developed mathematical model
- Development of experimental procedure for verification of the simulation
- Evaluation of the designed location, detection, and characterization system

REFERENCE

- Agrawal, A. (2008). A Theoretical, Numerical and Experimental Investigation of Guided Wave Propagation in Hollow Cylinders. Master Thesis, Carnegie Mellon University. Retrieved from www.researchgate.net/.../276129611.
- Blackledge J.M. (2006). "Digital Signal Processing". Dublin Institute of Technology, School of Electrical and Electronic Engineering. ARROW@DIT
- Brunone, B. and Ferrante, M. (2001). Detecting Leaks in Pressurized Pipes by Means of Transients. *Journal of Hydraulic Research*, IAHR 39(5): 539–547. Retrieved from www.journal.au.edu.
- Changhang, X., Jing, X., Wuyang, Z., Qingzhao K., Guoming, C., Gangbing, S. (2017). Experimental Investigation on the Detection of Multiple Surface Cracks Using Vibrothermography with a Low-Power Piezoceramic Actuator. *Sensors*, 17, 2705; doi:10.3390/s17122705.
- Enrique, S., Rui, S., Ricardo, P. (2016). Damage Detection Based on Power Dissipation Measured with PZT Sensors through the Combination of Electro-Mechanical Impedances and Guided Waves. *Sensors*, 16, 639; doi:10.3390/s16050639.
- Finnmore, E. J., Franzini, J. B. (2002). "Fluid Mechanics with Engineering Applications". 10 editions, Boston, McGraw-Hill. ISBN 0-07-243202-0; 0-07- 112196-X. Retrieved from www.docs.google.com
- Golmohamadi, M. (2015). "Pipeline Leak Detection". Masters Theses, Missouri University of Science and Technology. Scholars' Mine. Retrieved from http://scholarsmine.mst.edu/masters_theses/7397
- Guofeng, D., Qingzhao, K., Hua, Z., Haichang, G. (2017). "Multiple Cracks Detection in Pipeline Using Damage Index Matrix Based on Piezoceramic Transducer-Enabled Stress Wave Propagation". *Sensors*, 17, 1812; doi:10.3390/s17081812.
- Junxiao, Z., Liang, R., Siu-Chun, H., Ziguang, J., Gangbing, S. (2017). "Gas Pipeline Leakage Detection Based on PZT Sensors". *Smart Materials and Structures*. Smart Mater. Struct. 26 (2017) 025022 (7pp), doi:10.1088/1361-665X/26/2/025022.
- Kia, X., Qingshan, D., Lujun, C., Siuchun, H., Gangbing, S. (2018). "Damage Detection of a Concrete Column Subject to Blast Loads Using Embedded Piezoceramic Transducers". *Sensors*, 18, 1377. doi:10.3390/s18051377.
- Olugboji, O. A. (2011). Development of an Impact Monitoring System for Petroleum Pipelines. AU J.T. 15(2): 115-120. Retrieved from www.journal.au.edu/au techno/2011/oct2011/journal1152_article08.pdf.
- Olugboji, O. A and Yisa, J. J. (2012). Event Reconstruction by Inverse Methods. *International Journal Of Electronics; Mechanical And Mechatronics Engineering*. Vol.4, Num 3, 735 - 746. Retrieved from www.aydin.edu.tr/ijemme/articles/vol4num3/1_Olugboji_editted.pdf
- Park, H. W., Sohn, H., Law, K .H., and Farrar, C. R., (2007). Time Reversal Active Sensing for Health Monitoring of a Composite Plate. *Journal of Sound and Vibration*. Vol. 302, No. 1-2, 50-66. Retrieved from www.sciencedirect.com/science/article/pii/S0022460X06008388.
- Razi, P.; Esmaeel, R.A.; Taheri, F. (2013). Improvement of a Vibration-based Damage Detection Approach for Health Monitoring of Bolted Flange Joints in Pipelines. *Struct. Health Monit.* 2013, 12, 207–224.
- Shi, Y., Ying, L., Shuai, Z., Gangbing, S., Putian, Z. (2018). Pipeline Damage Detection Using Piezoceramic Transducers: Numerical Analyses with Experimental Validation. *Sensors*, 18, 2106. doi:10.3390/s18072106.
- Wang, X., Lambert, M., Simpson, A., Liggett, J. and Vítkovský, J. (2002). "Leak Detection in Pipeline Systems Using the Damping of Fluid Transients." *Journal of Hydraulic Engineering*, ASCE 128(7): 697–711. Retrieved from <https://www.researchgate.net/publication/256103533>.
- Záruba, J. (1993). "Water Hammer in Pipe-line Systems". Vol. 43, Amsterdam, Elsevier. ISBN 0-444-98722-3. Retrieved from www.elsevier.com



Analysis of Maximum Power Point Tracking (MPPT) Techniques under Different Atmospheric Conditions: Technical Review

*Dania, D. E¹, Tsado, J², Nwohu, M³, & Olatomiwa, L⁴

¹Electrical and Electronic Engineering Department, Federal University of Technology, PMB 65 Minna Niger State, Nigeria

²Electrical and Electronic Engineering Department, Federal University of Technology, PMB 65 Minna Niger State, Nigeria

³Electrical and Electronic Engineering Department, Federal University of Technology, PMB 65 Minna Niger State, Nigeria

⁴Electrical and Electronic Engineering Department, Federal University of Technology, PMB 65 Minna Niger State, Nigeria

*Corresponding author email: davedania4@gmail.com +2348037007448

ABSTRACT

The use of solar photovoltaic (PV) a renewable energy technology is on the rise. However, it has challenges. It has high initial cost and low energy conversion efficiency. It produces variable power that depends on atmospheric conditions that involve uniform radiation, rapidly varying radiations, temperature variations and partial shading conditions (PSCs). Further, it produces maximum power only at the maximum power point (MPP). The MPP characteristics under the different atmospheric conditions are divergent. In addition, the MPP varies continuously as the atmospheric conditions changes and it not the same as the operating point. Hence, Maximum power point tracking (MPPT) techniques is required to extract the maximum power produced whatever the atmospheric and load conditions. This work studied the effect of different atmospheric conditions and the load on the MPP. It examined the performance of MPPT techniques under different atmospheric conditions. The study reviewed published literature on MPPT techniques covering the three broad classifications of offline, online and hybrid MPPT techniques. The online MPPT techniques consist of Conventional, Artificial intelligence, and Emerging or nature inspired MPPT techniques. The study showed that MPPT techniques have been developed that considered tracking MPP under uniform radiation and PSCs, very few under rapidly varying radiations and almost negligible under temperature variations. The study showed that offline and conventional MPPT techniques fail to track MPP under rapidly varying and PSCs, however, Artificial intelligence and Emerging MPPT techniques could track MPP under PSCs. Moreover, oscillations about MPP occur amongst some MPPT techniques.

Keywords: *Atmospheric conditions, Maximum power point (MPP), MPPT Techniques, Partial shading conditions (PSCs).*

1 INTRODUCTION

The use of solar photovoltaic (PV) a renewable energy technology is on the rise. Solar PV is a technology that converts sunlight directly into direct current electricity by the photovoltaic effect using the solar cell. The solar cell is the basic unit of the PV system, is a large area P-N junction semiconductor device that is manufactured from mainly silicon and other conductive materials (Timmons et al., 2014).

Solar PV is modular. It does not produce pollution or green gas emission, it has long life span, and it has low maintenance with absence of moving parts. It does not require fuel to produce power. It produces power instantly (Sace, 2010). Despite these benefits, solar power has challenges.

The challenges of solar PV include high initial installation cost. It has low energy conversion efficiency that ranges from 6% to 20% (Green et al., 2015) this depends on the type of material used in the fabrication of the solar cell. Additionally, solar PV produces variable power that depends on irradiance and temperature that in

turn are dependent on atmospheric conditions that involve uniform radiation, rapidly varying radiations, temperature variations and partial shading conditions (PSCs) (Berrera et al., 2009; Sreekanth and Raglend, 2012). Likewise, solar PV has nonlinear characteristics, and it produces maximum power only at the maximum power point (MPP). The MPP varies continuously as the atmospheric conditions changes, and its characteristics are divergent under the different atmospheric conditions. Furthermore, the MPP and the load operating point are not the same.

The above challenges signpost that it is vital to extract the maximum power produced at all times whatever the atmospheric and load conditions. Achieving this requires locating and operating the solar PV at the MPP at all times. This essential but challenging task is performed by Maximum power point tracking (MPPT) techniques. The MPPT track the MPP, and at MPP, it uses the duty cycle to affect maximum power transfer to the load. MPPT techniques improve the efficiency of the PV system and are of economic benefit.

Because of the significance of MPPT techniques, this study investigated the effect of different atmospheric

conditions and the load on the maximum power point (MPP). In addition, the study examined the existing MPPT techniques to ascertain their performance under the different atmospheric conditions.

The study reviewed published literature on MPPT techniques covering the three broad classifications of offline, online and hybrid MPPT techniques. The online MPPT techniques consist of conventional, artificial intelligence, and emerging or nature inspired MPPT techniques

The rest of the paper is arranged as follows. Section 2 presents the solar PV model and its characteristics, and it describes the effects of different atmospheric conditions and load on maximum power point (MPP). The section also gives a brief description and review of the MPPT techniques used in the study. Section 3 presents the results and discussions. Section 4 presents the conclusion.

2 METHODOLOGY

This section presents the solar PV model and its characteristics, and it describes the effects of different atmospheric conditions and load on maximum power point (MPP). The section also gives a brief description and review of the MPPT techniques used in the study.

2.1 SUBSECTION

This section presents the solar PV model and its characteristics, and it describes the effects of different atmospheric conditions and load on maximum power point (MPP).

1. SOLAR CELL CHARACTERISTICS

The solar cell is modeled as a current source in parallel with a diode, shunt resistance and series resistance this is as shown in Figure 1. The current source represents the photo-generated current that depends on the solar radiation and temperature, the diode represents the p-n junction area of the solar cell, the shunt resistance represents the leakage current, and the series resistance represents the internal resistance to the current flow. In this work, the single model is considered.

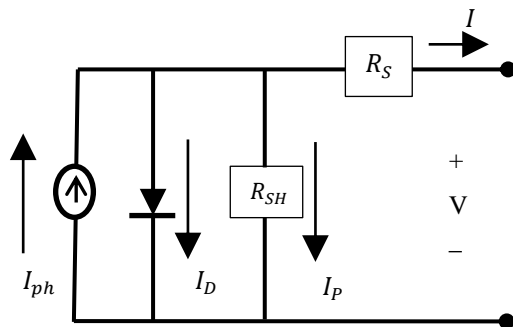


Figure 1: Simplified Equivalent Circuit Model for a Photovoltaic Cell

The current source which represents the photo-generated current that depends on the solar radiation and temperature, is given as in equation (1)

$$I_{ph} = \frac{G}{G_{ref}} [I_{sc} + K_i(T - T_{ref})] \quad (1)$$

where,

I_{ph} is the photocurrent at nominal PV at standard test condition (STC), I_{sc} is the cell short-circuit current at reference temperature and radiation, K_i is the short circuit current temperature coefficient, G is irradiance (W/m^2), G_{ref} is the solar radiation in $1000 W/m^2$ at standard test conditions (STC), T is temperature (K), $T_{ref} = 25$ °C, and $AM = 1.5$. All of these parameters are supplied by the manufacturer specifications.

Similarly based on the model the voltage-current (V-I) characteristic equation of a solar cell is given as in equation (2)

$$I = I_{ph} - I_o \left[\exp \left(\frac{q(V+I \cdot R_S)}{nKT} \right) - 1 \right] - \left[\frac{V+I \cdot R_S}{R_{SH}} \right] \quad (2)$$

where,

I is the Cell current, V is the cell voltage, I_{ph} is the light-generated current or photocurrent, I_o is the Reverse saturation current, R_S is the series resistance, R_{SH} is the shunt resistance, n is ideality factor, K is Boltzmann's constant, T is the cell's working temperature, q is electron charge.

As is often the case, $I_{ph} \approx I_{sc}$ therefore equation (2) is expressed as shown in equation (3)

$$I = I_{sc} - I_o \left[\exp \left(\frac{q(V+I \cdot R_S)}{nKT} \right) - 1 \right] - \left[\frac{V+I \cdot R_S}{R_{SH}} \right] \quad (3)$$

Further, I_o the cell saturation current varies with temperature according to equation (4)

$$I_o = I_{rr} \left[\frac{T}{T_{ref}} \right]^3 \exp \left(\frac{qE_G}{KA} \left[\frac{1}{T_{ref}} - \frac{1}{T} \right] \right) \quad (4)$$

where,

T is the cell working temperature, T_{ref} is the cell reference temperature, I_{rr} is the cell reverse saturation temperature at T_{ref} , E_G is the band gap of the semiconductor used in the cell.

Subsequently, based on equation (3) the typical I-V, P-V characteristic curve for the solar cell/module/array is determined as shown in Figure 2. In addition, based on Figure 2 the important parameters widely used to describe the cell electrical performance are the open-circuit voltage V_{oc} , the short-circuit current I_{sc} , current at maximum power point I_{mpp} , voltage at maximum power point V_{mpp} , and power at maximum power point P_{mpp} .

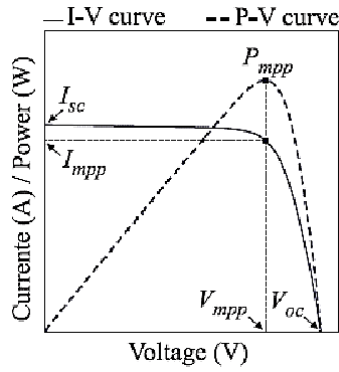


Figure 2: I-V and P-V characteristics important performance parameters

The short circuit current I_{sc} corresponds to the short circuit condition when the impedance is low and is calculated when the voltage equals zero that is I (at $V=0$) = I_{sc} . Moreover, the open circuit voltage (V_{oc}) is described by equation (5), it occurs when there is no current passing through the cell that is V (at $I=0$) = V_{oc} .

$$V_{oc} = \frac{nKT}{q} \ln \left[\frac{I_{sc}}{I_o} + 1 \right] \quad (5)$$

where, I_{sc} , I_o , n , K , T , and q retain the same meaning.

Further, P_{mpp} the power at maximum power point is given by equation (6)

$$P_{mpp} = V_{mpp} I_{mpp} = \gamma V_{mpp} I_{mpp} \quad (6)$$

where

V_{mpp} is terminal voltage of PV module at maximum power point (MPP), I_{mpp} is output current of PV module at maximum power point (MPP), γ is the cell fill factor, which is a measure of the quality of the cell and it is given by equation (7).

$$\text{Fill factor } \gamma = \frac{I_{mpp} V_{mpp}}{I_{sc} V_{oc}} \quad (7)$$

2. EFFECT OF DIFFERENT ATMOSPHERIC CONDITIONS AND LOAD ON MAXIMUM POWER POINT (MPP)

A brief description of the effect of different atmospheric conditions and load on maximum power point (MPP) now follows.

Under uniform radiation and under uniform illumination at constant temperature, change in solar irradiance is proportional to change in the photocurrent as expressed in equation (1). The change in irradiance has more effect on the short circuit current and minimal effect on open circuit voltage as shown in Figure 3. Moreover, increase or decrease in irradiance translates to increase or decrease in maximum power produced, and the MPP under this condition is mono as shown in Figure 4. Tracking the MPP is less cumbersome. However, the case is different under temperature variations.

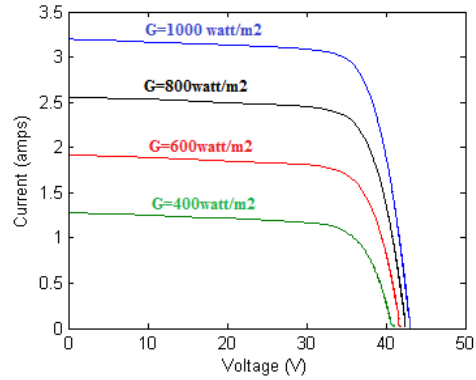


Figure 3: Irradiance and I-V characteristics

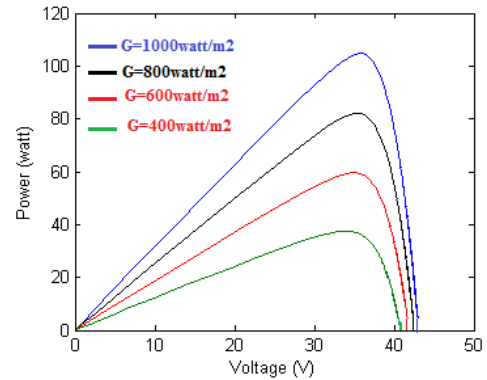
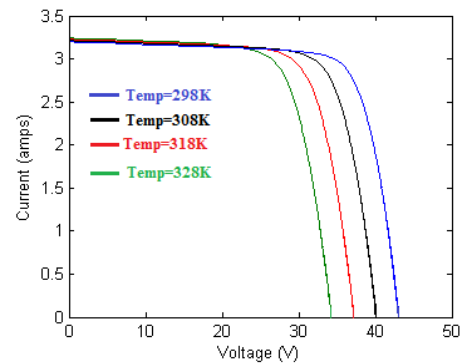
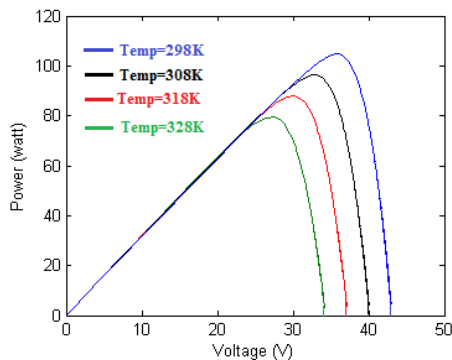


Figure 4: Irradiance and P-V characteristics

Under temperature variations, increase in temperature results in reduction of output voltage as shown in Figure 5(a) and as expressed in equation (4) and equation (5), where I_o the diode saturation current increases with rise in temperature. Conversely, rise in temperature has marginal increase in current as shown in Figure 5(a) and as expressed in equation (1). Overall, increase in temperature results to decrease in the maximum power produced while decrease in temperature results to increase in maximum power produced, this is as shown in Figure 5(b). The MPP is mono. Yet the case is different under rapidly varying radiations.



(a) I-V characteristics for 25°C, 35°C, 45°C, and 55°C



(b) P-V characteristics for 25°C, 35°C, 45°C, and 55°C

Figure 5: Temperature variations and the I-V and P-V characteristics

Under rapidly varying radiations, because the radiation changes abruptly, the maximum power point changes abruptly too, it is erratic. As such tracking the MPP has its own peculiar challenge. Nevertheless, the MPP is still mono. In contrast, under partial shading conditions (PSCs) the MPP characteristics is at variant to the others conditions earlier discussed.

Partial shading conditions (PSCs) results when part of the surface of the cell or module or array is shaded from direct illumination, from clouds, buildings, trees, leaves, or pollution. Shading reduces the output current, as it is directly proportional to the irradiance on the illuminated area of the cell as indicated in equation (1), but the output voltage is unchanged. Because of bypass diode added to protect the module against damage, the characteristics curve then becomes complex the current –voltage curve appears as staircase this is as shown in Figure 6. Also, the power- voltage curve shows multiple maximum power points, however, only one of them is the global maximum power point (GMPP) this is as shown in Figure 6 (Liu, Y. H., Chen, J. H., & Huang, J. W. , 2015).

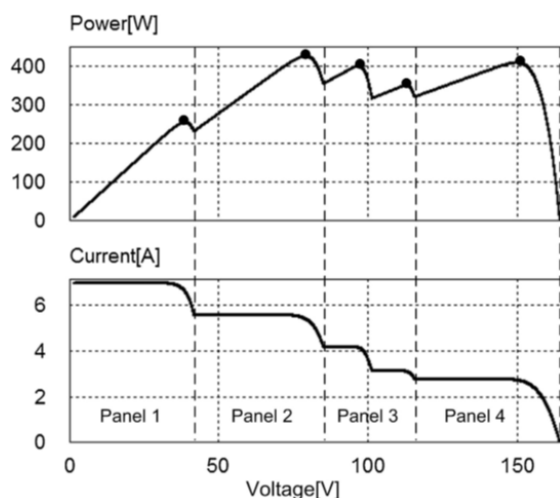


Figure 6: PV array under partial shading Daraban, et al., 2014)

In addition, partial shading cause losses in system output power, hot spot effects, and system safety and

reliability problems (Kazmi *et al.*, 2009; Kotak and Tyagi, 2013). Thus, under partial shading conditions (PSCs), the MPP is not mono but multiple peaks, this creates a challenge in tracking.

In the case of the load, the operating point is different from MPP, therefore, the use of a dynamic impedance matching network whatever atmospheric and load conditions is vital to carry out transfer of maximum power to the load at the MPP. The MPPT techniques perform this task.

2.2 FIGURES AND TABLES

Maximum power point tracking (MPPT) tracks and locate the MPP whatever the atmospheric conditions, and at the MPP, it simultaneously transfers the maximum power to the load. The MPPT techniques consist of the tracking and control unit and the DC-DC converter, and the typical block diagram is as shown in Figure 7.

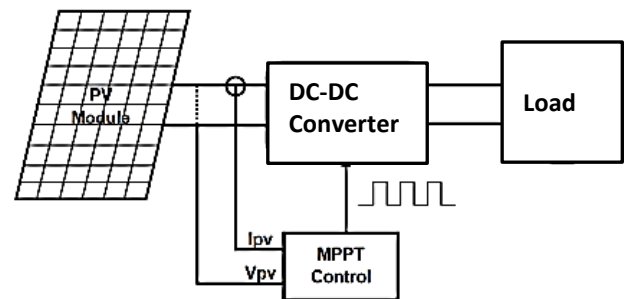


Figure 7: Typical block diagram of MPPT in a PV System

The tracking and control unit track and locate the MPP, at the same time it uses either maximum power point voltage V_{mpp} or current I_{mpp} as indicated in Figure 2, to set the duty cycle that is used to switch on and off the DC-DC converter. However, the voltage at MPP V_{mpp} is mostly used. The DC-DC converter then performs the transfer of maximum power to the load. Many different tracking algorithms are used. Likewise, different DC-DC topologies are also used depending upon the specific requirements.

Many MPPT techniques have been proposed and some implemented by researchers. These techniques differ in many characteristics such as required sensors, cost, complexity, convergence speed, range of effectiveness, correct tracking when irradiation and or change in temperature, hardware needed for the implementation or popularity.

Several authors have classified the MPPT techniques differently. However, in this work we adopt the broad classifications of offline MPPT techniques, online MPPT techniques and hybrid MPPT techniques. Besides, the online MPPT techniques include conventional MPPT

techniques, artificial intelligence and emerging or nature inspired MPPT techniques.

1. OFFLINE MPPT TECHNIQUES

Offline method uses reference signal such as open circuit voltage (V_{oc}), short circuit current (I_{sc}), solar insolation, and temperature which is used to generate the control signal to track MPP. The offline MPPT techniques appraised include Fractional open circuit voltage (FOCV), Fractional short circuit current (FSCC), Curve fitting (CF) methods, and Look up table (LUT) methods.

A brief description of these offline MPPT techniques now follows. The Fractional open circuit voltage (FOCV), is based on the premise the open circuit voltage V_{oc} varies with the irradiance and temperature. The FOCV uses the linear relationship between voltage at MPP and the open circuit voltage as expressed in equation (8).

$$V_{mpp} = K_1 V_{oc} \quad (8)$$

where K_1 is a constant depending on the characteristics of the PV array it ranges between (0.71 and 0.78). in this method the open circuit voltage V_{oc} is measured periodically, this leads to temporary power loss. This method only gives an approximation not the true MPP. The method fails to track MPP under rapidly varying, temperature variations and PSCs (Logeswaran, and SenthilKumar, 2014).

The Fractional short circuit current (FSCC) is similar to the fractional open circuit voltage method. The short current I_{sc} and current at maximum power point (MPP) I_{mpp} are linearly related as shown in equation (9).

$$I_{mpp} = K_2 I_{sc} \quad (9)$$

The coefficient of proportionality K_2 is determined for each PV array, and it ranges between 0.78 and 0.92. However, measurement of the short circuit current while the system is operating is a problem. In addition, this method fails to track MPP under rapidly varying, temperature variations and partial shading conditions (PSCs) (Logeswaran, and SenthilKumar, 2014).

The Curve fitting (CF) method requires prior knowledge of PV technical data, panel characteristics, mathematical model and equation to calculate the PV array output in terms of the voltage corresponding to the MPP. It performs large number of calculations that slows it down. Likewise, it requires large memory. Besides, it fails to track MPP under rapidly varying radiations and partial shading conditions (PSCs).

The Look up table (LUT) methods depends on stored data from previous knowledge of PV panel characteristics and technical data. For varying atmospheric conditions, the system becomes complex, making the system slow. In addition, because not all possible scenarios could be predicted, the system is prone to fail when it meets conditions that are not stored. In addition, because it is offline, it fails to track MPP under PSCs.

2. ONLINE MPPT TECHNIQUES

Online techniques are independent from prior knowledge of PV modules characteristics. In this method, usually the instantaneous values of the PV output current and voltage are used to generate the control signal that is applied to the PV system. The Online MPPT techniques include conventional techniques, Artificial Intelligence techniques and Emerging or nature inspired techniques. Brief description of the online techniques now follows.

The conventional MPPT techniques methods are based on hill-climbing principle that consists of moving the operation point of the photovoltaic (PV) array in the direction in which power increase, and if power decreases the operation, point is moved in the other direction. Two popular MPPT techniques based on the hill-climbing principle are Perturb and Observe (P&O) and Incremental Conductance (Icond) MPPT methods.

In P&O method, the MPPT algorithm is based on the calculation of the PV output power and observing the change in power by sampling both the PV array current and voltage. The technique operates by periodically incrementing or decrementing the solar array voltage (Atallah, *et al.*, 2014). The algorithm for this technique is shown in figure 8.

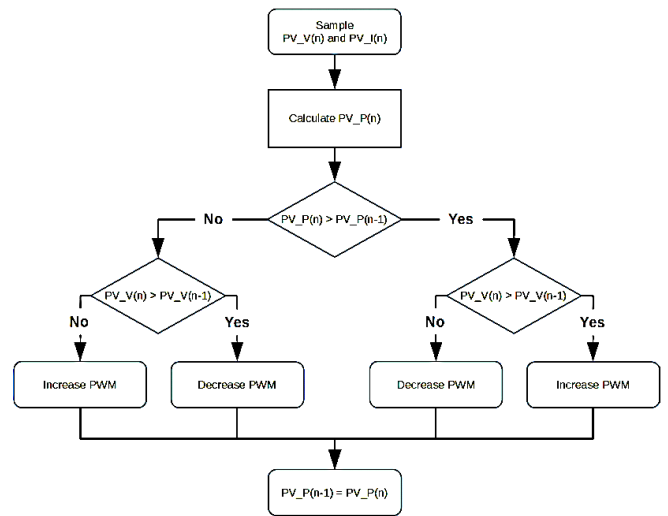


Figure 8: Flow chart of P&O Algorithm

If a given perturbation leads to increase in power, then the subsequent perturbation is generated in the same direction and vice versa. The duty cycle of the DC converter is varied and the process is repeated until the maximum power point has been reached.

A shortcoming of this method is that the system oscillates about the MPP. The technique never actually tracks the real MPP. In addition, reducing the perturbation step size can minimize the oscillation. However, small step size slows down the MPPT. For different values of irradiance and cell temperatures, the PV array would exhibit different characteristic curves. Additionally, apart from the oscillations around the MPP and the P&O can get lost and track the MPP in the wrong direction during rapidly changing atmospheric conditions. In addition, the

P&O fails to track the Global maximum power point (G_{MPP}) under partial shading conditions because there are multiple maxima in the curve (Logeswaran, and SenthilKumar, 2014).

The incremental conductance (Icond) MPPT uses equations (9) – (12) to arrive at the MPP.

$$dP/dV = d(IV)/dV = I + VdI/dV = 0 \quad (9)$$

$$dI/dV = -I/V \text{ At MPP} \quad (10)$$

$$dI/dV >= -I/V \text{ At left of MPP} \quad (11)$$

$$dI/dV <= -I/V \text{ At right of MPP} \quad (12)$$

where V and I are PV array output current and voltage respectively, the left hand side of equations represents Incremental conductance of PV module and the right hand side represents the instantaneous conductance. It is obvious that when the ratio of change in the output conductance is equal to the negative output conductance, solar array will operate at the maximum power point as shown in equation (10). By comparing the conductance at each sampling time, the MPPT will track the maximum power of the PV module. However, the speed of tracking depends on the size of the increment of the reference voltage. In addition, one drawback of this method is that it cannot differentiate between rapidly changing radiations. Additionally, this method fails to track (G_{MPP}) under partial shading conditions (Logeswaran, and SenthilKumar, 2014).

Conversely, artificial intelligence, techniques use complex mathematical models that involve the use of high computational efforts to obtain results. Hence, the system modeling allows the determination of the MPP with high accuracy. Some MPPT techniques under this category include Differential evolution (DE), Genetic algorithm (GA), Artificial neural network (ANN), and Fuzzy logic controller (FLC). The brief description of these techniques is discussed next.

Differential evolution (DE) requires a few parameters in the algorithm. A population of particles is required in DE and a few iterations are needed in order to generate the final solution. The differences in the particles are used to mutate each other in every iteration. The process starts with initialization of initial population of target vectors within the boundary constraints. The population vector of this system could be the reference voltage or current or duty cycle. DE technique could track MPP under PSCs (Tajuddin, *et al.*, 2013).

The genetic algorithms are a family of computational models inspired by evolution. They are parallel global probabilistic search techniques based on the principle of population genetics. These algorithms encode a potential solution to a specific problem on a single chromosome and apply recombination operators to them to preserve critical information. The GA MPPT technique oscillates about MPP under PSCs (Daraban, *et al.*, 2014).

The Artificial neural network techniques involve the use of a multi-layer feed-forward neural network (MFFNN) to track the MPP. The network consists of three layers: input layer, hidden layer and output layer. The

number of neurons in hidden layer is determined by trial and error. The input variables can be the PV array parameters like V_{oc} and I_{sc} , atmospheric data like irradiance and temperature, or any combination of these. The output is usually one or several reference signals like a duty cycle signal used to drive the power converter to operate at or close to the MPP. The ANN MPPT technique could track MPP under PSCs. but it has to be trained (Messalti, *et al.*, 2017) and it specific for that module or array.

The Fuzzy logic controller uses fuzzy logic to make decisions and control the output of the controller. The main components in fuzzy logic based MPPT controller are fuzzification, rule-base, inference and defuzzification. There are two inputs to the controller these are error e (k) and change in error Δe (k). The Fuzzification block converts the crisp inputs to fuzzy inputs, while the rules are formed in rule base and are applied in inference block. The defuzzification converts the fuzzy output to the crisp output. The fuzzy inference is carried out by using Mamdani's method, and the defuzzification uses the centre of gravity to compute the output, which is the change in duty cycle. The FLC technique could track MPP under the different atmospheric conditions, but with oscillation about MPP under PSCs. (Islam, *et al.*, 2018).

Another online category involves Emerging or nature inspired MPPT techniques, some of include Particle swarm optimisation (PSO), Firefly optimisation algorithm (FOA), Ant colony optimization (ACO), Cuckoo search (CS), and Radial movement optimization (RMO)

The Particle swarm optimisation (PSO) is a stochastic search method, modelled after the behaviour of bird flocks. The PSO algorithm maintains a swarm of individuals called particles, where each particle represents a candidate solution. The PSO algorithm is applied to realize the MPPT control of a PV system, where in the P-V characteristics exhibits multiple local MPP. However, the PSO experience under PSCs (Koad, *et al.*, 2016).

The Firefly optimisation algorithm (FOA) is Meta heuristic algorithm inspired by flashing of fireflies. One important rule of this algorithm is all fireflies are unisex. It means that regardless of sex, any firefly can be attracted to any other brighter one. Second rule is that flashing light (brightness) is determined from the objective function. Firefly algorithm is superior to other methods in terms of tracking speed, convergence to track global MPP and possesses good tracking efficiency. However, the FA MPPT oscillates (Hemalatha, *et al.*, 2016).

The Ant colony optimization (ACO) is implemented by making mimicking the ant behaviour. The process starts with randomly initializing the ants. The objective function is framed by including each panel exposure to irradiation and temperature. The Ant MPPT could track MPP under PSCs with oscillation about MPP as the start, but steady state the oscillation is absent. Then only simulations results available (Titri, *et al.*, 2017).

The Cuckoo search (CS) technique is an optimisation algorithm inspired by parasitic reproduction of cuckoo birds. The CS MPPT was applied under partial shading conditions and simulation results was reported (Rezk, et al., 2017).

The Radial movement optimization (RMO) technique is a swarm-based stochastic optimization technique. It has several similarities with other techniques such as PSO and DE. The Radial Movement Optimization (RMO) was used under partial shading conditions (PSCs), the result was compared with PSO, and the oscillation about the maximum power point (MPP) was less compared to PSO (Seyedmahmoudian, *et al.*, 2016).

The third MPPT classification involves hybrid MPPT techniques. Hybrid method is a combination of offline and online method. Hybrid techniques are the combination of two or more different categories that is used to achieve the desired objective. The MPP is tracked in two steps. The first step places the operating point close to MPP and the second step fine-tunes the operating point close to MPP. Some examples are the use of fuzzy logic controller (FLC) and genetic algorithms (GA) for optimization (Larbes, *et al.*, 2009). Another one is a Hopfield neural network (HNN) optimized FLC. HEN is utilised to tune automatically the FLC membership functions instead of adopting the trial-and-error approach (Subiyanto and Shareef, 2012).

3 RESULTS AND DISCUSSION

The results of the study and the discussions are presented below.

3.1 EQUATIONS

The results of the study are presented in Tables 1- 6.

TABLE 1: COMPARISON OF MPPT TECHNIQUES UNDER DIFFERENT ATMOSPHERIC CONDITIONS

Main grouping of MPPT Techniques	Atmospheric conditions			
	Uniform radiation	Rapidly varying radiations	Temperature variations	Partial shading conditions (PSCs)
Offline MPPT Technique				
Fractional Short Circuit Current (FSCC)	✓	–	–	–
Fractional open circuit voltage(FOCV)	✓	–	–	–
Look-up Table Methods	✓	–	–	–
Curve Fitting (CF) Based Methods	✓	–	–	–
Online MPPT Techniques(Conventional)	✓	–	–	–
Perturbation and	✓	–	–	–

observation (P&O)				
Incremental conductance (Icond)	✓	–	–	–
Online MPPT Techniques((Artificial intelligence)				
Artificial Neural Network (ANN)	✓	✓	✓	✓
Fuzzy Logic Control (FLC)	✓	✓	✓	✓
Differential Evolution (DE)	✓	✓	✓	✓
Genetic Algorithm (GA)	✓	✓	✓	✓
Online MPPT Techniques (Emerging)				
Firefly Optimization Algorithm(FOA)	✓	✓	✓	✓
Ant colony optimization algorithm(ACO)	✓	✓	✓	✓
Particle swarm optimization (PSO)	✓	✓	✓	✓
Cuckoo search (CS)	✓	✓	✓	✓
Radial Movement Optimization (RMO)	✓	✓	✓	✓

TABLE 2: COMPARISON OF MPPT TECHNIQUES VERSUS MPP TRACKING COMPLEXITY UNDER UNIFORM RADIATION

Main grouping of MPPT Techniques	Uniform radiation	Complexity
Offline MPPT Technique		
Fractional Short Circuit Current (FSCC)	✓	Simple
Fractional open circuit voltage(FOCV)	✓	Simple
Look-up Table Methods	✓	Medium
Curve Fitting (CF) Based Methods	✓	Medium
Online MPPT Techniques(Conventional)		
Perturbation and observation (P&O)	✓	Medium
Incremental conductance (Icond)	✓	Medium
Online MPPT Techniques((Artificial intelligence)		
Artificial Neural Network (ANN)	✓	Complex
Fuzzy Logic Control (FLC)	✓	Complex
Differential Evolution (DE)	✓	Complex
Genetic Algorithm (GA)	✓	Complex
Online MPPT Techniques (Emerging)		Complex
Firefly Optimization Algorithm(FOA)	✓	Complex
Ant colony optimization algorithm(ACO)	✓	Complex
Particle swarm optimization (PSO)	✓	Complex
Cuckoo search (CS)	✓	Complex
Radial Movement Optimization (RMO)	✓	Complex

TABLE 3: COMPARISON OF MPPT TECHNIQUES VERSUS MPP TRACKING COMPLEXITY UNDER RAPIDLY VARYING RADIATIONS

Main grouping of MPPT Techniques	Rapidly varying radiations	Complexity
Offline MPPT Technique		
Fractional Short Circuit Current (FSCC)	–	Simple
Fractional open circuit voltage(FOCV)	–	Simple
Look-up Table Methods	–	Medium
Curve Fitting (CF) Based Methods	–	Medium
Online MPPT Techniques(Conventional)		
Perturbation and observation (P&O)	–	Medium
Incremental conductance (Icond)	–	Medium
Online MPPT Techniques((Artificial intelligence)		
Artificial Neural Network (ANN)	✓	Complex
Fuzzy Logic Control (FLC)	✓	Complex
Differential Evolution (DE)	✓	Complex
Genetic Algorithm (GA)	✓	Complex
Online MPPT Techniques (Emerging)		
Firefly Optimization Algorithm(FOA)	✓	Complex
Ant colony optimization algorithm(ACO)	✓	Complex
Particle swarm optimization (PSO)	✓	Complex
Cuckoo search (CS)	✓	Complex
Radial Movement Optimization (RMO)	✓	Complex

TABLE 4: COMPARISON OF MPPT TECHNIQUES VERSUS MPP TRACKING COMPLEXITY UNDER TEMPERATURE VARIATIONS

Main grouping of MPPT Techniques	Temperature variations	Complexity
Offline MPPT Technique		
Fractional Short Circuit Current (FSCC)	–	Simple
Fractional open circuit voltage(FOCV)	–	Simple
Look-up Table Methods	–	Medium
Curve Fitting (CF) Based Methods	–	Medium
Online MPPT Techniques(Conventional)		
Perturbation and observation (P&O)	–	Medium
Incremental conductance (Icond)	–	Medium
Online MPPT Techniques((Artificial intelligence)		
Artificial Neural Network (ANN)	✓	Complex
Fuzzy Logic Control (FLC)	✓	Complex
Differential Evolution (DE)	✓	Complex
Genetic Algorithm (GA)	✓	Complex

Online MPPT Techniques (Emerging)		Complexity
Firefly Optimization Algorithm(FOA)	✓	Complex
Ant colony optimization algorithm(ACO)	✓	Complex
Particle swarm optimization (PSO)	✓	Complex
Cuckoo search (CS)	✓	Complex
Radial Movement Optimization (RMO)	✓	Complex

TABLE 5: COMPARISON OF MPPT TECHNIQUES VERSUS MPP TRACKING MPP COMPLEXITY UNDER PARTIAL SHADING CONDITIONS (PSCS)

Main grouping of MPPT Techniques	Partial Shading Conditions (PSCS)	Complexity
Offline MPPT Technique		
Fractional Short Circuit Current (FSCC)	–	Simple
Fractional open circuit voltage(FOCV)	–	Simple
Look-up Table Methods	–	Medium
Curve Fitting (CF) Based Methods	–	Medium
Online MPPT Techniques(Conventional)		
Perturbation and observation (P&O)	–	Medium
Incremental conductance (Icond)	–	Medium
Online MPPT Techniques((Artificial intelligence)		
Artificial Neural Network (ANN)	✓	Complex
Fuzzy Logic Control (FLC)	✓	Complex
Differential Evolution (DE)	✓	Complex
Genetic Algorithm (GA)	✓	Complex
Online MPPT Techniques (Emerging)		
Firefly Optimization Algorithm(FOA)	✓	Complex
Ant colony optimization algorithm(ACO)	✓	Complex
Particle swarm optimization (PSO)	✓	Complex
Cuckoo search (CS)	✓	Complex
Radial Movement Optimization (RMO)	✓	Complex

TABLE 6: QUALITATIVE COMPARISON BETWEEN THE METHODS

Type	Emerging Techniques	Artificial intelligence methods	Conventional methods
Tracking Speed	Fast	Medium	Slow
Tracking Accuracy	Accurate	Accurate	Low
Implementation complexity	Medium	Low	Low
Dynamic response	Good	Oscillatory	Oscillatory
Periodic tuning	Not Required	Not Required	Not Required
Steady State Oscillations	Zero	Zero	Zero

3.2 TABULATION

Table 1 show all the MPPT techniques compared under the different atmospheric conditions. The different categories of MPPT techniques are able to track MPP under uniform radiation condition. However, the results differ, because offline techniques give only approximation while conventional techniques are able to track the MPP. Even at that some of the conventional ones like P&O, oscillate about the MPP (Patel, *et al.*, 2013, Kalpana, *et al.*, 2013). It is also clear that the conventional MPPT techniques are not able to track true MPP under rapidly varying radiations, temperature variations and partial shading conditions (PSCs) conditions (Kumar, *et al.*, 2015.). On the other hand, although artificial intelligence MPPT techniques are able to track MPP under the different atmospheric conditions, they have their shortcomings. They are more complex than conventional techniques. For instance, ANN MPPT has to be trained for each PV system. In addition, at PSCs they experience oscillation (Cheema and Kaur, 2014). The implementation complexity of MPPT under uniform radiation is shown in Table 2.

Table 3 shows comparison of MPPT techniques under rapidly varying radiations. As indicated the offline MPPT techniques and conventional MPPT techniques fail to track MPP under rapidly varying conditions. However, online MPPT techniques involving Artificial intelligence and Emerging MPPT techniques were able to track MPP under rapidly varying radiations, even though implementation complexity is high.

Table 4 shows comparison of MPPT techniques under temperature variations condition. Here offline and conventional MPPT techniques fail to track MPP under temperature variations. However, online techniques involving Artificial intelligence and Emerging techniques are able to track MPP under temperature variations, but with more complexity..

Table 5 shows comparison of MPPT techniques under partial shading conditions (PSCs). The table shows that offline MMPT techniques and conventional MPPT techniques fail to track MPP under PSCs. Conversely online techniques involving Artificial intelligence and Emerging techniques are able to track MPP under partial shading conditions even though the implementation complexity is high as compared to conventional or offline MPPT techniques.

Additionally, the Emerging MPPT methods have the advantage that they are fast as indicted in Table 6, but they are complex to implement (Husain, *et al.*, 2016). Besides only simulation results are presently available, practical implementation and evaluation is in progress,

Also, whereas Hybrid techniques could track MPP under the different atmospheric conditions as revealed in Table 1, however, hybrid techniques involving conventional MPPT methods is not able to track MPP under PSCs conditions.

4 CONCLUSION

This paper shows that the different atmospheric conditions have different effect on the maximum power point (MPP), as well as the load. This paper also shows that not all the MPPT techniques able to track true MPP under different atmospheric conditions. The work shows that many MPPT techniques have been developed to track MPP under uniform radiation, partial shading conditions, but very few under rapidly varying radiations and very scanty development under temperature variations. In addition, the work shows that all the different classification of MPPT techniques is able to MPP under uniform radiation, though with varied results. Additionally, the work shows that offline MPPT techniques and conventional (online) MPPT techniques fail to track MPP under rapidly varying, temperature variations, and partial shading conditions (PSCs). While Artificial Intelligence and Emerging MPPT techniques and some hybrid MPPT techniques are able to track MPP under PSCs. In addition, the study shows that the use of emerging techniques is on the increase, because of its fastness to locate the GMPP, however results available are simulation results.

The paper shows that tracking the MPP under the different atmospheric is vital and is on active research area.

REFERENCE

- Atallah, A. M., Abdelaziz, A. Y., & Jumaah, R. S. (2014). Implementation of perturb and observe MPPT of PVsystem with direct control method using buck and buck-boost converters. *Emerging Trends in Electrical, Electronics & Instrumentation Engineering: An international Journal (EEIEJ)*, 1(1), 31-44.
- Berrera, M., Dolara, A., Faranda, R., & Leva, S. (2009, June). Experimental test of seven widely-adopted MPPTalgorithms. In *2009 IEEE BucharestPowerTech* (pp. 1-8). IEEE.
- Cheema, T. S., & Kaur, J. (2014). Fuzzy logic based MPPT algorithm for solar PV systems. *Int J Innov ResDev*, 3,367-70.
- Daraban, S., Petreus, D., & Morel, C. (2014). A novel MPPT (maximum power point tracking) algorithm based on amodified genetic algorithm specialized on tracking the global maximum power point in photovoltaic systems affected by partial shading. *Energy*, 74, 374-388.
- Green, M. A., Emery, K., Hishikawa, Y., Warta, W., & Dunlop, E. D. (2015). Solar cell efficiency tables (Version 45). *Progress in photovoltaics: research and applications*, 23(1), 1-9.
- Hemalatha, C., Rajkumar, M. V., & Krishnan, G. V. (2016). Simulation and Analysis for MPPT Control with Modified firefly algorithm for photovoltaic

- system. *International Journal of Innovative Studies in Sciences and Engineering Technology*, 2(11), 48-52.
- Husain, M. A., Jain, A., & Tariq, A. (2016). A novel fast mutable duty (FMD) MPPT technique for solar PV system with reduced searching area. *Journal of Renewable and Sustainable Energy*, 8(5), 054703.
- Islam, H., Mekhilef, S., Shah, N., Soon, T., Seyedmahmoudian, M., Horan, B., & Stojcevski, A. (2018). Performance evaluation of maximum power point tracking approaches and photovoltaic systems. *Energies*, 11(2), 365.
- Kalpana, C., Babu, C. S., & Kumari, J. S. (2013). Design and Implementation of different MPPT Algorithms for PV System. *International Journal of Science, Engineering and Technology Research (IJSETR)* Volume, 2(10), 1926-1933.
- Kazmi, S. M. R., Goto, H., Ichinokura, O., & Guo, H. J. (2009, September). An improved and very efficient MPPT controller for PV systems subjected to rapidly varying atmospheric conditions and partial shading. In 2009 Australasian Universities Power Engineering Conference (pp. 1-6). IEEE. [RPV & PSCs]
- Koad, R. B., Zobaa, A. F., & El-Shahat, A. (2016). A novel MPPT algorithm based on particle swarm optimization for photovoltaic systems. *IEEE Transactions on Sustainable Energy*, 8(2), 468-476.
- Kotak, V. C., & Tyagi, P. (2013). DC to DC Converter in maximum power point tracker. *International Journal of Advanced Research in Electrical, Electronics and Instrumentation Engineering*, 2(12), 6115-6125.
- Larbes, C., Cheikh, S. A., Obeidi, T., & Zerguerras, A. (2009). Genetic algorithms optimized fuzzy logic control for the maximum power point tracking in photovoltaic system. *Renewable energy*, 34(10), 2093-2100.
- Liu, Y. H., Chen, J. H., & Huang, J. W. (2015). A review of maximum power point tracking techniques for use in partially shaded conditions. *Renewable and Sustainable Energy Reviews*, 41, 436-453.
- Logeswaran, T., & SenthilKumar, A. (2014). A review of maximum power point tracking algorithms for photovoltaic systems under uniform and non-uniform irradiances. *Energy Procedia*, 54, 228-235.
- Messalti, S., Harrag, A., & Loukriz, A. (2017). A new variable step size neural networks MPPT controller: Review, simulation and hardware implementation. *Renewable and Sustainable Energy Reviews*, 68, 221-233.
- Patel, J., Sheth, V., & Sharma, G. (2013). Design & Simulation of Photovoltaic System Using Incremental MPPT Algorithm. *International Journal of Advanced Research in Electrical, Electronics and Instrumentation Energy*, ISSN (Print), 2320-3765.
- Rezk, H., Fathy, A., & Abdelaziz, A. Y. (2017). A comparison of different global MPPT techniques based on metaheuristic algorithms for photovoltaic system subjected to partial shading conditions. *Renewable and Sustainable Energy Reviews*, 74, 377-386.
- Sace, A. (2010). Technical Application Papers No. 10 Photovoltaic plants. A Division of ABB SpALV Breakers.
- Seyedmahmoudian, M., Horan, B., Rahmani, R., Maung Than Oo, A., & Stojcevski, A. (2016). Efficient photovoltaic system maximum power point tracking using a new technique. *Energies*, 9(3), 147.
- Sreekanth, S., & Raglend, I. J. (2012, March). A comparative and analytical study of various incremental algorithms applied in solar cell. In 2012 International Conference on Computing, Electronics and Electrical Technologies (ICCEET) (pp. 452-456). IEEE.
- Subiyanto, A. M., & Shareef, H. (2012). Hopfield neural network optimized fuzzy logic controller for maximum power point tracking in a photovoltaic system. *International Journal of Photoenergy*, 2012, 1-13.
- Tajuddin, M. F. N., Ayob, S. M., Salam, Z., & Saad, M. S. (2013). Evolutionary based maximum power point tracking technique using differential evolution algorithm. *Energy and Buildings*, 67, 245-252.
- Timmons, D., Harris, J. M., & Roach, B. (2014). The economics of renewable energy. *Global Development And Environment Institute, Tufts University*, 52.
- Titri, S., Larbes, C., Toumi, K. Y., & Benatchba, K. (2017). A new MPPT controller based on the Ant colony optimization algorithm for Photovoltaic systems under partial shading conditions. *Applied Soft Computing*, 58, 465-479.



DEVELOPMENT OF BRIQUETTE-POWERED WATER DISTILLER

*Muhammadu M. M¹, Unugbai, J. A², Bako M. D.³, Abubakar J. A.

^{1,2,3}Department of Mechanical Engineering, Federal University of Technology, P. M. B.

65, Gidann-Kwanu, Minna, Nigeria

⁴Department of Mechanical Engineering, Kaduna Polytechnic, Kaduna, Nigeria.

*Corresponding author: masin.muhammadu@futminna.edu.ng +2348032551955

ABSTRACT

Human beings can survive for weeks without food but the possibility of man being able to live without water for a few numbers of days is slim. Poor quality of water and unsatisfactory sanitation are seriously dangerous to man. Portable water is therefore of great importance to man. It was reported by WHO that nearly 1 billion people have no satisfactory access to portable water and that drinking of contaminated water leads to the occurrence of about 5 million deaths annually. The aim of this study is to develop a briquette-powered water distiller which will produce drinkable water for human consumption and hence reduce these death occurrences. The briquettes were made using carbonized sawdust and gelatinized starch mixed together uniformly in the proportion of 4479.2 cm³ of the carbonized sawdust to 306.06 cm³ of the gelatinized starch. Afterwards, the combustion chamber which consisted of the stove rest, ash filter, fuel rack and riser was fabricated. The stainless steel pot had a frustum shape with its height, larger and smaller diameters were 16.5 cm, 36.0 cm and 25.0 cm. Their lengths were both 100 cm. The material for the inner pipe was stainless steel while that for the outer pipe was galvanized mild steel. The gross calorific value of the briquettes produced was 20.3 KJ/kg. The fabricated water distiller was used to purify untreated water and in the process, 4.91 litres of portable water was produced from 10 litres of feed water.

Keywords: *Portable, water, distillers, energy, biomass, briquettes*

1 INTRODUCTION

Water is a chemical substance that is transparent, virtually colourless and has no taste and odour. Portable water is important to human beings and other living things. In the past decades, accessibility to portable water has increased in virtually all over the world, even though about 1 billion people are yet to have access to portable water while more than 2.5 billion people do not have access to satisfactory sanitation (1-4). Bad quality of water and poor sanitation are very dangerous. Drinking of contaminated water leads to about 5 million death occurrences annually. According to the World Health Organization (WHO), provision of portable water can stop 1.4 million deaths of children caused by diarrhoea every year (5-8).

For water to be safe for human consumption, it must undergo purification which will require the separation of undissolved particles, dissolved substances and dangerous microbial organisms. A water distiller is an effective treatment device used for producing portable water (9-12). It comprises majorly the heat source, boiling chamber, condensing and water storage units. Untreated water is turned into vapour by heating and then the vapour is allowed to condensed back to its liquid form in the condensing unit. Majority of the impurities in the untreated water will remain in the boiling chamber after distillation, thus making the condensed water to be virtually free of impurities (13-15).

The conversion of water into vapour needs considerable quantity of heat. While some water distillers were powered by electricity, some were powered by fossil fuels to produce the needed heat. Some water distillers also made use of renewable energy as their source of heat. Examples of some of the renewable energy used were solar energy, geothermal power, biomass and biogas (biofuels).

Briquette is obtained by the compression of loose biomass materials and/or pulverized solid fuels into solid products of higher densities than those of the parent materials usually with the application of high pressure and heat. Some additives may be added to the raw materials to produce better briquette fuels. The various materials used for biomass briquette fuels are usually industrial organic wastes, forest products and residues, food crops, energy crops, sugar crops, aquatic plants, algae and mosses, landfills, kelps and lichens, bio renewable and agricultural wastes (16-19).

It should be noted that the use of electricity to power water distillers comes at a huge cost as it is an expensive source of energy, also using fossil fuels and firewood to power water distillers can lead to significant harmful effects on the climate system of the Earth and the ecosystems beside the huge cost of providing these fuels. Although solar energy serves as a cheaper means of powering water distillers when compared with these other sources already mentioned, the machines using this source of energy usually have low production rate of distilled water (20).



The use of briquettes provides a cheaper means of powering water distillers in addition to its being environmentally friendly (21-22).

2.0 Materials and methods

The briquette-powered water distiller consisted of heating stove fed with sawdust briquettes. The stove was positioned in the combustion chamber. This distiller also had the boiling unit which comprised a skirt and a covered pot whose capacity is about 12.2 litres, the condenser with the ability to produce portable water from steam generated, the tank for storing the distilled water produced, the reservoir for the coolant and the chimney to aid convection. The capacity of water to be distilled was 10 litres which was equivalent to 10 kg of water.

The materials needed for this work were 0.5 mm thick stainless steel sheets used for constructing the combustion chamber and the boiling unit, stainless steel and mild steel pipes used for making the condenser, 0.8 mm thick mild steel sheets for making both the chimney and the outer cover for the combustion chamber, hoses and pipes, insulator used for lagging the riser (a mixture of gypsum and sawdust), water used as coolant in the condenser, plastic containers for storing the distillate and coolant, ingredients for making the sawdust briquettes, consumables and machines used.

The methods used for this study are as follows:

This machine was constructed at the Hamstring Engineering Workshop located within the Technology Incubation Centre, off David Mark Road, Minna, Nigeria. The work began on 25th February, 2019 and ended on 3rd May, 2019. The briquettes to power the machine had already been produced before this time in the same workshop. The various units of the water-distilling machine produced were the combustion chamber, the boiling unit, the condensing unit and the chimney.

The ingredients for the sawdust briquettes were sawdust, starch and water. The sawdust was obtained from the mixture of Gmelina (*Gmelina arborea* Roxb) and Teak (*Tectona grandis*) timbers at the Sango Sawmill in Minna, Nigeria on 27th October, 2018. It was dried in the sun up till 3rd November, 2018 before it was made to undergo Torrefaction in order to drive off moisture and other unnecessary volatiles present in the sawdust thereby producing a carbonized substance called bio coal. The starch obtained from cassava tubers was bought from the Kure Ultra-Modern Market in Minna, Nigeria. These ingredients were used to make the briquettes. About 4479.2 cm³ (680.39 g) of the carbonized sawdust was measured and poured into an empty bowl. This was then properly mixed with 306.06 cm³ (992.25 g) of the gelatinized starch to give a uniform mixture. This mixture was then poured into the mould of the briquetting machine after which the die of the machine was used to manually compress the mixture into briquettes. The moulded briquettes were then removed and dried in the sun for three days. Afterwards, they were kept in a cool

place and exposed to draught within the place. The diameter of the briquettes produced was 3.33 cm and the average height of each briquette was 3.41 cm. The average mass of each briquette was 30.86 g.

The combustion chamber contained the removable stove which consisted of the stove rest whose length, breadth and height were respectively 39 cm x 23 cm x 5 cm; the fuel rack whose length, width and height were respectively 22 cm x 22 cm x 8 cm. Directly below the fuel rack was the ash filter with a respective length and breadth of 19.5 cm and 18.3 cm. The riser was directly placed above the rack and its height and diameter were 20 cm and 17 cm respectively. It was lagged round about by a mixture of gypsum and sawdust with the thickness of insulation being 22.5 cm.

The boiling unit consisted of the stainless steel pot skirt whose diameter was 39 cm while its depth was 18 cm. The pot itself which was positioned inside the skirt had larger and smaller diameters of 36 cm and 25 cm respectively. Its depth was 16.5 cm while its material was also stainless steel. The mass of the pot was around 765g and was covered with a lid whose diameter was 38 cm. The lid had two openings. From the first opening comes a stainless steel pipe which is to channel the steam from the pot to the condenser while the other opening had a PVC pipe which is to help in directing the cooling water from the exit of the condenser to the inside of the pot. The diameters of the stainless steel and PVC pipes were 25 mm and 15 mm respectively.

The condensing unit consisted of the condenser, the tank for storing the coolant and the container for storing the distilled water produced. The condenser was an indirect-contact heat exchanger in which heat was transferred through the wall which separated the steam from the cooling water. This was a counter-flow heat exchanger where the cooling water flow in opposite direction to that of the steam. The condenser had two pipes which are concentric with the steam flowing in the inner pipe while the coolant flowed in the outer pipe. The pipe for the steam was made of stainless steel having a diameter and length of 25 mm and 1 m respectively. The pipe for the cooling water was made of galvanized steel having a respective diameter and length of 60 mm and 1 m.

The chimney was used to aid convection of the heated air in the system. It is made of mild steel material. Its length and diameter were 2 m and 12 cm respectively.

The various parts of the water-distilling machine were assembled together to form the water distiller. Plate I shows the set-up arrived at after the various parts of the water distiller had been assembled together.



Plate I: The set-up of the water distiller from various parts. Where: 1- Tank for coolant, 2- Condenser, 3- Distillates container, 4- Fuel rack inlet, 5- Chimney, 6- Pot and 7- Stove respectively.

With the water-distilling machine fully set, it was tested within the compound of the Technology Incubation Centre, Minna, Nigeria. On this day, the pot in the boiling unit was filled with 10 litres of feed water (well water). Forty-two pieces of briquettes, which were capable of turning this feed water to steam, were then put into the fuel rack of the combustion chamber. These briquettes were ignited with the aid of kerosene. Once the fuel was ignited, the timing of the process began. The test began at 12:45 pm and ended at 1:55 pm. By 1:55 pm, all the briquettes were completely burnt and 4.91 litres of distilled water were produced.

3.0 Discussion of results

Four samples of the briquettes were taken to the National Cereals Research Institute, Badeggi, Nigeria; to carry out proximate and ultimate analyses on them. In the same vein, two samples of the briquettes were also taken to the Department of Chemical Engineering, University of Ilorin, Nigeria; in order to determine the calorific value of the briquettes. Some of the distilled water produced was taken for various tests of purity at the Centre for Genetic Engineering and Biotechnology of Federal University of Technology, Minna, Nigeria; to determine how portable the distilled water produced was, the various results obtained from these tests were presented as follows as indicated Tables 1-2:

Result of the proximate analysis of the briquettes produced
TABLE 1: PROXIMATE ANALYSIS OF THE BRIQUETTES PRODUCED

COMPONENT COMPOSITION	PERCENTAGE (%)
CARBON	62.20
NITROGEN	2.01
OXYGEN	18.91
SULPUR	0.35
ASH CONTENT	11.81

RESULT OF ULTIMATE ANALYSIS OF THE BRIQUETTES PRODUCED

TABLE 2: ULTIMATE ANALYSIS OF THE BRIQUETTES

Component composition	Percentage (%)
Mixed content	31.53
Volatile Matter	50.00
Moisture content	4.30
Ash content	14.17

RESULT OF THE CALORIFIC VALUE TEST OF THE BRIQUETTES PRODUCED

The calorific value of the briquettes produced was 20.30 mj/kg. Table 3 shows the data obtained from the calorific value test done using the bomb calorimeter at the Department of Chemical Engineering in University of Ilorin, Nigeria. the parameters used were:
mass of fuel sample was 1.0 g;
Energy equivalent of the bomb calorimeter was 2330 cal/⁰c;
Amount of water used in the bomb calorimeter was 1500 ml;
Nichrome fuse wire used was 15 cm/0.018 g;
Cotton thread used was 5 cm/0.040 g.

TABLE 3: RESULT OBTAINED FROM THE CALORIFIC VALUE TEST DONE USING BOMB CALORIMETER.

PERIOD	TEMPERATURE (°C)	TIME (MIN S)	PERIOD	TEMPERATURE (°C)	TIME (MINS)
INITIAL	27.00				

A	0.00	1:00	07	2.31	10.00
B	0.00	2:00	08	2.35	11.00
C	0.00	3:00	09	2.39	12.00
D	0.00	4:00	010	2.43	13.00
E	0.00	5:00	011	2.45	14.00
12	2.48	15.00			
01	0.00	6:00	13	2.51	16.00
02	0.17	6.15	14	2.53	17.00
03	1.15	6.45	15	2.55	18.00
04	1.43	7.00	16	2.57	19.00
05	2.04	8.00	17	2.59	20.00
06	2.23	9.00	18	2,60	21.00

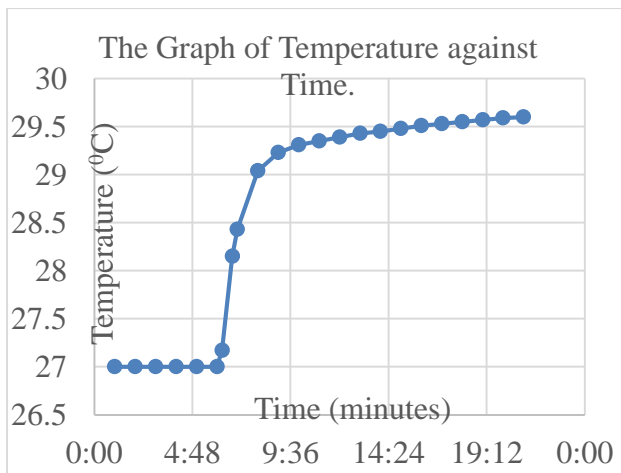


Figure 1: The characteristic temperature-time curve of a bomb calorimeter.

TABLE 4: RESULT OF THE MICROBIAL ANALYSIS OF THE FEED WATER USED.

Test	Count (cfu/ml)	Limit
Total coliform count	5.78×10^6	0

Total faecal coliform count	0	0
Total aerobic mesophilic bacteria count	5.78×10^6	1.0×10^2
Total Salmonella species	0	0
Total Pseudomonas aeruginosa count	0	0
Total Staphylococcus aureus count	0	0
Total Yeast/Mould count	0	1.0×10^2

TABLE 5: RESULT OF THE MICROBIAL ANALYSIS OF THE DISTILLED WATER PRODUCED.

Test	Count (cfu/ml)	Limit
Total coliform count	0	0
Total faecal coliform count	0	0

Total aerobic mesophilic bacteria count	0	1.0 x 10 ²
Total Salmonella species	0	0
Total Pseudomonas aeruginosa count	0	0
Total Staphylococcus aureus count	0	0
Total Yeast/Mould count	0	1.0 x 10 ²

TABLE 6: Result of the physicochemical analysis of both the feed and distilled water.

Sample	Conductivity (µS/cm)	pH value (mg/l)	Total hardness (mg/l)	TDS (mg/l)	Calcium (mg/l)	Magnesium
Feed water	1411	6.11	236.0	903.04	84.0	5.82
Distilled water	41	6.50	3.0	26.24	0.16	0.09

4.0 Discussion of results

From Table 1, the briquettes produced had a moisture content of about 4.30 %. This value was low and so its effect on the calorific value of the fuel was minimal. This therefore made the heating value of the briquettes produced to be high which agreed with (22).

The gross calorific value of the briquettes made was 20.30 MJ/kg. First and foremost, this meant that the briquettes could sustain combustion since its heating value was more than the 11.66 MJ/kg required by solid fuels like briquettes to sustain combustion (12, 21). Secondly, this heating value was also close to those values stated for briquettes made from sawdust in the literatures reviewed. According to (2), the heating value of briquettes from sawdust was around 17.93 MJ/kg while (20) stated that the value was about 19.52 MJ/kg.

From Figure 1, it could be seen that the temperature was steady for the first five minutes with it being at 27 °C. This occurred before the fuel sample in the bomb calorimeter was ignited. At this stage, the water in the calorimeter was continuously stirred for about five minutes to obtain a uniform temperature. Immediately after the five minutes elapsed, ignition of the fuel sample took place and there was a sharp increase in the temperature of the water in the calorimeter for up to the ninth minute of the test in which the temperature rose to about 29.2 °C. After this stage, the increase in temperature became gradual until it rose to about 29.6 °C where it became steady again and the test was stopped. Afterwards, the gross calorific value of the fuel sample was determined.

Table 4 showed the result obtained from the microbial analysis of the feed water before it was distilled off by the water distiller constructed. The water was found to contain E. Coli, the microorganisms which are pathogenic bacteria and are also called indicator organisms for water pollution. The water was therefore not good for human consumption. From Table 5, it could be seen that these E. Coli microorganisms were no longer present in the water after distillation had taken place which made it to be good for human consumption.

From Table 6, it could be seen that the conductivity of the water distilled off reduced significantly from 1411 µS/cm before distillation to 41 µS/cm after distillation, its pH value changed from 6.11 before distillation to 6.50 after distillation. Similarly, its total hardness also decreased considerably from 236.0 mg/l before distillation to 3.0 mg/l after distillation while the total dissolved solids (TDS) of the water before and after distillation were respectively 903.04 mg/l and 26.24 mg/l thereby resulting in a great reduction of the TDS present in the water after distillation. In the same vein, the amount of calcium available in the water changed greatly well from 84.0 mg/l before distillation to 0.16 mg/l after distillation just as the amount of magnesium present in it also changed from 5.82 mg/l before distillation to 0.09 mg/l



after distillation. The various values obtained for all these tested parameters after distillation were well below the safe limit for portability which made the water obtained after distillation to be good for human consumption.

5.0 Conclusion

In this paper, development of briquette-powered water distiller had been carried out by designing and fabricating a water distiller which made use of briquettes as its source of energy. The fabricated water distiller was used to purify untreated water and in the process, 4.91 litres of portable water was produced from 10 litres of feed water.

REFERENCES

1. Abduhamed, A.J., Adam, N.M., Hairuddin, A.A. & Kareem, H.K. (2016). Design and Fabrication of a Heat Exchanger of Portable Solar Water Distiller System. *International Food Research Journal*, 23, 15-22.
2. Roy, M.M. & Corscadden, K.W. (2012). An Experimental Study of Combustion and Emissions of Biomass Briquettes in a Domestic Wood Stove. *Applied Energy Journal*, 99, 206-212. doi:10.1016/j.apenergy.2012.05.003
3. Alberta State. (2006). *Alberta*. Retrieved May 2, 2016, from alberta.ca/index.aspx: <http://www1.agric.gov.ab.ca/..agdex 715>
4. Alpesh, M., Arjun, V., Nitin, B. & Dharmesh, L. (2011). Design of Solar Distillation System. *International Journal of Science and Technology*, 29, 67-74.
5. Asif, J.S. (2016). *Design, Construction and Performance Analysis of a Solar Powered Dual Mode Desalination System for Water Purification*. University of Dhaka. Dhaka: Institute of Energy, 1-84.
6. Azzeddine, F, Marwa, S., Farah, M., Maitha, A., Muna, O., Shamsa, H. & Hamda, A. (2017). A Versatile Solar and Electric Water Distiller. *International Journal on System Modelling and Simulation*, 2(2), 18-22. doi:10.24178/ijms.2017.2.2.18
7. Bates, R.B. & Ghoniem, A.F. (2012). Biomass Torrefaction: Modelling of Volatile and Solid Product Evolution Kinetics. *124*, pp. 460-469. *Bioresource Technology*. doi:10.1016/j.biortech.2012.07.018
8. Eze, J.I., Onyekwere, O. & Elijah, I.R. (2011). Solar Powered Distillation of Lagos Bar Beach Water. *Global Journal of Science Frontier Research*, 11(6), 53-58.
9. Gangadhar, N., Mukunda, S. & Sathish, S. (2012). Design and Fabrication of Solar Distillator. *International Journal on Theoretical and Applied Research in Mechanical Engineering*, 1(1), 47-51.
10. Kamran, H., Muhammad, M.K., Ijlal, S.A., Muhammad, O., Muhammad, A. & Abdul, W. (2013). Solar Power Water Distillation Unit. *Journal of Physics*, 1-5. doi:10.1088/1742-6596/450/1/012015
11. Manoj, K.S., Gohil, P. & Nikita, S. (2015). Biomass Briquette Production: A Propagation of Non - Conventional Technology and Future Pollution Free Thermal Energy Sources. *American Journal of Engineering Research*, 4(2), 44-50.
12. Mathias, A.M. (2013). *How Solar Powered Distillation of Water Works*. Energy Informative. Retrieved August 14, 2013, from HYPERLINK ["http://www.energyinformative.org"](http://www.energyinformative.org) <http://www.energyinformative.org>
13. Oyawale, F.A., Odior, A.O. & Ismaila, M.M. (2010). Design and Fabrication of Water Distiller. *Journal of Engineering Trends in Engineering and Applied Sciences*, 1(2), 169-174.
14. Sahoo, U., Singh, S.K., Barbate, I., Kumar, R. & Pant, P.C. (2016). Experimental Study of an Inclined Flat Plate - Type Solar Water Distillation System. *Springer Open Journal*, 3(5), 1-5.
15. Shashikanth, M., Binod, K., Yennam, L., P mohan, S.K., Nikhila, A. & Sonika, V. (2015). Solar Water Distillation Using Energy Storage Material. *Science Direct Procedia Earth and Planetary Science*, 368-375.
16. Shull, A. (2012). *The Design and Creation of a Portable Water Purification System*. Andrews University, Department of Engineering and Computer Science. Retrieved from <http://www.digitalcommons.andrews.edu/Honours/39>, 1-32.
17. Singh, R.V., Rahul, D., Hasan, M.M., & Tiwari, G.N. (2011). Comparative Energy and Exergy Analysis of Various Passive Solar Distillation Systems. *World Renewable Energy Congress*. Sweden: Linkoping, 3929-3936.
18. The watersite. (n.d.). Retrieved from <http://www.thewatersite.com>
19. World Health Organization. (2008). *Safe Water and Global Health*. Geneva. Retrieved July 25, 2010, from <http://www.who.int>.
20. Lee, C.C. (2007). *Handbook of Environmental Engineering Calculations*. New York, NY: Mc Graw - Hill Companies, Inc.
21. Storlarski, M.J., Szczukowski, S., Tworowski, J., Krzyaniak, m., Gulczynski, P. & Mleczek, M. (2013). Comparison of Quality and Production Cost of Briquettes made from Agricultural and Forest Origin Biomass. *Renewable Energy Journal*, 57, 20-26.
22. Solano, D., Vinyes, P. & Arranz, P. (2016). Biomass Briquetting Process: A Guideline Report. Beirut: A UNDP - CEDRO Publication. Retrieved October 2016, 1-5, 9-17.



IMPACT OF SVC AND DG COORDINATION ON VOLTAGE CONSTRAINED AVAILABLE TRANSFER CAPABILITY (VSATC)

*Sadiq A. A¹, Adamu S. S², Abubakar I. N¹, & Yusuf L¹

¹Electrical and Electronics Engineering Department, Federal University of Technology, PMB 65
Minna Niger State, Nigeria

²Electrical Engineering Department, Bayero University, Kano, Nigeria

*Corresponding Author email: ahmad.abubakar@futminna.edu.ng +2348057879333

ABSTRACT

Rapidly increasing power demand and inadequate generation and transmission capacity have set the trends towards Distributed Generation (DG) and Flexible AC Transmission System (FACTS) aimed at sustainable power delivery. FACTS and DG are often deployed to relieve congestions, improve voltage stability, and enhance transmission capability. However, FACTS and DG placement are often achieved separately. Hence their coordination in power systems operation is paramount for improved power transfer and minimal power losses for optimal power delivery. This paper demonstrates the coordination of SVC and DG in the IEEE 14 bus network for the enhancement of Voltage Constrained Available Transfer Capability (VSATC) and power loss reduction using Multi-Objective Particle Swarm Optimization (MOPSO). Since the objectives are opposite and parallel, hence the need for the transformation of ATC to minimization, which was achieved by negating its value during dominance determination stage. Voltage constrained ATC is obtained using continuation power flow (CPF) and computed at the CPF nose curve. Result show improved ATC with increasing DG penetration level. At high DG penetration (80%), ATC improved by 6.6% while losses reduced by 18.4% when compared to SVC and DG without coordination. Also, the Pareto front of ATC versus power loss indicates parabolic like characteristics.

Keywords: CPF, DG, FACTS, MOPSO, VSATC.

1 INTRODUCTION

Utilities around the world are embracing the market-driven and deregulated framework of the electrical power supply, thereby replacing a percentage of centralised power systems operations. A key feature of deregulation is the open access to transmission infrastructure, which results in the increased volume of the power transfer transaction. The increased in transactions are often constrained by transmission capacity, congestion, and voltage instability (Reddy, 2016; Sharma & Kumar, 2016; Yunfei, Zhinong, Guoqiang, & Yichu, 2015). Consequently, utilities seek to maximise the utilisation of the existing transmission infrastructure. One approach of maximising the utilisation of the existing transmission infrastructure is through optimal deployment of Flexible Alternating Current Transmission Systems (FACTS) devices. FACTS technology enables power flow re-distribution through the use of circuit parameters to relieve congestion, improve voltage stability at load centers, and enhance transmission capability (Ahmad Abubakar Sadiq, Adamu, & Buhari, 2019; Varshini & Kalpana, 2012).

On the other hand, “green politics” and issues of right of way within deregulation also prompt utilities, customers, and power system operators to prefer small capacity generators, connected to the load centers, often called Distributed Generation (DG). The financial risk of DGs is small, and possess technical potentials for ancillary

services in addition to meeting load demand (Nwohu, Olatomiwa, Ambafi, Ahmad, & Mogaji, 2017). Therefore, DGs are sited at the distribution level while large wind farms in addition to FACTS at the transmission level (Bavithra, Raja, & Venkatesh, 2016; S Kabir, Krause, Bansal, & Jayashri, 2014; S Kabir, Krause, & Haider, 2014; Shahariar Kabir, Krause, & Bartlett, 2013; Khan, Mallick, Rafi, & Mirza, 2015; Musa, Usman, & Adamu, 2013). Accordingly, a comprehensive assessment of the impacts of FACTS and DG placement in power systems operation to meet the increased power transaction is paramount. A primary index of transmission infrastructure performance and hence the viability of economic transfer transaction is the Available Transfer Capability (ATC) (A.A. Sadiq, Nwohu, & Okenna, 2014).

In (Rahman, Mahmud, Oo, Pota, & Hossain, 2016; Rahman, Mahmud, Pota, & Hossain, 2014), DSTATCOM and DG coordination are demonstrated for reactive power management to improve voltage profile and alleviate the severity of faults. Similarly, (Tolabi, Ali, & Rizwan, 2015) implements a Fuzzy - ACO approach to optimally place DSTATCOM and photovoltaic for power loss, voltage profile, and load balancing. (Venkateswarlu, Ram, & Raju, 2013) Examines the impacts of SVC and DG to increase network loading level and Voltage Stability Constrained ATC (VSATC) using Newton's Raphson (NR) power flow, while (Mahdad & Srairi, 2016) uses adaptive differential search algorithm to optimize the location and sizes of

multiple SVC and DG for power loss reduction and voltage deviation. The studies in (Rahman et al., 2016, 2014; Tolabi et al., 2015), ignores ATC enhancement with DFACTS and DG coordination. Although (Venkateswarlu et al., 2013) considered VSATC as critical loading factor, however, the computation of VSATC at the point where NR load flow fails to converge is an infeasible operating condition and the power balance equality constrained is violated; in addition, SVC and DG placement were not optimal but only based on the identified weak bus. In (Mahdad & Srairi, 2016), while a differential search algorithm was used, it did not consider ATC as an objective. This paper, therefore, demonstrates the coordination of SVC and DG in the IEEE 14 bus test network, for the enhancement of VSATC and power loss reduction using Multi-Objective Particle Swarm Optimization (MOPSO).

2 METHODOLOGY

2.1 SVC MODELING

At steady-state operation, the static var compensator (SVC) acts as a source or absorber of VAR. The SVC is therefore modelled as positive or negative load depending on whether it is absorbing or injecting reactive power respectively (A A Sadiq, Adamu, & Buhari, 2019; Venkateswarlu et al., 2013). The equivalent reactive load at the SVC installed bus is given by equation (1) while the modified residual Var is expressed by the equation (2). SVC capacity is constrained according to the equation (3).

$$Q_i^{new} = Q_i^{old} \pm Q_{svc} \quad (1)$$

$$\Delta Q_i^{new} = [(Q_{i,g} - Q_{i,d}) - Q_p^{cal}] + Q_{svc} \quad (2)$$

$$0 \leq Q_{svc} \leq 100 \text{ MVAR} \quad (3)$$

2.2 DG MODEL

In addition to the provision of ancillary service of local bus voltage control, DG is modelled as a generator with maximum and minimum active power capacity constrained by equation (4). Herein, to regulate the local bus voltage, the PQ bus with DG installed is modified into a PV bus.

$$5 \text{ MW} \leq P_{DG} \leq 100 \text{ MW} \quad (4)$$

The DG penetration specifies the maximum quantity of active power being injection as a percentage of the total network load (Mahdad & Srairi, 2016) and defines by the equation (5).

$$\sum_{i=1}^{ndg} P_{dg}^i \leq \mu \sum_{j \in PQ_{load}} P_{load}^j \quad (5)$$

In the equation (5), the total active power injected by DGs is a percentage of the active power demand, and the penetration is μ .

2.3 CPF FOR ATC

To solve the power flow equation, Continuation Power Flow (CPF) introduces a loading parameter λ to parameterise the power flow equations, thereby avoids singularity and ill-conditioning. The documentation of CPF for ATC assessment is given in (Ahmad Abubakar Sadiq et al., 2019), while at the CPF's nose point, the ATC evaluate to the maximum loading limit as expressed in equation (6), such that the i^{th} bus critical real power loading at the CPF nose point is expressed by the equation (7).

$$ATC = \sum_{i \in sink} P_L^{i,crit} - \sum_{i \in sink} P_L^{i,base} \quad (6)$$

$$P_L^{i,crit} = (1 + \lambda^{crit}) P_L^{i,base} \quad (7)$$

2.4 MOPSO

In this paper, the problem formulation involves two parallel and opposite objectives: ATC maximisation and minimisation of real power losses, hence a multi-objective formulation. Since the objectives are on two different fronts, there is a need to transform one of the objectives into minimisation or maximisation. Consequently, in the MOPSO algorithm, the ATC is transformed into minimisation by negating its value during the dominance determination stage. For a general minimisation problem, equation (8) defines the minimisation problem formulation of SVC and DG coordination for 2 objectives (Jumaat, Musirin, Othman, & Mokhlis, 2013; Zeinalzadeh, Mohammadi, & Moradi, 2015). The fitness vector of objectives is expressed by the equation (9), which is subject to power flows equality constraints in addition to the constraints equations (3) and (4).

$$\text{minimize } f(x, \lambda) = [f_1(x, \lambda), f_2(x, \lambda)] \quad (8)$$

$$\vec{f}(x, \lambda) = \begin{cases} -ATC = \sum_{i \in sink} P_L^{i,crit} - \sum_{i \in sink} P_L^{i,base} \\ P^{loss} = \sum_{k=1}^{nl} g_k [V_i^2 + V_j^2 - 2V_i V_j \cos(\delta_i - \delta_j)] \end{cases} \quad (9)$$

3 RESULTS AND DISCUSSION

As a form of validation, the CPF implementation and the methodology described in (Venkateswarlu et al., 2013) were compared and shown in Figure 1. Both CPF and Newton load flow is implemented in MATPOWER 7.0. As shown in Figure 1, both NR and CPF by MATPOWER

obtains similar ATC except in the case when Gen4 and Gen5 are the only sources supplying the additional increase in load demand, which is attributed to the generators reaching their respective reactive power limits and hence the likelihood of singularity.

Observe from Figure 1 that, under the case of interest, (with SVC_DG), both approaches obtain similar ATC,

with Newton's approach having slightly higher ATC. Consequently, for the active power loss objective, CPF approach is adopted, since the ATC computation at the point where NR fails to converge present an infeasible operating condition; the power losses are therefore not valid as the constraints of power balance equation become violated.

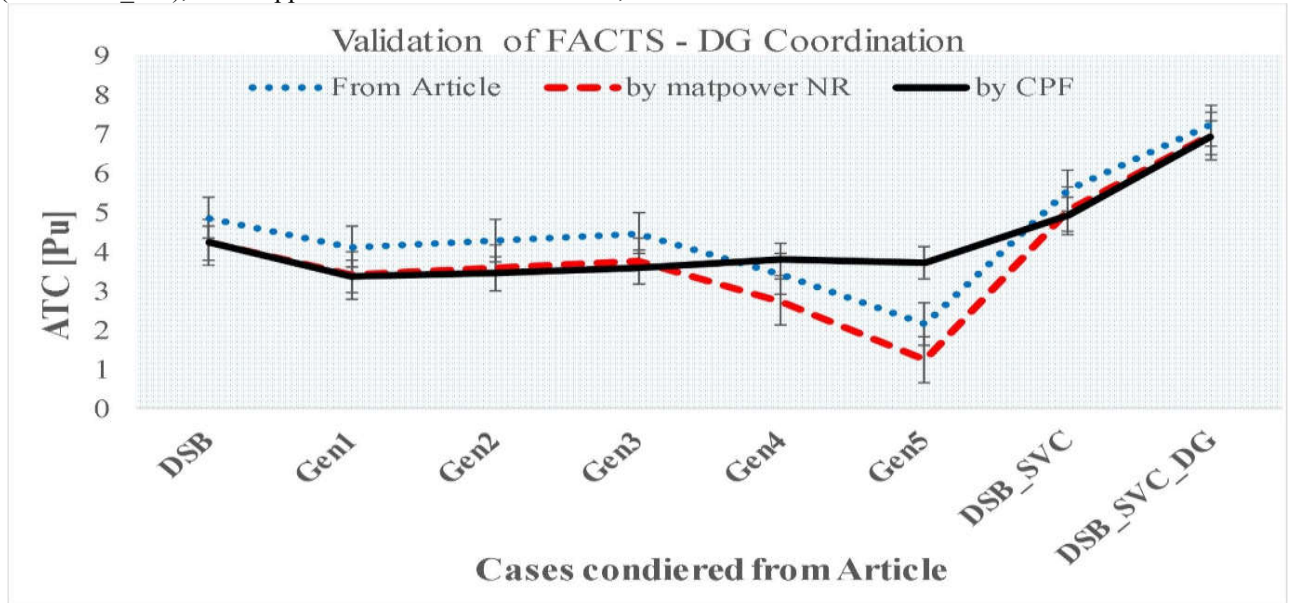


Figure 1: Comparison of NR and CPF approaches

For the multilateral power transfer transaction where all the generators are supplying the increase in load at all the load buses, Figure 2 shows the Pareto front of ATC versus Ploss

with different increasing DG penetration. The Pareto depicts a diving shape of, and the ATC increases with the increase in DG penetration.

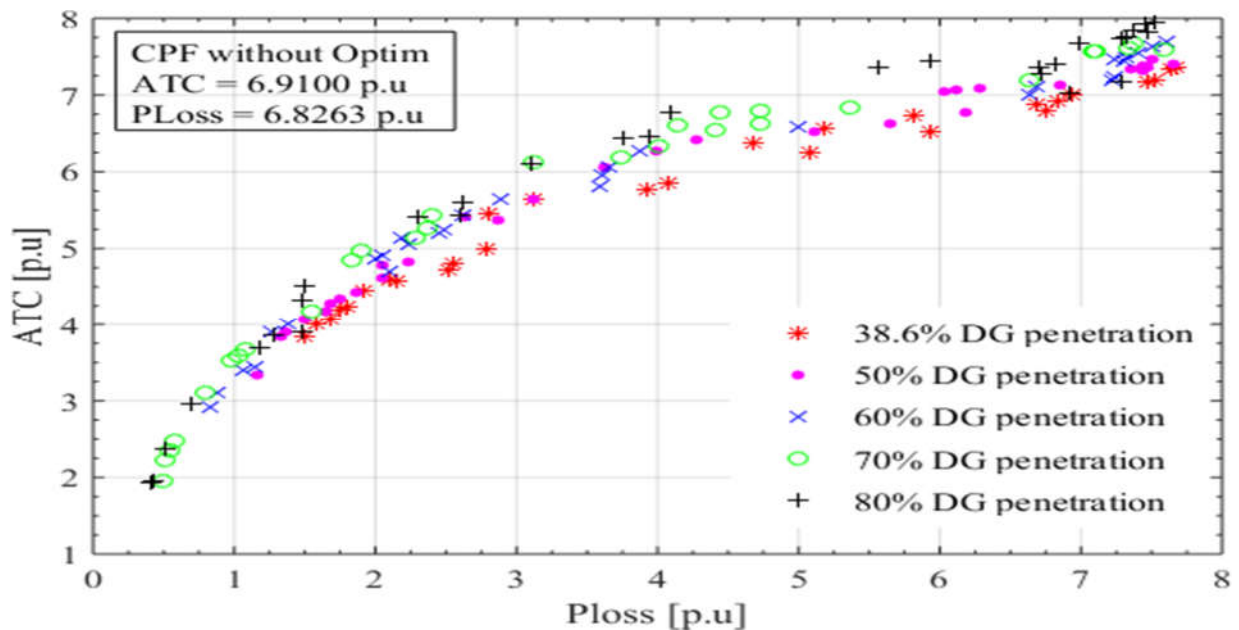


Figure 2: Pareto plot (ATC vs Ploss) for SVC & DG coordination

The Pareto front of Figure 2 with cursor values of nondominated solution within 50% and 80% is depicted in Figure 3. As shown, at 80% DG penetration, the ATC improves to 7.366 p.u with SVC and DG coordination against 6.91 p.u without coordination. Similarly, the active power losses also reduce from 6.826 p.u without coordination to 5.572 p.u with SVC and DG coordination.

At 80% DG penetration, the improvement in ATC and reduction in losses represent about 6.6% and 18.4% respectively.

TABLE 1 gives the selected optimal solution of the SVC and DG coordination for 50% to 80% DG penetration.

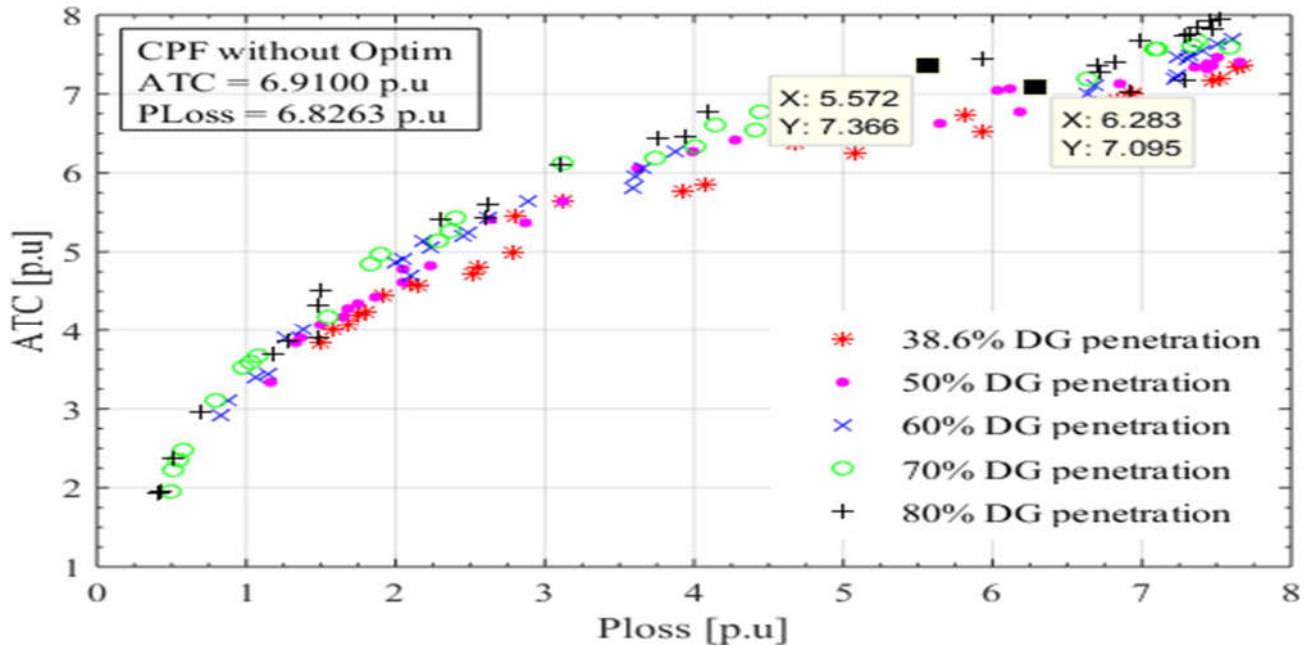


Figure 3: Pareto plot (ATC vs Ploss) with ATC and Ploss cursor values

TABLE 1: SELECTED NONDOMINATED SOLUTIONS FOR VARIOUS DG PENETRATION

% DG	Fitness Values		SVC Solution		DG Solution		
	ATC [p.u]	Ploss [p.u]	SVC bus no.	SVC Size [MVAR]	DG bus no.	PDG [MW]	Vbsvc [p.u]
50	7.09	6.28	14	54.76	9	128.83	1.084
60	7.10	6.68	14	63.60	10	152.93	1.009
60	7.19	6.64	14	58.49	10	181.3	1.009
80	7.36	5.57	14	65.83	7	207.2	1.100

4 CONCLUSION

This paper demonstrates the impacts of SVC and DG coordination for the improvement of VSATC and active power losses. It can be concluded that at higher DG penetration of 80%, for the multilateral transaction where all the generators are supplying the increase in load demand, ATC improves by 6.6% while the active power losses reduced by 18.4% with SVC and DG coordination.

REFERENCES

Bavithra, K., Raja, S. C., & Venkatesh, P. (2016). Optimal Setting of FACTS Devices using Particle Swarm Optimization for ATC Enhancement in Deregulated Power System. *IFAC-PapersOnLine*,

49(1), 450–455.

<https://doi.org/10.1016/j.ifacol.2016.03.095>

Jumaat, S. A., Musirin, I., Othman, M. M., & Mokhlis, H. (2013). MOPSO Approach for FACTS Device Installation in Power System. In *Proceedings of the 2013 IEEE 7th International Power Engineering and Optimization Conference, PEOCO 2013* (pp. 564–569).

<https://doi.org/10.1109/PEOCO.2013.6564611>

Kabir, S, Krause, O., Bansal, R., & Jayashri, R. (2014). Dynamic Voltage Stability Analysis of Sub-Transmission Networks with Large-Scale Photovoltaic Systems. In *IEEE Power & Energy Society General Meeting, Conference & Exposition-National Harbor, MD, USA* (pp. 1–5).

Kabir, S, Krause, O., & Haider, A. (2014). Design of an Optimal Placement Algorithm for Large Scale Photovoltaic in Sub-Transmission Networks. In *IEEE 3rd International Conference on the Developments in Renewable Energy Technology (ICDRET) - Dhaka, Bangladesh* (pp. 1–6). <https://doi.org/10.1109/ICDRET.2014.6861669>

Kabir, Shahariar, Krause, O., & Bartlett, S. (2013). Impact of Large-Scale Photovoltaic System on Short and Long Term Voltage Stability in Sub-Transmission Network. In *Australasian Universities Power*

- Engineering Conference, AUPEC* (pp. 1–6). Hobart, T AS, Australia,: Australasian Universities.
- Khan, I., Mallick, M. a., Rafi, M., & Mirza, M. S. (2015). Optimal Placement of FACTS Controller Scheme For Enhancement of Power System Security in Idian Scenario. *Journal of Electrical Systems and Information Technology*, 2(2), 161–171. <https://doi.org/10.1016/j.jesit.2015.03.013>
- Mahdad, B., & Srairi, K. (2016). Adaptive Differential Search Algorithm for Optimal Location of Distributed Generation in the presence of SVC for Power Loss Reduction in Distribution System. *Engineering Science and Technology, an International Journal*, 19(3), 1266–1282. <https://doi.org/10.1016/j.jestch.2016.03.002>
- Musa, H., Usman, B., & Adamu, S. S. (2013). Improvement of Voltage Stability Index Using Distributed Generation for Northern Nigeria Sub-Transmission Region. In *International Conference on Computing, Electrical and Electronic Engineering (ICCEEE)* (pp. 410–412). IEEE.
- Nwohu, M. N., Olatomiwa, L., Ambafi, J., Ahmad, S. A., & Mogaji, A. (2017). Optimal Deployment of Distributed Generators using Ant Colony Optimization to Minimize Line Losses and Improve Voltage Profiles on Distribution Network. In *Proceedings of the World Congress on Engineering and Computer Science WCECS 2017* (Vol. I, pp. 25–30). San Francisco, USA: WCECS.
- Rahman, M. S., Mahmud, M. A., Oo, A. M. T., Pota, H. R., & Hossain, M. J. (2016). Agent-based Reactive Power Management of Power Distribution Networks with Distributed Energy Generation. *Energy Conversion and Management*, 120, 120–134. <https://doi.org/10.1016/j.enconman.2016.04.091>
- Rahman, M. S., Mahmud, M. A., Pota, H. R., & Hossain, M. J. (2014). Distributed Multi-Agent Scheme for Reactive Power Management with Renewable Energy. *Energy Conversion and Management*, 88, 573–581. <https://doi.org/10.1016/j.enconman.2014.09.002>
- Reddy, S. S. (2016). Multi-Objective based Congestion Management using Generation Rescheduling and Load Shedding. *IEEE Transactions on Power Systems*, 8950(c), 1–12. <https://doi.org/10.1109/TPWRS.2016.2569603>
- Sadiq, A.A., Nwohu, M. N., & Okenna, A. E. (2014). Available transfer capability (ATC) as an index for transmission network performance – A case study of Nigerian 330kV transmission grid. *International Journal on Electrical Engineering and Informatics*, 6(3). <https://doi.org/10.15676/ijeei.2014.6.3.3>
- Sadiq, A A, Adamu, S. S., & Buhari, M. (2019). Optimal distributed generation planning in distribution networks : A comparison of transmission network models with FACTS Point of Common Coupling. *Engineering Science and Technology, an International Journal*, 22(1), 33–46. <https://doi.org/10.1016/j.jestch.2018.09.013>
- Sadiq, Ahmad Abubakar, Adamu, S. S., & Buhari, M. (2019). Available transfer capability enhancement with FACTS using hybrid PI-PSO. *Turkish Journal of Electrical Engineering & Computer Sciences*, 27(4), 2881–2897. <https://doi.org/10.3906/elk-1812-54>
- Sharma, P., & Kumar, A. (2016). Thevenin’s Equivalent based P-Q-V Voltage Stability Region Visualization and Enhancement with FACTS and HVDC. *International Journal of Electrical Power and Energy Systems*, 80, 119–127. <https://doi.org/10.1016/j.ijepes.2016.01.026>
- Tolabi, H. B., Ali, M. H., & Rizwan, M. (2015). Simultaneous Reconfiguration, Optimal Placement of DSTATCOM, and Photovoltaic Array in a Distribution System based on Fuzzy-ACO Approach. *IEEE Transactions on Sustainable Energy*, 6(1), 210–218. <https://doi.org/10.1109/TSTE.2014.2364230>
- Varshini, G. Y. S., & Kalpana, N. (2012). Enhancement of Available Transfer Capability using Particle Swarm Optimization Technique with Interline Power Flow Controller. In *Third International Conference on Sustainable Energy and Intelligent Systems (SEISCON 2012)* (pp. 331–334). Tamilnadu, India: IET. <https://doi.org/10.1049/cp.2012.2234>
- Venkateswarlu, A. N., Ram, S. S. T., & Raju, P. S. (2013). Impact of SVC and DG on Voltage Stability Constrained Available Transfer Capability. *International Journal of Engineering Trends and Technology (IJETT)*, 4(7), 3040–3044.
- Yunfei, C., Zhinong, W., Guoqiang, S., & Yichu, L. (2015). Fast Calculation of Available Transfer Capability Incorporating Uncertainty of Wind Generation. In *5th International Conference on Electricity Utility Deregulation and Restructuring and Power Technology. November 26-29* (pp. 2486–2490). Changsha, China: IEEE. <https://doi.org/10.1109/DRPT.2015.7432671>
- Zeinalzadeh, A., Mohammadi, Y., & Moradi, M. H. (2015). Optimal multi objective placement and sizing of multiple DGs and shunt capacitor banks simultaneously considering load uncertainty via MOPSO approach. *International Journal of Electrical Power and Energy Systems*, 67. <https://doi.org/10.1016/j.ijepes.2014.12.010>



CONSTRUCTION OF A SOLAR POWERED BATTERY FORGE

*Adimula, M. G.¹, Abubakre, O. K.², Muriana, R. A.³

¹Department of Materials and Metallurgical Engineering, Federal University of Technology, PMB 65 Minna Niger State, Nigeria

²School of Infrastructure, Process Engineering and Technology. Federal University of Technology, PMB 65 Minna Niger State, Nigeria

³ Department of Materials and Metallurgical Engineering, Federal University of Technology, PMB 65 Minna Niger State, Nigeria

email: muyiwagideon72@yahoo.com, +2347032065069

ABSTRACT

The ancient art of blacksmithing in our era nowadays is declining because of the conception and interpretation given to it by young folks and some educated class in our society. This paper identifies the challenges that comes with the traditional forge and pin point on the way to modify it into a consolidated equipment that measures up to the standard of modern equipment, yet easy to operate and handled. People disregard the profession of blacksmith because of the rigor and stress involved in the operation of the equipment, the dirtiness of the job, the exposure to heat and other elements that can pose danger to the life of the operator. Using this equipment will improve the outlook of the blacksmith job and also encourage youths and any interested individual to proudly go into Blacksmithing as a lucrative and viable source of income. If these problems are decisively tackled, there will be an increase in the number of young people coming into the business and it can also serve as a means to reduce the rate of unemployment in our society.

Keywords: Battery, Blacksmith, Charcoal, Forge.

1 INTRODUCTION

Forge is one of the oldest heating technologies that ever existed. It is one of the instruments used by a Smith. A blacksmith is a person that is specialized in shaping of metals by heating and forging the metal into desired tools, parts or shapes (Adebayo *et al.*, 2017). He heats the metal to soften it, using a forge, and then hammering it on an anvil into shapes. The first evidence of smithing by hammering iron into shapes is a dagger found in Egypt dating to 1350 B.C. History shows that the dagger was produced by the Hittites who invented Forging and tempering, but they kept their Ironworking technique secret until they were scattered across Greece and the Balkans. Blacksmithing is an ancient craft that is dated back to the first millennium BC, but some people believed it was imported from elsewhere, others argued that it emerged from Africa independently (Aliyu *et al.* 2008). In Nigeria, Iron was smelted in Northern Nigeria by the Nok around 500 BC, and by the end of the fourth century (AD), the knowledge had spread across the region. However, their knowledge of metallurgy brings about development in almost every area of life e.g. production of farming implements, domestic utensils, working tools and weapons.

The Smith uses the forge to heat any metal that he wants to work on. A traditional forge uses heated charcoal as the source of its heat. The heat of the charcoal is sustained through air supplied by the air generator, which comes in form of bellows, squirrel cage, hand cranked blower, and so on. Since the hottest part of the hearth is the center of the charcoal, therefore the smith places the metal in this hot spot for maximum heating. After the metal is well heated

to soften it, the smith brings the softened metal to an anvil or a hard surface, then hammers the metal into any shape he desires (Folayan, 2001).

1.1 LITERATURE REVIEW

BLACKSMITH FORGE

There are different means of heating metals which include Furnace. Furnace is equipment used to generate high temperature for the purpose of heating. However, some people calls furnace Oven or Kiln. In the smithing work, they can be liken to a forge, which does the same work of heating the material placed inside it (Lillico, 1995). A conventional blacksmith forge usually consist of some components:

- 1) The hearth
- 2) The air channel
- 3) The Air generator (Bellow or Fan)

1.1.1 The hearth

The hearth is the outer opening where the fuel is placed. It is made locally from refractory clay, cast iron because of its corrosion resistance, and sometimes, mild steel where the work is intermittent. It has different shapes as designed by the smith, but the most common is conical shape of hearth. The reason for the conical shape is for effective distribution of air to the fuel, which in turn leads to optimal burning of the fuel to produce high Temperature heat. However, some hearth are now mordernized and can be made with any container that can withstand heat or serve the purpose of the hearth. The basic function of the hearth is to hold the charcoal and



also to place the metal to be heated (Cline-cole *et. al.*, 1994). The hearth has a hole at its base, through which the air enters into it.

1.1.2 The air channel (Tuyere)

The air channel is a medium through which the air passes from the air generator to the hearth. In a local smith workshop, it is mostly hidden under the ground, in which one end is attached to the base of the hearth, and the other end is attached to the air exit of the air generator. It is mostly constructed in a tubular form, so as to allow unobstructed flow of air.

1.1.3 The air generator

The air generator is the component that produces fast moving air molecules and forces it through the air channel, to the hearth. The air generator comes in different forms;

- Bellow
- Electric blower (AC or DC)
- Hand crank blower
- Electric paddle type
- Squirrel cage

Any of the listed air generator can be used depending on the type of forge or design, as desired by the user.

The arrangement of the three components earlier mentioned can be used to generate heat, which can be used in a smith work shop, for heat treatment purpose or for other metallurgical effect such as Hardening, annealing and tempering. The fire produced from the forge is controlled in three major ways:

- Amount of Air
- Volume of Fuel
- Shape of Fuel/Fire

In a typical forge that uses coal, a firepot will be placed at the center of a flat hearth. The tuyere is fixed to the firepot at the base. During its operation, the center of the coal where the air enters the hearth is the hot core of the fire, and this core will be surrounded with pack of hot, but not burning coal. Around this unburnt coke, we have a transitional layer of coal that is transformed into coke by the heat of the fire. All these layers are surrounded by horse shoe shape of raw coal layer. It is usually kept damp and packed tightly to maintain the shape of the heart of the fire. It also prevent the coal from burning directly so that it cooks first into coke (Sinha *et. al.*, 1973)

When these separate units, that is, the hearth, the air channel and the blower is combined together into a single unit, it saves the cumbersomeness of the whole unit being operated separately. There will be ease of operating the equipment, because once the switch is on, no more effort is needed to make it operational.

1.2 CHARCOAL FUEL

For the purpose of saving cost, the fuel used in this work is charcoal fuel because we can obtain it easily and it is relatively cheap. It is also a very good source of heat when ignited.

1.3 CALORIFIC VALUE OF THE CHARCOAL

The calorific value of a fuel can also be referred to as the heating value of that fuel, and it is the amount of heat given out when a particular amount of the fuel is burned. It is usually measured in energy per unit of the substance, which can be mass, such as kcal/kg, J/mol, kJ/kg, Btu/m³. The heating value is usually determined by a Bomb calorimeter. Various grade of charcoal is produced from different species of trees and their calorific value has also been determined (Adeleke, 2003).

Calculation of heating value of charcoal is of great importance in converting it to a useful form of fuel and also its direct usage. Some of the formulas are:

$$Q = 145.44 C + 620.28 H + 40.5 S - 77.54 (O) \quad (1)$$

$$Q = 151.2 C + 499.77 H + 45.0 S - 47.7 (O) \quad (2)$$

$$Q = [654.3H - 100 - A + 424.62] [C/3 + H - S/8] \quad (3)$$

$$Q = 144.54 C + 610.2 H + 40.5 S - 62.46 (O) \quad (O) < 15\% \quad (4)$$

$$Q = 144.54 C + 610.2 H + 40.5 S - [65.88 - 30.96(O) - 100 -] (O) \quad (O) > 15\% \quad (5)$$

1.4 SOLAR POWER

When the sun shines, the sunlight hits the solar panel at an elevated level, and the solar panel converts the sun energy into a Direct current (DC). The DC current flows into the inverter. The work of the inverter is to simply convert the electricity from DC current into AC current. The AC current is then connected for usage to home appliances. The solar panel can also be connected directly to an appliance that operates with direct current DC.

1.4.1 ADVANTAGES OF SOLAR POWER

- Solar power is free of pollution and there is no greenhouse gases emission
- It reduces dependence on fossil fuels
- It is renewable power sources that can be gotten every day of the year, cloudy day even have some amount of solar energy.
- It needs less or no maintenance, because they last for over 30 years.
- Job opportunities are created by the solar panel manufacturing company.
- Excess power generated can be sold to Power Company.



- 7) If the power generated is enough to use at home, there is no need to depend on grid.
- 8) It can be installed at any place or location in a field
- 9) Batteries can be used to store extra power for use when there is no solar ray.
- 10) It is safer than the existing traditional electric current

1.4.2 DISADVANTAGES OF SOLAR POWER

- 1) Initial cost of material and installation is high
- 2) Due to no solar power at night, a large battery power bank is needed to store power during the day.
- 3) Devices that operates on DC power are more expensive.
- 4) Depending on a geographical location, there is variation of solar panel size to their power generation.
- 5) There is lower production during the winter.
- 6) Cars powered with solar are not as fast as cars powered with a typical gas.
- 7) Production of solar panels in mass are reduced due to lack of materials so as to lower the cost for affordability.

1.5 BATTERY

A battery is referred to as a device that consist of one or more electrochemical cells, which has external terminals where electrical gadgets and devices can be connected for power. In the battery, the positive terminal is cathode and the negative terminal is anode when supplying power. Batteries convert chemical energy into electrical energy. A battery consist of some number of voltaic cells (A voltaic cell or galvanic cell is an electrochemical cell that obtain its electrical energy from a spontaneous redox reactions occurring within the cell). A conductive electrolyte containing metal cations connects two half cells in series.

The voltage developed across the terminals of the cells depends on the release of energy of the chemical reactions of its electrolytes and electrodes. Though, Zinc-carbon and Alkaline cells both have different chemistry, they produce the same electromotive force of 1.5 volts. Also, NiCd and NiMH cells have different chemistry, but produce approximately the same electromotive force of 1.2 volts.

1.6 CATEGORIES AND TYPES OF BATTERIES

Batteries are classified into Primary batteries and Secondary batteries.

1.6.1 Primary Batteries: they are manufactured to be used until they are exhausted, then discarded. They cannot be recharged because their chemicals are not reversible.

1.6.2 Secondary Batteries: They can be recharged by applying electric current to the cell, because their

chemical reaction is reversible. This allow them to be used and recharged multiple times over.

The oldest type of rechargeable battery is the Lead-acid battery. They are widely used in automotives. The liquid electrolyte is placed in a container with lid or screw cap to prevent the liquid from spilling and it must be kept in an upright position and a well-ventilated area to ensure that the hydrogen produced during overcharging is safely dispersed. Other types of batteries are the gel batteries (it has a semi-solid electrolyte), Absorbed glass mat (It absorbs the electrolyte in a special fibre glass matting). One of the best type of battery for storing charges from a solar panel is a deep cycle battery. They are also applicable in small electric vehicles, some industrial equipments like golf cart, forklifts, scissors lifts and floor cleaner.

2 METHODOLOGY

The idea adopted in this paper is the consolidation of different units or components that make up the forge into one mobile unit.

2.1 MATEIALS FOR CONSTRUCTION

The materials that will be used for the construction of this unit must be strong and rigid, it must be durable at relatively high temperatures. Also, the material must be machineable, so that it can be reshaped and remodeled into a desired shape. The materials that will be used are: Square pipe Mild steel (25mm by 25mm), Flat bar Mild steel (2mm by 20mm), mild steel sheet (0.7mm thickness), Rubber fittings, Solar panel (12V, 80watt), Electronic parts, Wire, Screws, 12V DC fan.

2.2 MATERIALS FOR DIFFERENT COMPONENT OF THE FORGE

2.2.1 MATERIAL FOR HEATING CHAMBER

The materials that will be used for constructing the heating unit is 1.0mm is thick mild steel and it is selected based on the following requirement:

- 1) Ease of fabrication and machining
- 2) Ability to withstand high operating temperature both when the unit is to be used as a forge and as a heat treatment unit.
- 3) Ability to withstand internal pressure. A steel has a very high tensile strength ranging from 276Mpa to 2070Mpa (Singh, 2003)

Therefore, the materials to be used for the construction of the heating unit are: Mild steel sheet of 1.0mm thickness, Mild steel Flat bar of 2.0mm thickness, Glass fibre material for insulation, and Mild steel rod of 10mm diameter.



2.2.2. MATERIAL USED FOR AIR CHANNEL

The material to be used for air channel is mild steel sheet. This sheet is carefully cut into a square hollow channel that connects the hearth to the blower.

2.2.3 MATERIAL USED FOR BLOWER

A DC fan will be used as a blower in the construction of this unit. This dc fan will be mounted on a constructed casing that will help channel the air generated to the air channel that leads to the hearth where the combustion takes place. The casing is shaped in such a way to force air through a narrow section air channel.

2.2.4 MATERIALS USED FOR HEARTH

The hearth will be constructed using a mild steel sheet, due to the intermittent usage of the equipment. It will be shaped in a way to hold the charcoal in a kind of position that will allow equal distribution of air to the fuel (Charcoal).

2.2.5 Volume of the heating chamber

The heating chamber is in a cuboid shape, thus the space inside the cuboid is as given by:

$$V_{hc} = l \times b \times h \quad (6)$$

Where V_{hc} = Volume of heating chamber
 l = Length
 b = Breadth
 h = Height

2.3 Furnace Dimensions

The furnace dimension will depend on the following factors. (Tyler *et. al.*, 2001)

- (i) Productivity of the furnace.
- (ii) Size and shape of the billets.
- (iii) Mass of metal in the furnace at that instance.

The mass of metal, M will be given by the equation:

$$M_m = p \times \tau \quad (7)$$

. Where:

p = productivity, kg/hr;

τ = the heating time, hr

2.3.1 DETERMINATION OF THE EFFECTIVENESS OF INSULATORS (Q)

For single layer insulation, heat loss per m^2 of hot surface is:

$$q = \frac{T_1 - T_2}{R} = \frac{T_1 - T_m}{R + R_s} \quad (8)$$

Where:

R = thermal resistance of insulator per m^2 (m^2k/w)

R_s = thermal resistance of outer surface of insulation system (m^2k/w)

2.3.2 AMOUNT OF FUEL BURNED PER HOUR

Singh (2003) postulates that the heat supplied by fuel is given by the following equation:

$$Q_s = M_f \times LCV \quad (9)$$

Where Q_s = heat supplied
 M_f = Mass of fuel burned
 LCV = Lower calorific value

And the calorific value of the charcoal is obtained by using (Singh, 2003):

$$LCV = HCV - \frac{9}{100} \times H \times 2442 \text{ kJ/kg} \quad (10)$$

2.3.3 DETERMINATION OF THE PERIPHERAL DISCHARGE VELOCITY

The peripheral discharge velocity of the air at the outlet of the fan is expressed in terms of the diameter of the impeller with the shaft speed, is;

$$U = \pi D_2 N / 60 \quad (11)$$

Where U = Peripheral discharge velocity
 D = Diameter of impeller
 N = Shaft speed

2.4 METHOD OF OPERATION OF FORGE

The metal sheets and pipes will be joined together using an electric arc welding machine with gauge 12 electrode, the skeletal frame will be constructed first to give the equipment a rigid and balanced structure. The inner wall will be fixed first, which will serve as a platform for the lagging. The external wall will then be fixed to cover the lagging material. A square hole will be made at the base of the constructed box (which is the heating chamber). This represents the hole that will allow the passage of air from the blower to the hearth. The hearth will be constructed to form a hollow truncated pyramid that is opened at both end, it will be fixed upside down directly on the square hole at the base of the heating chamber. An air channel will be constructed to link the blower to the hearth using metal sheet.

The blower will be connected to a simple electric circuit which will also be connected to the battery. The equipment

carries out its function by simply heating the heated charcoal through the air produced by the blower.

The charcoal will be manually lit with fire, after other pieces of the stock of charcoal is red hot, and then the blower is powered on by a battery which will keep the blower on. The air channel directs the air to the hearth. The air channel enters the hearth through its base. The air combines with the heated charcoal to increase the heat being produced on the hearth. When the charcoals are red hot, then the blacksmith can then place the work piece in the heated charcoal through the opening within the front door.



Figure 1: Heating chamber of a Solar powered battery forge



Figure 2: Assembled Solar powered Battery forge

3 RESULTS AND DISCUSSION

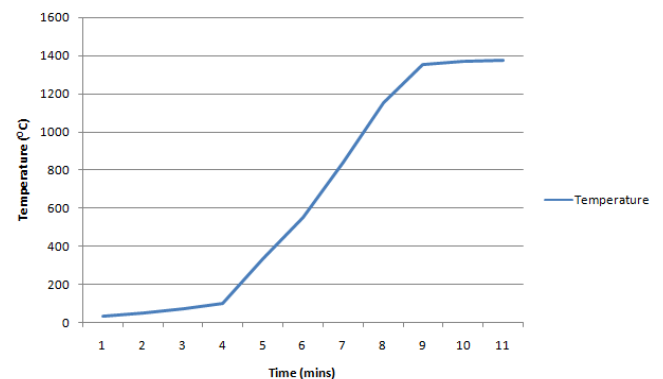
Charcoal is used as the fuel for this test. The test will determine the time taken for a specimen placed in the heating chamber to get hot when aided with a blower in the Solar Powered forge. The thermocouple can be used to obtain the temperature reading in the heating chamber. Table 3.1 shows the plot of temperature against heating time.

TEMPERATURE (°C)	TIME (mins)
35	0
51	3
76	6
101	9
335	12
550	15
842	18
1150	21
1355	24
1370	27

Table 3.1: Table of Temperature and Heating time

Table 3.1 Shows temperature values against the corresponding time read by higher capacity thermocouple

The room temperature is 35°C as measured by the thermocouple. The whole charcoal in the hearth will be heated by placing the already heated charcoal in the other unheated charcoal. Then the temperature rise in the heating chamber is measured until it gets to the maximum temperature and the graph plotted as seen in Graph 3.1.



Graph 4.1: Plot of Temperature against Time

The illustration in Graph 4.1 shows that the heating chamber reaches 1370°C Temperature within the period of 27 minutes. The temperature was initially slow, but after 4 minutes it began to rise steadily and faster till it got to a high Temperature of 1370°C where it remain constant. This shows the efficiency of this equipment, as heating of specimen in an enclosed chamber is more efficient compared to heating of specimen in open air hearth of the local blacksmith.



All Figures and Tables inserted should be properly referenced in the discussion of the results. Results and discussion entails the use of words to describe the implication of the results expected/obtained. Often, Figures, Tables and Plates are powerful means for proper technical result reporting and discussion. Examples of Figures and Tables are given in Figure1 and Table1.

4 CONCLUSION

This equipment will encourage young ones and the present age people to embrace the work of blacksmith as against their belief about the dirtiness of the job, because of the portability, modification and easy-to-operate nature of the equipment. It will also make the work of blacksmithing, which is already fading away, to be popular and acceptable to our society.

This equipment will also increase the efficiency of heating, and this means that the heating time of any work piece placed in the heated coal will be reduced. Since there will be steady and stable air supply from the blower, which is powered by a battery, there will be enough air fuel mixture which will make the charcoal to be hotter. This will make the work piece to get hot and soft within a short period, it will also make the work to be faster and increase the number of products produced within a short time.

The enclosed heating chamber will prevent the operator of this equipment from getting hurt from the heat coming from the heating chamber.

The mobility and portability of this equipment will make this job a desired type of occupation, especially among the youth.

With this equipment, unemployment will be reduced. Based on the effectiveness of the equipment and the importance of its product in the society, more unemployed individual can take advantage of it as a source of income.

However, it is recommended that this equipment is well marketed to the Small and Medium Entrepreneurs, so as to create awareness of its existence. Also, there should be some added gadget like solar panels, for charging the batteries in case there is no power supply from the power station

REFERENCE

Adebayo, R.A. & Oke, P.K. (2017) ‘ Development of a Forging Machine for Improved Blacksmithing in Nigeria. Current Journal of Applied Science and Technology. 25(4): 1-11, 2017

Adeleke A.F. (2003) Investigation into charcoal production techniques (unpublished) B.Eng project Report, Department of Mechanical Engineering, ABU Zaria

Aliyu, A.B., Yunusa & A.A. Adamu (2008) ‘Investigative Study of Archaeo-Metallurgy of Katsina State’, *Continental Journal of Engineering Science* 3(12):1-12.

Cherkassky, V.M. (1977). Pumps, Fans, and Compressors, MIR Publishers. Moscow. Pp 43-44, 174- 198.

Cline-Cole, R.A. (1994) ‘Political Economy, Fuel Wood Relations and Vegetation Conservation: Kasar Kano, Northern Nigeria, 1850-1915’, *Forest and Conservation History* 38(2)67-78.

Folayan, J.D. (2001) Design of a coal fired crucible type furnace, undergraduate project, Department of Mechanical Engineering, ABU Zaria.

Harvey, E.F; (1982) Pressure Components Construction (Design and materials application)

Lillico, J.W. (1995). The Blacksmith’s Craft. An introduction to smithing for apprentices and Craftmen. Rural Development Commission. 13(1): 1-3.

Singh, S. (2003) (Ed) Mechanical Engineers Hand Book Khana Publishers, New Delhi,India.

Sinha, K.P and Joel D.B. (1973) “Foundry technology” 1st edition London ILIFFE Books Ltd.



Financial Assessment of the Flood Risk Preparedness of Some Selected States in Nigeria

*Idachaba, A¹, Makinde, J² & Oke, A³

¹Project Management Department, Federal University of Technology, PMB 65 Minna Niger State, Nigeria

² Project Management Department, Federal University of Technology, PMB 65 Minna Niger State, Nigeria

³ Quantity Surveying Department, Federal University of Technology, PMB 65 Minna Niger State, Nigeria

*Corresponding author email: adidachaba88@gmail.com, +2348068900669

ABSTRACT

The impact of flooding transcends cultures, religions and geographies; such impact is associated with loss of properties and lives as well as disruption in community and business life. Flood risks are exacerbated by socio-economic factors including the action and inaction of governments. Previous studies on flooding within the study area have focused on the causes of flooding, the health effects of flood incidents and residents' coping measures. This paper will undertake a financial assessment of flood risk preparedness of some selected states within the north-central geopolitical zone of Nigeria with the view to highlighting the importance attached to flood risk in government budgets. This will be achieved through a review of literature to learn how studies of flood disaster costs were carried out in order to design an appropriate methodology for carrying out the research. The findings and methodologies applied in 15 papers on flood impact that were published between 2013 and 2018 were reviewed. Most of the papers adopted a quantitative approach; interviews, where used, served solely as a means of building up estimates of flood disaster costs. The suggestion that flood disaster costs research is best carried out using a quantitative approach was adopted in this paper and will be operationalized through questionnaires and document study. This will enable conclusions to be drawn as to the financial preparedness of governments to tackle flood disasters.

Keywords: *Costs; disaster; flood; risk; methodology.*

1 INTRODUCTION

The United Nations International Strategy for Disaster Reduction (UNISDR) produced by the UN Office for Disaster Risk Reduction has described floods as one of the most wide-ranging natural hazards globally. On the average floods affect about 70 million people each year (UNISDR, 2011). This means that the impact of flooding transcends cultures, religions and geographies; floods lead to loss of lives, disruption in community and business lives, damages to properties and assets. The risks of flooding are exacerbated by local socio-economic factors, which include increased population growth in coastal areas, non-sustainable agricultural practices as well as the impact of ongoing climate change. The recognition that flooding is a complex phenomenon, having political, economic, social and environmental dimensions consequently means that solely engineering solutions to flood problems will not suffice (Surminski and Eldridge, 2015). Similar to climate change however, flood damage has been on an increasing trend over the last century (Pielke, 2000), and annual damage costs are predicted to rise even more rapidly in the future (Ciscar *et al.*, 2011).

Increased flood problems in the states within the north-central geopolitical zone (such as Benue, Kogi and Niger States) and other areas of Nigeria have regularly (usually on an annual basis) disrupted socio-economic

activities and caused displacement of persons in affected areas. In Nigeria, flooding is associated with misery (Adeoye *et al.*, 2009). A case in point is that of the 2012 flood which occurred within the flood plains of the rivers Niger, Benue and their tributaries in Nigeria (Nigeria Hydrological Services Agency, 2013).

In September 2012 about twenty-seven states in Nigeria were affected by flood that covered one-third of the arable land and resulted in the deaths of more than three hundred persons. A further two million persons were displaced from their homes and farmland used for maize production and vegetable gardening (Shabu and Musa, 2015). The flood also destroyed other crops such as sorghum, millet, groundnut, beans, yam, cassava and sweet potatoes which were farmed along the banks of River Benue and its distributaries.

Previous studies on flooding within the study area have focused on the causes of flooding, the health effects of flood incidence and residents' coping measures (Ologunorisa and Tersoo; 2006, Ocheri and Okele, 2012; Shabu and Tyonum, 2013). Some of the studies looked at the social and economic impact of flooding (Oruonye, 2012; Duru and Chibo, 2014). Mngutyo and Ogwuche (2013) examined the control of flooding by government; however a financial analysis of the preparedness of governments to cope with flood incidents was not undertaken. Given the huge costs of flood damage in

Nigeria, and the low level of insurance uptake in the Nigerian economy, it becomes necessary to examine financially the level of preparedness of states that are susceptible to flooding in the north-central geopolitical zone of Nigeria.

This study is significant because it seeks to document expenditure on flood disaster management by government agencies and provide concise data on the size of government budgets for flood related activities. This knowledge will benefit both researchers and policy makers in the field of flood risk management because it is difficult to come across empirical data on the costs of flood management in Nigeria. The compilation of budgets for drainage, city planning and water transportation with specific reference to flood management is rare in the literature.

The aim of this paper is to undertake a financial assessment of flood risk preparedness of some selected states within the north-central geopolitical zone of Nigeria with the view to highlighting the importance attached to flood risk in government budgets. Three states within the north-central geopolitical zone will be covered in the study; these are the Benue, Kogi and Niger States, which are states through which pass Nigeria's two major rivers – the Niger and the Benue. The specific objectives of the study are to review literature to learn how studies of flood disaster costs were carried out and to design an appropriate methodology for carrying out the research.

1.1 FLOOD DISASTER RISKS

According to Arnell and Gosling (2016) by the turn of the millennium approximately 623 million people lived in flood-prone areas. This has made the search for more holistic management of flood an urgent necessity; structural mitigation measures such as dams and flood ways are no longer sufficient. Countries must move towards “more adaptive and integrated” approaches (Ward *et al.*, 2013). Simonovic and Carson (2003) have defined flood risk management in terms of the very wide range of activities aimed at reducing the potentially harmful impact of floods on people, economic activities and the environment. In the light of predictions of increasing trends in flood management costs (Pielke, 2000), Ciscar *et al.*, (2011) estimates that Europe's current annual flood damage costs are £5.2 Billion.

Nabangchang *et al.* (2015) examined the costs of the 2011 Bangkok flood, as an example of a 50-year flood. The inundation of greater Bangkok proceeded in three distinct phases. From March to April heavy rainfall led to flooding in southern Thailand; 61 deaths were recorded, in addition to damages to 600,000 homes and transportation infrastructure. In the second phase which occurred in mid-October, the Central Region, which is home to most of the industrial estates in Thailand, was flooded. Up to 3 meters of water was observed in areas. There was a resultant disruption in supply chains globally.

The final phase of the 2011 flood was documented by mid-November; it was estimated that 5.3 million people (8% of the total population of Thailand) were affected.

In their assessment of climate change implications for global river flood risk, Arnell and Gosling (2016) agreed that climate change has the potential to substantially change human exposure to the flood hazard. They however found considerable uncertainty in the magnitude of this impact, particularly as it involves rainfall. A key conclusion was that based on current projections, by 2050 approximately 450 million flood-prone people and 430 thousand km² of flood-prone cropland would be exposed to a doubling of flood frequency. This makes it imperative that preparations to mitigate such impact be started early. The roles played by politics, administration, and civil society may be key to surviving flood disasters. Thielen *et al.* (2016) reviewed how the measures that politics, administration, and civil society have implemented since 2002 helped with flood management. They found considerable improvements in consideration of flood hazards in urban development and comprehensive property-level mitigation and preparedness measures.

Planning for sustainable development requires the collection of relevant information the levels of risk that different areas are exposed to. The study carried out by Oriola and Chibuikwe (2016) attempted to accomplish this in the riverine communities of Edu Local Government Area of Kwara state, Nigeria. This resulted in the identification of three distinct risk zones; High, Moderate and low-risk areas. Three settlements fall into low-risk areas with elevations above 196m, two settlements located at between 110m and 196m are within moderate risk zone and six settlements in High-risk area with elevations below 110m. To limit exposure to flood damage, the study recommended public enlightenment on the implications of interactions between Man and the environment.

Rufat *et al.* (2015) profiled key drivers of social vulnerability to floods, based on a meta-analysis of 67 flood disaster case studies (1997–2013). Demographic characteristics, socioeconomic status, and health were identified as the leading empirical drivers of social vulnerability. Risk perception and coping capacity are poorly reflected in many social vulnerability indicators; yet these factors were prominent in the cases that were studied. Increase in river discharge on a global scale will drive increase in the frequency of floods in many regions of the globe (Parvin *et al.*, 2016). Rise in river volumes will be caused by increased precipitation and reduced evapo-transpiration.

1.2 FLOOD DISASTER COSTS

There has been a lot of interest in research into the costs of floods; however there does not appear to be a standard method of deriving such costs. While many estimates rely on the value of insured property, in many

areas of the world than are prone to flooding, an insurance culture has yet to take root. Thielen *et al.* (2016) found that with reference to floods of the year 2005, the June 2013 flooding in Central European countries caused damage amounting to €11.6 billion in Germany. Flood disaster costs are more difficult to estimate in Nigeria, where a lot of the flood recovery effort is informal and unstructured.

Parvin *et al.* (2016) reported on previous research showing that in Bangladesh, agricultural wages declined by 5% in flood-prone areas and by 14% in severely exposed areas during “extreme” floods. Households also experience up to 65% reduction in incomes during flood disasters. In Nigeria, Awopetu *et al.* (2013) used a post-2012 flood survey to show that 48% of respondents’ houses were swept away and about 12,000 people were displaced. Flood disaster costs in the 2010-2012 period in Pakistan included \$16 billion of physical capital losses and an estimated total flood recovery cost of US\$ 439.7 million for 2014 alone (Mujahid *et al.*, 2016).

Losses arising from flood disasters in the UK will likely be compounded by an absence of formal incentive mechanisms for risk reduction in the existing and proposed flood management schemes (Surminski and Eldridge, 2015). Although the mortality rate of natural disasters in Pakistan has declined the number of people affected by such disasters had risen almost three-fold. Population growth plays a large role in the increase in vulnerability to flood disaster risks.

In Nigeria, Shabu and Musa (2015) concluded that the absence of buffer Dams contributed to the increased socio-economic impact of the 2012 flood disaster. In addition, large segments of the population still live in highly unstable and vulnerable conditions; poverty is one reason why floodplain encroachment is increasing. In some cases where dams have been built, inflow of water beyond the retention capacity of the dam may result in unplanned releases of water which causes flooding of downstream low-lying areas (Ramirez and Rajasekar, 2015).

1.3 FLOOD DISASTER PREVENTION

Governments the world over have attended to the prevention of flood disasters with varying levels of commitment. Thielen *et al.* (2016) reviewed the considerable improvements in flood management in Germany from 2002 onwards. The research found that efforts targeted at prevention of floods included an increased consideration of flood hazards in spatial planning and urban development, more comprehensive property-level mitigation and preparedness measures, and a more targeted maintenance of flood defense systems. These efforts had the salutary effect of a reduction of damage during the 2013 floods.

Preemptive mapping of land in terms of flood risk susceptibility has been proposed by Oriola and Chibuike

(2016). This approach was applied by the researchers in Edu Local Government Area of Kwara State. The results revealed three distinct risk zones - High, Moderate and Low. Settlements at average elevations of more than 196m above sea level were classified as low-risk areas; elevations of 110m - 196m are prone to moderate risk zone while high-risk areas are at elevations lower than 110m. Such flood risk mapping can assist in guiding the types of activities and constructions that will be allowed in different areas of the study area. The study by Ramirez and Rajasekar (2015) described a similar mapping and modeling activity in the Surat area of India. The construction of the flood model of Surat utilized topography produced using elevation data collected from an extensive differential global positioning system survey and measurements of river cross-sections. The research modeled arrival of dam release discharge from the Ukai dam at Surat, flooding within Surat caused by dam release, and identified Surat infrastructure and population exposed to flooding.

Rufat *et al.* (2015) identified risk perception and coping capacity as serving as drivers of social vulnerability to damaging flood events. These drivers can be leveraged to improve flood prevention efforts. When populations at risk are aware of the risk facing them and the ways in which they can better cope with floods, the impact of flood disasters can be reduced considerably.

1.4 RELATED WORKS

A total of 15 papers dealing with different aspects of floods and the impact of flooding that spanned the six years from 2013 to 2018 were reviewed in this section and are presented in Table 1. Three of the studies were carried out in Nigeria; three in the UK; there was one paper each from Thailand, Vietnam, Malaysia, India, the European Union, Pakistan, Bangladesh, Germany and Sri Lanka. Only seven of the papers dealt specifically with the costs associated with flooding.

TABLE 1: SUMMARY OF FINDINGS OF RELATED WORKS

Author	Year	Place	Summary of findings
Awopetu <i>et al.</i>	2013	Nigeria	Flood victims expressed willingness to relocate from the flood prone area.
Surminski and Eldridge	2015	UK	Absence of formal incentive mechanisms for risk reduction in the existing and proposed flood insurance schemes.
Kantamani <i>et al.</i>	2015	UK	New estimates of England’s flooding costs for commercial and residential properties were found to be £1.6 Billion per year.

Author	Year	Place	Summary of findings
Nabangchang <i>et al.</i>	2015	Thailand	Median household economic costs were US\$3089, similar for poor and non-poor households as a percentage of annual household expenditures (53% and 48% respectively).
Chau <i>et al.</i>	2015	Vietnam	The estimated value of direct losses to the four main crops for a 1:10-, 1:20- and 1:100-year flood represent a percentage loss in value of 12, 56 and 62 %, respectively.
Shabu and Musa	2015	Nigeria	438,536 business outfits were affected and aggregate working days lost in trade and commerce was 881,400 days.
Ramirez and Rajasekar	2015	India	Modeled dam release discharge from the Ukai dam arrival, flooding within Surat and infrastructure and population exposed to flooding.
Rufat <i>et al.</i>	2015	EU	Demography, socioeconomic status, and health are leading empirical drivers of social vulnerability to damaging flood events.
Arnell and Gosling	2016	UK	Climate change has the potential to substantially change human exposure to the flood hazard, but that there is considerable uncertainty in the magnitude of this impact
Mujahid <i>et al.</i>	2016	Pakistan	Confirmed a suitable long run relationship among GDP growth and its determinants: agriculture growth, non-agriculture growth, investment and affected areas by flood.
Parvin <i>et al.</i>	2016	Bangladesh	Floods disrupt the agriculture, infrastructure, employment, and food distribution systems, but majority of the people are willing to live in this place despite floods.
Thieken <i>et al.</i>	2016	Germany	Considerable improvement in increased consideration of flood hazards in spatial planning and urban development,.

Author	Year	Place	Summary of findings
Oriola and Chibuike	2016	Nigeria	Classified study area into three risk zones; High (below 110m), Moderate (between 110m and 196m) and Low (above 196m).
Nayan <i>et al.</i>	2017	Malaysia	Goods (Mean = 1.56, SD = 0.894) and premises / stalls / kiosks (mean = 1.56, SD = 0531) suffered highest losses.
De Silva and Kawasak i	2018	Sri Lanka	Low income households that depend fully on natural resources are most vulnerable to financial losses incurred through floods and droughts.

The three papers from Nigeria were focused mainly on socio-economic issues associated with flooding. Two of the papers (Awopetu *et al.*, 2013; Shabu and Musa, 2015) reviewed the 2012 flood in Benue state, while the third (Oriola and Chibuike, 2016) suggested how flood risk mapping could help ameliorate the effects of flood disasters. One of the UK papers recommended how insurance could be employed to mitigate flood impact (Surminski and Eldridge, 2015) while the second paper estimated flood water levels in properties and concluded that current estimates of flood disaster costs were too optimistic (Kantamaneni *et al.*, 2015). The third paper from the UK (Arnell and Gosling, 2016) attempted to develop predictions of flood impact up to the year 2050. It suggested that considerable uncertainty still surrounds such predictions.

The rest nine papers were on a variety of subjects that had floods as the common thread running through them. Nabangchang *et al.* (2015) in Thailand, Chau *et al.* (2015) in Vietnam, Mujahid *et al.*, (2016) and Parvin *et al.* (2016) all dealt with the effects of local floods in their respective study areas. Ramirez and Rajasekar (2015) in India described a methodology for modeling flood disaster risk from dam releases. Rufat *et al.* (2016) worked in the EU and reviewed the indicators for measuring social vulnerability to flood disasters. The research found that risk perception and coping capacities were often ignored in the development of such vulnerability indicators.

2 METHODOLOGY

The paper reviewed seven papers that were of a similar nature to this study because of their focus on the costs associated with flood disasters. The review was done for their methodological orientation and the results are presented in Table 2.

TABLE 2: RESEARCH METHODOLOGIES OF RELATED STUDIES

Author	Aim of study	Research Methodology
Awopetu <i>et al.</i> (2013)	Examined effect of flood on socio-economic status of residents.	Quantitative approach
Kantamaneni <i>et al.</i> (2015)	Evaluated damage costs for properties.	Conceptual framework.
Nabangchang <i>et al.</i> (2015)	Estimated economic costs of households' in the 2011 Greater Bangkok flood.	Primary data collected using in-person interviews.
Chau <i>et al.</i> (2015)	Estimated direct damage to crops.	Used ex-post data.
Shabu and Musa (2015)	Evaluated short and long term impacts of the 2012 flood disaster.	ECLAC methodology adopted.
Parvin <i>et al.</i> (2016)	Drew a "flood impact tree" to explore coping strategies.	Field investigation; questionnaire survey, focus group discussions.
De Silva and Kawasaki (2018)	Investigated relationship between disaster risk, poverty, and vulnerability of households.	Questionnaire survey.
<i>This study (Idachaba et al.)</i>	<i>To undertake a financial assessment of flood risk preparedness.</i>	<i>Archival budget data; structured, close-ended questionnaire survey.</i>

Kothari (2004) defines research design to be the arrangement for the collection and analysis of data in a manner that aims to combine relevance to the research purpose with economy in procedure. Based on a review of research methodologies employed in previous studies of a related nature, this paper will adopt a single method approach of a quantitative nature.

3 CONCLUSION

This paper has reviewed relevant literature on flood disaster costs; based on the findings from the review, a research methodology has been designed for the study. Further development of this study will employ the quantitative research approach proposed to collect data and examine government budgets for disaster management and urban development. This will enable conclusions be drawn as to financial preparedness of governments to tackle flood disasters.

REFERENCE

- Adeoye, N.O., Ayanlade, A. and Babatimehin, O. (2009). Climate Change and Menace of Floods in Nigerian Cities: Socio-economic Implications. *Advances in Natural and Applied Sciences*, 3(3), 369-377.
- Arnell, N. W. and Gosling, S. N., (2016). The impacts of climate change on river flood risk at the global scale. *Climatic Change* 134:387-401
- Awopetu, R. G., Awopetu, S. O. and Awopetu, M. S., (2013). The impact of flood on the socio-economic status of residents of Wadata and Gado-villa communities in the Makurdi metropolitan area of Benue State, Nigeria. *WIT Transactions on The Built Environment*, 133, 1-8.
- Chau, V N, Cassells S. and Holland, J. (2015). Economic impact upon agricultural production from extreme flood events in Quang Nam, central Vietnam. *Nat Hazards* 75:1747-1765
- Ciscar, J. C., Iglesias, A., Feyen, L., Szabó, L., Van Regemorter, D., Amelung, B., ... & Soria, A. (2011). Physical and economic consequences of climate change in Europe. *Proceedings of the National Academy of Sciences*, 108(7), 2678-2683.
- De Silva, M.M.G.T. and Kawasaki, A. (2018). Socioeconomic Vulnerability to Disaster Risk: A Case Study of Flood and Drought Impact in a Rural Sri Lankan Community. *Ecological Economics* 152, 131-140
- Duru, P. N. and Chibo, C. N. (2014). Flooding in Imo State Nigeria: The Socio-Economic Implication for Sustainable Development. *Humanities and Social Sciences Letters*, 2(3), 129-140.
- Kantamaneni, K., Alrashed, I., Phillips, M., and Jenkins, R., (2015). Flood Crunch: A Fiscal Appraisal For Commercial And Residential Properties In England. *Regional and Sectoral Economic Studies* 15(1) 17-24.
- Kothari, C. R. (2004). *Research methodology: Methods and techniques*. New Delhi: New Age International.
- Mngutyo I. D. and Ogwuche, J. (2013). Comparative analysis of the effects of annual flooding on the maternal health of women floodplain and non floodplain dwellers in Makurdi urban area, Benue State, Nigeria. *Wudpecker Journal of Geography and Regional Planning*, 007 - 013.
- Mujahid, N., Malik, N. and Tahir, S. (2016). The Macroeconomics of Flood: A Case Study of Pakistan. *Journal of Environment and Earth Science* 6(5) 67-80.
- Nabangchang, O., Allaire, M., Leangcharoen, P., Jarungrattanapong, R. and Whittington, D. (2015). Economic costs incurred by households in the 2011 Greater Bangkok flood, *Water Resour. Res.*, 51, 58-77, doi:10.1002/2014WR015982.
- Nayan, N., Mahat, H., Hashim, M., Saleh, Y., Rahaman, Z. A. and See, K. L. (2017). Flood Aftermath Impact on Business: A Case Study of Kuala Krai, Kelantan,



- Malaysia. *International Journal of Academic Research in Business and Social Sciences* 2017, 7(6) 836-845.
- Nigeria Hydrological Services Agency (2013). 2013 Flood Outlook. Nigeria Hydrological Services Agency.
- Ocheri, M. I. and Okele, E. (2012). Social Impact and People's Perception of Flooding in Makurdi Town, Nigeria. *Special Publication of the Nigerian Association of Hydrological Sciences*, 97-105.
- Ogunorisa, E. T. and Tersoo, T. (2006). The Changing Rainfall Pattern and its Implication for flood Frequency in Makurdi, Northern Nigeria. *Journal of Applied Science and Environmental Management*, 10(3) 1-3.
- Oriola, E. O. and Chibuike, C. C. (2016). GIS for sustainable living in the riverine communities in edu local government area of Kwara State, Nigeria. *GEOGRAFIA Online Malaysian Journal of Society and Space* 12(1) 1–7.
- Oruonye, E. D. (2012). Socio-Economic Impact Assessment of Flash Flood in Jalingo Metropolis, Taraba. *International Journal of Environmental Sciences*, 1(3), 135-140.
- Parvin, G. A., Shimi, A. C., Shaw, R. and Biswas, C., (2016). Flood in a Changing Climate: The Impact on Livelihood and How the Rural Poor Cope in Bangladesh. *Climate* 4(60); 1-15; doi:10.3390/cli4040060.
- Pielke Jr, R. A., & Downton, M. W. (2000). Precipitation and damaging floods: Trends in the United States, 1932-97. *Journal of Climate*, 13(20), 3625-3637.
- Ramirez, J. and Rajasekar, U. (2015). Modelling Flood Impact In Surat, India. *Proceedings of TIFAC-IDRiM Conference 28th –30th October 2015 New Delhi, India*.
- Rufat, S., Tate, E., Burton, C. G. and Maroof, A. S. (2015). Social vulnerability to floods: review of case studies and implications for measurement. *International Journal of Disaster Risk Reduction* 14, 470–486.
- Shabu, T. and Musa, S. D. (2015). Downstream Socio-Economic Impact of Dam Failure: A Case Study of 2012 River Flooding in Benue State, Nigeria. *Journal of Environmental Issues and Agriculture in Developing Countries*, Volume 7, Number 3, 19-28.
- Shabu, T. and Tyonum, E. T. (2013). Residents Coping Measures in Flood Prone Areas of Makurdi Town, Benue State. *Applied Ecology and Environmental Sciences*, 1 (6), 120-125.
- Simonovic, S. P., & Carson, R. W. (2003). Flooding in the Red River Basin—Lessons from post flood activities. *Natural Hazards*, 28(2-3), 345-365.
- Surminski, S. and Eldridge, J. (2015). Flood insurance in England: an assessment of the current and newly proposed insurance scheme in the context of rising flood risk. *Journal of Flood Risk Management*; Accepted version. doi: 10.1111/jfr3.12127.
- Thieken, A. H., S. Kienzler, H. Kreibich, C. Kuhlicke, M. Kunz, B. Mühr, M. Müller, A. Otto, T. Petrow, S. Pisi, and K. Schröter. (2016). Review of the flood risk management system in Germany after the major flood in 2013. *Ecology and Society* 21(2):51. <http://dx.doi.org/10.5751/ES-08547-210251>.
- UNISDR (2011) Global Assessment Report on Disaster Risk Reduction: Revealing Risk, Redefining Development. Information Press, Oxford.
- Ward, P. J., Jongman, B., Weiland, F. S., Bouwman, A., van Beek, R., Bierkens, M. F., ... & Winsemius, H. C. (2013). Assessing flood risk at the global scale: model setup, results, and sensitivity. *Environmental research letters*, 8(4), 044019.



DEVELOPMENT OF SPIN DRYER MACHINE

¹Alhassan T. Yahaya, ²Muhammadu M. M.

^{1,2}Department of Mechanical Engineering, Federal University of Technology P.M.B 65, Gidan Kwanu Minna, Niger State, Nigeria.

Corresponding Author: yahayat73@gmail.com

ABSTRACT

A spin dryer is a dryer that uses centrifugal force and air interaction to dry BSG at ambient temperature, it is independent of sunshine. The major problem facing breweries in the country is how to utilize the spent grains after brewing due to its high moisture content. A spin spent grain dryer machine capable of drying 3kg of spent grain in 30min was designed, fabricated and evaluated. Fundamental design analysis and calculations were carried out to determine the selected materials for appropriate strength and sizes of the machine elements. The major parts of the machine include; internal basket with mesh diameter of 0.5mm, 2hp electric motor, the outer drum and the frame assembly. The results obtained after testing the machine shows the drying rate of the machine was 27.7g/min at a speed of 2840rpm and moisture content of 27.7% on weight basis. The efficiency of the machine was evaluated to be 72.3%. The operation of the machine is simple and its maintenance is also easy. It is thus found useful in the small scale spent grain processing industry.

Keywords: *Spin, Spent grain, Basket, Centrifugal force, Development.*

1.0 INTRODUCTION

Dehydration is one of the most important process of preventing post-harvested agricultural foods and seafood products from deterioration and wastage. In Nigeria, the problem of postharvest processing of raw food and food storage have prevented the micro and small scale farmers, food producers, and produce merchants from thriving well in their business. A large amount of agro-industrial waste is produced annually around the world from the benefited agricultural products or in food industrialization. The disposal of these residues in the environment results in a lot of inconvenience to the ecosystem, due to its significant nutritional value and high concentration of organic compounds that confers a high biochemical oxygen demand to the waste's degradation. In this context, brewing industry is among these activities, which includes in its production stages, the

processing and fermentation of vegetable feedstock, such as barley malt and other grains, and hops, generating several by-products. Many factors, such as environmental policies, possible scarcity of non-renewable sources, and problems related to the improper use of renewable raw materials, leads to the development of new processes that could generate less waste or reused. Beer is the fifth most consumed beverage in the world apart from tea, carbonates, milk and coffee with an estimated annual world production exceeding 1.34 billion hectolitres in 2002 (Fillaudeau et al., 2006). In recent years, the use of solar energy has become other of the day. Solar radiation is the main source of energy for drying. The use of solar energy in the agricultural sector to dry grains, fruits, and vegetables is viable, economical and ideal for farmers in many developing countries. However, this pose problem for most products during rainy season, preservation by using

only solar energy proves difficult (Barki et al., 2012). Hence, there is need for alternative means of drying. Spin dryer operate continuously at night and in cloudy days or when raining. It is very fast, it has been used for laundry purposes, this study modified the technology into spin grain dryer to solve problems which other dryers had in drying products; such as longer drying time, high cost of maintenance, complexity of operation and environmental factors and preservation of nutritive values.

2.0 METHODOLOGY

Stainless steel material was used for construction of parts of the machine that have direct contact with the brewer spent grain (BSG) because of its high resistance to corrosion. A 50 x 50 mm angle iron was used for the construction of the machine frame in order to give a rigid support and ensure stability of the machine when in operation (Gbabo et al., 2012). It is driven by a 1.5kw (2hp) motor, as the motor spins the basket, the moisture content is drain through mesh to the drum. The drum encloses the basket of mesh diameter 0.5mm, this outer casing collect water from the basket to prevent the splashing of the water and drain it through a spout. Stainless steel material is used to construct the basket in order to prevent corrosion of the material since it is in contact with water.

2.1 Description of Machine Parts

The Machine consist of the outer casing: This is made up of mild sheet of metal with diameter of 0.302m and 0.204m height. It is being mounted on the machine frame made up of angle iron assembly. A liquid outlet valve was fitted to the bottom side of the drum in order to allow out flow of extracted liquid

from the grain and discharging it as shown in **Figure 2**. The basket is made of height 0.166m and diameter 0.194m. Its wall is smooth with perforated openings of diameter 0.5mm, in order to allow fluid drainage and prevent spent grain losses. This is a flat bar with ball bearing at its mid-point. This is to prevent the basket from wobbling while spinning.



Figure. 1.0: Vertical Section of Spin dryer Machine

2.1 Materials Selection

The properties considered in selecting the materials needed for the development of spin dryer according to (Gana et al 2013), are:

- Physical properties such as size and shape.
- Mechanical properties which include; strength, toughness, wear resistance etc.
- Chemical properties: this includes resistance to oxidation and all forms of corrosion since the machine is to be used in processing wet substance.

- Material availability: the materials used were selected based on their availability such that they can be obtained from the market with ease.
- Cost of materials: materials used can be made available at a cheaper price.
- Strength of material: to avoid operational failure, the strength of the materials used was ascertained.
- For construction of the proto-type, ordinary mild steel was used but painted to reduce corrosion.

2.2 Design Considerations and Specifications

The following parameters were used during the development of the machine:

- Density of mild steel = 7840 kg/m^3
- Power of electric motor = $2\text{hp} = 1.5\text{KW}$
- Selected length of shaft = 0.339m
- Acceleration due to gravity, $g = 9.81\text{g/m}^2$
- Motor speed (N) = 2840rpm
- Allowable shear stress of mild steel is 56MPa for shaft without keyway (Khurmi and Gupta, 2005).
- Combined shock and fatigue factor applied to bending and torsional moment, k_b and k_t are 1.5 and 0.3 respectively (Khurmi and Gupta, 2005).
- Coefficient of friction between belt and pulley = 0.3

2.3 Theory of the design

The theory of design of spin dryer is based on the effect of a centrifugal force on the spent grains inside the basket. The spent grains were pushed towards the wall of the basket by centrifugal forces, which were compressed to the wall of the basket and the moisture content was removed as the basket was spinning (Gbabo 2005). A centrifugal force is a force

which acts away from the centre of rotation. Centrifugal forces are commonly identified with the following effects such as when a passenger in a car is “thrown” to one side when a sharp turn is made, the passenger is in a rotating frame and thinks centrifugal force pushes him outward. Centrifugal force arises due to Newton’s first law of motion known as law of inertia. (the tendency of a body to be in a state of uniform motion or in a state of rest)

2.4 Design analysis of components

The analysis of the design is aimed at determining the necessary parameters for selection of the various machine elements. The machine is designed to carry a maximum load of 3kg . This was done in order to avoid failures of machine parts during operation of the machine.

2.4.1 Determination of Power Required

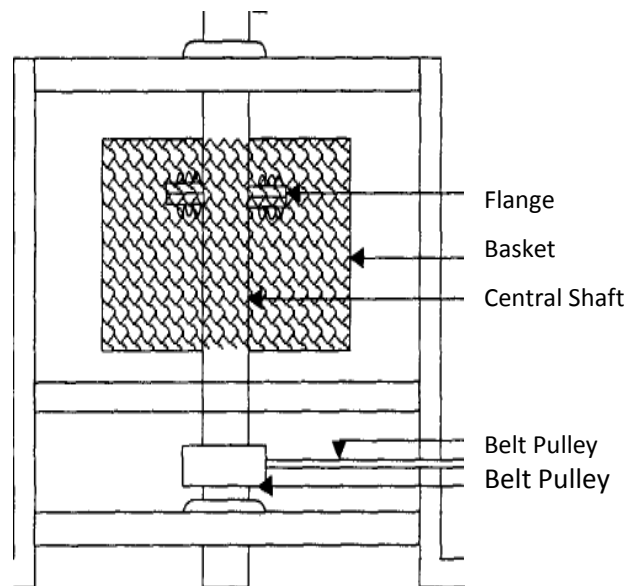


Figure 2: Vertical section of spin dryer



$$P = F_T V$$

1

Where

P = the power required rotate the basket and its content (W)

F_T = the total weight of the basket, its content and central shaft (N)

Velocity of the basket at full speed (m/s) is given by equation 2 below:

$$V = \frac{2\pi N}{60} = \frac{2 * \pi * 2840}{60} = 297.4 \text{ m/s} \quad 2$$

The required torque is given by equation 3 below:

$$T = F r_b = 4.8 * 9.81 * 0.097 = 4.57 \text{ Nm} \quad 3$$

The power required to spin the basket is a function of weight of the basket, its content and that of the shaft. It is given by equations 1 to 6 according to (Khurmi and Gupta 2005).

$$P = \frac{2\pi NT}{60} = \frac{2 * \pi * 2840 * 4.57}{60} = 1359.14 \text{ W} \quad 4$$

$$\omega = \frac{2\pi N}{60} = \frac{2 * \pi * 2840}{60} = 87.96 \text{ rad/sec} \quad 5$$

Where; P= power required by the machine (W)

F = the total force required (N)

T = the torque (Nm)

M = total mass (4.8kg)

ω = angular velocity of the basket (rpm)

M_1 = mass of material to be dried (3kg)

M_2 = mass of basket (0.3kg)

M_3 = mass of shaft and pulley (1.5kg)

π = constant

g= acceleration due to gravity =9.81m/s²

d_b = Diameter of the basket (m)

r_b = radius of the basket (m)

N = number of revolution per minute of the basket (rpm)

2.5 Centrifugal force generated in the spinning basket

Centrifugal force is the force which acts radially away from the centre of rotation. It is set up in the basket due to rotation of the basket while in operation. In line with the principle of centrifugal force, the direction of the force is from the centre of the basket towards the circumference of the basket as shown in **Figure 1**. This is given by equation 6 as:

$$F_c = M r_b \omega^2 = 4.8 * 0.097 * 87.96^2 = 3.602 \text{ KN} \quad 6$$

2.6 Stress in the spinning basket

The stress in the basket is due to the action of the centrifugal force on the wall of the basket which is computed in order to assist in the determination of the thickness of the basket. It was determined using the equations reported by (Gbabo et al, 2003)

$$\sigma_b = \frac{M \omega^2 r_b}{\pi D_b H_b} = \frac{M \omega^2}{2\pi H_b} = \frac{4.8 * 87.96^2}{2 * \pi * 0.166} = 35.6 \text{ KN} \quad 7$$

σ_b = stress on the wall of basket (N/m²)

H_b = height of the basket (m)

2.7 Design of basket thickness

The thickness of the basket to withstand the centrifugal force generated is given by the equation reported by (Gbabo and Igbeka 2003)

$$t_b = \frac{\sigma_b d_b}{2 \tau_b} = \frac{35600 * 0.194}{2 * 56000000} = 0.063 \text{ mm} \quad 8$$

t_b = thickness of the basket (mm)

σ_b = stress on the wall of the basket (Pa)

d_b = diameter of the basket (m)



τ_b = shear stress of stainless steel used for the basket (Pa)

2.8 Design of Shaft

Shaft is a rotating member of circular cross-section solid or hollow in nature, which transmits power and rotational motion. Elements such as gears, pulleys (sheaves), flywheels, clutches, and sprockets are mounted on the shaft to transmit power from the driving device (motor or engine) through a machine. It is the member on which press fit, keys, dowel, pins and splines are usually attached to. Shaft rotates on rolling contact bearings or bush bearings. Various types of retaining rings, thrust bearings, grooves and steps in the shaft are used to take up axial loads and locate the rotating elements. Couplings are used to transmit power from drive shaft (e.g., motor) to the driven shaft (gearbox and wheels).

2.8.1 Torque on the shaft (twisting moment)

The high speed rotating shaft is attached to the basket is subjected to a twisting

moment. In order for the shaft not to fail, the value of the torque generated must be within the permissible limit. This was determined as expressed by (Gbabo et al 2003).

$$T_s = \frac{60P}{2\pi N} = \frac{60 \times 1500}{2 \times 3.142 \times 2840} = 5.04 Nm \quad 9$$

T_s = Torque on the shaft (Nm)

N = speed of the shaft (rpm)

P = power transmitted (Watt)

π = constant (3.14)

2.8.2 Torsional shear stress

The torsional shear stress of the shaft was computed as a function of the twisting moment, diameter and second moment of area as expressed by (Webb 1982):

$$\tau_t = \frac{T_s d_s}{2J}$$

τ_t = the torsional shear stress (N/m²)

d_s = diameter of shaft (m)

$J = \frac{\pi d_s^4}{32}$ where J is the polar moment of area (m⁴)

By substituting J into equation above we have

$$\tau_t = \frac{16T_s}{\pi d_s^3} \quad 10$$

2.8.3 Diameter of Shaft

The diameter of the shaft to transmit power to the internal basket is dependent on the

torque (T_s) on the shaft and the permissible shear stress of the material of make. According to American Society of Mechanical Engineers (ASME) code for the design of

transmission shafts, the maximum permissible working stresses in tension or compression may be taken as 112 MPa for shafts without allowance for keyways and that of maximum permissible shear stress may be taken as 56 MPa for shafts with allowance for key ways. From equation 10, diameter of the shaft can be calculated as:

$$d^3 = \frac{16T_s}{\pi \tau_t} = \frac{16 \times 5.04}{\pi \times 56000000} \rightarrow d = 0.018m \quad 11$$

2.8.4 Length of the Belt

Belts are used to transmit power from one shaft to another by means of pulleys which rotate at the same speed or at different speeds.



In an open belt drive, both the pulleys rotate in the same direction.

$$L = \frac{\pi}{2}(d_1 + d_2) + 2X + \frac{(d_1 - d_2)^2}{4X} \quad 12$$

$$L = \frac{\pi}{2}(9.9 + 5.5) + 2 \times 27.2 + \frac{(9.9 - 5.5)^2}{4 \times 27.2} = 78.8 \text{ cm}$$

d_1 and d_2 = diameter of the driver and driven pulleys (9.9 and 5.5cm)

x = Distance between the centres of two pulleys (27.2)

L = Total length of the belt.

2.9 Belt Velocity Ratio

Velocity ratio of belt is the ratio between the velocities of the driver and the driven pulley.

$$\frac{N_2}{N_1} = \frac{d_1}{d_2} \quad 13$$

N_2 = Speed of the driver pulley

N_1 = Speed of the driven pulley

2.9.1 Power Transmitted by the Belt

Power transmitted by belt is the product of effective driving force at the circumference of the driven or driven pulley ($T_1 - T_2$) and the velocity of belt (v).

$$P = (T_1 - T_2) v \quad 14$$

$$2.3 \log_{10} \left[\frac{T_1}{T_2} \right] = \mu \theta \quad 15$$

T_1 and T_2 = tensions in the tight and slack side of the belt respectively.

θ = angle of lap of the belt with pulley in radian, where

$$\theta = \frac{L_1}{r_1} \quad 16$$

r_1 and r_2 = radii of the driving and driven pulley

L_1 = length of belt lapping the pulley (18.8cm)

3.0 Results and Discussion

The BSG were obtained from Nigerian Breweries Ibadan. Brewery BSG were collected from the spent grain silo shortly after being removed from the mashing process. The performance of BSG spin dryer was evaluated in accordance with procedures reported by (Gbabo et al. 2012). Four groups of experiments were carried out to investigate the performance of the machine. The experiments were carried out at Etsu Yahaya Abubakar Farm centre Bida, Niger State Nigerian on 8th July, 2019.

3.1 Design of the experiments

In the first set of experiments, the speed level of 2840rpm was taking and various masses of 0.5, 1, 2 and 3kg of BSG was introduced into the basket for a period of 30seconds respectively. Mass of BSG after spinning were in each case read and rate of dehydration was evaluated and recorded in table 2 bellow.

Table 2: Mass of water removed and rate of dehydration at 2840rpm for 30min

Mass of moist BSG Before spinning (kg)	Mass of BSG after spinning (kg)	Mass of water removed (kg)	Rate of dehydration (g/min)
0.5	0.292	0.208	6.93
1.0	0.585	0.415	13.8
2.0	1.376	0.624	20.8
3.0	2.169	0.831	27.7



The equation for determining drying rate was given by (Adamade et al., 2014).

$$R_t = \frac{M_m - M_d}{t} = \frac{3 - 0.831}{30} = 27.7 \text{g/min} \quad 17$$

R_t = rate of dehydration of water (Kg/s)

M_m = Mass of BSG before spinning (kg)

M_d = Mass of BSG after spinning (kg)

t = time taken for dehydration (min)

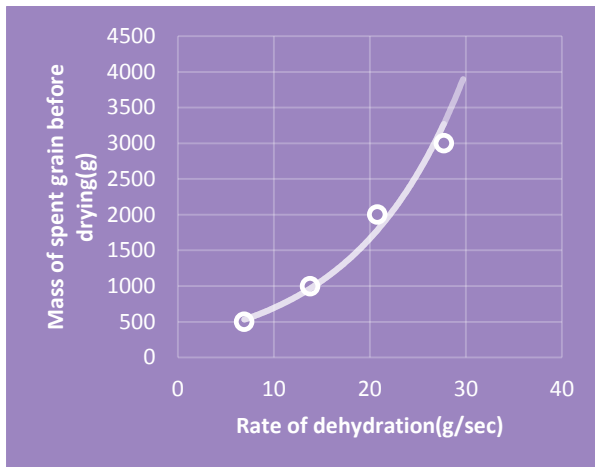


Figure 3: Graph of mass of spent grain against rate of dehydration at speed of 2840rpm for 30sec.

From the graph of mass of wet spent grain against rate of dehydration of spent grain at constant speed of 2840rpm and 30sec, it is observed that the out flow rate of moisture content of the spent grain increases with increase in mass of the moist spent grain up to the maximum loading capacity of the dryer. This is indicated by upward sloping of the graph from left to right.

In the second experiment, the dehydration time for a mass of 3kg of BSG at four speed levels were determined and recorded in table 3 below

Table 3: Time taken to dehydrate 3kg of BSG & water removed at four speed levels

Speed (rpm)	Time (min)
2840	93.80
1420	130.70
710	201.10
355	306.60

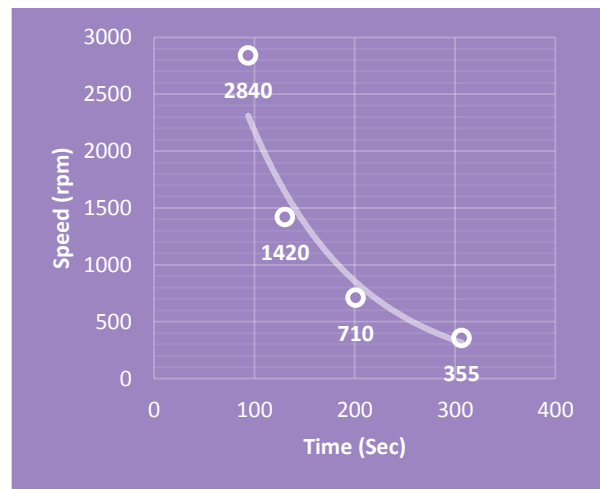


Figure 4: Graph of dehydration time of 3kg of spent grain against speed

From graph of speed against time taken to dry spent grain, we observed that the higher the speed, the lower the time take to dry spent grain and the lower the speed, the longer the period of dehydration of spent grain. This is indicated by the downward sloping of the graph from top left hand corner to the right.

3.2 Efficiency of the Dryer

Efficiency point out the how best the machine can carry out the drying of the sample. It is expressed as the ratio of output to the input.



There are some factors that affect drying efficiency some of which are ambient air condition, type of material to dry and design and operation of the dryer. The equation for computing the efficiency was given by (Adamade et al., 2014).

$$\eta = \frac{M_d}{M_m} \times 100\% = \frac{2.169}{3} \times 100\% = 72.3\%$$

η = Efficiency of the spin dryer

3.3 Moisture Content (M_c)

Water is found in all food products. Too little or too much can alter food properties. Moisture content can affect the physical and chemical properties of food, which directly correlate to the freshness and stability of food products for consumers. It determines the food quality, shelf life and legal labelling requirements. The moisture content on wet basis is given by the equation 19 below according to (Odujukan, R. O. et al 2013).

$$M_c = \frac{M_m - M_d}{M_m} \times 100\% = \frac{3 - 2.169}{3} \times 100\% = 27.7\%$$

4.0 Conclusion

The objective of this project was well achieved as the spin dryer was able to dry moisture content in the spent grains within a possible time-frame. The dryer was found to be effective, easy to operate and affordable. The dryer has loading capacity of 3kg and can dry 3kg of spent grain in 30min, it has no heat source.

The dryer was able to keep consistent drying time considerably. The moisture content of the spent grain was found to 27.7% on weight basis; this is in agreement with (Elshatey et al 2004) whose equilibrium moisture content is

within the range of 20 – 30%. This was achieved by spin dryer in approximately 5 – 8min, this is significant when compared with that reported by (K.S. Tonui et al., 2014) which took 4h drying daily in 3days to achieve the same purpose using solar dryer. The developed dryer is compact easy to maintain and be move from one place to another easily. Efficiency of the dryer was found to be 72.3% and drying rate of 6.93g/min which is in agreement with many other modern drying technologies. It is faster than the open sun drying method and solar dryer which has thermal efficiency estimated to be about 57.7% with average drying rate of 0.0077 kg/h, according to (K.S. Tonui et al., 2014).

REFERENCES

- Alexander, T. Shinbrot, and F. J. Muzzio. (2002). Scaling surface velocities in rotating cylinders as a function of vessel radius, rotation rate, and particle size," *Powder Technology*, vol. 126, pp. 174-190.
- Al-Hadithi, A.N., Muhsen, A.A., Yaser, A.A. (1985). Study of the possibility of using some organic acids as preservatives for brewery by-products. *Journal of Agriculture and Water Resources Research* 4, 229–242.
- Bartolomé B, Gómez-Córdovés C, Sancho AI et al. (2003). Growth and release of hydroxycinnamic acids from brewer's spent grain by *Streptomyces avermitilis* CECT 3339. *Enzyme Microb Technol* 32:140–144.
- Bena, B. and R.J. Fuller, (2002). Natural convection solar dryer with biomass back-up heater. *Sol. Energy*, 72:75-83.
- Blending Efficiency and Milk



- Consistency of a Grain Drinks *Academic Research*
- El-Shafey, E.I., Gameiro, M., Correia, P., de Carvalho, J. (2004). Dewatering of brewers' spent grain using a membrane filter press: a pilot plant study. *Separation Science and Technology* 39, 3237–3261.
- Emagbetere E., Adeyemi I., Olabisi A., Oghenekowho P. (2017). Design and Development of a Low-Cost Washing Machine Suitable for Polythene Materials. *Asian Journal of current research* 2(1): 22-32.
- FAO (2011). Successes and failures with animal nutrition practices and technologies in developing countries. Proceedings of the FAO Electronic Conference, 1-30 September 2010, Rome, Italy.
- Fillaudeau, L., Blanpain-Avet, P. and Daufin, G. (2006) Water, Wastewater and Waste Management in Brewing Industries. *Journal of Cleaner Production*, 14, 463-471.
- Forson, F.K., M.A.A. Nazha, F.O. Akuffo and H. Rajakaruna, (2007). Design of mixed-mode natural convection solar crop dryers: *Application of principles and rules of thumb. Renew. Energ.J.*, 32: 1-14.
- Gana, I. M., Gbabo, A., and Osunde, Z. (2013). Development of Grain Drinks Processing Machine Using Stainless Steel Materials. *Journal of Engineering and Applied Science*, 2 (1), 1 – 9.
- Gbabo A., J.C. Igbeka. (2003). Development and Performance of a Sugar Centrifuge, *Journal of Sugar Technology* Vol. 5 (3), 131 – 136.
- Gbabo, A. (2005). Development and Testing of Rotary Dryer for the Indigenous Cottage Sugar Industry in Nigeria *Journal of Sugar Tech.*, 7(2&3), 57-66.
- Gbabo, A., Gana, I. M., and Solomon, M. D. (2012). Effect of Blade Types On The grains in superheated steam. *Journal of Food Engineering*. (67) 457-465. *Internationa.l*2(3), 2223-9944.
- Khurmi, R. S. J.K. Gupta, J. K. (2005). *A Textbook of Machine Design (ed)*. Eurasia Publishing House, New Delhi. pp 5098-5101.
- Mujumdar, A. S., & Devahastin, S. (2000). Fluidized bed drying. Developments in drying vol. food dehydration (pp. 59–111). Bangkok: Kasetsart University Press.
- Mussatto S.I., Dragone, G., Roberto I.C, (2006). Brewer spent grain: Generation, characteristics and potential applications. *Journal of Cereal Science*, 43(1), pp1-14.
- Mussatto SI, Aguilar CN, Rodrigues LR and Teixeira JA, (2009). Fructooligosaccharides and β -fructofuranosidase production by *Aspergillus japonicas* immobilized on lignocellulosic materials. *JMol Catal B* 59:76–81.
- Mussatto SI, Roberto IC (2006). Chemical characterization and liberation of pentose sugars from brewer's spent grain. *J. Chem. Technol. Biotechnol.* 81: 268-274.



- Odunukan, R. O., Akinyemi, D. O., Tanimola, O. A. & Bankole, Y. O., (2013). Design, construction and performance analysis of brewery waste dryer, *Asian Journal of Basic and Applied Sciences* Vol. 3, No. 2.
- Robertson, G. L. and Lupien, J. R. (2008). Using Food Science and Technology to Improve Nutrition and Promote National Development, *International Union of Food Science and Technology*.
- Salihu A., & Muntari, B. (2011). Brewer spent grain: A review of its potentials and Applications, *Journal of Biotechnology* Vol. 10(3), pp. 324-331.
- Santos M., Jimé'nez J.J., Bartolome' B., Go'mez-Cordove's C, del Nozal, M.J., (2006). Variability of brewers' spent grain within a brewery. *Food Chemistry* 80, 2003, p17-21.
- Tang Z, Cenkowski S, Izydorczyk M., (2005). Thin-layer drying of spent grains in superheated steam. *Journal of Food Engineering*. (67) 457-465.
- Tang, Z., & Cenkowski, S. (2001). Equilibrium moisture content of spent grains in superheated steam under atmospheric pressure. *Transactions of the ASAE*,44(5),1261–1264.
- Tonui, K.S., Mutai, E.B.K., Mutuli, D.A., Mbugu, D.O. (2013). Design and Evaluation of Solar Grain Dryer with a Back-up Heater. *Journal of Applied Sciences, Engineering and Technology* 7(15): 3036-3043.
- Varun, Sunil, Avdhesh S., Naveen S., (2012). Construction and Performance Analysis of an Indirect Solar Dryer Integrated with Solar Air Heater. *Journal of Modeling Optimisation and Computing*. (38) pp3260-3269.



ASSESSMENT OF QUALITY CONTROL MANAGEMENT IN SACHET WATER PACKAGING

T.J Bolaji and A.A. Abdullahi

*Department of Mechanical Engineering, Federal University of Technology, Minna,
P.M.B. 65, Minna, Niger State, Nigeria.*

ABSTRACT

Too many Small and Medium Enterprises (SMEs), the applicability and utility of Quality Control Management (QCM) remains a challenge. It is generally recognized that (SMEs) face unique challenges, which affect their growth and profitability and hence, diminish their ability to contribute effectively to sustainable development. This paper is focused on assessing quality control management of sachet water packaging company. Four (4) different sets of questionnaires as well as structured open-ended interviews were employed as the data collection tools. In all two hundred and eighty (280) respondents were sampled in the study. SPSS, Excel, tables and graphs were utilized in the data analysis. For the period investigated, the non-defective products is 99.55% of the total water production output with a percentage defectives of 0.45% made of production. From the operating characteristic curves (OC) and average outgoing quality (AOQ) curves, for varying acceptable percentage defectives for a given constant sample size, important sampling plan parameters such as producer's risk, consumer's risk and average outgoing quality level (AOQL) are also presented. The findings of the study established that, there is a positive relationship between quality management and company performance. The study concluded that QCM strategy was the most appropriate quality management strategy to be adopted to turn around the quality fortunes of sachet water company.

Keywords: *Acceptable defectives, defective, control chart, non-defective, sachet water, sample size.*

1 INTRODUCTION

Small and Medium Industries (SMIs) have been widely acknowledged as the springboard for sustainable economic development. According to Deming (1986) developing countries including Nigeria, have since the 1970s shown increased interest in the promotion of small and medium scale enterprises for three main reasons: the failure of past industrial policies to generate efficient self-sustaining growth; increased emphasis on self-reliant approach to development and the recognition that dynamic and growing SMIs can contribute substantially to a wide range of developmental objectives. These objectives include efficient use of resources, employment creation, mobilization of domestic savings for investments, encouragement, expansion and development of indigenous entrepreneurship and technology as well as income distribution, among others.

In today's world, organizations are facing the growing challenges from global competition and more sophisticated customers in terms of what they want and their changing needs. Competition has become a major challenge which chief executives must meet effectively to

remain in business. Organizations have started adopting appropriate management strategies in the field of quality, to succeed in the market place and small scale enterprises are of no exception. Most managers agree that for an organization to be successful it must change continually in response to significant development, such as customer needs, technological breakthroughs and government regulations (Eke, 2001). Globalization of market and operations forces organizations to rethink their quality problems and in turn their overall organization competitiveness. In order to be successful in this global market, organizations should dedicate themselves to improving productivity and quality in a timely and collaborative manner (Dobyns and Crawford, 1994). Quality Control Management (QCM) techniques, supported by management commitment and good organization will provide objective means of improving quality and hence the overall organization competitiveness. QCM is an integrated approach to satisfy internal and external customers, planning and managing processes. It involves quality planning, quality control, quality assurance and quality improvement. It is among the new techniques that modern organizations now

employ with very good effect to secure and keep their customers permanently satisfied (Dodoo, 2006).

The only major sachet water production defect is water leakage from the sachets. The water leakages or defects are caused by (i) incorrect use of machines sealing temperatures it under set or overset temperatures causes poor sealed sachets and burnt sealed sachets respectively that later result to water leakage (ii) electric power supply fluctuating causing vary set temperature (iii) variation of thickness of supplied polythene during manufacturing, requiring varying sealing temperatures to properly seal the plastic sachets (iv) damaged or pierced supplied caused by plastic roll during transportation or manufacturing or (v) dist or sticky Teflon surfaces used for sealing sachets can result to leakage or product defects (Sadiq and Adeyemi, 2012).

2 METHODOLOGY

2.1 DATA COLLECTION

Daily production data comprising of useful output products, and defectives, made of production floor and sales return defectives were collected and recorded for 50 days of production. The data used in this study was obtained from both primary and secondary sources. The secondary data was derived from books, journals and published literature. An extensive range of books and statistical data were used and are listed in full in the reference section. Also an extensive review of literature was undertaken to establish the definitions of quality, quality control management, and the influence of quality on organisational performance. The outcome of the literature review served as a theoretical basis for the development of the questionnaires used in the study.

The primary data for the study was obtained through questionnaires administered to employees of the study companies and also consumers and distributors/retailers of sachet water products. The questionnaires were designed with the objectives of the study in mind. The second

questionnaire was a consumer survey that centered on consumer perception of the quality if the packaged water available on the market. In the administration of the questionnaire, consumers who could not read or write English were assisted in answering the questionnaire by interpreting it where possible. The third questionnaire was targeted at the distributors and retailers of the products of the selected case companies for the study. This was intended to give a measure of the performance and market value of the products of these companies. Also additional primary data was obtained through interpersonal interview and personnel observations were other types of Primary data that was used.

3 RESULTS AND DISCUSSION

The total quantity of material input must be balanced with the sum of non-defectives products i.e. useful output products, defectives on production floor and defectives returns from sales. For the period of investigation covered, the percentage defective is 0.45%, while non-defective products accounts for 99.55% of the total production. For the investigation period, the 0.45% defective indicates that for every 10000 packs, about 45 packs is due to defective products caused especially by sachets leakage.

3.0.1 Control Chart

Table 3.1 Control Data for Case Studies

Days	Mean Defects	
	(x)	MR
1	29.8	
2	30.4	0.6
3	34	3.6
4	31.8	2.2
5	38	6.2

6	26.6	11.4
7	29.8	3.2
8	30.2	0.4
9	32.4	2.2
10	34	1.6
11	39.6	5.6
12	35.8	3.8
13	36.8	1
14	38	1.2
15	42	4
16	41.2	0.8
17	31.2	10
18	34.2	3
19	32.4	1.8
20	35.8	3.4
Sum (Σ)	684	66
Mean	$\bar{X} = 34.2$	$\overline{MR} = 3.47$

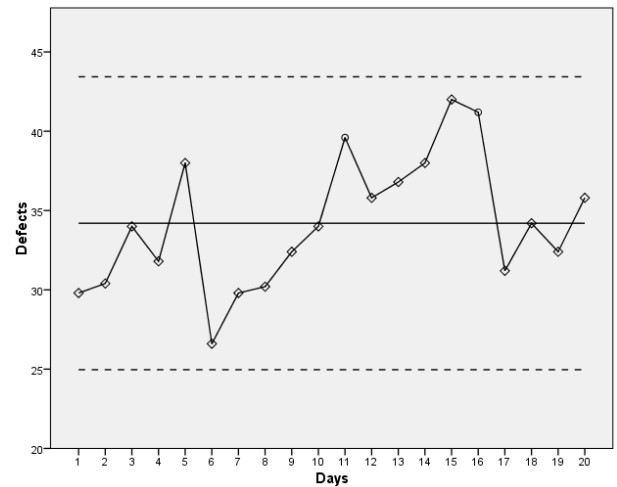


Figure 3.1: Control Chart for Packaging Sachet Water

Centre line, CL = 34.2

Upper control limit, UCL = 43.43

Lower control limit, LCL = 24.97

The process is in control since none of the plotted points fall outside either UCL or LCL. But day 11 and 16 violate control rules, which are; 6 points in a row trending up and 2 points out of the last 3 above + 2sigma respectively.

3.0.2 Operating Characteristic (OC) Curve

By using equation (3.11), the probabilities of acceptance (P_a), for various fraction defectives, p , are calculated for varying acceptance of $c = 2\%$ and 3% , at a constant defective sample sizes of 200. Figure 3.2 shows the OC curves for sample sizes of 200, packs under a constant acceptable defectives, $c = 2\%$ and 3% .

3.0.3 Average Outgoing Quality

By using equation (3.14), the average fractional defectives of outgoing defectives for varying acceptance defectives, c , and constant sample size of $n = 200$ are calculated and plotted to give Figure 3.3. Table 3.2 shows the average outgoing quality level (AOQL) with their corresponding fractional defective. The AOQL values are found to increase with increasing acceptable defectives at a constant sample size of 200

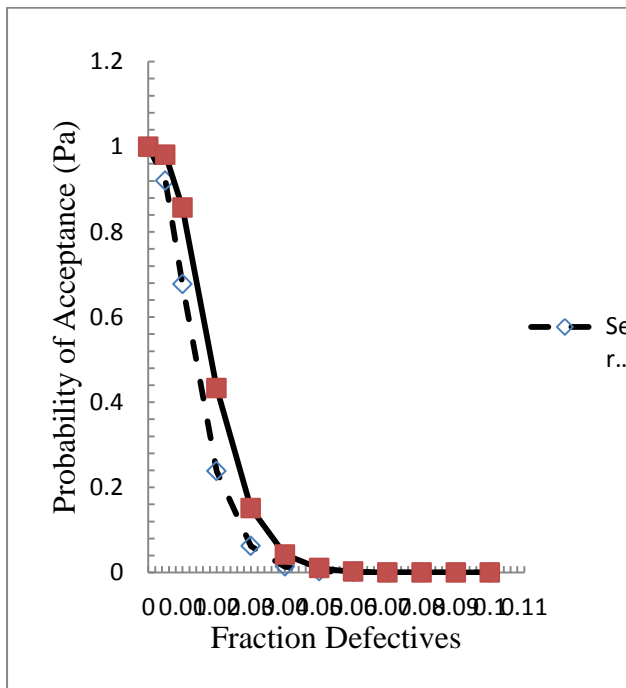


Figure 3.2: Operating Characteristic Curve for varying Acceptance

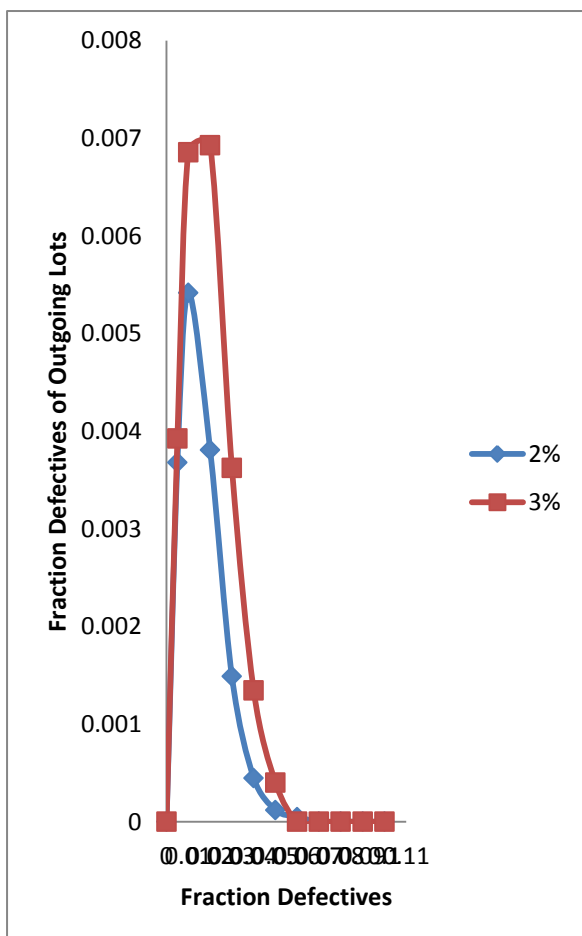


Figure 3.3: Average Outgoing Quality

From Figure 3.2, the optimum inspection acceptable defect plans so that the plan has to be accepted by both the producer and consumer of the supplied lot. The supplier's risk of rejecting good quality lots are called producer's risk (α), and consumer's risk, (β). The producer's risk (α) is the risk that the acceptable plan will fail to verify a sampling lot's quality and, thus, most often the producer's risk is set at 0.05, or 5 percent. The probability of accepting a lot with LTPD quality is the consumer's risk (β). A common value for the consumer's risk is 0.10, or 10 percentage.

The acceptable quality level (AQL) for high quality supplied lots and the lot tolerance percentage defective (LTPD) for low quality acceptable defective are calculated and tabulated in table 4.2, for acceptable defective, c and increasing acceptable defective at a constant acceptable defectives $n=200$. For $c= 2\%$, the plan provides a produce's risk and consumer's risk of 0.08 and 0.062, respectively. The result show that, produce's risk valve is higher than the values usually acceptable for plans. For 3%, the plan provides a produce's risk and consumer's risk of 0.019 and 0.151, respectively. The result show that, consumer's risk valve is higher than the values usually acceptable for plans. This demonstrate the following, increasing c while holding n constant decreases the producer's risk and increase the consumer's risk. The AOQL values are found to increase with increasing acceptable defectives at a constant sampling size of 200.

3.1 EQUATIONS

A measurement by attributes mean taking samples and using a single decision, the item is good (acceptable) or it is bad (defective). The functional defective products (defects) in a sample or a day can be estimated by;

$$p' = \frac{c}{n} \quad (3.1)$$

Where c = the number of defectives in a sample

n = the sample size/ the number of defective products produced in a sample

$$\bar{X} = \frac{\text{Total defective products}}{\text{Number of days}} \quad (3.2)$$

Moving Range (MR) can be defined as the absolute value of the first difference (the difference between two consecutive data points) of the data.

$$S = \frac{\overline{MR}}{d_2} \quad (3.3)$$

$$MR = |x_i - x_{i-1}|$$

$$\text{Moving Range } (\overline{MR}) = \frac{1}{m-1} \sum_{i=2}^m |x_i - x_{i-1}| \quad (3.4)$$

From A factor, d_2 can be determined as;

$$A_2 = 3/d_2 \sqrt{n} \quad (3.5)$$

According to Douglas (2014), individuals control limits for an observation $n=2$ and $A_2=1.880$

$$\text{Then; } d_2 = 3/A_2 \sqrt{n} \quad (3.6)$$

$$d_2 = 3/1.880 \sqrt{2}$$

$$d_2 = 1.128$$

Since average defective and moving range determined, control limit can be calculated from;

$$\text{Upper control limit (UCL)} = \bar{X} + 3 \frac{\overline{MR}}{1.128} \quad (3.7)$$

$$\text{Control limit (CL)} = \bar{X} \quad (3.8)$$

$$\text{Lower control limit (LCL)} = \bar{X} - 3 \frac{\overline{MR}}{1.128} \quad (3.9)$$

Where \bar{X} is the average of all the individuals defective and \overline{MR} is average moving ranges of two observations defective.

3.1.1 Operating Characteristic Curve

This refers to a graph of attributes of a sampling plan considered during management of a project which depicts the percent of lots or batches which are expected to be acceptable under the specified sampling plan and for a

specified process quality. Analysts create a graphic display of the performance of a sampling plan by plotting the probability of accepting the lot for a range of proportions of defective (fraction defective) units. The specified sampling plan may be demands of the project and could yield the results of acceptance or rejection based on specified criteria. It helps in the selection of sampling plans.

- (i) It aids in the selection of plans that are effective in reducing risks.
- (ii) It can help in keeping the high cost of inspection.

A sample of material of size, N , is submitted for review, a sample of n things is chosen indiscriminately from the parcel and exposed to examination or testing for imperfections. In acknowledgment test by qualities every one of these n things is named good (acceptable) or bad (defective) after the assessment. It is typical models that if over $c\%$ inadequate things are found from the example of n , the part will be rejected, yet the parcel will be acknowledged whether there is $c\%$ or less damaged.

$$P(\text{defectives}) = f(d) = \frac{n!}{d!(n-d)!} p^d (1-p)^{n-d} \quad (3.10)$$

$$P_a = P\{d \leq c\} = \sum_{d=0}^c \frac{n!}{d!(n-d)!} p^d (1-p)^{n-d} \quad (3.11)$$

Where; P_a = Probability of Acceptance

P = Fraction defectives

c = Defective acceptance

Two levels of quality are considered in the design of an acceptance sample plan. The first is the producer's risk (α), also known as Acceptable Quality Level (AQL), which is set at 0.005 or 5 percent.

$$1 - \alpha = P\{d \leq c\} = \sum_{d=0}^c \frac{n!}{d!(n-d)!} p^d (1-p)^{n-d} \quad (3.12)$$

The second level of quality is the lot tolerance proportion defective (LTPD), or the worst level of quality

that the consumer can tolerate. The LTPD is a definition of bad quality that the consumer would like to reject. Recognizing the high cost of defects, operations managers have become more cautious about accepting materials of poor quality from suppliers. Thus, sampling plans have lower LTPD values than in the past. The probability of accepting a lot with LTPD quality is the consumer's risk (β). A common value for the consumer's risk is 0.10, or 10 percent.

$$\beta = P\{d \leq c\} = \sum_{d=0}^c \frac{n!}{d!(n-d)!} p^d (1-p)^{n-d} \quad (3.13)$$

3.1.2 Average Outgoing Quality (AOQ)

The AOQ curve gives the average outgoing quality (left axis) as a function of the incoming quality (bottom axis). It is to check the performance of the plan. The maximum value of the AOQ curve is called the Average Outgoing Quality Level (AOQL). Regardless of the incoming quality, the defective or defect rate going to the customer should be no greater than the AOQL over an extended period of time. Individual lots might be worse than the AOQL but over the long run, the quality should not be worse than the AOQL.

The AOQ curve and AOQL assume rejected lots are 100% inspected, and is only applicable to this situation. They also assume the inspection is reasonably effective at removing defectives or defects, shows how outgoing quality (y-axis) depends on the incoming quality (bottom axis). The average outgoing quality is only applicable to the characteristics defective units, defects per unit, and defects per quantity and assumes rejected lots are 100% inspected and all defectives/defects are removed.

The AOQ curve initially increases as more defectives/defects are produced, more are released. As more and more lots are rejected, 100% inspections become more common and the AOQ curve starts to decrease as a result. The equation for AOQ is;

$$AOQ = \frac{P \times Pa (N-n)}{N} \quad (3.14)$$

Where; P = Fraction defective

Pa = probability of accepting the lot

N = lot size

n = sample size

3.2 TABULATION

Table 3.2: Important Parameters

Acceptable defectives	LTPD	AQL	AOQL(Fraction Defect)
2%	0.062	0.08	0.0055 (0.0445)
3%	0.151	0.019	0.006892(0.0531)

4 CONCLUSION

- For the given period of investigation, the non defective product is 99.55% of the total production output with the percentage defectives is 6.42%, made up of 0.45% defective from production.
- It is proposed that the concept of Quality Control Management can be utilized by sachet/bottle water companies to effectively manage quality of output and achieve company performance. The study has established TQM as the best quality management strategy for Minna's sachet water company.
- From the operating characteristic (OC) curves and average outgoing quality (AOQ) curves obtained from constant sample sizes and given varying acceptable defective, $c = 2\%$ and 3% , important sampling plan parameters such as acceptable quality level(AQL), lot tolerance percent defective (LTPD) and average outgoing level (AOQL) are determined and presented.

ACKNOWLEDGEMENTS

The authors wish to acknowledge the assistance provided by FUTMIN Table Water, Top Supreme Table



Water, COE Venture Table water, Muntuci Table Water and Pepper Table Water, in the form of facilities and resources that enhanced the successful completion of this work.

REFERENCES

1. Deming, W.E., (1986). *Out of the Crisis*. MIT Centre for Advanced Engineering Study., Massachusetts: Cambridge Press.
2. Eke, A.O. (2001), "SWOT Analysis and Managing Change", in Erurum UJT (ed), *Managing Service Quality in the Nigerian Public Sector*. Enugu: Smart Link Publishers.
3. Dobyns, B. & Crawford, J. (1994) *Organisational Changes and Development: A System View*. California: Good Year Publishing Company.
4. Dodoo, D.K. et al (2006). Quality of "sachet" waters in the Cape Coast Municipality of Ghana. *Journal of Environmental Science and Health – Part A Toxic/hazardous substances and environmental engineering*, 41(3), 329-342.
5. Sadiq, I.O., and Adeyemi, M.B. (2012). "Quality Control in a typical water Packaging Industry", *International Science Press* 3(1), pp. 17-21.
6. Douglas C.M. (2014). *Introduction to Statistical Quality Control*, 6th Edition. John Wiley and Sons Publishers, New York, U.S.A.
7. Dale, B.G., Boaden, R.J., and Lascelles D.M., (1994). *Total Quality Management- An Overview, Managing Quality* (edited by Dale, B.G.), New York: Prentice Hall.



SURVEY OF TRACTOR USAGE AND PARTS BREAKDOWN IN NIGER STATE, NIGERIA

*Dauda, S. M¹, Abdulmalik M.K.², Isyaku M. I.¹ Francis A.A.¹, Ahmad D³,

¹Agricultural and Bioresources Engineering Department, Federal University of Technology, PMB 65 Minna, Niger State, Nigeria

²Agricultural Engineering Department, Niger State Agricultural Development Programme Minna

³Department of Biological and Agricultural Engineering, Universiti Putra Malaysia 43400 Serdang, Selangor DarulEhsan, Malaysia

*Corresponding author email: smdauda@futminna.edu.ng, +2348038964659

ABSTRACT

An investigation into the level of farm tractor breakdown was carried out to determine the component wear in a tractor. The nature, frequency and magnitude of wear of these component as well as their causes were also under focus. The study was carried out by administering questionnaire and observation to find out the common component of the tractor that wears easily. The findings of this study are as follow: The tractor owners, operators, engineers, mechanics and managers is male dominated, the age group of most of the respondents is between 30-59 years, there educational background was low, majority of the operators (92.68 %) learnt how to operate the tractor from other tractor operators rather than through a formal tractor training school, the most dominant tractor make used by respondents was Mahindra (49.6 %), about 95.1 % (117) of the respondents reported that their steering pump casing wear more than three times during the farming season

Keywords: Tractor, Malfunctioning, Breakdown, Component, Failure.

1 INTRODUCTION

The use of motorized machines for farming activities started with the advent of steam engine in the early nineteenth century and since then gradual development has lead to the use of internal combustion engine as result from limitations of human muscles as sources of power in agriculture and quest for appreciable increase in agricultural production due to population explosion and globalization, hence the need for comprehensive agricultural mechanization. Farm mechanization is the utilization of machines for farm operations. These machines include all types of implements and devices for supplying of power on the farm such as plough, harrows, seeder/seed drills and planters, cultivators, harvesters, haying machines and tractors. (Aduayi and Ekong, 2011). The tractor is the most important machinery because it is the prime mover for all the implements. It is the most used and most prone to wear and tear. It is also the most expensive item of all farm machinery. Ellis and Wain—wright (1994), put the cost of machinery used in developing countries including Nigeria, at about 30% of the total investment in agriculture while Igbeka (2014) stated that the cost of operating machinery is the largest single farm expenditure due to machine failure or breakdown. A failure or breakdown is the malfunctioning of part,

component or the whole machine to carry out its specified function, partially or completely. It is as a result of inherent failure in the machine or due to misuse (Apollos, 2001). In most cases, misuse is the cause of breakdown. Misuse is a deliberate act by the user, which reduces the reliability, maintainability and operability of a given machine. It involves the use of a machine in such a way not envisaged by the designer, which may cause damage in or shorten the life of machine. Tractor misuse include use of adulterated fuel, use of machine for undesigned purposes, overloading or over speeding, incorrect adjustments and improper housing. The effects of misuse include decreases in the design and useful life of machine, disruption of production schedules, and increase in downtime and overhead costs due to maintenance. Usman and Bobboi (2003) observed that the main cause of early failure in farm tractors is the failure to adopt preventive maintenance practice. This leads to frequent tractor breakdown and high operating costs. Tuft and Hitts (2015) reported that most machines of the same make and model are designed to have same performance efficiency and life span but the subsequent differences observed in practice are due to the operators, environmental and maintenance activities. High frequent breakdown, high incidence of un-serviceability, unavailability of spare parts, handling from unskilled operators and technicians, old age of

tractors and lack of agricultural workshops and tools and insufficient experts or technicians are the objectives of this investigative study.

2 METHODOLOGY

2.1 STUDY AREA

The study was conducted in Niger State in the North Central region of Nigeria. Niger State is located in the guinea savannah agro-ecological zone of Nigeria at latitude 3.20° East and longitude 11.3° North. The state experience distinct dry and wet season's with annual rainfall varying from 1,100 mm in the Northern part of the state to 1,600 mm in the southern parts. Almost all crops that can be grown in the southern forest zone and the northern savanna zone of Nigeria can thrive well in the state. The lowest minimum temperature occur usually between December and January when most part of the state come under the influence of the tropical continental air mass which blows from the north, the dry season in Niger state commences in October.

2.2 Data Collection

About 180 questionnaires was designed and 10 each administered in 18 local government areas, that is 6 from each of the senatorial zone, only the tractor owners, operators, mechanics, engineers and managers were accessed. But only 123 received were used in the analysis of various factors and conditions of this research. Data was collected between September and October, 2018. The questionnaire was designed to obtain information on the causes of agricultural tractor steering pump problems and the major constraints affecting tractor steering pump maintenance and repair. Some information were gotten from oral interviews carried out.

2.3 Data Analysis

The data obtained from the survey were summarized using descriptive statistics. The summarized data were presented in the form of tables and graphs. Tables were used to help focus on specific numbers in the results. Bar charts were used to compare respondent responses for the different categories in a question. Frequencies and percentages were used to describe the composition of sample.

3 RESULTS AND DISCUSSION

3.1 Sex and Age of Group Distribution (Tractor Owners, Mechanics, Engineers, Manager and Operators)

The questionnaire was administered to 180 tractor owner, operator, engineer, mechanic and manager. The respondents included 122 male and one female. Out of

123 respondents, 28 were tractor owners, 15 were engineers, 17 were mechanics, 41 were tractor operators while 24 were managers. The result shows that tractor owners, operator, engineers, mechanics and manager is male dominated. Table 1 shows the age group distribution of all respondent

Table 1: The Age Group Distribution of All Respondents

Age Group	Frequency	Percentage (%)
30-39	28	22.76
40-49	46	37.40
50-59	24	19.51
60-69	9	7.32
Total	123	100

3.2 Educational Background of All the Respondents

Education has an immense impact on the human society (Goel, 2007). Education is the knowledge of putting one's potentials to maximum use. Education is one of the factors affecting the capability of the tractor users. The literacy status of a tractor user may influence understanding about the use of tractor and its associated implements because he can study the operation manual and understand all the instructions (Bhutta, *et al* 1997). The educational background of tractor owner, tractor operator, mechanics, engineers and manager is presented in figure.1. Generally, the educational background of the respondents was low. About 62 % of the respondents had Arabic/ Islamic knowledge, no formal education or had between one and six years of formal education. 22 % of the respondents were makaranta graduate. 21.1 % of the respondents had no formal education while 18.7 % had between one and six years of formal education (primary school level education). About 16.3 % of the respondents had middle school level education; approximately 6.5 % had junior secondary school level education, while about 7.3 % had senior secondary school level education. Approximately 8.1 % of the respondents had technical school level education and polytechnic level education.

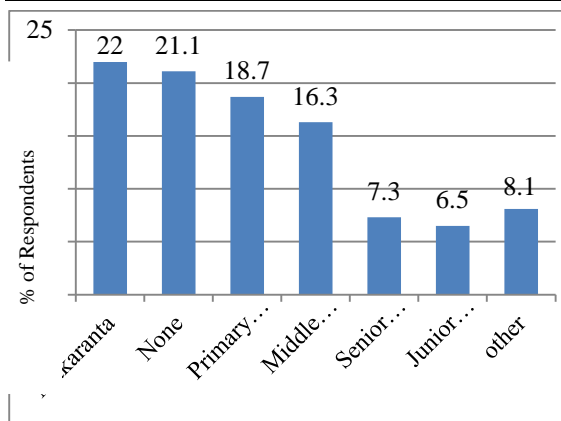


Figure 1: Educational Background of the respondent

3.3 Tractor Operators Background Training and Experience

Table 2 displays the background training of the tractor operators. It can be seen that the majority of the operators (92.68 %) learnt how to operate the tractor from other tractor operators rather than through a formal tractor operator training school. Only 7.32 % of the operators had formal tractor operator training. While formal tractor operator training is structured, informal tractor operator training is not structured. This means that different tractor operators would train their subordinates, based on their own limited experience producing ‘gaps’ in their (subordinate) training

Table 2: Tractor Operator Training

Mode of Tractor operator Training	Frequency	Percentage (%)
From another Tractor operator	38	92.68
Government Sponsored (Ministry of Agriculture and Rural Development)	3	7.32
Total	41	100

Table 3.2: Tractor Operator Training

Figure 3.2 illustrates the years of experience of the 41 tractor operators. Tractor operators with one to ten years of operating experience constituted 36.8 % of the respondents. This was followed by those with 11 to 20 years of experience (27.6 %); and 21 to 30 years of experience (17.2 %). Tractor operators with 31 to 40 years of operating experience represented 13.8 % of the

respondents while those with 41 to 50 years experience made up 4.6 % of the respondents.

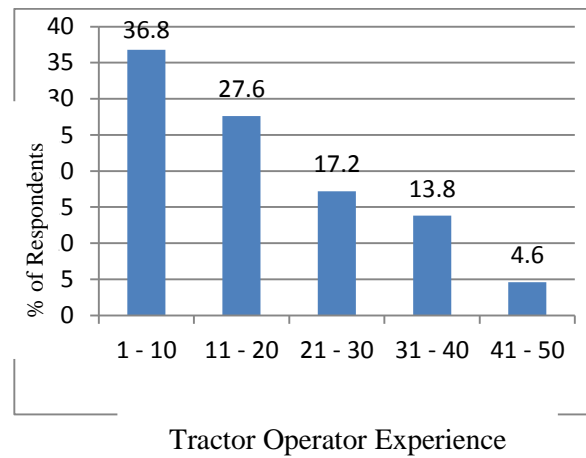


Figure 2. Experience of respondents

3.4 Tractor Makes

In figure 3, the maker of tractors used by respondents is depicted. Mahindra, Massey Ferguson, and ford consisted of 73.2 % of the make of tractor in the state. The most dominant tractor make used by respondents was Mahindra (49.6 %). Massey Ferguson constituted (13.8 %) while Ford represented (9.8 %) of the make of tractors in the study area. John Deere, styre and Fiat formed 16.3 % of the make of tractors that is john Deere had (5.7 %), Styr had (5.7 %) and Fiat constituted (4.9 %) while other make of tractors formed 10.5 % which included New Holland (3.26 %), Etcher (3.25 %), Farmtrac (1.7 %), swaraj (1.63 %), and universal (0.66 %).

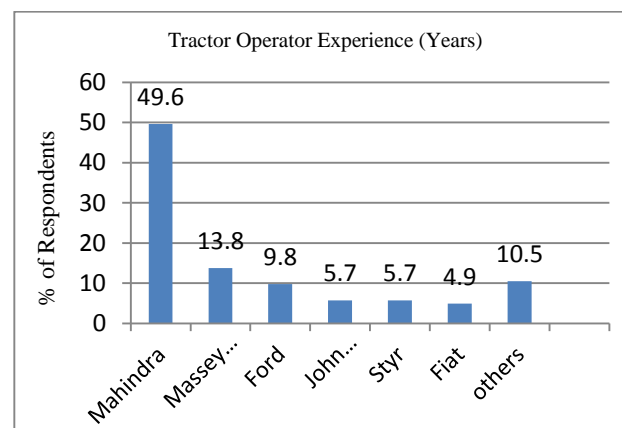


Figure 3. Distribution of Make of Tractors at the Study Area

3.5 Nature of Tractor Purchase and Tractor Size

Table 3 shows the nature of tractor purchase obtained from the survey. About 58.5 % of the respondents reported that their tractors were purchased as brand new while 41.5 % of the respondents indicated that theirs were purchased as “second hand”.

Table 3: Nature of Tractor Purchase

Tractor Purchase	Frequency	Percentage (%)
New	72	58.5
Second Hand	51	41.5
Total	123	100

Figure 4: presents the results of the tractor Size found from the administration of the questionnaires. Out of the 123 respondents, 56.9 % did not know their tractor size in (hp). About 17.9 % indicated their tractor size to be about 65 hp while 23.5 % reported their tractor size to be 70 hp (8.9 %), 45 hp (8.1 %) and 55 hp (6.5 %). The other 1.6 % of the respondents indicated their tractor engine size 30 hp.

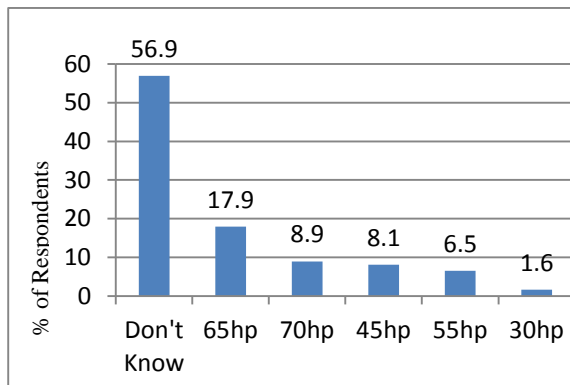


Figure 3 Tractor Engine size

3.6 The Tractor Steering Pump

When respondents were asked about the working condition of their tractor steering pump, 59.3 % of them indicated that their tractor steering pump was not in working order while 40.7 % said that their tractor steering pump was in working order. This is shown in table 4.

Table 4: Tractor Steering Pump

Tractor Steering Pump	Frequency	Percentage (%)
In order	50	40.7
Not in order	73	59.3
Total	123	100

3.7 The Tractor Steering Pump Casing

Table 5 presents the respondent responses about steering pump casing analyzed in figure 5. As can be seen, 95.1 % (117) of the respondents reported that their steering pump casing wear more than three times during the farming season, 3.2 % (4) reported that their casing wears at least twice in a season while 1.7 % (2) indicated that theirs did not wear during the farming season.

Table 5: Wear In Tractor Steering Pump Casing during the Farming Season

Wear	Frequency	Percentage (%)
Wear More than three Times	117	95.1
wear at least twice	4	3.2
Did Not Wear	2	1.7
Total	123	100

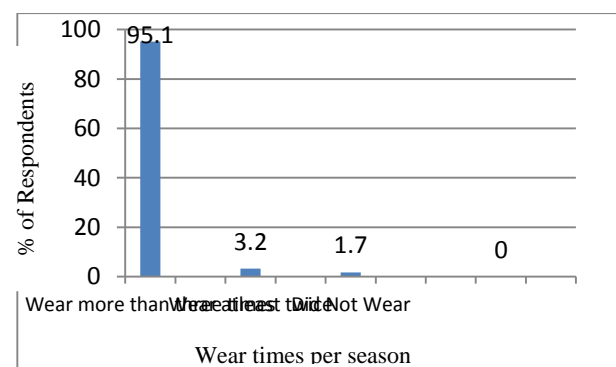


Figure 4

3.8 Use of Tractor Steering Pump Manual and Maintenance and Repairs

Reading the manual is important because it tells the owner or operator how to set the steering pump and what

part to check before one takes it to the field (Wehrspann, 2003). The respondents were asked if they have access to their operators' manual. About 57.7 % of the respondents said that they do have access to it while the remaining 42.3 % indicated that they do not have access to their manual (Table 6). Furthermore, 78 % of the respondents indicated that they do not follow the pump manufacturer's instruction in the maintenance of their pump while 22 % reported that they follow the pump manufacturer's instruction in the maintenance of their pumps

Table 6: Tractor Steering Pumps Manual and Manufacturers Instruction

Access to pump Operator manual	Frequency Instructions	Percentage (%)	Manufacturer's
Yes	71	57.7	
No	52	42.3	
Total	123	100	

3.9 Tractor Mechanics and Well Equipped Repair Workshops

Table 7 shows the responses provided by the participating respondents on availability and proficiency of tractor mechanics at the study area. Of the 123 respondents, 3.3 % said that tractor mechanics are readily available and 96.7 % said that tractor mechanics are not readily available. Similarly, 3.3 % indicated that the tractor mechanics are proficient and 96.7 % of the respondents reported that the tractor mechanics are not proficient.

Table 7: Availability of tractor mechanics

Availability of mechanics	Frequency	Percentage (%)	Proficiency of mechanics	Frequency	Percentage (%)
Of tractor Mechanics	(%)	in tractor repair	(%)		
Yes	4	3.3	Proficient	4	3.3
No	119	96.7	Not Proficient	119	96.7
Total	123	100	Total	123	100

Almost 27.6 % of the respondents perceived having well equipped tractor repair workshops while 72.4 % believed that they did not have well equipped tractor repair workshops. Table 8 also shows that only 81.3 % of the respondent sought help outside their town

for the repairs of their tractors. About 18.7 % does not seek help for repairs outside their home town.

Table 8: Well equipped tractor repair workshop

Well equipped repairs outside (%)	Frequency	Percentage (%)	Seek helps for repairs outside (%)	Frequency	Percentage (%)
Yes	34	27.6	Seek help	100	81.3
No	89	72.4	Does not Seek help	23	18.7
Total	123	100	Total	123	100

4.0 CONCLUSION

Based on the results obtained, the following conclusions are drawn. The result shows that tractor owners, operator, engineers, mechanics and manager is male dominated. The age group of most of the respondents is between 30-59 years. Generally, the educational background of the respondents was low. The majority of the operators (92.68 %) learnt how to operate the tractor from other tractor operators rather than through a formal tractor operator training school. The most dominant tractor make used by respondents was Mahindra (49.6 %). About 95.1 % (117) of the respondents reported that their steering pump casing wear more than three times during the farming season. The respondents perceived the causes of steering pump failure to be wear, leakages, cracks in the pump casing, use of fake spare parts for maintenance and repair, use of adulterated fluid and old age of the pump, exposure to extreme dust and over usage that is mis use of the pump during farming operation.

5.0 REFERENCES

- Aduayi, E.A and Ekong, E. E (2011); *General Agriculture and Soils*. Cassel Ltd, London
- Apollos, S.K. (2001). Agricultural Machinery Misused in Nigeria, Basic issues. Proceeding of the Annual Conference of the Nigerians Institutions of Agricultural Engineers. Vol. 23, Pp 59-64.
- Bhutta, M.S, Tanveer, T. and Awan, H.M. (1997): Technical Skill of Tractor Operator: A



-
- Case Study in Multan, Pakistan. *Agricultural Mechanization in Asia, Africa and Latin America*, 28 (1): pp 18-22.
- Ellis J.J. and Wain —Wright K.P. (1994). *Criteria Affecting Agricultural Rehabilitation Scheme*. Silsoe Research Institute, Bedford. Pp. 47-52.
- Goel, M. (2007): *The Importance of Education*. Available online: <http://searchwarp.com/swa230219.htm>
- Igbeka, J.C. (2014). *Development in Rice Production Mechanization*. *Journal of Agricultural Mechanization*. Macmillan Publisher Limited., London, Pp. 55.
- Tuft, R. A. and Hitts, J. A. (2015). *Failure, Cause, Frequency and Repairs for Forest Harvesting Equipment*. Paper presented as ASAE Paper No. 82 – 1598. St. Joseph M149085.
- Usman, A. M. and Bobboi, U. (2003). *Farm Tractor Maintenance; Types, Procedures and Related Problems in Nigeria*; *Proceedings of the Nigerian Institution An Official*
- Wehrspann, J. (2003): *10 biggest causes of Machinery breakdowns (and how to prevent them)*, Available online: http://farmindustrynews.com/mag/farming_biggest_causes_machinery/



DEVELOPMENT OF AN INSPECTION METHODOLOGY FOR PEUGEOT 508

Bala Dauda¹, James Oseni Abu²

¹Department of Mechanical Engineering, Federal University of Technology, Minna, Nigeria

²Department of Mechanical Engineering, Federal University of Technology, Minna, Nigeria

ABSTRACT

The inability of a car component to function effectively as designed for reliability when put to use is an issue in automobile industry. That is why monitoring of a car quality standard is very important to ensure safe and efficient operation of the brand through critical inspections. The structural integrity of a car depends on the quality of certain structural components within the body-frame, engine compartment, external and interior features. It is evident that the reliability of a car is measured within the durability period. Therefore, the research methodology is aimed at essential improvement by pursuing root causes of defects on the brand (Peugeot 508) with the help of computerized and pneumatic machines. These defects may be as a result of improper surface finishing, variation in features tolerances, irregular frame cavities, improper wheel rimming and unsuitable body frame material thickness that can stand the test of time when subjected to road performance. The inspections were carried out successfully, and the objectives were achieved. During the course of the research, it was recommended that suitable alloyed material thickness with high level of resistance capacity to deformation and good surface finishing with close tolerance limits should be used on the brand.

Keywords: Development, Improvement, Inspection, Manufacturing, Methodology and Quality.

1 INTRODUCTION

Development of an inspection methodology and the improvement of the Peugeot 508 brand is an integrative philosophy of management for continuously improving on the product quality and processes used all over the world. It involves a variety of activities such as product design, data collection, process and material selection, production planning and control, materials handling, packaging, marketing and sales as a vital methodology. In this conversion process, the key factors that dictate the productivity and competitiveness of one manufacturer over another are the ease, the quickness and the economy of manufacturing of the quality products. These factors are especially important for American manufacturers owing to the increasing globalization of all aspect of product manufacture including technology, labour and market (Newman and Jain, 1995).

To achieve a reliable economy and quality control in manufacturing through critical inspection methodology, manufacturing practitioners and researchers in the past advocated for complete automation in all manufacturing activities. The used of advanced technologies were seen as the key to achieving a competitive edge in the world market. Generally, it was believed that human workers had difficulties in providing the required quality, uniformity, reliability, repeatability and documentation for competitive manufacturing which made the case for complete automation of all manufacturing activities completed. While these ideas were not narrowly confined, fully automated factories based on hard automation are

not yet viable due to technical, economic and cybernetic reasons (Mital *et al.*, 1994).

Hard automation does not yield itself to situations where a product is to be changed frequently because of user's needs, costs and engineering improvements. Also, automated equipment such as robots and vision systems for inspection provide flexibility but not capability. For robots to be capable, they must have the necessary intelligence and must be able to sense the working environment to see, touch, feel pressure and sense their own movement; acquire knowledge and judgment to carry out tasks properly and act according to the skilled worker (for example, accept parts that may not have the exact tolerance or not properly oriented); perform tasks reliably to impart the required 3-D motions to the product and communicate with the operator by voice, written sentences, and other appropriate forms of communication. Currently, humans must either work with automated systems or supervise them and must intervene when problems are generated. For instance, when a robot drops a part or when a computer is unable to make an inspection decision after searching or identifying a defect ((Friedrich, 2002).

One of the aspects of Technology Driven Train Inspection (TDTI) initiative is the development of the system known as Automated Inspection of Structural Components (AISC), which is currently underway at the University of Illinois at Urbana-Champaign (UIUC). AISC focuses on developing technology to aid in the inspection of freight car under-bodies for defective structural components through the use of machine vision. A machine vision

system requires data using digital cameras organizes and analyzes the images using computer algorithms and useful information such as types and location of defects to the appropriate repair personnel (Anand *et al.*, 1993).

The machine vision algorithms use visual cues to locate areas of interest on the freight car and then analyze each component to determine its variance from the baseline case. While manual inspections are subject to inaccuracies and delays due to time constraints and human fatigue. AISC will work collectively with other automated inspection systems (for example, machine vision systems for inspecting safety appliances car components and brake shoes) to inspect freight cars efficiently and objectively and will not suffer from monotony or fatigue. AISC will also maintain health records of every car that undergoes inspection, allowing potential structural defects to be monitored so that components are repaired prior to failure. Additionally, applying these new technologies to the inspection processes, has the potential to enhance safety and efficiency for both train crew members and mechanical personnel. A primary benefit of AISC and other automated inspection systems is the facilitation of preventive or condition-based maintenance (Faieza and Mousavi, 1999).

Condition-based maintenance involves the monitoring of certain parameters related to component health or degradation and the subsequent corrective actions taken prior to component failure. Despite the advantages of condition-based maintenance, current structural component repair and billing practices engender corrective maintenance which does not occur, until some critical defects are detected. Due to the reactive nature of corrective maintenance, repairs cannot be planned as effectively, resulting in higher expenses and less efficient repairs. For example, it is more economical to patch a cracked cross-bearer before it breaks than to replace a fully broken cross-bearer, but it is very important to replace another one in order to make the car reliable to stand the test of time. Having recognized the needs for preventative maintenance, railroads have begun implementing other technologies similar to AISC that monitor subtle indicators of the car component health (De-sa and Zachmann 1993).

Inspections are key in maintaining quality production. Therefore, developments of inspection methodologies are critical in automobile industries to improve on quality of a product through defect detection and analysis improvement. Also, integrate quality and reliability in manufacturing processes provides sufficient information services and active feedback to various customers quality requirements for the manufacturing and design processes. These procedures have to be taken to meet market quality requirements, and improve on customers satisfaction in

order to make the product competitive in the world market which can only be achieved via perpetual and consistent evaluation (Friedrich, 2002)

The automotive industry is currently one of the world largest economic contributors with 91.5 million motor vehicles produced globally (European Automobile Manufacturers Association, 2016). Major transitions are currently happening within the automotive industry and it is important for car makers to keep the momentum moving in supplying demand for customers. Since the introduction of moving assembly line, automotive industry has become one of biggest market players in developing new advance technologies (Gusikhin *et al.*, 2007). Technology has always driven the transformation inside the automotive industry.

The development of this industry into a digital business creates opportunities for disruption to increase from external threats or within the automotive industry itself. Automotive companies accepted that digital technological inspections as part of their core process with technological trends such as 3D printing, mobile advancement, cloud and virtual systems; Internet of things has expanded traditional barriers of automotive industry (Zhou, 2012).

2 METHODOLOGY

The necessary Equipment that contributed to the actualization of this inspection at Peugeot Automobile Nigeria Limited (PAN) Kaduna State include:

- i. Hydraulic and electrical operated car elevator
- ii. Pneumatic polishing and dusting machine
- iii. Trolley, roller and belt conveyers
- iv. Electrical and pneumatic hoists
- v. Computerised wheel balancing
- vi. Computerised wheel alignment machine
- vii. Hydraulic wheel fitting machine
- viii. Pneumatic bolt and nut fastening machine
- ix. Cable lifter

2.1 INSPECTION UNIT PROCESSES

The inspections that were carried out at PAN usually commence at the chassis line, right from the factory, when each car is gradually coming to a completion stage. For a wheel to be ready for use at the production line, it must pass through critical measurements, using a wheel fitting machine and a computerised wheel balancer. Wheel alignment machines are mostly used after the completion of the production processes. The wheels are properly fitted together with tyres, with the help of a manually operated fitting machine, and measured with a computerised wheel balancer to ensure that all the wheels are properly balanced with the aid of some weights of different kilogram (kg) attached to them. The balancing of every wheel depends on the measurement and the weight to make it balanced. Also, the wheel alignment has to be

taken by moving the car on an elevator, and then lifting it up to the required level where the wheels can be aligned with the help of a computerised wheel alignment machine, to ensure that all the wheels are in a straight line ready for road performance.

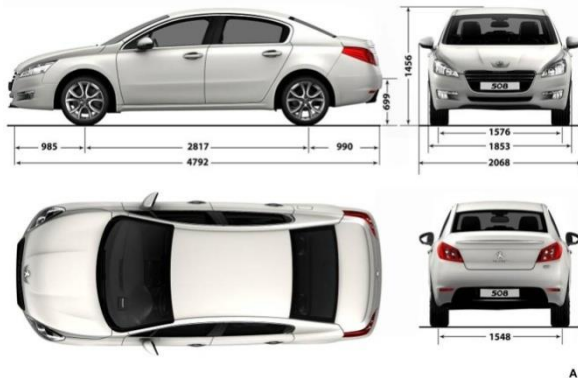


Plate I: Inspected designed Peugeot 508 dimensioned in (mm) (PAN Manual, 2017)

Inspections are vital to detect defects on cars and to develop some critical measures in order to improve on the products in the manufacturing industry. Developments of these methods are key in assessing the effect of product reliability and quality of spare parts required for acceptable field performance. The research is to develop an essential technique on how to improve on manufactured products in automobile industry. The inspection method is to set a standard for product requiring a reliability test. Also, Provide necessary input to unit and product-level life cycle cost analysis and product failure rates, and how often a part will be replaced. The need for this reliability research inspection is also paramount in developing essential methodologies by standardizing manufactured product and combine data with analysis by showing the infrequency of structural defects indicated and proffer alternative solutions to data acquisition were necessary. These has the potential to provide more objective information on the car structural condition, improved utilization of car inspection and repair resources, increase car performance and employee safety and improvements to overall road network efficiency.

2.3 INSPECTION PROCEDURES

Two basic procedures were used during the course of the inspection evaluation. An inspection method for data collection, design analysis and material selection in manufacturing, are basic tools for improving on quality products in all levels of production. To minimize or eradicate defects on the brands, reliability which can be called in a simple term (Plan-Do-Check-Act Cycle) has to be taken into consideration to achieve the required

purpose. These methods composed of five phases, each bearing acronyms DMAIC and DMADV (Deming *et al.*, 2010).

DMAIC: Is used for improving on existing manufacturing processes. DMAIC is also pronounced as “Duh-may-ick”

DMADV: Is used for creating a new product or design process in manufacturing. DMADV is also pronounced as “Duh-mad-vee”

DMAIC (Duh-may-ick): This project method used in manufacturing processes features five phases from the acronym which are:

- i. Define the project problems; listen to the voice of customers and the project goals specifically.
- ii. Measure key aspects of the current process, inspect the areas of application and collect relevant data.
- iii. Analyze the important data to investigate and verify the causes and effects relationship, determine what the relationships are and attempt to ensure that all factors have been considered. Seek out the root cause of defects under investigation.
- iv. Improve or optimize the current process based upon data analysis using techniques such as design of experiments, standard work to create a new future state process and set up pilot runs to establish process capability.
- v. Control the future state process to ensure that any deviations from target are corrected before they result in defects. Implement control systems such as statistical process control, production boards visual workplaces and monitoring the process continuously (Taguchil *et al.*, 1986a).

DMADV (Duh-may-vee): This project design method used in manufacturing processes features five phases from the acronym which are:

- i. Define design goals that are consistent with customer demands, identify relevant information regarding the design process, understanding why the design goals and the enterprise strategy.
- ii. Measure and identify CTQs (characteristics to Critical to Quality), product capabilities, production process capability, suitable measures to be adopted for the design processes and risks involved.
- iii. Analyze to develop and design alternatives, create a high level design and evaluate design capability to select the best design.
- iv. Design details, optimize the design, note the relevant procedures to be used and plan for design verification. This phase may require simulations to authenticate the design process.

Verify the design, set up pilot runs, implement the production process and hand it over to the process owners (Taguchi *et al.*, 1986b).

These inspection procedures facilitate improvement on the quality of products and processes in manufacturing which may be used all over the world as a yardstick. It capitalizes on the involvement of management, workforce, suppliers and even customers to meet or exceed user's expectations. Also, to seek on how to improve on the quality of process outputs by identifying and removing the causes of defects (errors) and minimizing variability in manufacturing and business processes. It uses a set of quality management methods, including statistical methods creates a special infrastructure for people in the industry.

3 RESULTS AND DISCUSSION

An inspection was carried out to help illustrate the construction of control limits for counts data. 54 cars were inspected at PAN, and some observed numbers of defects were equally recorded.

Table 1: Results for inspected car samples and their number of defects

Car No:	1	2	3	4	5	6	7	8	9	10	11	12	13	14	15	16
Defect No:	30	33	31	34	36	29	31	26	32	26	28	29	30	34	28	32
	17	18	19	20	21	22	23	24	25	26	27	28	29	30	31	32
	24	29	31	26	23	27	32	36	25	33	24	25	26	30	29	31
	36	37	38	39	40	41	42	43	44	45	46	47	48	49	50	51
	26	28	25	28	34	24	26	31	33	28	34	26	29	30	23	27

3.1 INSPECTION FOR CONTROL LIMITS

The number of defects that occur are counted in the inspection unit. More often than not, an inspection unit is a single unit or item of product, for example, a car. However, sometimes the inspection unit could consist of five or ten cars. The size of inspection units may depend on the recording facility, measuring equipment and operator. Suppose defects occur in a given inspection unit, according to the Poisson distribution with parameter A, and the number of defects X, It is also known that both the mean and the variance of this distribution are equal to C. Then the K-control chart is (Shewhart *et al.*, 1986):

$$UCL = A + K\sqrt{A} \quad (1).$$

$$LCL = A - K\sqrt{A} \quad (2).$$

If the LCL comes out negative, then there is no lower control limit. This control scheme assumes that a standard value for A is valuable. If this is not the case, the A may be estimated as the average of the number of defects in a preliminary sample of inspection units, call it \bar{A} . Usually, $k = 3$, therefore equation (1) and (2) becomes;

$$UCL = A + 3\sqrt{A} \quad (3).$$

$$LCL = A - 3\sqrt{A} \quad (4).$$

Where,

UCL = Upper Control Limit

LCL = Lower Control Limit

CL = Centre Line = A = Mean value

K = constant

3.2 CALCULATIONS

From the table 1, we have;

X = Total number of samples (cars) = 54

C = Total number of defects = 1569

$$A = \frac{\text{Total number of defects}}{\text{Total number of samples}} = \frac{X}{C} = \frac{1569}{54} = 29.06$$

Note: The CL (A) can be approximately represented as 29 on the plotted chart for accuracy

To determine the Upper Control Limit (UCL) for sample defects

From equation (3), we substitute our obtained values in order to get UCL

$$UCL = A + 3\sqrt{A} = 29.06 + 3\sqrt{29.06}$$

$$UCL = 29.06 + 3(5.3907) = 29.06 + 16.1722$$

$$UCL = 45.23$$

Note: The UCL can be approximately represented as 45 on the plotted chart for accuracy.

To determine the Upper Control Limit (LCL) for sample defects

From equation (4), we substitute our obtained values in order to get LCL

$$LCL = A - 3\sqrt{A} = 29.06 - 3\sqrt{29.06}$$

$$LCL = 29.06 - 3(5.3907) = 29.06 - 16.1722$$

LCL = 12.89

Note: The LCL can be approximately represented as 13 on the plotted chart for accuracy

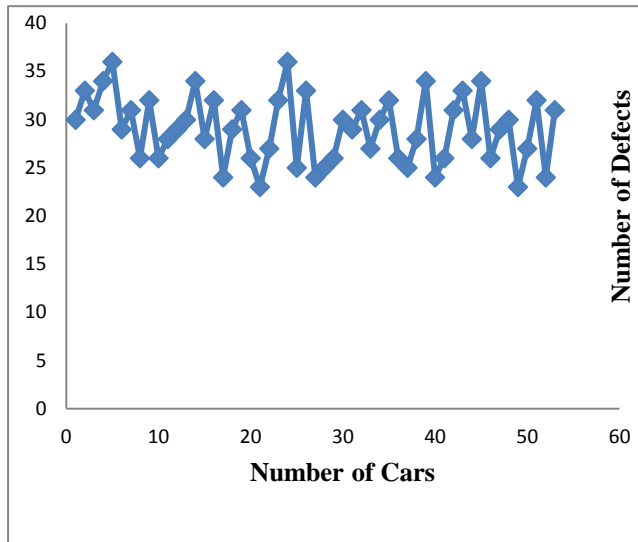


Figure 2: Chart for Car samples and their no: of defects

Control charts in manufacturing processes are basically used to monitor quality products, depending on the number of process characteristics to be monitored. From the calculated values obtained, it was obvious that the Centre line (mean value) for the car samples defects is approximately 29, and the UCL is approximately 45 while the LCL is approximately 13.

Limits in production processes, tells you where you belong based on the number data points. Where limits are placed during the course of evaluation, it will determine the risk of undertaking the research. For example, if the first 40 of 54 points fall above centre line and the last 14 fall below centre line, we know the reason why. That is to say, the first 40 is at the upper limit, while the last 14 is at the lower limit. Statistical methods to detect sequences or non-random patterns can be applied to interpret control charts. To be sure, “in control” implies all points are between control limits and form random pattern when the chart is plotted.

During the inspection analysis, it was noticed that there was a little compromise on the quality standard of the metal frame thickness and some of the brand features, that makes defects to be on the increase on cars. Also, wide range of tolerances on the car cavities and improper surface finishing contributed to the enormous defects of the brand. After fixing the car fittings, there were some gaps on the brand positions, like head lights, boot, doors, liners and some of the interior features which could not be

rectified easily because of wide or close range of tolerances, as they were manufactured from the factory.

From the observations, the conditions to be considered when selecting materials for the cars were:

- i. Highly alloyed metal sill (sheet) thickness with very good surface finishing ability
- ii. A reliable thickness of materials that are highly resistant to deformation
- iii. Trim leather materials that can adapt to all weather conditions
- iv. Materials that can withstand close range tolerances

4 CONCLUSION

Inspections are key in maintaining and exceeding the quality standard of a manufacturing product. Therefore, inspection methodology developments are critical in automobile industry to improve on quality of products through defect detection, and data collection analysis. Also, integrated quality and reliability in manufacturing processes provide sufficient information, and active feedback from customers in manufacturing and design processes. These procedures have to be taken up to meet market quality requirements, and improve on customers satisfaction. This will make the product more competitive, through perpetual and consistent evaluation.

Inspection creates some important measures for quality reliability in enhancing a good management technique for material selection, and controlling the quality standards of the manufactured product. Also, it minimises and eradicates the number of errors by improving on the quality assurance of products, in order to achieve a defect free brand through total quality management. The feasibility of an automated inspection system is capable of detecting structural defects in car under-frames, and presents an inspection approach using machine vision techniques, including multi-scale image segmentation. The method foster a pronounce avenue for making the brand satisfactory to the customers needs by promoting the products and making the manufacturing industries to be more competitive to other world class automobile industry.

The development of this technology, in conjunction with additional preventive maintenance systems, has the potential to provide more relevant information on the car structural condition, improved utilization of car inspection and repair resources, increased training and employee safety, and improvements to overall road network efficiency of the brand.

ACKNOWLEDGEMENTS

It is my pleasure to express my profound gratitude to almighty God, for the gift of life, wisdom and understanding throughout this period of great endeavours.



My appreciation also goes to my entire family members, for their unceasing prayers, support and encouragement that kept me thus far and making this paper a reality.

I sincerely wish to appreciate the efforts of my wonderful supervisor; Engr Dr J. O. Abu for his wonderful supervision, guidance and directions throughout the period of this project. I also want to express my gratitude to the Head of Department and the entire staff of Mechanical Engineering Department, Federal University of Technology Minna. I do appreciate all your kind gestures, contributions and efforts to impact knowledge throughout the duration of this paper. In the same vein, I say a big thank you to Peugeot Automobile Nigeria Limited (PAN) Kaduna, for allowing me to carry out my experimental analysis.

In conclusion, I also wish to acknowledge my colleagues, friends and well-wishers for their wonderful encouragement and contributions throughout the pursuit of this work. May the almighty God richly bless and reward you all. Amen!

REFERENCES

- Adler, P.S. (1991). Capitalizing on new manufacturing technologies: current problems and emergent trends in US industry in *People and Technology in the Workplace*, 2, 79-103.
- Anand, S., Kopardekar, P., and Mital, A. (1993). Manual Hybrid and Automated Inspection Literature and Current Research, *Integrated Manufacturing Systems*, 4, 18-29.
- Deming, D., Taguchi, and Shahart, J. (2010). Automation and Work Design for Quality Control and Reliability, *Journal of Manufacturing Technology*, 3, 12-18.
- De-sa, A., & Zachmann, G. (1999). Virtual Reality as a tool for verification of assembly and maintenance process. *Computer & Graphics*, 23(3), 389-403.
- European Automobile Manufacturers Association. (2016). Retrieved May 21, 2016, from <http://www.acea.be/statistics/tag/category/world-production>
- Faieza, A., & Mousavi, M. (2009). A Review of Haptic Feedback in Virtual Reality For Manufacturing Industry. *Journal of Mechanical Engineering*, 40(1), 68-71.
- Farrant, A., Menassa, R., Sansome, A., and Thomas, B., (2012). Automotive manufacturing using spatial augmented reality. *The International Journal of Virtual Reality for manufacturing* 11(1), 33-41.
- Flynn, B.B., Schroeder, R., and Sakakibara, S. (1995). Determination of quality performance in high and low quality plants, *Journal for Quality Management*, 5, 9-25.
- Friedrich, W. (2002). Augmented Reality development, production and service. 1st International Symposium on Mixed and Augmented Reality (ISMAR) (3-4).
- Gusikhin, O., Rychtyckyj, N., & Filev, D. (2007). Intelligent systems in the automotive industry : applications and trends. *Knowledge and Information System*, Volume 12 (2), 147-168.
- Hou, T., Lin, L., & G, D. C. (1993). An empirical study of hybrid inspection systems and allocation of inspection functions. *International Journal of Human Factors in Manufacturing* 3(4), 351-367.
- Mital, A. (1995). Integrating humans in advanced manufacturing technology: identification and ranking of research needs, *Journal of Design and Manufacturing*, 5, 275-286.
- Mital, A., Kullarni, M., Motorwala, A., Sinclair, M., and Siemieniuch, C. (1994b). Allocation of functions to humans and machines in a manufacturing environment, *International Journal of Industrial Ergonomics*, 14, 33-49.
- Newman, T. S., and Jain, A. K. (1995). A survey of automated visual inspection, *Computer Vision and Image Understanding*, 61(2), 231-62.
- Zhou, J., Lee, I., Thomas, B., Menassa, R., Farrant, A., & Sansome, A. (2012). Manufacturing using spatial augmented reality. *The International Journal of Virtual Reality* 11(1), 33-41.



DESIGN AND FABRICATION OF BANANA FIBER EXTRACTOR MACHINE AND PERFORMANCE EVALUATION FOR THE REINFORCEMENT OF COMPOSITES

Odi Kinsley Chika¹, Ademoh N A²

¹Federal University of Technology Minna, Niger State, Nigeria

²Federal University of Technology Minna, Niger State, Nigeria

ABSTRACT

The use of many products from banana plant (pseudo stem) is becoming excessively demanding in Nigeria but the means of extracting the fibre and converting it into useful wants is tagged with various problems such as longer extraction time, poor production rate and treatment. Therefore, this study is targeted at overcoming the limitations associated with means of extracting the banana fibre and treatment that may be involved. In this work, two methods of banana fibre extraction were adopted; manual and mechanized method. Mechanical method employed involves selection of appropriate materials, design, fabrication and assembly of the various components of the machine parts. The design analysis obtained show that a 2 horse power electric motor could drive the machine efficiently. The total length of flat-belt to drive the pulley was 1.33m at an angle of lap on the smaller pulley of 2.58 rad and velocity of 4.46m/s. The resultant load of 292.2 N act on a diameter shaft of 14mm with maximum bending moment of 17.946 Nm. Also, a force of 300 N, 350 N and 400 N could pulp a corresponding thickness of banana ribs of approximately, 8.12 mm, 8.54 mm and 9.0 mm, respectively and the torque require by rolling drum to pulp rib was 25.8 Nm. The machine capacity was calculated to be 31.5 kg/per day. From the test result obtained, the banana fibre extraction machine could extract a sliced stem of maximum width of 150mm and thickness of 10 mm respectively, while the length varies. The alkaline treatment was done using 8% of sodium hydroxide (NaOH) solution.

Keywords: *banana fibre, extraction time, limitations, pseudo stem, sodium hydroxide, treatment,*

1 INTRODUCTION

Banana (*Musa paradisiaca*, family of Musaceae) is a central fruit crop of the tropical and subtropical regions of the world grown on about 8.8 million hectares (Mohapatra *et al.*, 2010). As a diet, banana is an affluent source of carbohydrate with calorific value of 67 calories per 100g fruit and is one of the most well-liked and widely traded fruits across the world (Emaga *et al.*, 2008; Kumar *et al.*, 2012). Banana plant (Scientific name: *Musa acuminata*) or plantain plant (*balbisiana* hybrids) does not only give delicious fruit but also provides quality of natural fiber. All species of banana plants have fibers in abundance and these fibers are obtained after the fruit is harvested and are in the group of bast fibers. After the fruit production, the trunk of banana plant (Pseudo stem) is thrown as agricultural waste to great extent.

These pseudo stems can be efficiently utilized in the production of good banana fiber. The pseudo stem can be profitably utilized for numerous applications and preparation of various products like bags, baskets, ropes, footwears, socks, decorative papers, floor mats, rugs, currency paper, and home furnishings can be made with banana fibre according to Mohiuddin, *et al.*, (2014).

In recent years, attention has been given to the use of banana fibres as reinforcement in thermoplastic companies because of its low density, light weight, appropriate stiffness, high disposability and renewability/ recyclability, mechanical properties and structural applications.

The traditional process such as retting method, chemical method and biological method are time consuming and may even cause damage to fibers extraction, therefore, the researcher gave much attention to mechanized techniques, processing and automated mechanism for banana fiber extraction in order to abolish manual and other methods and to improve the quality and processing time. Hence, this brought the purpose of this study which is to design and fabrication of fiber extractor machine and generation of fiber for the reinforcement of composites using banana stem (pseudo stem).

There has been lot of research on use of natural fibers as reinforcements. Banana fiber, a ligno-cellulosic fiber, obtained from the pseudo-stem of banana fiber (*Musa sapientum*), is a bast fiber with relatively good mechanical properties. Banana plant is a large perennial herb with leaf sheaths that form pseudo stem. Its height can be (3.0-8.2 meters) surrounded with 8-12 large leaves. The leaves are up to 2.7 meters long and 0.61 meter wide. Banana plant is available throughout Thailand and Southeast Asian, India,

Uganda, China, Bangladesh, Indonesia, Malaysia, Philippines, Hawaii, and some Pacific islands.

In Africa countries today, Uganda is the largest banana producer followed by Burundi, Cameroon, Kenya, Egypt, Tanzania, and Rwanda. Nigeria is among the largest banana producing countries in Africa providing about 2.73 million tons of banana per year. Also, it is the largest plantain producing country in West Africa. It is widely produced in the South and Central regions of Nigeria such as; Oyo, Edo, Ondo, Bayelsa, Delta, Akwa Ibom, Rivers, Ogun States, Cross River, Ebonyi, Abia, Ekiti, Imo, Plateau, Osun, Kogi, Anambra and Enugu. <http://www.finelib.com>

It grows easily as it sets out young shoots and is most commonly found out in hot tropical climates. All species of banana plants have fibers in abundance. These fibers are obtained after the fruit is harvested and are in the group of bast fibers. After the fruit production, the trunk of banana plant (Pseudo stem) is thrown as agricultural waste to great extent.

These pseudo stems can be efficiently utilized in the production of good banana fiber. The pseudo stem can be profitably utilized for numerous applications and preparation of various products like bags, baskets, ropes, footwear, socks, decorative papers, floor mats, rugs, currency paper, home furnishings can be made with banana fibre according to Mohiuddin, *et al.*, (2014)

However, Kulkarni *et al.*, (1983) were the first to report on the fiber yield, structure and properties of banana fibers. Subsequently, evaluated yield, structure and properties of banana fibers gathered from a few commercially cultivated varieties and observed that variations exist in both structure and properties of fibers from different regions along the length and across the thickness of the pseudo stem. They also reported differences in tensile and structural properties among fibers belonging to different varieties and showed that the matrix in which the cells are embedded in the fiber had a role in deciding the tensile strength of the fiber.

2 METHODOLOGY

The following materials and instruments were used during and after the fiber extraction

- Cutlass: This was used to cut and sliced the banana stem from the base after the fruit was harvested.
- Kitchen Knife: This was used to separate the pseudo stem to the required measurement of length and width.
- Scrapper: This was used to force the non-fibrous or banana stem tissue out, there by retaining the fiber.
- Sodium Hydroxide (NaOH): This is an alkaline reagent used to treat the fiber after production.

- Measurement Tape: This was used to determine the length and width of the banana sliced pseudo stem before fiber extractions.

Banana pseudo stems were obtained from a village called Ado Kuchi, near Nyanya/Marraba in Karu L.G.A, Nassarawa State. Both manual and mechanized methods were employed to extract the fiber. These methods were considered necessary for this study because, the traditional retting technique of extracting banana fibers is faced with various problems such as longer extraction time, high cost of locally fabricated machine and poor fiber production rate. In this research work, two methods of fiber extraction were promptly used; these are manual and mechanical method.

Manual method: This is also called hand scrapping method which involved the use of scrapper or blunt metal to scrap or force non fibrous tissues of sliced pseudo stem away by human force until fiber strands are extracted. The matured stem of the banana plant was used for the extraction of the fibers. Banana plants are usually cut down as soon as the fruits are harvested. Some harvested trunks were collected, peeled and sliced accordingly and the brown-green skin was thrown away while retaining the cleaner or white portion and then separated them manually with the aid of cutlass and knife into 60cm length and 15cm width, and these sheaths were removed, as each series of leaf sheaths produced different grade of fibers. With the use of scrapper or blunt metal edge, to force out the non-fibrous material, left with extracted fiber. Extracted fibers were sun-dried and later washed in the solution of clean water and detergent to whiten the fiber and free the knotted ones accordingly. Manual extraction of banana fiber from plant required certain care to prevent damages to the fiber.

Mechanical method: This method is the best way to obtain fiber of both quality and quantity in an eco-friendly way. The fiber extractor machine consists of a rotating drum mounted on a shaft, on the circumference of the drum mounted several blades that will create a beating action as the drum is rotated by 220V single phase electrical drive or prime mover machine. As the drum rotates, the sliced banana pseudo-stem is fed between the drum and feeding roller. Owing to the crushing, beating and pulling action, the pulpy material is removed when it is half way through. The pseudo stems are slowly pulled manually by hand from the drum and eventually, the fibers are collected.

2.1 BANANA FIBER EXTRACTION MACHINE

This is a simple machine consisting of double rollers which roll on fixed support to extract the fiber. The rollers are provided with rotating shaft, horizontal stainless-steel blades with blunt metal edges. From the designed calculation, the power required to drive the extractor was 1.210kw or 1.6HP. Therefore, two horse power (2HP) electric motor was selected as the next nearest standard

motor available in the market to drive the extractor machine. The banana fiber extractor or the decorticator machine is a machine with multiple sub-assemblies and components performing different functions. The proposed banana fiber extracting machine is shown in the figure 1 below. Sheikh S.A and Awate N.P., (2016).

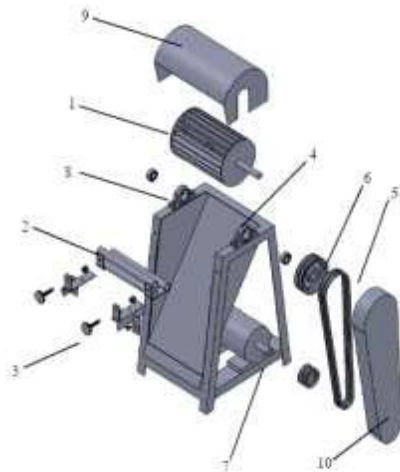


Figure 1: proposed fabricated banana fiber machine

The components parts are as follows;

- (1) Roller drum with beating blade and shaft
- (2) Inlet (3) Bearings (4) Frame
- (5) Belt Drive (6) Pulleys (7) Electric motor
- (8) Screw Guide (9) Drum Compartment (10) Belt cover.

2.2 DESIGN CALCULATIONS OF BANANA STEM

The assumption or measured values of banana stem are shown in table 1 below.

Table 1: Assumptions or measured values of banana sliced stem

Components	Values
Length of sliced banana stem	600mm
Width of sliced banana stem	150mm
Thickness of sliced banana stem	10mm
Maximum deflection of stem after feeding y	4mm
Modulus elasticity of banana stem E_b	29Gpa
Area moment of Inertial of stem, I	450mm ²

3 RESULTS AND DISCUSSION

In this work, two methods of banana fiber extraction were adopted; manual and mechanized method. Manual method involves the use of scrapper and human force while mechanical method involves the use of

electrical/mechanical machine to extract the fiber. Mechanical method employed involves selection of appropriate materials, design, fabrication and assembly of the various components of the machine parts. The design calculations were employed in the fabrication of the machine. The machine was tested to ascertain the efficient of the device. At the design stage, the computation of the length, width and thickness of the banana sliced stem were determined. The thicknesses of banana sliced stem used for this test are: 8.0mm, 7.0mm, 8.50mm, 8.54mm, 9.0mm and 10.0mm. The test was done on a steady voltage supply of 220V single phase induction motor using a stop watch to determine the extraction time. The machine capacity was calculated to be 31.5kg/per day. From the test result obtained, the banana fiber extraction machine could extract a sliced stem of maximum width of 150mm and thickness of 10 mm respectively, while the length varies. The results obtained from the test are summarized in the Table 3 below.

3.1 DESIGN OF THE MACHINE COMPONENT

The major components of the banana extractor machine such as the frame, pulley, shaft, roller drum, drum compartment, belt drive, electric motor and bearings were all designed to ensure efficiency. For instance, the motor shaft should be able to withstand the loading in motion, the frame which housed all other components should be able to withstand vibration and loads on it. The mathematical analysis of the concepts used for developing the fiber extractor machine were all proved from equations (1 – 23).

3.2 DESIGN OF THE MACHINE SHAFT

Design was done in order to safeguard against bending and torsional stresses. From equations given by Khurmi and Gupta (2008) and Shigley and Mischke (2001). The belt is to inclined at an angle of 30° to the horizontal. The forces acting on the pulley comprise of vertical and horizontal forces as follows;

(a) Forces exerted by Pulley

- (i) Vertical load acting on shaft at position of pulley,

$$F_{PV} = WP + (T_1 + T_2) \times \sin 30^\circ \quad (1)$$

Where; F_{PV} is vertical load acting on shaft at position of pulley

W_P is the Weight of pulley

T_1 is the tension on tight side of belt drive

T_2 is the tension on slack side of belt drive

- (ii) Horizontal load acting on shaft at position of pulley,

$$F_{PH} = (T_1 + T_2) \times \sin 30^\circ \quad (2)$$

Where F_{PH} is the horizontal load acting on shaft at position of pulley

(b) Vertical load on shaft exerted by Roller drum assembly F_R ,

$$F_R = W_R + F_{RT} \quad (3)$$

Where: W_R is the Weight of Roller drum.

F_{RT} is the Tangential force exerted by roller drum as a result of rotation.

F_R is the vertical load on shaft exerted by Roller drum assembly

$$F_{RT} = \frac{T}{R} \quad (4)$$

Where; T is the torque developed by the machine.

R is the radius of roller drum.

Khurmi, R.S., & Gupta, J.K. (2008)

3.2.1 Diameter of the machine shaft

Using equivalent twisting moment T_e , we have that

$$T_e = \sqrt{[(K_b \times M_b)^2 + (K_t \times T)^2]} = \frac{\pi}{16} \tau \times d^3 \quad (5)$$

Using equivalent bending moment, M_e , we have,

$$M_e = \frac{1}{2} [K_b \times M_b + \sqrt{(K_b \times M_b)^2 + (K_t \times T)^2}] \\ = \frac{1}{2} [K_b \times M_b + T_e] = \frac{\pi}{32} \sigma_b \times d^3 \quad (6)$$

Using ASME code equation; Hall et al. (2002)

$$d^3 = \frac{16}{\pi S_s} \sqrt{(K_b M_b)^2 + (K_t M_t)^2} \quad (7)$$

Where:

K_b = the Combined shock and fatigue factor for bending.

M_b = the Bending moment, Nm

M_t = the torsional moment, Nm

T = the Twisting moment or torque acting upon the shaft, N

T_e = the equivalent twisting moment, Nm

τ = the Shear stress induced due to twisting moment, Nm

πS_s = the allowable stress without keyway, N/m²

σ_b = the Bending stress induced due to bending moment an

d = the Diameter of the shaft, mm

3.2.2 Length of open belt drive

From theory of machine by Khurmi and Gupta., (2010) the expression for the length of an open belt drive is obtained as;

$$L = \pi(r_1 + r_2) + 2\chi + \frac{(r_1 + r_2)^2}{\chi} \quad (8)$$

Where;

r_1 = the radius of larger pulley

r_2 = the radius of smaller pulleys and

χ = the distance between the centres of two pulleys.

3.2.3 Velocity ratio of the belt drive

The velocity ratio of belt drive could be expressed as;

$$\frac{N_2}{N_1} = \frac{d_1}{d_2} \quad (9)$$

Where:

d_1 = the Diameter of the driver.

d_2 = the Diameter of the follower.

N_1 = the Speed of the driver in rpm and

N_2 = the Speed of the follower in revolution per minute (rpm)

Considering the thickness of the belt (t), the velocity ratio becomes;

$$\frac{N_2}{N_1} = \frac{d_1 + t}{d_2 + t} \quad (10)$$

3.2.4 Determination of angle of contact or lap

R.S. Khurmi, J.K.Gupta (2010)

The angle of contact or lap, Θ is expressed in radian (rad)

$$\Theta = (180^\circ - 2\alpha) \frac{\pi}{180} \text{ (rad)} \quad (11)$$

And the centrifugal tension T_c ,

$$T_c = MV^2 \quad (12)$$

where, M = Mass of belt per unit length in kg

V = Linear velocity of belt

3.2.5 Maximum tension on the belt

The maximum tension on the belt (T) is equal to the total tension in the tight side of the belt (T_t)

$$T = \sigma \cdot b \cdot t \quad (13)$$

Where σ is the Maximum safe stress in N/mm²

b is the Width of the belt in mm, and

t is the Thickness of the belt in mm

T_t is tension on the tight side.

$$T = T_t + T_c \quad (14)$$

$$T_t = T - T_c \quad (15)$$

where, T = Maximum tension and T_c = Centrifugal tension. Oreko et al. (2018)

3.2.6 The force or torque needed to pulp the banana rib

The modulus of elasticity E could be expressed as

$$E = \frac{fl^3}{48yl} \quad (16)$$

Where:

E = the modulus of elasticity

y = the Deflection in mm

f = the pulping force/load in N

I = the moment of inertia and

l = the length of material/ banana rib

Rearranging the equation (15), we have

$$EI = \frac{F}{48y} l^3 \quad (17)$$

where, EI is the flexural rigidity of the banana rib.

$$\text{Also, } I = \frac{B}{12} H^3 \quad (18)$$

Where: I = the moment of inertia

B = the breadth of banana rib in mm

H = the height/thickness of banana rib in mm.

3.2.7 Torque needed to pulp the banana rib

The torque required to pulp the rib is expressed as

$$T = f \times r \quad (19)$$

where, f = the force needed to pulp the banana rib

r = the radius of the rolling drum

3.2.8 Power required to drive the drum

R.S. Khurmi, J.K.Gupta (2010)

The power required to drive the rolling drum is given as:

$$P = \frac{2\pi TN}{60} \quad (20)$$

where; P = the power transmitted to shaft
T = the torque in Nm and
N = the speed of the shaft in (rpm).

3.2.9 Power Transmitted by Belt Drive

R.S. Khurmi, J.K.Gupta (2010)

The power transmitted by a belt is given as;

$$P = (T_1 - T_2)V \text{ (Watts)} \quad (21)$$

Where:

T₁ = the Tension in the tight side of belt in newton, (N)

T₂ = the Tension in the slack side of belt in newton, (N)

V = the Velocity of the belt in metre per second, m/s.

The ratio of driving tensions for flat belt drive is given as;

$$2.3 \log \left(\frac{T_1}{T_2} \right) = \mu \cdot \Theta \quad (22)$$

The above expression gives the relation between the tight side and the slack side tensions, in terms of coefficient of friction and an angle of contact.

Where:

Θ = the Angle of contact in radians and

μ = the Coefficient of friction between the belt and pulley

3.2.10 Bearings Selection

The bearings were selected base on the diameter of the shaft, load carrying capacity and the working mechanism of the machine following the SKF general catalogue and selected bearings were pressed smoothly to fit into the shaft because if hammered the bearings may develop cracks, Hall, *et al* (2002). The selected bearing number is 6206.

$$\text{Bearing Life} = \frac{60 \times N \times \text{Operating Time}}{10^6} \quad (23)$$

Where: N is the Number of revolutions.

Oreko, *et al* (2018).

3.3 DESIGN CALCULATIONS OF BANANA FIBER MACHINE

The summary of results gotten from calculated components of machine design are shown in table 2 below.

Table 2: Results of sizing design analysis

S/N	Component Name	Measure Size	Values
1	Motor pulley	Diameter (d ₁)	60mm
2	Driven pulley	Diameter (d ₂)	90mm
3	Motor pulley	Speed (N ₁)	1420rpm
4	Driven pulley	Speed (N ₂)	448rpm
5	Belt drive	Velocity (V)	4.46m/s

6	Tight side of belt drive	Tension (T ₁)	333.8N
7	Slack side of belt drive	Tension (T ₂)	448N
8	Power require by machine	Power (P)	1.210kw
9	Torque develop by machine	Torque (T)	25.8N
10	Shaft diameter	Diameter (d)	14mm
11	Belt drive	Thickness	12mm
12	Power transmitted by motor	Power (P)	1.6 = 2hp
13	Force need to pulp the rib	Force (N)	286.76N
14	Weight of pulley	Weight (N)	19.62N
15	Centre of pulleys	Distance, x	450mm
16	Belt drive	Length (L)	1.33mm
17	Motor pulley	Angle of lap (Θ)	2.58rad
18	Mass of the belt drive	Mass (M)	0.07127kg/m
19	Driving pulley	Radius (r ₁)	30mm
20	Driver pulley	Radius (r ₂)	95mm
21	Load on shaft	Vertical (F _{pv})	263.42N
22	Load on shaft	Horizontal (F _{ph})	243.8N
23	Bending moment	Resultant (RBM)	17.946Nm
24	Roller drum	Radius (r)	90mm
25	Roller drum	Weight (wt)	92.2N
26	Force pulling motor at slop	Force (N)	66.22N
27	Power transmitted by belt drive	Power (P)	802.8W
28	Centrifugal tension on belt	Tension (T)	1.42N
29	Maximum tension on belt	Tension (T)	335.2N

3.4 DESIGN BANANA FIBER MACHINE TEST

The analysis of the test run result of design and fabricated banana fiber machine are computed in table 3 below.



Plate I: front view of designed banana fiber machine

The view of a complete design and fabricated banana fibre machine is shown in plate 1 above shows the view of designed and fabricated banana fiber machine.

S / N	Vol (V)	Length (mm)	Width (mm)	Thickness (mm)	Extracting time (s)
1	220	100	30	8.00	12
2	220	150	30	7.00	13
3	220	300	80	8.50	22
4	220	350	86	8.54	24
5	220	550	100	9.00	29
6	220	600	150	10.00	32

Table 3: Test run result of banana fiber machine

$$\text{Machine average extracting time} = \frac{\text{Total value of extracting time}}{\text{number of test run activity}}$$

$$= \frac{132}{6} = 22$$

Therefore, the average extracting time for fiber machine extractor is 22 seconds

4 CONCLUSION

The design and fabrication of banana fiber extraction machine was achieved with higher efficiency. This machine will reduce manual extraction time and is suitable for mass production. It is portable and easy to maintain, assemble and disassemble by the operators. The factors affecting quality of fiber are roller speed, feed angle and clearance angle also affect the production quantity of fiber. During the design and fabrication of this machine, all these aforementioned factors were considered. By considering these factors effectively, the qualities and quantities of production of fiber could be increased. The design analysis obtained show that a 2 horse power electric motor could drive the machine efficiently. The total length of flat-belt to drive the pulley was 1.33m at an angle of lap on the smaller pulley of 2.58rad and velocity of 4.46m/s. The resultant load of 292.2N act on a diameter shaft of 14mm with maximum bending moment of 17.946Nm. Also, a force of 300N, 350N and 400N could pulp a corresponding thickness of banana ribs of approximately, 8.12mm, 8.54mm and 9.0mm, respectively and the torque require by rolling drum to pulp rib was 25.8Nm. The machine capacity was calculated to be 315kg/per day. From the test result obtained, the banana fiber extraction machine could extract a sliced stem of maximum width of 150mm and thickness of 10 mm respectively, while the length varies. The alkaline treatment was done using 8% of sodium hydroxide (NaOH) solution to increase mechanical properties.

ACKNOWLEDGEMENTS

My most sincere gratitude goes to Almighty God, the most beneficent, the giver of life, the wiser than the wisest, the greater than the greatest, the Mightier than the Mightiest, the better than the best, the merciful father for giving me life, guiding and providing all that I needed to make my course of study a huge success despite all odds.

My profound gratitude goes to Hamstring Engineering Company Minna, Niger State for their effort, invaluable assistance and encouragement throughout the research work and to Mr Clement the owner of the banana farm at Nyanya/Marraba in Karu L.G.A, Nassarawa State.

To be candid, I must appreciate the effort of HOD, Mechanical Engineering and the others staff in Mechanical Engineering Federal University of Technology, Minna for providing the necessary academic background that metamorphosed into the academic adventure.

To God be the Glory..... Amen!!!

REFERENCES

- Das P.K., Nag D., Debnath S., and Nayak L.K., (2008) Machinery for extraction and traditional spinning of plant fibres, National Institute of Research on Jute & Allied Fibre Technology, ICAR, 12, Regent Park, Kolkata 700 040, West Bengal.
- Emaga, T. H., Andrianaivo, R. H. Wathelet, B.Tchango, J. T. and Paquot, M (2008). "Effects of the stage of

- maturation and varieties on the chemical composition of banana and plantain peels” *Food Chemistry*, 103: 590-600.
- Food and Agricultural Organization (FAO), Geneva, (2009); www.fao.org/production/faostat.
- Hall, A.S., Holowenko, A.E., and Laughlin, H.G. (2002). *Schaum’s outline series theory and problems of machine design*. (1st ed.). New York; McGraw-Hill Companies Inc., p12-22,113-115.
- Kumar S.S., Anbumalar .V. (2015); A literature review “selection and evaluation of natural fibers” Department of Mechanical Engineering, Velammal College of Engineering and Technology, Madurai, Tamil Nadu, India. *International Journal of Innovative Science, Engineering & Technology*, Vol. 2 ; ISSN 2348 – 7968.
- Kumar S.S., Anbumalar .V. (2015); A literature review “selection and evaluation of natural fibers” Department of Mechanical Engineering, Velammal College of Engineering and Technology, Madurai, Tamil Nadu, India. *International Journal of Innovative Science, Engineering & Technology*, Vol. 2 ; ISSN 2348 – 7968.
- Khurmi, R. S. and Gupta, J. K. ((2010). *A Textbook of Theory of Machine*, (latest Edition). S. Chand publishing House (PVT) Ltd. Ram Nagar, New Delhi, India. 110-055., p325-360.
- Khurmi, R. S. and Gupta, J. K. ((2013). *A Textbook of Machine Design*, (8th Edition). New Delhi; Eurasia Publishing House (PVT) Ltd, 365-369.
- Mohapatra, D., Mishra, S. and Sutar, N. (2010). Banana and its by-product utilization: an overview. *Journal Scientific & Industrial Research*, 69: 323-329.
- Mohiuddin A.K.M., Saha, M.K., Hossain, M.S. and Ferdoushi, A. 2014. Usefulness of banana bio-products: A review from the agriculturists, 12(1): 148-158.
- Mohiuddin A. K. M., Manas Kanti Saha, Md. Sanower Hossian and Aysa Ferdoushi (2014); A Review on Usefulness of Banana (*Musa paradisiaca*) Wastes in Manufacturing of Bio-products, *A Scientific Journal of Krishi Foundation, The Agriculturists* 12(1): 148-158.
- Mukhopadhyay, S., Fanguero, R., Yusuf, A. and Senturk, U. 2008. Banana fibers variability and fracture behaviour. *Journal Engineered Fibres and Fabrics*, 3(2): 39-45.
- Oreko B. U., Okiy S., Emagbetere E., and Okwu M. (2018). “Design and development of plantain fibre extraction machine”. Faculty of Engineering, University of Nigeria, Nsukka. Vol. 37, No. 2, pp. 397 – 406.
- Rahamaththulla, S., Premnath, S., Ravi, V., S. Madheswaran, N. Jayakumar., (2018), Design and Fabrication of Banana Fiber Extracting Machine, *International Journal for Scientific Research & Development*, Bannari Amman Institute of Technology, India. ISSN (online): 2321-0613, P390 – 393.
- Sheikh, A.S. and Awata, N. P. (2016) “A Review Paper on Design and Development of Banana Fibre Extraction Machine”. *International Journal of Engineering Sciences and Research Technology*, Vol. 3, 841-846
- Shigley, J.E., and Mischke, C.R (2001). *Mechanical Engineering Design*. (6th edition). New York; McGraw-Hill Companies, Inc.



OPTIMISATION OF BIODIESEL PRODUCTION FROM SANDBOX (*HURA CREPITANS*) SEED OIL

*Usman M., Adebayo S., Aliyu M. Dauda, S. M.,
Agricultural and Bioresources Engineering Department, Federal University of Technology,
PMB 65 Minna Niger State, Nigeria

*Corresponding author email: moh.usman@futminna.edu.ng

ABSTRACT

Transesterification reaction is the most common method of biodiesel production from fats or vegetable oil. In this research, Sandbox (*Hura crepitans*) seed oil is used as feedstock extracted by solvent extraction using N-hexane as solvent. The study evaluates properties of the oil for its suitability in biodiesel production, biodiesel yields as it is affected by the reacting conditions such as methanol-oil molar ratio, reaction temperature, catalyst concentration and reaction time, the reaction conditions are optimized using a two-step four factor factorial design. Results indicate that the feedstock is suitable for biodiesel production, catalyst concentration and reaction times interaction are the important factors that has greater effect on the yield of ethyl ester. The optimum yield condition for Sandbox (*Hura crepitans*) were 0.2wt/wt molar ratio, 30°C temperature, 0.4wt% catalyst concentration and 60 min reaction time yielding 93% ethyl ester (biodiesel), and all the measured properties of Sandbox (*Hura crepitans*) of biodiesel met with ASTM6751 standard exception of high polarization rate and slightly high viscosity that can be normalized by appropriate blending. The result showed that only molar ratio showed a negative effect on the reaction. Hence adhering to the standards for high quality biodiesel and economically cheap production process.

Keywords: Biodiesel; Process Optimization; Renewable Energy; Sandbox

1 INTRODUCTION

Hura crepitans seed which is highly rich in non-edible oil which falls into group of underutilized species of plants. *Hura crepitans* commonly known as sand box, possum wood, monkey no climb or dynamite tree is about 25m tall with very spiny trunk and branches and it is commonly planted as shade (Okolie *et al.*, 2012), it has gained much attention as a feedstock for biodiesel production (Srivastava *et al.*, 2018).

In the world today, there is ever increasing demand for petroleum resource, although, high speculations concerning its dwindling supplies, unstable price, non-renewable nature and environmental problems has led to an extensive research on the seek for the alternative resource attributes of the petroleum as the most important source of energy (Nakpong and Wootthikanokkhan, 2010).

There are four ways in which vegetable oils and fats can be converted into biodiesel namely; transesterification, blending, micro-emulsions and pyrolysis (Verma and Sharma, 2016; Silitonga *et al.*, 2018). The most common method to produce biodiesel is transesterification of vegetable oils and animal fats in the presence of a catalyst such as acid, alkali or enzyme (Gashaw and Lakachew, 2014; Rodionova *et al.*, 2017). This is due to complications faced in biodiesel production of the presence of Free

Fatty Acids (FFAs) in non-edible oils. Adoption of homogeneous base catalyst, results in formation of soaps causing strenuous separation thus decreasing ester yield (Marchetti *et al.*, 2007). Therefore, high FFA feedstock, acid catalyst is preferred to produce biodiesel, but it demands more reaction time and alcohol (Meher *et al.*, 2006). For oils or fats having high FFA acid esterification is advantageous, as acid catalyze the FFA esterification to produce fatty acid methyl ester (FAME). (Verma and Sharma, 2016) Moreover, Type of alcohol, molar ratio and reaction time play significant role in biodiesel yield and its properties. literature are available on optimisation of process variables of biodiesel production from different oils using Response Surface Methodology (RSM) but little work is reported particularly on Sandbox seed oil and comparison of impact of different alcohols on biodiesel production to optimize the reaction parameters.

Saydut *et al.*, (2016), used RSM to optimise biodiesel production from sunflower oil, Ethanol was used as alcohol for transesterification reaction and highest yield of 97.8% was obtained which was close to predicted yield of 99.2%. Galeano *et al.*, (2017) produced biodiesel from palm oil on ethanolysis using 0.2–1 wt.% NaOH at temperature between 60 and 80 C and ethanol to oil molar ratio 6:1. Highest yield of 96% with 100% conversion of fatty acids into



methyl esters was obtained on 1 h of reaction. Avramović et al., (2015) produced fatty acid ethyl esters from sunflower oil with yield of 95% on using heterogeneous catalyst Calcium zincate at 78 °C reaction temperature. Yatish et al., 2016 optimised sunflower biodiesel production with RSM technique and achieved yield of 98.6% which was well close to predicted value of 98.9%. Optimum reaction conditions found were temperature in range of 50–59 °C ethanol-to-oil molar ratio of 12:1, 0.75% catalyst and reaction time of 15 min. Keera et al., (2018) did ethanolysis of castor and soybean oils and found out yield more than 90% for soybean oil biodiesel and around 30% for castor biodiesel. Avramović et al., (2015) applied RSM to ethanolysis of sunflower oil for production of biodiesel and obtained good relation between predicted and actual values of yield obtained with 93.7% accuracy. applied a response

surface methodology to determine the optimum condition for the production of biodiesel production from *Raphanus sativus* using two levels three factor experimental design (2³ experimental design): the ethanol:oil molar ratio (6:1 and 12:1), the catalyst concentration in relation to oil mass (0.4 and 0.8 wt% NaOH) and the alcoholysis temperature (45 and 65 °C), this process yield 95.8% methyl ester. From the above literature, it is noted that, there has been limited study on the use of non-edible feedstock (*Hura crepitans*) and optimization of reaction parameters on biodiesel production.

Table 1: A summary of applications of transesterification for biodiesel production

s/no	Method	Material	Conditions	References
1	Methanolysis (Complete Factorial design)	Palm oil	0.2-1wt% NaOH, 60oC - 80oC and 0.1 mole ratio	Narvaez et al, Rubio-Caballero et al, Nie et al, 2006, Thliveros et al., 2014
2	Heterogeneous catalysis (RMS)	Sunflower	50–59 oC and 12:1 Mole ratio	Vujicic et al., 2010, Lee et al., 2014, lee and Wilson, 2015
3	Ethanolysis (RMS)++	castor and soybean oils	-	da Costa Barbosa, 2010, Caldas et al., 2016
4	Alcoholysis (RMS)	<i>Raphanus sativus</i>	6:1 and 12:1 mole ratio, 0.4 and 0.8 wt% NaOH and 45 and 65 °C temperature.	Domingos and Saad, 2008
5	Ethanolysis (RSM and ANN)	<i>Sunflower</i>	50 and 59 °C, 12:1 mole ratio, catalyst loading of 0.75% and reaction time of 15min	Stamenković et al., 2013

2 Materials and Methods

Sandbox seed were collected from Okene in Kogi state, all chemicals such as KOH, alcohols, Sulphoric acid, N-Hexane methanol and ethanol were of AR grade and 99% pure and were purchased from Tunga market in Minna, Niger state.

2.1 Materials Pretreatment

The raw sand box seed collected is removed from husk casing dried in an electric oven for about 24hr at about 65°C to enhance crushing of the seed in order to reduce the size and provide increased contact between the seed the solvent during the extraction process.

Experimental Setup

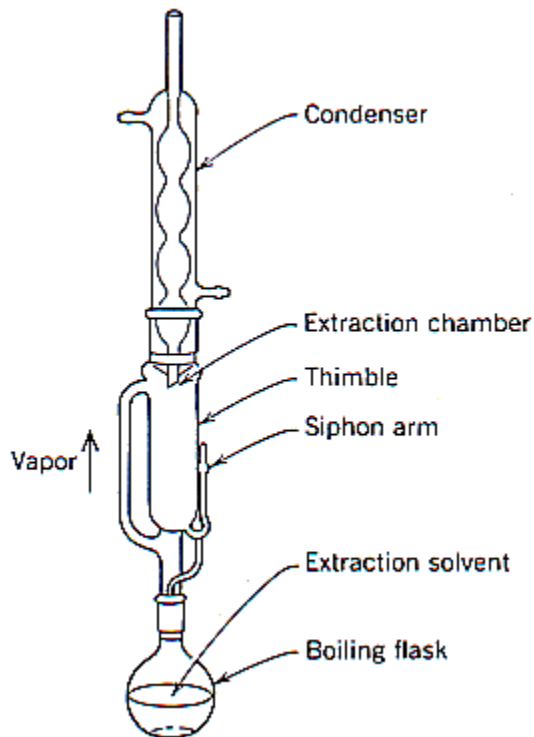


Fig 2.1: Experimental set up for extraction of oil from sandbox seed

The extraction of oil was done using soxhlet extractor, the soxhlet extraction is a set up with the reflux condenser which cools the vapor to convert it to liquid. Weight of the filter paper and stepping pin are taking as (W_1). The samples were then wrapped in filter paper and stepped, the weight of the filter paper, stepping pin and the sample is taking as (W_2). soxhlet extractor uses a method in which the material to be extracted is placed in the extraction chamber which is soaked by the condensed solvent, it dissolves the oil from the sample a for a period of time, the solvent is then removed and replaced with a fresh one, the whole set-up was put on a heating mantle that provides heat which gently heats up the solvent. After each run, the sample was dried for 10 minutes and weighed (W_3). The percentage oil yield is calculated from the formula below;

$$\text{Weight of extracted oil} = (w_2 - w_1) - (w_3 - w_1) \quad (3.1)$$

Where,

W_1 = Weight of the filter paper and the stepping pin

W_2 = Weight of the sample, filter paper and the stepping pin

W_3 = Weight of sample, filter paper and stepping pin after extraction.

The solvent was recovered from the extract by distillation using the soxhlet extractor. This was done by removing the thimble from the upper of the extractor, then the mixture of the solvent and the extracted oil in the round bottom flask was heated to 30-35°C, at this temperature N-hexane which has the boiling point 40 °C will evaporate with the aid of water cooling condenser, the solvents were collected in a flask separately from the extracting column, while the oil will be collected in the round bottom flask.

2.2 Analytical Procedure

The oil sample extracted from sandbox seed is analysed for kinetic viscosity, specific gravity, saponification value, free fatty acid content, peroxide value, iodine value and refractive index to ascertain its suitability for biodiesel production. The biodiesel produced is also characterized for its suitability in internal combustion engine, parameters analysed were; viscosity, specific gravity, pour point, flash point, cloud point, acid value cetane number and iodine value.

2.3 Design of Experiment

A factorial design, was employed using four variables to analyse the response patterns and optimise the process variables. The effect of the A (reaction temperature (C)), B (molar ratio of alcohol to oil), C (catalyst concentration (wt.%)) and D (reaction time (min)) at three variable levels in the reaction process is shown in Table 2. A total of 16 experiments were conducted separately for getting the experimental response of yield of sand box oil methyl ester (FAME). The above variables were independent variables selected for optimisation. The experimental matrix is shown in table 3.

Table2: Factorial Design Levels

Variable	Symbl	Levels		
		- α	0	+ α
Mole ratio	A	0.2	0.35	0.5
Temperature	B	30	45	60
Catalyst con.	C	0.25	0.3	0.4
Reaction time	D	30	45	60



Table 3: Design Matrix and Responds

Run No.	Ethanol: oil ratio [wt/wt]	Temperature [°C]	Catalyst conc [wt%]	Reaction time [s]	Ethyl ester conc [wt%]
1	0.2	30	0.25	30	90.00
2	0.5	30	0.25	30	89.16
3	0.2	45	0.25	30	88.88
4	0.5	45	0.25	30	89.44
5	0.2	30	0.4	30	93.81
6	0.5	30	0.4	30	87.69
7	0.2	45	0.4	30	96.44
8	0.5	45	0.4	30	90.55
9	0.2	30	0.25	60	88.32
10	0.5	30	0.25	60	94.87
11	0.2	45	0.25	60	90.00
12	0.5	45	0.25	60	87.75
13	0.2	30	0.4	60	89.44
14	0.5	30	0.4	60	86.60
15	0.2	45	0.4	60	88.32
16	0.5	45	0.4	60	85.44

The Design Expert 9.0.6.2 software was used for the regression and graphical analysis of the data. The highest value of biodiesel yield was taken as the response of the design experiment for transesterification process. The experimental data obtained by the above procedure were analysed by the factorials design and the general model were developed following the polynomial function equation 1 and 2

$$Y = b_0 + \sum_{i=1}^n b_i X_i + \sum_{i=1}^n b_{ii} X_i^2 + \sum_{I=1}^{j-1} \sum_{j=1}^n b_{ij} X_j X_I \quad 1$$

$$Y = b_0 + b_1 A + b_2 B + b_3 C + \dots \quad 2$$

4.0 Results and Discussion

4.1 Characterization of Sandbox (*Hura crepitans*) seed oil

Sandbox (*Huracrepitans*) seed oil were used as the biodiesel feedstock in this research, the properties such as Kinetic Viscosity, specific gravity, free fatty acid, acid value, peroxide value and saponification of the oil were determined to confirm it suitability for biodiesel production as shown in Table 1. The colour of the oil is golden yellow. The oil yield from the seed is 54.4%, this is although higher than oil yield from coconut seed but less than yield from ground nut seed and palm oil (Kareem et al., 2017) The specific gravity is 0.91 which is slightly less than 0.93 for Jatropher and higher than 0.89 for palm

karnel (Musa and Folorusho, 2012; Beccles, 2013). the kinetic viscosity is the measure of resistance of the oil to flow when it is subjected to shear stress (Kareem et al., 2017), the value obtained is 19.69 mm²/s at 40°C which is less than 29.8 mm²/s obtained for coconut and 30.1 mm²/s for palm karnel (Gillies et al., 2012; Krishnan and Dass, 2012), this indicate that the biodiesel from this oil will have better atomized injection in internal combustion engine. the saponification value of the oil is 207.57 mg KOH/g slightly lower than the value obtained by (Otoikhian et al., 2016) for sesame and Orodu et al., for pineapple peel, while greater than (190 mg KOH/g) for Jatropher, (193.55 mg KOH/g) (Umaru et al., 2016) less than (250 mg KOH/g) for crude palm karnel (David and Julius, 2010) it is determinant of the degree of soap formation by the oil during esterification, this value thus indicate high tendency of soap formation instead of biodiesel formation, this will best be corrected using two step reaction. Free Fatty acid composition of the oil is 12.342 and is higher than value for 1.189 for palm karnel Krishnan and Dass, 2012), which is also in line with other report (Otoikhian et al., 2016). Free Fatty acid are unattached fatty acid in fat and oil unrefined oil contains high percentage of Free Fatty acid but reduces through refining process, high value of free fatty acid interfere with separation of fatty acid and glycerol during transesterification leading to unsatisfactory conversion to biodiesel. (Beccles, 2013).



Table 4.: Physico-Chemical Properties of *Hura crepitans* Seed Oil

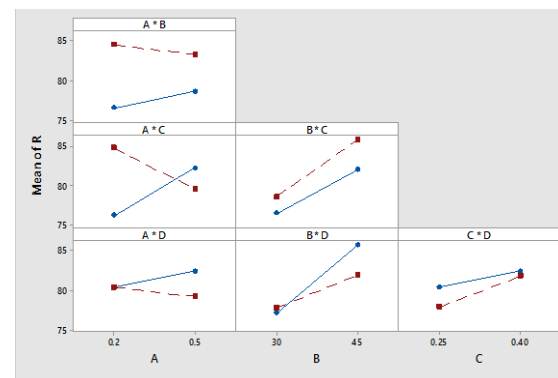
Properties	Obtained Values
Colour	Golden Yellow
Percentage Yield (%)	54.4
Kinetic Viscosity at 40°C [mm ² /s]	19.690
Specific Gravity at 30°C	0.911
Saponification Value (mg KOH/g)	207.57
Free Fatty Acid (as oleic acid; %)	12.342
Peroxide Value (mg Eq/kg)	4.400
Iodine Value (g/100)	163.510
Refractive Index	1.463
Acid Value (mg KOH/g)	24.684

Peroxide value obtained in this research is 4.40 mg Eq/kg, it is slightly greater than (4.073Eq/Kg) and lesser than (6.327±0.006Eq/Kg) for almond nut and frytol respectively (Al-Bachir, 2014). Fresh oils have peroxide values less than 10mEq/kg. The low values of Peroxide value are indicative of low levels of oxidative rancidity of the oils and also suggest high levels of antioxidant, peroxides are possibly not directly responsible for the taste and odour of rancid fats, their concentration is often useful in assessing the extent to which the rancidity has advanced (Atsu Barku *et al.*, 2012), Barku *et al.*, (2012) conclude that a rancid taste often begins to be noticeable when the Peroxide Value is above 20 Eq/kg. Iodine value 163.510 shows high degree of un-saturation of the oil and this categorize it under semi-drying group (iodine value > 100 and <130), which fall within range of iodine value obtained for corn oil (115-130) (Atsu Barku *et al.*, 2012) with sharp difference from (8-10) for coconut and (14-22) for palm kernel (Kareem *et al.*, 2017). The value obtained in this research suggest that the oil is inedible as accumulation of iodine in the body leads to development of goiter, and the oil can be used in production of shoe polish and alkaline resin. (Musa and Folorusho, 2012). Refractive index is 1.463 this value is low compare to other drying oil (1.47) and

(1.48) (Abiodun, *et al.*, 2014). It is attributed to the nature of the fatty acids present since refractive index decreases with the molecular weight of the fatty acids. It can also be related to its lower iodine value since refractive index decreases with unsaturation. Acid value defined as the amount (mg) of KOH necessary to neutralize the FFA in 1g of oil or fat sample 24.684 This high value may be due to the moisture contents, refining and deodorization processes. The value obtained is very high compared to palm oil (14.04mgKOH/g), cashew nut oil (0.82mgKOH/g) and rape seed of 7 mg KOH/g stated by Atsu Barku *et al.*, (2012).

4.2 Optimization of Biodiesel Production

Fig 2.11 showing the effect trends and interactions of the factor variables, this plots indicates level of



significance in factor reactions, only factor A*B (mole ratio and reaction temperature) and B*C (reaction temperature and catalyst concentration) show insignificant level of interaction. While other interactions are significant. This however provides basis for model assumption.

Fig2.11: Effect plot of interaction between factor R= yield of the (wt%), A =Methanol oil ratio, B is Temperature (°C), C is Catalyst Concentration (wt%), and D is Reaction time(Sec)

Table 4.2: analysis of the variance table

S/N	Factor	Factor Effects	Coef	Sum of square	Df	Mean Square	F-Value	P-value (%)
	Consta			80.7				
	nt							
1	A	-3.1	-1.5	31.9	1	31.9	13.8	10.3
2	B	1.8	0.6	6.8	1	6.8	2.9	2.2
3	C	5.6	2.8	108.16	1	108.1	46.6	34.7
4	D	6.6	3.3	160.0	1	160.0	68.9	51.3

5	AB	1.1	0.5	2.56	1	2.6	1.09	0.80
6	AC	-1.5	-0.8	6.76	1	6.8	2.9	2.2
7	BC	-0.4	-0.2	1.82	1	1.8	0.8	0.6
8	BD	0.7	0.5	1.96	1	1.8	0.8	0.6
9	CD	2.8	1.4	31.3	1	2.0	31.1	10.1
10	ABC	-0.4	-0.2	1.8	1	31.6	0.8	0.6
11	ABD	1.9	0.9	11.6	1	11.6	4.8	3.7
12	ACD	-1.5	-0.8	6.9	1	6.9	2.9	2.2
13	BCD	0.9	0.5	5.5	1	5.5	2.3	1.8
14	ABCD	1.9	0.9	10.6	1	10.6	4.4	3.2

The experimental data in table 4.1 were analyzed with Mini-tab statistic software on all four process variables in which catalyst concentration and reaction time show most significant effect as shown in Figure 4.0 and their interactions. The experimental result was then fit to regression model equation for predicting the yield. Where Y is the respond, A, B, C and D are coded independent variable.

The predicting model equation

Y is the respond, and the coded variables are A = 0.2-0.5 (wt/wt), B=30-45 (oC), C=0.25-0.4 (wt%) and D= 30-60 (min). the regression model for the response (Yield) is govern by the equation:

$$Y = 80.75 - 1.54A + 0.53B + 2.73C + 3.29D + 0.53AB - 0.78AC - 0.46BC + 0.23BD + 1.53CD - 0.21ABC + 0.98ABD - 0.73ACD + 0.46BCD + 0.96ABCD$$

$$(R^2 = 0.785) (R_{adj}^2 = 0.74)$$

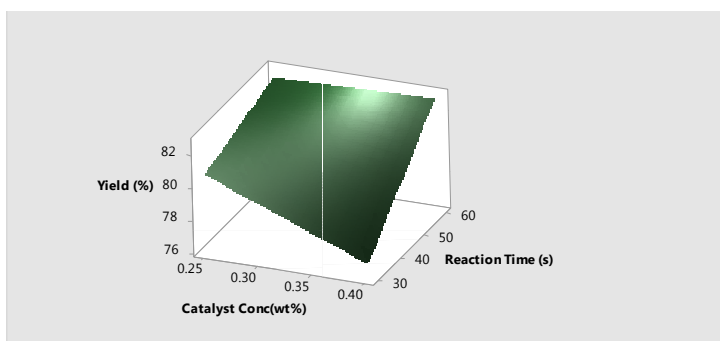


Figure 4.0: Influence of Catalyst concentration and reaction time on ethyl ester yield

This factor exhibits great positive effect on yield of biodiesel, the methyl ester yield increases with increasing time of reaction, this is possibly due to increased mixing of the ethanol in oil with time which is in accordance with (David *et al.*, 2010). Increased molar concentration inhibits the formation of more ethyl ester as indicated in Figure 4.0. But on the other hand, unnecessary prolong of the reaction

time leads to the hydrolysis of ester resulting on more formation of free fatty acid.

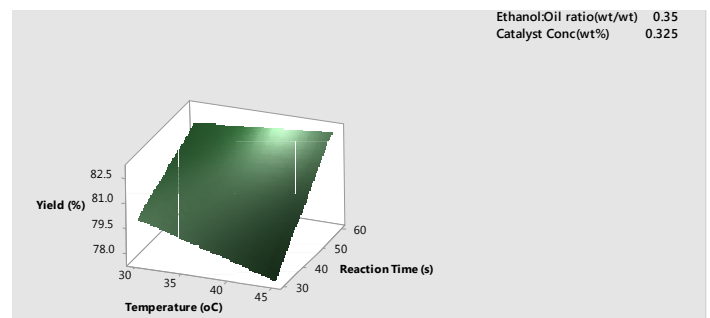


Figure 4.2: Influence of temperature and reaction time on Ethyl ester yield

Temperature has a very slight positive effect or influence on yield of biodiesel, making it possible to operate at low (room) temperature 30°C this is because increasing temperature leads to decrease in ethyl ester yield which is attributed to the formation triglyceride saponification and decomposition of unsaturated methyl esters and unreacted triglycerides in methanol at high temperature.

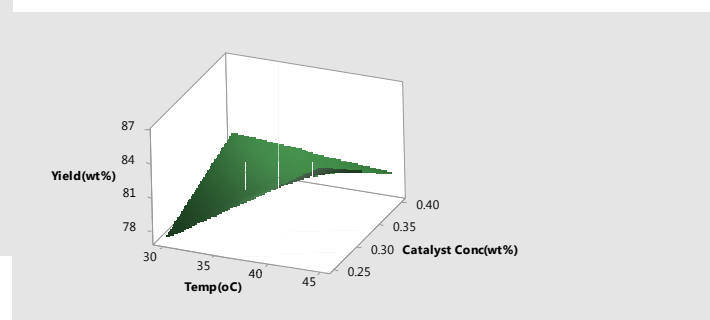


Figure 4.3: Influence of catalyst concentration and reaction time on the ethyl ester yield

The methanol to oil ratios show negative effect, this is obviously an indication of a decrease molar yield with increase molar ratio. This is due to the restriction of the reaction equilibrium and difficulties in separating excessive methanol from methyl esters and glycerol as such

0.2mole with yield 93% is the optimum molar concentration for the production of the biodiesel.

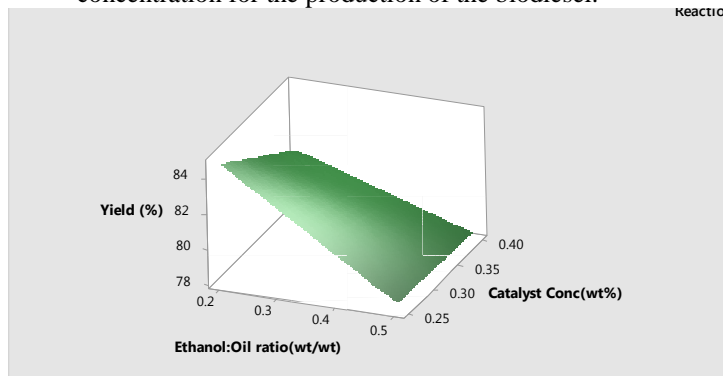


Figure 4.4: Influence of Molar ratio and catalyst concentration on ethyl ester yield

The molar ratio has a significant negative effect on the yield of biodiesel, increase concentration of potassium hydroxide other hand does not significantly affect yield of the biodiesel, though slightly increases the amount of free fatty acid produced through saponification.

4.4 Effect of Interactions

Catalyst and reaction time has significant positive effect on the biodiesel yield responses, this is due to action of catalyst in increasing the polarity of the feedstock with increasing time making the reaction mixture more susceptible to reaction producing more of yield of the biodiesel.

4.5 Biodiesel Characterization

The biodiesel were also characterized for properties such as specific gravity 0.93 which is though less than the ASTM D6751 standard which indicates the degree of impurity in the biodiesel such as water content and fatty acid composition, Viscosity at 40°C is 6.67mm/s² which are less than that of the oil by one sixth due to alkaline methanolysis that reduces the viscosity, the viscosity is slightly greater than ASTM D6751 biodiesel standard, which signifies there will formation of deposits in the internal combustion engine, clogging of the injector nozzle and production of dark exhaust gas, an heterogeneous alkaline catalysis will enhance a good viscosity (Nakpong and Wootthikanokkhan, 2010), though the value obtained compares relatively with (4.45mm²) for palm oil and (4.05mm²) for ground nut oil (Abiodun, et al., 2014). The flash point is the minimum temperature at which a liquid gives off enough vapour that is sufficient to form an ignitable mixture with air near its surface, the obtained in this research is 185°C which is in the range of ASTM D6751 standard, and is greater than (130°C) for Coconut and (174°C) for Palm oil (Abiodun, et al., 2014), The flash point of pure biodiesels is considerably higher than the prescribed limits, but can decrease rapidly with increasing amount of residual alcohol. As these two aspects are strictly correlated, the flash point can be used as an indicator of the

presence of methanol in the biodiesel. (Atsu Barku et al., 2012). Cloud point is particularly important as it relates to the length and degree of saturation of the fatty acid components of the oil, the temperature at which clouds of wax crystals first appear in the liquid when cooled. -5°C is obtained for conformity with the ASTM6751 standard, the parameter estimates the degree of saturation of the biodiesel. Minimum operating temperature in internal combustion engine of the biodiesel is determined by pour point which is -16°C for this research which is in conforming with the ASTM6751, insusceptibility to gel or crystallization, the problem of high pour point can be addressed by blending of the biodiesel (Saydut *et al.*, 2016). Acid value is 23.964 mgKOH/g, this value is greater than ASTM6751 standard, and is greater than value reported by (Silitonga *et al.*, 2018) this indicate high polymerization rate with the degree of unsaturation of the fatty acids. Cetane number is 51.251 which is slightly higher than (50 max) for conventional diesel and within the range of the ASTM6751 biodiesel standard, since it is the measure of a fuel's willingness to ignite when it is compressed. It rates the ignition potentials of a diesel fuel, just as octane number determines the quality of gasoline (petrol). The higher the Cetane number, the more efficient is the fuel biodiesel has a higher Cetane number than petroleum diesel because of the presence of oxygen molecules (Opra and Obot, 2009), hence this biodiesel has higher ignition potential than conventional diesel. The iodine value measures the degree of unsaturation and tendency of biodiesel to polymerize, high iodine value means high degree of unsaturation, value obtained is 141.00 g/100 which is slightly greater than (121.19±0.01 g/100) for fryol (Atsu Barku et al., 2012). Biodiesel with high IV tends to polymerize and form deposits on injector nozzles, piston rings and piston ring grooves. The tendency of polymerization increases with the degree of unsaturation of the fatty acids.

5.0 CONCLUSION

Sandbox (Hura crepitans) seed oil have a high value of saponification value, and relatively low acid value, density and viscosity which are characteristics that determine suitability of the oil for biodiesel production.

- Catalyst concentration and reaction time show highest percentage contribution effect on the transesterification process and subsequently on ethyl ester yield
- Increasing reaction time and catalyst concentration increases the ethyl ester yield with decreasing molar ratio and temperature.

REFERENCES

- Abiodun, O. A., Akinoso, R., Olosunde, O. O., Adegbite, J. A., & Omolola, O. A. (2014). Nutritional quality and essential oil compositions of *Thaumatococcus danielli* (Benn.) tissue and seed. *Food chemistry*, 160, 286-291.

- Al-Bachir, M. (2014). Physicochemical properties of oil extracts from gamma irradiated almond (*Prunus amygdalus* L.). *Innovative Romanian Food Biotechnology*, 14.
- Avramović, J. M., Veličković, A. V., Stamenković, O. S., Rajković, K. M., Milić, P. S., & Veljković, V. B. (2015). Optimization of sunflower oil ethanolysis catalyzed by calcium oxide: RSM versus ANN-GA. *Energy Conversion and Management*, 105, 1149-1156.
- Avramović, J. M., Veličković, A. V., Stamenković, O. S., Rajković, K. M., Milić, P. S., & Veljković, V. B. (2015). Optimization of sunflower oil ethanolysis catalyzed by calcium oxide: RSM versus ANN-GA. *Energy Conversion and Management*, 105, 1149-1156.
- Barku, V. A., Nyarko, H. D., & Dordunu, P. (2012). Studies on the physicochemical characteristics, microbial load and storage stability of oil from Indian almond nut (*Terminalia catappa* L.). *Studies*, 8.
- Barku, V. A., Nyarko, H. D., & Dordunu, P. (2012). Studies on the physicochemical characteristics, microbial load and storage stability of oil from Indian almond nut (*Terminalia catappa* L.). *Studies*, 8.
- Beccles, R. (2013). Biofuel as the solution of alternative energy production. *Future of Food: Journal on Food, Agriculture and Society*, 1(1), 22-26.
- Caldas, B. S., Nunes, C. S., Souza, P. R., Rosa, F. A., Visentainer, J. V., Oscar de Olivera, S., & Muniz, E. C. (2016). Supercritical ethanolysis for biodiesel production from edible oil waste using ionic liquid [HMim][HSO₄] as catalyst. *Applied Catalysis B: Environmental*, 181, 289-297.
- da Costa Barbosa, D., Serra, T. M., Meneghetti, S. M. P., & Meneghetti, M. R. (2010). Biodiesel production by ethanolysis of mixed castor and soybean oils. *Fuel*, 89(12), 3791-3794.
- Domingos, A. K., Saad, E. B., Wilhelm, H. M., & Ramos, L. P. (2008). Optimization of the ethanolysis of *Raphanus sativus* (L. Var.) crude oil applying the response surface methodology. *Bioresource Technology*, 99(6), 1837-1845.
- Galeano, J. D., Mitchell, D. A., & Krieger, N. (2017). Biodiesel production by solvent-free ethanolysis of palm oil catalyzed by fermented solids containing lipases of *Burkholderia contaminans*. *Biochemical engineering journal*, 127, 77-86.
- Gashaw, A., & Lakachew, A. (2014). Production of biodiesel from non-edible oil and its properties. *International Journal of Science, Environment and Technology*, 3(4), 1544-1562.
- Gillies, S. A., Futardo, A., & Henry, R. J. (2012). Gene expression in the developing aleurone and starchy endosperm of wheat. *Plant biotechnology journal*, 10(6), 668-679.
- Kareem, S. O., Falokun, E. I., Balogun, S. A., Akinloye, O. A., & Omeike, S. O. (2017). Enzymatic biodiesel production from palm oil and palm kernel oil using free lipase. *Egyptian journal of petroleum*, 26(3), 635-642.
- Keera, S. T., El Sabagh, S. M., & Taman, A. R. (2018). Castor oil biodiesel production and optimization. *Egyptian journal of petroleum*, 27(4), 979-984.
- Krishnan, D., & Dass, D. M. (2012). A kinetic study of biodiesel in waste cooking oil. *African Journal of Biotechnology*, 11(41), 9797-9804.
- Lee, A. F., & Wilson, K. (2015). Recent developments in heterogeneous catalysis for the sustainable production of biodiesel. *Catalysis Today*, 242, 3-18.
- Lee, A. F., Bennett, J. A., Manayil, J. C., & Wilson, K. (2014). Heterogeneous catalysis for sustainable biodiesel production via esterification and transesterification. *Chemical Society Reviews*, 43(22), 7887-7916.
- Nakpong, P., & Wootthikanokkhan, S. (2010). High free fatty acid coconut oil as a potential feedstock for biodiesel production in Thailand. *Renewable Energy*, 35(8), 1682-1687.
- Nie, K., Xie, F., Wang, F., & Tan, T. (2006). Lipase catalyzed methanolysis to produce biodiesel: optimization of the biodiesel production. *Journal of Molecular Catalysis B: Enzymatic*, 43(1-4), 142-147.
- Okolie, P. N., Uaboi-Egbenni, P. O., & Ajekwene, A. E. (2012). Extraction and quality evaluation of sandbox tree seed (*Hura crepitans*) oil. *World Journal of Agricultural Sciences*, 8(4), 359-365.
- Orodu, V. E. and Inengite, A. K. (2018). Extraction and Physicochemical Analysis of Oil Extracted from Pineapple (*ANANAS COMOSUS*) Peels, *World Journal of Pharmaceutical Research*, Volume 7, Issue 18, 154-166.
- Otoikhian, S. K., Aluyor, E. O., & Audu, T. O. K. (2016). Mechanical Extraction and Fuel Properties Evaluation of *Hura crepitans* Seed Oil. *Chem Technol Ind J*, 11(6), 104.
- Rodionova, M. V., Poudyal, R. S., Tiwari, I., Voloshin, R. A., Zharmukhamedov, S. K., Nam, H. G., ... & Allakhverdiev, S. I. (2017). Biofuel production: challenges and opportunities. *International Journal of Hydrogen Energy*, 42(12), 8450-8461.
- Sani, F. M., Abdulmalik, I. O., & Rufai, I. A. (2013). Performance and emission characteristics of compression ignition engines using biodiesel as a fuel: a review. *Asian J Nat Appl Sci*, 2(4), 65-72.
- Saydut, A., Erdogan, S., Kafadar, A. B., Kaya, C., Aydin, F., & Hamamci, C. (2016). Process optimization for production of biodiesel from hazelnut oil, sunflower oil and their hybrid feedstock. *Fuel*, 183, 512-517.



- Silitonga, A. S., Masjuki, H. H., Ong, H. C., Sebayang, A. H., Dharma, S., Kusumo, F., ... & Chen, W. H. (2018). Evaluation of the engine performance and exhaust emissions of biodiesel-bioethanol-diesel blends using kernel-based extreme learning machine. *Energy*, *159*, 1075-1087.
- Srivastava, N., Srivastava, M., Gupta, V. K., Manikanta, A., Mishra, K., Singh, S., ... & Mishra, P. K. (2018). Recent development on sustainable biodiesel production using sewage sludge. *3 Biotech*, *8*(5), 245.
- Stamenković, O. S., Rajković, K., Veličković, A. V., Milić, P. S., & Veljković, V. B. (2013). Optimization of base-catalyzed ethanolysis of sunflower oil by regression and artificial neural network models. *Fuel processing technology*, *114*, 101-108.
- Thliveros, P., Kiran, E. U., & Webb, C. (2014). Microbial biodiesel production by direct methanolysis of oleaginous biomass. *Bioresource technology*, *157*, 181-187.
- Umaru, M., Aris, M. I., Munnir, S. M., Aliyu, A. M., Aberuagba, F., & Isaac, A. J. (2016). Statistical Optimization of Biolubricant Production from *Jatropha Curcas* Oil using Trimethylolpropane as a Polyol. In *Proceedings of the World Congress on Engineering and Computer Science* (Vol. 2).
- Verma, P., & Sharma, M. P. (2016). Review of process parameters for biodiesel production from different feedstocks. *Renewable and Sustainable Energy Reviews*, *62*, 1063-1071.
- Vujicic, D., Comic, D., Zarubica, A., Micic, R., & Boskovic, G. (2010). Kinetics of biodiesel synthesis from sunflower oil over CaO heterogeneous catalyst. *Fuel*, *89*(8), 2054-2061.
- Yatish, K. V., Lalithamba, H. S., Suresh, R., Arun, S. B., & Kumar, P. V. (2016). Optimization of scum oil biodiesel production by using response surface methodology. *Process Safety and Environmental Protection*, *102*, 667-672.



A Multi-source Broadband Radio Frequency Energy Harvester with Cascaded Diversity Combiner for Mobile Devices

*Themelandu, J. C.¹, Onwuka, E. N.², David, M.³, Zubair, S.⁴, and Ojerinde O. A.⁵

¹Department of Electrical Engineering, School of Engineering and Technology
Federal Polytechnic, P.M. B. 55, Bida, Niger State, Nigeria

²Department of Telecommunication Engineering, School of Electrical Engineering and Technology, Federal University of Technology, P.M.B. 65, Minna, Niger State, Nigeria

³Department of Telecommunication Engineering, School of Electrical Engineering and Technology, Federal University of Technology, P.M.B. 65, Minna, Niger State, Nigeria

⁴Department of Telecommunication Engineering, School of Electrical Engineering and Technology, Federal University of Technology, P.M.B. 65, Minna, Niger State, Nigeria

⁵Department of Telecommunication Engineering, School of Electrical Engineering and Technology, Federal University of Technology, P.M.B. 65, Minna, Niger State, Nigeria

*Corresponding author email: ihemelandu.pg823917@st.futminna.edu.ng, +2347037063240

ABSTRACT

Radio frequency (RF) energy harvesting has been established as a viable alternative for powering mobile devices without increasing greenhouse gas (GHG) emission which is a threat to the environment. However, low RF power harvestable from various sources and low radio frequency-to-direct current (RF-DC) conversion efficiency has made it a very difficult task to harvest sufficient power to operate mobile devices such as smartphones. Considering the anticipated deluge of mobile devices and high data rates in the forth-coming fifth generation (5G) mobile networks, which will place a strict demand on the already dwindling global energy needs, this paper presents a RF energy harvester model aimed at harvesting sufficient power for the operation of smartphones and other mobile devices.

Keywords: *Radio frequency, conversion efficiency, RF power, greenhouse gas, smartphones, mobile devices*

1 INTRODUCTION

Spectrum crisis and high power consumption are some of the challenges that have emerged in mobile communications, which the fourth generation (4G) wireless communication networks have failed to address. Moreover, it is expected that the fifth generation (5G) with its huge promising facilities, which include capacity for 100 billion devices worldwide, massive multi-input-multi-output (MIMO) systems, 7.6 billion subscribers and up to 10 GB/s individual user speed, will require enormous amount of operating power (Wang, Haider, Gao, You, Yang, Yuan, Aggoune, Haas, Fletcher & Hepsaydir, 2014). It is therefore not surprising that energy efficiency demand is increasing globally due to high energy costs and environmental issues (Lakshmanan, Mohammed, Palanivelan, & Kumar, 2016).

Globally, a rapid increase of mobile traffic, estimated at over 60 % per year, is anticipated due to the increase in the number of smartphones and tablet terminals (Kimura, Seki, Kubo, & Taniguchi, 2015). As the increase in the demand and usage of smartphones will directly translate to increased data services, there will certainly be increased demand for energy to power the devices. Increase in energy consumption in wireless networks directly leads to increase in greenhouse gas (GHG) emission. This has been recognized as a big threat to the environment. Therefore, there has been a call on wireless network researchers and engineers to shift focus a little from wide-spread access and large capacity to energy efficient based designs (Lakshmanan *et al.*, 2016).

Reducing energy consumption is a major challenge in recent wireless systems that adopt 4G/5G technologies. 5G

is expected to address all of these challenges (Kimura *et al.*, 2015). Recently, interest has increased with respect to powering wireless network nodes using renewable energy sources such as thermal, vibration, solar, acoustic, wind and ambient radio frequency (RF) power, which are used to reduce energy costs and harmful effects on the environment caused by carbon dioxide (CO₂) emission (Liu, Zhang, Yu, & Xie, 2015). According to Lakshmanan et al (2016) 9 % of total carbon emission is attributed to mobile communications. Specifically, radio access part consumes 70 % of its total power. European member states recently signed agreement to reduce greenhouse gas emission by 20 % by 2020. Also, Vodafone group agreed to reduce CO₂ emission by 50 %. (Wu, Li, Chen, Ng, & Schober, 2017).

The major advantages of 5G over 4G according to Qasrawi and Al-qasrawi (2016), include better spectrum allocation, longer battery life, higher bit rates in larger portion of the coverage area, higher total capacity for many users at the same time via both licensed and unlicensed spectrum, lower outage probability and lower infrastructure costs. All of these cannot be achieved without a sustainable source of energy. Low latency and highly reliable communication is accommodated by 4G in terms of throughput and user density but challenges such as delay reduction and reliability improvement cannot be realized in 4G. Figure 1 shows some of the differences between 4G and 5G:

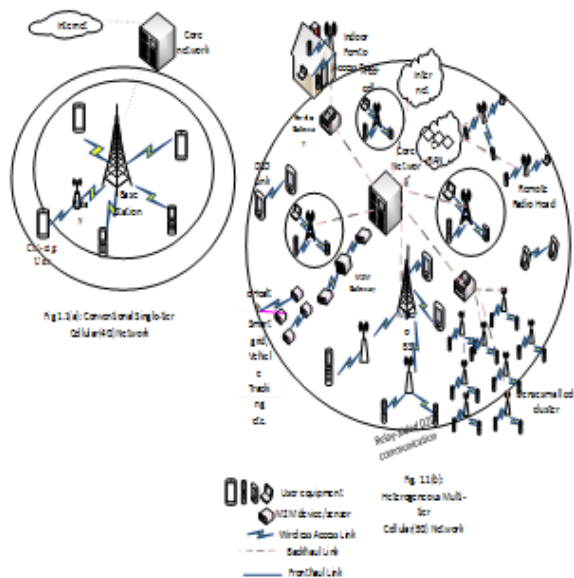


Figure 1: Differences between 4G and 5G Networks.
(Qasrawi & Al-qasrawi, 2016)

It is projected that by 2021 over 28 billion devices will be connected to 5G wireless networks and over 15 billion of these will be machine-to-machine (M2M) connections. This is to make provision for Internet of Things (IoT) communications, which is one of the most important

missions of 5G (Ercan, Sunay, & Akyildiz, 2018). For more than a century research and design of wireless networks has been concentrated on optimization metrics such as data rate, throughput, latency et cetera. However, in the last decade, energy efficiency has become a new area of concern due to economic, operational and environmental factors (Buzzi, I, Klein, Poor, Yang, & Zappone, 2016). The energy challenge in Nigeria and other developing countries is peculiar as there is, generally, insufficient energy and what is available is mainly fossil fuel, and these developing countries are notably dependent on wireless networks for communications. In order to ameliorate this pitiable situation and to prepare for the global expectation of massive connection of smartphones and other mobile devices in the next generation of wireless networks (5G), there is urgent need to develop a green system that will ensure that mobile devices are always powered and therefore improve energy efficiency and reduce greenhouse gas (GHG) emission.

2 THE LOOMING GLOBAL ENERGY CRISIS

Energy supply grossly inadequate to meet energy demand is termed energy crisis according to Machado (2018) (History.com, 2018, Kinney 2015).

Since the middle of 1960s, nations of the world have suffered the effects of energy crises, the toughest being the one between 1973 and 1974 during the oil embargo by members of organization of Arab Petroleum Exporting countries (OAPEC). It greatly affected countries such as United States, Great Britain, Germany, Switzerland, Norway and Denmark (History.com, 2018). It has been predicted that the next energy crisis will be between 2018 and 2030. This will be as a result of dwindling capital spending in the global oil business from 2014 till date (Martenson, 2017, Constable, 2019 and Tambari, 2019). Other reports warning of looming global energy crisis include Weyer (2019), Mrza (2018).

Energy crisis is of two kinds: Naturally occurring scarcity of fuel in the form of dwindling supply from coal mines, oil wells and man-made crisis due to embargo, insensitivity and lack of political will of the ruling class to take necessary actions to boost energy supply (Kinney, 2015). Energy crisis will continue to loom over humanity until strategic steps are taken to solve it. There is ever-increasing demand for energy, which is being satisfied mainly with conventional energy from coal, oil and gas, despite calls and agreements at various international conferences such as Villach conference, 1985; Vienna convention, 1987; Toronto conference, 1988; conference in Rio de Janeiro, 1992; Kyoto conference, 1997 (History.aip.org, 2019) to reduce the use of these conventional sources that deplete the protective Ozone layer and has caused continuous climate change (including global warming).

Global warming due to emissions of greenhouse gasses (GHG) from fossil fuel was first reported in 1896 by Arrhenius (History .aip.org, 2019). Since the first report of global warming, the major international body on climate change, the intergovernmental Panel on Climate Change (IPCC) has been issuing warnings on the consequences of not reducing greenhouse gas (GHG) emissions. Notably in 2007, IPCC issued a warning that serious effects of warming had become evident and that cost of reducing GHG emissions would be far less than the damage they will cause (History. aip.org, 2019). The solutions to global energy crises, global warming and its devastating effects have been identified by scientists and engineers as follows:

- i. Energy efficiency,
- ii. Electrifying transportation,
- iii. Pulling carbon dioxide (CO₂) out of the atmosphere by reforestation and using carbon capture technology, and
- iv. rapid deployment of renewable energy.(Worland, 2018)

Energy efficiency is defined as the harnessing of technology to avoid or reduce energy waste, and thereby make efficient use of available energy (Shinn, 2018). The solution proposed in this paper, which is a multi-source broadband, radio frequency (RF) energy harvester to capture some of the RF energy radiated from broadcast radio, television (TV) and global system for mobile communication (GSM) transmitting stations, is in line with the above four identified solution lines. It is efficient because it is converting the waste from radiated RF power to useful energy, it is renewable and therefore sustainable, it clean because it reduces the unwanted radiations in the environment. The captured energy will be used to charge batteries in mobile phones and similar devices.

3 RELATED WORKS

Some interesting works have been done in the area of RF energy harvesting. A few of the related works are examined in this section. Key challenges facing the technology of RF energy harvesting include: low amount of harvested energy; short transmitter- harvester (T – H) distances, which are usually too short for practical purposes; inefficient RF- to- DC energy converter; use of dedicated RF sources et cetera..

In an effort to increase the amount of harvested RF energy, Altinel and Kurt (2017) proposed the idea of using diversity combiner for RF energy harvesting. This idea is captured in their model shown in Figure 2.

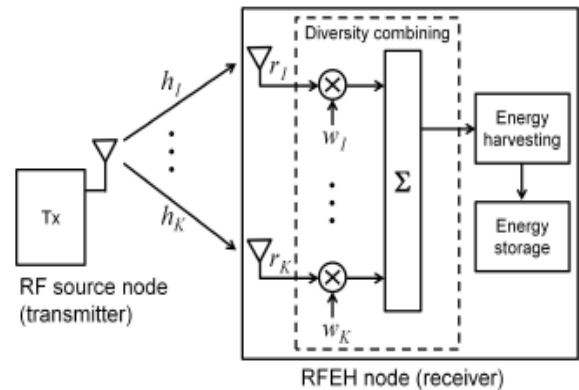


Figure 2: RF Energy Harvesting System with Diversity combining (Altinel and Kurt, 2017)

The signals received are combined in the diversity combiner, using maximal ratio combining (MRC). The harvested energy is stored in a super capacitor or rechargeable battery. Considering one transmitter-harvester pair and assuming K receive antennas, the received signal at the kth antenna is given by:

$$r_k = \sqrt{P_T} h_k x + z_k, \quad k = 1, 2, 3, \dots, K \quad (1)$$

where P_T is the average transmit power

h_k is the channel coefficient

x is the transmitted signal

z_k is the additive white Gaussian noise (AWGN)

(Altinel and Kurt, 2017)

This work focuses on RF energy harvesting, so the noise component of equation (1) also contributes to power to be harvested. Therefore, the received power from kth antenna, $P_{R,k}$ is

$$P_{R,k} = P_T |h_k|^2 |x|^2 + |z_k|^2 \quad (2)$$

The received power having gone through conversion (RF – to DC), the harvested power from kth antenna of the Transmitter- Harvesting node pair, say TV VHF, is

$$P_{H Tv VHF} = \eta \left[P_T |h_k|^2 |x|^2 + |z_k|^2 \right] \quad (3)$$

where η ; which is $0 < \eta < 1$, is the conversion efficiency (ie RF power to DC power). This depends on the performance of the RF energy harvesting system harvested energy from kth antenna in VHF.Channel is

$$E_{H,K} = \eta T [P_T |h_k|^2 |x|^2 + |z_k|^2] \quad (4)$$

where T is the period of harvesting.

Considering contribution of diversity combining, the received signal is

$$y_k = \sqrt{P_t} w_k h_k x + w_k z_k \quad k = 1, 2, 3 \dots K \quad (5)$$

where w_k is aggregate value of combiner weight coefficient with respect to k th antenna (Altinel and Kurt, 2017).

Therefore, total harvested power with diversity combiner in place is

$$P_h = \eta P_T \left[\sum_{k=1}^K w_k h_k x \right]^2 + \eta \left[\sum_{k=1}^K w_k z_k \right]^2 \quad (6)$$

and the maximum harvestable power ($P_{h, max}$) is

$$P_{h, max} = \sum_{k=1}^k \left\{ \eta P_T |w_k|^2 |h_k|^2 + \eta |w_k|^2 |z_k|^2 \right\} \quad (7)$$

Their major concern in this work is to investigate the performance of three different diversity combiner techniques on RF energy harvesting with respect to amount of energy harvested. The three combiner techniques are maximal ratio combining (MRC), equal gain combining (EGC) and selection combining (SC). The power consumption of the diversity combiners was also taken into account. Their results showed that the net harvested power depends on the power consumption of the circuit during the combining process. MRC gave the best performance in the RF-EH; followed by EGC and the worst result came from the harvester with SC. There is need therefore, not only to employ the adequate diversity combiner technique but also to carefully select the components in the combiner circuitry in order to reduce power consumption in the combiners and increase the net harvestable power.

Considering both destructive and constructive interferences at any given location by factoring path lengths and path differences between target sources, the total received power from any number of RF sources is given by

$$P_T^r = G_r \left(\frac{\lambda}{4\pi} \right)^2 \left[\sum_{i=1}^k \frac{P_i G_i}{R_i^2} + \sum_{\substack{i=1 \\ i \neq j}}^k \sum_{j=1}^k \frac{\sqrt{G_i G_j P_i P_j}}{R_i R_j} \cos(k(\Delta r_{ij})) \right] \quad (8)$$

where P_i and G_i are transmission power and the gain of the transmitting antenna of RF sources and $\Delta r = |R_i - R_j|$, differences of distances between the RF sources and the harvesting node and G_r is the gain of the receiving antenna (Naderi, Chowdhury and Basagni, 2015)

Radio frequency (RF) wireless charging model is given by

$$P_H = \eta P_T^r \quad (9)$$

where P_H is the harvested power, P_T^r is the received power at the harvesting node, and η is the RF - to - DC conversion efficiency.

Therefore, harvested power from K RF sources is

$$P_H = \eta \left[G_r \left(\frac{\lambda}{4\pi} \right)^2 \left[\sum_{i=1}^K \frac{P_i G_i}{R_i^2} + \sum_{\substack{i=1 \\ i \neq j}}^k \sum_{j=1}^k \frac{\sqrt{G_i G_j P_i P_j}}{R_i R_j} \cos(k(\Delta r_{ij})) \right] \right] \quad (10)$$

where $k = 6$

Considering the contribution of the cascaded diversity combiner, the harvested power from k RF sources

$$P_H \text{ diversity} =$$

$$\eta [|w|^2] \left[G_r \left(\frac{\lambda}{4\pi} \right)^2 \left[\sum_{i=1}^k \frac{P_i G_i}{R_i^2} + \sum_{\substack{i=1 \\ i \neq j}}^k \sum_{j=1}^k \frac{\sqrt{G_i G_j P_i P_j}}{R_i R_j} \cos(k(\Delta r_{ij})) \right] \right] \quad (11)$$

Kim, Vyas, Bito, Niotaki, Collado, Georgiadis, and Tenzleris (2014) reviewed in detail various ambient technologies and the possibility of applying them in the development of self-sustaining wireless platforms. A prototype RF energy harvester that harvests from a digital TV transmission at UHF band (512-566 MHz) 6.3 km away from the proposed harvester was presented. Also a high-efficiency dual-band ambient energy harvester at 915 MHz and 2.45 GHz as well as an energy harvester for on-body application at 460 MHz were presented to confirm the capabilities of ambient UHF/RF energy harvesting as a suitable technology for Internet of Things and Smart skin

applications. The harvested energy here, though at a reasonable distance, can only operate very low power devices. To power devices such as smartphones and tablets, there is need to make the harvester broadband to enable it harvest sufficient power from varied RF sources such as AM, FM, and TV transmitters.

Naderi, Chowdhury, and Basagni (2015) discussed formulation of expressions for power harvesting rates in plane 2D and 3D dimensions and the placement of multiple RF Energy Transmitters (ETs). These harvesters were used in recharging the nodes of wireless sensor network (WSN). The authors studied distribution of total available and harvested power within the entire WSN system. They provided a closed matrix forms for estimating harvestable power at any given point in space. Energy transfer in the WSN is analyzed using power outage probability and harvested voltage considering the effects of constructive and destructive interference of the transmitted energy. The results indicate that received power within the entire network and interference power from concurrent energy transfers are characterized with Log-Normal distributions while the harvested voltage has a Rayleigh distribution.

An optimized RF energy harvesting system operating in GSM 900 band for the purpose of powering wireless sensor network is presented by Rengalakshmi and Brinda (2016). The RF energy harvester was improved by optimizing the impedance matching network and rectifier. Agilent Advanced Design System (ADS) software was used for simulation and analysis. The harvester is to receive power from a dedicated microwave source to operate a health monitoring system. DC output voltage from the RF energy harvester is 4.03 v for a load resistance of 5 K Ω . Power conversion efficiency of the proposed system is 72 %. In order to increase DC output voltage and current there is need for a broadband antenna and randomly placed multiple RF sources. This will ensure continuous reception of RF power.

The design, simulation, analysis and comparison of multiple stage voltage multiplier for a RF energy harvesting in the ISM band (2.4 GHz) was reported by Panda and Deshmukh (2016) in the work "Novel Technique for wireless Power Transmission Using ISM Band RF Energy Harvesting for Charging Applications". It is proposed for powering mobile devices, Mp3 players, digital cameras, laptops et cetera. Target distance is 3-5 m between the RF sources and receive antenna. Advanced design system (ADS) simulator was used for simulation and analysis. The results were compared with existing systems and showed an improvement in terms of harvested voltage, current, and with respect to distance. DC output voltage obtained is 7 v at a distance of 5 meters. This is too short a distance to be practical.

A design and simulation of five-stage voltage multiplier with π type matching circuit for RF energy harvesting

system was presented by Shahabuddin, Shalu, and Akter (2018). RF energy source used in this work was GSM-900 band. Specifically, input power range of -30 dBm at 915 MHz was used. Simulation was carried out with ADS simulator and the output voltage of 9.6 v and maximum voltage of 33.9 v at -20 dBm were obtained across a load resistance of 180 k Ω . A comparison of the work with previous ones showed that increase in the number of stages of voltage multiplier increases the output voltage and the π type matching circuit performed better than other matching circuits. Leon-Gil, Cortes-Loredo, Fabian-Mijangos, Martinez-Flores, Tovar-Padilla, Cardona-Castro, and Alvarez-Quintana (2018) developed a RF energy harvester based on a four-stage full wave Cockcroft-Walton voltage multiplier with conversion efficiency of up to 90 %. RF input source from AM broadcast (Medium and Short Wave) was used. An output power of 62 μ W over 1.5 M Ω output impedance was obtained at a distance of 2.5 km from the harvester and thus was able to power low-power electronic calculator. This is impressive, but the harvested power could be enhanced by harvesting from both AM and FM transmitters. This will enable the powering of higher power devices such as mobile phones.

4 THE PROPOSED MODEL

Most of the previous works reviewed could only develop RF energy harvesters placed few meters away from the transmitters. The farthest is 6.3 km, but the harvested power could only operate a wireless sensor node. None of the previous researchers considered combining RF sources from TV, Radio broadcasting and GSM for the same RF energy harvester. Most of the previous RF energy harvesters are limited to powering wireless sensors which are low-power devices in comparison to smartphones. Such amount of harvested power cannot power mobile hand-held devices such as mobile phones, tablets and the like. To support mobile wireless communications in the 5G era, which promises billions of mobile hand-held and wearable devices without, at the same time, endangering the environment via GHG effect from fossil fuels, it is imperative to power mobile devices of the future with green energy sources such as RF. Therefore, a multi-source, broadband RF energy harvester with a cascaded diversity combiner is proposed with the anticipation that enough power will be harvested to ensure always powered mobile devices both in the urban and rural areas. It is believed that for a desired level of RF power to be harvested such as could keep a mobile device always powered, anywhere and anytime, a few factors have to be considered: (i) the effective isotropic radiated power (EIRP) of transmitters should be reasonably high to enable RF energy harvester receive sufficient power at practical distances, (ii) to make the harvester applicable for mobile devices, multiple RF sources that are easily available in the mobile environment should be considered, as this will enable a mobile device to always have RF sources to harvest from wherever it may

be, (iii) considering the challenges of multipath fading, an efficient space diversity combiner is needed to enhance the power receivable at harvester antenna. A good combiner output can go a long way to counter the additional challenge of the currently low efficient energy converters, (iv) to reduce power losses due to impedance mismatch, it is important to have well designed impedance matching circuits that will ensure maximum power transfer of the enhanced RF power from the diversity combiner to the RF-DC converter. To achieve all these, the harvester model of figure 3 is proposed. This will reduce the burning of fossil fuel in generators used at phone charging centres commonly found in developing countries.

The proposed model is shown in Figure 3. Each of the antennas will be connected to the same energy harvesting circuit via a cascaded combiner (MRC/MRC). It is intended to harvest from each of the six RF sources using an array of 4 directional antennas arranged circularly to cover 360 degrees. This arrangement will provide higher gain than using omnidirectional antennas, which are usually of lower gain. Each array of 4 antennas is connected to one diversity combiner (MRC). The output of the first stage of the cascaded diversity combiner will feed the second stage which is a 6-input-1-output MRC. This second stage feeds an enhanced RF power to the impedance matching circuit. The harvested energy will be used to charge a mobile phone battery.

5 CONCLUSION

This paper presented an RF energy harvester model that is anticipated will help alleviate the energy challenges in the forth-coming 5G networks. It briefly discussed the energy challenges currently facing the world in general and specifically pointed out how it will affect the 5G mobile network standards. It noted that the global energy crisis will impact negatively on the future of mobile communications if technology did not move fast to address the challenges. The paper also noted that whatever energy solutions that is proposed must be environmentally friendly. Literature generally agrees that renewable energy is a viable direction to go in search of sustainable energy solutions. The paper, therefore, focused on RF energy harvesting for powering mobile communication devices and pointed out some gaps in literature. It concluded with a proposed RF energy harvester model, which is believed will close major gaps in literature.

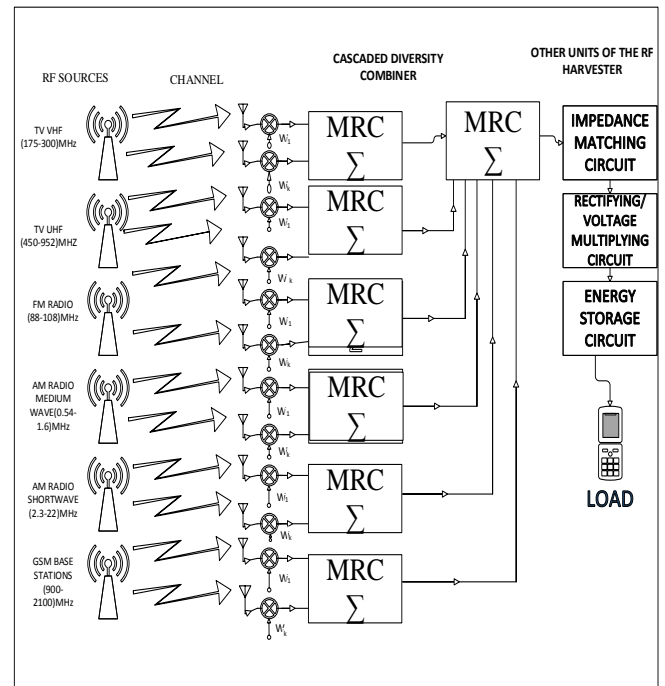


Figure 3: Proposed model for the research.

ACKNOWLEDGEMENT

The authors wish to acknowledge the valuable contributions offered by Onu Christian toward the completion of this work.

REFERENCES

- Altinel, D., & Kurt, G. K. (2017.). Diversity Combining for RF Energy Harvesting.
- Buzzi, S., Chih-Lin, I., Klein, T. E., Poor, H. V., Yang, C., & Zappone, A. (2016). A survey of energy-efficient techniques for 5G networks and challenges ahead. *IEEE Journal on Selected Areas in Communications*, 34(4), 697–709.
- Constable, S. (2019). Supplies of Energy Set to fall-Report from International Energy Agency 2019 www.thestreet.com Retrieved 23/5/2019
- Ercan, A. Ö., Sunay, M. O., & Akyildiz, I. F. (2018). Rf energy harvesting and transfer for spectrum sharing cellular iot communications in 5g systems. *IEEE Transactions on Mobile Computing*, 17(7), 1680–1694.
- History.aip.org (2019). Discovery of Global Warming. www.history.aip.org Retrieved 23/5/2019
- History.com (2018). Energy Crisis (1970's). www.history.com Retrieved 23/5/2019
- Kim, S., Vyas, R., Bito, J., Niotaki, K., Collado, A., Georgiadis, A., and Tentzeris, M. M. (2014). Ambient RF energy-harvesting technologies for self-sustainable standalone wireless sensor platforms. *Proceedings of the IEEE*, 102(11), 1649–1666.
- Kimura, D., Seki, H., Kubo, T., & Taniguchi, T. (2015).



- Wireless network technologies toward 5G. *APSIPA Transactions on Signal and Information Processing*, 4.
- Kinney, C. (2015). Energy Crisis : Definition and Solutions. www.Study.com Retrieved 23/5/2019
- Lakshmanan, M., Mohammed, V. N., Palanivelan, M., & Kumar, P. S. (2016). Energy Control in 4G Networks. *Indian Journal of Science and Technology*, 9(35).
- Leon-Gil, J. A., Cortes-Loredo, A., Fabian-Mijangos, A., Martinez-Flores, J. J., Tovar-Padilla, M., Cardona-Castro, M. A., ... Alvarez-Quintana, J. (2018). Medium and Short Wave RF Energy Harvester for Powering Wireless Sensor Networks. *Sensors*, 18(3), 768.
- Liu, Y., Zhang, Y., Yu, R., and Xie, S. (2015). Integrated energy and spectrum harvesting for 5G wireless communications. *IEEE Network*, 29(3), 75–81.
- Machado, J. (2018). What is the Meaning of an Energy Crisis ? www.Quora.com Retrieved 23/5/2019
- Martenson, C. (2017). The Looming Energy Shock. www.PeakProsperity.com Retrieved 21/5/2019
- Mrza, F. (2018). World Oil Crisis Looms as Supply Levels under threat. www.arabnews.com Retrieved 23/5/2019
- Naderi, M. Y., Chowdhury, K. R., & Basagni, S. (2015). Wireless sensor networks with RF energy harvesting: Energy models and analysis. In *Wireless Communications and Networking Conference (WCNC), 2015 IEEE* (pp. 1494–1499). IEEE.
- Panda, N., & Deshmukh, S. M. (2016). Novel Technique for Wireless Power Transmission using ISM Band RF Energy Harvesting for Charging Application.
- Qasrawi, I. Al, & Al-qasrawi, I. S. (2016). Proposed Technologies for Solving Future 5G Heterogeneous Networks Challenges Proposed Technologies for Solving Future 5G Heterogeneous Networks Challenges, (August). <https://doi.org/10.5120/ijca2016909924>
- Rengalakshmi, P., & Brinda, R. (2016). Rectifier for RF Energy Harvesting. *International Journal of Computer Applications*, 143(10).
- Shahabuddin, A. A., Shalu, P. D., & Akter, N. (2018). Optimized Process Design of RF Energy Harvesting Circuit for Low Power Devices. *International Journal of Applied Engineering Research*, 13(2), 849–854.
- Shinn, L. (2018). Energy Efficiency: the Clean Facts. NDRC
- Tambari, A. (2019). Averting the Looming Energy Crisis. www.dailytrust.com.ng Retrieved 23/5/2019
- Wang, C.-X., Haider, F., Gao, X., You, X.-H., Yang, Y., Yuan, D., ... Hepsaydir, E. (2014). Cellular architecture and key technologies for 5G wireless communication networks. *IEEE Communications Magazine*, 52(2), 122–130.
- Weyer, M. V. (2019). An Energy Crisis is Looming, but Ministers are Distracted by Brexit. www.spectator.co.uk Retrieved 23/5/2019
- Worland, J. (2018). Scientists Just Laid out Paths to solve Climate Change. We aren't on Track to do any of them. United Nations
- Wu, Q., Li, G. Y., Chen, W., Ng, D. W. K., & Schober, R. (2017). An overview of sustainable green 5G networks. *IEEE Wireless Communications*, 24(4), 72–80.



ARTIFICIAL NEURAL NETWORK (ANN), A FORMIDABLE TOOL FOR ATMOSPHERIC FORECASTING. A REVIEW

Usman M.N., Aku I.G. & Oyedum O.D.

Department of Physics, Federal University of Technology, PMB 65 Minna Niger State, Nigeria
musman1965@yahoo.com, +2348162075591

ABSTRACT

Forecasting weather is the eminent role of science and technology that predict the future condition of a weather for particular area. Unlike traditional methods, advanced weather forecasting involves a combination of computer models and knowledge of trends and patterns. Weather forecasting has turned out to be an important area of research in the past few decades which has affect the life of people. The purpose of this study was to review how frequently ANN is being used for weather forecasting, ANN performances and ways to improve it. This paper reviews the recent past and present uses of Artificial Neural Network for weather forecasting. Available literatures of some algorithm, techniques and parameter employed by different researchers to apply ANN for Weather Forecasting was presented. At the end, this review has shown that using Artificial Neural Network (ANN) approach for weather forecasting yields good results and can be considered as an alternative to traditional metrological approaches, BPNN found to be widely used and ENN can perform more than individual ANN. This study also highlighted the capabilities of ANN in predicting several weather phenomenon's such as temperature, rainfall, thunderstorms, others.

Keywords: *Artificial Neural Network, BPNN, Forecasting Techniques, Weather*

1 INTRODUCTION

Currently, weather forecasting is in high demand for several applications in agriculture, air traffic services, floods, and energy and environment control. Weather forecasting is an expectation of what the weather will resemble in next 1 hour, tomorrow, or 1 week from now. It includes a combination of models, perceptions, and learning of patterns with precedents (Saba and Rehman 2012; Norouzi et al. 2014). By utilizing these techniques, sensible exact estimates could be made up to 7 days ahead. Weather forecast are furnish by collecting required data (i.e. parameters) about the specified location status of the atmosphere (Gurung, 2017). Accurate weather predictions are important for planning our day to day activities. Farmers need information to help them plan for the planting and harvesting of their crops. Airlines need to know about the local weather conditions in order to schedule flights (www.learner.org/exhibits/weather/forecasting.html).

All these helps us to make more informed daily decision and may even help keep us out of danger.

Most early forecasting was based on observations of weather patterns. Over the years, this observations has resulted in traditional wisdom a good idea of which is inaccurate, day-to-day analysis of the weather is to be predicted and these forecasting should be communicated for the end users for taking decisions. It is a most challenging issue since the decisions that are taken are mostly with uncertainty (Krishna, 2015). Many have highlighted that most of the changes in the climatic conditions are mostly due to the global weather changes. Therefore if these weather changes are identified,

effective prediction techniques can be planned (Krishna, 2015). However, unlike traditional methods, modern Weather forecasting involves a combination of computer models, observation (by use of instruments, balloons and satellites), and knowledge of trends and patterns (used by Local weather observers and weather stations). Using these methods, reasonably accurate forecasts can be made. Though, there is limited success in forecasting the weather parameters using the numerical model (Karmakar and Kowar, 2012).

Artificial Neural Network came into existence in 1986 which is able to reduce this limited success and drawing considerable attention in various researched work across the world, as it can handle the complex non-linearity problems better than the conventional existing statistical techniques. No other model (except the neural network model) so far has been able to forecast long-range weather parameter so accurately (Sanjeev *et al.*, 2008). Neural Networks has numerous applications in real life for machine vision and to search suitable solutions as compared to the traditional numerical models. For instance, currently, neural networks are employed in documents analysis and recognition (Rehman and Saba 2014; Neamah et al. 2014; Alkawaz et al. 2016), flood control (Joorabchi et al. 2007; Saba 2016), biometrics classification stock market, weather forecasting and rice yield forecast (Phetchanchai et al. 2010; Elsafi 2014). Recent research exhibits that neural networks are promising non-linear tools if proper training and testing is conducted as well attention is given to learning parameters.

The modern application of science and technology help predict the state of the atmosphere in future time for a given location, it is so important due to its effectiveness



in human life. Today, weather forecasts are made by collecting quantitative data about the current state of the atmosphere and using scientific understanding of atmospheric processes to project how the atmosphere will evolve. The chaotic nature of the atmosphere implies the need of massive computational power is required (Devi, 2012). Weather forecasting has become an important field of research in the last few decades which has impacts the lives of many people. It is found that architecture of ANN is the most widespread techniques used for weather forecasting. This is why the researcher want to review the application of ANN in weather forecasting and its impact. The aims of this study is to find out frequently used ANN for weather forecasting, ANN performances and how to improve it so as to help validate ANN as formidable tool for weather forecast.

1.1 STATEMENT OF THE PROBLEM

Accurate weather forecasting is very significant in our daily activities. It is becoming absolutely necessary for scientists, farmers, global food security and disaster management to understand weather phenomena in order to plan and be prepared for the future. Throughout the centuries, attempts have been made to produce forecasts based on weather changes but due to the chaotic nature of weather parameters and their direct impact on our society, the inaccuracies and errors in weather forecasting have been found to be of significant. Researchers have been developing different tools like Artificial Neural Networks that can be suitable for weather forecasting with minimal errors. It is in line with this the researcher want to review frequent use of ANN for weather forecasting and its associated techniques and applications. This effort will guarantee further research on Improving the accuracy of the method.

2 THE REVIEW

Recent studies have reported that ANN may offer a promising alternative for the hydrological forecasting because unlike most computer applications, an ANN is not “programmed,” rather it is “taught” to give an acceptable answer to a particular problem. Time series models have been widely used in a broad range of scientific applications to forecast the variables including hydrology (Aghelpour and Mohammadi, 2019). Furthermore, the unique structure of the neural networks, together with the non-linear transfer functions combined with each neuron in the input, processing, and output layers, allows the neural network to approximate complex non-linear relationships without any assumption (Dibike and Coulibaly 2006). The results of other studies demonstrated the satisfactory performance of time series model for predicting temperature in other applications (Ye

et al. 2013; Asamoah-Boaheng 2014; John et al. 2014; Musa 2014).

Many studies have been carried out to estimate or to forecast the weather variables. For example, Aggarwal et al., (2012). Have used the ANN model for maximum and minimum temperatures prediction. The data was from the first decade of the twenty first century and a model was used according to the seasonal trend; this model had a good accuracy and was able to forecast the monthly values for these two variables for 12 months. In this respect, neural networks have also been widely used for predicting the temperature, rainfall and other weather parameters (El Houari et al. 2015; Shereef and Baboo 2011; Hayati and Mohebi 2007; Bassam et al. 2017).

Shrivastava, et al., (2017). It is found that suitability of ANN for Weather Forecasting has greatly improved the performance and the result accuracy. It is also found that the different type of Neural Networks package supports different types of training and learning algorithms like Artificial Neural Network (ANN), Back Propagation Neural Network (BPN). Since weather forecasting is a dynamic and non-linear process so ANN can be used for prediction of weather. From the research it is also found that ANN is the best approach than Numerical and traditional methods. On the contrary BPN is the best algorithm to use the neural network for weather forecasting. The development of neural network model of Back Propagation type is focused in Kassem (2009) paper. He estimates the hourly total and diffuse solar radiation on horizontal surface and result is compared during testing phase statistically by three Methods; Root Mean Square Error (RMSE), Mean Bias Error (MBE), and Coefficient Of Determination (R), giving a value of 4.284 W/m, -0.60 W/m and 0.9309, respectively when estimating hourly total solar radiation. In contrast, the RMSE, MBE and R values of estimating hourly diffuse solar radiation were 2.450 W/m, -3.449 W/m and 0.7802, respectively. These results indicate that this methodology can be used to estimate the hourly total and diffuse solar radiation on horizontal surface.

Krishnamurthy et al, (2000). Have demonstrated the performance of multimodel ensemble forecast analysis that showed superior forecast skills as compared to other individual models used. The parameters used for comparison among these models include global weather, hurricane track and intensity forecasts, and seasonal climate simulations.

Abhishek Saxena et al, (2013). Presented the review of weather prediction using artificial neural networks and studied the benefit of using it. It yields good results and can be considered as an alternative to traditional meteorological approach. The study expressed the



**3rd International Engineering Conference (IEC 2019)
Federal University of Technology, Minna, Nigeria**



capability of artificial neural network in predicting various weather phenomena such as temperature, thunderstorms, rainfall, wind speed and concluded that major architecture like BP, MLP are suitable for predicting weather phenomenon. But due to the nonlinear nature of the weather dataset, prediction accuracy obtained by these techniques is still below the satisfactory level.

Sawale and Gupta (2013). Proposed an artificial neural network method for the prediction of weather for future in a given location. Back Propagation Neural Network is used for initial modeling. Then Hopfield Networks are fed with the result outputted by BPN model. The attributes include temperature, humidity and wind speed. Three years data of weather is collected comprising of 15000 instances. The prediction error is very less and learning process is quick. This can be considered as an alternative to the traditional meteorological approaches. Both algorithms are combined effectively. It is able to determine non-linear relationship that exists between the historical data attributes and predicts the weather in future.

Olaiya (2012), investigates the use of data mining techniques in forecasting maximum temperature, rainfall, evaporation and wind speed. This was carried out using Artificial Neural Network and Decision Tree algorithms and meteorological data collected between 2000 and 2009 from the city of Ibadan, Nigeria. It was observed that with enough data ANN's can detect the relationships between weather parameters and use these for predicting the future weather conditions.

Khalili (2011), presented ANN modeling for daily rainfall forecasting in Mashhad synoptic station. The ANN model is used as a black box model, and it was found that the hidden dynamics of rainfall through the past information of the system. The obtained results of validation phase that include Correlation Coefficient (R), Root Mean Square Error (RMSE) and Mean Absolute Error (MAE) for daily prediction using GS531 and GS651. Has proved that ANN model gave satisfactory prediction performance.

Devi (2012), showed that these neural networks are useful in forecasting the weather and the working of most powerful prediction algorithm called back propagation algorithm was explained in detail stating that neural network can predict the future temperature with less error. Sharma, 2014 has presented how neural network are useful in forecasting the weather and the working of most powerful prediction algorithm BPN was explained. The trained sets are predicted by BPNN with least errors.

Karmakar (2014), identified impact of learning rate and momentum factor in prediction of chaotic motion through BPN system and clearly declared that the optimum value of learning rate and momentum factor is dynamic and always depending on input parameters and

targeted parameter in BPN system. However no contributions have been found to identify optimum value of learning rate and momentum factor for most favorable performance of BPN. Similarly the optimum architecture of BPN is equally pre requisite in terms of number neurons in hidden layer, number of input vectors, number of output neurons etc. It is observed that weather forecasting modeling through BPN has sufficiently suitable to explain chaotic nature of weather data time series and significant for prediction of future.

Sanam et al, (2017), found that, simulation results of neural network shows the training algorithm performs well in the process of convergence characteristics, and improve the convergence rate, a satisfactory approximation. The major finding of this paper was that fuzzy logic system can predict the temperature more accurately than the other methods including B.P neural networks. Malik et al, Proposed a new technique of weather forecasting by using Feed-forward ANN. The data is taken from Rice Research center (Kaul) Haryana. The data is trained by LM algorithm. And it is found that this is the fastest method among other weather forecasting methods.

Saba, et al, (2017), presented a hybrid neural model and experimental results have exhibited that hybrid neural model outperforms than individual feed forward neural networks (MLP & RBF). It is also observed that hybrid model not only have better generalization ability but also better learning ability. Several statistical measures are adopted to verify the weather forecasting results of individual neural networks and hybrid neural model. In comparison to the regression models, hybrid neural model forecast weather at high precision. Future work may include training of hybrid neural model using synthetic data, online training, self-error detection, and correction.

Mislana et al, (2015), present a BPNN algorithm that was used to model and predict rainfall in Tenggara, East Kalimantan - Indonesia. After testing the three architectures with different epochs; the best MSE value was obtained with 2-50-20-1 architecture the results of this study have showed that BPNN models can be used as a predictive algorithm that provides a good predictive accuracy. The prediction results have demonstrated the suitability of the area Tenggara that has an equatorial type of two peak rainy seasons in April and November. Future work is suggested to include a comparison of a few ANN methods and the optimization process in order to obtain more accurate prediction results.

Chatterjee and Deyz, (2018), proposed a novel hybrid neural based approach to build a robust and accurate model for rainfall prediction. The proposed model is tested by using a dataset collected by Dum Dum meteorological center situated at state West Bengal of eastern part of India. The hybrid model is supported by a feature selection phase. The experimental results have



revealed that the feature selection phase can significantly improve classifier performance for rainfall prediction. Besides, the extensive comparative analysis reveals that the proposed HNN model is highly efficient in predicting rainfall.

Gurung, (2017), reports a detailed survey on forecasting weather using different neural network architectures and techniques over twenty to thirty years. Several analyses shown that most of the research fellow has used Neural Network Back Propagation (BPN) said that the forecasting weather system can be efficient with the help of Neural Network Back Propagation method and by the execution of this forecasting system it is demonstrated that how can an intelligent system be resourcefully combined with a neural network prediction model for predicting the status of weather. Back propagation neural network approach for weather forecasting is capable of yielding good results and can be considered as an alternative to traditional meteorological approaches.

Geetha and Nasira, (2014). From the model we can conclude that artificial neural networks can be used as an aid to model a weather forecasting system for predicting maximum and minimum temperature. The accuracy (81.78%) was as a result of training 1000 cycles, with the learning rate of 0.3 and with momentum 0.2. The performance is measured in terms of its RMSE (Root Mean Square Error) correlation. Though there are many data mining methodologies, ANN are better at finding the strength of connections between attributes, can learn from training and exhibit intelligence in making predictions. Also, the model can be extended in predicting other weather parameters like rainfall, cyclonic storms, hurricanes, snowfall and tornadoes.

Ibeh, et al., (2012). Renewable energy is consider as the key source for the future as it is the vital and essential ingredients to human activities of all kind, and can only be acquired through measurement or prediction. The result of this work, clearly indicate the importance of using ANN approaches for predicting the global solar radiation on horizontal surface reaching the earth at different location in Warri – Nigeria. From the close relationship that exist between measured and ANN predicted results, it is clear that ANN model is a good model for solar radiation prediction.

Harshani and Nagahamulla et al., (2012). Rainfall forecasting was done using Ensemble neural network (ENN) by. In ENN, finite numbers of ANN are trained for the same task and their results are combined using the weighted average method. Here, each ANN is assigned a weight to minimize mean square error. The study area selected to be Colombo, where daily observed data of forty one years was used by dividing it in four climatic seasons every year with twenty six variables. The performance is compared with Backpropagation neural

network (BPN), radial basis function network (RBFN) and general regression neural network GRNN). Results show that, ENN model predicts rainfall more accurately than individual BPN, RBFN and GRNN. The paper compares ANN with BPN, RBFN and GRNN and the comparison shows that ANN gives more accuracy compared to others.

Elkateb et al. (1998), monthly peak load demand of Jeddah area for the past nine years was used for investigation. The first seven years data was used for training while the prediction was carried out for the following two years. First, Minitab statistical software package was used for peak load prediction using Autoregressive Integrated Moving Average (ARIMA) technique, and an average error value of 11.7% is achieved. Next, an Artificial Neural Network (ANN) was utilized and several suggestions are implemented to build an adaptive form of ANN. Direct ANN implementation shown poor performance. Also, Fuzzy Neural Network (FNN) was also examined but showed comparatively better performance. The modeling of the trend of peak load demand is incorporated by introducing “time index feature” and that clearly enhanced the performance of both ANN (6.8% error) and FNN (4.7% error).

Abdulkadir, et al, (2012). The modelling of rainfall data of Ilorin using ANN, automated in ALYUDA Forecaster showed that ANN is a good method of optimization, since error observed in the comparison of actual and model output is minimal. The neural network summary yielded 76% of good forecasts for rainfall in Ilorin with correlation coefficient of 0.88. This showed that the trained network is reliable and fit to be used for the subsequent quantitative prediction of rainfall. It can therefore be concluded that forecasting using ANN is a very versatile tool in water resources management modelling.

Mekanika, et al., (2011). Investigate the effectiveness of Artificial Neural Networks on monthly rainfall forecasting for a highland region. A monthly feed forward multilayer perceptron neural network (ANN) rainfall forecasting model was developed for a station in the west mountainous region of Iran. The model was trained based on Levenberg-Marquardt algorithm. The ANN model has been constructed to depict the non-linear relationship among rainfall series. It was shown that ANN has the ability of forecasting rainfall for one year in advance. The results may be applicable for future water resources management, drought forecasting and municipal decision making and planning. The results of this study are from one stations only, thus the results need to be explored further through similar studies in the region at similar and also different elevation.

Dubey (2015), in this paper, different artificial neural networks have been created for the rainfall prediction of Pondicherry, a coastal region in India.



These ANN models were created using three different training algorithms namely, feed-forward back propagation algorithm, layer recurrent algorithm and feedforward distributed time delay algorithm. The number of neurons for all the models was kept at 20. The mean squared error was measured for each model and the best accuracy was obtained by feed-forward distributed time delay algorithm with MSE value as low as .0083. The input data set comprises of parameters affecting rainfall such as minimum temperature, maximum temperature, vapor pressure, potential evapotranspiration and crop evapotranspiration. The results obtained from all the models were then compared to each other using the Mean Square Error (MSE) and subsequently the conclusions were drawn.

Mishra, et al (2018). Artificial Neural Network (ANN) technique has been used to develop one-month and two month ahead forecasting models for rainfall prediction using monthly rainfall data of Northern India. In these model, Feed Forward Neural Network (FFNN) using Back Propagation Algorithm and Levenberg - Marquardt training function has been used. The performance of both the models has been assessed based on Regression Analysis, Mean Square Error (MSE) and Magnitude of Relative Error (MRE). Proposed ANN model showed optimistic results for both the models for forecasting and found one month ahead forecasting model perform better than two months ahead forecasting model. This paper also gives some future directions for rainfall prediction and time series data analysis research.

Chelang, et al., (2018), in this study an application of BPNN back propagation neural network with different input combinations and different number of hidden layer neurons was used to forecast daily precipitation at two stations of Huston ,Texas and Dallas regions using different weather parameters Temperature , relative humidity, sea level pressure and wind speed. This was done by using two different methods which are Back Propagation Neural Networks BPNN and Adaptive Neuro Inference System ANFIS. Two case studies were selected for this operation which are Huoston, Texas and Dallas, Texas. The high performance of the applied models in forecasting the daily precipitation was concluded especially by using auxiliary weather data with the lagged day precipitation values since the BPNN and ANFIS were able to learn from continuous input data.

Abhishek et al., (2012). Develops an ANN model to forecast average monthly rainfall. He selected data from Udupi, Karnataka which is eight months data for fifty years making 400 entries for input and output. The data is normalized by finding mean and standard deviation of each parameter. Then training is done on 70% of data and the remaining 30% data is used for testing and validation. The model used is a three layered ANN with

backpropagation learning. Later after testing, the results are compared with actual output. It showed higher degree of similarity in output. Thus it is proved that ANN model is accurate in prediction. Authors concluded that, learnngdm is the best learning function for training whereas trainlm is the best training function.

Anad, et al., (2011). Uses Artificial Neural Network (ANN) for predicting and classify thunderstorms. ANN has designed to forecasts the occurrence of thunderstorm in two geographical regions. Thus, it is concluded from the results that ANN can be effectively utilized for the prediction and classification of thunderstorm with appreciable level of accuracy. Recently ANN technique has been used for rainfall forecasting in Alexandria, Egypt. Shafie et al., (2011). Comparison with linear regression models was made on the basis of mean error (BIAS), mean absolute error (MAE), root mean square error (RMSE), and the correlation coefficient (CC) and it was observed that both the models had the ability to predict the extreme values, maximum and minimum values. However, the ability to predict the mid-range values is better for the ANN model

3 RESULTS AND DISCUSSION

It is always difficult to analyze results in the area of weather forecasting due to several subjective issues like train/test data variety, neural architecture, learning parameters and activation functions but weather forecasting can be done in a variety of different ways and using even more complex methods to analyze data such as an ANN or a genetic algorithm. Additionally, most of the researchers employed individual neural network for forecasting.

However, from this study, it shows that ANN can be more reliable and useful in weather forecasting and the widely used algorithm for prediction is back propagation neural network.

The Ensemble Neural Network which that can combine several models in to one predictive model as an input can predict more accurately than any individual FNN, BPNN, RBFN and GRNN. With ENN, the bias, variance are reduced in order to improving predictions. Which shows that ENN has high performances than the rest ANN

The performances (speed and accuracy) neural network model can be improved when input data is well prepared, when more data is employed for initial training. Also, avoiding overfitting and underfitting during training data set can enhance the ANN performances. For a neural network model to be more accurate, the mean square error has to be as low as possible.

However, few available techniques, parameters, algorithm employed in ANN forecasting are presented in the table below.

TABLE 1: SOME ALGORITHM, TECHNIQUES, PARAMETERS IN ANN FORECASTING

Author	Algorithm	Techniques	Parameters	Applications
Abdulkadir <i>et al</i> 2012	ALYUDA Forecaster	ANN	rainfall	Monthly rainfall prediction in Ilorin
Ibeh <i>et al</i> 2012	MLP	ANN	max temperature, solar radiations	Solar radiation prediction in Warri
Elkateb <i>et. al.</i> (1998).	Minitab	ARIMA, ANN	temperature, relative humidity rainfall and vapour pressure	Monthly weather prediction in Jeddah
Dubey 2015	FFBP, LR, FFDTD	ANN	Minimum temperature, maximum temperature, vapor pressure.	Monthly rainfall prediction of Pondicherry
Mekanika, 2011	Levenberg-Marquardt	ANN	-	Monthly rainfall prediction in Iran
Saxena <i>et al.</i> 2013	BP, MLP	ANN	temperature, thunderstorms, rainfall, wind speed	Weather prediction
Oliya and Adeyemo 2012	C4.5	Decision Tree, ANN	maximum temperature, rainfall, evaporation and wind speed	Weather prediction and climate change studies
Harshani and Nagahamulla <i>et al.</i> , 2012	BPN, RBFN, GRNN	ENN, ANN	-	Rainfall prediction in Colombo
Gaurav and Gupta., 2013	BPN, HFN	ANN	temperature, humidity and wind speed	Future weather prediction
Khalili <i>et al.</i> , in 2011	GS531, GS651, black box model	ANN	-	Daily prediction in Mashhad
Bojja and Sanam (2017)	fuzzy logic	ANN	-	Temperature prediction
Mislana, and Hardwinartoc, 2015	BPNN	ANN	-	Rainfall prediction in Tenggarong
Geetha and Nasira, 2014	RapidMiner 5.3	ANN	temperature, pressure, humidity, dew point	Temperature prediction

Chatterjee and Deyz, 2018	-	HNN	-	rainfall prediction in Bengal
Mishra, et al 2018	BP, Levenberg – Marquardt	ANN	-	Rainfall prediction
Chelang and Kayis 2018	BPNN, ANFIS	ANN	temperature , RH, sea level pressure and wind speed	Daily precipitation prediction in Houston, Texas and Dallas, Texas
Kassem (2009)	BPNN	ANN	-	Hourly total and diffuse solar radiation estimation.
Abhishek et al., 2012	BPN	ANN	-	Average monthly rainfall prediction
Devi et al., 2012	BPNN	ANN	max, min temperature	Temperature prediction

4 CONCLUSION

In this work, a review study is conducted for the applications of ANN related to weather forecasting; using ANN approach for weather forecasting yields good results and can be regarded as an alternative to traditional approaches. BPNN is commonly used in ANN forecasting among other ANN architectures while ENN can predict more accurately. More data should be used for good predictions. Additionally, this study also highlighted the capabilities of ANN in predicting several atmospheric phenomenon's such as temperature, rainfall, thunderstorms, others.

Hence, ANN has proved to be a formidable tool for atmospheric forecasting

REFERENCES

- A Geetha, G M Nasira Artificial Neural Networks' Application in Weather Forecasting. International Journal of Computational Intelligence and Informatics, Vol. 4: No. 3, October - December 2014
- Abhishek Aggarwal, Vikas Kumar, Ashish Pandey and Imran Khan (2012). An application of Time series analysis for weather forecasting, International Journal of Engineering Research and Applications, ISSN: 2248-9622, Vol. 2, issue 2 974-980
- Abhishek Saxena, Neeta Verma, Dr K. C. Tripathi, "A Review Study of Weather Forecasting Using Artificial Neural Network Approach", International Journal of Engineering Research & Technology (IJERT) Vol. 2 Issue 11, November – 2013
- Abhishek, K., et al., *A Rainfall Prediction Model using Artificial Neural Network*. 2012 IEEE Control and System Graduate Research Colloquium (ICSGRC 2012), 2012
- Akash D Dubey. Artificial Neural Network Models for Rainfall Prediction in Pondicherry International Journal of Computer Applications (0975 – 8887) Volume 120 – No.3, June 2015
- Amartya Raj Gurung, "Forecasting Weather System Using Artificial Neural Network (ANN): A Survey Paper" *International Journal of Latest Engineering Research and Applications (IJLERA) ISSN: 2455-7137 Volume – 02, Issue – 10, October – 2017, PP – 42-50*
- Bojja.P & Sanam, N. (2017). Design and Development of Artificial Intelligence System For Weather Forecasting Using, *12(3)*, 685-689.
- Ch. Jyosthna Devi, B. Syam Prasad Reddy, K. Vagadhan Kumar, B. Musala Reddy, N. Raja Nayak, "ANN Approach for Weather Prediction using Back Propagation," International Journal of

- Engineering Trends and Technology-
Volume3Issue1- 2012.
- Charaniya, N.A. and S.V. Dudul, *Design of Neural Network Models for Daily Rainfall Prediction*. International Journal of Computer Applications, 2013. **61**(14, January 2013): p. 23-26.
- Chelang A .Arslan and Enas Kayis. Weather Forecasting Models Using Neural Networks & Adaptive Neuro Fuzzy Inference for Two Case Studies at Huoston, Texas and Dallas States. Journal of Asian Scientific Research ISSN (e):2223-1331 ISSN (p):2226-5724. Vol. 8, No. 1, 1-12 © 2018 AESS Publications. All Rights Reserved.
- Devi, C. J., Reddy, B. S. P., Kumar, K. V., Reddy, B. M., & Raja, N. (2012). ANN Approach for Weather Prediction using Back Propagation, 3, 19-23.
- El-Shafie, A. H., El-Shafie, A., El Mazoghi, H. G., Shehata, A. and Taha, M. R. (2011), Artificial neural network technique for rainfall forecasting applied to Alexandria, Egypt, International Journal of the Physical Sciences 6, 1306-1316
- F. Mekanika, T.S. Leeb and M. A. Imteaza. Rainfall modeling using Artificial Neural Network for A mountainous region in West Iran. 19th International Congress on Modelling and Simulation, Perth, Australia, 12–16 December 2011
- Gaurav J. Sawale, Dr. Sunil R. Gupta, “Use of Artificial Neural Network in Data Mining For Weather Forecasting”, International Journal of Computer Science and Applications Vol. 6, No.2, Apr 2013.
- Gazzaz, N. M., Yusoff, M. K., Aris, A. Z., Juahir, H., & Ramli, M. F. (2012). Artificial neural Network modeling of the water quality index for Kinta River (Malaysia) using water quality variables as predictors. *Marine pollution bulletin*, 64(11), 2409-2420.
- Gyanesh Shrivastava Application of Artificial Neural Networks in Weather Forecasting *International Journal of Computer Applications (0975 – 8887) Volume 51– No.18, August 2012*
- Gyanesh Shrivastava, Sanjeev Karmakar, Manoj Kumar Kowar, Pulak Guhathakurta, 2012, “Application of artificial neural networks in weather forecasting: A comprehensive literature Review”, International Journal of Computer Applications (0975 – 8887), Volume 51– No.18.
- Harshani R. K. Nagahamulla, Uditha R. Ratnayake, AsangaRatnaweera,” An Ensemble of Artificial Neural Networks in Rainfall Forecasting,” The International Conference on Advances in ICT for Emerging Regions - ICTer 2012: 176-181
- Ibeh G.F, Agbo G.A, Agbo, P.E, Ali, P.A Application of Artificial Neural Networks for Global Solar Radiation Forecasting With Temperature, Advances in Applied Science Research, 2012, 3 (1):130-134
- Jyosthna Devi ANN Approach for Weather Prediction Using Back Propagation *International Journal of Engineering Trends and Technology- Volume3Issue1- 2012*
- Karmakar Sanjeev et al., 2008, “Development of Artificial Neural Network Models for Long Range Meteorological Parameters Pattern Recognition over the Smaller Scale Geographical Region”, IEEE Computer Society, Washington, DC, USA. 8-10 Dec. 2008, pp.1 – 6
- Khalili, N., Khodashenas, S. R., Davary, K., & Rainfall forecasting for Mashhad Synoptic Station using Artificial Neural Networks, 19, 118- 123.
- Kumar Abhishek, Abhay Kumar, Rajeev Ranjan, Sarthak Kumar, “A Rainfall Prediction Model Using Artificial Neural Network”, IEEE Control and System Graduate Research Colloquium (ICSGRC 2012), pp 82-87.
- M. Ali Akcayol, Can Cinar, Artificial neural network based modeling of heated catalytic converter Performance, Applied Thermal Engineering 25 (2005) 2341-2350.
- M. M. Elkateb, et. al., (1998). A comparative study of medium-weather-dependent load forecasting Using enhanced artificial/fuzzy neural network and statistical techniques. Neurocomputing. 23. 3-13.10.1016/S0925-2312 (98)00076-9.
- Malik, P., & Arora, B. (2014). An Effective Weather Forecasting Using Neural Network, 2(2), 209-212
- Meera Narvekar, Priyanca Fargose, 2015 Daily Weather Forecasting using Artificial Neural

- Network *International Journal of Computer Applications (0975 – 8887) Volume 121 – No.22, July 2015*
- Mislana, Haviluddinb, Sigit Hardwinartoc, Sumaryonod, Marlon Aipassae Rainfall Monthly Prediction Based on Artificial Neural Network: A Case Study in Tenggara Station, East Kalimantan – Indonesia *International Conference on Computer Science and Computational Intelligence (ICCSCI 2015)*
- Mohsen Hayati and Zahra Mohebi, “Temperature Forecasting based on Neural Network Approach”, *World Applied Sciences Journal 2(6): 613-620, 2007, ISSN 1818-4952, IDOSI Publications, 2007.*
- Neelam Mishra, Hemant Kumar Soni Development and Analysis of Artificial Neural Network Models for Rainfall Prediction by Using Time-Series Data. *I.J. Intelligent Systems and Applications, 2018, 1, 16-23. Published Online January 2018 in MECS (<http://www.mecspress.org/>)*
- Nourani, V., Elkiran, G., & Abba, S. I. (2018). Wastewater treatment plant performance analysis Using artificial intelligence—an ensemble approach. *Water Science and Technology.*
- Olaiya, F., & Adeyemo, A. B. (2012). Application of Data Mining Techniques in Weather Prediction and Climate Change Studies. *International Journal of Information Engineering and Electronic Business, 4(1), 51-59. <https://doi.org/10.5815/ijieeb.2012.01.07>*
- Paras, Sanjay Mathur, Avinash Kumar, and Mahesh Chandra, 2009, A Feature Based Neural Network Model for Weather Forecasting *International, Journal of Computational Intelligence Volume 4 Number3.*
- S. Chatterjee, b. Dattay, n. Deyz hybrid neural network Based rainfall prediction supported by Flower pollination algorithm doi: 10.14311/nnw.2018.28.027
- Saba, T., Rehman, A. & Al Ghamdi, J.S. *App Water Sci (2017) 7: 3869. <https://doi.org/10.1007/s13201-017-0538-0>*
- Sanjeev Karmakar Manoj Kumar Kowar Application of Artificial Neural Networks in Weather Forecasting *International Journal of Computer Applications (0975 – 8887) Volume 51– No.18, August 2012*
- Shabib Aftab, Munir Ahmad, Noreen Hameed, Muhammad Salman Bashir, Iftikhar Ali, Zahid Nawaz Rainfall Prediction using Data Mining Techniques: A Systematic Literature Review *IJACSA) International Journal of Advanced Computer Science and Applications, Vol. 9, No. 5, 2018*
- Singh, K. P., Basant, A., Malik, A., & Jain, G. (2009). Artificial neural network modeling of the River water quality a case study, *220, 888–895.*
- T. S. Abdulkadir, A. W. Salami and A. G. Kareem Artificial Neural Network Modeling of Rainfall In Ilorin, Kwara State, Nigeria. *Journal of Research Information in Civil Engineering, 9(1), 2012*
- Vamsi Krishna A Review of Weather Forecasting Models-Based on Data Mining and Artificial Neural Networks Vol 6 • Number 2 April – Sep 2015 pp. 214-222.
- Vertika Shrivastava., Sanjeev Karmakar and Sunita Soni, 2017. Suitability of neural Network for weather forecasting: a comprehensive literature review DOI: <http://dx.doi.org/10.24327/ijrsr.2017.0812.1243>

Development of a Model for Generation of Examination Timetable Using Genetic Algorithm

Ahmed A¹, *Umar B. U¹, Abdullahi I. M², Maliki. D³, Anda. I⁴. and Kamaldeen J. A⁵.
^{1,2,3,5}Department of Computer Engineering, Federal University of Technology, Minna, Niger-state,
Nigeria

*Corresponding author email: buhariumar@futminna.edu.ng, +2348058001775

ABSTRACT

Examination time table scheduling problem is one of the complexes, NP-complete and typical combinatorial optimization problem faced by the university community across the globe. Many researchers have studied the problem due to its NP-complete nature and highly- multi-constrained problem which seeks to find possible scheduling for courses. Creating an examination timetable for university is a very difficult, time-consuming and the wider complex problem of scheduling, especially when the number of students and courses are high. Several factors are responsible for the problem: increases number of students, the aggregation of schools, changes in educational paradigms, among others. In most universities, the examination time table schedule is usually ended up with various courses clashing with one another. In order to solve this problem of time table scheduling for University examination and effective utilization of resources, this research proposed a model for examination time table generation using Genetic Algorithm (GA) probabilistic operators. GA has been successful in solving many optimization problems, including University time table. This is based on the fact that GA is accurate, precise, free from human error and robust for complex space problem. GA theory was also covered with emphasis on the use of fitness function and time to evaluate the result. The effects of altered mutation rate and population size are tested. By using Genetic algorithm, we are able to reduce the time required to generate a timetable which is more accurate, precise and free of human errors. The implication of this research is a solution, minimizing the time taken in timetable allocation and the clashing that usually characterize time table schedule.

Keywords: *Genetic algorithm, timetable, constraints, chromosomes, fitness function.*

1 INTRODUCTION

The Timetable Problem is one of the complex problems faced in any university in the world. It is a highly-constrained combinatorial problem that seeks to find possible scheduling for the university course offerings. There are many algorithms and approaches adopted to solve this problem, but one of the effective approaches to solve it is the use of metaheuristics. Genetic algorithms were successfully useful to solve many optimization problems including the university Timetable Problem. In this paper, we present a near-optimal solution for problem of time table scheduling using GA. The GA method was implemented in MATLAB (Assi, Halawi, & Haraty, 2018). The University timetabling problem is a typical scheduling problem that appears to be a tedious job in every academic institute once or twice a year (Datta, Deb, & Fonseca, 2006). In earlier days, time table scheduling was done manually with a single person or some group involved in task of scheduling it manually, which takes a lot of effort and time. Planning timetables are one of the most complex and error-prone applications.

Timetabling is the task of creating a timetable while satisfying some constraints. There are basically two types of constraints, soft constraints and hard constraints. Soft constraints are those if we violate them in scheduling, the output is still valid, but hard constraints are those which, if we violate them; the timetable is no longer valid (Doulaty, Derakhshi, & Abdi, 2013). The search space of a timetabling problem is too vast, many solutions exist in the search space and few of them are not feasible. Feasible solutions here mean those which do not violate hard constraints and as well try to satisfy soft constraints. We need to choose the most appropriate one from feasible solutions. Most appropriate ones here mean those which do not violate soft constraints to a greater extent (Doulaty et al., 2013). The goal is to have the near-optimal solution for the time table scheduling problem using GA. GAs are used in optimized searching processes and scheduling process. This GA is generally applied to the problem of where optimization is the key goal. A timetable problem is basically related to finding the exact time allocation within limited time period of number of events (courses-lectures) and assigning to them number of resources (teachers, students and Lecture Halls) while satisfying

Hard Constraints and Soft constraints (Deeba Kannan, 2019).

Also, this is based on the fact that GA is accurate, precise, free from human error and robust for complex space problem. GA theory was also covered with emphasis on the use of fitness function and time to evaluate the result. The effects of altered mutation rate and population size are tested. By using Genetic algorithm, we are able to reduce the time required to generate a timetable which is more accurate, precise and free of human errors. The implication of this research is a solution, minimizing the time taken in timetable allocation and the clashing that usually characterize time table schedule.

The remaining part of this paper is organized as follows: section II deals with time tables issues. section III discussed GA; related works are discussed IV; V presents the proposed methodology and the implementation, while VI presents the results and discussion. Finally, section VII presents the conclusion.

2. TIMETABLING ISSUES

2.1 Examination Timetabling Problem

The examination timetabling problem is a well-known non-deterministic polynomial-time (NP) and is a hard optimization problem (solving problems without violation of the university's terms) faced by all educational institutions. However, the approach that the institutions adopt in preparing examination timetables depends on the variations in the institution's requirements and constraints (Burke, Eckersley, McCollum, Petrovic, & Qu, 2003; Burke et al., 2003).

The Federal University of Technology, Minna (FUTMINNA) like any other institutions of higher learning, face a similar problem and is used as the case study in this paper. Preparing the examination timetable takes much of the administrator's time and when it involves all the different programs, the task is overwhelming (Ross, Corne, & Fang, 1994; Birbas, Daskalaki, & Housos, 2009). Timetabling is complicated due to many factors. Below are some of the problems that university administrations usually face when preparing the final examination schedule (Birbas et al., 2009):

- a. Limited time to prepare.
- b. A limited number of rooms.
- c. Limited number of staffs to prepare the schedule.
- d. Last-minute timetable changes.
- e. Inadequate staff to invigilate.
- f. Late submission of examination grades by Lecturers.
- g. Absence of invigilators or students (sick or vacation leaves) at the appointed time.

3 GENETIC ALGORITHM

Genetic Algorithm (GA) is an optimization method that imitates the behaviour of biological evolution to solve

particular problems programmatically. In aligning with a specific problem at hand, a quantitative evaluation is performed by a fitness function to each candidate solution by implementing GA that makes the solution better, i.e. improves the fitness level (Birbas et al., 2009). The algorithm evaluates each candidate at random according to the fitness function (Birbas et al., 2009). However, by chance, a few may succeed but with weak or imperfect results. These positive solution candidates are stimulated, reserved and permitted to reproduce (Obaid, Ahmad, Mostafa, & Mohammed, 2012). GA has been widely used in many areas that are difficult for humans to handle. The solutions are more credible, efficient, faster, and higher complexity than humans can solve. In many cases, genetic algorithms produce solutions that are far better than the programmer who wrote the algorithm. The Basic outline of GA in the step next below.

```
Create a population of creatures.
Evaluate the fitness of each creature.
While the population is not fit enough:
{
Kill all relatively unfit creatures.
While population size < max;
{
Select two population members.
Combine their genetic material to create a new creature.
Cause a few random mutations on the new creature.
Evaluate the new creature and place it in the population.
}}
```

3.1 GA Operators

Chromosome representation: Chromosome is a set of parameters which define a proposed solution to the problem that the genetic algorithm is trying to solve. The chromosome is often represented as a simple string. The fitness of a chromosome depends upon how well that chromosome solves the problem at hand.

Initial population: The first step in the functioning of a GA is the generation of an initial population. Each member of this population encodes a possible solution to a problem. After creating the initial population, each individual is evaluated and assigned a fitness value according to the fitness function. It has been recognized that if the initial population to the GA is good, then the algorithm has a better possibility of finding a good solution and that, if the initial supply of building blocks is not large enough or good enough, then it would be difficult for the algorithm to find a good solution.

Selection: This operator selects chromosomes in the population for reproduction. The fitter the chromosome, the more times it is likely to be selected to reproduce (Mitchell, 1998).

Crossover: In genetic algorithms, a crossover is a genetic operator used to vary the programming of a chromosome or chromosomes from one generation to the next. It is analogous to reproduction and biological crossover, upon which genetic algorithms are based. A crossover is a process of taking more than one parent solutions and producing a child's solution from them. There are methods for selection of the chromosomes. This operator randomly chooses a locus and exchanges the subsequences before and after that locus between two chromosomes to create two offspring.

Mutation: Mutation is a genetic operator used to maintain genetic diversity from one generation of a population of genetic algorithm chromosomes to the next. It is analogous to biological mutation. The mutation alters one or more gene values in a chromosome from its initial state. In mutation, the solution may change entirely from the previous solution. Hence GA can come to a better solution by using mutation. This operator randomly flips some of the bits in a chromosome (Mitchell, 1998).

Fitness Function: The fitness function is defined over the genetic representation and measures the quality of the represented solution. The fitness function is always problem dependent. In particular, in the fields of genetic Programming and genetic algorithms, each design solution, are commonly represented as a string of numbers referred to as a chromosome. After each round of testing, or simulation, the idea is to delete the 'n' worst design solutions and to breed 'n' new ones from the best design solutions.

4 RELATED WORKS

Different approaches have been proposed to solve the university timetable problem by a different researcher. These research are: (Elsaka, 2017), (Matias, Fajardo, & Medina, 2018), (Dener & Calp, 2019), (Dener & Calp, 2019), (Soyemi, Akinode, & Oloruntoba, 2017), (Mohammed, 2017), (Rozaimie, Shafee, Hadi, & Mohamed, 2017), (Al-Jarrah, Al-Sawalqah, & Al-Hamdan, 2017), (Sani & Yabo, 2016), (Mittal, Doshi, Sunasra, & Nagoure, 2015), (Amaral & Pais, 2016) and (Abdelfattah & Shawish, 2016). Numerous works of some of these are presented in this section below.

Research by (Bhaduri, 2009) solved the problem with an evolutionary technique such as the Mimetic Hybrid Algorithm, Genetic Artificial Immune Network (GAIN) and compared the result with that obtained from genetic algorithm. His result showed that GAIN was able to reach the optimal feasible solution faster than that of GA but not as effective as GA.

Mei Rui 2010, in his paper, performed analysis and the summarization of the existing problems. A mathematical model for the course timetable system was proposed. At the same time, through the use of the pattern recognition

technology in artificial intelligence, aiming at this mathematical model a new university course timetable system design program is proposed and realized. This program not only can well solve the shortages of the existing course timetable system but also is simple and easy to operate, has strong versatility.

A genetic algorithm (GA) based model to generate examination schedules such that they focus on students' success in addition to satisfying the hard constraints required for feasibility. The model is based on the idea that student success is positively related to adequate preparation and resting time between exams. Therefore, the main objective of the system is to maximize the time length among exams (i.e., paper spread) considering the difficulties of exams. Two different genetic algorithm models were developed to optimize the paper spread. In the first genetic algorithm model, a high penalty approach was used to eliminate infeasible solutions throughout generations. The second genetic algorithm model controls whether or not each chromosome joining the population satisfies the hard constraints. The model presented can be implemented in software to make it use practical. On the other hand, the models presented can be extended to include the fuzziness that may arise when understanding the difficulties of exams. Only constraints set by the institutions and lecturers have been taken into account (Kalayci & GUNGOR, 2012).

The author in (Parkavi, 2012), developed an e-College Time table Retrieval System Based on Service Oriented Architecture which provides support for staffs, HODs, Principal, Directors and other societies interested in e-college time table retrieval systems, as well as for students. This system provides the facility for coordinator to enter the time table or change the time table and the staffs to access the time table using their PDAs or by using their smartphones, alerts can be transferred about their duties over the mobiles and exchanging of duties can also be done using the mobile devices with the help of web services. The system is expensive due to the involvement of many entities and takes time to develop. Network failure can lead to inadequate message dissemination. Extra alerts sent over the media or internet require extra spending.

Research in Mugdha K. P., Rakhe S. S., Prachi A. P. & Naveena N. T. (2014), authors focused on the development of a web application for automatic time table generation. A mechanized system was designed with a computer-aided timetable generator. The system allows interaction between the staff and students and at the same time enable them to upload their queries, notes, presentations and e-books. The application makes the procedure of time table generation easier consistently which may otherwise need to be done using spreadsheet manually which might lead to constraints problem that is

strenuous to establish when time table is generated physically. The purpose of the algorithm is to generate a timetable schedule mechanically. Keeping in mind the generality of the algorithm operation, it can further be modified to more particular scenarios, e.g. University, examination schedules, etc. A number of hours which are spent on creating a fruitful timetable can be reduced ultimately through the mechanization of the timetable issue. The cost of developing a site to operate only time table schedule can be minimized by developing a simple standalone application and also, the security aspect i.e. how secure the site is may allow hackers to easily penetrate and easy pasting of irrelevant posts is achieved by any students which are a disadvantage to the system too.

Also, research by (Mittal, Doshi, Sunasra, & Nagoure, 2015) developed an automatic timetable scheduler by using Genetic algorithm. The time requires to generate time table was able to reduce drastically and generate a timetable which is more accurate, precise and free of human errors. The first phase contains all the common compulsory classes of the institute, which are scheduled by a central team. The second phase contains the individual departmental classes. Presently, this timetable is prepared manually, by manipulating those of earlier years, with the only aim of producing a feasible timetable.

5 PROPOSED METHODOLOGY AND IMPLEMENTATION

In order to deal with timetabling issues, we are proposing a system which would automatically generate a timetable for the institute. Course and lectures will be scheduled in accordance with all possible constraints and given inputs and thus a timetable will be generated. The structure of time table generator consists of input data, relation between the input data, system constraints and application of a genetic algorithm. Figure 1, present flowchart for Timetable Generator.

5.1 The Structure for Time Table Generation

A. Input Data

The input data contains:

1. *Subject*: Data describes the name of courses in the current term.
2. *Room*: Data describes the room number and their capacity.
3. *Time intervals*: It indicates starting time along with the duration of a lecture.

B. Hard and Soft Constraints

A timetable must serve and overcome a number of constraints. Constraints are universally used to deal with timetabling problems. In GA, the types of constraints are soft and hard. Hard constraints in constructing an examination timetable should have no violation, an example is, a class cannot be at different locations at the same time. While Soft constraints are constraints that can be violated but violations must be minimized. Below are the lists of hard and soft constraints used in this research.

Hard constraints

- a) No students should write two exams on the same day.
- b) No two venues should be assigned for the same exam.
- c) No two exams should be allocated to the same venue.
- d) A number of days should not be violated.

Soft constraints

- a) The Capacity of the venues should be considered.
- b) Carryover students should be considered.

C. The Parameters for the implementation

Population Size = 60
Number of Generation = 100
Partially mapped Crossover
Single point Mutation
Rank Selection
Crossover probability = 0.8
Mutation rate = 0.03

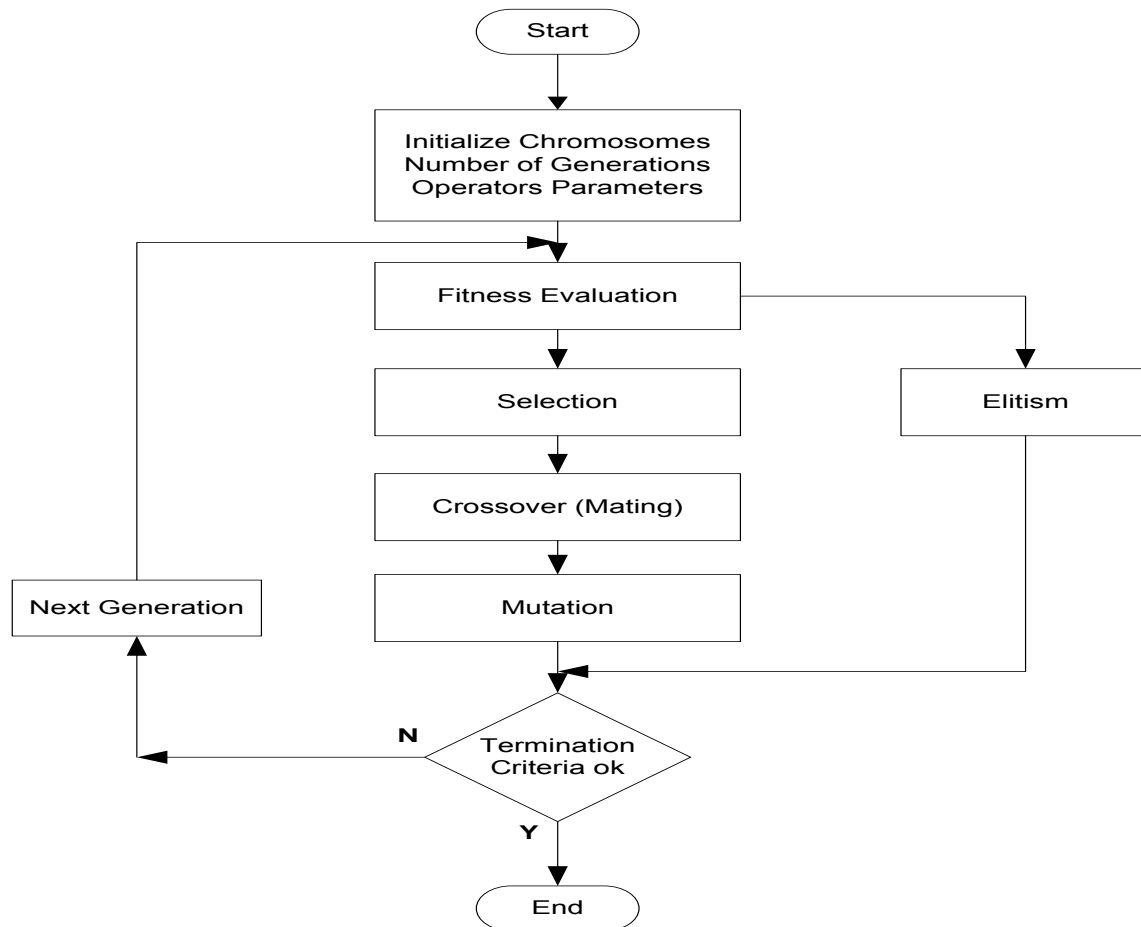


Figure 1: Flowchart of the Timetable Generator

6 RESULT AND DISCUSSION

The experiments aim to quantitatively determine the best results. The experiments focus on the best fitness that could be obtained with a fixed population size and generation iterations. Thus, the best value is assumed to have the lowest fitness value out of all values generated for each population size used.

In this paper, the time at which each result is generated and the fitness value of the generated result are used as the evaluation metrics. The results are presented in table 1, figure 2 and 3 respectively.

Figure 2 shows the minimum and maximum fitness value of the generated timetable against the population size, while figure 3 shows the maximum time of the generated timetable against different population size.

From the result in figure 2, it can be deduced that the fitness value is inversely proportional to the population size and directly proportional to the time spent to give results for each timetable i.e., the higher the population size, the better and smaller the fitness value and at the same time the longer it takes to give results for higher population size and vice versa.

The implication of this result is a solution, minimizing the time taken in timetable allocation and the clashing that usually characterize time table schedule.

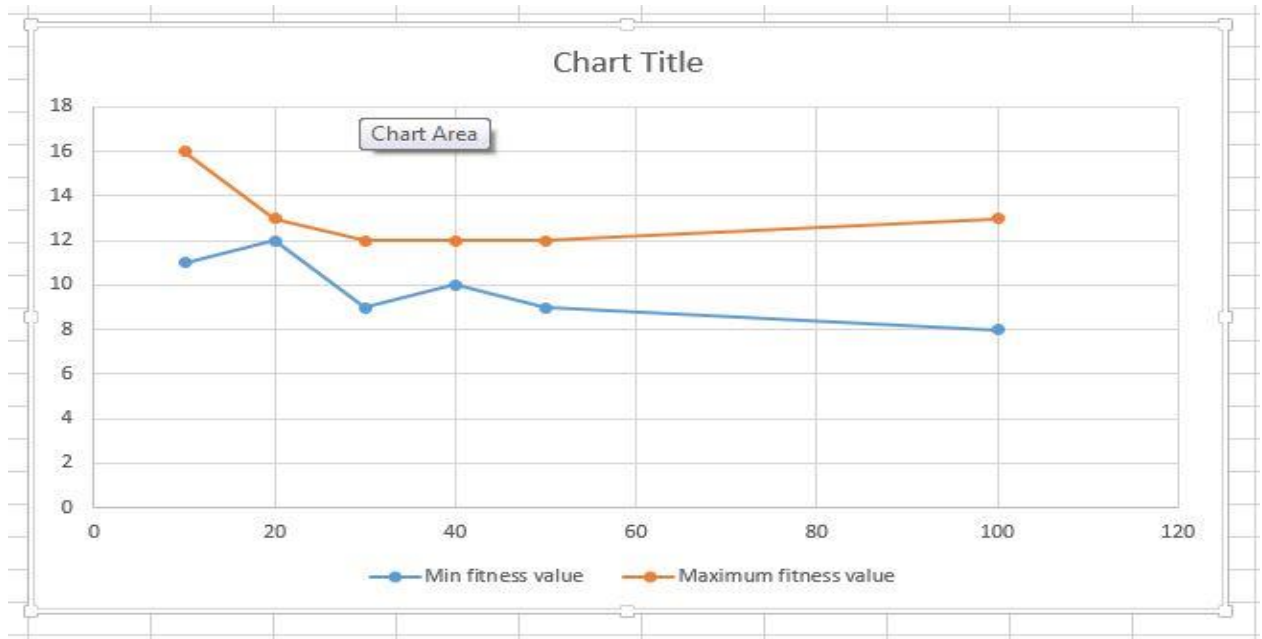


Figure 2: Population Size against Fitness Value

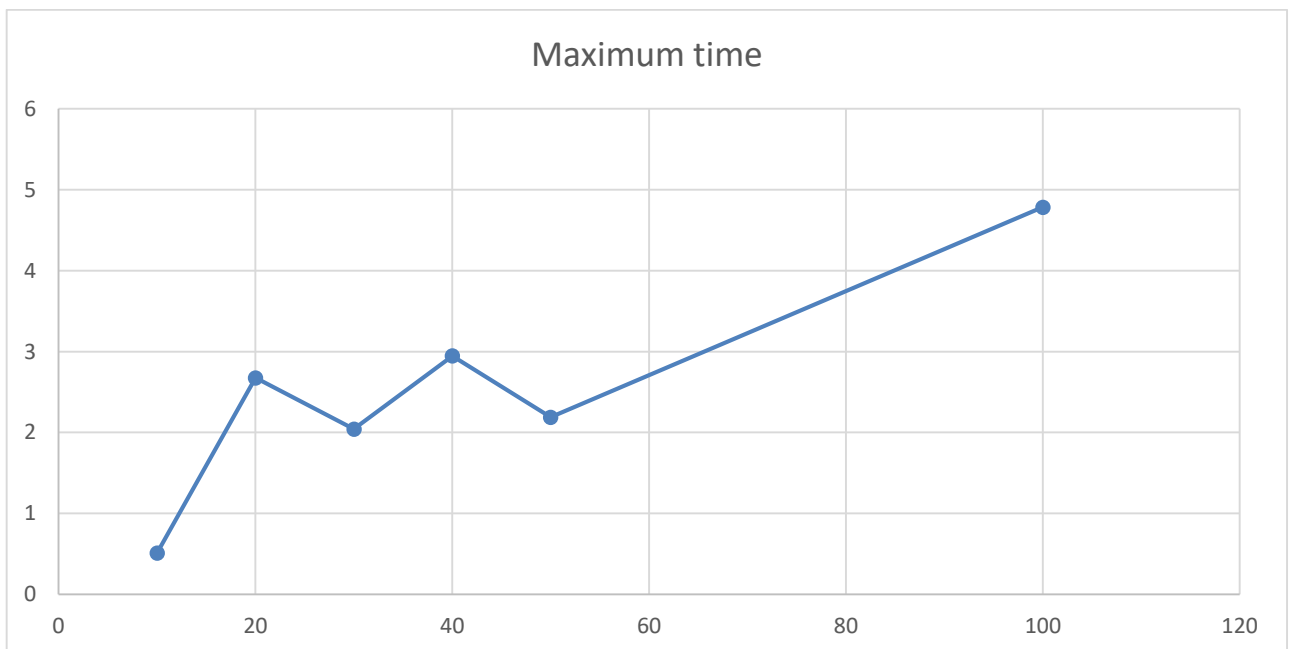


Figure 3: Maximum Time against Population Size

Table 1: Result Obtain for Proposed Timetable Generation using GA

S/n	Population size	Min fitness value	Meantime	Mean fitness value	Maximum fitness value	Maximum time
1	10	11	0.2744	11.8900	16	0.5084
2	20	12	1.5085	12.0300	13	2.6747
3	30	9	1.1091	9.6200	12	2.0425
4	40	10	1.6266	10.8300	12	2.9448
5	50	9	1.1002	9.7800	12	2.1885
6	100	8	8.2872	10.3300	13	4.7846

7 CONCLUSION

University time table scheduling is an NP problem. Many techniques exist for solving University time table scheduling problem. This research addresses the problem of time complexity and the clashes that usually associated with most university time table scheduling using GA. The undertaking is created in a manner that; no exam conflicts happen given elements to tailor the timetable as of a wish. This research also talks about the execution of a Genetic Algorithm (GA) to locate the best answer for examination timetabling issue. Furthermore, the selected operators' viability and effectiveness are concentrated on. An assortment of GA operators has been acquainted all together with meet the difficulties and the requests of examination timetabling issue. The proposed algorithm is tested with genuine information and the results present optimal solution for time table scheduling problem. The algorithm's conduct is investigated taking into account the varieties of the selected parameters. The best results are obtained with the moderate populace of 60 chromosomes, partially mapped crossover single point mutation, and rank selection. Consequently, the algorithm can initialize the population of examination timetable solutions that are feasible (satisfies hard constraints) at all time. The implication of this research is a solution, minimizing the time taken in timetable allocation and the clashing that usually characterize time table schedule.

REFERENCES

- Abdelfattah, M., & Shawish, A. (2016). *Automated academic schedule builder for University's faculties*. Paper presented at the Proceedings of the World Congress on Engineering.
- Al-Jarrah, M. A., Al-Sawalqah, A. A., & Al-Hamdan, S. F. (2017). DEVELOPING A Course TIMETABLE SYSTEM FOR ACADEMIC DEPARTMENTS USING GENETIC ALGORITHM. *Jordanian Journal of Computers and Information Technology (JJCIT)*, 3(1).
- Amaral, P., & Pais, T. C. (2016). Compromise ratio with weighting functions in a Tabu Search multi-criteria approach to examination timetabling. *Computers & Operations Research*, 72, 160-174.
- Assi, M., Halawi, B., & Haraty, R. A. (2018). Genetic Algorithm Analysis using the Graph Coloring Method for Solving the University Timetable Problem. *Procedia Computer Science*, 126, 899-906.
- Bhaduri, A. (2009). *University time table scheduling using genetic artificial immune network*. Paper presented at the Advances in Recent Technologies in Communication and Computing, 2009. ARTCom'09. International Conference on.
- Birbas, T., Daskalaki, S., & Housos, E. (2009). School timetabling for quality student and teacher schedules. *Journal of Scheduling*, 12(2), 177-197.
- Burke, E., Eckersley, A., McCollum, B., Petrovic, S., & Qu, R. (2003). Similarity measures for exam timetabling problems.
- Datta, D., Deb, K., & Fonseca, C. M. (2006). Solving class timetabling problem of IIT Kanpur using

- multi-objective evolutionary algorithm. *KanGAL Report*, 2006006, 1-10.
- Deeba Kannan, K. B. a. S. R. (2019). Solving Timetable Scheduling Problems Using Genetic Algorithm. *International Journal of Recent Technology and Engineering (IJRTE)*, 7 (5C), 168 - 170.
- Dener, M., & Calp, M. H. (2019). Solving the exam scheduling problems in central exams with genetic algorithms. *arXiv preprint arXiv:1902.01360*.
- Doulaty, M., Derakhshi, M. F., & Abdi, M. (2013). Timetabling: A state-of-the-art evolutionary approach. *International Journal of Machine Learning and Computing*, 3(3), 255.
- Elsaka, T. (2017). *Autonomous generation of conflict-free examination timetable using constraint satisfaction modelling*. Paper presented at the 2017 International Artificial Intelligence and Data Processing Symposium (IDAP).
- Kalayci, C. B., & GUNGOR, A. (2012). A Genetic Algorithm Based Examination Timetabling Model Focusing on Student Success for the Case of the College of Engineering at Pamukkale University, Turkey. *Gazi University Journal of Science*, 25(1), 137-153.
- Matias, J. B., Fajardo, A. C., & Medina, R. M. (2018). *A fair course timetabling using genetic algorithm with guided search technique*. Paper presented at the 2018 5th International Conference on Business and Industrial Research (ICBIR).
- Mei Rue (2010). Computer and Automation Engineering. *The 2nd International Conference (Volume: 4)*
- Mittal, D., Doshi, H., Sunasra, M., & Nagoure, R. (2015). Automatic timetable generation using genetic algorithm. *International Journal of Advanced Research in Computer and Communication Engineering*, 4(2), 245-248.
- Mohammed, M. A. (2017). A Review of Genetic Algorithm Application in Examination Timetabling Problem*" Mazin Abed Mohammed," Mohd Khanapi Abd Ghani," Omar Ibrahim Obaid," Salama A. Mostafa,"Mohd Sharifuddin Ahmad," Dheyaa Ahmed Ibrahim and" MA Burhanuddin" Biomedical Computing and Engineering Technologies (BIOCORE) Applied Research Group. *Journal of Engineering and Applied Sciences*, 12(20), 5166-5181.
- Mitchell, M. (1998). *An introduction to genetic algorithms*: MIT press.
- Mugdha K. P., Rakhe S. S., Prachi A. P. & Naveena N. T. (2014). Web Application for Automatic Timetable Generation. *International Journal of Current Engineering and Technology* 2277 – 4106.
- Obaid, O. I., Ahmad, M., Mostafa, S. A., & Mohammed, M. A. (2012). Comparing performance of genetic algorithm with varying crossover in solving examination timetabling problem. *J. Emerg. Trends Comput. Inf. Sci*, 3(10), 1427-1434.
- Parkavi, A. (2012). An e-College Time table Retrieval System Based on Service Oriented Architecture. *International Journal of Advances in Computing and Information Technology*.
- Ross, P., Corne, D., & Fang, H.-L. (1994). Improving evolutionary timetabling with delta evaluation and directed mutation. *Parallel Problem Solving from Nature—PPSN III*, 556-565.
- Rozaimiee, A., Shafee, A. N., Hadi, N. A. A., & Mohamed, M. A. (2017). A framework for university's final exam timetable allocation using genetic algorithm. *World Applied Sciences Journal*, 35(7), 1210-1215.
- Sani, H., & Yabo, M. (2016). Solving timetabling problems using genetic algorithm technique. *International Journal of Computer Applications*, 134(15).
- Soyemi, J., Akinode, J., & Oloruntoba, S. (2017). *Electronic Lecture Time-Table Scheduler Using Genetic Algorithm*. Paper presented at the 2017 IEEE 15th Intl Conf on Dependable, Autonomic and Secure Computing, 15th Intl Conf on Pervasive Intelligence and Computing, 3rd Intl Conf on Big Data Intelligence and Computing and Cyber Science and Technology Congress (DASC/PiCom/DataCom/CyberSciTech).



Smart Protection of Vehicle using Multifactor Authentication (MFA) Technique

*S. Aliyu, Umar Abdullahi, Majeedat Pomam, Mustapha Hafiz, Adeiza Sanusi, and Sodiq Akanmu
Department of Telecommunication Engineering, Federal University of Technology, PMB 65 Minna
Niger State, Nigeria

*Corresponding author email: salihu.aliyu@futminna.edu.ng, +2347039335074

ABSTRACT

In typical third world country like Nigeria, the incessant increase in car theft has called for provision of an immediate solution. Occurrence of car theft is not limited to public places such as market, and bank arena, several car thefts have occurred on gun-point. There is no doubt that modern cars have some level of pre-installed anti-theft device by the manufacturers, however, poor user authentication has led to its inability to solve the problem of car theft. Therefore, this paper proposed a multiple factor authentication approach to provide reliable car user authentication. The proposed approach is capable of preventing unauthorized user from accessing the car, thus securing the it from theft. Traditional approach of unlocking/locking cars involve the use of two buttons, one for locking and the other for unlocking. This approach lacks user authentication, consequently, it is prone to unauthorized access. To solve this problem, a password authentication approach was introduced. After unlocking the car, user biometric, fingerprint, is required as a second means of authentication before the car ignition can be activated. In the event of theft, a user authentication request pops up at a random time to authenticate the current user. In the absence of genuine user, the car is deactivated and an SMS containing the current car location is sent to the genuine user as well as security personnel. This is made possible through the use of GSM/GPS communication module. The proposed system herewith is simple to use and can be used by any model of vehicle and it is very reliable and efficient.

Keywords: *Biometric; Fingerprint; GPS; GSM; Atmega16 Microcontroller; Multifactor Authentication .*

1 INTRODUCTION

Vehicles (automobiles generally) are stolen everyday yet people keep purchasing them; this is so because they serve as means of easily transporting oneself from one place to the other. In Nigeria today, vehicle theft has become so ubiquitous such that car owners are conscious of where and how they park their cars. Car theft is an illegal act of possessing vehicles. In consensus with the National Insurance Crime Bureau (NICB), Nationwide in 2010, one million, two hundred thousand motor vehicle thefts were estimated, i.e. about 416.7 cars were stolen per 100,000 residents (All, Ijeh-Ogbo, & Gbadamosi, 2005; Modi & Sukhadia, 2017).

The alarming rate at which vehicles are stolen has brought about the need for vehicle anti-theft systems – which are systems designated to thwart the illegal possession of valuable items such as automobiles. Anti-theft systems have been in existence since stealing became human's source of livelihood. However, most previously proposed systems fell short of proper user authentication, therefore, the proposed system has been designed such that vehicle driver can be well authenticated, and can easily be shut down and tracked in the event of theft. To achieve user or driver authentication, it was designed with a multi-level authentication; failure to provide an appropriate means of

identification at either level restrains the user from gaining complete access into the vehicle.

2 RELATED WORKS

Several systems have been proposed in the literature for car security. Xiao & Feng, (2009), proposed a low-cost extendable framework for embedded smart vehicle security system. It consists of a FDS, a GPS module, a GSM module and a control platform. The FDS is based on Adaboost algorithm which can detect people's faces in the vehicle when nobody ought to be in the car, and either alarms loudly or soundlessly. Other modules aid in the transmission of the important data to car owners and, it helps to watch guard vehicles at all the time, even when the car is lost. Alarm is sent to the control center of the system whenever intrusion is detected. Whenever the vehicle is on silent mode, no alarm is made, but some modules function to inform the owner and law enforcement agency about the exact location of the car. This system is not expensive, efficient and can be used to track vehicles.

Hasan et al., (2009), presented an arrangement that permits an owner to remotely locate the vehicle. The present position of the car is read by the system using the GPS while it sends data through GPRS (General Packet Radio Service) service to a web server utilizing the POST mechanism of the HTTP protocol. The vehicle's location is then stored in the database for live and previous tracking.



It is useful for the parents to watch over their children's safety, but it lacks unauthorized access denial and it requires one to log into the website before tracking can be done.

Hameed et al., (2010), presented a vehicle monitoring and tracking system with an enhancement in mobility and database facilities. This system can send SMS and MMS to an authorized user for speedy response most especially if the car is in close range. The images of the unauthorized users are transmitted to the user and/or police through local GSM/GPRS service provider. Whenever there is a hijack, local security agent and owner can track down the car using GPS which can be linked to Google Earth Map for ease of location. The system makes use of microcontroller, GPRS modem, and a PC. This system is cost-effective, has a real life application, but it cannot prevent unauthorized access into the car.

Wankhade & Dahad, (2011), proposed a system that deals with the design and development of a theft control system for an automobile, used to prevent vehicle theft. The system makes use of an embedded system based on GSM technology. A cell phone is interfaced with the microcontroller, which in turn, is connected to the engine. Information in the form of SMS is sent to the central insurance system. The microcontroller unit reads the SMS and, using the triangulation method, it extracts the exact location (latitude and longitude) of the vehicle and sends it to the user's mobile. STATUS can be sent to the GSM module by the user. This module verifies the authenticity of the message before replying with an SMS that contains the location (latitude and longitude) the vehicle. This system lacks the ability to prevent unauthorized persons from getting into the car.

Rashidi, Ariff, & Ibrahim, (2011), proposed a car monitoring system using Bluetooth. Once an alarm is triggered, a message is transmitted to the owner's phone via Bluetooth informing him/her of an intrusion. A PIR sensor is used to monitor movements around the car. Alert messages are sent to the user, if the microcontroller keeps on receiving signal from the PIR sensor for seven minutes. This system is restrained to the distance covered by the Bluetooth; however, the owner can only receive alerts if within the range of the Bluetooth.

Almomani, Alkhalil, Ahmad, & Jodeh, (2011), developed a GPS car tracking and management system which is aimed at making vehicle tracking easier and available for any user and fleet companies. It provides mobile software that enables ubiquitous tracking services and web-based tracking software. It enables users to remotely track and control the speed of their vehicles. It makes use of GPS tracker, a GSM modem and a PC.

Bagavathy, Dhaya, & Devakumar, (2011), proposed an emergency response system for smart cars to prevent theft using ARM (Advanced RISC Machine) processor. This system has an FDS which detects the face of the person trying to gain access into the vehicle during the time nobody should be in the car. FDS obtains images in a tiny

digital camera. Principal Component Algorithm (PCA) – Linear Discriminant Analysis (LDA) is used to provide the face authentication in the security system. A camera module is used for downloading images from the system. It recognizes the input after the image has been captured. The result is processed as a character signal (authentic or not). The microcontroller executes some actions based on the result of the character signal. Though this system can deny access to unauthorized users, it cannot be used to track vehicles.

Kamble, (2012), wrote a paper on a smart vehicle tracking system. The proposed system is a tracking system useful in the determination of the geographical location of a vehicle. Also, it can be used to transmit the information remotely to a server. The system incorporates the use of GPS, GSM and microcontroller to achieve the predefined goals. To find the location of the vehicle, a user request is sent to the number at the modem, which instantly replies to that mobile showing the vehicle's position. The proposed system is limited to vehicle tracking only, i.e. it cannot deny access to unauthorized users.

Sehgal, Singhal, Mangla, Singh, & Kulshrestha, (2012), proposed an embedded interface for GSM based car security system. It makes use of an 8-bits AT89S52 interfaced with a GSM module. Its control mechanism is based on Dual Tone Multi-access Frequency tones generated when the number keys are pressed. The system has real life application and it is marketable due to its cost-effectiveness, but it cannot be used to track vehicles in event of theft.

Padmapriya & Kalajames, (2012), developed a real time smart car lock security system using an improved face detection and recognition technique based on skin color information. The face is detected by Adaboost algorithm; in addition, it employs the use of PCA algorithm to recognize a specific face which compares the faces in the database with the newly captured ones. A webcam is placed in the car door, which records video frames. When an unauthorized user tries to open the door, the owner is alerted, else, the door will open and access will be gained into the car. This system is efficient, cost-effective and can be utilized for tracking vehicles using GPS. However, the technique used for authentication is quite slow.

Khan & Mishra, (2012), described a system that can provide tele-monitoring system for commercial vehicles. It comprises of GPS, GSM and an AMR microcontroller. If a password-like SMS is received from the owner, the vehicle is stopped automatically. This system is applicable in traffic surveillance. It can be used to remotely monitor a vehicle but, it does not prevent unauthorized access. The components used are; GPS, GSM, satellite and ARM LPC2138 microcontroller.

Katta & Sudharsan, (2012), introduced an integrated system to provide and assist the travelers, transport courier companies, cars, and bike users obtain a real-time dynamic vehicle tracking and traveled route information with the time stamps. It is an integration of Geographical

Information and Communication Technology (Geo-ICT) and Sensor Network (SN) was used to develop a real time monitoring system and take necessary decision in delivery of information. It gathers information automatically using sensors, and transmitting through Xbee enabled devices and GPS for locating vehicles.

Ramani et al., (2013), made use of GPS and GSM technology for a tracking and locking systems. The components used includes; GSM, GPS, and a microcontroller. The system was designed in two modes: sleep mode when the owner is the operator and active mode when there is an intruder, where the IR sensor senses the signals and SMS is sent to the microcontroller. The controller sends signals containing the vehicle's location. Depending on the command received, the vehicle's speed is gradually decreased and finally come to a stop. In addition, all the doors are locked. To open the door or restart the engine, authorized person needs to enter the passwords. With this system, vehicles can be easily tracked without the escape of the criminal, but it can only detect intrusion if there is an interruption in any door of the car.

Pethakar, Srivastava, & Suryawanshi, (2013), developed a GPS and GSM based vehicle tracking and worker security system, which enables a company to track the vehicle's location. The system utilizes GPS, GSM, RFID and a microcontroller. The proposed system consists of three units – the vehicle unit, emergency button and company unit. The vehicle unit is placed inside the car. Whenever the car picks up the worker, he/she needs to swipe the RF card number, with its database records; it sends the worker's id, cab id and the cab position co-ordinates to the company unit via GSM module. The emergency button is a part of the vehicle unit; there are three to four emergency buttons in the car. These buttons are placed such that workers can easily access them. If worker finds himself/herself in a problem, he/she will press the button; microcontroller will detect the action and send a signal to the GSM which will communicate with the company unit and police. Microcontroller will also send a signal to the relay which turns off the vehicle ignition and stops the vehicle. Company unit consist of GSM modem, RS232 cable and computer. The GSM modem will receive the message through the GSM. This message will be transferred to the computer through the serial port. The worker name, id and cab position coordinates get displayed on the computer. Its use is limited to the use of the RF cards.

Kotte & Yanamadala, (2013), described a tracking system capable of continuous monitoring a vehicle on PC via Google Earth Application. The main components used in constructing this system is; GPS, GSM and MCU; it comprises of two major design units which includes: In-vehicle unit (the core part, installed in the vehicle) and the tracking monitoring station. All the information sent by the in-vehicle unit is stored in the database, maintained by the tracking server. The in-vehicle unit has a tracking server which it uses to transmit the vehicle's location to its owner.

It is not cost-effective and it is mainly proposed for tracking vehicles.

Verma & Bhatia, (2013), described a monitoring system that informs the owner of the location and the route traveled by the vehicle. It has a web application that provides the user with the exact vehicle's location. This system comprises of GPS, GSM, AT mega microcontroller MAX232, 16x2 LCD and software interfaced with all the required modules and a web application. The GPS module is used for getting the co-ordinates of the vehicle while the GSM module is used for transmitting received data. The microcontroller is the central unit which controls every other component of the system; the LCD is used to display location of vehicle. This system can calculate the distance traveled by the vehicle, however, monitoring is via internet.

Oladimeji, Oshevire, Omitola, & Adedokun, (2013), described a system that can be used to proffer a lasting solution to the endemic act of vehicle theft. The components used in realizing this system include; GSM, GPRS modem module, HyperTerminal software and PC. This module supervises the entire system communication with one or more remote disabling receivers, which act as the interface circuitry between the controller and the motor vehicle subsystem.

Monisha, Leo, & Sakthi, (2014), described a system that uses microcontroller (PIC16F877A), with regulated power supply, GPS receiver for location of information, GSM modem/mobile phone for remote communication and LED indicators. This system consists of three modules; the SMS ignition module: which is user defined, when the car starts, it sends SMS to the car owner, the user is only able to start the vehicle if there is a reply. The malfunction mode helps to send message to the service center, whenever the vehicle develops a fault. The accident alert module sends SMS to a hospital or to the next of kin whenever an accident occurs. The GSM is used to send the text message containing the vehicle's co-ordinates gotten from the GPS. The GSM and GPS modules communicate with the microcontroller with the aid of a serial device. The proposed system has the capability to deny an unauthorized person to access the vehicle; however, authentication takes time because without a reply from the authorized user, the vehicle cannot be started.

Sehgal, Singhal, Mangla, Singh, & Kulshrestha, (2012), described a system that makes use of GSM and GPS for controlling and securing vehicles. Whenever there's an intrusion, the user can send a predefined text to the system via an SMS in order to automatically switching off the car's ignition system. The proposed system cannot detect intrusion, it lacks access denial ability to unauthorized users and it requires internet connection.

Prakash & Sirisha, (2014), developed a system that utilizes GSM technology with CAN bus along with RFID system for vehicle theft control. Once the car is ignited, an SMS containing the vehicle's co-ordinates are sent to the owner's number. On receiving this message, the owner sends a reply to either stop the vehicle or allow the vehicle

to run through a keypad. On receiving the locking code, the speed of the car will be decreased. Similarly, whenever there's an intrusion, an alarm is sounded. The speed of the vehicle can be remotely controlled. The system requires RFID to be placed on every road; which makes the system practically unrealistic.

All, Ijeh-Ogbo, & Gbadamosi, (2015), proposed a system that can be used to protect vehicle theft via GSM network. Commands are sent to and fro the system via a GSM module. SMS messages are sent from GSM/GPRS modem module to the user's mobile phone whenever an alarm situation occurs. Time snapshots of the vehicle's driver can be taken using DM642 media processor. Any phone could be used to send out commands and remotely demobilize the vehicle but no unauthorized access denial and no authentication is required.

B. Bhatt, P. Kalani, N. Parmar, (2015), developed a smart vehicle security system using GSM and GPS. The component used in the system includes; GSM modem, GPS receiver, 8051 microcontrollers, relay, interrupt switch, vibration sensor etc. If the interrupt switch is pressed, and the vehicle is started then controller will not give any alert, because only the owner knows where it is. If the vehicle is started without pressing the interrupt switch, then an intrusion is detected, thus the microcontroller sends an alert to the owner with the location of the vehicle through SMS via GSM. Then the owner can stop the engine by sending "stop" to the controller through GSM to the microcontroller and relay engine will stop. If accident occurs at that time, information about the accident is sent simultaneously with the location of the vehicle via SMS to the stored number.

Singh, Sethi, Biswal, & Pattanayak, (2015), developed a smart anti-theft system that uses GPS and GSM system to prevent theft and to determine the exact location of vehicle. The system contains GPS module, GSM modem, infrared sensors, Dual Tone Multi Frequency decoder IC MT8870DE, 8051 microcontrollers, relay switch, vibration sensor, paint spray and high voltage mesh. The circuit is subdivided into two; one is for detecting the motion of the thief using infrared sensors, and the other is for DTMF tone detecting – for switching on/off the relay. When the thief tries to unlock the car, the infrared sensors placed near the car door will sense the motion or movement and will send the signal to 8051 microcontrollers which sends the triggering signal to relay; simultaneously, the microcontroller sends the triggering signal thrice, to the GSM mobile thereof, calling the user to inform him/her of the intruder. The user then sends the DTMF tone to the system placed in the car. The DTMF tone is decoded using IC MT8870DE which controls the relays to activate the security. It provides real time information such as location, speed and expected arrival time of the user.

In a nutshell, after carrying out several reviews on previous work relating to this project, it became apparent that these developed systems lacked, majorly, user authentication; thus traditional car security systems cannot

deny access to unauthorized users and cannot detect intrusion in the case of hijack/theft. However, the proposed system herewith is aimed at solving some of the limitations of previous systems by incorporating the use of various smart devices in order for it to be track able and to be able to deny access to unauthorized users, and detect intrusion in case of hijack.

3 METHODOLOGY

The GSM/GPS based vehicle anti-theft and monitoring system was designed and constructed into two sub-systems: the handheld system and the in-built system. The block diagrams of the sub-systems are depicted in the Figure 1 and Figure 2 respectively. Communications between the GSM module and the microcontroller, the GPS module and the microcontroller, and the Fingerprint module and the microcontroller was achieved by interfacing them with a serial multiplexer, since ATMEGA 16 can accommodate only one serial device

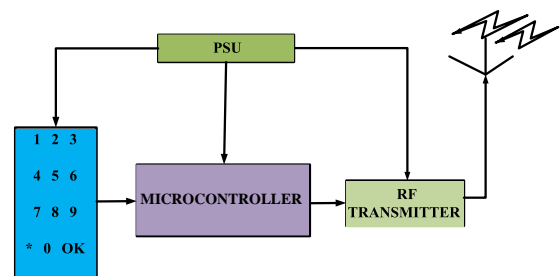


Figure 1. Block Diagram of the Handheld System

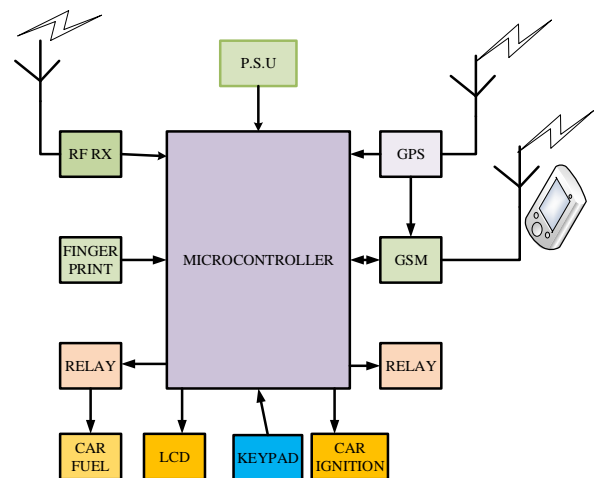


Figure 2. Block Diagram of the in-built System

3.1 THE COMMUNICATION UNIT

This unit comprises of a GSM module, which sends and receives messages (SMS) to and fro the vehicle's owner. The microcontroller works based on the reply the GSM module receives; and a GPS module, which aids in tracking and monitoring the vehicle at any particular point in time. With the aid of this module, the location (longitude and latitude) of the vehicle can be determined.

3.2 THE AUTHENTICATION UNIT

This unit is made up of a fingerprint module. Its purpose in this system is to scan the finger of the person driving the vehicle at any point in time. It serves as a means of easily sensing intrusion through verification of the current user.

3.3 THE IMMOBILIZING UNIT AND RELAY PARAMETERS

This unit is made up of two relays interconnected with the ignition engine of the vehicle and its fuel pump. As we all know, a relay is a switching device so was it employed in this design to switch ON the ignition of the vehicle while simultaneously permitting the flow of fuel into the combustion engine and vice-versa. Since a relay requires 12V to operate, a transistor was used to amplify the voltage being supplied by the microcontroller to the relay. The calculations behind the values chosen is as follows:

$$R_B = \frac{V_{BB} - V_{BE}}{I_B} \quad (1)$$

$$I_C = \beta I_B \quad (2)$$

$$V_{CE} = V_{BB} - I_C R_C \quad (3)$$

$$Relay = 1000\Omega$$

$$V_{RELAY} = 12V$$

$$Relay = \frac{V_{RELAY}}{R_{RELAY}} = \frac{12}{1000} = 0.012A$$

$$V_{BE} = 0.7V \text{ and } V_{BB} = 12V$$

$$I_C = I_{RELAY} = 0.012A$$

$$\therefore R_B = \frac{12 - 0.7}{0.012} = 941.67\Omega$$

3.4 DISPLAY UNIT

An LM016L, 16-character-by-2-line, dot matrix Alphanumeric Liquid Crystal Display (LCD) was used in this project as the display unit. An LM016L has 11 data lines is required. The control lines include: RW, RS, and EN. The Read/Write RW, control line reads data from the LCD when it is 1 while data is written when it is 0. The Register Select RS, Line treats data as an instruction when it is ZERO and, it displays data on the screen when it is ONE. The Enable Line is used to inform the LCD that data has been sent to it. To send data to the LCD, EN is set to LOW, while simultaneously setting the RW and the RS

lines appropriately. Pin 3 of the LCD is interfaced with a variable resistor which is connected to the power supply. This variable resistor is used to adjust the contrast of the LCD.

3.5 CONTROL UNIT

ATmega16 is an 8-bit, high performance Atmel AVR family with low power consumption. It is a 40pin microcontroller with 16KB programmable flash memory, 1024bytes RAM and 512bytes EEPROM that allows both temporary and permanent storage of data. The Atmel AVR processor's memory is a modified form of Harvard Architecture, in which the program and data memory uses separate buses for ease of access and increased capacity. An Atmel AVR microcontroller has four categories of memories: data memory, registers, I/O registers, and SRAM program flash memory, each with a distinct address.

3.6 HANDHELD SYSTEM

This comprises of an Atmega16 microcontroller, an RF module (transmitter), a HT12E encoder, and a three-by-four matrix keypad. This unit is used to grant access to a user when the user inputs a pre-defined password. It communicates wirelessly with the in-built system via its RF module which transmits an encoded signal (encodes using HT12E) at a frequency of 433MHz to its receiving counterpart in the in-built device where it is decoded (using HT12D). Also, by pressing the 'OK' button on the remote device, the system is placed on a 'PARK' mode, though ideally, the system remains on 'PARK' mode once the system is activated. The components are further explained.

RF Module: This is the simplest pass-through integrated circuit. It permits users to set their own baud rates. It transmits data wirelessly to the receiver. It operates within the frequency range of 315-434MHz; with a data rate of 2,400bps. The transmitter operates with a voltage supply ranging from 2V to 12V, while the receiver operates with a voltage supply ranging from 4.5V to 5.5V.

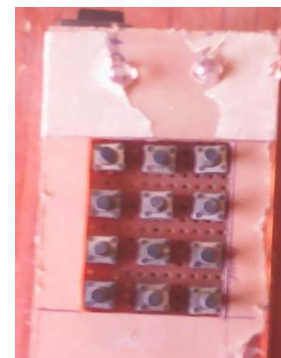


Figure 3. Image of the Hand held device

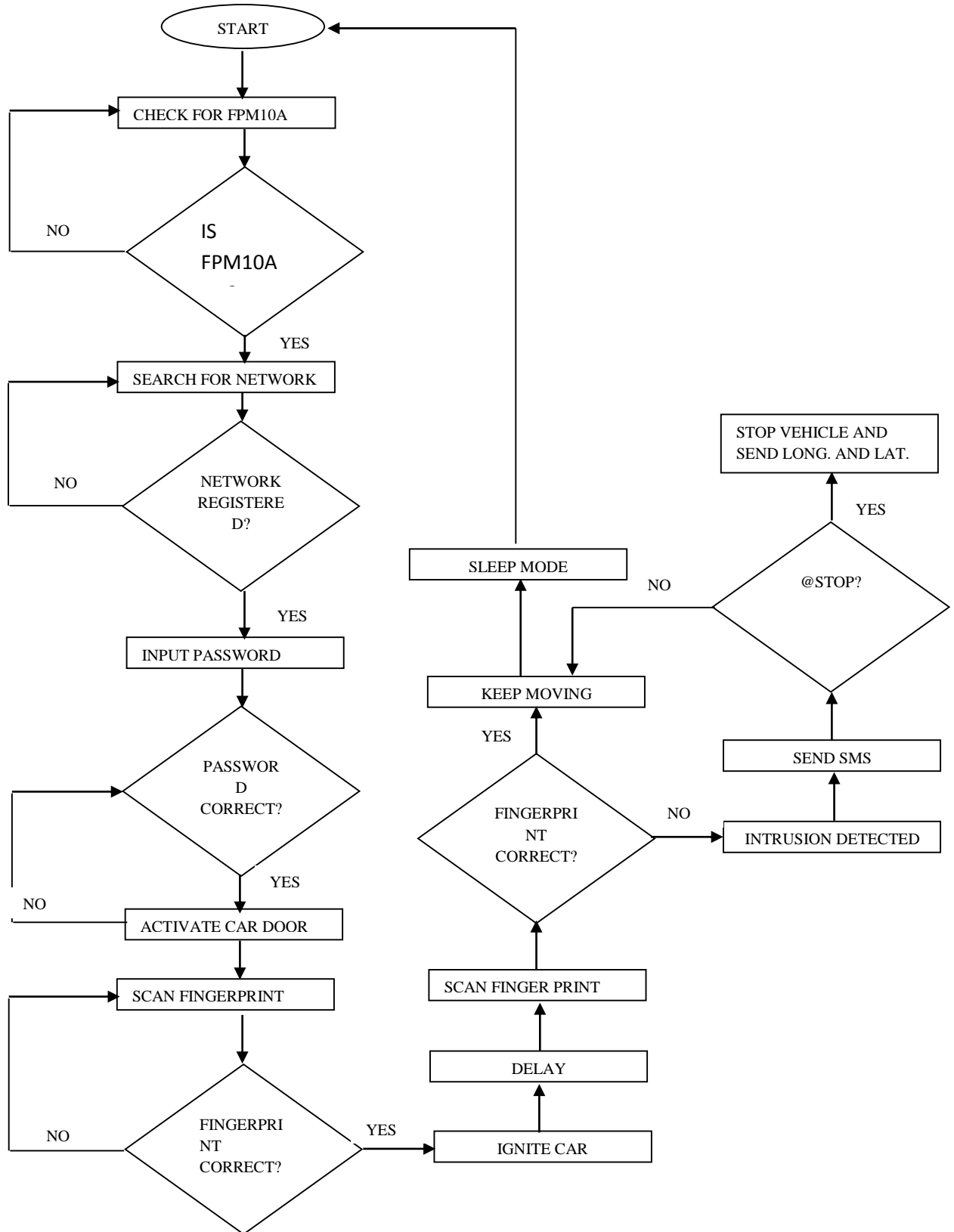


Figure 4. Software Flowchart

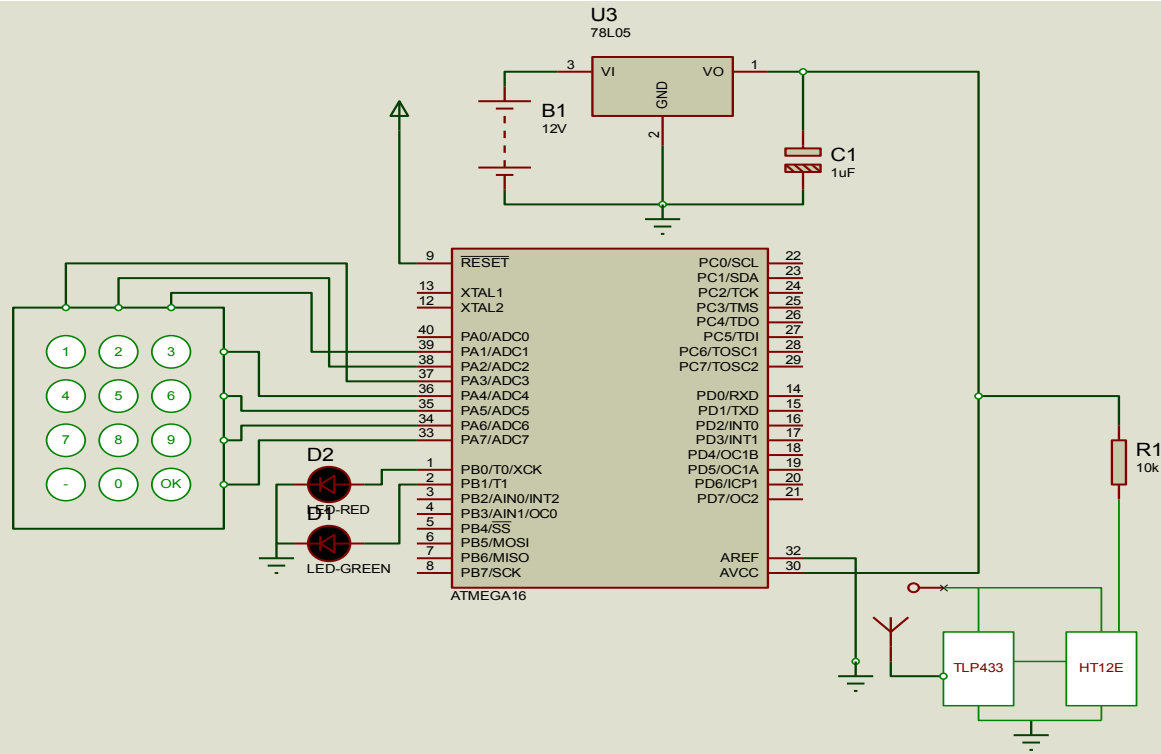


Fig. 5: Circuit Diagram of the remote device

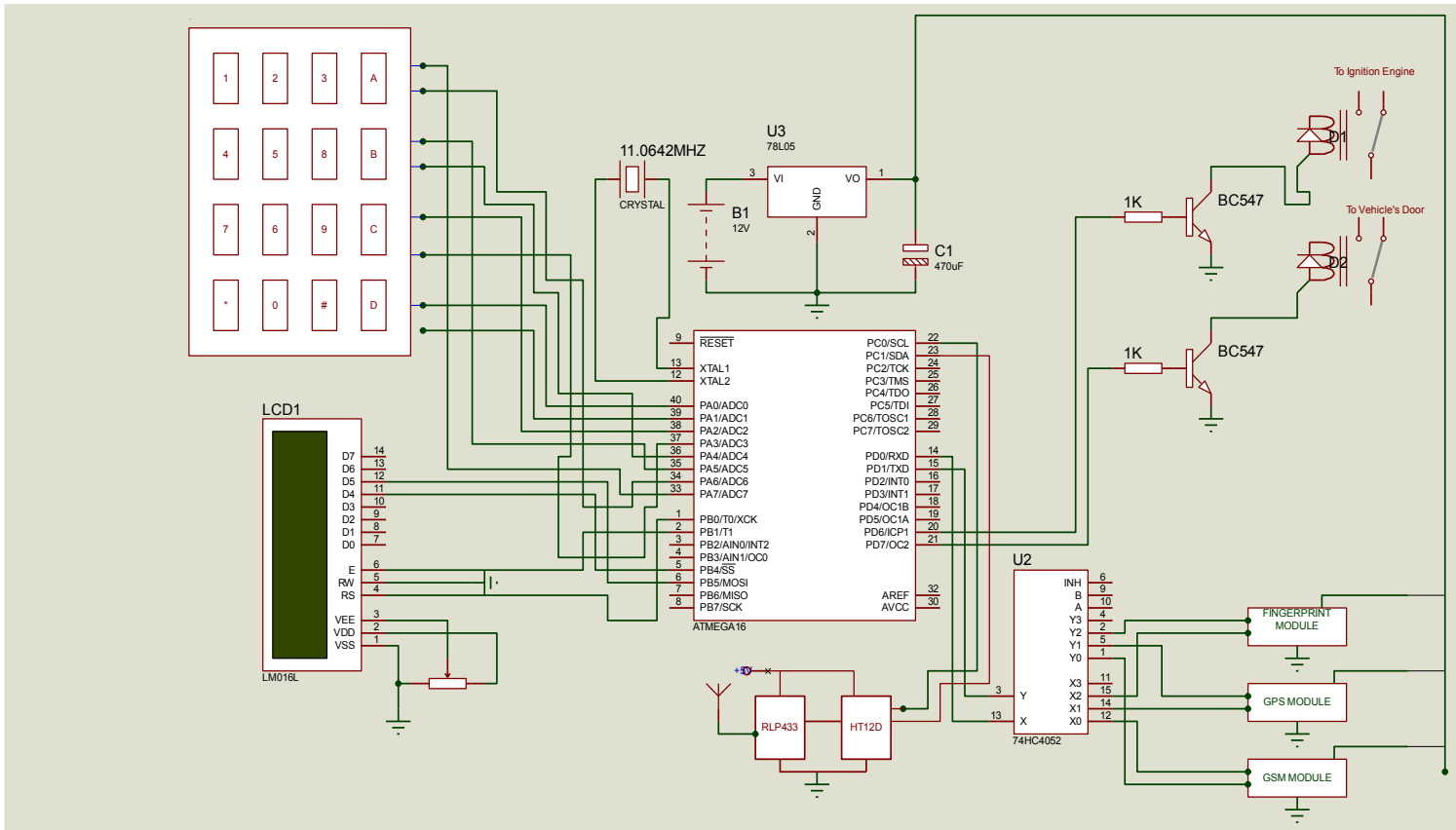


Fig. 6: Circuit Diagram of the in-built system

4 RESULTS AND DISCUSSION

This was achieved by carrying out some test on the various units of the system. The approaches used to achieve this are discussed below:

A. Display Unit

In order to verify this unit, the commands sent and received were compared with that displayed on the LCD. Also, the variable resistor was adjusted until the desired contrast was obtained.

B. Immobilizer Unit

The accuracy of this unit was tested by using the fingerprint of an unauthorized user when a request for the fingerprint of the user was made. When this was done, an intrusion was detected and, instantly, an SMS was sent to a predefined phone number, informing the user of an intrusion

After receiving the '@STOP' command from the user, the voltage supply to the relay was cut-off thus, stopping the fuel supply and car ignition while it simultaneously sent the current location (Longitude and Latitude) of the vehicle to the number from which it received the command.

C. Authentication Unit Test

The fingerprint was tested by scanning a correct thumb and a wrong thumb when the fingerprint of the user was requested. Table 1 shows the test result;

TABLE 1: FINGERPRINT TEST RESULT

S/NO	INPUT	RESULT	No. of instances
1	Correct Fingerprint identified	Image found with ID No: 000	10
2	Wrong Fingerprint rejection	Image not found in the database	9
3	Correct Fingerprint rejection	Image not found in the database	1
4	Wrong Fingerprint acceptance		0

D. Handheld System

The handheld device was tested by inputting the password (1234) in order to activate the vehicle; the red LED blinks at each input. In the event of correct password entered by the user, the car doors unlock and allow the user access to the car. However, that's not all, second level authentication is carried out while the user is in the car before the ignition of the car is activated. The handheld unit is as shown in Figure 3.

E. Change of Ownership Mode

This mode results when the password or fingerprint needs to be changed particularly due to transfer of ownership. The steps listed below are to be adhered to while changing the system's ownership: -

- i) Switch OFF the system;
- ii) Switch the system ON while pressing 'D' on the Keypad, which takes the system to CONFIG. MODE;
- iii) Press '*' on the keypad, so as to input the old password;
- iv) Press 'D' to enter; this will ask you to input the new password;
- v) Press 'D' to enter and empty the fingerprint database;
- vi) Scan your fingerprint twice to change ownership.



Figure 7: Result for inputting the correct password combination



Figure 8: Result for scanning the correct finger



Figure 9: Result for scanning wrong finger



Figure 10: CONFIG. MODE



Figure 11: Result from change of password

Figure 7 depicts the result gotten when a correct password is inputted on the remote access control; this activates the car's door. Figure 8 shows the result of scanning the owner's thumb print; this ignites the car, while Figure 9 shows the result gotten when an unauthorized user scans his/her thumb. Figure 10 is the result gotten when the system was taken to the configure mode. In configuration mode, user can change their password or change of ownership can be carried out. Figure 11 is the snapshot of the prompt that comes up after going into the CONFIG. MODE. In the event of theft at gun point, a user does not need to panic as a user authentication request will pop up at a random time with few hours after the stealing event. The car is deactivated and its current location is sent to the genuine owner as well as security personnel after user authentication fails.

5 CONCLUSION

In this paper, a multifactor authentication system for car security and tracking was presented. The system was tested and, the results showed that the proposed system is highly reliable and can be used with any model of car. The proposed system has been designed such that ownership can be changed unlike the previous systems. In addition, the system can be used to thwart intrusion, deny access to unauthorized users and to track/monitor vehicles. A typical challenge that the device can face includes when it runs out of call card. This will disallow the user from receive location message in the event of theft. A post-paid subscription can be used to solve this problem.

REFERENCES

- All, K. S., Ijeh-Ogbo, C., & Gbadamosi, S. L. (2005). Design and Construction of a Remotely Controlled Vehicle Anti-Theft System Via GSM Network. *International Journal of Education and Research*, 3(5), 326–330.
- All, K. S., Ijeh-Ogbo, C., & Gbadamosi, S. L. (2015). Design And Construction of a Remotely Controlled Vehicle Anti-Theft System Via GSM Network. *International Journal of Education and Research*, 3(5), 405–418.
- Almomani, I. M., Alkhalil, N. Y., Ahmad, E. M., & Jodeh, R. M. (2011). Ubiquitous GPS Vehicle Tracking and Management System.
- B. Bhatt, P. Kalani, N. Parmar, N. S. (2015). "Smart Vehicle Security System Using GSM and GPS." *International Journal of Engineering and Computer Science (IJECS)*, 4(6), 12508–12511.



- Bagavathy, P., Dhaya, R., & Devakumar, T. (2011). Real Time Car Theft Decline System Using ARM Processor. In *Proc. of Int. Conf. on Advances in Recent Technologies in Communication and Computing (IET)* (pp. 101–105).
- Hameed, S. A., Khalifa, O., Ershad, M., Zahudi, F., Sheyaa, B., & Asender, W. (2010). Car Monitoring, Alerting and Tracking Model Enhancement with Mobility and Database Facilities. In *International Conference on Computer and Communication Engineering (ICCCE 2010)*, Kaula Lumpur, Malaysia (pp. 11–13).
- Hasan, K. S., Rahman, M., Haque, A. L., Rahman, M. A., Rahman, T., & Rasheed, M. M. (2009). Cost effective GPS-GPRS based object tracking system. In *Proceedings of the international multiconference of engineers and computer scientists* (Vol. 1, pp. 18–20).
- Kamble, K. P. (2012). Smart Vehicle Tracking System. *International Journal of Distributed and Parallel Systems*, 3(4), 91.
- Katta, S., & Sudharsan, D. (2012). "IVTrace: A Cost-Effective Vehicle Tracking System-A Prototype". *International Journal of Engineering and Technology (IJET)*, 2(7), 1162–1171.
- Khan, A., & Mishra, R. (2012). GPS–GSM based tracking system. *International Journal of Engineering Trends and Technology*, 3(2), 161–164.
- Kotte, S., & Yanamadala, H. B. (2013). Advanced Vehicle Tracking System on Google Earth Using GPS and GSM. *International Journal of Computer Trends and Technology (IJCTT)*–volume, 6.
- Modi, R. . . & Sukhadia, R. . . (2017). IoT based Gateway for Electricity Energy Meter by using ZigBee. *International Journal of Advanced Research in Electrical, Electronics and Instrumentation Engineering*, 6(1), 210–218.
<https://doi.org/10.15662/IJAREEIE.2017.0601031>
- Monisha, R., Leo, J. J., & Sakthi, B. T. T. S. (2014). Car authentication and accident intimation system using GPS and GSM. *Interantional Journal of Innovative Research Computer and Communications Engineering*, 2(1), 1–7.
- Oladimeji, T. T., Oshevire, P. O., Omitola, O. O., & Adedokun, O. E. (2013). Design and Implementation of Remotely Controlled Vehicle Anti-Theft System via GSM Network. *Wireless Sensor Network*, 5(8), 151.
- Padmapriya, S., & Kalajames, E. A. (2012). Real Time Smart Car Lock Security System Using Face Detection and Recognition.
- Pethakar, S. S., Srivastava, N., & Suryawanshi, S. D. (2013). GPS and GSM based Vehicle Tracing and Employee Security System. *International Journal of Computer Applications*, 62(6).
- Prakash, C. B., & Sirisha, K. (2014). Design and Implementation of a Vehicle Theft Control Unit using GSM and CAN Technology. *International Journal of Innovative Research in Electronics and Communications (IJIREC)*, 1(4), 46–53.
- Ramani, R., Valarmathy, S., Suthanthira Vanitha, N., Selvaraju, S., Thiruppathi, M., & Thangam, R. (2013). Vehicle tracking and locking system based on gsm and gps. *International Journal of Intelligent Systems and Applications*, 5(9), 86.
- Rashidi, F. R. M., Ariff, M. H., & Ibrahim, M. Z. (2011). Car Monitoring using Bluetooth Security System, 424–428.
- Sehgal, V. K., Singhal, M., Mangla, B., Singh, S., & Kulshrestha, S. (2012). An embedded interface for GSM based car security system. In *Computational Intelligence, Communication Systems and Networks (CICSyN), 2012 Fourth International Conference on* (pp. 9–13). IEEE.
- Singh, P., Sethi, T., Biswal, B. B., & Pattanayak, S. K. (2015). A Smart Anti-theft System for Vehicle Security. *International Journal of Materials, Mechanics and Manufacturing*, 3(4), 249–254.
- Verma, P., & Bhatia, J. S. (2013). Design and development of GPS-GSM based tracking system with Google map based monitoring. *International Journal of Computer Science, Engineering and Applications*, 3(3), 33.
- Wankhade, P. P., & Dahad, S. O. (2011). Real time vehicle locking and tracking system using GSM and GPS Technology-An anti-theft system. *International Journal of Technology and Engineering System (IJTES)*, 2(3).
- Xiao, J., & Feng, H. (2009). A Low-cost Extendable Framework for Embedded Smart Car Security System, 829–833.



DEVELOPMENT OF PRODUCTION FRAME WORK TO MITIGATE CORROSION IN UNDER GROUND TANKS

Emenuwe Vincent¹, Aliyu Abdullahi²

Department of Mechanical Engineering, Federal University of Technology, Minna

ABSTRACT

Corrosion is a major concern for managers of petrol stations. This is because corrosion failure will adversely affect the lifespan of tanks. Leaks caused by corrosion are commonly-identified problems in buried metal tanks which can lead to catastrophic failures, causing significant socio-economic losses. Unlike in the pipelines where periodic inspection of the buried pipelines is vital, in the case of underground tanks appropriate mitigating measures via construction is preferable. The development of corrosion- protection techniques, corrosion-induced deterioration of tanks remains a major problem globally, and billions of dollars are spent every year on cleaning of leakages into water/soil. To date, ways to mitigate corrosion for underground fuel storage tanks has not been explored comprehensively by other researchers. Corrosion mitigation in UST is best achieved through proper development of production frame-work. This was achieved through variation of two major welding parameters (electrode type and current) and subsequent post heat treatment, microstructural examination and corrosion subjection. A current of 80A, 90A and 100A were varied with Electrodes E6010, E6013 and E7018 respectively. A total of 36 coupons were gotten in all. Eighteen (18) coupons were subjected to post heat treatment. Nine coupons in each case of the post heat treated and non-heat treated ones were taken for microstructural examination and the rest were subjected to corrosion in aqueous acidified sandy soil in bath for 30 days. It was observed that the heat treated coupons has a more refined grain sizes than non-heat treated counterparts equally more corrosion resistance.

Keywords: *Corrosion, Development, Framework, Microstructural, Mitigate, Welding.*

1 INTRODUCTION

In many industries today including diesel tank fabrication, engineers are concerned with efficient weldment and ways to prolong the life of the structures. Welding has proven to be the best method of joining metals together. According to Wema (2003), the reasons are not far-fetched. In the first place, weld joints are fluid tight for tanks and vessels. Also, weld structures can be altered easily and economically. It has also been proven that welded joints have considerable corrosion resistance when compared to other joining processes and different types of joints are possible in weld joining processes.

In the construction or production of Underground Storage tank (UST), mild steel plates are welded together. The weld joints and the Heat Affected Zone (HAZ) plays a major role in the behavior of the UST in application. HAZ is the adjacent zone to the weld metal. It is the portion of the base metal that has not been completely melted; but whose microstructure or mechanical properties have been altered by the heat of welding. The microstructural features of the welds and the HAZ are responsible for any emerging properties in the weldment.

Mild steel plate like other metallic materials, when subjected to salty environment, it is bound to corrode. Corrosion, which is the deterioration of a metal as a result of chemical reactions between it and the surrounding environment, is severe at the welded and HAZ than the parent material due to compositional variation (Foss,

2008) The cycle of heating and cooling in the welding process affects the microstructure and surface composition of welds and adjacent base metal. Variation in composition occurs due to effects of segregation in micro and macro scales, precipitation of secondary phases, formation of unmixed zones, recrystallization and grain growth in HAZ, contamination of the solidifying weld pool, and dilution at the weld fusion, weld interface and HAZ. The compositional differences create a potential difference between the welded portion and the parent material. In an underground tank, the percolation of water cannot be exempted, the water molecule can penetrate the microscopic pits and crack any exposed metal. The hydrogen atoms present in water molecules can combine with other element or compound like carbon iv oxide (CO₂) to form acids, which will eventually cause more steel surface to be exposed. If chloride or carbonates ions are present, as is the case of salt water, the corrosion is likely to occur quickly (Schmitt, 2006). The corrosion of UST is a serious challenge to the industry due to the enormity of consequences. Apart from the losses that would be incurred by the tank owners for reinstallation and clean up, there is fuel loss and the environment is equally contaminated. The contamination is in two folds. Firstly, the contamination of the fuel in the tank which can result to poor efficiency of the fuel. In the second place, the fuel leaking into the soil may percolate into surrounding drinking water resulting to pollution. It is unfortunate that in Nigeria no effort or attention has been paid to this industrial problem. The American Environmental Protection Agency EPA has been

investigating and instituted several measures to curb this challenge. EPA's July 2016 research report on corrosion in underground tanks storing diesel fuel shows moderate or severe corrosion of metal components inside 35 of 42 – or 83 percent – of examined diesel fuel tanks. Since the corrosion may potentially lead to releases in the environment and many UST owners may be unaware their systems are affected, EPA usually alert owners (ASTM, 2003).

This project essence is to develop a production framework to curb or minimize corrosion failures in our USTs. This is achievable through best choice of welding parameters which is the chief means of tank fabrication; post heat treatment by annealing to reduce the lock up stresses the welded portion and HAZ; and the use of efficient corrosion protection (Wahid, 1993).

2 METHODOLOGY

The materials used are outlined below:

- Samples of 5mm mild steel plate

WELDING MATERIAL

- Vernial caliper
- Measuring tape
- Miller Welding Machine
- Bosch Hand cutting machine
- Cutting and filing disc.

HEAT TREATMENT/METALLOGRAPHIC MATERIALS

- Heat treatment machine
- Thermometer
- Viella echant
- Olymos microscope model:

CORROSION EXPERIMENT MATERIALS

- Distilled water
- Measuring cylinders
- Pipette for measuring out acids
- Plastic beakers for containing the solutions
- 5litres of 95-97% concentrated H₂SO₄ analytical grade
- 5litres of 95-97% concentrated Hydrochloric acid analytical grade
- Sodium chloride analytical grade
- Sodium sulphate analytical grade

The experiment method comprises sample preparation, welding of samples, post heat treatment of selected samples, and subjection to corrosion

2.1 Experimental design and Grouping of samples:

The factorial method for Design of Experiment was used to determine the number of samples ($3^2 \times 2^2$). Base on consideration of varying two major welding parameters (current and electrode types) at three levels of experiments with heat treatment and corrosion rate determination as a factor also, a total of thirty-six (36) coupons is needed. Hence, a total of seventy-two (72) samples of workpiece is required and these are grouped into 'X', 'Y' and 'Z'. Each comprising of twenty-four (24) test pieces.

Samples preparation: This involves the purchase of mild steel plate. The plate density is 7.85gm/cm³ and was manufactured by Visco Chemicals, Houston.

Characterisation of the work piece to ascertain the percentage composition of various elemental constituents was taken from the manufacturers' specification.

A sheet of 5mm mild steel plate is cut into seventy-two (72) test pieces each of 50mm x 80mm dimension. Cutting of samples was done with Bosch hand cutting machine (Model:). To achieved this, 60mm diameter cutting disc was fixed to the hand cutting machine was then connected to electricity for powering.

2.2 Manual Metal Arc Welding

Carrying out Metal Arc Welding of workpiece 'X' at constant current 80amps (C₈₀) but different welding Electrodes to obtain twelve samples (four each):

X1 at welding Electrode E1(E6010) represented as E1C₈₀

X2 at welding Electrode E2(E6013) represented as E2C₈₀

X3 at welding Electrode E3(E7018) represented as E3C₈₀

The procedure used in carry out the MMAW process used is outlined below

1. Placing the steel plate flat on the bench and brushing to free it of dirt and scales.
2. Attaching the ground bead securely to the plate
3. Setting the welding machine amperage to 80
4. Fitting the electrode into the holder (E1, E2, E3), each at a time.
5. Turning on the welding machine
6. Dropping the hood over the face and striking an arc by brushing the base metal with the electrode. The distance between the electrode and the base metal was approximately equal to the diameter of the electrode. Upon sticking of the electrode to the base metal, a quick twist was made to frees the electrode. But if not, free the electrode through the electrode holder. Then, subsequent retry to stabilize the arc.
7. Striking an arc and laying of several beads on the sample
8. Chip the weld beads thoroughly and then wire brush.

9. Laying of more beads on each of the samples to complete welding process

By still using the listed electrodes, and carrying out MAW as outlined above while varying the current to 90A. Further 12 coupons were gotten.

Y1 at welding Electrode E1(E6010) represented as E1C₉₀

Y2 at welding Electrode E2(E6013) represented as E2C₉₀

Y3 at welding Electrode E3(E7018) represented as E3C₉₀

Similarly, by using 100Amps

Z1 at welding Electrode E1(E6010) represented as E1C₁₀₀

Z2 at welding Electrode E2(E6013) represented as E2C₁₀₀

Z3 at welding Electrode E3(E7018) represented as E3C₁₀₀

2.3 POST HEAT TREATMENT OF THE SELECTED SAMPLES

Same as Workpiece 'X', but with post heat treatment of welded samples to obtain four samples 'Y'

Y1 at welding Electrode E1

Y2 at welding Electrode E2

Y3 at welding Electrode E3

Same as Workpiece 'Y' but with post heat treatment to obtain four samples and different welding current.

Z1 at welding current C1

Z2 at welding current C2

Z3 at welding current C3

2.4 MICROSTRUCTURAL EXAMINATION OF SAMPLES

Carrying Metallography and Microstructural studies of all samples.

The samples were sectioned and mounted in Electro-lite™, a conductive mounting compound, using the LECO PR-32 mounting press. The mounted samples were prepared using grit steps of 240, 320, 400 and 600. The samples were then polished using 6µm, 3µm and 1µm polish clothes followed by a final polishing step of colloidal silica. The samples were then etched using Viella's Reagent. LOM micrographs were taken of each simulated HAZ microstructure from 5x through 100x. Several etchants were attempted before finding a few that had the desired effect of showing grain boundaries and carbides in the microstructure. One etchant that was found to be successful was Viella's Reagent. The other was a solution that consisted of 1-part nitric acid, 2 parts

sulfuric acid, and 3 parts distilled water. After polishing and etching, light optical microscopy was performed on the samples using an Olympus GX-51 scope. Images were captured at 5x to 100x magnification.

2.4 Subjection of samples to active corrosive medium and observation.

The metal coupons were buried in an acidic soil environment for a maximum of 30 days. On days 10 and 20, duplicate sets of the buried coupons were retrieved for analysis and the last set of coupons was retrieved on the last day of exposure (30 days). Monitoring of the buried coupons at intervals was to determine what corrosion effect had taken place on the coupons at the end of each observational period and to compare the effect of time on the rates of corrosion on the heat treated and non-heat-treated coupon types in the acidic soil environments under study. After retrieval from the soil bath, the coupons were taken to the laboratory for cleaning and analyses to determine the weight loss and corrosion rates. Being in acidified soil bath environments, the retrieved coupons did not have any oil residues on them but as expected, they were found to be covered with soil debris when they were recovered.

In the laboratory, outer soil debris on the coupons was carefully removed. They were then cleaned with inhibited acid (15% HCl) to remove corrosion products on the surface of the coupons according to ASTM G1 (Standard Practice for Preparing, Cleaning, and Evaluating Corrosion Test Specimens). The coupons were then rinsed under running water. Next, the coupons were placed in an oven at 70°C for 15 minutes to dry them. After drying, they were placed in a desiccator to cool after which they were weighed to a constant weight using a Mettler Toledo weighing balance (New Classic ML 204, Switzerland). The weight of the retrieved coupons before cleaning was compared to the initial weight, the difference indicating the metal loss during the exposure period. The corresponding average percentage weight loss (APWL) and corrosion rate (CR) were calculated.

Corrosion rate was calculated assuming uniform corrosion over the entire surface of the coupons. The corrosion rate in mils per year (mpy) was calculated from the weight loss using the formula:

$$CR = \frac{W}{(D \times A \times t)} \times k$$

where:

W = weight loss in grams

k = constant (22,300)

D = metal density in g/cm³
A = coupon area (inch²)
t = time (days)

Table 2. Corrosion of heat treated coupons in acidified

Caption.

3 RESULTS AND DISCUSSION

The table below depicts the results gotten from the immersion of the coupon on the acidified sandy soil.

Table 1. Corrosion of non-heat treated coupons in acidified aqueous sandy soil

ELECTRODE → CURRENT↓	E6010			E6013			E7018		
	Initial Wt	Final Wt	Weight Loss	Initial Wt	Final Wt	Weight Loss	Initial Wt	Final Wt	Weight Loss
C80	28.982	28.501	0.481	28.982	28.611	0.371	28.982	28.655	0.327
C90	28.983	28.526	0.457	28.983	28.652	0.331	28.983	28.764	0.219
C100	28.983	28.530	0.453	28.983	28.666	0.317	28.983	28.780	0.203

The choice of acidified sandy soil is due to the recommendations by EPA as the final choice for back filling of UST. From Table 1, increase in current in each case of the electrodes results in decrease in weight loss upon subjection to acidified aqueous sandy soil. From equation 1, weight loss is directly proportional to the rate of corrosion. Hence, with increase in current, the better corrosion resistant within the current range under consideration. The same is true of table 2. Generally, within the scope of study, Electrode E7018 at current of 100Amps gives the best corrosion resistant.

ELECTRODE → CURRENT↓	E6010			E6013			E7018		
	Initial Wt	Final Wt	Weight Loss	Initial Wt	Final Wt	Weight Loss	Initial Wt	Final Wt	Weight Loss
C80	28.982	28.721	0.261	28.982	28.730	0.252	28.982	28.900	0.082
C90	28.983	28.834	0.149	28.983	28.800	0.183	28.983	28.950	0.033
C100	28.983	28.875	0.108	28.983	28.820	0.163	28.983	28.980	0.003

4 CONCLUSION

Corrosion in an underground tank which are usually made of mild steel is inevitable. Therefore, deliberate effort must be made to mitigate this menace. This can be achieved through proper development of production framework. The method of joining plates in UST construction is via mainly arc welding. The welding parameters such as electrode type, current variation etc., has significant effect on the microstructural properties of material which also inadvertently affects corrosion rate. A study of the variation of metal arc welding process parameters in mild steel for UST and the resultant corrosion resistance were presented. It was discovered that proper choice of welding parameters and post heat treatment reduces corrosion rate. And also, the problem of UST corrosion can be achieved through refining the grain structure of the welded part.

ACKNOWLEDGEMENTS

My profound gratitude goes to Almighty God who is the giver of knowledge through which this study was possible.

My profound gratitude goes to Hamstring Engineering Company Minna, Niger State for their effort, invaluable assistance and encouragement throughout the research work

I am also highly indebted to of HOD, Mechanical Engineering and all the staff in Mechanical Engineering Federal University of Technology, Minna for providing excellent studying environment which has metamorphosed into the academic success.

REFERENCES

- ASTM Standard G1, 2003, Standard Practice for Preparing, Cleaning, and Evaluating Corrosion Test Specimens, ASTM International, West Conshohocken, PA, 2003, DOI: 10.1520/G0001-03, www.astm.org
- ASM international, 1987. Handbook Committee. *ASM Handbook, Volume 13: Corrosion*. Materials Park, OH: ASM international.
- Bockris, J. O. M., Drazic, D. & Despic, A. R. (1961). The electrode kinetics of the deposition and dissolution of iron, *Electrochimica Acta*, 4, 325.
- de Waard, C. & Lotz, U. (1993). Prediction of CO₂ Corrosion of Carbon Steel. Paper presented at the NACE Corrosion/93, paper no. 069.
- Espan, T., Kapusta, S. D. & Simon Thomas, M. J. J. (2001), Case study: extreme corrosion of a 20" oil pipeline in the niger delta region. Paper presented at the NACE Corrosion/01, paper no. 629.
- Foss, M., Gulbrandsen, E. & Sjoblom, J. (2008). Interaction of carbon dioxide corrosion inhibitors with corrosion products deposit, paper presented at the NACE Corrosion/08, paper no. 343.
- Gaudet M. J (2010), "Mechanical behavior and fracture properties of the heat affected zone for dual torch welded X80 steel" Thesis, The University of British Columbia.
- Morita, N. & Boyd, P. A. (1994). Typical sand production problems: case studies and strategies for sand control. Paper presented at the SPE paper no. 27343.
- Nešić, S & Lee, J. (2003). A mechanistic model for carbon dioxide corrosion of mild steel in the presence of protective iron carbonate films – Part 3: Film growth model. *Corrosion*, 59(7), 616-628.
- Nippes EF, (1959), The weld heat-affected zone, *Weld Journal*; (vol.1):1s–17s. Pg 38.
- Savage W. F., (1980), Solidification, segregation, and weld imperfections (Houdremont lecture). *Weld World*; 18 (5/6): Pg. 89–114.
- Savage W. F, Nippes E. F, Miller T. W. (1976), Microsegregation in 70Cu–30ni weld metal. *Weld J*; 55 (6): 165s–173s.
- Schmitt, G. (2006). Fundamental aspects of CO₂ metal loss corrosion - Part II: influence of different parameters on CO₂ corrosion mechanisms. Paper presented at the NACE Corrosion/06, paper no.06112.
- Wahid A, Olson. D.L.. Matlock D.K, and Cross, C.E. 1993, *Corrosion of Weldments, Welding, Brazing, and Soldering*, Vol 6, ASM Handbook, ASM International,, p 1065–1069.
- Weman, Klas (2003). *Welding processes handbook*. New York: CRC Press LLC. ISBN 0-8493-1773-8.



PHYSICAL PROPERTY MODIFICATION OF VEGETABLE BIO-CUTTING OIL USING GARLIC AS EP ADDITIVE

Sanni John

Mechanical Engineering Department, Federal University of Technology, PMB 65 Minna Niger State, Nigeria

sanijohn08@gmail.com, +2348072533223

ABSTRACT

This study examined the physical property improvement of castor oil and watermelon oil with the addition of garlic powder particle as anti-wear agent. Samples with addition of garlic powder particles were prepared and tested using a heated viscometer. All the laboratory tests carried out were in accordance with the specification of the American Society for testing and materials (ASTM). The results of the tests obtained from the blend show that the properties such as viscosity, density, increases with increase in additive concentration, while flash point decreases as the concentration of the additive increases.

Keywords: Additives, flash point, garlic, kinematic viscosity, Nanoparticles, specific gravity.

1 INTRODUCTION

Growing regulations over pollution and contamination of the eco-system due to the use of mineral oil as metalworking fluids (MWFs) have increased the need for renewable and biodegradable metalworking fluids (MWFs) (Fox et al, 2007). However, most MWF consist of petroleum based oil and chemically derives additive that have adverse effect on environment due to improper disposal, toxicity and non-biodegradability. The hazardous effect associated with mineral MWFs have become a global concern and With a view to maintaining domestic energy security and addressing environmental concerns, there is an increasing demand for environmentally acceptable and biodegradable products suitable for use as MWFs (katna, Singh, agrawal and Jain. 2017). The use of vegetable/bio-lubricant oils for lubrication purposes has been in practice for many years due to the environmental impact of commercial fossil fuels (Zainal et al., 2018). Bio-lubricants are extracted from vegetable oils which have good lubricity and viscosity index (Lawal et al., 2012). However, consumer acceptance requires overcoming certain limitation such as thermal oxidative instabilities, high pour point and limited viscosity range which prevent their use in extreme condition (Sripada et al; 2013).

To overcome these limitations, and In order to improve performance characteristics of MWFs some chemical components are added, they are called additives. The most common used additives are antioxidants and extreme pressure agents (EP). Conventional EP additives used in MWFs are sulphur, chlorine and phosphorous. These EP additives prevent high wear caused by contact between metal to metal under high load (Xue et al., 1997). These additives are showing some restrictions on its use due to their toxic nature and impact on the environment, as industry is facing increasingly rigorous environmental regulations. Compared with the traditional organic MWFs additives that contain Phosphorus, Sulphur and Chlorine elements, MWFs additives with environmental friendly

feature are certainly becoming more desirable in the future, and research for the green MWFs additives with Good tribological properties and low environmental impact becomes important (Peng et al., 2009).

Didam, (2014), studied the performance of five different vegetable oil namely moringa, jatropha, castor, neem and water melon as cutting fluids. This oil provided great lubricating properties and showed comparable performance with regards to temperature, tool wear and surface finish. But the quantity of sulphur in all oil sample were low, Sulphur was not found in water melon and jatropha oil. Sulphur is used as EP additive in cutting fluid (Lawal et al, 2003). Since %wt. of sulphur in all the oil sample were low it was recommended that green additives with sulphur containing compound be made to improve performance of the oils, this necessitate the use of environmentally friendly antioxidant such as garlic as EP additive to be use in the present study in order to promote the culture of green and renewable MWFs. In this study, garlic particles have been selected as EP additives in watermelon, castor and investigated.

2 METHODOLOGY

2.1 MATERIALS

Castor oil and watermelon oil was used as the base fluids because of its performance as cutting oil (Didam 2014). Garlic was selected as additive because they are sulphur containing non-hazardous substance, though this compound is present in combined state. Sulphur is used as an extreme pressure additive in lubricant and cutting fluids (Lawal et al, 2003). The performance of MWFs can be improved by adding substances that contain phosphorus, sulphur, and chlorine as EP additives (Brinksmeier et al., 2013).

PREPARATION OF GARLIC NANOFLUID BASE CUTTING OIL

The garlic powder particle was added to the cutting oil at different concentrations (0-2%) by weight percent. The required quantity of garlic particles was accurately weighed using a precision electronic weighing balance and mixed with the cutting oil using a mechanical stirrer for mixing the powder particle additives in the cutting oil. The time of agitation was fixed as 30 minutes for suspension with sufficient time for sedimentation to begin. After the device and the machine are agitated for 30 minutes, the nano-lubricant was obtained.

DETERMINATION OF KINEMATIC VISCOSITY OF CUTTING OIL

Viscosity of cutting oil containing different nanoparticle concentration is investigated using rotary viscometer test method. In this method, a metal spindle is rotated in the oil at a constant rpm, and the torque required to rotate the spindle immersed in the test fluid is measured. The absolute viscosity can be determined based on the internal resistance to rotation provided by the shear stress of the test oil. The viscosity of additive free castor and watermelon oil and different concentrations of garlic additive in cutting oil are estimated using rotary viscometer test method

DETERMINATION OF FLASH POINT OF NANO-CUTTING OIL

The pensky-Martens Closed Cup Test (ASTM D93) method was used to determining the flash point of oil under investigation. The test cup was filled with about 75ml of each sample of oil under investigation. The sample was stirred continuously with a thermometer and temperature was recorded to the nearest 0.25°C immediately the sample stabilized. the ignition source was lowered into the vapor space of the test cup in 0.5 and left it in lowered position for 1sec and quickly raised again to it upward position. The observed flash point reading on the temperature measuring device at the time ignition source application caused a distinct flash in the interior of the test cup was recorded accordingly.

DETERMINATION OF SPECIFIC GRAVITY OF NANO-CUTTING OIL.

Specific gravity of the oils was determined using the procedure of ASTM method D-1298. The sample was poured into a clean measuring cylinder and was stirred continuously with a thermometer; the temperature was recorded to the nearest 0.25°C immediately the sample stabilized. Once the thermometer was removed, the hydrometer was depressed about two scale division into

the oil and it was released. Sufficient time was allowed for the hydrometer to remain stationary and at this point the reading was taken. The actual value of the specific gravity was read at 150°C. From the petroleum measurement table using the value obtained from the experiment at the observed temperature.

3.0 RESULTS AND DISCUSSION

The effect of garlic additive on each vegetable cutting oil properties is presented in the following figures below. These properties include physiochemical properties such as viscosity, flash point and specific gravity.

VISCOSITY

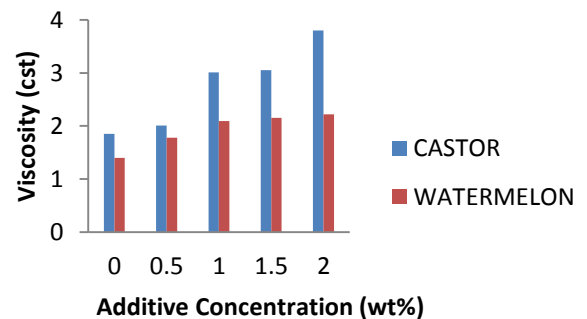


Figure 3.1 Effect of garlic on kinematic viscosity of castor and watermelon cutting oil

Viscosity is a measure of the flow of fluid at a definite temperature. Results as shown in Figure 3.1 above indicate that the higher the concentration of garlic additive from 0%-2% in both castor and watermelon oil blend, the higher the viscosity. As mentioned by Farhanah et al. (2015) that the higher viscosity usually has high anti-friction and anti-wear ability. This is as a result of change of internal viscous of shear stress. as the impact of lower temperature on liquid viscosity does not weaken the intermolecular forces and the forces between molecules of the measured range of nanofluids.

FLASH POINT

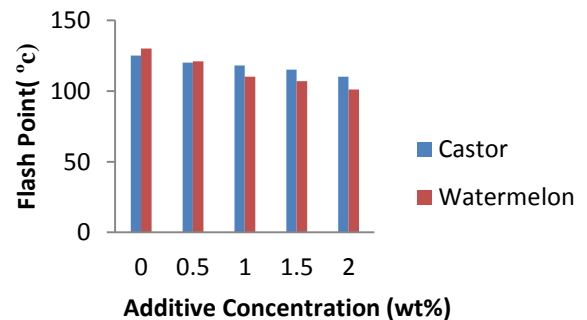


Figure 3.2 Effects of garlic additive on flash point of castor and watermelon oil

Flash point is the lowest temperature of the cutting oil at which the application of a test flame causes the vapour of the oil to ignite under a specified condition of test. Flash point is just a specific value for safe guard. Figure 3.2 above shows the experimental result of garlic additive concentration on the flash point of the blended both castor and watermelon oil. Figure 3.2 above which is a plot of flash point against additive concentration shows that the more the additive concentration in both castor and watermelon mixed with garlic powder, the lower the value of flash point temperature. For castor oil blend with garlic particle there was sharp decrease in flash point temperature from 120°C to 110°C at 0.5%-2% concentration of garlic while flash point of watermelon also decrease from 130°C to 101°C. The reason for the decrease in flash point was the presence of sulphur from garlic release into both watermelon and castor oil. As sulphur when present in oil reduce flash point. Therefore much additive should be avoided to maintain a safe flash point when blending oil with additive.

SPECIFIC GRAVITY

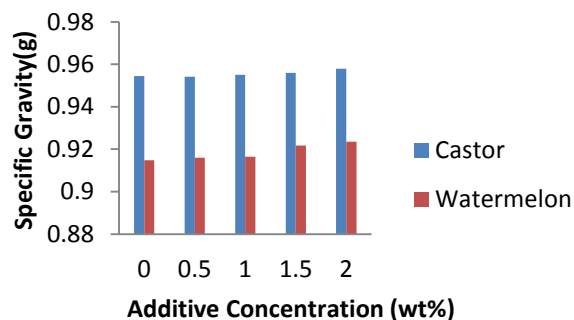


Figure 3.3 Effects of garlic additive on specific gravity of castor and watermelon oil

Density could be defined as the mass per unit volume of a substance. Density is of paramount importance in cutting oil to ensure effective and efficient working of the cutting oil. Figure 3.3 shows the experimental result of the effect of garlic additive on the density of the oil blend at a particular temperature as results shows that the more the additive concentration on the oil blend, the higher the density of oil. The test temperature for the density is 150C and the ASTM specification for the density of cutting oil it was observed that at the density of 0.9148-0.9545, further increase in the additive concentration does not produce further increase in density.

4.0 CONCLUSION

The present work focuses on the physical property modification of vegetable oil cutting of kinematic viscosity, density and flash point of garlic particles dispersed in castor and watermelon oil nanolubricants. The results show that the kinematic viscosity increase with respect to increasing nanoparticle concentration due to the change of internal viscous of shear stress. due to the impact of lower temperature on liquid viscosity does not weakens the intermolecular forces. However, further investigations need to be done on the tribological performance of garlic particle as additive to both castor and watermelon oil to extend the present work.

ACKNOWLEDGEMENTS

The authors of this work would like to acknowledge the selfless contributions of Prof. N.A. Ademoh of the Department of mechanical engineering, Federal University of Technology, Minna. Also the supports of laboratory staff National Research Institute for Chemical Technology (NARICT) Zaria Kaduna state Nigeria were highly appreciated.

REFERENCE

1. Brinksmeier, E.; Huesmann, A.-G.; Schulz, J.(2012) Investigation of the Mechanism between Sulfur Containing Metal Working Fluids and Metal Surfaces by Scratch Experiments. In Proceedings of the Lubmat, Bilbao, Spain, 6–8 June 2012.
2. Farhanah, A.N., Syahrullail, S. and Sapawe, N., (2015). Tribological performance of raw and chemically modified RBD palm kernel. In Proceedings of Malaysian International Tribology Conference 2015, 207-208.
3. Katna, R., Singh, K., Agrawal, N. and Jain, S. (2017). Green Manufacturing-Performance of a Biodegradable Cutting Fluid. Materials and Manufacturing Processes, 32, 1522-1527.
4. Lawal, S. A., Abolarin, M. S., Ugheoke, B. I and Onche, E.O. (2003); Performance evaluation of cutting fluids developed from fixed oils;Leonado electronic journal of practices and technology; Retrieved from <http://www.lejpt.academicdirect>.
5. Lawal SA, Choudhury IA, Nukman Y. (2012). Application of vegetable oil-based metalworking



- fluids in machining ferrous metals a review. *Int J Mach Tools Manuf* 2012;52:1–12.
6. Lawal, SA, Choudhury, IA, Nukman Y, (2012). Application of vegetable oil-based metalworking fluids in machining ferrous metals—a review. *Int J Mach Tools Manuf* .52:1–12.
 7. Peng, D., et al., (2009). Tribological properties of diamond and SiO₂ nanoparticles added in paraffin. *Tribology International*, 42(6): p. 911-917.
 8. Sukirno* and Ningsih Y.R (2016). Utilization of sulphurized palm oil as cutting fluid base oil for broaching process. *International Conference on Recent Trends in Physics 2016 (ICRTP2016)* IOP Publishing *Journal of Physics: Conference Series* 755 (2016) 011001 doi:10.1088/1742-6596/755/1/011001
 9. Xue QJ, Liu WM and Zhang ZJ. (1997). Friction and wear properties of the surface modified the TiO₂ nanoparticle additive in liquid paraffin n. *Wear*..213(1-2):29-32.[http://dx.doi.org/10.1016/S0043-1648\(97\)00200-7](http://dx.doi.org/10.1016/S0043-1648(97)00200-7).
 10. Zainal, N.A. Zulkifli, N.W. Gulzar, M. Masjuki, H.H. (2018). A review on the chemistry, production, and technological potential of bio based lubricants, *Renewable and Sustainable Energy Reviews* 82 80–102.



SOIL MOISTURE AND NUTRIENTS CONTROL: AN AUTOMATED DESIGN PROPOSAL

Mustapha Mohammed¹, Elijah David Kure¹ & Yusuf Mubarak¹

¹Department of Computer Engineering, Nuhu Bamalli Polytechnic Zaria, Kaduna State.

ABSTRACT

Agriculture is the bedrock of economic growth, development and poverty eradication in the developing countries. Agriculture can be said to be a panacea for economic growth and human existence. This propose research work focuses on developing a close loop system that will automatically water and apply fertilizer to a farmland through the feedback signal received from the moisture and pH sensors. The water pump and the solenoid verves will remain OFF and CLOSE only when there is a signal from the sensors that indicate shortage of moisture or any of the three basic soil elements (NPK) required by the plant for better growth and yield. This approach will help to reduce the farmer (human resource) manual efforts in the area of Irrigation and fertilizer application which could lead to much higher yield of productivity. The novelty of this design is not in any kind a new invention, but rather applying the known technologies and knowledge and using them in appropriate areas in optimum amount to bring out an outstanding automated system from simple modules or components.

Keywords: *Automation, Irrigation, Soil Moisture, Soil nutrients, Control.*

1 INTRODUCTION

Agriculture is the bedrock of economic growth, development and poverty eradication in the developing countries. Agriculture can be said to be a panacea for economic growth and human existence. The quest for long-run economic growth will either be won or lost in the agricultural sector. [1] The Agricultural activities in Nigeria today is largely a single season farming that is the raining season, this is due to the weather conditions experienced in the country. The single season farming is not sufficient to meet the demand of the Nigerian populace not to talk of exporting the farm produce so as to boost the GDP of the nation. The key reason behind many farmers not engaging in all year crop production activities is because of the seasonal rain fall. Rain or water supply is one the basic requirements of all plants. No plant cannot survive without water supply to it. To

address this challenge, irrigation farming can be the panacea.

Plant production is also affected by the soil nutrients. Soil is a critical part of successful agriculture and is the original source of the nutrients that we use to grow crops. The nutrients move from the soil into plants. Nutrients are also a part of the food animals eat. In the end, we benefit from healthy soil. The healthiest soils produce the healthiest and most abundant food supplies. [2] Monitoring and control of the soil nutrients can boost the yield in no small way.

Building or maintaining healthy soil improves the productivity of cropland, rangeland and woodland. Healthy soil requires less maintenance, making lawns, gardens and landscapes easier to care for. Healthy soil also helps reduce erosion from wind and water, thus protecting air and water quality. Other benefits include: Increased plant growth and crop yields,

Increased retention and cycling of nutrients such as carbon, nitrogen, phosphorus and other nutrients, Increased capacity for soil to hold moisture and nutrients, Enhanced ability to filter and buffer potential organic and inorganic pollutants and Time and money saved by reducing water, fertilizer, pesticide and herbicide uses. [3]

2 METHODOLOGY

This chapter outline the materials used in the design, their working principles and design specifications and the design method used. The design method shows how the materials were put together to work as a unit so as to meet the desire need of the design.

2.1 MATERIALS USED IN THE DESIGN

The design of the automatic irrigation and soil fertility measurement and control system adopted the following materials in the implementation of the design. They are as follows;

- i. pH sensors (3)
- ii. Moisture sensors (3)
- iii. Signal Conditioning Circuits (3)
- iv. ESP32 Microcontroller board (4)
- v. Arduino Integrated Development Environment
- vi. 12V D.C Relay (2)
- vii. Solenoid Valves (2)

pH sensors: The pH value of a solution is measured using a pH electrode. It consists essentially of a pair of electrodes, measurement and reference electrode, both submerged in the solution of unknown pH.

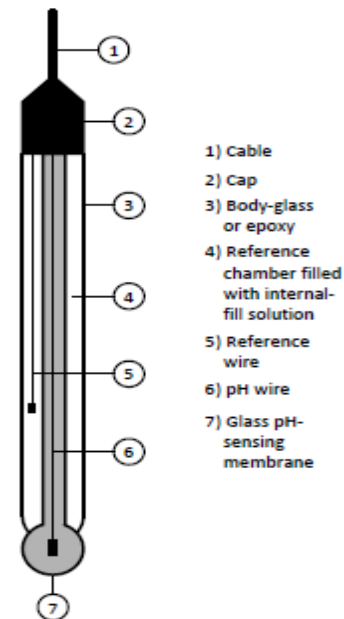


Figure 1: pH Electrode (Source: Texas Instruments)

These two electrodes essentially form two half cells. Although the potential developed in the reference cell is constant, the potential of the measurement cell depends on the concentration of hydrogen ions in the solution and is governed by the Nernst equation:

$$E = E_0 + \frac{RT \ln(aC)}{nF} \quad (1)$$

Where:

- E= e.m.f of the half-cell
- E₀= e.m.f of the half-cell under saturated condition
- R= Gas constant (8.314 J/ 0 C)
- T= Absolute temperature (K)
- N= valance of the ion
- F= Faraday Constant = 96493 C
- a= Activity co-efficient (0 1) ≤ ≤ a ; for a very dilute solution, a → 1
- C= molar concentration of ions.

Moisture sensors: Soil moisture is the water that is held in the spaces between soil particles. Surface soil moisture is the water that is in the upper 10 cm of soil, whereas root zone soil moisture is the water that is available to plants, which is generally considered to be in the upper 200 cm of soil. The Moisture sensor is used to measure the water content (moisture) of soil. when the soil is having water shortage, the module output is at high level, else the output is at low level. This sensor reminds the user to water their plants and also monitors the moisture content of soil. It has been widely used in agriculture, land irrigation and botanical gardening. The figure below shows the soil electrode chosen for this design.



Figure 2: Soil Moisture Sensor

(Source: <https://www.delmhorst.com>).

pH Signal Conditioning Circuit: The board in figure 12 have the ability to supply a voltage output to the analogue pin of a microcontroller that will represent a pH value just like any other sensor. Ideally, one will want a pH 0 represent 0v and a pH of 14 to represent 5V. But there is a twist with pH sensor, by default the pH probe have pH 7 set to 0V (or near it, it differs from one pH probe to another, that is why we have to calibrate the probe as you will see later on), This means that the voltage will go into the minuses when reading acidic PH values and that cannot be read by the analogue Microcontroller port. The offset pot is used to change this so that a pH 7 will read the expected 2.5V to the Microcontroller analogue pin, the analogue pin can read voltages between 0V and 5V hence the

2.5V that is halfway between 0V and 5V as a pH 7 is halfway between pH 0 and pH 14. One will need to turn the offset potentiometer to get the right offset, the offset pot is the blue pot nearest to the BNC connector.

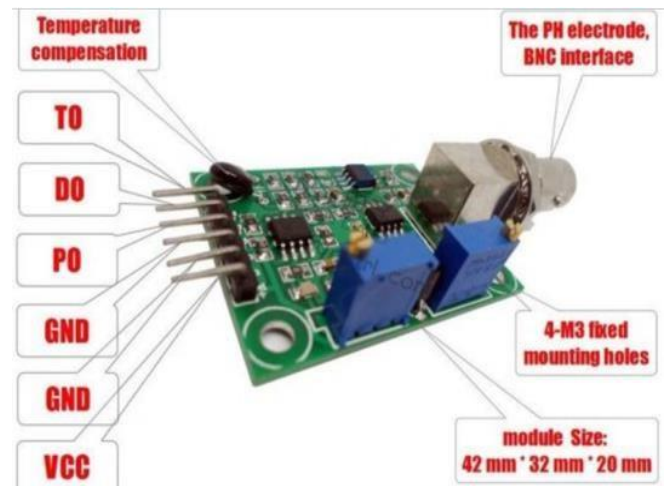


Figure 3: pH Signal Conditioning Module Board

pH Signal Conditioning Module Board Pinout

TO – Temperature output

DO – 3.3V Output (from pH limit pot)

PO – PH analog output ==> **ADC pin of ESP32**

Gnd – Gnd for PH probe (can come from Arduino GND pin) ==> **GND of ESP32**

Gnd – Gnd for board (can also come from Arduino GND pin) ==> **GND of ESP32**

VCC – 5V DC (can come from Arduino 5V pin) ==> **5V pin of ESP32**

POT 1 – Analog reading offset (Nearest to BNC connector)

POT 2 – PH limit setting

ESP32 Node Microcontroller Board: ESP32-DevKitC V4 is a small-sized ESP32-based development board produced by Espressif. Most of the I/O pins are broken out to the pin headers on both sides for easy interfacing. Developers can either connect peripherals with jumper wires or mount ESP32-DevKitC V4 on a breadboard.

There are many versions of ESP32 chip available in the market. ESP32 devkit uses ESP-WROOM-32 module. But the functionality of all GPIO pins is the same across all ESP32 development boards.

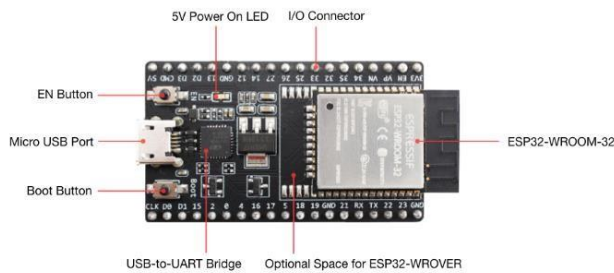


Figure 4: Functional Description of ESP32
(Source: www.espressif.com)

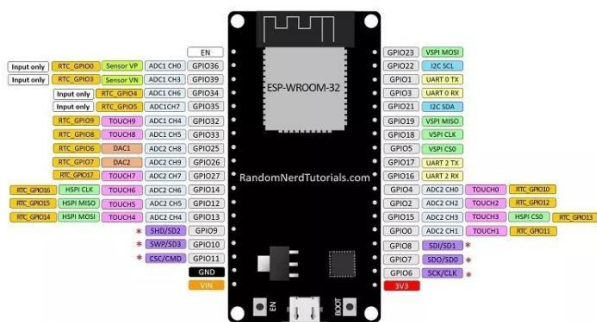


Figure 5: ESP32 Pinout Reference
(Source: www.espressif.com)

The ESP32 peripherals include:

- 18 Analog-to-Digital Converter (ADC) channels
- 3 SPI interfaces
- 3 UART interfaces
- 2 I2C interfaces
- 16 PWM output channels
- 2 Digital-to-Analog Converters (DAC)
- 2 I2S interfaces

- 10 Capacitive sensing GPIOs

Arduino Integrated Development Environment:

The Arduino Integrated Development Environment - or Arduino Software (IDE) - contains a text editor for writing code, a message area, a text console, a toolbar with buttons for common functions and a series of menus. It connects to the Arduino, Genuino, ESP8266, ESP32 e.t.c hardware to upload programs and communicate with them. [30]

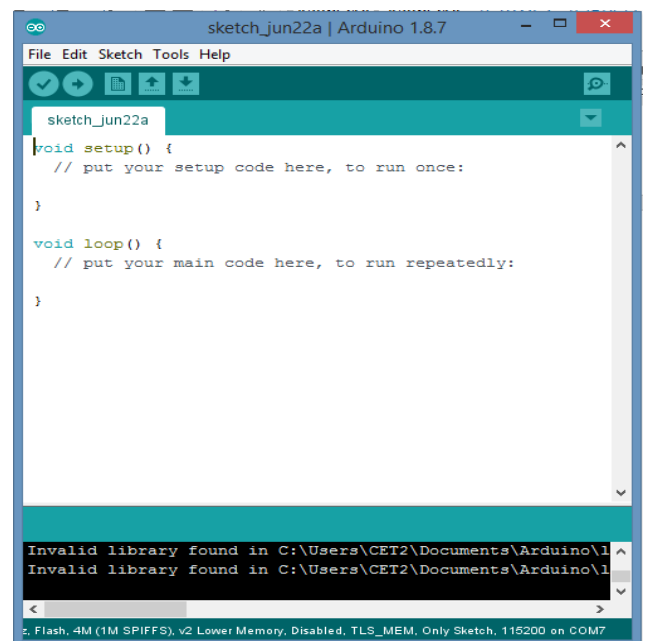


Figure 6: Arduino Integrated Development Environment version 1.8.7

12V DC Electromechanical Relay: A DC relay uses a single coil of wire wound around the iron core to make the electromagnet. When the DC coil is energized, the magnetism generated in the core is steady because the DC just keeps going.



Figure 7: Figure 18: 12V DC Relay

(Source: www.amazon.com)

Relays are switches that open and close circuits electromechanically or electronically. Relays control one electrical circuit by opening and closing contacts in another circuit. As relay diagrams show, when a relay contact is normally open (NO), there is an open contact when the relay is not energized. When a relay contact is Normally Closed (NC), there is a closed contact when the relay is not energized. In either case, applying electrical current to the contacts will change their state. Relays are generally used to switch smaller currents in a control circuit and do not usually control power consuming devices except for small motors and Solenoids that draw low amps. Nonetheless, relays can "control" larger voltages and amperes by having an amplifying effect because a small voltage applied to a relays coil can result in a large voltage being switched by the contacts. Protective relays can prevent equipment damage by detecting electrical abnormalities, including overcurrent, undercurrent, overloads and reverse currents. In addition, relays are also widely used to switch starting coils, heating elements, pilot lights and audible alarms.

Solenoid Valve: A solenoid valve is an electromechanical device in which the

solenoid uses an electric current to generate a magnetic field and thereby operate a mechanism which regulates the opening of fluid flow in a valve.



Figure 8: Solenoid Valve

(Source: www.amazon.com)

A solenoid valve is a combination of two basic functional units:

- A solenoid (electromagnet) with its core.
- A valve body containing one or more orifices.

Flow through an orifice is shut off or allowed by the movement of the core when the solenoid is energized or de-energized.

2.2 DESIGN METHOD

The method employed in this research work is classified into two; Hardware connection and software interfacing of the components.

- Design of Sensor Nodes:** The primary thing in the design of the sensor node is the interfacing of the pH and Moisture sensor with the ESP32 Wi-fi board. To interface the sensors with the microcontroller, it will involve both hardware and software connections.

- Hardware Design of Sensor Nodes:** The soil moisture probe, pH probe, pH signal conditioning board interfaced with ESP32 Wi-fi board forms the Sensor node. The primary responsibility of the sensor node is to sense the moisture and pH level of the soil, process it and present the result wirelessly to the control unit. The wiring diagram of the sensor node is shown in figure 21 below.

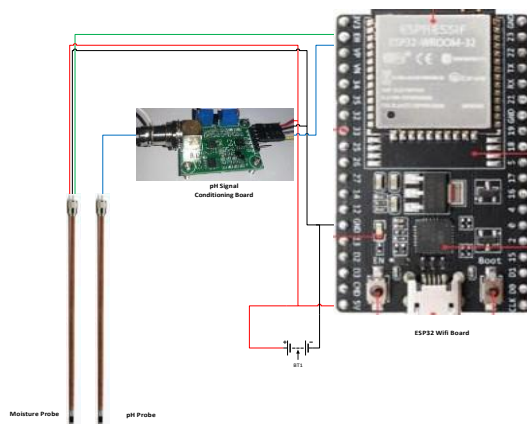


Figure 9: Moisture sensor and pH sensor Interfaced with ESP32

The wiring diagram of Figure 21 above shows the signal and the power supply connections from the moisture sensor to the ESP32 board. The sensor receives 5V power from the ESP32 board and creates a voltage proportional to the dielectric permittivity of the soil. Dielectric permittivity of the soil is the moisture level or the amount of water that is held in the spaces between soil particles. The voltage created by the moisture sensor is carried by the signal line to one of the Analogue-to-digital (ADC) pin of the ESP32 Wifi board which described the level of water content of the soil. The sense voltage usually is high enough to drive the input of ADC directly without signal conditioning.

The pH probe being a passive sensor does not require power supply to it. It consists essentially of a pair of electrodes, measurement and reference electrode. These two electrodes essentially form two half cells. Although the potential developed in the reference cell is constant, the potential of the measurement cell depends on the concentration of hydrogen ions in the solution. The pH sensor through electrochemical reaction generate a signal voltage which is directly proportional to the amount of ions measured by the measurement electrode. The signal voltage is usually in milli Volt which requires signal conditioning. Ideally, one will want a pH 0 to represent 0v and a pH of 14 to represent 5V. But there is a twist with pH sensor as seen in table 2 above. By default, the pH probe has pH 7 set to 0V this means that the voltage will go into the minuses when reading acidic pH values and that cannot be read by the analogue Pin of the Microcontroller. This is another reason for signal conditioning.

The weak signal in milli volts will be amplified by the signal conditioning circuit to a higher voltage level in volts. The voltages in minuses was taken care of by the op-amp and the voltage divider which have an offset potentiometer. The offset potentiometer is used to change the minuses, so that a pH 7 will read the expected 2.5V to the Microcontroller analogue pin, the analogue pin can read voltages between 0V and 5V hence the 2.5V that is halfway between 0V and 5V as a pH 7 is halfway between pH 0 and pH 14. One will need to turn the offset potentiometer to get the right offset, the offset pot is the blue pot nearest to the BNC connector.

- Software Design of Sensor Nodes:** The software design is essentially the design of signal flow and processing pattern of the microcontroller. It tells which pin the microcontroller will pick input signal and which one it will give out output. It also specifies the desire operation the microcontroller will carry out on the signal before outputting it. flowchart is always used in designing software program before writing of code on the Integrated Development Environment (IDE) for compilation and uploading of the Hex file on the microcontroller. The software designed for the sensor node, included individual flowcharts of both sensors as shown below

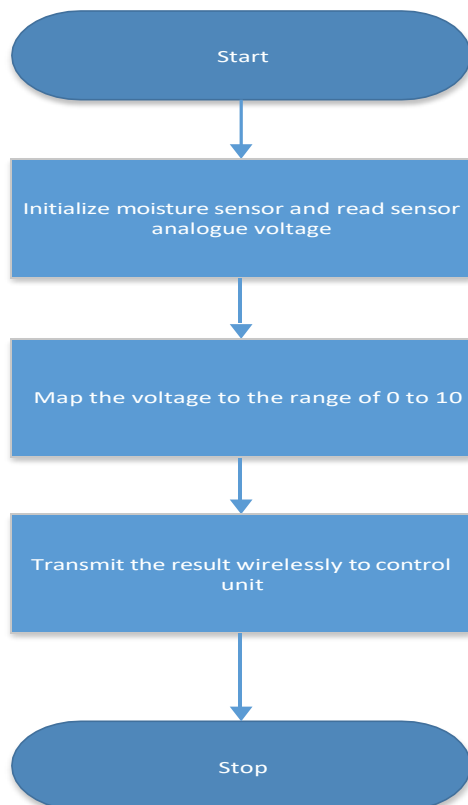


Figure 10: Flowchart of Moisture level sensing

Figure 10 shows the flowchart of the moisture level sensing employed in the design of the system. the sensor was initialized, by initializing we mean that the sensor was set to clear all previous signals in the sensor so as to avoid error in measurement. After that, then the signal voltage was read at the GPIO39 pin which is one of the analogue pins of the esp32 board. The ADC converted the signal voltage to values between 0 to 1023. This range of values was mapped to the range of 0-10, with 0-3 indicating low moisture, 4-7 indicating Normal moisture and 7-10 indicating High moisture. This results of measurement were transmitted to the control unit for necessary action when the condition of threshold value is met.

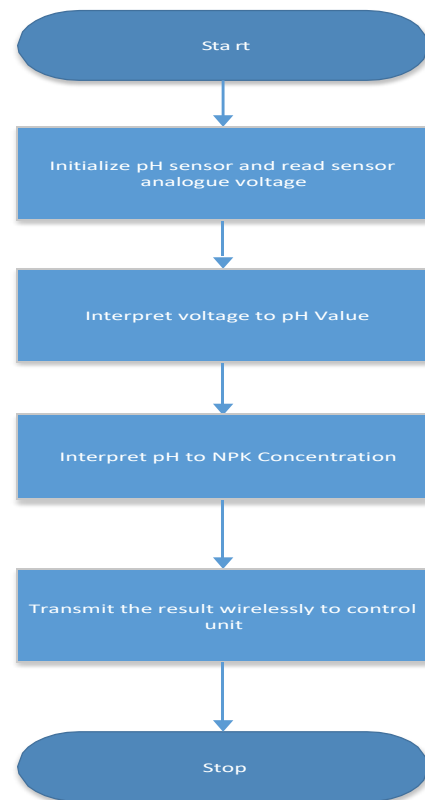


Figure 11: Flowchart of pH level sensing and NPK Concentration

ii. Design of Control Unit

• Hardware Design

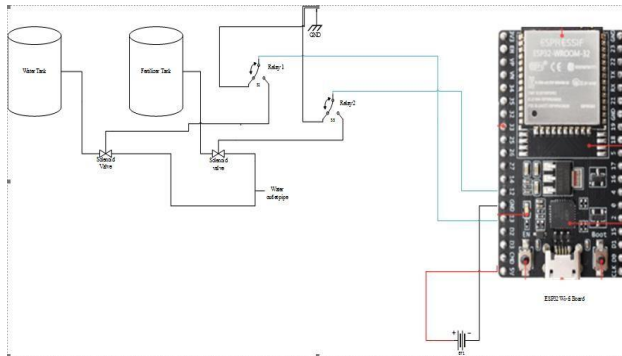


Figure 12: Relay and Solenoid valve interfacing with ESP32 at the Control Unit.

Software Design:

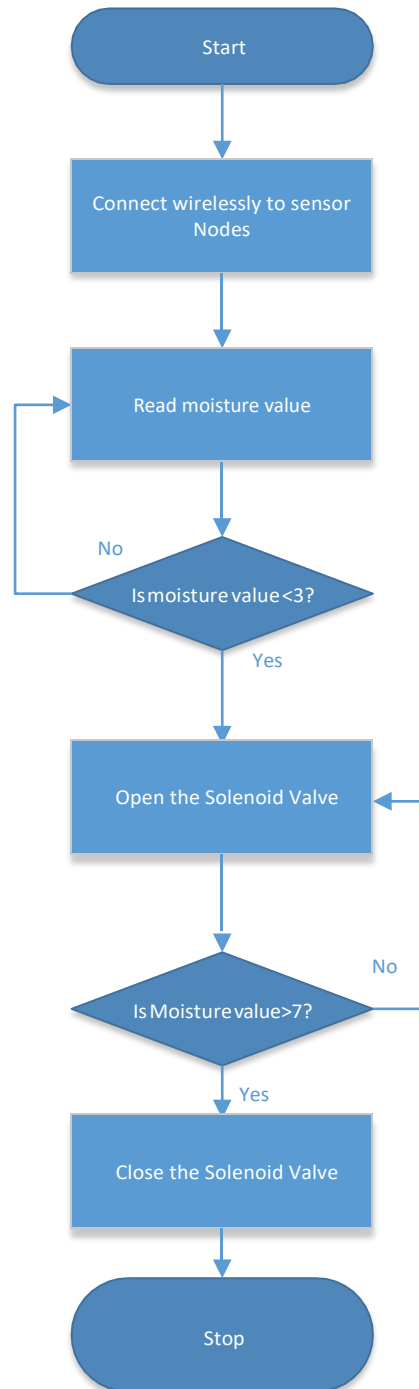


Figure 13: Flowchart of pH level sensing and NPK Concentration



**3rd IEC
2019**



ISBN: 978 - 978 - 52341 - 6 - 9